RH-TRU 72-B

Safety Analysis Report

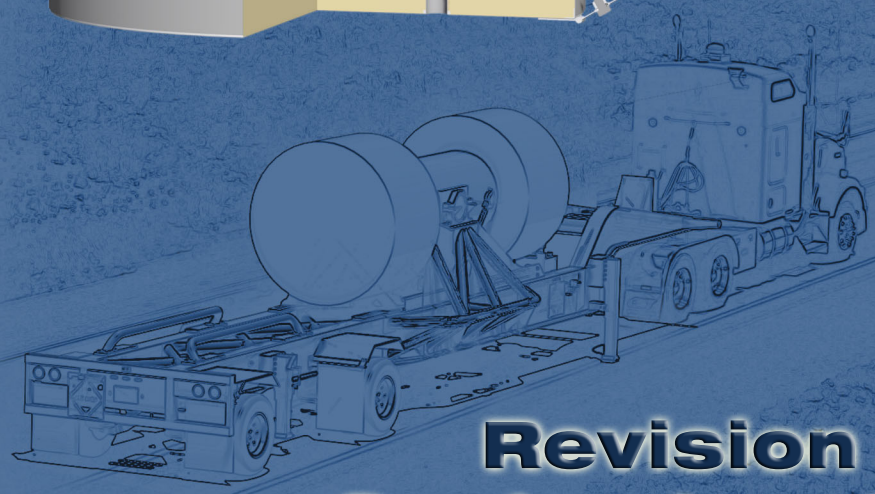

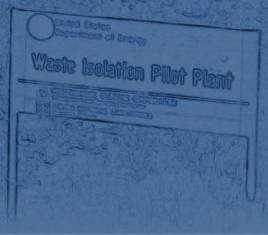

Revision 4
September 2005

This page intentionally left blank to facilitate duplex printing.

TABLE OF CONTENTS

1.0 GENERAL INFORMATION 1.1-1

1.1 Introduction 1.1-1

1.2 Package Description 1.2-1

1.2.1 Packaging 1.2-1

1.2.2 Operational Features 1.2-5

1.2.3 Contents of Packaging 1.2-6

1.2.4 Package Evaluation 1.2-6

1.3 Appendices 1.3-1

1.3.1 Packaging General Arrangement Drawings 1.3.1-1

1.3.2 Glossary of Terms and Acronyms 1.3.2-1

2.0 STRUCTURAL EVALUATION 2.1-1

2.1 Structural Design 2.1-1

2.1.1 Discussion 2.1-2

2.1.2 Design Criteria 2.1-2

2.2 Weights and Centers of Gravity 2.2-1

2.3 Mechanical Properties of Materials 2.3-1

2.4 General Standards for All Packages 2.4-1

2.4.1 Minimum Package Size 2.4-1

2.4.2 Tamper Indicating Feature 2.4-1

2.4.3 Positive Closure 2.4-1

2.4.4 Chemical and Galvanic Reactions 2.4-1

2.5 Lifting and Tie-down Standards for All Packages 2.5-1

2.5.1 Lifting Devices 2.5-1

2.5.2 Tie-down Devices 2.5-5

2.6 Normal Conditions of Transport 2.6-1

2.6.1 Heat 2.6-1

2.6.2 Cold 2.6-7

2.6.3 Reduced External Pressure 2.6-7

2.6.4 Increased External Pressure 2.6-7

2.6.5 Vibration 2.6-8

2.6.6 Water Spray 2.6-9

2.6.7 Free Drop 2.6-9

2.6.8 Corner Drop 2.6-39

2.6.9 Compression 2.6-39

2.6.10 Penetration 2.6-40
2.7 Hypothetical Accident Conditions 2.7-1
2.7.1 Free Drop 2.7-1
2.7.2 Crush 2.7-23
2.7.3 Puncture 2.7-23
2.7.4 Thermal 2.7-32
2.7.5 Immersion – Fissile Material 2.7-36
2.7.6 Immersion – All Packages 2.7-36
2.7.7 Deep Water Immersion Test 2.7-36
2.7.8 Summary of Damage 2.7-37
2.8 Special Form 2.8-1
2.9 Fuel Rods 2.9-1
2.10 Appendices 2.10-1
2.10.1 Finite Element Analysis (FEA) Models 2.10.1-1
2.10.2 Drop Analysis Codes Description 2.10.2-1
2.10.3 Drop Impact Evaluation Results 2.10.3-1
2.10.4 Slapdown Assessment 2.10.4-1
2.10.5 Buckling Design Criteria and Detailed Evaluation 2.10.5-1
2.10.6 Closure Bolt Stress Evaluations 2.10.6-1
2.10.7 Static and Dynamic Testing 2.10.7-1
2.10.8 Fabrication Stresses Due to Lead Pour 2.10.8-1

3.0 THERMAL EVALUATION 3.1-1
3.1 Discussion 3.1-1
3.2 Summary of Thermal Properties of Materials 3.2-1
3.3 Technical Specifications of Components 3.3-1
3.4 Thermal Evaluation for Normal Conditions of Transport 3.4-1
3.4.2 Maximum Temperatures 3.4-2
3.4.3 Minimum Temperatures 3.4-2
3.4.4 Maximum Internal Pressure 3.4-2
3.4.5 Maximum Thermal Stresses 3.4-11
3.4.6 Evaluation of Package Performance for Normal Conditions of Transport 3.4-11
3.5 Hypothetical Accident Thermal Evaluation 3.5-1
3.5.1 Thermal Model 3.5-1
3.5.2 Package Conditions and Environment 3.5-2
3.5.3 Package Temperatures 3.5-3
3.5.4 Maximum Internal Pressure 3.5-3

3.5.5 Maximum Thermal Stresses 3.5-4
3.5.6 Evaluation of Package Performance for the Hypothetical Accident Thermal Conditions 3.5-4
3.6 Appendices 3.6-1
3.6.1 Thermal Model Details 3.6.1-1
3.6.2 Finite Difference Thermal Analysis and Results 3.6.2-1
3.6.3 Polyurethane Foam Performance Tests 3.6.3-1
3.6.4 Designating an Alternative Seal Material 3.6.4-1

4.0 CONTAINMENT 4.1-1
4.1 Containment Boundary 4.1-1
4.1.1 Containment Vessel 4.1-1
4.1.2 Containment Penetrations 4.1-3
4.1.3 Seals and Welds 4.1-3
4.1.4 Closure 4.1-4
4.2 Requirements for Normal Conditions of Transport 4.2-1
4.2.1 Containment of Radioactive Material 4.2-1
4.2.2 Pressurization of Containment Vessel 4.2-1
4.2.3 Containment Criterion 4.2-1
4.3 Containment Requirements for the Hypothetical Accident Conditions 4.3-1
4.3.1 Fission Gas Products 4.3-2
4.3.2 Containment of Radioactive Material 4.3-2
4.3.3 Containment Criterion 4.3-3

5.0 SHIELDING EVALUATION 5.1-1
5.1 Discussion and Results 5.1-1
5.2 Source Specification 5.2-1
5.2.1 Gamma Source 5.2-2
5.2.2 Neutron Source 5.2-2
5.3 Model Specification 5.3-1
5.3.1 Description of Radial and Axial Shielding Configuration 5.3-1
5.3.2 Shield Regional Densities 5.3-1
5.4 Shielding Evaluation 5.4-1
5.4.1 Gamma Shielding Evaluation 5.4-1
5.4.2 Neutron Shielding Evaluation 5.4-3
5.4.3 Total Radiation Source 5.4-4
5.5 Appendices 5.5-1
5.5.1 HAC at 1m Co-60 Point Source Gamma Shielding Analysis 5.5.1-1

5.5.2 Derivation of MCNP Neutron Subcritical Multiplication Factor 5.5.2-1
5.5.3 Screening Methodology for Neutron Emitting Isotopes 5.5.3-1
5.5.4 Screening Methodology for Gamma Emitting Isotopes 5.5.4-1
5.5.5 Evaluation of the Effect of NCT to HAC Changes on Neutron Dose Rates 5.5.5-1
5.5.6 Evaluation of the Effect of NCT-to-HAC Changes on Gamma Dose Rates 5.5.6-1
5.5.7 MCNP Input Files for the Shielding Analyses 5.5.7-1

6.0 CRITICALITY EVALUATION 6.1-1

6.1 Discussion of Results 6.1-1

6.2 Package Contents 6.2-1
6.2.1 Applicability of Case A Limits – General Payload 6.2-1
6.2.2 Applicability of Case B Limits – Special Reflector Payload 6.2-3
6.2.3 Applicability of Case C Limits – Machine-Compacted Payload 6.2-3
6.2.4 Applicability of Case D Limits – LEU Payload 6.2-4

6.3 Model Specifications 6.3-1
6.3.1 Contents Models 6.3-1
6.3.2 Package Model 6.3-3
6.3.3 Single Package Models 6.3-5
6.3.4 Array Models 6.3-5
6.3.5 Package Regional Densities 6.3-5

6.4 Criticality Calculations 6.4-1
6.4.1 Calculational or Experimental Method 6.4-1
6.4.2 Fuel Loading or Other Contents Loading Assumptions 6.4-1
6.4.3 Criticality Results 6.4-2

6.5 Critical Benchmark Experiments 6.5-1
6.5.1 Benchmark Experiments and Applicability 6.5-1
6.5.2 Details of Benchmark Calculations 6.5-3
6.5.3 Results of Benchmark Calculations 6.5-3

7.0 OPERATING PROCEDURES 7.1-1

7.1 Procedures for Loading the Package 7.1-1

7.2 Procedures for Unloading the Package 7.2-1

7.3 Preparation of an Empty Package for Transport 7.3-1
7.3.1 Shipment of the Package as LSA Material 7.3-1

7.4 Appendices 7.4-1
7.4.1 Preshipment Leakage Rate Test 7.4.1-1

8.0 ACCEPTANCE TESTS AND MAINTENANCE PROGRAM 8.1-1
8.1 Acceptance Tests 8.1-1
8.1.1 Visual Inspection 8.1-1
8.1.2 Structural and Pressure Tests 8.1-1
8.1.3 Fabrication Leakage Rate Tests 8.1-2
8.1.4 Component Tests 8.1-9
8.1.5 Tests for Shielding Integrity 8.1-16
8.1.6 Thermal Acceptance Tests 8.1-17
8.1.7 Lead Installation Tests 8.1-18
8.2 Maintenance Program 8.2-1
8.2.1 Structural and Pressure Tests 8.2-1
8.2.2 Maintenance/Periodic Leakage Rate Tests 8.2-2
8.2.3 Subsystems Maintenance 8.2-6
8.2.4 Valves, Rupture Discs, and Gaskets 8.2-8
8.2.5 Shielding 8.2-8
8.2.6 Thermal 8.2-8
8.2.7 Criticality Control Materials 8.2-8
8.3 Appendices 8.3-1
8.3.1 Lead Installation Procedure 8.3.1-1

9.0 QUALITY ASSURANCE 9.1-1
9.1 Introduction 9.1-1
9.2 Quality Assurance Requirements 9.2-1
9.2.1 U.S. Nuclear Regulatory Commission 9.2-1
9.2.2 U.S. Department of Energy 9.2-1
9.2.3 Transportation to/from WIPP 9.2-1
9.3 Quality Assurance Program 9.3-1
9.3.1 NRC Regulatory Guide 7.10 ..... 9.3-1
9.3.2 Design 9.3-1
9.3.3 Fabrication, Assembly, and Testing 9.3-1
9.3.4 Procurement 9.3-1
9.3.5 Use 9.3-1
9.3.6 Maintenance and Repair 9.3-2

LIST OF TABLES

Table 1.2-1 – Overall Component Weights 1.2-7
Table 2.1-1 – Containment Components Allowable Stress Limits 2.1-8

Table 2.1-2 – Non-Containment Components Allowable Stress Limits 2.1-9
Table 2.1-3 – Shell Buckling Geometries 2.1-9
Table 2.2-1 – RH-TRU 72-B Package Component Weights, Centers of Gravity, and Mass Moments of Inertia 2.2-2
Table 2.3-1 – Mechanical Properties of Steel Used in the RH-TRU 72-B Package 2.3-3
Table 2.3-2 – Mechanical Properties of Lead Used in the RH-TRU 72-B Package 2.3-4
Table 2.3-3 – Crush Stress vs. Strain for 11½ lb/ft³ Nominal Density Polyurethane Foam 2.3-4
Table 2.5-1 – Material Properties for Type 304 Stainless Steel at 143 ºF 2.5-13
Table 2.5-2 – Data Used in Tie-down Trunnion Lifting Stress Analysis 2.5-14
Table 2.5-3 – Trunnion Stress Analysis for a Vertical Lift 2.5-15
Table 2.5-4 – Trunnion Stress Analysis for a Horizontal Lift 2.5-16
Table 2.6-1 – Summary of NCT Material Properties for Analysis 2.6-41
Table 2.6-2 – Maximum NCT Temperatures 2.6-42
Table 2.6-3 – Package Parameters for Pressure Stress Calculations 2.6-42
Table 2.6-4 – Unit Pressure Stress Results for P1 – P6 ..... 2.6-43
Table 2.6-5 – Unit Pressure Stress Results for P7 – P10 ..... 2.6-43
Table 2.6-6 – Maximum Pressure Stress Results for P1 – P10 ..... 2.6-43
Table 2.6-7 – Package Stresses Due to Side Drop 2.6-44
Table 2.6-8 – NCT End Drop, OC Lid Bending 2.6-44
Table 2.6-9 – NCT Top-End Drop, IV Shell with 42.5*g* Acceleration 2.6-45
Table 2.6-10 – NCT Bottom-End Drop, IV Shell with 42.5*g* Acceleration 2.6-45
Table 2.6-11 – Fabrication Induced OC Inner Shell Hoop Stress, Interface Pressure, and Axial Load That Can Be Supported 2.6-46
Table 2.6-12 – OC Shell Stresses with Maximum End Drop Fab Condition 2.6-46
Table 2.6-13 – NCT Fab & End Drop, OC Inner Shell with 42.5*g* at -20 ºF 2.6-46
Table 2.6-14 – NCT Fab & End Drop, OC Inner Shell with 42.5*g* at 70 ºF 2.6-47
Table 2.6-15 – NCT Fab & End Drop, OC Inner Shell with 42.5*g* at 160 ºF 2.6-47
Table 2.6-16 – NCT End Drop, Lead Pressure and Hoop Stress Summary 2.6-48
Table 2.6-17 – NCT End Drop, OC Shell Stresses with Zero Fabrication Condition with 42.5*g* Acceleration 2.6-48
Table 2.6-18 – NCT End Drop, OC Inner Shell with 42.5*g* at -20 ºF 2.6-48
Table 2.6-19 – NCT End Drop, OC Inner Shell with 42.5*g* at 70 ºF 2.6-49
Table 2.6-20 – NCT End Drop, OC Inner Shell with 42.5*g* at 160 ºF 2.6-49

Table 2.6-21 – OC Shell Stresses with Max Oblique Drop Fab Condition 2.6-50
Table 2.6-22 – NCT Fab & Oblique Drop, OC Inner Shell with 17.9*g* at -20 ºF 2.6-50
Table 2.6-23 – NCT Fab & Oblique Drop, OC Inner Shell with 17.9*g* at 70 ºF 2.6-51
Table 2.6-24 – NCT Fab & Oblique Drop, OC Inner Shell with 17.9*g* at 160 ºF 2.6-51
Table 2.6-25 – NCT Oblique Drop, IV Shell with 17.9*g* at 70 ºF 2.6-52
Table 2.6-26 – NCT Oblique Drop, Canister Shell with 17.9*g* at 200 ºF 2.6-52
Table 2.6-27 – OC Shell Stresses with Max Side Drop Fab Condition 2.6-53
Table 2.6-28 – NCT Fab & Side Drop, OC Inner Shell with 19.3*g* at -20 ºF 2.6-53
Table 2.6-29 – NCT Fab & Side Drop, OC Inner Shell with 19.3*g* at 70 ºF 2.6-54
Table 2.6-30 – NCT Fab & Side Drop, OC Inner Shell with 19.3*g* at 160 ºF 2.6-54
Table 2.6-31 – NCT Side Drop, IV Shell with 19.3*g* at 160 ºF 2.6-55
Table 2.6-32 – NCT Side Drop, Canister Shell with 19.3*g* at 200 ºF 2.6-55
Table 2.6-33 – NCT Fab & Side Drop, OC Shells' Welds with 19.3*g* at -20 ºF 2.6-56
Table 2.7-1 – Summary of HAC Material Properties for Analysis 2.7-38
Table 2.7-2 – Fabrication Induced OC Inner Shell Hoop Stress, Interface Pressure, and Axial Load That Can Be Supported 2.7-39
Table 2.7-3 – OC Shell Stresses with Maximum End Drop Fab Condition 2.7-39
Table 2.7-4 – HAC Fab & End Drop, OC Inner Shell with 89.7*g* at -20 ºF 2.7-39
Table 2.7-5 – HAC Fab & End Drop, OC Inner Shell with 89.7*g* at 70 ºF 2.7-40
Table 2.7-6 – HAC Fab & End Drop, OC Inner Shell with 89.7*g* at 160 ºF 2.7-40
Table 2.7-7 – HAC End Drop, Lead Pressure and Hoop Stress Summary 2.7-41
Table 2.7-8 – HAC End Drop, OC Shell Stresses with Zero Fabrication Condition with 89.7*g* Acceleration 2.7-41
Table 2.7-9 – HAC End Drop, OC Inner Shell with 89.7*g* at -20 ºF 2.7-41
Table 2.7-10 – HAC End Drop, OC Inner Shell with 89.7*g* at 70 ºF 2.7-42
Table 2.7-11 – HAC End Drop, OC Inner Shell with 89.7*g* at 160 ºF 2.7-42
Table 2.7-12 – OC Shell Stresses with Max Oblique Drop Fab Condition 2.7-43
Table 2.7-13 – HAC Fab & Oblique Drop, OC Inner Shell with 48.1*g* at -20 ºF 2.7-43
Table 2.7-14 – HAC Fab & Oblique Drop, OC Inner Shell with 48.1*g* at 70 ºF 2.7-44
Table 2.7-15 – HAC Fab & Oblique Drop, OC Inner Shell with 48.1*g* at 160 ºF 2.7-44
Table 2.7-16 – HAC Oblique Drop, IV Shell with 48.1*g* at 70 ºF 2.7-45
Table 2.7-17 – HAC Oblique Drop, Canister Shell with 48.1*g* at 200 ºF 2.7-45
Table 2.7-18 – OC Shell Stresses with Max Side Drop Fab Condition 2.7-46

Table 2.7-19 – HAC Fab & Side Drop, OC Inner Shell with 81.2*g* at -20 ºF 2.7-46
Table 2.7-20 – HAC Fab & Side Drop, OC Inner Shell with 81.2*g* at 70 ºF 2.7-47
Table 2.7-21 – HAC Fab & Side Drop, OC Inner Shell with 81.2*g* at 160 ºF 2.7-47
Table 2.7-22 – HAC Side Drop, IV Shell with 81.2*g* at 160 ºF 2.7-48
Table 2.7-23 – HAC Side Drop, Canister Shell with 81.2*g* at 200 ºF 2.7-48
Table 2.7-24 – HAC Fab & Side Drop, OC Shells' Welds with 81.2*g* at -20 ºF..... 2.7-49
Table 2.7-25 – Stress-Strain Values for Type 304 Stainless Steel at 212 ºF 2.7-49
Table 2.7-26 – Stresses Due to 300 psig Pressure 2.7-50
Table 2.7-27 – Thermal Stress Summary 2.7-50
Table 2.7-28 – Buckling Geometry Parameters per Code Case N-284 ..... 2.7-51
Table 2.7-29 – Stresses for 290 psig External Pressure + Fabrication 2.7-51
Table 2.7-30 – Buckling Summary for 290 psig External Pressure + Fab 2.7-52
Table 2.10.1-1 – Input Listing for Trunnion Loading the OC Outer Shell..... 2.10.1-3
Table 2.10.1-2 – Input Listing for IV Radius Transition Zone Stresses Due to Pressure . 2.10.1-11
Table 2.10.1-3 – Input Listing for IV Radius Transition Zone Stresses Due to 1*g* Acceleration 2.10.1-15
Table 2.10.1-4 – Containment Assembly Node and Element Numbering 2.10.1-20
Table 2.10.2-1 – CASKDROP Sample Problem Output Files 2.10.2-7
Table 2.10.2-2 – Sample Inputs to the SLAPDOWN Program 2.10.2-13
Table 2.10.2-3 – Sample Force-Deflection to the SLAPDOWN Program..... 2.10.2-13
Table 2.10.2-4 – Sample of SLAPDOWN General Output..... 2.10.2-14
Table 2.10.2-5 – Sample of SLAPDOWN Time History Output 2.10.2-15
Table 2.10.2-6 – Comparison of SLAPDOWN and SCANS Results..... 2.10.2-16
Table 2.10.3-1 – Polyurethane Foam Data used in CASKDROP..... 2.10.3-3
Table 2.10.3-2 – CASKDROP Output File for NCT End Drop, Cold (-20 ºF)..... 2.10.3-4
Table 2.10.3-3 – CASKDROP Output File for NCT End Drop, Warm (140 ºF)..... 2.10.3-5
Table 2.10.3-4 – CASKDROP Output File for NCT Side Drop, Cold (-20 ºF) 2.10.3-6
Table 2.10.3-5 – CASKDROP Output File for NCT Side Drop, Warm (140 ºF) 2.10.3-7
Table 2.10.3-6 – CASKDROP Output File for HAC End Drop, Cold (-20 ºF) 2.10.3-8
Table 2.10.3-7 – CASKDROP Output File for HAC End Drop, Warm (140 ºF) 2.10.3-9
Table 2.10.3-8 – CASKDROP Output File for HAC Side Drop, Cold (-20 ºF)..... 2.10.3-10
Table 2.10.3-9 – CASKDROP Output File for HAC Side Drop, Warm (140 ºF)..... 2.10.3-11

Table 2.10.3-10 – Summary of End and Side Drop Impact Accelerations and Impact Limiter Deflections 2.10.3-12

Table 2.10.3-11 – Maximum Package Responses as a Function of Initial Impact Angle (-20 ºF Cases) 2.10.3-13

Table 2.10.3-12 – Maximum Package Responses as a Function of Initial Impact Angle (140 ºF Cases) 2.10.3-14

Table 2.10.3-13 – Summary of Impact Limiter Separation Moments 2.10.3-15

Table 2.10.3-14 – Time-History Details from the Maximum Impact Force Condition SLAPDOWN Analyses (NCT, -20 ºF, 1-foot Drop) 2.10.3-15

Table 2.10.3-15 – Time-History Details from the Maximum Impact Force Condition SLAPDOWN Analyses (HAC, -20 ºF, 30-foot Drop) 2.10.3-16

Table 2.10.4-1 – Impact Force and Maximum Deflections for Cold (-20 ºF) HAC Slapdown Cases 2.10.4-3

Table 2.10.4-2 – Impact Force and Maximum Deflections for Warm (140 ºF) HAC Slapdown Cases 2.10.4-3

Table 2.10.4-3 – Force-Deflection Data for Cold (-20 ºF) and Warm (140 ºF) HAC 0º Slapdowns 2.10.4-4

Table 2.10.4-4 – Shear and Moment During Slapdown 2.10.4-5

Table 2.10.4-5 – Thrust and Moment Due to HAC Cold (-20 ºF) Slapdown Cases 2.10.4-5

Table 2.10.4-6 – Thrust and Moment Due to HAC Warm (140 ºF) Slapdown Cases 2.10.4-5

Table 2.10.4-7 – Stresses and Margins of Safety Due to HAC Cold (-20 ºF) Slapdown 2.10.4-6

Table 2.10.4-8 – Stresses and Margins of Safety Due to HAC Warm (140 ºF) Slapdown 2.10.4-6

Table 2.10.4-9 – Comparison of Allowable and Predicted Deformations for Warm (140 ºF) Slapdown 2.10.4-6

Table 2.10.5-1 – Geometry, Geometric Parameters, and Material Data Used in Buckling Evaluations 2.10.5-10

Table 2.10.5-2 – Temperature Dependent Material Properties for Type 304 Stainless Steel 2.10.5-10

Table 2.10.5-3 – Theoretical Elastic Buckling Stress Values (General Temperature Independent Form) 2.10.5-11

Table 2.10.5-4 – Temperature Dependent Theoretical Elastic Buckling Stresses for Each RH-TRU 72-B Package Shell 2.10.5-11

Table 2.10.5-5 – Temperature Dependent Capacity Reduction Factors 2.10.5-12

Table 2.10.5-6 – Upper Bounds for Compressive Stresses and In-Plane Shear Stresses 2.10.5-12

Table 2.10.5-7 – Compressive Membrane and In-Plane Shear Stress Summary for the Outer Cask Inner Shell 2.10.5-13

Table 2.10.5-8 – Compressive Membrane and In-Plane Shear Stress Summary for the Outer Cask Outer Shell 2.10.5-14
Table 2.10.5-9 – Compressive Membrane and In-Plane Shear Stress Summary for the Inner Vessel 2.10.5-15
Table 2.10.5-10 – Worst-Case Load Combinations for the Outer Cask Inner Shell 2.10.5-16
Table 2.10.5-11 – Worst-Case Load Combinations for the Outer Cask Outer Shell 2.10.5-16
Table 2.10.5-12 – Worst-Case Load Combinations for the Inner Vessel 2.10.5-17
Table 2.10.5-13 – Interaction Equation Checks 2.10.5-19
Table 2.10.6-1 – Outer Cask NCT Bolt Stresses, Torque Coefficient = 0.13 ..... 2.10.6-9
Table 2.10.6-2 – Outer Cask NCT Bolt Stresses, Torque Coefficient = 0.20 ..... 2.10.6-10
Table 2.10.6-3 – Inner Vessel NCT Bolt Stresses, Torque Coefficient = 0.13 ..... 2.10.6-11
Table 2.10.6-4 – Inner Vessel NCT Bolt Stresses, Torque Coefficient = 0.20 ..... 2.10.6-12
Table 2.10.6-5 – Outer Cask HAC Bolt Stresses, Torque Coefficient = 0.13 ..... 2.10.6-13
Table 2.10.6-6 – Outer Cask HAC Bolt Stresses, Torque Coefficient = 0.20 ..... 2.10.6-14
Table 2.10.6-7 – Inner Vessel HAC Bolt Stresses, Torque Coefficient = 0.13 ..... 2.10.6-15
Table 2.10.6-8 – Inner Vessel HAC Bolt Stresses, Torque Coefficient = 0.20 ..... 2.10.6-16
Table 2.10.7-1 – Static Crush Test Summary 2.10.7-13
Table 2.10.7-2 – Static Test Article Stress-Strain Properties 2.10.7-13
Table 2.10.7-3 – End Crush CASKDROP Output 2.10.7-14
Table 2.10.7-4 – Side Crush CASKDROP Output 2.10.7-15
Table 2.10.7-5 – Oblique Crush CASKDROP Output 2.10.7-16
Table 2.10.7-6 – Dynamic Drop Test Summary 2.10.7-17
Table 2.10.7-7 – Dynamic Test Article Stress-Strain Properties 2.10.7-17
Table 2.10.7-8 – End Drop CASKDROP Output 2.10.7-18
Table 2.10.7-9 – Side Drop CASKDROP Output 2.10.7-19
Table 2.10.7-10 – Oblique Drop CASKDROP Output 2.10.7-20
Table 2.10.7-11 – Oblique Drop SLAPDOWN Output 2.10.7-21
Table 2.10.7-12 – Free Drop Test Result Summary 2.10.7-22
Table 2.10.8-1 – Mechanical Properties of Stainless Steel (Type 304) 2.10.8-12
Table 2.10.8-2 – Mechanical Properties of Lead (Copperized) 2.10.8-12
Table 2.10.8-3 – Steel Shell Geometry at 70 ºF 2.10.8-12
Table 2.10.8-4 – Initial Shell Conditions Before Lead Solidification 2.10.8-12
Table 2.10.8-5 – Stress-Free OC Inner Shell Dimensions 2.10.8-13

Table 3.1-1 – Maximum NCT Temperatures for RH-TRU 72-B Package 3.1-3
Table 3.1-2 – Maximum HAC Temperatures for RH-TRU 72-B Package 3.1-4
Table 3.2-1 – Thermal Properties of Materials 3.2-3
Table 3.2-2 – Conductivity of Air 3.2-3
Table 3.2-3 – Radiation Properties of Materials 3.2-4
Table 3.4-1 – Insolation Values 3.4-11
Table 3.4-2 – Maximum NCT Temperatures (ºF) for RH-TRU 72-B Package 3.4-12
Table 3.4-3 – Paper Waste NCT Package Temperature Variations with Decay Heat 3.4-12
Table 3.4-4 – Metallic Waste NCT Package Temperature Variations with Decay Heat 3.4-13
Table 3.4-5 – RH-TRU 72-B Pressure Increase Contributions 3.4-13
Table 3.5-1 – Maximum HAC Temperatures for RH-TRU 72-B Package 3.5-5
Table 3.6.1-1 – Thermal Properties of Materials 3.6.1-5
Table 3.6.1-2 – Conductivity of Air 3.6.1-5
Table 3.6.1-3 – Solar Loads (Insolation) for the Thermal Model 3.6.1-6
Table 3.6.1-4 – External Radiation Input for the Thermal Model 3.6.1-7
Table 5.1-1 – Summary of HAC Activity Limits 5.1-4
Table 5.1-2 – RH-TRU Radionuclide Inventory 5.1-7
Table 5.3-1 – Summary of Shield Regional Densities 5.3-2
Table 5.4-1 – Mass Attenuation Coefficients from ANSI/ANS 6.4.3-1991 ..... 5.4-6
Table 5.4-2 – Iron Exposure Buildup Factor Coefficients from ANSI/ANS 6.4.3-1991 ..... 5.4-6
Table 5.4-3 – Gamma Flux-to-Dose Rate Conversion Factors from ANSI/ANS 6.1.1-1977 .. 5.4-7
Table 5.4-4 – Neutron Flux-to-Dose Rate Conversion Factors from ANSI/ANS 6.1.1-1977 .. 5.4-7
Table 5.4-5 – Neutron Dose Rate Calculations 5.4-8
Table 5.5.2-1 – Dose Rate Increase from Neutron Multiplication 5.5.2-3
Table 5.5.2-2 – Typical MCNP Input File for the Neutron Multiplication Calculations 5.5.2-4
Table 5.5.5-1 – Dose Rates as a Function of Neutron Source (Pu-239) Location and Self-Shielding 5.5.5-4
Table 5.5.5-2 – Listing of MCNP File for Neutron Case “nopun”; No Puncture Bar Damage 5.5.5-5
Table 5.5.5-3 – Listing of MCNP File for Neutron Case “pun”; Includes Puncture Bar Damage 5.5.5-6
Table 5.5.6-1 – Dose Rates as a Function of a Representative Photon Cs-137 Source (E = 0.6617 MeV) Location and Self-Shielding 5.5.6-5

Table 5.5.6-2 – Dose Rates as a Function of a Representative Photon Co-60 Source (E = 1.21 MeV) Location and Self-Shielding 5.5.6-6

Table 5.5.6-3 – Listing of MCNP File for Cs-137 Photon Case "mpun"; Includes Puncture Bar Damage 5.5.6-8

Table 5.5.6-4 – Listing of MCNP File for Co-60 Photon Case "hpun"; Includes Puncture Bar Damage 5.5.6-9

Table 6.1-1 – Fissile Material Limit per RH-TRU 72-B Package 6.1-4

Table 6.1-2 – Summary of Criticality Analysis Results 6.1-4

Table 6.2-1 – Special Reflector Material Parameters that Achieve the Reactivity of a 25%/75% Polyethylene/Water Mixture Reflector 6.2-5

Table 6.3-1 – Fissile Contents Model Properties for 315 g Pu Spheres (Case A)$^{\Phi}$ 6.3-8

Table 6.3-2 – Fissile Contents Model Properties for Various Pu Spheres with Pu-240 Added as Indicated (Case A)$^{\Phi}$ 6.3-9

Table 6.3-3 – Fissile Contents Model Properties for 100 g Pu Spheres (Case B) 6.3-10

Table 6.3-4 – Fissile Contents Model Properties for 245 g Pu Spheres (Case C) 6.3-12

Table 6.3-5 – Fissile Contents Model Properties for 0.96 wt% U-235 FEM (Case D) 6.3-12

Table 6.3-6 – Fissile Contents Model Properties for 0.96 wt% U-235 FEM (Case D with Variable Beryllium Moderator and H/U-235=500) 6.3-13

Table 6.3-7 – Structural Model Properties for the RH-TRU 72-B Package (All Cases) 6.3-13

Table 6.3-8 – Reflector Model Properties for the RH-TRU 72-B Package by Case 6.3-14

Table 6.4-1 – Single-Unit, NCT and HAC, Case A, Sphere Centered, 315 FGE, k_s vs. H/Pu Ratio with Different Moderator/Reflector Combinations 6.4-12

Table 6.4-2 – Single-Unit, NCT and HAC, Case A, Sphere Top and Radially Displaced, 315 FGE, H/Pu at 900, k_s vs. Variable Interspersed Moderation Volume Fraction in the IV 6.4-13

Table 6.4-3 – Infinite-Unit, NCT and HAC, Case A, Sphere Top and Radially Displaced, 315 FGE, k_s vs. H/Pu Ratio with Different Moderator/Interspersed Moderator Combinations 6.4-13

Table 6.4-4 – Infinite-Unit, NCT and HAC, Case A, Sphere Top and Radially Displaced, 315 FGE, k_s vs. Variable Interspersed Moderator at H/Pu Ratios of Interest 6.4-14

Table 6.4-5 – Infinite-Unit, NCT and HAC, Case A, Sphere Top and Radially Displaced, k_s vs. H/Pu Ratio for Limiting Pu-240/Pu-239 Combinations with Optimum Moderator/Reflector 6.4-15

Table 6.4-6 – Infinite-Unit, NCT and HAC, Case B, Sphere Centered, 100 FGE, k_s vs. H/Pu Ratio with Different Reflector Conditions 6.4-16

Table 6.4-7 – Infinite-Unit, NCT and HAC, Case B, Sphere Centered, 100 FGE, k_s vs. H/Pu Ratio with Different Moderator Conditions in 100% Be Reflector 6.4-17

Table 6.4-8 – Infinite-Unit, NCT and HAC, Case B, Sphere Centered, 305 FGE, k_s vs. H/Pu Ratio with the Indicated Moderator Conditions 6.4-19

Table 6.4-9 – Infinite Unit, NCT and HAC, Case C, Sphere Top Side, 245 FGE, k_s vs. H/Pu Ratio with Different Moderator/Reflector Combinations 6.4-21

Table 6.4-10 – Single-Unit, NCT and HAC, Case D, Cylindrical Fissile Region, 0.96 wt% U-235 FEM, k_s vs. H/U-235 Ratio 6.4-21

Table 6.4-11 – Infinite-Unit, NCT and HAC, Case D, Cylindrical Fissile Region, 0.96 wt% U-235, k_s vs. H/U-235 Ratio and Variable Density Interspersed Moderation Conditions . 6.4-22

Table 6.4-12 – Single-Unit, NCT and HAC, Case D, Be Reflected, Cylindrical Fissile Region, 0.96 wt% U-235 FEM, k_s vs. H/U-235 Ratio 6.4-23

Table 6.4-13 – Infinite-Unit, NCT and HAC, Case D, Be Reflected, Short, Squat, Cylindrical Fissile Region, 0.96 wt% U-235 FEM, k_s vs. H/U-235 Ratio and Variable Interspersed Moderation Between Packages 6.4-24

Table 6.4-14 – Infinite-Unit, NCT and HAC, Case D, Be Reflected, Short, Squat, Cylindrical Fissile Region, 0.96 wt% U-235 FEM, Moderated to H/U-235=500, k_s vs. Be in Moderator 6.4-25

Table 6.4-15 – Fissile Payload Limits 6.4-26

Table 6.5-1 – ^{239}Pu Benchmark Experiment Description 6.5-6

Table 6.5-2 – ^{239}Pu Benchmark Case Parameters and Computed Results 6.5-7

Table 6.5-3 – Calculation of Pu-239 USL with Be 6.5-15

Table 6.5-4 – Low Enriched U-235 Benchmark Experiment Description 6.5-15

Table 6.5-5 – Low Enriched U-235 Benchmark Case Parameters, Computed Results and Reported Experimental Benchmark Uncertainty 6.5-16

Table 6.5-6 – Calculation of Low Enriched U-235 USL 6.5-19

Table 8.1-1 – Compressive Stress Ranges at Room Temperature (psi) 8.1-18

LIST OF FIGURES

Figure 1.1-1 – RH-TRU 72-B Package 1.1-3

Figure 1.1-2 – RH-TRU 72-B Package Components 1.1-4

Figure 1.1-3 – View of the RH-TRU 72-B Closure Regions 1.1-5

Figure 1.2-1 – Inner Vessel Containment Components 1.2-8

Figure 1.2-2 – Outer Cask Containment Components 1.2-9

Figure 2.1-1 – ASME Code, Section III, Figure I-9.4 ..... 2.1-10

Figure 2.2-1 – RH-TRU 72-B Package Component Weight Breakdown 2.2-3

Figure 2.3-1 – True Stress/Strain for Type 304 Stainless at 212 ºF 2.3-5

Figure 2.3-2 – Crush Stress vs. Strain for 11½ lb/ft³ Nominal Density Polyurethane Foam ... 2.3-6

Figure 2.3-3 – Tensile Curves at a Strain Rate of 0.05 in/in/min 2.3-7

Figure 2.3-4 – Strain Rate Effects on Tensile Curves at 100 ºF and 250 ºF 2.3-7

Figure 2.3-5 – Tensile Curves at a Strain Rate of 0.005 in/in/min 2.3-8
Figure 2.3-6 – Compression Curves at a Strain Rate of 0.005 in/in/min 2.3-8
Figure 2.3-7 – Total Strain vs. Creep Time 2.3-9
Figure 2.3-8 – Stress vs. Creep Time Curves 2.3-10
Figure 2.5-1 – Lifting Trunnion Geometry 2.5-17
Figure 2.5-2 – Horizontal Lift Loading Configuration 2.5-17
Figure 2.5-3 – Attachment Loads for WRC Bulletin 107 ..... 2.5-18
Figure 2.5-4 – Figure 1A from WRC Bulletin 107 ..... 2.5-19
Figure 2.5-5 – Figure 2A from WRC Bulletin 107 ..... 2.5-20
Figure 2.5-6 – Figure 3A from WRC Bulletin 107 ..... 2.5-21
Figure 2.5-7 – Figure 4A from WRC Bulletin 107 ..... 2.5-22
Figure 2.5-8 – Figure 1B from WRC Bulletin 107 ..... 2.5-23
Figure 2.5-9 – Figure 1B-1 from WRC Bulletin 107 ..... 2.5-24
Figure 2.5-10 – Figure 2B from WRC Bulletin 107 ..... 2.5-25
Figure 2.5-11 – Figure 2B-1 from WRC Bulletin 107 ..... 2.5-26
Figure 2.5-12 – Figure 3B from WRC Bulletin 107 ..... 2.5-27
Figure 2.5-13 – Figure 4B from WRC Bulletin 107 ..... 2.5-28
Figure 2.5-14 – Lifting Trunnion Weld Evaluation 2.5-29
Figure 2.5-15 – Center-Pivot Trailer Configuration 2.5-29
Figure 2.5-16 – Lift-Off Trailer Configuration 2.5-30
Figure 2.5-17 – Center-Pivot Trunnion Loading Configuration 2.5-30
Figure 2.5-18 – Tie-down Loading Configuration 2.5-31
Figure 2.5-19 – Center-Pivot Trailer Free-Body Diagram for Tie-down 2.5-31
Figure 2.5-20 – Lift-Off Trailer Free-Body Diagram for Tie-down 2.5-32
Figure 2.6-1 – Package Locations for Pressure Stress Calculations 2.6-57
Figure 2.6-2 – Figure I-9.2.2 from Appendix I of the ASME Code 2.6-58
Figure 2.6-3 – Free-Body Diagrams of Axial Forces in OC Components 2.6-59
Figure 2.6-4 – OC Bottom-End Plate Configuration 2.6-60
Figure 2.6-5 – Axial Pressure Distribution Due to Lead 2.6-61
Figure 2.6-6 – NCT Cold (-20 ºF) Outer Cask Stresses 2.6-62
Figure 2.6-7 – NCT Cold (-20 ºF) Inner Vessel Stresses 2.6-63
Figure 2.6-8 – NCT Cold (-20 ºF) Canister Stresses 2.6-64
Figure 2.6-9 – NCT Cold (-20 ºF) Thrust 2.6-65

Figure 2.6-10 – NCT Cold (-20 ºF) Shear 2.6-66
Figure 2.6-11 – NCT Cold (-20 ºF) Bending Moment 2.6-67
Figure 2.6-12 – Comparison of *g*-Loads Used for Calculating Cold (-20 ºF) NCT Stresses . 2.6-68
Figure 2.6-13 – NCT Hot (140 ºF) Outer Cask Stresses 2.6-69
Figure 2.6-14 – NCT Hot (140 ºF) Inner Vessel Stresses 2.6-70
Figure 2.6-15 – NCT Hot (140 ºF) Canister Stresses 2.6-71
Figure 2.6-16 – NCT Hot (140 ºF) Thrust 2.6-72
Figure 2.6-17 – NCT Hot (140 ºF) Shear 2.6-73
Figure 2.6-18 – NCT Hot (140 ºF) Bending Moment 2.6-74
Figure 2.6-19 – NCT Cold (-20 ºF) Shear Due to a Distributed Payload 2.6-75
Figure 2.6-20 – NCT Cold (-20 ºF) Moment Due to a Distributed Payload 2.6-76
Figure 2.6-21 – NCT Cold (-20 ºF) Shear Due to a Concentrated Payload 2.6-77
Figure 2.6-22 – NCT Cold (-20 ºF) Moment Due to a Concentrated Payload 2.6-78
Figure 2.6-23 – NCT Hot (140 ºF) Shear Due to a Distributed Payload 2.6-79
Figure 2.6-24 – NCT Hot (140 ºF) Moment Due to a Distributed Payload 2.6-80
Figure 2.6-25 – NCT Hot (140 ºF) Shear Due to a Concentrated Payload 2.6-81
Figure 2.6-26 – NCT Hot (140 ºF) Moment Due to a Concentrated Payload 2.6-82
Figure 2.7-1 – HAC Cold (-20 ºF) Outer Cask Stresses 2.7-53
Figure 2.7-2 – HAC Cold (-20 ºF) Inner Vessel Stresses 2.7-54
Figure 2.7-3 – HAC Cold (-20 ºF) Canister Stresses 2.7-55
Figure 2.7-4 – HAC Cold (-20 ºF) Thrust 2.7-56
Figure 2.7-5 – HAC Cold (-20 ºF) Shear 2.7-57
Figure 2.7-6 – HAC Cold (-20 ºF) Bending Moment 2.7-58
Figure 2.7-7 – Comparison of *g*-Loads Used for Calculating Cold (-20 ºF) HAC Stresses ... 2.7-59
Figure 2.7-8 – HAC Hot (140 ºF) Outer Cask Stresses 2.7-60
Figure 2.7-9 – HAC Hot (140 ºF) Inner Vessel Stresses 2.7-61
Figure 2.7-10 – HAC Hot (140 ºF) Canister Stresses 2.7-62
Figure 2.7-11 – HAC Hot (140 ºF) Thrust 2.7-63
Figure 2.7-12 – HAC Hot (140 ºF) Shear 2.7-64
Figure 2.7-13 – HAC Hot (140 ºF) Bending Moment 2.7-65
Figure 2.7-14 – HAC Cold (-20 ºF) Shear Due to a Distributed Payload 2.7-66
Figure 2.7-15 – HAC Cold (-20 ºF) Moment Due to a Distributed Payload 2.7-67
Figure 2.7-16 – HAC Cold (-20 ºF) Shear Due to a Concentrated Payload 2.7-68

Figure 2.7-17 – HAC Cold (-20 ºF) Moment Due to a Concentrated Payload 2.7-69
Figure 2.7-18 – HAC Hot (140 ºF) Shear Due to a Distributed Payload 2.7-70
Figure 2.7-19 – HAC Hot (140 ºF) Moment Due to a Distributed Payload 2.7-71
Figure 2.7-20 – HAC Hot (140 ºF) Shear Due to a Concentrated Payload 2.7-72
Figure 2.7-21 – HAC Hot (140 ºF) Moment Due to a Concentrated Payload 2.7-73
Figure 2.7-22 – Finite Element Model for Puncture on the OC Lid 2.7-74
Figure 2.7-23 – Stress and Deformation for Puncture on the OC Lid 2.7-74
Figure 2.7-24 – OC Gas Samping Port Region 2.7-75
Figure 2.7-25 – Package Orientation for the Puncture Drop 2.7-76
Figure 2.7-26 – Geometry of the Puncture Bar at the Gas Sampling Port 2.7-77
Figure 2.7-27 – Figure I-9.2.1 from Appendix I of the ASME Code 2.7-78
Figure 2.10.1-1 – Finite Element Analysis Model of the Center-Pivot Trunnion Interface 2.10.1-7
Figure 2.10.1-2 – Center-Pivot Trunnion Longitudinal and Vertical Cosine-Distributed Loads . 2.10.1-8
Figure 2.10.1-3 – OC Outer Shell Stress Intensities 2.10.1-9
Figure 2.10.1-4 – Stress Intensity Linearization at the Bottom-Right Corner of the Trunnion Base 2.10.1-10
Figure 2.10.1-5 – Finite Element Analysis Model of the IV Bottom Transition Due to Pressure 2.10.1-13
Figure 2.10.1-6 – IV Bottom Transition Stress Intensities Due to Pressure 2.10.1-14
Figure 2.10.1-7 – Finite Element Analysis Model of the IV Bottom Transition Due to 1*g* Acceleration 2.10.1-17
Figure 2.10.1-8 – IV Bottom Transition Stress Intensities Due to 1*g* Acceleration 2.10.1-18
Figure 2.10.1-9 – Containment Assembly Oblique Analysis Model 2.10.1-21
Figure 2.10.2-1 – Impact Limiter Force and Centroid Development 2.10.2-17
Figure 2.10.2-2 – Strain Determination 2.10.2-18
Figure 2.10.2-3 – Determination of Impact Limiter Separation Moments 2.10.2-19
Figure 2.10.2-4 – Example Problem 2.10.2-20
Figure 2.10.2-5 – CASKDROP Program Input Windows 2.10.2-21
Figure 2.10.2-6 – SLAPDOWN Analytical Model 2.10.2-22
Figure 2.10.3-1 – Impact Limiter Deflection and Residual Clearance for the NCT Oblique Drop, Cold (-20 ºF) 2.10.3-17
Figure 2.10.3-2 – Impact Limiter Separation Moments for the NCT Oblique Drop, Cold (-20 ºF) 2.10.3-17

Figure 2.10.3-3 – Impact Limiter Deflection and Residual Clearance for the NCT Oblique Drop, Warm (140 ºF) 2.10.3-18
Figure 2.10.3-4 – Impact Limiter Separation Moments for the NCT Oblique Drop, Warm (140 ºF) 2.10.3-18
Figure 2.10.3-5 – Impact Limiter Deflection and Residual Clearance for the HAC Oblique Drop, Cold (-20 ºF) 2.10.3-19
Figure 2.10.3-6 – Impact Limiter Separation Moments for the HAC Oblique Drop, Cold (-20 ºF) 2.10.3-19
Figure 2.10.3-7 – Impact Limiter Deflection and Residual Clearance for the HAC Oblique Drop, Warm (140 ºF) 2.10.3-20
Figure 2.10.3-8 – Impact Limiter Separation Moments for the HAC Oblique Drop, Warm (140 ºF) 2.10.3-20
Figure 2.10.4-1 – Free-Body Diagram for Slapdown Loads 2.10.4-7
Figure 2.10.4-2 – Shear Diagram for Package During Slapdown 2.10.4-8
Figure 2.10.4-3 – Moment Diagram for Package During Slapdown 2.10.4-8
Figure 2.10.7-1 – End Orientation Test 2.10.7-23
Figure 2.10.7-2 – End Orientation, Post-Test Configuration 2.10.7-23
Figure 2.10.7-3 – End Orientation, View of Open End 2.10.7-24
Figure 2.10.7-4 – End Crush Data Versus Prediction 2.10.7-24
Figure 2.10.7-5 – Side Orientation Test 2.10.7-25
Figure 2.10.7-6 – Side Orientation, Post-Test Configuration 2.10.7-26
Figure 2.10.7-7 – Side Crush Data Versus Prediction 2.10.7-27
Figure 2.10.7-8 – Oblique Orientation Test 2.10.7-28
Figure 2.10.7-9 – Oblique Orientation, Post-Test Configuration 2.10.7-29
Figure 2.10.7-10 – Oblique Orientation, Post-Test Side View 2.10.7-29
Figure 2.10.7-11 – Oblique Crush Data Versus Prediction 2.10.7-30
Figure 2.10.7-12 – End Drop Configuration 2.10.7-31
Figure 2.10.7-13 – End Drop, Post-Test Configuration 2.10.7-32
Figure 2.10.7-14 – Side Drop Configuration 2.10.7-33
Figure 2.10.7-15 – Side Drop, Crush Gage Detail (Before Test) 2.10.7-34
Figure 2.10.7-16 – Side Drop, Post-Test Configuration 2.10.7-34
Figure 2.10.7-17 – Oblique Drop Configuration 2.10.7-35
Figure 2.10.7-18 – Oblique Drop, Post-Test Configuration 2.10.7-36
Figure 2.10.7-19 – Oblique Drop, Post-Test Configuration (Detail) 2.10.7-36

Figure 2.10.7-20 – Oblique Free Drop, Measurement of Deflection 2.10.7-37
Figure 2.10.7-21 – Drawing 9715-015, *RH-72B Dummy Package*, Sheet 1 ..... 2.10.7-39
Figure 2.10.7-22 – Drawing 9715-015, *RH-72B Dummy Package*, Sheet 2 ..... 2.10.7-40
Figure 2.10.7-23 – Drawing 9715-010, *Impact Limiter Test Article RH-72B*, Sheet 1 ..... 2.10.7-41
Figure 2.10.7-24 – Drawing 9715-010, *Impact Limiter Test Article RH-72B*, Sheet 2 ..... 2.10.7-42
Figure 2.10.7-25 – Drawing 9715-010, *Impact Limiter Test Article RH-72B*, Sheet 3 ..... 2.10.7-43
Figure 2.10.7-26 – Drawing 9715-010, *Impact Limiter Test Article RH-72B*, Sheet 4 ..... 2.10.7-44
Figure 2.10.8-1 – Free-Body Diagram of Molten Lead in the Lead Column 2.10.8-13
Figure 3.4-1 – Paper Waste NCT Package Temperature Versus Decay Heat 3.4-14
Figure 3.4-2 – Metallic Waste NCT Package Temperature Versus Decay Heat 3.4-14
Figure 3.5-1 – IV and OC O-ring Seal Temperatures – 50W Payload 3.5-6
Figure 3.5-2 – Payload Temperatures – 50W Payload 3.5-6
Figure 3.5-3 – Center-Pivot Trunnion Region Temperatures – 50W Payload 3.5-7
Figure 3.5-4 – OC Wall Temperatures – 50W Payload 3.5-7
Figure 3.5-5 – Payload Temperatures – 50W Payload 3.5-8
Figure 3.5-6 – IV and OC O-ring Seal Temperatures – 300W Payload 3.5-8
Figure 3.5-7 – Payload Temperatures – 300W Payload 3.5-9
Figure 3.5-8 – Center-Pivot Trunnion Region Temperatures – 300W Payload 3.5-9
Figure 3.5-9 – OC Wall Temperatures – 300W Payload 3.5-10
Figure 3.5-10 – Payload Temperatures – 300W Payload 3.5-10
Figure 3.6.1-1 – Thermal Model Stations for RH-TRU 72-B Package Model 3.6.1-8
Figure 3.6.1-2 – Node Layout for the Impact Limiters and Packaging Body 3.6.1-9
Figure 3.6.1-3 – Thermal Model Node Layout at the Package Lid-End 3.6.1-10
Figure 3.6.1-4 – Payload Node Layout (Non-Metallic Shown) 3.6.1-11
Figure 3.6.1-5 – Center-Pivot Trunnion Node Layout 3.6.1-12
Figure 3.6.1-6 – Lid-End Impact Limiter Node Layout 3.6.1-13
Figure 3.6.1-7 – Side Drop and Puncture Bar Damage Node Layout 3.6.1-14
Figure 4.1-1 – Inner Vessel Containment Components 4.1-5
Figure 4.1-2 – Outer Cask Containment Components 4.1-6
Figure 5.1-1 – HAC Radial Shielding Configuration 5.1-8
Figure 5.4-1 – Axial View for MCNP Neutron Point Source Calculations 5.4-9
Figure 5.5.2-1 – Axial View of Geometry Model for Neutron Multiplication Showing Sphere, Reflector, and Puncture Bar Vicinity 5.5.2-6

Figure 5.5.2-2 – Plan View of Geometry Model for Neutron Multiplication Showing Sphere, Reflector, and Puncture Bar Vicinity 5.5.2-7

Figure 5.5.2-3 – Expanded Axial View for Neutron Multiplication Showing Detector 5.5.2-8

Figure 5.5.3-1 – Neutron Source Strength at 1,000 mrem/hr vs. Average Neutron Energy 5.5.3-3

Figure 5.5.3-2 – Total Neutron Source Strength per Curie as a Function of Maximum Allowable Activity (Curies) 5.5.3-4

Figure 5.5.4-1 – Intensity Factor vs. Gamma Energy for a Dose Rate of 1,000 mrem/hr at 1 Meter with a 1×10^8 Curie Source Activity 5.5.4-3

Figure 5.5.4-2 – Effective Activity vs. Gamma Energy for a Dose Rate of 1,000 mrem/hr at 1 Meter 5.5.4-4

Figure 5.5.5-1 – Axial View for Source and Attenutation Variations (NCT to HAC) Showing Detectors 5.5.5-7

Figure 6.3-1 – Simplified Drawing of RH-TRU 72-B Package 6.3-15

Figure 6.3-2 – KENO-V.a NCT and HAC Single Unit, Case A through C, Sphere Centered Model Representation (Top and Side Views) 6.3-16

Figure 6.3-3 - KENO-V.a NCT and HAC Single Unit, Case A through C, Sphere Centered Top Model Representation (Top and Side Views)[8] 6.3-17

Figure 6.3-4 – KENO-V.a NCT and HAC Single Unit, Case A through C, Sphere Centered Top and Displaced Radially, Model Representation (Top and Side Views)[8] 6.3-18

Figure 6.3-5 – KENO-V.a NCT and HAC Infinite Unit, Case D, Cylindrical Fissile Region Model Representation (Top and Side Views) 6.3-19

Figure 6.3-6 – KENO-V.a NCT and HAC Single-Unit, Case D, Cylindrical Fissile Region Models with Various Be Reflector Regions (Long, Skinny; Short, Squat; and Encapsulated Location Models both Top and Side Views) 6.3-20

Figure 7.4-1 – Pressure Rise Leakage Rate Test Schematic 7.4.1-2

Figure 8.1-1 – Testing the IV Lid Seal Integrity 8.1-19

Figure 8.1-2 – Testing the OC Lid Seal Integrity 8.1-19

This page intentionally left blank.

1.0 GENERAL INFORMATION

This chapter of the Safety Analysis Report (SAR) for the Remote-Handled Transuranic (RH-TRU) 72-B waste shipping package presents a general introduction and description of the RH-TRU 72-B package. The RH-TRU 72-B package is presented in Figure 1.1-1, and schematics of the key components are presented as Figure 1.1-2 and Figure 1.1-3. Figure 1.1-2 presents an exploded view of all packaging components. Figure 1.1-3 presents a detailed view of the closure/seal areas. Drawing X-106-500-SNP, presenting all design details associated with the RH-TRU 72-B packaging, and Drawings X-106-501-SNP and X-106-502-SNP, presenting design details associated with the RH-TRU payload canister, are included in Appendix 1.3.1, *Packaging General Arrangement Drawings*. Terminology and notation used throughout the report is presented in Appendix 1.3.2, *Glossary of Terms and Acronyms*. All details relating to payloads and payload preparation for shipment in a RH-TRU 72-B package are presented in the *Remote-Handled Transuranic Waste Authorized Methods for Payload Control* (RH-TRAMPAC)[1].

1.1 Introduction

The Remote-Handled Transuranic Waste Shipping Package (Model No. RH-TRU 72-B) has been developed as a safe means of transporting, via ground transportation, remote-handled transuranic (RH-TRU) wastes from various sites around the United States. The RH-TRU 72-B package is a Category I packaging. RH-TRU waste is transported within the RH-TRU 72-B package by highway and rail. Limits for allowable external temperature and radiation levels have been established to ensure compliance with 10 CFR §71.43[2] and §71.47. The design is optimized for minimum weight and maximum safety during loading, transport, and unloading operations.

The RH-TRU 72-B package provides two levels of testable containment for the payload during both normal conditions of transport (NCT) and hypothetical accident conditions (HAC).

The packaging is composed of an IV that provides an inner containment boundary, an OC that provides an outer containment boundary and acts as an environmental barrier, and energy-absorbing impact limiters at each end of the OC. The containment boundary provided by the IV consists of a 1½-inch thick bottom plate, a 3/8-inch thick, 32-inch outside diameter shell, a lid-end forging, and a 6½ inch thick lid. IV lid closure is accomplished using eight (8), 7/8-inch diameter bolts. The actual containment boundary provided by the OC consists of a 5-inch thick bottom plate, a 1-inch thick, 32⅜-inch inside diameter inner shell, a lid-end forging, and a 6-inch thick lid. OC lid closure is accomplished using eighteen (18), 1¼-inch diameter bolts. Polyurethane foam filled energy absorbers (impact limiters) are attached to each end of the OC using six (6), 1¼-inch diameter bolts, to limit the consequences of NCT and HAC.

The RH-TRU 72-B package is designed for truck and rail transport. The maximum allowable total weight of the loaded RH-TRU 72-B package is 45,000 pounds. The empty package weighs

[1] U.S. Department of Energy (DOE), *Remote-Handled Transuranic Waste Authorized Methods for Payload Control* (RH-TRAMPAC), U.S. Department of Energy, Carlsbad Field Office, Carlsbad, New Mexico.

[2] Title 10, Code of Federal Regulations, Part 71 (10 CFR 71), *Packaging and Transportation of Radioactive Material*, Final Rule, 01-26-04.

approximately 37,000 pounds. The maximum allowable total weight of the loaded payload canister is 8,000 pounds. The payload of the RH-TRU 72-B package consists of one payload canister of waste. The payload canister is part of the packaging contents and, as such, is not required to meet the containment requirements of 10 CFR §71.51[2]. The authorized contents are defined by the RH-TRAMPAC[1].

Authorization is sought for shipment of the RH-TRU 72-B package by ground transportation as a Type B(M)F-96 package per the definitions delineated in Subpart E of 10 CFR 71[2].

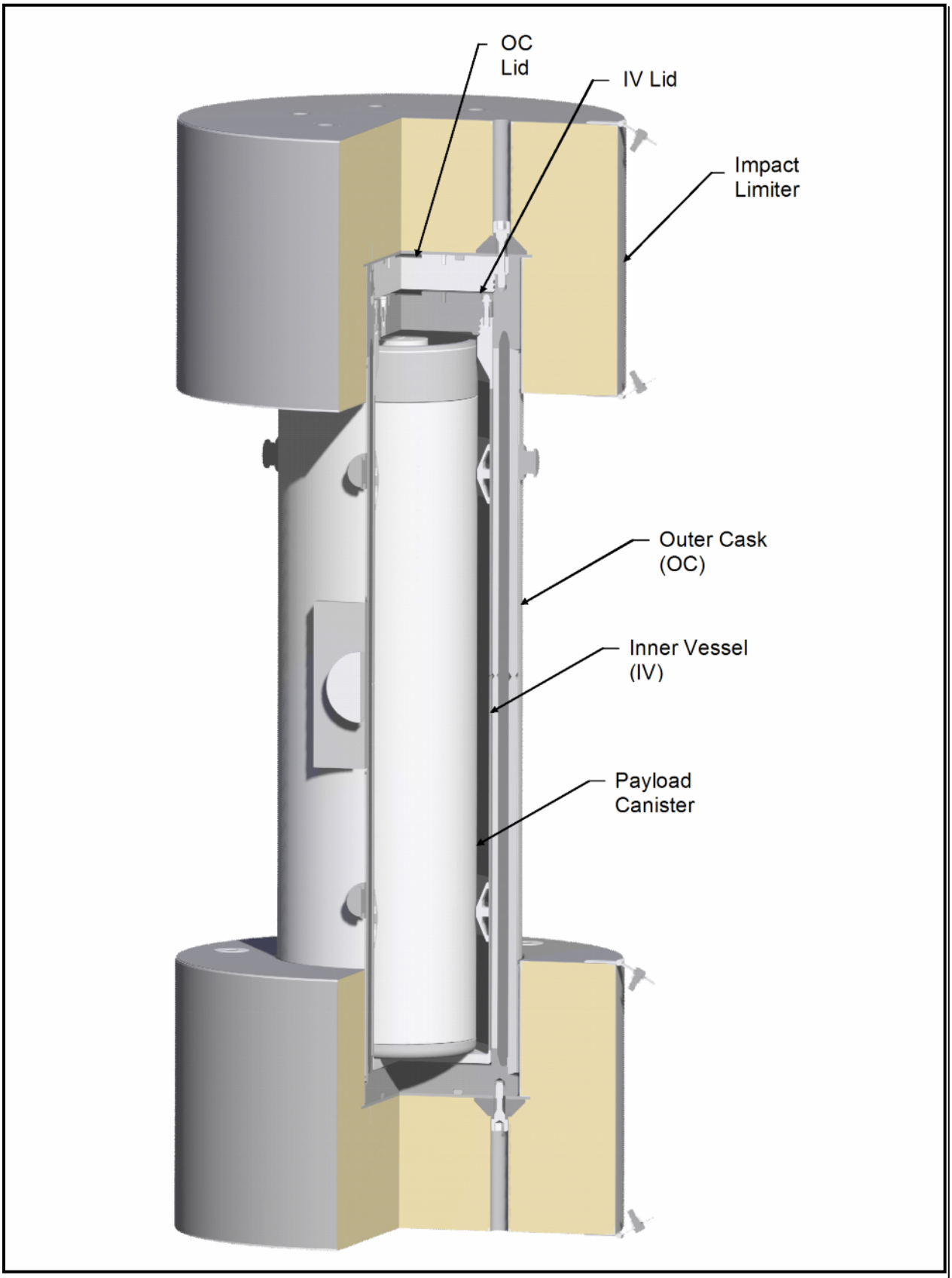

Figure 1.1-1 – RH-TRU 72-B Package

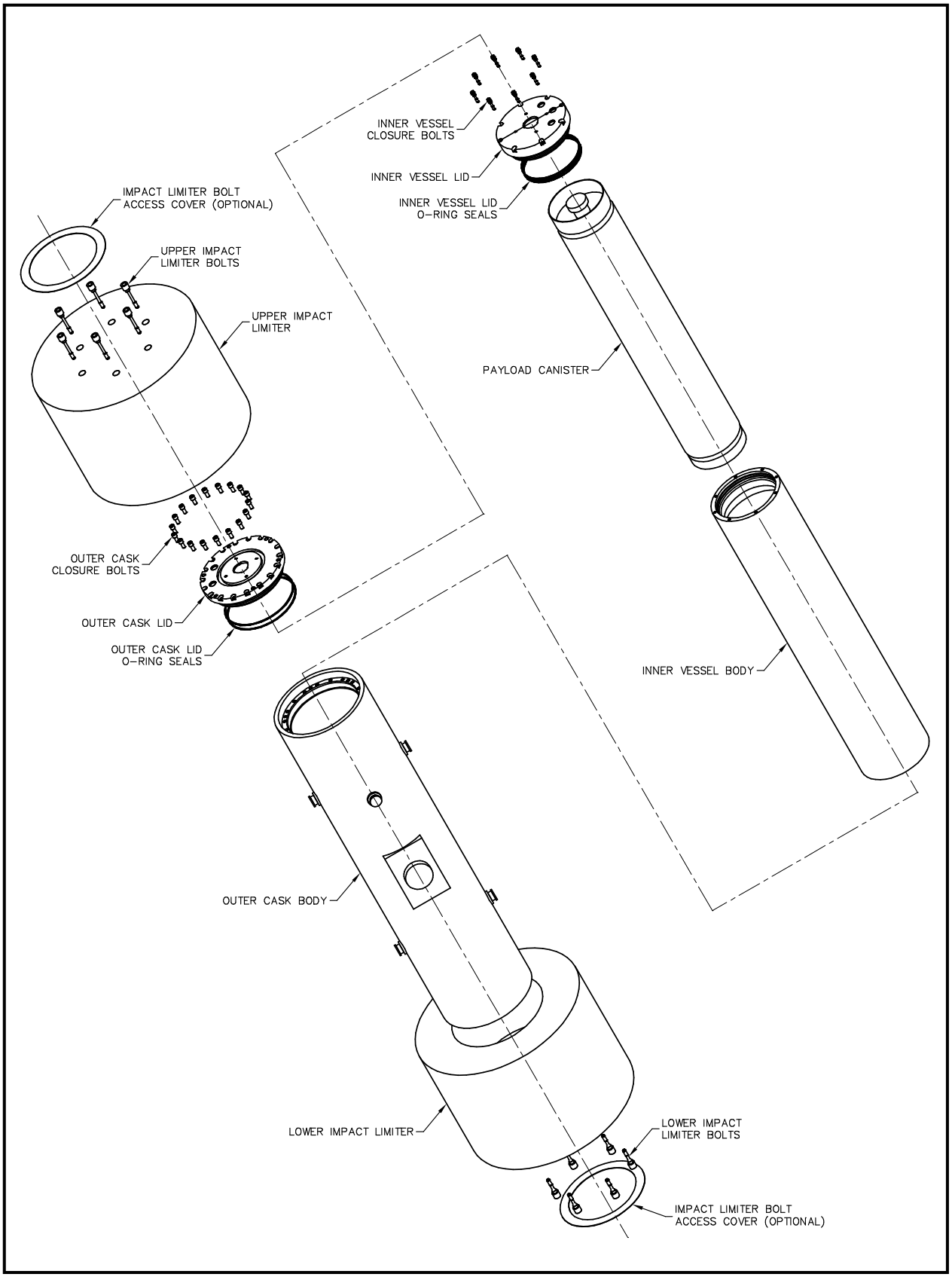

Figure 1.1-2 – RH-TRU 72-B Package Components

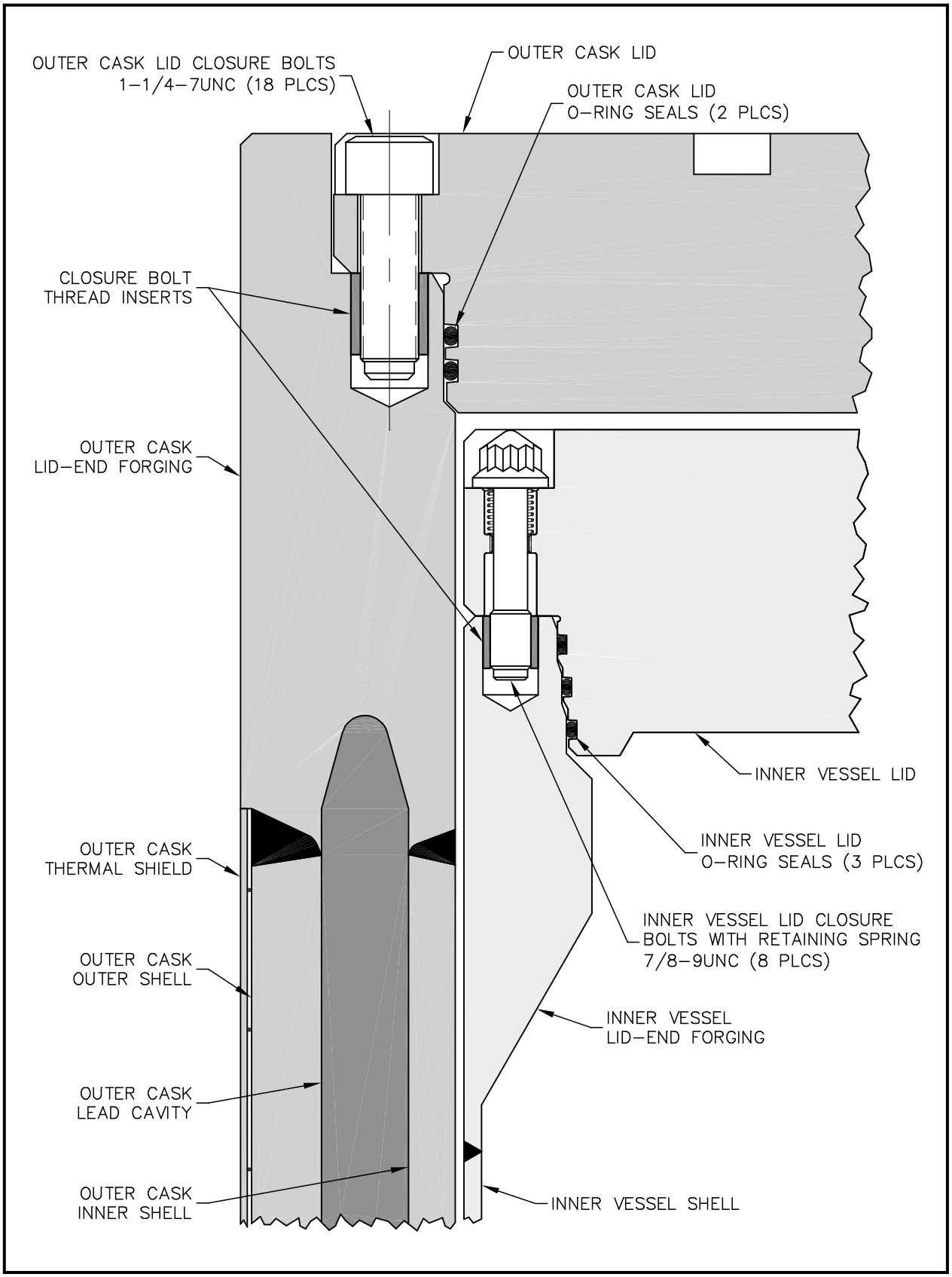

Figure 1.1-3 – View of the RH-TRU 72-B Closure Regions

This page intentionally left blank.

1.2 Package Description

This section presents a basic description of the RH-TRU 72-B package and the contents that may be transported. The *Packaging General Arrangement Drawing* for the RH-TRU 72-B package is presented in Appendix 1.3.1, *Packaging General Arrangement Drawings*.

1.2.1 Packaging

1.2.1.1 General Design Description, Containment Boundary and Closure Identification, Overall Dimensions and Materials of Construction

The RH-TRU 72-B package provides double containment for the radioactive contents. The inner vessel (IV) provides an inner containment boundary for the package payload (loaded payload canister). The outer cask (OC) provides an outer containment boundary for the payload and also acts as an environmental barrier. The lead-shielded OC is protected at each end by energy absorbing impact limiters that consist of stainless steel skins filled with medium density, closed-cell polyurethane foam. These impact limiters also provide thermal insulation that protects seal areas during the hypothetical accident condition (HAC) thermal event. The OC is passively cooled due to the relatively low, maximum heat loading of 300 thermal watts per payload canister. The maximum design pressure of the RH-TRU 72-B package is 150 psig. The maximum temperatures for the major components of the RH-TRU 72-B package under normal conditions of transport (NCT) and HAC are presented in Chapter 3.0, *Thermal Evaluation*. The overall arrangement of the RH-TRU 72-B package and design details of the IV and OC are presented in Appendix 1.3.1, *Packaging General Arrangement Drawings*. The IV, OC, and impact limiters are more fully described in the following sections.

1.2.1.1.1 Inner Vessel

The IV structure is fabricated primarily of ASTM A240, Type 304, stainless steel for the shells, and ASTM A240, Type 304, or ASTM A182, Type F304, austenitic stainless steel for the lid and end closure. Non-Type 304 stainless members include butyl rubber O-ring seals, and Nitronic 60 port closure bolts. The specification for the butyl rubber O-ring seal material is ASTM D2000[1] M4AA710 A13 B13 F17 F48 Z Trace Element. Certification of compliance with this specification is provided by the supplier for Rainier Rubber Compound RR0405-70, or equivalent. Eight (8), 7/8-9UNC, ASTM A320, Grade L43, carbon steel closure bolts secure the IV lid to the IV body.

With reference to Appendix 1.3.1, *Packaging General Arrangement Drawings*, the IV containment boundary consists of the following components:

1. A 1½-inch thick, Type 304 or Type F304 stainless steel bottom closure;
2. A 3/8-inch thick, 32-inch outside diameter, Type 304 stainless steel shell, with a full-length, full penetration seam weld;

[1] ASTM D2000-01, *Standard Classification System for Rubber Products in Automotive Applications,* American Society for Testing and Materials, Philadelphia, PA, Volume 09.02, 2001.

3. A full-penetration girth weld joining the shell to the bottom forging;
4. An upper-end (lid-end), Type F304 stainless steel ring forging;
5. A full-penetration girth weld joining the upper-end ring forging to the shell;
6. A 6½-inch thick, Type 304 or Type F304 stainless steel lid;
7. A butyl rubber containment O-ring seal that forms the seal between the upper end forging and the lid (the containment O-ring seal is the middle of the three IV closure seals);
8. A Type 304 or Type 316 stainless steel gas sampling port insert, containing a Nitronic 60 closure bolt with butyl O-ring seal (the upper O-ring seal is the containment seal);
9. A 1/4-inch bevel weld which seals the gas sampling port insert to the lid;
10. A Type 304 or Type 316 stainless steel backfill port insert, containing a Nitronic 60 closure bolt with butyl O-ring seal;
11. A 1/4-inch bevel weld which seals the backfill port insert to the lid;
12. A Type 304 or Type 316 stainless steel test port insert; and
13. A 1/4-inch bevel weld that seals the test port insert to the lid.

The inside diameter of the IV is 31¼ inches. Two (2) intermediate support rings and a pair of optional guide rails are located inside the IV for payload canister support. Including the support rings, guide rails, and upper forging, a 26½-inch diameter by 121½-inch long cavity is provided within the IV for the packaging payload.

The specific IV containment components are illustrated in Figure 1.2-1.

The weight of the IV is approximately 4,023 pounds, the overall length is 130 inches, and the outside diameter is 32 inches.

1.2.1.1.2 Outer Cask

The OC is fabricated primarily of ASTM A240, Type 304, stainless steel for the shells, and ASTM A240, Type 304, or ASTM A182, Type F304, austenitic stainless steel for the lid and end closure. Non-Type 304 stainless members include the cast lead shell, butyl rubber O-ring seals (identical material as described for the IV per Section 1.2.1.1.1, *Inner Vessel*), and Nitronic 60 port closure bolts. Eighteen (18), 1¼-7UNC, ASTM A320, Grade L43, carbon steel closure bolts secure the OC lid to the OC body. The body of the OC is constructed of two concentric stainless steel shells that sandwich the cast lead shell.

With reference to Appendix 1.3.1, *Packaging General Arrangement Drawings*, the OC containment boundary consists of the following components:

1. A 5-inch thick, Type 304 or Type F304 stainless steel bottom closure;
2. A 1-inch thick, 34⅜-inch outside diameter, Type 304 stainless steel inner shell, with a full length, full penetration seam weld;
3. A full-penetration girth weld joining the inner shell to the bottom forging;
4. An upper end (lid-end), Type F304 stainless steel ring forging;

5. A full-penetration girth weld joining the upper end ring forging to the inner shell;

6. A 6-inch thick, Type 304 or Type F304 stainless steel lid;

7. A butyl rubber containment O-ring seal that forms the seal between the upper-end forging and the lid (the containment O-ring seal is the innermost of the two OC closure seals);

8. A Type 304 or Type 316 stainless steel gas sampling port insert, containing a Nitronic 60 closure bolt with butyl O-ring seal;

9. A 1/4-inch bevel weld which seals the gas sampling port insert to the lid;

10. A Type 304 or Type 316 stainless steel test port insert; and

11. A 1/4-inch bevel weld which seals the test port insert to the lid.

12. A 32⅜-inch diameter by 130¾-inch long cavity is provided within the OC for the IV.

The specific OC containment components are illustrated in Figure 1.2-2.

The 1½-inch thick, 41⅛-inch outside diameter outer shell and the 1⅞-inch thickness of cast lead filling the annular space between the inner and outer shells are non-containment. A thermal shield of ten (10) gauge stainless steel sheet surrounds the outside of the outer shell. The thermal shield is spaced outward from the outer shell by a twelve (12) gauge wire wrap on a 3-inch pitch spacing.

The overall external dimensions of the OC are an outside diameter of 41⅝ inches and a length of 141¾ inches. The total weight of the OC is computed to be approximately 27,883 pounds, with 10,739 pounds comprising the 1⅞-inch thick cast lead shell.

Several protrusions from the OC external cylindrical surface extend through the thermal shield. The protrusions include two (2) trunnions (180º apart) near the base end of the OC, that can be used as pivot points during loading and unloading the package onto or from the trailer, to secure the OC in an upright position during payload canister loading and unloading, and for stabilizing the package during transport, and four (4) trunnions (90º apart) near the lid end of the OC, that can be used for lifting the entire package as well as stabilizing the package during transport. At approximately mid length of the package are two (2) larger trunnions (180º apart) used for package tie-down to the trailer during transport, and used for pivoting the package during some loading and unloading operations.

As discussed in Appendix 8.3.1, *Lead Installation Procedure*, installation of the cast lead into the OC is done in a carefully controlled manner. Temperatures of the inner and outer shells are continuously monitored and controlled during the lead fill and cooldown processes. In addition, the weld connecting the outer shell to the bottom end plate is made after the cooldown process is complete and the entire OC has reached a uniform temperature. The lead pour process is described in Appendix 8.3.1, *Lead Installation Procedure*, subsequent shielding integrity testing is described in Section 8.1.5, *Tests for Shielding Integrity*, and fabrication verification testing is described in Section 8.1.3, *Fabrication Leakage Rate Tests*.

1.2.1.1.3 Impact Limiters

The impact limiter skins are fabricated from 300 series stainless steel. Non-stainless members include the closed-cell polyurethane foam and the ASTM A320, Grade L43, impact limiter attachment bolts. The polyurethane foam has a nominal density of 11½ pounds per cubic foot. Six (6), 1¼-7UNC bolts necked down to a 1-inch diameter secure each impact limiter to the OC.

The outside diameter of each impact limiter is 76 inches and the length is 46 inches. The approximate weight of each impact limiter is 2,547 pounds.

1.2.1.1.4 Payload Canister

All RH-TRU waste will be loaded directly into the payload canister or into inner containers within the payload canister. The RH-TRU payload canister design must meet the requirements of Appendix 1.3.1, *Packaging General Arrangement Drawings*. The payload canister uses a 26-inch outside diameter 1/4-inch thin-wall cylinder fabricated of carbon or stainless steel as the outer shell. Including a lift pintle at the top of the payload canister, the overall length is 120½ inches.

The payload canister is basically a one- or two-piece construction unit (fixed or removable lid versions, respectively, either of which may be configured with a through-pintle fill port and plug) capable of transporting RH-TRU waste.

1.2.1.2 Gross Weight

Gross shipping weight of the RH-TRU 72-B package is 45,000 pounds, maximum. A summary of overall component weights is detailed in Table 1.2-1.

1.2.1.3 Neutron Moderation and Absorption

The RH-TRU 72-B package contains no specific neutron moderators or absorbers.

1.2.1.4 Receptacles, Valves, Testing and Sampling Ports

The OC lid has a seal test port and a combination vent/sampling port. The seal test port accesses the volume between the two O-ring seals on the OC lid, thereby verifying assembly prior to shipping the loaded package. The IV lid has a seal test port, a combination vent/sampling port, and a helium backfill port. The seal test port accesses the volume between the upper and middle (containment) O-ring seals on the IV lid, thereby verifying assembly prior to shipping the loaded package. The helium backfill port accesses the volume between the lower and middle (containment) O-ring seals on the IV lid, thereby allowing a helium atmosphere to be introduced below the containment O-ring seal for the purpose of conducting helium leakage rate tests (note that preshipment leakage rate tests use pressure rise testing without helium, as delineated in Appendix 7.4.1, *Preshipment Leakage Rate Test*). For both the IV and OC lids, the vent port is opened at the loading end of shipment for ease of lid installation, and is used as a sampling port at the receiving end of shipment to determine contamination levels and to equalize pressure. Air or helium fills all void spaces within the packaging for NCT. There are no receptacles or valves utilized on this package. A more detailed discussion of the package test and vent port features is provided in Chapter 4.0, *Containment*.

1.2.1.5 Heat Dissipation

The package design heat capacity is 300 thermal watts maximum. The RH-TRU 72-B package dissipates this relatively low internal heat load entirely by passive heat transfer. No special devices or features are needed or utilized to enhance the normal dissipation of heat. A more detailed discussion of the package thermal characteristics is provided in Chapter 3.0, *Thermal Evaluation*.

1.2.1.6 Coolants

There are no coolants utilized within the RH-TRU 72-B package.

1.2.1.7 Protrusions

There are no outer or inner protrusions on the package other than the eight (8) external lifting, handling and tie-down trunnions discussed in Section 2.5, *Lifting and Tie-down Standards for All Packages*, all of which are located well within the envelope protected by the impact limiters. Refer to Appendix 1.3.1, *Packaging General Arrangement Drawings*, for more detail.

1.2.1.8 Lifting and Tie-down Devices

Of the eight trunnions located on the exterior of the package, four are intended for lifting (four trunnions near the lid-end) and six for tie-down (two pivot trunnions, two trunnions near the lid, and the two trunnions near the base). The two trunnions nearest the base of the package and two of the four near the lid of the package are also used to stabilize the package during loading and unloading. A more detailed discussion of the package lifting and tie-down features is provided in Section 2.5, *Lifting and Tie-down Standards for All Packages*.

1.2.1.9 Pressure Relief System

No pressure relief systems are utilized for the IV or OC. Plastic pipe plugs are included on the impact limiters' skins to preclude excessive pressurization of the impact limiters in a hypothetical fire transient event.

1.2.1.10 Shielding

Radiation attenuation is achieved through the 1⅞ inches of lead and 2⅞ inches of steel maintained between the outside diameter of the payload canister and the exterior surface of the package. The bottom of the package is shielded by 6½ inches of steel. A minimum of 12½ inches shields the top end. Further details are provided in Chapter 5.0, *Shielding Evaluation*.

1.2.2 Operational Features

The RH-TRU 72-B package is not considered to be operationally complex. All operational features are readily apparent from an inspection of the drawing provided in Appendix 1.3.1, *Packaging General Arrangement Drawings*, and the previous discussions presented in Section 1.2.1, *Packaging*.

Generally, the package is designed so that it may be rotated, after removing the impact limiters, to a vertical orientation (about the center-pivot trunnions) and secured in place for loading and unloading operations, while still on the trailer. In order to rotate the package, the impact limiters must first be removed. Alternatively, the package may be upended and removed from the trailer using a crane and lifting yoke attached to two of the trunnions near the package lid.

Both the OC and IV are fitted with four-point eyebolt holes and a pintle receptacle where a pintle can be installed. The lids can be lifted with standard eyebolts and four-point rigging. The lid can also be lifted using the pintle grapple that is used for handling the payload canister.

The IV lid also incorporates use of captured, spring-loaded closure bolts and stepped O-ring sealing surfaces to improve installation efficiency in remote environments. Captured closure bolts aid installation and removal in remote environments. Stepped sealing surfaces help minimize potential for lid binding and help reduce lid installation forces required.

Detailed operational procedures are listed in Chapter 7.0, *Operating Procedures*.

To improve remote and non-remote lid installation operations, there are tapered lid alignment guide pins on the OC and IV to assist in lid rotational alignment for bolt installation.

1.2.3 Contents of Packaging

The RH-TRU 72-B package is designed to transport remote-handled transuranic (RH-TRU) materials for the U.S. Department of Energy (DOE). RH-TRU payload materials transported in the RH-TRU 72-B package must meet the restrictions set forth in the *Remote-Handled Transuranic Waste Authorized Methods for Payload Control* (RH-TRAMPAC)[2].

1.2.4 Package Evaluation

1.2.4.1 Structural

Chapter 2.0, *Structural Evaluation*, summarizes the effects on the RH-TRU 72-B package of tests specified by 10 CFR 71[3] for NCT and HAC. Maximum stresses were found to be below allowables for various types of stress combinations, given in Table 2.1-1 and Table 2.1-2 of Section 2.1.2, *Design Criteria*. The corresponding margins of safety are presented in Chapter 2.0, *Structural Evaluation*, where margins of safety are calculated for both NCT and HAC allowables for all structural components.

1.2.4.2 Thermal

Chapter 3.0, *Thermal Evaluation*, summarizes a thermal evaluation of the packaging to assure that containment integrity would not be compromised due to changes from thermal loadings. Maximum temperatures were found for major package components under both NCT and HAC. These values are summarized in Section 3.1, *Discussion*, and are found to be within the operating limits of the materials of the corresponding components.

1.2.4.3 Containment

Chapter 4.0, *Containment*, summarizes that containment of the payload is verified by evaluating the containment boundary, including the containment vessel, containment penetrations, seals and welds, and positive closure. Requirements for NCT are addressed, including containment of radioactive material, pressurization of the containment vessel, and NCT containment criteria. Similarly, requirements for HAC, including fission gas products, containment of radioactive

[2] U.S. Department of Energy (DOE), *Remote-Handled Transuranic Waste Authorized Methods for Payload Control* (RH-TRAMPAC), U.S. Department of Energy, Carlsbad Field Office, Carlsbad, New Mexico.

[3] Title 10, Code of Federal Regulations, Part 71 (10 CFR 71), *Packaging and Transportation of Radioactive Material*, Final Rule, 01-26-04.

material, and HAC containment criteria, are addressed. These containment verification requirements are discussed in Chapter 4.0, *Containment*.

1.2.4.4 Shielding

Chapter 5.0, *Shielding Evaluation*, summarizes the shielding evaluation and describes the process by which compliance with radiation dose rate limits, as specified in 10 CFR §71.47(b)[3] for NCT, and 10 CFR §71.51(a)(2) for HAC, is determined. Measurement of the radiation dose rates will be performed as specified in 10 CFR §71.47(b) for an exclusive use shipment: 200 mrem/hr on the external surface of the package, 10 mrem/hr at any point 2 meters from the surface of the package (conservative location), and 2 mrem/hr in any normally occupied space (if required).

1.2.4.5 Criticality

The presence and location of the stainless steel in the package walls and a half-thickness of the impact limiters are shown in Chapter 6.0, *Criticality Evaluation*, to be all that is required for maintaining criticality safety for infinite arrays of undamaged or damaged packages, as dictated by 10 CFR 71[3] for NCT or HAC. KENO calculations are performed to verify that the authorized quantity of fissile material in a single RH-TRU 72-B package meets the requirements of 10 CFR §71.55. Additional KENO calculations are then done to show that an infinite array of undamaged or damaged RH-TRU 72-B packages meet the requirements of 10 CFR §71.59. Details of the models used and the results obtained are included in Chapter 6.0, *Criticality Evaluation*. Based on an unlimited number of damaged or undamaged RH-TRU 72-B packages, the criticality safety index (CSI), per 10 CFR §71.59, is 0.0.

1.2.4.6 Acceptance Tests

Acceptance tests were devised to ensure that the RH-TRU 72-B package performs as required before its first use, and a maintenance program was created to ensure its continued performance. These procedures are described in Section 8.1, *Acceptance Tests*, and Section 8.2, *Maintenance Program*, and comply with Subpart G of 10 CFR 71[3].

Table 1.2-1 – Overall Component Weights

Component	Weight	
	(lbs)	(kg)
Outer Cask	27,883	12,647
Inner Vessel	4,023	1,825
Impact Limiters	5,094	2,311
Loaded Canister	8,000	3,629
TOTAL	***45,000***	***20,412***

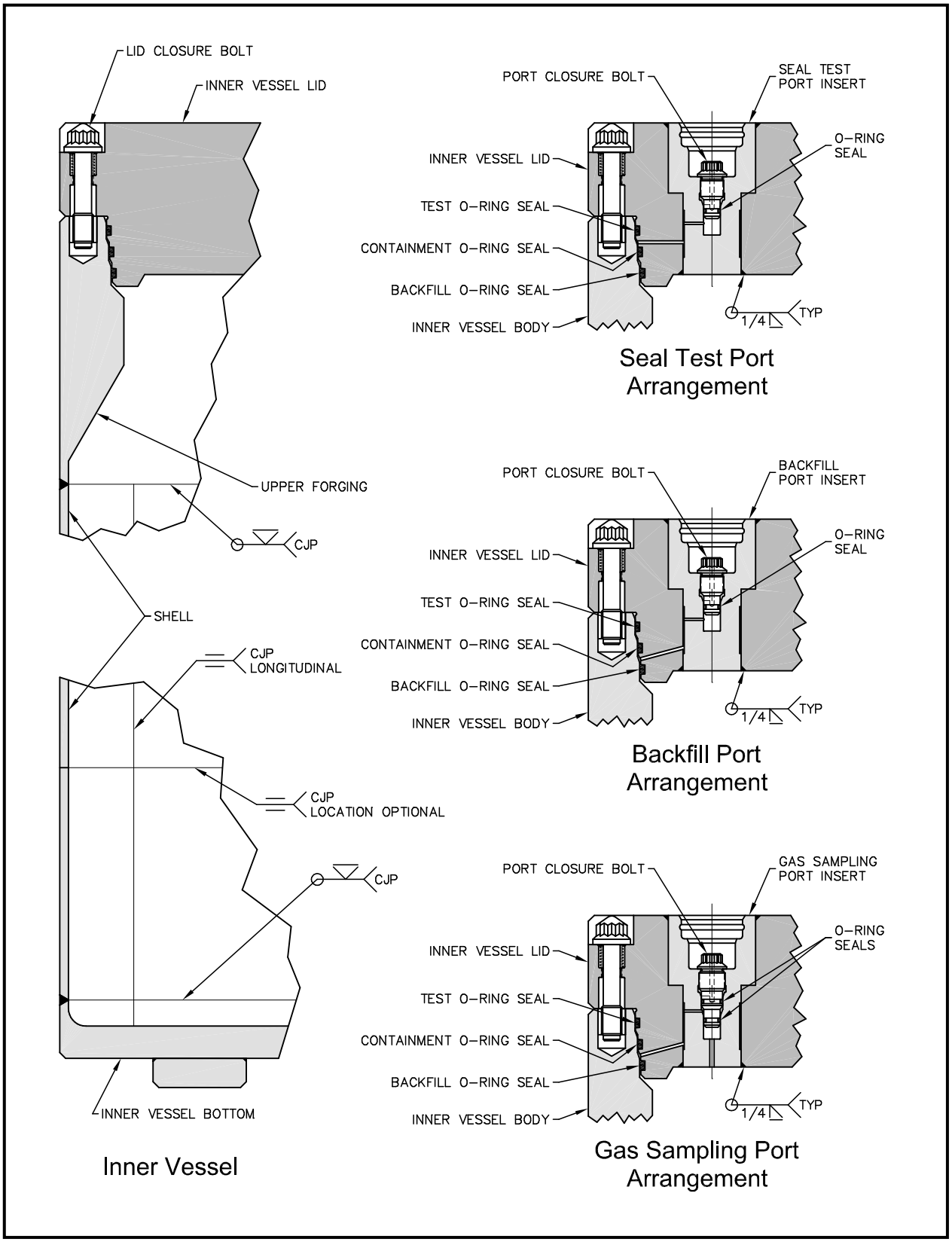

Figure 1.2-1 – Inner Vessel Containment Components

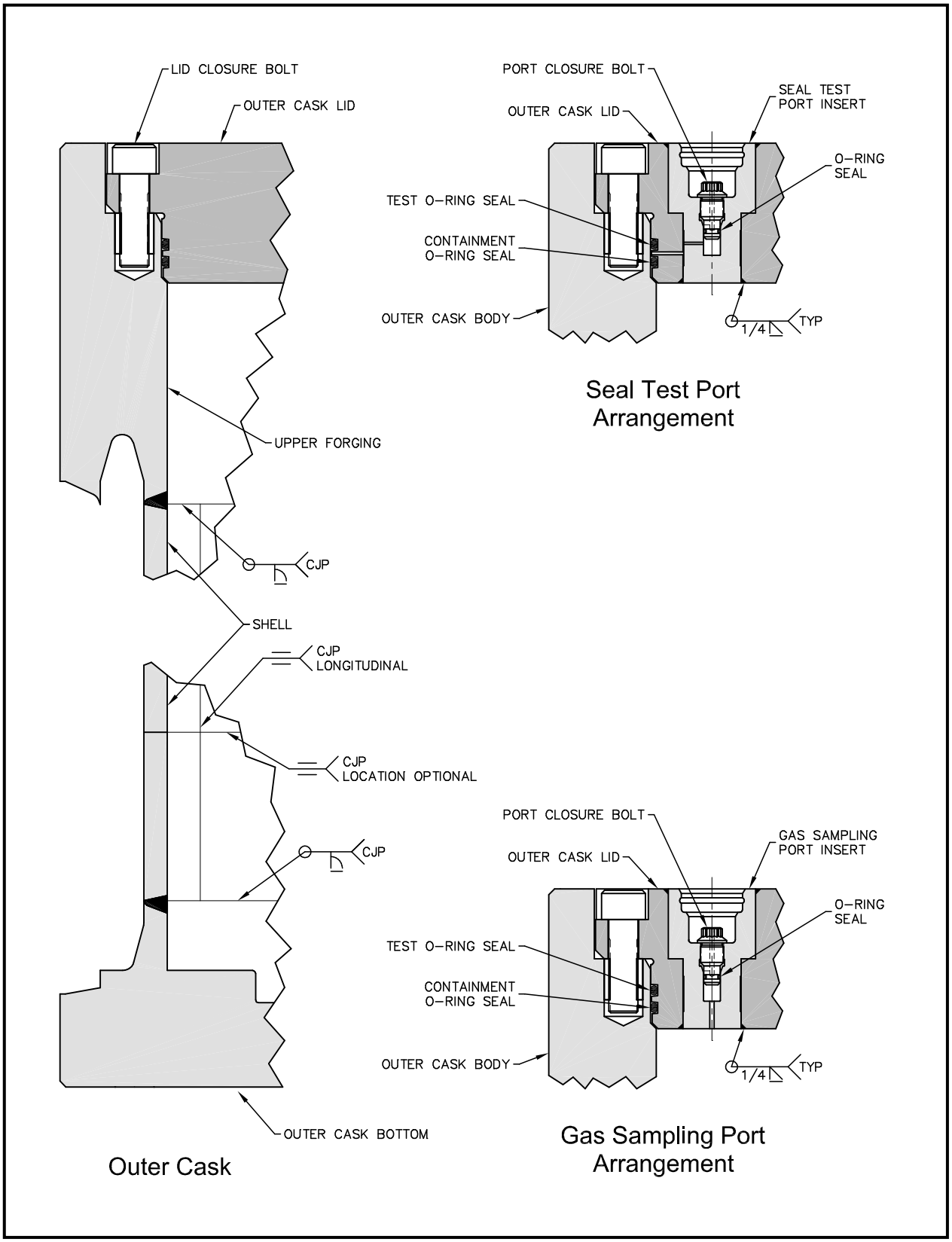

Figure 1.2-2 – Outer Cask Containment Components

This page intentionally left blank.

1.3 Appendices

1.3.1 *Packaging General Arrangement Drawings*

1.3.2 *Glossary of Terms and Acronyms*

This page intentionally left blank.

1.3.1 Packaging General Arrangement Drawings

This page intentionally left blank.

REVISION HISTORY			
REV	DESCRIPTION	REL	DATE
1	INITIAL RELEASE	BH	3/17/99
2	SEE DCN 1/1, 2/1 AND 3/1	B. HARGIS	1/24/01
3	SEE DCN 1/2, 2/2, 3/2 & 4/2	BH	11/25/02
4	SEE DCR 51301-01		

NOTES, UNLESS OTHERWISE SPECIFIED:

1 PRIOR TO ASSEMBLY, ALL COMPONENTS SHALL BE CLEANED OF CUTTING OILS, MARKING DYES, WELDING FLUX, SPATTER, SCALE, GRIME, AND ALL OTHER FOREIGN MATERIALS. FINISHED ASSEMBLY AND ALL INTERIOR SURFACES SHALL BE CLEANED AND VISUALLY OR WIPE TEST INSPECTED IN ACCORDANCE WITH ASTM-A380.

2 NOMINAL WEIGHT OF EMPTY PACKAGE: 37,000 LBS.
MAXIMUM ALLOWABLE WEIGHT OF PACKAGE: 45,000 LBS.
MAXIMUM ALLOWABLE WEIGHT OF CONTENTS: 8,000 LBS.

3 IDENTIFICATION: PACKAGE SHALL BE IDENTIFIED ON OUTER CASK WITH STAINLESS STEEL NAMEPLATES SEAL WELDED ALL AROUND IN ACCORDANCE WITH THE REQUIREMENTS OF 10 CFR 71.85 (c).

4 LEAD TO BE CAST IN PLACE, PER APPENDIX 8.3.1 OF THE SAR. LEAD SHALL MEET THE REQUIREMENTS OF QQ-L-171e GRADE A OR C OR OPTIONALLY, ASTM B29-92 PURE OR CHEMICAL COPPER LEAD.

5 ACCEPTANCE OF THE AS-INSTALLED LEAD SHIELDING SHALL BE DETERMINED BY GAMMA SCAN, AFTER COOL DOWN TO AMBIENT TEMPERATURE. ACCEPTANCE IS BASED ON AN OBSERVED ABSENCE OF ANY SIGNIFICANT VOIDS AND CONFIRMATION THAT A MINIMUM ACCEPTABLE THICKNESS EXISTS FOR THE LEAD AT ALL LOCATIONS. SPECIFIC METHODS AND ACCEPTANCE CRITERIA FOR THE GAMMA SCAN ARE SET OUT IN SECTION 8.1.5 OF THE SAR.

6 THERMAL SHIELD TO BE INSTALLED AFTER ACCEPTABLE GAMMA SCAN OF LEAD IS COMPLETE.

8 THIS WELD TO BE MADE AFTER LEAD POUR AND COOL DOWN TO AMBIENT TEMPERATURE.

9 ALL WELDING PROCEDURES AND PERSONNEL SHALL BE QUALIFIED IN ACCORDANCE WITH ASME CODE, SECTION IX.

10 INDICATED WELDS SHALL BE LIQUID PENETRANT INSPECTED ON ROOT PASS AND EACH WELD LAYER, IF A MULTI-PASS WELD, AND ON THE COMPLETED WELD IF A SINGLE PASS WELD IN ACCORDANCE WITH ASME B & PV CODE, SECTION III, DIVISION I, SUBSECTION NB, ARTICLE NB-5000 AND SECTION V, ARTICLE 6.

11 INDICATED WELDS SHALL BE LIQUID PENETRANT INSPECTED ON ROOT AND FINAL PASS IN ACCORDANCE WITH ASME B & PV CODE, SECTION III, DIVISION I, SUBSECTION NF, ARTICLE NF-5000 AND SECTION V, ARTICLE 6.

12 ALL WELDS SHALL BE VISUALLY INSPECTED IN ACCORDANCE WITH AWS D1.1.

13 INDICATED WELDS SHALL BE RADIOGRAPH INSPECTED IN ACCORDANCE WITH ASME B & PV CODE, SECTION III, DIVISION I, SUBSECTION NB, ARTICLE NB-5000, AND SECTION V, ARTICLE 2.

14 INDICATED WELDS SHALL BE ULTRASONIC TESTED PER ASME B & PV CODE, SECTION III, DIVISION I, SUBSECTION NB, ARTICLE NB-5000, AND SECTION V, ARTICLE 5.

15 TAMPER INDICATING SEAL SHALL BE INSTALLED AT ONE LOCATION CONNECTING THE UPPER IMPACT LIMITER TO THE OUTER CASK. PAD EYES MAY BE INSTALLED ON UPPER AND LOWER LIMITERS FOR INTERCHANGEABILITY.

16 INDICATED ITEM(S) SHALL BE LOAD TESTED TO 150% OF THE MAXIMUM WORKING LOAD.

18 DESIGN PRESSURE IS 150 psig. INNER VESSEL AND OUTER CASK CONTAINMENT BOUNDARIES SHALL BE SUBJECTED TO AN INTERNAL TEST PRESSURE EQUAL TO A MINIMUM OF 150% OF THE DESIGN PRESSURE PER 10 CFR 71.85 (b).

19 INNER VESSEL AND OUTER CASK CONTAINMENT BOUNDARIES SHALL BE HELIUM LEAK TESTED TO DEMONSTRATE A LEAKAGE RATE NOT TO EXCEED 1 X 10^{-7} STANDARD CUBIC CENTIMETERS PER SECOND IN ACCORDANCE WITH ANSI N14.5.

NOTE: PRIOR TO LEAD POUR, THE INNER SHELL OF THE OUTER CASK SHALL BE HELIUM LEAKAGE TESTED.

20 INDICATED HOLES ARE PROVIDED FOR THE INSTALLATION OF AN IV HANDLING FIXTURE FOR LIFTING AND HANDLING OF IV LID, IV ASSEMBLY, AND/OR LOADED IV.

21 INDICATED HOLES ARE PROVIDED FOR THE INSTALLATION OF AN OC HANDLING FIXTURE FOR LIFTING AND HANDLING OF THE OC LID. EACH LOCATION SHALL BE STENCILED OR OTHERWISE LABELED WITH THE FOLLOWING WARNING: "LID LIFT ONLY".

22 PINTLE SOCKETS LOCATED AT CENTER OF IV AND OC ARE PROVIDED FOR LID HANDLING ONLY. EACH LOCATION SHALL BE STENCILED OR OTHERWISE LABELED WITH FOLLOWING WARNING: "LID LIFT ONLY".

23 TORQUE INDICATED BOLTS (1-1/4-7UNC) TO 600-700 FT-LBS. OPTIONALLY COAT THREADS WITH A NICKEL BEARING LUBRICANT PRIOR TO ASSEMBLY.

24 TORQUE INDICATED BOLTS (7/8-9UNC) TO 100-200 FT-LBS. OPTIONALLY COAT THREADS WITH A NICKEL BEARING LUBRICANT PRIOR TO ASSEMBLY.

26 OPTIONAL: HARD CHROME OR NICKEL PLATE SURFACE.

27 OUTER CASK INNER AND OUTER SHELLS, AND INNER VESSEL SHELL SHALL COMPLY WITH THE TOLERANCE REQUIREMENTS OF ASME CODE, SECTION III, DIVISION I, SUBSECTION NE, ARTICLE NE-4220.

28 MATERIAL: POLYURETHANE FOAM 11.5 LB. PER CUBIC FOOT DENSITY ±15%. INSTALLATION TECHNIQUES, ACCEPTANCE TESTS AND ACCEPTABLE DEVIATIONS IN PROPERTIES ARE SUMMARIZED IN SECTION 8.1.4.1 OF THE SAR.

29 THREADS PER ANSI B1.1.

31 CADMIUM OR THIN DENSE CHROME PLATE. OPTIONAL FOR THREAD INSERTS.

33 MATERIAL: ASTM A-276 TYPE 304 STAINLESS STEEL.

34 MATERIAL: ASTM A-240, TYPE 304 STAINLESS STEEL PLATE.

35 MATERIAL: BUTYL PER RAINIER RUBBER RR0405-70 OR EQUIVALENT MEETING THE REQUIREMENTS OF ASTM D2000 M4AA710 A13 B13 F17 F48 Z TRACE ELEMENT.

36 O-RING SHALL BE LIGHTLY COATED WITH VACUUM GREASE PRIOR TO ASSEMBLY. SEAL SURFACES MAY ALSO, AS AN OPTION, BE COATED WITH A THIN COAT OF VACUUM SEAL GREASE.

39 AS BUILT MINIMUM THICKNESS SHALL COMPLY WITH TOLERANCES GIVEN IN ASTM-A480. AT GROUND WELD JOINTS, MINIMUM THICKNESS MAY BE REDUCED UP TO .050 INCHES.

40 INSTALL BOLT, NUT AND FLAT WASHER IN IMPACT LIMITER LIFTING LUGS PRIOR TO TRANSPORT.

41 MATERIAL: ASTM A-182, TYPE F304 STAINLESS STEEL FORGING. (OPTIONAL FOR INNER VESSEL AND OUTER CASK LIDS AND END PLATES AND INNER VESSEL PAYLOAD SPACERS.)

42 'CJP' INDICATES COMPLETE JOINT PENETRATION.

44 QUALITY ASSURANCE REQUIREMENTS - 10 CFR 71, SUBPART H.

45 TORQUE PORT PLUG BOLTS TO 15-20 FT-LBS.

46 DIMENSIONS ARE "BETWEEN WELDS".

47 THE TOTAL AXIAL CLEARANCE BETWEEN THE INNER VESSEL AND THE OUTER CASK CAVITY SHALL VARY FROM 1/16 TO 1 5/16.

48 PLUG WELD AND GRIND FLUSH AFTER INSTALLATION OF FOAM.

49 TOLERANCES FOR STOCK PLATE, SHEET, TUBING AND ANGLE COMPONENTS ARE TO BE PER THE APPLICABLE ASTM STANDARD FOR THE SPECIFIED MATERIAL.

50 INSERT MATERIAL SHALL MEET ASTM A434 WITH 140,000 PSI MINIMUM TENSILE STRENGTH.

51 OUTER DIAMETER OF IV LID SHALL NOT EXCEED OUTER DIAMETER OF ADJACENT IV BODY FORGING.

52 MODIFY 1 INCH LEG AS NECESSARY TO FIT FLAT ON BOTTOM FLANGE. ANGLE IS OPTIONAL AND IS USED AS A MANUFACTURING AID ONLY.

53 FOR EACH HEAT/LOT, PERFORM AND DOCUMENT A CHARPY TEST ON THREE (3) SPECIMENTS. TEST MUST DEMONSTRATE AT LEAST 20 FT-LB ABSORBED ENERGY AT -40°F.

54 BACKING BARS OPTIONAL.

55 EXPOSED EXTERNAL OUTER CASK SURFACES MAY BE OPTIONALLY ABRASIVE BLASTED IN ACCORDANCE WITH SSPC-SP-6 AND/OR PAINTED WITH A LOW HALOGEN PAINT.

NOTES NOT USED 7, 17, 25, 30, 32, 37, 38 AND 43.

ITEM	QTY	NEXT ASSY

ORIGINAL SIGNATURES ON FILE

TOLERANCES, UNLESS OTHERWISE SPECIFIED:

LINEAL DIMENSION RANGE	FRACTIONAL	ANGULAR
0-2"	±1/16	±2°
2"-6"	±1/8	
6"-18"	±1/4	
18"-48"	±1/2	
> 48"	±3/4	

Prepared for

U.S. Department of Energy

by PACKAGING TECHNOLOGY, INC.

RH-TRU 72-B PACKAGING
SAR DRAWING

WASTE ISOLATION PILOT PLANT WIPP

SCALE: NONE | WT. N/A
REV: 4 | SHEET 1 OF 8
DWG SIZE D | DWG NO. X-106-500-SNP
CADFILE: 97015SAR014.DWG

X-106-500-SNP	2	4

REVISION HISTORY

REV	DESCRIPTION	REL	DATE
0	INITIAL RELEASE	BH	3/17/99
2	SEE DCN 1/1, 2	B. HARGIS	1/24/01
3	SEE DCN 1/2, 2/2, 3/2 & 4/2	BH	11/25/02
4	SEE DCR 51301-01		

FIGURE WITHHELD UNDER 10 CFR 2.390

ITEM	QTY	NEXT ASSY

ORIGINAL SIGNATURES ON FILE

ANCES, UNLESS OTHERWISE SPECIFIED:

LINEAL DIMENSION RANGE	FRACTIONAL	ANGULAR
0–2"	±1/16	±2°
2"–6"	±1/8	
6"–18"	±1/4	
18"–48"	±1/2	
> 48"	±3/4	

Prepared for

U.S. Department of Energy

by PACKAGING TECHNOLOGY, INC.

RH-TRU 72-B PACKAGING SAR DRAWING

WASTE ISOLATION PILOT PLANT WIPP

SCALE: 3/8 | WT. N/A

REV: 4 | SHEET 2 OF 8

DWG SIZE D | DWG NO. X-106-500-SNP

CADFILE: 97015SAR024.DWG

X-106-500-SNP	3	4

REVISION HISTORY

REV	DESCRIPTION	REL	DATE
0	INITIAL RELEASE	BH	3/17/99
2	SEE DCN 1/1, 2/1 AND 3/1	B. HARGIS	1/24/01
3	SEE DCN 1/2, 2/2, 3/2 & 4/2	BH	11/25/02
4	SEE DCR 51301-01		

FIGURE WITHHELD UNDER 10 CFR 2.390

ITEM	QTY	NEXT ASSY

ORIGINAL SIGNATURES ON FILE

ES, UNLESS OTHERWISE SPECIFIED:

LINEAL DIMENSION RANGE	FRACTIONAL	
0–2"	±1/16	±2
2"–6"	±1/8	
6"–18"	±1/4	
18"–48"	±1/2	
> 48"	±3/4	

Prepared for

U.S. Department of Energy

by PACKAGING TECHNOLOGY, INC.

RH-TRU 72-B PACKAGING
SAR DRAWING

WASTE ISOLATION PILOT PLANT WIPP

SCALE: 3/8	WT. N/A
REV: 4	SHEET 3 OF 8
DWG SIZE D	DWG NO. X-106-500-SNP
	CADFILE: 97015SAR034.DWG

X-106-500-SNP	4	4

REVISION HISTORY

REV	DESCRIPTION	REL	DATE
1	INITIAL RELEASE	BH	3/17/99
2	SEE DCN 1/1, 2/1 AND 3/1	B. HARGIS	1/24/01
3	SEE DCN 1/2, 2/2, 3/2 & 4/2	BH	11/25/02
4	SEE DCR 51301-01		

FIGURE WITHHELD UNDER 10 CFR 2.390

ITEM	QTY	NEXT ASSY

ORIGINAL SIGNATURES ON FILE

TOLERANCES, UNLESS OTHERWISE SPECIFIED:

LINEAL DIMENSION RANGE	FRACTIONAL	ANGULAR
0–2"	±1/16	±2°
2"–6"	±1/8	
6"–18"	±1/4	
18"–48"	±1/2	
> 48"	±3/4	

Prepared for

U.S. Department of Energy

by PACKAGING TECHNOLOGY, INC.

RH-TRU 72-B PACKAGING SAR DRAWING

WASTE ISOLATION PILOT PLANT WIPP

SCALE: 1/4 | WT. N/A

REV: 4 | SHEET 4 OF 8

DWG SIZE D | DWG NO. X-106-500-SNP

CADFILE: 97015SAR044.DWG

X-106-500-SNP	5	4

REVISION HISTORY

REV	DESCRIPTION	REL	DATE
1	INITIAL RELEASE	BH	3/17/99
2	SEE DCN 1/1, 2	B. HARGIS	1/24/01
3	SEE DCN 1/2, 2/2, 3/2 & 4/2	BH	11/25/02
4	SEE DCR 51301-01		

FIGURE WITHHELD UNDER 10 CFR 2.390

ITEM	QTY	NEXT ASSY

ORIGINAL SIGNATURES ON FILE

NLESS OTHERWISE SPECIFIED:

LINEAL DIMENSION RANGE	FRACTIONAL	ANGULAR
0-2"	±1/16	±2°
2"-6"	±1/8	
6"-18"	±1/4	
18"-48"	±1/2	
> 48"	±3/4	

Prepared for

U.S. Department of Energy

by PACKAGING TECHNOLOGY, INC.

RH-TRU 72-B PACKAGING
SAR DRAWING

WASTE ISOLATION PILOT PLANT WIPP

SCALE: 1/4 | WT. N/A

REV: 4 | SHEET 5 OF 8

DWG SIZE D | DWG NO. X-106-500-SNP

CADFILE: 97015SAR054.DWG

X-106-500-SNP	6	4

REVISION HISTORY

REV	DESCRIPTION	REL	DATE
1	INITIAL RELEASE	BH	3/17/99
2	SEE DCN 1/1, 2/1 AND 3/1	B. HARGIS	1/24/01
3	SEE DCN 1/2, 2/2, 3/2 & 4/2	BH	11/25/02
4	SEE DCR 51301-01		

FIGURE WITHHELD UNDER 10 CFR 2.390

ITEM	QTY	NEXT ASSY

ORIGINAL SIGNATURES ON FILE

LERANCES, UNLESS OTHERWISE SPECIFIED:

LINEAL DIMENSION RANGE	FRACTIONAL
0–2"	±1/16
2"–6"	±1/8
6"–18"	±1/4
18"–48"	±1/2
> 48"	±3/4

Prepared for

U.S. Department of Energy

by PACKAGING TECHNOLOGY, INC.

RH–TRU 72–B PACKAGING SAR DRAWING

WASTE ISOLATION PILOT PLANT WIPP

SCALE: 1/8 | WT. N/A

REV: 4 | SHEET 6 OF 8

DWG SIZE D | DWG NO. X–106–500–SNP

CADFILE: 97015SAR064.DWG

X-106-500-SNP	7	4

REVISION HISTORY

REV	DESCRIPTION	REL	DATE
1	INITIAL RELEASE	BH	3/17/99
2	SEE DCN 1/1, 2	B. HARGIS	1/24/01
3	SEE DCN 1/2, 2/2, 3/2 & 4/2	BH	11/25/
4	SEE DCR 51301-01		

FIGURE WITHHELD UNDER 10 CFR 2.390

ITEM	QTY	NEXT ASSY

ORIGINAL SIGNATURES ON FILE

ES, UNLESS OTHERWISE SPECIFIED:

LINEAL DIMENSION RANGE	FRACTIONAL	ANGULAR
0-2"	±1/16	±2°
2"-6"	±1/8	
6"-18"	±1/4	
18"-48"	±1/2	
> 48"	±3/4	

Prepared for

U.S. Department of Energy

by PACKAGING TECHNOLOGY, INC.

RH-TRU 72-B PACKAGING SAR DRAWING

WASTE ISOLATION PILOT PLANT WIPP

SCALE: 1/4 | WT. N/A

REV: 4 | SHEET 7 OF 8

DWG SIZE D | DWG NO. X-106-500-SNP

CADFILE: 97015SAR074.DWG

X-106-500-SNP	8	4

REVISION HISTORY

REV	DESCRIPTION	REL	DATE
1	INITIAL RELEASE	BH	3/17/99
2	SEE DCN 1/1, 2/1 AND 3/1	B. HARGIS	1/24/01
3	SEE DCN 1/2, 2/2, 3/2 & 4/2	BH	11/25/02
4	SEE DCR 51301-01		

FIGURE WITHHELD UNDER 10 CFR 2.390

ITEM	QTY	NEXT ASSY

ORIGINAL SIGNATURES ON FILE

TOLERANCES, UNLESS OTHERWISE SPECIFIED:

LINEAL DIMENSION RANGE	FRACTIONAL	ANGULAR
0-2"	±1/16	±2°
2"-6"	±1/8	
6"-18"	±1/4	
18"-48"	±1/2	
> 48"	±3/4	

Prepared for

U.S. Department of Energy

by PACKAGING TECHNOLOGY, INC.

RH-TRU 72-B PACKAGING SAR DRAWING

WASTE ISOLATION PILOT PLANT WIPP

SCALE: 1/2 | WT. N/A

REV: 4 | SHEET 8 OF 8

DWG SIZE D | DWG NO. X-106-500-SNP

CADFILE: 97015SAR084.DWG

X-106-501-SNP	1	4

REVISION HISTORY

REV	DESCRIPTION	REL	DATE
0	INITIAL RELEASE	BH	8/5/99
	±E DCN 1/0	BH	8/16/99
		BH	9/29/00
3	SEE DCN 1/2 & 2/2	BH	8/6/01
4	SEE DCR 51301-01		

FIGURE WITHHELD UNDER 10 CFR 2.390

ITEM	QTY	NEXT ASSY

ORIGINAL SIGNATURES ON FILE

Prepared for

U.S. Department of Energy

by PACKAGING TECHNOLOGY, INC.

RH-TRU
WASTE CANISTER ASSEMBLY
FIXED LID DESIGN

WASTE ISOLATION PILOT PLANT WIPP

SCALE: 1/4	WT. N/A
REV: 4	SHEET 1 OF 1
DWG SIZE D	DWG NO. X-106-501-SNP
	CADFILE: 97015CAN014.DWG

X-106-502-SNP	1	2

REVISION HISTORY

REV	DESCRIPTION	REL	DATE
0	INITIAL RELEASE	BH	9/29/00
1	SEE DCN 1/0 & 2/0	BH	8/6/01
2	SEE DCR 51301-01		

FIGURE WITHHELD UNDER 10 CFR 2.390

ITEM	QTY	NEXT ASSY

ORIGINAL SIGNATURES ON FILE

Prepared for

U.S. Department of Energy

by PACKAGING TECHNOLOGY, INC.

RH-TRU
WASTE CANISTER ASSEMBLY
REMOVABLE LID DESIGN

WASTE ISOLATION PILOT PLANT WIPP

SCALE: 1/4	WT. N/A
REV: 2	SHEET 1 OF 1
DWG SIZE D	DWG NO. X-106-502-SNP
	CADFILE: 97015CAN022.DWG

1.3.2 Glossary of Terms and Acronyms

ASME – American Society of Mechanical Engineers.

ASME B&PVC – ASME Boiler and Pressure Vessel Code.

Bolt Hole Access Debris Ring – An optional ring covering the six impact limiter attachment bolt access tubes on each impact limiter.

Cask – The assembly of components comprising the RH-TRU 72-B packaging (see ***Packaging***).

Center-Pivot Trunnions – The two circular trunnions located at the OC's center of length that serve as the package's main tie-down points, and allow uprighting of the package while situated on a transport trailer.

Impact Limiters – Polyurethane foam-filled impact energy absorbers and thermal insulators that are located at each end of the OC.

Impact Limiter Attachment Bolts – The six 1¼-7UNC socket head cap screws used to secure each impact limiter to the OC body.

Inner Vessel – The assembly (comprised of an IV lid and IV body) providing a secondary level of containment for the payload.

IV – Inner Vessel (secondary containment vessel).

IV Alignment Lug – The flat external protuberance located at the bottom of the IV body for aligning the IV with the mating socket in the OC body bottom.

IV Backfill Port – The penetration into IV lid that allows tracer gas backfill between the lower (backfill) O-ring seal and the middle (containment) O-ring seal.

IV Backfill Port Closure Bolt – The IV backfill port closure assembly consisting of a cross-drilled bolt and an O-ring seal.

IV Backfill Port Insert – The replaceable IV backfill port component that provides the interface for the IV backfill port closure bolt.

IV Body – The assembly consisting of the IV seal flange, cylindrical shell, and bottom closure.

IV Closure Bolts – The eight 7/8-9UNC socket head cap screws used to secure the IV lid to the IV body; each assembly consists of a necked-down bolt, a spring, and an optional stainless steel washer to enhance remote operations.

IV Closure Bolt Thread Insert – The optional thread insert to allow thread replacement, if necessary.

IV Gas Sampling Port – The penetration through the IV lid that allows venting and gas sampling of the IV cavity.

IV Gas Sampling Port Closure Bolt – The IV gas sampling port closure assembly consisting of a cross-drilled bolt and an O-ring seal.

IV Gas Sampling Port Insert – The replaceable IV gas sampling port component that provides the interface for the IV gas sampling port closure bolt.

IV Lid – The monolithic mating closure for the IV body.

IV Lid Pintle Socket – The bayonet-type recess at the lid's centerline for handling the IV lid.

IV Lower O-ring Seal – The lower elastomeric O-ring seal in the IV seal flange that forms the tracer gas boundary for leakage rate testing.

IV Middle O-ring Seal – The middle elastomeric O-ring seal in the IV seal flange that forms the containment boundary.

IV Seal Test Port – The penetration into the IV lid that allows testing between the middle (containment) O-ring seal and upper (test) O-ring seal.

IV Seal Test Port Closure Bolt – The IV upper seal test port closure assembly consisting of a cross-drilled bolt and an O-ring seal.

IV Seal Test Port Insert – The replaceable IV upper seal test port component that provides the interface for the IV upper seal test port closure bolt.

IV Upper O-ring Seal – The upper elastomeric O-ring seal in the IV seal flange that forms the test boundary for leakage rate testing.

HAC – Hypothetical Accident Conditions.

Lift/Tie-down Trunnions – The four circular trunnions located near the OC's closure end; two lift/tie-down trunnions serve as the package's lift points, and two serve as secondary tie-down points.

NCT – Normal Conditions of Transport.

OC – Outer Cask (primary containment vessel).

OC Body – The assembly consisting of the OC seal flange, inner and outer cylindrical shells, lead biological shielding, thermal shield, and bottom closure.

OC Closure Bolts – The eighteen 1¼-7UNC socket head cap screws used to secure the OC lid to the OC body.

OC Closure Bolt Thread Insert – The optional thread insert to allow thread replacement, if necessary.

OC Gas Sampling Port – The penetration through the OC lid that allows venting and gas sampling of the OC cavity.

OC Gas Sampling Port Closure Bolt – The OC gas sampling port closure assembly consisting of a cross-drilled bolt and an O-ring seal.

OC Gas Sampling Port Insert – The replaceable OC gas sampling port component that provides the interface for the OC gas sampling port closure bolt.

OC Lid – The monolithic mating closure for the OC body.

OC Lid Pintle Socket – The bayonet-type recess at the lid's centerline for handling the OC lid.

OC Lower O-ring Seal – The lower elastomeric O-ring seal in the OC seal flange that forms the containment boundary.

OC Seal Test Port – The penetration into the OC lid that allows testing between the lower (containment) O-ring seal and upper (test) O-ring seal.

OC Seal Test Port Closure Bolt – The OC seal test port closure assembly consisting of a cross-drilled bolt and an O-ring seal.

OC Seal Test Port Insert – The replaceable OC seal test port component that provides the interface for the OC seal test port closure bolt.

OC Thermal Shield – The thin shell outside the heavy OC outer shell that prevents hot gasses and flames from directly impinging on the OC surface in the event of a HAC fire.

OC Upper O-ring Seal – The upper elastomeric O-ring seal in the OC seal flange that forms the test boundary for leakage rate testing.

Outer Cask – The assembly (comprised of an OC lid and OC body) providing a primary level of containment for the payload.

Package – The packaging with its radioactive contents, or payload, as presented for transportation as defined in 10 CFR §71.4. Within this SAR, the package is denoted as the RH-TRU 72-B package.

Packaging – The assembly of components necessary to ensure compliance with packaging requirements as defined in 10 CFR §71.4. Within this SAR, the packaging is denoted as the RH-TRU 72-B packaging.

Payload – Remote-handled transuranic (RH-TRU) waste or other authorized contents contained within the approved payload container. In this SAR, the payload includes a payload canister (RH-TRU canister). Payload requirements are defined by the RH-TRAMPAC.

Payload Canister – The receptacle containing the RH-TRU waste.

RH-TRAMPAC – Remote-Handled Transuranic Waste Authorized Methods for Payload Control defines the authorized contents for the RH-TRU 72-B packaging.

RH-TRU 72-B Package – The package consisting of a RH-TRU 72-B packaging and the payload.

RH-TRU 72-B Packaging – The packaging consisting of an outer cask (OC), an inner vessel (IV), and two impact limiters.

RH-TRU Waste – Remote-Handled Transuranic Waste.

RTV – Room Temperature Vulcanizing.

SAR – Safety Analysis Report (this document).

Tamper Indicating Device – A lock-wire or equivalent device that is installed between the closure-end impact limiter and the OC body prior to each shipment.

Tie-down Trunnions – The two circular trunnions located near the OC's bottom end, serving as secondary tie-down points.

This page intentionally left blank.

2.0 STRUCTURAL EVALUATION

This chapter presents structural evaluations demonstrating that the RH-TRU 72-B package design meets all applicable structural criteria. The energy absorbing external impact limiters, outer cask (OC), and inner vessel (IV) are evaluated and shown to provide adequate protection for the package payload (loaded payload canister). Normal conditions of transport (NCT) and hypothetical accident condition (HAC) evaluations, using analytical and experimental techniques, are performed in accordance with 10 CFR 71[1] requirements. Analytical demonstration techniques comply with the methodology presented in NRC Regulatory Guide 7.6[2].

2.1 Structural Design

Component tests have been performed to verify mechanical properties and physical performance. These tests are described within subsequent sections where appropriate. For example, component testing of package external impact limiters has been carried out to refine the design and to characterize the behavior and performance of the impact limiters. Burn tests, on the polyurethane foam used in the impact limiters, have been performed to establish foam characteristics during exposure to the hypothetical fire event. These tests were performed in conjunction with the NuPac 125-B cask[3] development program. Since that package utilizes the same type and density of foam as used in the RH-TRU 72-B package, the test results are directly applicable. These results are presented in Appendix 3.6.3, *Polyurethane Foam Performance Tests*. As indicated by the preceding discussions, detailed test results are typically relegated to the appendices herein.

The RH-TRU 72-B package bears a strong resemblance to the NuPac 125-B cask[3]. Analytical techniques, successfully utilized for the licensing of the NuPac 125-B cask, are generally repeated for the RH-TRU 72-B package. Additionally, parallels between the two packages are frequently taken advantage of herein to simplify and clarify the analysis methodologies.

The following table summarizes NuPac 125-B cask[3] test results that are specifically considered when evaluating the RH-TRU 72-B package design:

Section	72-B Evaluation	Utilization of Previous 125-B Data
2.7.1	Free Drop	Accelerometer traces from 125-B testing indicate the 125-B and 72-B packages can be reasonably treated as rigid bodies, thus helping to justify static application of impact accelerations.
2.7.1.1(9)	End Drop Lead Slump	Conservatism of the 72-B evaluation approach is demonstrated by reference to the fact that no lead slump was observed in end drop testing of a prototypic 125-B package body.

[1] Title 10, Code of Federal Regulations, Part 71 (10 CFR 71), *Packaging and Transportation of Radioactive Material*, Final Rule, 01-26-04.

[2] U. S. Nuclear Regulatory Commission, Regulatory Guide 7.6, *Design Criteria for the Structural Analysis of Shipping Package Containment Vessels*, Revision 1, March 1978.

[3] Nuclear Packaging, Inc., *Safety Analysis Report for the NuPac 125-B Fuel Shipping Package*, USNRC Certificate of Compliance 71-9200, U.S. Department of Energy, Washington, D.C.

Section	72-B Evaluation	Utilization of Previous 125-B Data
2.7.8	Side Punch Lead Deformation	72-B lead deformation is established by comparing to 125-B testing which employed a prototypic package body. 72-B testing only used an all steel, dummy package mass simulation and could not be used for this assessment.
3.6.3	Polyurethane Foam Burn Performance	Burn tests of 125-B foam, which is essentially identical to 72-B foam, are directly referenced.

2.1.1 Discussion

The RH-TRU 72-B, Type B(M)F-96, package consists of three basic components: (1) the energy-absorbing external impact limiters that protect the ends of the OC, (2) the OC (primary containment), and (3) the IV (secondary containment). The polyurethane foam-filled impact limiters serve the dual purposes of limiting *g*-loads acting on the package under drop conditions and providing thermal insulation for the hypothetical accident fire event. By selecting a proper density foam, *g*-loads acting upon the package are limited to acceptable levels.

The basic structure of the OC consists entirely of stainless steel (Type 304 or 304L) materials and is comprised of a 5-inch thick bottom closure plate, which welds directly to an outer shell (1½-inch thick, 41⅛-inch OD) and an inner shell (1-inch thick, 34⅜-inch OD). The annular region between these shells (1⅞-inch thick) is filled with lead shielding. The top closure consists of a thick-walled forging (ring) which welds directly to the inner and outer shells and a 6-inch thick closure plate (lid) which bolts to the body forging via eighteen (18), ASTM A320, Grade L43, 1¼-7UNC bolts. The bottom closure plate, inner shell, top forging and top closure plate form the outer containment boundary. Lifting and handling trunnions are attached to the outer, 1½-inch thick shell.

The basic structure of the IV is fabricated of stainless steel (Type 304 or 304L) materials and consists of a 1½-inch thick bottom closure plate which welds directly to a 3/8-inch thick shell (32-inch OD). At the top end, the shell is welded to a thick upper forging and final closure is provided by a 6½-inch thick closure plate (lid). The closure lid plate attaches to the upper forging via eight (8), ASTM A320, Grade L43, 7/8-9UNC bolts. The inner containment boundary, therefore, consists of the bottom closure plate, shell, upper forging, and the top closure plate. The IV is designed so that, with the package vertical, the IV top or bottom closure plate will rest on the corresponding OC closure plate.

2.1.2 Design Criteria

2.1.2.1 Basic Design Criteria (Allowable Stresses)

This section defines the stress allowables for primary-membrane, primary-bending, secondary, peak, bearing, shear, and buckling stresses for containment structures and fasteners, and non-containment structures and fasteners.

NRC Regulatory Guide 7.6[2] is used in conjunction with NRC Regulatory Guide 7.8[4] to evaluate the integrity of the RH-TRU 72 B-package. Where the loads specified by NRC Regulatory

[4] U. S. Nuclear Regulatory Commission, Regulatory Guide 7.8, *Load Combinations for the Structural Analysis of Shipping Packages for Radioactive Material*, Revision 1, March 1989.

Guide 7.6[2] conflict with those given in the current version of 10 CFR 71, the latter is used. Material properties and design stress intensity values, S_m, used in the analyses can be found in Table 2.3-1 and Table 2.3-2.

2.1.2.1.1 Containment Structures

NRC Regulatory Guide 7.6[2] was used for all package containment boundaries for both NCT and the HAC. Material data used in the evaluation correspond to the design stress values, S_m, yield strengths, S_y, and ultimate strengths, S_u, given in the ASME Code, Section III, Class I[5]. The primary containment is considered to be the 32⅜-inch inside diameter, 1-inch thick inner OC shell, the OC upper forging, the 6-inch thick bolted OC closure lid, and the 5-inch thick OC bottom plate. The secondary containment is considered to be the 1½-inch thick IV bottom plate, the 31¼-inch inside diameter, 3/8-inch thick IV shell, the IV upper forging, and the 6½-inch thick bolted IV closure lid. A summary of allowable stresses used for containment structures and fasteners is presented in Table 2.1-1. These data are consistent with Regulatory Guide 7.6[2] and Section NB-3000 and Appendix F of the ASME Code, Section III[5].

2.1.2.1.2 Non-Containment Structures

Structural evaluations of non-containment boundaries, such as the OC outer shell, and tie-down and center-pivot trunnions, use allowable stresses for NCT and HAC as presented in Table 2.1-2. The impact limiters are allowed to exceed yield for all conditions. The acceptance criterion for all impact related loads within the impact limiters is that no package "hard points" directly come into contact with the impact surface. Adherence to this criterion is assured by designing the impact limiters so that no impact limiter deformation for any regulatory drop event ever exceeds the maximum strain level achieved in polyurethane foam crush tests. Foam samples have been tested to strains of up to 87%. Static testing of prototypic, half-scale RH-TRU 72-B package impact limiters imposed strains of up to 97% (for 35º from vertical orientation, see Appendix 2.10.7, *Static and Dynamic Testing*). For purposes of this Safety Analysis Report, a strain limit of 85% is imposed for the polyurethane foam. Requirements for foam mechanical properties are presented in Section 2.3, *Mechanical Properties of Materials*. For lifting and handling loads, the "non-containment" NCT allowables of Table 2.1-2 are utilized in conjunction with a load factor of three (3), per 10 CFR §71.45.

2.1.2.2 Miscellaneous Structural Failure Modes

2.1.2.2.1 Brittle Fracture

With the exception of the closure bolts and the canister (if ASTM A516, Grade 55, 60, or 70 carbon steel is used for payload canister construction), all containment, and nearly all non-containment structural components, are fabricated of Type 304, Type F304, or Type 304L austenitic stainless steel. Since this material does not undergo a ductile-to-brittle transition in the temperature range of interest (to -40 ºF), it is safe from brittle fracture.

[5] American Society of Mechanical Engineers (ASME) Boiler and Pressure Vessel Code, Section III, *Rules for Construction of Nuclear Power Plant Components*, Division 1, Subsection NB and Appendices, 1986 Edition.

The closure bolts are fabricated from ASTM A320, Grade L43, alloy steel, an ASME Section III, Class I, material. As such, it is in compliance with the applicable brittle fracture requirements of ASME Section III, Subsection NB. As part of the manufacturing process, bolts with a diameter greater than 1-inch must be examined in accordance with ASME Section III, Subsection NB, Paragraph NB-2580, and tested in accordance with ASME Section III, Subsection NB, Paragraph NB-2333. Per Section 5 of NUREG/CR-1815[6], bolts are generally not considered as fracture critical components because multiple load paths exist and because bolted systems are designed to be redundant. However, for purposes of comparison, the nil ductility transition (NDT) temperature of the closure bolts will be calculated and compared with the requirements of NUREG/CR-1815[6].

According to Section 6.2.1.1 of the ASTM A320, Grade L43, specification, the minimum impact energy absorption is 20 ft-lbs at -150 ºF. The Charpy impact measurement may be transformed into a fracture toughness value by using the empirical relation developed in Section 4.2 of NUREG/CR-1815[6], as follows:

$$K_{ID} = \sqrt{5E(C_v)} = 53{,}665 \text{ psi-in}^{1/2}$$

where K_{ID} = dynamic fracture toughness, psi in^{½} and the elastic modulus, E = 28.8(10)^6 psi at -150 ºF (from Table I-6.0 in Appendix I of the ASME Code[5]), and the Charpy impact measurement, C_v = 20 ft-lbs.

The dynamic fracture toughness is translated to an equivalent nil-ductility transition (NDT) temperature by using the Design Reference K_{ID} curve given as Figure 2 of NUREG/CR-1815[6]. By interpolation, the temperature relative to the NDT temperature is found as:

$$T - NDT = 30\,°F$$

Accordingly, the NDT temperature is:

$$NDT = -150 - (+30) = -180\,°F$$

For Category I fracture critical components, and for section thicknesses of 1.25 inches (i.e., bolt diameter), Figure 3 of NUREG/CR-1815[6] gives the minimum offset, "A", as approximately 40 ºF. Thus, the maximum NDT temperature value is:

$$T_{NDT} = LST - A = -20 - 40 = -60\,°F$$

where the maximum NDT temperature is T_{NDT} per NUREG/CR-1815[6], the lowest service temperature, LST = -20 ºF per NRC Regulatory Guide 7.6[2], and A = 40 ºF per Figure 3 of NUREG/CR-1815[6].

The ASTM A320, Grade L43, closure bolts experience a ductile-to-brittle transition temperature at -180 ºF, whereas the criterion of NUREG/CR-1815[6] prescribes a maximum NDT temperature of -60 ºF. The 120 ºF margin between criteria requirements and material capability provides conservative assurance that brittle fracture failures will not occur in these ferritic closure-bolt materials.

[6] U.S. Nuclear Regulatory Commission, *Recommendations for Protecting Against Failure By Brittle Fracture in Ferritic Steel Shipping Containers Up to Four Inches Thick*, NUREG/CR-1815, June 1981.

The RH-TRU payload canisters are fabricated from Type 304 (or Type 304L) austenitic stainless steel, or ASTM A516, Grade 55, 60, or 70 carbon steel. This carbon steel conforms to the fine austenitic grain size requirement of ASTM A20/A20M. Because of the fine grain structure, coupled with the less than 0.40-inch thickness, the potential for brittle fracture of the payload canister steel is minimized.

2.1.2.2.2 Fatigue

2.1.2.2.2.1 Normal Operating Cycles

Normal operating cycles do not present a fatigue concern for the RH-TRU 72-B package components which have no stress concentrations. This is because the allowable stress for NCT ($3.0S_m$) will not exceed the allowable fatigue stress limit for the expected number of operating cycles. From Table I-1.2 in Appendix I of the ASME Code[5], the maximum value of the stress intensity (S_m) at the maximum normal operating temperature established herein, 200 ºF, is 20,000 psi for the Type 304 stainless steel used in the RH-TRU 72-B package. The expected number of operating cycles (defined as the process of going from an empty package, to one with maximum heat load, at the maximum normal operating temperature, and back again) for the RH-TRU 72-B package is below 10,000. From Figure I-9.2.1 in Appendix I of the ASME Code[5], the fatigue allowable stress intensity amplitude, S_a, of the alternating stress component (one-half of the alternating stress range) for 10,000 cycles is 64,000 psi. This value, when multiplied by the ratio of elastic modulus, $27.6(10)^6/28.3(10)^6$, gives a fatigue allowable alternating stress intensity amplitude of 62,400 psi. The non-fatigue allowable stress intensity range, from Section NB 3222.2 of the ASME Code[5], however, is 60,000 psi ($3.0S_m$). Since one-half of this range (30,000 psi) is less than the fatigue allowable alternating stress intensity (62,400 psi), the non-fatigue allowable stress criterion will govern.

Areas of stress concentration for the package occur at the IV and at the OC closure bolts. The maximum cyclic stress in the OC closure bolts is due to the preload. From Equation 5.4 of Bickford[7], the preload, P, is given by:

$$P = \frac{T}{KD}$$

where the torque is T, the torque coefficient is K, and the nominal bolt diameter is D.

<u>OC Closure Bolts</u>:

For these bolts, the pre-load torque is 600 – 700 lb-ft, or a maximum of 8,400 lb-in. The nominal bolt diameter is 1¼ inches, hence D = 1.25 inches. The torque coefficient is taken as K = 0.13 for cadmium and/or lubricated plated bolts. Therefore, the maximum bolt pre-load is:

$$P = \frac{8{,}400}{(0.13)(1.25)} = 51{,}692 \text{ lb}$$

[7] John H. Bickford, *An Introduction to the Design and Behavior of Bolted Joints*, 1981, Marcell Dekker, Inc.

From Appendix H of Bickford[7], the tensile stress area of the bolt, A = 0.969 in^2. The corresponding stress in the bolts, S, is:

$$S = \frac{P}{A} = \frac{51{,}692}{0.969} = 53{,}346 \text{ psi}$$

From Paragraph NB-3232.3(c) of the ASME Code[5], the fatigue strength reduction factor is assumed to be 4.0. In addition, from Table I-6.0 in Appendix I of the ASME Code[5], the modulus of elasticity at 160 ºF is 27.3(10)^6 psi. Since Figure 2.1-1 (Figure I-9.4 in Appendix I of the ASME Code[5]) is based upon a modulus of elasticity of 30.0(10)^6 psi, the equivalent stress range, S_{range}, is given by:

$$S_{range} = (53{,}346)(4)\frac{30.0(10)^6}{27.3(10)^6} = 234{,}490 \text{ psi}$$

The alternating component is one-half of the stress range, or 117,245 psi. From Figure 2.1-1, using the $3.0S_m$ curve, the allowable number of operating cycles is about 460. Operational procedures specify replacement of these bolts prior to the completion of 460 service cycles.

<u>IV Closure Bolts</u>:

For these bolts, the pre-load torque is 100 – 200 lb-ft, or a maximum of 2,400 lb-in. The nominal bolt diameter is 7/8 inch, hence D = 0.875 inches. The torque coefficient is taken as K = 0.13 for cadmium and/or lubricated plated bolts. Therefore, the maximum bolt pre-load is:

$$P = \frac{2{,}400}{(0.13)(0.875)} = 21{,}099 \text{ lb}$$

From Appendix H of Bickford[7], the tensile stress area of the bolt, A = 0.407 in^2. The corresponding stress in the bolts, S, is:

$$S = \frac{P}{A} = \frac{21{,}099}{0.407} = 51{,}840 \text{ psi}$$

The equivalent stress range, S_{range}, is given by:

$$S_{range} = (51{,}840)(4)\frac{30.0(10)^6}{27.3(10)^6} = 227{,}868 \text{ psi}$$

The alternating component is one-half of the stress range, or 113,934 psi. From Figure 2.1-1, using the $3.0S_m$ curve, the allowable number of operating cycles is about 550. Operational procedures specify replacement of these bolts prior to the completion of 550 service cycles.

2.1.2.2.2.2 Normal Vibration Over the Road

The criterion applied to analyze over-the-road vibration will be limited to the *g*-loading requirements established by 10 CFR 71. The vertical loading, 2*g*, will be used to evaluate the fatigue life of the RH-TRU 72-B package. Refer to Section 2.6.5, *Vibration*, for further discussion.

2.1.2.2.2.3 Extreme Total Stress Intensity Range

Per Paragraph C.7 of NRC Regulatory Guide 7.6[2], "The extreme total stress intensity range (including stress concentrations) between the initial state, the fabrication state, the normal operating conditions, and the accident conditions should be less than twice the adjusted value (adjusted to account for modulus of elasticity at the highest temperature) of S_a at 10 cycles given by the appropriate design fatigue curves." Evaluation of stresses per this criterion is addressed in Section 2.7.4.4, *Comparison with Allowable Stresses*.

2.1.2.2.2.3 Buckling

Buckling, per Paragraph C.5 of NRC Regulatory Guide 7.6[2], is an unacceptable failure mode for the containment vessels. The intent of this provision is to preclude large deformations that would compromise the validity of linear analysis assumptions and quasi-linear stress allowables, as given in Paragraph C.6 of NRC Regulatory Guide 7.6[2].

There are two shells within the RH-TRU 72-B package where buckling prevention criteria are applicable: the inner shell of the OC and the IV shell. For additional conservatism, the OC outer shell will also be evaluated. For reference purposes, the principal geometric features of these shells are listed in Table 2.1-3.

To demonstrate that buckling will not occur for these three shell geometries, the methodology of ASME Code Case N 284[8] is directly applied. The basic steps involved are summarized below. Details of the buckling assessments are presented in Appendix 2.10.5, *Buckling Design Criteria and Detailed Evaluation*.

1. Theoretical elastic buckling stresses are determined for hoop and axial compression and in-plane shear loadings using classical theory.
2. Capacity reduction factors are applied which account for the difference between classical theory and predicted instability stresses for fabricated shells.
3. Plasticity reduction factors are applied for those cases where elastically determined buckling stresses are above the proportional limit.
4. Elastic and inelastic buckling checks that employ appropriate factors of safety and appropriate interaction equations are made using worst-case applied compressive and in-plane shear stresses.

Consistent with the NRC Regulatory Guide 7.6[2] philosophy, factors of safety corresponding to ASME Code Level A and D Service conditions are employed respectively for NCT and HAC loadings, with applicable factors of safety of 2.0 for NCT and 1.34 for HAC, as specified in ASME Code Case N 284[8].

[8] American Society of Mechanical Engineers (ASME) Boiler and Pressure Vessel Code, Section III, *Rules for Construction of Nuclear Power Plant Components*, Division 1, Class MC, Code Case N-284, *Metal Containment Shell Buckling Design Methods*, August 25, 1980 approval date.

Table 2.1-1 – Containment Components Allowable Stress Limits

Stress Category	NCT	HAC
Containment Structure Allowable Stress Limits		
Primary Membrane Stress Intensity	S_m	Lesser of: $2.4S_m$, $0.7S_u$
Primary Membrane + Bending Stress Intensity	$1.5S_m$	Lesser of: $3.6S_m$, S_u
Range of Primary + Secondary Stress Intensity	$3.0S_m$	N/A
Bearing Stress	S_y	Sealing Surfaces: S_y Elsewhere: S_u
Pure Shear Stress	$0.6S_m$	$0.42S_u$
Peak	Per Section 2.1.2.2.2, *Fatigue*	
Buckling	Per Section 2.1.2.2.3, *Buckling*	
Containment Fastener Allowable Stress Limits		
Membrane Stress Intensity①	Lesser of: $2.0S_m$, S_y	S_y
Membrane + Bending Stress Intensity①	Lesser of: $3.0S_m$, S_y	S_y

Notes:

① Not considering stress concentrations; stress concentration is considered in Section 2.1.2.2.2, *Fatigue*.

Table 2.1-2 – Non-Containment Components Allowable Stress Limits

Stress Category	NCT	HAC
Non-Containment Structure Allowable Stress Limits		
Primary Membrane Stress Intensity	Greater of: S_m, S_y	$0.7S_u$
Primary Membrane + Bending Stress Intensity	Greater of: $1.5S_m$, S_y	S_u
Range of Primary + Secondary Stress Intensity	Greater of: $3.0S_m$, S_y	N/A
Bearing Stress	S_y	Sealing Surfaces: S_y Elsewhere: S_u
Pure Shear Stress	Greater of: $0.6S_m$, $0.6S_y$	$0.42S_u$
Peak	Per Section 2.1.2.2.2, *Fatigue*	
Buckling	Per Section 2.1.2.2.3, *Buckling*	
Non-Containment Fastener Allowable Stress Limits		
Membrane Stress Intensity①	Greater of: $2.0S_m$, S_y	Greater of: S_y, $0.7S_u$
Membrane + Bending Stress Intensity①	Greater of: $3.0S_m$, S_y	S_u

Notes:

① Not considering stress concentrations; stress concentration is considered in Section 2.1.2.2.2, *Fatigue*.

Table 2.1-3 – Shell Buckling Geometries

Shell	Dimensions (inches)		
	Mean Radius (R)	Thickness (t)	Length (L)
OC Inner Shell	16.690	1.000	121.25
OC Outer Shell	19.815	1.500	121.62
IV Shell	15.813	0.375	111.75

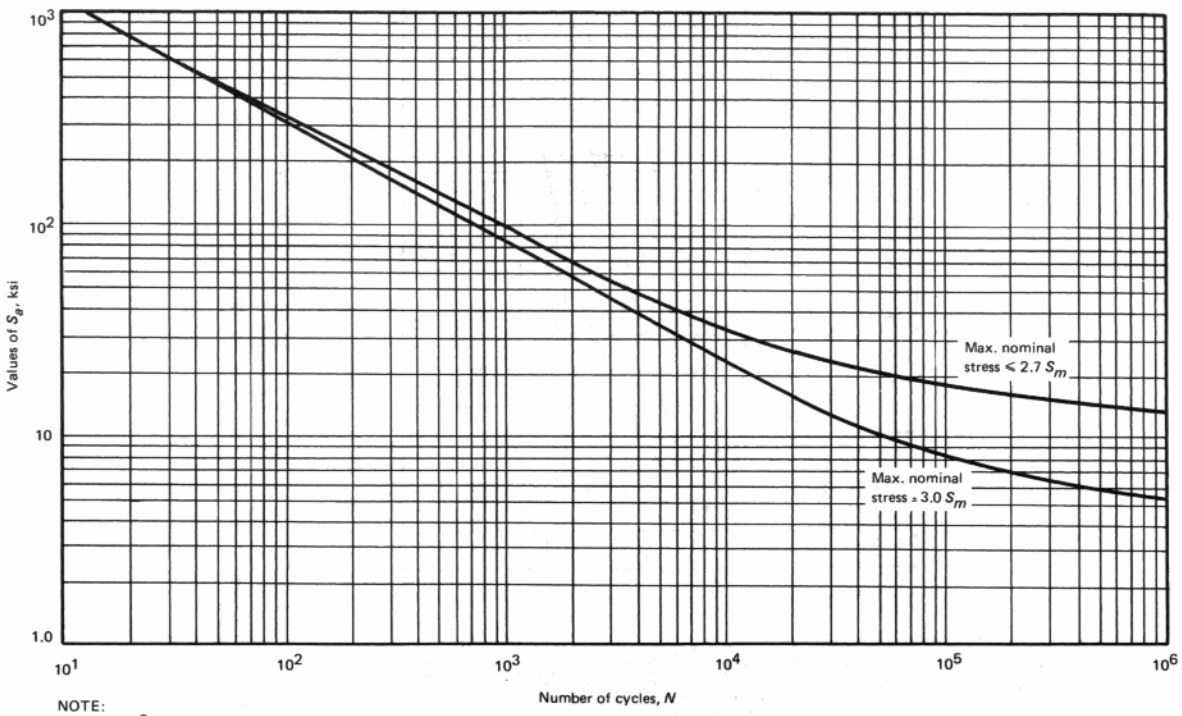

NOTE:
E = 30 X 10^6 psi

FIG. I-9.4 DESIGN FATIGUE CURVES FOR HIGH STRENGTH STEEL BOLTING FOR TEMPERATURES NOT EXCEEDING 700°F
Table I-9.1 Contains Tabulated Values and a Formula for Accurate Interpolation of These Curves

TABLE I-9.1
TABULATED VALUES OF S_a, ksi, FROM FIGS. I-9.0[1,2]

		Number of Cycles [Note (3)]																	
Figure	Curve	1E1	2E1	5E1	1E2	2E2	5E2	8.5E2 [Note (4)]	1E3	2E3	5E3	1E4	1.2E4 [Note (4)]	2E4	5E4	1E5	2E5	5E5	1E6
I-9.1	UTS 115–130 ksi	420	320	230	175	135	100	. . .	78	62	49	44	43	36	29	26	24	22	20
I-9.1	UTS ≤80 ksi	580	410	275	205	155	105	. . .	83	64	48	38	. . .	31	23	20	16.5	13.5	12.5
I-9.2.1	. . .	708	512	345	261	201	148	. . .	119	97	76	64	. . .	55.5	46.3	40.8	35.9	31	28.3
I-9.2.2 (see Table I-9.2.2)																			
I-9.3	S_y = 18.0 ksi	260	190	125	95	73	52	. . .	44	36	28.5	24.5	. . .	21	17	15	13.5	12.5	12.0
I-9.3	S_y = 30.0 ksi	260	190	125	95	73	52	. . .	44	36	28.5	24.5	. . .	19.5	15	13	11.5	9.5	9.0
I-9.3	S_y = 45.0 ksi	260	190	125	95	73	52	46	39	24.5	15.5	12	. . .	9.6	7.7	6.7	6.0	5.2	5.0
I-9.4	MNS ≤2.7 S_m [Note (5)]	1150	760	450	320	225	143	. . .	100	71	45	34	. . .	27	22	19	17	15	13.5
I-9.4	MNS = 3 S_m [Note (5)]	1150	760	450	300	205	122	. . .	81	55	33	22.5	. . .	15	10.5	8.4	7.1	6	5.3

NOTES:
(1) All notes on the referenced figures apply to these data.
(2) Interpolation between tabular values is permissible based upon data representation by straight lines on a log-log plot. Accordingly, for $S_i > S > S_j$

$$\frac{N}{N_i} = \left(\frac{N_j}{N_i}\right)^{[\log(S_i/S)]/\log(S_i/S_j)}$$

where S, S_i, and S_j are values of S_a; N, N_i, and N_j are corresponding numbers of cycles from design fatigue data.
Example: From the data given in the Table above, use the interpolation formula above to find the number of cycles N for S_a = 53.5 ksi when UTS ≤ 80 ksi in Fig. I-9.1:

$$\frac{N}{2000} = \left(\frac{5000}{2000}\right)^{\log(64/53.5)/\log(64/48)}$$

$$N = 3540 \text{ cycles}$$

(3) The number of cycles indicated shall be read as follows: IEJ = I × 10^J, e.g., 5E2 = 5 × 10^2 or 500.
(4) These data points are included to provide accurate representation of curves at branches or cusps.
(5) MNS is the Maximum Nominal Stress.

Figure 2.1-1 – ASME Code, Section III, Figure I-9.4

2.2 Weights and Centers of Gravity

The maximum total weight of the RH-TRU 72-B package, including a maximum payload of 8,000 pounds, is 45,000 pounds. The package is nearly symmetrical and, therefore, the center of gravity (CG) is very near the geometric center of the package. Though no significant deviation from this assumption is anticipated when the package is in service, a worst-case CG offset of 6.46 inches from the geometric center of the package is calculated in Section 2.5.2.1, *Center-Pivot and Tie-down Trunnion Loads*. This small offset is derived from a highly conservative assumption that payload is comprised of a 44.2-inch long, 26.5 inch diameter solid metal slug, weighing 6,900 pounds and located at the extreme end of the payload cavity. Using this assumption, the mass moment of inertia of the packaging can be recalculated. From Table 2.2-1, the mass moment of inertia of the package, less the payload canister, is 278,601 – 26,691 = 251,910 lb-in-s^2. (Figure 2.2-1 provides the component-numbering schematic for components identified in Table 2.2-1).

The mass moment of inertia of the assumed offset payload slug, I_m, can be calculated as:

$$I_m = \frac{m}{48}\left(3d^2 + 4l^2\right) = 3{,}691\ \text{lb-in-s}^2$$

where the mass of the payload, m = 6,900/386.4 = 17.857 lb-s^2/in, the diameter, d = 26.50 inches, and the length, l = 44.2 inches.

As calculated in Section 2.5.2.1, *Center-Pivot and Tie-down Trunnion Loads*, the distance of the offset payload CG from the package geometric center is approximately 26½ inches. The mass moment of inertia for the package with the extreme offset payload is thus 251,910 + 3,691 + [(26.5)^2 × 17.857] = 268,141 lb-in-s^2. This represents a difference of only [(278,601 – 268,141)/278,601] × 100 = 4% from the nominal value calculated in Table 2.2-1. Such a small difference in inertial characteristics will have a negligible effect on the dynamic response of the package to oblique impacts.

As a bounding case for side impacts, a worst-case assumption for payload distribution is made in Paragraph (3) of Section 2.6.7.3, *Flat Side Drop*, for normal conditions of transport (NCT) and Paragraph (3) of Section 2.7.1.3, *Flat Side Drop*, for hypothetical accident conditions (HAC). This assumption conservatively assumes the entire payload weight is lumped at one end of the inner vessel (IV). The analysis results are discussed in Appendix 2.10.1.5, *Containment Assembly Analysis for Side Drops*. Loading of the analysis model was accomplished by imposing the maximum linear acceleration derived from the impact analysis for a symmetrically loaded package.

Table 2.2-1 – RH-TRU 72-B Package Component Weights, Centers of Gravity, and Mass Moments of Inertia

Component	Approximate Weight (lb)	Distance to Center of Gravity① (in)	Approximate Mass Moment of Inertia② (lb-in-s^2)
1.0 Bottom Impact Limiter	2,547	-1.05	40,224
2.0 Outer Cask (OC)	27,883	71.11	145,287
2.1 Bottom Base Plate	1,967	2.57	24,773
2.2 Lead Shielding	10,739	67.07	38,592
2.3 Inner Shell	3,688	65.63	13,435
2.4 Outer Shell	6,587	65.43	25,147
2.5 Upper Forging	2,000	133.60	20,462
2.6 Lid	1,667	138.93	19,544
2.7 Trunnions	624	72.94	783
2.8 Thermal Shield/Wire	611	65.57	2,551
3.0 Inner Vessel (IV)	4,023	92.19	28,744
3.1 Bottom End Plate	354	5.77	4,149
3.2 Shell	1,216	63.38	3,907
3.3 Upper Forging	604	126.74	5,328
3.4 Lid	1,382	132.93	13,566
3.5 Spacers	467	67.50	1,794
4.0 Payload Canister	8,000	67.00	26,691
5.0 Upper Impact Limiter	2,547	142.80	37,655
TOTAL	**45,000**	**72.24**	**278,601**

Notes:

① The reference datum is the base of the outer cask (OC)

② The transverse-axis mass moment of inertia is about the transverse neutral axis of the package.

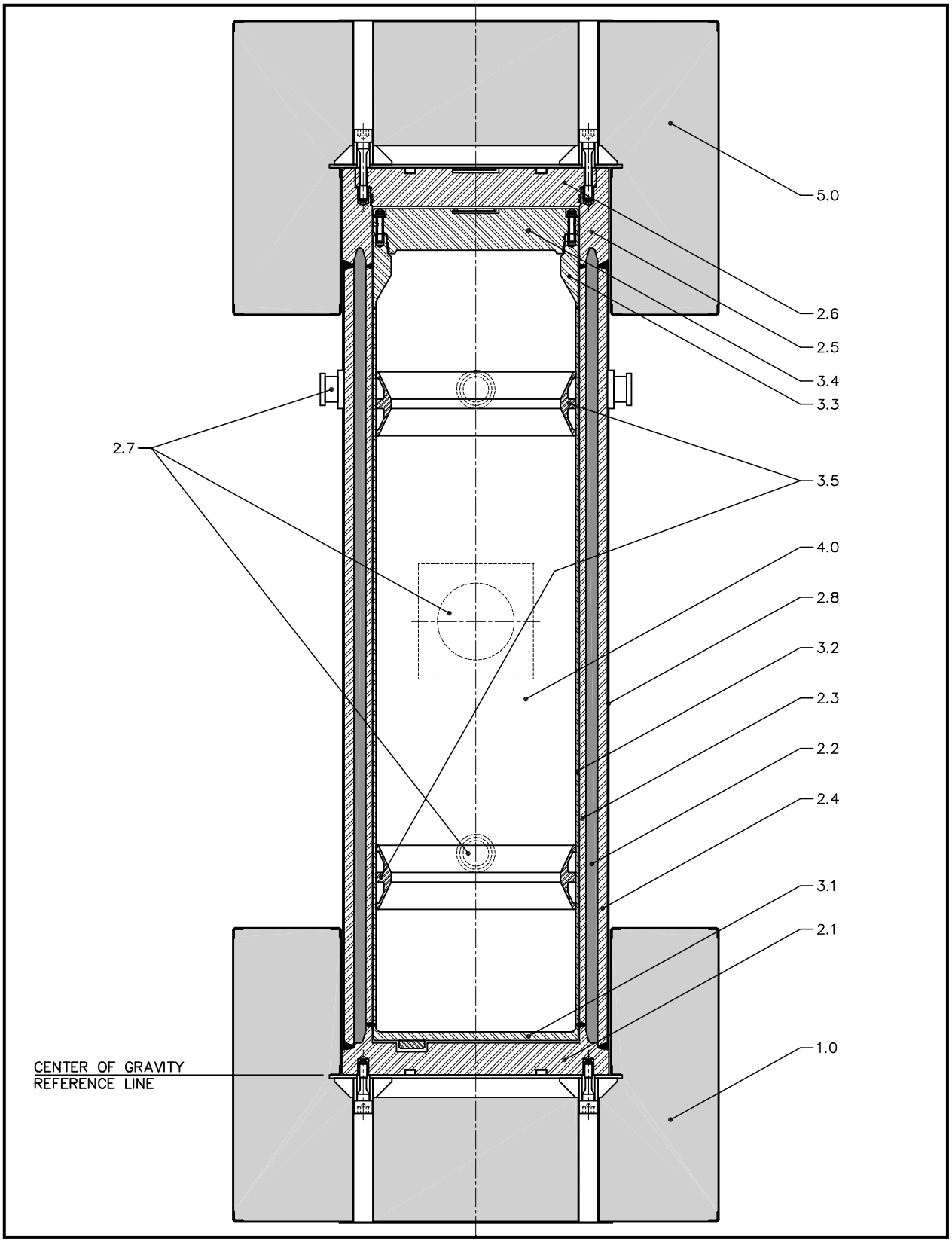

Figure 2.2-1 – RH-TRU 72-B Package Component Weight Breakdown

This page intentionally left blank.

2.3 Mechanical Properties of Materials

The RH-TRU 72-B package is fabricated primarily from Type 304, austenitic stainless steel, structural polyurethane foam, high strength alloy steel bolts, and lead. Appendix 1.3.1, *Packaging General Arrangement Drawings*, defines the specific material used for each item of the RH-TRU 72-B package. Table 2.3-1 presents material properties for the Type 304 stainless steel, the ASTM A320 fasteners, and ASTM A516 carbon steel, and Table 2.3-2 presents material properties for the lead used in the RH-TRU 72-B package. Material properties are linearly interpolated between or, if necessary, linearly extrapolated beyond the temperature values shown. For instance, when temperatures outside the tabulated ranges are of interest (e.g., low temperature properties to -40 ºF), the data are extrapolated. When a particular analysis requires data extrapolation, it is addressed within the applicable section of the SAR.

The stress-strain curve for Type 304 stainless steel at 212 ºF is presented as Figure 2.3-1. This is the same curve employed in the T-3[1] and 125-B[2] SARs. It is further noted that this curve is reasonably consistent with the ASME Code[3] minimum material property data. The ASME Code specifies a modulus of elasticity of $27.53(10)^6$ at 212 ºF versus the $27.7(10)^6$ psi value shown in Figure 2.3-1. In addition, the yield stress at 0.2% offset strain in Figure 2.3-1 (setting $0.002 = a[\sigma - \sigma_p]^b$) is found to be 25,000 psi, as compared with the ASME Code specified 24,700 psi minimum yield stress. Therefore, it is concluded that the Figure 2.3-1 stress-strain curve corresponds very closely to ASME minimum material property data and is justified for use herein.

The applicable stress-strain curves (at room temperature (approximately 70 – 75 ºF), at -20 ºF, and at 140 ºF) for polyurethane foam with density of about 11½ lb/ft^3 used in the RH-TRU 72-B package impact limiters are presented as Figure 2.3-2 and tabulated in Table 2.3-3. Extensive testing of numerous foam samples at various densities (including densities of approximately 11½ lb/ft^3) resulted in the nominal (room temperature) curve shown in Figure 2.3-2.

A ±10% bound on the nominal room temperature curves indicates the acceptance criteria (per Section 8.1.4.1, *Polyurethane Foam*) associated with the foam actually installed within the impact limiters. To be acceptable, when averaged for all pours into a given limiter, parallel- and perpendicular-to-rise stress-strain curves taken at room temperature (70 – 75 ºF) for a production unit impact limiter must fall within ±10% of the corresponding nominal room temperature curves. Stress-strain curves for individual pours must fall within ±15% of nominal. Also shown in Figure 2.3-2 are curves corresponding to foam at -20 ºF and at 140 ºF. The -20 ºF (minimum foam temperature) curve is an upper-bound curve and corresponds to -20 ºF nominal foam, increased by 10%. The 140 ºF (maximum foam temperature) curve is a lower-bound curve and corresponds to 140 ºF nominal foam decreased by 10%. Drop analyses herein typically consider the -20 ºF and the 140 ºF foam curves in order to bound, respectively, package acceleration (*g*) loads and impact-limiter deformations.

---

[1] U.S. Department of Energy, *Safety Analysis Report for the T-3 Spent Fuel Shipping Package*, NRC Certificate of Compliance No. 71-9132, U.S. Department of Energy, Washington, D.C.

[2] U.S. Department of Energy, *Safety Analysis Report for the NuPac 125-B Fuel Shipping Package*, NRC Certificate of Compliance No. 71-9200 U.S. Department of Energy, Washington, D.C.

[3] American Society of Mechanical Engineers (ASME) Boiler and Pressure Vessel Code, Section III, *Rules for Construction of Nuclear Power Plant Components*, Division 1, Subsection NB and Appendices, 1986 Edition.

Appendix 2.10.7, *Static and Dynamic Testing*, presents the results from static crush and dynamic, 30-foot free drop testing of prototypic half-scale impact limiters. As discussed in Appendix 2.10.7, *Static and Dynamic Testing*, when properly correlated with the observed test results, analytic evaluation techniques (described and implemented in Appendix 2.10.2, *Drop Analysis Codes Description*, and Appendix 2.10.3, *Drop Impact Evaluation Results*, respectively) are shown to accurately predict impact limiter behavior.

To adequately address fabrication stresses due to lead shrinkage on the inner shell of the outer cask (OC), stress-strain and creep data are required for lead. The lead used in the package is per Federal Specification QQ-L-171e, or per ASTM B29-79 (for copper-bearing material). The composition of the lead is primarily lead (99.9% minimum) and copper (0.04 to 0.08%). Stress-strain and creep data are therefore extracted from WADC Technical Report 57-695[4] for a copperized lead with a composition of 99.94% lead and 0.0577% copper. Stress-strain curves and creep data from the reference are presented in Figure 2.3-3 through Figure 2.3-8.

ASTM A276 and ASTM A269 stainless steels are used for various portions of the impact limiters. These materials are not ASME Code materials, but are acceptable for use as these components are non-structural in nature. Other materials used in the package that are non-structural in nature are the butyl rubber used for the O-ring seals and the 300-series stainless steel used for the thermal shield wire wrap. Some additional minor non-structural items for the impact limiters are manufactured from plastic, stainless steel, or an alloy steel.

The optional thread inserts used for the inner vessel (IV) and OC lid closure bolts are manufactured from ASTM A434 steel, which is not an ASME code material. However, the room temperature tensile strength of the inserts is rated at a minimum value of 140,000 psi. The inserts have been used in high-temperature aerospace applications with very little weakening at temperatures up to 500 ºF. The inserts will be certified to meet material strength requirements equivalent to the minimum properties of the base material before being installed in the RH-TRU 72-B package.

[4] Thomas Tietz, *Determination of the Mechanical Properties of a High Purity Lead and a 0.058% Copper-Lead Alloy*, WADC Technical Report 57-695, ASTIA Document No. 151165, Stanford Research Institute, April 1958.

Table 2.3-1 – Mechanical Properties of Steel Used in the RH-TRU 72-B Package

Material Specification	Type or Grade	T (ºF)	Strength (ksi) Yield① S_y	Ultimate② S_u	Allowable③ S_m	Elastic Modulus④ (10^6 psi)	Coefficient of Thermal Expansion⑤ (10^{-6} in/in/ºF)
ASTM A240	304	70	—	—	—	28.3	8.46
ASTM A276		100	30.0	75.0	20.0	—	8.55
		200	25.0	71.0	20.0	27.6	8.79
		300	22.5	66.0	20.0	27.0	9.00
		400	20.7	64.4	18.7	26.5	9.19
		500	19.4	63.5	17.5	25.8	9.37
		600	18.2	63.5	16.4	25.3	9.53
		700	17.7	63.5	16.0	24.8	9.69
ASTM A240	304L	70	—	—	—	28.3	8.46
ASTM A276		100	25.0	70.0	16.7	—	8.55
		200	21.3	66.2	16.7	27.6	8.79
		300	19.1	60.9	16.7	27.0	9.00
		400	17.5	58.5	15.8	26.5	9.19
		500	16.3	57.8	14.8	25.8	9.37
		600	15.5	57.0	14.0	25.3	9.53
		700	14.9	56.2	13.5	24.8	9.69
ASTM A182	F304	70	—	—	—	28.3	8.46
ASME SA182		100	30.0	70.0	20.0	—	8.55
(forgings)		200	25.0	66.2	20.0	27.6	8.79
		300	22.5	61.5	20.0	27.0	9.00
		400	20.7	60.0	18.7	26.5	9.19
		500	19.4	59.3	17.5	25.8	9.37
ASTM A320	L43	70	—	—	—	27.8	6.20
(fasteners)		100	105.0	125.0	35.0	—	6.27
		200	99.0	—	33.0	27.1	6.54
		300	95.7	—	31.9	26.7	6.78
		400	91.8	—	30.6	26.1	6.98
		500	88.5	—	29.5	25.7	7.16
ASTM A516	55	70	—	—	—	29.5	5.42
		100	30.0	55.0	18.3	—	5.53
		200	27.3	55.0	18.3	28.8	5.89
		300	26.6	55.0	17.7	28.3	6.26
		400	25.7	55.0	17.2	27.7	6.61
		500	24.5	55.0	16.2	27.3	6.91

Notes:

① ASME Code[3], Table I-2.1, Table I-2.2, Table I-13.3.

② ASME Code[3], Table I-1.3, Table I-3.1, Table I-3.2.

③ ASME Code[3], Table I-1.1, Table I-1.2, Table I-1.3.

④ ASME Code[3], Table I-6.0.

⑤ ASME Code[3], Table I-5.0; mean from 70 ºF.

⑥ Steel density is 0.283 lb/in^3, and Poisson's ratio is 0.3.

Table 2.3-2 – Mechanical Properties of Lead Used in the RH-TRU 72-B Package

Material Specification	Type or Grade	T (ºF)	Strength (psi)					Elastic Modulus④ (10^6 psi)	Coefficient of Thermal Expansion⑤ (10^{-6} in/in/ºF)
			Proportional① S_p		Yield② S_y		Ultimate③ S_u		
			Tens	Comp	Tens	Comp	Tens		
QQ-L-171e	A or C	-99	—	—	—	—	—	2.50	15.28
ASTM B29-79		70	—	—	—	—	—	2.34	16.07
(copper bearing)		100	276	215	584	490	1,570	2.30	16.21
		175	293	107	509	428	1,162	2.20	16.58
		250	277	107	498	391	844	2.09	16.95
		325	189	93	311	320	642	1.96	17.54
		440	—	—	—	—	—	1.74	18.50
		620	—	—	—	—	—	1.36	20.39

Notes:

① WADC Technical Report 57-695[4], Page 21, 26.

② WADC Technical Report 57-695[4], Page 21, 26.

③ WADC Technical Report 57-695[4], Page 14.

④ NUREG/CR-0481[5], Page 66.

⑤ NUREG/CR-0481[5], Page 56; mean from 70 ºF.

⑥ Lead density is 0.41 lb/in^3, Poisson's ratio is 0.45, and the melting point is 620 ºF.

Table 2.3-3 – Crush Stress vs. Strain for 11½ lb/ft³ Nominal Density Polyurethane Foam

Strain	Parallel-to-Rise (psi)			Perpendicular-to-Rise (psi)		
	Upper Bound, Cold (-20 ºF)	Nominal, Room Temp (75 ºF)	Lower Bound, Hot (140 ºF)	Upper Bound, Cold (-20 ºF)	Nominal, Room Temp (75 ºF)	Lower Bound, Hot (140 ºF)
0%	0	0	0	0	0	0
5%	574	372	282	499	324	245
10%	579	376	285	536	348	264
20%	581	377	286	559	363	275
30%	622	404	306	599	389	294
40%	692	449	340	672	436	331
50%	835	543	411	823	534	405
60%	1,163	755	572	1,170	760	575
65%	1,485	964	731	1,529	993	752
70%	2,051	1,332	1,009	2,146	1,394	1,056
75%	3,083	2,002	1,516	3,200	2,078	1,574
80%	5,511	3,578	2,711	5,527	3,589	2,719

[5] H. J. Rack, and G. A. Knorovsky, *An Assessment of Stress-Strain Data Suitable for Finite Element Elastic-Plastic Analysis of Shipping Containers*, NUREG/CR-0481, SAND77-1872, Sandia National Laboratories, Albuquerque, New Mexico, September 1978.

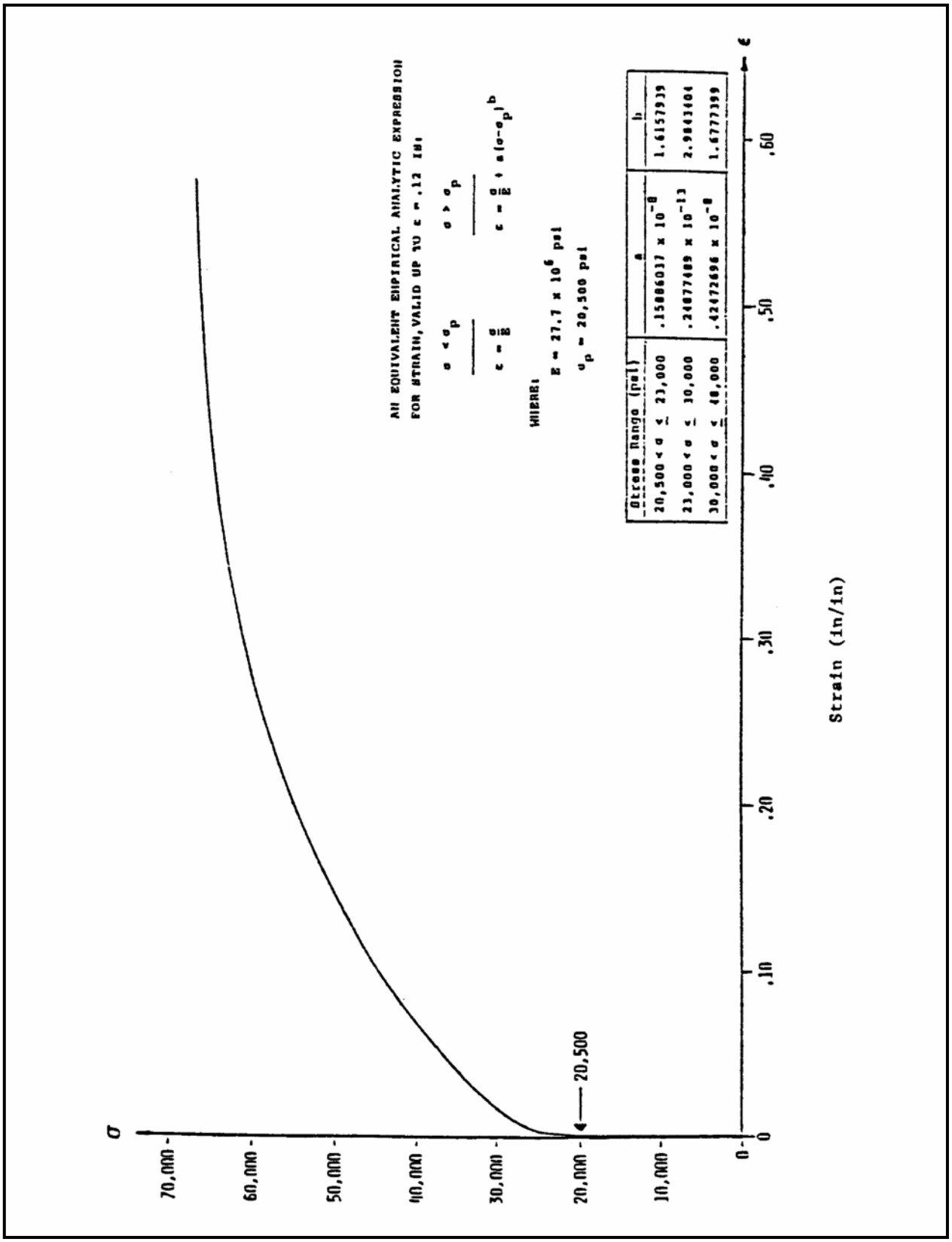

Figure 2.3-1 – True Stress/Strain for Type 304 Stainless at 212 ºF

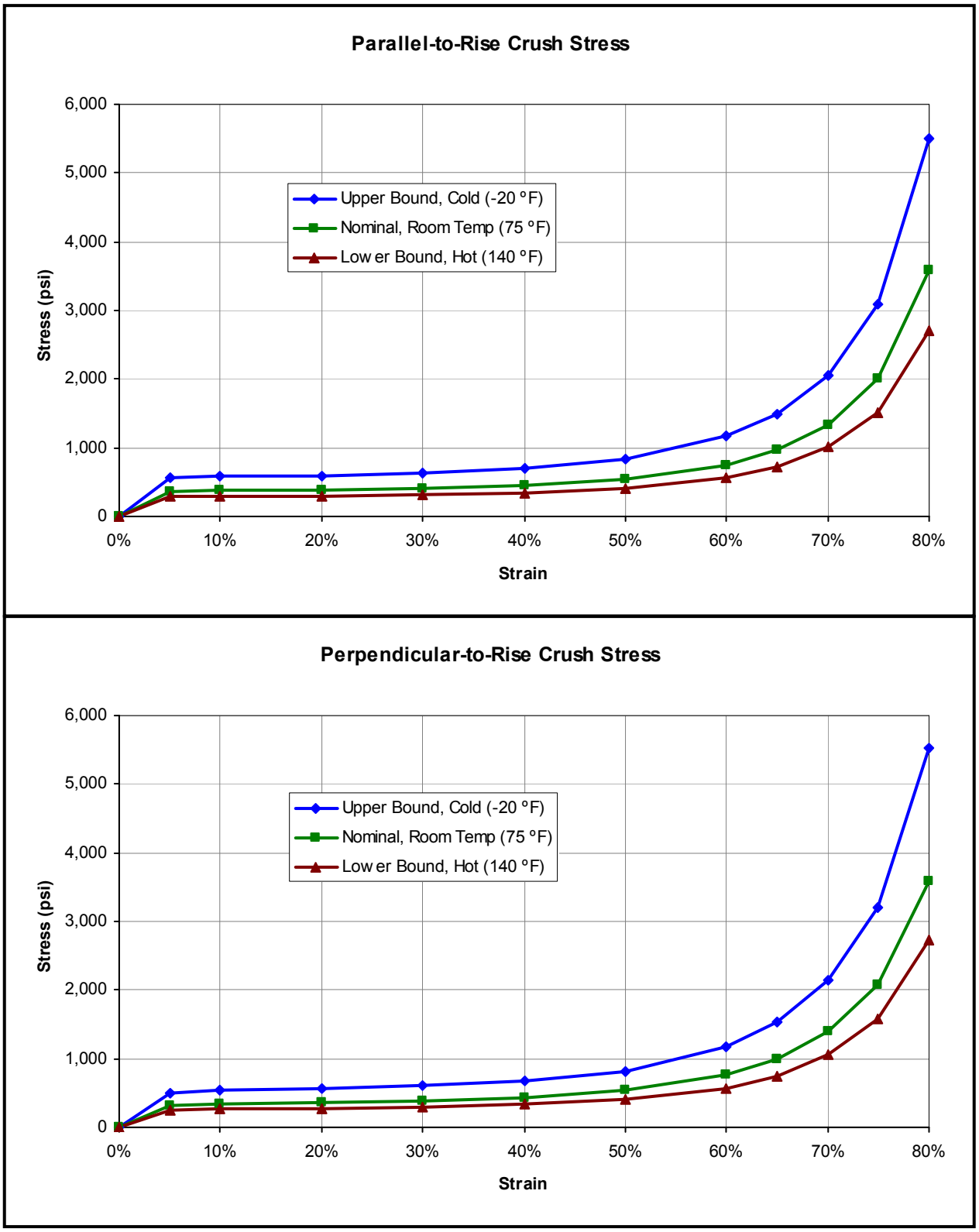

Figure 2.3-2 – Crush Stress vs. Strain for 11½ lb/ft³ Nominal Density Polyurethane Foam

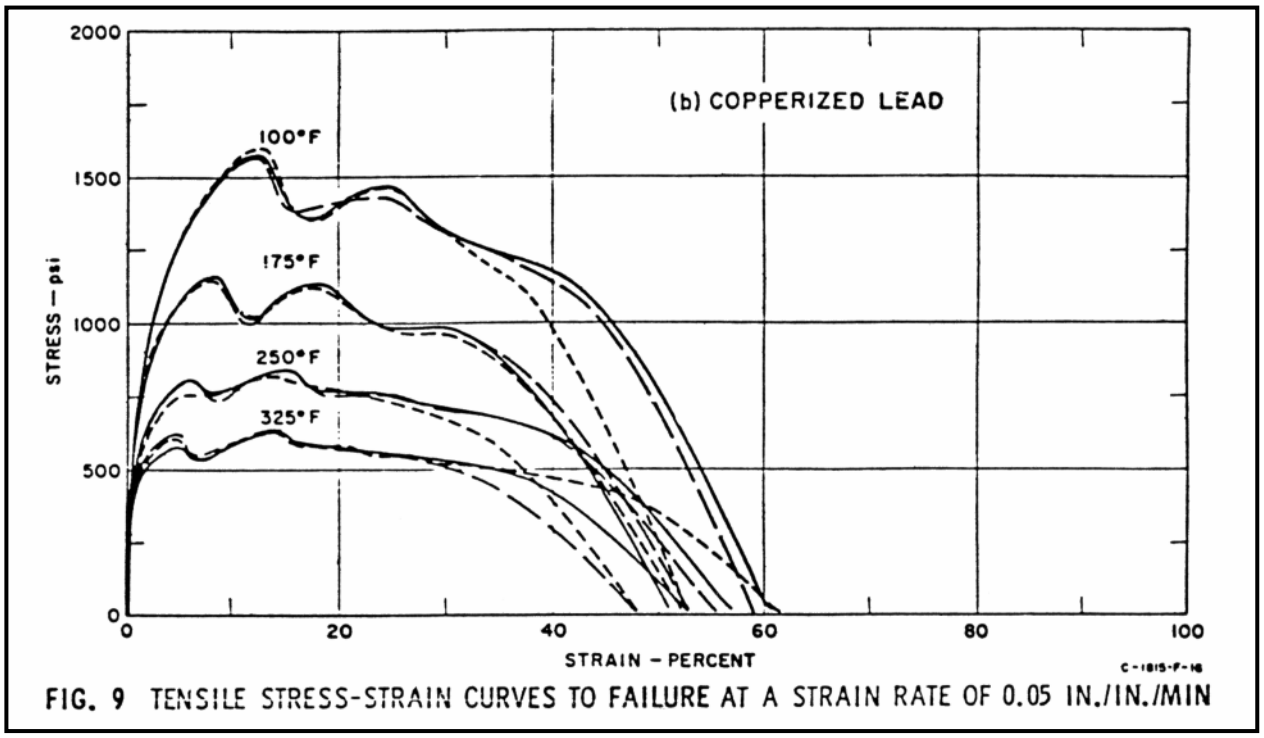

Figure 2.3-3 – Tensile Curves at a Strain Rate of 0.05 in/in/min

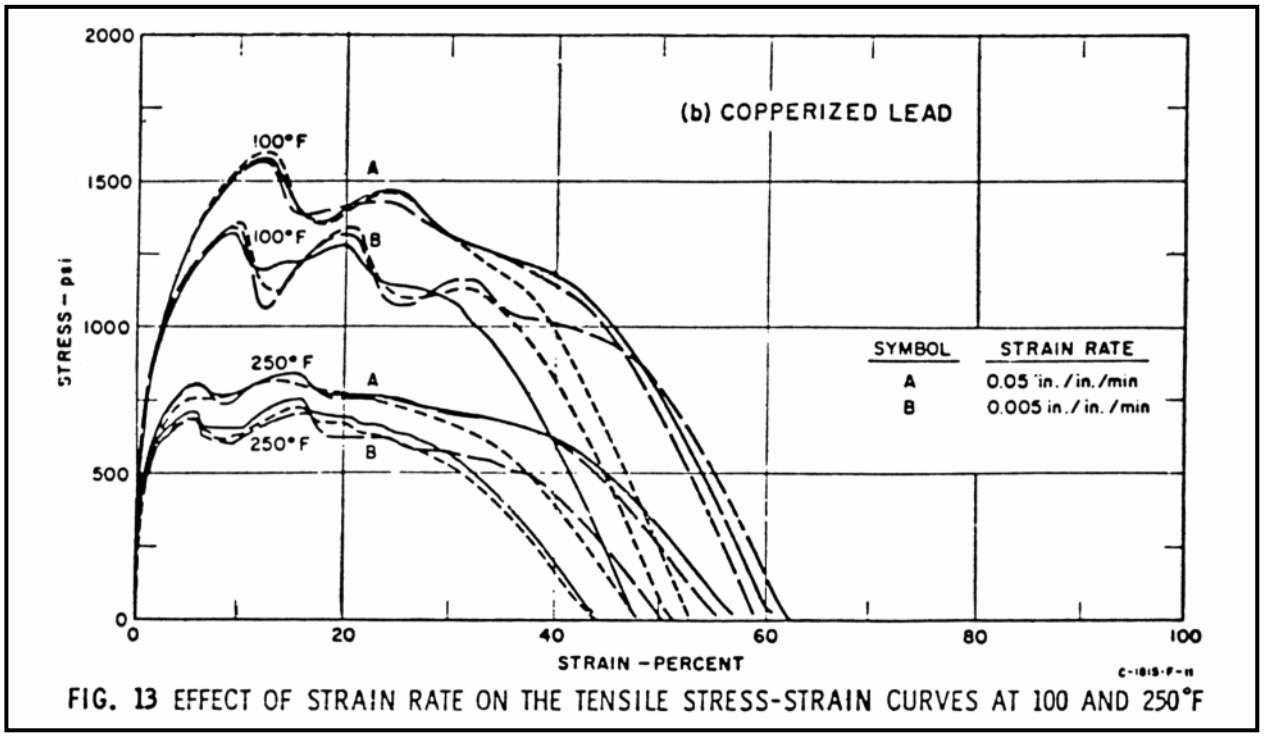

Figure 2.3-4 – Strain Rate Effects on Tensile Curves at 100 ºF and 250 ºF

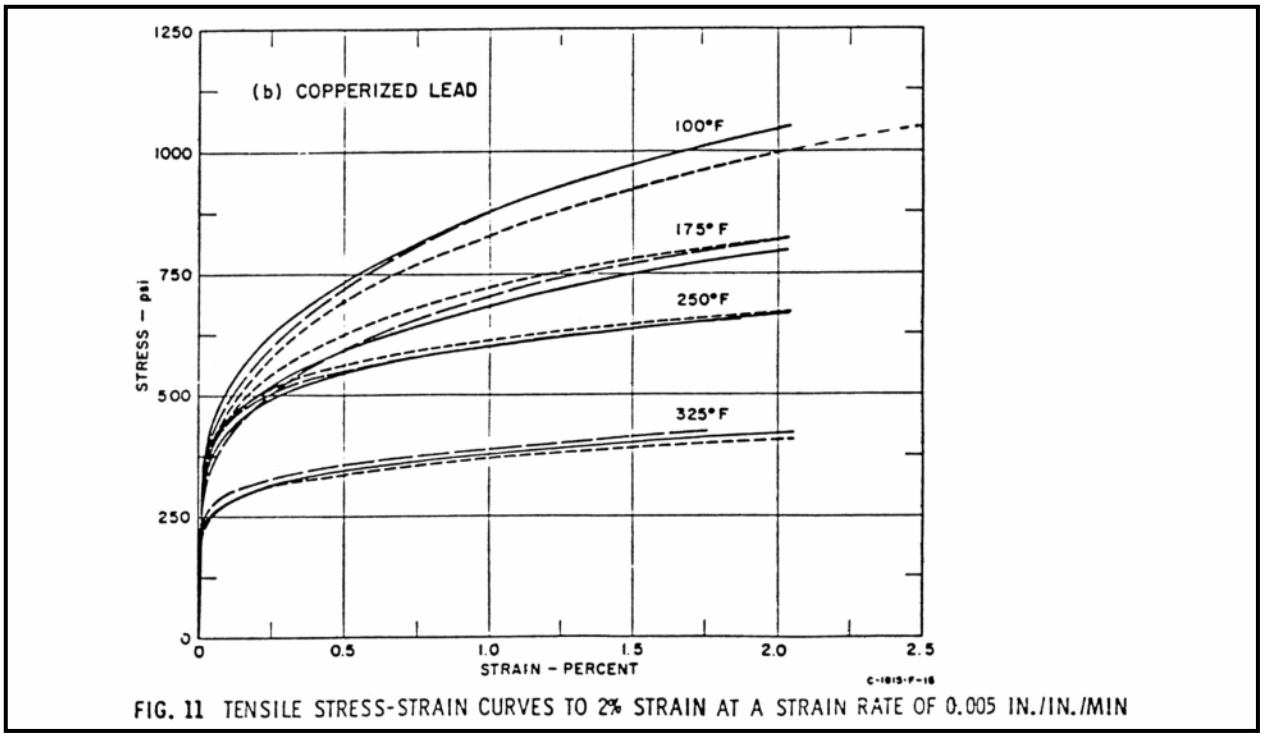

FIG. 11 TENSILE STRESS-STRAIN CURVES TO 2% STRAIN AT A STRAIN RATE OF 0.005 IN./IN./MIN

Figure 2.3-5 – Tensile Curves at a Strain Rate of 0.005 in/in/min

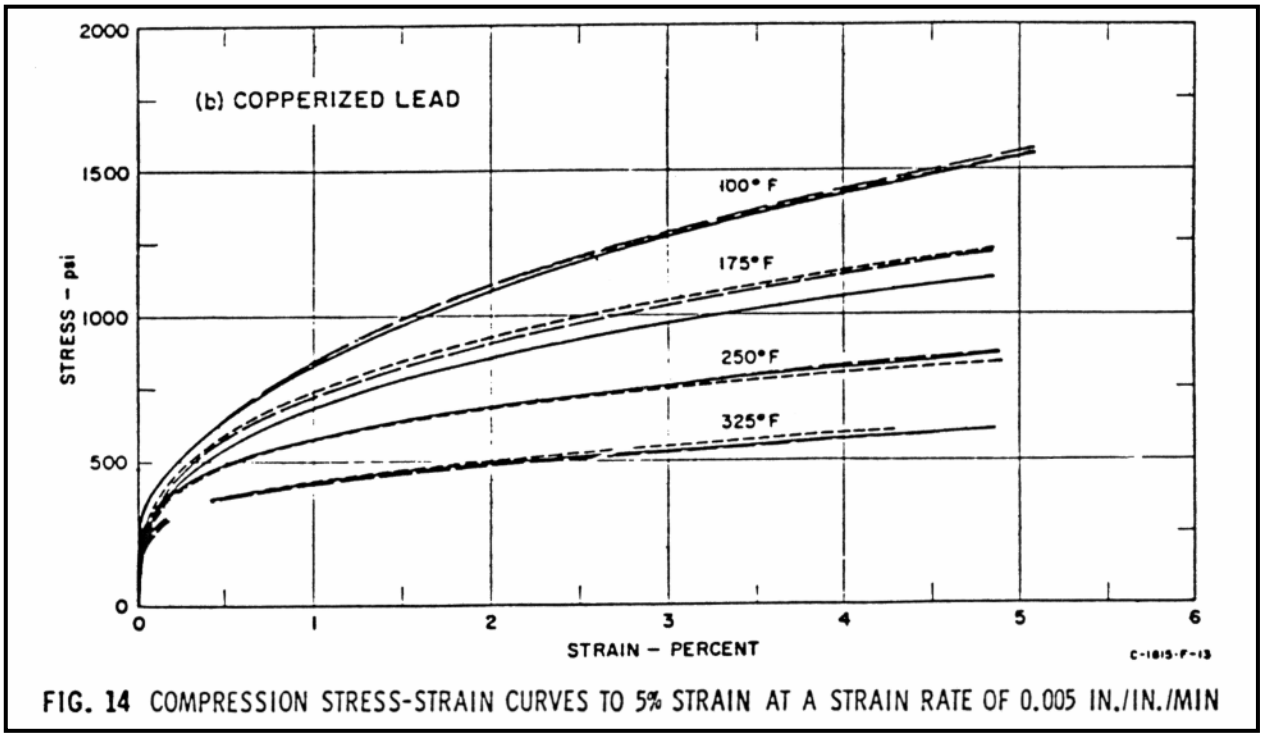

FIG. 14 COMPRESSION STRESS-STRAIN CURVES TO 5% STRAIN AT A STRAIN RATE OF 0.005 IN./IN./MIN

Figure 2.3-6 – Compression Curves at a Strain Rate of 0.005 in/in/min

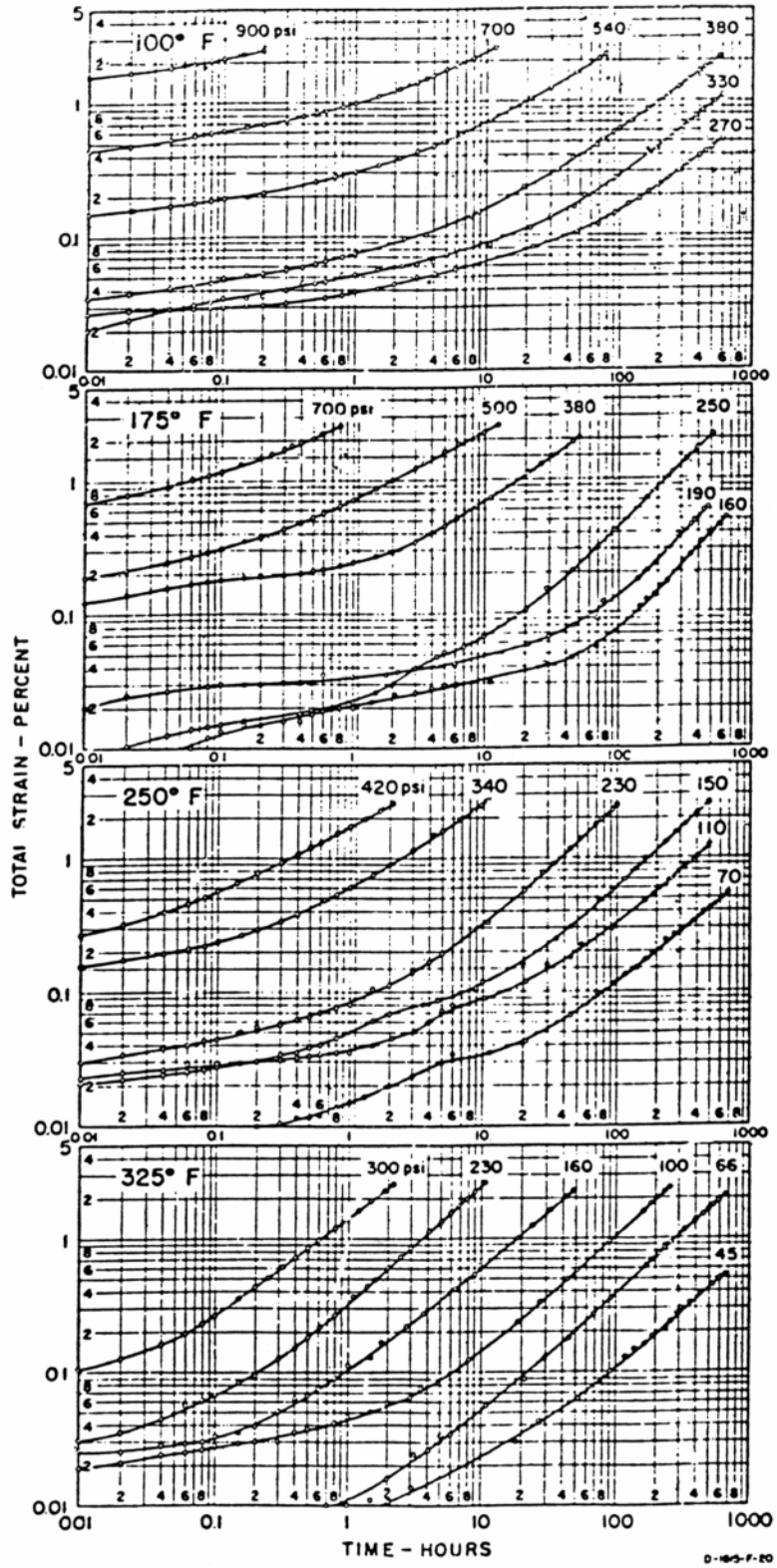

FIG. 20 TOTAL STRAIN VS CREEP TIME FOR COPPERIZED LEAD

Figure 2.3-7 – Total Strain vs. Creep Time

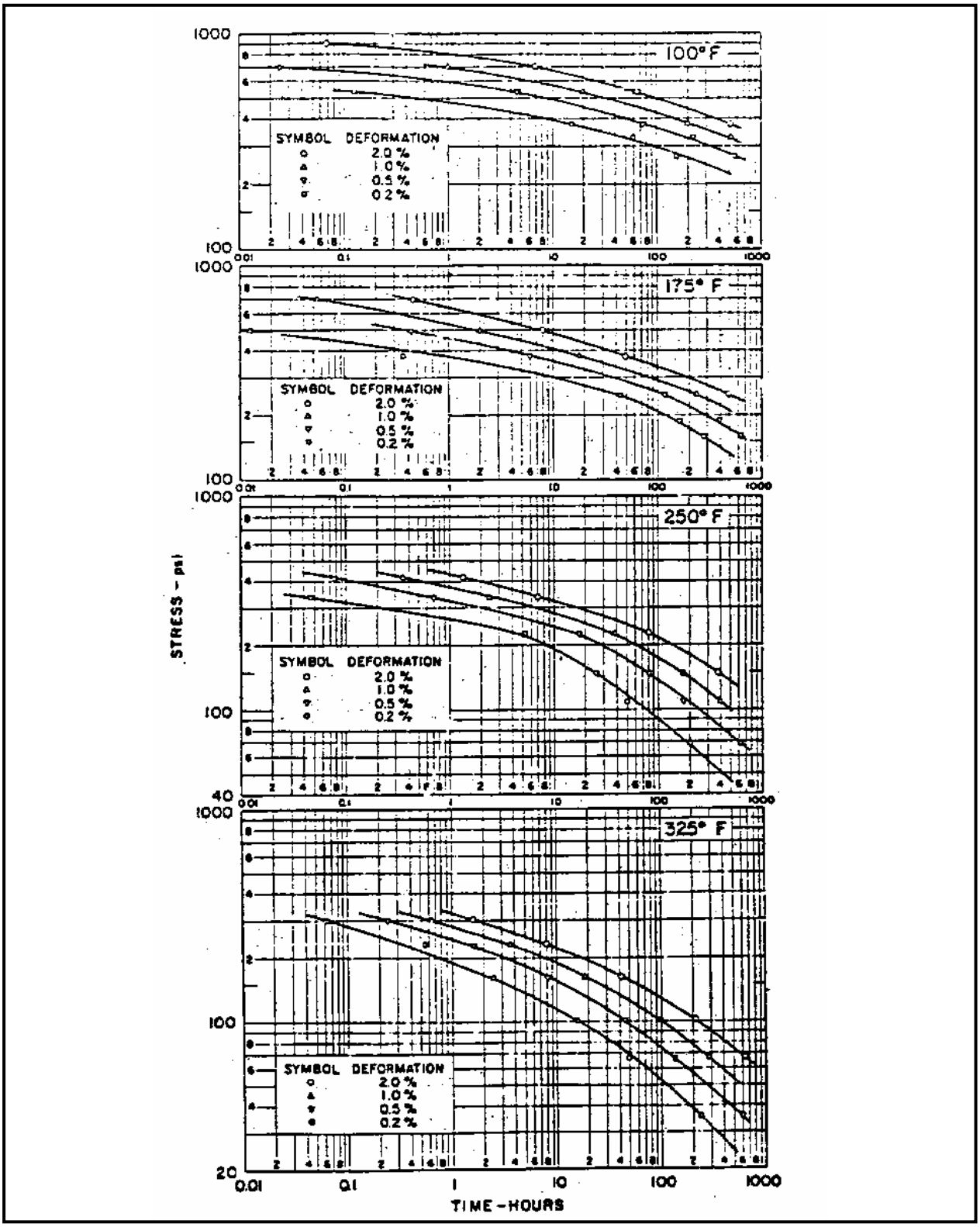

Figure 2.3-8 – Stress vs. Creep Time Curves

2.4 General Standards for All Packages

This section demonstrates that the general standards for all packages are met.

2.4.1 Minimum Package Size

The minimum transverse dimension of the package (not including the outer cask (OC) thermal shield and without the impact limiters) is 41⅛ inches, and the minimum longitudinal dimension is 141¾ inches.

2.4.2 Tamper Indicating Feature

A "lock-wire", or equivalent, is utilized between two tie points on the closure end of the package during a loaded shipment. Specifically, one tie point is affixed to the OC thermal shield, and one tie point is affixed to the closure end impact limiter. Failure of said device will indicate purposeful tampering in accordance with 10 CFR §71.43(b)[1].

2.4.3 Positive Closure

Inadvertent opening of the package closures cannot occur for the RH-TRU 72-B package. Following installation of the package payload, the inner vessel (IV) lid is secured via eight (8), 7/8-9UNC bolts. The OC closure lid is then secured via eighteen (18), 1¼-7UNC bolts, thus eliminating access to the IV closure. The closure-end impact limiter is attached using six (6), 1¼-7UNC bolts. When installed, the impact limiter eliminates access to the OC closure. With this double containment closure and the presence of the impact limiter, inadvertent opening of the package cannot occur.

2.4.4 Chemical and Galvanic Reactions

The materials from which this package is fabricated (i.e., stainless steel, carbon steel, lead, and polyurethane foam) will not cause significant chemical, galvanic, or other reactions in air or water environments. These materials have been previously used in radioactive material (RAM) packages for transport of similar chemical material without incident. This RAM packaging history, combined with successful use of these materials in similar industrial environments, ensures that the integrity of the package will not be compromised by any chemical, galvanic or other reactions. The materials of construction and the payload are evaluated below for potential reactions.

2.4.4.1 RH-TRU 72-B Package Materials of Construction

The RH-TRU 72-B package is primarily constructed of Type 304 stainless steel. This material is highly corrosion-resistant to most environments. The actual metallic structure of the RH-TRU 72-B package is composed entirely of this and appropriate weld material. The weld material and

[1] Title 10, Code of Federal Regulations, Part 71 (10 CFR 71), *Packaging and Transportation of Radioactive Material*, Final Rule, 01-26-04.

processes have been selected in accordance with the ASME Boiler and Pressure Vessel Code[2] to provide as good or better material properties than the base material, including corrosion resistance. Both the base and weld materials are 300-series stainless steel, which is highly resistant to corrosion. These materials also have approximately the same electrochemical potential, minimizing any galvanic corrosion that could occur.

The polyurethane foam used in the impact limiter of the RH-TRU 72-B package is the same as that which has been successfully used in a number of transportation packages, such as the NuPac 125-B (Docket 71-9200), the CNSI 1-13C II (Docket 71-9152), the NuPac 10-142 (Docket 71-9208), and the NuPac PAS-1 (Docket 71-9184). All of these packages have had a long and successful record of performance demonstrating that the foam does not impose any adverse conditions on the packaging. The polyurethane foam in the impact limiters is a closed-cell foam that is very low in free halogens. The foam material is sealed inside a dry cavity in each impact limiter, to prevent exposure to the elements. Even if moisture were available, for leaching trace chlorides from the foam, very little chloride would be available, since the material is a closed-cell foam and water does not penetrate the material to allow significant leaching.

The butyl rubber and other elastomers used in the O-ring seals contain no corrosives that would adversely affect the packaging. These materials are organic in nature and non-corrosive to the stainless steel body of the RH-TRU 72-B package.

2.4.4.2 RH-TRU 72-B Package Materials of Construction and Payload Compatibility

The materials of construction of the RH-TRU 72-B package have been evaluated for compatibility with the authorized contents as described in the *Remote-Handled Transuranic Waste Authorized Methods for Payload Control* (RH-TRAMPAC)[3].

Corrosive materials are prohibited from the payloads. All payloads are contained in the payload canister. Typically, the payload may be further confined within drums and liners. This configuration ensures that the chemistry of the payloads has very little interaction with the IV. However, the evaluation of compatibility is based on complete interaction of payload materials with the packaging.

Since corrosives are prohibited from the payload, the only potential material that could be, in theory, of concern for the IV is the release of free chlorides. Gaseous free chlorides could potentially be available only from the radiolysis of polyvinyl chloride and/or halogenated organic compounds within the payload. In both cases, the total quantity of gaseous free chlorides that would be available for diffusion into the IV is very small. The distribution of volatile organic compounds is discussed in Appendix 4.4 of the *RH-TRU Payload Appendices*[4]. The source term for gaseous-free chlorides in the payload and the potential for stress corrosion cracking are discussed in Appendix 4.2 of the *RH-TRU Payload Appendices*.

---

[2] American Society of Mechanical Engineers (ASME) Boiler and Pressure Vessel Code, Section III, *Rules for Construction of Nuclear Power Plant Components*, Division 1, Subsection NB and Appendices, 1986 Edition.

[3] U.S. Department of Energy (DOE), *Remote-Handled Transuranic Waste Authorized Methods for Payload Control* (RH-TRAMPAC), U.S. Department of Energy, Carlsbad Field Office, Carlsbad, New Mexico.

[4] U.S. Department of Energy (DOE), *RH-TRU Payload Appendices*, U.S. Department of Energy, Carlsbad Field Office, Carlsbad, New Mexico.

Any small quantities of free-gaseous chlorides that could potentially be generated in the waste would be retarded from diffusing out of a payload container due to the high solubility in absorbed water and/or moisture. The potential for free-gaseous chloride generation and interactions within payload containers is discussed in detail in Appendix 4.2 of the *RH-TRU Payload Appendices*[4].

2.4.4.3 Seal Material and Payload

The butyl rubber O-ring seal material was evaluated for chemical compatibility with identified payload chemicals by review of the published literature on the performance of the seal material in the presence of the chemical. This evaluation determined that only a few payload constituents were potentially incompatible with butyl rubber under expected operating conditions. Those chemicals determined to potentially pose a problem were a few volatile organic compounds (VOC's). Specifically, they were Freon-113, carbon tetrachloride, methylene chloride, and 1,1,1-trichloroethane. All of these compounds are highly-volatile and, in general, volatilize or permeate through the waste-confinement materials prior to the closure of payload containers. A discussion of the occurrence of VOCs in the waste and headspace (void volumes) of confinement layers is presented in Appendix 4.4 of the *RH-TRU Payload Appendices*[4]. Estimates of VOC concentrations in the IV headspace is also provided in Appendix 4.4 of the *RH-TRU Payload Appendices*.

The very small quantities of these compounds could have a small effect on the O-ring seal material. All of these compounds interact with butyl rubber by permeating and straining the polymer structure, causing the O-ring seal to swell. The O-ring seal will not readily lose its shape due to the crosslinking that occurs during manufacturing. Butyl rubber is a co-polymer of polyisobutylene with a small amount of polyisoprene. The polyisoprene allows cross-linking of the polymer chains that make up the O-ring seal material. This cross-linking limits the amount of swelling that can occur, as does the amount of compression the material experiences. If a sufficient quantity of solvent is present, the O-ring seal material can swell to the point where some softening of the material occurs, reducing its sealing force. This reduction of sealing force is offset by the osmotic pressure generated by the swelling. The force due to swelling may well be greater than the sealing force lost due to softening of the material.

The combined effect of the very small quantities of incompatible solvents found in the payload, combined with the mechanism of attack on the butyl, indicate that the payload will not significantly degrade the performance of the seals. Additionally, exposure to gamma radiation in the doses expected will not adversely effect the performance of the O-ring seals. IV O-ring seals will be inspected before each shipment to determine if damage is present. A more detailed discussion is provided in Appendix 4.4 of the *RH-TRU Payload Appendices*[4].

2.4.4.4 Chemical Compatibility Determination for RH-TRU Waste

The design of the RH-TRU 72-B package is for transport of waste that is limited to solid or solidified material. Corrosives, pressurized containers, explosives, radioactive and non-radioactive pyrophorics greater than 1%, and liquid volumes greater than 1% are prohibited. These restrictions ensure that the waste in the payload is in a non-reactive form for safe transport in the RH-TRU 72-B package.

In addition to the above restrictions, the chemical components in the payload are restricted to those that have been evaluated as described in the RH-TRAMPAC[3] and Appendix 4.1 of the *RH-TRU Payload Appendices*[4].

2.5 Lifting and Tie-down Standards for All Packages

This section addresses the lifting and tie-down design requirements. The RH-TRU 72-B package incorporates eight (8) trunnions for all package lifting and tie-down loads. The design criteria of ANSI N14.6[1] and 10 CFR §71.45[2] are used for the lifting and tie-down analyses. Lifting devices for the lids (non-structural member) are described in Section 1.2.2, *Operational Features*, and are identified in Appendix 1.3.1, *Packaging General Arrangement Drawings*.

Material properties are based on a temperature of 143 ºF for the outer cask (OC), and are summarized in Table 2.5-1 for ASTM A240 and ASTM A182, Type 304, stainless steels, based on non-containment allowable stresses from Table 2.1-2 in Section 2.1.2.1.2, *Non-Containment Structures*. The 143 ºF temperature is the maximum normal condition OC temperature (see Section 3.1, *Discussion*). The remaining material for the OC is ASTM A276, Type 304, stainless steel. This is not an ASME Code material, but it has a chemical composition and mechanical properties that are virtually identical to those of the ASTM A240 material. Therefore, the properties listed in Table 2.5-1 for ASTM A240 stainless steel are also valid for ASTM A276 stainless steel.

2.5.1 Lifting Devices

2.5.1.1 Lifting Trunnion Loads

The RH-TRU 72-B package has four trunnions provided for lifting which are located 90º apart on a cross-sectional plane near the lid-end of the package. Two trunnions are intended for primary use while two additional trunnions provide redundancy as desired for lifting and handling safety.

10 CFR §71.45[2] criteria are applicable to the lifting trunnions. These criteria require the device to lift three times the combined package weight while maintaining stresses less than yield.

The following analysis uses WRC Bulletin 107[3]. Loads are applied first in the longitudinal direction to simulate vertical lift, and then in the circumferential direction to represent horizontal lift. Figure 2.5-1 illustrates the load components on the lifting trunnion.

$$d_o = ½(1.5) + 1.03 + (0.75)(1.6) = 2.98 \text{ in}$$

Analyzing the two trunnions carrying the lifting load, the critical load for each trunnion is:

$$V_L = \frac{3(\text{Package Weight})}{2} = \frac{3(45{,}000)}{2} = 67{,}500 \text{ lb}$$

[1] ANSI N14.6-1993, *Special Lifting Devices for Shipping Containers Weighing 10,000 Pounds (4,500 Kg) or More,* American National Standards Institute, Inc. (ANSI).

[2] Title 10, Code of Federal Regulations, Part 71 (10 CFR 71), *Packaging and Transportation of Radioactive Material*, Final Rule, 01-26-04.

[3] K. R. Wickman, A. G. Hopper, and J. L. Mershon, *Local Stresses in Spherical and Cylindrical Shells Due to External Loadings*, Welding Research Council Bulletin 107, Welding Research Council, New York, June 1977.

The trunnion bending moment then becomes:

$$M_L = V_L d_o = (67{,}500)(2.98) = 201{,}150 \text{ in - lb}$$

The critical lifting load for the horizontally oriented package is determined by assuming that the package is lifted from the horizontal orientation at the tie-down trunnion location nearest the lid-end, and that the package rotates about the opposite tie-down trunnions (see Figure 2.5-2). The center of gravity of the package is assumed to be 8 inches from the center-pivot trunnion toward the lid-end (this offset distance of 8 inches is derived in Section 2.5.2.1, *Center-Pivot and Tie-down Trunnion Loads*).

Summing moments about the assumed pivot point results in the following:

$$(36.25 + 36.25)(2V_C) - (36.25 + 8.0)(135{,}000) = 0$$

Solving for V_C:

$$V_C = \frac{(44.25)(135{,}000)}{2(72.50)} = 41{,}200 \text{ lb}$$

Using the same moment arm for the tie-down trunnions as before:

$$M_C = V_C d_o = (41{,}200)(2.98) = 122{,}770 \text{ in - lb}$$

The above moment arm, d_o, assumes load V_C is applied at the most conservative location.

There are no torsional forces, M_T, or forces acting on the trunnions normal to the OC outer shell, P, during lifting. The OC outer shell is not considered a pressure boundary, so there is no internal pressure acting on the outer shell. Therefore, loads V_L and M_L are the only loads applied in the trunnion analysis.

2.5.1.2 OC Outer Shell Stresses

The analysis method used to determine these stresses is from WRC Bulletin 107[3]. Required parameters and input data used in the tie-down trunnion lifting stress analysis are presented in Table 2.5-2.

Analysis results are given in Table 2.5-3 (vertical lift) and Table 2.5-4 (horizontal lift). The maximum combined stress intensity (membrane plus bending) in the OC outer shell is 18,390 psi. The resulting margin of safety (MS) against the allowable yield strength, σ_y, is:

$$MS = \frac{\sigma_y}{S} - 1 = \frac{28{,}000}{18{,}390} - 1 = +0.52$$

The corresponding maximum membrane stress intensity is equal to twice the maximum shear stress, or 9,550 psi. For this case, the resulting margin of safety against the allowable yield strength, σ_y, is:

$$MS = \frac{\sigma_y}{S} - 1 = \frac{28{,}000}{9{,}550} - 1 = +1.93$$

2.5.1.3 Trunnion Stresses

Bearing stress in the trunnion is found by applying the lifting load, V, over the projected area (length = 1.6 inches) of the 4-inch diameter trunnion (see Figure 2.5-1):

$$S_b = \frac{V}{A_b} = \frac{67{,}500}{(4.0)(1.6)} = 10{,}547 \text{ psi}$$

The margin of safety for bearing is then:

$$MS = \frac{\sigma_y}{S_b} - 1 = \frac{28{,}000}{10{,}547} - 1 = +1.65$$

2.5.1.4 Lifting Trunnion Attachment Weld

The maximum lateral force acting on the trunnion base plate weld through the lifting trunnion is V = 67,500 pounds, as derived in Section 2.5.1.1, *Lifting Trunnion Loads*. To conservatively evaluate base plate weld requirements due to this force and due to the accompanying bending moment, an additional offset of the force from the weld due to the curvature of the OC outer shell will be accounted for as follows (see Figure 2.5-14 for a pictorial representation of θ and e):

$$\theta = \frac{6.0}{20.56} = 0.292 \text{ rad} = 16.7°$$

and

$$e = 20.56\left[1 - \cos\left(\frac{\theta}{2}\right)\right] = 0.22 \text{ in}$$

The total offset of load, V, is thus 0.22 + 2.23 = 2.45 inches. The bending moment acting on the weld is then M = (2.45)(V) = (2.45)(67,500) = 165,375 in-lb. To determine minimum weld throat size, relationships from *Design of Weldments*[4] may be employed in the following calculation to calculate the unit shear load, f_s, and unit bending load, f_b:

$$f_s = \frac{V}{L_w} = 3{,}581 \text{ lb/in}$$

and

$$f_b = \frac{M}{S_w} = 5{,}850 \text{ lb/in}$$

where the trunnion load, V = 67,500 pounds, the unit thickness weld length, $L_w = \pi D = \pi(6.0) =$ 18.85 in/in, the trunnion bending moment, M = 165,375 in-lb, and the unit thickness weld section modulus, $S_w = (\pi/4)D^2 = (\pi/4)(6.0)^2 = 28.27 \text{ in}^3/\text{in}$.

[4] Omer W. Blodgett, *Design of Welded Structures*, The James F. Lincoln Arc Welding Foundation, Cleveland, Ohio, June 1966.

The total unit weld load, f_{total}, is the vector sum of these two components:

$$f_{total} = \sqrt{f_s^2 + f_b^2} = \sqrt{(3{,}581)^2 + (5{,}850)^2} = 6{,}859 \text{ lb/in}$$

Using a shear stress allowable of $0.6S_y = 0.6(28{,}000) = 16{,}800$ psi, and assuming a bevel weld, the minimum acceptable weld size, w, is:

$$w = \frac{6{,}859}{16{,}800} = 0.408 \text{ in}$$

The attachment weld for the trunnion is a 5/8-inch bevel weld, resulting in a weld margin of safety of:

$$MS = \frac{0.625}{0.408} - 1 = +0.53$$

2.5.1.5 Excessive Lifting Trunnion Loads

To preclude damage to the package due to inadvertent overloading of the lifting trunnions, the trunnion weld should fail before the OC outer shell stress reaches ultimate strength. The specified allowable tensile stress for the outer shell material is 73,400 psi at an outer shell temperature of 143 ºF. The outer shell will reach ultimate strength when the membrane stress of the shell reaches ultimate stress. During excessive loading, plastic hinges will occur at areas of peak bending stress. The ultimate strength of the OC outer shell is therefore based on the shell membrane stress reaching ultimate stress.

The maximum outer shell membrane stress intensity induced by the 67,500 pound lifting load is 2,847 + 751 = 3,598 psi for the vertical lift case (see Table 2.5-3). Therefore, the smallest possible load required to induce failure in the OC outer shell is:

$$V_{shell} = (67{,}500)\left(\frac{73{,}400}{3{,}598}\right) = 1{,}377{,}015 \text{ lb}$$

The weld failure load for the 5/8-inch trunnion outer shell bevel weld can be derived as:

$$f_{fail} = (0.6)(73{,}400)(0.625) = 27{,}525 \text{ lb/in}$$

This weld load would result from a failure load, V_{weld}, applied to the trunnion as derived from the following equation:

$$f_{fail} = \sqrt{\left(\frac{V_{weld}}{L_{weld}}\right)^2 + \left(\frac{M_{weld}}{S_{weld}}\right)^2} = 27{,}525 \text{ lb/in}$$

where V_{weld} is the load needed to induce failure of weld, the length of the weld, $L_{weld} = 18.85$ in/in, the moment in the weld due to V_{weld}, $M_{weld} = (2.45)V_{weld}$, and the elastic section modulus, $S_{weld} = 28.27$ in^3/in. Substituting:

$$\sqrt{\left(\frac{V_{weld}}{18.85}\right)^2 + \left(\frac{(2.45)V_{weld}}{28.27}\right)^2} = 27{,}525\,\text{lb/in}$$

Solving results in a maximum weld failure load, V_{weld} = 270,883 pounds. Therefore, the trunnion weld will fail under excessive loading before the OC outer shell fails. The margin of safety against OC outer shell failure is then

$$MS = \frac{1{,}377{,}015}{270{,}883} - 1 = +4.08$$

2.5.2 Tie-down Devices

2.5.2.1 Center-Pivot and Tie-down Trunnion Loads

The RH-TRU 72-B package can be transported on either of two types of trailers. Each trailer design incorporates a specially engineered tie-down system to secure the package. The first, the Center-Pivot Trailer (CPT), utilizes an onboard uprighting system which allows the package to be unloaded while still attached to the trailer (see Figure 2.5-15). The second, the Lift-Off Trailer (LOT), requires an external crane to upright the package, lift it off the trailer, and place it in an unloading area away from the trailer (see Figure 2.5-16). The CPT uses two of the upper lifting trunnions as well as the center-pivot and lower trunnions for tie-down attachments. Thus, only the two remaining upper trunnions, both vertically oriented, one on the top surface of the package and the other on the lower surface of the package, need to be evaluated for inadvertent tie-down use. Inspection of the trailer design shows that the top trunnion is not in a useable position while the bottom trunnion is inaccessible because of trailer structure.

Because the LOT requires access to the upper lifting trunnions for the crane attachment, only the center-pivot and lower trunnions are used for tie-down attachments. The vertically oriented trunnions near the lid are unusable or inaccessible as discussed above. The horizontally oriented trunnions near the lid end are accessible for inadvertent use, but any attachment to them with chains or cable would be much less rigid than the engineered tie-down system components and thus would not experience significant loads.

The analysis of the two tie-down systems is given below. Worst-case tie-down loads on the lifting and tie-down trunnions and the center-pivot trunnions are determined for both trailer designs described above. The lifting and tie-down trunnion loads are shown to be smaller than those experienced during the lifting procedure analyzed in Section 2.5.1, *Lifting Devices*. The center-pivot trunnion loads are shown to be nearly the same for either trailer configuration.

Transport loads applied to the center-pivot trunnions are assumed to act at the center of a 2½-inch wide bearing area that interfaces with the transporter support system, as shown in Figure 2.5-17.

Due to the center-pivot arrangement as primary support for the package in transit, the response of the system to transportation induced loads will depend strongly on the location of the center of gravity (CG) of the loaded package. Nominally, for an empty package, the package CG will be approximately 3 inches from the pivot point of the trunnions, toward the lid-end of the package. A uniformly loaded canister placed inside the package will result in the CG being shifted back to a

location about 1⅞ inches from the pivot point, toward the lid-end (refer to Table 2.2-1). For this case, where the package CG is very near the support point, trunnion loading in response to the regulatory requirements of 10*g* longitudinal, 5*g* transverse and 2*g* vertical is fairly straightforward.

However, if the package CG is offset significantly from the support point, additional loading will be induced into the center-pivot trunnions in the form of reacting couples. To conservatively bound the worst-case CG offset, and thus the worst-case trunnion loading situation, the payload canister CG will be calculated for a worst-case load imbalance. It will be assumed that an entire payload will consist of a solid steel slug with a density of 0.283 lb/in^3 and weighing 6,900 pounds (the maximum useful canister payload weight), and that this slug is located at the extreme top end of the canister.

The inside diameter of the canister spacer is 26½ inches, so it will be assumed that the steel slug has a 26½-inch outside diameter. The length of the slug will thus be:

$$L = \frac{6{,}900/0.283}{(\pi/4)(26.5)^2} = 44.2\,\text{in}$$

The payload canister is 121 inches long. Therefore, the CG of the steel slug, which is approximately 31 inches from the top of the canister (the worst-case load imbalance occurs when the steel slug is shifted to the top of the canister instead of the bottom), will be approximately 26½ inches from the center-pivot trunnions (towards the lid-end). The CG of the 1,100 pound canister is less than 3½ inches from the pivot point (geometric center) of the package, toward the bottom of the package. The weight of the empty package is 37,000 pounds (45,000 – 8,000).

The offset distance of the CG of the package from the pivot point (toward the lid-end of the package) with the unbalanced load is:

$$L_{offset} = \frac{(37{,}000)(-3.02) + (1{,}100)(3.50) + (6{,}900)(-26.5)}{45{,}000} = 6.46\,\text{in}$$

To allow for uncertainties in the location of the canister CG (the lead pig at the bottom-end of the payload canister is optional), a total package CG offset distance of 8 inches (in either direction) will be conservatively used to calculate the tie-down loads.

The 10*g* longitudinal load (in the direction of travel) will not be affected by the offset of the package CG in the longitudinal direction. Therefore, the longitudinal load on each of the two primary center-pivot trunnions is:

$$F_L = \frac{10(45{,}000)}{2} = 225{,}000\,\text{lb/trunnion}$$

The 5*g* transverse load will result in reaction loading on the center-pivot trunnions, as shown in Figure 2.5-18. To derive reaction loads R_1, R_2, and R_3, equations of force and moment balance for static equilibrium are used:

$$\sum F_{trans} = F_T - R_1 = 0$$

$$\sum F_{long} = R_2 - R_3 = 0$$

$$\sum M_o = 2(23.05)R_3 - (8.0)F_T = 0$$

Solving the equations simultaneously for the unknown reactions yields $F_T = R_1 = 225{,}000$ pounds, and $R_2 = R_3 = 39{,}050$ pounds.

Shown, in Figure 2.5-19 and Figure 2.5-20, the two trailer designs support the package differently. The CPT design uses the upper trunnions and the center-pivot trunnions for the tie-down system. The LOT design uses the lower trunnions and the center-pivot trunnions for the tie-down system. As such, the CPT and LOT analyses are identical, although on different sets of trunnions.

For either design, the 2*g* vertical load will result in the following worst-case loading on the center-pivot and upper/lower trunnions:

$$R_4 = F_v\left(\frac{a}{L}\right) = 19{,}862\text{ lb} = 9{,}931\text{ lb/trunnion}$$

$$R_5 = F_v + R_4 = 109{,}862\text{ lb} = 54{,}931\text{ lb/trunnion}$$

where the vertical force, $F_v = 2W = 2(45{,}000) = 90{,}000$ pounds based on a package weight, $W = 45{,}000$ pounds, $a = 8.0$ inches, and $L = 36.25$ inches.

The 2*g* vertical upload will result in the same loading case as above since there are trunnion caps for the center-pivot trunnions.

The worst-case forces from either trailer design on the center-pivot trunnions are required to be imposed simultaneously on the package tie-down system (force components for each direction must be summed and applied to the trunnions), as listed below:

<u>Longitudinal Forces</u>: $F_L = 225{,}000 + 39{,}050 = 264{,}050$ pounds (transversely loaded trunnion)
$F_L = 225{,}000 - 39{,}050 = 185{,}950$ pounds (non-transversely loaded trunnion)

<u>Transverse Forces</u>: $F_T = 225{,}000$ pounds (transversely loaded trunnion only)

<u>Vertical Forces</u>: $F_V = 54{,}931$ pounds (each trunnion)

A calculation was also performed to determine the forces associated with yawing. Yawing can occur during rapid negotiations of curves in highways, as the result of tracking due to grooves in highway lanes, or as the result of rapid lane changes.

The yawing calculation assumed a rotation of the package about a vertically oriented axis through the package's centroid. For conservatism, the center-pivot trunnions' resistance to yawing was neglected.

The package's mass moment of inertia about its vertical axis has been previously determined to be 278,601 lb-sec^2-in (see Table 2.2-1). The package's average angular acceleration during a rapid turning event was estimated utilizing the following assumptions:

1. The turning angle for the front wheels of the tractor can vary between -35º to +35º.
2. The corresponding steering wheel movement varies between -1.5 and +1.5 revolutions.
3. The driver can turn the steering wheel a quarter revolution per second.

4. The angular acceleration at the package location on the trailer is the same as the angular acceleration of the tractor.
5. The tractor-trailer is initially traveling in a straight line and therefore, has no initial angular velocity.

Using the above listed assumptions, the average angular acceleration for the turning event was estimated as shown below:

- Average steering wheel angular velocity $\omega_s = (\pi/2)$ rad/sec
- Average tractor wheel angular velocity ω_{avg}
  $= \omega_s$ (rad/sec) × (35º tractor wheel rotation/1.5 steering wheel rotation)
  $= (\pi/2)(35/540) = 0.102$ rad/sec
- Average angular acceleration (α) over a 1 second interval
  $= \omega_{avg}/\Delta t = (0.102 \text{ rad/sec})/(1 \text{ sec}) = 0.102 \text{ rad/sec}^2$

Using the values for mass moment of inertia and angular acceleration determined above, the torque developed during the turning event is estimated as:

$$\text{Torque} = I_{package}\alpha = (278{,}601)(0.102) = 28{,}417 \text{ in - lb}$$

If this torque is entirely reacted at the center-pivot trunnions, the reacting forces are very low, since the moment arm for the reacting forces is approximately 36 inches. Using this approximate moment arm, each reacting force is approximately 790 pounds (28,417/36). These reacting loads are insignificant when compared with the previously determined horizontal reaction of 264,050 pounds for the center-pivot trunnions.

If the torque is entirely reacted at the center-pivot trunnion and at an adjustable side post located at a lid-end tie-down trunnion, as previously illustrated, the reacting force is 1,907/3.0, or approximately 636 pounds, since the moment arm between the center-pivot trunnions and the lid-end tie-down trunnions is approximately 3 feet. Since the reacting load is very small, the required brace cross-sectional area for the side post is also very small.

A tracking type of yaw can lead to a cyclic stress being applied to the center-pivot trunnions. This corresponding cyclic stress would be very low, since simultaneous application of all of the worst-case center-pivot trunnion loads (F_L = 264,050 lbs, F_T = 225,000 lbs and F_V = 54,931 lbs) results in a maximum stress intensity of 21,892 psi per Section 2.5.2.2, *OC Outer Shell Stresses*. By ratioing, the cyclic stress due to yawing would be under 50 psi, and therefore, would be insignificant with regard to fatigue failure.

2.5.2.2 OC Outer Shell Stresses

The maximum transportation-induced load acting on the two tie-down trunnions at the bottom-end of the package is the load R_4 arising from the 2*g* vertical force. This load, tangent to the OC outer shell, is 9,931 pounds per trunnion. This circumferential load is significantly less than the circumferential lifting load V_C = 67,500 pounds. Since the margin of safety against outer shell yielding for that load case was +0.52 (see Section 2.5.1.2, *OC Outer Shell Stresses*), it may be concluded that an even greater margin exists for transportation induced trunnion loading.

The center-pivot trunnions and the OC outer shell are analyzed for the combined imposition of the worst-case loads calculated above. For conservatism, the strengthening of the OC outer shell by the OC inner shell and lead shielding is neglected in the ANSYS® finite element analysis.

The stresses in the OC outer shell due to the tie-down loads imposed on the center-pivot trunnion are determined using the finite element analysis described in Appendix 2.10.1.1, *Tie-down Trunnion Analysis*. The maximum membrane-plus-bending stress intensity resulting from the combined transport loads is 21,892 psi. This stress intensity occurs midway between the two center-pivot trunnions, near the end of the OC outer shell. Since the maximum OC outer shell temperature under NCT is 143 ºF, the maximum allowable (or yield) stress, obtained from Table 2.5-1, is 28,000 psi. The corresponding margin of safety, for combined worst-case transportation induced loading, is:

$$MS = \frac{28{,}000}{21{,}892} - 1 = +0.28$$

The OC outer shell is therefore adequate under worst-case inertial loads.

2.5.2.3 Center-Pivot Trunnion Stresses

Center-pivot trunnion bearing stress is derived by applying the vector sum of the transport loads which act in a direction perpendicular to the trunnion (F_V and F_L) to the projected area of the 12.0-inch diameter center-pivot trunnion. The width of the bearing surface on the trunnion is assumed to be 2.5 inches. Therefore, the bearing stress is:

$$S_B = \frac{\sqrt{F_V^2 + F_L^2}}{DW} = \frac{\sqrt{(54{,}931)^2 + (264{,}050)^2}}{(12.0)(2.5)} = 8{,}990\ \text{psi}$$

The bearing stress margin of safety (using a yield stress of 28,000 psi) is then:

$$MS = \frac{28{,}000}{8{,}990} - 1 = +2.11$$

2.5.2.4 Center-Pivot Trunnion Attachment Welds

The welds attaching the 12-inch diameter center-pivot trunnion to the 18.0-inch wide, 28.0-inch long center-pivot trunnion base, and the weld attaching the base to OC outer shell, are both analyzed in this section.

The trunnion weld is evaluated using the same method found in Section 2.5.1.4, *Lifting Trunnion Attachment Weld*. The transportation load is offset from the trunnion weld by a distance of 0.4 + ½(2.5) = 1.65 inches. The equivalent transportation load acting perpendicular to the trunnion will be the vector sum of forces F_V and F_L, as used in Section 2.5.2.3, *Center-Pivot Trunnion Stresses*:

$$F_{eq} = \sqrt{F_V^2 + F_L^2} = \sqrt{(54{,}931)^2 + (264{,}050)^2} = 269{,}703\ \text{lb}$$

The bending moment acting on the center-pivot trunnion weld is then:

$$M_{eq} = (269{,}703)(1.65) = 445{,}010\ \text{in-lb}$$

Trunnion weld force components are thus:

$$f_s = \frac{F_{eq}}{L_w} = \frac{269{,}703}{37.7} = 7{,}154 \text{ lb/in}$$

$$f_b = \frac{M_{eq}}{S_w} = \frac{445{,}010}{113.1} = 3{,}935 \text{ lb/in}$$

where the unit thickness weld length, $L_w = \pi(12.0 \text{ in}) = 37.7$ inches, and the unit thickness weld section modulus, $S_w = (\pi/4)(12.0)^2 = 113.1 \text{ in}^2$. The total weld force is:

$$f_{total} = \sqrt{f_s^2 + f_b^2} = \sqrt{(7{,}154)^2 + (3{,}935)^2} = 8{,}165 \text{ lb/in}$$

Using a shear stress allowable of $0.6S_y = 0.6(28{,}000) = 16{,}800$ psi, and assuming a full penetration bevel weld, the minimum acceptable weld size, w, is:

$$w = \frac{8{,}165}{16{,}800} = 0.486 \text{ in}$$

Since the trunnion is attached to the base plate with a full penetration, 1½-inch bevel weld, the minimum weld margin of safety is:

$$MS = \frac{1.5}{0.486} - 1 = +2.09$$

For the center-pivot trunnion base weld, the maximum load offset from the weld will include offset "e" due to curvature of the OC outer shell (refer to Section 2.5.1.4, *Lifting Trunnion Attachment Weld*, for the analysis methodology):

$$\theta = 2\left[\sin^{-1}\left(\frac{9.0}{20.56}\right)\right] = 51.9°$$

and

$$e = 20.56\left[1 - \cos\left(\frac{\theta}{2}\right)\right] = 2.07 \text{ in}$$

The maximum offset is thus 2.07 + 1.03 + 1.65 = 4.75 inches. This rectangular weld pattern will be analyzed by simultaneously applying the relevant separate load components, and conservatively assuming the above maximum offset applies to each. For the vertical load, F_V:

$$f_{sV} = \frac{F_V}{L_w} = \frac{54{,}931}{92} = 597 \text{ lb/in}$$

$$f_{bV} = \frac{M_V}{S_{wV}} = \frac{(54{,}931)(4.75)}{612} = 426 \text{ lb/in}$$

and, for the longitudinal force, F_L:

$$f_{sL} = \frac{F_L}{L_w} = \frac{264{,}050}{92} = 2{,}870 \text{ lb/in}$$

$$f_{bL} = \frac{M_L}{S_{wL}} = \frac{(264{,}050)(4.75)}{765} = 1{,}640 \text{ lb/in}$$

where, the unit thickness weld length, $L_w = 2(b + d) = 2(18.0 + 28.0) = 92.0$ inches, the unit thickness weld section modulus in the vertical direction is, $S_{wV} = bd + d^2/3 = (28.0)(18.0) + (18)^2/3 = 612 \text{ in}^2$, and the unit thickness weld section modulus in the longitudinal direction is, $S_{wL} = bd + d^2/3 = (18.0)(28.0) + (28)^2/3 = 765 \text{ in}^2$. The equivalent weld force components are:

$$f_{s,eq} = \sqrt{f_{sV}^2 + f_{sL}^2} = \sqrt{(597)^2 + (2{,}870)^2} = 2{,}931 \text{ lb/in}$$

$$f_{b,eq} = \sqrt{f_{bV}^2 + f_{bL}^2} = \sqrt{(426)^2 + (1{,}640)^2} = 1{,}694 \text{ lb/in}$$

Finally, the total equivalent weld load is:

$$f_{total} = \sqrt{f_{s,eq}^2 + f_{b,eq}^2} = \sqrt{(2{,}931)^2 + (1{,}694)^2} = 3{,}385 \text{ lb/in}$$

Using a shear stress allowable of $0.6S_y = 0.6(28{,}000) = 16{,}800$ psi, and assuming a full penetration bevel weld, the minimum acceptable weld size, w, is:

$$w = \frac{3{,}385}{16{,}800} = 0.201 \text{ in}$$

Since the trunnion is attached to the base plate with a full penetration, 1½-inch bevel weld, the minimum weld margin of safety is:

$$MS = \frac{1.5}{0.201} - 1 = +6.46$$

2.5.2.5 Excessive Center-Pivot Trunnion Loading

To preclude damage to the package due to inadvertent overloading of the center-pivot trunnions, the trunnion welds should fail before the OC outer shell stress reaches the ultimate tensile strength of the material. The specified ultimate tensile strength for the outer shell material, obtained from Table 2.5-1, is 73,400 psi. The outer shell will reach ultimate strength when the membrane stress of the shell reaches ultimate stress. During excessive loading, plastic hinges will occur at areas of peak bending stress. The ultimate strength of the OC outer shell is therefore based on the shell membrane stress reaching ultimate stress.

The stresses in the OC outer shell due to the tie-down loads imposed on the center-pivot trunnion are determined using the finite element analysis described in Appendix 2.10.1.1, *Tie-down Trunnion Analysis*. The maximum outer shell membrane stress intensity from the combined tie-down loads is 12,040 psi at the bottom-right corner of the center-pivot trunnion block. Therefore, the smallest

possible load required to induce failure in the OC outer shell for loads acting perpendicular to the trunnion is:

$$V_{shell} = \left(\frac{73{,}400}{12{,}040}\right)\sqrt{(264{,}050)^2 + (54{,}931)^2} = 1{,}644{,}204 \text{ lb}$$

Note that this value is conservatively small, since the shell stress intensity level of 12,040 psi includes effects of the load component which acts to compress the center-pivot trunnion. This load component does not affect the trunnion welds.

Using a shear stress allowable of $0.6S_u = 0.6(73{,}400) = 44{,}040$ psi, the weld failure load for the trunnion attachment weld (3/4-inch bevel weld) can be derived as:

$$f_{fail} = (44{,}040)(0.75) = 33{,}030 \text{ lb/in}$$

This weld load would result from a failure load V_{weld} applied to the trunnion which can be derived from the following equation:

$$f_{fail} = \sqrt{\left(\frac{V_{weld}}{L_{weld}}\right)^2 + \left(\frac{M_{weld}}{S_{weld}}\right)^2}$$

where the weld failure load, $f_{fail} = 33{,}030$ lb/in, the load needed to induce failure of weld is V_{weld}, the length of the weld, $L_{weld} = \pi D = \pi(12.0) = 37.7$ inches, the moment in weld due to V_{weld}, $M_{weld} = (1.65)V_{weld}$, and the section modulus, $S_+ = (\pi/4)D^2 = (\pi/4)(12.0)^2 = 113.1$ in^2. Therefore:

$$f_{fail} = \sqrt{\left(\frac{V_{weld}}{37.7}\right)^2 + \left(\frac{(1.65)V_{weld}}{113.1}\right)^2} = 33{,}030$$

Solving for V_{weld} yields a maximum weld failure load of 1,091,100 pounds. Therefore, the trunnion weld will fail under excessive loading before the OC outer shell fails. The margin of safety against package outer shell failure is then:

$$MS = \frac{1{,}644{,}204}{1{,}091{,}100} - 1 = +0.51$$

It is thus demonstrated that the package center-pivot trunnions meet regulatory requirements.

Table 2.5-1 – Material Properties for Type 304 Stainless Steel at 143 ºF

Material Property	Value (psi)
Elastic Modulus, E	$27.9(10)^6$
Yield Strength, S_y	28,000
Ultimate Strength, S_u	73,400
Design Stress, S_m	20,000
Allowable Normal Primary Membrane Stress Intensity	28,000
Allowable Normal Primary Membrane + Bending Stress Intensity	30,000
Normal Pure Shear Stress	16,800
Normal Bearing Stress	28,000

Table 2.5-2 – Data Used in Tie-down Trunnion Lifting Stress Analysis

Applied Loads (see Figure 2.5-3)	Vertical Lift	Horizontal Lift
Circumferential Moment, M_C (in-lb)	0	122,770
Longitudinal Moment, M_L (in-lb)	201,150	0
Circumferential Shear, V_C (lb)	0	41,200
Longitudinal Shear, V_L (lb)	67,500	0
Geometry and Geometric Parameters	**Formula**	**Value**
Outer Shell Thickness, T (in)	T	1.50
Outer Shell Mean Radius (in)	R_m	19.813
Trunnion Base Radius (in)	r_o	3.00
Outer Shell Parameter	$\lambda = R_m/T$	13.209
Trunnion Attachment Parameter	$\beta = 0.875(r_o/R_m)$	0.132

Figure No.	Parameter	Value	Stress Formula①	Vertical Lift Result (psi)	Horizontal Lift Result (psi)
Figure 2.5-6	$\frac{N_\phi}{M_C/R_m^2\beta} =$	0.30	$K_n\left(\frac{N_\phi}{M_C/R_m^2\beta}\right)\left(\frac{M_C}{R_m^2\beta T}\right) =$	0	474
Figure 2.5-4	$\frac{M_\phi}{M_C/R_m\beta} =$	0.10	$K_b\left(\frac{M_\phi}{M_C/R_m\beta}\right)\left(\frac{6M_C}{R_m\beta T^2}\right) =$	0	12,518
Figure 2.5-12	$\frac{N_\phi}{M_L/R_m^2\beta} =$	1.1	$K_n\left(\frac{N_\phi}{M_L/R_m^2\beta}\right)\left(\frac{M_L}{R_m^2\beta T}\right) =$	2,847	0
Figure 2.5-8 Figure 2.5-9	$\frac{M_\phi}{M_L/R_m\beta} =$	0.054	$K_b\left(\frac{M_\phi}{M_L/R_m\beta}\right)\left(\frac{6M_L}{R_m\beta T^2}\right) =$	11,075	0
Figure 2.5-7	$\frac{N_x}{M_C/R_m^2\beta} =$	0.41	$K_n\left(\frac{N_x}{M_C/R_m^2\beta}\right)\left(\frac{M_C}{R_m^2\beta T}\right) =$	0	648
Figure 2.5-5	$\frac{M_x}{M_C/R_m\beta} =$	0.059	$K_b\left(\frac{M_x}{M_C/R_m\beta}\right)\left(\frac{6M_C}{R_m\beta T^2}\right) =$	0	7,386
Figure 2.5-13	$\frac{N_x}{M_L/R_m^2\beta} =$	0.29	$K_n\left(\frac{N_x}{M_L/R_m^2\beta}\right)\left(\frac{M_L}{R_m^2\beta T}\right) =$	751	0
Figure 2.5-10 Figure 2.5-11	$\frac{M_x}{M_L/R_m\beta} =$	0.086	$K_b\left(\frac{M_x}{M_L/R_m\beta}\right)\left(\frac{6M_L}{R_m\beta T^2}\right) =$	17,639	0
n/a	n/a	n/a	$\frac{V_C}{\pi r_o T} =$	0	2,914
n/a	n/a	n/a	$\frac{V_L}{\pi r_o T} =$	4,775	0

Note:

① The stress concentration factors, K_n (membrane) and K_b (bending), are assumed to be 1.0.

Table 2.5-3 – Trunnion Stress Analysis for a Vertical Lift

Stress Formula	A_U	A_L	B_U	B_L	C_U	C_L	D_U	D_L
$K_n\left(\frac{N_\phi}{M_C/R_m^2\beta}\right)\left(\frac{M_C}{R_m^2\beta T}\right) =$					– 0	– 0	+ 0	+ 0
$K_b\left(\frac{M_\phi}{M_C/R_m\beta}\right)\left(\frac{6M_C}{R_m\beta T^2}\right) =$					– 0	+ 0	+ 0	– 0
$K_n\left(\frac{N_\phi}{M_L/R_m^2\beta}\right)\left(\frac{M_L}{R_m^2\beta T}\right) =$	– 2,847	– 2,847	+ 2,847	+ 2,847				
$K_b\left(\frac{M_\phi}{M_L/R_m\beta}\right)\left(\frac{6M_L}{R_m\beta T^2}\right) =$	– 11,075	+ 11,075	+ 11,075	– 11,075				
Summation of Circumferential Stresses, σ_ϕ	– 13,922	+ 8,228	+ 13,922	– 8,228	– 0	+ 0	+ 0	– 0
$K_n\left(\frac{N_x}{M_C/R_m^2\beta}\right)\left(\frac{M_C}{R_m^2\beta T}\right) =$					– 0	– 0	+ 0	+ 0
$K_b\left(\frac{M_x}{M_C/R_m\beta}\right)\left(\frac{6M_C}{R_m\beta T^2}\right) =$					– 0	+ 0	+ 0	– 0
$K_n\left(\frac{N_x}{M_L/R_m^2\beta}\right)\left(\frac{M_L}{R_m^2\beta T}\right) =$	– 751	– 751	+ 751	+ 751				
$K_b\left(\frac{M_x}{M_L/R_m\beta}\right)\left(\frac{6M_L}{R_m\beta T^2}\right) =$	– 17,639	+ 17,639	+ 17,639	– 17,639				
Summation of Longitudinal Stresses, σ_x	– 18,390	+ 16,888	+ 18,390	– 16,888	– 0	+ 0	+ 0	– 0
$\frac{V_C}{\pi r_o T} =$	+ 0	+ 0	– 0	– 0				
$\frac{V_L}{\pi r_o T} =$					– 4,775	– 4,775	+ 4,775	+ 4,775
Summation of Shear Stresses, τ	+ 0	+ 0	– 0	– 0	– 4,775	– 4,775	+ 4,775	+ 4,775
Stress Intensity, S	18,390	16,888	18,390	16,888	9,550	9,550	9,550	9,550

Table 2.5-4 – Trunnion Stress Analysis for a Horizontal Lift

Stress Formula	A_U	A_L	B_U	B_L	C_U	C_L	D_U	D_L
$K_n\left(\frac{N_\phi}{M_C/R_m^2\beta}\right)\left(\frac{M_C}{R_m^2\beta T}\right) =$					– 474	– 474	+ 474	+ 474
$K_b\left(\frac{M_\phi}{M_C/R_m\beta}\right)\left(\frac{6M_C}{R_m\beta T^2}\right) =$					– 12,518	+ 12,518	+ 12,518	– 12,518
$K_n\left(\frac{N_\phi}{M_L/R_m^2\beta}\right)\left(\frac{M_L}{R_m^2\beta T}\right) =$	– 0	– 0	+ 0	+ 0				
$K_b\left(\frac{M_\phi}{M_L/R_m\beta}\right)\left(\frac{6M_L}{R_m\beta T^2}\right) =$	– 0	+ 0	+ 0	– 0				
Summation of Circumferential Stresses, σ_ϕ	– 0	+ 0	+ 0	– 0	– 12,992	+ 12,044	+ 12,992	– 12,044
$K_n\left(\frac{N_x}{M_C/R_m^2\beta}\right)\left(\frac{M_C}{R_m^2\beta T}\right) =$					– 648	– 648	+ 648	+ 648
$K_b\left(\frac{M_x}{M_C/R_m\beta}\right)\left(\frac{6M_C}{R_m\beta T^2}\right) =$					– 7,386	+ 7,386	+ 7,386	– 7,386
$K_n\left(\frac{N_x}{M_L/R_m^2\beta}\right)\left(\frac{M_L}{R_m^2\beta T}\right) =$	– 0	– 0	+ 0	+ 0				
$K_b\left(\frac{M_x}{M_L/R_m\beta}\right)\left(\frac{6M_L}{R_m\beta T^2}\right) =$	– 0	+ 0	+ 0	– 0				
Summation of Longitudinal Stresses, σ_x	– 0	+ 0	+ 0	– 0	– 8,034	+ 6,738	+ 8,034	– 6,738
$\frac{V_C}{\pi r_o T} =$	+ 2,914	+ 2,914	– 2,914	– 2,914				
$\frac{V_L}{\pi r_o T} =$					– 0	– 0	+ 0	+ 0
Summation of Shear Stresses, τ	+ 2,914	+ 2,914	– 2,914	– 2,914	– 0	– 0	+ 0	+ 0
Stress Intensity, S	5,828	5,828	5,828	5,828	12,992	12,044	12,992	12,044

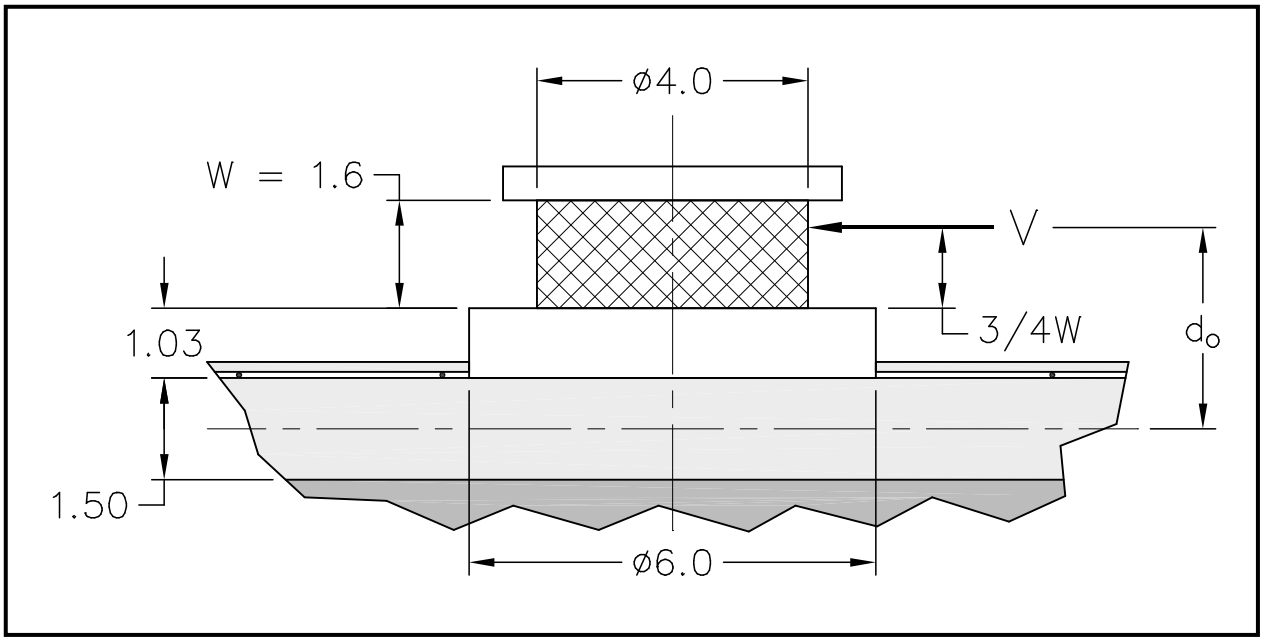

Figure 2.5-1 – Lifting Trunnion Geometry

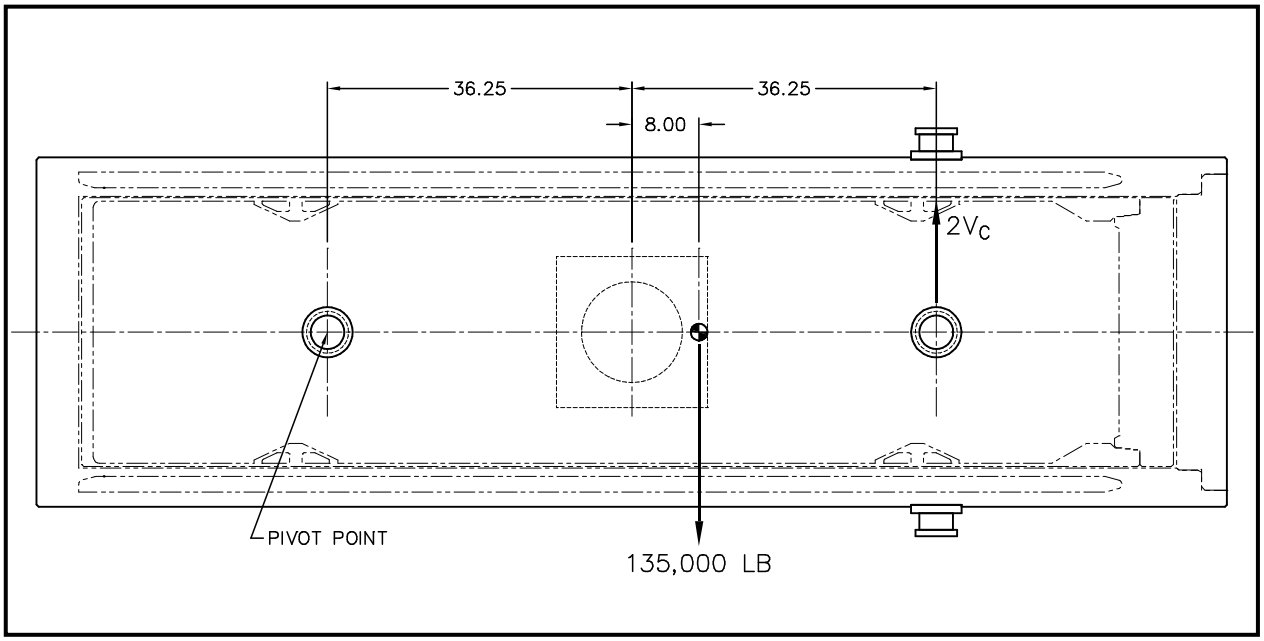

Figure 2.5-2 – Horizontal Lift Loading Configuration

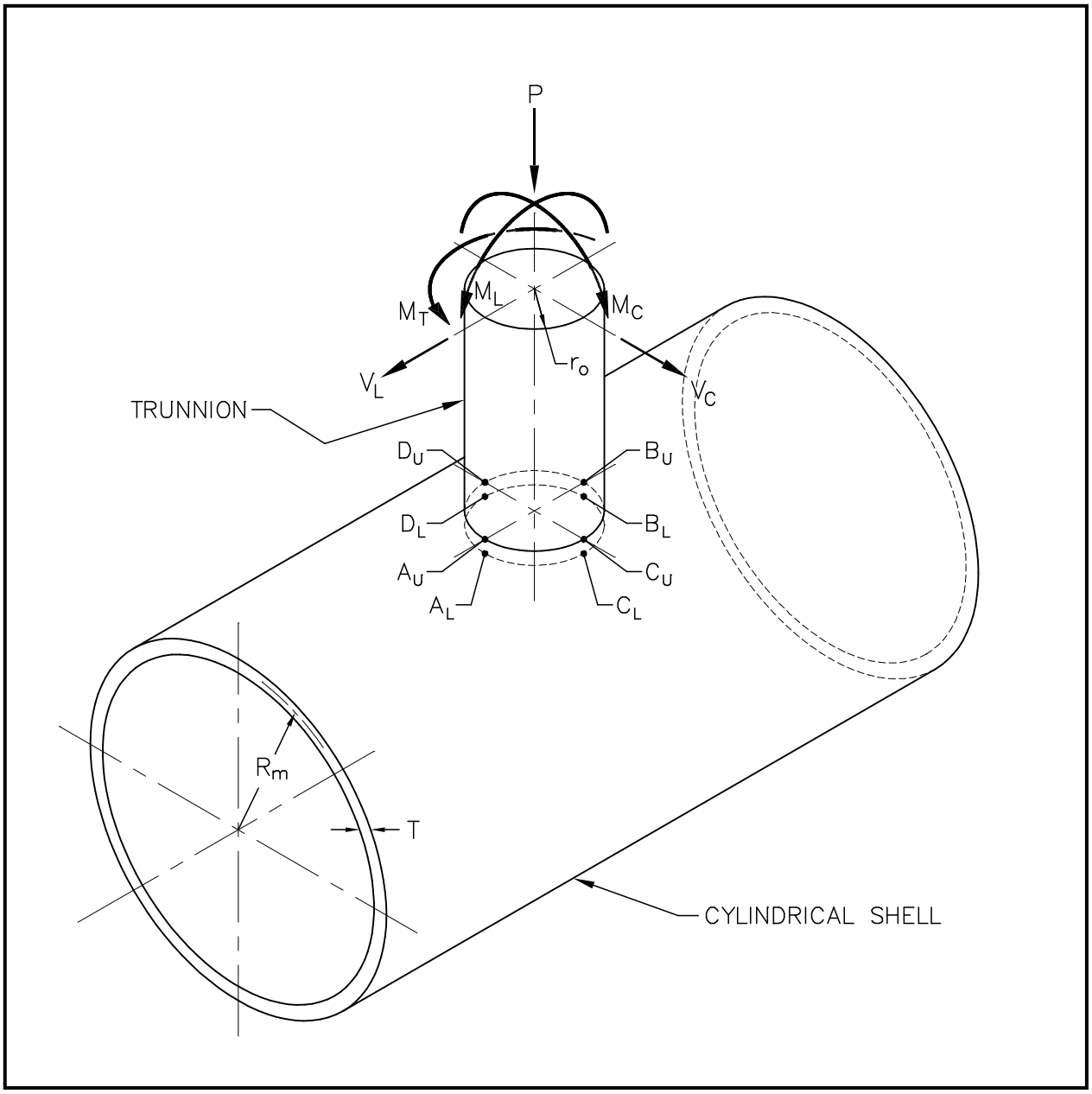

Figure 2.5-3 – Attachment Loads for WRC Bulletin 107

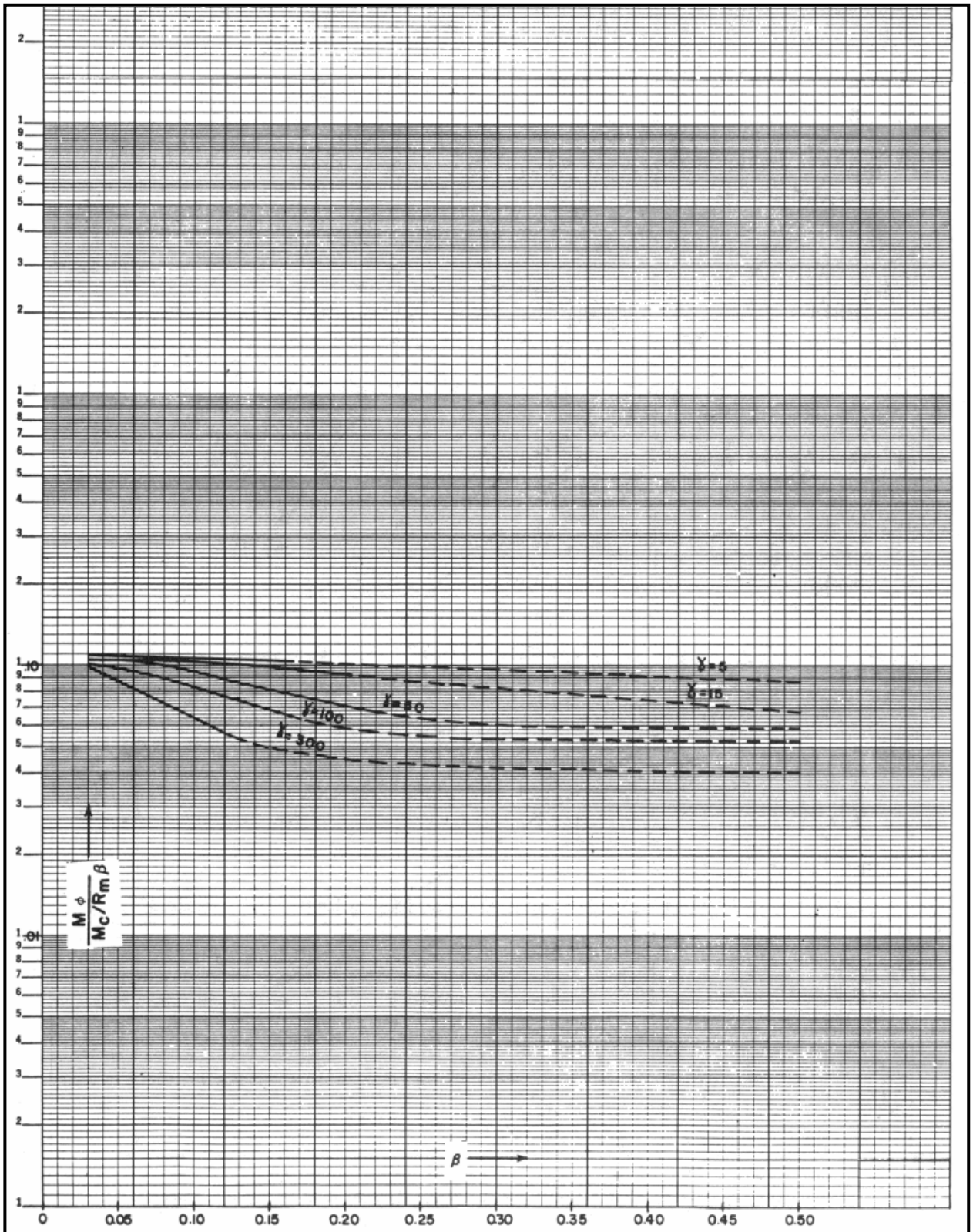

Fig. 1A—Moment $M_\phi/(M_r/R_m\beta)$ due to an external circumferential moment M_r on a circular cylinder

Figure 2.5-4 – Figure 1A from WRC Bulletin 107

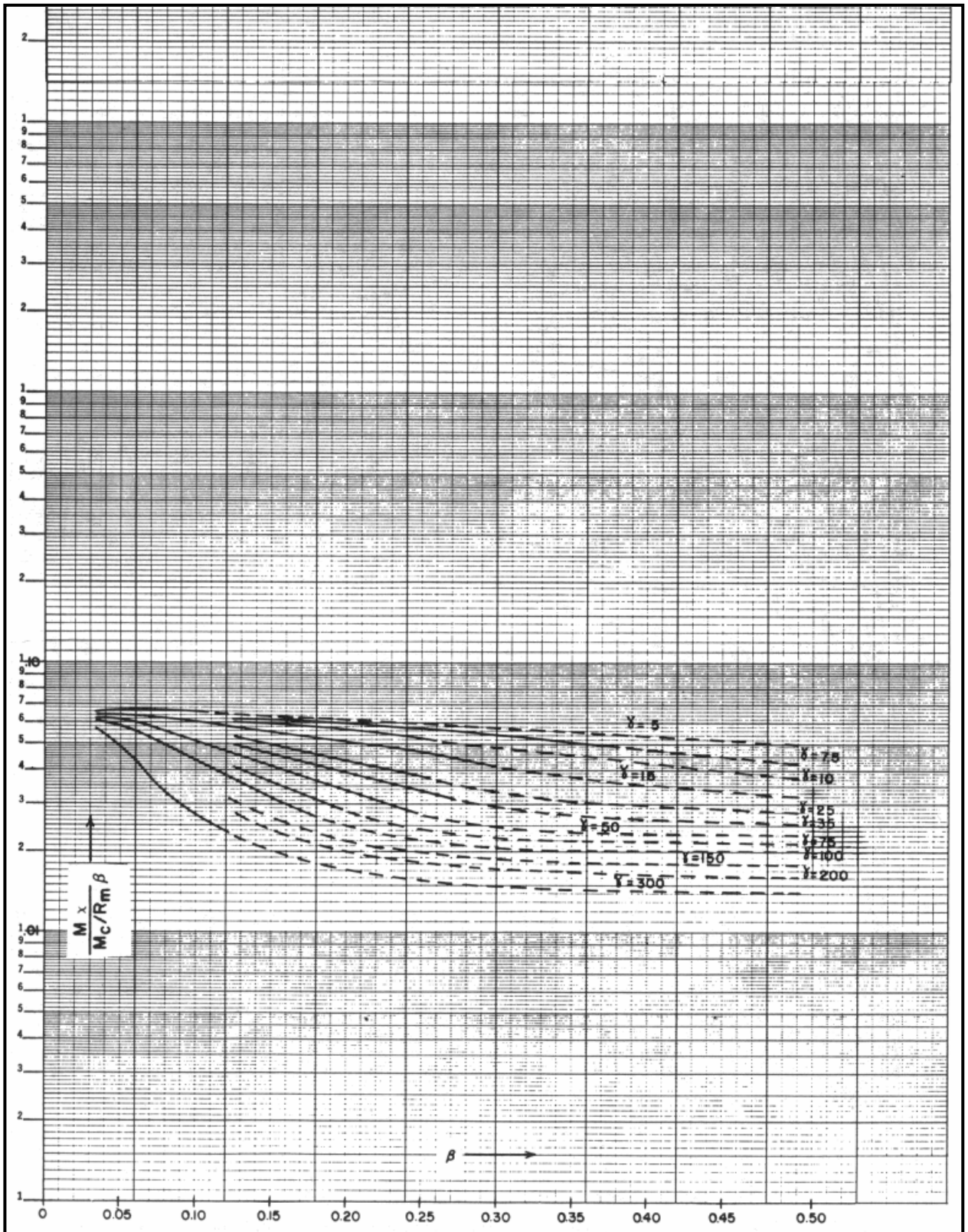

Figure 2.5-5 – Figure 2A from WRC Bulletin 107

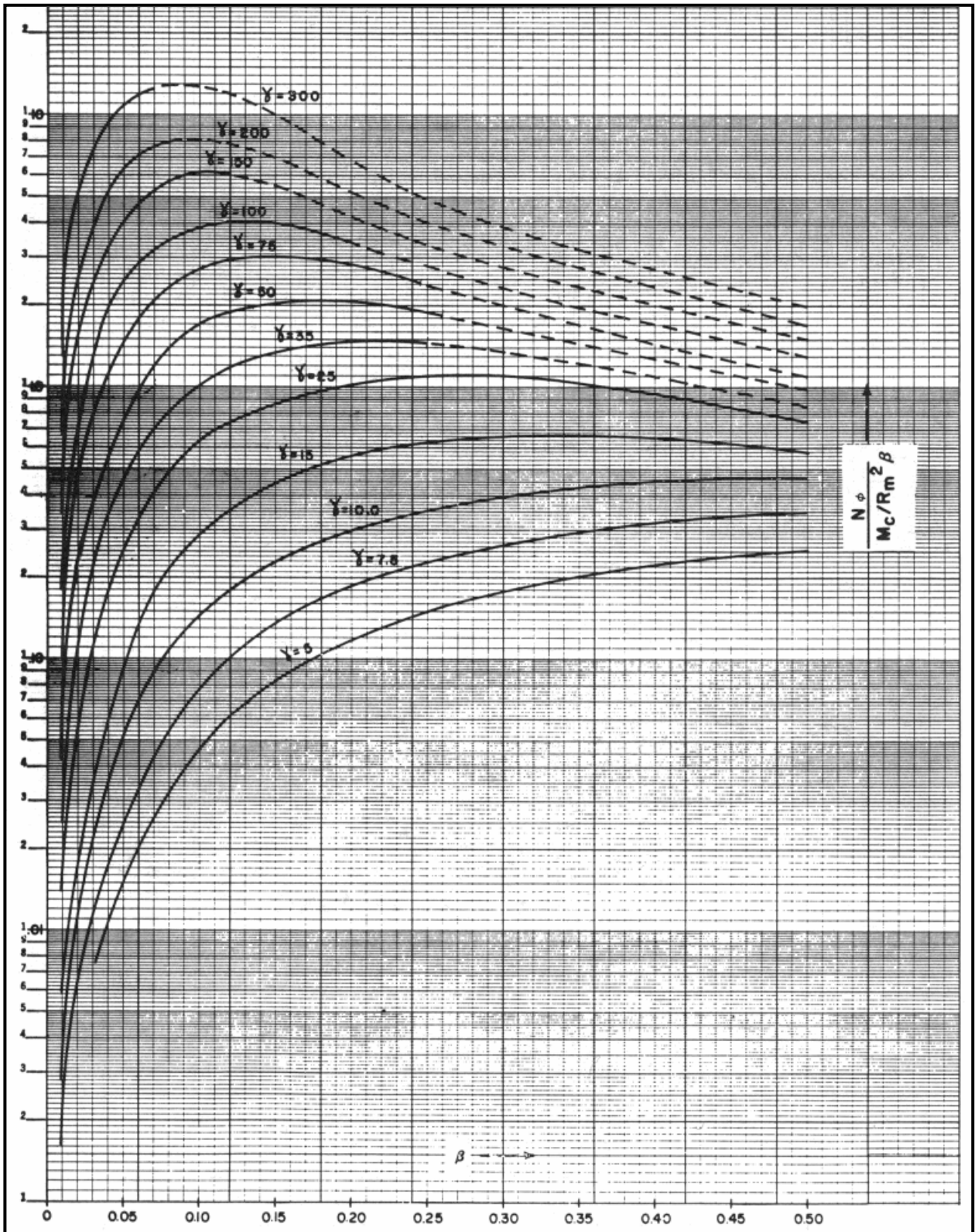

Fig. 3A—Membrane force $N_\phi/(M_c/R_m^2\beta)$ due to an external circumferential moment M_c on a circular cylinder

Figure 2.5-6 – Figure 3A from WRC Bulletin 107

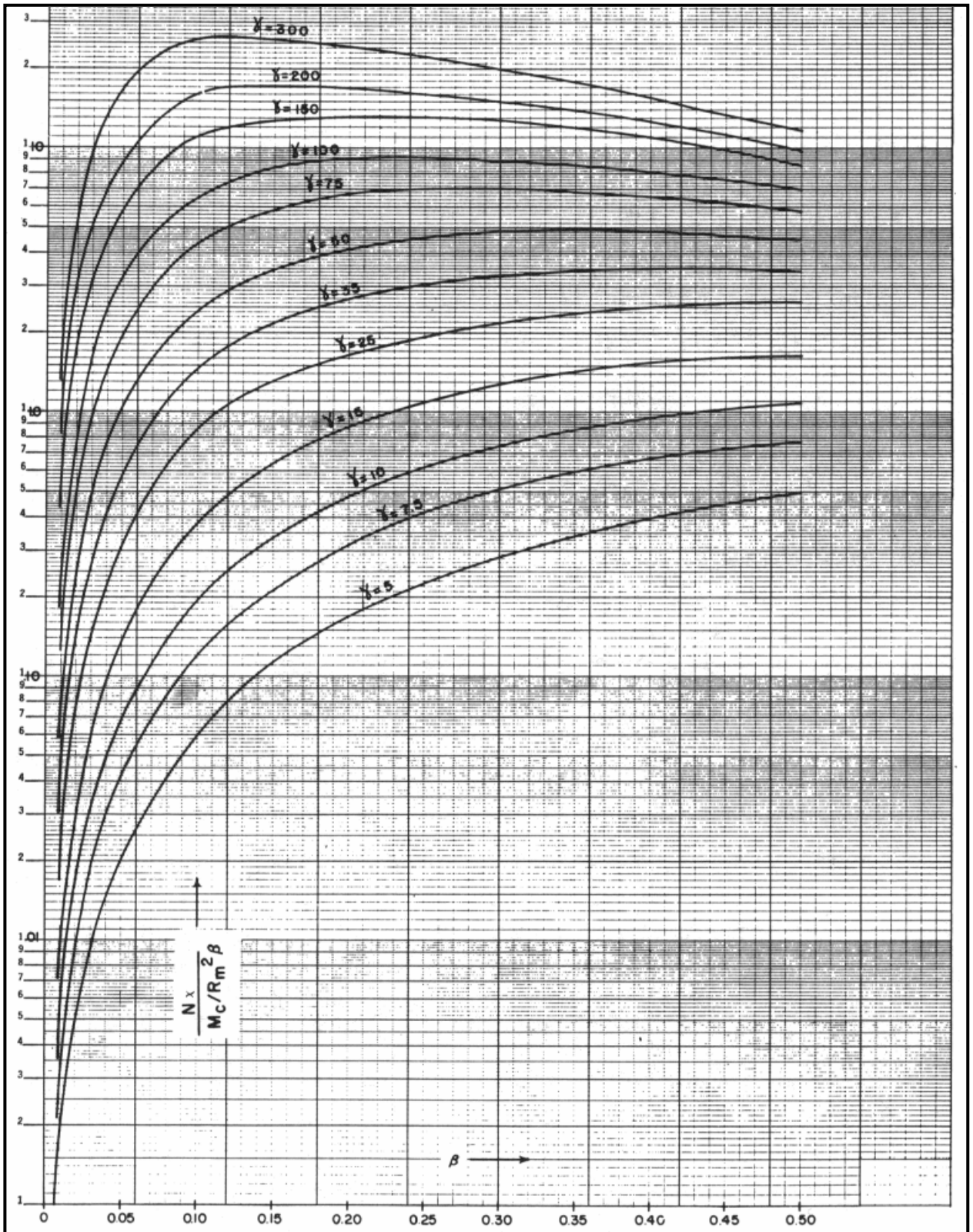

Fig. 4A—Membrane force $N_x/(M_c/R_m^2\beta)$ due to an external circumferential moment M_c on a circular cylinder

Figure 2.5-7 – Figure 4A from WRC Bulletin 107

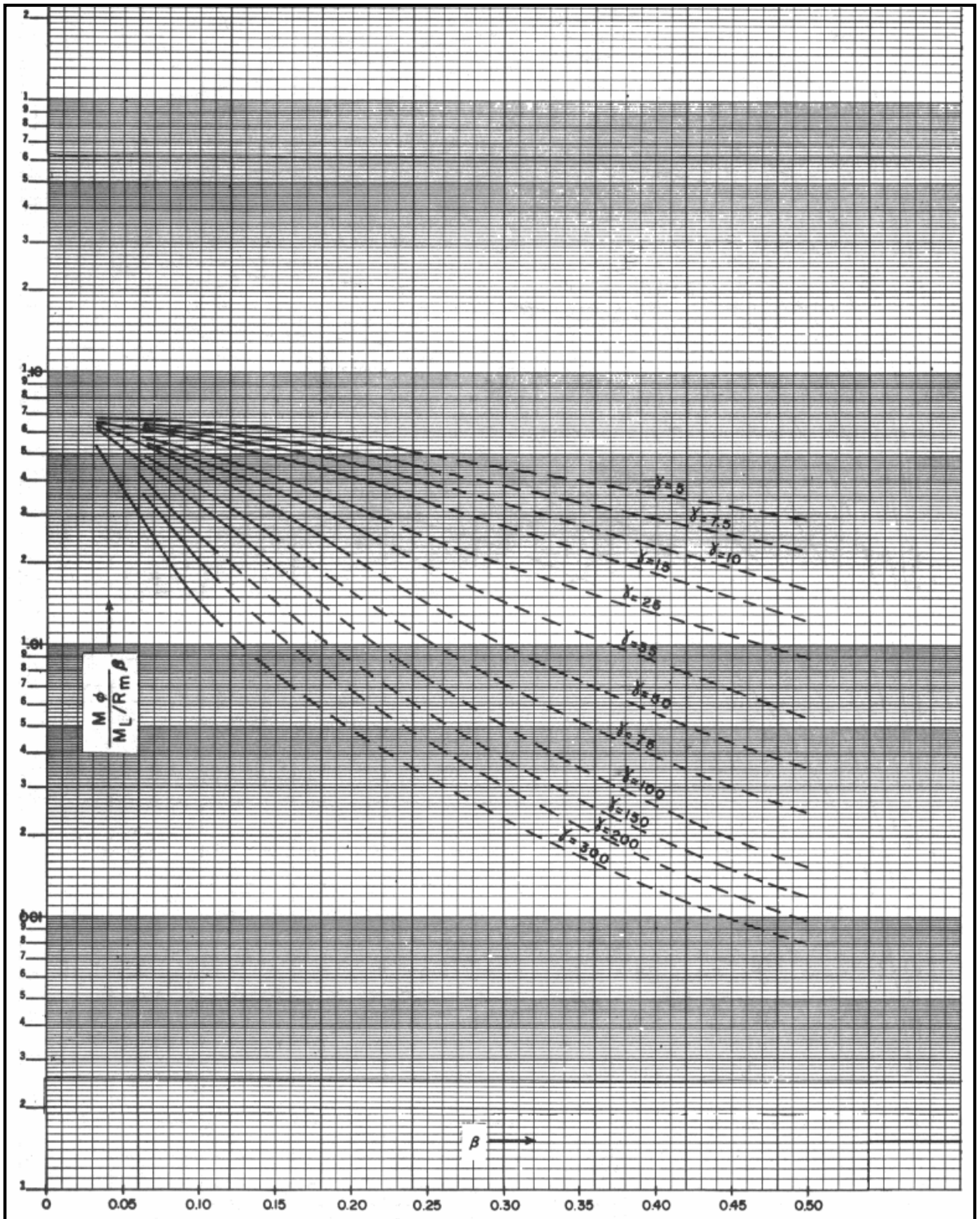

Fig. 1B—Moment $M_\phi/(M_L/R_m\beta)$ due to an external longitudinal moment M_L on a circular cylinder (Stress on the longitudinal plane of symmetry)

Figure 2.5-8 – Figure 1B from WRC Bulletin 107

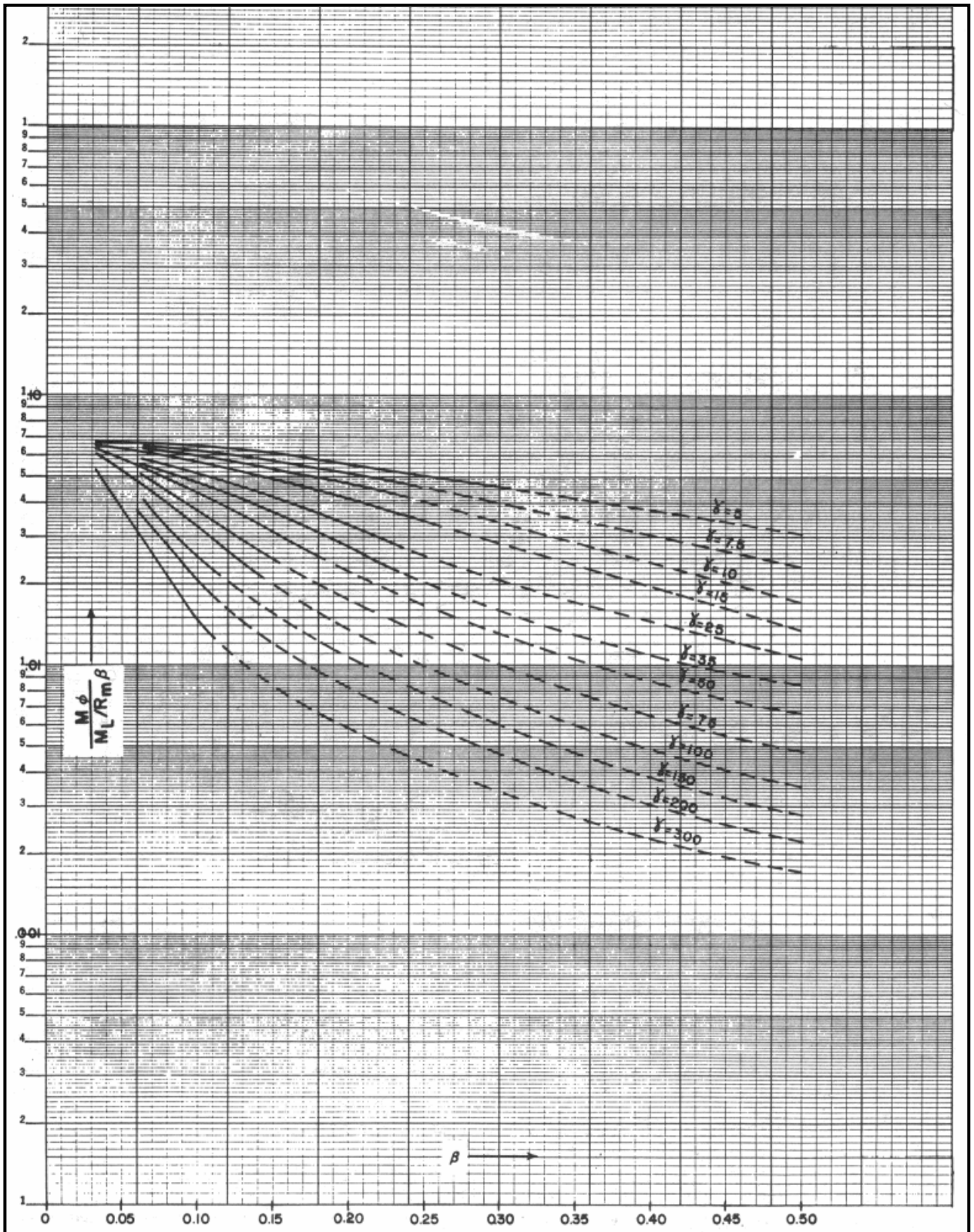

Fig- 1B-1—Moment $M_\phi/(M_L/R_m\beta)$ due to an external longitudinal moment M_L on a circular cylinder

Figure 2.5-9 – Figure 1B-1 from WRC Bulletin 107

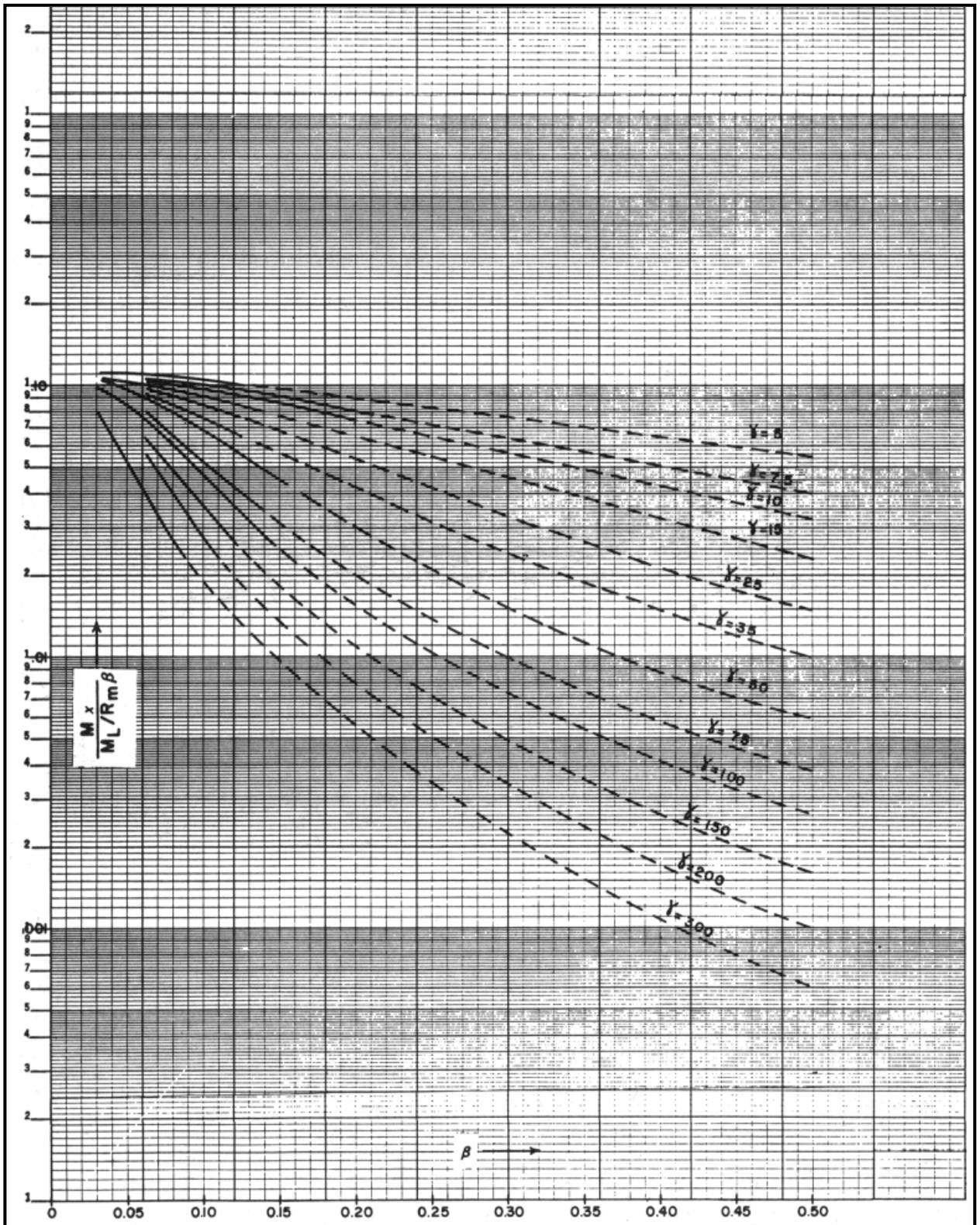

Fig. 2B-Moment $M_x/(M_L/R_m\beta)$ due to an external longitudinal moment M_L on a circular cylinder (Stress on longitudinal plane of symmetry)

Figure 2.5-10 – Figure 2B from WRC Bulletin 107

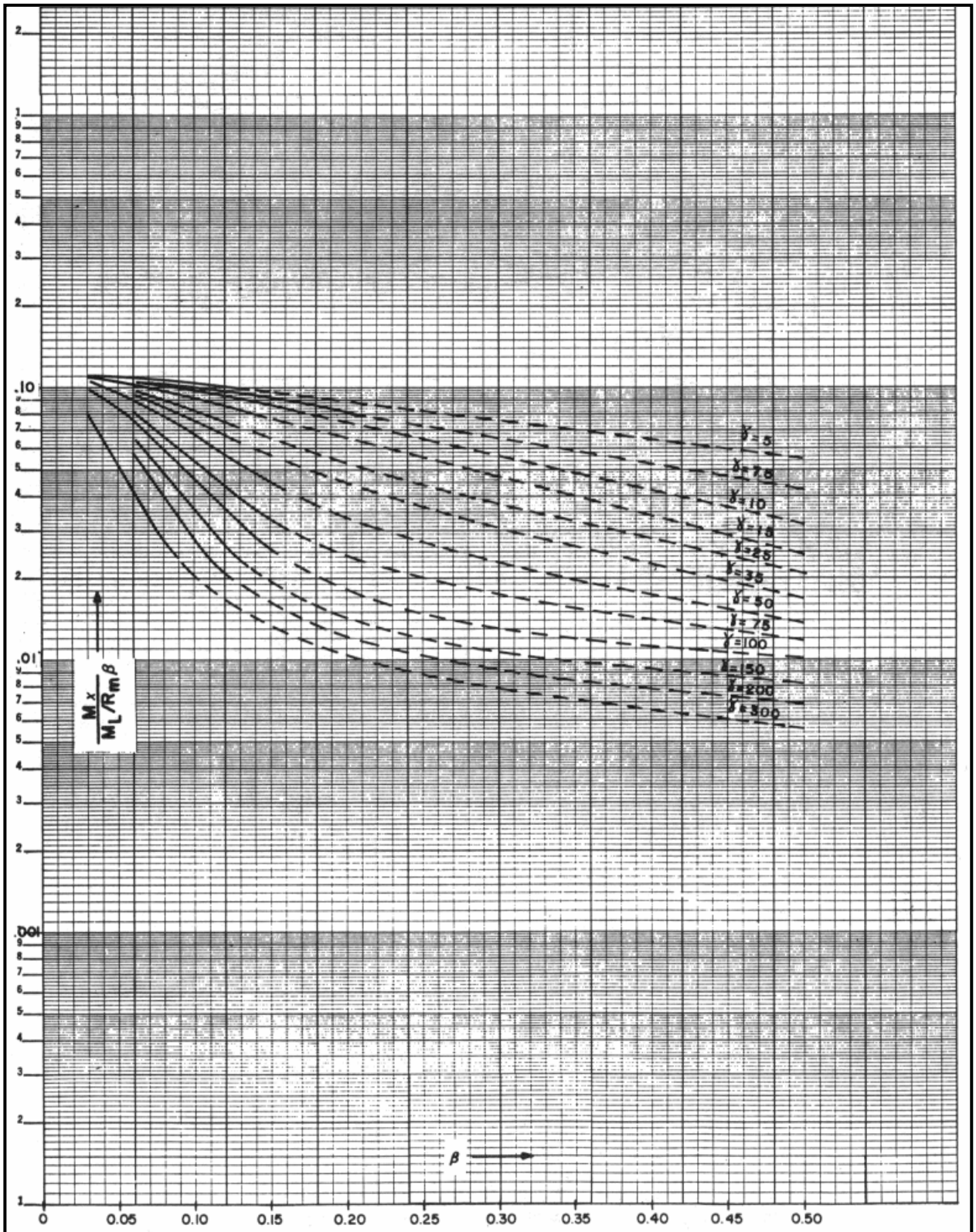

Fig. 2B-1—Moment $M_x/(M_L/R_m\beta)$ due to an external longitudinal moment M_L on a circular cylinder

Figure 2.5-11 – Figure 2B-1 from WRC Bulletin 107

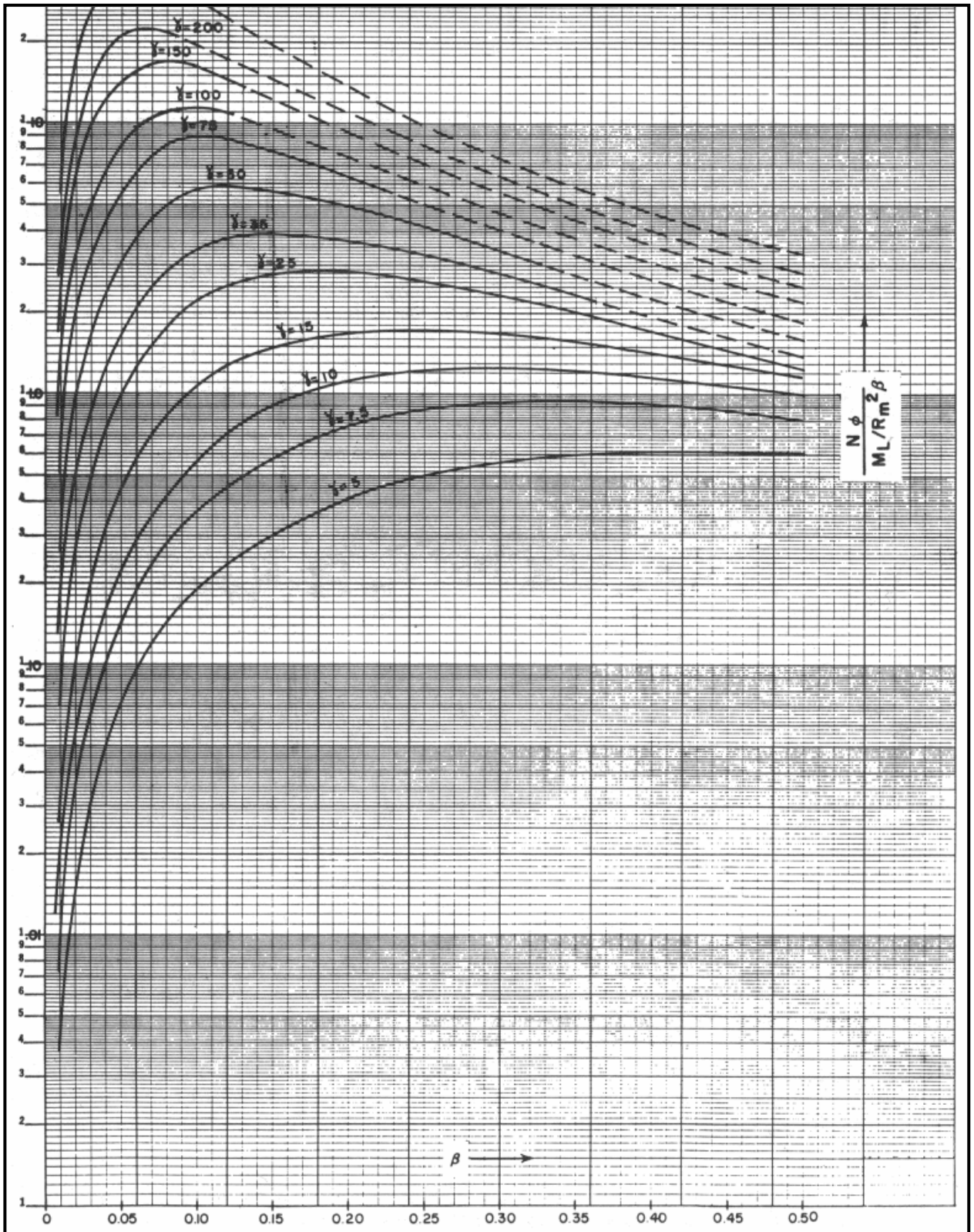

Fig. 3B—Membrane force $N_\phi/(M_L/R_m^2\beta)$ due to an external longitudinal moment M_L on a circular cylinder

Figure 2.5-12 – Figure 3B from WRC Bulletin 107

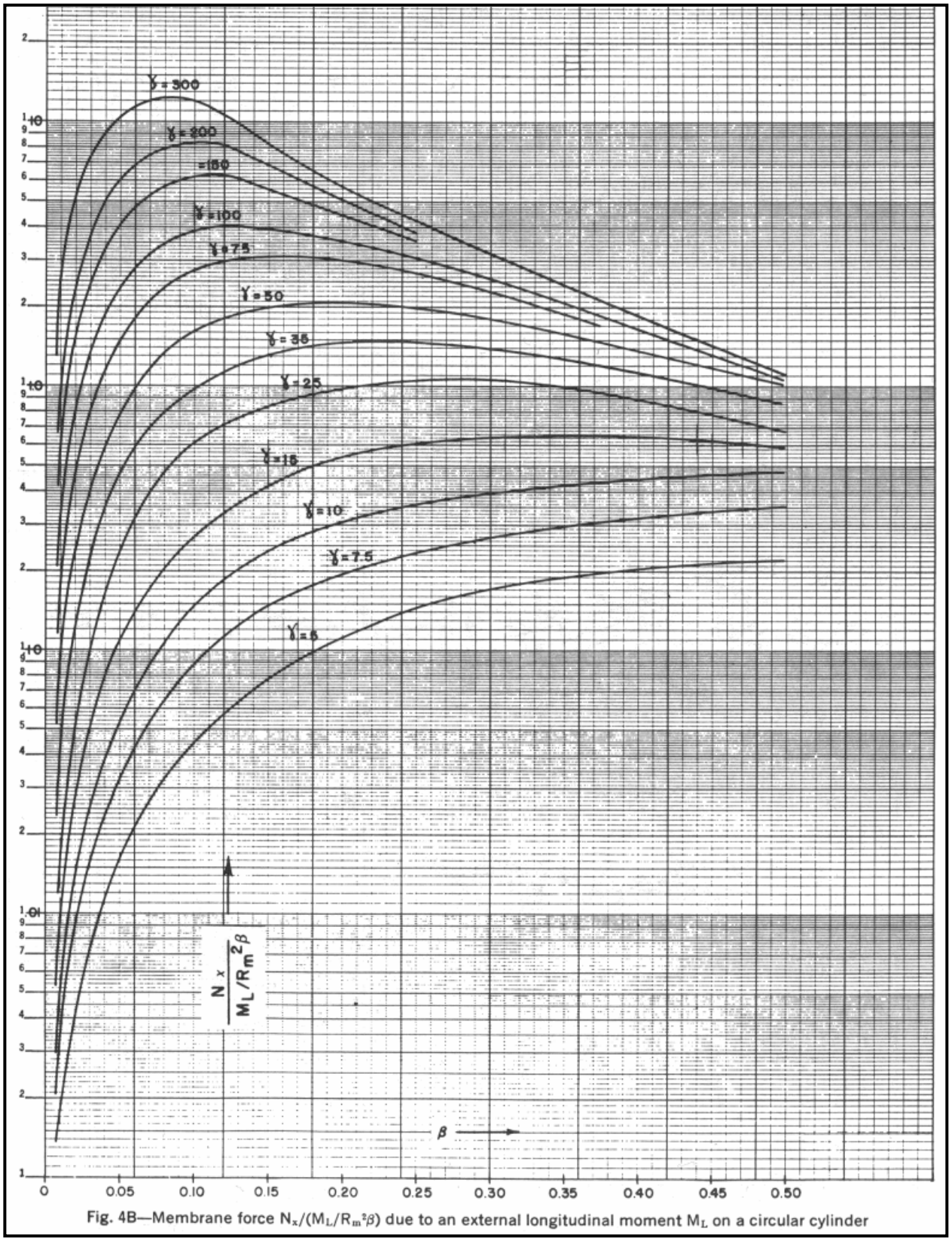

Figure 2.5-13 – Figure 4B from WRC Bulletin 107

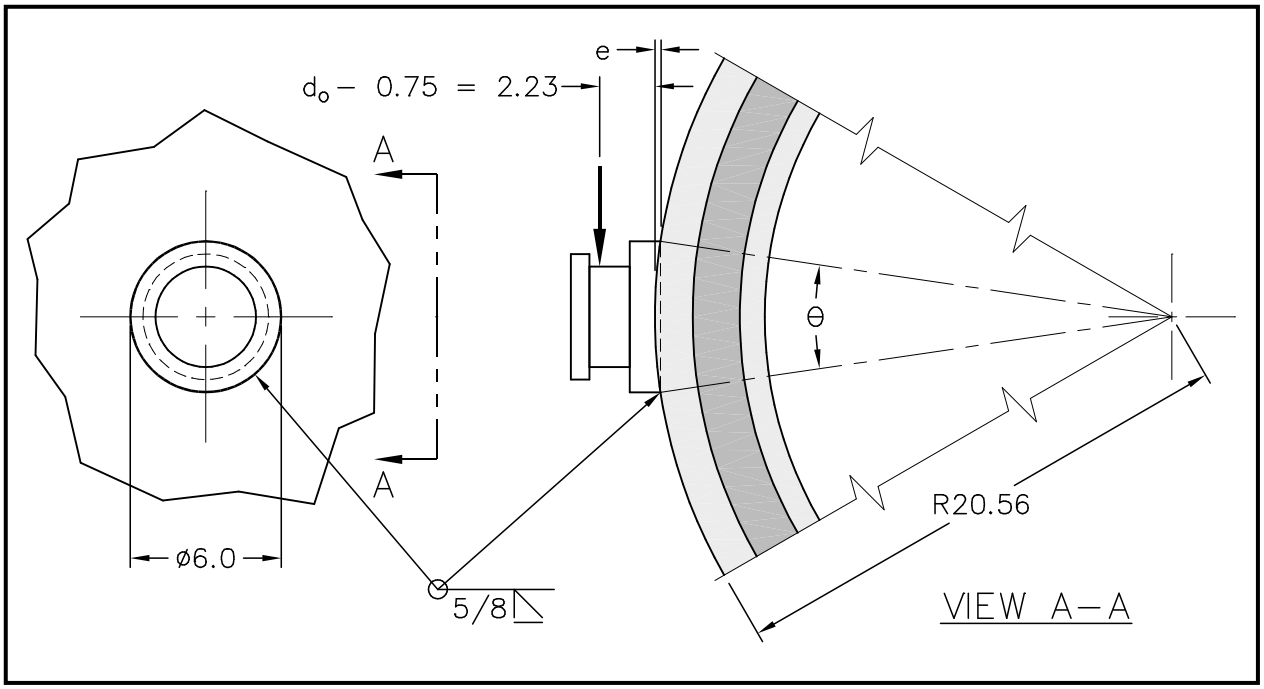

Figure 2.5-14 – Lifting Trunnion Weld Evaluation

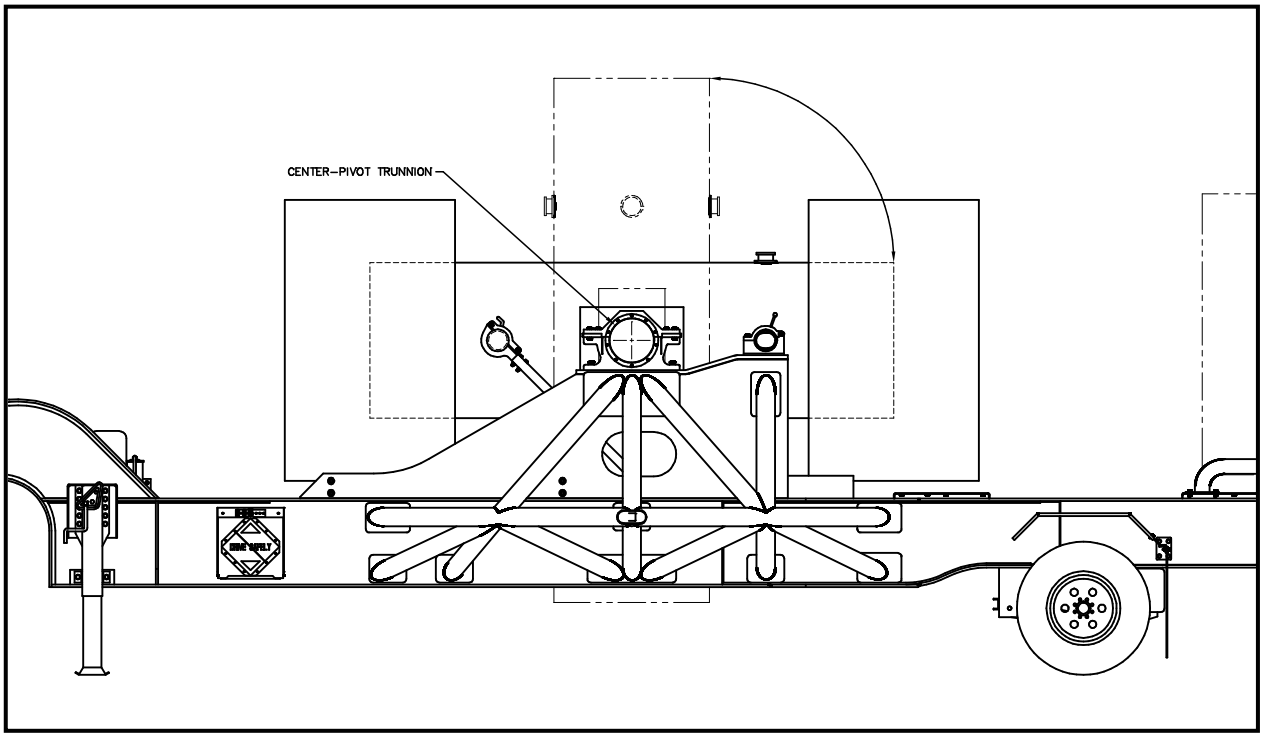

Figure 2.5-15 – Center-Pivot Trailer Configuration

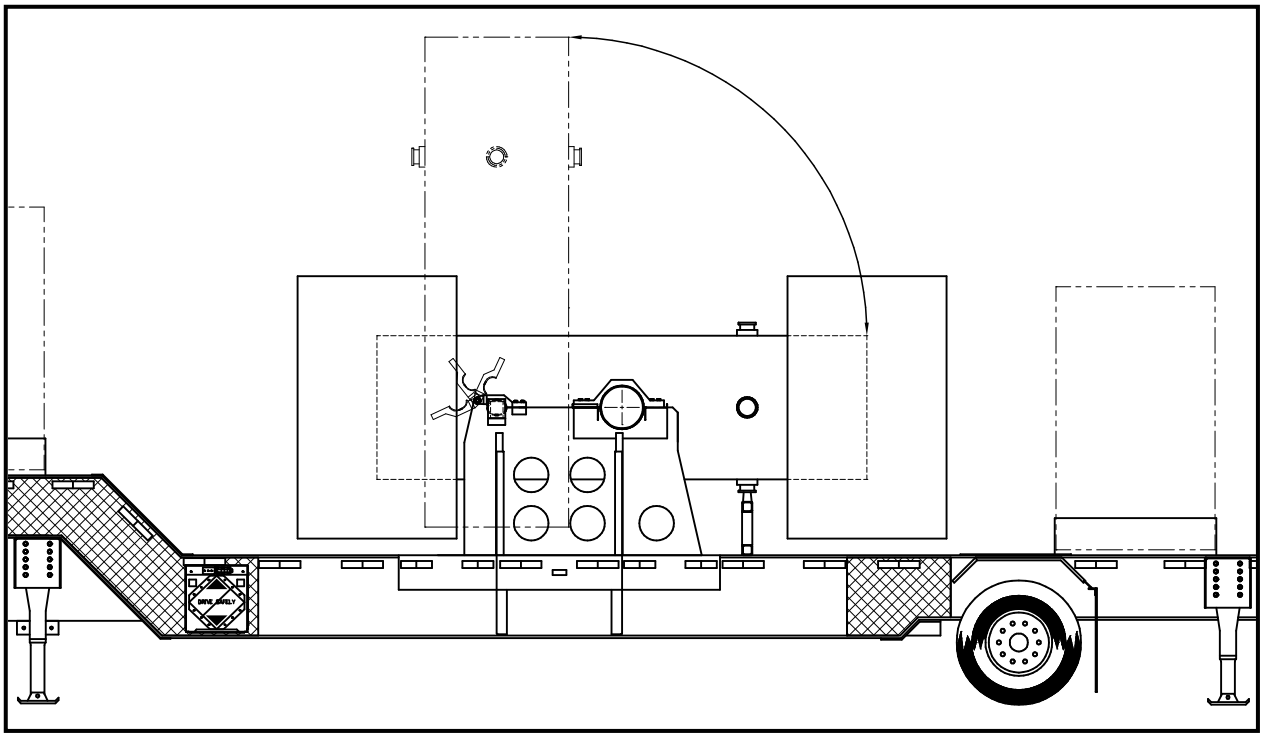

Figure 2.5-16 – Lift-Off Trailer Configuration

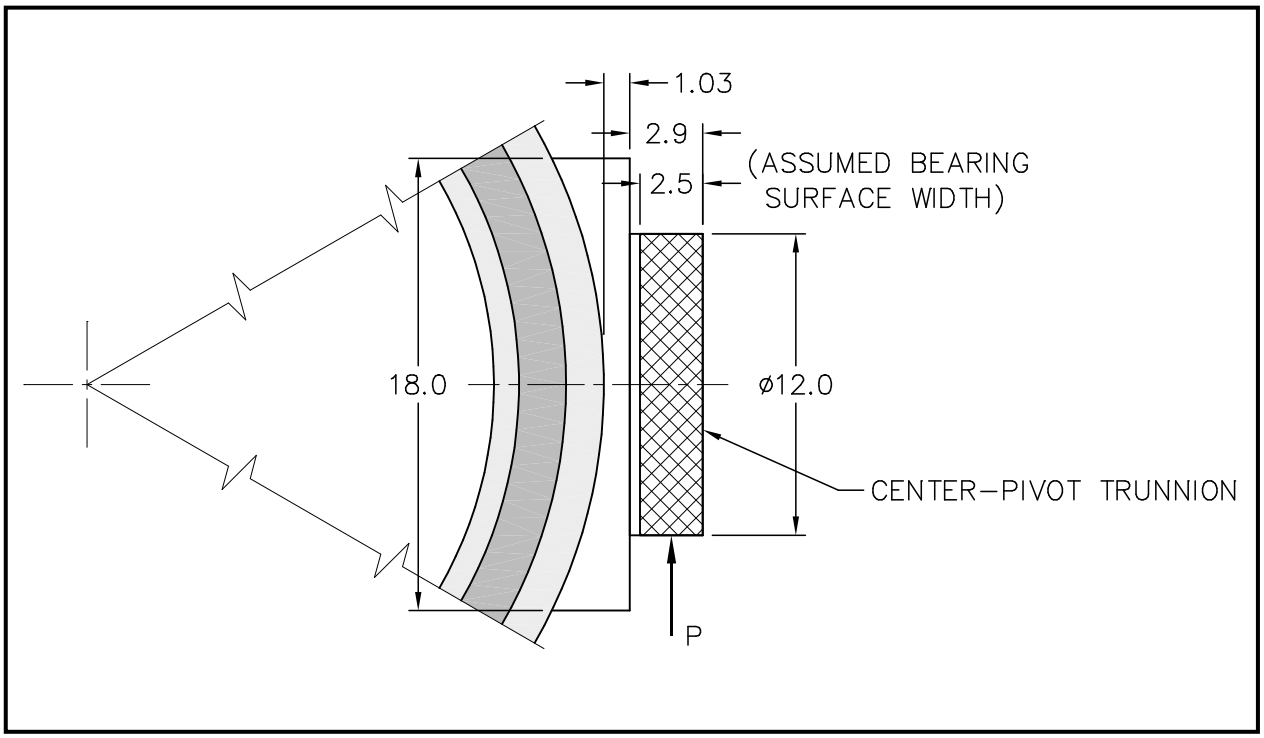

Figure 2.5-17 – Center-Pivot Trunnion Loading Configuration

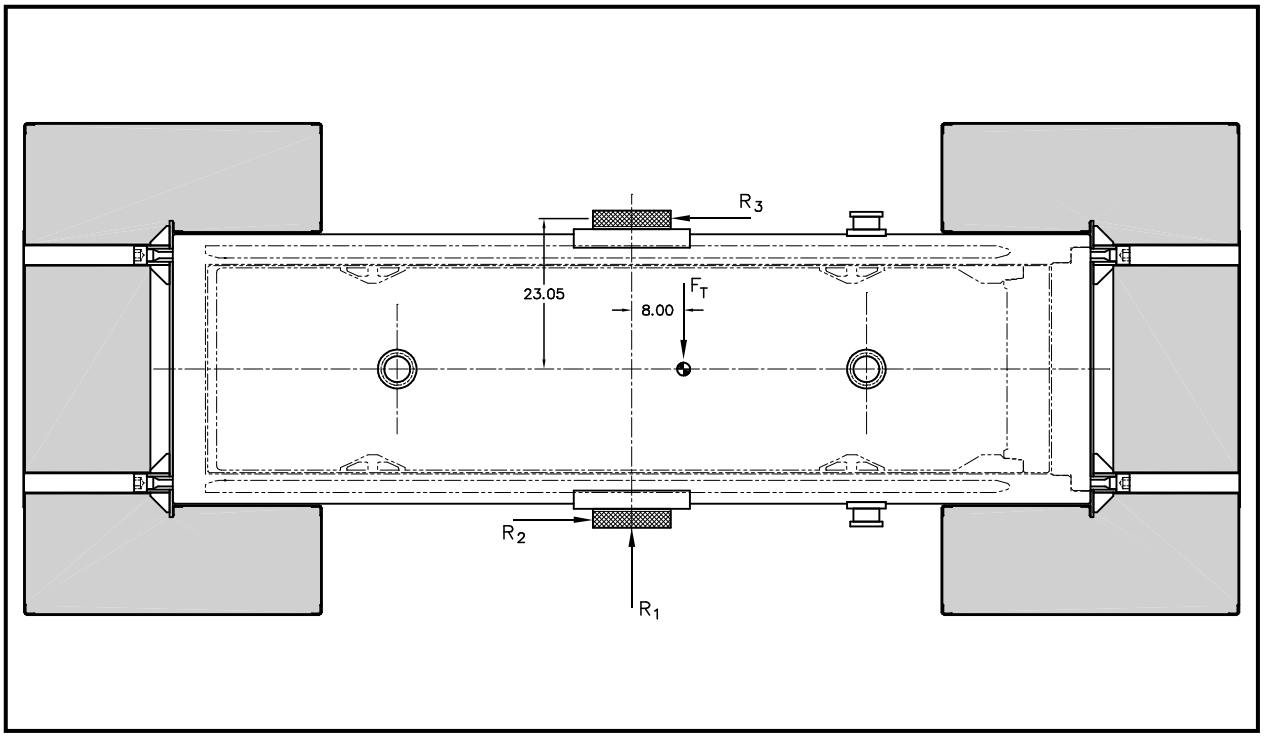

Figure 2.5-18 – Tie-down Loading Configuration

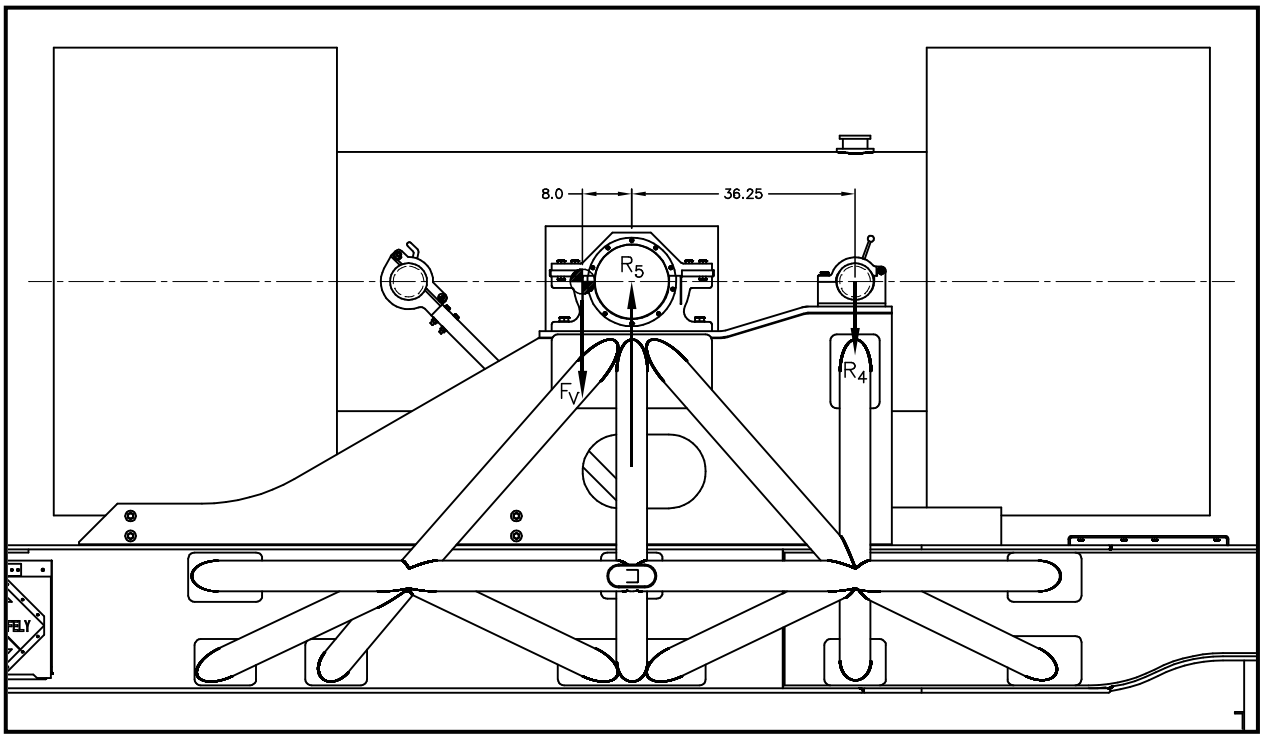

Figure 2.5-19 – Center-Pivot Trailer Free-Body Diagram for Tie-down

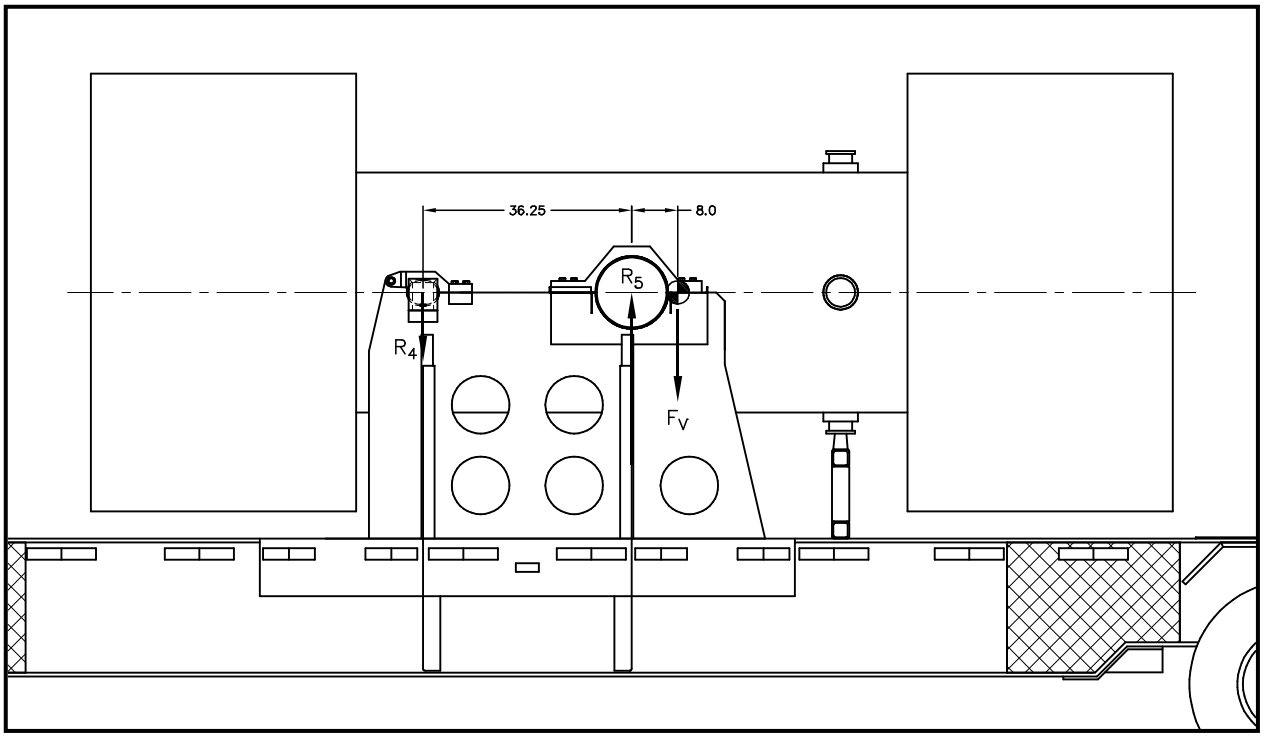

Figure 2.5-20 – Lift-Off Trailer Free-Body Diagram for Tie-down

2.6 Normal Conditions of Transport

The RH-TRU 72-B package, when subjected to normal conditions of transport (NCT) as specified in 10 CFR §71.71[1], meets the performance requirements specified in Subpart E of 10 CFR 71. This conclusion is demonstrated in the following subsections, where each normal condition is addressed and shown to meet the applicable design criteria (except buckling) previously discussed in Section 2.1.2, *Design Criteria*. Buckling evaluations for all buckling sensitive package components are presented in Appendix 2.10.5, *Buckling Design Criteria and Detailed Evaluation*.

Properties of Type 304 stainless steel and lead used in subsequent analyses are summarized in Table 2.6-1.

2.6.1 Heat

The thermal evaluation for the NCT heat condition is presented in Section 3.4, *Thermal Evaluation for Normal Conditions of Transport*. The NCT heat condition consists of exposing the package to direct sunlight and 100 ºF still air per the requirements of 10 CFR §71.71(c)(1)[1], with insolation per NRC Regulatory Guide 7.8[2]. A maximum internal heat load of 50 watts (combustible payload) and 300 watts (non-combustible payload) is used for the evaluation.

2.6.1.1 Summary of Pressures and Temperatures

The conditions of normal heat result in rather modest temperatures throughout the package. Maximum temperatures for the various package components are presented in Table 2.6-2. As indicated, all package structural component temperatures remain below 160 ºF. For many of the analyses herein, a 160 ºF maximum temperature for both the inner vessel (IV) and outer cask (OC) is conservatively employed. The payload canister temperature reaches a maximum of 167 ºF. Therefore a 200 ºF maximum temperature for analysis of the canister is conservatively employed.

The only differential expansions of significance are the radial expansions of the RH-TRU 72-B package cylindrical shells relative to their respective end plates or end attachment hardware. Worst-case temperature differences between shells and their end hardware are available from Section 3.4.5, *Maximum Thermal Stresses*. The difference in temperature between inner and outer shells of the OC (<0.5 ºF) is negligible. It is noted from the thermal analysis results (see Section 3.1, *Discussion*) that the temperatures of the OC shells and lead are greater than the stress free temperature of 89.9 ºF, determined in Appendix 2.10.8, *Fabrication Stresses Due to Lead Pour*, where fabrication stresses are discussed. Therefore, fabrication induced stresses due to lead shrinkage on the inner shell of the OC are relieved under the normal heat condition.

Initial pressure in both the IV and the OC is one (1) atmosphere (14.7 psia). Per Section 3.4.4, *Maximum Internal Pressure*, the design pressure is 150 psig for any package component.

---

[1] Title 10, Code of Federal Regulations, Part 71 (10 CFR 71), *Packaging and Transportation of Radioactive Material*, Final Rule, 01-26-04.

[2] U. S. Nuclear Regulatory Commission, Regulatory Guide 7.8, *Load Combinations for the Structural Analysis of Shipping Packages for Radioactive Material*, Revision 1, March 1989.

2.6.1.2 Differential Thermal Expansion – Radial Expansions of Shells Relative to Their End Hardware

A 3 ºF maximum temperature difference can exist between the OC end-closure plate and the OC inner and outer shells per Section 3.4.5, *Maximum Thermal Stresses*. Treating the end plate as rigid, maximum stresses in the inner and outer shells of the OC are determined as follows (very conservatively assuming a step change in temperature between the shells and their end hardware of 3 ºF):

For the OC inner shell, with a mean shell radius, R_i =16.69 inches, and the coefficient of thermal expansion, $\alpha = 8.69(10)^{-6}$ in/in/ºF, taken at a maximum assumed shell temperature of 160 ºF, the imposed radial deflection is:

$$\delta_i = R_i\alpha(\Delta T) = (16.69)(8.69\times10^{-6})(3) = 0.000435\,\text{in}$$

For the OC outer shell, with a mean shell radius, R_o =19.813 inches, the imposed radial deflection is:

$$\delta_o = R_o\alpha(\Delta T) = (19.813)(8.69\times10^{-6})(3) = 0.000517\,\text{in}$$

Rotations, θ, at the shell ends are set equal to zero. From Table 30, Cases 8 and 10, of Roark[3]:

$$\delta = \frac{V_o}{2D\lambda^3} - \frac{M_o}{2D\lambda^2}$$

$$\theta = -\frac{V_o}{2D\lambda^2} + \frac{M_o}{D\lambda}$$

Shell parameters D and λ for the OC inner shell are:

$$D = \frac{Et^3}{12(1-\mu^2)} = \frac{(27.8\times10^6)(1.0)^3}{12(1-(0.3)^2)} = 2.546\times10^6\ \text{in-lb}$$

$$\lambda = \sqrt[4]{\frac{3(1-\mu^2)}{R^2t^2}} = \sqrt[4]{\frac{3(1-(0.3)^2)}{(16.69)^2(1.0)^2}} = 0.3146\,\text{in}^{-1}$$

where the mean inner shell radius, R = 16.69 inches, the shell thickness, t = 1.00 inch, the elastic modulus, $E = 27.8(10)^6$ psi at 160 ºF, and Poisson's ratio, μ = 0.3.

With the displacement of the inner shell, δ_i = 0.000435 inches and the slope, θ = 0 radians, solving for V_o and M_o from the above equations yields V_o = 137.9 lb/in, and M_o = 219.2 in-lb/in.

The stress components, from Table 30, Cases 8 and 10, of Roark[3] are:

$$\sigma_1 = 0.0\,\text{psi}\ \ (\text{axial membrane stress})$$

[3] R. J. Roark, W. C. Young, *Formulas for Stress and Strain*, 5th Edition, McGraw-Hill, Inc., New York, NY, 1975.

$$\sigma_2 = \frac{2V_o\lambda R}{t} - \frac{2M_o\lambda^2 R}{t} = 724\,\text{psi (hoop membrane stress)}$$

$$\sigma_1' = \frac{6M_o}{t^2} = 1{,}315\,\text{psi (axial bending stress)}$$

$$\sigma_2' = \mu\sigma_1' = 395\,\text{psi (hoop bending stress)}$$

Repeating the above analysis for the OC outer shell yields the following:

$$D = \frac{Et^3}{12(1-\mu^2)} = \frac{(27.8\times10^6)(1.5)^3}{12(1-(0.3)^2)} = 8.592\times10^6\ \text{in-lb}$$

$$\lambda = \sqrt[4]{\frac{3(1-\mu^2)}{R^2t^2}} = \sqrt[4]{\frac{3(1-(0.3)^2)}{(19.813)^2(1.5)^2}} = 0.2358\,\text{in}^{-1}$$

where the mean inner shell radius, R = 19.813 inches, the shell thickness, t = 1.50 inches, the elastic modulus, E = 27.8(10)^6 psi at 160 ºF, and Poisson's ratio, μ = 0.3.

With the displacement of the outer shell, δ_o = 0.000517 inches and the slope, θ = 0 radians, solving for V_o and M_o from the above equations yields V_o = 233 lb/in, and M_o = 494 in-lb/in.

The stress components, from Table 30, Cases 8 and 10, of Roark[3] are:

$$\sigma_1 = 0.0\,\text{psi (axial membrane stress)}$$

$$\sigma_2 = \frac{2V_o\lambda R}{t} - \frac{2M_o\lambda^2 R}{t} = 725\,\text{psi (hoop membrane stress)}$$

$$\sigma_1' = \frac{6M_o}{t^2} = 1{,}317\,\text{psi (axial bending stress)}$$

$$\sigma_2' = \mu\sigma_1' = 395\,\text{psi (hoop bending stress)}$$

The above analyses are now repeated for the IV. From Section 3.4.5, *Maximum Thermal Stresses*, the thermal gradient for the IV shell is 5 ºF. Maximum temperature for the IV is taken as 160 ºF for these calculations. For the IV shell, with a mean shell radius, R_i =15.81 inches, and the coefficient of thermal expansion, α = 8.69(10)$^{-6}$ in/in/ºF, the imposed radial deflection is:

$$\delta = R\alpha(\Delta T) = (15.81)(8.69\times10^{-6})(5) = 0.000687\,\text{in}$$

Shell parameters D and λ for the IV shell are:

$$D = \frac{Et^3}{12(1-\mu^2)} = \frac{(27.8\times10^6)(0.375)^3}{12(1-(0.3)^2)} = 1.343\times10^5\ \text{in-lb}$$

$$\lambda = \sqrt[4]{\frac{3(1-\mu^2)}{R^2 t^2}} = \sqrt[4]{\frac{3(1-(0.3)^2)}{(15.81)^2(0.375)^2}} = 0.5279\,\text{in}^{-1}$$

where the mean inner shell radius, R = 15.81 inches, the shell thickness, t = 0.375 inches, the elastic modulus, $E = 27.8(10)^6$ psi at 160 ºF, and Poisson's ratio, $\mu = 0.3$.

With the displacement of the inner shell, $\delta = 0.000687$ inches and the slope, $\theta = 0$ radians, solving for V_o and M_o from the above equations yields $V_o = 54.3$ lb/in, and $M_o = 51.4$ in-lb/in.

The stress components, from Table 30, Cases 8 and 10, of Roark[3] are:

$$\sigma_1 = 0.0\,\text{psi}\ \ (\text{axial membrane stress})$$

$$\sigma_2 = \frac{2V_o\lambda R}{t} - \frac{2M_o\lambda^2 R}{t} = 1{,}208\,\text{psi}\ \ (\text{hoop membrane stress})$$

$$\sigma_1' = \frac{6M_o}{t^2} = 2{,}193\,\text{psi}\ \ (\text{axial bending stress})$$

$$\sigma_2' = \mu\sigma_1' = 658\,\text{psi}\ \ (\text{hoop bending stress})$$

Since these thermal stresses are deformation limited, they can be classified as secondary stresses. The NCT allowable for range of primary-plus-secondary stress intensity is $3.0S_m$, or 60,000 psi for the Type 304 stainless steel used within the RH-TRU 72-B package. Conservatively combining the highest NCT secondary stress intensity determined above (2,193 psi) with the highest NCT primary membrane-plus-bending stress intensity anywhere in the package, excluding bolts (11,153 psi at the center of the OC lid for pressure-plus-end drop loading, per Table 2.6-8 of Section 2.6.7.1, *Flat End Drop*) results in a primary-plus-secondary stress intensity of 11,153 + 2,193 = 13,346 psi. By conservatively assuming fully reversing stress states, the range of primary-plus-secondary stress intensity becomes:

$$SI_{range} = 2(13{,}346) = 26{,}692\,\text{psi}$$

and the corresponding margin of safety is:

$$MS = \frac{60{,}000}{26{,}692} - 1 = +1.25$$

Per the above discussion, the remainder of this section does not specifically address thermal stresses when load combinations are made. In other words, the design is governed by primary, load-controlled stresses and the corresponding limits specified in Section C.2 of NRC Regulatory Guide 7.6[4] rather than by primary-plus-secondary stresses and the $3.0S_m$ limit specified in Section C.4. However, buckling evaluations presented in Appendix 2.10.5, *Buckling Design Criteria and Detailed Evaluation*, do consider secondary thermal stresses.

[4] U. S. Nuclear Regulatory Commission, Regulatory Guide 7.6, *Design Criteria for the Structural Analysis of Shipping Package Containment Vessels*, Revision 1, March 1978.

2.6.1.3 Stress Calculations

This section presents calculations of pressure induced stresses on the various package components. Unit pressure is first considered and appropriate factors are then applied to arrive at stresses for particular loading cases of interest. Locations of interest for the RH-TRU 72-B package are shown in Figure 2.6-1.

The only significant mechanical loading on the RH-TRU 72-B package is dead weight. As free drop cases impose higher mechanical loadings on the package than does dead weight alone, combinations of pressure loads and mechanical loadings due to free drop govern the design and are presented in Section 2.6.7, *Free Drop*. Fatigue is not a concern as discussed in Section 2.1.2.2.2, *Fatigue*.

2.6.1.3.1 Stresses Due To Unit Pressures

Referring to Figure 2.6-1, geometries and temperatures for the various locations (P1 through P10) are summarized in Table 2.6-3.

For locations P1, P2, and P3 (away from the cylinder ends),

$$\sigma_1 = \frac{pr}{2t} \text{ (axial membrane stress)}$$

$$\sigma_2 = \frac{pr}{t} \text{ (hoop membrane stress)}$$

$$\sigma_1' = 0 \text{ (axial bending stress)}$$

$$\sigma_2' = 0 \text{ (hoop bending stress)}$$

For locations P4 and P5 (at the OC cylinder ends), stresses are determined from Table 29, Case 1c, and Table 30, Cases 8 and 10, of Roark[3]:

$$\sigma_1 = \frac{pr}{2t} \text{ (axial membrane stress)}$$

$$\sigma_2 = \frac{pr}{t} - \frac{2V_o\lambda r}{t} + \frac{2M_o\lambda^2 r}{t} \text{ (hoop membrane stress)}$$

$$\sigma_1' = -\frac{6M_o}{t^2} \text{ (axial bending stress)}$$

$$\sigma_2' = -\frac{\mu 6M_o}{t^2} \text{ (hoop bending stress)}$$

where shell parameters D and λ are:

$$D = \frac{Et^3}{12(1-\mu^2)}$$

$$\lambda = \sqrt[4]{\frac{3(1-\mu^2)}{r^2t^2}}$$

In addition, the radial displacement, δ, and axial slope, θ, are as follows:

$$\delta = \frac{pr^2}{Et}\left(1-\frac{\mu}{2}\right) - \frac{V_o}{2D\lambda^3} + \frac{M_o}{2D\lambda^2} = 0$$

$$\theta = \frac{V_o}{2D\lambda^2} - \frac{M_o}{D\lambda} = 0$$

where the elastic modulus, $E = 27.8(10)^6$ psi at 160 ºF, Poisson's ratio, $\mu = 0.3$, and the unit pressure, $p = 1.0$ psi.

For locations P4 and P5 it is necessary to solve the two equations ($\delta = 0 = ...$) and ($\theta = 0 = ...$) simultaneously for V_o and M_o in each case. This yields the following results:

$$V_o = 3.604 \text{ lb/in (for P4)}$$

$$M_o = 7.644 \text{ in - lb/in (for P4)}$$

$$V_o = 2.701 \text{ lb/in (for P5)}$$

$$M_o = 4.292 \text{ in - lb/in (for P5)}$$

For location P6, a radius transition is provided between the shell and the end plate. The complicated geometry of this transition precludes the use of classical stress analysis techniques. Therefore, a finite element analysis has been performed for this structure to obtain the stresses associated with P6. For more details of this finite element model see Appendix 2.10.1.2, *Inner Vessel Radius Transition Zone Stresses Due to Pressure*.

Table 2.6-4 summarizes the results for locations P1 through P6.

Locations P7 through P10 are considered utilizing Table 24, Case 10a, of Roark[3]. Assuming a simply-supported plate with a uniform loading, the bending moment, M_o, and stress, σ, are:

$$M_o = \frac{pa^2(3+\mu)}{16}$$

$$\sigma = \frac{6M_o}{t^2} = \frac{3pa^2(3+\mu)}{8t^2}$$

where a is the plate radius, t is the plate thickness, Poisson's ratio, $\mu = 0.3$, and the unit pressure, $p = 1.0$ psi.

Table 2.6-5 summarizes the results for locations P7 through P10.

2.6.1.3.2 Stresses Due to Maximum Pressures

The maximum internal pressure acting on any component in the RH-TRU 72-B Package is 150 psig. Utilizing the unit stresses developed in Section 2.6.1.3.1, *Stresses Due To Unit Pressures*, maximum pressure stress results are shown in Table 2.6-6 for P1 – P10.

2.6.1.4 Comparison with Allowable Stresses

As discussed in Section 2.6.1.3, *Stress Calculations*, load combinations and comparisons with allowable stress limits are presented in Section 2.6.7, *Free Drop*, where worst-case combined load cases are addressed.

2.6.2 Cold

For the cold condition, a -40 ºF steady state ambient temperature and no internal heat generation are assumed. This results in a uniform temperature throughout the package of -40 ºF. The materials of construction for the package are not adversely affected by the -40 ºF condition. In particular, brittle fracture is not a concern, as discussed in Section 2.1.2.2.1, *Brittle Fracture*.

The only concern identified with the cold condition is with shrinkage of the lead onto the inner shell of the OC. As shown in Appendix 2.10.8, *Fabrication Stresses Due to Lead Pour*, a hoop stress of -1,837 psi and an axial stress of -1,979 psi can develop in the inner shell when cooled to -40 ºF. This case is independent of other load cases and will not, therefore, limit the package design. However, a -20 ºF case must be considered as a possible initial condition for other load cases, per 10 CFR §71.71(b)[1]. The hoop stress is -1,821 psi, and the axial stress is -1,963 psi at -20 ºF, per Appendix 2.10.8, *Fabrication Stresses Due to Lead Pour*. These stresses are determined by conservatively neglecting the beneficial effects of lead creep.

An additional discussion of fabrication induced stresses due to lead shrinkage onto the OC inner shell is contained in Section 2.6.7.1, *Flat End Drop*. The analysis therein assesses the consequences of a flat end drop of the package. In order to arrive at appropriate initial conditions for the drop, a special process of molten lead cooldown is followed, to properly control solidification.

2.6.3 Reduced External Pressure

The effect of reduced external pressure of 3.5 psia (11.2 psig internal pressure), per 10 CFR §71.71(c)(3)[1], is considered negligible to the RH-TRU 72-B package. This conclusion is based upon the calculations presented in Section 2.6.1.3.2, *Stresses Due to Maximum Pressures*, which assesses package survivability at a NCT internal pressure of 150 psig.

2.6.4 Increased External Pressure

The effect of increased external pressure of 20 psia (5.3 psig external pressure), per 10 CFR §71.71(c)(4)[1], is considered negligible to the RH-TRU 72-B package due to the thick OC outer shell and end closures. Additionally, Section 2.6.7, *Free Drop*, addresses a multiplicity of different loading cases in excess of the prescribed requirements.

2.6.5 Vibration

The effect of vibrations normally incident to transport are considered to be negligible. This conclusion is drawn based on the small stresses obtained throughout the OC and IV for the side drop event discussed in Section 2.6.7.3, *Flat Side Drop*. Per that section, the NCT side drop results in a 19.3*g* lateral acceleration on the package that translates to stresses in the package, as given in Table 2.6-7.

As a conservative worst-case, normal vibration *g*-loads are assumed equal to the normal vertical loading imposed on tie-downs. Utilizing the specification in 10 CFR §71.45(b)(1)[1] of 2*g* in the vertical direction, the maximum combined stress, S, is found by ratioing to be 489 psi in the IV. This stress is well below the endurance limit for Type 304 stainless steel at 160 ºF. From Figure 2.6-2 (Figure I-9.2.2 from Appendix I of the ASME Code[5]), for 10^9 cycles, and correcting for the ratio of elastic moduli at room temperature and 160 ºF, the minimum allowable alternating stress intensity, S_a, becomes

$$S_a = (14{,}000)\left(\frac{27.8(10)^6}{28.3(10)^6}\right) = 13{,}753\ \text{psi}$$

The IV shell vibratory stress margin of safety is:

$$MS = \frac{S_a}{S} - 1 = \frac{13{,}753}{489} - 1 = +27.1$$

e tie-down trunnions must also resist the 2*g* vibration loading. The maximum center-pivot trunnion load, P, with an inertia load of 2*g* is:

$$P = \frac{(2g)(45{,}000)}{2\ \text{trunnions}} = 45{,}000\ \text{lb}$$

The center-pivot trunnion was evaluated with a vertical load (i.e., no longitudinal or transverse loads included), P_v = 54,931 pounds, as discussed in Appendix 2.10.1.1, *Tie-down Trunnion Analysis*, with a resulting maximum OC outer shell stress intensity, S_{max} =1,972 psi.

With a maximum temperature for the trunnions taken at 160 ºF, and assuming 10^9 cycles of stress, the allowable alternating stress intensity, S_a, has previously been calculated to be 13,753 psi. The center-pivot trunnion vibratory stress minimum margin of safety is therefore:

$$MS = \frac{S_a}{S} - 1 = \frac{13{,}753}{1{,}972} - 1 = +5.97$$

Therefore, the requirements of 10 CFR §71.71(c)(5)[1] have been met.

[5] American Society of Mechanical Engineers (ASME) Boiler and Pressure Vessel Code, Section III, *Rules for Construction of Nuclear Power Plant Components*, Division 1, Subsection NB and Appendices, 1986 Edition.

2.6.6 Water Spray

Due to the materials of construction utilized for the RH-TRU 72-B package, the water spray test requirement, per 10 CFR §71.71(c)(6)[1], will have a negligible effect on this package.

2.6.7 Free Drop

The RH-TRU 72-B shipping package weighs 45,000 pounds. Subpart F of 10 CFR 71[1] requires that a package in excess of 33,000 pounds weight be dropped one (1) foot onto a flat, essentially unyielding, horizontal surface, striking the surface in a position for which maximum damage is expected. The following subsections address free drops at all angles with respect to horizontal. It is shown that all conditions of 10 CFR §71.71[1] have been met.

The analyses in this section extract accelerations from impact analysis results summarized in Appendix 2.10.3, *Drop Impact Evaluation Results*, and statically apply them to the package. The durations of impact loadings are relatively long as the result of using soft (relative to the steel structures) energy absorbing impact limiters to protect the package during free drop events. The package frequencies are high as the result of using relatively thick, stiff shells for the OC. To verify these assertions, the impact duration and natural frequency of the package will be approximated using simple, conservative calculations. For illustration purposes, end impact will be analyzed, since flat end drop immediately mobilizes the largest area of the impact limiter, the flat end surface. Consequently, the impact duration for end drop can be expected to be the least of all drop orientations, and will thus conservatively bound impact durations for the other free drop orientations.

For the purpose of approximating impact duration, the package is considered to be a rigid mass on a constant force damper, which is the impact limiter. The assumption of a constant force response from the impact limiter is based on the conservative presumption that all of the foam is mobilized in pure compression throughout the duration of the event. This type of response is referred to as "fully effective" in the drop analysis results presented in Appendix 2.10.3, *Drop Impact Evaluation Results*. Such a response will result in greater energy absorption in less time, thus minimizing impact duration.

This system can be represented by the following single degree of freedom equation:

$$M\frac{\partial^2 y}{\partial t^2} = F_y - Mg$$

where the package mass, $M = W/g = 45{,}000/386.4 = 116.5$ lb-sec^2/in, the package weight, $W = 45{,}000$ lb, the gravitational constant, $g = 386.4$ in/sec^2, the direction of the drop, assumed positive upward, is y, the time is t, and the impact limiter crush force for flat end drop is F_y.

For the assumed constant force response, the impact limiter reaction force is:

$$F_y = \sigma_c A$$

where the polyurethane foam "plateau" stress, $\sigma_c \approx 700$ lb/in^2 at 40% strain per Table 2.3-3 for the parallel-to-rise orientation cold condition, the impact limiter cross-sectional area, $A = (\pi/4)D^2 = 4{,}536.5$ in^2, and the impact limiter diameter, $D = 76.0$ inches.

Since the impact limiter reaction force is independent of time, the governing equation may be integrated once to yield:

$$M\frac{dy}{dt} = (F_y - Mg)t + c$$

where the vertical velocity, dy/dt = v_y, and the constant of integration is c. To evaluate the constant of integration, consider that, at time t = 0 seconds (instant of initial impact):

$$v_y = v_o = \sqrt{2gh} = -527.5 \text{ in/sec}$$

where the drop height, h = 30 ft = 360 inches, and the gravitational constant, g = 386.4 in/sec^2. Inserting t = 0 seconds and $v_y = v_o$ into the previous equation and solving for c results in:

$$c = Mv_o$$

With this constant now defined, and recognizing that W = Mg, the governing equation can be solved for time t:

$$t = -\frac{W(v_y - v_o)}{g(\sigma_c A - W)}$$

The duration of the impact, t, can be determined by realizing that, at the end of the impact event, v_y = 0 in/sec. Substituting in the appropriate quantities, the minimum free drop impact duration may thus be approximated as:

$$t = -\frac{(45{,}000)(0 - 527.5)}{(386.4)[(700)(4{,}536.5) - 45{,}000]} = 0.02 \text{ sec}$$

The corresponding fundamental natural period of the package will now be determined. The response of the OC is assumed to dominate the package system for end impact, and the mass and damping effect of the IV and payload are ignored. The OC is modeled as a massless spring with a rigid mass (closure components plus impact limiter) at each end. From the tables on Page 1-12 of *Shock and Vibration Handbook*[6], the governing equation for the assumed vibratory system is:

$$\omega_n = \sqrt{\frac{k(m_1 + m_2)}{m_1 m_2}}$$

where the fundamental angular natural frequency of the spring-mass system is ω_n, the spring constant of the massless spring, k = AE/L, the cross-section area of the OC is A, the modulus of elasticity of the OC material is E, the length of the OC shells is L, the mass of bottom impact limiter and base plate, $m_1 = W_1/g$, the weight of bottom impact limiter and base plate is W_1, the mass of the top impact limiter, upper forging, and lid, $m_2 = W_2/g$, the weight of the top impact limiter, upper forging, and lid is W_2, and the gravitational constant, g = 386.4 in/sec^2.

The fundamental natural frequency of the spring-mass system, f_n, is:

[6] Cyril M. Harris, *Shock and Vibration Handbook*, 3rd edition, McGraw-Hill, Inc., New York, NY, 1988.

$$f_n = \frac{\omega_n}{2\pi}$$

and the fundamental natural period of the spring-mass system, τ_n, is:

$$\tau_n = \frac{1}{f_n} = \frac{2\pi}{\omega_n} = 2\pi\sqrt{\frac{m_1 m_2}{k(m_1 + m_2)}} = 2\pi\sqrt{\frac{W_1 W_2}{kg(W_1 + W_2)}}$$

The composite equivalent axial stiffness, EA, of the OC can be determined from the method described in Section 2.1.3 of NUREG/CR-3966[7]:

$$EA = E_1 A_1 + E_2 A_2 + E_3 A_3$$

where the modulus of elasticity of the OC inner shell is E_1, the cross-sectional area of OC inner shell, $A_1 = \pi(r_2^2 - r_1^2)$, the modulus of elasticity of the lead column is E_2, the cross-sectional area of lead column, $A_2 = \pi(r_3^2 - r_2^2)$, the modulus of elasticity of the OC outer shell is E_3, the cross-sectional area of OC outer shell, $A_3 = \pi(r_4^2 - r_3^2)$, the OC inner shell inner radius is r_1, the OC inner shell outer radius and lead column inner radius is r_2, the OC outer shell inner radius and lead column outer radius is r_3, and the OC outer shell outer radius is r_4.

From Table 2.2-1 in Section 2.2, *Weights and Centers of Gravity*, W_1 = 2,547 lb (bottom impact limiter) + 1,967 lb (base plate) = 4,514 lb, and W_2 = 2,547 lb (top impact limiter) + 2,000 lb (upper forging) + 1,667 lb (lid) = 6,214 lb. From the drawings in Appendix 1.3.1, *Packaging General Arrangement Drawings*, r_1 = 16.19 inches, r_2 = 17.19 inches, r_3 = 19.07 inches, r_4 = 20.57 inches, and L = 124.25 inches.

From Table 2.6-1, $E_1 = E_3 = 28.3(10)^6$ lb/in^2 for Type 304 stainless steel, and $E_2 = 2.34(10)^6$ lb/in^2 for lead.

Substituting the above quantities into the appropriate equations results in:

$$EA = [28.3(10)^6](104.9) + [2.34(10)^6](214.2) + [28.3(10)^6](186.8) = 8.75(10)^9 \text{ lb}$$

$$k = \frac{EA}{L} = \frac{8.75(10)^9}{124.25} = 70.43(10)^6 \text{ lb/in}$$

$$\tau_n = 2\pi\sqrt{\frac{(4{,}514)(6{,}214)}{[70.43(10)^6](386.4)(4{,}514 + 6{,}214)}} = 0.002 \text{ sec}$$

Since the fundamental natural period of the package is an order of magnitude less than the minimum impact duration, it may be concluded that dynamic effects of the package arising from the impact will be negligible.

In addition, inspection of accelerometer data available from NuPac 125-B quarter-scale drop tests (NRC Certificate of Compliance No. 9200[8]) indicates that this type of package responds essentially

[7] T. A. Nelson, R. C. Chun, *Methods for Impact Analysis of Shipping Containers*, NUREG/CR-3966, Lawrence Livermore National Laboratory, Livermore, CA, November 1987.

as a rigid body (e.g., for end and oblique drops, all axial accelerometer traces are very nearly the same and, for side drop, the accelerations for all accelerometers oriented in the direction of the drop are nearly identical). This observation further justifies static application of *g*-loads.

2.6.7.1 Flat End Drop

Analysis of RH-TRU 72-B package behavior for the end drop event is performed in the following steps:

(1) Analyze the impact force using the CASKDROP computer program.

(2) Analyze the OC lid for bending assuming the IV and payload canister act as a uniform load on a simply supported plate (no impact limiter support).

(3) Analyze the OC lid for bending, as performed in (2), but with the impact limiter foam pressure acting in the opposite direction (impact limiter support).

(4) Analyze the stresses in the OC lid bolts.

(5) Analyze the IV stresses.

(6) Analyze the axial and hoop stresses in the OC shells and lead (maximum fabrication stress condition assumed).

(7) Analyze the axial and hoop stresses in the OC shells and lead (zero fabrication stress condition assumed).

(8) Analyze the payload canister stresses.

(9) Determine the amount of lead slump.

Material properties and allowable stresses corresponding to maximum enveloping temperature of 160 ºF for the Type 304 stainless steel OC and IV and lead are given in Table 2.6-1. Buckling is addressed in Appendix 2.10.5, *Buckling Design Criteria and Detailed Evaluation*.

Where possible, the analyses in this section are performed on the basis of a unit (1*g*) axial acceleration, with actual acceleration numbers being substituted at the final point of calculating stresses. From Table 2.10.3-10 in Appendix 2.10.3, *Drop Impact Evaluation Results*, the maximum *g*-load for the NCT flat end drop case is 42.5*g* (i.e., at -20 ºF and fully effective foam).

(1) End Drop Computer Analysis Using CASKDROP

The end drop analysis was performed utilizing the energy balance computer program, CASKDROP, documented in Appendix 2.10.2.1, *Description of the CASKDROP Computer Code*. Two cases were run assuming fully effective impact limiters, and considering the variations in foam strength due to temperature effects and the possible variations in foam strength from nominal values (see Section 2.3, *Mechanical Properties of Materials*). Fully effective impact limiter cases consider the entire impact limiter impact area available for crush. Based on the half-scale test results documented in Appendix 2.10.7, *Static and Dynamic Testing*, the fully effective impact limiter assumption is realistic. Output for each of the end drop cases is presented in Appendix

[8] Nuclear Packaging, Inc., *Safety Analysis Report for the NuPac 125-B Fuel Shipping Package*, USNRC Certificate of Compliance 71-9200, U.S. Department of Energy, Washington, D.C.

2.10.3, *Drop Impact Evaluation Results*. The worst-case deflections and accelerations are utilized for all analyses. From Appendix 2.10.3, *Drop Impact Evaluation Results*, the maximum NCT acceleration and maximum impact limiter deflection for a one-foot end drop is 42.5*g* at -20 ºF (Table 2.10.3-2) and 0.86 inches at 140 ºF (Table 2.10.3-3), respectively.

(2) OC Lid Bending Analysis Assuming No Impact Limiter Support

The OC lid is 6.00 inches thick and the welded end closure plate is 5.00 inches thick. The welded end closure plate is reasonably treated as a fixed-edge plate. Treating the bolted lid as a simply supported plate is conservative.

Therefore, to conservatively bound the problem, a 5-inch thick plate is analyzed as simply supported. The unit stress in the OC lid, σ, may be calculated by utilizing Table 24, Case 10a, of Roark[3], assuming a uniform load across the entire area:

$$\sigma = \frac{6M}{t^2} = \frac{3qa^2(3+\mu)}{8t^2} = 216 \text{ psi}/g$$

where the unit pressure, q = W/A = 13,690/1,110 = 12.33 lb/in^2, the IV weight + canister weight + OC lid weight, W = 13,690 pounds, the exterior OC lid area, A = $\pi(18.80)^2$ = 1,110 in^2, the exterior OC lid radius, a = 18.80 inches, Poisson's ratio, μ = 0.3, and the OC lid thickness, t = 5.00 inches.

Applying 42.5*g* acceleration from the NCT end drop analysis (Table 2.10.3-10 in Appendix 2.10.3, *Drop Impact Evaluation Results*) the bending stress, σ, becomes:

$$\sigma = (216)(42.5) = 9{,}180 \text{ psi}$$

Table 2.6-8 combines this stress with that due to a 150 psig normal pressure loading. As shown, the resultant margin of safety is +1.69. This margin is somewhat conservative as accelerations applied to the lid are those corresponding to a drop at -20 ºF, whereas allowables are taken at a temperature of 160 ºF.

(3) OC Lid Bending Analysis Assuming Full Impact Limiter Support

As analyzed above, assume the OC lid is supported across the impact plane by the foam. As before, the unit stress in the OC lid, σ, may be calculated by utilizing Table 24, Case 10a, of Roark[3], assuming a uniform load across the entire area:

$$\sigma' = \frac{6M'}{t^2} = \frac{3q'a^2(3+\mu)}{8t^2} = 494 \text{ psi}/g$$

where the unit pressure, q′ = W/A = 45,000/1,110 = 40.54 lb/in^2, the total package weight, W = 45,000 pounds, the exterior OC lid area, A = $\pi(18.80)^2$ = 1,110 in^2, the exterior OC lid radius, a = 18.80 inches, Poisson's ratio, μ = 0.3, and the OC lid thickness, t = 5.00 inches.

Once again applying 42.5*g* acceleration from the NCT end drop analysis (Table 2.10.3-10 in Appendix 2.10.3, *Drop Impact Evaluation Results*) the bending stress, σ ', becomes:

$$\sigma' = (494)(42.5) = 20{,}995 \text{ psi}$$

Internal pressure would reduce this bending stress, but is conservatively ignored. From Table 2.6-1, the NCT allowable primary membrane-plus-bending stress intensity, S_a = 30,000 psi at 160 ºF for Type F304 stainless steel. Therefore, the minimum OC lid bending stress margin of safety, MS, is:

$$MS = \frac{S_a}{\sigma'} - 1 = \frac{30{,}000}{20{,}995} - 1 = +0.43$$

(4) OC Lid Bolt Stresses

OC bolt stresses under end impact conditions are computed and summarized within Table 2.10.6-1 and Table 2.10.6-2 from Appendix 2.10.6, *Closure Bolt Stress Evaluations*. Assuming an impact acceleration of 42.5*g* acting on the full weight of the lid (1,667 pounds), IV (4,023 pounds), and canister (8,000 pounds), the maximum bolt stress intensity is 56,702 psi, including pressure stress effects. This value exceeds the maximum bolt preload stress of 53,346 psi (51,692 lb/0.969 in^2). This stress conservatively neglects impact limiter reaction forces that would reduce estimated bolt impact stresses to near zero, if considered. From Table 2.6-1, the NCT allowable containment fastener primary membrane-plus-bending stress intensity, S_a = 67,600 psi at 160 ºF for ASTM A320, Grade L43, bolting material. With a total tensile stress of 56,702 psi, the resultant minimum margin of safety is computed as +0.19, in Table 2.10.6-5 of Appendix 2.10.6, *Closure Bolt Stress Evaluations*.

An assessment of OC bolt and thread insert engagement is provided in Appendix 2.10.6, *Closure Bolt Stress Evaluations*, and shown to have a minimum margin of safety of +0.13.

A detailed analysis of the OC lid bolts for various drop angles and torque coefficients is presented in Appendix 2.10.6, *Closure Bolt Stress Evaluations*.

(5) IV Stresses

The IV is designed so that, on end impact, the end closures (lid and bottom plate) will be flush against the end closures of the OC. This will tend to minimize bending stresses in IV end plates. IV analyses are performed for both top-end down and bottom-end down flat end drop.

Top-End Down: The IV bottom plate is loaded only by self-weight for the top-end down drop. Conservatively assuming a simply supported plate, the unit stress in the IV bottom plate, σ, may be calculated by using Table 24, Case 10a, of Roark[3]:

$$\sigma = \frac{6M}{t^2} = \frac{3qa^2(3+\mu)}{8t^2} = 62.0 \text{ psi}/g$$

where the unit pressure, q = W/A = 354/804.2 = 0.44 lb/in^2, the IV bottom plate weight, W = 354 pounds, the IV bottom plate area, A = $\pi(16.00)^2$ = 804.2 in^2, the IV bottom plate radius, a = 16.00 inches, Poisson's ratio, μ = 0.3, and the IV bottom plate thickness, t = 1.50 inches.

Applying 42.5*g* acceleration from the NCT end drop analysis (Table 2.10.3-10 in Appendix 2.10.3, *Drop Impact Evaluation Results*) the bending stress, σ, becomes:

$$\sigma = (62.0)(42.5) = 2{,}635 \text{ psi}$$

Internal pressure would reduce this bending stress, but is conservatively ignored. From Table 2.6-1, the NCT allowable primary membrane-plus-bending stress intensity, S_a = 30,000 psi at 160 ºF for Type F304 stainless steel. Therefore, the minimum IV bottom plate bending stress margin of safety, MS, is:

$$MS = \frac{S_a}{\sigma} - 1 = \frac{30{,}000}{2{,}635} - 1 = +10.4$$

The stresses resulting in the radius transition between the bottom plate and the IV shell are analyzed by the ANSYS® model shown in Appendix 2.10.1.3, *Inner Vessel Radius Transition Zone Stresses Due to 1g Acceleration*. A unit acceleration (1*g*) is applied to the model and scaled for final drop loading results. The maximum stress intensity, SI, in the radius transition is 110 psi for a 1*g* acceleration.

For the NCT end drop loading of 42.5*g*, the maximum radius transition stress intensity, SI, is:

$$SI = (110)(42.5) = 4{,}675 \text{ psi}$$

The stress in the radius transition is opposite in nature to the stresses resulting from internal pressure; hence, stresses from internal pressure are conservatively ignored in this calculation. From Table 2.6-1, the NCT allowable primary membrane-plus-bending stress intensity, S_a = 30,000 psi at 160 ºF for Type F304 stainless steel. Therefore, the minimum IV radius transition bending stress margin of safety, MS, is:

$$MS = \frac{S_a}{SI} - 1 = \frac{30{,}000}{4{,}675} - 1 = +5.42$$

The maximum stress acting on the shell away from the transition region will be a compressive membrane stress due to self-weight:

$$\sigma = -\frac{P}{A} = -54.67 \text{ psi}/g$$

where the weight of IV bottom plate (354 pounds), spacers (467 pounds), and shell (1,216 pounds), P = 2,037 pounds, and the shell cross-sectional area, $A = \pi[(16.00)^2 - (15.625)^2] = 37.26 \text{ in}^2$.

Applying 42.5*g* acceleration from the NCT end drop analysis (Table 2.10.3-10 in Appendix 2.10.3, *Drop Impact Evaluation Results*), the axial stress, σ, becomes:

$$\sigma = (-54.67)(42.5) = -2{,}323 \text{ psi}$$

Table 2.6-9 combines this stress with that due to a 150 psig normal pressure loading. As shown, the resultant margin of safety is +2.09. This margin is somewhat conservative, as accelerations applied to the IV shell are those corresponding to a drop at -20 ºF, whereas allowables are taken at a temperature of 160 ºF. A detailed buckling analysis for this load combination is presented in Appendix 2.10.5, *Buckling Design Criteria and Detailed Evaluation*.

The IV lid is supported during top-end down end drop by the OC lid, which is of comparable thickness and diameter. Because the OC lid will tend to limit deflections of the IV lid, it may be

assumed that the large margins of safety derived for the OC lid in both backed and unbacked bending will be applicable to the IV lid.

Bottom-End Down: For bottom-end impact, the IV bottom plate will be supported by the OC bottom plate. The IV bottom plate is of approximately the same diameter, yet of significantly smaller thickness than the OC lid. Therefore, the IV bottom plate will see lower stresses than the OC bottom plate when forced into the OC bottom plate. This is because the OC closure will limit deflections of the IV closure, thereby assuring margins of safety in excess of the already conservative values presented for the OC closures.

The maximum stress acting on the IV shell away from the transitions with the upper flange forging and lower bottom plate will be a compressive membrane stress due to self-weight:

$$\sigma = -\frac{P}{A} = -98.47 \text{ psi}/g$$

where the weight of IV lid (1,382 pounds), flange (604 pounds), shell (1,216 pounds), and spacers (467 pounds), P = 3,669 pounds, and the shell cross-sectional area, $A = \pi[(16.00)^2 - (15.625)^2] = 37.26 \text{ in}^2$.

Applying 42.5*g* acceleration from the NCT end drop analysis (Table 2.10.3-10 in Appendix 2.10.3, *Drop Impact Evaluation Results*) the axial stress, σ, becomes:

$$\sigma = (-98.47)(42.5) = -4{,}185 \text{ psi}$$

Table 2.6-10 combines this stress with that due to a 150 psig NCT pressure loading. As shown, the resultant margin of safety is +1.72. This margin is somewhat conservative, as accelerations applied to the shell are those corresponding to a drop at -20 ºF, whereas allowables are taken at a temperature of 160 ºF. A detailed buckling analysis for this load combination is presented in Appendix 2.10.5, *Buckling Design Criteria and Detailed Evaluation*.

The IV lid is loaded only by self-weight for a bottom-down end drop. Conservatively assuming a simply supported circular plate, the unit bending stress may be calculated by using Table 24, Case 10a, of Roark[3]:

$$\sigma = \frac{6M}{t^2} = \frac{3qa^2(3+\mu)}{8t^2} = 12.9 \text{ psi}/g$$

where the unit pressure, $q = W/A = 1{,}382/804.2 = 1.72 \text{ lb/in}^2$, the IV lid weight, W = 1,382 pounds, the IV lid area, $A = \pi(16.00)^2 = 804.2 \text{ in}^2$, the IV lid radius, a = 16.00 inches, Poisson's ratio, $\mu = 0.3$, and the IV lid thickness, t = 6.50 inches.

Applying 42.5*g* acceleration from the NCT end drop analysis (Table 2.10.3-10 in Appendix 2.10.3, *Drop Impact Evaluation Results*), the bending stress, σ, becomes:

$$\sigma = (12.9)(42.5) = 548 \text{ psi}$$

Internal pressure would reduce this bending stress, but is conservatively ignored. From Table 2.6-1, the NCT allowable primary membrane-plus-bending stress intensity, $S_a = 30{,}000$ psi at 160 ºF for Type F304 stainless steel. Therefore, the minimum IV lid bending stress margin of safety, MS, is:

$$MS = \frac{S_a}{\sigma} - 1 = \frac{30{,}000}{548} - 1 = +54.7$$

IV bolt stresses under end impact conditions are computed and summarized within Table 2.10.6-3 and Table 2.10.6-4 from Appendix 2.10.6, *Closure Bolt Stress Evaluations*. Assuming an impact acceleration of 42.5*g* acting on the full weight of the lid (1,382 pounds) and canister (8,000 pounds), the maximum bolt stress intensity is 56,179 psi, including pressure stress effects. This value exceeds the maximum bolt preload stress of 51,840 psi (21,099 lbs/0.407 in²). These stresses neglect impact limiter reaction forces, which would reduce estimated bolt impact stresses to near zero, if considered. However, for added conservatism, all impact limiter forces have been neglected. From Table 2.6-1, the NCT allowable containment fastener primary membrane-plus-bending stress intensity, S_a = 67,600 psi at 160 ºF for ASTM A320, Grade L43, bolting material. With a total tensile stress of 56,179 psi, the resultant minimum margin of safety is computed as +0.20, in Table 2.10.6-5 of Appendix 2.10.6, *Closure Bolt Stress Evaluations*.

An assessment of IV bolt and thread insert engagement is provided in Appendix 2.10.6, *Closure Bolt Stress Evaluations*, and shown to have a minimum margin of safety of +0.18.

A detailed analysis of the IV lid bolts for various drop angles and torque coefficients is presented in Appendix 2.10.6, *Closure Bolt Stress Evaluations*.

(6) Stresses in the OC Shells and Lead (Maximum Fabrication Stress Condition Assumed)

The principal concern for the OC under NCT end drop is with buckling of the inner shell. As shown by the following stress calculations and the detailed buckling evaluations presented in Appendix 2.10.5, *Buckling Design Criteria and Detailed Evaluation*, buckling will not occur as the result of the hoop and axial compressive stresses which develop in the OC inner shell under the NCT end drop event.

Various initial conditions can be assumed for the NCT end drop event. In particular, a temperature must be assumed in order to establish an initial fabrication stress for the inner shell. A lower assumed temperature will result in a higher initial hoop stress on the inner shell (see Appendix 2.10.8, *Fabrication Stresses Due to Lead Pour*), but higher allowable stresses. For purposes of this analysis, drops at 160 ºF (conservatively bounding the maximum OC lead and inner and outer shell NCT temperatures per Section 3.4.2, *Maximum Temperatures*), 70 ºF, and -20 ºF are considered. Regardless of temperature, the maximum inertia load of 42.5*g* (for -20 ºF drop case) is conservatively employed.

To adequately bound the consequences of the drop event at a given temperature, two initial lead conditions are also considered. The first assumes that the lead has shrunk onto the inner shell and away from the outer shell. In addition, due to the combined effects of friction between the lead and inner shell, and axial shrinkage of the lead relative to the stainless shells, axial gaps will develop between the lead and the steel structures at the top and bottom end of the lead column. These axial gaps are important in that, until friction is overcome, under increased axial loading, the lead will impose a direct axial load on the inner shell. Once friction is overcome, the lead will become supported at its base (the bottom of the lead column) and will grow radially outward due to the "Poisson effect" under increased axial loading. This radial growth will tend to relieve the initial fabrication hoop stress as the lead separates from the inner shell. If sufficient axial load develops, the lead would grow out to the outer shell creating tensile hoop stresses therein, and under further

loading would eventually flow back inward into the inner shell, thereby developing compressive hoop stresses in the inner shell.

From Appendix 2.10.8, *Fabrication Stresses Due to Lead Pour*, the hoop stress in the inner shell due to fabrication is -1,413 psi at 70 ºF, and -1,821 psi at -20 ºF. Extrapolating, the hoop stress in the inner shell is -1,038 psi at 160 ºF. (Note that the outer shell hoop stress is considered to be negligible since the lead separates from the outer shell upon cooling.)

The equivalent pressure at the lead/inner shell interface, p, is:

$$p = \frac{\sigma t}{r}$$

where the shell thickness, t = 1.00 inch, and the shell radius, r = 16.69 inches. Therefore, the interface pressure is 62.2 psi at 160 ºF, 84.7 psi at 70 ºF, and 109.1 psi at -20 ºF.

With a coefficient of friction, *f*, for lead on stainless steel assumed to fall in the 0.5 to 1.0 range[9], the load, P, which can be supported by friction at the lead/inner shell interface, may be determined as follows:

$$P = \pi D L p f$$

where inner shell outside diameter, D = 34.38 inches, the lead column height, L = 123.5 inches, the interface pressure is p, and the coefficient of friction, $f = 0.5 – 1.0$.

Applying the above interface pressures, the total axial load that may be supported for each case is provided in Table 2.6-11.

With the total lead weight equal to 10,739 pounds, per Table 2.2-1 in Section 2.2, *Weights and Centers of Gravity*, the minimum *g*-load that can be supported by friction is 414,842/10,739 = 38.6*g*. This minimum *g*-load is based on the total lead weight that can be supported with the package at an assumed (conservatively high) maximum NCT temperature of 160 ºF. At -20 ºF, the minimum *g*-load is 727,641/10,739 = 67.8*g*. Since this *g*-load exceeds the maximum NCT end drop of 42.5*g* at -20 ºF, the lead will not slip under the cold end drop condition. Axial stress in the inner shell is, therefore, governed by the cold case and is determined, with reference to Table 2.2-1 and Figure 2.6-3(a), as follows:

$$w_1 = \eta W_1 = 264{,}095 \text{ lb}$$

$$w_2 = \eta W_2 = 305{,}915 \text{ lb}$$

$$w_3 = \eta W_3 = 156{,}740 \text{ lb}$$

$$w_L = \eta W_L = 456{,}408 \text{ lb}$$

$$w_4 = \eta W_4 = 510{,}978 \text{ lb}$$

[9] Theodore Baumeister, *Mark's Standard Handbook for Mechanical Engineers*, Ninth Edition, McGraw-Hill Book Company, New York, NY, 1987, Table 3.2.1.

$$q_2 = \frac{w_4}{A_4} = 620.5 \text{ lb/in}^2$$

$$q_1 = \frac{w_1 + w_2 + w_3 + w_L + w_4}{A_5} = 1{,}246.4 \text{ lb/in}^2$$

where the impact acceleration, $\eta = 42.5g$, the weight of the top impact limiter, OC lid, and OC flange, W_1 = 6,214 pounds, the weight of the OC outer shell and thermal shield, W_2 = 7,198 pounds, the weight of the package inner shell, W_3 = 3,688 pounds, the weight of the lead, W_L = 10,739 pounds, the weight of the loaded payload canister and IV, W_4 = 12,023 pounds, the area of the OC bottom, $A_4 = \pi R_i^2 = 823.5$ in^2, the radius of the OC bottom (inside), R_i = 16.19 inches, the weight of the loaded payload canister and IV, $A_5 = \pi R_o^2 = 1{,}359.2$ in^2, and the radius of the OC bottom (outside), R_o = 20.8 inches.

Free-body diagrams of the OC shells and end plate are illustrated in Figure 2.6-3(b).

The reaction forces R_1 and R_2 can be calculated by distributing W_1 to the inner and outer shells based on their relative stiffnesses. The stiffnesses of the shells are directly dependant on their cross-sectional areas. Therefore, R_1 and R_2 are calculated as follows:

$$R_1 = W_1\left(\frac{A_3}{A_2 + A_3}\right) = 94{,}972 \text{ lb}$$

$$R_2 = W_1\left(\frac{A_2}{A_2 + A_3}\right) = 169{,}123 \text{ lb}$$

where the cross-sectional area of the inner shell, $A_3 = \pi(R_{io}^2 - R_{ii}^2) = 104.87$ in^2, the inner shell outer radius, R_{io} = 17.19 inches, the inner shell inner radius, R_{ii} = 16.19 inches, the cross-sectional area of the outer shell, $A_2 = \pi(R_{oo}^2 - R_{oi}^2) = 186.75$ in^2, the outer shell outer radius, R_{oo} = 20.565 inches, and the outer shell inner radius, R_{oi} = 19.065 inches.

Assuming reaction R_3 does not affect the deflection of the bottom-end plate (conservative for the maximum R_3), the differential deflection may be calculated. As shown in Figure 2.6-4, utilizing Table 24, Case 10a, of Roark[3], assuming a simply supported circular plate with a uniform load, the differential deflection, $\delta_1 - \delta_2$, may be determined as follows:

$$\delta_1 - \delta_2 = y_c + \frac{M_c r^2}{2D(1+\mu)} - \frac{qr^4 G_{11}}{D} = \frac{128{,}863}{E} \text{ in}$$

given:

$$y_c = \frac{qa^4(5+\mu)}{64D(1+\mu)} = \frac{536{,}965}{E} \text{ in}$$

$$M_c = \frac{qa^2(3+\mu)}{16} = 50{,}686 \text{ in - lb/in}$$

$$D = \frac{Et^3}{12(1-\mu^2)} = (11.4469)E \text{ in - lb}$$

$$G_{11} = \frac{1}{64}\left\{1 + 4\left(\frac{r_o}{r}\right)^2 - 5\left(\frac{r_o}{r}\right)^4 - 4\left(\frac{r_o}{r}\right)^2\left[2 + \left(\frac{r_o}{r}\right)^2\right]\ln\left(\frac{r}{r_o}\right)\right\}\langle r - r_o\rangle^0 = \frac{1}{64}$$

where the net pressure, $q = -(q_1 - q_2) = -(1{,}264.4 - 620.5) = 625.9$ lb/in^2, the outside plate/pressure radius, a = 19.815 inches, the mean inner shell radius, r = 16.69 inches, the inner pressure radius, $r_o = 0.0$ inches, the bottom-end plate thickness, t = 5.0 inches, and Poisson's ratio, $\mu = 0.3$.

Also, from the free-body diagrams of the OC inner and outer shells (see in Figure 2.6-3(b)), and axial stiffness relations for the shells ($\delta = PL/AE$ for an end load, and $\delta = PL/2AE$ for self-weight, i.e., a uniformly distributed load), the deflections, δ_1 and δ_2, and reactions, R_3 and R_4, may be found:

$$\delta_1 = \frac{(R_3 - R_1)L}{A_3E} - \frac{(w_3 - w_L)L}{2A_3E}$$

$$\delta_2 = \frac{(R_4 - R_2)L}{A_2E} - \frac{w_2L}{2A_2E}$$

where the shell length, L = 124.65 inches and, as before, the cross-sectional area of the inner shell, $A_3 = 104.87$ in^2, and the cross-sectional area of the outer shell, $A_2 = 186.75$ in^2. Substituting values:

$$\delta_1 = R_3\left(\frac{1.1886}{E}\right) - \frac{477{,}278}{E}$$

$$\delta_2 = R_4\left(\frac{0.6675}{E}\right) - \frac{214{,}989}{E}$$

Summing vertical forces:

$$R_3 + R_4 = w_1 + w_2 + w_3 + w_L = 1{,}183{,}158 \text{ lb}$$

Solving the above equations simultaneously yields the following:

$$R_3 = \frac{\frac{128{,}863}{E} + \frac{477{,}278}{E} - \frac{214{,}989}{E} + (1{,}183{,}158)\left(\frac{0.6675}{E}\right)}{\frac{1.1886}{E} + \frac{0.6675}{E}} = 636{,}232 \text{ lb}$$

$$R_4 = 1{,}183{,}158 - 636{,}232 = 546{,}926 \text{ lb}$$

Therefore, the axial compressive stress in the OC inner shell, σ_3, and outer shell, σ_2, is:

$$\sigma_3 = -\frac{R_3}{A_3} = -6{,}067 \text{ psi}$$

$$\sigma_2 = -\frac{R_4}{A_2} = -2{,}929 \text{ psi}$$

where, as before, the cross-sectional area of the inner shell, $A_3 = 104.87$ in^2, and the cross-sectional area of the outer shell, $A_2 = 186.75$ in^2.

It has been shown above, based upon the stated assumptions, that the elastic modulus, E, is independent of the axial stresses calculated. Therefore, the shell stresses are summarized, with reference to Appendix 2.10.8, *Fabrication Stresses Due to Lead Pour*, for hoop stresses, as given in Table 2.6-12.

Table 2.6-13, Table 2.6-14, and Table 2.6-15 present the corresponding margins of safety for the more critical inner shell. Zero internal pressure is used in order to maximize compressive stresses in the inner shell. Note that axial stresses will actually decrease with increasing drop temperature since *g*-loads are lower at higher temperatures (due to decreased foam strength with increased temperature); this effect is conservatively ignored in Table 2.6-13, Table 2.6-14, and Table 2.6-15.

Buckling is addressed in Appendix 2.10.5, *Buckling Design Criteria and Detailed Evaluation*.

(7) Stresses in the OC Shells and Lead (Zero Fabrication Stress Condition Assumed)

The second initial lead condition assumes the fabrication stress has fully crept away, resulting in a stress-free column of lead just in contact with the inner and outer shells. This is potential worst-case since any axial load imposed on the lead will directly load in the radial direction both the inner and outer shells (i.e., the lead need not flow away from the inner shell, into the outer shell, and back into the inner shell to develop a compressive hoop stress in the inner shell).

For this condition, initial stresses in the lead and the steel shells are taken as zero. As an axial load is applied to the lead and the shells, the lead will attempt to move downward and outward, and develop pressures on both the inner and outer shells, as shown in Figure 2.6-5.

For the purpose of this analysis, let $p_i = p_o = p$. This assumption is considered reasonable once lead starts to flow.

Conservatively assuming that the lead receives no axial support at its base, but rather is supported solely by friction at the inner and outer shells, the maximum value of the pressure, p_{max}, is determined based on a lead weight, $W_L = 10{,}739$ pounds, being acted on by an end drop acceleration, $\eta = 42.5g$, resulting in a total lead force, w_L, of:

$$w_L = \eta W_L = 456{,}408 \text{ lb}$$

For the maximum pressure, p_{max}, use the minimum expected coefficient of friction, $f = 0.5$, resulting in a force, w, of:

$$w = p_{max}(2\pi r_L)(L - d)f$$

where the mean lead shell radius, $r_L = ½(r_o^2 + r_i^2) = 18.1275$ inches, the lead shell outer radius, $r_o = 19.065$ inches, the lead shell inner radius, $r_i = 17.19$ inches, and the shell length, L = 123.5 inches. Letting $w = w_L = 456{,}408$ pounds, the maximum pressure, p_{max}, is:

$$p_{max} = \frac{8{,}014}{(123.5 - d)} \text{ psi}$$

Assuming lead flow initiates at the yield strength of the lead, σ_y, the height of the lead column, d, required to yield the lead cross-section due to the 42.5*g* NCT acceleration is:

$$\sigma_y = \rho d(42.5g)$$

where σ_y is lead's yield strength at temperature, and the lead density, $\rho = 0.41$ lb/in^3. Therefore:

$$d = (0.05739)\sigma_y$$

For lead temperatures of 160 ºF, 70 ºF, and -20 ºF, and conservatively estimating an upper bound on the lead properties delineated in Figure 2.3-3 through Figure 2.3-6 of Section 2.3, *Mechanical Properties of Materials*, the pressures and hoop stresses may be summarized as shown in Table 2.6-16.

The maximum axial stress in the shells is determined using the same approach as developed in the preceding calculations in Paragraph (6) of Section 2.6.7.1, *Flat End Drop*, except that one-half of the lead weight is considered to act on each shell rather than all lead weight being carried on the inner shell. Again, no support is considered at the base of the lead.

Repeating the previous calculational approach:

$$\delta_1 - \delta_2 = \frac{128{,}863}{E} \text{ in}$$

$$\delta_1 = \frac{(R_3 - R_1)L}{A_3 E} - \frac{\left(w_3 + \frac{w_L}{2}\right)L}{2A_3 E} = R_3\left(\frac{1.1886}{E}\right) - \frac{228{,}775}{E}$$

$$\delta_2 = \frac{(R_4 - R_2)L}{A_2 E} - \frac{\left(w_2 + \frac{w_L}{2}\right)L}{2A_2 E} = R_4\left(\frac{0.6675}{E}\right) - \frac{178{,}254}{E}$$

where the shell length, L = 124.65 inches and, as before, the cross-sectional area of the inner shell, $A_3 = 104.87$ in^2, and the cross-sectional area of the outer shell, $A_2 = 186.75$ in^2.

Summing vertical forces as before:

$$R_3 + R_4 = w_1 + w_2 + w_3 + w_L = 1{,}183{,}158 \text{ lb}$$

Solving the above equations simultaneously yields the following:

$$R_3 = \frac{\frac{128{,}863}{E} + \frac{228{,}775}{E} - \frac{178{,}254}{E} + (1{,}183{,}158)\left(\frac{0.6675}{E}\right)}{\frac{1.1886}{E} + \frac{0.6675}{E}} = 523{,}218 \text{ lb}$$

$$R_4 = 1{,}183{,}158 - 523{,}218 = 662{,}940 \text{ lb}$$

Therefore, the axial compressive stress in the OC inner shell, σ_3, and outer shell, σ_2, is:

$$\sigma_3 = -\frac{R_3}{A_3} = -4{,}989 \text{ psi}$$

$$\sigma_2 = -\frac{R_4}{A_2} = -3{,}550 \text{ psi}$$

It has been shown above, based upon the stated assumptions, that the elastic modulus, E, is independent of the axial stresses calculated. Therefore, the shell stresses are summarized at temperatures of 160 ºF, 70 ºF, and -20 ºF for a NCT drop load of 42.5*g* in Table 2.6-17.

Table 2.6-18, Table 2.6-19, and Table 2.6-20 present the corresponding margins of safety for the more critical inner shell. Zero internal pressure is used in order to maximize compressive stresses in the inner shell. Again, it is noted that the margins presented for the 70 ºF and 160 ºF cases are conservative in that at these temperatures, *g*-loads will actually be less than the 42.5*g* considered herein.

Buckling is addressed in Appendix 2.10.5, *Buckling Design Criteria and Detailed Evaluation*.

(8) Discussion of Payload Canister Behavior in End Drop

Hoop and axial stresses in the canister are addressed for the one-foot NCT end drop condition. Hoop stress in the canister is maximized by assuming a water-filled canister. The maximum axial stress, σ_a, in the canister shell for a 1*g* load is defined as:

$$\sigma_a = \frac{P}{A} = 87.14 \text{ psi}$$

where the worst-case weight of an empty canister, the fixed-lid version, P = 1,762 pounds, the canister cross-sectional shell area, $A = \pi(r_o^2 - r_i^2) = 20.22 \text{ in}^2$, and the canister shell's outer and inner radii, r_o = 13.00 inches and r_i = 12.75 inches, respectively.

For the 42.5*g* end drop load, the axial shell stress, σ_a, is:

$$\sigma_a = (87.14)(42.5) = 3{,}703 \text{ psi (compression)}$$

The canister shell hoop stress, σ_h, is defined as:

$$\sigma_h = \frac{pr}{t} = 225.1 \text{ psi}$$

where the hydrostatic pressure, $p = \gamma h = (0.0361)(121) = 4.37$ psi, the density of water, $\gamma = 0.0361$ lb/in^3, the canister height, h = 121 inches, the mean canister radius, r = 12.875 inches, and the canister shell thickness, t = 0.25 inches.

For the 42.5*g* end drop load, the hoop shell stress, σ_h, is:

$$\sigma_h = (225.1)(42.5) = 9{,}567 \text{ psi (tension)}$$

The maximum canister shell stress intensity (SI) is therefore, 3,703 + 9,567 = 13,270 psi. From Table 2.6-1, the NCT allowable primary membrane stress intensity, S_a = 21,300 psi at 200 ºF for worst-case Type 304L stainless steel as the material of construction. The margin of safety (MS) for the canister shell is then:

$$MS = \frac{S_a}{SI} - 1 = \frac{21{,}300}{13{,}270} - 1 = +0.61$$

(9) Lead Slump

An upper-bound value for the amount of lead slump that could occur may be determined from Equation 2.16 of the *Package Designers Guide*[10]. From this equation for the one-foot NCT drop of a bare package (i.e., no impact limiters), the maximum lead slump is determined to be 0.068 inches. This amount of slump equates to an approximate impact deceleration of 354.7*g*. Since the maximum deceleration for NCT has been determined to be 42.5*g*, the maximum possible lead slump can be determined from the ratio of the accelerations as (42.5/354.7)(0.068) = 0.008 inches. This value is insignificant for the RH-TRU 72-B package.

Even though an upper-bound lead slump value has been determined, lead slump is not expected to be a problem for the RH-TRU 72-B package. By comparison to the NuPac 125-B cask[8] (NRC Certificate of Compliance 71-9200), the RH-TRU 72-B package provides a more restrictive structure to lead slump. Comparatively, the RH-TRU 72-B package has thicker containment shells and thinner lead than the scaled NuPac 125-B cask. Similar methods of fabrication will also be used for both packages. It can therefore be assumed that lead slump for the RH-TRU 72-B package will be bounded by the magnitude of lead slump for the NuPac 125-B cask. The quarter-scale end drop test of the NuPac 125-B cask resulted in no measurable lead slump due to a 30-foot drop. It can then be concluded that no lead slump will occur during the much less critical one-foot end drop for the RH-TRU 72-B package.

2.6.7.2 Corner and Oblique Drops

Analysis of RH-TRU 72-B package behavior during the corner drop event, including oblique drop orientations, is performed in the following steps:

(1) Determine the force-deflection relations for a range of initial impact angles, using the CASKDROP computer program. Utilize the force-deflection data from CASKDROP as input to the computer program SLAPDOWN to determine the package response for various initial impact angles.

[10] L. B. Shappert, *Package Designers Guide, A Guide for the Design, Fabrication, and Operation of Shipping Packages for Nuclear Applications*, ORNL-NSIC-68, Oak Ridge National Laboratory, Oak Ridge, Tennessee, February 1970.

(2) Based on the accelerations and rotations predicted in (1), determine the equivalent "static" forces on the OC and IV, considered as a rigid body with distributed and lumped masses.

(3) Based on the loads from (2), analyze the OC shells and IV as simple beams, finding the internal forces: shear, moment, and thrust. Compute stresses for the maximum value of each of these forces, and by inspection of the relative magnitudes of these maximum component stresses, select load cases for further analysis which will have the maximum combined stresses.

(4) Analyze the OC shells for stress, assuming the two shells act as parallel beams, under the loads determined in (3).

(5) Analyze the IV for stress under the loads determined in (3).

(6) Analyze the payload canister for stress under the loads determined in (3).

(7) Analyze impact limiter attachment forces.

(8) Based on the forces from (7), calculate the impact limiter attachment stresses.

(9) Analyze the stresses in the OC and IV lid bolts.

(10) Calculate the maximum impact limiter deformations and residual clearances for package hard spots.

Material properties and allowable stresses corresponding to the maximum enveloping temperature of 160 ºF for the Type 304 stainless steel OC and IV and lead are given in Table 2.6-1. Buckling is addressed in Appendix 2.10.5, *Buckling Design Criteria and Detailed Evaluation*.

(1) Corner Drop Computer Analysis (CASKDROP and SLAPDOWN)

Analytic predictions of package performance for drop orientations impacting upon the corner of the package employ two computer programs: CASKDROP and SLAPDOWN, documented in Appendix 2.10.2, *Drop Analysis Codes Description*. CASKDROP uses an energy-balance technique to determine loads and deformations of the impact limiter. Since CASKDROP assumes all drop energy is absorbed in deformation of the impact limiter, it provides valid results when the impact orientation places the center-of-gravity (CG) directly over the impacted corner, approximately 68º from the horizontal for the RH-TRU 72-B package. At other impact orientations, the force-deflection values generated by CASKDROP are used in SLAPDOWN, a dynamic analysis program that considers rotational motion effects. For initial impact angles between the CG-over-corner and vertical, dynamic effects (such as a secondary slapdown) are negligible, and results at the upper, or secondary impact limiter are unimportant. For such cases, CASKDROP is used to conservatively calculate the primary impact results.

Two (2) cases were run which accounted for variations in foam strength due to temperature effects and the possible variations in foam strength from nominal values (see Section 2.3, *Mechanical Properties of Materials*). Detailed output for each of the two analysis cases is presented in Appendix 2.10.3, *Drop Impact Evaluation Results*. Note that the load and stress evaluations presented in this section are typically based on the results from the -20 ºF foam stress case. Impact limiter responses (i.e., attachment forces, deformations, and residual clearances) presented herein directly consider both analytic cases.

(2) Equivalent "Static" Loads:

The OC and IV are treated as rigid bodies under longitudinal, transverse and angular accelerations, along with an angular velocity. The two bodies are assumed to move together, and the forces between them, needed to make them do so, are found. The centers of gravity of the two bodies are assumed to be coincident.

Slapdown impacts are not governing, as shown in Appendix 2.10.4, *Slapdown Assessment*. The only potentially serious slapdown loading problem will affect package impact limiter attachment fastener and OC lid fastener integrity. These load cases are addressed in Paragraphs (7) and (9), below.

(3) Internal Forces

The OC shells are analyzed as if they are two beams acting in parallel. The payload canister is analyzed as one beam attached to the IV at the two spacer disk locations, and the IV connects to the OC via a series of interface (gap) elements. A schematic representation of the finite element analysis model used is presented as Figure 2.10.1-9 in Appendix 2.10.1.4, *Containment Assembly Analysis for Oblique Drops*.

Maximum stresses are given as functions of impact angle for the cold foam (-20 ºF) conditions in Figure 2.6-6, Figure 2.6-7, and Figure 2.6-8 for the OC, IV, and payload canister, respectively, based on maximum thrust, shear, and bending moment given in Figure 2.6-9, Figure 2.6-10, and Figure 2.6-11, respectively. The stresses shown in Figure 2.6-6, Figure 2.6-7, and Figure 2.6-8 were calculated using slightly different *g*-loadings than those found in Appendix 2.10.3, *Drop Impact Evaluation Results*. A comparison of the *g*-loading from Appendix 2.10.3, *Drop Impact Evaluation Results* for the NCT cold free drop and those data used in calculating the peak stresses is presented in Figure 2.6-12. Since the *g*-loads match closely for all the orientations considered here, scaling of the previously calculated stresses is an appropriate method for evaluating package components.

In a similar manner, the values from Figure 2.6-13, Figure 2.6-14, and Figure 2.6-15, showing the maximum stresses for the OC, IV, and payload canister, respectively, for hot foam (140 ºF) conditions are also scaled accordingly, based on maximum thrust, shear, and bending moment given in Figure 2.6-16, Figure 2.6-17, and Figure 2.6-18.

The stresses are computed as follows:

$$S_t = \frac{P}{A} \times \frac{g_{new}}{g_{old}} = \text{stress due to thrust, psi}$$

$$S_v = \frac{V}{A} \times \frac{g_{new}}{g_{old}} = \text{stress due to shear, psi}$$

$$S_m = \frac{Mc}{I} \times \frac{g_{new}}{g_{old}} = \text{stress due to bending moment, psi}$$

where P is the thrust force (lb), V is the shear force (lb), and M is the bending moment (in-lb). The distance to the neutral axis, c = 20.565 inches for the OC outer shell, c = 17.19 inches for the OC inner shell, c = 16.00 inches for the IV shell, and c = 13.00 inches for the payload canister. The

moment of intertia, I = 51,334 in^4 for the OC, I = 4,718 in^4 for the IV, and I = 1,676 in^4 for the payload canister. Finally, the area, A = 292 in^2 for the OC, A = 38 in^2 for the IV, and A = 20 in^2 for the payload canister.

From Figure 2.6-6, it can be deduced that an 85º impact angle with cold foam (-20 ºF), yields the worst stresses for the OC. Similarly, from Figure 2.6-7 and Figure 2.6-8, it can be deduced that an 85º impact angle with cold foam also yields the worst stresses for the IV and payload canister.

Although the maximum thrust, shear, and bending moment do not occur at the same location for each component, the true maximums are used to provide a conservative analysis. The figures are based on a *g*-load of 15.7*g*, whereas the impact of an 85º angle is 17.9*g*. The scale factor is therefore 17.9/15.7 = 1.14.

For the OC, these maximums are P_{max} = 444,680 × 1.14 = 506,935 pounds, V_{max} = 155,730 × 1.14 = 177,532 pounds, and M_{max} = 12,754,000 × 1.14 = 14,539,560 in-lb. For the IV, the maximums are P_{max} = 57,278 × 1.14 = 65,297 pounds, V_{max} = 69,976 × 1.14 = 79,773 pounds, and M_{max} = 923,570 × 1.14 = 1,052,870 in-lb. Finally, for the payload canister, the maximums are P_{max} = 125,100 × 1.14 = 142,614 pounds, V_{max} = 7,956 × 1.14 = 9,070 pounds, and M_{max} = 106,350 × 1.14 = 121,239 in-lb.

(4) OC Stresses

The maximum membrane stress in the OC inner shell, for the load case selected in Paragraph (3), is:

$$S_m = \frac{Mc}{I} + \frac{P}{A} = \frac{(14{,}539{,}560)[17.19 - (½)(1.0)]}{51{,}334} + \frac{506{,}935}{292} = 6{,}463 \text{ psi}$$

The maximum membrane-plus-bending stress in the OC inner shell is:

$$S_{mb} = \frac{Mc}{I} + \frac{P}{A} = \frac{(14{,}539{,}560)(17.19)}{51{,}334} + \frac{506{,}935}{292} = 6{,}605 \text{ psi}$$

Similarly, the maximum stresses in the OC outer shell are:

$$S_m = \frac{Mc}{I} + \frac{P}{A} = \frac{(14{,}539{,}560)[20.565 - (½)(1.5)]}{51{,}334} + \frac{506{,}935}{292} = 7{,}348 \text{ psi}$$

$$S_{mb} = \frac{Mc}{I} + \frac{P}{A} = \frac{(14{,}539{,}560)(20.565)}{51{,}334} + \frac{506{,}935}{292} = 7{,}561 \text{ psi}$$

In addition, shear stress must be added in the calculation of the membrane stress intensities for the OC inner and outer shells. The shear stress is:

$$S_v = \frac{V}{A} = \frac{177{,}532}{292} = 608 \text{ psi}$$

Axial fabrication stresses used in the oblique drop analyses are scaled from those used in the end drop analysis (see Table 2.6-12 from Section 2.6.7.1, *Flat End Drop*) using the respective *g*-loadings of the package (17.9/42.5). Fabrication stresses for the oblique drop analyses are given in Table 2.6-21.

Table 2.6-22, Table 2.6-23, and Table 2.6-24 present the corresponding margins of safety for the more critical OC inner shell. Zero internal pressure is used in order to maximize compressive stresses in the OC inner shell. Again, note that the margins presented for the 70 ºF and 160 ºF cases are conservative in that at these temperatures, *g*-loads will actually be less than the 17.9*g* conservatively considered herein.

(5) IV Stresses

The maximum membrane stress in the IV shell, for the load case selected in Paragraph (3), is:

$$S_m = \frac{Mc}{I} + \frac{P}{A} = \frac{(1{,}052{,}870)[16.00 - (½)(0.38)]}{4{,}718} + \frac{65{,}297}{38} = 5{,}247 \text{ psi}$$

The maximum membrane-plus-bending stress in the IV shell is:

$$S_{mb} = \frac{Mc}{I} + \frac{P}{A} = \frac{(1{,}052{,}870)(16.00)}{4{,}718} + \frac{65{,}297}{38} = 5{,}289 \text{ psi}$$

In addition, shear stress must be added in the calculation of the membrane stress intensity for the IV shell. The shear stress is:

$$S_v = \frac{V}{A} = \frac{79{,}773}{38} = 2{,}099 \text{ psi}$$

Table 2.6-25 presents stress and margin of safety results for the IV for the worst-case load combination.

(6) Discussion of Payload Canister Behavior in Oblique Drops

The maximum membrane stress in the payload canister shell, for the load case selected in Paragraph (3), is:

$$S_m = \frac{Mc}{I} + \frac{P}{A} = \frac{(121{,}239)[13.00 - (½)(0.25)]}{1{,}676} + \frac{142{,}614}{20} = 8{,}062 \text{ psi}$$

The maximum membrane-plus-bending stress in the payload canister shell is:

$$S_{mb} = \frac{Mc}{I} + \frac{P}{A} = \frac{(121{,}239)(13.00)}{1{,}676} + \frac{142{,}614}{20} = 8{,}071 \text{ psi}$$

In addition, shear stress must be added in the calculation of the membrane stress intensity for the payload canister shell. The shear stress is:

$$S_v = \frac{V}{A} = \frac{9{,}070}{20} = 454 \text{ psi}$$

Table 2.6-26 presents stress and margin of safety results for the payload canister shell for the worst load combination. The NCT allowable stress, S_a, from Table 2.1-2 in Section 2.1.2.1.2, *Non-Containment Structures*, is the greater of S_m or S_y for primary membrane stress intensity. From Table 2.3-1 in Section 2.3, *Mechanical Properties of Materials*, the allowable stress, S_a = 21,300

psi at 200 ºF is based on S_y using worst-case Type 304L stainless steel as the material of construction (conservative maximum payload canister temperature; see Table 2.6-2). Buckling is addressed in Appendix 2.10.5, *Buckling Design Criteria and Detailed Evaluation*.

(7) Impact Limiter Attachment Forces

The maximum NCT impact limiter attachment moment, $2.16(10)^6$ in-lb, is given in Table 2.10.3-13 of Appendix 2.10.3, *Drop Impact Evaluation Results*. Six, ASTM A320, Grade L43, 1¼-7UNC bolts (necked down to a 1.0-inch diameter) secure each impact limiter to the package structure. Assuming that tension varies linearly from one side of the package to the other, the moment is resisted by the six bolts as follows:

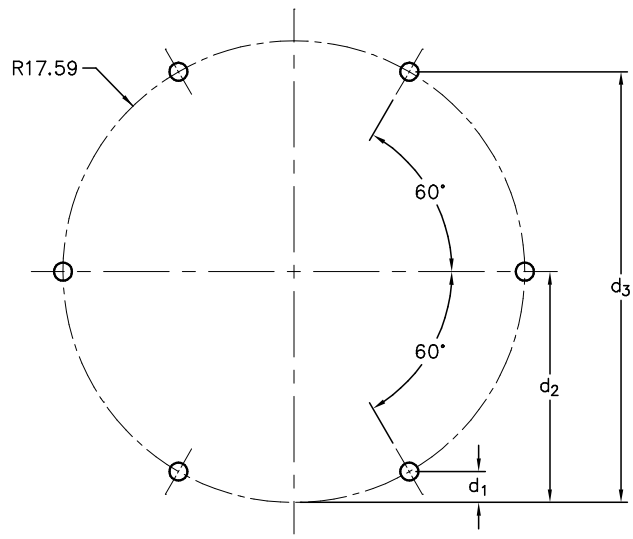

$$M = 2P_{max}\left(\frac{d_1^2 + d_2^2 + d_3^2}{d_3}\right) = (84.8)P_{max}$$

where $d_1 = (17.59)(1 - \sin 60^\circ) = 2.36$ inches, $d_2 = 17.59$ inches, and $d_3 = (17.59)(1 + \sin 60^\circ) = 32.82$ inches.

Thus, for a maximum separation moment of $2.16(10)^6$ in-lb, the maximum force in the bolts, P_{max}, is:

$$P_{max} = \frac{M}{84.8} = \frac{2.16(10)^6}{84.8} = 25{,}472 \text{ lb}$$

(8) Impact Limiter Attachment Stresses

The tensile stress area of a 1¼-7UNC bolt of 0.969 in^2 exceeds the cross-sectional area of the 1.0-inch diameter shaft ($A = 0.785$ in^2). Therefore, maximum impact limiter attachment bolt stress is:

$$S_B = \frac{P_{max}}{A} = \frac{25{,}472}{0.785} = 32{,}448 \text{ psi}$$

From Table 2.6-1, the NCT allowable non-containment fastener primary membrane stress intensity, S_a = 101,400 psi at 160 ºF for ASTM A320, Grade L43, bolting material. Therefore, the impact limiter attachment bolt margin of safety is:

$$MS = \frac{S_a}{S_B} - 1 = \frac{101{,}400}{32{,}448} - 1 = +2.13$$

Bolt engagement is checked by using, from the preceding calculations, the maximum bolt force, P = 25,472 pounds. Per Appendix 1.3.1, *Packaging General Arrangement Drawings*, the minimum engagement length for these fasteners, L = 1.75 inches. The shear area per inch of engagement for a 1¼-7UNC-2B internal thread, A = 2.9441 in^2/in[11]. The resultant shear stress is therefore:

$$\tau = \frac{P}{LA} = \frac{25{,}472}{(1.75)(2.9441)} = 4{,}944 \text{ psi}$$

From Table 2.6-1, the NCT allowable pure shear stress intensity, S_a = 12,000 psi at 160 ºF, conservatively assuming the threads are Type F304 stainless steel. Therefore, the thread shear margin of safety is:

$$MS = \frac{S_a}{\tau} - 1 = \frac{12{,}000}{4{,}944} - 1 = +1.43$$

Thread insert engagement is checked by using the same maximum force from above, P = 25,472 pounds, to determine the maximum thread insert force. The engagement length for the thread inserts is 1.75 inches. The shear area per inch of engagement for a 1¾-12UN-2B internal thread is 3.9804 in^2/in[11]. The resultant shear stress is therefore:

$$\tau = \frac{P}{LA} = \frac{25{,}472}{(1.75)(3.9804)} = 3{,}657 \text{ psi}$$

From Table 2.6-1, the NCT allowable pure shear stress intensity, S_a = 12,000 psi at 160 ºF, for Type F304 stainless steel. Therefore, the thread shear margin of safety is:

$$MS = \frac{S_a}{\tau} - 1 = \frac{12{,}000}{3{,}657} - 1 = +2.28$$

(9) Stresses in the OC and IV Lid Bolts

Four basic loading mechanisms exist for the OC and IV closure bolts:

- Longitudinal impact forces inducing tensile bolt stresses which attempt to separate the lid from the body (OC or IV),
- Lateral impact forces inducing bolt shear,
- Pressure forces inducing tensile bolt stresses, and
- Bolt preload effects.

[11] *Table Speeds Calculation of Strength of Threads*, Product Engineering, November 27, 1961, pp41-49.

Maximum longitudinal impact forces are experienced during vertical or near-vertical impact. These forces are conservatively assessed in Section 2.6.7.1, *Flat End Drop*. In this early analysis, conservatism is assured by neglecting the external energy absorber forces imposed upon the lid that directly react impact associated with bolt tensile stresses. Thus, in this earlier end drop analysis, all impact forces are conservatively reacted by direct uniform bolt tension.

Similarly, maximum lateral impact forces are experienced during side impacts and have been assessed in Section 2.6.7.3, *Flat Side Drop*. In this section, lateral impact forces are assumed to be carried by one or more of three bounding mechanisms. The first and most probable mechanism assumes frictional forces between the lid and body carry all lateral forces. Bolt preloads are shown to be sufficient to assure a positive margin of safety.

The second lateral force reacting mechanism demonstrates that in the absence of bolt preload forces, all loads are carried in bearing between the stepped lid and the body. Under this mechanism, clearances are such that no lateral loads are imposed via bearing stresses upon the bolts themselves. Specifically, the maximum radial clearance between the OC lid and body is 0.017 inches, and the minimum bolt radial clearance is 0.034 inches. Similarly, the IV lid-to-body gap is 0.011 inches, and the minimum bolt radial clearance is 0.015 inches, precluding the possibility of shear loading the bolts.

In the third and least likely lateral force reacting mechanism, friction force resistance capability is assumed degraded (to zero) by internal pressure effects and all lateral forces are shown to be resisted by bolt shear.

Although the consequences of both maximum lateral and longitudinal impact forces are addressed in the analysis of end and side drops, corner and oblique drops pose a somewhat different set of circumstances. Specifically, friction forces between lid and body, associated with bolt preloads, may not exist (or be sufficient) to carry lateral loads where longitudinal impact forces are sufficiently large as to relieve the normal forces between lid and body. In these circumstances, associated only with corner and oblique loads, lateral forces may be imposed on the bolts. Such circumstances are addressed in analyses discussed below.

(a) Stresses in the OC Lid Bolts

Comprehensive analysis of all oblique orientations is summarized in Table 2.10.6-1 and Table 2.10.6-2 of Appendix 2.10.6, *Closure Bolt Stress Evaluations*. The minimum margin of safety is found at a near-vertical orientation of 85º with respect to horizontal. At this orientation angle, direct tensile stress due to impact, pressure effects, and preload effects is estimated at 55,504 psi. The associated shear stress is 149 psi. From Table 2.6-1, the NCT allowable containment fastener primary membrane stress intensity, S_a = 67,600 psi at 160 ºF for ASTM A320, Grade L43, bolting material. The resultant margin of safety is computed at +0.22.

As described in Appendix 2.10.6, *Closure Bolt Stress Evaluations*, bolt impact stresses are calculated assuming a triangular distribution of bolt forces and external impact forces arbitrarily (and conservatively) applied at the corner of the package. Thus, external energy absorber forces are not employed to reduce bolt tensile forces. For near vertical impacts, this assumption is most conservative.

The margin of safety for bolt engagement need not be calculated since it is greater than for the end drop case possessing a margin of safety of +0.19. An assessment of OC bolt and thread insert

engagement is provided in Appendix 2.10.6, *Closure Bolt Stress Evaluations*, and shown to have a minimum margin of safety of +0.13.

(b) Stresses in the IV Lid Bolts

The bolts must resist only preloads, pressure stresses, and lateral forces. No impact forces exist since all axial loads are transmitted directly to the OC lid; both surfaces are flat and parallel.

Comprehensive analysis of all impact orientations is summarized in Table 2.10.6-3 and Table 2.10.6-4 of Appendix 2.10.6, *Closure Bolt Stress Evaluations*. The minimum margin of safety is found at a near-horizontal orientation of 5º with respect to horizontal. This differs from the OC conditions because impact loads are directly transferred to the OC lid (in direct bearing) and do not contribute to bolt stresses. At an angle of 5º, total direct tension, due to pressure and preload effects, is estimated at 53,737 psi, with an associated shear stress of 2,199 psi. From Table 2.6-1, the NCT allowable containment fastener primary membrane stress intensity, S_a = 67,600 psi at 160 ºF for ASTM A320, Grade L43, bolting material. The resultant margin of safety is computed as +0.25.

Bolt engagement stresses are nearly identical to end impact values since the dominant tensile stress component is due to pressure, which is identical in both analyses. An assessment of IV bolt and thread insert engagement is provided in Appendix 2.10.6, *Closure Bolt Stress Evaluations*, and shown to have a minimum margin of safety of +0.18.

(10) Impact Limiter Deformations and Residual Clearances

Maximum impact limiter deformations and residual clearances due to normal corner/oblique drops are directly available from Figure 2.10.3-3 in Appendix 2.10.3, *Drop Impact Evaluation Results*. Per that section, maximum crush of an impact limiter corner is 9.68 inches for the 140 ºF foam stress case, and occurs for a drop angle of 45º with respect to horizontal. Minimum residual clearance for the main package body is 13.4 inches for the 140 ºF foam stress case, and occurs for a drop angle of 5º with respect to horizontal. These deformations and residual clearances are of little consequence for the RH-TRU 72-B package.

2.6.7.3 Flat Side Drop

Analysis of RH-TRU 72-B package behavior for the side drop event is performed in the following steps:

(1) Analyze the impact force using the CASKDROP computer program.

(2) Based on the accelerations predicted in (1), determine the equivalent "static" forces on the OC and IV, considered as a rigid body with distributed and lumped masses.

(3) Based on the loads from (2), analyze the OC shells and IV as simple beams, finding the internal forces: thrust, shear, and moment. Compute stresses for the maximum value of each of these forces.

(4) Analyze the OC shells for stress, assuming the two shells act as parallel beams, under the loads determined in (3).

(5) Analyze the IV for stress under the loads determined in (3).

(6) Analyze the payload canister for stress under the loads determined in (3).

(7) Analyze the OC lid for bearing against the top OC ring forging, analyze the OC closure bolts, and analyze the top OC ring forging for shear.

(8) Analyze the OC end plate welds for shear.

(9) Analyze the IV lid for bearing against the IV ring forging, analyze the IV closure bolts, and analyze the IV ring forging.

(10) Calculate the maximum impact limiter deformations and residual clearances for package hard spots.

Material properties and allowable stresses corresponding to maximum enveloping temperature of 160 ºF for the Type 304 stainless steel OC and IV are given in Table 2.6-1. Buckling is addressed in Appendix 2.10.5, *Buckling Design Criteria and Detailed Evaluation*.

Where possible, the analyses in this section are performed on the basis of a unit (1*g*) axial acceleration, with actual acceleration numbers being substituted at the final point of calculating stresses.

(1) Side Drop Computer Analysis Using CASKDROP

The side drop analysis was performed utilizing the energy-balance computer program, CASKDROP, documented in Appendix 2.10.2.1, *Description of the CASKDROP Computer Code*. Two cases were run which accounted for variations in foam strength due to temperature effects and the possible variations in foam strength from nominal values (see Section 2.3, *Mechanical Properties of Materials*). Each of these two cases consists of two different loading studies for a total of four different cases. The two different loading cases are as follows: (1) distributed payload within the canister, and (2) concentrated payload and canister weight at either of the IV spacer disk supports.

The drop cases consider the impact limiter as fully effective, as defined in Appendix 2.10.3, *Drop Impact Evaluation Results*. Worst-case deflections and accelerations obtained from the bounding cases are utilized for all analyses. The maximum resultant acceleration for the NCT side drop is 19.3*g* for cold (-20 ºF) foam per Table 2.10.3-10, and the maximum impact limiter deflection is 2.12 inches for warm (140 ºF) foam per Table 2.10.3-5 of Appendix 2.10.3, *Drop Impact Evaluation Results*.

(2) Equivalent "Static" Loads

The OC and IV are treated as rigid bodies under transverse acceleration. The two bodies are assumed to move together, and the forces between them needed to make them do so, is found. The centers of gravity of the two bodies are assumed to be coincident.

(3) Internal Forces

The OC shells are analyzed as if they are two beams acting in parallel. The payload canister is analyzed as one beam attached to the IV at the two spacer disk locations, and the IV connects to the OC via a series of interface (gap) elements. A schematic representation of the finite element analysis model used is presented as Figure 2.10.1-9 in Appendix 2.10.1.4, *Containment Assembly Analysis for Oblique Drops*.

Worst-case loading conditions on the OC and IV are found to occur under the following combinations of temperature and payload distribution: cold (-20 ºF) foam with a distributed payload for the OC, and cold (-20 ºF) foam with a concentrated payload for the IV.

Shear and moment diagrams for cold (-20 ºF) foam with a distributed payload are shown in Figure 2.6-19 and Figure 2.6-20, and with a concentrated payload in Figure 2.6-21 and Figure 2.6-22 with each component on the same figure. As discussed in Section 2.6.7.2, *Corner and Oblique Drops*, the figures were created using slightly different impact *g*-loadings than given in Appendix 2.10.3, *Drop Impact Evaluation Results*. The difference, however, is small. The figures were created using a side drop g load of 20.3*g*, which is comparable to the actual side drop *g*-load of 19.3*g*. Therefore, scaling of the shear and moments is appropriate. Similarly, the shear and moment diagrams for hot (140 ºF) foam with a distributed payload, shown in Figure 2.6-23 and Figure 2.6-24, and with a concentrated payload in Figure 2.6-25 and Figure 2.6-26, are scaled accordingly.

As previously discussed, the cold foam yields the worst stresses. The OC experiences worst-case stresses under a distributed payload, while the IV experiences its worst stresses due to a concentrated payload/canister force. The canister stresses are calculated for the distributed payload case and included only for the sake of consistency with other sections herein. Although the maximum shear and moment do not occur at the same location for each component, the maximums will be used to determine combined stresses, since this approach provides a conservative analysis. The figures are based on a *g*-load of 20.3*g*, whereas the actual side drop impact is 19.3*g*. The scale factor is therefore 19.3/20.3 = 0.951.

The maximum shear, V_{max}, and moment, M_{max}, for the OC are:

$$V_{max} = (385{,}325)(0.951) = 366{,}444 \text{ lb}$$

$$M_{max} = (12{,}551{,}000)(0.951) = 11{,}936{,}000 \text{ in-lb}$$

The maximum shear, V_{max}, and moment, M_{max}, for the IV are:

$$V_{max} = (88{,}456)(0.951) = 84{,}122 \text{ lb}$$

$$M_{max} = (1{,}462{,}600)(0.951) = 1{,}390{,}930 \text{ in-lb}$$

The maximum shear, V_{max}, and moment, M_{max}, for the payload canister, with only the distributed payload considered, are:

$$V_{max} = (50{,}084)(0.951) = 47{,}630 \text{ lb}$$

$$M_{max} = (547{,}920)(0.951) = 521{,}072 \text{ in-lb}$$

Maximum stresses can be calculated from the maximum shear and moments (given above) as follows:

$$S_v = \frac{V}{A} = \text{stress due to shear, psi}$$

$$S_m = \frac{Mc}{I} = \text{stress due to bending moment, psi}$$

where V is the shear force (lb) and M is the bending moment (in-lb). The distance to the neutral axis, c = 20.565 inches for the OC outer shell, c = 17.19 inches for the OC inner shell, c = 16.00 inches for the IV shell, and c = 13.00 inches for the payload canister. The moment of intertia, I = 51,334 in^4 for the OC, I = 4,718 in^4 for the IV, and I = 1,676 in^4 for the payload canister. Finally, the area, A = 292 in^2 for the OC, A = 38 in^2 for the IV, and A = 20 in^2 for the payload canister.

(4) OC Stresses

The maximum membrane stress in the OC inner shell, for the load case selected in Paragraph (3), is:

$$S_m = \frac{Mc}{I} = \frac{(11{,}936{,}000)[17.19 - (½)(1.0)]}{51{,}334} = 3{,}881 \text{ psi}$$

The maximum membrane-plus-bending stress in the OC inner shell is:

$$S_{mb} = \frac{Mc}{I} = \frac{(11{,}936{,}000)(17.19)}{51{,}334} = 3{,}997 \text{ psi}$$

Similarly, the maximum stresses in the OC outer shell are:

$$S_m = \frac{Mc}{I} = \frac{(11{,}936{,}000)[20.565 - (½)(1.5)]}{51{,}334} = 4{,}607 \text{ psi}$$

$$S_{mb} = \frac{Mc}{I} = \frac{(11{,}936{,}000)(20.565)}{51{,}334} = 4{,}782 \text{ psi}$$

In addition, shear stress must be added in the calculation of the membrane stress intensities for the OC inner and outer shells. The shear stress is:

$$S_v = \frac{V}{A} = \frac{366{,}444}{292} = 1{,}255 \text{ psi}$$

Hoop fabrication stresses used in the NCT side drop analyses are identical to those used in the end drop analysis (refer to Table 2.6-12 in Section 2.6.7.1, *Flat End Drop*), and axial fabrication stresses are -1,963 psi per Appendix 2.10.8.5, *Axial Stress Evaluation after Cooldown from 620 ºF to -20 ºF*. Fabrication stresses for the side drop analyses are given in Table 2.6-27.

Table 2.6-28, Table 2.6-29, and Table 2.6-30 present the corresponding margins of safety for the more critical OC inner shell. Zero internal pressure is used in order to maximize compressive stresses in the inner shell. Again, it is noted that the margins presented for the 70 ºF and 160 ºF cases are conservative since at these temperatures, *g*-loads will actually be less than the 19.3*g* considered herein.

(5) IV Stresses

The maximum membrane stress in the IV shell, for the load case selected in Paragraph (3), is:

$$S_m = \frac{Mc}{I} = \frac{(1{,}390{,}930)[16.00 - (½)(0.38)]}{4{,}718} = 4{,}661 \text{ psi}$$

The maximum membrane-plus-bending stress in the IV shell is:

$$S_{mb} = \frac{Mc}{I} = \frac{(1{,}390{,}930)(16.00)}{4{,}718} = 4{,}717 \text{ psi}$$

In addition, shear stress must be added in the calculation of the membrane stress intensity for the IV shell. The shear stress is:

$$S_v = \frac{V}{A} = \frac{84{,}122}{38} = 2{,}214 \text{ psi}$$

Table 2.6-31 presents stress and margin of safety results for the IV for the worst-case load combination selected in Paragraph (3).

(6) Discussion of Payload Canister Behavior in Side Drops

The maximum membrane stress in the payload canister shell, for the load case selected in Paragraph (3), is:

$$S_m = \frac{Mc}{I} = \frac{(521{,}072)[13.00 - (½)(0.25)]}{1{,}676} = 4{,}003 \text{ psi}$$

The maximum membrane-plus-bending stress in the payload canister shell is:

$$S_{mb} = \frac{Mc}{I} = \frac{(521{,}072)(13.00)}{1{,}676} = 4{,}042 \text{ psi}$$

In addition, shear stress must be added in the calculation of the membrane stress intensity for the payload canister shell. The shear stress is:

$$S_v = \frac{V}{A} = \frac{47{,}630}{20} = 2{,}382 \text{ psi}$$

Table 2.6-32 presents stress and margin of safety results for the canister shell for the load combination selected in Paragraph (3). Allowable stresses were conservatively determined for 200 ºF material temperature. Buckling is addressed in Appendix 2.10.5, *Buckling Design Criteria and Detailed Evaluation*.

(7) OC Lid Analysis

Since the clearance between the OC lid and sealing surface is less than the clearance between the bolt and bolt hole, the lid will displace laterally to bear against the sealing surface in the forging before lateral loading of the lid bolts occurs. Therefore, the following analysis addresses the stress resulting from lateral loading of the body ring forging by the lid.

In the most unlikely event that the lid displaces laterally to bear upon the body ring forging, lateral loads will be transferred by bearing. The following calculations demonstrate the adequacy of this load transfer mechanism.

The weight of the OC lid may be carried in bearing against the lid-end OC ring forging if sliding occurs at the lid-to-forging interface. The side drop acceleration of 19.3*g* is utilized in a Hertzian analysis to determine the bearing stress between the two cylinders. Because this analysis is sensitive to very small variations in the diametric gap between the cylinders, the worst-case tolerance stackup has been factored into the following calculation using Table 33, Case 2c, from Roark and Young[12], assuming the elastic modulus, E, and Poisson's ratio, μ, are equal for the mating materials:

$$S_b = 0.591\sqrt{\frac{PE}{LK_D}} = 3{,}903 \text{ psi}$$

where the OC lid weight with 19.3*g*, P = (1,667)(19.3) = 32,173 pounds, the elastic modulus, $E = 27.8(10)^6$ psi at 160 ºF from Table 2.3-1 in Section 2.3, *Mechanical Properties of Materials*, the contact length, L = 0.664 inches (approximately), and the diametral stiffness, K_D, is:

$$K_D = \frac{D_1 D_2}{D_1 - D_2} = 30{,}886 \text{ in}$$

where the outer cylinder diameter, D_1 = 32.896 inches, and the inner cylinder diameter, D_2 = 32.861 inches.

From Table 2.6-1, the NCT allowable sealing surface bearing stress intensity, S_a = 27,000 psi at 160 ºF for Type F304 stainless steel. Therefore, the bearing stress margin of safety is:

$$MS = \frac{S_a}{S_b} - 1 = \frac{27{,}000}{3{,}903} - 1 = +5.92$$

The lip of the forging that supports the OC lid is loaded in shear by the lid. Conservatively assuming only one-half of the lip is effective in resisting the 19.3*g* load, the shear stress is:

$$S_v = \frac{V}{\frac{1}{2}\pi(R_o^2 - R_i^2)} = 269 \text{ psi}$$

where the weight of the lid is the shear load with 19.3*g*, V = (1,667)(19.3) = 32,173 pounds, the outside radius of the lip, R_o = 20.81 inches, and the inside radius of the lip, R_i = 18.89 inches.

From Table 2.6-1, the NCT allowable shear stress intensity, S_a = 12,000 psi at 160 ºF for Type F304 stainless steel. Therefore, the shear stress margin of safety is:

$$MS = \frac{S_a}{S_v} - 1 = \frac{12{,}000}{269} - 1 = +43.6$$

[12] R. J. Roark, W. C. Young, *Formulas for Stress and Strain*, 5th Edition, McGraw-Hill, Inc., New York, NY, 1975.

(8) Welds Joining the OC Shells to the End Closure Plate

The worst-case shear load at the joints of the OC shells to the end closure plate is taken as the maximum shear load determined from Figure 2.6-19 at the package locations corresponding to the welded joints (0 inches and 120 inches). Therefore, the maximum shear load at the welded joints, V = 353,152 pounds.

Since the welds are full penetration bevel welds, the effective shear area for shells may be found by the following equation (i.e., conservatively use half the total weld area):

$$A_w = \frac{2\pi(R_i t_i + R_o t_o)}{2} = 145.8\,\text{in}^2$$

where the mean OC inner shell radius, R_i = 16.69 inches, the OC inner shell thickness, t_i = 1.00 inches, the mean OC outer shell radius, R_o = 19.81 inches, and the OC outer shell thickness, t_o = 1.50 inches.

The direct shear stress in the OC shells' welds is:

$$\tau_w = \frac{V}{A_w} = 2{,}422\ \text{psi}$$

Table 2.6-33 presents stress and margin of safety results for the OC shells' welds under worst-case load combinations.

(9) IV Lid Analysis

Since the clearance between the lid and sealing surface is less than the clearance between the bolt and bolt hole, the IV lid will displace laterally to bear against the sealing surface in the forging before lateral loading of the bolts. Therefore, the following analysis addresses the stress resulting from lateral loading of the IV body ring forging by the IV lid.

In the most unlikely event that the lid displaces laterally to bear upon the body ring forging, lateral loads will be transferred by bearing. The following calculation demonstrates the adequacy of this load transfer mechanism.

The weight of the IV lid may be carried in bearing against the IV body ring forging if sliding occurs at the lid-to-forging interface.

This analysis accounts for only the uppermost race surface being in contact with the forging for bearing. As with Paragraph (7), the side drop acceleration of 19.3*g* is utilized in a Hertzian analysis to determine the bearing stress between two cylinders for the worst-case tolerance stackup using the following calculation using Table 33, Case 2c, from Roark and Young[12], assuming the elastic modulus, E, and Poisson's ratio, μ, are equal for the mating materials:

$$S_b = 0.591\sqrt{\frac{PE}{LK_D}} = 4{,}657\ \text{psi}$$

where the IV lid weight with 19.3*g*, P = (1,382)(19.3) = 26,673 pounds, the elastic modulus, E = 27.8(10)^6 psi at 160 ºF from Table 2.3-1 in Section 2.3, *Mechanical Properties of Materials*, the contact length, L = 0.32 inches (approximately), and the diametral stiffness, K_D, is:

$$K_D = \frac{D_1 D_2}{D_1 - D_2} = 37{,}321 \text{ in}$$

where the outer cylinder diameter, D_1 = 28.006 inches, and the inner cylinder diameter, D_2 = 27.985 inches.

From Table 2.6-1, the NCT allowable sealing surface bearing stress intensity, S_a = 27,000 psi at 160 ºF for Type F304 stainless steel. Therefore, the bearing stress margin of safety is:

$$MS = \frac{S_a}{S_b} - 1 = \frac{27{,}000}{4{,}657} - 1 = +4.80$$

The lip of the forging that supports the IV lid is loaded in shear by the lid. Conservatively assuming only one-half of the lip is effective in resisting the 19.3*g* load, the shear stress is:

$$S_v = \frac{V}{\frac{1}{2}\pi(R_o^2 - R_i^2)} = 283 \text{ psi}$$

where the weight of the lid is the shear load with 19.3*g*, V = (1,382)(19.3) = 26,673 pounds, the outside radius of the lip, R_o = 16.00 inches, and the inside radius of the lip, R_i = 14.00 inches.

From Table 2.6-1, the NCT allowable shear stress intensity, S_a = 12,000 psi at 160 ºF for Type F304 stainless steel. Therefore, the shear stress margin of safety is:

$$MS = \frac{S_a}{S_v} - 1 = \frac{12{,}000}{283} - 1 = +41.4$$

(10) Impact Limiter Deformations and Residual Clearances

Maximum impact limiter deformations and residual clearances due to NCT side drop are directly available from Appendix 2.10.3, *Drop Impact Evaluation Results*. Per Table 2.10.3-10 in Appendix 2.10.3, *Drop Impact Evaluation Results*, maximum crush of an impact limiter side is 2.12 inches for the 140 ºF foam stress case resulting in a minimum residual clearance for the main package body of 14.88 inches (based on a 16.00 inch nominal radial thickness). These deformations and residual clearances are of little consequence for the RH-TRU 72-B package.

2.6.8 Corner Drop

This test does not apply to the RH-TRU 72-B package since the package weight is in excess of 100 kg (220 pounds) and the materials of construction do not include wood or fiberboard.

2.6.9 Compression

This test does not apply to the RH-TRU 72-B package since the package weight is in excess of 5,000 kg (11,000 pounds).

2.6.10 Penetration

Due to the lack of sensitive external protuberances, the one meter (40-inch) drop of a 13-pound hemispherical headed, 1¼-inch diameter, steel cylinder is of negligible consequence to the RH-TRU 72-B package.

Table 2.6-1 – Summary of NCT Material Properties for Analysis

Material Property	Material Property Value (psi)					Reference
	-40 °F	-20 °F	70 °F	160 °F	200 °F	
ASTM A240/A276, Type 304 Stainless Steel						
Elastic Modulus, E ($\times 10^6$)	28.9	28.8	28.3	27.8	27.6	Table 2.3-1
Design Stress Intensity, S_m	20,000	20,000	20,000	20,000	20,000	
Yield Strength, S_y	30,000	30,000	30,000	27,000	25,000	
Ultimate Strength, S_u	75,000	75,000	75,000	72,600	71,000	
Stress Intensity Allowable for Containment Structures (Table 2.1-1)						
Primary Membrane	20,000	20,000	20,000	20,000	20,000	
Primary Membrane-Plus-Bending	30,000	30,000	30,000	30,000	30,000	
ASTM A182/SA182, Type F304, Stainless Steel						
Elastic Modulus, E ($\times 10^6$)	28.9	28.8	28.3	27.8	27.6	Table 2.3-1
Design Stress Intensity, S_m	20,000	20,000	20,000	20,000	20,000	
Yield Strength, S_y	30,000	30,000	30,000	27,000	25,000	
Ultimate Strength, S_u	70,000	70,000	70,000	67,700	66,200	
Stress Intensity Allowable for Containment Structures (Table 2.1-1)						
Primary Membrane	20,000	20,000	20,000	20,000	20,000	
Primary Membrane-Plus-Bending	30,000	30,000	30,000	30,000	30,000	
Pure Shear	12,000	12,000	12,000	12,000	12,000	
Bearing (Sealing Surfaces)	30,000	30,000	30,000	27,000	25,000	
Stress Intensity Allowable for Non-Containment Structures (Table 2.1-2)						
Primary Membrane	30,000	30,000	30,000	27,000	25,000	
Primary Membrane-Plus-Bending	30,000	30,000	30,000	30,000	30,000	
ASTM A240/A276, Type 304L Stainless Steel						
Elastic Modulus, E ($\times 10^6$)	28.9	28.8	28.3	27.8	27.6	Table 2.3-1
Design Stress Intensity, S_m	16,700	16,700	16,700	16,700	16,700	
Yield Strength, S_y	25,000	25,000	25,000	22,800	21,300	
Ultimate Strength, S_u	70,000	70,000	70,000	67,700	66,200	
Stress Intensity Allowable for Non-Containment Structures (Table 2.1-2)						
Primary Membrane	25,000	25,000	25,000	22,800	21,300	
Primary Membrane-Plus-Bending	25,050	25,050	25,050	25,050	25,050	
ASTM A320, Grade L43, Alloy Steel						
Elastic Modulus, E ($\times 10^6$)	27.8	27.8	27.8	27.3	27.1	Table 2.3-1
Design Stress Intensity, S_m	35,000	35,000	35,000	33,800	33,000	
Yield Strength, S_y	105,000	105,000	105,000	101,400	99,000	
Ultimate Strength, S_u	125,000	125,000	125,000	125,000	125,000	
Stress Intensity Allowable for Containment Fasteners (Table 2.1-1)						
Primary Membrane	70,000	70,000	70,000	67,600	66,000	
Primary Membrane-Plus-Bending	105,000	105,000	105,000	101,400	99,000	
Stress Intensity Allowable for Non-Containment Fasteners (Table 2.1-2)						
Primary Membrane	105,000	105,000	105,000	101,400	99,000	
Primary Membrane-Plus-Bending	105,000	105,000	105,000	101,400	99,000	
Lead						
Elastic Modulus, E ($\times 10^6$)	2.44	2.43	2.34	2.22	2.16	Table 2.3-2

Table 2.6-2 – Maximum NCT Temperatures

Location	Temperature, ºF	
	50 Watt Payload	300 Watt Payload
Canister Shell	132	167
Inner Vessel Shell	127	150
Outer Cask Inner Shell	126	143
Outer Cask Lead Shell	126	143
Outer Cask Outer Shell	126	143
Thermal Shield	125	142
Outer Cask Upper Ring Forging	126	137
Inner Vessel Lid	127	141
Outer Cask Lid	126	137
Inner Vessel O ring Seals	126	140
Outer Cask O ring Seals	126	137
Impact Limiter Shell	133	142
Trunnions	126	143

Table 2.6-3 – Package Parameters for Pressure Stress Calculations

Location	Temperature (ºF)	Radius (in)	Thickness (in)	Diameter (in)	Thickness (in)
P1	160	19.813	1.50	—	—
P2	160	16.69	1.00	—	—
P3	160	15.81	0.375	—	—
P4	160	19.813	1.50	—	—
P5	160	16.69	1.00	—	—
P6	160	15.81	0.375	—	—
P7	160	—	—	41.60	5.00
P8	160	—	—	37.60	6.00
P9	160	—	—	32.00	6.50
P10	160	—	—	32.00	1.50

Table 2.6-4 – Unit Pressure Stress Results for P1 – P6

Location	Temperature (ºF)	λ (in^{-1})	D (lb-in)	V_o (lb-in)	M_o (in-lb/in)	σ_1 (psi)	σ_2 (psi)	σ_1' (psi)	σ_2' (psi)
P1	160	—	—	—	—	6.60	13.21	0.0	0.0
P2	160	—	—	—	—	8.35	16.69	0.0	0.0
P3	160	—	—	—	—	21.08	42.16	0.0	0.0
P4	160	0.2357	$8.592(10)^6$	3.604	7.644	6.60	1.94	-20.43	-6.13
P5	160	0.3146	$2.546(10)^6$	2.701	4.292	8.35	2.44	-25.83	-7.75
P6	160	—	—	—	—	21.67	-37.74	-220.2	-68.66

Table 2.6-5 – Unit Pressure Stress Results for P7 – P10

Location	Temperature (ºF)	M_o (in-lb/in)	σ (psi)
P7	160	89.23	21.42
P8	160	72.90	12.15
P9	160	52.80	7.50
P10	160	52.80	140.80

Table 2.6-6 – Maximum Pressure Stress Results for P1 – P10

Shell / End Plate Location	Axial Membrane σ_1 (psi)	Hoop Membrane σ_2 (psi)	Axial Bending① σ_1' (psi)	Hoop Bending① σ_2' (psi)	Radial Bending σ (psi)
P1	990	1,982	0	0	—
P2	1,252	2,504	0	0	—
P3	3,162	6,324	0	0	—
P4	990	291	-3,064	-920	—
P5	1,252	366	-3,874	-1,162	—
P6	3,251	-5,661	-33,030	-10,299	—
P7	—	—	—	—	3,213
P8	—	—	—	—	1,823
P9	—	—	—	—	1,125
P10	—	—	—	—	21,120

Notes:

① σ_1' and σ_2' are positive when tensile on the shell outside diameter.

Table 2.6-7 – Package Stresses Due to Side Drop

Component	Membrane-Plus-Bending Stress Intensity (psi)
OC Outer Shell	4,782
OC Inner Shell	3,997
IV Shell	4,717

Table 2.6-8 – NCT End Drop, OC Lid Bending

Evaluation Parameters	
Loading Condition:	NCT Flat End Drop, -20 ºF Foam
Structural Material:	ASTM A240, Type F304, Stainless Steel
Stress Condition:	Primary Membrane-Plus-Bending
Structural Criterion:	Containment Boundary
Stress Allowable (from Table 2.1-1):	$1.5S_m$
Material Temperature:	160 ºF
Allowable Stress, S_a:	30,000 psi

Load Condition	Stress Components (psi)				Reference Section
	Radial σ_r	Hoop σ_t	Axial σ_z	Shear τ_{rz}	
Internal Pressure	1,823	0	-150	0	2.6.1.3.2
End Drop	9,180	9,180	0	0	2.6.7.1(2)
Direct Stress Summation	11,003	9,180	-150	0	—
Principal Stresses	11,003	9,180	-150	—	—
Stress Differences	11,153	9,330	1,823	—	—
Maximum Stress Intensity (SI)	11,153	—	—	—	—
Allowable Stress Intensity (S_a)	30,000	—	—	—	—
Margin of Safety ($MS = S_a/SI - 1$)	+1.69	—	—	—	—

Table 2.6-9 – NCT Top-End Drop, IV Shell with 42.5*g* Acceleration

Evaluation Parameters	
Loading Condition:	NCT Flat End Drop, -20 ºF Foam
Structural Material:	ASTM A240, Type 304, Stainless Steel
Stress Condition:	Primary Membrane
Structural Criterion:	Containment Boundary
Stress Allowable (from Table 2.1-1):	S_m
Material Temperature:	160 ºF
Allowable Stress, S_a:	20,000 psi

Load Condition	Stress Components (psi)				Reference Section
	Radial σ_r	Hoop σ_t	Axial σ_z	Shear τ_{rz}	
Internal Pressure	-150	6,324	3,162	0	2.6.1.3.2
End Drop	0	0	-2,323	0	2.6.7.1(5)
Direct Stress Summation	-150	6,324	839	0	—
Principal Stresses	6,324	-150	839	—	—
Stress Differences	5,485	-989	6,474	—	—
Maximum Stress Intensity (SI)	6,474	—	—	—	—
Allowable Stress Intensity (S_a)	20,000	—	—	—	—
Margin of Safety (MS = S_a/SI – 1)	+2.09	—	—	—	—

Table 2.6-10 – NCT Bottom-End Drop, IV Shell with 42.5*g* Acceleration

Evaluation Parameters	
Loading Condition:	NCT Flat End Drop, -20 ºF Foam
Structural Material:	ASTM A240, Type 304, Stainless Steel
Stress Condition:	Primary Membrane
Structural Criterion:	Containment Boundary
Stress Allowable (from Table 2.1-1):	S_m
Material Temperature:	160 ºF
Allowable Stress, S_a:	20,000 psi

Load Condition	Stress Components (psi)				Reference Section
	Radial σ_r	Hoop σ_t	Axial σ_z	Shear τ_{rz}	
Internal Pressure	-150	6,324	3,162	0	2.6.1.3.2
End Drop	0	0	-4,185	0	2.6.7.1(5)
Direct Stress Summation	-150	6,324	-1,023	0	—
Principal Stresses	6,324	-150	-1,023	—	—
Stress Differences	7,347	873	6,474	—	—
Maximum Stress Intensity (SI)	7,347	—	—	—	—
Allowable Stress Intensity (S_a)	20,000	—	—	—	—
Margin of Safety (MS = S_a/SI – 1)	+1.72	—	—	—	—

Table 2.6-11 – Fabrication Induced OC Inner Shell Hoop Stress, Interface Pressure, and Axial Load That Can Be Supported

Temperature (ºF)	Hoop Stress (psi)	Interface Pressure (psi)	Coefficient of Friction	Axial Load (lb)
160	-1,038	62.2	0.5	414,842
			1.0	829,685
70	-1,413	84.7	0.5	564,906
			1.0	1,129,812
-20	-1,821	109.1	0.5	727,641
			1.0	1,455,283

Table 2.6-12 – OC Shell Stresses with Maximum End Drop Fab Condition

Temperature (ºF)	Inner Shell Stresses (psi)		Outer Shell Stresses (psi)	
	Hoop σ_t	Axial σ_z	Hoop σ_t	Axial σ_z
160	-1,038	-6,067	0	-2,929
70	-1,413	-6,067	0	-2,929
-20	-1,821	-6,067	0	-2,929

Table 2.6-13 – NCT Fab & End Drop, OC Inner Shell with 42.5*g* at -20 ºF

Evaluation Parameters	
Loading Condition:	NCT Flat End Drop, -20 ºF Foam
Structural Material:	ASTM A240, Type 304, Stainless Steel
Stress Condition:	Primary Membrane
Structural Criterion:	Containment Boundary
Stress Allowable (from Table 2.1-1):	S_m
Material Temperature:	-20 ºF
Allowable Stress, S_a:	20,000 psi

Load Condition	Stress Components (psi)				Reference Section
	Radial σ_r	Hoop σ_t	Axial σ_z	Shear τ_{rz}	
Fabrication and End Drop	0	-1,821	-6,067	0	2.6.7.1(6)
Direct Stress Summation	0	-1,821	-6,067	0	—
Principal Stresses	0	-1,821	-6,067	—	—
Stress Differences	6,067	4,246	1,821	—	—
Maximum Stress Intensity (SI)	6,067	—	—	—	—
Allowable Stress Intensity (S_a)	20,000	—	—	—	—
Margin of Safety ($MS = S_a/SI - 1$)	+2.30	—	—	—	—

Table 2.6-14 – NCT Fab & End Drop, OC Inner Shell with 42.5*g* at 70 ºF

Evaluation Parameters	
Loading Condition:	NCT Flat End Drop, -20 ºF Foam
Structural Material:	ASTM A240, Type 304, Stainless Steel
Stress Condition:	Primary Membrane
Structural Criterion:	Containment Boundary
Stress Allowable (from Table 2.1-1):	S_m
Material Temperature:	70 ºF
Allowable Stress, S_a:	20,000 psi

Load Condition	Stress Components (psi)				Reference Section
	Radial σ_r	Hoop σ_t	Axial σ_z	Shear τ_{rz}	
Fabrication and End Drop	0	-1,413	-6,067	0	2.6.7.1(6)
Direct Stress Summation	0	-1,413	-6,067	0	—
Principal Stresses	0	-1,413	-6,067	—	—
Stress Differences	6,067	4,654	1,413	—	—
Maximum Stress Intensity (SI)	6,067	—	—	—	—
Allowable Stress Intensity (S_a)	20,000	—	—	—	—
Margin of Safety (MS = S_a/SI – 1)	+2.30	—	—	—	—

Table 2.6-15 – NCT Fab & End Drop, OC Inner Shell with 42.5*g* at 160 ºF

Evaluation Parameters	
Loading Condition:	NCT Flat End Drop, -20 ºF Foam
Structural Material:	ASTM A240, Type 304, Stainless Steel
Stress Condition:	Primary Membrane
Structural Criterion:	Containment Boundary
Stress Allowable (from Table 2.1-1):	S_m
Material Temperature:	160 ºF
Allowable Stress, S_a:	20,000 psi

Load Condition	Stress Components (psi)				Reference Section
	Radial σ_r	Hoop σ_t	Axial σ_z	Shear τ_{rz}	
Fabrication and End Drop	0	-1,038	-6,067	0	2.6.7.1(6)
Direct Stress Summation	0	-1,038	-6,067	0	—
Principal Stresses	0	-1,038	-6,067	—	—
Stress Differences	6,067	5,029	1,038	—	—
Maximum Stress Intensity (SI)	6,067	—	—	—	—
Allowable Stress Intensity (S_a)	20,000	—	—	—	—
Margin of Safety (MS = S_a/SI – 1)	+2.30	—	—	—	—

Table 2.6-16 – NCT End Drop, Lead Pressure and Hoop Stress Summary

Temperature (ºF)	σ_y (psi)	d (in)	p_{max} (psi)	$\sigma_t = p_{max}R/t$ (psi)	
				Inner Shell	Outer Shell
160	~600	34.4	89.9	-1,500	1,188
70	~800	45.9	103.3	-1,724	1,365
-20	~1,000	57.4	121.2	-2,023	1,601

Table 2.6-17 – NCT End Drop, OC Shell Stresses with Zero Fabrication Condition with 42.5*g* Acceleration

Temperature (ºF)	Inner Shell Stresses (psi)		Outer Shell Stresses (psi)	
	Hoop σ_t	Axial σ_z	Hoop σ_t	Axial σ_z
160	-1,500	-4,989	1,188	-3,550
70	-1,724	-4,989	1,365	-3,550
-20	-2,023	-4,989	1,601	-3,550

Table 2.6-18 – NCT End Drop, OC Inner Shell with 42.5*g* at -20 ºF

Evaluation Parameters	
Loading Condition:	NCT Flat End Drop, -20 ºF Foam
Structural Material:	ASTM A240, Type 304, Stainless Steel
Stress Condition:	Primary Membrane
Structural Criterion:	Containment Boundary
Stress Allowable (from Table 2.1-1):	S_m
Material Temperature:	-20 ºF
Allowable Stress, S_a:	20,000 psi

Load Condition	Stress Components (psi)				Reference Section
	Radial σ_r	Hoop σ_t	Axial σ_z	Shear τ_{rz}	
Fabrication and End Drop	0	-2,023	-4,989	0	2.6.7.1(7)
Direct Stress Summation	0	-2,023	-4,989	0	—
Principal Stresses	0	-2,023	-4,989	—	—
Stress Differences	4,989	2,966	2,023	—	—
Maximum Stress Intensity (SI)	4,989	—	—	—	—
Allowable Stress Intensity (S_a)	20,000	—	—	—	—
Margin of Safety ($MS = S_a/SI - 1$)	+3.01	—	—	—	—

Table 2.6-19 – NCT End Drop, OC Inner Shell with 42.5*g* at 70 ºF

Evaluation Parameters	
Loading Condition:	NCT Flat End Drop, -20 ºF Foam
Structural Material:	ASTM A240, Type 304, Stainless Steel
Stress Condition:	Primary Membrane
Structural Criterion:	Containment Boundary
Stress Allowable (from Table 2.1-1):	S_m
Material Temperature:	70 ºF
Allowable Stress, S_a:	20,000 psi

Load Condition	Stress Components (psi)				Reference Section
	Radial σ_r	Hoop σ_t	Axial σ_z	Shear τ_{rz}	
Fabrication and End Drop	0	-1,724	-4,989	0	2.6.7.1(7)
Direct Stress Summation	0	-1,724	-4,989	0	—
Principal Stresses	0	-1,724	-4,989	—	—
Stress Differences	4,989	3,265	1,724	—	—
Maximum Stress Intensity (SI)	4,989	—	—	—	—
Allowable Stress Intensity (S_a)	20,000	—	—	—	—
Margin of Safety (MS = S_a/SI – 1)	+3.01	—	—	—	—

Table 2.6-20 – NCT End Drop, OC Inner Shell with 42.5*g* at 160 ºF

Evaluation Parameters	
Loading Condition:	NCT Flat End Drop, -20 ºF Foam
Structural Material:	ASTM A240, Type 304, Stainless Steel
Stress Condition:	Primary Membrane
Structural Criterion:	Containment Boundary
Stress Allowable (from Table 2.1-1):	S_m
Material Temperature:	160 ºF
Allowable Stress, S_a:	20,000 psi

Load Condition	Stress Components (psi)				Reference Section
	Radial σ_r	Hoop σ_t	Axial σ_z	Shear τ_{rz}	
Fabrication and End Drop	0	-1,500	-4,989	0	2.6.7.1(7)
Direct Stress Summation	0	-1,500	-4,989	0	—
Principal Stresses	0	-1,500	-4,989	—	—
Stress Differences	4,989	3,489	1,500	—	—
Maximum Stress Intensity (SI)	4,989	—	—	—	—
Allowable Stress Intensity (S_a)	20,000	—	—	—	—
Margin of Safety (MS = S_a/SI – 1)	+3.01	—	—	—	—

Table 2.6-21 – OC Shell Stresses with Max Oblique Drop Fab Condition

Temperature (ºF)	Inner Shell Stresses (psi)		Outer Shell Stresses (psi)	
	Hoop σ_t	Axial σ_z	Hoop σ_t	Axial σ_z
160	-1,038	-2,555	0	-1,234
70	-1,413	-2,555	0	-1,234
-20	-1,821	-2,555	0	-1,234

Table 2.6-22 – NCT Fab & Oblique Drop, OC Inner Shell with 17.9*g* at -20 ºF

Evaluation Parameters	
Loading Condition:	NCT 85º Oblique Drop, -20 ºF Foam
Structural Material:	ASTM A240, Type 304, Stainless Steel
Stress Condition:	Primary Membrane
Structural Criterion:	Containment Boundary
Stress Allowable (from Table 2.1-1):	S_m
Material Temperature:	-20 ºF
Allowable Stress, S_a:	20,000 psi

Load Condition	Stress Components (psi)				Reference Section
	Radial σ_r	Hoop σ_t	Axial σ_z	Shear τ_{rz}	
Fabrication	0	-1,821	-2,555	0	2.6.7.2(4)
Oblique Drop	0	0	-6,463	608	2.6.7.2(4)
Direct Stress Summation	0	-1,821	-9,018	608	—
Principal Stresses	41	-1,821	-9,059	—	—
Stress Differences	9,100	7,238	1,862	—	—
Maximum Stress Intensity (SI)	9,100	—	—	—	—
Allowable Stress Intensity (S_a)	20,000	—	—	—	—
Margin of Safety ($MS = S_a/SI - 1$)	+1.20	—	—	—	—

Table 2.6-23 – NCT Fab & Oblique Drop, OC Inner Shell with 17.9*g* at 70 ºF

Evaluation Parameters	
Loading Condition:	NCT 85º Oblique Drop, -20 ºF Foam
Structural Material:	ASTM A240, Type 304, Stainless Steel
Stress Condition:	Primary Membrane
Structural Criterion:	Containment Boundary
Stress Allowable (from Table 2.1-1):	S_m
Material Temperature:	70 ºF
Allowable Stress, S_a:	20,000 psi

Load Condition	Stress Components (psi)				Reference Section
	Radial σ_r	Hoop σ_t	Axial σ_z	Shear τ_{rz}	
Fabrication	0	-1,413	-2,555	0	2.6.7.2(4)
Oblique Drop	0	0	-6,463	608	2.6.7.2(4)
Direct Stress Summation	0	-1,413	-9,018	608	—
Principal Stresses	41	-1,413	-9,059	—	—
Stress Differences	9,100	7,646	1,454	—	—
Maximum Stress Intensity (SI)	9,100	—	—	—	—
Allowable Stress Intensity (S_a)	20,000	—	—	—	—
Margin of Safety (MS = S_a/SI – 1)	+1.20	—	—	—	—

Table 2.6-24 – NCT Fab & Oblique Drop, OC Inner Shell with 17.9*g* at 160 ºF

Evaluation Parameters	
Loading Condition:	NCT 85º Oblique Drop, -20 ºF Foam
Structural Material:	ASTM A240, Type 304, Stainless Steel
Stress Condition:	Primary Membrane
Structural Criterion:	Containment Boundary
Stress Allowable (from Table 2.1-1):	S_m
Material Temperature:	160 ºF
Allowable Stress, S_a:	20,000 psi

Load Condition	Stress Components (psi)				Reference Section
	Radial σ_r	Hoop σ_t	Axial σ_z	Shear τ_{rz}	
Fabrication	0	-1,038	-2,555	0	2.6.7.2(4)
Oblique Drop	0	0	-6,463	608	2.6.7.2(4)
Direct Stress Summation	0	-1,038	-9,018	608	—
Principal Stresses	41	-1,038	-9,059	—	—
Stress Differences	9,100	8,021	1,079	—	—
Maximum Stress Intensity (SI)	9,100	—	—	—	—
Allowable Stress Intensity (S_a)	20,000	—	—	—	—
Margin of Safety (MS = S_a/SI – 1)	+1.20	—	—	—	—

Table 2.6-25 – NCT Oblique Drop, IV Shell with 17.9*g* at 70 ºF

Evaluation Parameters	
Loading Condition:	NCT 85º Oblique Drop, -20 ºF Foam
Structural Material:	ASTM A240, Type 304, Stainless Steel
Stress Condition:	Primary Membrane
Structural Criterion:	Containment Boundary
Stress Allowable (from Table 2.1-1):	S_m
Material Temperature:	70 ºF
Allowable Stress, S_a:	20,000 psi

Load Condition	Stress Components (psi)				Reference Section
	Radial σ_r	Hoop σ_t	Axial σ_z	Shear τ_{rz}	
Oblique Drop	0	0	-5,247	2,099	2.6.7.2(5)
Direct Stress Summation	0	0	-5,247	2,099	—
Principal Stresses	736	0	-5,983	—	—
Stress Differences	6,719	5,983	736	—	—
Maximum Stress Intensity (SI)	6,719	—	—	—	—
Allowable Stress Intensity (S_a)	20,000	—	—	—	—
Margin of Safety (MS = S_a/SI – 1)	+1.98	—	—	—	—

Table 2.6-26 – NCT Oblique Drop, Canister Shell with 17.9*g* at 200 ºF

Evaluation Parameters	
Loading Condition:	NCT 85º Oblique Drop, -20 ºF Foam
Structural Material:	ASTM A240, Type 304L, Stainless Steel
Stress Condition:	Primary Membrane
Structural Criterion:	Non-containment Boundary
Stress Allowable (from Table 2.1-1):	S_m
Material Temperature:	200 ºF
Allowable Stress, S_a:	21,300 psi

Load Condition	Stress Components (psi)				Reference Section
	Radial σ_r	Hoop σ_t	Axial σ_z	Shear τ_{rz}	
Oblique Drop	0	0	-8,062	454	2.6.7.2(6)
Direct Stress Summation	0	0	-8,062	454	—
Principal Stresses	25	0	-8,087	—	—
Stress Differences	8,112	8,087	25	—	—
Maximum Stress Intensity (SI)	8,112	—	—	—	—
Allowable Stress Intensity (S_a)	21,300	—	—	—	—
Margin of Safety (MS = S_a/SI – 1)	+1.63	—	—	—	—

Table 2.6-27 – OC Shell Stresses with Max Side Drop Fab Condition

Temperature (ºF)	Inner Shell Stresses (psi)		Outer Shell Stresses (psi)	
	Hoop σ_t	Axial① σ_z	Hoop σ_t	Axial σ_z
160	-1,038	-1,963	0	0
70	-1,413	-1,963	0	0
-20	-1,821	-1,963	0	0

Note:

① Axial compressive stress in the inner shell per Appendix 2.10.8.5, *Axial Stress Evaluation after Cooldown from 620 ºF to -20 ºF*.

Table 2.6-28 – NCT Fab & Side Drop, OC Inner Shell with 19.3*g* at -20 ºF

Evaluation Parameters	
Loading Condition:	NCT Flat Side Drop, -20 ºF Foam
Structural Material:	ASTM A240, Type 304, Stainless Steel
Stress Condition:	Primary Membrane
Structural Criterion:	Containment Boundary
Stress Allowable (from Table 2.1-1):	S_m
Material Temperature:	-20 ºF
Allowable Stress, S_a:	20,000 psi

Load Condition	Stress Components (psi)				Reference Section
	Radial σ_r	Hoop σ_t	Axial σ_z	Shear τ_{rz}	
Fabrication	0	-1,821	-1,963	0	2.6.7.3(4)
Side Drop	0	0	-3,881	1,255	2.6.7.3(4)
Direct Stress Summation	0	-1,821	-5,844	1,255	—
Principal Stresses	258	-1,821	-6,102	—	—
Stress Differences	6,360	4,281	2,079	—	—
Maximum Stress Intensity (SI)	6,360	—	—	—	—
Allowable Stress Intensity (S_a)	20,000	—	—	—	—
Margin of Safety (MS = S_a/SI – 1)	+2.14	—	—	—	—

Table 2.6-29 – NCT Fab & Side Drop, OC Inner Shell with 19.3*g* at 70 ºF

Evaluation Parameters	
Loading Condition:	NCT Flat Side Drop, -20 ºF Foam
Structural Material:	ASTM A240, Type 304, Stainless Steel
Stress Condition:	Primary Membrane
Structural Criterion:	Containment Boundary
Stress Allowable (from Table 2.1-1):	S_m
Material Temperature:	70 ºF
Allowable Stress, S_a:	20,000 psi

Load Condition	Stress Components (psi)				Reference Section
	Radial σ_r	Hoop σ_t	Axial σ_z	Shear τ_{rz}	
Fabrication	0	-1,413	-1,963	0	2.6.7.3(4)
Side Drop	0	0	-3,881	1,255	2.6.7.3(4)
Direct Stress Summation	0	-1,413	-5,844	1,255	—
Principal Stresses	258	-1,413	-6,102	—	—
Stress Differences	6,360	4,689	1,671	—	—
Maximum Stress Intensity (SI)	6,360	—	—	—	—
Allowable Stress Intensity (S_a)	20,000	—	—	—	—
Margin of Safety (MS = S_a/SI – 1)	+2.14	—	—	—	—

Table 2.6-30 – NCT Fab & Side Drop, OC Inner Shell with 19.3*g* at 160 ºF

Evaluation Parameters	
Loading Condition:	NCT Flat Side Drop, -20 ºF Foam
Structural Material:	ASTM A240, Type 304, Stainless Steel
Stress Condition:	Primary Membrane
Structural Criterion:	Containment Boundary
Stress Allowable (from Table 2.1-1):	S_m
Material Temperature:	160 ºF
Allowable Stress, S_a:	20,000 psi

Load Condition	Stress Components (psi)				Reference Section
	Radial σ_r	Hoop σ_t	Axial σ_z	Shear τ_{rz}	
Fabrication	0	-1,038	-1,963	0	2.6.7.3(4)
Side Drop	0	0	-3,881	1,255	2.6.7.3(4)
Direct Stress Summation	0	-1,038	-5,844	1,255	—
Principal Stresses	258	-1,038	-6,102	—	—
Stress Differences	6,360	5,064	1,296	—	—
Maximum Stress Intensity (SI)	6,360	—	—	—	—
Allowable Stress Intensity (S_a)	20,000	—	—	—	—
Margin of Safety (MS = S_a/SI – 1)	+2.14	—	—	—	—

Table 2.6-31 – NCT Side Drop, IV Shell with 19.3*g* at 160 ºF

Evaluation Parameters	
Loading Condition:	NCT Flat Side Drop, -20 ºF Foam
Structural Material:	ASTM A240, Type 304, Stainless Steel
Stress Condition:	Primary Membrane
Structural Criterion:	Containment Boundary
Stress Allowable (from Table 2.1-1):	S_m
Material Temperature:	160 ºF
Allowable Stress, S_a:	20,000 psi

Load Condition	Stress Components (psi)				Reference Section
	Radial σ_r	Hoop σ_t	Axial σ_z	Shear τ_{rz}	
Side Drop	0	0	-4,661	2,214	2.6.7.3(5)
Direct Stress Summation	0	0	-4,661	2,214	—
Principal Stresses	884	0	-5,545	—	—
Stress Differences	6,429	5,545	884	—	—
Maximum Stress Intensity (SI)	6,429	—	—	—	—
Allowable Stress Intensity (S_a)	20,000	—	—	—	—
Margin of Safety (MS = S_a/SI – 1)	+2.11	—	—	—	—

Table 2.6-32 – NCT Side Drop, Canister Shell with 19.3*g* at 200 ºF

Evaluation Parameters	
Loading Condition:	NCT Flat Side Drop, -20 ºF Foam
Structural Material:	ASTM A240, Type 304L, Stainless Steel
Stress Condition:	Primary Membrane
Structural Criterion:	Non-containment Boundary
Stress Allowable (from Table 2.1-1):	S_m
Material Temperature:	200 ºF
Allowable Stress, S_a:	21,300 psi

Load Condition	Stress Components (psi)				Reference Section
	Radial σ_r	Hoop σ_t	Axial σ_z	Shear τ_{rz}	
Side Drop	0	0	-4,003	2,382	2.6.7.3(6)
Direct Stress Summation	0	0	-4,003	2,382	—
Principal Stresses	1,110	0	-5,113	—	—
Stress Differences	6,223	5,113	1,110	—	—
Maximum Stress Intensity (SI)	6,223	—	—	—	—
Allowable Stress Intensity (S_a)	21,300	—	—	—	—
Margin of Safety (MS = S_a/SI – 1)	+2.42	—	—	—	—

Table 2.6-33 – NCT Fab & Side Drop, OC Shells' Welds with 19.3*g* at -20 ºF

Evaluation Parameters	
Loading Condition:	NCT Flat Side Drop, -20 ºF Foam
Structural Material:	ASTM A240, Type 304, Stainless Steel
Stress Condition:	Primary Membrane
Structural Criterion:	Containment Boundary
Stress Allowable (from Table 2.1-1):	S_m
Material Temperature:	-20 ºF
Allowable Stress, S_a:	20,000 psi

Load Condition	Stress Components (psi)				Reference Section
	Radial σ_r	Hoop σ_t	Axial σ_z	Shear τ_{rz}	
Fabrication	0	-1,821	-1,963	0	2.6.7.3(4)
Side Drop	0	0	-3,881	2,422	2.6.7.3(4)(8)
Direct Stress Summation	0	-1,821	-5,844	2,422	—
Principal Stresses	873	-1,821	-6,717	—	—
Stress Differences	7,590	4,896	2,694	—	—
Maximum Stress Intensity (SI)	7,590	—	—	—	—
Allowable Stress Intensity (S_a)	20,000	—	—	—	—
Margin of Safety (MS = S_a/SI – 1)	+1.64	—	—	—	—

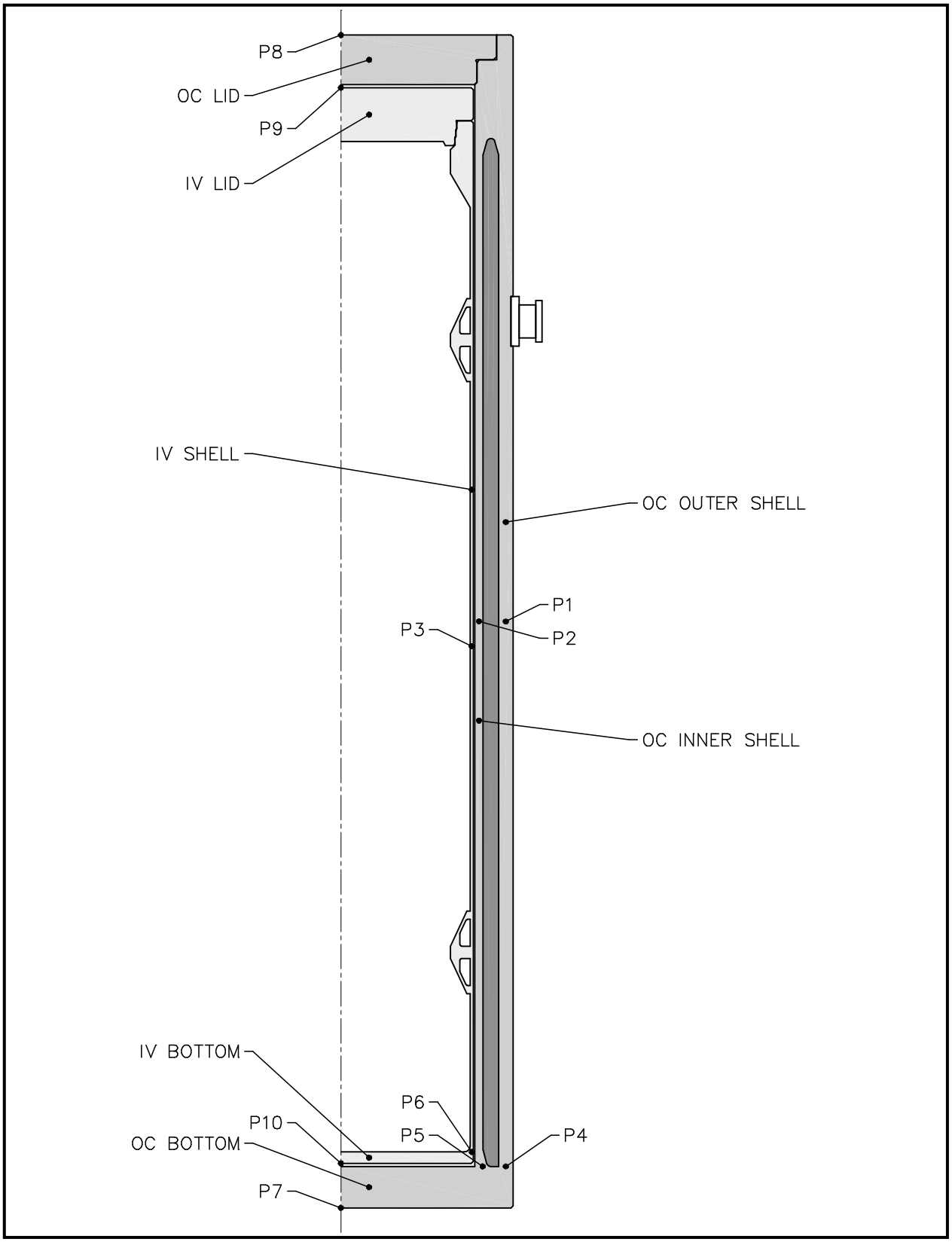

Figure 2.6-1 – Package Locations for Pressure Stress Calculations

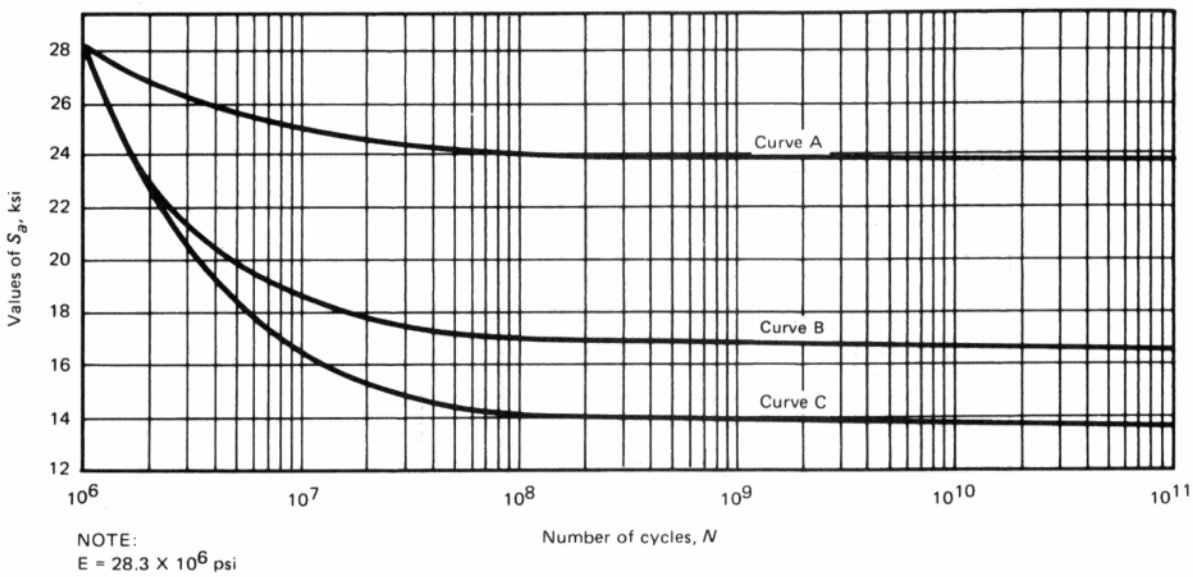

Criteria for the Use of the Curves in This Figure
[Notes (1)–(5)]

Curve	Elastic Analysis of Material Other Than Welds and Adjacent Base Metal	Elastic Analysis of Welds and Adjacent Base Metal
A	$(P_L + P_b + Q)_{Range} \leq 27.2$ ksi	. . .
B	$(P_L + P_b + Q)_{Range} > 27.2$ ksi and S_a is corrected for applied mean stress	$(P_L + P_b + Q)_{Range} \leq 27.2$ ksi
C	$(P_L + P_b + Q)_{Range} > 27.2$ ksi	$(P_L + P_b + Q)_{Range} > 27.2$ ksi

NOTES:
(1) Range applies to the individual quantities P_L, P_b, and Q and applies to the set of cycles under consideration.
(2) Thermal bending stresses resulting from axial and radial gradients are excluded from Q.
(3) Curve A is also to be used with inelastic analysis with $S_a = \frac{1}{2} \Delta \epsilon_t E$, where $\Delta \epsilon_t$ is the total effective strain range.
(4) The maximum effect of retained mean stress is included in Curve C.
(5) The adjacent base metal is defined as three wall thicknesses from the center line of the weld.

FIG. I-9.2.2 DESIGN FATIGUE CURVES FOR AUSTENITIC STEELS, NICKEL–CHROMIUM–IRON ALLOY, NICKEL–IRON–CHROMIUM ALLOY, AND NICKEL–COPPER ALLOY FOR $S_a \leq 28.2$ ksi, FOR TEMPERATURES NOT EXCEEDING 800°F

Figure 2.6-2 – Figure I-9.2.2 from Appendix I of the ASME Code

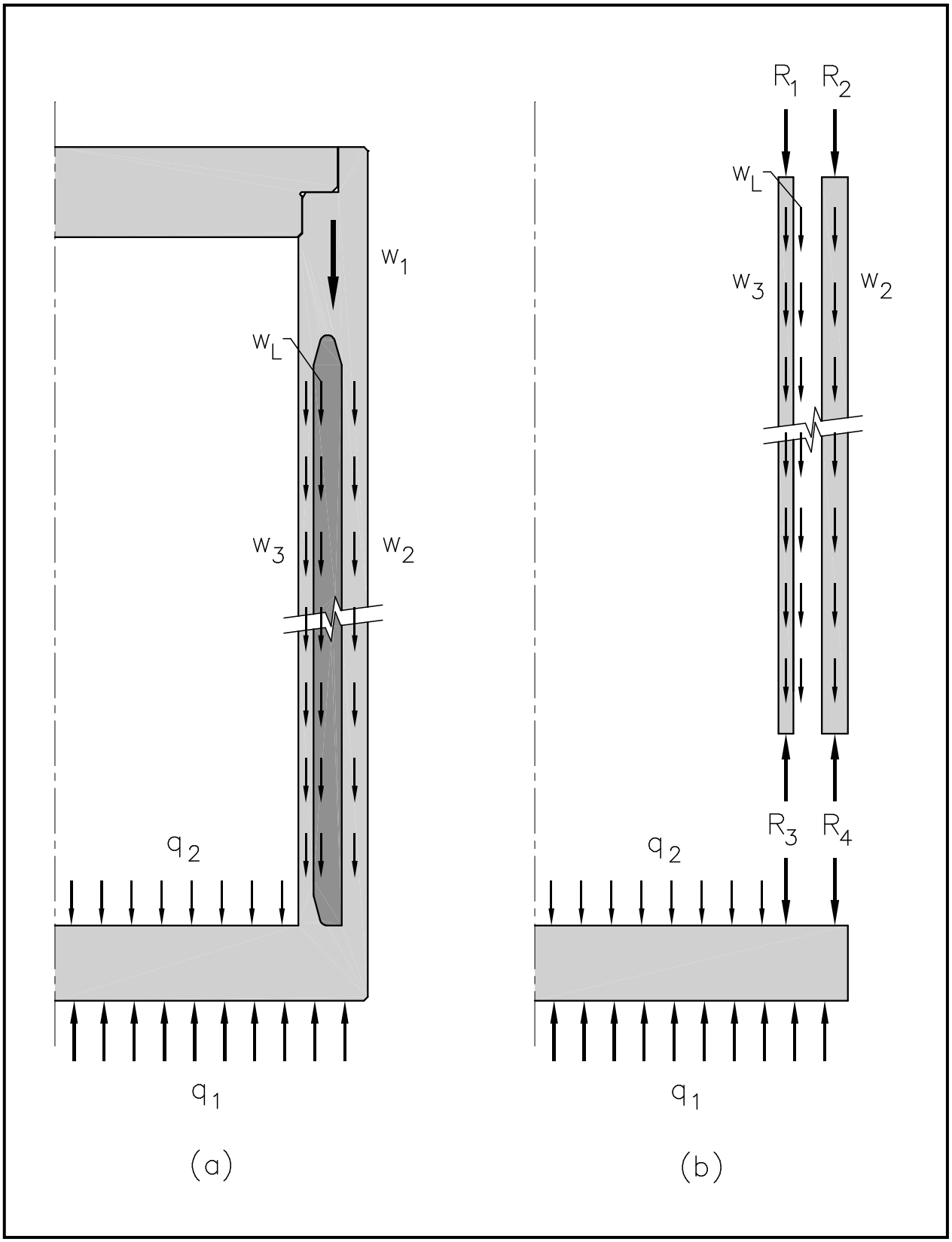

Figure 2.6-3 – Free-Body Diagrams of Axial Forces in OC Components

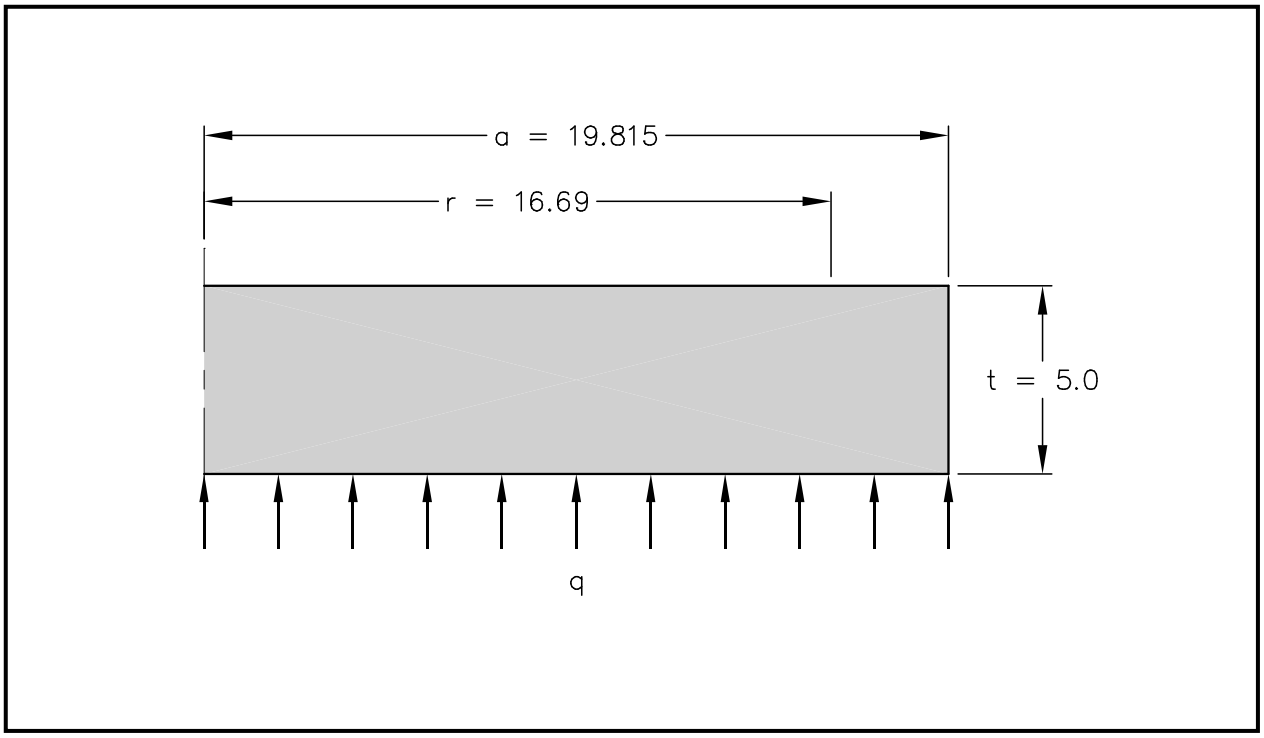

Figure 2.6-4 – OC Bottom-End Plate Configuration

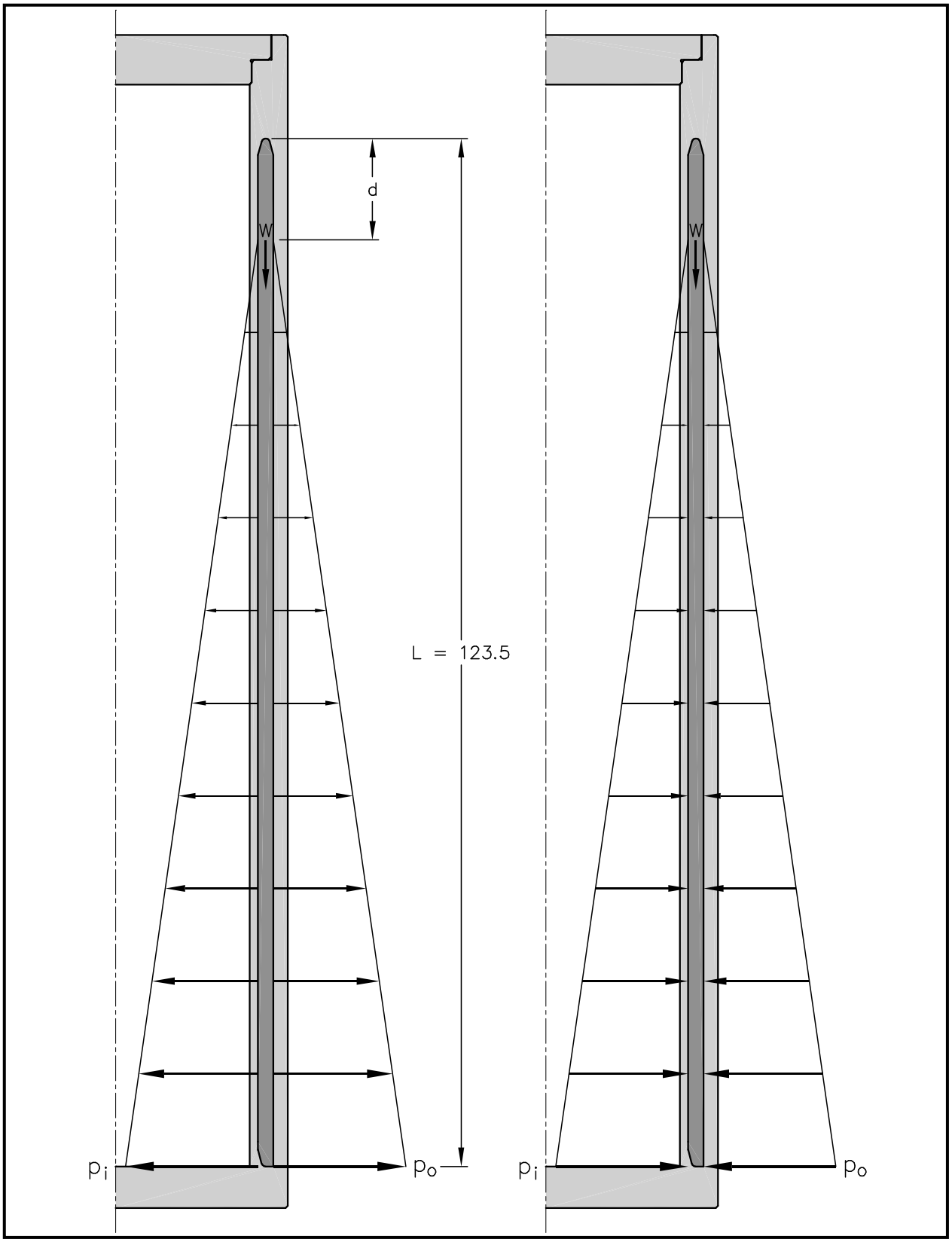

Figure 2.6-5 – Axial Pressure Distribution Due to Lead

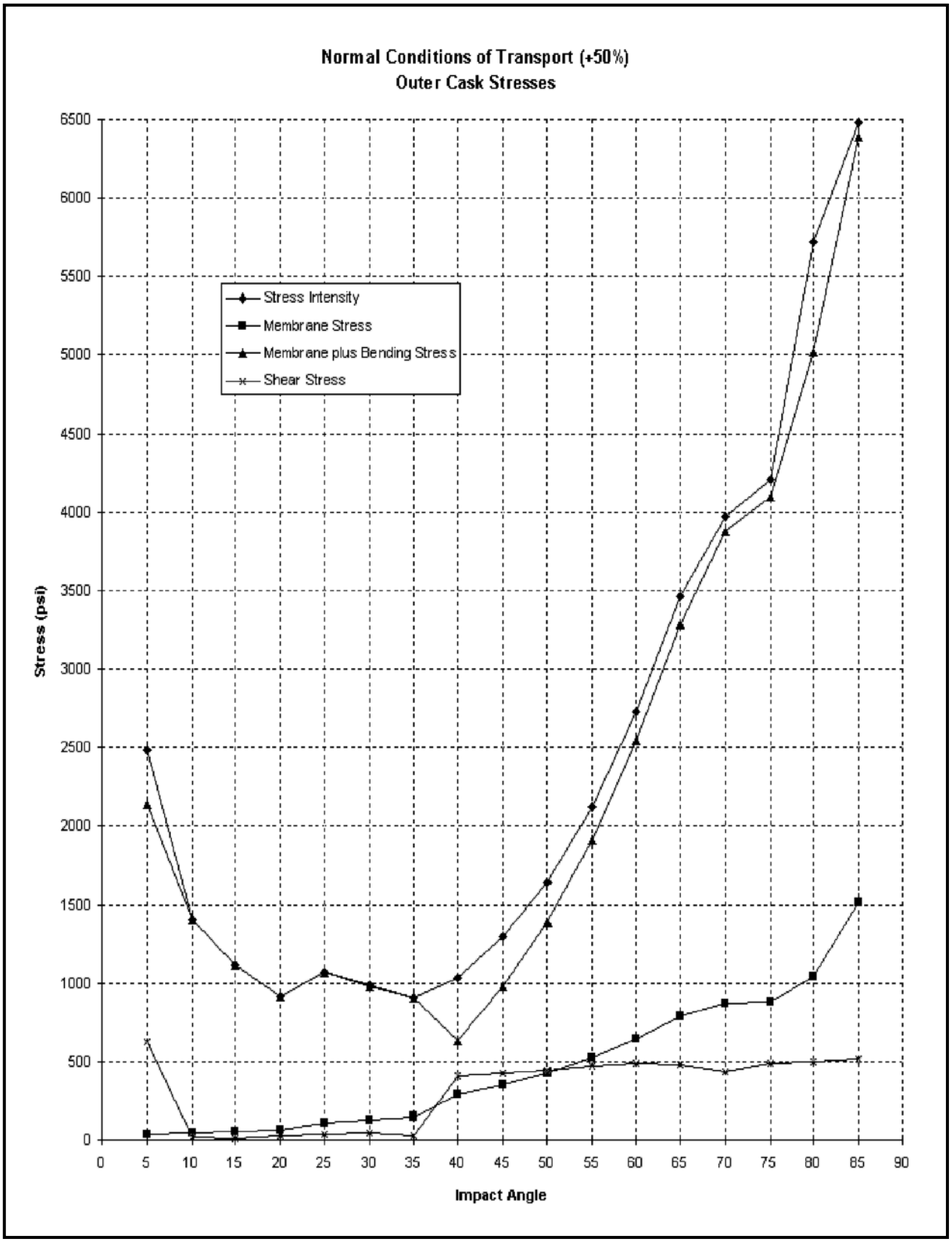

Figure 2.6-6 – NCT Cold (-20 ºF) Outer Cask Stresses

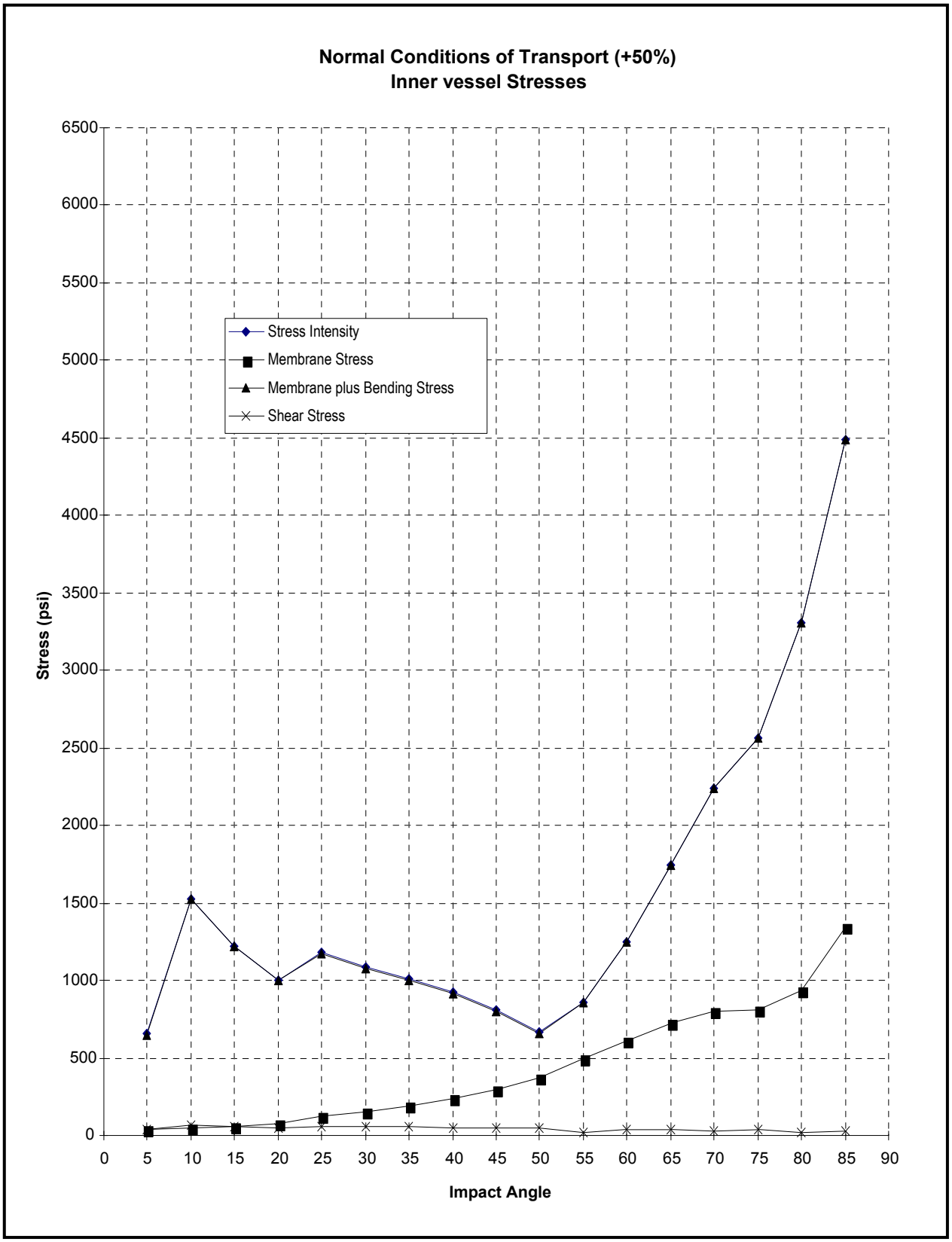

Figure 2.6-7 – NCT Cold (-20 ºF) Inner Vessel Stresses

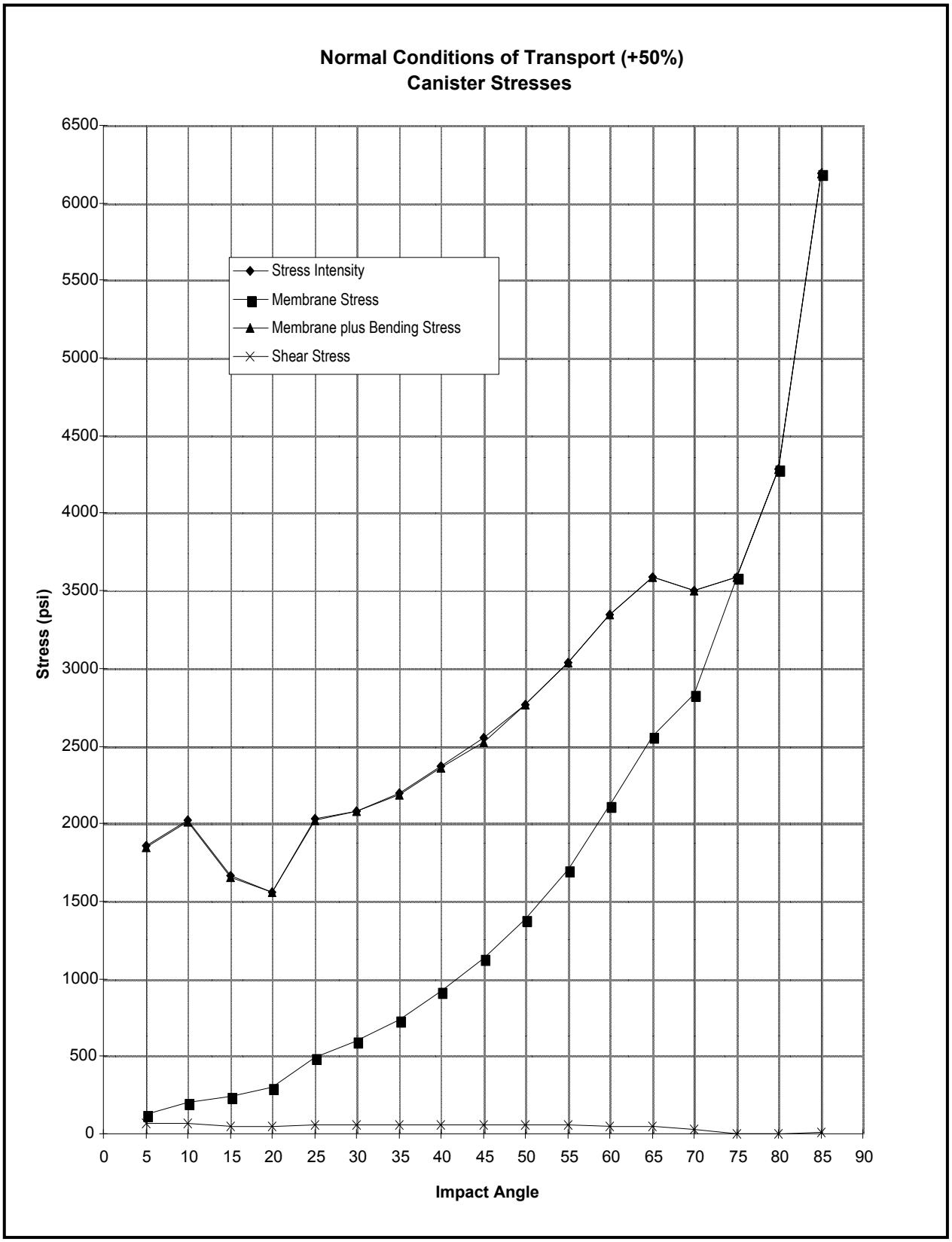

Figure 2.6-8 – NCT Cold (-20 ºF) Canister Stresses

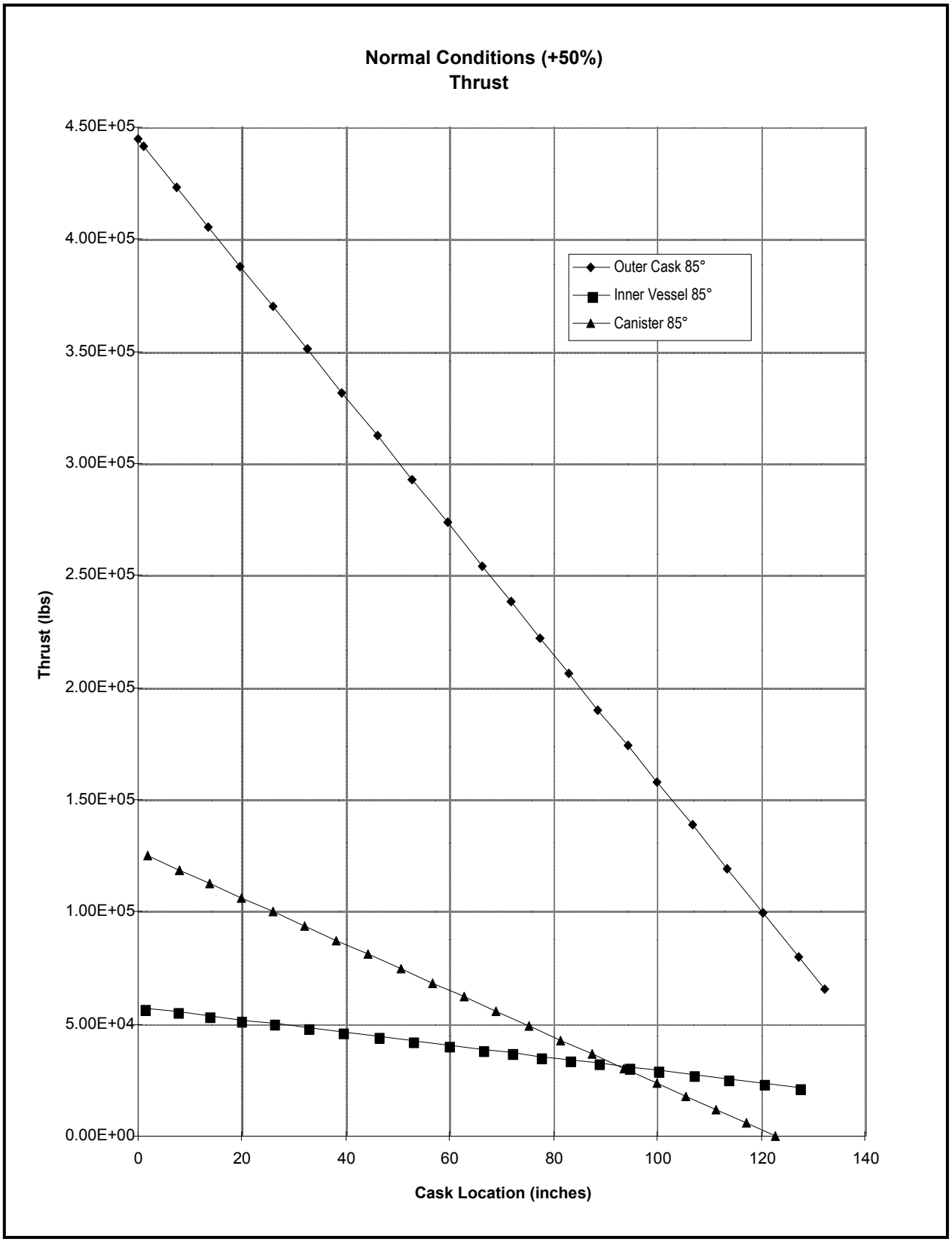

Figure 2.6-9 – NCT Cold (-20 ºF) Thrust

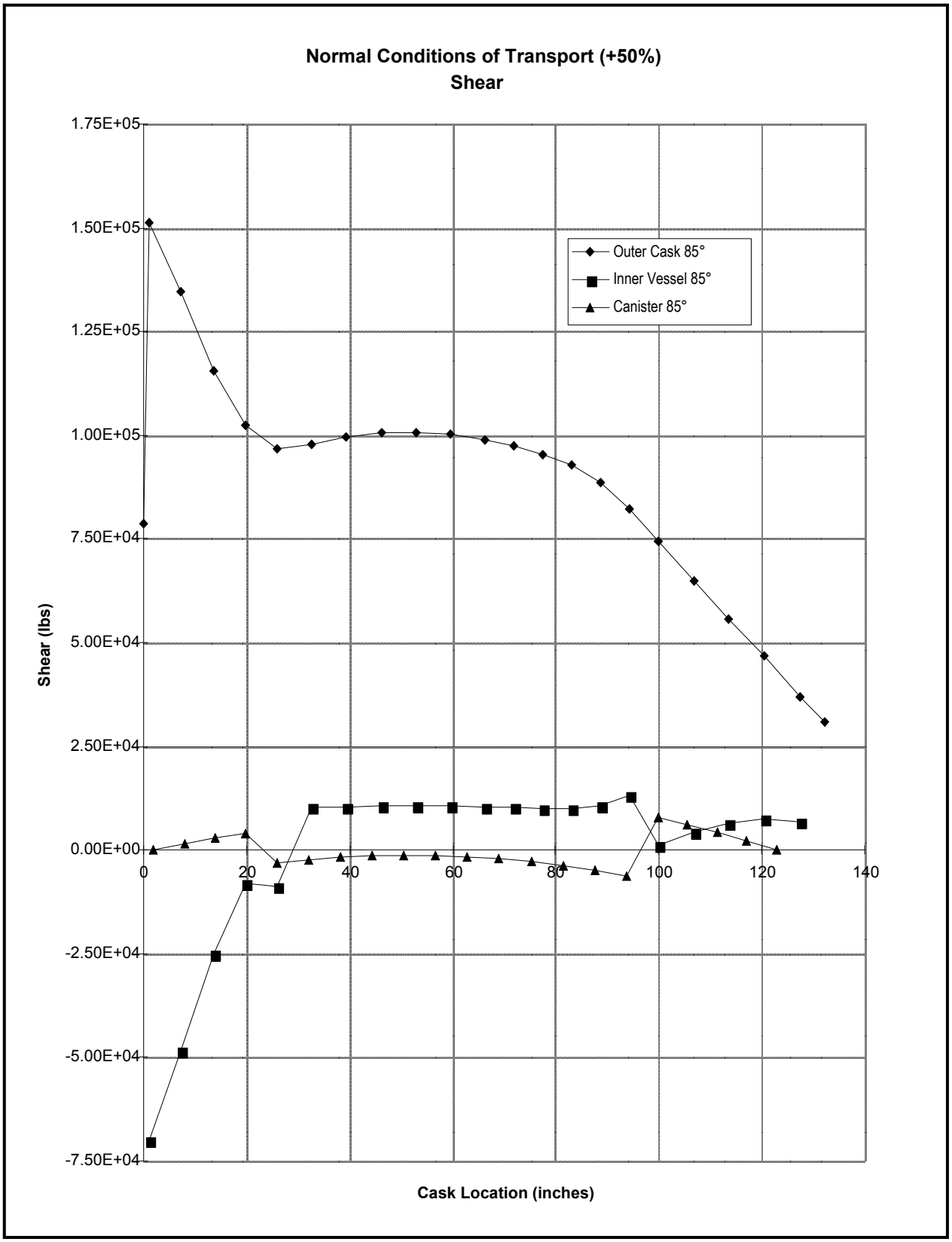

Figure 2.6-10 – NCT Cold (-20 ºF) Shear

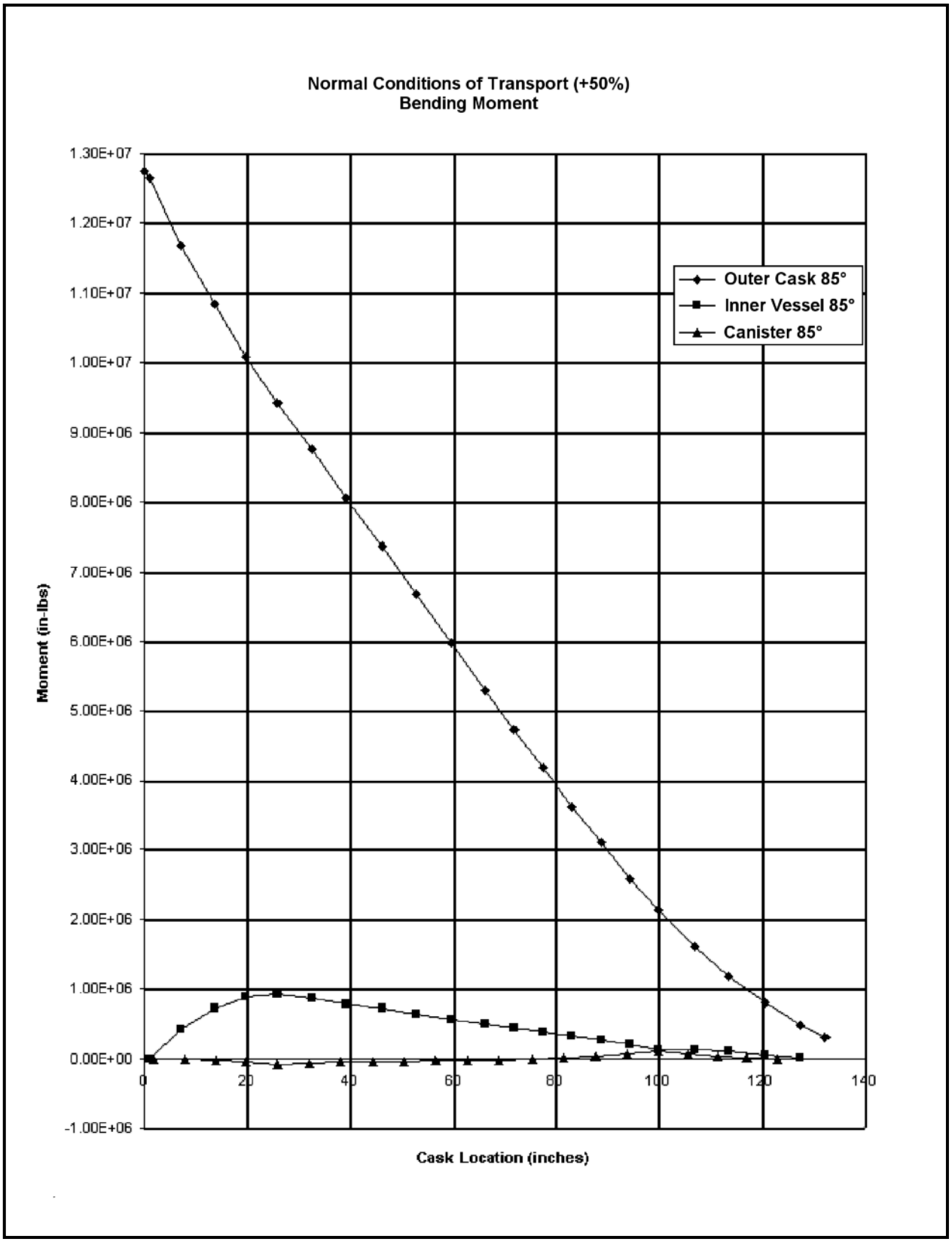

Figure 2.6-11 – NCT Cold (-20 ºF) Bending Moment

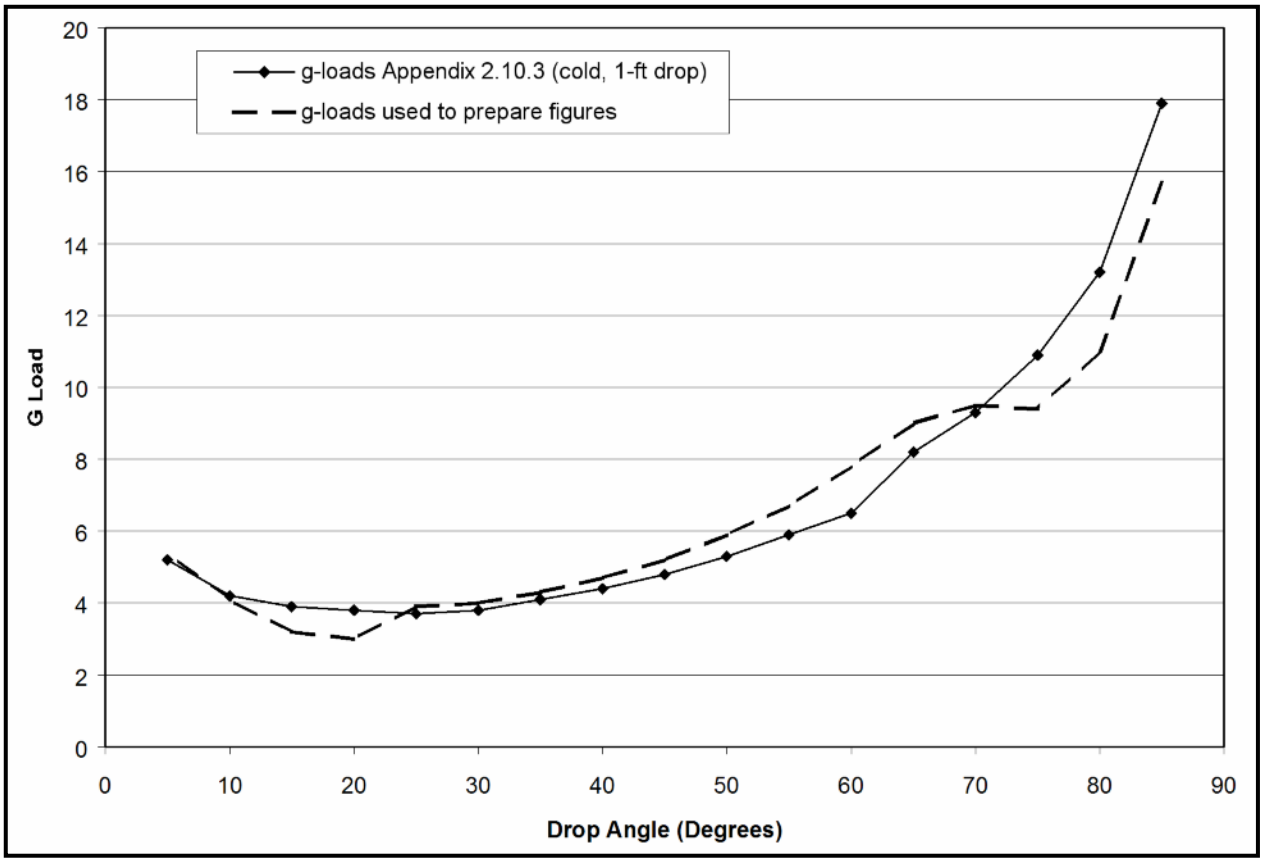

Figure 2.6-12 – Comparison of *g*-Loads Used for Calculating Cold (-20 ºF) NCT Stresses

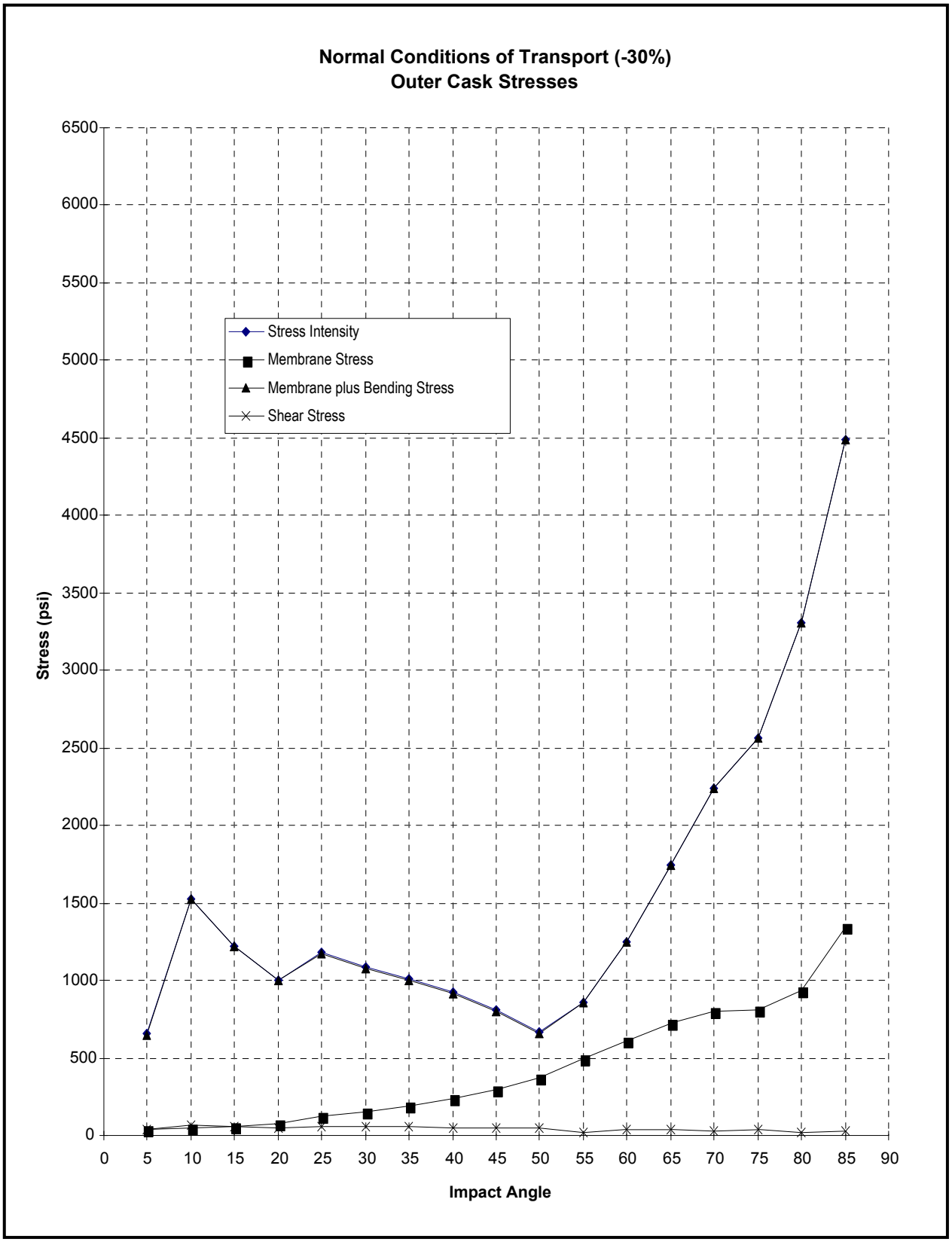

Figure 2.6-13 – NCT Hot (140 ºF) Outer Cask Stresses

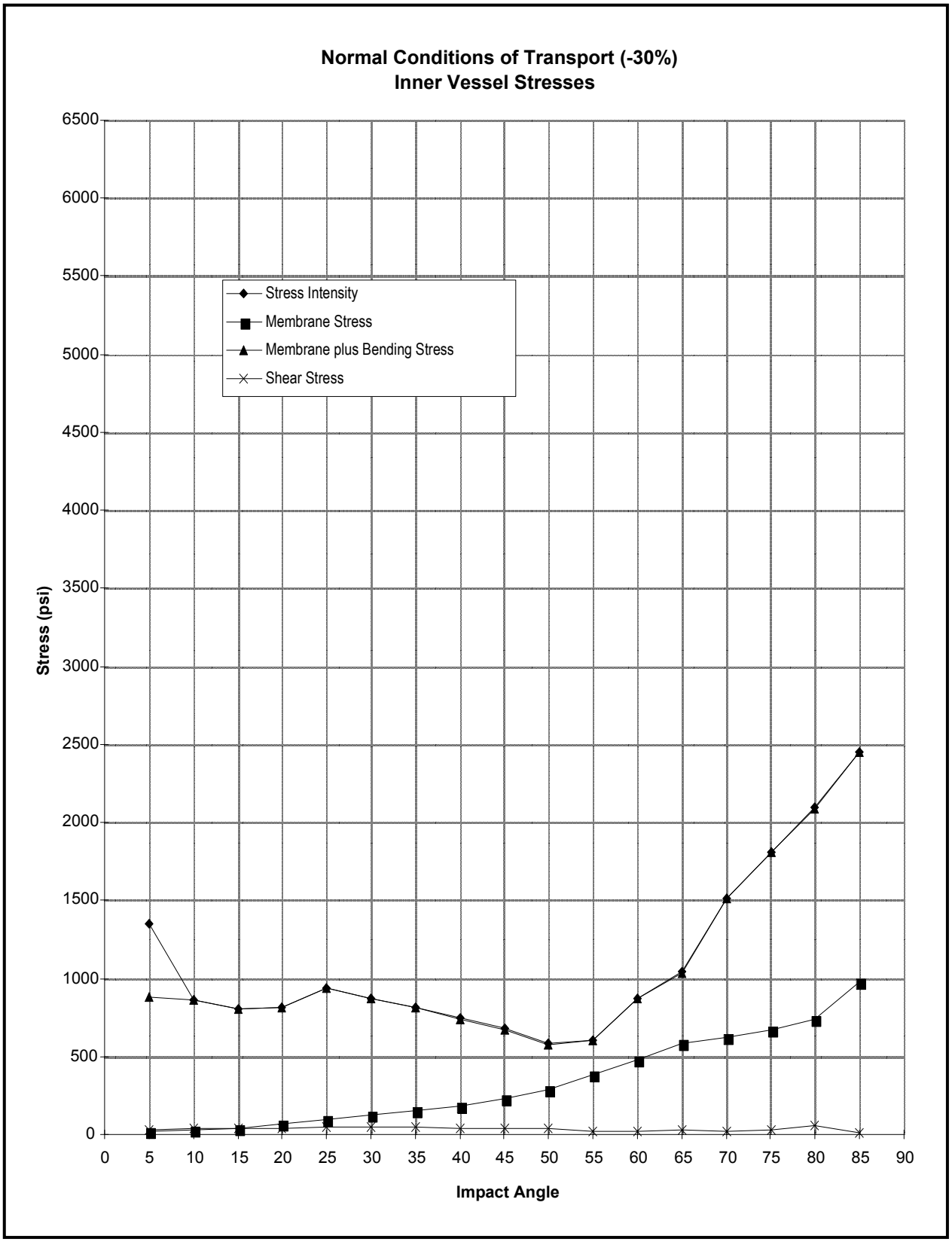

Figure 2.6-14 – NCT Hot (140 ºF) Inner Vessel Stresses

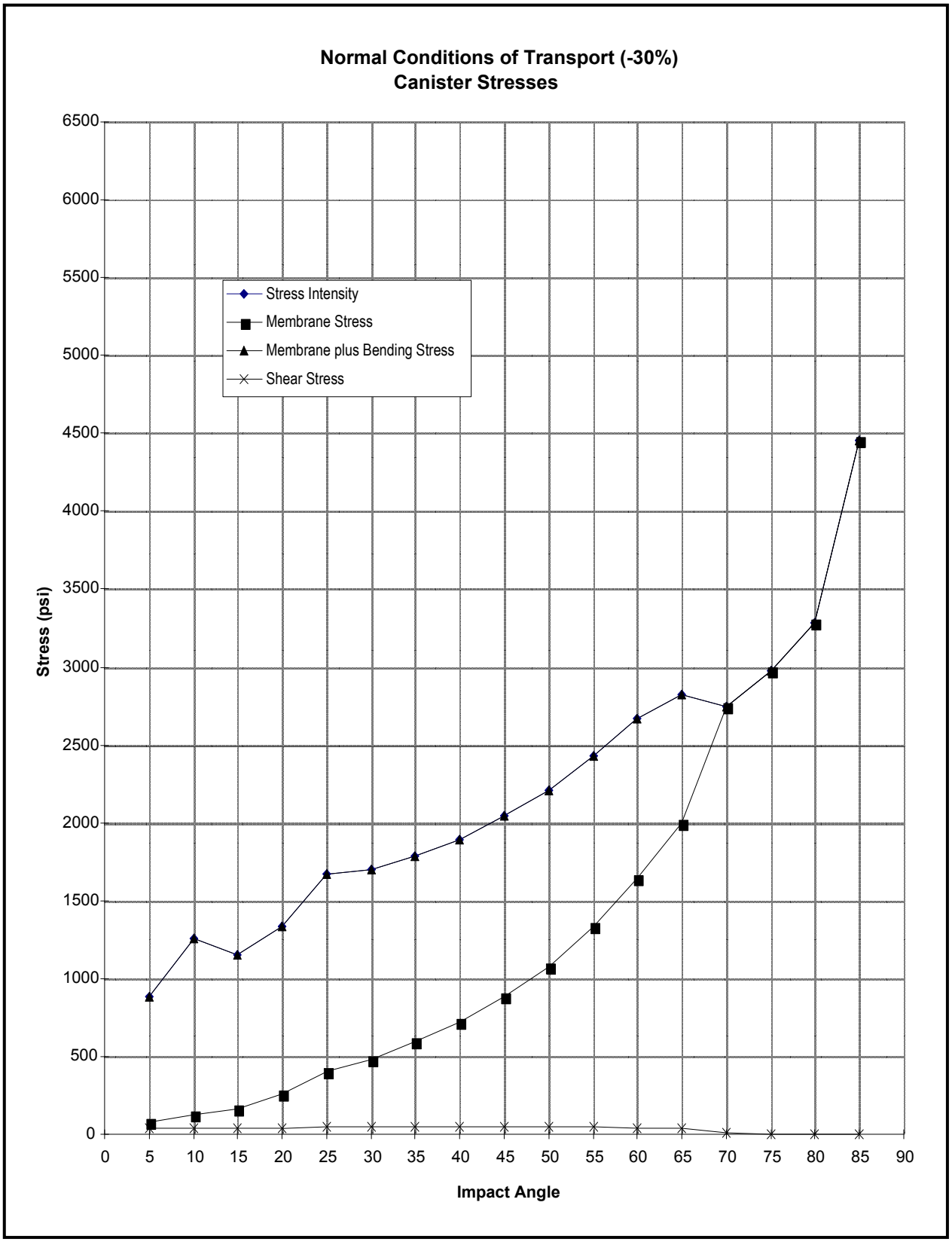

Figure 2.6-15 – NCT Hot (140 ºF) Canister Stresses

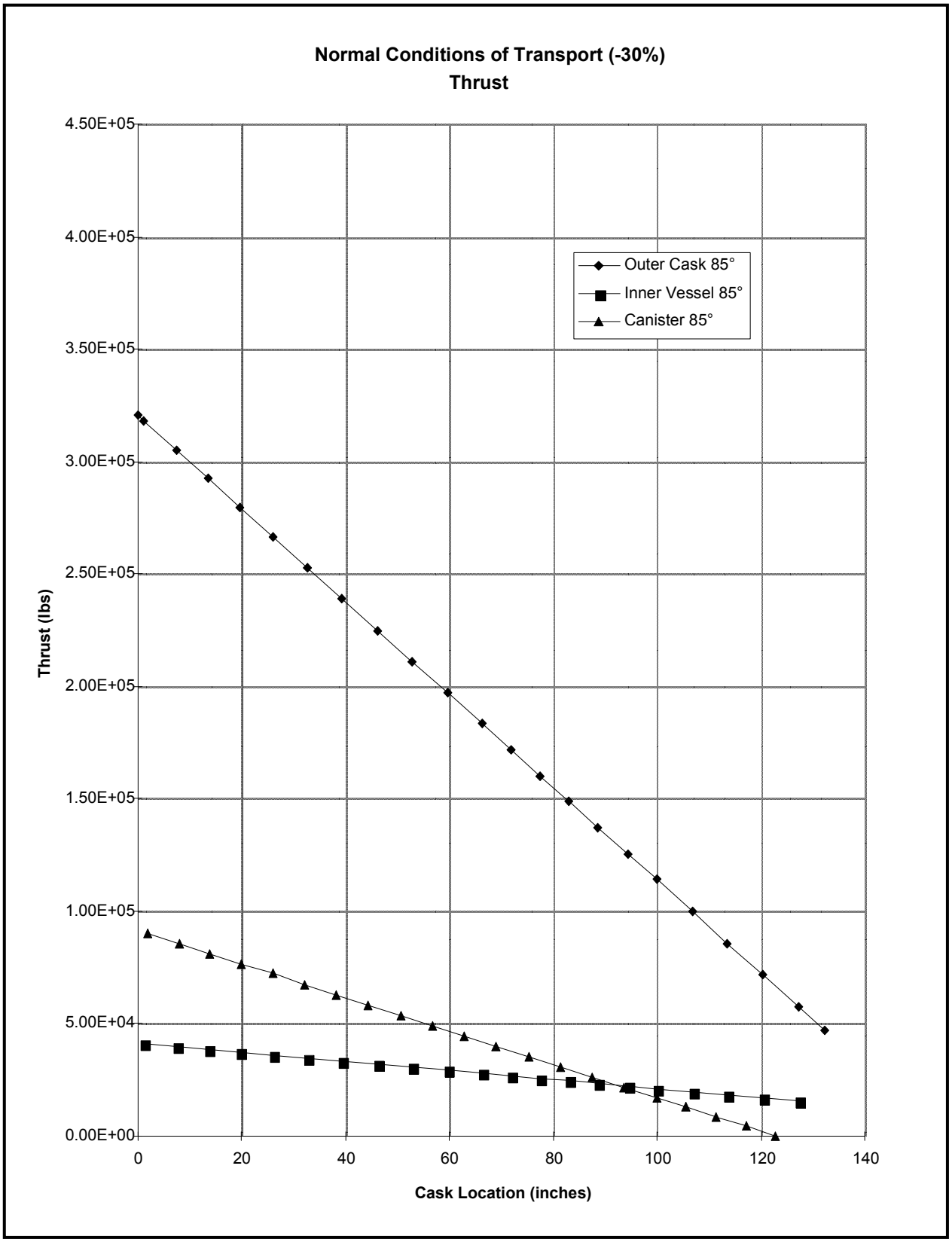

Figure 2.6-16 – NCT Hot (140 ºF) Thrust

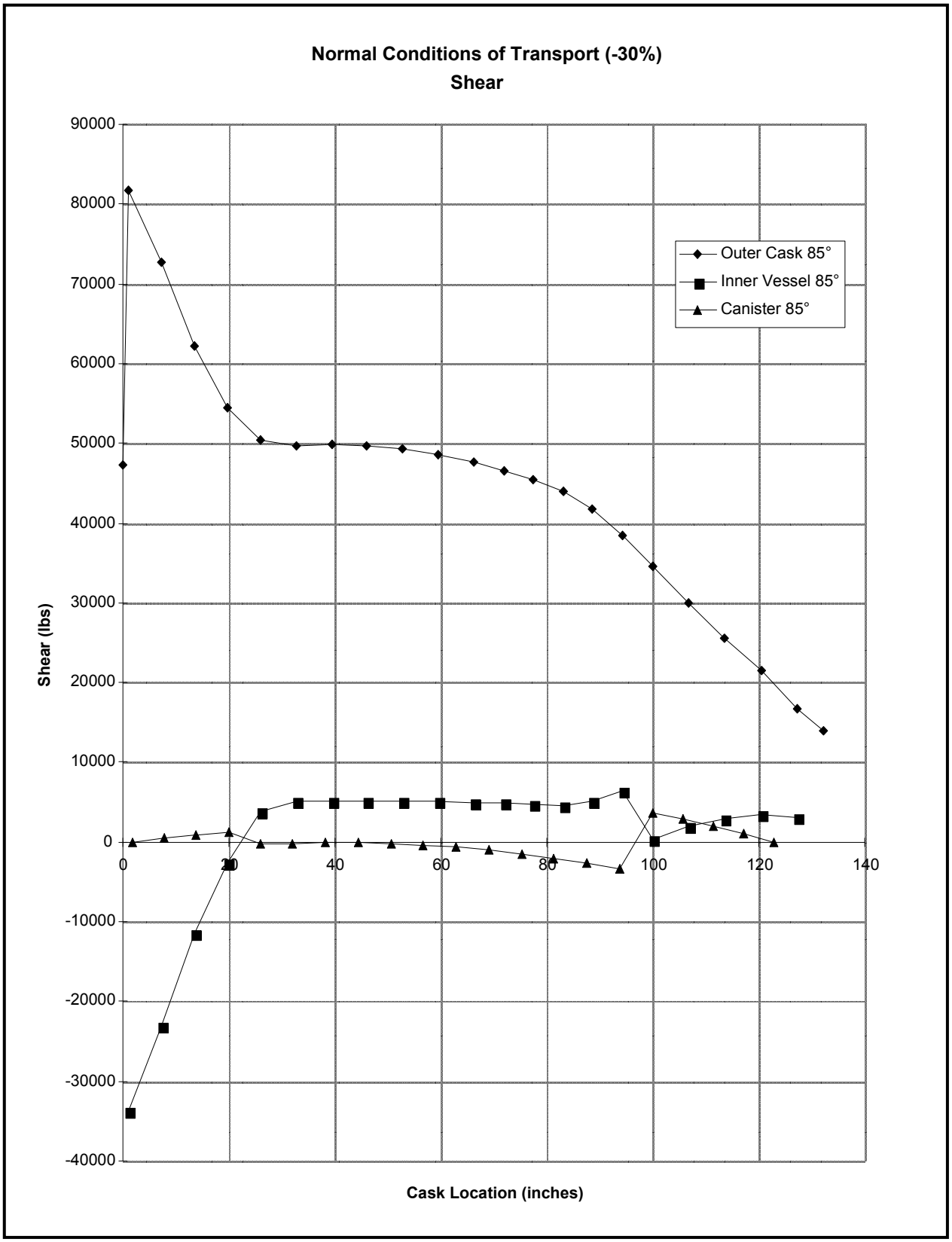

Figure 2.6-17 – NCT Hot (140 ºF) Shear

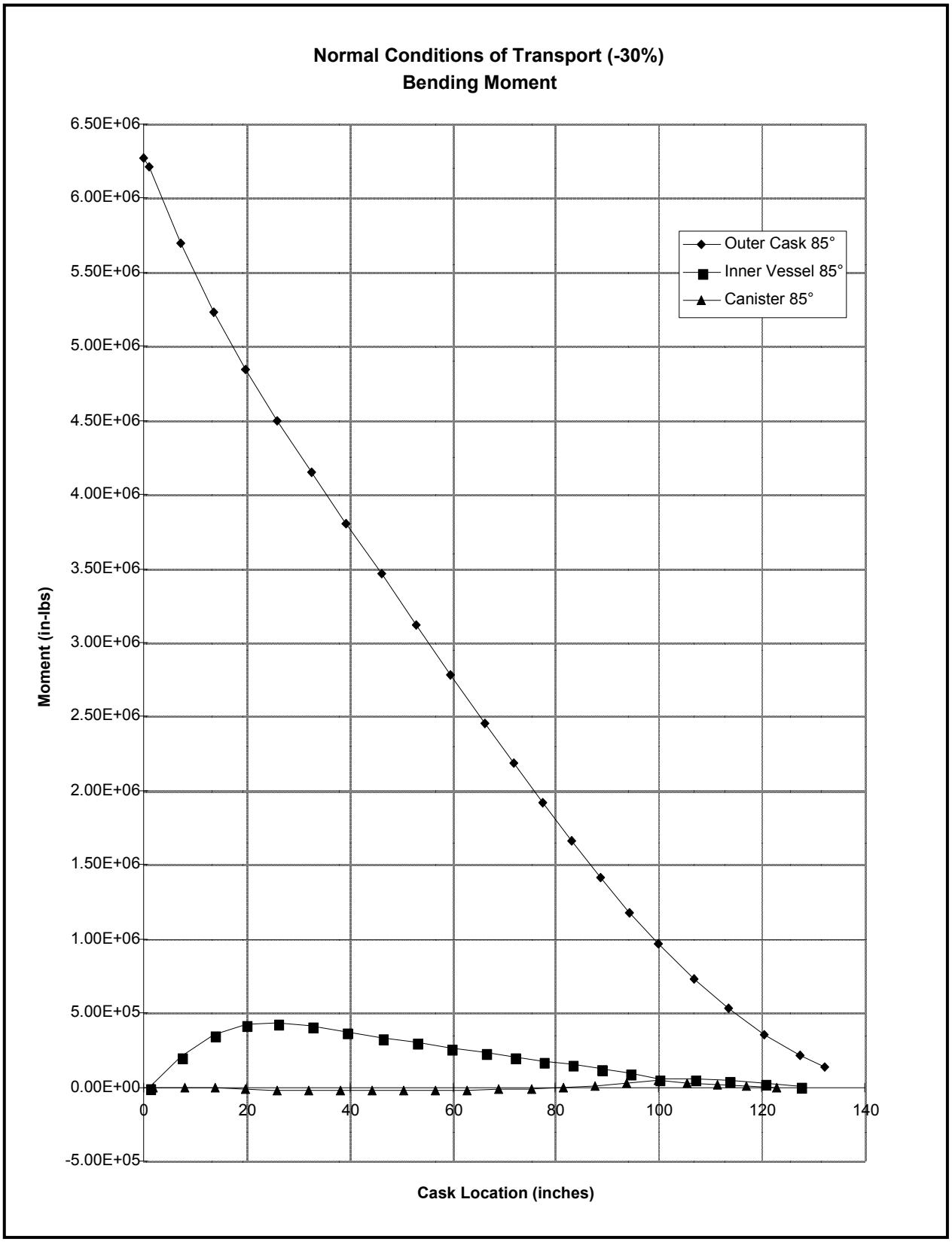

Figure 2.6-18 – NCT Hot (140 ºF) Bending Moment

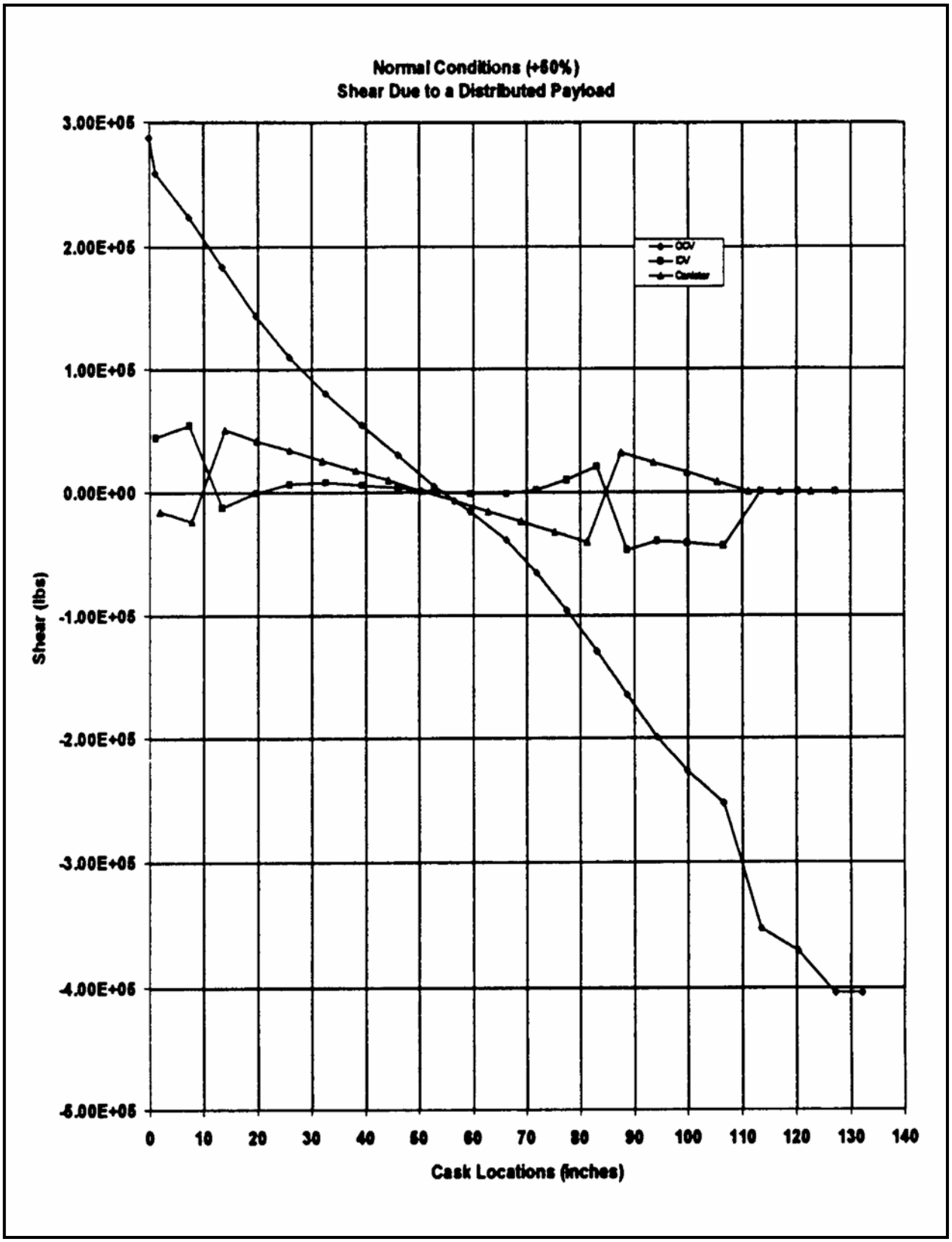

Figure 2.6-19 – NCT Cold (-20 ºF) Shear Due to a Distributed Payload

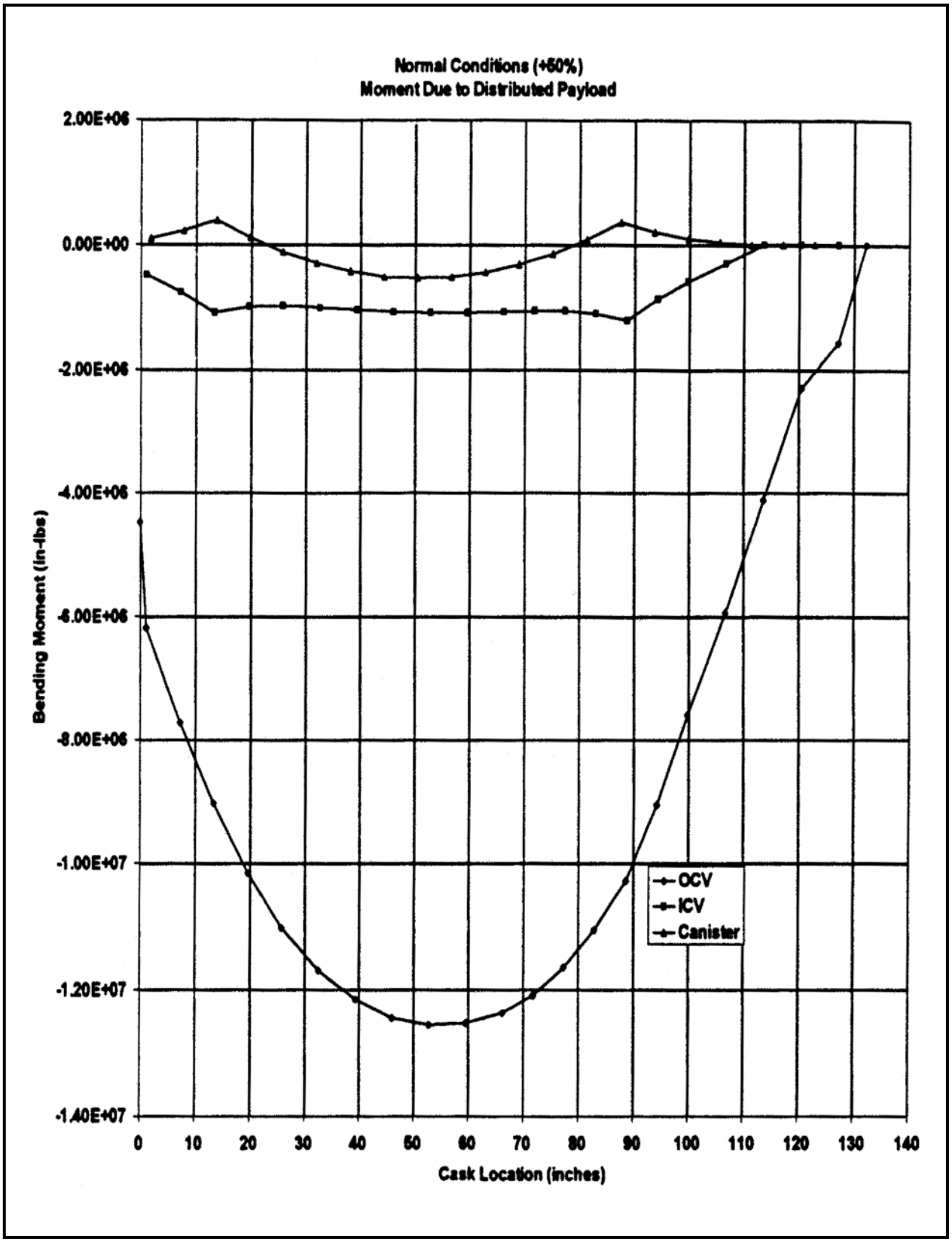

Figure 2.6-20 – NCT Cold (-20 ºF) Moment Due to a Distributed Payload

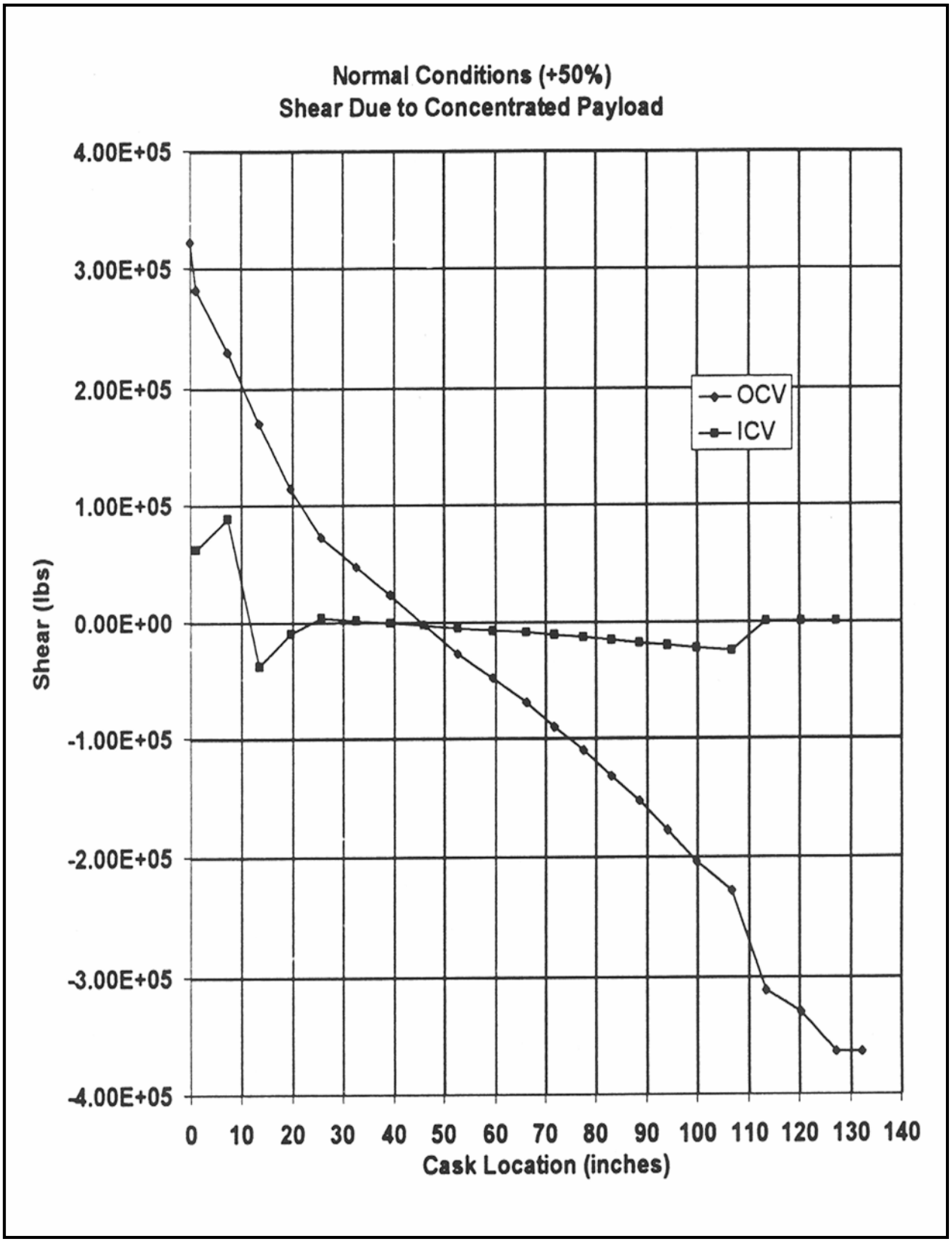

Figure 2.6-21 – NCT Cold (-20 ºF) Shear Due to a Concentrated Payload

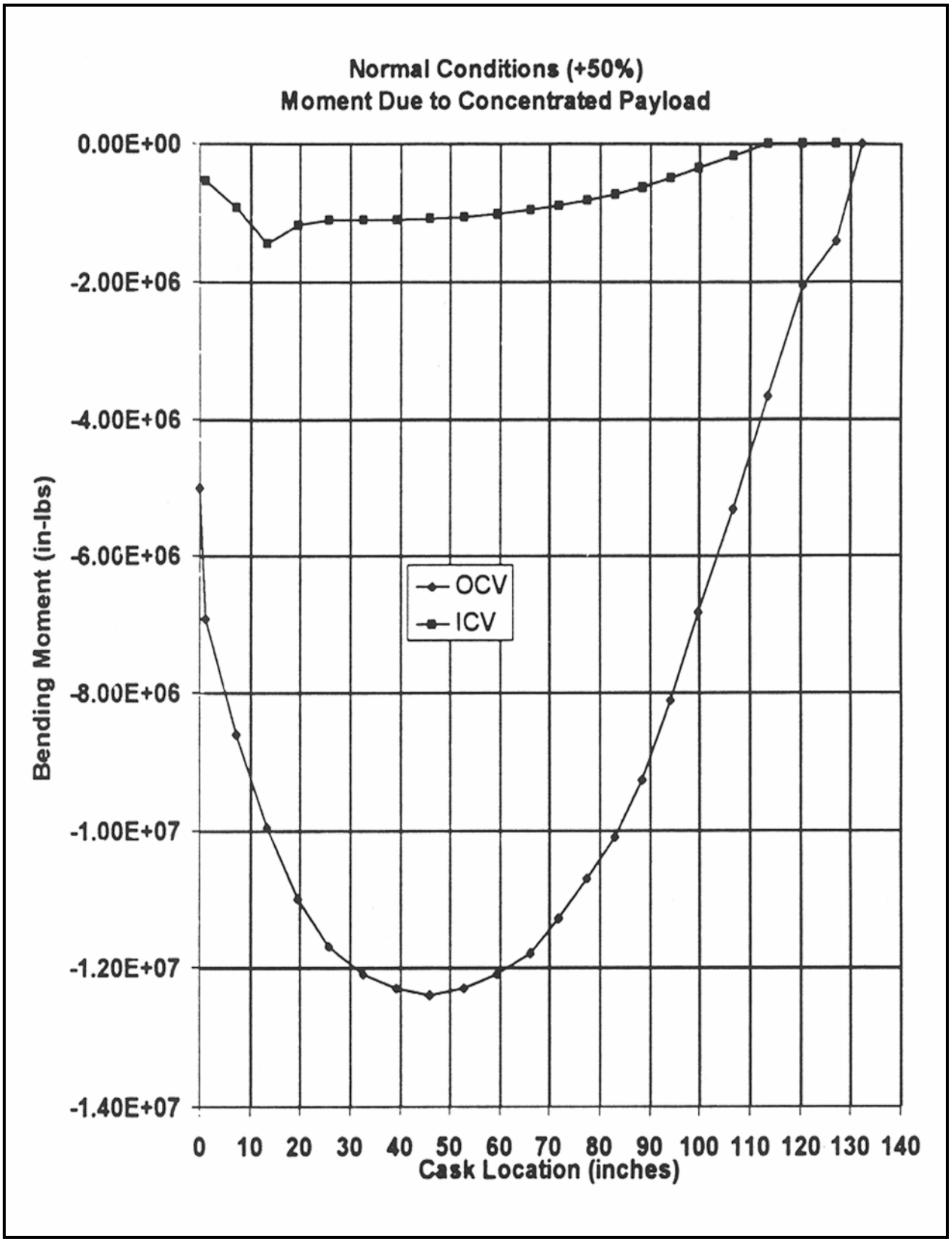

Figure 2.6-22 – NCT Cold (-20 ºF) Moment Due to a Concentrated Payload

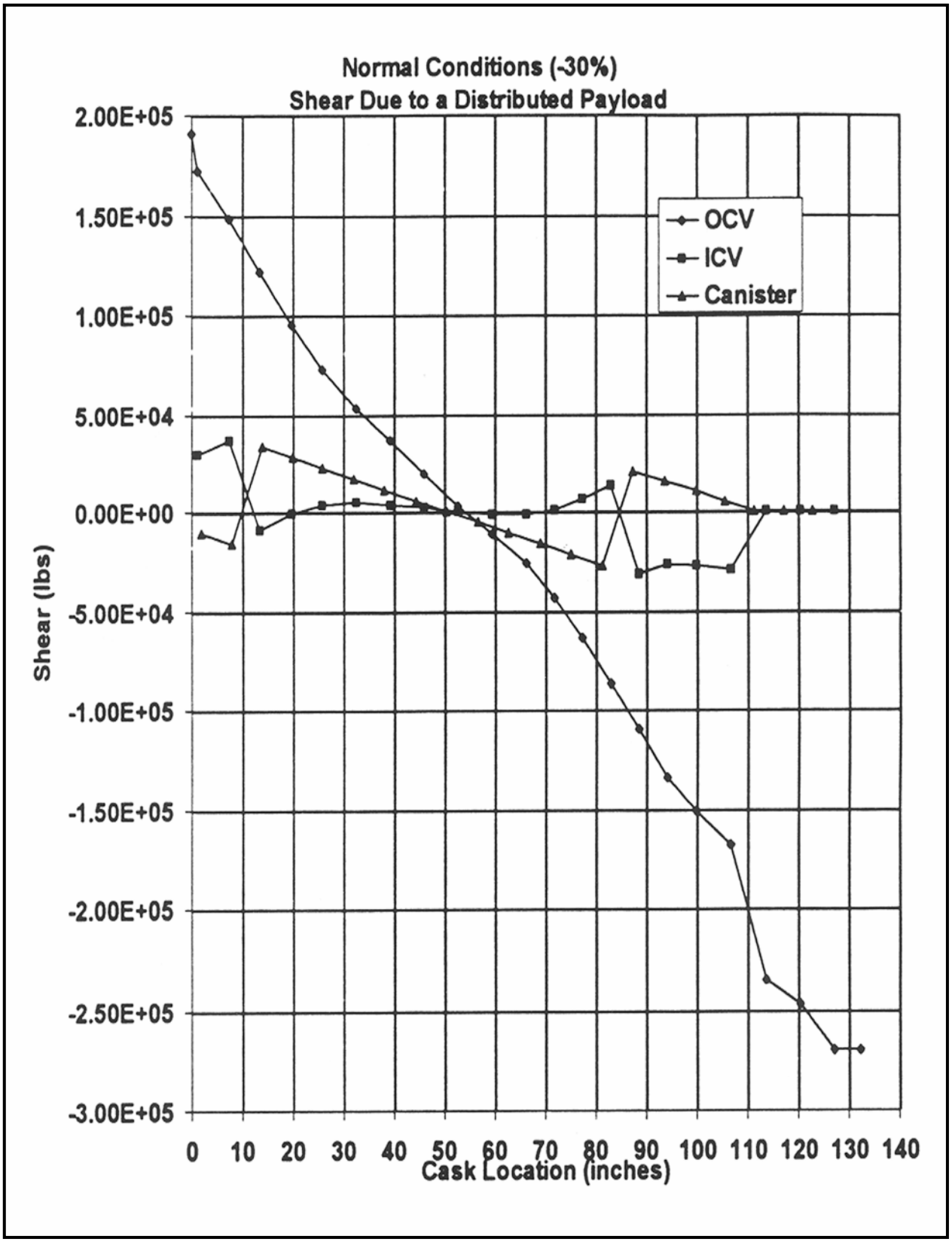

Figure 2.6-23 – NCT Hot (140 ºF) Shear Due to a Distributed Payload

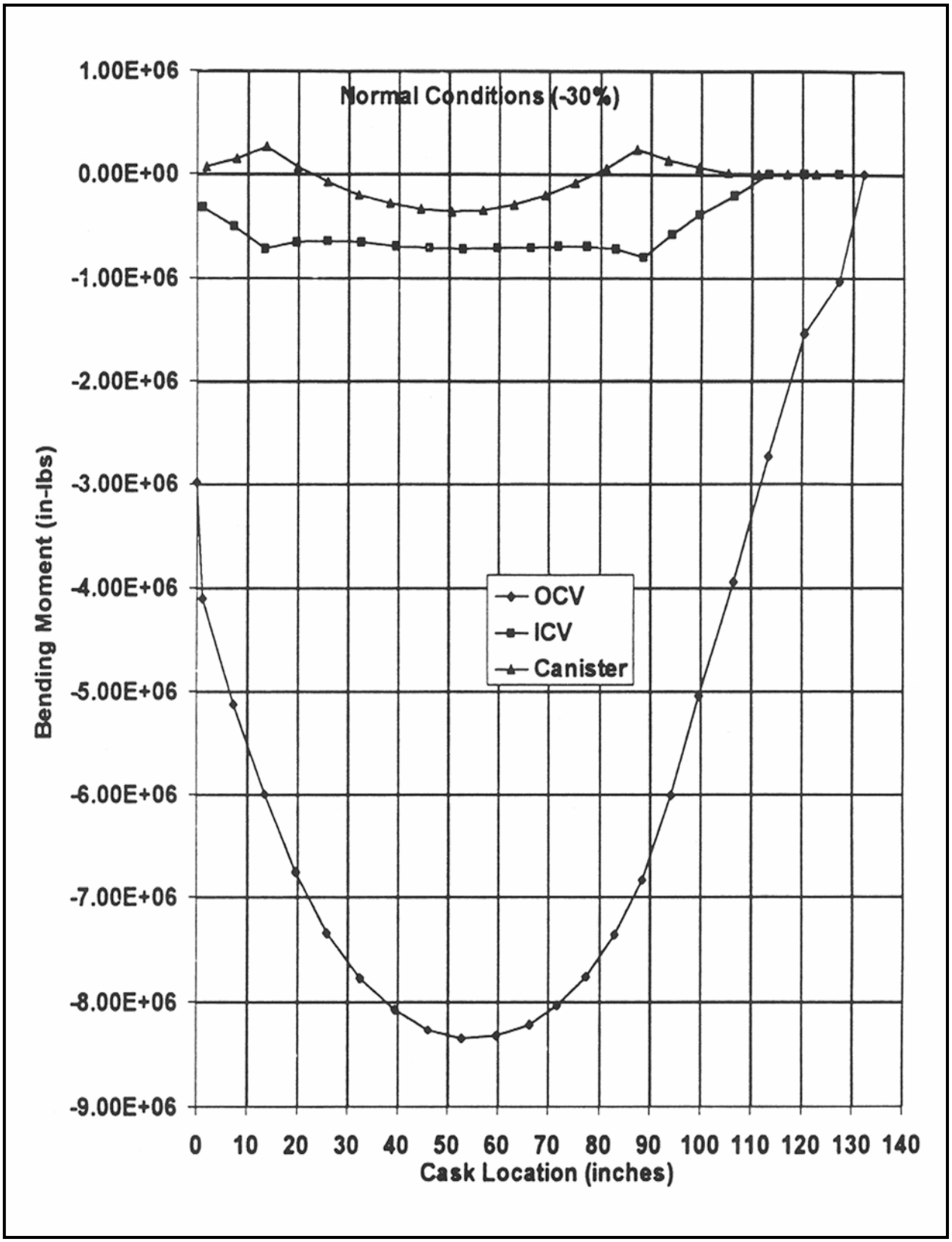

Figure 2.6-24 – NCT Hot (140 ºF) Moment Due to a Distributed Payload

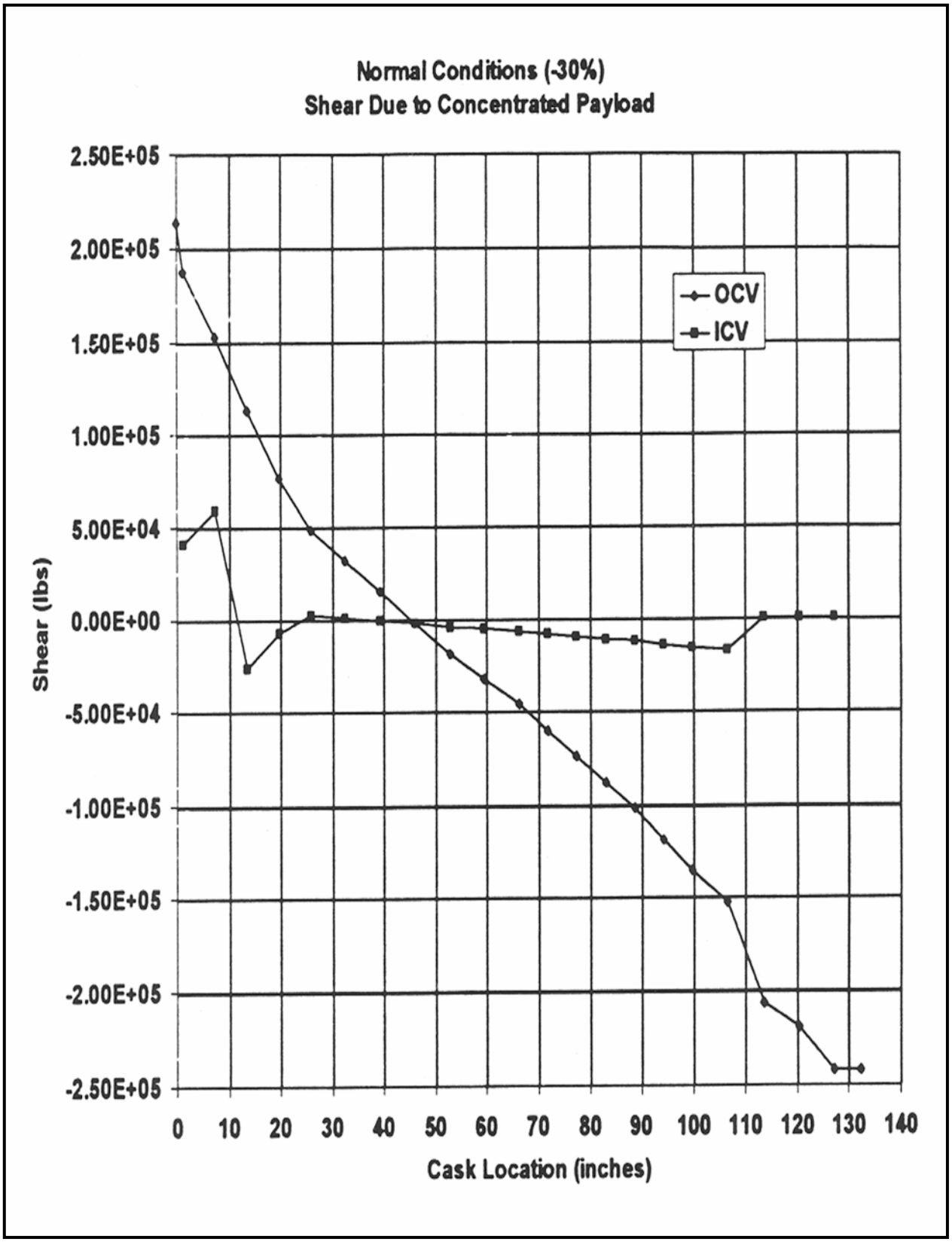

Figure 2.6-25 – NCT Hot (140 ºF) Shear Due to a Concentrated Payload

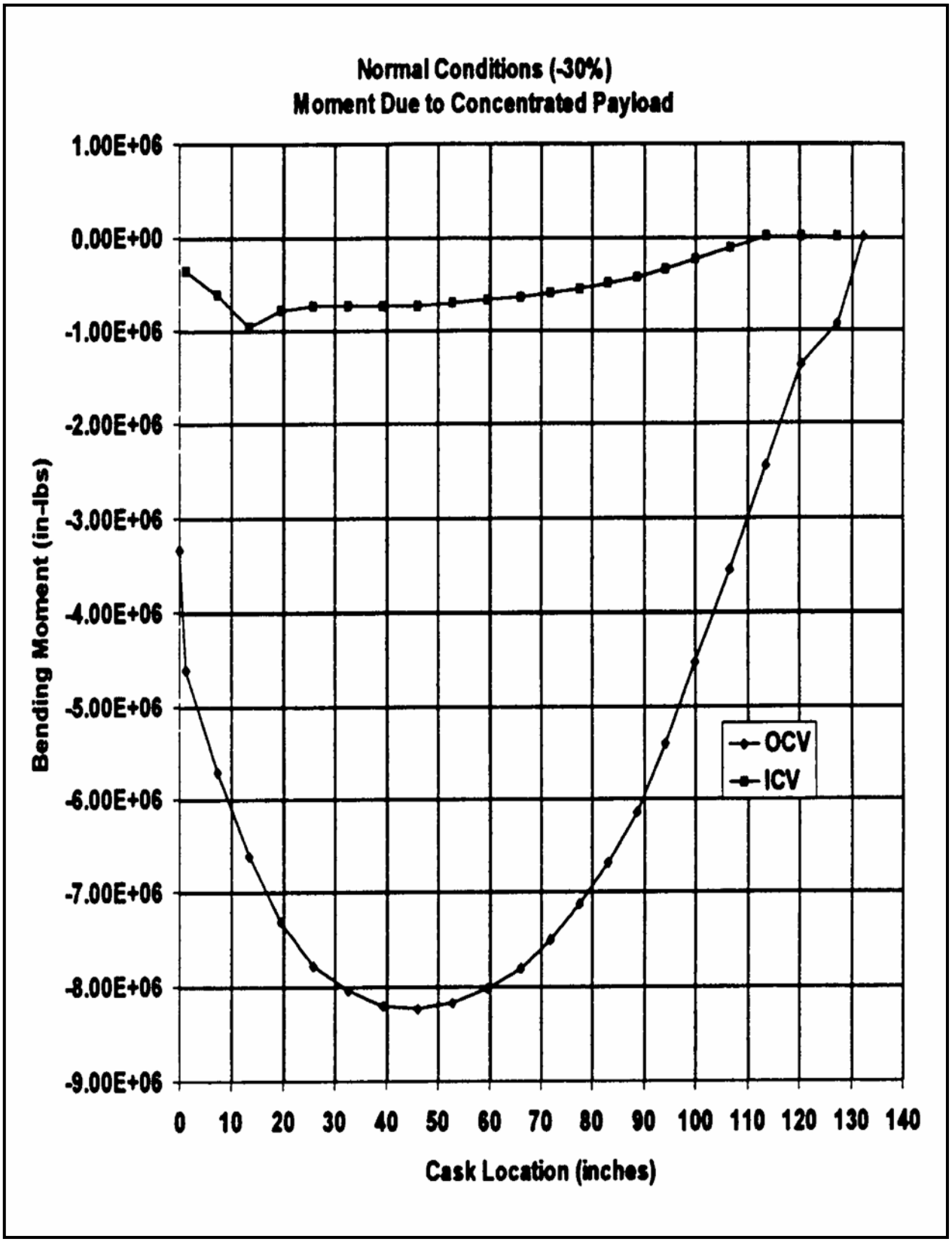

Figure 2.6-26 – NCT Hot (140 ºF) Moment Due to a Concentrated Payload

2.7 Hypothetical Accident Conditions

The RH-TRU 72-B package, when subjected to the sequence of hypothetical accident conditions (HAC) as specified in 10 CFR §71.73[1], meets the performance requirements specified in Subpart E of 10 CFR 71. With the exception of buckling, this is demonstrated in the following subsections where each HAC is addressed and shown to meet the applicable design criteria previously discussed in Section 2.1.2, *Design Criteria*. Buckling evaluations for all buckling-sensitive package components are presented in Appendix 2.10.5, *Buckling Design Criteria and Detailed Evaluation*. The structural response of the payload canister is briefly summarized in this section.

2.7.1 Free Drop

Subpart F of 10 CFR 71[1] requires that a 30-foot free drop be considered for the RH-TRU 72-B package. The drop is to be onto a flat, essentially unyielding, horizontal surface, and the package is to strike the surface in a position for which maximum damage is expected. Per 10 CFR §71.73(b)[1], the initial temperature for the free drop is to be the worst-case constant ambient air temperature between -20 ºF and 100 ºF. Internal heat generation from the payload and insolation are also considered when it is conservative to do so. Regarding initial internal pressure, the design pressure of 150 psig must be considered unless a lower internal pressure consistent with the ambient temperature assumed to precede and follow the drop is more unfavorable.

The analyses in this section extract accelerations from impact analysis results summarized in Appendix 2.10.3, *Drop Impact Evaluation Results*, and statically apply them to the package. Static application is justified since the natural frequencies of the package are relatively high and the duration of the impact loadings relatively long. The package frequencies are high as the result of using relatively thick, stiff shells for the outer cask (OC).

The durations of impact loadings are relatively long as the result of using soft (relative to the steel structures) energy absorbing impact limiters to protect the package during free drop events. In addition, inspection of accelerometer data available from the NuPac 125-B quarter-scale drop tests[2] indicates that the package responds essentially as a rigid body (e.g., for end and oblique drops, all accelerometer traces are very nearly the same, and for side drop, the accelerations for all accelerometers oriented in the direction of the drop are nearly identical). This observation further justifies static application of *g*-loads.

2.7.1.1 Flat End Drop

Analysis of RH-TRU 72-B package behavior during the end impact is performed in the following steps:

(1) Analyze the impact force using the CASKDROP computer program.

[1] Title 10, Code of Federal Regulations, Part 71 (10 CFR 71), *Packaging and Transportation of Radioactive Material*, Final Rule, 01-26-04.

[2] Nuclear Packaging, Inc., *Safety Analysis Report for the NuPac 125-B Fuel Shipping Package*, USNRC Certificate of Compliance 71-9200, U.S. Department of Energy, Washington, D.C.

(2) Analyze the OC lid for bending assuming the inner vessel (IV) and payload canister act as a uniform load on a simply supported plate (no impact limiter support).

(3) Analyze the OC lid for bending, as performed in (2), but with the impact limiter foam pressure acting in the opposite direction (impact limiter support).

(4) Analyze the stresses in the OC lid bolts.

(5) Analyze the IV stresses.

(6) Analyze the axial and hoop stresses in the OC shells and lead (maximum fabrication stress condition assumed).

(7) Analyze the axial and hoop stresses in the OC shells and lead (zero fabrication stress condition assumed).

(8) Analyze the payload canister stresses.

(9) Determine the amount of lead slump.

Material properties and allowable stresses corresponding to maximum enveloping temperature of 160 ºF for the stainless steel OC and IV, and lead, and 200 ºF for the carbon steel payload canister are given in Table 2.7-1. Buckling is addressed in Appendix 2.10.5, *Buckling Design Criteria and Detailed Evaluation*.

The nine steps of this HAC end drop analysis are carried out in the same fashion as was done for the normal conditions of transport (NCT) end drop analysis presented in Section 2.6.7.1, *Flat End Drop*. In most cases, HAC results can be obtained directly from NCT results by applying the ratio of the maximum HAC *g*-load to the maximum NCT *g*-load. This ratio is 89.7/42.5 = 2.11.

(1) End Drop Computer Analysis Using CASKDROP

The end drop analysis was performed utilizing the energy-balance computer program, CASKDROP, documented in Appendix 2.10.2.1, *Description of the CASKDROP Computer Code*. Two cases were considered assuming fully effective impact limiters and considering the variations in foam strength due to temperature effects and the possible variations in foam strength from nominal values (see Section 2.3, *Mechanical Properties of Materials*). Fully effective impact limiter cases consider the entire impact limiter impact area available for crush. Based on NuPac 125-B quarter-scale test results[2] (i.e., observed impact limiter displacements and package acceleration), the fully effective impact limiter assumption is realistic. Output for each of the two end drop cases is presented in Appendix 2.10.3, *Drop Impact Evaluation Results*. Worst-case deflections and accelerations are utilized for all analyses. From Table 2.10.3-10 of Appendix 2.10.3, *Drop Impact Evaluation Results*, the maximum HAC acceleration and impact limiter deflection for a 30-foot end drop are 89.7*g* (cold foam) and 8.67 inches (hot foam), respectively.

(2) OC Lid Bending Analysis Assuming No Impact Limiter Support

From Paragraph (2) in Section 2.6.7.1, *Flat End Drop*, the maximum OC lid bending stress, σ, for a unit (1*g*) acceleration is 216 psi/*g*. Applying 89.7*g* acceleration, the bending stress is:

$$\sigma = (216)(89.7) = 19{,}375 \text{ psi}$$

Combining this bending stress with the stresses due to a 150-psig internal pressure (1,823 psi bending stress, -150 psi radial stress) results in a stress intensity (SI) of 19,375 + 1,823 + 150 = 21,348 psi.

From Table 2.7-1, the HAC allowable primary membrane-plus-bending stress intensity, S_a = 67,700 psi at 160 ºF for Type F304 stainless steel. Therefore, the OC lid bending stress margin of safety is:

$$MS = \frac{S_a}{SI} - 1 = \frac{67{,}700}{19{,}375} - 1 = +2.17$$

(3) OC Lid Bending Analysis Assuming Full Impact Limiter Support

From Paragraph (3) in Section 2.6.7.1, *Flat End Drop*, the maximum OC lid bending stress, σ, for a unit (1*g*) acceleration is 494 psi/*g*. Applying 89.7*g* acceleration, the bending stress is:

$$\sigma = (494)(89.7) = 44{,}312 \text{ psi}$$

Note that internal pressure would reduce this bending stress; therefore, the stress intensity (SI) is 44,312 psi. From Table 2.7-1, the HAC allowable primary membrane-plus-bending stress intensity, S_a = 67,700 psi at 160 ºF for Type F304 stainless steel. Therefore, the OC lid bending stress margin of safety is:

$$MS = \frac{S_a}{SI} - 1 = \frac{67{,}700}{44{,}312} - 1 = +0.53$$

(4) OC Lid Bolt Stresses

OC bolt stresses under end impact conditions are computed and summarized in Table 2.10.6-5 and Table 2.10.6-6 of Appendix 2.10.6, *Closure Bolt Stress Evaluations*. The minimum margin of safety occurs at an impact angle of 85º. For this angle, the maximum deceleration is 90.7*g*. Assuming this deceleration acts on the full weight of the OC lid (1,667 pounds), IV (4,023 pounds), and payload canister (8,000 pounds), the maximum bolt stress intensity is 78,233 psi, assuming uniform loading of the 18 lid bolts. These values include pressure stress effects. This stress conservatively neglects impact limiter reaction forces that would reduce estimated bolt impact stresses to near zero, if considered. From Table 2.7-1, the HAC allowable containment fastener primary membrane-plus-bending stress intensity, S_a = 101,400 psi at 160 ºF for ASTM A320, Grade L43, bolting material. With a total tensile stress of 78,233 psi, the resultant minimum margin of safety is computed as +0.30, in Table 2.10.6-5 of Appendix 2.10.6, *Closure Bolt Stress Evaluations*.

An assessment of OC bolt and thread insert engagement is provided in Appendix 2.10.6, *Closure Bolt Stress Evaluations*, and shown to have a minimum margin of safety of +0.93.

A detailed analysis of the OC lid bolts for various drop angles and torque coefficients is presented in Appendix 2.10.6, *Closure Bolt Stress Evaluations*.

(5) IV Stresses

The IV is designed so that, on end impact, the end closures (lid and bottom plate) will be flush against the end closures of the OC. This will tend to minimize bending stresses in IV end plates. IV analyses are performed for both top-end down and bottom-end down flat end drop.

Top-End Down: From Paragraph (5) in Section 2.6.7.1, *Flat End Drop*, the maximum bottom plate bending stress for a unit (1*g*) acceleration is 62.0 psi/*g*. Applying 89.7*g* maximum acceleration, the bending stress becomes:

$$\sigma = (62.0)(89.7) = 5{,}561 \text{ psi}$$

Note that internal pressure would reduce this bending stress, but is conservatively ignored; therefore, the stress intensity (SI) is 5,561 psi. From Table 2.7-1, the HAC allowable primary membrane-plus-bending stress intensity, S_a = 67,700 psi at 160 ºF for Type F304 stainless steel. Therefore, the IV bottom plate bending stress margin of safety is:

$$MS = \frac{S_a}{SI} - 1 = \frac{67{,}700}{5{,}561} - 1 = +11.2$$

From Paragraph (5) in Section 2.6.7.1, *Flat End Drop*, the maximum IV shell stress for a unit (1*g*) acceleration resulting from the top-end down drop is -54.67 psi/*g*. Applying 89.7*g* maximum acceleration, the membrane stress becomes:

$$\sigma = (-54.67)(89.7) = -4{,}904 \text{ psi}$$

Combining this stress with stresses due to a 150-psig internal pressure (3,162 psi axial membrane, 6,324 psi hoop membrane, and -150 psi radial) results in a stress intensity (SI) of 6,324 – (-4,904 + 3,162) = 8,066 psi.

From Table 2.7-1, the HAC allowable primary membrane stress intensity, S_a = 48,000 psi at 160 ºF for Type 304 stainless steel. Therefore, the IV shell stress margin of safety is:

$$MS = \frac{S_a}{SI} - 1 = \frac{48{,}000}{8{,}066} - 1 = +4.95$$

A detailed buckling analysis for this load combination is presented in Appendix 2.10.5, *Buckling Design Criteria and Detailed Evaluation*.

The IV lid is supported during top-end down end drop by the OC lid, which is of comparable thickness and diameter. Because the OC lid will tend to limit deflections of the IV lid, it may be assumed that the large margins of safety derived for the OC lid in both backed and unbacked bending will be applicable to the IV lid.

Bottom-End Down: For the bottom-end impact, the IV bottom plate will be supported by the OC bottom plate. The IV bottom-end closure is of approximately the same diameter, yet of significantly smaller thickness than the OC end closure. The IV bottom plate will therefore see lower stresses than the OC bottom plate when forced into the OC bottom plate. This is because the OC closure will limit deflections of the IV closure, thereby assuring margins of safety in excess of the already conservative values presented for the OC closures.

From Paragraph (5) in Section 2.6.7.1, *Flat End Drop*, the maximum IV shell stress for a unit (1*g*) acceleration resulting from the bottom-end down drop is -98.47 psi/*g*. Applying 89.7*g* maximum acceleration, the membrane stress becomes:

$$\sigma = (-98.47)(89.7) = -8{,}833 \text{ psi}$$

Combining this stress component with those due to a 150-psig internal pressure (3,162 psi axial membrane, 6,324 psi hoop membrane, and -150 psi radial) results in a stress intensity (SI) of 6,324 – (-8,833 + 3,162) = 11,995 psi.

From Table 2.7-1, the HAC allowable primary membrane stress intensity, S_a = 48,000 psi at 160 ºF for Type 304 stainless steel. Therefore, the IV shell stress margin of safety is:

$$MS = \frac{S_a}{SI} - 1 = \frac{48{,}000}{11{,}995} - 1 = +3.00$$

A detailed buckling analysis for this load combination is presented in Appendix 2.10.5, *Buckling Design Criteria and Detailed Evaluation*.

From Paragraph (5) in Section 2.6.7.1, *Flat End Drop*, the maximum IV lid bending stress for a unit (1*g*) acceleration resulting from the bottom-end down drop is 12.9 psi/*g*. Applying the 89.7 g's acceleration results in:

$$\sigma = (12.9)(89.7) = 1{,}157 \text{ psi}$$

Internal pressure would reduce this bending stress, but is conservatively ignored. From Table 2.7-1, the HAC allowable primary membrane-plus-bending stress intensity, S_a = 67,700 psi at 160 ºF for Type F304 stainless steel. Therefore, the minimum IV lid bending stress margin of safety, MS, is:

$$MS = \frac{S_a}{\sigma} - 1 + \frac{67{,}700}{1{,}157} - 1 = +61.2$$

Per Table 2.10.6-7 and Table 2.10.6-8 of Appendix 2.10.6, *Closure Bolt Stress Evaluations*, the maximum total IV bolt tensile stress is estimated at 53,737 psi, including pressure and preload effects. It should be observed that no impact loads are applied to IV bolts since loads are directly transferred to the OC lid in direct compression. This stress of 53,737 psi results in a margin of safety of +0.89 based on an allowable, S_a = 101,400 psi. It should be noted that the estimated stress includes a preload stress of 51,840 psi (21,099 lbs/0.407 in^2). In conventional bolting analyses, per established codes (e.g., American Institute of Steel Construction and Appendix F, Section III, of the ASME Boiler and Pressure Vessel Code), preload effects are neglected when assessing the capacity of a bolted connection. This conclusion is because preloads have little effect upon the ultimate capacity of a bolted connection[3]. Thus, the reported margin of safety is extraordinarily conservative, when compared with the methodology of conventional codes.

An assessment of IV bolt and thread insert engagement is provided in Appendix 2.10.6, *Closure Bolt Stress Evaluations*, and shown to have a minimum margin of safety of +1.79.

[3] Joseph E. Shigley and Larry D. Mitchell, *Mechanical Engineering Design*, 4th Edition, McGraw-Hill, 1983.

A detailed analysis of the IV lid bolts for various drop angles and torque coefficients is presented in Appendix 2.10.6, *Closure Bolt Stress Evaluations*.

(6) Stresses in the OC Shells and Lead (Maximum Fabrication Stress Condition Assumed)

The principal concern for the OC under HAC end drop conditions is with buckling of the inner shell. As shown by the following stress calculations and the detailed buckling evaluation presented in Appendix 2.10.5, *Buckling Design Criteria and Detailed Evaluation*, buckling will not occur as the result of the hoop and axial compressive stresses that develop in the OC inner shell under HAC end drop conditions.

Various initial conditions can be assumed for the HAC end drop event. In particular, a temperature must be assumed in order to establish an initial fabrication stress for the inner shell. A lower assumed temperature will result in a higher initial hoop stress on the inner shell (see Section 2.6.2, *Cold*), but higher allowable stresses. For purposes of this analysis, drops at 160 ºF (conservatively bounding the maximum lead and OC shells normal temperatures per Section 3.4.2, *Maximum Temperatures*), 70 ºF, and -20 ºF are considered. Regardless of temperature, the maximum *g*-load of 89.7*g* for the -20 ºF drop case is conservatively employed.

To adequately bound the consequences of the drop event at a given temperature, two initial lead conditions are also considered. The first assumes that the lead has shrunk onto the inner shell and away from the outer shell. In addition, due to the combined effects of friction between the lead and inner shell, and axial shrinkage of the lead relative to the stainless shells, axial gaps will develop between the lead and the steel structures at the top and bottom end of the lead column. These axial gaps are important in that, until friction is overcome, under increased axial loading, the lead will impose a direct axial load on the inner shell. Once friction is overcome, the lead will become supported at its base (the bottom of the lead column) and will grow radially outward due to the "Poisson effect" under increased axial loading. This radial growth will tend to relieve the initial fabrication hoop stress as the lead separates from the inner shell. If sufficient axial load develops, the lead would grow out to the outer shell creating tensile hoop stresses therein, and under further loading would eventually flow back inward into the inner shell, thereby developing compressive hoop stresses in the inner shell.

From Appendix 2.10.8, *Fabrication Stresses Due to Lead Pour*, the hoop stress in the inner shell due to fabrication is -1,413 psi at 70 ºF, and -1,821 psi at -20 ºF. Extrapolating, the hoop stress in the inner shell is -1,038 psi at 160 ºF. (Note that the outer shell hoop stress is considered to be negligible since the lead separates from the outer shell upon cooling.)

The equivalent pressure at the lead/inner shell interface, p, is:

$$p = \frac{\sigma t}{r}$$

where the shell thickness, t = 1.00 inch, and the shell radius, r = 16.69 inches. Therefore, the interface pressure is 62.2 psi at 160 ºF, 84.7 psi at 70 ºF, and 109.1 psi at -20 ºF.

With a coefficient of friction, *f*, for lead on stainless steel assumed to fall in the 0.5 to 1.0 range[4], the load, P, that can be supported by friction at the lead/inner shell interface, may be determined as follows:

$$P = \pi DLpf$$

where inner shell outside diameter, D = 34.38 inches, the lead column height, L = 123.5 inches, the interface pressure is p, and the coefficient of friction, $f = 0.5 – 1.0$.

Applying the above interface pressures, the total axial load that may be supported for each case is provided in Table 2.7-2.

With the total lead weight equal to 10,739 pounds, per Table 2.2-1 in Section 2.2, *Weights and Centers of Gravity*, the minimum *g*-load that can be supported by friction is 414,842/10,739 = 38.6*g*. The maximum *g*-load that can be supported by friction is 1,455,283/10,739 = 135.5*g* (-20 ºF with friction coefficient of 1.0). Since end drop *g*-loads range from 51.1*g* at the maximum foam temperature of 140 ºF to 89.7*g* at the minimum foam temperature of -20 ºF, lead slippage may or may not occur. The following analysis assumes no slippage for the HAC 89.7*g* load. This assumption conservatively maximizes loading on the inner shell. Axial stress in the OC inner and outer shells are therefore determined by ratioing the NCT end drop results available in Paragraph (6) of Section 2.6.7.1, *Flat End Drop*, by a factor of 89.7/42.5 = 2.11. Table 2.7-3 summarizes the axial and hoop stress results.

Table 2.7-4, Table 2.7-5, and Table 2.7-6 present the corresponding margins of safety for the more critical inner shell at temperatures of -20 ºF, 70 ºF, and 160 ºF, respectively. Zero internal pressure is used in order to maximize compressive stresses in the inner shell. Note that axial stresses will actually decrease with increasing drop temperature since *g*-loads are lower at higher temperatures (due to decreased foam strength with increased temperature). This effect is conservatively ignored in Table 2.7-4, Table 2.7-5, and Table 2.7-6.

Buckling is addressed in Appendix 2.10.5, *Buckling Design Criteria and Detailed Evaluation*.

(7) Stresses in the OC Shells and Lead (Zero Fabrication Stress Condition Assumed)

The second initial lead condition assumes that the fabrication stress has fully crept away resulting in a stress free column of lead just in contact with the OC inner and outer shells. This is a potential worst case since any axial load imposed on the lead will directly load, radially, both the inner and outer shells (i.e., the lead need not flow away from the inner shell, into the outer shell and back into the inner shell to develop a compressive hoop stress in the inner shell).

For this condition, initial stresses in the lead and the steel shells are taken as zero. As axial load is applied to the lead and shells, the lead will attempt to move downward and outward and develop pressures on both the inner and outer shells, as shown in Figure 2.6-5 in Paragraph (7) of Section 2.6.7.1, *Flat End Drop*.

For the purpose of this analysis, let $p_i = p_o = p$. This assumption is considered reasonable once lead starts to flow.

[4] Theodore Baumeister, *Mark's Standard Handbook for Mechanical Engineers*, Ninth Edition, McGraw-Hill Book Company, New York, NY, 1987, Table 3.2.1.

Conservatively assuming that the lead receives no axial support at its base, but rather is supported solely by friction at the inner and outer shells, the maximum value of the pressure, p_{max}, is determined based on a lead weight, W_L = 10,739 pounds, being acted on by an end drop acceleration, $\eta = 89.7g$, resulting in a total lead force, w_L, of:

$$w_L = \eta W_L = 963{,}288 \text{ lb}$$

For the maximum pressure, p_{max}, use the minimum expected coefficient of friction, $f = 0.5$, resulting in a force, w, of:

$$w = p_{max}(2\pi r_L)(L - d)f$$

where the mean lead shell radius, $r_L = ½(r_o^2 + r_i^2) = 18.1275$ inches, the lead shell outer radius, $r_o = 19.065$ inches, the lead shell inner radius, $r_i = 17.19$ inches, and the shell length, L = 123.5 inches. Letting $w = w_L$ = 963,288 pounds, the maximum pressure, p_{max}, is:

$$p_{max} = \frac{16{,}915}{(123.5 - d)} \text{ psi}$$

Assuming lead flow initiates at the yield strength of the lead, σ_y, the height of the lead column, d, required to yield the lead cross-section due to the 89.7*g* HAC acceleration is:

$$\sigma_y = \rho d(89.7g)$$

where σ_y is lead's yield strength at temperature, and the lead density, $\rho = 0.41$ lb/in^3. Therefore:

$$d = (0.02719)\sigma_y$$

For lead temperatures of 160 ºF, 70 ºF, and -20 ºF, and conservatively estimating an upper bound on the lead properties delineated in Figure 2.3-3 through Figure 2.3-6 of Section 2.3, *Mechanical Properties of Materials*, the pressures and hoop stresses may be summarized as shown in Table 2.7-7.

The maximum axial stress in the shells is determined by multiplying the results available from Paragraph (7) of Section 2.6.7.1, *Flat End Drop*, by the ratio of HAC-to-NCT end drop *g*-loads. The resultant stresses in the OC inner and outer shells for the HAC end drop load of 89.7*g* are summarized in Table 2.7-8.

Table 2.7-9, Table 2.7-10, and Table 2.7-11 present the corresponding margins of safety for the more critical inner shell. Zero internal pressure is used in order to maximize compressive stresses in the inner shell. Again, it is noted that the margins presented for the 70 ºF and 160 ºF cases are conservative since at these temperatures, *g*-loads will actually be less than the 89.7*g* conservatively considered. Buckling is addressed in Appendix 2.10.5, *Buckling Design Criteria and Detailed Evaluation*.

(8) Discussion of Payload Canister Behavior in End Drop

Hoop and axial stresses in the canister are addressed for the thirty-foot HAC end drop condition. Stresses resulting due to a 1*g* load, from Paragraph (8) of Section 2.6.7.1, *Flat End Drop*, are

scaled by the 89.7*g* HAC drop loading. The payload canister shell hoop stress due to a 1*g* load is 225.1 psi, and the axial stress due to a 1*g* load is 87.14 psi.

The HAC end drop hoop (σ_h) and axial (σ_a) stresses are:

$$\sigma_h = (225.1)(89.7) = 20{,}191 \text{ psi (tension)}$$

$$\sigma_a = (87.14)(89.7) = 7{,}816 \text{ psi (compression)}$$

The maximum canister shell stress intensity (SI) is therefore, 20,191 + 7,816 = 28,007 psi. From Table 2.7-1, the HAC allowable primary membrane stress intensity, S_a = 38,500 psi at 200 ºF using worst-case ASTM A516, Grade 55, carbon steel as the material of construction (conservative maximum canister temperature; see Table 2.6-2 in Section 2.6, *Normal Conditions of Transport*). Therefore, the margin of safety (MS) for the payload canister shell is:

$$MS = \frac{S_a}{SI} - 1 = \frac{38{,}500}{28{,}007} - 1 = +0.37$$

(9) Lead Slump

As discussed in Paragraph (9) of Section 2.6.7.1, *Flat End Drop*, an upper-bound for lead slump can be determined from Eq. 2.16 of the Package Designers Guide[5]. The upper-bound lead slump per foot of drop for a bare package is determined to be 0.068 inches. For the 30-foot HAC drop, the upper bound limit would be 2.03 inches, which corresponds to an approximate deceleration of 354.7*g*. The maximum deceleration for the package with impact limiters was determined to be 89.7*g*. Ratioing these deceleration levels yields an upper lead slump value of 0.513 inches, which is insignificant.

As previously noted in Paragraph (9) of Section 2.6.7.1, *Flat End Drop*, lead slump of the NuPac 125-B cask[2] (NRC Certificate of Compliance 71-9200) is expected to bound lead slump of the RH-TRU 72-B package. Quarter-scale testing of the NuPac 125-B cask showed no measurable lead slump due to the 30-foot end drop. Even though an upper bound value was determined, it can therefore be concluded that lead slump will not be a problem for the RH-TRU 72-B package.

2.7.1.2 Corner and Oblique Drops

Analysis of the RH-TRU 72-B package behavior during the HAC corner drop, including oblique drop orientations, uses the same methods as those used for the NCT corner drop. HAC corner and oblique drops lead to the possibility of a secondary impact, or slapdown, of the package on the end opposite the initially impacted end. This possibility is addressed in Appendix 2.10.4, *Slapdown Assessment*. In that section, the consequences of slapdown are shown to be less severe for the RH-TRU 72-B package than those associated with a flat side drop from a height of 30 feet. For this reason, slapdown is not a limiting case for the package and is not further addressed in this section.

[5] L. B. Shappert, *Package Designers Guide, A Guide for the Design, Fabrication, and Operation of Shipping Packages for Nuclear Applications*, ORNL-NSIC-68, Oak Ridge National Laboratory, Oak Ridge, Tennessee, February 1970.

Analysis of RH-TRU 72-B package behavior during the corner drop event, including oblique drop orientations, is performed in the following steps:

(1) Determine the force-deflection relations for a range of initial impact angles, using the CASKDROP computer program. Utilize the force-deflection data from CASKDROP as input to the computer program SLAPDOWN to determine the package response for various initial impact angles.

(2) Based on the accelerations and rotations predicted in (1), determine the equivalent "static" forces on the OC and IV, considered as a rigid body with distributed and lumped masses.

(3) Based on the loads from (2), analyze the OC shells and IV as simple beams, finding the internal forces: shear, moment, and thrust. Compute stresses for the maximum value of each of these forces, and by inspection of the relative magnitudes of these maximum component stresses, select load cases for further analysis which will have the maximum combined stresses.

(4) Analyze the OC shells for stress, assuming the two shells act as parallel beams, under the loads determined in (3).

(5) Analyze the IV for stress under the loads determined in (3).

(6) Analyze the payload canister for stress under the loads determined in (3).

(7) Analyze impact limiter attachment forces.

(8) Based on the forces from (7), calculate the impact limiter attachment stresses.

(9) Analyze the stresses in the OC and IV lid bolts.

(10) Calculate the maximum impact limiter deformations and residual clearances for package hard spots.

Material properties and allowable stresses corresponding to the maximum enveloping temperature of 160 ºF for the Type 304 stainless steel OC and IV and lead are given in Table 2.7-1. Buckling is addressed in Appendix 2.10.5, *Buckling Design Criteria and Detailed Evaluation*.

(1) Corner Drop Computer Analysis (CASKDROP and SLAPDOWN)

Analytic predictions of package performance for drop orientations impacting upon the corner of the package employ two computer programs: CASKDROP and SLAPDOWN, documented in Appendix 2.10.2, *Drop Analysis Codes Description*. CASKDROP uses an energy-balance technique to determine loads and deformations of the impact limiter. Since CASKDROP assumes all drop energy is absorbed in deformation of the impact limiter, it provides valid results when the impact orientation places the center-of-gravity (CG) directly over the impacted corner, approximately 68º from the horizontal for the RH-TRU 72-B package. At other impact orientations, the force-deflection values generated by CASKDROP are used in SLAPDOWN, a dynamic analysis program that considers rotational motion effects. For initial impact angles between the CG-over-corner and vertical, dynamic effects (such as a secondary slapdown) are negligible, and results at the upper, or secondary impact limiter are unimportant. For such cases, CASKDROP is used to conservatively calculate the primary impact results.

Two (2) cases were run which accounted for variations in foam strength due to temperature effects and the possible variations in foam strength from nominal values (see Section 2.3, *Mechanical*

Properties of Materials). Detailed output for each of the two analysis cases is presented in Appendix 2.10.3, *Drop Impact Evaluation Results*. Note that the load and stress evaluations presented in this section are typically based on the results from the -20 ºF foam stress case. Impact limiter responses (i.e., attachment forces, deformations, and residual clearances) presented herein directly consider both analytic cases.

(2) Equivalent "Static" Loads:

Equivalent static loads acting on the RH-TRU 72-B package as the result of a HAC corner/oblique drop are determined in exactly the same manner as for the NCT corner/oblique drop (see Paragraph (2) in Section 2.6.7.2, *Corner and Oblique Drops*).

Slapdown impacts are not governing, as shown in Appendix 2.10.4, *Slapdown Assessment*. The only potentially serious slapdown loading problem will affect package impact limiter attachment fastener and OC lid fastener integrity. These load cases are addressed in Paragraphs (7) and (9) , below.

(3) Internal Forces

The OC shells are analyzed as if they are two beams acting in parallel. The payload canister is analyzed as one beam attached to the IV at the two spacer disk locations, and the IV connects to the OC via a series of interface (gap) elements. A schematic representation of the finite element analysis model used is presented as Figure 2.10.1-9 in Appendix 2.10.1.4, *Containment Assembly Analysis for Oblique Drops*.

Maximum stresses are given as functions of impact angle for the cold foam (-20 ºF) conditions in Figure 2.7-1, Figure 2.7-2, and Figure 2.7-3 for the OC, IV, and payload canister, respectively, based on maximum thrust, shear, and bending moment given in Figure 2.7-4, Figure 2.7-5, and Figure 2.7-6, respectively. The stresses shown in Figure 2.7-1, Figure 2.7-2, and Figure 2.7-3 were calculated using slightly different *g*-loadings than those found in Appendix 2.10.3, *Drop Impact Evaluation Results*. A comparison of the *g*-loading from Appendix 2.10.3, *Drop Impact Evaluation Results* for the HAC cold free drop and those data used in calculating the peak stresses is presented in Figure 2.7-7. Since the *g*-loads match closely for all the orientations considered here, scaling of the previously calculated stresses is an appropriate method for evaluating package components.

In a similar manner, the values from Figure 2.7-8, Figure 2.7-9, and Figure 2.7-10, showing the maximum stresses for the OC, IV, and payload canister, respectively, for hot foam (140 ºF) conditions are also scaled accordingly, based on maximum thrust, shear, and bending moment given in Figure 2.7-11, Figure 2.7-12, and Figure 2.7-13.

The stresses are computed as follows:

$$S_t = \frac{P}{A} \times \frac{g_{new}}{g_{old}} = \text{stress due to thrust, psi}$$

$$S_v = \frac{V}{A} \times \frac{g_{new}}{g_{old}} = \text{stress due to shear, psi}$$

$$S_m = \frac{Mc}{I} \times \frac{g_{new}}{g_{old}} = \text{stress due to bending moment, psi}$$

where P is the thrust force (lb), V is the shear force (lb), and M is the bending moment (in-lb). The distance to the neutral axis, c = 20.565 inches for the OC outer shell, c = 17.19 inches for the OC inner shell, c = 16.00 inches for the IV shell, and c = 13.00 inches for the payload canister. The moment of intertia, I = 51,334 in^4 for the OC, I = 4,718 in^4 for the IV, and I = 1,676 in^4 for the payload canister. Finally, the area, A = 292 in^2 for the OC, A = 38 in^2 for the IV, and A = 20 in^2 for the payload canister.

From Figure 2.7-1, it can be deduced that a 5º impact angle with cold foam (-20 ºF), yields the worst stresses for the OC. Similarly, from Figure 2.7-2 and Figure 2.7-3, it can be deduced that a 5º impact angle with cold foam also yields the worst stresses for the IV and payload canister. Although the maximum thrust, shear, and bending moment do not occur at the same location for each component, the true maximums are used to provide a conservative analysis. The figures are based on a *g*-load of 32.2*g*, whereas the impact of a 5º angle is 48.1*g*. The scale factor is therefore 48.1/32.2 = 1.49.

For the OC, these maximums are P_{max} = 30,366 × 1.49 = 45,245 pounds, V_{max} = 939,900 × 1.49 = 1,400,451 pounds, and M_{max} = 34,873,000 × 1.49 = 51,960,770 in-lb. For the IV, the maximums are P_{max} = 2,596 × 1.49 = 3,868 pounds, V_{max} = 191,350 × 1.49 = 285,112 pounds, and M_{max} = 4,260,000 × 1.49 = 6,347,400 in-lb. Finally, for the payload canister, the maximums are P_{max} = 12,107 × 1.49 = 18,039 pounds, V_{max} = 163,610 × 1.49 = 243,779 pounds, and M_{max} = 1,992,000 × 1.49 = 2,968,080 in-lb.

(4) OC Stresses

The maximum membrane stress in the OC inner shell, for the load case selected in Paragraph (3), is:

$$S_m = \frac{Mc}{I} + \frac{P}{A} = \frac{(51{,}960{,}770)[17.19 - (½)(1.0)]}{51{,}334} + \frac{45{,}245}{292} = 17{,}049 \text{ psi}$$

The maximum membrane-plus-bending stress in the OC inner shell is:

$$S_{mb} = \frac{Mc}{I} + \frac{P}{A} = \frac{(51{,}960{,}770)(17.19)}{51{,}334} + \frac{45{,}245}{292} = 17{,}555 \text{ psi}$$

Similarly, the maximum stresses in the OC outer shell are:

$$S_m = \frac{Mc}{I} + \frac{P}{A} = \frac{(51{,}960{,}770)[20.565 - (½)(1.5)]}{51{,}334} + \frac{45{,}245}{292} = 20{,}212 \text{ psi}$$

$$S_{mb} = \frac{Mc}{I} + \frac{P}{A} = \frac{(51{,}960{,}770)(20.565)}{51{,}334} + \frac{45{,}245}{292} = 20{,}971 \text{ psi}$$

In addition, shear stress must be added in the calculation of the membrane stress intensities for the OC inner and outer shells. The shear stress is:

$$S_v = \frac{V}{A} = \frac{1{,}400{,}451}{292} = 4{,}796 \text{ psi}$$

Axial fabrication stresses used in the oblique drop analyses are scaled from those used in the end drop analysis (see Table 2.6-12 from Section 2.6.7.1, *Flat End Drop*) using the respective *g*-loadings of the package (48.1/42.5). Fabrication stresses for the oblique drop analyses are given in Table 2.7-12.

Table 2.7-13, Table 2.7-14, and Table 2.7-15 present the corresponding margins of safety for the more critical OC inner shell. Zero internal pressure is used in order to maximize compressive stresses in the OC inner shell. Again, note that the margins presented for the 70 ºF and 160 ºF cases are conservative in that at these temperatures, *g*-loads will actually be less than the 48.1*g* conservatively considered herein.

(5) IV Stresses

The maximum membrane stress in the IV shell, for the load case selected in Paragraph (3), is:

$$S_m = \frac{Mc}{I} + \frac{P}{A} = \frac{(6{,}347{,}400)[16.00 - (½)(0.38)]}{4{,}718} + \frac{3{,}868}{38} = 21{,}372 \text{ psi}$$

The maximum membrane-plus-bending stress in the IV shell is:

$$S_{mb} = \frac{Mc}{I} + \frac{P}{A} = \frac{(6{,}347{,}400)(16.00)}{4{,}718} + \frac{3{,}868}{38} = 21{,}628 \text{ psi}$$

In addition, shear stress must be added in the calculation of the membrane stress intensity for the IV shell. The shear stress is:

$$S_v = \frac{V}{A} = \frac{285{,}112}{38} = 7{,}503 \text{ psi}$$

Table 2.7-16 presents stress and margin of safety results for the IV for the worst-case load combination.

(6) Discussion of Payload Canister Behavior in Oblique Drops

The maximum membrane stress in the payload canister shell, for the load case selected in Paragraph (3), is:

$$S_m = \frac{Mc}{I} + \frac{P}{A} = \frac{(2{,}968{,}080)[13.00 - (½)(0.25)]}{1{,}676} + \frac{18{,}039}{20} = 23{,}703 \text{ psi}$$

The maximum membrane-plus-bending stress in the payload canister shell is:

$$S_{mb} = \frac{Mc}{I} + \frac{P}{A} = \frac{(2{,}968{,}080)(13.00)}{1{,}676} + \frac{18{,}039}{20} = 23{,}924 \text{ psi}$$

In addition, shear stress must be added in the calculation of the membrane stress intensity for the payload canister shell. The shear stress is:

$$S_v = \frac{V}{A} = \frac{243{,}779}{20} = 12{,}189 \text{ psi}$$

Table 2.7-17 presents stress and margin of safety results for the canister shell for the worst load combination. Buckling is addressed in Appendix 2.10.5, *Buckling Design Criteria and Detailed Evaluation*.

(7) Impact Limiter Attachment Forces

The maximum HAC impact limiter attachment moment, $2.76(10)^6$ in-lb, is given in Table 2.10.3-13 of Appendix 2.10.3, *Drop Impact Evaluation Results*. The NCT analysis given in Paragraph (7) of Section 2.6.7.2, *Corner and Oblique Drops*, addressed a $2.16(10)^6$ in-lb moment, resulting in a 25,472-pound maximum attachment force. By ratio, the maximum HAC attachment force is 32,548 pounds.

(8) Impact Limiter Attachment Stresses

The tensile stress area of a 1¼-7UNC bolt of 0.969 in^2 exceeds the cross-sectional area of the 1.0-inch diameter shaft (A = 0.785 in^2). Therefore, maximum impact limiter attachment bolt stress is:

$$S_B = \frac{P_{max}}{A} = \frac{32{,}548}{0.785} = 41{,}462 \text{ psi}$$

From Table 2.7-1, the HAC allowable non-containment fastener primary membrane stress intensity, S_a = 101,400 psi at 160 ºF for ASTM A320, Grade L43, bolting material. Therefore, the impact limiter attachment bolt margin of safety is:

$$MS = \frac{S_a}{S_B} - 1 = \frac{101{,}400}{41{,}462} - 1 = +1.45$$

From Paragraph (8) of Section 2.6.7.2, *Corner and Oblique Drops*, a 32,448 psi bolt stress corresponds to a shear stress in the internal threads of the thread insert equal to 4,944 psi. For the 41,462 psi HAC bolt stress, the corresponding shear stress, τ = 6,317 psi.

From Table 2.7-1, the HAC allowable shear stress for the internal threads, S_a = 28,400 psi at 160 ºF, conservatively using Type F304 stainless steel. Therefore, the margin of safety is:

$$MS = \frac{S_a}{\tau} - 1 = \frac{28{,}400}{6{,}317} - 1 = +3.50$$

From Paragraph (8) of Section 2.6.7.2, *Corner and Oblique Drops*, a 32,448 psi bolt stress corresponds to a shear stress in the external threads of the insert equal to 3,657 psi. For the 41,462 psi accident condition bolt stress, the corresponding shear stress, τ = 4,673 psi.

From Table 2.7-1, the HAC allowable shear stress for the external threads, S_a = 28,400 psi at 160 ºF for Type F304 stainless steel. Therefore, the margin of safety is:

$$MS = \frac{S_a}{\tau} - 1 = \frac{28{,}400}{4{,}673} - 1 = +5.08$$

(9) Stresses in the OC and IV Lid Bolts

This evaluation directly parallels the analysis and rationale of that used for NCT, as discussed in Paragraph (9) of Section 2.6.7.2, *Corner and Oblique Drops*.

(a) Stresses in the OC Lid Bolts

Comprehensive analysis of all oblique orientations is summarized in Table 2.10.6-5 and Table 2.10.6-6 of Appendix 2.10.6, *Closure Bolt Stress Evaluations*. The minimum margin of safety is found at a near-vertical orientation of 85º with respect to horizontal. At this orientation angle, direct tensile stress due to impact, pressure effects, and preload effects is estimated at 78,219 psi. The associated shear stress is 756 psi. From Table 2.7-1, the HAC allowable containment fastener primary membrane stress intensity, S_a = 101,400 psi at 160 ºF for ASTM A320, Grade L43, bolting material. The resultant margin of safety is +0.30.

As described in Appendix 2.10.6, *Closure Bolt Stress Evaluations*, bolt impact stresses are calculated assuming a triangular distribution of bolt forces and external impact forces arbitrarily (and conservatively) applied at the corner of the package. Thus, external energy absorber forces are not employed to reduce bolt tensile forces. For near vertical impacts (≥80º), a uniform force distribution is employed.

Note that a yield criterion for closure bolts is very conservative for bore-sealed packages such as the RH-TRU 72-B package, since sealing is dependent on radial, not axial, geometry. This fact was graphically demonstrated by a successful leak test of the quarter-scale NuPac 125-B cask[2] with "loose" (i.e., untightened) bolts. For face-sealed packages, a yield criterion may be quite appropriate since sealing in this instance depends upon unchanging geometry in the axial direction.

An assessment of OC bolt and thread insert engagement is provided in Appendix 2.10.6, *Closure Bolt Stress Evaluations*, and shown to have a minimum margin of safety of +0.93.

(b) Stresses in the IV Lid Bolts

Comprehensive analysis of the IV bolts for all impact orientations is summarized in Table 2.10.6-7 and Table 2.10.6-8 of Appendix 2.10.6, *Closure Bolt Stress Evaluations*. The minimum margin of safety is found at a near-horizontal orientation of 5º with respect to horizontal. This differs from OC conditions because impact loads are directly transferred to the OC lid (in direct bearing) and do not contribute to bolt stresses. At an angle of 5º, total direct tension, due to pressure and preload effects, is estimated at 53,737 psi. The associated shear stress is 20,338 psi. From Table 2.7-1, the HAC allowable containment fastener primary membrane stress intensity, S_a = 101,400 psi at 160 ºF for ASTM A320, Grade L43, bolting material. The resultant margin of safety is +0.50.

An assessment of IV bolt and thread insert engagement is provided in Appendix 2.10.6, *Closure Bolt Stress Evaluations*, and shown to have a minimum margin of safety of +1.79.

(10) Impact Limiter Deformations and Residual Clearances

Maximum impact limiter deformations and residual clearances due to HAC corner/oblique drops are directly available from

Figure 2.10.3-7 in Appendix 2.10.3, *Drop Impact Evaluation Results*. Per that appendix, maximum crush of an impact limiter corner is 23.7 inches for the 140 ºF foam stress case and occurs for a drop angle of 55º with respect to horizontal.

Minimum residual clearance for the main package body is 4.69 inches for the 140 ºF foam stress case and occurs for a drop angle of 40º with respect to horizontal. These deformations and residual clearances are of little consequence for the RH-TRU 72-B package.

2.7.1.3 Flat Side Drop

Analysis of RH-TRU 72-B package behavior for the side drop event is performed in the following steps:

(1) Analyze the impact force using the CASKDROP computer program.

(2) Based on the accelerations predicted in (1), determine the equivalent "static" forces on the OC and IV, considered as a rigid body with distributed and lumped masses.

(3) Based on the loads from (2), analyze the OC shells and IV as simple beams, finding the internal forces: thrust, shear, and moment. Compute stresses for the maximum value of each of these forces.

(4) Analyze the OC shells for stress, assuming the two shells act as parallel beams, under the loads determined in (3).

(5) Analyze the IV for stress under the loads determined in (3).

(6) Analyze the payload canister for stress under the loads determined in (3).

(7) Analyze the OC lid for bearing against the top OC ring forging, analyze the OC closure bolts, and analyze the top OC ring forging for shear.

(8) Analyze the OC end plate welds for shear.

(9) Analyze the IV lid for bearing against the IV ring forging, analyze the IV closure bolts, and analyze the IV ring forging.

(10) Calculate the maximum impact limiter deformations and residual clearances for package hard spots.

Material properties and allowable stresses corresponding to the maximum enveloping temperature of 160 ºF for the Type 304 stainless steel OC and IV are given in Table 2.7-1. Buckling is addressed in Appendix 2.10.5, *Buckling Design Criteria and Detailed Evaluation*.

Where possible, the analyses in this section are performed on the basis of a unit (1*g*) axial acceleration, with actual acceleration numbers being substituted at the final point of calculating stresses.

(1) Side Drop Computer Analysis Using CASKDROP

The side drop analysis was performed utilizing the energy-balance computer program, CASKDROP, documented in Appendix 2.10.2.1, *Description of the CASKDROP Computer Code*. Two cases were run which accounted for variations in foam strength due to temperature effects and the possible variations in foam strength from nominal values (see Section 2.3, *Mechanical Properties of Materials*). Each of these two cases consists of two different loading studies for a total of four different cases. The two different loading cases are as follows: (1) distributed payload within the canister, and (2) concentrated payload and canister weight at either of the IV spacer disk supports.

The drop cases consider the impact limiter as fully effective, as defined in Appendix 2.10.3, *Drop Impact Evaluation Results*. The worst-case deflections and accelerations obtained from the bounding cases are utilized for all analyses. The maximum resultant acceleration for the HAC side drop is 81.2*g* (-20 ºF foam), and the maximum impact limiter deflection is 11.5 inches (140 ºF foam) per Table 2.10.3-10 of Appendix 2.10.3, *Drop Impact Evaluation Results*.

(2) Equivalent "Static" Loads

The OC and IV are treated as rigid bodies under transverse acceleration. The two bodies are assumed to move together, and the forces between them needed to make them do so, is found. The centers of gravity of the two bodies are assumed to be coincident.

(3) Internal Forces

The OC shells are analyzed as if they are two beams acting in parallel. The payload canister is analyzed as one beam attached to the IV at the two spacer disk locations, and the IV connects to the OC via a series of interface (gap) elements. A schematic representation of the finite element analysis model used is presented as Figure 2.10.1-9 in Appendix 2.10.1.4, *Containment Assembly Analysis for Oblique Drops*.

To avoid plastic deformation of the payload canister shell, the payload must very nearly be restricted to a uniformly distributed load over the entire length of the canister. Since, this uniformly distributed payload weight does not necessarily impose the worst loading conditions on the OC and IV, the concentrated payload weight is considered at either of the spacer disk supports. Maximum loading conditions are found to occur under the following conditions:

- OC – cold foam (-20 ºF), distributed payload
- IV – cold foam (-20 ºF), concentrated payload

Shear and moment diagrams for -20 ºF foam with a distributed payload are shown in Figure 2.7-14 and Figure 2.7-15, respectively, and with a concentrated payload in Figure 2.7-16 and Figure 2.7-17, respectively, with each component on the same figure. As discussed in Section 2.7.1.2, *Corner and Oblique Drops*, the figures were created using slightly different impact *g*-loadings than given in Appendix 2.10.3, *Drop Impact Evaluation Results*. The difference, however, is small because the figures were created using a side drop *g*-loading of 81.4*g*, which is comparable to the actual side drop *g*-load of 81.2*g*. Therefore, scaling of the shear and moments is appropriate. Similarly, the shear and moment diagrams for hot foam (140 ºF) with a distributed payload, shown in Figure 2.7-18 and Figure 2.7-19, and with a concentrated payload, shown in Figure 2.7-20 and Figure 2.7-21, are scaled accordingly.

As previously discussed, the cold foam yields the worst stresses. The OC experiences worst-case stresses under a distributed payload, while the IV experiences its worst stresses due to a concentrated payload/canister force. The payload canister stresses for the distributed load case are included only for the sake of consistency with other sections herein. Although the maximum shear and moment do not occur at the same location for each component, the maximums will be used to determine combined stresses as this provides a conservative analysis. The figures are based on a side drop *g*-loading of 81.4*g*, whereas the actual side drop impact is 81.2*g*. Therefore, the scale factor is 81.2/81.4 = 0.998.

The maximum shear, V_{max}, and moment, M_{max}, for the OC are:

$$V_{max} = (1{,}625{,}100)(0.998) = 1{,}621{,}850 \text{ lb}$$

$$M_{max} = (50{,}329{,}000)(0.998) = 50{,}228{,}342 \text{ in - lb}$$

The maximum shear, V_{max}, and moment, M_{max}, for the IV are:

$$V_{max} = (354{,}760)(0.998) = 354{,}050 \text{ lb}$$

$$M_{max} = (5{,}864{,}000)(0.998) = 5{,}852{,}272 \text{ in - lb}$$

The maximum shear, V_{max}, and moment, M_{max}, for the payload canister, with only the distributed payload considered, are:

$$V_{max} = (200{,}830)(0.998) = 200{,}428 \text{ lb}$$

$$M_{max} = (2{,}197{,}100)(0.998) = 2{,}192{,}706 \text{ in - lb}$$

Maximum stresses can be calculated from the maximum shear and moments (given above) as follows:

$$S_v = \frac{V}{A} = \text{stress due to shear, psi}$$

$$S_m = \frac{Mc}{I} = \text{stress due to bending moment, psi}$$

where V is the shear force (lb) and M is the bending moment (in-lb). The distance to the neutral axis, c = 20.565 inches for the OC outer shell, c = 17.19 inches for the OC inner shell, c = 16.00 inches for the IV shell, and c = 13.00 inches for the payload canister. The moment of intertia, I = 51,334 in^4 for the OC, I = 4,718 in^4 for the IV, and I = 1,676 in^4 for the payload canister. Finally, the area, A = 292 in^2 for the OC, A = 38 in^2 for the IV, and A = 20 in^2 for the payload canister.

(4) OC Stresses

The maximum membrane stress in the OC inner shell, for the load case selected in Paragraph (3), is:

$$S_m = \frac{Mc}{I} = \frac{(50{,}228{,}342)[17.19 - (½)(1.0)]}{51{,}334} = 16{,}331 \text{ psi}$$

The maximum membrane-plus-bending stress in the OC inner shell is:

$$S_{mb} = \frac{Mc}{I} = \frac{(50{,}228{,}342)(17.19)}{51{,}334} = 16{,}820 \text{ psi}$$

Similarly, the maximum stresses in the OC outer shell are:

$$S_m = \frac{Mc}{I} = \frac{(50{,}228{,}342)[20.565 - (½)(1.5)]}{51{,}334} = 19{,}388 \text{ psi}$$

$$S_{mb} = \frac{Mc}{I} = \frac{(50{,}205{,}300)(20.565)}{51{,}334} = 20{,}122 \text{ psi}$$

In addition, shear stress must be added in the calculation of the membrane stress intensities for the OC inner and outer shells. The shear stress is:

$$S_v = \frac{V}{A} = \frac{1{,}621{,}850}{292} = 5{,}554 \text{ psi}$$

Fabrication stresses applicable to HAC side drop analyses are identical to those used in the NCT side drop analyses (refer to Table 2.6-27 in Section 2.6.7.1, *Flat End Drop*). Fabrication stresses for the side drop analyses are given in Table 2.7-18.

Table 2.7-19, Table 2.7-20, and Table 2.7-21 present the corresponding margins of safety for the more critical OC inner shell. Zero internal pressure is used in order to maximize compressive stresses in the inner shell. Again, it is noted that the margins presented for the 70 ºF and 160 ºF cases are conservative since at these temperatures, *g*-loads will actually be less than the 81.2*g* considered herein.

(5) IV Stresses

The maximum membrane stress in the IV shell, for the load case selected in Paragraph (3), is:

$$S_m = \frac{Mc}{I} = \frac{(5{,}852{,}272)[16.00 - (½)(0.38)]}{4{,}718} = 19{,}611 \text{ psi}$$

The maximum membrane-plus-bending stress in the IV shell is:

$$S_{mb} = \frac{Mc}{I} = \frac{(5{,}852{,}272)(16.00)}{4{,}718} = 19{,}847 \text{ psi}$$

In addition, shear stress must be added in the calculation of the membrane stress intensity for the IV shell. The shear stress is:

$$S_v = \frac{V}{A} = \frac{354{,}050}{38} = 9{,}317 \text{ psi}$$

Table 2.7-22 presents stress and margin of safety results for the IV for the worst-case load combination selected in Paragraph (3).

(6) Discussion of Payload Canister Behavior in Side Drops

The maximum membrane stress in the payload canister shell, for the load case selected in Paragraph (3), is:

$$S_m = \frac{Mc}{I} = \frac{(2{,}192{,}706)[13.00 - (½)(0.25)]}{1{,}676} = 16{,}844 \text{ psi}$$

The maximum membrane-plus-bending stress in the payload canister shell is:

$$S_{mb} = \frac{Mc}{I} = \frac{(2{,}192{,}706)(13.00)}{1{,}676} = 17{,}008 \text{ psi}$$

In addition, shear stress must be added in the calculation of the membrane stress intensity for the payload canister shell. The shear stress is:

$$S_v = \frac{V}{A} = \frac{200{,}428}{20} = 10{,}021 \text{ psi}$$

Table 2.7-23 presents stress and margin of safety results for the canister shell for the load combination selected in Paragraph (3). Allowable stresses were conservatively determined for 200 ºF material temperature. Buckling is addressed in Appendix 2.10.5, *Buckling Design Criteria and Detailed Evaluation*.

(7) OC Lid Analysis

Since the clearance between the OC lid and sealing surface is less than the clearance between the bolt and bolt hole, the lid will displace laterally to bear against the sealing surface in the forging before lateral loading of the lid bolts occurs. Therefore, the following analysis addresses the stress resulting from lateral loading of the body ring forging by the lid.

In the most unlikely event that the lid displaces laterally to bear upon the body ring forging, lateral loads will be transferred by bearing. The following calculations demonstrate the adequacy of this load transfer mechanism.

The weight of the OC lid may be carried in bearing against the lid-end OC ring forging if sliding occurs at the lid-to-forging interface. The side drop acceleration of 81.2*g* is utilized in a Hertzian analysis to determine the bearing stress between the two cylinders. Because this analysis is sensitive to very small variations in the diametric gap between the cylinders, the worst-case tolerance stackup has been factored into the following calculation using Table 33, Case 2c, from Roark and Young[6], assuming the elastic modulus, E, and Poisson's ratio, μ, are equal for the mating materials:

$$S_b = 0.591\sqrt{\frac{PE}{LK_D}} = 8{,}006 \text{ psi}$$

where the OC lid weight with 81.2*g*, P = (1,667)(81.2) =135,360 pounds, the elastic modulus, E = 27.8(10)^6 psi at 160 ºF from Table 2.3-1 in Section 2.3, *Mechanical Properties of Materials*, the contact length, L = 0.664 inches (approximately), and the diametral stiffness, K_D, is:

$$K_D = \frac{D_1 D_2}{D_1 - D_2} = 30{,}886 \text{ in}$$

where the outer cylinder diameter, D_1 = 32.896 inches, and the inner cylinder diameter, D_2 = 32.861 inches.

[6] R. J. Roark, W. C. Young, *Formulas for Stress and Strain*, 5th Edition, McGraw-Hill, Inc., New York, NY, 1975.

From Table 2.7-1, the HAC allowable sealing surface bearing stress, S_a = 27,000 psi at 160 ºF for Type F304 stainless steel. Therefore, the margin of safety is:

$$MS = \frac{S_a}{S_b} - 1 = \frac{27{,}000}{8{,}006} - 1 = +2.37$$

The lip of the forging that supports the OC lid is loaded in shear by the lid. Conservatively assuming only one-half of the lip is effective in resisting the 81.2*g* load, the shear stress is:

$$S_v = \frac{V}{\frac{1}{2}\pi(R_o^2 - R_i^2)} = 1{,}131\,\text{psi}$$

where the weight of the lid is the shear load with 81.2*g*, V = (1,667)(81.2) = 135,360 pounds, the outside radius of the lip, R_o = 20.81 inches, and the inside radius of the lip, R_i = 18.89 inches.

From Table 2.7-1, the HAC allowable shear stress, S_a = 28,400 psi at 160 ºF for Type F304 stainlesss steel. Therefore, the margin of safety is:

$$MS = \frac{S_a}{S_v} - 1 = \frac{28{,}400}{1{,}131} - 1 = +24.1$$

(8) Welds Joining the OC Shells to the End Closure Plate

The worst-case shear load at the joints of the OC shells to the end closure plate is taken as the maximum shear load determined from Figure 2.7-14 at the package locations corresponding to the welded joints (0 inches and 120 inches). Therefore, the maximum shear load at the welded joints, V = 1,485,800 pounds.

Since the welds are full penetration bevel welds, the effective shear area for shells may be found by the following equation (i.e., conservatively use half the total weld area):

$$A_w = \frac{2\pi(R_i t_i + R_o t_o)}{2} = 145.8\,\text{in}^2$$

where the mean OC inner shell radius, R_i = 16.69 inches, the OC inner shell thickness, t_i = 1.00 inches, the mean OC outer shell radius, R_o = 19.81 inches, and the OC outer shell thickness, t_o = 1.50 inches.

The direct shear stress in the OC shells' welds is:

$$\tau_w = \frac{V}{A_w} = 10{,}191\,\text{psi}$$

Table 2.7-24 presents stress and margin of safety results for the OC shells' welds under worst-case load combinations.

(9) IV Lid Analysis

Since the clearance between the lid and sealing surface is less than the clearance between the bolt and bolt hole, the IV lid will displace laterally to bear against the sealing surface in the forging

before lateral loading of the bolts. Therefore, the following analysis addresses the stress resulting from lateral loading of the IV body ring forging by the IV lid.

In the most unlikely event that the lid displaces laterally to bear upon the body ring forging, lateral loads will be transferred by bearing. The following calculation demonstrates the adequacy of this load transfer mechanism.

The weight of the IV lid may be carried in bearing against the IV body ring forging if sliding occurs at the lid-to-forging interface.

This analysis accounts for only the uppermost race surface being in contact with the forging for bearing. As with Paragraph (7), the side drop acceleration of 81.2*g* is utilized in a Hertzian analysis to determine the bearing stress between two cylinders for the worst-case tolerance stackup using the following calculation using Table 33, Case 2c, from Roark and Young[6], assuming the elastic modulus, E, and Poisson's ratio, μ, are equal for the mating materials:

$$S_b = 0.591\sqrt{\frac{PE}{LK_D}} = 9{,}552 \text{ psi}$$

where the IV lid weight with 81.2*g*, P = (1,382)(81.2) = 112,218 pounds, the elastic modulus, $E = 27.8(10)^6$ psi at 160 ºF from Table 2.3-1 in Section 2.3, *Mechanical Properties of Materials*, the contact length, L = 0.32 inches (approximately), and the diametral stiffness, K_D, is:

$$K_D = \frac{D_1 D_2}{D_1 - D_2} = 37{,}321 \text{ in}$$

where the outer cylinder diameter, D_1 = 28.006 inches, and the inner cylinder diameter, D_2 = 27.985 inches.

From Table 2.7-1, the HAC allowable sealing surface bearing stress, S_a = 27,000 psi at 160 ºF for Type F304 stainless steel. Therefore, the bearing stress margin of safety is:

$$MS = \frac{S_a}{S_b} - 1 = \frac{27{,}000}{9{,}552} - 1 = +1.83$$

The lip of the forging that supports the IV lid is loaded in shear by the lid. Conservatively assuming only one-half of the lip is effective in resisting the 81.2*g* load, the shear stress is:

$$S_v = \frac{V}{\frac{1}{2}\pi(R_o^2 - R_i^2)} = 1{,}191 \text{ psi}$$

where the weight of the lid is the shear load with 81.2*g*, V = (1,382)(81.2) = 112,218 pounds, the outside radius of the lip, R_o = 16.00 inches, and the inside radius of the lip, R_i = 14.00 inches.

From Table 2.7-1, the HAC allowable shear stress, S_a = 28,400 psi at 160 ºF for Type F304 stainlesss steel. Therefore, the shear stress margin of safety is:

$$MS = \frac{S_a}{S_v} - 1 = \frac{28{,}400}{1{,}191} - 1 = +22.8$$

(10) Impact Limiter Deformations and Residual Clearances

Maximum impact limiter deformations and residual clearances due to NCT side drop are directly available from Appendix 2.10.3, *Drop Impact Evaluation Results*. Per Table 2.10.3-10 in Appendix 2.10.3, *Drop Impact Evaluation Results*, maximum crush of an impact limiter side is 11.52 inches for the 140 ºF foam stress case resulting in a minimum residual clearance for the main package body of 5.48 inches (based on a 16.00 inch nominal radial thickness). These deformations and residual clearances are of little consequence for the RH-TRU 72-B package.

2.7.2 Crush

Subpart F of 10 CFR 71[1] requires performing a dynamic crush test in accordance with the requirements of 10 CFR §71.73(c)(2)[1]. Since the RH-TRU 72-B package weight exceeds 1,100 pounds, the dynamic crush test is not required.

2.7.3 Puncture

Subpart F of 10 CFR 71[1] requires that a 40-inch free drop of the RH-TRU 72-B package onto the upper end of a solid, vertical, cylindrical, mild steel bar mounted on an essentially unyielding, horizontal surface be considered. The bar must have a 6-inch diameter, with the top horizontal and its edge rounded to a radius of not more than 0.25 inches. The package is to be oriented in a position for which maximum damage is expected and the length of the pin is to be such that maximum damage will occur.

2.7.3.1 Side Puncture

For impact occurring on the side of the RH-TRU 72-B package, the required OC outer shell thickness, t, for puncture integrity is determined using three independent equations as follows:

(1) Nelms' Equation[7]

$$t = \left(\frac{W}{S_u}\right)^{0.71} = 0.712 \text{ in}$$

where the weight of the package, W = 45,000 pounds, and the ultimate strength of Type 304 stainless steel, S_u = 72,600 psi at 160 ºF (Table 2.7-1). Therefore, given an OC outer shell thickness, t_o = 1.50 inches, the thickness-basis margin of safety resisting puncture is:

$$MS = \frac{t_o}{t} - 1 = \frac{1.50}{0.712} - 1 = +1.11$$

For purposes of comparison, utilize Nelms' equation to calculate the package weight, W_p, necessary to puncture a 1½-inch thick stainless steel shell:

[7] L. B. Shappert, *Package Designers Guide – A Guide for the Design, Fabrication, and Operation of Shipping Packages for Nuclear Applications*, ORNL-NSIC-68, Oak Ridge National Laboratory, Oak Ridge, Tennessee, February 1970.

$$W_p = S_u t^{\left(\frac{1}{0.71}\right)} = 128{,}515 \text{ pounds}$$

Therefore, the OC outer shell energy-basis margin of safety resisting puncture is:

$$MS = \frac{W_p}{W} - 1 = \frac{128{,}515}{45{,}000} - 1 = +1.86$$

(2) Sakamoto's Equation[8]

$$\frac{E}{S_u} = \left[0.0030 + (0.047)\left(\frac{t}{D}\right) + (0.002)\left(\frac{d}{D}\right) + (0.006)\left(\frac{r}{d}\right)\right]\left\{t^{[1.585-(0.11)r]}\right\}\left\{d^{[1.465+(0.077)r]}\right\}$$

where the puncture drop energy, E = W × h, the weight of the package, W = 45,000 pounds (20,412 kg = 20.412 metric tons), the drop height, h = 40 inches (1,016 mm), the ultimate strength of Type 304 stainless steel, S_u = 72,600 psi at 160 ºF per Table 2.7-1 (51.04 kg/mm), the OC outer shell outside diameter, D = 41.13 inches (1,044.7 mm), the puncture bar diameter, d = 6.0 inches (152.4 mm), and the puncture bar edge radius, r = 0.25 inches (6.35 mm). Substituting the known quantities results in the following equation:

$$\frac{(20.412)(1{,}016)}{51.04} = [0.003542 + (0.000045)t]\left\{t^{0.8865}\right\}\{18{,}426.5\}$$

Solving, the required OC outer shell thickness, t = 7.135 mm = 0.281 inches. Therefore, given an outer shell thickness, t_o = 1.50 inches, the thickness-basis OC outer shell margin of safety is:

$$MS = \frac{t_o}{t} - 1 = \frac{1.50}{0.281} - 1 = +4.34$$

For purposes of comparison, utilize Sakamoto's equation to calculate the package weight to puncture a 1½-inch (38.1 mm) thick shell:

$$W_p = \left(\frac{S_u}{h}\right)\left[0.0030 + (0.047)\left(\frac{t}{D}\right) + (0.002)\left(\frac{d}{D}\right) + (0.006)\left(\frac{r}{d}\right)\right]\left\{t^{[1.585-(0.11)r]}\right\}\left\{d^{[1.465+(0.077)r]}\right\}$$

Substituting the known quantities results in the following equation and solving, the package weight, W_p = 122.63 metric tons. Therefore, the OC outer shell energy-basis margin of safety is:

$$MS = \frac{W_p}{W} - 1 = \frac{122.63}{20.412} - 1 = +5.01$$

Because 10 CFR §71.73(c)(2)[1] specifies a puncture bar radius, r, of not more than 0.25 inches, a 0.0-inch radius is also considered. This assumption results in t = 0.552 inches and the OC outer shell thickness-basis margin of safety is:

[8] I. Sakamoto, K. Hinkino, A. Onodera, Y. Sakai, S. Maezawa, *An Experimental Study on Puncture Resistance of Spent Fuel Shipping Packages by Drop Impact Test*, 4th International Symposium on Packaging and Transportation of Radioactive Materials, Miami Beach, Florida, September 1984, pp. 262-276.

$$MS = \frac{t_o}{t} - 1 = \frac{1.50}{0.552} - 1 = +1.72$$

On an energy-basis, the OC outer shell margin of safety is +1.84.

(3) Shieh's Equation[9]

$$\frac{W}{S_u} = \frac{0.37\left[1 + \frac{6}{D} + \left(\frac{41}{D}\right)^2\right]e^{\left(\frac{t}{3}\right)}t^{1.68}}{1 + (0.1)t^{0.87}}$$

where the parameters (in inches) apply:

$$0.5 < t < D/30;\ \ 45 < D < 90;\ \ 2D < L < 3D$$

These conditions are not met for the RH-TRU 72-B package geometry under consideration, but are sufficiently close to warrant solving for required OC outer shell thickness, t. Substituting and solving for the OC outer shell thickness, t = 0.776 inches. Therefore, the OC outer shell thickness-basis margin of safety resisting puncture is:

$$MS = \frac{t_o}{t} - 1 = \frac{1.50}{0.776} - 1 = +0.93$$

For purposes of comparison, utilize Shieh's equation to calculate the package weight to puncture a 1½-inch thick OC outer shell:

$$W_p = \frac{(0.37)S_u\left[1 + \frac{6}{D} + \left(\frac{41}{D}\right)^2\right]e^{\left(\frac{t}{3}\right)}t^{1.68}}{1 + (0.1)t^{0.87}} = 163{,}933 \text{ pounds}$$

Therefore, the OC outer shell energy-basis margin of safety is:

$$MS = \frac{W_p}{W} - 1 = \frac{163{,}933}{45{,}000} - 1 = +2.64$$

(4) Conclusion

The lowest thickness-basis margin of safety using any of the three documented empirical equations is +0.93. On an energy-basis, the margin of safety is much larger.

2.7.3.2 Package Bending Due to Side Puncture

To determine the overall effect on the package, consider the puncture impact occurring at the center of length of the package. Applying a unit acceleration and conservatively ignoring the strength of the lead, the membrane stress induced in the OC inner shell by the bending moment is:

[9] R. C. Shieh, *Empirical Equations for Puncture Analysis of Lead-Shielded Spent Fuel Shipping Packages*, Transporation Branch, U.S. Nuclear Regulatory Commission, Washington, D.C.

$$S_{mi} = \frac{Mc}{I} = \frac{\left(\frac{w_C L^2}{8} + \frac{W_{IL} L}{2}\right) c_i}{I} = 289 \text{ psi}$$

where the package weight per unit length, less impact limiters, $w_C = W_C/L = 281.52$ lb/in, the package weight, less impact limiters, $W_C = 39{,}906$ pounds, the package length, L = 141.75 inches, the impact limiter weight, $W_{IL} = 2{,}547$ pounds, the mid-plane OC inner shell radius, $c_i = ½(R_{io} + R_{ii}) = 16.69$ inches, the OC inner shell outer radius, $R_{io} = 17.19$ inches, the OC inner shell inner radius, $R_{ii} = 16.19$ inches, and the OC inner and outer shell moment of inertia, I, is:

$$I = \left(\frac{\pi}{4}\right)\left[\left(R_{oo}^4 - R_{oi}^4\right) + \left(R_{io}^4 - R_{ii}^4\right)\right] = 51{,}334 \text{ in}^4$$

where the the OC outer shell outer radius, $R_{oo} = 20.565$ inches, the OC outer shell inner radius, $R_{oi} = 19.065$ inches, the OC inner shell outer radius, $R_{io} = 17.19$ inches, and the OC inner shell inner radius, $R_{ii} = 16.19$ inches.

Correspondingy, the membrane stress induced in the OC outer shell by the bending moment is:

$$S_{mo} = \frac{Mc}{I} = \frac{\left(\frac{w_C L^2}{8} + \frac{W_{IL} L}{2}\right) c_o}{I} = 343 \text{ psi}$$

where the mid-plane OC outer shell radius, $c_o = ½(R_{oo} + R_{oi}) = 19.815$ inches.

The impact acceleration can be estimated from the puncture bar cross-section area, A_P, and dynamic flow stress, σ_f, of the 6-inch diameter, mild steel puncture bar. Assuming a dynamic flow stress for the mild steel puncture bar is the mean of the yield and ultimate strengths for ASTM A36 carbon steel, $\sigma_f = ½(36{,}000 + 58{,}000) = 47{,}000$ psi, the acceleration, η, is:

$$\eta = \frac{P_f}{W} = 29.5g$$

where the puncture bar force, $P_f = \sigma_f \times A_P = 1{,}328{,}878$ pounds, the puncture bar cross cross-sectional area, $A_P = \pi(3.0)^2 = 28.274$ in^2, and the package weight, W = 45,000 pounds.

Thus, the OC inner shell membrane stress, $S_{mi} = (29.5)(289) = 8{,}526$ psi, and OC outer shell membrane stress, $S_{mo} = (29.5)(343) = 10{,}119$ psi.

Shear stress, τ, for the OC shells is determined by using an effective shear area equal to half the cross-sectional area, A, of the OC inner and outer shells, as follows:

$$\tau = \frac{V}{½A} = 4{,}546 \text{ psi}$$

where the maximum shear force, $V = ½W\eta = 663{,}750$ pounds, the package weight, W = 45,000 pounds, the acceleraton, $\eta = 29.5g$, the cross-sectional area, A, of the OC inner and outer shells is:

$$A = \pi\left[\left(R_{oo}^2 - R_{oi}^2\right) + \left(R_{io}^2 - R_{ii}^2\right)\right] = 292 \text{ in}^2$$

The two principal stresses in the OC inner shell on the side of the package opposite the point of puncture bar impact, σ_1 and σ_2, are:

$$\sigma_{1,2} = \frac{S_{mi}}{2} \pm \sqrt{\left(\frac{S_{mi}}{2}\right)^2 + \tau^2} = 10{,}495 \text{ psi}, \ -1{,}969 \text{ psi}$$

The corresponding OC inner shell stress intensity, SI, is:

$$SI = |\sigma_1 - \sigma_2| = 12{,}464 \text{ psi}$$

From Table 2.7-1, the HAC allowable primary membrane stress intensity, S_a = 48,000 psi at 160 ºF for Type 304 stainless steel. Therefore, the OC inner shell margin of safety is:

$$MS = \frac{S_a}{SI} - 1 = \frac{48{,}000}{12{,}464} - 1 = +2.85$$

The two principal stresses in the OC outer shell on the side of the package opposite the point of puncture bar impact, σ_1 and σ_2, are:

$$\sigma_{1,2} = \frac{S_{mi}}{2} \pm \sqrt{\left(\frac{S_{mi}}{2}\right)^2 + \tau^2} = 11{,}861 \text{ psi}, \ -1{,}742 \text{ psi}$$

The corresponding OC outer shell stress intensity, SI, is:

$$SI = |\sigma_1 - \sigma_2| = 13{,}604 \text{ psi}$$

From Table 2.7-1, the HAC allowable primary membrane stress intensity, S_a = 48,000 psi at 160 ºF for Type 304 stainless steel. Therefore, the OC outer shell margin of safety is:

$$MS = \frac{S_a}{SI} - 1 = \frac{48{,}000}{13{,}604} - 1 = +2.53$$

These are the maximum global stresses that arise from puncture bar impact on the package side. For impacts at locations other than the center of the package's side, a portion of the drop kinetic energy will be converted into rotational energy of the package, and the package stress levels will be correspondingly lower.

2.7.3.3 End Puncture

To evaluate the effects of puncture bar impact on the OC end closures, both closures will be analyzed. The top closure is a 6-inch thick bolted lid. For conservatism, it is analyzed as a simply supported circular plate using Table 24, Case 16, from Roark and Young[6]:

$$M_{max} = \left(\frac{W}{4\pi}\right)\left[(1+\mu)\ln\frac{a}{r_o'} + 1\right] = 369{,}998 \text{ in - lb/in}$$

where the center load, $W = W_P\eta = 1{,}327{,}500$ pounds, the package weight, $W_P = 45{,}000$ pounds, the puncture bar acceleration, $\eta = 29.5g$, Poisson's ratio, $\mu = 0.3$, the lid radius, a = 20.565 inches, and the effective load radius, $r_o' = 3.0$ inches.

For a lid thickness, t = 6.0 inches, the maximum lid bending stress is:

$$\sigma = \frac{6M_{max}}{t^2} = 61{,}666 \text{ psi}$$

Internal pressure acts in the opposite direction to relieve this bending stress, so zero internal pressure is assumed. From Table 2.7-1, the HAC allowable primary membrane-plus-bending stress intensity, $S_a = 67{,}700$ psi at 160 ºF for Type F304 stainless steel. Therefore, the OC lid bending stress margin of safety is:

$$MS = \frac{S_a}{\sigma} - 1 = \frac{67{,}700}{61{,}666} - 1 = +0.10$$

The 5-inch thick bottom closure plate is analyzed as a fixed-edge circular plate using Table 24, Case 17, from Roark and Young[6]:

$$M_{max} = \left(\frac{W}{4\pi}\right)\left[(1+\mu)\ln\frac{a}{r_o'}\right] = 264{,}359 \text{ in - lb/in}$$

For a bottom closure thickness, t = 5.0 inches, the maximum bottom closure bending stress is:

$$\sigma = \frac{6M_{max}}{t^2} = 63{,}446 \text{ psi}$$

From Table 2.7-1, the HAC allowable primary membrane-plus-bending stress intensity, S_a = 67,700 psi at 160 ºF for Type F304 stainless steel. Therefore, the OC bottom closure bending stress margin of safety is:

$$MS = \frac{S_a}{\sigma} - 1 = \frac{67{,}700}{63{,}446} - 1 = +0.07$$

Note that both stress values are conservative, since backing of the plates by the IV and payload caniser is neglected. For impacts other than at the center of the plates, part of the drop kinetic energy will be converted to rotational energy, and stress levels will be lower than shown. Therefore, the end closures are adequate for the puncture event.

2.7.3.4 Puncture on the Lifting Trunnions

A puncture bar impacting a lifting trunnion from the side will, at worst, fail the attachment weld, without compromising the integrity of the OV outer shell. Justification for this assumption can be found in Section 2.5.1.5, *Excessive Lifting Trunnion Loads*.

The effects of a puncture bar axially impacting a lifting trunnion will be no worse than a direct strike of the puncture bar onto the OC outer shell because the trunnion is mounted on a 6-inch diameter base that is welded to the outer shell. The puncture force acting through this base will

have an equivalent effect on the outer shell as the 6-inch diameter puncture bar itself. Since it has been shown that a puncture bar impact on the outer shell will not compromise the integrity of the outer shell (see Section 2.7.3.1, *Package Bending Due to Side Puncture*), puncture bar impact directly onto a lifting trunnion will likewise not detrimentally affect the package integrity. In fact, the effect will be less than that of a puncture bar impact on the outer shell since the lifting trunnions are removed from the center of gravity of the package and some of the drop's kinetic energy will be converted to rotational energy without imposing the full puncture load.

2.7.3.5 Puncture on the Center-Pivot Trunnions

To evaluate the effects of a puncture bar impact on the side of a center-pivot trunnion, reference is made to Section 2.5.2.4, *Center-Pivot Trunnion Attachment Welds*, where it is demonstrated that the weld attaching the trunnion to the trunnion base will always fail before the weld attaching the trunnion base to the OC outer shell. It may be assumed, therefore, that a puncture bar impact on the side of the center-pivot trunnion will have no worse effect than that of separating the trunnion from the trunnion mount, and the integrity of the OC outer shell will not be compromised. As with the lifting trunnions, the puncture bar load will be offset from the package center-of-gravity in this impact orientation; therefore, the full punch force is not developed on the trunnion.

A direct puncture bar impact onto the face of one of the center-pivot trunnions will impose a maximum load, $P = \sigma_f \times A_P = 1{,}328{,}878$ pounds, as determined in see Section 2.7.3.1, *Package Bending Due to Side Puncture*. The shear area of the trunnion mount weld, $A_w = 2(L_w + H_w) \times T_w = 138$ in^2, where the trunnion mount length, $L_w = 28$ inches, the trunnion mount height, $H_w = 18$ inches, and the weld thickness, $T_w = 1.5$ inches for a full penetration weld. The resulting shear stress, $\tau = P/A_w = 9{,}630$ psi.

From Table 2.7-1, the HAC allowable shear stress intensity, $S_a = 28{,}400$ psi at 160 ºF for Type F304 stainless steel. Therefore, the minimum weld margin of safety is:

$$MS = \frac{S_a}{\tau} - 1 = \frac{28{,}400}{9{,}630} - 1 = +1.95$$

2.7.3.6 Puncture Bar Impact on Containment Penetrations

The OC has two containment penetrations: the closure lid and the gas sampling port. The effects of a puncture impact on these structures are addressed in the following sections.

2.7.3.6.1 Puncture Bar Impact on the OC Closure Lid

As shown in Section 2.7.3.3, *End Puncture*, the stress in the OC closure lid due to a puncture impact in the center of the lid exceeds the yield point of the lid material at temperature. The stress, 61,666 psi, is determined by a conservative analysis technique, but since it is above the material's yield point, some plastic deformation can be expected. However, the following analysis shows that the ability of the lid's O-ring seals to remain leaktight is not affected by the resulting plastic deformation.

Since the containment seal is located on the inside of the lid, i.e., the side that goes into tension due to the inward deformation of the lid, compression of the seal is shown to increase slightly, thus improving its performance. The amount and direction of permanent deformation is determined with a nonlinear finite element analysis using ANSYS® Revision 5.4[10]. The closure lid, including the flange and two O-ring seal grooves, is modeled axisymmetrically, as shown in Figure 2.7-22. The closure lid thickness is 6 inches, and the outer diameter is 37.59 inches. PLANE42, two-dimensional structural solid elements are used. The model is loaded over a 3-inch radius, with a pressure based on the maximum load that can be sustained by the puncture bar. For ASTM A36 mild steel, the maximum load that can be applied, assuming no buckling of the puncture bar, is bounded by the flow stress in the material. The flow stress taken as the average of the yield and ultimate strengths of ASTM A36. Thus, the average stress is ½(36,000 + 58,000) = 47,000 psi, which for purposes of this analysis, is conservatively rounded up to 50,000 psi. The lid is supported beneath the flange at the OC inner radius. All of the load spreading effect of the impact limiter foam and 1/2-inch thick plate adjacent to the lid is conservatively ignored.

Nonlinear stress-strain material properties are taken the closure lid analysis of the NuPac 125-B cask[2], and summarized in Table 2.7-25 from Figure 2.3-1 in Section 2.3, *Mechanical Properties of Materials*. Although the temperature of the lid is bounded by 160 ºF, the material properties from the reference are for a conservatively higher temperature of 212 ºF. The modulus of elasticity is $27.7(10)^6$ psi, and the proportional limit is 20,500 psi. The input commands necessary to run the model are given in *Data Package for the RH-TRU 72-B Waste Shipping Package*[11].

Results are shown in Figure 2.7-23. One point on the containment O-ring seal groove, node 280, moves 0.0104 inches radially outward, consistent with the expected deformation under the applied loading. This movement equates to a small increase in containment O-ring seal compression. Therefore, containment is not affected by the puncture event.

2.7.3.6.2 Puncture at the OC Gas Sampling Port

The consequence of a puncture bar impact on the OC gas sampling port is not significant, as demonstrated below. For contact between the puncture bar and the head of the port closure bolt, the worst-case is for impact at an oblique angle. As shown in the following analysis, the puncture bar cannot penetrate deeply enough to contact the gas sampling port closure bolt head. Figure 2.7-24 shows a detail of the gas sampling port region with the impact limiter installed.

The following conservative assumptions are made in the analysis:

- The package is assumed to contact the puncture bar at an angle of 45º to the horizontal. This angle ensures the maximum initial penetration of the puncture bar into the sampling port opening. The sampling port is assumed to be oriented with respect to the package so it will fall a maximum distance before contacting the puncture bar (see Figure 2.7-25).
- The analysis conservatively ignores any energy absorbtion contributed by the crushed foam in the impact limiter.

[10] ANSYS®, Inc., Revision Release 5.4, Houston, PA.

[11] U.S. Department of Energy, *Data Package for the RH-TRU 72-B Waste Shipping Package*, Current Revision, U.S. Department of Energy, Carlsbad Field Office, Carlsbad, New Mexico.

- The analysis conservatively ignores any resistance to impact contributed by the 1/2-inch thick stainless steel plate on the inner surface of the impact limiter (adjacent to the OC lid) or the perpendicular stiffening ring (see Figure 2.7-24).
- Although the package center of gravity is not over the impact point, the analysis conservatively assumes that no energy is transformed into rotational energy.

The impact between the puncture bar and the package closure lid can be modeled as a steel plate being perforated by a missile. This analysis is described by Equation 2-7 in Section 2.2 of *Design of Structures for Missile Impact*[12]. The thickness of the perforation is calculated by:

$$T = \frac{\left(\tfrac{1}{2}MV_s^2\right)^{2/3}}{672D} = 1.36\,\text{in}$$

where the mass of the package, M = 45,000 pounds = 1,397.5 slugs, the velocity of the puncture bar relative to the package, $V = (2gh)^{1/2} = 22.27$ ft/s, the acceleration due to gravity, $g = 32.2$ ft/s^2, the total drop height, h = 92.4 inches = 7.7 feet (see Figure 2.7-25), and D is the effective diameter of the missile's projected area, calculated as follows. Because the puncture bar is making contact with an annular area, the effective diameter is the diameter of a circle that has an area, A, equal to the difference between the areas of the 6-inch diameter puncture bar and the 2.625-inch diameter opening as follows:

$$A = \left(\frac{\pi}{4}\right)\left[(6)^2 - (2.625)^2\right] = 22.86\,\text{in}^2$$

Therefore, the effective puncture bar diameter is:

$$D = \sqrt{\left(\frac{4}{\pi}\right)A} = 5.40\,\text{in}$$

The geometric interface between the obliquely oriented puncture bar and the cylindrical test port opening must also be considered. Figure 2.7-26 shows that at the time of initial contact between the puncture bar and the lid, the puncture bar has already slightly penetrated the upper plane of the lid. The distance of penetration can be solved geometrically by considering the view shown in Figure 2.7-26. The end of the bar has an elliptical profile (in the 45º oblique plane) equal to

$$\frac{x^2}{a^2} + \frac{y^2}{b^2} = 1$$

where the ellipse's major axis, a = 3 inches, and the ellipse's minor axis, b = 3(sin 45º) = 2.12 inches for an oblique bar angle of 45º. Given that the puncture bar contacts the opening at the value of x = ½(2.625) inches, y = 1.91 inches.

$$y = b\sqrt{1 - \frac{x^2}{a^2}} = 1.91\,\text{in}$$

[12] Bechtel Power Corporation, *Design of Structures for Missile Impact*, BC-TOP-9-A, Rev. 2, September 1974.

The depth of penetration, d, at incipient contact, is:

$$d = b - y = 2.12 - 1.91 = 0.21 \text{ in}$$

Therefore, the maximum penetration is the sum of T and d:

$$p_{max} = T + d = 1.36 + 0.21 = 1.57 \text{ in}$$

As shown in Figure 2.7-26, the distance from the top of the port closure bolt to the top of the closure lid, e = 1.64 inches. Therefore, the margin of safety is:

$$MS = \frac{e}{p_{max}} - 1 = \frac{1.64}{1.57} - 1 = +0.04$$

The positive margin demonstrates that the puncture bar cannot contact the gas sampling port closure bolt despite the very conservative assumptions incorporated in the analysis.

The most conservative assumption is the neglect of the substantial steel structures in the adjacent impact limiter, i.e., the 1/2-inch thick inner plate and vertical stiffening ring. These structures also make extrusion of compressed foam into the port opening impossible. Finally, note that even if contact with the closure port bolt is made, the bolt seal is a bore-type O-ring seal. Since any impact-related motion of the bolt would be along the bolt axis, the ability of the O-ring seal to seal would not be affected.

2.7.4 Thermal

The HAC fire transient, presented in Section 3.5, *Hypothetical Accident Thermal Evaluation*, provides maximum temperatures and pressures.

2.7.4.1 Summary of Pressures and Temperatures

The maximum HAC fire temperatures for the various package components are presented in Table 2.7-27. Maximum internal pressure resulting from the fire transient is 178.8 psig for any package component, from Section 3.5.4, *Maximum Internal Pressure*. The stresses resulting from the HAC thermal pressure are addressed in Section 2.7.4.3, *Pressure Stress Calculations*.

2.7.4.2 Differential Thermal Expansion

Differential thermal expansions due to the HAC fire are of little consequence for the RH-TRU 72-B package. All stresses resulting from differential expansions can be classified as secondary, displacement limited stresses. As limits on secondary stresses do not apply for HAC, per Table 2.1-1 in Section 2.1.2.1.1, *Containment Structures*, differential thermal expansions in themselves do not compromise the integrity of the package.

Through-wall (and through-thickness) thermal gradients also result in secondary stresses and again are of little consequence for the package. To address the requirement specified in

Paragraph C.7 of NRC Regulatory Guide 7.6[13], and discussed in Section 2.1.2.2.2.3, *Extreme Total Stress Intensity Range*, a finite element analysis was performed to determine maximum stresses associated with the HAC fire transient event. Details of this analysis are as follows.

The ANSYS® finite element program was used to determine thermal stresses. The analysis utilized an axisymmetric finite element model, with isoparametric solids representing the OC inner and outer shells, upper forging, lid, and base. The package's lead shielding is poured into the cavity between the OC inner and outer shells at an approximate temperature of 620 ºF. As the lead cools and solidifies, it will shrink both radially and longitudinally. This shrinkage produces gaps between the lead and the OC outer and inner shells, forging, and base. During the HAC fire event, the lead will absorb heat and expand, but will not close the gaps until the 620 ºF solidification temperature is reached. Therefore, thermal expansion of the lead will not contribute to the stress state in the OC inner and outer shells. Consequently, the lead is not included in evaluation of the OC for the HAC fire event of 10 CFR §71.73(c)(4)[1].

Critical temperatures from the thermal analysis performed in Chapter 3.0, *Thermal Evaluation*, are used as boundary temperatures for this thermal stress model. The thermal case utilized is that of the damaged package (i.e., side drop and puncture bar damage) in the HAC fire event. Thus, the model considers the local hot spots near the trunnions and the hot spot near the sealing region due to the puncture bar hole. An ANSYS® thermal analysis is performed with these boundary temperatures. This thermal analysis determined the remaining node temperatures as initial conditions for the ANSYS® structural analysis used to determine thermal stresses.

Time-history results of the HAC fire transient analysis (see Section 3.5, *Hypothetical Accident Thermal Evaluation*) indicate the maximum component temperatures and gradients can be expected at about one-half hour into the fire event (when impinging flame terminates). Accordingly, temperatures at this time step are taken from the appropriate tables in Section 3.5, *Hypothetical Accident Thermal Evaluation*, and applied to the proper nodal locations of the finite element model. Temperatures at finite element model nodes other than those directly transferable from the thermal model are interpolated from known temperatures using the ANSYS® thermal routine.

A uniform model temperature of 70 ºF is input as the initial stress-free condition. Temperature dependent material properties are input in tabular form to assure utilization of correct properties at each nodal temperature. The maximum package stress intensity, SI = 73,609 psi at node 4652, occurs in the OC outer shell at the trunnion locations.

2.7.4.3 Pressure Stress Calculations

Stresses from a unit internal pressure are calculated at 10 points on the containment vessels, as discussed in Section 2.6.1.3.1, *Stresses Due To Unit Pressures*, and shown in Figure 2.6-1. Table 2.7-26 summarizes the stresses at these points under a very conservative 300 psig internal pressure, as calculated from the unit pressure stresses in Table 2.6-4 and Table 2.6-5 in Section 2.6.1.3.2, *Stresses Due to Maximum Pressures*.

---

[13] U. S. Nuclear Regulatory Commission, Regulatory Guide 7.6, *Design Criteria for the Structural Analysis of Shipping Package Containment Vessels*, Revision 1, March 1978.

[15] American Society of Mechanical Engineers (ASME) Boiler and Pressure Vessel Code, Section III, *Rules for Construction of Nuclear Power Plant Components*, Division 1, Subsection NB and Appendices, 1986 Edition.

The radius transition at location P6 is analyzed using an ANSYS® finite element model. Stresses resulting in the radius transition due to a 1.0-psi internal pressure are reported in Section 2.6.1.3.1, *Stresses Due To Unit Pressures*. The bending stress at location P6, between the flat head and the cylindrical shell, is a secondary stress per NRC Regulatory Guide 7.6[13], and need not be considered for this Level D Accident Pressure Condition. The maximum local axial and hoop membrane stresses at location P6 are 6,501 psi and -11,322 psi, respectively, for 300 psig internal pressure. The maximum local membrane stress intensity at 300 psig is 6,501 – (-11,322) = 17,823 psi.

The stress in the OC lid bolts, S_B, due to a 300 psig internal pressure, P, is:

$$S_B = \frac{PA_P}{NA_t} = 14{,}619 \text{ psi}$$

where the area the internal pressure acts upon, $A_P = (\pi/4)D^2 = 849.92$ in^2, the sealing diameter, D = 32.896 inches, the number of bolts, N = 18, and the tensile stress area of a 1¼-7UNC bolt, $A_t = 0.969$ in^2.

The stress in the IV lid bolts, S_B, due to a 300 psig internal pressure, P, is:

$$S_B = \frac{PA_P}{NA_t} = 56{,}759 \text{ psi}$$

where the area the internal pressure acts upon, $A_P = (\pi/4)D^2 = 616.02$ in^2, the sealing diameter, D = 28.006 inches, the number of bolts, N = 8, and the tensile stress area is the shank area for the modified 7/8-9UNC bolt, $A_t = 0.407$ in^2.

Stress calculations for differential thermal expansion are presented in Section 2.7.4.2, *Differential Thermal Expansion*.

2.7.4.4 Comparison with Allowable Stresses

The margins of safety for stresses due to HAC thermal pressure, using NRC Regulatory Guide 7.6[13] HAC allowables, are presented in Table 2.7-27. Allowable stress intensities are conservatively based on a HAC temperature of 300 ºF for the IV and 500 ºF for the OC, except where noted. Furthermore, the allowable stress intensities for locations P1 – P6 (i.e., shell regions) are based on Type 304 stainless steel, and the allowable stress intensities for locations P7 – P10 (i.e., end closures) are conservatively based on Type F304 stainless steel. Calculated stress intensities are presented in Section 2.7.4.3, *Pressure Stress Calculations*.

The maximum stress in the OC lid bolts is 14,619 psi. The HAC allowable stress for ASTM A320, Grade L43, bolts, S_a = 88,500 psi at 500 ºF ($S_a = S_y$ per Table 2.1-1 in Section 2.1.2.1.1, *Containment Structures*, where S_y is taken from Table 2.3-1 in Section 2.3, *Mechanical Properties of Materials*). Therefore, the OC lid bolt margin of safety is:

$$MS = \frac{S_a}{S_B} - 1 = \frac{88{,}500}{14{,}619} - 1 = +5.05$$

The maximum stress in the IV lid bolts is 56,759 psi. The HAC allowable stress for ASTM A320, Grade L43, bolts, S_a = 95,700 psi at 300 ºF ($S_a = S_y$ per Table 2.1-1 in Section 2.1.2.1.1, *Containment Structures*, where S_y is taken from Table 2.3-1 in Section 2.3, *Mechanical Properties of Materials*). Therefore, the IV lid bolt margin of safety is:

$$MS = \frac{S_a}{S_B} - 1 = \frac{95{,}700}{56{,}759} - 1 = +0.69$$

From Section 2.7.4.2, *Differential Thermal Expansion*, the maximum stress intensity is 73,609 psi. To conservatively evaluate the stress state in relation to the requirements from Paragraph C.7 of NRC Regulatory Guide 7.6[13], the worst-case thermal/secondary stress intensity is used. Note that the stress intensity, SI = 73,609 psi, occurs in the OC outer shell, not the containment structure. It has also been demonstrated elsewhere herein that the maximum combined primary membrane-plus-bending stress intensity (due to fabrication stress, dead weight, internal pressure, and HAC drop loading) is in conformance with NRC Regulatory Guide 7.6[13]. Therefore, it is permissible and conservative to assume that the maximum allowable value for the primary stresses, S_u, actually develops within the structure.

Assuming an average through-wall temperature of 600 ºF, the ultimate strength of Type 304 stainless steel plate used for the OC shells, S_u = 63,500 psi per Table 2.3-1 in Section 2.3, *Mechanical Properties of Materials*. Adding this stress to the worst-case thermal stress intensity, the total primary-plus-secondary stress intensity becomes 63,500 + 73,609 = 137,109 psi. The maximum possible stress range will be twice this value, or 2 × 137,109 = 274,218 psi. This value is very conservative because it addresses the peak thermal stresses at the trunnions and combines it with the assumed maximum stress of S_u, and because it assumes the maximum non-thermal stress will exist at the same location as the HAC thermal stress. It could be shown that the actual stress range is significantly lower than this value, including structural discontinuity effects. However, for this calculation, the maximum stress range of 274,218 psi is used. The appropriate alternating stress will be one-half this value, S_{alt} = ½(274,218) = 137,109 psi. As required by NRC Regulatory Guide 7.6[13], the maximum alternating stress intensity (S_{alt}) should be modified by the ratio of the elastic modulus for which the design fatigue curves are based, $E_{70} = 28.3(10)^6$ psi, and the elastic modulus used in the analysis, $E_{600} = 25.3(10)^6$ psi, per Table 2.3-1 in Section 2.3, *Mechanical Properties of Materials* Therefore, the adjusted alternating stress is:

$$S_{alt} \text{ at } 600\,°F = S_{alt}\left(\frac{E_{70}}{E_{600}}\right) = (137{,}109)\left(\frac{28.3(10)^6}{25.3(10)^6}\right) = 153{,}367 \text{ psi}$$

NRC Regulatory Guide 7.6[13] requires that the maximum stress intensity range be less than twice the adjusted value of the allowable alternating stress intensity, S_a, at 10 cycles from the appropriate design fatigue curve. For Type 304 stainless steel, S_a = 708,000 psi per Figure 2.7-27 (Figure I-9.2.1 from Appendix I of the ASME Code[15]). The maximum adjusted stress intensity range is twice the adjusted alternating stress, S_{max} = 2 × 153,367 = 306,734 psi. Therefore, the margin of safety is:

$$MS = \frac{S_a}{S_{max}} - 1 = \frac{708{,}000}{306{,}734} - 1 = +1.31$$

Recognizing the grossly conservative assumptions that are utilized in the preceding evaluation (e.g., use of allowable primary stresses rather than actual stresses, assuming fully reversing primary and secondary stress states to determine ranges, assuming worst-case primary stresses occur simultaneously with the worst-case HAC fire transient stresses, etc.), it is apparent that the actual margin of safety will be significantly larger than +1.31. Regardless, the requirement of Paragraph C.7 of NRC Regulatory Guide 7.6[13] is met.

2.7.5 Immersion – Fissile Material

The criticality evaluation presented in Chapter 6.0, *Criticality Evaluation*, considers the effect of water in-leakage. Thus, the requirement of 10 CFR §71.73(c)(5)[1] is met.

2.7.6 Immersion – All Packages

The effect of a 21 psig external pressure due to immersion in 50 feet of water, as required by 10 CFR §71.73(c)(6)[1], is of negligible consequence for the RH-TRU 72-B package.

2.7.7 Deep Water Immersion Test

A 290 psig external water pressure, for Type B packages containing more than 10^5 A_2, as required by 10 CFR §71.61[1], results in shell and end closure stresses less than those evaluated in Section 2.7.4, *Thermal*, for 300 psig internal pressure. Therefore, reported margins of safety will be greater.

As shown in the following sections, buckling of the OC inner (containment) shell is not of consequence due to the effect of a 290 psig external pressure. The cylindrical portion of the OC is evaluated using ASME Boiler and Pressure Vessel Code Case N-284[16]. Consistent with Regulatory Guide 7.6[13] philosophy, a factor of safety of 1.34 is applied for HAC buckling evaluations per ASME Code Case N-284[16], corresponding to ASME Code, Service Level D conditions.

Buckling analysis geometry parameters are summarized in Table 2.7-28, and loading parameters are summarized in Table 2.7-29. The cylindrical shell buckling analysis utilizes an OC temperature of 70 ºF. The stresses are determined using an external pressure of 290 psig. The hoop stress, σ_θ, and axial stress, σ_ϕ, are found from:

$$\sigma_\theta = \frac{Pr}{t} \qquad \sigma_\phi = \frac{Pr}{2t}$$

where P is the applied external pressure of 290 psi, r is the mean radius, and t is the cylindrical shell thickness. Conservatively included also with the pressure stresses for the OC inner shell are the hoop and axial fabrication stresses, σ_h = 1,413 psi (at 70 ºF), and σ_a = 1,963 psi, respectively, identified in Appendix 2.10.8, *Fabrication Stresses Due to Lead Pour*.

[16] American Society of Mechanical Engineers (ASME) Boiler and Pressure Vessel Code, Section III, *Rules for Construction of Nuclear Power Plant Components*, Division 1, Class MC, Code Case N-284, *Metal Containment Shell Buckling Design Methods*, August 25, 1980.

Buckling analysis methodology is addressed in Appendix 2.10.5, *Buckling Design Criteria and Detailed Evaluation*. As shown in Table 2.7-30, since all interaction check parameters are less than 1.0, as required, the design criteria are satisfied.

Thus, the effect of a 290 psig external water pressure, for Type B packages containing more than 10^5 A_2, as required by 10 CFR §71.61[1], is of negligible consequence for the RH-TRU 72-B package.

2.7.8 Summary of Damage

The analyses presented in the preceding sections demonstrate that the HAC test sequence will not result in any significant structural damage to the RH-TRU 72-B package. Nearly all permanent damage occurs in the external impact limiters, as desired. Minor damage can occur to packaging components, as summarized in the remainder of this section.

For the 30-foot free drop event, a conservatively maximum bounding lead slump of 0.513 inches is estimated, as detailed in Paragraph (9) of Section 2.7.1.1, *Flat End Drop*. However, as demonstrated in testing of the NuPac 125-B cask[2], no measurable lead slump would actually be expected to occur in the RH-TRU 72-B package as a result of a flat end drop. For the 40-inch drop onto a 6-inch diameter puncture bar, occurring on the side of the package at midlength, localized package damage can occur at the impact point. However, overall bending response of the package remains elastic. Additionally, the OC outer shell will not be perforated, and no melting of the lead shielding occurs in the ensuing HAC fire event.

Localized puncture damage occurs in the form of a reduction in lead thickness adjacent to the point of impact of the puncture bar. Puncture drop results from the NuPac 125-B quarter-scale testing program[2] are analyzed to provide a conservative estimate of similar damage that could be expected for the RH-TRU 72-B package. The 40-inch side drop on the puncture bar caused, at most, a 35% localized reduction in the thickness of the lead shielding on the NuPac 125-B cask[2]. This estimate is conservative for the RH-TRU 72-B package because it is significantly lower in weight than the NuPac 125-B cask[2], and puncture-induced deformations are expected to be less.

These permanent deformations are of little consequence for the RH-TRU 72-B package, as they represent only minor changes in package geometry. In particular, damage is not sufficient to compromise “leaktightness” of the IV or OC containment boundaries. Lead deformation is only of concern relative to shielding. The worst-case puncture damage is therefore addressed in the shielding evaluation in Chapter 5.0, *Shielding Evaluation*. For these reasons, the integrity of the package is not considered to be compromised by the HAC test sequence set forth in 10 CFR 71[1].

Table 2.7-1 – Summary of HAC Material Properties for Analysis

Material Property	Material Property Value (psi)					Reference
	-40 °F	-20 °F	70 °F	160 °F	200 °F	
ASTM A240/A276, Type 304 Stainless Steel						
Elastic Modulus, E ($\times 10^6$)	28.9	28.8	28.3	27.8	27.6	Table 2.3-1
Design Stress Intensity, S_m	20,000	20,000	20,000	20,000	20,000	
Yield Strength, S_y	30,000	30,000	30,000	27,000	25,000	
Ultimate Strength, S_u	75,000	75,000	75,000	72,600	71,000	
Stress Intensity Allowable for Containment Structures (Table 2.1-1)						
Primary Membrane	48,000	48,000	48,000	48,000	48,000	
Primary Membrane-Plus-Bending	72,000	72,000	72,000	72,000	71,000	
Pure Shear	31,500	31,500	31,500	30,500	29,800	
Bearing (Sealing Surfaces)	30,000	30,000	30,000	27,000	25,000	
ASTM A182/SA182, Type F304, Stainless Steel						
Elastic Modulus, E ($\times 10^6$)	28.9	28.8	28.3	27.8	27.6	Table 2.3-1
Design Stress Intensity, S_m	20,000	20,000	20,000	20,000	20,000	
Yield Strength, S_y	30,000	30,000	30,000	27,000	25,000	
Ultimate Strength, S_u	70,000	70,000	70,000	67,700	66,200	
Stress Intensity Allowable for Containment Structures (Table 2.1-1)						
Primary Membrane	48,000	48,000	48,000	47,400	46,300	
Primary Membrane-Plus-Bending	70,000	70,000	70,000	67,700	66,200	
Pure Shear	29,400	29,400	29,400	28,400	27,800	
Bearing (Sealing Surfaces)	30,000	30,000	30,000	27,000	25,000	
ASTM A516, Grade 55, Carbon Steel						
Elastic Modulus, E ($\times 10^6$)	29.5	29.5	29.5	29.3	28.8	Table 2.3-1
Design Stress Intensity, S_m	18,300	18,300	18,300	18,300	18,300	
Yield Strength, S_y	30,000	30,000	30,000	28,400	27,300	
Ultimate Strength, S_u	55,000	55,000	55,000	55,000	55,000	
Stress Intensity Allowable for Non-Containment Structures (Table 2.1-2)						
Primary Membrane	38,500	38,500	38,500	38,500	38,500	
Primary Membrane-Plus-Bending	55,000	55,000	55,000	55,000	55,000	
Pure Shear	23,100	23,100	23,100	23,100	23,100	
ASTM A320, Grade L43, Alloy Steel						
Elastic Modulus, E ($\times 10^6$)	27.8	27.8	27.8	27.3	27.1	Table 2.3-1
Design Stress Intensity, S_m	35,000	35,000	35,000	33,800	33,000	
Yield Strength, S_y	105,000	105,000	105,000	101,400	99,000	
Ultimate Strength, S_u	125,000	125,000	125,000	125,000	125,000	
Stress Intensity Allowable for Containment Fasteners (Table 2.1-1)						
Primary Membrane	105,000	105,000	105,000	101,400	99,000	
Primary Membrane-Plus-Bending	105,000	105,000	105,000	101,400	99,000	
Stress Intensity Allowable for Non-Containment Fasteners (Table 2.1-2)						
Primary Membrane	105,000	105,000	105,000	101,400	99,000	
Primary Membrane-Plus-Bending	125,000	125,000	125,000	125,000	125,000	

Table 2.7-2 – Fabrication Induced OC Inner Shell Hoop Stress, Interface Pressure, and Axial Load That Can Be Supported

Temperature (ºF)	Hoop Stress (psi)	Interface Pressure (psi)	Coefficient of Friction	Axial Load (lb)
160	-1,038	62.2	0.5	414,842
			1.0	829,685
70	-1,413	84.7	0.5	564,906
			1.0	1,129,812
-20	-1,821	109.1	0.5	727,641
			1.0	1,455,283

Table 2.7-3 – OC Shell Stresses with Maximum End Drop Fab Condition

Temperature (ºF)	Inner Shell Stresses (psi)		Outer Shell Stresses (psi)	
	Hoop σ_t	Axial σ_z	Hoop σ_t	Axial σ_z
160	-1,038	-12,801	0	-6,180
70	-1,413	-12,801	0	-6,180
-20	-1,821	-12,801	0	-6,180

Table 2.7-4 – HAC Fab & End Drop, OC Inner Shell with 89.7*g* at -20 ºF

Evaluation Parameters	
Loading Condition:	HAC Flat End Drop, -20 ºF Foam
Structural Material:	ASTM A240, Type 304, Stainless Steel
Stress Condition:	Primary Membrane
Structural Criterion:	Containment Boundary
Stress Allowable (from Table 2.1-1):	$2.4S_m$
Material Temperature:	-20 ºF
Allowable Stress, S_a:	48,000 psi

Load Condition	Stress Components (psi)				Reference Section
	Radial σ_r	Hoop σ_t	Axial σ_z	Shear τ_{rz}	
Fabrication and End Drop	0	-1,821	-12,801	0	2.7.1.1(6)
Direct Stress Summation	0	-1,821	-12,801	0	—
Principal Stresses	0	-1,821	-12,801	—	—
Stress Differences	12,801	10,980	1,821	—	—
Maximum Stress Intensity (SI)	12,801	—	—	—	—
Allowable Stress Intensity (S_a)	48,000	—	—	—	—
Margin of Safety ($MS = S_a/SI - 1$)	+2.75	—	—	—	—

Table 2.7-5 – HAC Fab & End Drop, OC Inner Shell with 89.7*g* at 70 ºF

Evaluation Parameters	
Loading Condition:	HAC Flat End Drop, -20 ºF Foam
Structural Material:	ASTM A240, Type 304, Stainless Steel
Stress Condition:	Primary Membrane
Structural Criterion:	Containment Boundary
Stress Allowable (from Table 2.1-1):	$2.4S_m$
Material Temperature:	70 ºF
Allowable Stress, S_a:	48,000 psi

Load Condition	Stress Components (psi)				Reference Section
	Radial σ_r	Hoop σ_t	Axial σ_z	Shear τ_{rz}	
Fabrication and End Drop	0	-1,413	-12,801	0	2.7.1.1(6)
Direct Stress Summation	0	-1,413	-12,801	0	—
Principal Stresses	0	-1,413	-12,801	—	—
Stress Differences	12,801	11,388	1,413	—	—
Maximum Stress Intensity (SI)	12,801	—	—	—	—
Allowable Stress Intensity (S_a)	48,000	—	—	—	—
Margin of Safety (MS = S_a/SI – 1)	+2.75	—	—	—	—

Table 2.7-6 – HAC Fab & End Drop, OC Inner Shell with 89.7*g* at 160 ºF

Evaluation Parameters	
Loading Condition:	HAC Flat End Drop, -20 ºF Foam
Structural Material:	ASTM A240, Type 304, Stainless Steel
Stress Condition:	Primary Membrane
Structural Criterion:	Containment Boundary
Stress Allowable (from Table 2.1-1):	$2.4S_m$
Material Temperature:	160 ºF
Allowable Stress, S_a:	48,000 psi

Load Condition	Stress Components (psi)				Reference Section
	Radial σ_r	Hoop σ_t	Axial σ_z	Shear τ_{rz}	
Fabrication and End Drop	0	-1,038	-12,801	0	2.7.1.1(6)
Direct Stress Summation	0	-1,038	-12,801	0	—
Principal Stresses	0	-1,038	-12,801	—	—
Stress Differences	12,801	11,763	1,038	—	—
Maximum Stress Intensity (SI)	12,801	—	—	—	—
Allowable Stress Intensity (S_a)	48,000	—	—	—	—
Margin of Safety (MS = S_a/SI – 1)	+2.75	—	—	—	—

Table 2.7-7 – HAC End Drop, Lead Pressure and Hoop Stress Summary

Temperature (ºF)	σ_y (psi)	d (in)	p_{max} (psi)	$\sigma_t = p_{max}R/t$ (psi)	
				Inner Shell	Outer Shell
160	~600	16.31	157.8	-2,633	2,085
70	~800	21.75	166.2	-2,774	2,197
-20	~1,000	27.19	175.6	-2,931	2,321

Table 2.7-8 – HAC End Drop, OC Shell Stresses with Zero Fabrication Condition with 89.7*g* Acceleration

Temperature (ºF)	Inner Shell Stresses (psi)		Outer Shell Stresses (psi)	
	Hoop σ_t	Axial σ_z	Hoop σ_t	Axial σ_z
160	-2,633	-10,530	2,085	-7,493
70	-2,774	-10,530	2,197	-7,493
-20	-2,931	-10,530	2,321	-7,493

Table 2.7-9 – HAC End Drop, OC Inner Shell with 89.7*g* at -20 ºF

Evaluation Parameters	
Loading Condition:	HAC Flat End Drop, -20 ºF Foam
Structural Material:	ASTM A240, Type 304, Stainless Steel
Stress Condition:	Primary Membrane
Structural Criterion:	Containment Boundary
Stress Allowable (from Table 2.1-1):	$2.4S_m$
Material Temperature:	-20 ºF
Allowable Stress, S_a:	48,000 psi

Load Condition	Stress Components (psi)				Reference Section
	Radial σ_r	Hoop σ_t	Axial σ_z	Shear τ_{rz}	
Fabrication and End Drop	0	-2,931	-10,530	0	2.7.1.1(7)
Direct Stress Summation	0	-2,931	-10,530	0	—
Principal Stresses	0	-2,931	-10,530	—	—
Stress Differences	10,530	7,599	2,931	—	—
Maximum Stress Intensity (SI)	10,530	—	—	—	—
Allowable Stress Intensity (S_a)	48,000	—	—	—	—
Margin of Safety ($MS = S_a/SI - 1$)	+3.56	—	—	—	—

Table 2.7-10 – HAC End Drop, OC Inner Shell with 89.7*g* at 70 ºF

Evaluation Parameters	
Loading Condition:	HAC Flat End Drop, -20 ºF Foam
Structural Material:	ASTM A240, Type 304, Stainless Steel
Stress Condition:	Primary Membrane
Structural Criterion:	Containment Boundary
Stress Allowable (from Table 2.1-1):	$2.4S_m$
Material Temperature:	70 ºF
Allowable Stress, S_a:	48,000 psi

Load Condition	Stress Components (psi)				Reference Section
	Radial σ_r	Hoop σ_t	Axial σ_z	Shear τ_{rz}	
End Drop	0	-2,774	-10,530	0	2.7.1.1(7)
Direct Stress Summation	0	-2,774	-10,530	0	—
Principal Stresses	0	-2,774	-10,530	—	—
Stress Differences	10,530	7,756	2,774	—	—
Maximum Stress Intensity (SI)	10,530	—	—	—	—
Allowable Stress Intensity (S_a)	48,000	—	—	—	—
Margin of Safety (MS = S_a/SI – 1)	+3.56	—	—	—	—

Table 2.7-11 – HAC End Drop, OC Inner Shell with 89.7*g* at 160 ºF

Evaluation Parameters	
Loading Condition:	HAC Flat End Drop, -20 ºF Foam
Structural Material:	ASTM A240, Type 304, Stainless Steel
Stress Condition:	Primary Membrane
Structural Criterion:	Containment Boundary
Stress Allowable (from Table 2.1-1):	$2.4S_m$
Material Temperature:	160 ºF
Allowable Stress, S_a:	48,000 psi

Load Condition	Stress Components (psi)				Reference Section
	Radial σ_r	Hoop σ_t	Axial σ_z	Shear τ_{rz}	
End Drop	0	-2,633	-10,530	0	2.7.1.1(7)
Direct Stress Summation	0	-2,633	-10,530	0	—
Principal Stresses	0	-2,633	-10,530	—	—
Stress Differences	10,530	7,897	2,633	—	—
Maximum Stress Intensity (SI)	10,530	—	—	—	—
Allowable Stress Intensity (S_a)	48,000	—	—	—	—
Margin of Safety (MS = S_a/SI – 1)	+3.56	—	—	—	—

Table 2.7-12 – OC Shell Stresses with Max Oblique Drop Fab Condition

Temperature (ºF)	Inner Shell Stresses (psi)		Outer Shell Stresses (psi)	
	Hoop σ_t	Axial σ_z	Hoop σ_t	Axial σ_z
160	-1,038	-6,866	0	-3,315
70	-1,413	-6,866	0	-3,315
-20	-1,821	-6,866	0	-3,315

Table 2.7-13 – HAC Fab & Oblique Drop, OC Inner Shell with 48.1*g* at -20 ºF

Evaluation Parameters	
Loading Condition:	HAC 5º Oblique Drop, -20 ºF Foam
Structural Material:	ASTM A240, Type 304, Stainless Steel
Stress Condition:	Primary Membrane
Structural Criterion:	Containment Boundary
Stress Allowable (from Table 2.1-1):	$2.4S_m$
Material Temperature:	-20 ºF
Allowable Stress, S_a:	48,000 psi

Load Condition	Stress Components (psi)				Reference Section
	Radial σ_r	Hoop σ_t	Axial σ_z	Shear τ_{rz}	
Fabrication	0	-1,821	-6,866	0	2.7.1.2(4)
Oblique Drop	0	0	-17,049	4,796	2.7.1.2(4)
Direct Stress Summation	0	-1,821	-23,915	4,796	—
Principal Stresses	926	-1,821	-24,841	—	—
Stress Differences	25,767	23,020	2,747	—	—
Maximum Stress Intensity (SI)	25,767	—	—	—	—
Allowable Stress Intensity (S_a)	48,000	—	—	—	—
Margin of Safety ($MS = S_a/SI - 1$)	+0.86	—	—	—	—

Table 2.7-14 – HAC Fab & Oblique Drop, OC Inner Shell with 48.1*g* at 70 ºF

Evaluation Parameters	
Loading Condition:	HAC 5º Oblique Drop, -20 ºF Foam
Structural Material:	ASTM A240, Type 304, Stainless Steel
Stress Condition:	Primary Membrane
Structural Criterion:	Containment Boundary
Stress Allowable (from Table 2.1-1):	$2.4S_m$
Material Temperature:	70 ºF
Allowable Stress, S_a:	48,000 psi

Load Condition	Stress Components (psi)				Reference Section
	Radial σ_r	Hoop σ_t	Axial σ_z	Shear τ_{rz}	
Fabrication	0	-1,413	-6,866	0	2.7.1.2(4)
Oblique Drop	0	0	-17,049	4,796	2.7.1.2(4)
Direct Stress Summation	0	-1,413	-23,915	4,796	—
Principal Stresses	926	-1,413	-24,841	—	—
Stress Differences	25,767	23,428	2,339	—	—
Maximum Stress Intensity (SI)	25,767	—	—	—	—
Allowable Stress Intensity (S_a)	48,000	—	—	—	—
Margin of Safety (MS = S_a/SI – 1)	+0.86	—	—	—	—

Table 2.7-15 – HAC Fab & Oblique Drop, OC Inner Shell with 48.1*g* at 160 ºF

Evaluation Parameters	
Loading Condition:	HAC 5º Oblique Drop, -20 ºF Foam
Structural Material:	ASTM A240, Type 304, Stainless Steel
Stress Condition:	Primary Membrane
Structural Criterion:	Containment Boundary
Stress Allowable (from Table 2.1-1):	$2.4S_m$
Material Temperature:	160 ºF
Allowable Stress, S_a:	48,000 psi

Load Condition	Stress Components (psi)				Reference Section
	Radial σ_r	Hoop σ_t	Axial σ_z	Shear τ_{rz}	
Fabrication	0	-1,038	-6,866	0	2.7.1.2(4)
Oblique Drop	0	0	-17,049	4,796	2.7.1.2(4)
Direct Stress Summation	0	-1,038	-23,915	4,796	—
Principal Stresses	926	-1,038	-24,841	—	—
Stress Differences	25,767	23,803	1,964	—	—
Maximum Stress Intensity (SI)	25,767	—	—	—	—
Allowable Stress Intensity (S_a)	48,000	—	—	—	—
Margin of Safety (MS = S_a/SI – 1)	+0.86	—	—	—	—

Table 2.7-16 – HAC Oblique Drop, IV Shell with 48.1*g* at 70 ºF

Evaluation Parameters	
Loading Condition:	HAC 5º Oblique Drop, -20 ºF Foam
Structural Material:	ASTM A240, Type 304, Stainless Steel
Stress Condition:	Primary Membrane
Structural Criterion:	Containment Boundary
Stress Allowable (from Table 2.1-1):	$2.4S_m$
Material Temperature:	70 ºF
Allowable Stress, S_a:	48,000 psi

Load Condition	Stress Components (psi)				Reference Section
	Radial σ_r	Hoop σ_t	Axial σ_z	Shear τ_{rz}	
Oblique Drop	0	0	-21,372	7,503	2.7.1.2(5)
Direct Stress Summation	0	0	-21,372	7,503	—
Principal Stresses	2,371	0	-23,743	—	—
Stress Differences	26,114	23,743	2,371	—	—
Maximum Stress Intensity (SI)	26,114	—	—	—	—
Allowable Stress Intensity (S_a)	48,000	—	—	—	—
Margin of Safety (MS = S_a/SI – 1)	+0.84	—	—	—	—

Table 2.7-17 – HAC Oblique Drop, Canister Shell with 48.1*g* at 200 ºF

Evaluation Parameters	
Loading Condition:	HAC 5º Oblique Drop, -20 ºF Foam
Structural Material:	ASTM A516, Grade 55, Carbon Steel
Stress Condition:	Primary Membrane
Structural Criterion:	Non-containment Boundary
Stress Allowable (from Table 2.1-1):	$2.4S_m$
Material Temperature:	200 ºF
Allowable Stress, S_a:	38,500 psi

Load Condition	Stress Components (psi)				Reference Section
	Radial σ_r	Hoop σ_t	Axial σ_z	Shear τ_{rz}	
Oblique Drop	0	0	-23,703	12,189	2.7.1.2(6)
Direct Stress Summation	0	0	-23,703	12,189	—
Principal Stresses	5,149	0	-28,852	—	—
Stress Differences	34,001	28,852	5,149	—	—
Maximum Stress Intensity (SI)	34,001	—	—	—	—
Allowable Stress Intensity (S_a)	38,500	—	—	—	—
Margin of Safety (MS = S_a/SI – 1)	+0.13	—	—	—	—

Table 2.7-18 – OC Shell Stresses with Max Side Drop Fab Condition

Temperature (ºF)	Inner Shell Stresses (psi)		Outer Shell Stresses (psi)	
	Hoop σ_t	Axial σ_z	Hoop σ_t	Axial σ_z
160	-1,038	-1,963	0	0
70	-1,413	-1,963	0	0
-20	-1,821	-1,963	0	0

Note:

① Axial compressive stress in the inner shell per Appendix 2.10.8.5, *Axial Stress Evaluation after Cooldown from 620 ºF to -20 ºF*.

Table 2.7-19 – HAC Fab & Side Drop, OC Inner Shell with 81.2*g* at -20 ºF

Evaluation Parameters	
Loading Condition:	HAC Flat Side Drop, -20 ºF Foam
Structural Material:	ASTM A240, Type 304, Stainless Steel
Stress Condition:	Primary Membrane
Structural Criterion:	Containment Boundary
Stress Allowable (from Table 2.1-1):	$2.4S_m$
Material Temperature:	-20 ºF
Allowable Stress, S_a:	48,000 psi

Load Condition	Stress Components (psi)				Reference Section
	Radial σ_r	Hoop σ_t	Axial σ_z	Shear τ_{rz}	
Fabrication	0	-1,821	-1,963	0	2.7.1.3(4)
Side Drop	0	0	-16,331	5,554	2.7.1.3(4)
Direct Stress Summation	0	-1,821	-18,294	5,554	—
Principal Stresses	1,554	-1,821	-19,848	—	—
Stress Differences	21,402	18,027	3,375	—	—
Maximum Stress Intensity (SI)	21,402	—	—	—	—
Allowable Stress Intensity (S_a)	48,000	—	—	—	—
Margin of Safety ($MS = S_a/SI - 1$)	+1.24	—	—	—	—

Table 2.7-20 – HAC Fab & Side Drop, OC Inner Shell with 81.2*g* at 70 ºF

Evaluation Parameters	
Loading Condition:	HAC Flat Side Drop, -20 ºF Foam
Structural Material:	ASTM A240, Type 304, Stainless Steel
Stress Condition:	Primary Membrane
Structural Criterion:	Containment Boundary
Stress Allowable (from Table 2.1-1):	$2.4S_m$
Material Temperature:	70 ºF
Allowable Stress, S_a:	48,000 psi

Load Condition	Stress Components (psi)				Reference Section
	Radial σ_r	Hoop σ_t	Axial σ_z	Shear τ_{rz}	
Fabrication	0	-1,413	-1,963	0	2.7.1.3(4)
Side Drop	0	0	-16,331	5,554	2.7.1.3(4)
Direct Stress Summation	0	-1,413	-18,294	5,554	—
Principal Stresses	1,554	-1,413	-19,848	—	—
Stress Differences	21,402	18,435	2,967	—	—
Maximum Stress Intensity (SI)	21,402	—	—	—	—
Allowable Stress Intensity (S_a)	48,000	—	—	—	—
Margin of Safety (MS = S_a/SI – 1)	+1.24	—	—	—	—

Table 2.7-21 – HAC Fab & Side Drop, OC Inner Shell with 81.2*g* at 160 ºF

Evaluation Parameters	
Loading Condition:	HAC Flat Side Drop, -20 ºF Foam
Structural Material:	ASTM A240, Type 304, Stainless Steel
Stress Condition:	Primary Membrane
Structural Criterion:	Containment Boundary
Stress Allowable (from Table 2.1-1):	$2.4S_m$
Material Temperature:	160 ºF
Allowable Stress, S_a:	48,000 psi

Load Condition	Stress Components (psi)				Reference Section
	Radial σ_r	Hoop σ_t	Axial σ_z	Shear τ_{rz}	
Fabrication	0	-1,038	-1,963	0	2.7.1.3(4)
Side Drop	0	0	-16,331	5,554	2.7.1.3(4)
Direct Stress Summation	0	-1,038	-18,294	5,554	—
Principal Stresses	1,554	-1,038	-19,848	—	—
Stress Differences	21,402	18,810	2,592	—	—
Maximum Stress Intensity (SI)	21,402	—	—	—	—
Allowable Stress Intensity (S_a)	48,000	—	—	—	—
Margin of Safety (MS = S_a/SI – 1)	+1.24	—	—	—	—

Table 2.7-22 – HAC Side Drop, IV Shell with 81.2*g* at 160 ºF

Evaluation Parameters	
Loading Condition:	HAC Flat Side Drop, -20 ºF Foam
Structural Material:	ASTM A240, Type 304, Stainless Steel
Stress Condition:	Primary Membrane
Structural Criterion:	Containment Boundary
Stress Allowable (from Table 2.1-1):	$2.4S_m$
Material Temperature:	160 ºF
Allowable Stress, S_a:	48,000 psi

Load Condition	Stress Components (psi)				Reference Section
	Radial σ_r	Hoop σ_t	Axial σ_z	Shear τ_{rz}	
Side Drop	0	0	-19,611	9,317	2.7.1.3(5)
Direct Stress Summation	0	0	-19,611	9,317	—
Principal Stresses	3,721	0	-23,332	—	—
Stress Differences	27,053	23,332	3,721	—	—
Maximum Stress Intensity (SI)	27,053	—	—	—	—
Allowable Stress Intensity (S_a)	48,000	—	—	—	—
Margin of Safety (MS = S_a/SI – 1)	+0.77	—	—	—	—

Table 2.7-23 – HAC Side Drop, Canister Shell with 81.2*g* at 200 ºF

Evaluation Parameters	
Loading Condition:	HAC Flat Side Drop, -20 ºF Foam
Structural Material:	ASTM A516, Grade 55, Carbon Steel
Stress Condition:	Primary Membrane
Structural Criterion:	Non-containment Boundary
Stress Allowable (from Table 2.1-1):	$2.4S_m$
Material Temperature:	200 ºF
Allowable Stress, S_a:	38,500 psi

Load Condition	Stress Components (psi)				Reference Section
	Radial σ_r	Hoop σ_t	Axial σ_z	Shear τ_{rz}	
Side Drop	0	0	-16,844	10,021	2.7.1.3(6)
Direct Stress Summation	0	0	-16,844	10,021	—
Principal Stresses	4,668	0	-21,512	—	—
Stress Differences	26,180	21,512	4,668	—	—
Maximum Stress Intensity (SI)	26,180	—	—	—	—
Allowable Stress Intensity (S_a)	38,500	—	—	—	—
Margin of Safety (MS = S_a/SI – 1)	+0.47	—	—	—	—

Table 2.7-24 – HAC Fab & Side Drop, OC Shells' Welds with 81.2*g* at -20 ºF

Evaluation Parameters	
Loading Condition:	HAC Flat Side Drop, -20 ºF Foam
Structural Material:	ASTM A240, Type 304, Stainless Steel
Stress Condition:	Primary Membrane
Structural Criterion:	Containment Boundary
Stress Allowable (from Table 2.1-1):	$2.4S_m$
Material Temperature:	-20 ºF
Allowable Stress, S_a:	48,000 psi

Load Condition	Stress Components (psi)				Reference Section
	Radial σ_r	Hoop σ_t	Axial σ_z	Shear τ_{rz}	
Fabrication	0	-1,821	-1,963	0	2.7.1.3(4)
Side Drop	0	0	-16,323	10,191	2.7.1.3(4)(8)
Direct Stress Summation	0	-1,821	-18,286	10,191	—
Principal Stresses	4,548	-1,821	-22,834	—	—
Stress Differences	27,382	21,013	6,369	—	—
Maximum Stress Intensity (SI)	27,382	—	—	—	—
Allowable Stress Intensity (S_a)	48,000	—	—	—	—
Margin of Safety ($MS = S_a/SI - 1$)	+0.75	—	—	—	—

Table 2.7-25 – Stress-Strain Values for Type 304 Stainless Steel at 212 ºF

True Stress, σ (psi)	True Strain, ε (in/in)
20,500	$7.401(10)^{-4}$
24,000	$1.805(10)^{-3}$
26,000	$4.555(10)^{-3}$
36,000	$4.684(10)^{-2}$
48,000	$1.209(10)^{-1}$

Table 2.7-26 – Stresses Due to 300 psig Pressure

Shell / End Plate Location①	Axial Membrane σ_1 (psi)	Hoop Membrane σ_2 (psi)	Axial Bending② σ_1' (psi)	Hoop Bending② σ_2' (psi)	Radial Bending σ (psi)
P1	1,980	3,963	0	0	—
P2	2,505	5,004	0	0	—
P3	6,324	12,648	0	0	—
P4	1,980	582	-6,129	-1,839	—
P5	2,505	753	-7,725	-2,319	—
P6	6,501	-11,322	-66,060	-20,598	—
P7	—	—	—	—	6,426
P8	—	—	—	—	3,645
P9	—	—	—	—	2,250
P10	—	—	—	—	42,240

Notes:

① Locations are shown in Figure 2.6-1 from Section 2.6.1.3, *Stress Calculations*.

② σ_1' and σ_2' are positive when tensile on the shell outside diameter.

Table 2.7-27 – Thermal Stress Summary

Stress Location	Stress Category	HAC Temperature (ºF)	Allowable Stress Intensity (psi)	Actual Stress Intensity (psi)	Margin of Safety
P1	Membrane	615	39,200	3,963	+8.89
P2	Membrane	500	42,000	5,004	+7.39
P3	Membrane	350	45,600	12,648	+2.61
P4	Membrane	500	42,000	1,980	+20.21
	Membrane + Bending	500	63,000	6,129	+9.28
P5	Membrane	500	42,000	2,505	+15.77
	Membrane + Bending	500	63,000	7,725	+7.16
P6	Membrane	300	46,200	17,823	+1.59
P7	Membrane + Bending	500	59,300	6,426	+8.23
P8	Membrane + Bending	500	59,300	3,645	+15.27
P9	Membrane + Bending	300	61,500	2,250	+26.33
P10	Membrane + Bending	300	61,500	42,240	+0.46

Table 2.7-28 – Buckling Geometry Parameters per Code Case N-284

Geometry and Material Input	
	OC
Mean Radius, inch	16.69
Shell Thickness, inch	1.000
Length, inch	121.25
Geometry Output (nomenclature consistent with ASME Code Case N-284)	
R =	16.69
T =	1.000
$(Rt)^{½}$ =	4.085
L_ϕ =	121.25
L_θ =	104.87
M_ϕ =	29.68
M_θ =	25.67
M =	25.67

Table 2.7-29 – Stresses for 290 psig External Pressure + Fabrication

Component	OC	
	Axial Stress, σ_ϕ	**Hoop Stress, σ_θ**
Pressure	2,420	4,840
Fabrication	1,963	1,413
Total	4,383	6,253

Table 2.7-30 – Buckling Summary for 290 psig External Pressure + Fab

Condition	Outer Cask	Remarks
Capacity Reduction Factors (-1511)		
$\alpha_{\phi L}$ =	0.2670	
$\alpha_{\theta L}$ =	0.8000	
$\alpha_{\phi\theta L}$ =	0.8000	
Plasticity Reduction Factors (-1610)		
η_{ϕ} =	1.0000	
η_{θ} =	1.0000	
$\eta_{\phi\theta}$ =	1.0000	
Theoretical Buckling Values (-1712.1.1)		
C_{ϕ} =	0.6050	
$\sigma_{\phi eL}$ =	1,025,854 psi	
$C_{\theta r}$ =	0.0291	
$\sigma_{\theta eL} = \sigma_{reL}$ =	49,274 psi	
$C_{\theta h}$ =	0.0291	
$\sigma_{\theta eL} = \sigma_{heL}$ =	49,274 psi	
$C_{\theta h}$ =	0.1369	
$\sigma_{\phi\theta eL}$ =	232,189 psi	
Elastic Interaction Equations (-1713.1.1)		
$\sigma_{\phi s}$ =	21,997 psi	
$\sigma_{\theta s}$ =	10,474 psi	
$\sigma_{\phi\theta s}$ =	0 psi	
Axial + Hoop ⇨ Check (a):	*N/A*	<1 ∴ OK
Axial + Hoop ⇨ Check (b):	*N/A*	<1 ∴ OK
Axial + Shear ⇨ Check (c):	0.0214	<1 ∴ OK
Hoop + Shear ⇨ Check (d):	0.2126	<1 ∴ OK
Axial + Hoop + Shear ⇨ Check (e):	*N/A*	<1 ∴ OK
Inelastic Interaction Equations (-1713.2.1)		
$\sigma_{\phi s}$ =	21,997 psi	
$\sigma_{\theta s}$ =	10,474 psi	
$\sigma_{\phi\theta s}$ =	0 psi	
Axial + Shear ⇨ Check (a):	0.0005	<1 ∴ OK
Hoop + Shear ⇨ Check (b):	0.0452	<1 ∴ OK

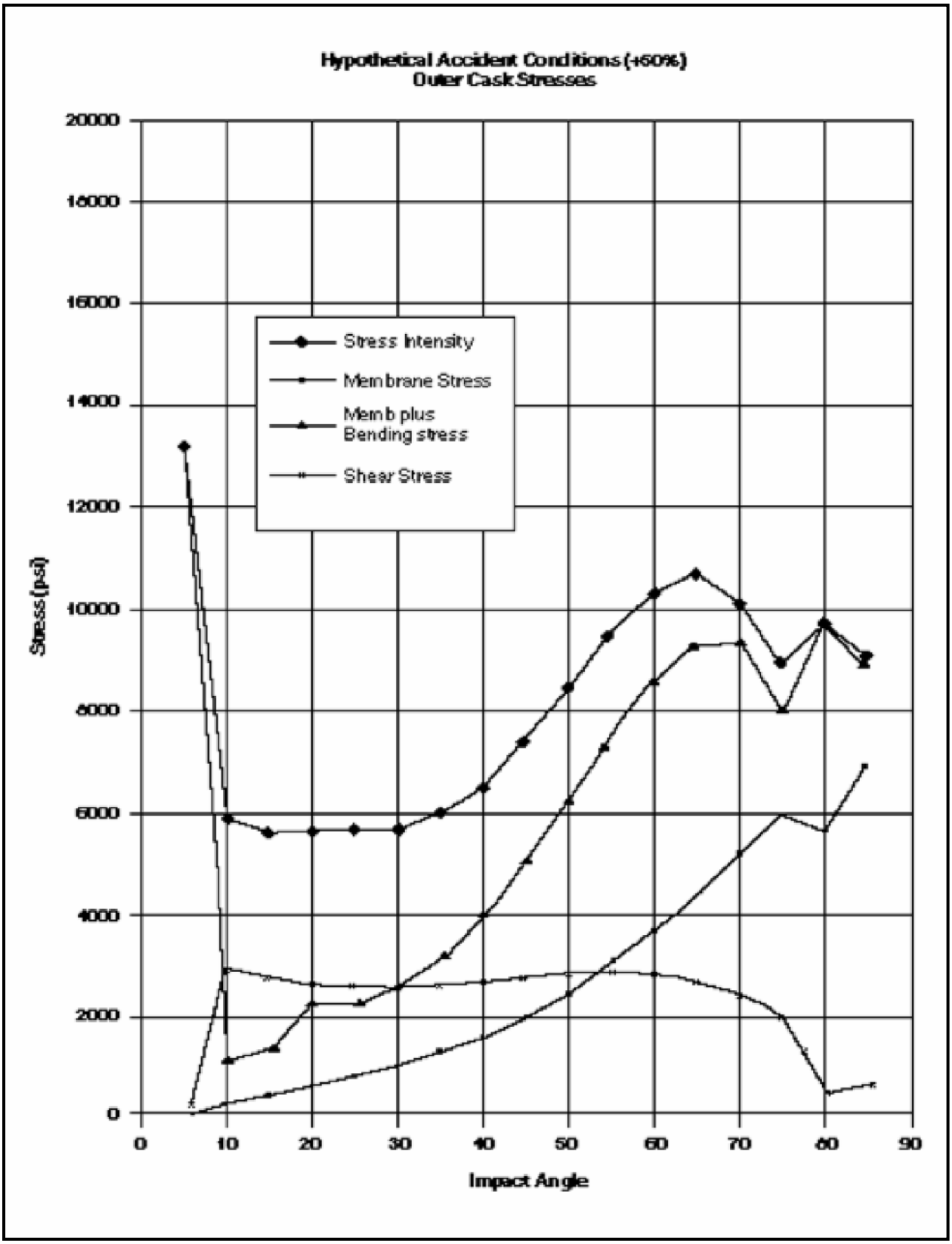

Figure 2.7-1 – HAC Cold (-20 ºF) Outer Cask Stresses

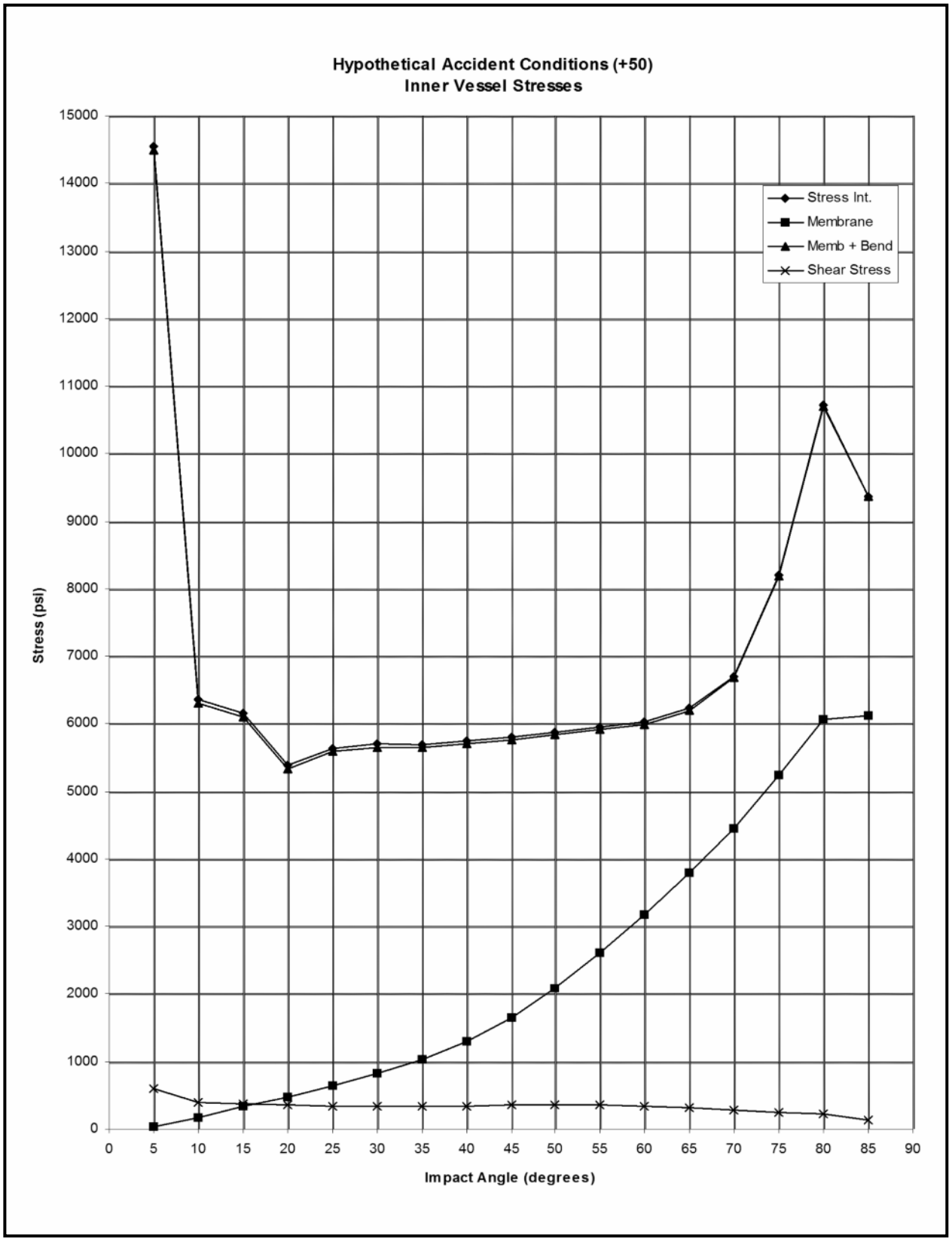

Figure 2.7-2 – HAC Cold (-20 ºF) Inner Vessel Stresses

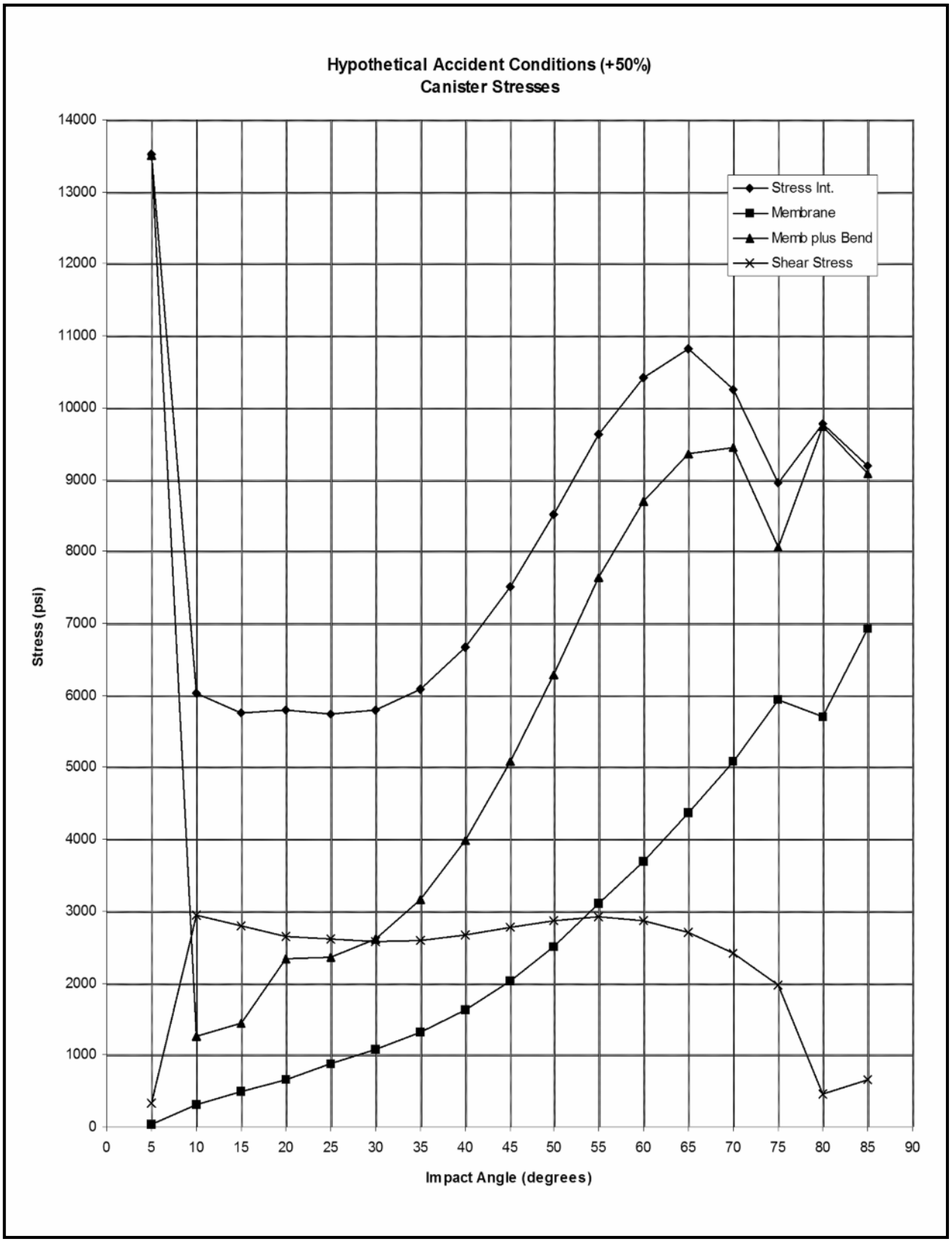

Figure 2.7-3 – HAC Cold (-20 ºF) Canister Stresses

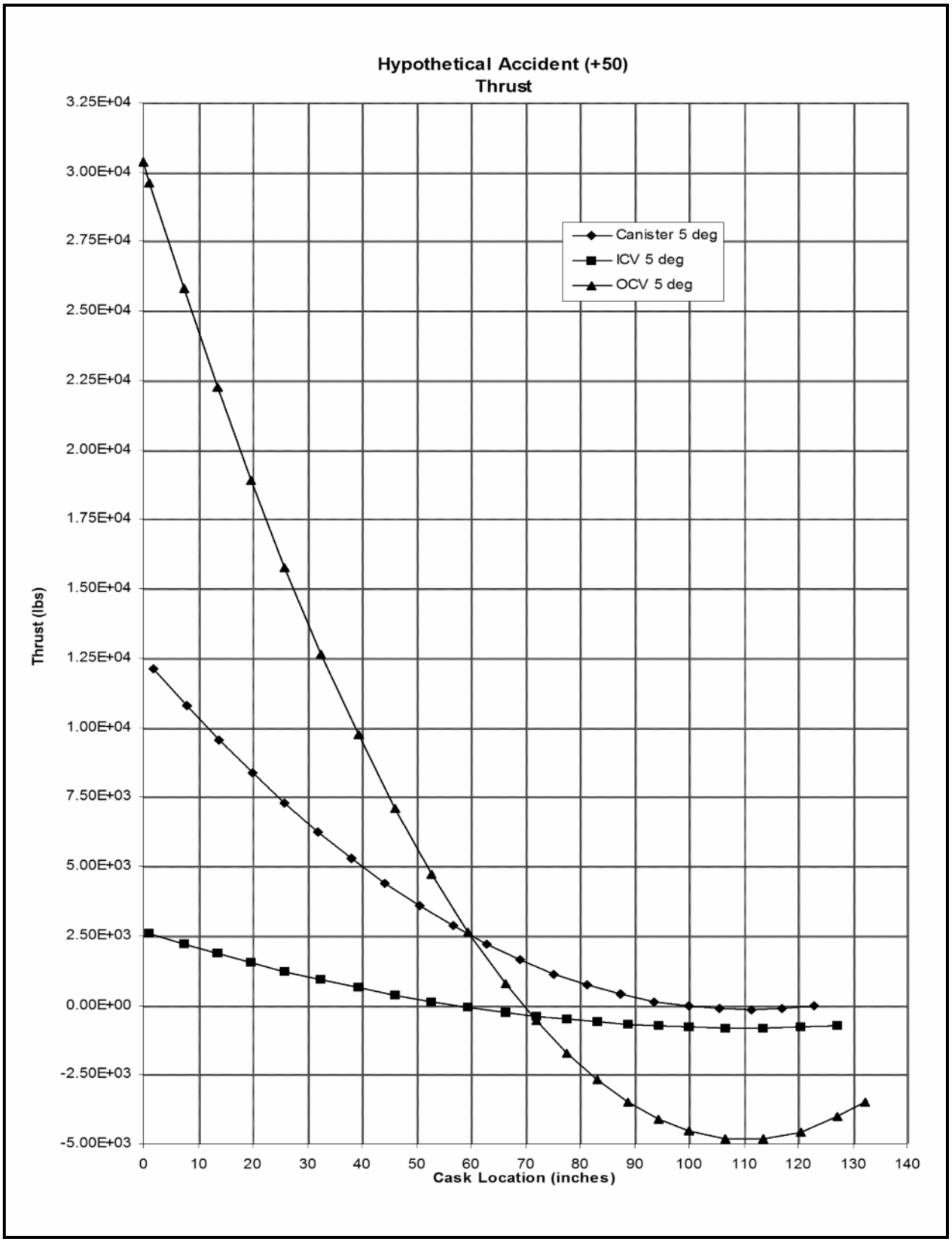

Figure 2.7-4 – HAC Cold (-20 ºF) Thrust

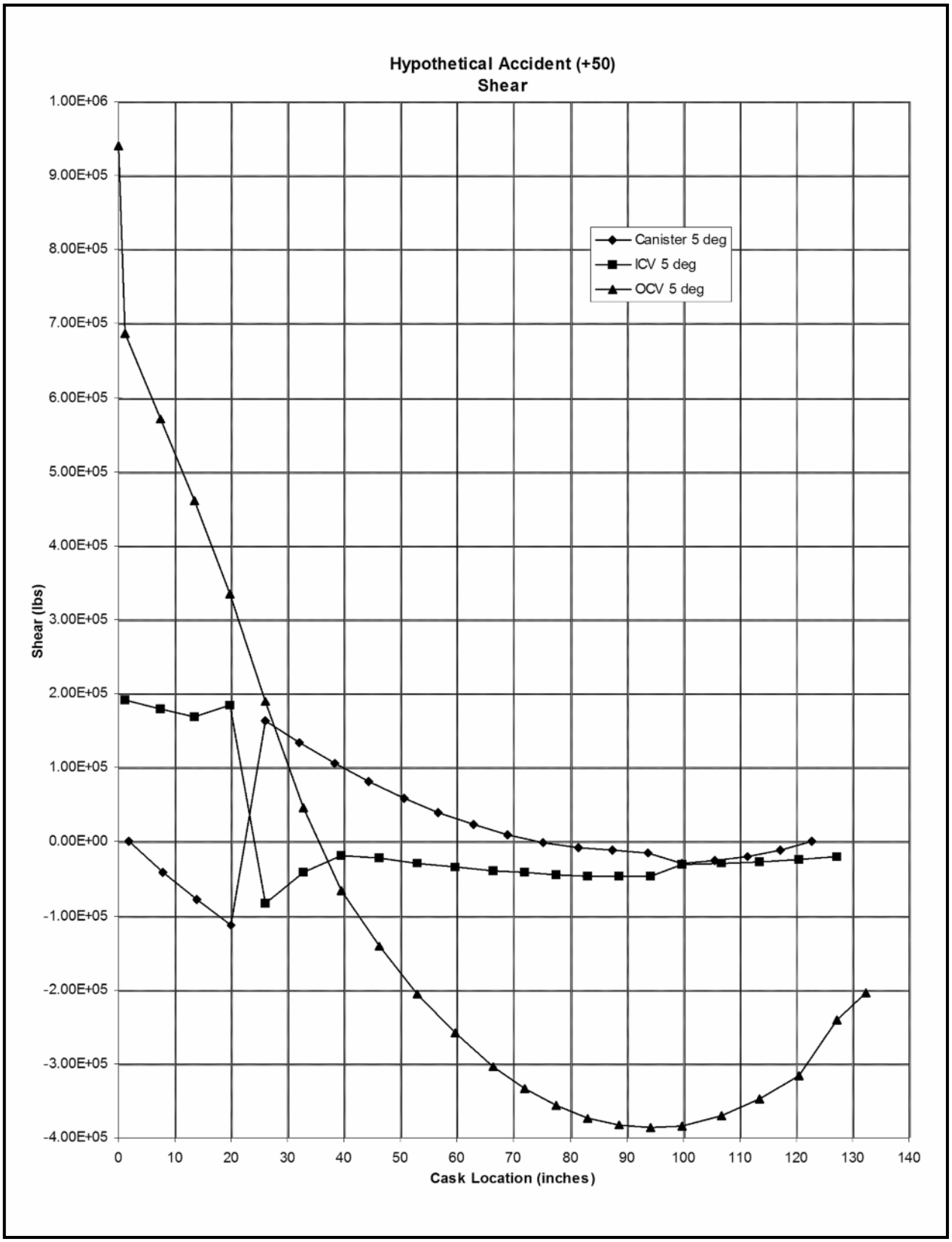

Figure 2.7-5 – HAC Cold (-20 ºF) Shear

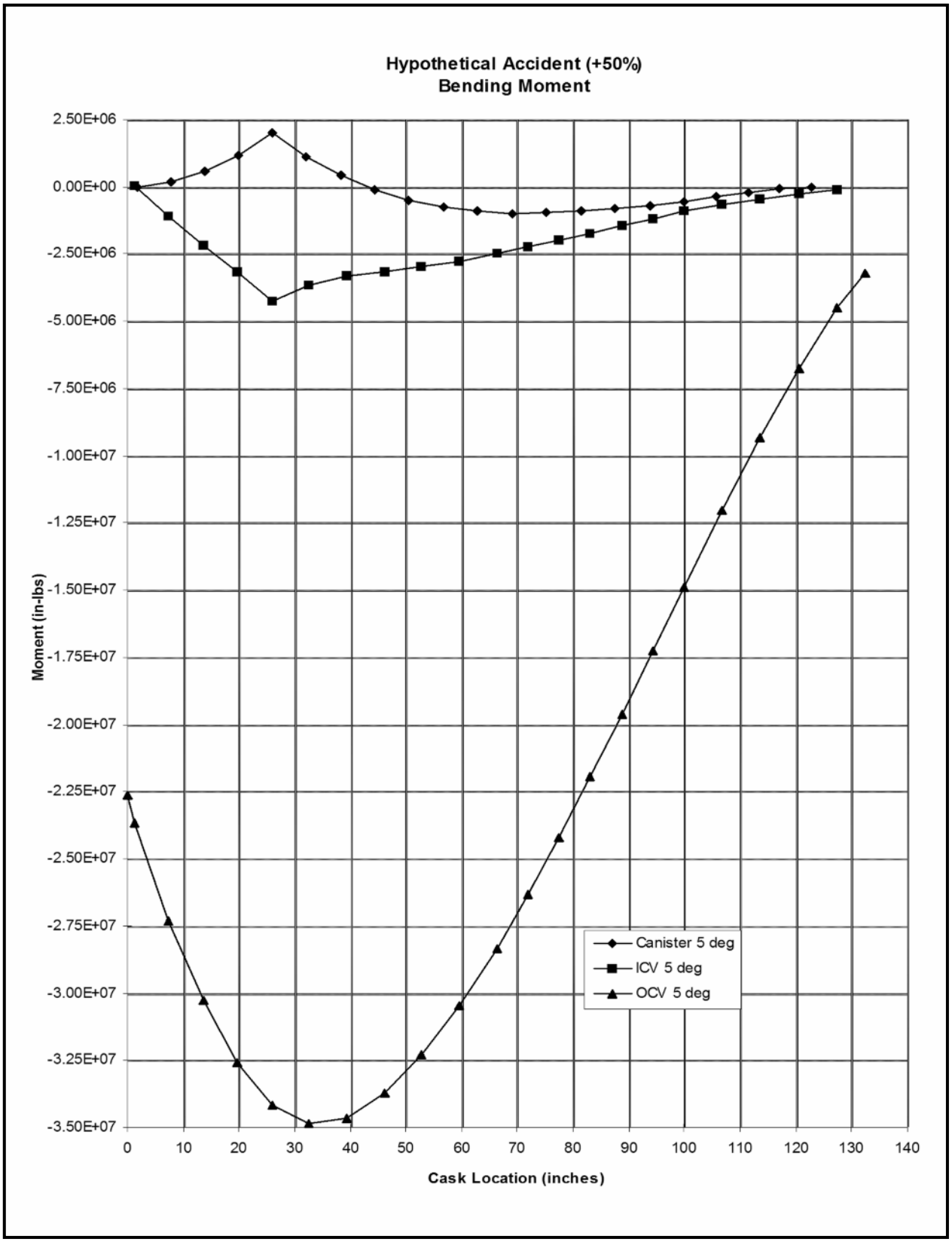

Figure 2.7-6 – HAC Cold (-20 ºF) Bending Moment

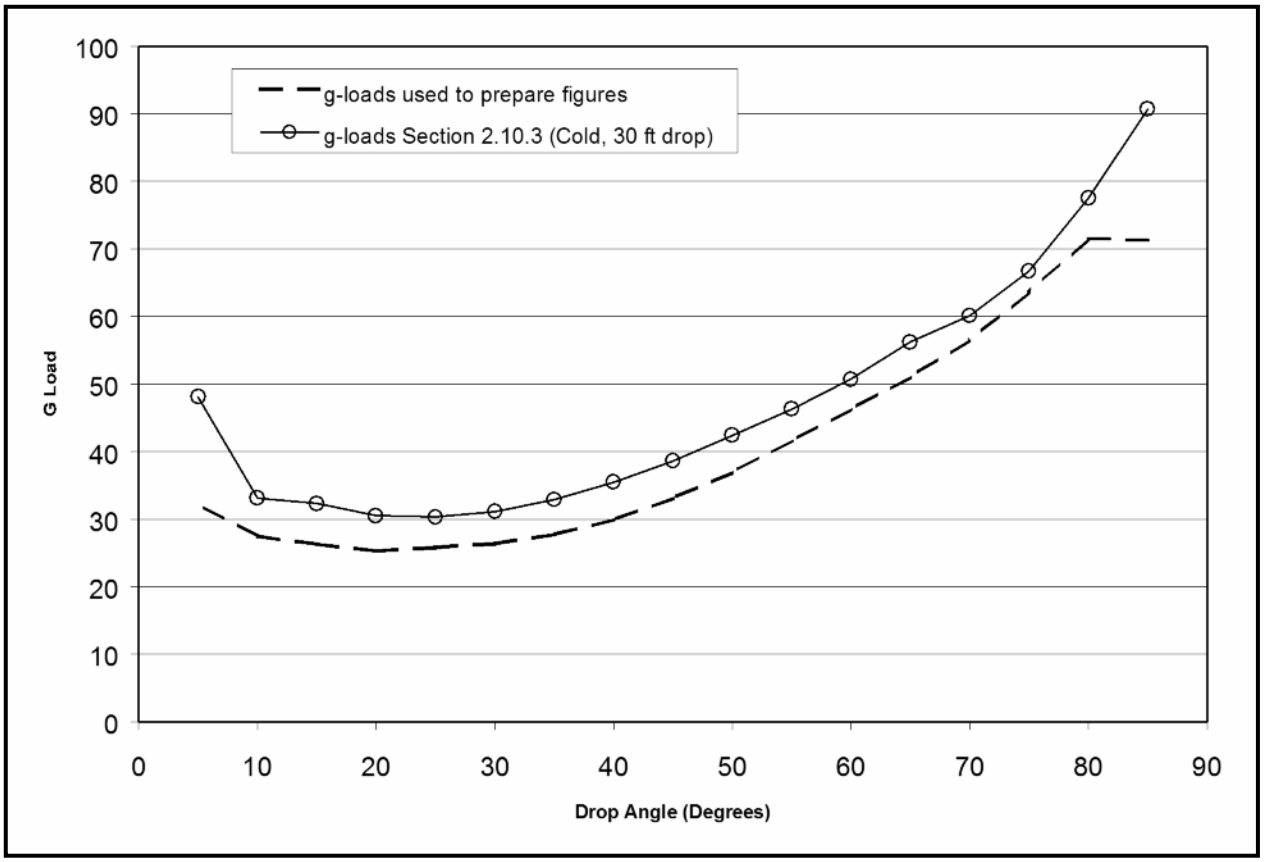

Figure 2.7-7 – Comparison of *g*-Loads Used for Calculating Cold (-20 ºF) HAC Stresses

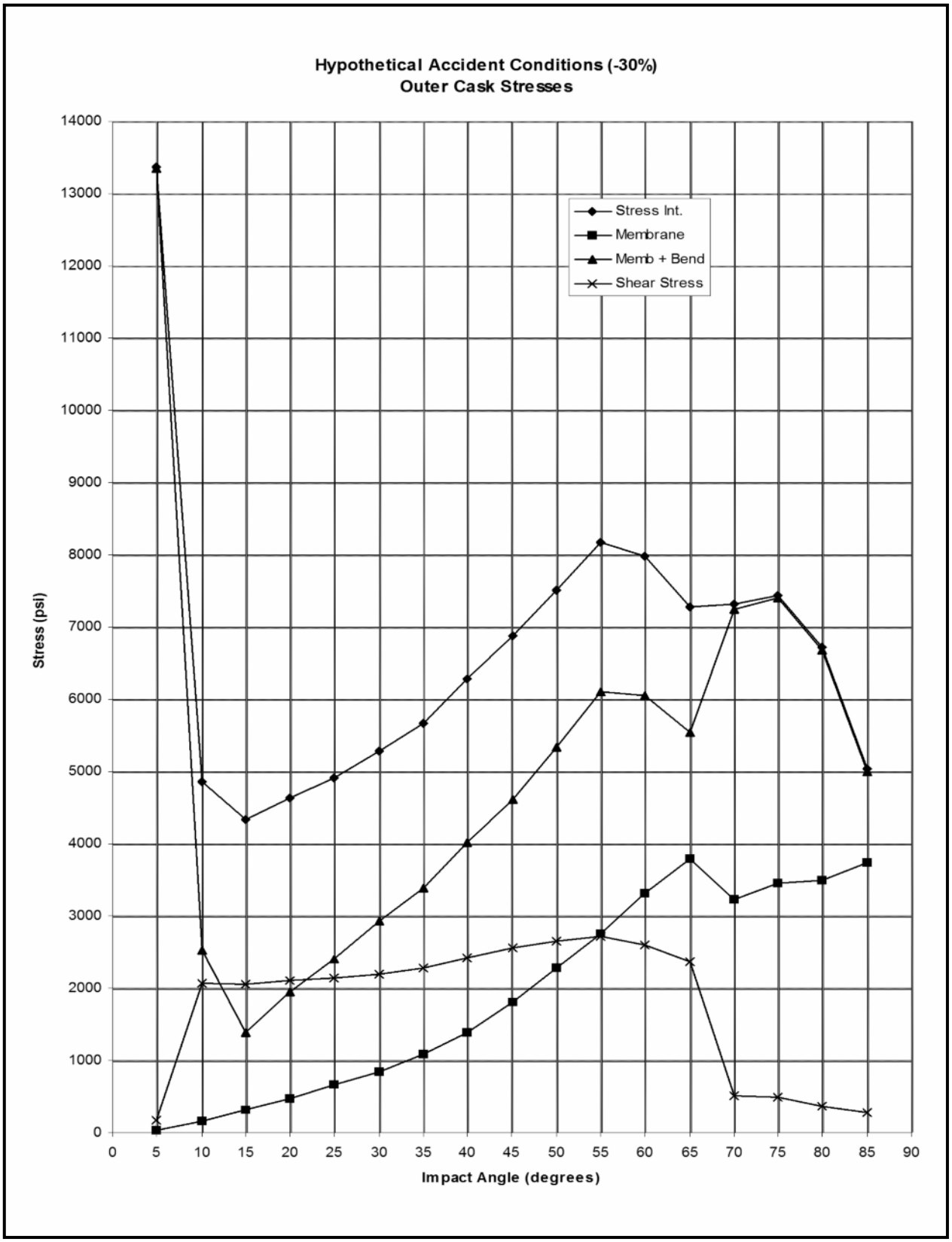

Figure 2.7-8 – HAC Hot (140 ºF) Outer Cask Stresses

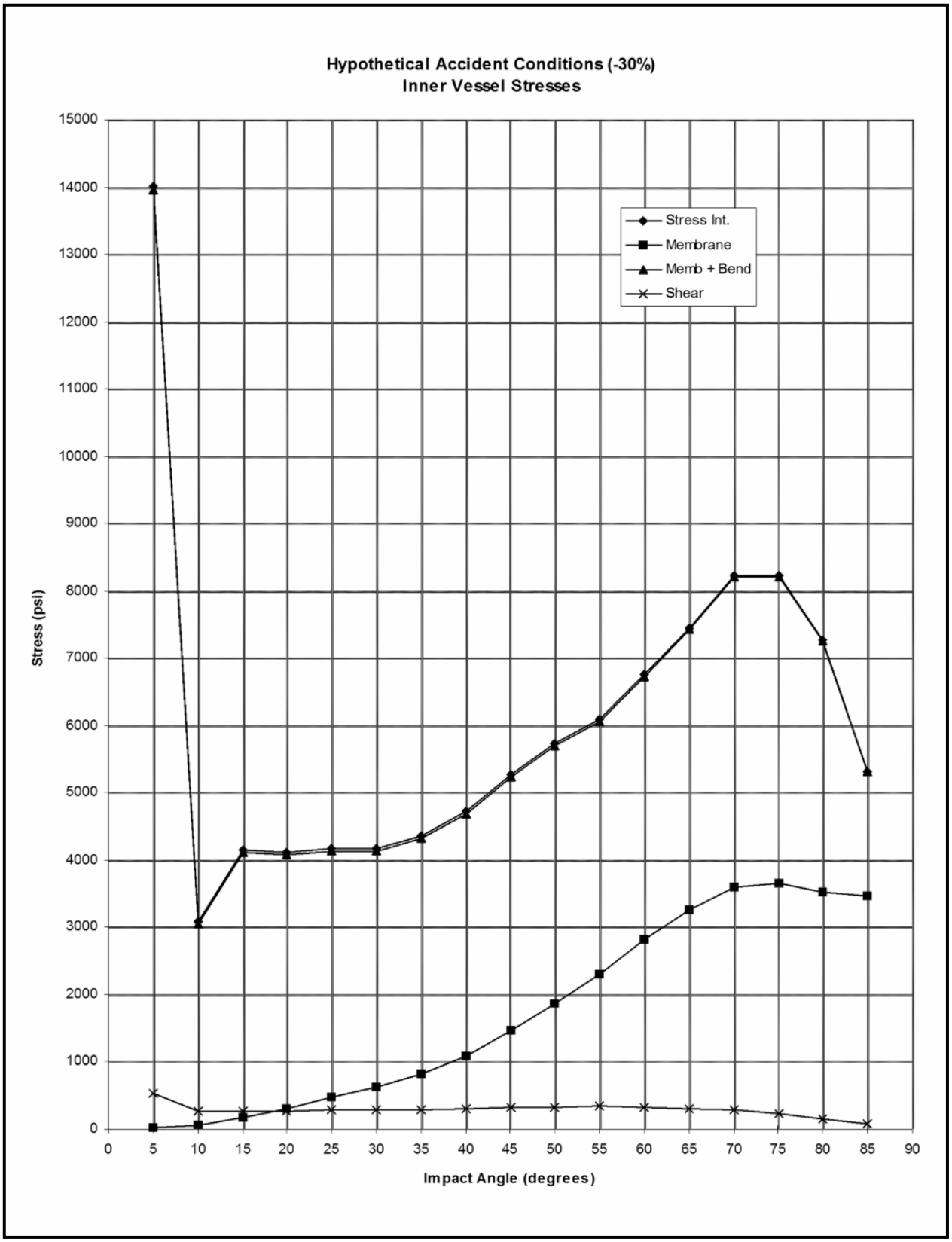

Figure 2.7-9 – HAC Hot (140 ºF) Inner Vessel Stresses

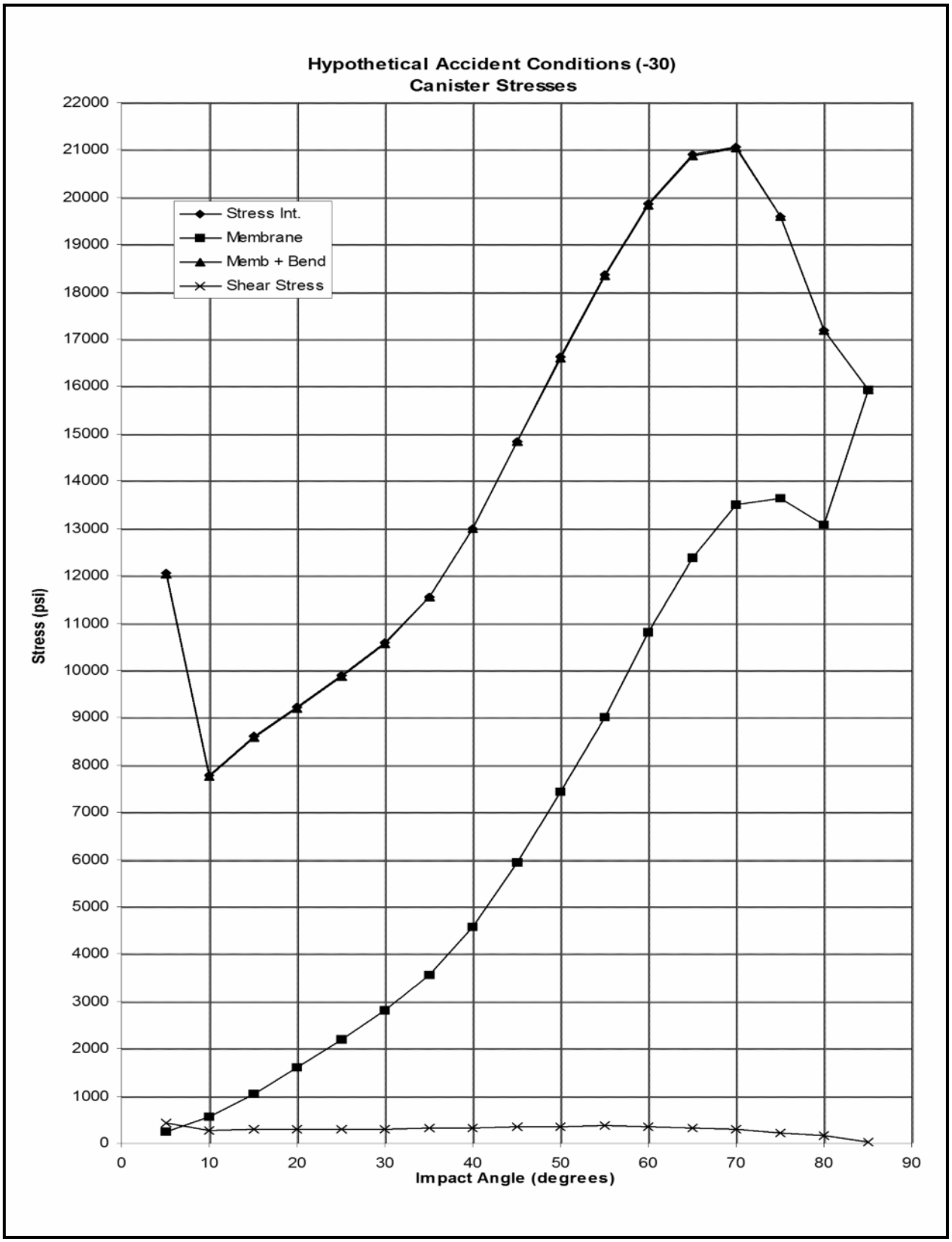

Figure 2.7-10 – HAC Hot (140 ºF) Canister Stresses

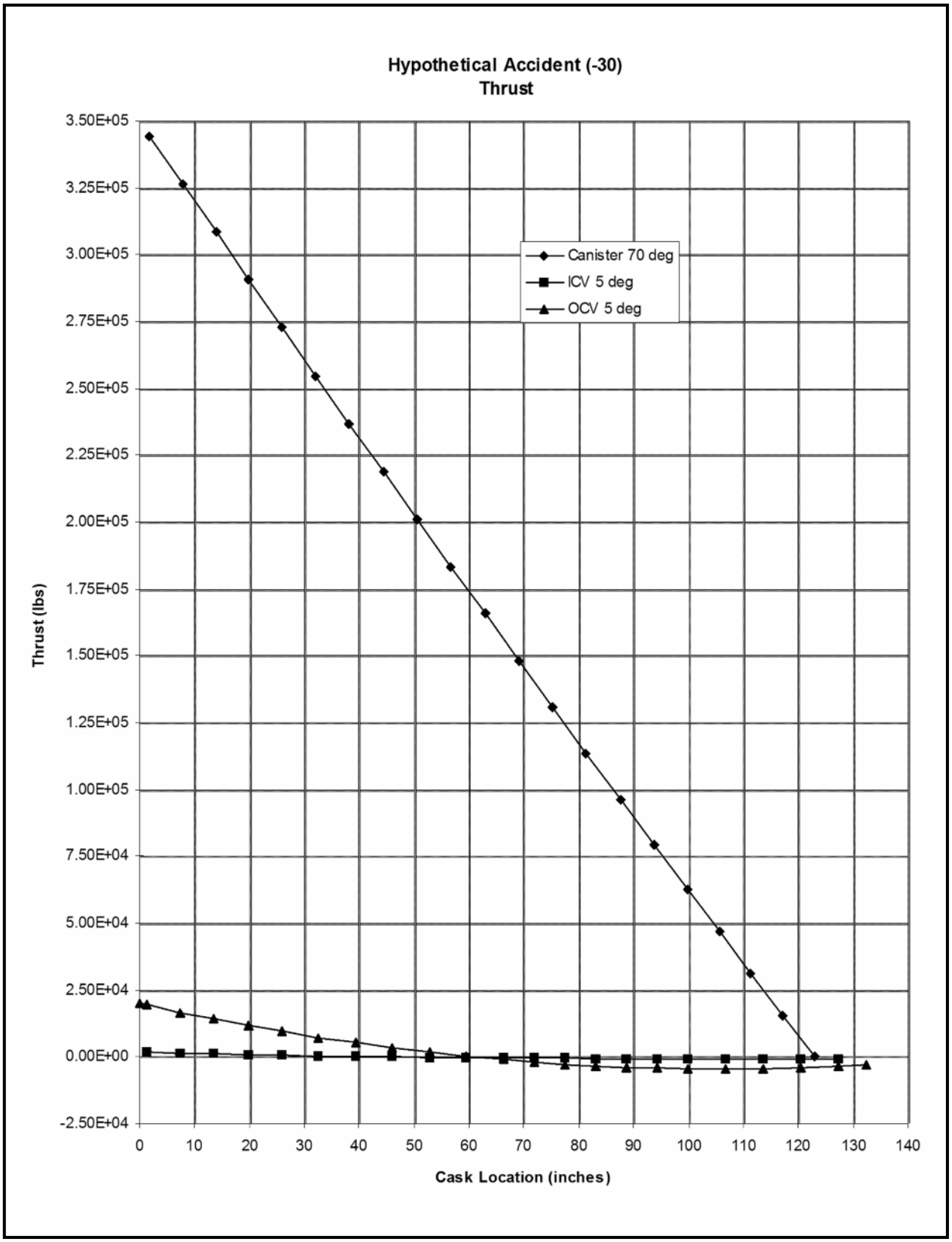

Figure 2.7-11 – HAC Hot (140 ºF) Thrust

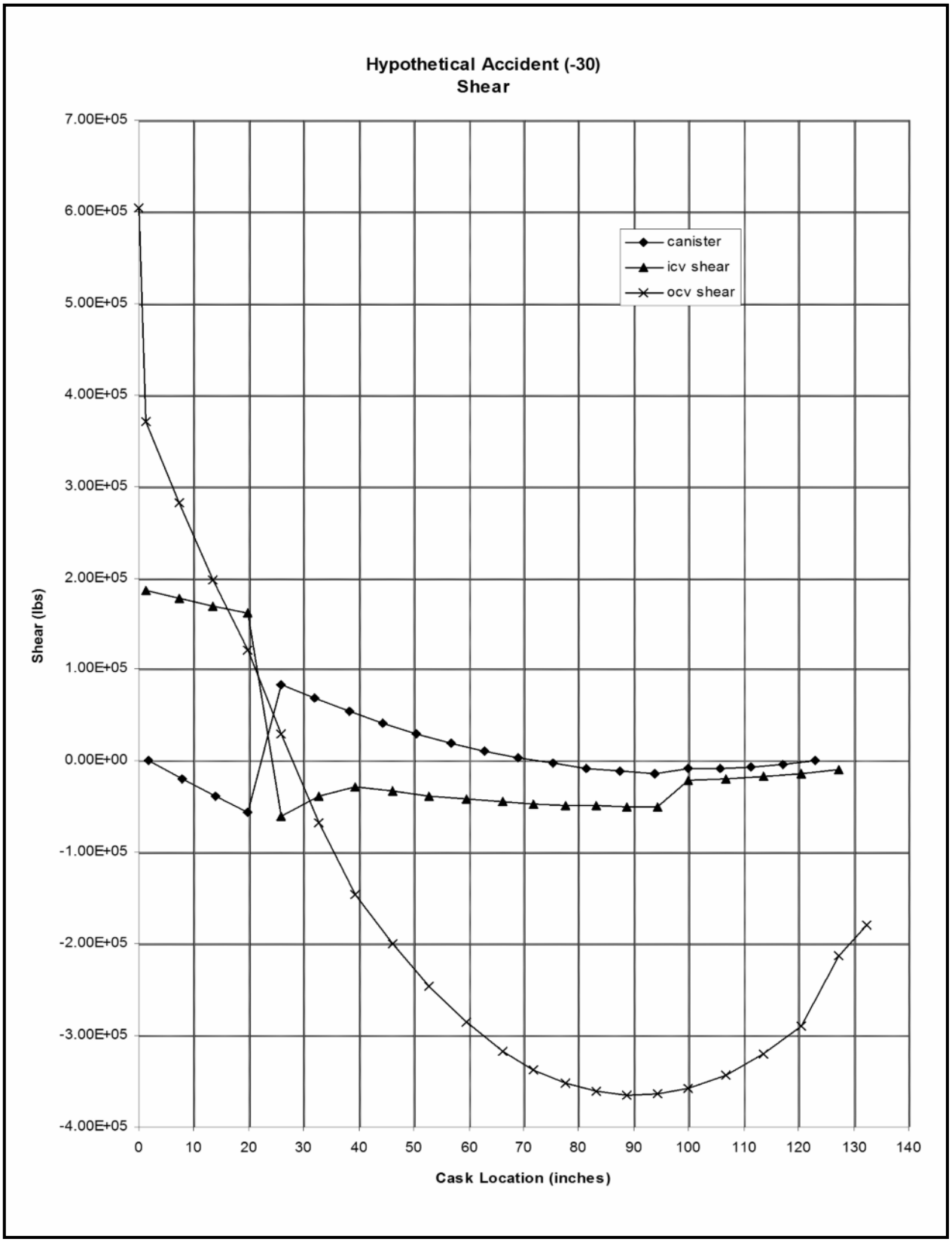

Figure 2.7-12 – HAC Hot (140 ºF) Shear

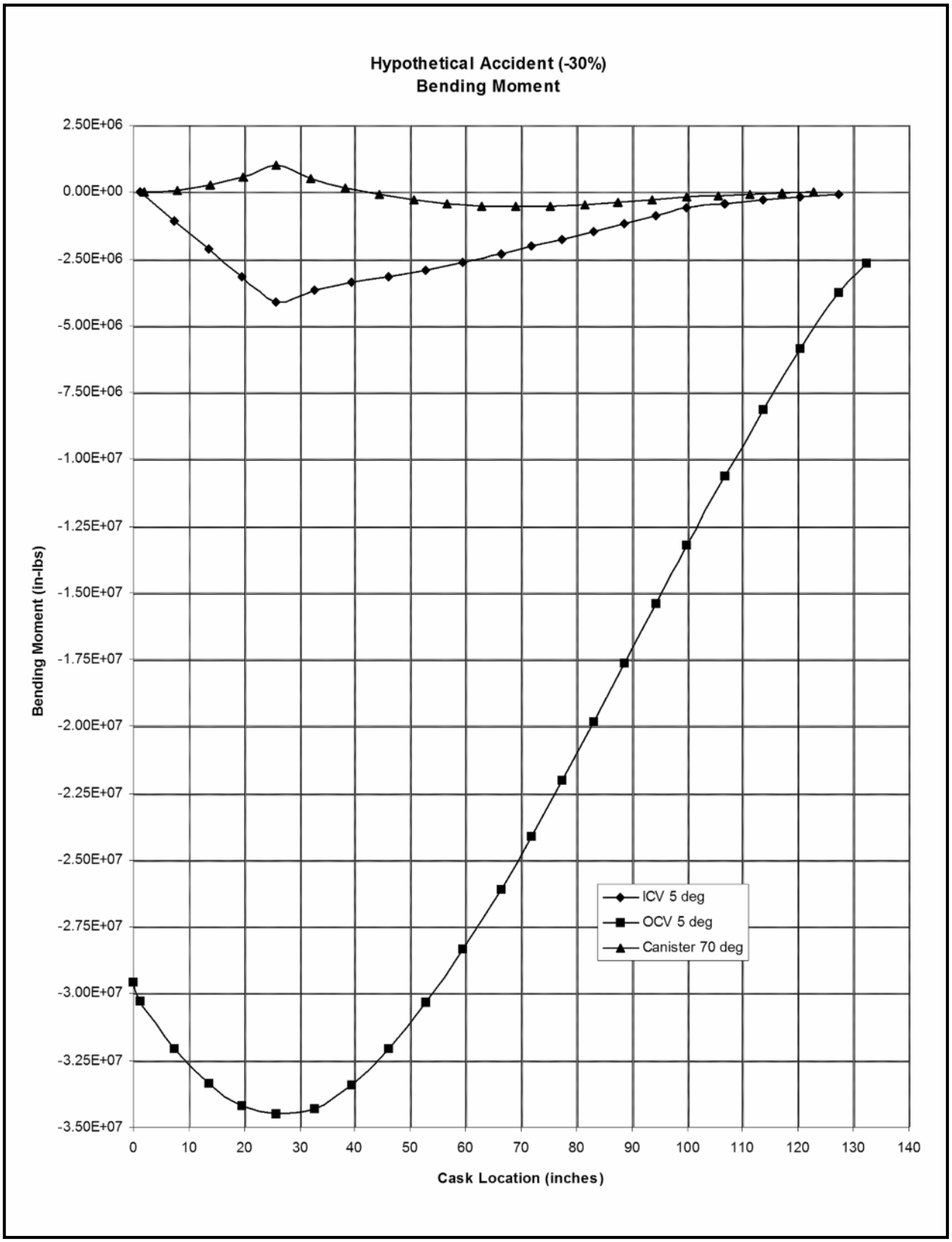

Figure 2.7-13 – HAC Hot (140 ºF) Bending Moment

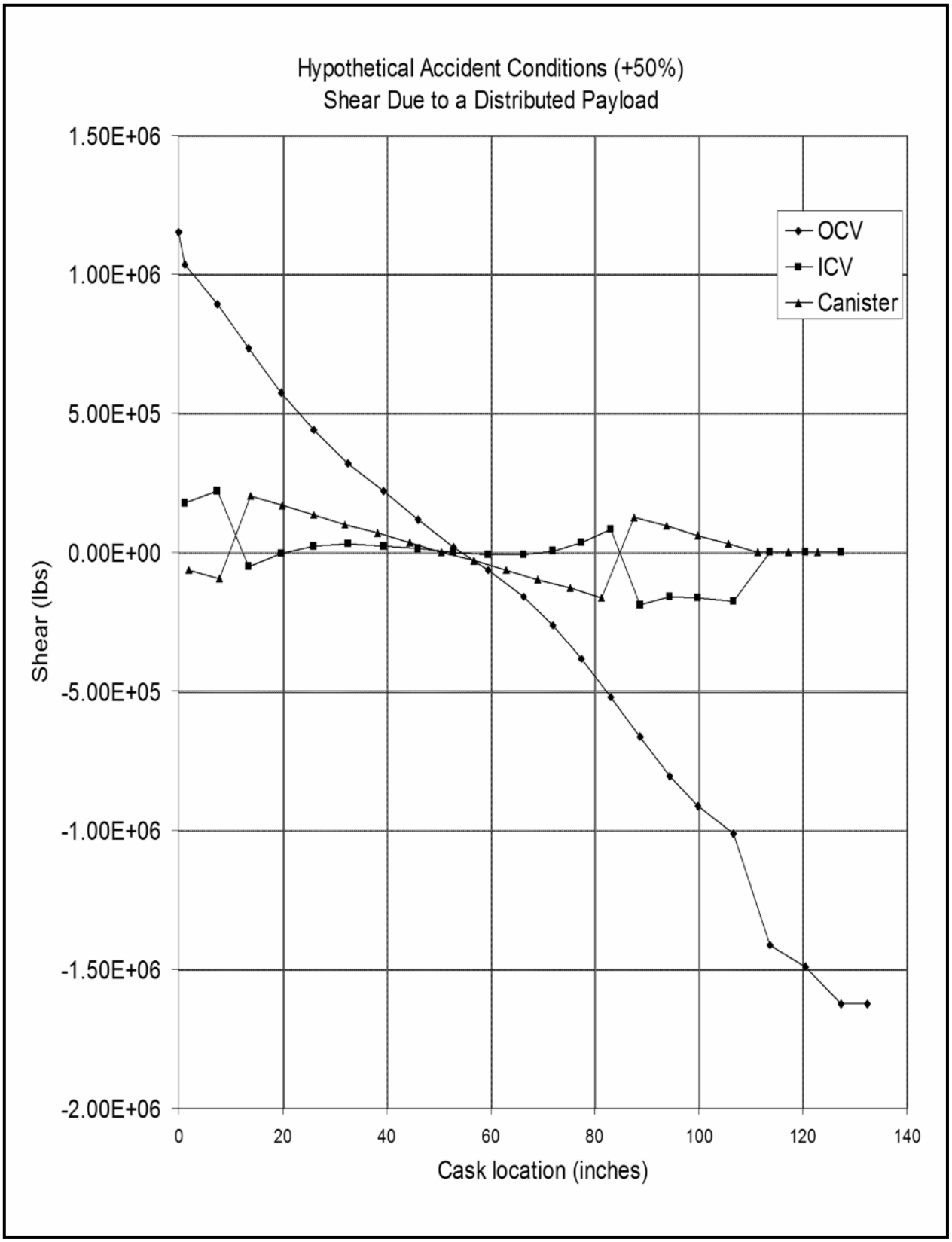

Figure 2.7-14 – HAC Cold (-20 ºF) Shear Due to a Distributed Payload

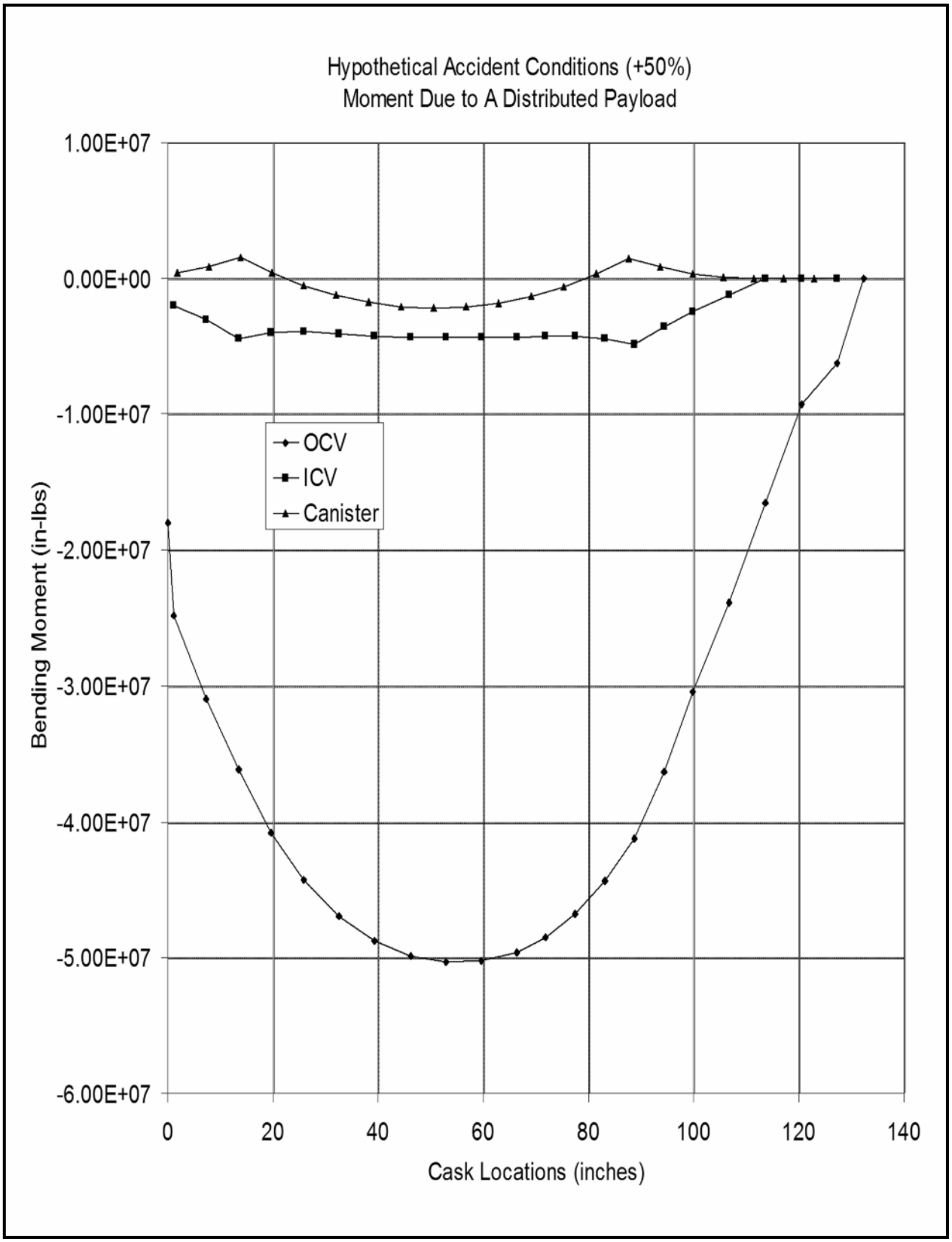

Figure 2.7-15 – HAC Cold (-20 ºF) Moment Due to a Distributed Payload

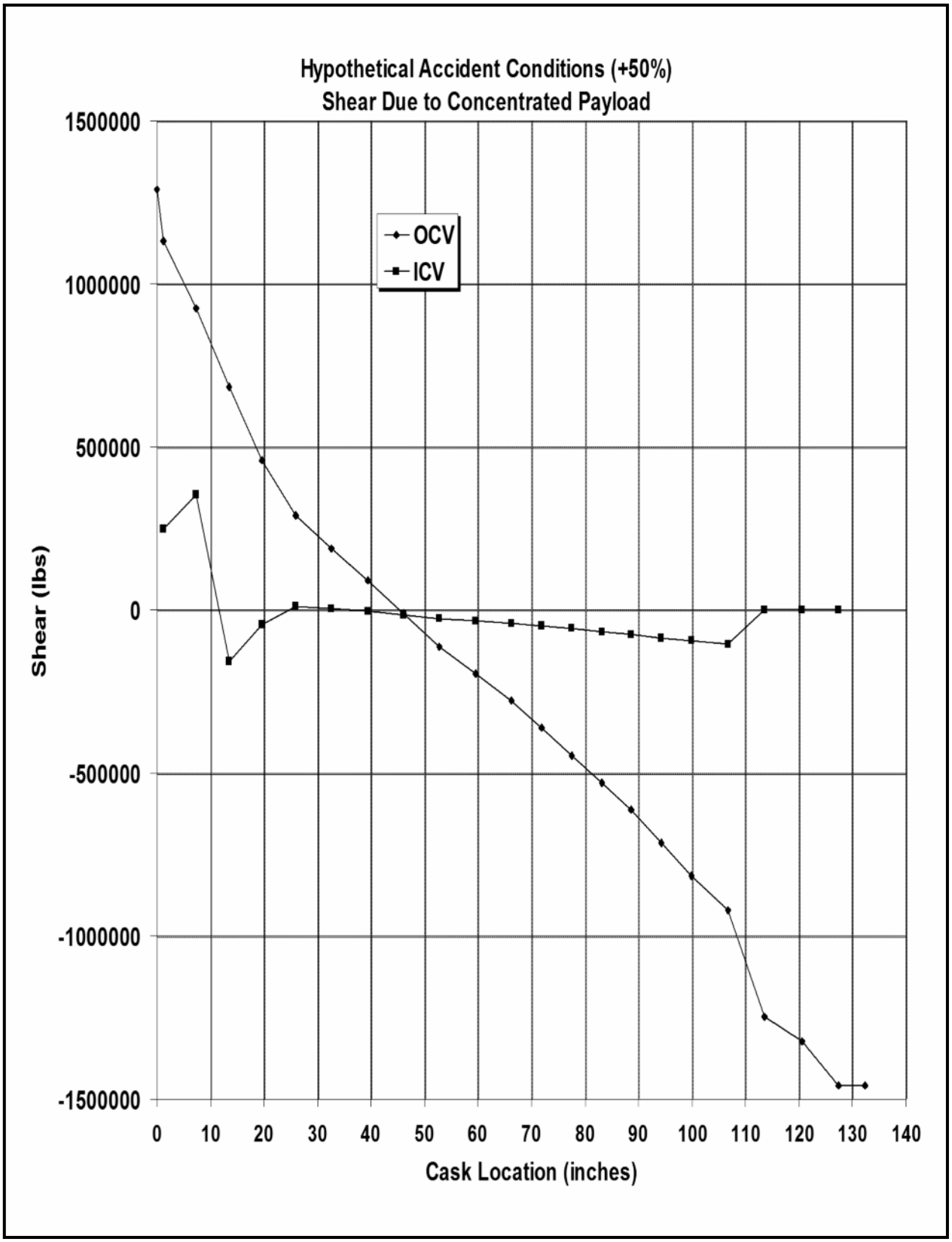

Figure 2.7-16 – HAC Cold (-20 ºF) Shear Due to a Concentrated Payload

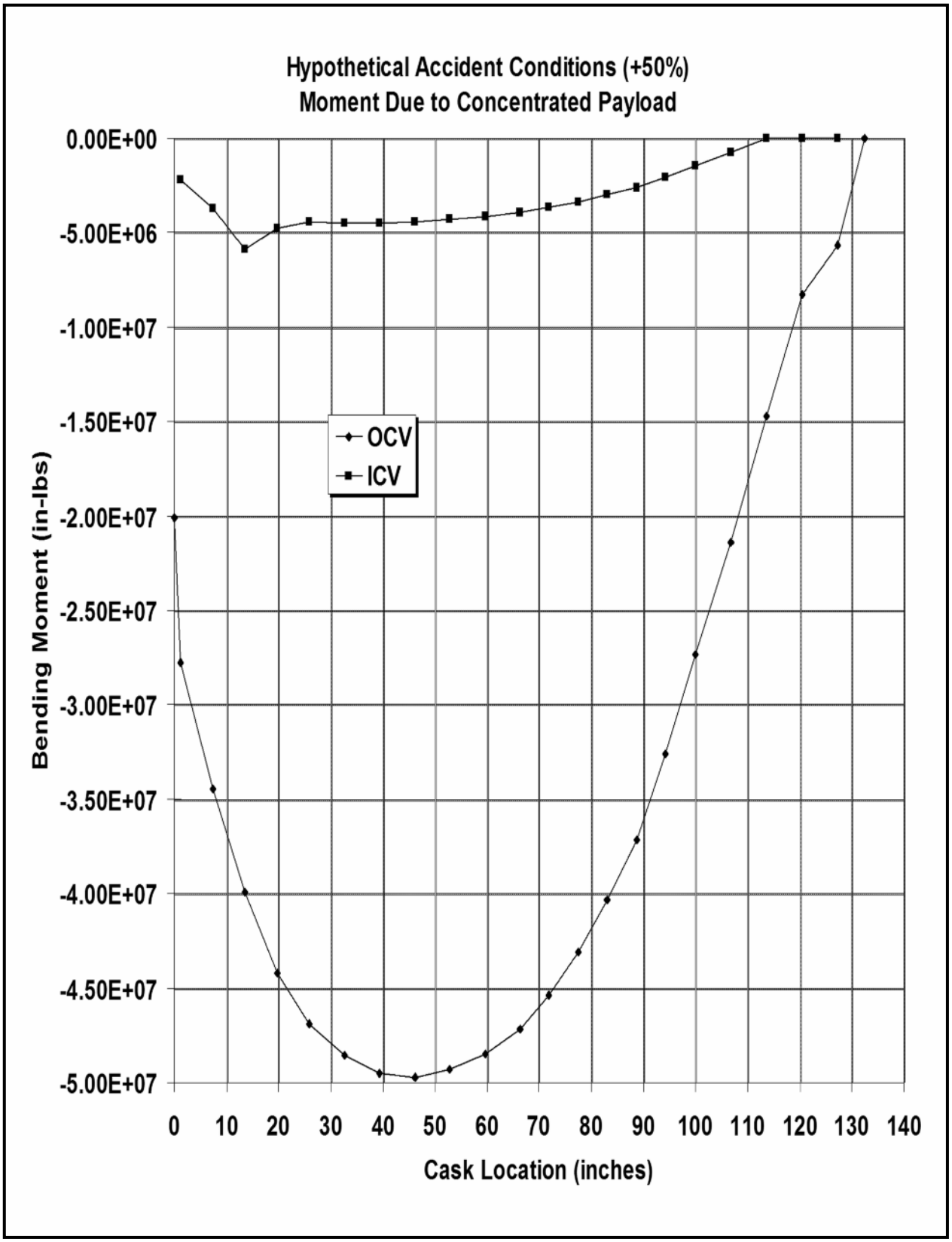

Figure 2.7-17 – HAC Cold (-20 ºF) Moment Due to a Concentrated Payload

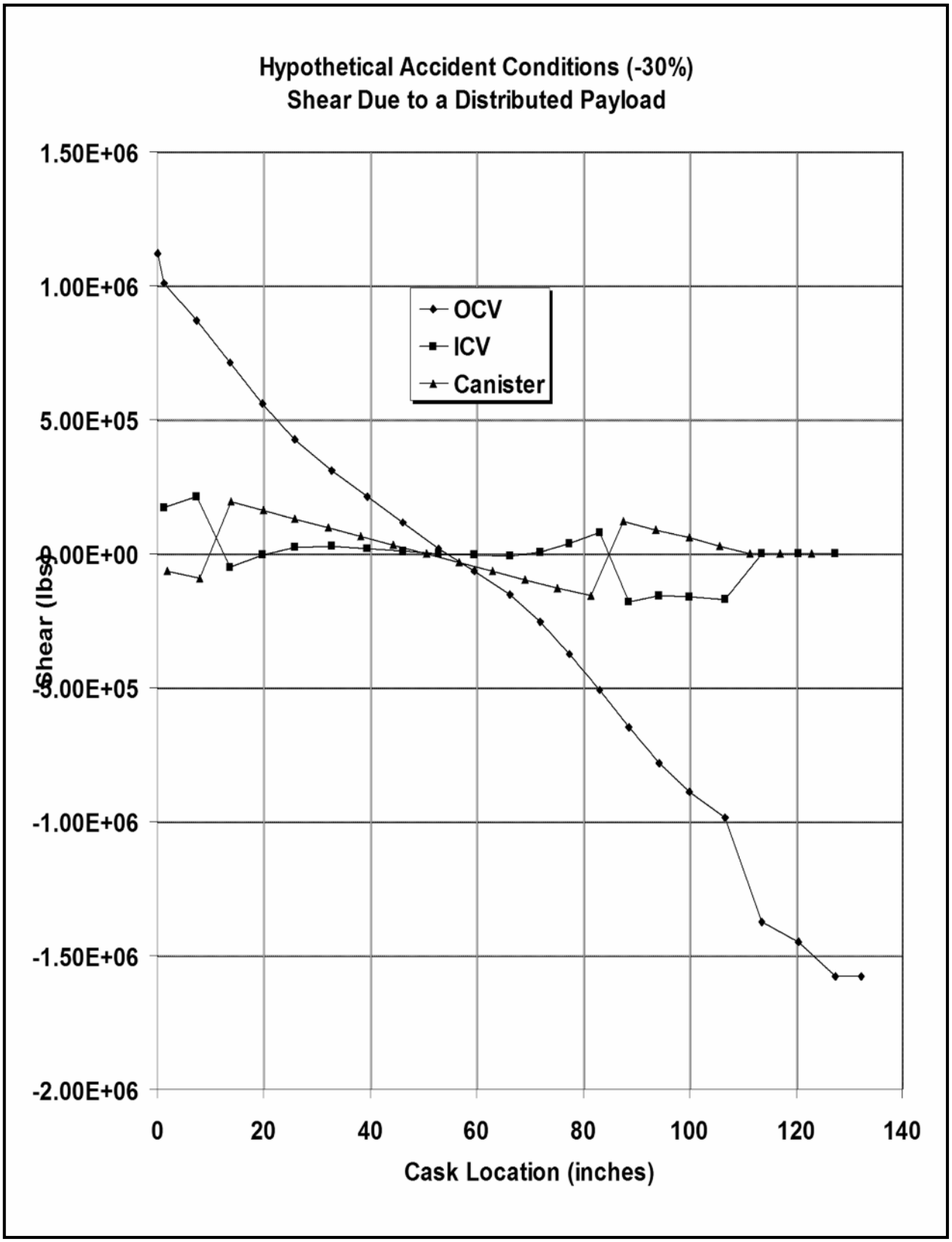

Figure 2.7-18 – HAC Hot (140 ºF) Shear Due to a Distributed Payload

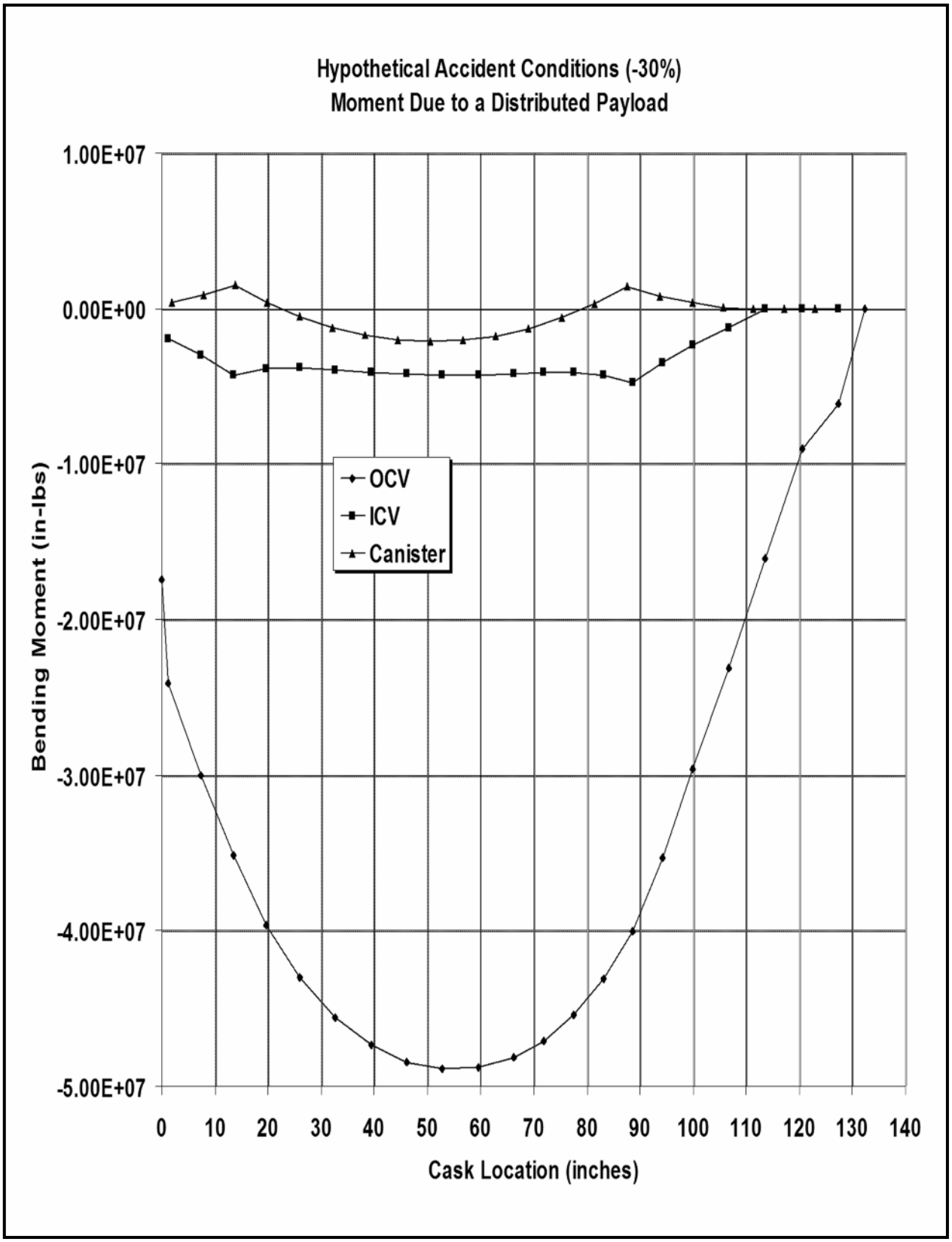

Figure 2.7-19 – HAC Hot (140 ºF) Moment Due to a Distributed Payload

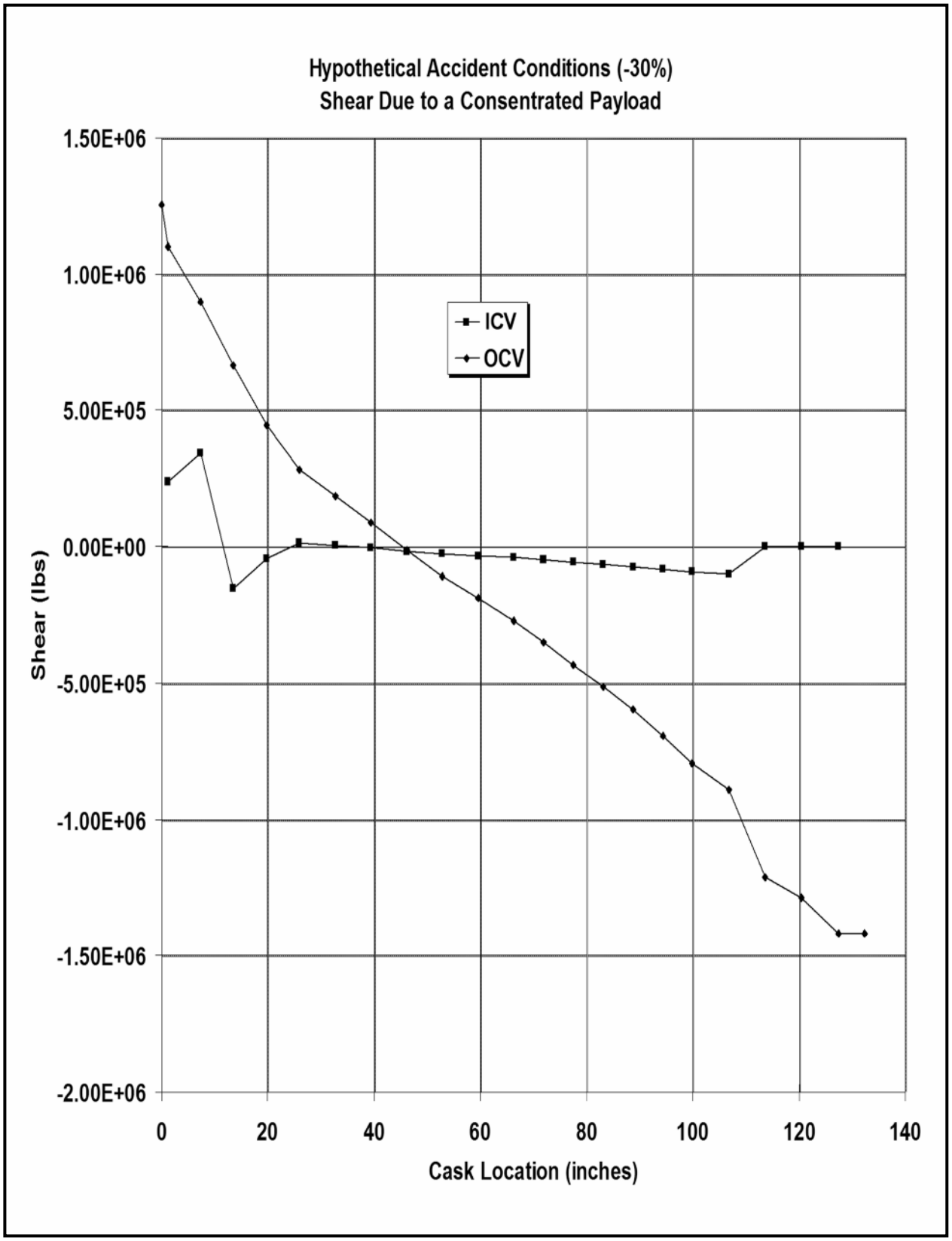

Figure 2.7-20 – HAC Hot (140 ºF) Shear Due to a Concentrated Payload

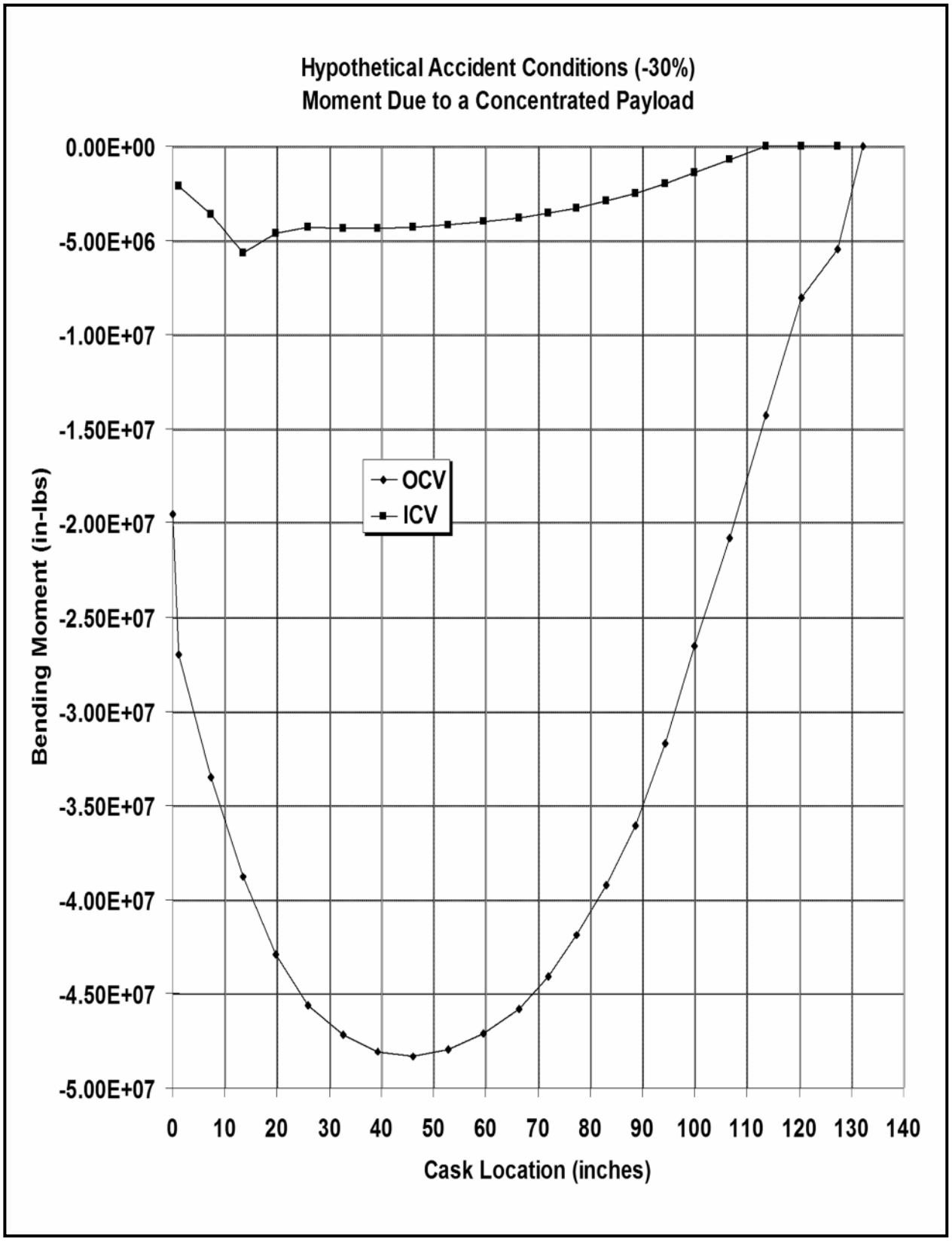

Figure 2.7-21 – HAC Hot (140 ºF) Moment Due to a Concentrated Payload

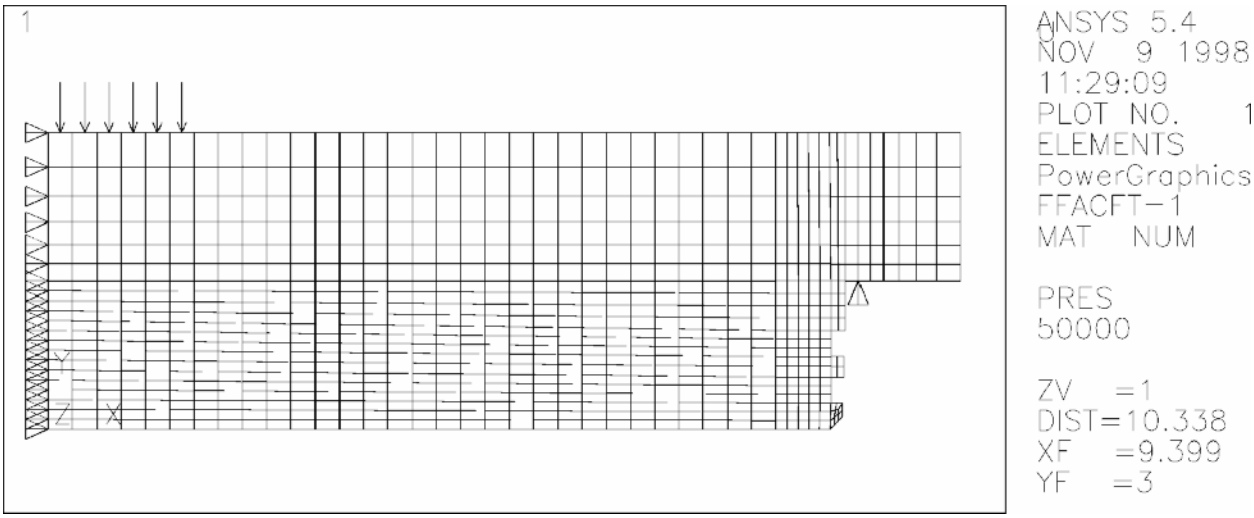

Figure 2.7-22 – Finite Element Model for Puncture on the OC Lid

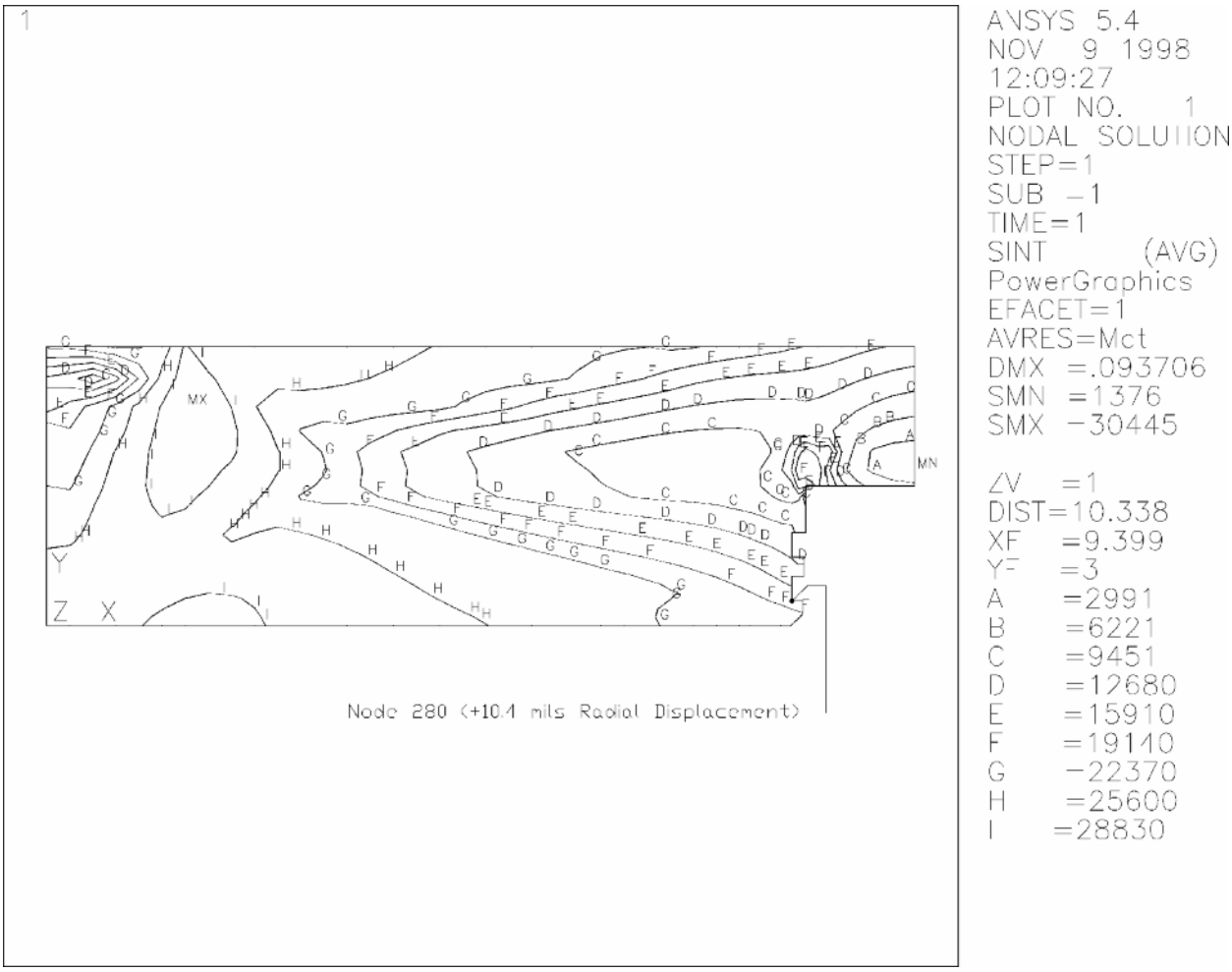

Figure 2.7-23 – Stress and Deformation for Puncture on the OC Lid

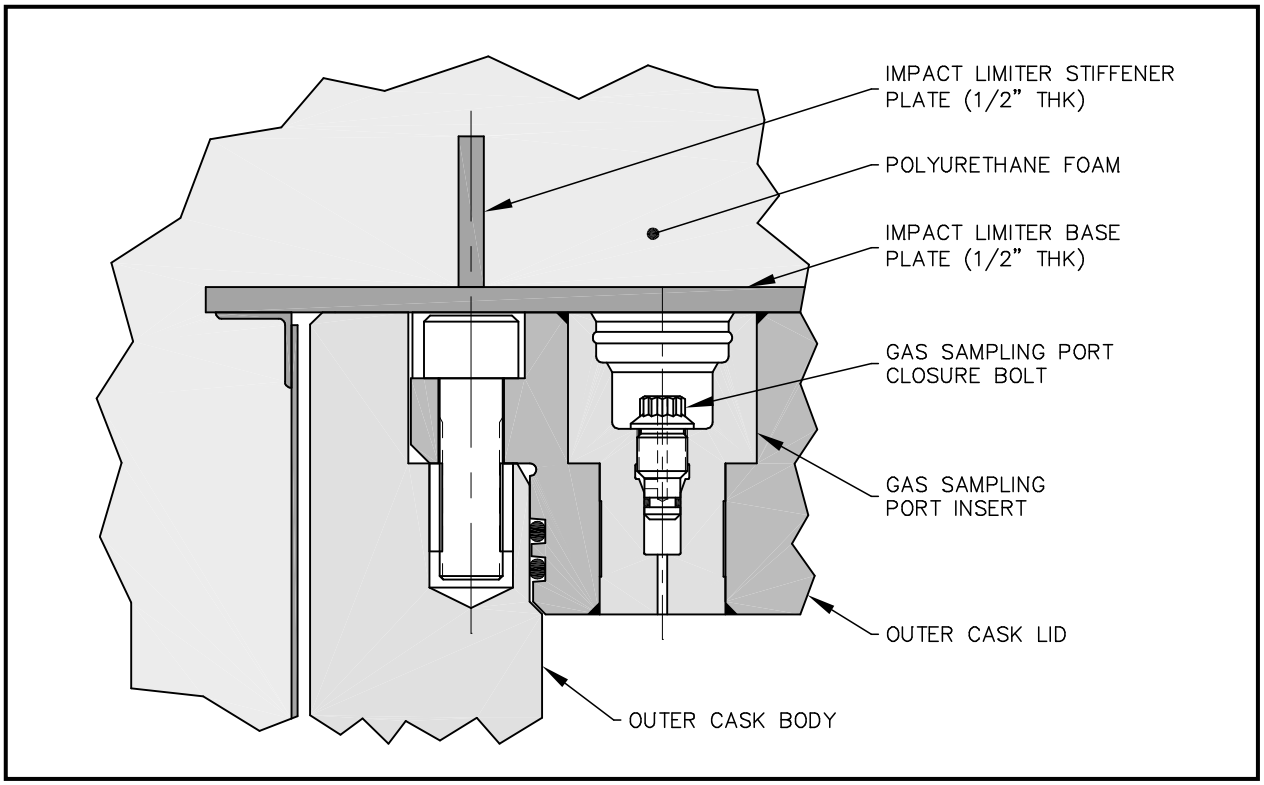

Figure 2.7-24 – OC Gas Samping Port Region

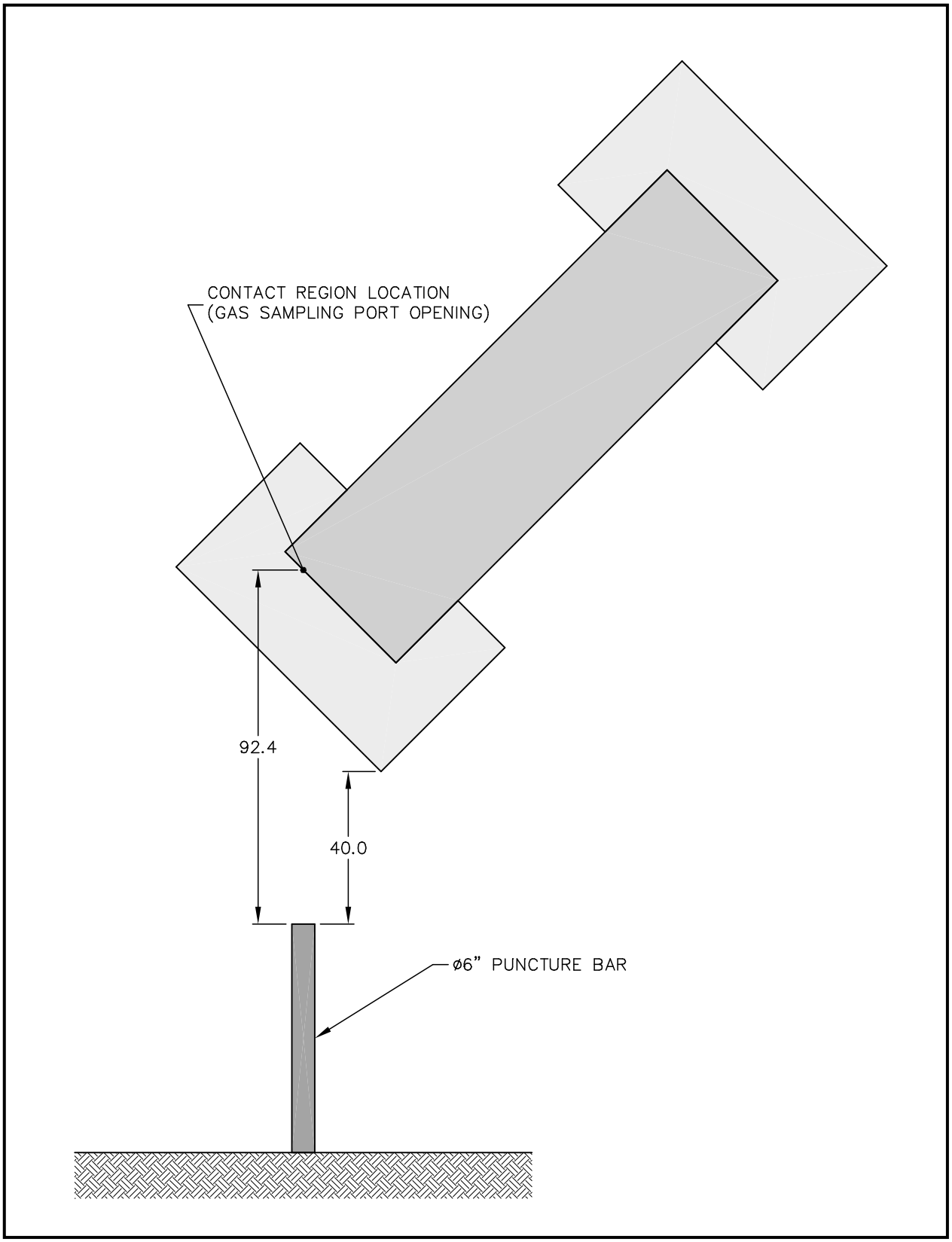

Figure 2.7-25 – Package Orientation for the Puncture Drop

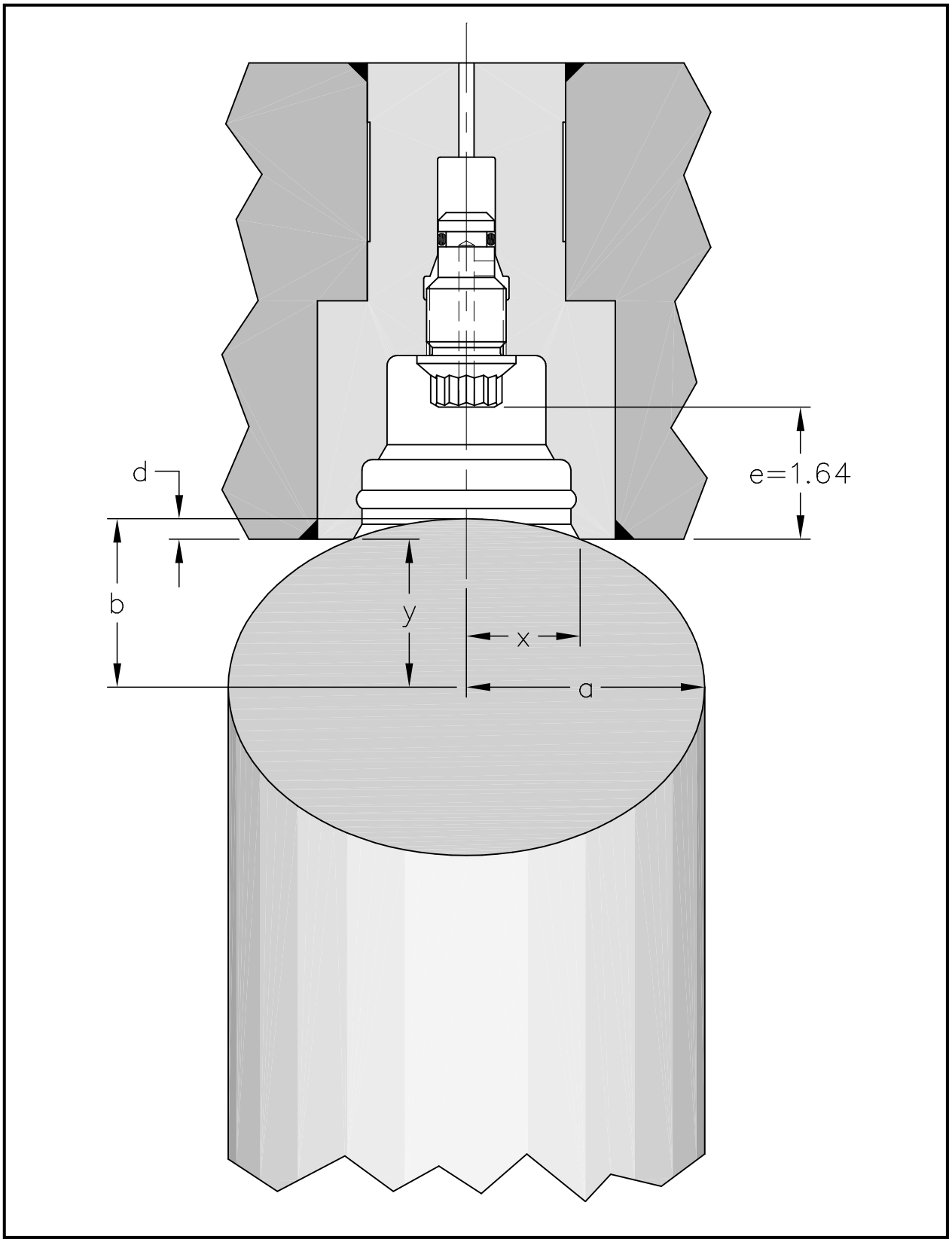

Figure 2.7-26 – Geometry of the Puncture Bar at the Gas Sampling Port

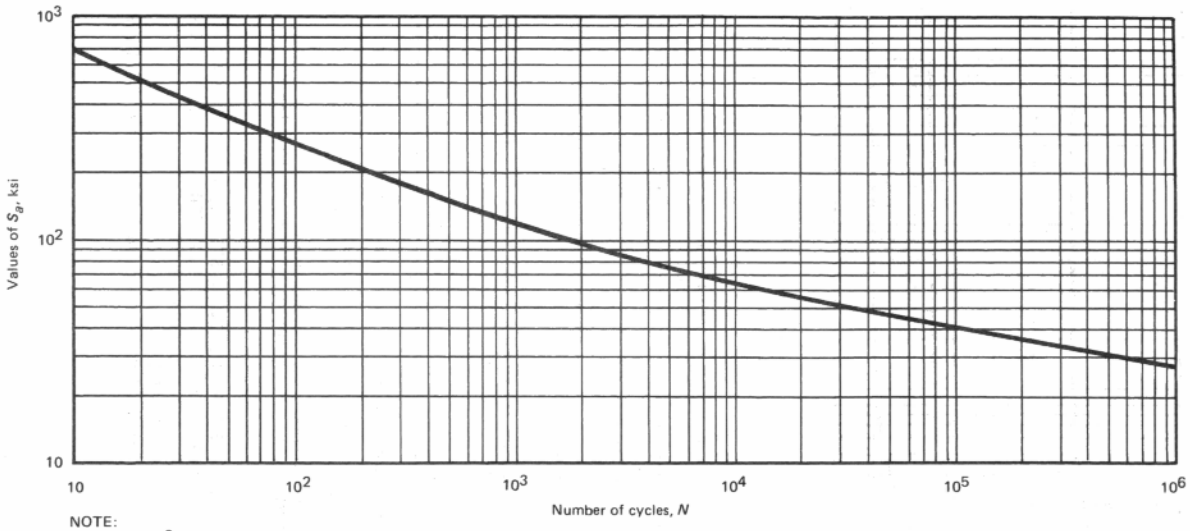

NOTE:
E = 28.3 X 10^6 psi

FIG. I-9.2.1 DESIGN FATIGUE CURVE FOR AUSTENITIC STEELS, NICKEL-CHROMIUM-IRON ALLOY, NICKEL–IRON–CHROMIUM ALLOY, AND NICKEL–COPPER ALLOY FOR S_a > 28.2 ksi, FOR TEMPERATURES NOT EXCEEDING 800°F
(For $S_a \leq$ 28.2 ksi, use Fig. I-9.2.2.)
Table I-9.1 Contains Tabulated Values and a Formula for Accurate Interpolation of This Curve

TABLE I-9.1
TABULATED VALUES OF S_a, ksi, FROM FIGS. I-9.0[1,2]

		Number of Cycles [Note (3)]																	
Figure	Curve	1E1	2E1	5E1	1E2	2E2	5E2	8.5E2 [Note (4)]	1E3	2E3	5E3	1E4	1.2E4 [Note (4)]	2E4	5E4	1E5	2E5	5E5	1E6
I-9.1	UTS 115–130 ksi	420	320	230	175	135	100	. . .	78	62	49	44	43	36	29	26	24	22	20
I-9.1	UTS ≤80 ksi	580	410	275	205	155	105	. . .	83	64	48	38	. . .	31	23	20	16.5	13.5	12.5
I-9.2.1	. . .	708	512	345	261	201	148	. . .	119	97	76	64	. . .	55.5	46.3	40.8	35.9	31	28.3
I-9.2.2 (see Table I-9.2.2)																			
I-9.3	S_y = 18.0 ksi	260	190	125	95	73	52	. . .	44	36	28.5	24.5	. . .	21	17	15	13.5	12.5	12.0
I-9.3	S_y = 30.0 ksi	260	190	125	95	73	52	. . .	44	36	28.5	24.5	. . .	19.5	15	13	11.5	9.5	9.0
I-9.3	S_y = 45.0 ksi	260	190	125	95	73	52	46	39	24.5	15.5	12	. . .	9.6	7.7	6.7	6.0	5.2	5.0
I-9.4	MNS ≤2.7S_m [Note (5)]	1150	760	450	320	225	143	. . .	100	71	45	34	. . .	27	22	19	17	15	13.5
I-9.4	MNS = 3S_m [Note (5)]	1150	760	450	300	205	122	. . .	81	55	33	22.5	. . .	15	10.5	8.4	7.1	6	5.3

NOTES:
(1) All notes on the referenced figures apply to these data.
(2) Interpolation between tabular values is permissible based upon data representation by straight lines on a log-log plot. Accordingly, for $S_i > S > S_j$

$$\frac{N}{N_j} = \left(\frac{N_i}{N_j}\right)^{[\log(S_i/S)]/\log(S_i/S_j)}$$

where S, S_i, and S_j are values of S_a; N, N_i, and N_j are corresponding numbers of cycles from design fatigue data.
Example: From the data given in the Table above, use the interpolation formula above to find the number of cycles N for S_a = 53.5 ksi when UTS ≤ 80 ksi in Fig. I-9.1:

$$\frac{N}{2000} = \left(\frac{5000}{2000}\right)^{\log(64/53.5)/\log(64/48)}$$

$$N = 3540 \text{ cycles}$$

(3) The number of cycles indicated shall be read as follows: IEJ = I × 10^J, e.g., 5E2 = 5 × 10^2 or 500.
(4) These data points are included to provide accurate representation of curves at branches or cusps.
(5) MNS is the Maximum Nominal Stress.

Figure 2.7-27 – Figure I-9.2.1 from Appendix I of the ASME Code

2.8 Special Form

Since the package is demonstrated to be leaktight and fully capable of meeting the requirements for a Type B package, no credit is taken for any special form characteristics the contents may possess.

This page intentionally left blank.

2.9 Fuel Rods

Since fuel rods are not transported within the RH-TRU 72-B package, this section does not apply.

This page intentionally left blank.

2.10 Appendices

2.10.1 *Finite Element Analysis (FEA) Models*

2.10.2 *Drop Analysis Codes Description*

2.10.3 *Drop Impact Evaluation Results*

2.10.4 *Slapdown Assessment*

2.10.5 *Buckling Design Criteria and Detailed Evaluation*

2.10.6 *Closure Bolt Stress Evaluations*

2.10.7 *Static and Dynamic Testing*

2.10.8 *Fabrication Stresses Due to Lead Pour*

This page intentionally left blank.

2.10.1 Finite Element Analysis (FEA) Models

The finite element analyses presented in the following subsections are performed using the ANSYS® finite element analysis program[1], with the exception of Appendix 2.10.1.4, *Containment Assembly Analysis for Oblique Drops*, and Appendix 2.10.1.5, *Containment Assembly Analysis for Side Drops*, where an earlier version of the ANSYS® finite element analysis program[2] is used. *Data Package for the RH-TRU 72-B Waste Shipping Package*[3] contains additional information regarding the finite element analyses and results for Appendix 2.10.1.4, *Containment Assembly Analysis for Oblique Drops*. Modeling details, including input file listings, are provided for case verification.

2.10.1.1 *Tie-down Trunnion Analysis*

2.10.1.2 *Inner Vessel Radius Transition Zone Stresses Due to Pressure*

2.10.1.3 *Inner Vessel Radius Transition Zone Stresses Due to 1g Acceleration*

2.10.1.4 *Containment Assembly Analysis for Oblique Drops*

2.10.1.5 *Containment Assembly Analysis for Side Drops*

2.10.1.1 Tie-down Trunnion Analysis

As shown in Figure 2.10.1-1, the model is comprised of half the outer cask (OC) outer shell and one center-pivot trunnion utilizing approximately 11,000 SOLID92, three-dimensional, 10-node tetrahedral solid elements. SOLID92 elements have a quadratic displacement behavior and are well suited to model irregular meshes and curved surfaces, providing exceptional accuracy for this application. Each element is defined by 10 nodes having three degrees of freedom at each node: translations in the nodal x-, y-, and z-directions.

Circumferential displacement constraints are applied at the symmetry boundary, and each end of the OC shell is constrained from displacing in all directions to simulate rigid ends.

As discussed in Section 2.5.2.1, *Center-Pivot and Tie-down Trunnion Loads*, a longitudinal force of 264,050 pounds, a transverse force of 225,000 pounds, and a vertical force of 54,931 pounds are applied simultaneously to the center-pivot trunnion. As shown in Figure 2.10.1-2, both the longitudinal and vertical forces are applied as cosine-distributed loads to simulate interaction with the corresponding center-pivot trunnion trailer interface, at the center of a 2½-inch wide bearing area that interfaces with the transporter support system, as shown in Figure 2.5-17 of Section 2.5.2.2, *OC Outer Shell Stresses*. Although transverse loads are reacted by the trunnion base, the transverse force is conservatively applied as a pressure load to the 12-inch diameter center-pivot trunnion face.

[1] ANSYS®, Inc., Revision Release 8.0A01, UP20031124, Houston, PA.

[2] ANSYS®, Inc., *ANSYS Engineering Analysis System User's Manual*, Report 1082, June 1, 1997, Version 940.

[3] U.S. Department of Energy, *Data Package for the RH-TRU 72-B Waste Shipping Package*, Current Revision, U.S. Department of Energy, Carlsbad Field Office, Carlsbad, New Mexico.

As shown in Figure 2.10.1-3, the maximum membrane-plus-bending stress intensity in the OC outer shell is 21,892 psi. For the case of a 2*g* only vertical force of 54,931 pounds, the maximum stress intensity in the outer shell is 1,972 psi.

In addition, stresses are linearized at the three locations exhibiting the highest stress intensity peaks: 1) at the top-right corner of the center-pivot trunnion base, 2) at the bottom-right corner of the center-pivot trunnion base, and 3) at the top-right end of the cylinder (i.e., location of highest stress). Stress linearization is performed to extract the maximum membrane stress intensity for the excessive tie-down load evaluation. As shown in Figure 2.10.1-4, the maximum membrane stress intensity is 12,040 psi.

The ANSYS® input file is provided in Table 2.10.1-1.

Table 2.10.1-1 – Input Listing for Trunnion Loading the OC Outer Shell

```
/PREP7                                                          ! Enter the pre-processing module
/UNITS,       BIN                                               ! Specify British (inches) for units

/TITLE,OC Outer Shell Stresses with Center-Pivot Trunnion Tie-down Loads

ET,       1,    SOLID92                                         ! Cylindrical outer shell
ET,       2,    SOLID92                                         ! Trunnion base
ET,       3,    SOLID92                                         ! Trunnion

MP,      EX,    1,         27900000                             ! Properties for stainless steel
MP,    NUXY,    1,           0.3000

K,      100,     0.0000,     0.0000,     0.0000                 ! Define the cylindrical shell keypoints
K,      101,     0.0000,   -20.5625,     0.0000
K,      102,    20.5625,     0.0000,     0.0000
K,      103,     0.0000,    20.5625,     0.0000
K,      104,     0.0000,   -19.0625,     0.0000
K,      105,    19.0625,     0.0000,     0.0000
K,      106,     0.0000,    19.0625,     0.0000

LARC,         101,  102,  100,    20.5625                       ! Define the shell lines
LARC,         102,  103,  100,    20.5625
LARC,         104,  105,  100,    19.0625
LARC,         105,  106,  100,    19.0625
L,            101,  104
L,            103,  106

AL,             1,    2,    3,    4,    5,    6                 ! Define the end-of-cylinder area

VOFFST,         1,  -120.0000,    6                             ! Extrude the area to form a volume

K,      113,    21.5938,     9.0000,   -46.0000                 ! Define the trunnion base keypoints
K,      114,    21.5938,    -9.0000,   -46.0000
K,      115,    21.5938,     9.0000,   -74.0000
K,      116,    21.5938,    -9.0000,   -74.0000

L,            113,  114                                         ! Define the trunnion base lines
L,            115,  116
L,            113,  115
L,            114,  116

AL,            19,   20,   21,   22                             ! Define the trunnion base area

VOFFST,         9,    -6.0000,    4                             ! Extrude the area to form a volume

VSBV,           1,    2, SEPO, KEEP, KEEP                       ! Cut the trunnion base at the shell outer surface
VSBV,           1,    3, SEPO, KEEP, KEEP
ASEL,           S, AREA,     ,   27,   28,    1
VSBA,           2,  ALL, SEPO, DELE, KEEP
VDELE,          1,    6,    5
ASEL,         ALL
VGLUE,          3,    4,    5

NUMCMP,      LINE                                               ! Compress line, area, and volume numbering for convenience
NUMCMP,      AREA
NUMCMP,      VOLU

LOCAL,         11,    1,    24.5000,     0.0000,   -60.0000,     ,     ,   90 ! Define the trunnion keypoints
K,      200,     0.0000,     0.0000,     0.0000
K,      201,     6.0000,     0.0000,     0.0000
KGEN,          24,  201,  201,    0,     0.0000,    15.0000,     0.0000,    1
KGEN,           2,  200,  224,    1,     0.0000,     0.0000,    -1.2500,  100
KGEN,           2,  300,  324,    1,     0.0000,     0.0000,    -3.0000,  100

LARC,         201,  202,  200,     6.0000                       ! Define the trunnion lines
*REPEAT,       23,    1,    1,    0,    0
LARC,         224,  201,  200,     6.0000
LARC,         301,  302,  300,     6.0000
*REPEAT,       23,    1,    1,    0
LARC,         324,  301,  300,     6.0000
LARC,         401,  402,  400,     6.0000
*REPEAT,       23,    1,    1,    0
LARC,         424,  401,  400,     6.0000
L,            201,  301
*REPEAT,       24,    1,    1
L,            301,  401
*REPEAT,       24,    1,    1
L,            200,  201
L,            200,  207
L,            200,  213
L,            200,  219
L,            300,  301
L,            300,  307
L,            300,  313
L,            300,  319
L,            400,  401
L,            400,  407
L,            400,  413
L,            400,  419
L,            200,  300
L,            300,  400

AL,            80,  152,  104,  153                             ! Define the trunnion areas
*REPEAT,       23,    1,    1,    1,    1
```

```
AL,          103,  175,  127,  152
AL,          104,  176,  128,  177
*REPEAT,      23,    1,    1,    1,    1
AL,          127,  199,  151,  176
AL,          200,   80,   81,   82,   83,   84,   85,  201
AL,          201,   86,   87,   88,   89,   90,   91,  202
AL,          202,   92,   93,   94,   95,   96,   97,  203
AL,          203,   98,   99,  100,  101,  102,  103,  200
AL,          204,  104,  105,  106,  107,  108,  109,  205
AL,          205,  110,  111,  112,  113,  114,  115,  206
AL,          206,  116,  117,  118,  119,  120,  121,  207
AL,          207,  122,  123,  124,  125,  126,  127,  204
AL,          208,  128,  129,  130,  131,  132,  133,  209
AL,          209,  134,  135,  136,  137,  138,  139,  210
AL,          210,  140,  141,  142,  143,  144,  145,  211
AL,          211,  146,  147,  148,  149,  150,  151,  208
AL,          152,  204,  212,  200
*REPEAT,       4,    6,    1,    0,    1
AL,          176,  208,  213,  204
*REPEAT,       4,    6,    1,    0,    1

VA,           85,   37,   38,   39,   40,   41,   42,   89,   97,   98       ! Define the trunnion volumes
*REPEAT,       3,    1,    6,    6,    6,    6,    6,    6,    1,    1,    1
VA,           88,   55,   56,   57,   58,   59,   60,   92,  100,   97
VA,           89,   61,   62,   63,   64,   65,   66,   93,  101,  102
*REPEAT,       3,    1,    6,    6,    6,    6,    6,    6,    1,    1,    1
VA,           92,   79,   80,   81,   82,   83,   84,   96,  104,  101

VSEL,          S, VOLU,     ,    8,   11,    1                        ! Cut the trunnion at the trunnion base
VSBA,        ALL,   27, SEPO, DELE, KEEP
VDELE,        16,   19,    1
VSEL,        ALL
VGLUE,       ALL

SMRTSIZE,       3                                                     ! Mesh the volumes into elements
VATT,           1,    1,    3
VMESH,          4,    7,    1
VMESH,         12,   15,    1
VATT,           1,    1,    2
VMESH,          8
VATT,           1,    1,    1
VMESH,          2,    3,    1

*AFUN,       DEG                                                      ! Use degrees for angular calculations
LT = 0                                                                ! Begin calculating the cosine distribution of lengths
*DO,            I,  308,  318,    1                                   ! Total the cosine lengths
   LT = LT + ABS(COS(KY(I)))
*ENDDO

TFX = 264050                                                          ! Define the total longitudinal force
*DO,            I,  308,  318,    1                                   ! Assign forces to the associated keypoints
   FKX = TFX*ABS(COS(KY(I)))/LT
   FK,          I,   FZ, -FKX
*ENDDO

TFZ = 54931                                                           ! Define the total vertical force
*DO,            I,  314,  324,    1                                   ! Assign forces to the associated keypoints
   FKZ = TFZ*ABS(SIN(KY(I)))/LT
   FK,          I,   FY,  FKZ
*ENDDO

TFY = 225000                                                          ! Define the total transverse force
TAY = 113.0973                                                        ! Define the total transverse area
TPY = TFY/TAY                                                         ! Define the total transverse pressure
ASEL,           S, AREA,     ,   85,   88,    1                       ! Select the trunnion surface for the transverse pressure
SFA,         ALL,     , PRES,  TPY

CSYS,           0                                                     ! Transfer back to the global cartesian coordinate system

NSEL,     S,  LOC,    Z,  -120.0000                                   ! Restrain axial nodes at the cylinder's free ends
NSEL,     A,  LOC,    Z,     0.0000
D,      ALL,   UZ,     0.0000,     ,     ,     ,   UX,   UY
NSEL,   ALL

NSEL,     S,  LOC,    X,     0.0000                                   ! Restrain hoop nodes at the cylinder's free ends
D,      ALL,   UX,     0.0000
NSEL,   ALL

SBCTRAN                                                               ! Transfer all loads from keypoints to nodes

WSORT,       ALL                                                      ! Reduce the solution wavefront

/RGB,       INDEX,  100,  100,  100,    0                             ! Invert colors (white background for output plot files)
/RGB,       INDEX,   80,   80,   80,   13
/RGB,       INDEX,   60,   60,   60,   14
/RGB,       INDEX,    0,    0,    0,   15

/DEV,        FONT,    1,Courier*New,  400,    0,  -16,    0,    0        Set the font sizes
/DEV,        FONT,    2,      Arial,  400,    0,  -13,    0,    0
/DEV,        FONT,    3,      Arial,  400,    0,  -13,    0,    0

TIFF,        COMP,    1                                               ! Set the graphics file parameters
TIFF,       ORIEN,HORIZ
TIFF,       COLOR,    2
TIFF,        TMOD,    1
/GFILE,      1800

/WINDOW,        1,   -1.0000,     1.6700,    -0.9260,     0.9260      ! Set the graphics window size to 9.00 x 6.25 ratio
```

```
/FOCUS,        1,   16.2700,    1.4100,   -53.5300                  ! Set the graphics window parameters
/DIST,         1,   34.0000
/VIEW,         1,    0.6500,    0.2400,     0.7200
/ANGLE,        1,    0.0000

/PNUM,      TYPE,   1                                               ! Show the elements types as different colors
/NUMBER,       1                                                    ! Turn on element colors only

EPLOT                                                               ! Plot elements to the screen
/SHOW,       PNG
EPLOT                                                               ! Plot elements to a file
/SHOW,     CLOSE

/FOCUS,        1,   15.4400,    0.0000,   -60.0000                  ! Set the graphics window parameters
/DIST,         1,   10.7700
/VIEW,         1,    1.0000,    0.0000,     0.0000
/ANGLE,        1,    0.0000

/PBC,          F,   1                                               ! Display applied forces
/NUMBER,      -1                                                    ! Turn off element numbers and colors

EPLOT                                                               ! Plot elements to the screen
/SHOW,       PNG
EPLOT                                                               ! Plot elements to a file
/SHOW,     CLOSE

FINISH

/SOLUTION                                                           ! Enter the solution module

ANTYPE, STATIC                                                      ! Specify a static problem
SOLCONTROL,    ON,   ON                                             ! Set solution controls

SOLVE                                                               ! Solve the problem

FINISH

/POST1                                                              ! Enter the post-processing module

SET,   LAST                                                         ! Retrieve the final load step's data

/GROPT,      AXDV,   ON                                             ! Define linerized stress graph parameters
/GROPT,      AXNM,   ON
/GROPT,     AXNSC,    1
/GROPT,     ASCAL,   ON
/GROPT,      LOGX,  OFF
/GROPT,      LOGY,  OFF
/GROPT,      FILL,  OFF
/GROPT,     CGRID,   ON
/GROPT,      DIG1,    6
/GROPT,      DIG2,    0
/GROPT,      REVX,  OFF
/GROPT,      REVY,  OFF
/GROPT,      DIVX
/GROPT,      DIVY,   11
/GROPT,      LTYP,    0
/AXLAB,         X
/AXLAB,         Y
/GTHK,       AXIS,    2
/GTHK,       GRID,    1
/GTHK,      CURVE,    3
/GRTYP,               0
/GRID,                3
/XRANGE,        DEFAULT
/YRANGE,              0,22000,    0

/NUMBER,       0                                                    ! Turn on element numbers and colors

PATH,          P1,    2,   30,   20                                 ! Linerized stress intensity along Path 1
PPATH,          1, 1386                                             !  (top-right corner of trunnion base)
PPATH,          2, 2475
PMAP,          ACCURATE
/OUTPUT,       TRUNNION,  OUT                                       ! Write output to a file
PRSECT                                                              ! Print path stresses at this location
/OUTPUT
PLSECT,         S,  INT                                             ! Plot linearized stress intensity to the display
/SHOW,       PNG
PLSECT,         S,  INT                                             ! Plot linearized stress intensity to a file
/SHOW,     CLOSE

PATH,          P2,    2,   30,   20                                 ! Linerized stress intensity along Path 2
PPATH,          1, 1390                                             !  (bottom-right corner of trunnion base)
PPATH,          2, 2477
PMAP,          ACCURATE
/OUTPUT,       TRUNNION,  OUT,     ,     APPEND                      ! Write output to a file
PRSECT                                                              ! Print path stresses at this location
/OUTPUT
PLSECT,         S,  INT                                             ! Plot linearized stress intensity to the display
/SHOW,       PNG
PLSECT,         S,  INT                                             ! Plot linearized stress intensity to a file
/SHOW,     CLOSE

PATH,          P3,    2,   30,   20                                 ! Linerized stress intensity along Path 3
PPATH,          1, 9528                                             !  (top-right of cylindrical shell)
PPATH,          2, 9683
PMAP,          ACCURATE
/OUTPUT,       TRUNNION,  OUT,     ,     APPEND                      ! Write output to a file
PRSECT                                                              ! Print path stresses at this location
/OUTPUT
```

```
PLSECT,         S,  INT                                          ! Plot linearized stress intensity to the display
/SHOW,        PNG
PLSECT,         S,  INT                                          ! Plot linearized stress intensity to a file
/SHOW,      CLOSE

/GRAPHICS,   FULL                                                ! Disable PowerGraphics

/FOCUS,         1,    16.2700,     1.4100,   -53.5300            ! Set the graphics window parameters
/DIST,          1,    34.0000
/VIEW,          1,     0.6500,     0.2400,     0.7200
/ANGLE,         1,     0.0000
/DSCALE,        1,     1.0000                                    ! Set displacment scaling to 1

ESEL,           S, TYPE,     ,    1                              ! Select the outer shell elements

PLNSOL,        SI                                                ! Plot stress intensity to the screen
/SHOW,        PNG
PLNSOL,        SI                                                ! Plot stress intensity to a file
/SHOW,      CLOSE
```

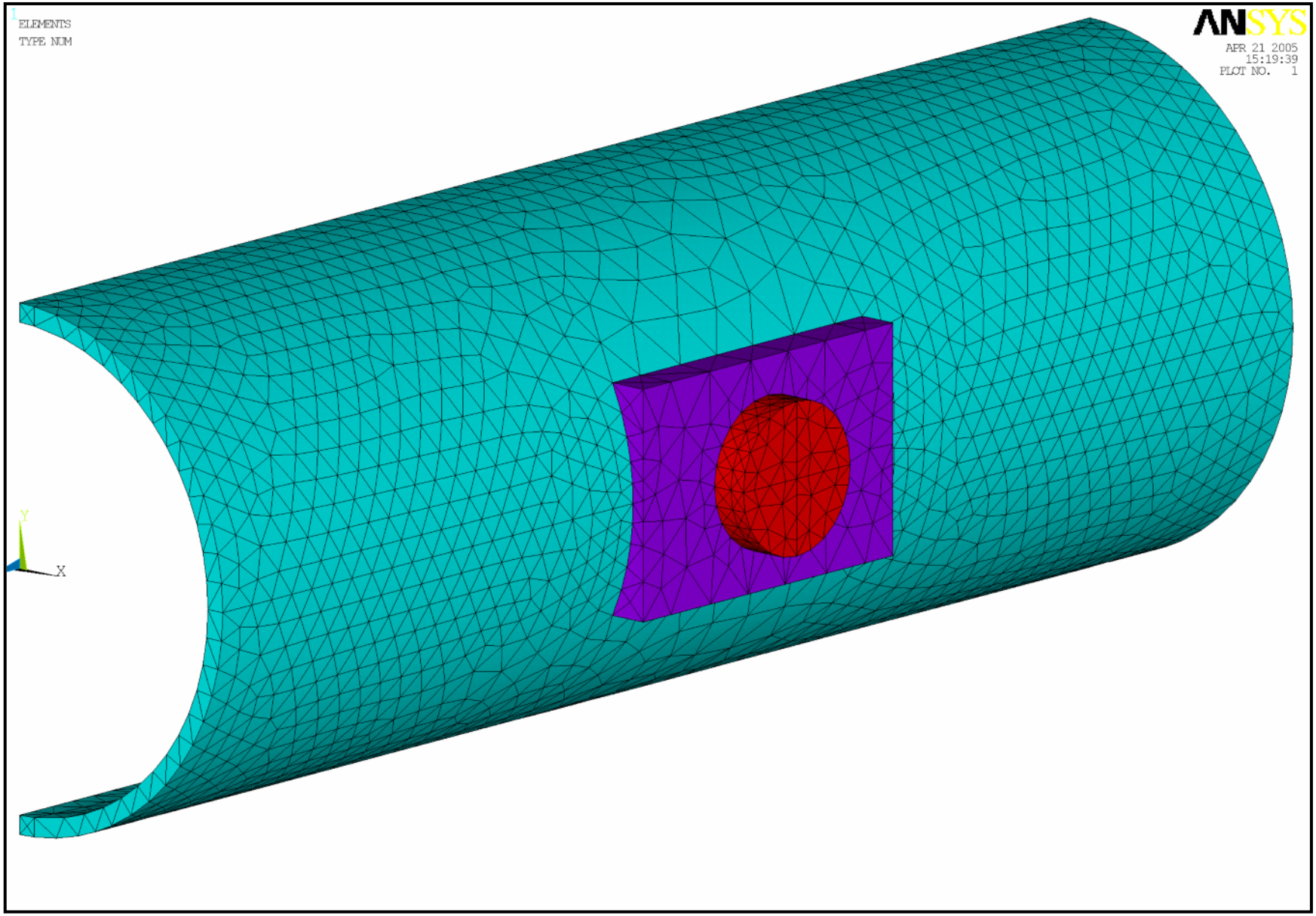

Figure 2.10.1-1 – Finite Element Analysis Model of the Center-Pivot Trunnion Interface

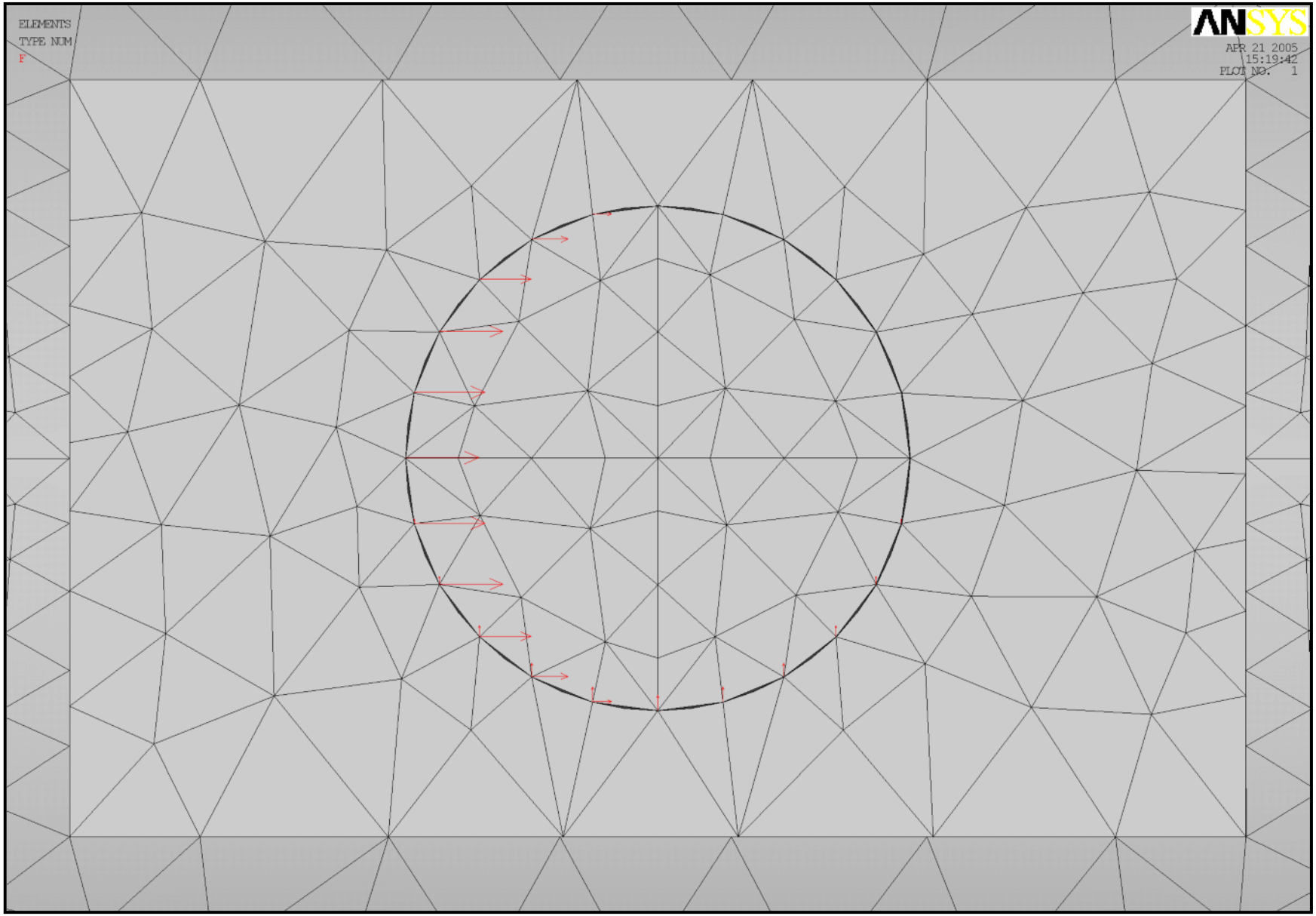

Figure 2.10.1-2 – Center-Pivot Trunnion Longitudinal and Vertical Cosine-Distributed Loads

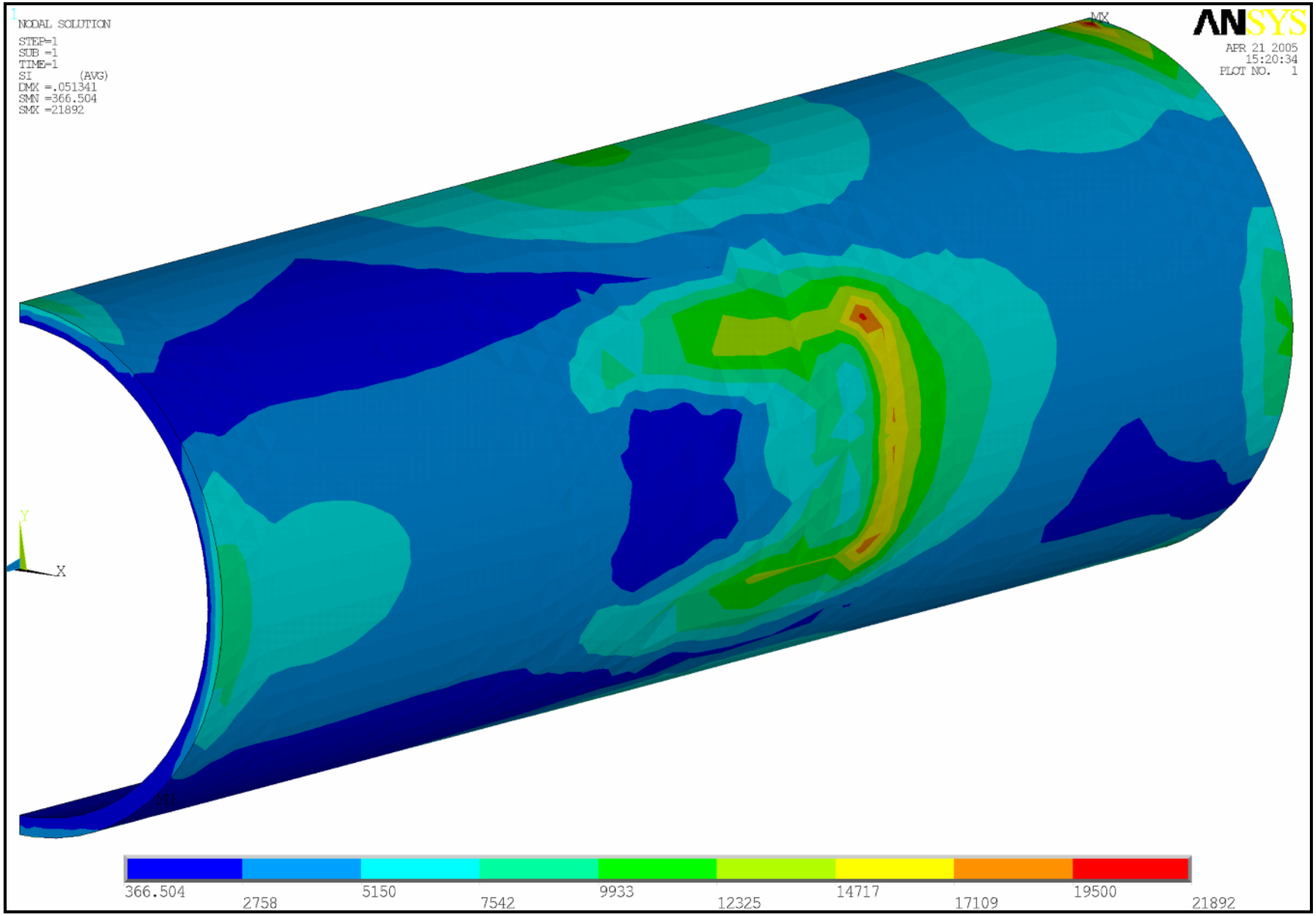

Figure 2.10.1-3 – OC Outer Shell Stress Intensities

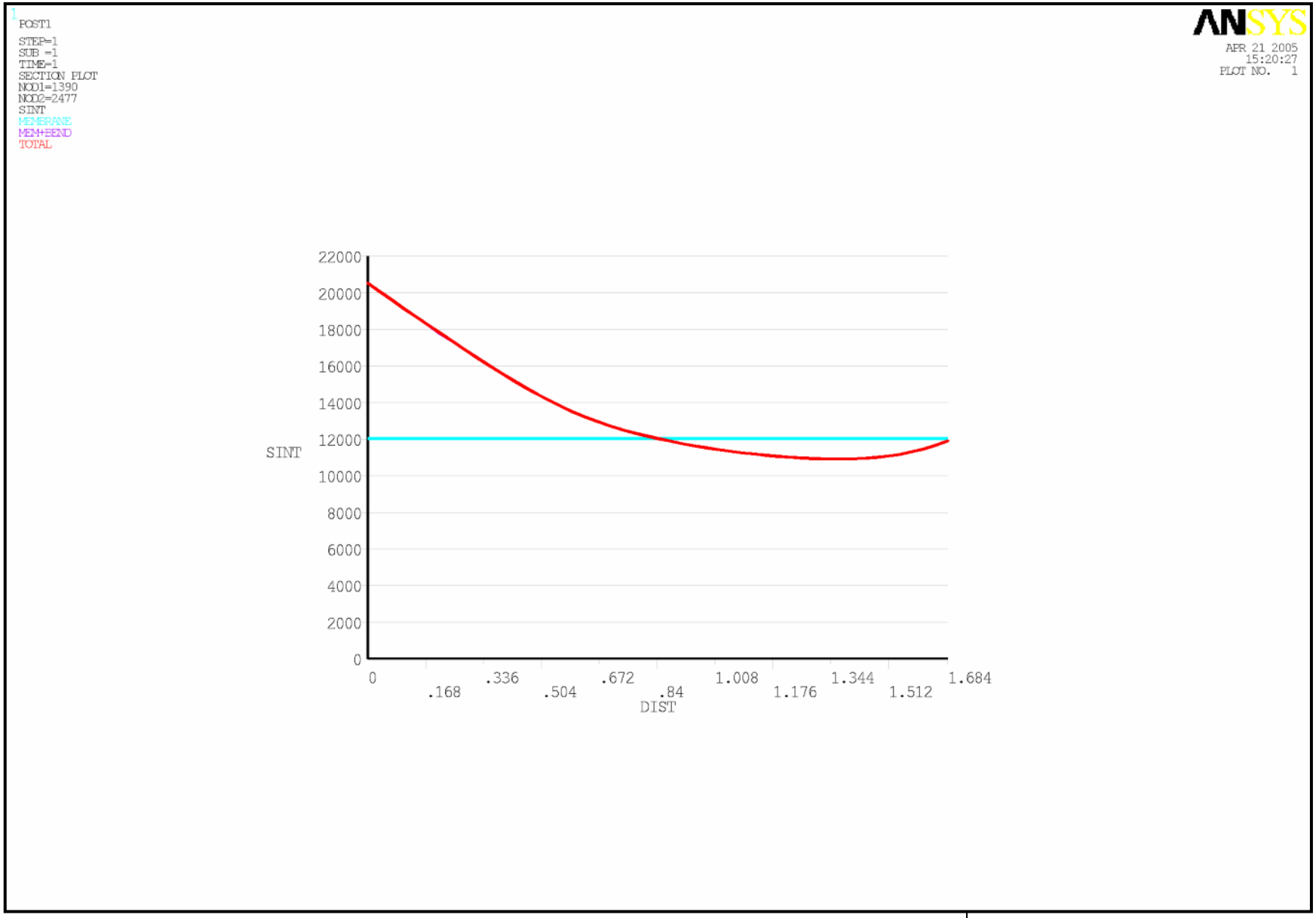

Figure 2.10.1-4 – Stress Intensity Linearization at the Bottom-Right Corner of the Trunnion Base

2.10.1.2 Inner Vessel Radius Transition Zone Stresses Due to Pressure

As shown in Figure 2.10.1-5, the model is comprised of the bottom transition in the inner vessel (IV) shell utilizing approximately 1,700 PLANE82, 8-node axisymmetric solid elements. PLANE82 elements have a quadratic displacement behavior and are well suited to model irregular meshes and curved surfaces, providing exceptional accuracy for this application. Each element is defined by 8 nodes having two degrees of freedom at each node: translations in the nodal x- and y-directions.

Radial displacement constraints are applied at the symmetry boundary, and the end of the IV shell is constrained from displacing in the axial direction.

An internal unit pressure of 1.0 psig is applied to the entire inside surface of the model.

As shown in Figure 2.10.1-6, the maximum stress intensity in the IV shell is 287 psi, occurring at the transition to the cylindrical shell. Stresses are linearized at this location to extract the maximum membrane and bending stress components in both the axial and hoop directions:

$$\sigma_1 = 21.67 \text{ psi (axial membrane stress)}$$

$$\sigma_2 = -37.74 \text{ psi (hoop membrane stress)}$$

$$\sigma_1' = -220.2 \text{ psi (axial bending stress)}$$

$$\sigma_2' = -68.66 \text{ psi (hoop bending stress)}$$

The ANSYS® input file is provided in Table 2.10.1-2.

Table 2.10.1-2 – Input Listing for IV Radius Transition Zone Stresses Due to Pressure

```
/PREP7                                                          ! Enter the pre-processing module

/UNITS,       BIN                                               ! Specify British (inches) for units

/TITLE,IV Shell Stresses at Bottom Corner Transition with 1-psig Internal Pressure

ET,       1,    PLANE82,     ,     ,    1                       ! Shell and Bottom

MP,      EX,    1,         27800000                             ! Properties for stainless steel
MP,    NUXY,    1,           0.3000

K,        1,     0.0000,     0.0000                             ! Define the keypoints
K,        2,    15.1250,     0.0000
K,        3,    16.0000,     0.0000
K,        4,    16.0000,     2.0000
K,        5,    16.0000,    13.5000
K,        6,     0.0000,     1.5000
K,        7,    15.1250,     1.5000
K,        8,    15.6250,     2.0000
K,        9,    15.6250,    13.5000
K,       10,    15.1250,     2.0000

L,              1,    2                                         ! Define the lines
*REPEAT,        4,    1,    1
L,              6,    7
LARC,           7,    8,   10,     0.5000
L,              8,    9
L,              1,    6
L,              2,    7
L,              4,    8
L,              5,    9

AL,             1,    9,    5,    8                             ! Define the bottom plate area
AL,             4,   11,    7,   10                             ! Define the cylinder area
AL,             2,    3,   10,    6,    9                       ! Define the transition area

SMRTSIZE,       2                                               ! Mesh the volumes into elements
LESIZE,         2,     ,     ,    9
```

```
LESIZE,         3,     ,     ,   21
LESIZE,         8,     ,     ,   16
LESIZE,         9,     ,     ,   16
LESIZE,        10,     ,     ,    4
LESIZE,        11,     ,     ,    4
AATT,           1,    1,    1
AMESH,          1
AMESH,          2
AMESH,          3

SFL,            5, PRES,     1.0000                                  ! Apply a unit pressure load to the inside surface
SFL,            6, PRES,     1.0000
SFL,            7, PRES,     1.0000

NSEL,     S,  LOC,    X,     0.0000                                  ! Restrain radial and axial nodes at the free ends
D,      ALL,   UX,     0.0000
NSEL,     S,  LOC,    Y,    13.5000
D,      ALL,   UY,     0.0000
NSEL,   ALL

SBCTRAN                                                              ! Transfer all loads from keypoints to nodes

WSORT,        ALL                                                    ! Reduce the solution wavefront

/RGB,       INDEX,  100,  100,  100,    0                            ! Invert colors (white background for output plot files)
/RGB,       INDEX,   80,   80,   80,   13
/RGB,       INDEX,   60,   60,   60,   14
/RGB,       INDEX,    0,    0,    0,   15

/DEV,        FONT,    1,Courier*New,  400,    0,  -16,    0,    0       Set the font sizes
/DEV,        FONT,    2,      Arial,  400,    0,  -13,    0,    0
/DEV,        FONT,    3,      Arial,  400,    0,  -13,    0,    0

PNGR,        COMP,    1                                              ! Set the graphics file parameters
PNGR,       ORIEN,HORIZ
PNGR,       COLOR,    2
PNGR,        TMOD,    1
/GFILE,      1800

/WINDOW,        1,    -1.0000,     1.6700,    -0.9260,     0.9260    ! Set the graphics window size to 9.00 x 6.25 ratio

/FOCUS,         1,     8.6120,     6.6770,     0.0000                ! Set the graphics window parameters
/DIST,          1,     7.5000
/VIEW,          1,     0.0000,     0.0000,     1.0000
/ANGLE,         1,     0.0000

EPLOT                                                                ! Plot elements to the screen
/SHOW,        PNG
EPLOT                                                                ! Plot elements to a file
/SHOW,      CLOSE

FINISH

/SOLUTION                                                            ! Enter the solution module

ANTYPE, STATIC                                                       ! Specify a static problem
SOLCONTROL,    ON,   ON                                              ! Set solution controls

SOLVE                                                                ! Solve the problem

FINISH

/POST1                                                               ! Enter the post-processing module

SET,   LAST                                                          ! Retrieve the final load step's data

PATH,          P1,    2,   30,   20                                  ! Linerized stress intensity along Path 1
PPATH,          1,    1                                              !  (center of IV bottom)
PPATH,          2,    3
PMAP,         ACCURATE
/OUTPUT,        IVPRES,  OUT                                         ! Write output to a file
PRSECT                                                               ! Print path stresses at this location
/OUTPUT

PATH,          P2,    2,   30,   20                                  ! Linerized stress intensity along Path 2
PPATH,          1, 5029                                              !  (top of radius transition in cylindrical shell)
PPATH,          2, 5087
PMAP,         ACCURATE
/OUTPUT,        IVPRES,  OUT,     ,     APPEND                       ! Write output to a file
PRSECT                                                               ! Print path stresses at this location
/OUTPUT

/GRAPHICS,   FULL                                                    ! Disable PowerGraphics

/FOCUS,         1,    14.0800,     1.2470,     0.0000                ! Set the graphics window parameters
/DIST,          1,     1.8000
/VIEW,          1,     0.0000,     0.0000,     1.0000
/ANGLE,         1,     0.0000

PLNSOL,        SI                                                    ! Plot stress intensity to the screen
/SHOW,        PNG
PLNSOL,        SI                                                    ! Plot stress intensity to a file
/SHOW,      CLOSE
```

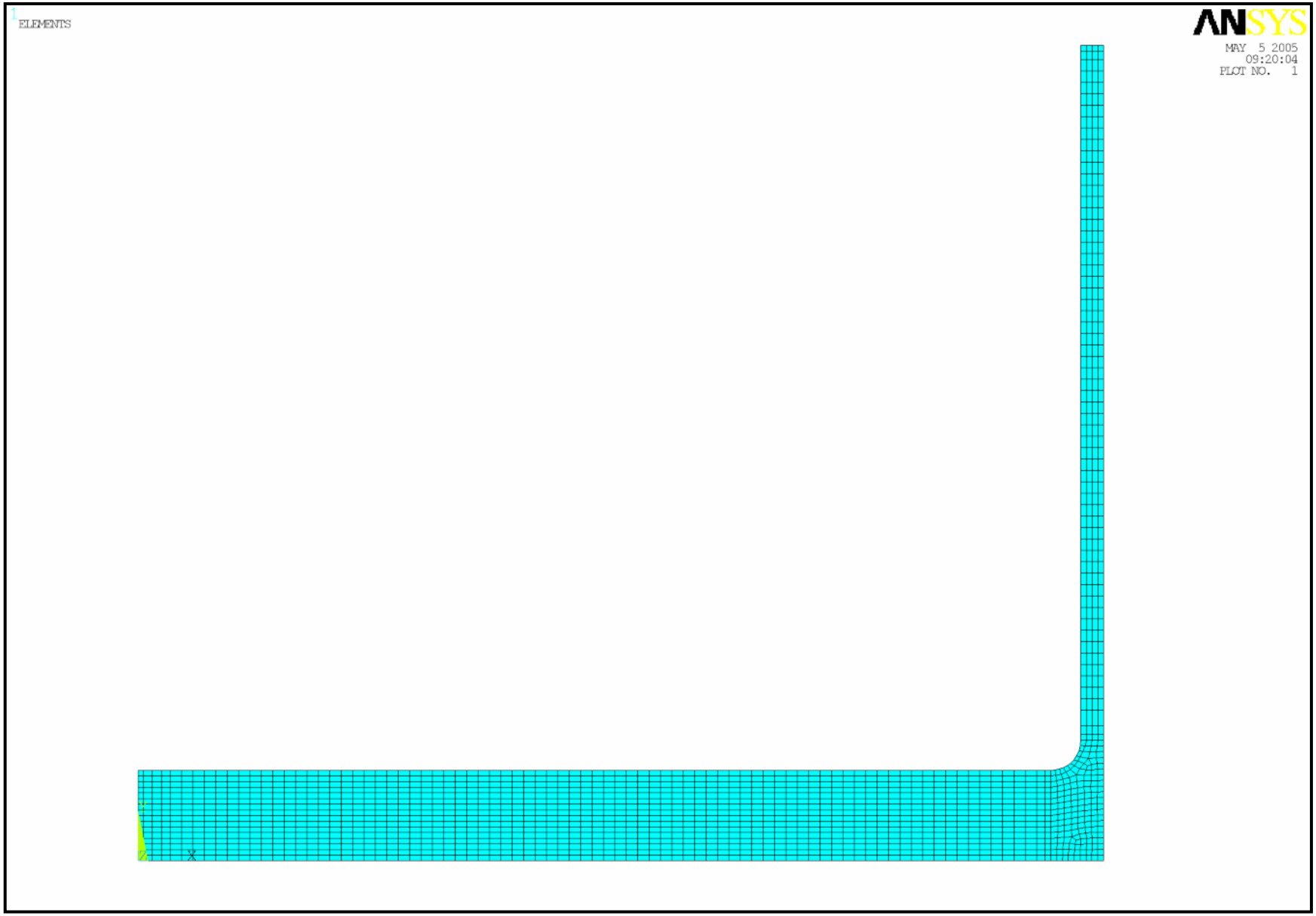

Figure 2.10.1-5 – Finite Element Analysis Model of the IV Bottom Transition Due to Pressure

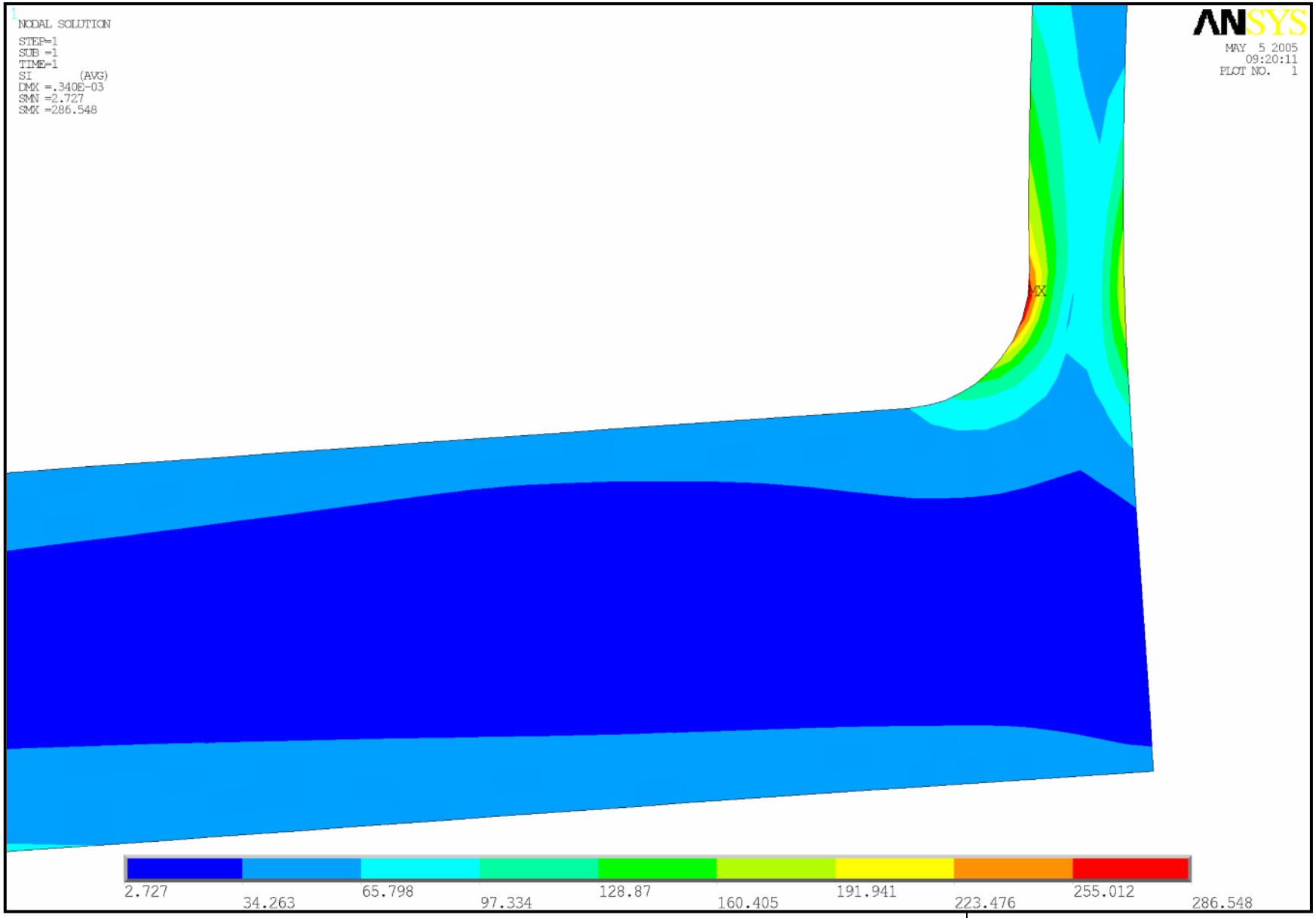

Figure 2.10.1-6 – IV Bottom Transition Stress Intensities Due to Pressure

2.10.1.3 Inner Vessel Radius Transition Zone Stresses Due to 1*g* Acceleration

As shown in Figure 2.10.1-7, the model is comprised of the bottom transition in the inner vessel (IV) shell utilizing approximately 1,700 PLANE82, 8-node axisymmetric solid elements. PLANE82 elements have a quadratic displacement behavior and are well suited to model irregular meshes and curved surfaces, providing exceptional accuracy for this application. Each element is defined by 8 nodes having two degrees of freedom at each node: translations in the nodal x- and y-directions.

Radial displacement constraints are applied at the symmetry boundary, and the end of the IV shell is constrained from displacing in the axial direction to simulate the entire structure.

A unit acceleration load of -386.0 in/s^2 is applied to the model in the axial direction.

As shown in Figure 2.10.1-8, the maximum stress intensity in the IV shell is 110 psi, occurring at the transition to the cylindrical shell.

The ANSYS® input file is provided in Table 2.10.1-3.

Table 2.10.1-3 – Input Listing for IV Radius Transition Zone Stresses Due to 1*g* Acceleration

```
/PREP7                                                          ! Enter the pre-processing module

/UNITS,       BIN                                               ! Specify British (inches) for units

/TITLE,IV Shell Stresses at Bottom Corner Transition with 1g Axial Acceleration

ET,       1,    PLANE82,     ,     ,    1                       ! Shell and Bottom

MP,      EX,    1,        27800000                              ! Properties for stainless steel
MP,    DENS,    1,       7.513E-04
MP,    NUXY,    1,          0.3000

K,        1,     0.0000,     0.0000                             ! Define the keypoints
K,        2,    15.1250,     0.0000
K,        3,    16.0000,     0.0000
K,        4,    16.0000,     2.0000
K,        5,    16.0000,    13.5000
K,        6,     0.0000,     1.5000
K,        7,    15.1250,     1.5000
K,        8,    15.6250,     2.0000
K,        9,    15.6250,    13.5000
K,       10,    15.1250,     2.0000

L,              1,    2                                         ! Define the lines
*REPEAT,        4,    1,    1
L,              6,    7
LARC,           7,    8,   10,     0.5000
L,              8,    9
L,              1,    6
L,              2,    7
L,              4,    8
L,              5,    9

AL,             1,    9,    5,    8                             ! Define the bottom plate area
AL,             4,   11,    7,   10                             ! Define the cylinder area
AL,             2,    3,   10,    6,    9                       ! Define the transition area

SMRTSIZE,       2                                               ! Mesh the volumes into elements
LESIZE,         2,     ,     ,    9
LESIZE,         3,     ,     ,   21
LESIZE,         8,     ,     ,   16
LESIZE,         9,     ,     ,   16
LESIZE,        10,     ,     ,    4
LESIZE,        11,     ,     ,    4
AATT,           1,    1,    1
AMESH,          1
AMESH,          2
AMESH,          3

ACEL,            0.0000,  -386.0000,     0.0000                 ! Apply a unit acceleration load to the model

NSEL,     S,  LOC,    X,     0.0000                             ! Restrain radial and axial nodes at the free ends
D,      ALL,   UX,     0.0000
NSEL,     S,  LOC,    Y,    13.5000
D,      ALL,   UY,     0.0000
NSEL,   ALL
```

```
SBCTRAN                                                          ! Transfer all loads from keypoints to nodes

WSORT,        ALL                                                ! Reduce the solution wavefront

/RGB,       INDEX,  100,  100,  100,    0                        ! Invert colors (white background for output plot files)
/RGB,       INDEX,   80,   80,   80,   13
/RGB,       INDEX,   60,   60,   60,   14
/RGB,       INDEX,    0,    0,    0,   15

/DEV,        FONT,    1,Courier*New,  400,    0,  -16,    0,    0        Set the font sizes
/DEV,        FONT,    2,      Arial,  400,    0,  -13,    0,    0
/DEV,        FONT,    3,      Arial,  400,    0,  -13,    0,    0

PNGR,        COMP,    1                                           ! Set the graphics file parameters
PNGR,       ORIEN,HORIZ
PNGR,       COLOR,    2
PNGR,        TMOD,    1
/GFILE,      1800

/WINDOW,        1,    -1.0000,     1.6700,    -0.9260,     0.9260       ! Set the graphics window size to 9.00 x 6.25 ratio

/FOCUS,         1,     8.6120,     6.6770,     0.0000                  ! Set the graphics window parameters
/DIST,          1,     7.5000
/VIEW,          1,     0.0000,     0.0000,     1.0000
/ANGLE,         1,     0.0000

EPLOT                                                            ! Plot elements to the screen
/SHOW,        PNG
EPLOT                                                            ! Plot elements to a file
/SHOW,      CLOSE

FINISH

/SOLUTION                                                        ! Enter the solution module

ANTYPE, STATIC                                                   ! Specify a static problem
SOLCONTROL,    ON,   ON                                          ! Set solution controls

SOLVE                                                            ! Solve the problem

FINISH

/POST1                                                           ! Enter the post-processing module

SET,   LAST                                                      ! Retrieve the final load step's data

PATH,          P1,    2,   30,   20                              ! Linerized stress intensity along Path 1
PPATH,          1,    1                                          !  (center of IV bottom)
PPATH,          2,    3
PMAP,         ACCURATE
/OUTPUT,        IVPRES,  OUT                                     ! Write output to a file
PRSECT                                                           ! Print path stresses at this location
/OUTPUT

PATH,          P2,    2,   30,   20                              ! Linerized stress intensity along Path 2
PPATH,          1, 5029                                          !  (top of radius transition in cylindrical shell)
PPATH,          2, 5087
PMAP,         ACCURATE
/OUTPUT,        IVPRES,  OUT,     ,     APPEND                     ! Write output to a file
PRSECT                                                           ! Print path stresses at this location
/OUTPUT

/GRAPHICS,   FULL                                                ! Disable PowerGraphics

/FOCUS,         1,    14.0800,     1.2470,     0.0000              ! Set the graphics window parameters
/DIST,          1,     1.8000
/VIEW,          1,     0.0000,     0.0000,     1.0000
/ANGLE,         1,     0.0000

PLNSOL,        SI                                                ! Plot stress intensity to the screen
/SHOW,        PNG
PLNSOL,        SI                                                ! Plot stress intensity to a file
/SHOW,      CLOSE
```

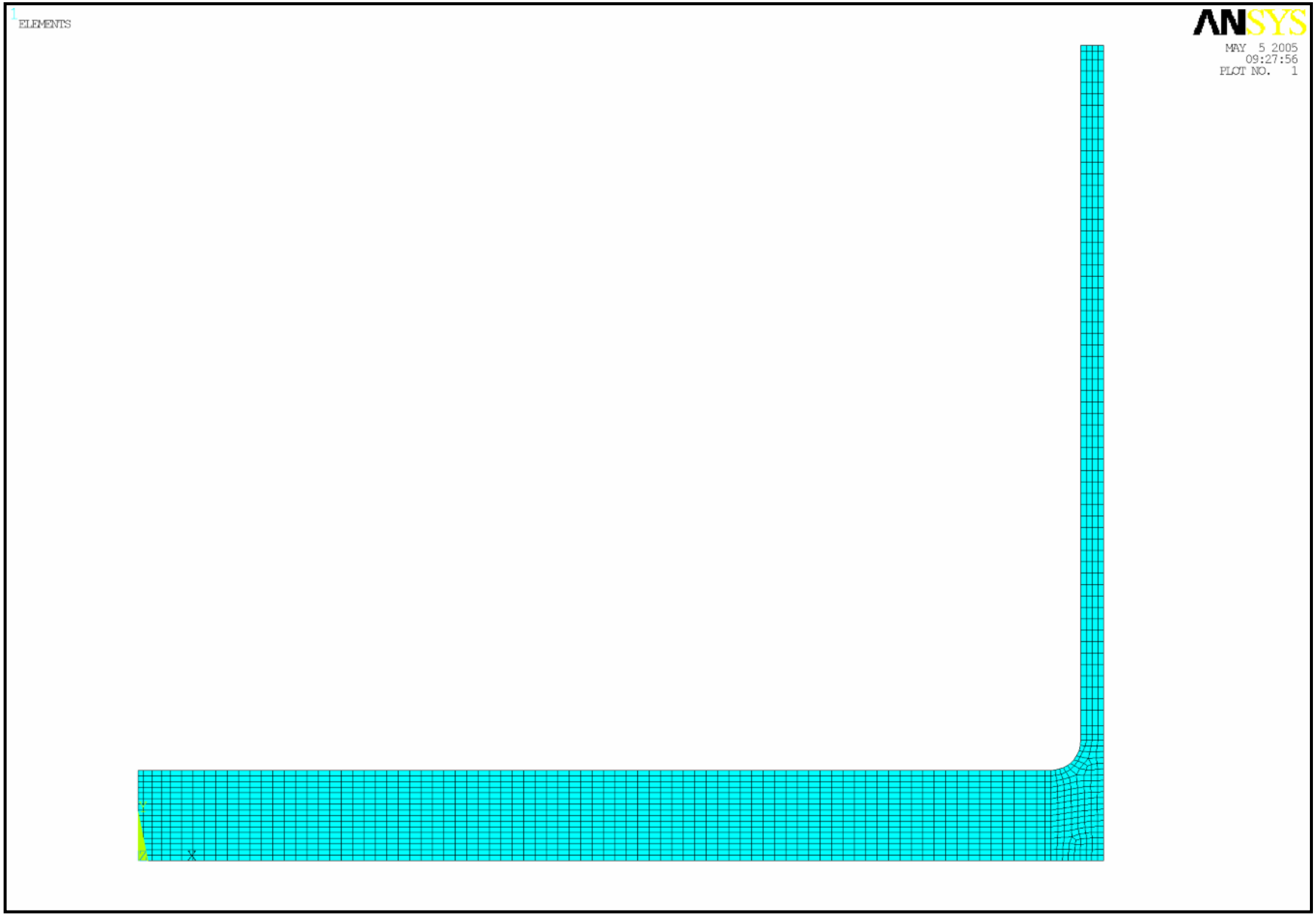

Figure 2.10.1-7 – Finite Element Analysis Model of the IV Bottom Transition Due to 1*g* Acceleration

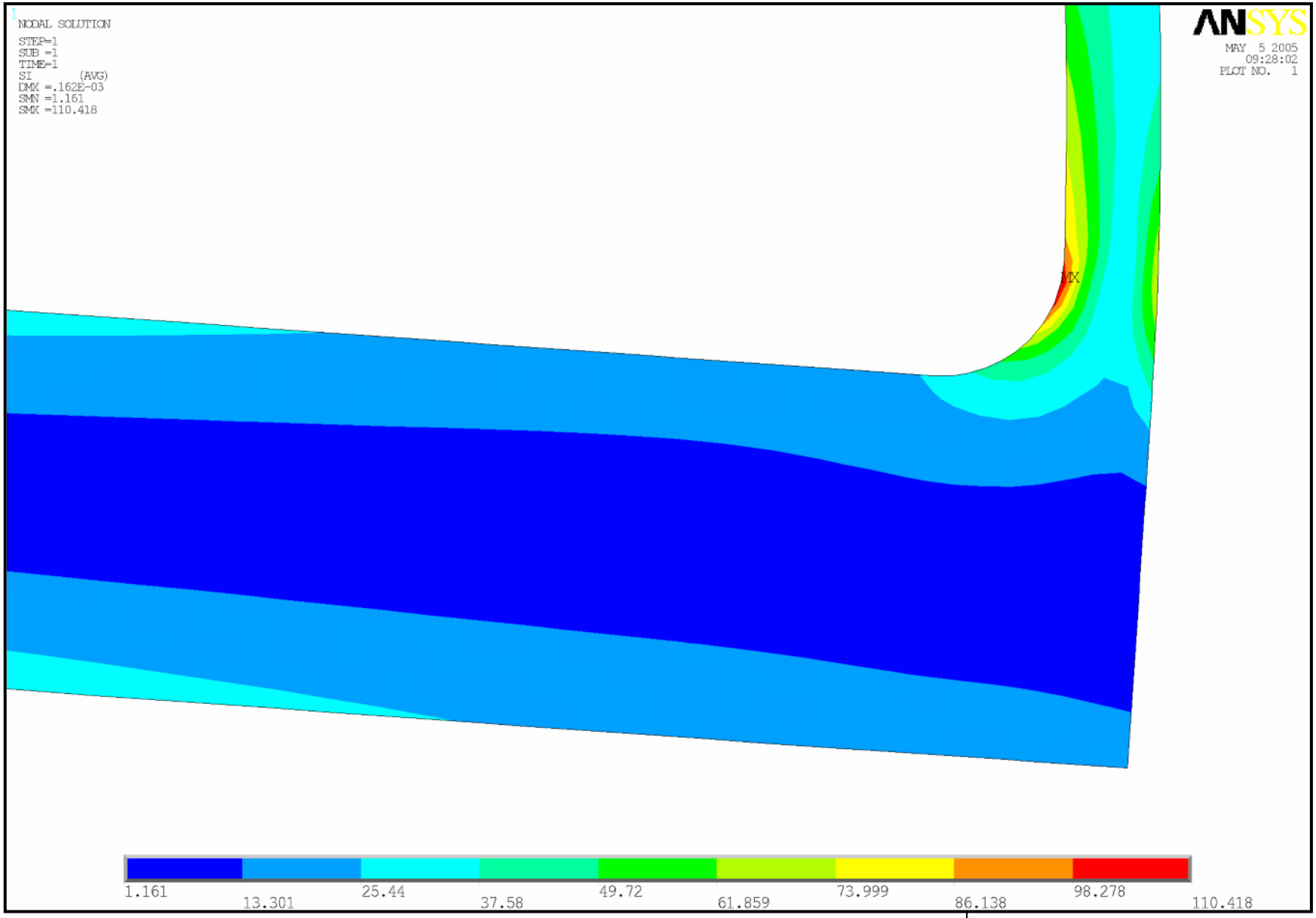

Figure 2.10.1-8 – IV Bottom Transition Stress Intensities Due to 1*g* Acceleration

2.10.1.4 Containment Assembly Analysis for Oblique Drops

The oblique drop finite element model represents all components of the RH-TRU 72-B package: the impact limiters, the outer cask (OC) and inner vessel (IV) base plates, shells, and lids, and the payload canister. Table 2.10.1-4 summarizes node and element numbering for each of the structural components. The model was built so that varying drop angles, accelerations, rotational velocities, rotational accelerations, and distances between impact and the center of gravity could be accommodated. These parameters are available from the SLAPDOWN program results and used as input to the finite element model (see Appendix 2.10.4, *Slapdown Assessment*).

The OC, IV, and payload canister are all modeled with two-dimensional, elastic beam elements (STIF3). The element is defined by two nodal points having three degrees of freedom at each node: translations in the nodal x- and y-directions, and rotation about the nodal z-axis. The elastic beam element is a uniaxial element with tension, compression, torsion, and bending capabilities. The OC is modeled only with the structural properties of the stainless steel inner and outer shells, assuming the lead provides no structural support. The material density of the OC beam is adjusted to include the mass of the lead. Similarly, the material densities of the IV and canister are adjusted to account for the mass of the contents and other components not included in the ANSYS® model.

The impact limiters, lids, and bases are modeled as generalized two-dimensional mass elements with rotary inertia (STIF21). These elements are defined by one node which has three degrees of freedom: translations in the nodal x- and y-directions, and rotation about the nodal z-axis. This element contributes only to the structural mass and has no displacement function.

The lower impact limiter also has five elements (1-5) associated with it that are two-dimensional, elastic beams (STIF3) being used as rigid connectors. These rigid connectors are needed so that the loads from the drop impact will be transmitted to the package properly.

Combination elements (STIF40) are used to interface between the OC and IV. The element is defined by two nodal points having one degree of freedom: either a translation in a nodal coordinate direction or a rotation about a nodal coordinate axis. The combination element is representative of a spring coupled to a gap in series. The combination elements are used to interface between the OC and IV so that the load of the IV on the OC is distributed properly for the various drop orientations considered. To properly model this aspect, a stiff spring (spring stiffness, $k = (10)^8$ lb/in) having no mass is used. The interface elements are modeled with an initial gap of $1(10)^{-6}$ inches, assuming that the IV and OC are initially in contact along the entire length of the IV. For this model, the combination elements are restricted to displacement in the nodal y-direction (or in the package's radial direction).

The origin of the nodal coordinate system is located at the center of gravity of the package (node 117) as shown in Figure 2.10.1-9. The nodal x-axis corresponds to the horizontal direction with respect to the ground, and the nodal y-axis corresponds to the vertical direction with respect to the ground.

Nodes 105 (OC base), 207 (IV base), and 307 (canister base) are coupled to move in the x-direction together since the bases of all the vessels rest directly on each other and would move together vertically. Nodes 107 (OC shell adjacent to the IV base) and 207 (IV base) are coupled to move in the y-direction since the IV base is laterally restricted in movement by the OC shell.

Nodes 127 (OC shell adjacent to the IV lid) and 227 (IV lid) are coupled to move in the y direction since the IV lid is laterally restricted in movement by the OC shell. Nodes 211 and 311 are coupled in the y-direction to simulate the spacer belt that is at that location to support the payload canister in the IV. Nodes 223 and 323 are coupled in the y-direction to simulate the spacer belt at the other location.

The model is restrained from translating and rotating in all directions at node 1, which represents the corner of impact.

As discussed previously the model is loaded with appropriate accelerations and velocities from SLAPDOWN program results.

In addition, a temperature of 160 ºF is utilized to determine the temperature dependent material property values of the OC and IV. The only material property affected by a temperature of 160 ºF is Young's modulus which, consistent with Table 2.3-1 in Section 2.3, *Mechanical Properties of Materials*, is set to $27.8(10)^6$ psi for Type 304 stainless steel. A temperature of 175 ºF is utilized to determine the temperature dependent material property values of the canister. Again, the only material property affected by a temperature of 175 ºF is Young's modulus which, consistent with Table 2.3-1 in Section 2.3, *Mechanical Properties of Materials*, is set to $28.9(10)^6$ psi for ASTM A516, Grade 55, carbon steel.

2.10.1.5 Containment Assembly Analysis for Side Drops

The side drop finite element model has the identical geometry as that for the oblique drops. Therefore, refer to Appendix 2.10.1.4, *Containment Assembly Analysis for Oblique Drops*, for geometry details. The side drop model, like the oblique model, requires the acceleration from the CASKDROP program results as input for the finite element model (see Appendix 2.10.2.1, *Description of the CASKDROP Computer Code*). However, the angle of impact, rotational velocity, rotational acceleration, and distance between impact and the center of gravity, parameters that are needed for the oblique finite element model, are not necessary for the side drop and therefore have been deleted.

Table 2.10.1-4 – Containment Assembly Node and Element Numbering

Component	Node Numbers	Element Numbers
Lower Impact Limiter	101 – 104	1 - 5, 30
Outer Cask Base Plate	105	31
Outer Cask Shells	106 – 128	6 - 27
Outer Cask Lid	129	32
Inner Vessel Base Plate	207	44
Inner Vessel Shell	207 – 227	34 - 43
Inner Vessel Lid	227	45
Payload Canister	307 – 327	46 - 65
Upper Impact Limiter	128 – 130	28, 29, 33

FIGURE WITHHELD UNDER 10 CFR 2.390

Figure 2.10.1-9 – Containment Assembly Oblique Analysis Model

This page intentionally left blank.

2.10.2 Drop Analysis Codes Description

2.10.2.1 Description of the CASKDROP Computer Code

This section briefly documents the methodology employed by the PacTec computer code CASKDROP. The computer program CASKDROP is used to demonstrate compliance of the package with 10 CFR §71.71(c)(7)[1] and 10 CFR §71.73(c)(1)[1] for normal conditions of transport (NCT) and hypothetical accident conditions (HAC) free drop analyses, respectively.

A summary of the appendix subsections is as follows:

- describes the CASKDROP analysis methodology.
- provides an example problem with input and output.

2.10.2.1.1 Using CASKDROP to Determine Impact Limiter Deformation Behavior

The package is protected by polyurethane foam-filled, energy absorbing end buffers, called impact limiters. For purposes of the regulatory free drop analyses using the CASKDROP computer program, the impact limiters are assumed to absorb, in plastic deformation of the polyurethane foam, all of the potential energy of the drop event. In other words, the drop analyses assume that none of the potential energy of the free drop event is transferred to kinetic or strain energy of the target (i.e., the "unyielding" surface assumption of 10 CFR 71), nor strain energy in the package body itself.

CASKDROP evaluates all angles of drop from 0º (horizontal) to 90º (vertical) by performing a quasi-static analysis that ignores rotational effects. At orientations where rotational effects are important, use of a dynamic analysis computer program such as SCANS[2] or SLAPDOWN[3] is required utilizing the force-deflection data developed by CASKDROP. Three orientations where rotational motions (or pitch) play no role in the evaluation of the free drop analyses are:

- END DROP on the circular end surface of the impact limiter,
- SIDE DROP on the cylindrical side surfaces of the impact limiters, and
- CORNER DROP with the package center of gravity directly over the impact limiter corner.

For all orientations of impact, the prediction of impact limiter deformation behavior can be approached from straightforward energy balance principles:

$$E = W(h + \delta) = \int_0^{\delta} F_x dx$$

[1] Title 10, Code of Federal Regulations, Part 71 (10 CFR 71), *Packaging and Transportation of Radioactive Material*, Final Rule, 01-26-04.

[2] *SCANS (Shipping Package ANalysis System), a Microcomputer Based Analysis System for Shipping Package Design Review*, NUREG/CR-4554, Version 1A, Lawrence Livermore National Laboratory, Livermore, California.

[3] G. D. Sjaardema, G. W. Wellman, *Numerical and Analytical Methods for Approximating the Eccentric Impact Response (Slapdown) of Deformable Bodies*, SAND 88-0616, Sandia National Laboratories, Albuquerque, New Mexico, March 1988.

where the package gross weight is W, the drop height is h, the maximum impact limiter deformation is δ, and the force imposed on target at an impact limiter deformation of x is F_x. The left-hand term represents the potential energy of the free drop. The right-hand term represents the strain energy of the deformed impact limiter(s).

Given a specific drop angle, θ, and impact limiter deformation, δ, as illustrated in Figure 2.10.2-1, the result is an impact limiter crush plane "footprint." Integration of the impact limiter crush plane yields a total crush force and centriodal distance of:

$$F = \iint \sigma\{\varepsilon\} dA$$

and,

$$\overline{X} = \left(\frac{1}{F}\right) \iint \overline{x}\sigma\{\varepsilon\} dA$$

respectively, where the total integrated force is F, the differential stress as a function of strain is $\sigma\{\varepsilon\}$, the differential area is dA (i.e., dA is a function of the "x" and "y" directions, or dx and dy), the total integrated centriodal distance from the package center of gravity is $\overline{X}$, and the differential centriodal distance from the package center of gravity is $\overline{x}$.

With reference to Figure 2.10.2-1, the geometric calculations for the impact surface (crush plane) and the associated strains are carried out using a translating X'-Y'-Z' coordinate system, with the X'-Y' plane corresponding to the crush plane. Due to the cylindrical nature of the problem, the overall crush plane is comprised of a segment of an ellipse corresponding to the outside surface of the impact limiter. The optional end hole requires removal of its associated elliptical segment. Similarly, the optional conical surface is an elliptical, parabolic, or hyperbolic segment depending on both the drop angle, θ, and angle of the cone.

Calculation of the differential strain is somewhat more complex. As illustrated in Figure 2.10.2-2, the differential strain, $\varepsilon\{x,y\}$, is calculated at the center of the differential area, dA. The differential strain is determined by calculating the amount of vertical deformation at the (x, y) location on the crush plane. The vertical distance from point (x, y) on the impact surface to the package or upper impact limiter surface is found and denoted z_{TOP}. Similarly, the vertical distance from point (x, y) on the impact surface to the undeformed lower impact limiter surface is found and denoted z_{BOT}. In equation format the differential strain at location (x, y) is simply:

$$\varepsilon = \frac{z_{BOT}}{z_{BOT} + z_{TOP}}$$

This strain is used to determine the corresponding crush stress from an implicit tabular definition of the crushable media stress-strain characteristics. For each differential area, dA, the differential force, dF, is found. The total force, F, is therefore the summation of the differential forces. Similarly, the centroidal distance, $\overline{X}$, is the summation of the moments, $\overline{x} \times dF$, divided by the total force, F.

Unbacked regions are defined as having an (x, y) location where z_{TOP} is calculated to occur outside the package's "shadow" (i.e., or backing, occurring on the impact limiter surface). Unbacked regions usually utilize the nominal crush strength of the crushable media (typically at

10% strain for polyurethane foam material) for integrated force purposes. The crush strength for unbacked regions is user-definable in the program CASKDROP.

For most drop angles, θ, and impact limiter deformations, δ, the impact limiter crush force, F, is transmitted to the package body in direct compression. Hence, the forces transmitted to the circumferential impact limiter attachments are essentially zero. However, for nearly vertical or horizontal orientations at small deformations where the crush force occurs beyond the edge of the package, the forces transmitted to the impact limiter attachments can be substantially large. It is important to note that only the nearly vertical or nearly horizontal orientations are required to produce the prying motion; all other orientations will always compress the impact limiter onto the package body. Figure 2.10.2-3 illustrates the near-vertical and near-horizontal orientations producing impact limiter separation forces.

For the near vertical orientation, the moment about point "a" determines whether a separation force exists at the impact limiter attachments. Assuming for this case that a counterclockwise moment is positive (i.e., will tend to "pry" the impact limiter off the package), the equation for the moment about point "a," M_a, is:

$$M_a = Fx_F + F_{IL}x_{IL}$$

Similarly, for the near horizontal orientation, the moment about point "b" determines whether a separation force exists at the impact limiter attachments. Assuming for this case that a clockwise moment is positive (i.e., will tend to "pry" the impact limiter off the package), the equation for the moment about point "b," M_b, is:

$$M_b = Fx_F - F_{IL}x_{IL}$$

If M_a or M_b are positive, a separation force will occur at the impact limiter attachments whereas if M_a or M_b are zero or negative, a separation force will not occur. Note that use of a conically shaped impact limiter typically eliminates the impact limiter separation force by causing the crush force, F, to almost always occur between points "a" and "b."

2.10.2.1.2 Example Problem for the CASKDROP Program

An example problem is illustrated in Figure 2.10.2-4. The CASKDROP program utilizes a variety of physical input data to determine package and impact limiter geometry. In all cases, the package and impact limiter are assumed axisymmetric. The package is cylindrical, as is the impact limiter. Two fundamental variations in the basic cylindrical shape of the impact limiter are an optional end hole and optional conical end. The end hole may extend part or all of the way from the outside surface of the impact limiter to the package end. The conical end may be a truncated or fully developed cone, defined by a cone diameter and a cone length at the outside surface of the impact limiter. By varying the impact limiter dimensions the result is a wide variety of possible impact limiter shapes, from a totally enclosing "overpack" to pointed end-only buffers.

The CASKDROP program was primarily developed as an impact limiter design tool. Geometry and analysis control input to the CASKDROP program is fully interactive allowing changes "on the fly." The top screenshot in Figure 2.10.2-5 illustrates the CASKDROP screen for data entry into the Input Window.

The CASKDROP program allows for three types of crushable media definition:

1. CONSTANT: a constant crush stress independent of calculated strain.
2. VARIABLE: a variable, user-defined stress-strain definition.
3. POLYFOAM: a built-in polyurethane foam database providing accurate stress-strain definition for 5 to 25 pound per cubic foot (pcf) density and temperatures of -20 ºF to +300 ºF based on extensive sample testing.

The example problem assumes 20-pcf polyurethane foam at a temperature of -20 ºF. A +60% bias is applied to the temperature-corrected stress-strain data to account for dynamic strain rate effects for the example problem. The bottom screenshot in Figure 2.10.2-5 illustrates the CASKDROP input screen for the polyurethane foam crush media for the example problem.

For the example problem, the CASKDROP program utilizes polyurethane foam where "parallel-to-rise" foam curing occurs in the axial direction and "perpendicular-to-rise" foam curing occurs in the radial direction, although the difference between these two directions is small. The user may optionally select the "parallel-to-rise" or "perpendicular-to-rise" properties to be reversed or global for all drop orientations. For orientations other than axial (end drop) and radial (side drop), the CASKDROP program interpolates foam properties using an ellipse function. For the case where crush stress "parallel-to-rise" is in the axial direction, σ_{PAR}, and crush stress "perpendicular-to-rise" is in the radial direction, σ_{PER}, the interpolation equation at drop angle, θ, is:

$$\sigma_\theta = \sqrt{\frac{1}{\frac{\sin^2\theta}{\sigma_{PAR}^2} + \frac{\cos^2\theta}{\sigma_{PER}^2}}}$$

Similarly, for the case where crush stress "perpendicular-to-rise" is in the axial direction, σ_{PER}, and crush stress "parallel-to-rise" is in the radial direction, σ_{PAR}, the interpolation equation is:

$$\sigma_\theta = \sqrt{\frac{1}{\frac{\sin^2\theta}{\sigma_{PER}^2} + \frac{\cos^2\theta}{\sigma_{PAR}^2}}}$$

The Control Window allows the user to specify various analysis and output controls. The Control Window is separated into Analysis, Crush, Angle, Static, Dynamic, Print, and File.

Three Analysis options are available: "dXY" defines the number of integration elements in the crush plane, 25 for the example problem; "Sln" defines the analysis methodology ("Global" versus "Local Strain Theory"), "Global" for the example problem; "ε/σ" defines the strain (or crush stress) value to be utilized in unbacked regions (e.g., if a value is specified between 0 and 1, it is assumed a strain value and the corresponding crush stress at that strain is used; if a value is specified greater than 1, it is assumed to be a crush stress), 0.1 for the example problem corresponding to a crush stress at 10% strain from the polyurethane foam database.

The "Crush" options define the incremental deformations to be analyzed. The example problem specifies analyzing for crush deformations from 0.25 inches to 20 inches in 0.25-inch increments. Specifying a "Max" value greater than the actual maximum available crush depth (as determined geometrically) flags the CASKDROP program not to exceed the maximum available crush depth.

Similarly, the "Angle" options define the incremental angular orientations to be analyzed. The example problem specifies analyzing for drop angles from 0º to 90º in 15º increments.

The "Static" options allow the user to specify quasi-static analyses providing "Full" display output, "Smry" (summary) output, or "Both". The example problem specifies "Full" output to the display only. Similarly, the "Dynamic" options allow the user to specify dynamic analyses providing "Full" display output, "Smry" (summary) output, or "Both". The example problem does not specify a dynamic analysis as that module is not completed in the CASKDROP program.

The "Print" and "File" options allow the user to specify "Full" display output, "Smry" (summary) output, or "Both" to the printer or a file. The example problem specifies "Full" output to an output file only.

The Output Window provides the location for Static and Dynamic display output. A quasi-static solution is achieved when the strain energy of the crushable media (SE) is equal to the free-falling kinetic energy of the package (KE), or SE/KE = 1. Table 2.10.2-1 provides a sample file output at 0º (side drop), at 45º, and at 90º (end drop).

2.10.2.2 Description of the SLAPDOWN Computer Code

Impact limiter deflections and package accelerations are calculated using the Sandia National Laboratories developed computer code SLAPDOWN[3]. This program solves the rigid-body equations of motion for a transportation package, given parameters such as weight, rotational moment of inertia, geometric relationships, and impact limiter force-deflection curves. The output consists of maximum impact limiter deformations and a time history of the parameters of motion (of principal interest, the acceleration at the center of gravity and angular acceleration). From these outputs, accelerations at any point on the package are found. Figure 2.10.2-6 shows a sample of geometric parameters, and Table 2.10.2-2 lists the required input parameters for the sample geometry.

To bound the dynamic impact analyses, the lower values of package weight and mass moment of inertia are used conservatively with the upper bound force-deflection curves to calculate the maximum impact accelerations, the condition for which the impact velocity of the secondary impact is greatest. The higher values of package weight and mass moment of inertia are used with the lower bound force-deflection curves to calculate the maximum crush distances. The center of gravity (CG) is taken as the geometric center of the package. Friction is assigned a value of zero, since this maximizes the impact forces and deflections for the secondary (slapdown) impact limiter.

The original VMS-based SLAPDOWN FORTRAN computer code is now IBM-PC compatible through the use of a PC-based FORTRAN compiler. Using a test input file, the current PC version gives identical results to the original VMS version running at Sandia National Laboratories.

Table 2.10.2-2 shows a listing of sample input for the SLAPDOWN program. Table 2.10.2-3 shows a listing of sample force-deflection data for the SLAPDOWN program. Table 2.10.2-4 shows a sample output of the SLAPDOWN program from the general output file. This is performed for a 15º primary oblique orientation. Note that the angle of secondary contact with a the ground surface is displayed at the end of the output list ("Tail Impact Angle"). The angle is

nearly zero, which is true in almost all cases. Table 2.10.2-5 shows a portion of the corresponding time history output file, showing the results only through the end of the primary impact. The time variable is given in the first column. In the second, third and fourth columns are given the results at the package center of gravity (SLAPDOWN node 2): the vertical position is in the column headed POSY(2) (inches), the velocity is in the column headed VELY(2) (in/s), and the acceleration is in the column headed ACCY(2) (in/s^2). The last three columns give the rotational parameters of angular position: the angle THETA (radians, horizontal is zero), the angular velocity OMEGA (rad/s) and the angular acceleration ALPHA (rad/s^2). Table 2.10.2-5 is an excerpt from the time history output file, and shows the beginning (primary portion) of the impact.

As further confirmation of the SLAPDOWN code analysis methodology, the sample problem described above is compared to output from the public domain program SCANS[2]. The results compare well, as demonstrated in Table 2.10.2-6. Input data for the comparison is taken from Table 2.10.2-2. A 15º initial impact angle is used for direct comparison.

Table 2.10.2-1 – CASKDROP Sample Problem Output Files

Side Drop *** PACKAGING TECHNOLOGY *** CASKDROP, v2.21
05-16-1995, 15:38:39 Jul 01, 1994

SAMPLE PROBLEM FOR QUALITY ASSURANCE CHECK (AREAS AND VOLUMES)	
Impact Limiter Weight (each) - 1,000 lbs	Cask and Payload Weight - 10,000 lbs
Impact Limiter Outside Diameter - 60.0000 in	Cask Outside Diameter - 40.0000 in
Impact Limiter Overall Length - 24.0000 in	Cask Overall Length - 48.0000 in
Impact Limiter Conical Diameter - 48.0000 in	Dynamic Unloading Modulus - 1.000E+07 lbs/in
Impact Limiter Conical Length - 10.0000 in	Rad Mass Moment of Inertia - 12,235 lb-in-s²
Impact Limiter End Thickness - 12.0000 in	Frictional Coefficient - 0.0000
Impact Limiter Hole Diameter - 20.0000 in	Drop Height - 30.0000 ft
Impact Limiter Hole Length - 8.0000 in	Drop Angle from Horizontal - 0.0000°
Unbacked Area Threshhold Strain - 0.1000 in/in	Crush Analysis Theory - Global
Unbacked Area Crush Stress - 2,675 psi	Number of Integration Incs - 25

POLYFOAM CRUSH STRESS (Axial: "‖" to rise)	
Density = 20.000 pcf Temp = -20.000 °F σ-yield = 2,552.3 psi Bias = 60.000%	
ε (in/in)	σ (psi)
0.000	0.0
0.100	2,552.3
0.200	2,687.0
0.300	2,868.8
0.400	3,302.9
0.500	4,115.1
0.600	6,074.3
0.650	7,942.0
0.700	10,925.0
0.750	15,001.8
0.800	26,829.5

POLYFOAM CRUSH STRESS (Radial: "⊥" to rise)	
Density = 20.000 pcf Temp = -20.000 °F σ-yield = 2,675.0 psi Bias = 60.000%	
ε (in/in)	σ (psi)
0.000	0.0
0.100	2,675.0
0.200	2,785.4
0.300	2,959.9
0.400	3,345.9
0.500	4,147.7
0.600	6,062.8
0.650	7,868.8
0.700	10,180.0
0.750	15,554.4
0.800	29,704.8

POLYFOAM CRUSH STRESS (Actual Data @ 0.0°)	
Density = 20.000 pcf Temp = -20.000 °F σ-yield = 2,675.0 psi Bias = 60.000%	
ε (in/in)	σ (psi)
0.000	0.0
0.100	2,675.0
0.200	2,785.4
0.300	2,959.9
0.400	3,345.9
0.500	4,147.7
0.600	6,062.8
0.650	7,868.8
0.700	10,180.0
0.750	15,554.4
0.800	29,704.8

DEFL (in)	MAX ε (%)	AREA (in²)	VOLUME (in³)	XBAR (in)	IMPACT FORCE (lbs)	ACCEL (g's)	I/L MOMENT (in-lbs)	STRAIN ENERGY (in-lbs)	KINETIC ENERGY (in-lbs)	SE/KE RATIO
0.250	2.50	221	37	0.00	106,881	8.9	0	13,360	4,323,000	0.00
0.500	5.00	318	105	0.00	289,508	24.1	0	62,909	4,326,000	0.01
0.750	7.50	396	194	0.00	518,875	43.2	0	163,957	4,329,000	0.04
1.000	10.00	465	302	0.00	733,200	61.1	0	320,466	4,332,000	0.07
1.250	12.49	528	425	0.00	955,009	79.6	0	531,492	4,335,000	0.12
1.500	14.99	587	565	0.00	1,107,366	92.3	0	789,289	4,338,000	0.18
1.750	17.49	644	719	0.00	1,270,225	105.9	0	1,086,488	4,341,000	0.25
2.000	19.99	699	886	0.00	1,371,441	114.3	0	1,416,697	4,344,000	0.33
2.250	22.49	752	1,068	0.00	1,509,207	125.8	0	1,776,778	4,347,000	0.41
2.500	24.99	804	1,262	0.00	1,668,937	139.1	0	2,174,046	4,350,000	0.50
2.750	27.49	855	1,469	0.00	1,761,221	146.8	0	2,602,815	4,353,000	0.60
3.000	29.99	906	1,690	0.00	1,946,101	162.2	0	3,066,230	4,356,000	0.70
3.250	32.49	955	1,921	0.00	2,044,813	170.4	0	3,565,095	4,359,000	0.82
3.500	34.98	1,005	2,167	0.00	2,249,052	187.4	0	4,101,828	4,362,000	0.94
3.614	36.13	1,027	2,285	0.00	2,326,676	193.9	0	4,363,372	4,363,372	1.00
3.750	37.48	1,053	2,424	0.00	2,419,003	201.6	0	4,956,582	4,365,000	1.14
4.000	39.98	1,101	2,692	0.00	2,640,297	220.0	0	5,588,994	4,368,000	1.28
4.250	42.48	1,149	2,975	0.00	2,759,520	230.0	0	6,263,971	4,371,000	1.43
4.500	44.98	1,197	3,267	0.00	2,956,003	246.3	0	6,978,412	4,374,000	1.60
4.750	47.48	1,244	3,571	0.00	3,208,534	267.4	0	7,748,979	4,377,000	1.77
5.000	49.98	1,292	3,889	0.00	3,357,376	279.8	0	8,569,718	4,380,000	1.96
5.250	52.48	1,339	4,219	0.00	3,603,141	300.3	0	9,439,782	4,383,000	2.15
5.500	54.97	1,385	4,556	0.00	3,906,997	325.6	0	10,378,550	4,386,000	2.37
5.750	57.47	1,432	4,909	0.00	4,215,273	351.3	0	11,393,833	4,389,000	2.60
6.000	59.97	1,479	5,275	0.00	4,573,066	381.1	0	12,492,376	4,392,000	2.84
6.250	62.47	1,520	5,650	0.00	4,961,100	413.4	0	13,684,147	4,395,000	3.11

Side Drop
05-16-1995, 15:38:39

*** PACKAGING TECHNOLOGY ***
(continued...)

CASKDROP, v2.21
Jul 01, 1994

DEFL (in)	MAX ε (%)	AREA (in^2)	VOLUME (in^3)	XBAR (in)	IMPACT FORCE (lbs)	ACCEL (g's)	I/L MOMENT (in-lbs)	STRAIN ENERGY (in-lbs)	KINETIC ENERGY (in-lbs)	SE/KE RATIO
6.500	64.97	1,559	6,035	0.00	5,404,072	450.3	0	14,979,793	4,398,000	3.41
6.750	67.47	1,597	6,430	0.00	5,893,283	491.1	0	16,391,963	4,401,000	3.72
7.000	69.97	1,632	6,834	0.00	6,440,254	536.7	0	17,933,655	4,404,000	4.07
7.250	72.47	1,666	7,246	0.00	7,087,717	590.6	0	19,624,651	4,407,000	4.45
7.500	74.96	1,698	7,667	0.00	8,001,352	666.8	0	21,510,785	4,410,000	4.88
7.750	77.46	1,730	8,095	0.00	9,446,226	787.2	0	23,691,732	4,413,000	5.37
8.000	79.96	1,760	8,532	0.00	11,484,412	957.0	0	26,308,062	4,416,000	5.96
8.250	82.46	1,790	8,976	0.00	13,964,555	1,163.7	0	29,489,183	4,419,000	6.67
8.500	84.96	1,818	9,427	0.00	16,801,077	1,400.1	0	33,334,887	4,422,000	7.54
8.750	87.46	1,846	9,885	0.00	19,931,256	1,660.9	0	37,926,428	4,425,000	8.57
9.000	89.96	1,873	10,350	0.00	23,276,639	1,939.7	0	43,327,415	4,428,000	9.78
9.250	92.45	1,899	10,822	0.00	26,896,391	2,241.4	0	49,599,044	4,431,000	11.19
9.500	94.95	1,925	11,300	0.00	30,724,250	2,560.4	0	56,801,624	4,434,000	12.81
9.750	97.45	1,950	11,784	0.00	34,740,688	2,895.1	0	64,984,741	4,437,000	14.65
10.000	99.95	1,974	12,275	0.00	38,887,797	3,240.6	0	74,188,302	4,440,000	16.71

Corner Drop
05-16-1995, 15:38:39

*** PACKAGING TECHNOLOGY ***

CASKDROP, v2.21
Jul 01, 1994

SAMPLE PROBLEM FOR QUALITY ASSURANCE CHECK (AREAS AND VOLUMES)

Impact Limiter Weight (each) -	1,000 lbs	Cask and Payload Weight -	10,000 lbs
Impact Limiter Outside Diameter -	60.0000 in	Cask Outside Diameter -	40.0000 in
Impact Limiter Overall Length -	24.0000 in	Cask Overall Length -	48.0000 in
Impact Limiter Conical Diameter -	48.0000 in	Dynamic Unloading Modulus -	1.000E+07 lbs/in
Impact Limiter Conical Length -	10.0000 in	Rad Mass Moment of Inertia -	12,235 lb-in-s²
Impact Limiter End Thickness -	12.0000 in	Frictional Coefficient -	0.0000
Impact Limiter Hole Diameter -	20.0000 in	Drop Height -	30.0000 ft
Impact Limiter Hole Length -	8.0000 in	Drop Angle from Horizontal -	45.0000°
Unbacked Area Threshhold Strain -	0.1000 in/in	Crush Analysis Theory -	Global
Unbacked Area Crush Stress -	2,611 psi	Number of Integration Incs -	25

POLYFOAM CRUSH STRESS (Axial: "‖" to rise)

Density = 20.000 pcf
Temp = -20.000 °F
σ-yield = 2,552.3 psi
Bias = 60.000%

ε (in/in)	σ (psi)
0.000	0.0
0.100	2,552.3
0.200	2,687.0
0.300	2,868.8
0.400	3,302.9
0.500	4,115.1
0.600	6,074.3
0.650	7,942.0
0.700	10,925.0
0.750	15,001.8
0.800	26,829.5

POLYFOAM CRUSH STRESS (Radial: "⊥" to rise)

Density = 20.000 pcf
Temp = -20.000 °F
σ-yield = 2,675.0 psi
Bias = 60.000%

ε (in/in)	σ (psi)
0.000	0.0
0.100	2,675.0
0.200	2,785.4
0.300	2,959.9
0.400	3,345.9
0.500	4,147.7
0.600	6,062.8
0.650	7,868.8
0.700	10,180.0
0.750	15,554.4
0.800	29,704.8

POLYFOAM CRUSH STRESS (Actual Data @ 45.0°)

Density = 20.000 pcf
Temp = -20.000 °F
σ-yield = 2,611.5 psi
Bias = 60.000%

ε (in/in)	σ (psi)
0.000	0.0
0.100	2,611.5
0.200	2,734.9
0.300	2,913.3
0.400	3,324.2
0.500	4,131.3
0.600	6,068.5
0.650	7,905.2
0.700	10,532.8
0.750	15,270.6
0.800	28,157.6

DEFL (in)	MAX ε (%)	AREA (in²)	VOLUME (in³)	XBAR (in)	IMPACT FORCE (lbs)	ACCEL (g's)	I/L MOMENT (in-lbs)	STRAIN ENERGY (in-lbs)	KINETIC ENERGY (in-lbs)	SE/KE RATIO
0.250	1.44	7	1	-8.30	1,351	0.1	0	169	4,323,000	0.00
0.500	2.88	20	4	-8.11	7,756	0.6	0	1,307	4,326,000	0.00
0.750	4.33	36	11	-7.90	21,631	1.8	0	4,981	4,329,000	0.00
1.000	5.79	55	22	-7.68	44,807	3.7	0	13,286	4,332,000	0.00
1.250	7.25	78	39	-7.44	78,737	6.6	0	28,729	4,335,000	0.01
1.500	8.71	102	61	-7.19	124,483	10.4	0	54,131	4,338,000	0.01
1.750	10.18	129	90	-6.92	182,320	15.2	0	92,481	4,341,000	0.02
2.000	11.66	158	126	-6.65	250,919	20.9	0	146,636	4,344,000	0.03
2.250	13.14	189	169	-6.39	327,791	27.3	0	218,975	4,347,000	0.05
2.500	14.63	222	221	-6.15	409,985	34.2	0	311,197	4,350,000	0.07
2.750	16.12	256	280	-5.92	495,229	41.3	0	424,349	4,353,000	0.10
3.000	17.64	290	349	-5.70	581,988	48.5	0	559,001	4,356,000	0.13
3.250	19.14	321	425	-5.53	666,955	55.6	0	715,119	4,359,000	0.16
3.500	21.04	350	509	-5.39	750,161	62.5	0	892,258	4,362,000	0.20
3.750	23.53	379	600	-5.30	832,241	69.4	0	1,090,058	4,365,000	0.25
4.000	26.04	407	698	-5.24	913,114	76.1	0	1,308,228	4,368,000	0.30
4.250	28.58	435	804	-5.21	993,967	82.8	0	1,546,613	4,371,000	0.35
4.500	31.14	462	916	-5.20	1,075,026	89.6	0	1,805,237	4,374,000	0.41
4.750	33.55	490	1,035	-5.22	1,157,389	96.4	0	2,084,289	4,377,000	0.48
5.000	35.86	517	1,161	-5.24	1,240,678	103.4	0	2,384,048	4,380,000	0.54
5.250	38.16	545	1,293	-5.27	1,325,202	110.4	0	2,704,783	4,383,000	0.62
5.500	40.44	573	1,433	-5.30	1,413,119	117.8	0	3,047,073	4,386,000	0.69
5.750	42.71	600	1,579	-5.33	1,503,231	125.3	0	3,411,616	4,389,000	0.78
6.000	44.96	628	1,733	-5.37	1,596,230	133.0	0	3,799,049	4,392,000	0.86
6.250	47.21	656	1,894	-5.40	1,692,397	141.0	0	4,210,127	4,395,000	0.96
6.359	48.17	668	1,966	-5.41	1,735,814	144.7	0	4,396,303	4,396,303	1.00
6.500	49.43	684	2,061	-5.42	1,792,981	149.4	0	4,837,403	4,398,000	1.10
6.750	51.75	711	2,236	-5.44	1,897,584	158.1	0	5,298,723	4,401,000	1.20
7.000	54.19	739	2,417	-5.46	2,009,560	167.5	0	5,787,116	4,404,000	1.31
7.250	56.65	767	2,605	-5.47	2,128,316	177.4	0	6,304,351	4,407,000	1.43

Corner Drop
05-16-1995, 15:38:39

*** PACKAGING TECHNOLOGY ***
(continued...)

CASKDROP, v2.21
Jul 01, 1994

DEFL (in)	MAX ε (%)	AREA (in^2)	VOLUME (in^3)	XBAR (in)	IMPACT FORCE (lbs)	ACCEL (g's)	I/L MOMENT (in-lbs)	STRAIN ENERGY (in-lbs)	KINETIC ENERGY (in-lbs)	SE/KE RATIO
7.500	59.12	795	2,800	-5.48	2,255,709	188.0	0	6,852,354	4,410,000	1.55
7.750	61.60	824	3,002	-5.48	2,392,365	199.4	0	7,433,363	4,413,000	1.68
8.000	64.10	852	3,212	-5.47	2,538,941	211.6	0	8,049,776	4,416,000	1.82
8.250	66.60	881	3,429	-5.47	2,701,943	225.2	0	8,704,887	4,419,000	1.97
8.500	69.12	909	3,652	-5.45	2,882,629	240.2	0	9,402,959	4,422,000	2.13
8.750	71.65	938	3,883	-5.43	3,079,002	256.6	0	10,148,162	4,425,000	2.29
9.000	74.19	967	4,121	-5.38	3,300,885	275.1	0	10,945,648	4,428,000	2.47
9.250	76.75	995	4,367	-5.32	3,573,055	297.8	0	11,804,891	4,431,000	2.66
9.500	79.31	1,024	4,619	-5.26	3,901,592	325.1	0	12,739,222	4,434,000	2.87
9.750	81.89	1,053	4,879	-5.17	4,292,510	357.7	0	13,763,484	4,437,000	3.10
10.000	84.49	1,082	5,146	-5.06	4,763,070	396.9	0	14,895,432	4,440,000	3.35
10.250	87.09	1,109	5,419	-4.95	5,316,128	443.0	0	16,155,332	4,443,000	3.64
10.500	89.71	1,134	5,698	-4.83	5,947,562	495.6	0	17,563,293	4,446,000	3.95
10.750	92.34	1,161	5,985	-4.74	6,665,548	555.5	0	19,139,932	4,449,000	4.30
11.000	94.98	1,184	6,270	-4.63	7,465,195	622.1	0	20,906,275	4,452,000	4.70
11.250	97.64	1,206	6,563	-4.54	8,360,345	696.7	0	22,884,467	4,455,000	5.14

End Drop *** PACKAGING TECHNOLOGY *** CASKDROP, v2.21
05-16-1995, 15:38:39 Jul 01, 1994

SAMPLE PROBLEM FOR QUALITY ASSURANCE CHECK (AREAS AND VOLUMES)

Impact Limiter Weight (each) -	1,000 lbs	Cask and Payload Weight -	10,000 lbs
Impact Limiter Outside Diameter -	60.0000 in	Cask Outside Diameter -	40.0000 in
Impact Limiter Overall Length -	24.0000 in	Cask Overall Length -	48.0000 in
Impact Limiter Conical Diameter -	48.0000 in	Dynamic Unloading Modulus -	1.000E+07 lbs/in
Impact Limiter Conical Length -	10.0000 in	Rad Mass Moment of Inertia -	12,235 lb-in-s²
Impact Limiter End Thickness -	12.0000 in	Frictional Coefficient -	0.0000
Impact Limiter Hole Diameter -	20.0000 in	Drop Height -	30.0000 ft
Impact Limiter Hole Length -	8.0000 in	Drop Angle from Horizontal -	90.0000°
Unbacked Area Threshhold Strain -	0.1000 in/in	Crush Analysis Theory -	Global
Unbacked Area Crush Stress -	2,552 psi	Number of Integration Incs -	25

POLYFOAM CRUSH STRESS (Axial: "‖" to rise)

Density = 20.000 pcf
Temp = -20.000 °F
σ-yield = 2,552.3 psi
Bias = 60.000%

ε (in/in)	σ (psi)
0.000	0.0
0.100	2,552.3
0.200	2,687.0
0.300	2,868.8
0.400	3,302.9
0.500	4,115.1
0.600	6,074.3
0.650	7,942.0
0.700	10,925.0
0.750	15,001.8
0.800	26,829.5

POLYFOAM CRUSH STRESS (Radial: "⊥" to rise)

Density = 20.000 pcf
Temp = -20.000 °F
σ-yield = 2,675.0 psi
Bias = 60.000%

ε (in/in)	σ (psi)
0.000	0.0
0.100	2,675.0
0.200	2,785.4
0.300	2,959.9
0.400	3,345.9
0.500	4,147.7
0.600	6,062.8
0.650	7,868.8
0.700	10,180.0
0.750	15,554.4
0.800	29,704.8

POLYFOAM CRUSH STRESS (Actual Data @ 90.0°)

Density = 20.000 pcf
Temp = -20.000 °F
σ-yield = 2,552.3 psi
Bias = 60.000%

ε (in/in)	σ (psi)
0.000	0.0
0.100	2,552.3
0.200	2,687.0
0.300	2,868.8
0.400	3,302.9
0.500	4,115.1
0.600	6,074.3
0.650	7,942.0
0.700	10,925.0
0.750	15,001.8
0.800	26,829.5

DEFL (in)	MAX ε (%)	AREA (in²)	VOLUME (in³)	XBAR (in)	IMPACT FORCE (lbs)	ACCEL (g's)	I/L MOMENT (in-lbs)	STRAIN ENERGY (in-lbs)	KINETIC ENERGY (in-lbs)	SE/KE RATIO
0.250	2.08	1,518	377	0.00	810,360	67.5	0	101,295	4,323,000	0.02
0.500	4.17	1,541	759	0.00	1,592,808	132.7	0	401,691	4,326,000	0.09
0.750	6.25	1,564	1,147	0.00	2,311,804	192.7	0	889,768	4,329,000	0.21
1.000	8.33	1,587	1,541	0.00	2,931,701	244.3	0	1,545,206	4,332,000	0.36
1.250	10.42	1,610	1,941	0.00	3,416,844	284.7	0	2,338,774	4,335,000	0.54
1.500	12.50	1,634	2,346	0.00	3,752,646	312.7	0	3,234,960	4,338,000	0.75
1.750	14.58	1,657	2,758	0.00	3,971,661	331.0	0	4,200,498	4,341,000	0.97
1.785	14.88	1,661	2,816	0.00	3,995,461	333.0	0	4,341,425	4,341,425	1.00
2.000	16.67	1,681	3,175	0.00	4,112,712	342.7	0	5,354,946	4,344,000	1.23
2.250	18.75	1,705	3,598	0.00	4,214,497	351.2	0	6,395,847	4,347,000	1.47
2.500	20.83	1,729	4,027	0.00	4,287,704	357.3	0	7,458,622	4,350,000	1.71
2.750	22.92	1,753	4,462	0.00	4,351,294	362.6	0	8,538,497	4,353,000	1.96
3.000	25.00	1,777	4,904	0.00	4,445,683	370.5	0	9,638,119	4,356,000	2.21
3.250	27.08	1,801	5,351	0.00	4,562,636	380.2	0	10,764,159	4,359,000	2.47
3.500	29.17	1,826	5,804	0.00	4,693,990	391.2	0	11,921,237	4,362,000	2.73
3.750	31.25	1,851	6,264	0.00	4,831,784	402.6	0	13,111,959	4,365,000	3.00
4.000	33.33	1,875	6,730	0.00	4,973,522	414.5	0	14,337,622	4,368,000	3.28
4.250	35.42	1,900	7,202	0.00	5,120,673	426.7	0	15,599,396	4,371,000	3.57
4.500	37.50	1,925	7,680	0.00	5,274,868	439.6	0	16,898,839	4,374,000	3.86
4.750	39.58	1,951	8,164	0.00	5,437,800	453.2	0	18,237,922	4,377,000	4.17
5.000	41.67	1,976	8,655	0.00	5,611,685	467.6	0	19,619,108	4,380,000	4.48
5.250	43.75	2,002	9,152	0.00	5,802,397	483.5	0	21,045,868	4,383,000	4.80
5.500	45.83	2,027	9,656	0.00	6,018,789	501.6	0	22,523,516	4,386,000	5.14
5.750	47.92	2,053	10,166	0.00	6,268,472	522.4	0	24,059,424	4,389,000	5.48
6.000	50.00	2,079	10,682	0.00	6,560,063	546.7	0	25,662,991	4,392,000	5.84
6.250	52.08	2,105	11,205	0.00	6,900,740	575.1	0	27,345,591	4,395,000	6.22
6.500	54.17	2,131	11,735	0.00	7,296,837	608.1	0	29,120,288	4,398,000	6.62
6.750	56.25	2,158	12,271	0.00	7,751,903	646.0	0	31,001,381	4,401,000	7.04
7.000	58.33	2,184	12,814	0.00	8,272,373	689.4	0	33,004,415	4,404,000	7.49
7.250	60.42	2,211	13,363	0.00	8,862,880	738.6	0	35,146,322	4,407,000	7.98

End Drop
05-16-1995, 15:38:39

*** PACKAGING TECHNOLOGY ***
(continued...)

CASKDROP, v2.21
Jul 01, 1994

DEFL (in)	MAX ε (%)	AREA (in^2)	VOLUME (in^3)	XBAR (in)	IMPACT FORCE (lbs)	ACCEL (g's)	I/L MOMENT (in-lbs)	STRAIN ENERGY (in-lbs)	KINETIC ENERGY (in-lbs)	SE/KE RATIO
7.500	62.50	2,238	13,919	0.00	9,556,877	796.4	0	37,448,792	4,410,000	8.49
7.750	64.58	2,265	14,482	0.00	10,454,871	871.2	0	39,950,260	4,413,000	9.05
8.000	66.67	2,606	15,051	0.00	11,632,851	969.4	0	42,711,226	4,416,000	9.67
8.250	68.75	2,633	15,706	0.00	13,506,993	1,125.6	0	45,853,706	4,419,000	10.38
8.500	70.83	2,660	16,368	0.00	14,954,954	1,246.2	0	49,411,449	4,422,000	11.17
8.750	72.92	2,688	17,037	0.00	16,218,008	1,351.5	0	53,308,070	4,425,000	12.05
9.000	75.00	2,715	17,712	0.00	18,519,890	1,543.3	0	57,650,307	4,428,000	13.02
9.250	77.08	2,743	18,394	0.00	22,571,268	1,880.9	0	62,786,702	4,431,000	14.17
9.500	79.17	2,771	19,084	0.00	27,794,818	2,316.2	0	69,082,462	4,434,000	15.58
9.750	81.25	2,799	19,780	0.00	33,405,583	2,783.8	0	76,732,513	4,437,000	17.29
10.000	83.33	2,827	20,483	0.00	39,286,171	3,273.8	0	85,818,982	4,440,000	19.33
10.250	85.42	2,827	21,190	0.00	45,050,964	3,754.2	0	96,361,124	4,443,000	21.69
10.500	87.50	2,827	21,897	0.00	51,018,884	4,251.6	0	108,369,855	4,446,000	24.37
10.750	89.58	2,827	22,604	0.00	57,507,705	4,792.3	0	121,935,678	4,449,000	27.41
11.000	91.67	2,827	23,311	0.00	64,451,479	5,371.0	0	137,180,576	4,452,000	30.81
11.250	93.75	2,827	24,017	0.00	74,690,773	6,224.2	0	154,573,358	4,455,000	34.70
11.500	95.83	2,827	24,724	0.00	85,563,336	7,130.3	0	174,605,121	4,458,000	39.17
11.750	97.92	2,827	25,431	0.00	96,435,898	8,036.3	0	197,355,026	4,461,000	44.24
12.000	100.00	2,827	26,138	0.00	107,308,461	8,942.4	0	222,823,071	4,464,000	49.92

Table 2.10.2-2 – Sample Inputs to the SLAPDOWN Program

Parameter	Description	Sample Value
Z1, Z2	Length from primary end to CG, and from CG to secondary end, respectively①	90.38 inches (both sides)
R1, R2	Length from package axis to impact limiter contact point, primary and secondary ends, respectively	63.0 inches (both ends)
$\mu 1$, $\mu 2$	Coefficient of friction, primary and secondary ends, respectively	0.0 (both ends)
M	Overall package mass	611.0 lb-s^2/in
I_{cg}	Radial mass moment of inertia about the package CG	3.1(10)^6 in-lb-s^2
v_o	Impact velocity	-527.5 in/s (30-ft drop)
Θ	Angle with respect to horizontal of primary impact	0º, 15º, etc, as required
K	Elastic rebound stiffness of the impact limiter material	10^7 lb/in

Notes:

① This dimension is measured from the package CG to the center of the cylindrical portion of the impact limiter, which is the location of the line of action of side drop impact force.

Table 2.10.2-3 – Sample Force-Deflection to the SLAPDOWN Program

Primary Impact Limiter		Secondary Impact Limiter	
Deflection (in)	Force (lb)	Deflection (in)	Force (lb)
0	0	0	0
1	207,100	1	2,383,000
2	583,900	2	3,363,000
3	1,069,000	3	3,963,000
4	1,640,000	4	4,450,000
5	2,285,000	5	4,885,000
6	2,998,000	6	5,289,000
7	3,767,000	7	5,671,000
8	4,444,000	8	6,041,000
9	5,146,000	9	6,310,000
10	5,756,000	10	6,513,000
11	6,304,000	11	6,721,000
12	6,818,000	12	6,936,000
13	7,223,000	13	7,157,000
14	7,573,000	14	7,384,000
15	7,926,000	15	7,614,000

Table 2.10.2-4 – Sample of SLAPDOWN General Output

```
SAMPLE PACKAGE, 15 DEGREE OBLIQUE

 ****** SEQUENCE OF EVENTS ******

 ** NOSE HIT     AT TIME  0.000E+00, VELOCITY = -5.275E+02, RATIO =  1.00
 ** NOSE REBOUND AT TIME  3.311E-02, VELOCITY =  1.507E+01, RATIO =  -.03
 ** NOSE UNLOAD  AT TIME  4.008E-02, VELOCITY =  1.346E+02, RATIO =  -.26
 ** TAIL HIT     AT TIME  7.318E-02, VELOCITY = -7.061E+02, RATIO =  1.34
 ** TAIL REBOUND AT TIME  1.037E-01, VELOCITY =  2.410E+01, RATIO =  -.05
 ** TAIL UNLOAD  AT TIME  1.106E-01, VELOCITY =  1.422E+02, RATIO =  -.27


 ****** RESULTS ******

 Event over at time    1.115E-01, Time step size  8.712E-04
 Time step multiplier  1.000E-01,  129 Plot times written to database


            DISPLACEMENT     VELOCITY     ACCELERATION

    NOSE      1.159E+01      1.346E+02      2.732E+04 (MAX)
                            -5.275E+02     -7.297E+03 (MIN)

    TAIL      1.206E+01      1.422E+02      2.927E+04 (MAX)
                            -7.061E+02     -6.478E+03 (MIN)

      CG                     2.781E+01      1.099E+04 (MAX)
                            -5.277E+02     -3.860E+02 (MIN)

 ANGULAR                     1.266E+00      2.025E+02 (MAX)
                            -4.623E+00     -1.880E+02 (MIN)

 MAXIMUM ENERGIES:  3.488E+07 (NOSE),  5.947E+07 (TAIL)
  IMPACT AT 80 IN FROM C.G. =       65.677830  (NOSE)
  IMPACT AT 80 IN FROM C.G. =       70.322280  (TAIL)
  TAIL IMPACT ANGLE =        1.906593 DEG.
```

Table 2.10.2-5 – Sample of SLAPDOWN Time History Output

TITLE: SAMPLE PACKAGE, 15 DEGREE OBLIQUE
02/20/1996 13:17:05

TIME,S	POSY(2)	VELY(2)	ACCY(2)	THETA	OMEGA	ALPHA
.0000,	.864E+02,	-.527E+03,	-.386E+03,	.262E+00,	.000E+00,	.000E+00,
.0009,	.859E+02,	-.528E+03,	-.230E+03,	.262E+00,	-.234E-02,	-.268E+01,
.0017,	.855E+02,	-.528E+03,	-.744E+02,	.262E+00,	-.701E-02,	-.536E+01,
.0026,	.850E+02,	-.528E+03,	.186E+03,	.262E+00,	-.156E-01,	-.985E+01,
.0035,	.846E+02,	-.527E+03,	.469E+03,	.262E+00,	-.284E-01,	-.147E+02,
.0044,	.841E+02,	-.526E+03,	.803E+03,	.262E+00,	-.462E-01,	-.205E+02,
.0052,	.836E+02,	-.525E+03,	.116E+04,	.262E+00,	-.695E-01,	-.267E+02,
.0061,	.832E+02,	-.524E+03,	.155E+04,	.262E+00,	-.985E-01,	-.333E+02,
.0070,	.827E+02,	-.522E+03,	.197E+04,	.262E+00,	-.134E+00,	-.406E+02,
.0078,	.823E+02,	-.520E+03,	.240E+04,	.261E+00,	-.176E+00,	-.479E+02,
.0087,	.818E+02,	-.518E+03,	.286E+04,	.261E+00,	-.224E+00,	-.559E+02,
.0096,	.814E+02,	-.515E+03,	.332E+04,	.261E+00,	-.280E+00,	-.638E+02,
.0105,	.809E+02,	-.512E+03,	.382E+04,	.261E+00,	-.343E+00,	-.723E+02,
.0113,	.805E+02,	-.508E+03,	.431E+04,	.261E+00,	-.413E+00,	-.808E+02,
.0122,	.800E+02,	-.504E+03,	.481E+04,	.260E+00,	-.491E+00,	-.894E+02,
.0131,	.796E+02,	-.499E+03,	.531E+04,	.260E+00,	-.577E+00,	-.981E+02,
.0139,	.792E+02,	-.494E+03,	.580E+04,	.259E+00,	-.669E+00,	-.107E+03,
.0148,	.787E+02,	-.489E+03,	.622E+04,	.259E+00,	-.769E+00,	-.114E+03,
.0157,	.783E+02,	-.483E+03,	.663E+04,	.258E+00,	-.874E+00,	-.121E+03,
.0166,	.779E+02,	-.477E+03,	.703E+04,	.257E+00,	-.985E+00,	-.128E+03,
.0174,	.775E+02,	-.470E+03,	.742E+04,	.256E+00,	-.110E+01,	-.134E+03,
.0183,	.771E+02,	-.463E+03,	.779E+04,	.255E+00,	-.122E+01,	-.141E+03,
.0192,	.766E+02,	-.456E+03,	.813E+04,	.254E+00,	-.135E+01,	-.147E+03,
.0200,	.762E+02,	-.449E+03,	.843E+04,	.253E+00,	-.149E+01,	-.152E+03,
.0209,	.759E+02,	-.441E+03,	.870E+04,	.252E+00,	-.162E+01,	-.157E+03,
.0218,	.755E+02,	-.434E+03,	.896E+04,	.250E+00,	-.176E+01,	-.161E+03,
.0227,	.751E+02,	-.426E+03,	.919E+04,	.249E+00,	-.191E+01,	-.165E+03,
.0235,	.747E+02,	-.417E+03,	.939E+04,	.247E+00,	-.205E+01,	-.169E+03,
.0244,	.744E+02,	-.409E+03,	.958E+04,	.245E+00,	-.220E+01,	-.172E+03,
.0253,	.740E+02,	-.401E+03,	.975E+04,	.244E+00,	-.236E+01,	-.175E+03,
.0261,	.737E+02,	-.392E+03,	.990E+04,	.242E+00,	-.251E+01,	-.178E+03,
.0270,	.733E+02,	-.383E+03,	.100E+05,	.239E+00,	-.267E+01,	-.180E+03,
.0279,	.730E+02,	-.374E+03,	.101E+05,	.237E+00,	-.283E+01,	-.182E+03,
.0287,	.727E+02,	-.365E+03,	.102E+05,	.235E+00,	-.299E+01,	-.184E+03,
.0296,	.723E+02,	-.356E+03,	.103E+05,	.232E+00,	-.315E+01,	-.185E+03,
.0305,	.720E+02,	-.347E+03,	.104E+05,	.229E+00,	-.331E+01,	-.186E+03,
.0314,	.717E+02,	-.338E+03,	.104E+05,	.226E+00,	-.347E+01,	-.187E+03,
.0322,	.714E+02,	-.329E+03,	.104E+05,	.223E+00,	-.364E+01,	-.188E+03,
.0331,	.711E+02,	-.320E+03,	.104E+05,	.220E+00,	-.380E+01,	-.188E+03,
.0340,	.709E+02,	-.311E+03,	.104E+05,	.217E+00,	-.397E+01,	-.188E+03,
.0348,	.706E+02,	-.303E+03,	.966E+04,	.213E+00,	-.412E+01,	-.175E+03,
.0357,	.703E+02,	-.295E+03,	.879E+04,	.210E+00,	-.426E+01,	-.160E+03,
.0366,	.701E+02,	-.288E+03,	.763E+04,	.206E+00,	-.438E+01,	-.140E+03,
.0375,	.698E+02,	-.283E+03,	.621E+04,	.202E+00,	-.448E+01,	-.115E+03,
.0383,	.696E+02,	-.279E+03,	.459E+04,	.198E+00,	-.455E+01,	-.870E+02,
.0392,	.693E+02,	-.277E+03,	.281E+04,	.194E+00,	-.460E+01,	-.559E+02,
.0401,	.691E+02,	-.276E+03,	.935E+03,	.190E+00,	-.462E+01,	-.231E+02,
.0409,	.688E+02,	-.276E+03,	-.386E+03,	.186E+00,	-.462E+01,	.000E+00,

Table 2.10.2-6 – Comparison of SLAPDOWN and SCANS Results

Parameter	SLAPDOWN Result	SCANS Result
Primary Impact Limiter Deflection, inches	11.6	11.6
Secondary Impact Limiter Deflection, inches	12.1	12.1
Primary Vertical Acceleration (CG), in/s^2	26.9	26.8
Secondary Vertical Acceleration (CG), in/s^2	28.5	28.5
Primary Angular Acceleration, radians/s^2	-188	-186
Secondary Angular Acceleration, radians/s^2	202	218

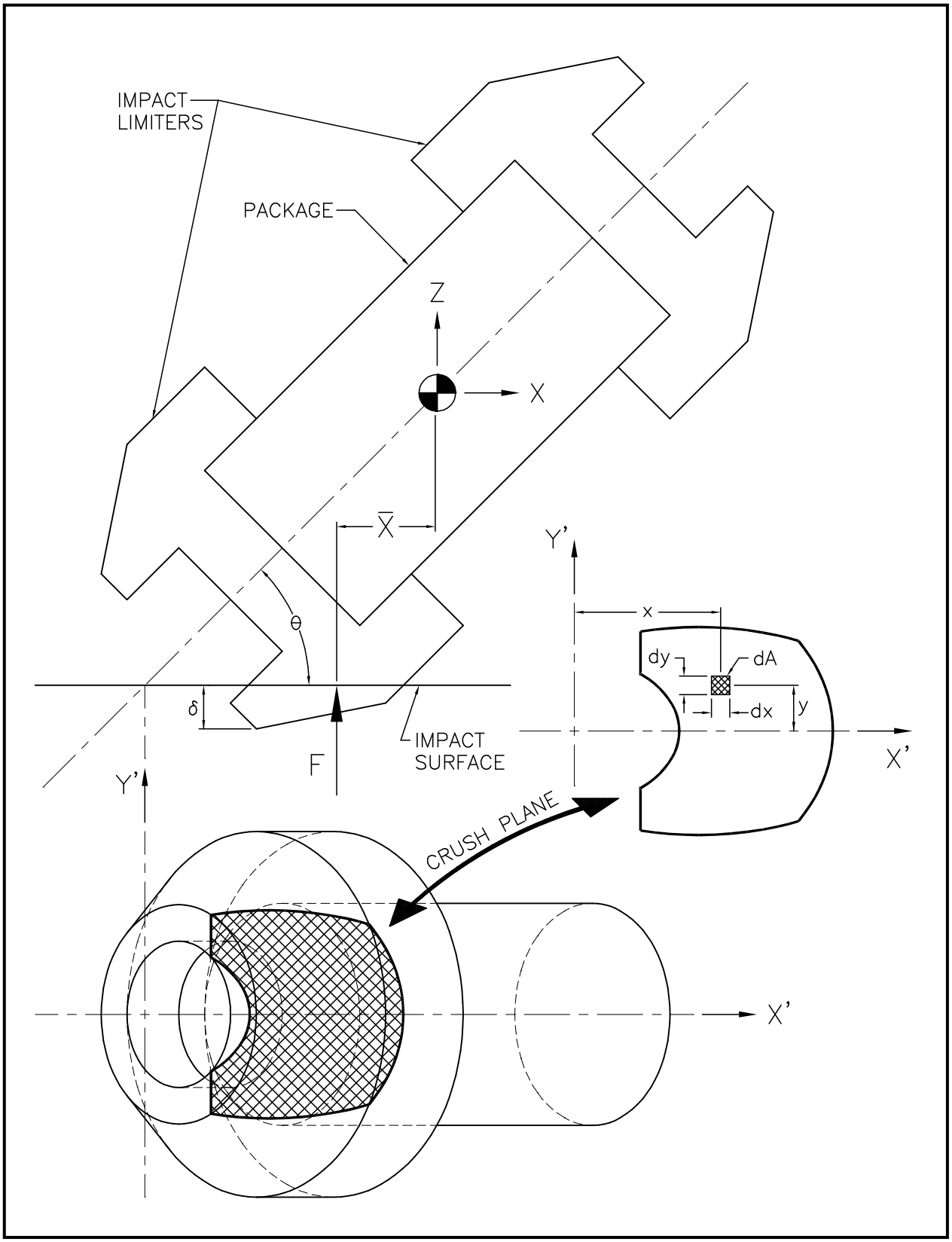

Figure 2.10.2-1 – Impact Limiter Force and Centroid Development

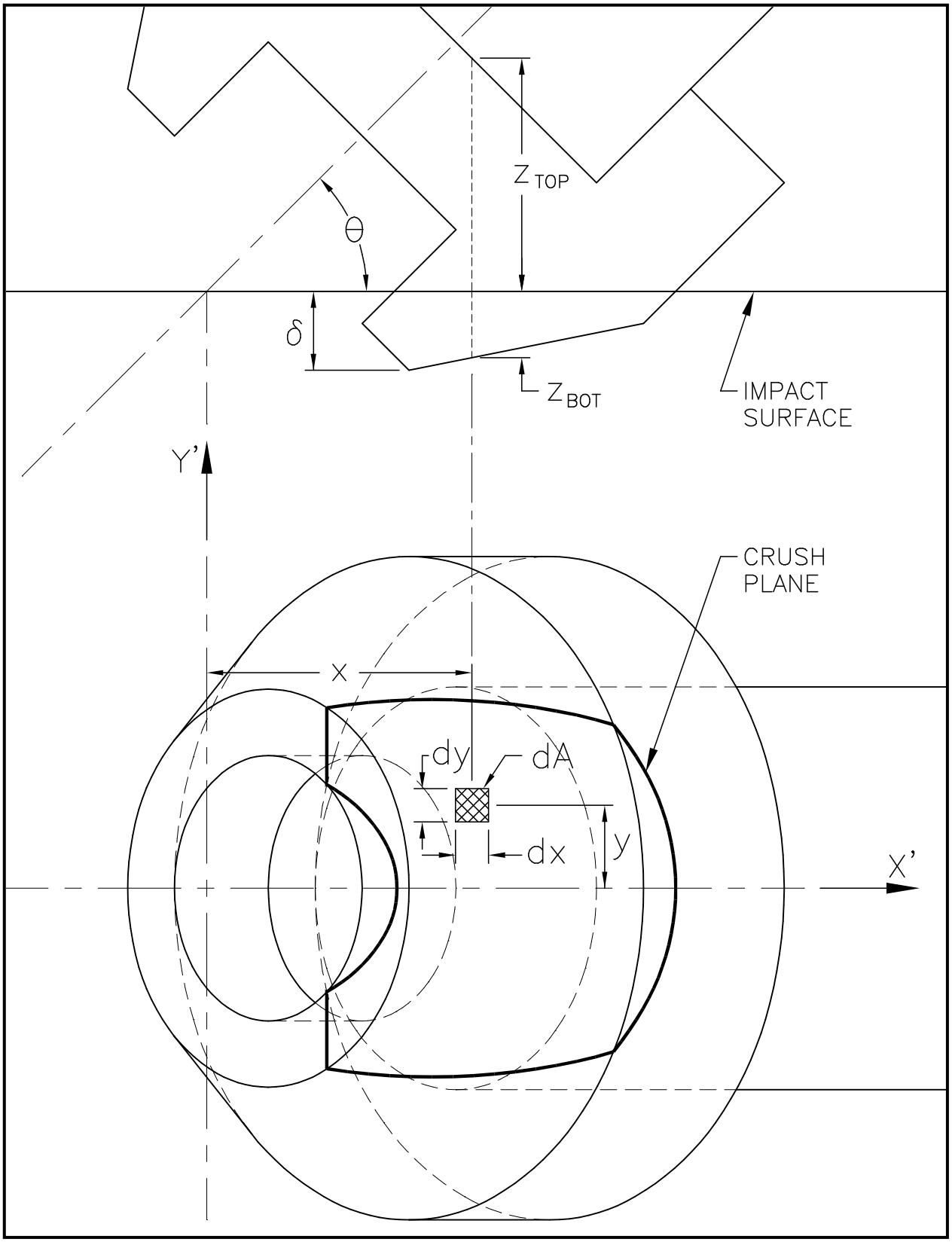

Figure 2.10.2-2 – Strain Determination

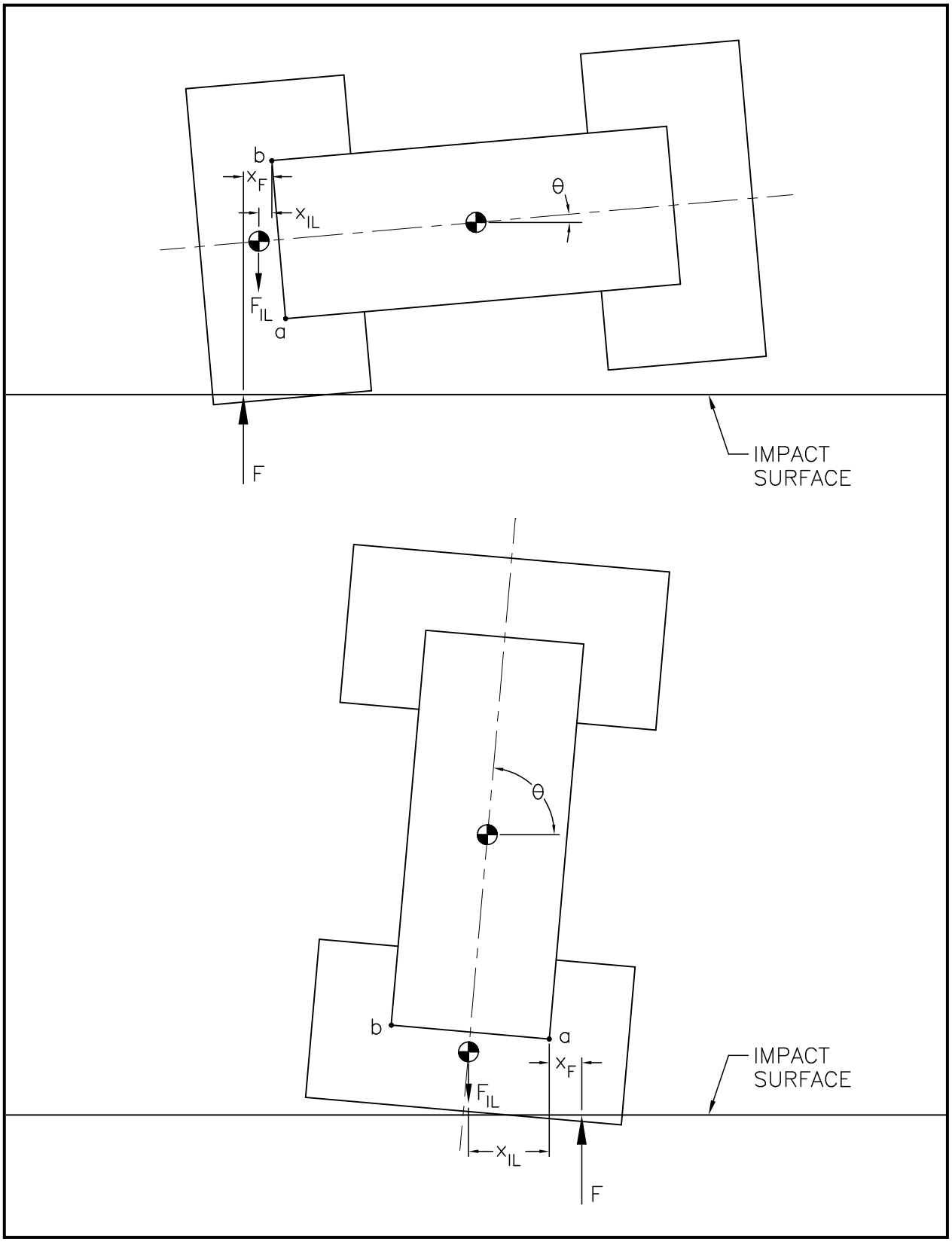

Figure 2.10.2-3 – Determination of Impact Limiter Separation Moments

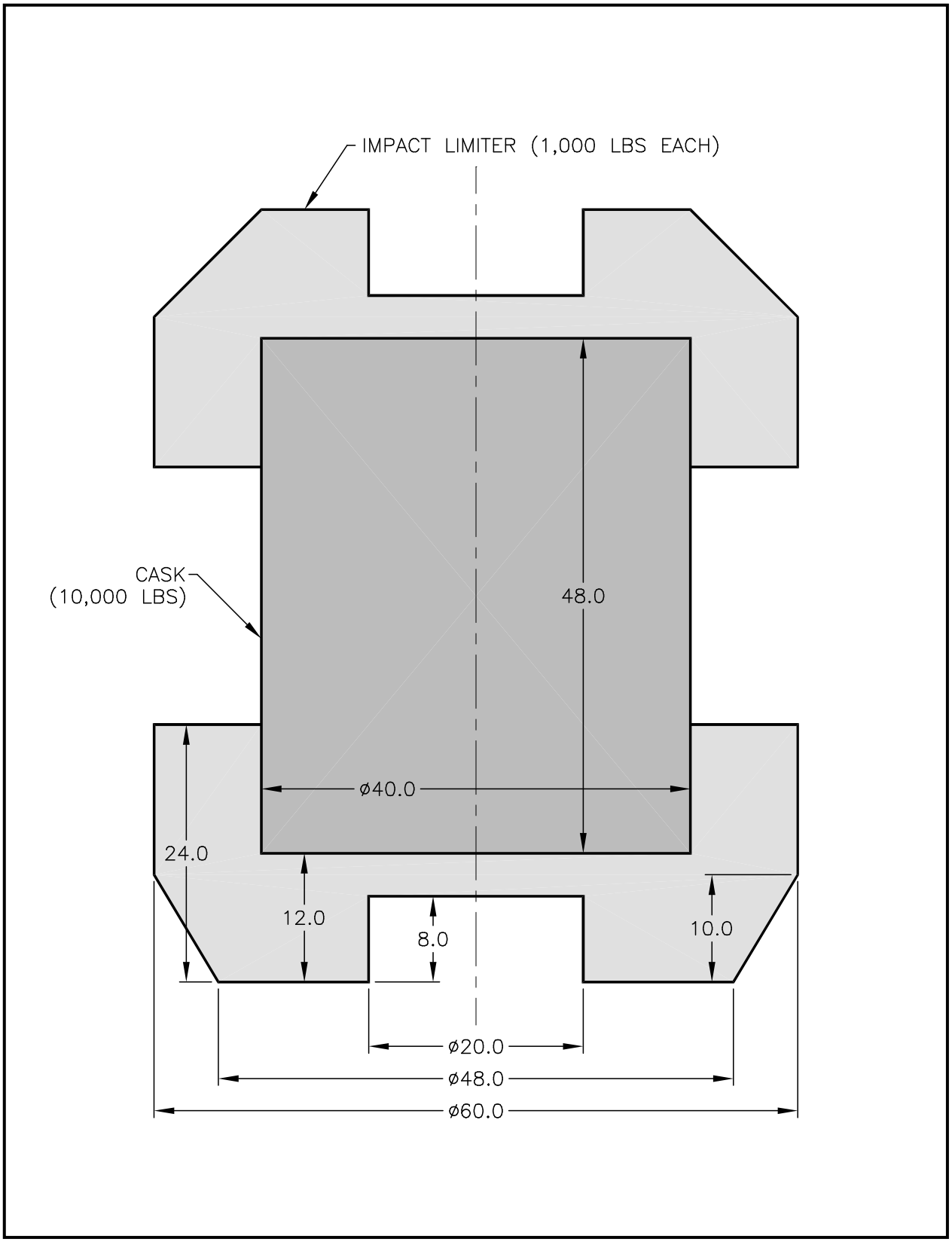

Figure 2.10.2-4 – Example Problem

Packaging Technology's Cask Drop Analysis Program, v2.21

Tuesday, May 16, 1995 3:38:19 pm

[Input Window]

Title: SAMPLE PROBLEM FOR QUALITY ASSURANCE CHECK (AREAS AND VOLUMES)

IL Weight (each, lbs):	1000	Cask/Payload Weight (lbs):	10000
IL Outside Diameter (in):	60	Cask Outside Diameter (in):	40
IL Overall Length (in):	24	Cask Overall Length (in):	48
IL Conical Diameter (in):	48	Free Drop Height (ft):	30
IL Conical Length (in):	10	Radial Mass MI (lb-in-s²):	12235.16
IL End Thickness (in):	12	Frictional Coefficient (μ):	0
IL End Hole Diameter (in):	20	Unloading Modulus (lbs/in):	10000000
IL End Hole Length (in):	8	Crush Media Specification:	PolyFoam

[Control Window]

Analysis	Crush (in)	Angle (°)	Static	Dynamic	Print	File
dXY: 25	Min: 0.25	Min: 0	Full √	Full	Full	Full √
Sln: Global	Max: 20	Max: 90	Smry	Smry	Smry	Smry
ε/σ: 0.1	Inc: 0.25	Inc: 45	Both	Both	Both	Both

[Output Window]

[PgUp]/[PgDn] keys toggle active window; [F10] exits program

Packaging Technology's Cask Drop Analysis Program, v2.21

Tuesday, May 16, 1995 3:38:29 pm

[Input Window]

Title: SAMPLE PROBLEM FOR QUALITY ASSURANCE CHECK (AREAS AND VOLUMES)

IL Weight (each, lbs):	1000	Cask/Payload Weight (lbs):	10000
IL Outside Di		r (in):	40
IL Overall		h (in):	48
IL Conical Di		t (ft):	30
IL Conical		in-s²):	12235.16
IL End Thi		nt (μ):	0
IL End Hole Di		bs/in):	10000000
IL End Hole		cation:	PolyFoam

[Polyurethane Foam Database]

D (pcf): 20.0000 T (°F): -20.00

σ (psi): 2552.3 Bias (%): 60

"‖" to rise		"⊥" to rise	
ε(in/in)	σ(psi)	ε(in/in)	σ(psi)
0.00	0.0	0.00	0.0
0.10	2,552.3	0.10	2,675.0
0.20	2,687.0	0.20	2,785.4
0.30	2,868.8	0.30	2,959.9
0.40	3,302.9	0.40	3,345.9
0.50	4,115.1	0.50	4,147.7
0.60	6,074.3	0.60	6,062.8
0.65	7,942.0	0.65	7,868.8
0.70	10,925.0	0.70	10,180.0
0.75	15,001.8	0.75	15,554.4
0.80	26,829.5	0.80	29,704.8
Orientation: Axial		Orientation: Radial	

[Control Window]

Analysis	Cr		Print	File
dXY: 25	Mi		ull	Full √
Sln: Global	Ma		mry	Smry
ε/σ: 0.1	In		oth	Both

[Output Window]

[F2] calculates stress data and [F3] toggles orientation; [F10] exits...

Figure 2.10.2-5 – CASKDROP Program Input Windows

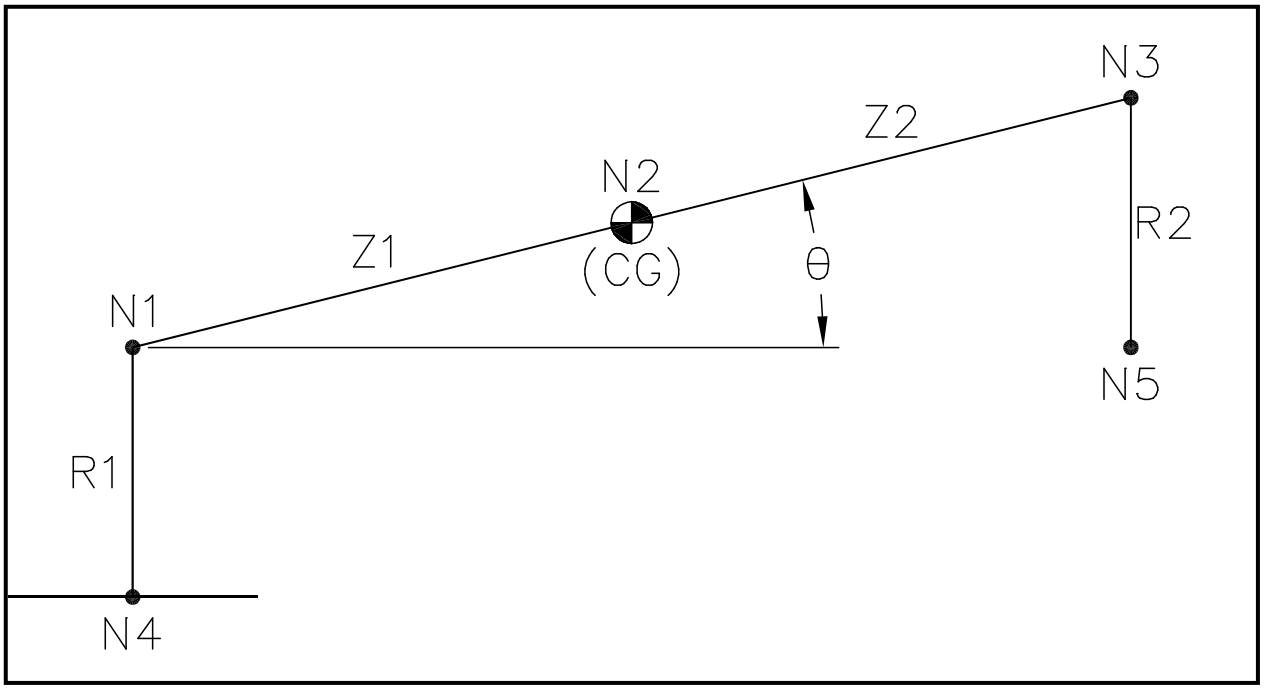

Figure 2.10.2-6 – SLAPDOWN Analytical Model

2.10.3 Drop Impact Evaluation Results

This appendix presents the impact analysis of the RH-TRU 72-B package for normal conditions of transport (NCT) 1-foot drops and hypothetical accident condition (HAC) 30-foot drops. The results are used in Section 2.6.7, *Free Drop*, and Section 2.7.1, *Free Drop*. Given the RH-TRU 72-B package and impact limiter geometry, and the impact limiter's foam material properties, the computer codes CASKDROP (described in Appendix 2.10.2.1, *Description of the CASKDROP Computer Code*) and SLAPDOWN (described in Appendix 2.10.2.2, *Description of the SLAPDOWN Computer Code*) are used to predict results for a combination of bounding foam strengths, orientations, and drop heights. Geometric inputs include limiter outside diameter, limiter overall length, limiter end thickness, package diameter, package length, package mass, and package mass moment of inertia. Mass properties are obtained from Section 2.2, *Weights and Centers of Gravity*.

Impact calculations are performed for end drop, side drop, and oblique angles from five to 85º from horizontal (in 5º increments). If the orientation is stable i.e., where the package center of gravity is supported such that no package rotation occurs, the program CASKDROP is used to report the impact results in the following tables. If the orientation is not stable, such that a secondary impact occurs, the program SLAPDOWN is used to calculate impact results. Program SLAPDOWN uses impact limiter force deflection data calculated by CASKDROP. For angles to the horizontal of 65º to 90º, package rotation is relatively small, and is conservatively neglected by using CASKDROP outputs. For these cases, CASKDROP conservatively overpredicts primary impact results. Secondary slapdown impacts are only important for relatively shallow angles, as discussed in Section 2.10.4, *Slapdown Assessment*.

Impact calculations use the upper- and lower-bound foam stress-strain data given in Table 2.3-3 in Section 2.3, *Mechanical Properties of Materials*. Lower-bound foam properties lead to maximum deflections and strains, and upper-bound properties lead to maximum impacts and stresses. Both parallel-to-rise and perpendicular-to-rise data is used. The parallel-to-rise direction is axial to the package. Depending on impact orientation, the parallel- and perpendicular-to-rise stress-strain data is combined using interpolation, as described in Appendix 2.10.2.1, *Description of the CASKDROP Computer Code*.

For HAC 30-foot drop cases, the foam strength is adjusted by a multiplying factor of 1.52 to bring the calculations into agreement with test results, as discussed in Appendix 2.10.7.3, *Correction Factors*. The factor of 1.52 was developed using 30-foot drop test data, and it includes a dynamic effect. Since the NCT 1-foot drop has a much smaller impact velocity and, therefore, a negligible dynamic effect, the foam strength data for NCT free drops is adjusted by the static factor of 1.19, rather than the full dynamic factor of 1.52. Table 2.10.3-1 summarizes all parallel-to-rise and perpendicular-to-rise stress data for NCT/HAC and warm/cold conditions.

Special circumstances are encountered in the modeling of end and side drop orientations. In the end drop, shear of some of the foam occurs, as described in Appendix 2.10.7.1, *Static Test Program*. To properly account for the shear, the diameter of the inner shell of the package is assumed to be equal to the whole diameter of the impact limiter, namely 75.9 inches (the full diameter is 76 inches). This approach was successful in predicting end orientation crush force-deflection curves in static testing.

Shear of the foam also occurs to a lesser extent in the side drop, as described in Appendix 2.10.7.1, *Static Test Program*. Thus, the inner shell is lengthened somewhat for purposes of calculation. The true end distance is 22.5 inches, but for side drop impacts, a half-effective end length of 11.25 inches is assumed. As before, this approach was successful in predicting side orientation crush force-deflection curves in static testing. These modeling modifications are designated "fully effective," and they are aids to bring the test and modeling results into better agreement. For orientation angles of 5º – 85º, no change to the impact limiter actual dimensions is made.

Significant results from the NCT 1-foot drop analyses are summarized in the following tables and figures:

- Table 2.10.3-2 – CASKDROP Output File for NCT End Drop, Cold (-20 ºF)
- Table 2.10.3-3 – CASKDROP Output File for NCT End Drop, Warm (140 ºF)
- Figure 2.10.3-1 – Impact Limiter Deflection and Residual Clearance for the NCT Oblique Drop, Cold (-20 ºF)
- Figure 2.10.3-2 – Impact Limiter Separation Moments for the NCT Oblique Drop, Cold (-20 ºF)
- Figure 2.10.3-3 – Impact Limiter Deflection and Residual Clearance for the NCT Oblique Drop, Warm (140 ºF)
- Figure 2.10.3-4 – Impact Limiter Separation Moments for the NCT Oblique Drop, Warm (140 ºF)
- Table 2.10.3-4 – CASKDROP Output File for NCT Side Drop, Cold (-20 ºF)
- Table 2.10.3-5 – CASKDROP Output File for NCT Side Drop, Warm (140 ºF)

Significant results from the HAC 30-foot drop analyses are summarized in the following tables and figures:

- Table 2.10.3-6 – CASKDROP Output File for HAC End Drop, Cold (-20 ºF)
- Table 2.10.3-7 – CASKDROP Output File for HAC End Drop, Warm (140 ºF)
- Figure 2.10.3-5 – Impact Limiter Deflection and Residual Clearance for the HAC Oblique Drop, Cold (-20 ºF)
- Figure 2.10.3-6 – Impact Limiter Separation Moments for the HAC Oblique Drop, Cold (-20 ºF)
- Figure 2.10.3-7 – Impact Limiter Deflection and Residual Clearance for the HAC Oblique Drop, Warm (140 ºF)
- Figure 2.10.3-8 – Impact Limiter Separation Moments for the HAC Oblique Drop, Warm (140 ºF)
- Table 2.10.3-8 – CASKDROP Output File for HAC Side Drop, Cold (-20 ºF)
- Table 2.10.3-9 – CASKDROP Output File for HAC Side Drop, Warm (140 ºF)

Maximum impact limiter deflections and residual clearances, and impact limiter separation moments given in Figure 2.10.3-1 though Figure 2.10.3-8 are presented as a function of the initial package impact angle, measured from horizontal.

A summary of the impact limiter deformations and package accelerations for the end and side impact orientations is represented in Table 2.10.3-10. A summary of the maximum package responses as a function of initial impact angle is presented in Table 2.10.3-11 and Table 2.10.3-12. A summary of the maximum impact limiter separation moments as a function of initial impact angle is represented in Table 2.10.3-13.

As shown in Table 2.10.3-13, the maximum impact limiter separation moments are similar for both normal and accident conditions. This is because the maximum moment occurs at a relatively small crush depth, i.e., the moment arm decreases with additional crush depth at a higher rate than the crush force increases.

Finally, Table 2.10.3-14 and Table 2.10.3-15 summarize the time-history from the upper bound (cold) foam strength SLAPDOWN analyses at the time of maximum impact force, F_{max}. The remaining values in the table come from the SLAPDOWN output file.

Table 2.10.3-1 – Polyurethane Foam Data used in CASKDROP

	NCT① (psi)				HAC② (psi)			
	Cold		Warm		Cold		Warm	
Strain	PAR	PER	PAR	PER	PAR	PER	PAR	PER
5%	683	594	336	292	872	758	429	373
10%	689	638	339	314	879	815	433	401
20%	692	665	340	327	883	849	435	418
30%	740	712	364	350	946	910	465	448
40%	824	800	405	393	1,052	1,022	518	503
50%	994	979	489	482	1,270	1,251	625	615
60%	1,385	1,392	681	685	1,768	1,778	870	875
65%	1,767	1,819	869	895	2,257	2,324	1,111	1,143
70%	2,441	2,554	1,201	1,256	3,118	3,262	1,534	1,605
75%	3,668	3,808	1,805	1,873	4,686	4,864	2,305	2,393
80%	—	—	3,226	3,235	—	—	4,120	4,133
87%	—	—	10,539	10,944	—	—	13,462	13,979

Notes:

① NCT data equal to data from Table 2.3-3 in Section 2.3, *Mechanical Properties of Materials*, multiplied by a 1.19 static factor.

② HAC data equal to data from Table 2.3-3 in Section 2.3, *Mechanical Properties of Materials*, multiplied by a 1.52 dynamic factor.

Table 2.10.3-2 – CASKDROP Output File for NCT End Drop, Cold (-20 ºF)

End Drop *** PACKAGING TECHNOLOGY *** CASKDROP, v2.31
02-01-1999, 09:42:06 Nov 13, 1997

72-B End Drop Analysis FULL SCALE SAR PREDICTION (One Foot)			
Impact Limiter Weight (each) -	2,547 lbs	Cask and Payload Weight -	39,906 lbs
Impact Limiter Outside Diameter -	76.0000 in	Cask Outside Diameter -	79.5000 in
Impact Limiter Overall Length -	46.0000 in	Cask Overall Length -	141.7500 in
Impact Limiter Conical Diameter -	0.0000 in	Dynamic Unloading Modulus -	1.000E+07 lbs/in
Impact Limiter Conical Length -	0.0000 in	Rad Mass Moment of Inertia -	304,239 lb-in-s²
Impact Limiter End Thickness -	22.5000 in	Frictional Coefficient -	0.0000
Impact Limiter Hole Diameter -	0.0000 in	Drop Height -	1.0000 ft
Impact Limiter Hole Length -	0.0000 in	Drop Angle from Horizontal -	90.0000°
Unbacked Area Threshhold Strain -	0.1000 in/in	Crush Analysis Theory -	Global
Unbacked Area Crush Stress -	689 psi	Number of Integration Incs -	50

VARIABLE CRUSH STRESS	
ε (in/in)	σ (psi)
0.000	0.0
0.050	683.0
0.100	689.0
0.200	692.0
0.300	740.0
0.400	824.0
0.500	994.0
0.600	1,385.0
0.650	1,767.0
0.700	2,441.0
0.750	3,668.0

DEFL (in)	MAX ε (%)	AREA (in²)	VOLUME (in³)	XBAR (in)	IMPACT FORCE (lbs)	ACCEL (g's)	I/L MOMENT (in-lbs)	STRAIN ENERGY (in-lbs)	KINETIC ENERGY (in-lbs)	SE/KE RATIO
0.500	2.22	4,536	2,268	0.00	1,661,112	36.9	0	415,278	562,500	0.74
0.585	2.60	4,536	2,652	0.00	1,911,833	42.5	0	566,304	566,304	1.00
1.000	4.44	4,536	4,536	0.00	2,900,495	64.5	0	1,555,680	585,000	2.66
1.500	6.67	4,536	6,805	0.00	3,360,835	74.7	0	3,121,012	607,500	5.14
2.000	8.89	4,536	9,073	0.00	3,245,452	72.1	0	4,772,584	630,000	7.58
2.500	11.11	4,536	11,341	0.00	3,035,136	67.4	0	6,342,731	652,500	9.72
3.000	13.33	4,536	13,609	0.00	2,955,584	65.7	0	7,840,411	675,000	11.62
3.500	15.56	4,536	15,878	0.00	2,975,047	66.1	0	9,323,069	697,500	13.37
4.000	17.78	4,536	18,146	0.00	3,050,583	67.8	0	10,829,476	720,000	15.04
4.500	20.00	4,536	20,414	0.00	3,139,253	69.8	0	12,376,935	742,500	16.67
5.000	22.22	4,536	22,682	0.00	3,207,174	71.3	0	13,963,542	765,000	18.25
5.500	24.44	4,536	24,951	0.00	3,255,426	72.3	0	15,579,192	787,500	19.78
6.000	26.67	4,536	27,219	0.00	3,294,103	73.2	0	17,216,574	810,000	21.26

Table 2.10.3-3 – CASKDROP Output File for NCT End Drop, Warm (140 ºF)

End Drop *** PACKAGING TECHNOLOGY *** CASKDROP, v2.31
02-09-1999, 16:42:40 Nov 13, 1997

72-B 90 Deg Drop FULL SCALE SAR PREDICTION (1 ft)			
Impact Limiter Weight (each) -	2,547 lbs	Cask and Payload Weight -	39,906 lbs
Impact Limiter Outside Diameter -	76.0000 in	Cask Outside Diameter -	75.9000 in
Impact Limiter Overall Length -	46.0000 in	Cask Overall Length -	141.8000 in
Impact Limiter Conical Diameter -	0.0000 in	Dynamic Unloading Modulus -	1.000E+07 lbs/in
Impact Limiter Conical Length -	0.0000 in	Rad Mass Moment of Inertia -	304,415 lb-in-s²
Impact Limiter End Thickness -	22.5000 in	Frictional Coefficient -	0.0000
Impact Limiter Hole Diameter -	0.0000 in	Drop Height -	1.0000 ft
Impact Limiter Hole Length -	0.0000 in	Drop Angle from Horizontal -	90.0000°
Unbacked Area Threshhold Strain -	0.1000 in/in	Crush Analysis Theory -	Global
Unbacked Area Crush Stress -	339 psi	Number of Integration Incs -	50

VARIABLE CRUSH STRESS	
ε (in/in)	σ (psi)
0.000	0.0
0.050	336.0
0.100	339.0
0.200	340.0
0.300	364.0
0.400	405.0
0.500	489.0
0.600	681.0
0.650	869.0
0.700	1,201.0
0.750	1,805.0
0.800	3,226.0
0.870	10,539.0

DEFL (in)	MAX ε (%)	AREA (in²)	VOLUME (in³)	XBAR (in)	IMPACT FORCE (lbs)	ACCEL (g's)	I/L MOMENT (in-lbs)	STRAIN ENERGY (in-lbs)	KINETIC ENERGY (in-lbs)	SE/KE RATIO
0.500	2.22	4,536	2,268	0.00	817,125	18.2	0	204,281	562,500	0.36
0.856	3.80	4,536	3,884	0.00	1,284,766	28.6	0	578,525	578,525	1.00
1.000	4.44	4,536	4,536	0.00	1,426,862	31.7	0	765,278	585,000	1.31
1.500	6.67	4,536	6,805	0.00	1,653,486	36.7	0	1,535,365	607,500	2.53
2.000	8.89	4,536	9,073	0.00	1,596,849	35.5	0	2,347,949	630,000	3.73
2.500	11.11	4,536	11,341	0.00	1,493,202	33.2	0	3,120,461	652,500	4.78
3.000	13.33	4,536	13,609	0.00	1,453,542	32.3	0	3,857,147	675,000	5.71
3.500	15.56	4,536	15,878	0.00	1,462,459	32.5	0	4,586,147	697,500	6.58
4.000	17.78	4,536	18,146	0.00	1,499,051	33.3	0	5,326,525	720,000	7.40
4.500	20.00	4,536	20,414	0.00	1,542,413	34.3	0	6,086,891	742,500	8.20
5.000	22.22	4,536	22,682	0.00	1,576,022	35.0	0	6,866,500	765,000	8.98
5.500	24.44	4,536	24,951	0.00	1,600,256	35.6	0	7,660,570	787,500	9.73
6.000	26.67	4,536	27,219	0.00	1,619,852	36.0	0	8,465,597	810,000	10.45

Table 2.10.3-4 – CASKDROP Output File for NCT Side Drop, Cold (-20 ºF)

Side Drop *** PACKAGING TECHNOLOGY *** CASKDROP, v2.31
02-11-1999, 10:19:49 Nov 13, 1997

72-B Side Drop Analysis FULL SCALE SAR PREDICTION (One Foot)			
Impact Limiter Weight (each) -	2,547 lbs	Cask and Payload Weight -	39,906 lbs
Impact Limiter Outside Diameter -	76.0000 in	Cask Outside Diameter -	42.1000 in
Impact Limiter Overall Length -	46.0000 in	Cask Overall Length -	141.7500 in
Impact Limiter Conical Diameter -	0.0000 in	Dynamic Unloading Modulus -	1.000E+07 lbs/in
Impact Limiter Conical Length -	0.0000 in	Rad Mass Moment of Inertia -	241,355 lb-in-s²
Impact Limiter End Thickness -	11.2500 in	Frictional Coefficient -	0.0000
Impact Limiter Hole Diameter -	0.0000 in	Drop Height -	1.0000 ft
Impact Limiter Hole Length -	0.0000 in	Drop Angle from Horizontal -	0.0000°
Unbacked Area Threshhold Strain -	0.1000 in/in	Crush Analysis Theory -	Global
Unbacked Area Crush Stress -	638 psi	Number of Integration Incs -	50

VARIABLE CRUSH STRESS	
ε (in/in)	σ (psi)
0.000	0.0
0.050	594.0
0.100	638.0
0.200	665.0
0.300	712.0
0.400	800.0
0.500	979.0
0.600	1,392.0
0.650	1,819.0
0.700	2,554.0
0.750	3,808.0

DEFL (in)	MAX ε (%)	AREA (in²)	VOLUME (in³)	XBAR (in)	IMPACT FORCE (lbs)	ACCEL (g's)	I/L MOMENT (in-lbs)	STRAIN ENERGY (in-lbs)	KINETIC ENERGY (in-lbs)	SE/KE RATIO
0.500	2.95	1,131	377	0.00	254,185	5.6	0	63,546	562,500	0.11
1.000	5.90	1,593	1,065	0.00	618,411	13.7	0	281,696	585,000	0.48
1.435	8.46	1,903	1,828	0.00	866,688	19.3	0	604,567	604,567	1.00
1.500	8.85	1,945	1,953	0.00	896,815	19.9	0	660,502	607,500	1.09
2.000	11.80	2,238	3,001	0.00	1,094,295	24.3	0	1,158,280	630,000	1.84
2.500	14.75	2,494	4,185	0.00	1,273,629	28.3	0	1,750,261	652,500	2.68
3.000	17.70	2,723	5,491	0.00	1,452,846	32.3	0	2,431,880	675,000	3.60
3.500	20.65	2,931	6,905	0.00	1,630,952	36.2	0	3,202,829	697,500	4.59
4.000	23.60	3,123	8,419	0.00	1,800,623	40.0	0	4,060,723	720,000	5.64
4.500	26.55	3,300	10,026	0.00	1,959,027	43.5	0	5,000,636	742,500	6.73
5.000	29.50	3,467	11,718	0.00	2,107,610	46.8	0	6,017,295	765,000	7.87
5.500	32.44	3,623	13,491	0.00	2,249,786	50.0	0	7,106,644	787,500	9.02
6.000	35.39	3,771	15,340	0.00	2,388,758	53.1	0	8,266,280	810,000	10.21
6.500	38.34	3,911	17,261	0.00	2,526,373	56.1	0	9,495,063	832,500	11.41
7.000	41.29	4,044	19,250	0.00	2,656,249	59.0	0	10,790,718	855,000	12.62
7.500	44.24	4,171	21,304	0.00	2,773,831	61.6	0	12,148,238	877,500	13.84
8.000	47.19	4,292	23,420	0.00	2,912,379	64.7	0	13,569,791	900,000	15.08
8.500	50.14	4,407	25,595	0.00	3,068,230	68.2	0	15,064,943	922,500	16.33
9.000	53.09	4,518	27,826	0.00	3,248,041	72.2	0	16,644,011	945,000	17.61
9.500	56.04	4,625	30,112	0.00	3,461,662	76.9	0	18,321,437	967,500	18.94
10.000	58.99	4,727	32,451	0.00	3,720,944	82.7	0	20,117,089	990,000	20.32
10.500	61.94	4,825	34,839	0.00	4,038,789	89.8	0	22,057,022	1,012,500	21.78
11.000	64.89	4,920	37,276	0.00	4,430,555	98.5	0	24,174,358	1,035,000	23.36
11.500	67.84	5,011	39,759	0.00	4,917,330	109.3	0	26,511,329	1,057,500	25.07
12.000	70.79	5,099	42,287	0.00	5,559,781	123.6	0	29,130,607	1,080,000	26.97
12.500	73.74	5,184	44,858	0.00	6,415,572	142.6	0	32,124,445	1,102,500	29.14
13.000	76.69	5,266	47,471	0.00	7,466,055	165.9	0	35,594,852	1,125,000	31.64
13.500	79.64	5,345	50,124	0.00	8,652,713	192.3	0	39,624,544	1,147,500	34.53
14.000	82.58	5,421	52,815	0.00	9,954,562	221.2	0	44,276,363	1,170,000	37.84
14.500	85.53	5,495	55,545	0.00	11,346,716	252.1	0	49,601,683	1,192,500	41.59
15.000	88.48	5,566	58,310	0.00	12,826,362	285.0	0	55,644,952	1,215,000	45.80
15.500	91.43	5,635	61,110	0.00	14,372,946	319.4	0	62,444,779	1,237,500	50.46
16.000	94.38	5,701	63,945	0.00	15,991,266	355.4	0	70,035,832	1,260,000	55.58
16.500	97.33	5,765	66,812	0.00	17,668,073	392.6	0	78,450,667	1,282,500	61.17

Table 2.10.3-5 – CASKDROP Output File for NCT Side Drop, Warm (140 ºF)

Side Drop *** PACKAGING TECHNOLOGY *** CASKDROP, v2.31
02-09-1999, 15:29:19 Nov 13, 1997

72-B 0 degrees (Full Scale) TAIL (One foot)			
Impact Limiter Weight (each) -	2,547 lbs	Cask and Payload Weight -	39,906 lbs
Impact Limiter Outside Diameter -	76.0000 in	Cask Outside Diameter -	42.1000 in
Impact Limiter Overall Length -	46.0000 in	Cask Overall Length -	141.8000 in
Impact Limiter Conical Diameter -	0.0000 in	Dynamic Unloading Modulus -	1.000E+07 lbs/in
Impact Limiter Conical Length -	0.0000 in	Rad Mass Moment of Inertia -	241,517 lb-in-s²
Impact Limiter End Thickness -	11.2500 in	Frictional Coefficient -	0.0000
Impact Limiter Hole Diameter -	0.0000 in	Drop Height -	1.0000 ft
Impact Limiter Hole Length -	0.0000 in	Drop Angle from Horizontal -	0.0000°
Unbacked Area Threshhold Strain -	0.1000 in/in	Crush Analysis Theory -	Global
Unbacked Area Crush Stress -	314 psi	Number of Integration Incs -	50

VARIABLE CRUSH STRESS	
ε (in/in)	σ (psi)
0.000	0.0
0.050	292.0
0.100	314.0
0.200	327.0
0.300	350.0
0.400	393.0
0.500	482.0
0.600	685.0
0.650	895.0
0.700	1,256.0
0.750	1,873.0
0.800	3,235.0
0.870	10,944.0

DEFL (in)	MAX ε (%)	AREA (in²)	VOLUME (in³)	XBAR (in)	IMPACT FORCE (lbs)	ACCEL (g's)	I/L MOMENT (in-lbs)	STRAIN ENERGY (in-lbs)	KINETIC ENERGY (in-lbs)	SE/KE RATIO
0.500	2.95	1,131	377	0.00	124,918	2.8	0	31,230	562,500	0.06
1.000	5.90	1,593	1,065	0.00	303,986	6.8	0	138,456	585,000	0.24
1.500	8.85	1,945	1,953	0.00	441,013	9.8	0	324,705	607,500	0.53
2.000	11.80	2,238	3,001	0.00	538,294	12.0	0	569,532	630,000	0.90
2.120	12.51	2,303	3,273	0.00	559,706	12.4	0	635,399	635,399	1.00
2.500	14.75	2,494	4,185	0.00	626,550	13.9	0	860,743	652,500	1.32
3.000	17.70	2,723	5,491	0.00	714,637	15.9	0	1,196,040	675,000	1.77
3.500	20.65	2,931	6,905	0.00	802,125	17.8	0	1,575,231	697,500	2.26
4.000	23.60	3,123	8,419	0.00	885,491	19.7	0	1,997,135	720,000	2.77
4.500	26.55	3,300	10,026	0.00	963,353	21.4	0	2,459,346	742,500	3.31
5.000	29.50	3,467	11,718	0.00	1,036,383	23.0	0	2,959,280	765,000	3.87
5.500	32.44	3,623	13,491	0.00	1,106,199	24.6	0	3,494,925	787,500	4.44
6.000	35.39	3,771	15,340	0.00	1,174,375	26.1	0	4,065,069	810,000	5.02
6.500	38.34	3,911	17,261	0.00	1,241,904	27.6	0	4,669,138	832,500	5.61
7.000	41.29	4,044	19,250	0.00	1,305,781	29.0	0	5,306,060	855,000	6.21
7.500	44.24	4,171	21,304	0.00	1,363,848	30.3	0	5,973,467	877,500	6.81
8.000	47.19	4,292	23,420	0.00	1,432,346	31.8	0	6,672,515	900,000	7.41
8.500	50.14	4,407	25,595	0.00	1,509,262	33.5	0	7,407,917	922,500	8.03
9.000	53.09	4,518	27,826	0.00	1,597,651	35.5	0	8,184,646	945,000	8.66
9.500	56.04	4,625	30,112	0.00	1,702,457	37.8	0	9,009,672	967,500	9.31
10.000	58.99	4,727	32,451	0.00	1,829,920	40.7	0	9,892,767	990,000	9.99
10.500	61.94	4,825	34,839	0.00	1,986,897	44.2	0	10,846,971	1,012,500	10.71
11.000	64.89	4,920	37,276	0.00	2,179,962	48.4	0	11,888,686	1,035,000	11.49
11.500	67.84	5,011	39,759	0.00	2,417,147	53.7	0	13,037,963	1,057,500	12.33
12.000	70.79	5,099	42,287	0.00	2,734,368	60.8	0	14,325,842	1,080,000	13.26
12.500	73.74	5,184	44,858	0.00	3,163,581	70.3	0	15,800,329	1,102,500	14.33
13.000	76.69	5,266	47,471	0.00	3,670,030	81.6	0	17,508,732	1,125,000	15.56
13.500	79.64	5,345	50,124	0.00	4,441,159	98.7	0	19,536,529	1,147,500	17.03
14.000	82.58	5,421	52,815	0.00	6,132,302	136.3	0	22,179,894	1,170,000	18.96
14.500	85.53	5,495	55,545	0.00	9,078,839	201.8	0	25,982,679	1,192,500	21.79
15.000	88.48	5,566	58,310	0.00	13,103,071	291.2	0	31,528,157	1,215,000	25.95
15.500	91.43	5,635	61,110	0.00	17,894,737	397.7	0	39,277,609	1,237,500	31.74
16.000	94.38	5,701	63,945	0.00	23,299,209	517.8	0	49,576,095	1,260,000	39.35
16.500	97.33	5,765	66,812	0.00	29,219,382	649.3	0	62,705,743	1,282,500	48.89

Table 2.10.3-6 – CASKDROP Output File for HAC End Drop, Cold (-20 ºF)

End Drop *** PACKAGING TECHNOLOGY *** CASKDROP, v2.31
02-09-1999, 10:29:48 Nov 13, 1997

72-B End Drop Analysis FULL SCALE SAR PREDICTION (30 ft)			
Impact Limiter Weight (each) -	2,547 lbs	Cask and Payload Weight -	39,906 lbs
Impact Limiter Outside Diameter -	76.0000 in	Cask Outside Diameter -	79.5000 in
Impact Limiter Overall Length -	46.0000 in	Cask Overall Length -	141.7500 in
Impact Limiter Conical Diameter -	0.0000 in	Dynamic Unloading Modulus -	1.000E+07 lbs/in
Impact Limiter Conical Length -	0.0000 in	Rad Mass Moment of Inertia -	304,239 lb-in-s²
Impact Limiter End Thickness -	22.5000 in	Frictional Coefficient -	0.0000
Impact Limiter Hole Diameter -	0.0000 in	Drop Height -	30.0000 ft
Impact Limiter Hole Length -	0.0000 in	Drop Angle from Horizontal -	90.0000°
Unbacked Area Threshhold Strain -	0.1000 in/in	Crush Analysis Theory -	Global
Unbacked Area Crush Stress -	879 psi	Number of Integration Incs -	50

VARIABLE CRUSH STRESS	
ε (in/in)	σ (psi)
0.000	0.0
0.050	872.0
0.100	879.0
0.200	883.0
0.300	946.0
0.400	1,052.0
0.500	1,270.0
0.600	1,768.0
0.650	2,257.0
0.700	3,118.0
0.750	4,686.0

DEFL (in)	MAX ε (%)	AREA (in²)	VOLUME (in³)	XBAR (in)	IMPACT FORCE (lbs)	ACCEL (g's)	I/L MOMENT (in-lbs)	STRAIN ENERGY (in-lbs)	KINETIC ENERGY (in-lbs)	SE/KE RATIO
0.500	2.22	4,536	2,268	0.00	2,121,086	47.1	0	530,271	16,222,500	0.03
1.000	4.44	4,536	4,536	0.00	3,703,284	82.3	0	1,986,364	16,245,000	0.12
1.500	6.67	4,536	6,805	0.00	4,290,028	95.3	0	3,984,692	16,267,500	0.24
2.000	8.89	4,536	9,073	0.00	4,141,244	92.0	0	6,092,510	16,290,000	0.37
2.500	11.11	4,536	11,341	0.00	3,871,467	86.0	0	8,095,688	16,312,500	0.50
3.000	13.33	4,536	13,609	0.00	3,769,226	83.8	0	10,005,861	16,335,000	0.61
3.500	15.56	4,536	15,878	0.00	3,794,042	84.3	0	11,896,678	16,357,500	0.73
4.000	17.78	4,536	18,146	0.00	3,891,134	86.5	0	13,817,972	16,380,000	0.84
4.500	20.00	4,536	20,414	0.00	4,005,722	89.0	0	15,792,186	16,402,500	0.96
4.653	20.68	4,536	21,110	0.00	4,036,322	89.7	0	16,409,407	16,409,407	1.00
5.000	22.22	4,536	22,682	0.00	4,094,493	91.0	0	17,817,239	16,425,000	1.08
5.500	24.44	4,536	24,951	0.00	4,158,401	92.4	0	19,880,463	16,447,500	1.21
6.000	26.67	4,536	27,219	0.00	4,209,808	93.6	0	21,972,515	16,470,000	1.33
6.500	28.89	4,536	29,487	0.00	4,261,154	94.7	0	24,090,255	16,492,500	1.46
7.000	31.11	4,536	31,755	0.00	4,324,629	96.1	0	26,236,701	16,515,000	1.59
7.500	33.33	4,536	34,023	0.00	4,406,678	97.9	0	28,419,528	16,537,500	1.72
8.000	35.56	4,536	36,292	0.00	4,508,003	100.2	0	30,648,198	16,560,000	1.85
8.500	37.78	4,536	38,560	0.00	4,629,057	102.9	0	32,932,463	16,582,500	1.99
9.000	40.00	4,536	40,828	0.00	4,770,292	106.0	0	35,282,300	16,605,000	2.12
9.500	42.22	4,536	43,096	0.00	4,933,137	109.6	0	37,708,157	16,627,500	2.27
10.000	44.44	4,536	45,365	0.00	5,122,922	113.8	0	40,222,171	16,650,000	2.42

Table 2.10.3-7 – CASKDROP Output File for HAC End Drop, Warm (140 ºF)

End Drop *** PACKAGING TECHNOLOGY *** CASKDROP, v2.31
02-09-1999, 15:06:40 Nov 13, 1997

72-B 90 Deg Drop FULL SCALE SAR PREDICTION (30 ft)			
Impact Limiter Weight (each) -	2,547 lbs	Cask and Payload Weight -	39,906 lbs
Impact Limiter Outside Diameter -	76.0000 in	Cask Outside Diameter -	79.5000 in
Impact Limiter Overall Length -	46.0000 in	Cask Overall Length -	141.8000 in
Impact Limiter Conical Diameter -	0.0000 in	Dynamic Unloading Modulus -	1.000E+07 lbs/in
Impact Limiter Conical Length -	0.0000 in	Rad Mass Moment of Inertia -	304,415 lb-in-s²
Impact Limiter End Thickness -	22.5000 in	Frictional Coefficient -	0.0000
Impact Limiter Hole Diameter -	0.0000 in	Drop Height -	30.0000 ft
Impact Limiter Hole Length -	0.0000 in	Drop Angle from Horizontal -	90.0000°
Unbacked Area Threshhold Strain -	0.1000 in/in	Crush Analysis Theory -	Global
Unbacked Area Crush Stress -	433 psi	Number of Integration Incs -	50

VARIABLE CRUSH STRESS	
ε (in/in)	σ (psi)
0.000	0.0
0.050	429.0
0.100	433.0
0.200	435.0
0.300	465.0
0.400	518.0
0.500	625.0
0.600	870.0
0.650	1,111.0
0.700	1,534.0
0.750	2,305.0
0.800	4,120.0
0.870	13,462.0

DEFL (in)	MAX ε (%)	AREA (in²)	VOLUME (in³)	XBAR (in)	IMPACT FORCE (lbs)	ACCEL (g's)	I/L MOMENT (in-lbs)	STRAIN ENERGY (in-lbs)	KINETIC ENERGY (in-lbs)	SE/KE RATIO
0.500	2.22	4,536	2,268	0.00	1,043,255	23.2	0	260,814	16,222,500	0.02
1.000	4.44	4,536	4,536	0.00	1,821,777	40.5	0	977,072	16,245,000	0.06
1.500	6.67	4,536	6,805	0.00	2,111,263	46.9	0	1,960,332	16,267,500	0.12
2.000	8.89	4,536	9,073	0.00	2,039,305	45.3	0	2,997,974	16,290,000	0.18
2.500	11.11	4,536	11,341	0.00	1,907,653	42.4	0	3,984,714	16,312,500	0.24
3.000	13.33	4,536	13,609	0.00	1,857,962	41.3	0	4,926,117	16,335,000	0.30
3.500	15.56	4,536	15,878	0.00	1,870,313	41.6	0	5,858,186	16,357,500	0.36
4.000	17.78	4,536	18,146	0.00	1,917,764	42.6	0	6,805,205	16,380,000	0.42
4.500	20.00	4,536	20,414	0.00	1,973,373	43.9	0	7,777,990	16,402,500	0.47
5.000	22.22	4,536	22,682	0.00	2,015,887	44.8	0	8,775,305	16,425,000	0.53
5.500	24.44	4,536	24,951	0.00	2,046,019	45.5	0	9,790,781	16,447,500	0.60
6.000	26.67	4,536	27,219	0.00	2,070,140	46.0	0	10,819,821	16,470,000	0.66
6.500	28.89	4,536	29,487	0.00	2,094,660	46.5	0	11,861,021	16,492,500	0.72
7.000	31.11	4,536	31,755	0.00	2,125,852	47.2	0	12,916,149	16,515,000	0.78
7.500	33.33	4,536	34,023	0.00	2,166,877	48.2	0	13,989,331	16,537,500	0.85
8.000	35.56	4,536	36,292	0.00	2,217,782	49.3	0	15,085,496	16,560,000	0.91
8.500	37.78	4,536	38,560	0.00	2,278,476	50.6	0	16,209,560	16,582,500	0.98
8.666	38.52	4,536	39,314	0.00	2,300,796	51.1	0	16,589,977	16,589,977	1.00
9.000	40.00	4,536	40,828	0.00	2,348,872	52.2	0	17,366,397	16,605,000	1.05
9.500	42.22	4,536	43,096	0.00	2,429,426	54.0	0	18,560,972	16,627,500	1.12
10.000	44.44	4,536	45,365	0.00	2,522,773	56.1	0	19,799,021	16,650,000	1.19
10.500	46.67	4,536	47,633	0.00	2,632,097	58.5	0	21,087,739	16,672,500	1.26
11.000	48.89	4,536	49,901	0.00	2,760,578	61.3	0	22,435,908	16,695,000	1.34
11.500	51.11	4,536	52,169	0.00	2,911,590	64.7	0	23,853,950	16,717,500	1.43
12.000	53.33	4,536	54,438	0.00	3,092,917	68.7	0	25,355,076	16,740,000	1.51
12.500	55.56	4,536	56,706	0.00	3,316,754	73.7	0	26,957,494	16,762,500	1.61
13.000	57.78	4,536	58,974	0.00	3,595,488	79.9	0	28,685,555	16,785,000	1.71
13.500	60.00	4,536	61,242	0.00	3,941,507	87.6	0	30,569,803	16,807,500	1.82
14.000	62.22	4,536	63,510	0.00	4,367,345	97.1	0	32,647,016	16,830,000	1.94
14.500	64.44	4,536	65,779	0.00	4,886,139	108.6	0	34,960,387	16,852,500	2.07
15.000	66.67	4,536	68,047	0.00	5,521,128	122.7	0	37,562,204	16,875,000	2.23
15.500	68.89	4,536	70,315	0.00	6,382,208	141.8	0	40,538,038	16,897,500	2.40
16.000	71.11	4,536	72,583	0.00	7,615,724	169.2	0	44,037,521	16,920,000	2.60
16.500	73.33	4,536	74,852	0.00	9,180,523	204.0	0	48,236,582	16,942,500	2.85
17.000	75.56	4,536	77,120	0.00	10,854,594	241.2	0	53,245,362	16,965,000	3.14

Table 2.10.3-8 – CASKDROP Output File for HAC Side Drop, Cold (-20 ºF)

72-B Side Drop Analysis FULL SCALE SAR PREDICTION (30 Foot)			
Impact Limiter Weight (each) -	2,547 lbs	Cask and Payload Weight -	39,906 lbs
Impact Limiter Outside Diameter -	76.0000 in	Cask Outside Diameter -	42.1000 in
Impact Limiter Overall Length -	46.0000 in	Cask Overall Length -	141.7500 in
Impact Limiter Conical Diameter -	0.0000 in	Dynamic Unloading Modulus -	1.000E+07 lbs/in
Impact Limiter Conical Length -	0.0000 in	Rad Mass Moment of Inertia -	241,355 lb-in-s²
Impact Limiter End Thickness -	11.2500 in	Frictional Coefficient -	0.0000
Impact Limiter Hole Diameter -	0.0000 in	Drop Height -	30.0000 ft
Impact Limiter Hole Length -	0.0000 in	Drop Angle from Horizontal -	0.0000°
Unbacked Area Threshhold Strain -	0.1000 in/in	Crush Analysis Theory -	Global
Unbacked Area Crush Stress -	815 psi	Number of Integration Incs -	50

VARIABLE CRUSH STRESS	
ε (in/in)	σ (psi)
0.000	0.0
0.050	758.0
0.100	815.0
0.200	849.0
0.300	910.0
0.400	1,022.0
0.500	1,251.0
0.600	1,778.0
0.650	2,324.0
0.700	3,262.0
0.750	4,864.0

DEFL (in)	MAX ε (%)	AREA (in²)	VOLUME (in³)	XBAR (in)	IMPACT FORCE (lbs)	ACCEL (g's)	I/L MOMENT (in-lbs)	STRAIN ENERGY (in-lbs)	KINETIC ENERGY (in-lbs)	SE/KE RATIO
0.500	2.95	1,131	377	0.00	324,284	7.2	0	81,071	16,222,500	0.00
1.000	5.90	1,593	1,065	0.00	789,118	17.5	0	359,422	16,245,000	0.02
1.500	8.85	1,945	1,953	0.00	1,144,778	25.4	0	842,896	16,267,500	0.05
2.000	11.80	2,238	3,001	0.00	1,397,243	31.0	0	1,478,401	16,290,000	0.09
2.500	14.75	2,494	4,185	0.00	1,626,309	36.1	0	2,234,289	16,312,500	0.14
3.000	17.70	2,723	5,491	0.00	1,855,001	41.2	0	3,104,616	16,335,000	0.19
3.500	20.65	2,931	6,905	0.00	2,082,242	46.3	0	4,088,927	16,357,500	0.25
4.000	23.60	3,123	8,419	0.00	2,298,917	51.1	0	5,184,217	16,380,000	0.32
4.500	26.55	3,300	10,026	0.00	2,501,445	55.6	0	6,384,308	16,402,500	0.39
5.000	29.50	3,467	11,718	0.00	2,691,558	59.8	0	7,682,558	16,425,000	0.47
5.500	32.44	3,623	13,491	0.00	2,873,426	63.9	0	9,073,804	16,447,500	0.55
6.000	35.39	3,771	15,340	0.00	3,051,045	67.8	0	10,554,922	16,470,000	0.64
6.500	38.34	3,911	17,261	0.00	3,226,824	71.7	0	12,124,389	16,492,500	0.74
7.000	41.29	4,044	19,250	0.00	3,392,747	75.4	0	13,779,282	16,515,000	0.83
7.500	44.24	4,171	21,304	0.00	3,543,103	78.7	0	15,513,244	16,537,500	0.94
7.788	45.94	4,241	22,516	0.00	3,654,879	81.2	0	16,550,469	16,550,469	1.00
8.000	47.19	4,292	23,420	0.00	3,720,284	82.7	0	17,329,091	16,560,000	1.05
8.500	50.14	4,407	25,595	0.00	3,919,504	87.1	0	19,239,038	16,582,500	1.16
9.000	53.09	4,518	27,826	0.00	4,149,136	92.2	0	21,256,198	16,605,000	1.28
9.500	56.04	4,625	30,112	0.00	4,421,782	98.3	0	23,398,928	16,627,500	1.41
10.000	58.99	4,727	32,451	0.00	4,752,752	105.6	0	25,692,561	16,650,000	1.54
10.500	61.94	4,825	34,839	0.00	5,158,773	114.6	0	28,170,443	16,672,500	1.69
11.000	64.89	4,920	37,276	0.00	5,659,424	125.8	0	30,874,992	16,695,000	1.85
11.500	67.84	5,011	39,759	0.00	6,281,177	139.6	0	33,860,142	16,717,500	2.03
12.000	70.79	5,099	42,287	0.00	7,101,512	157.8	0	37,205,814	16,740,000	2.22
12.500	73.74	5,184	44,858	0.00	8,194,556	182.1	0	41,029,831	16,762,500	2.45
13.000	76.69	5,266	47,471	0.00	9,536,501	211.9	0	45,462,595	16,785,000	2.71
13.500	79.64	5,345	50,124	0.00	11,052,547	245.6	0	50,609,857	16,807,500	3.01
14.000	82.58	5,421	52,815	0.00	12,715,792	282.6	0	56,551,942	16,830,000	3.36
14.500	85.53	5,495	55,545	0.00	14,494,454	322.1	0	63,354,504	16,852,500	3.76
15.000	88.48	5,566	58,310	0.00	16,384,939	364.1	0	71,074,352	16,875,000	4.21
15.500	91.43	5,635	61,110	0.00	18,360,939	408.0	0	79,760,821	16,897,500	4.72
16.000	94.38	5,701	63,945	0.00	20,428,655	454.0	0	89,458,220	16,920,000	5.29
16.500	97.33	5,765	66,812	0.00	22,571,122	501.6	0	100,208,164	16,942,500	5.91

Table 2.10.3-9 – CASKDROP Output File for HAC Side Drop, Warm (140 ºF)

72-B 0 degrees (Full Scale) TAIL			
Impact Limiter Weight (each) -	2,547 lbs	Cask and Payload Weight -	39,906 lbs
Impact Limiter Outside Diameter -	76.0000 in	Cask Outside Diameter -	42.1000 in
Impact Limiter Overall Length -	46.0000 in	Cask Overall Length -	141.8000 in
Impact Limiter Conical Diameter -	0.0000 in	Dynamic Unloading Modulus -	1.000E+07 lbs/in
Impact Limiter Conical Length -	0.0000 in	Rad Mass Moment of Inertia -	241,517 lb-in-s²
Impact Limiter End Thickness -	11.2500 in	Frictional Coefficient -	0.0000
Impact Limiter Hole Diameter -	0.0000 in	Drop Height -	30.0000 ft
Impact Limiter Hole Length -	0.0000 in	Drop Angle from Horizontal -	0.0000°
Unbacked Area Threshhold Strain -	0.1000 in/in	Crush Analysis Theory -	Global
Unbacked Area Crush Stress -	401 psi	Number of Integration Incs -	50

VARIABLE CRUSH STRESS	
ε (in/in)	σ (psi)
0.000	0.0
0.050	373.0
0.100	401.0
0.200	418.0
0.300	448.0
0.400	503.0
0.500	615.0
0.600	875.0
0.650	1,143.0
0.700	1,605.0
0.750	2,393.0
0.800	4,133.0
0.870	13,979.0

DEFL (in)	MAX ε (%)	AREA (in²)	VOLUME (in³)	XBAR (in)	IMPACT FORCE (lbs)	ACCEL (g's)	I/L MOMENT (in-lbs)	STRAIN ENERGY (in-lbs)	KINETIC ENERGY (in-lbs)	SE/KE RATIO
0.500	2.95	1,131	377	0.00	159,582	3.5	0	39,895	16,222,500	0.00
1.000	5.90	1,593	1,065	0.00	388,316	8.6	0	176,870	16,245,000	0.01
1.500	8.85	1,945	1,953	0.00	563,302	12.5	0	414,774	16,267,500	0.03
2.000	11.80	2,238	3,001	0.00	687,524	15.3	0	727,481	16,290,000	0.04
2.500	14.75	2,494	4,185	0.00	800,286	17.8	0	1,099,433	16,312,500	0.07
3.000	17.70	2,723	5,491	0.00	912,911	20.3	0	1,527,732	16,335,000	0.09
3.500	20.65	2,931	6,905	0.00	1,024,839	22.8	0	2,012,170	16,357,500	0.12
4.000	23.60	3,123	8,419	0.00	1,131,547	25.1	0	2,551,266	16,380,000	0.16
4.500	26.55	3,300	10,026	0.00	1,231,260	27.4	0	3,141,968	16,402,500	0.19
5.000	29.50	3,467	11,718	0.00	1,324,837	29.4	0	3,780,992	16,425,000	0.23
5.500	32.44	3,623	13,491	0.00	1,414,346	31.4	0	4,465,788	16,447,500	0.27
6.000	35.39	3,771	15,340	0.00	1,501,758	33.4	0	5,194,814	16,470,000	0.32
6.500	38.34	3,911	17,261	0.00	1,588,246	35.3	0	5,967,315	16,492,500	0.36
7.000	41.29	4,044	19,250	0.00	1,669,847	37.1	0	6,781,838	16,515,000	0.41
7.500	44.24	4,171	21,304	0.00	1,743,728	38.7	0	7,635,232	16,537,500	0.46
8.000	47.19	4,292	23,420	0.00	1,830,733	40.7	0	8,528,847	16,560,000	0.52
8.500	50.14	4,407	25,595	0.00	1,928,488	42.9	0	9,468,653	16,582,500	0.57
9.000	53.09	4,518	27,826	0.00	2,041,121	45.4	0	10,461,055	16,605,000	0.63
9.500	56.04	4,625	30,112	0.00	2,174,985	48.3	0	11,515,081	16,627,500	0.69
10.000	58.99	4,727	32,451	0.00	2,337,898	52.0	0	12,643,302	16,650,000	0.76
10.500	61.94	4,825	34,839	0.00	2,538,382	56.4	0	13,862,372	16,672,500	0.83
11.000	64.89	4,920	37,276	0.00	2,784,839	61.9	0	15,193,178	16,695,000	0.91
11.500	67.84	5,011	39,759	0.00	3,087,936	68.6	0	16,661,371	16,717,500	1.00
11.518	67.95	5,015	39,851	0.00	3,100,628	68.9	0	16,718,328	16,718,328	1.00
12.000	70.79	5,099	42,287	0.00	3,493,463	77.6	0	18,306,721	16,740,000	1.09
12.500	73.74	5,184	44,858	0.00	4,041,833	89.8	0	20,190,545	16,762,500	1.20
13.000	76.69	5,266	47,471	0.00	4,688,811	104.2	0	22,373,206	16,785,000	1.33
13.500	79.64	5,345	50,124	0.00	5,673,939	126.1	0	24,963,893	16,807,500	1.49
14.000	82.58	5,421	52,815	0.00	7,834,174	174.1	0	28,340,922	16,830,000	1.68
14.500	85.53	5,495	55,545	0.00	11,597,645	257.7	0	33,198,876	16,852,500	1.97
15.000	88.48	5,566	58,310	0.00	16,737,524	371.9	0	40,282,669	16,875,000	2.39
15.500	91.43	5,635	61,110	0.00	22,857,434	507.9	0	50,181,408	16,897,500	2.97
16.000	94.38	5,701	63,945	0.00	29,760,073	661.3	0	63,335,785	16,920,000	3.74
16.500	97.33	5,765	66,812	0.00	37,321,340	829.4	0	80,106,138	16,942,500	4.73

Table 2.10.3-10 – Summary of End and Side Drop Impact Accelerations and Impact Limiter Deflections

Drop Height (ft)	Drop Orientation	Impact Limiter Temperature (ºF)	Impact Acceleration (*g*)	Impact Limiter Deflection (in)
1	End	-20	42.5	0.59
		140	28.6	0.86
	Side	-20	19.3	1.44
		140	12.4	2.12
30	End	-20	89.7	4.65
		140	51.1	8.67
	Side	-20	81.2	7.79
		140	68.9	11.52

Table 2.10.3-11 – Maximum Package Responses as a Function of Initial Impact Angle (-20 ºF Cases)

Drop Height (ft)	Package Orientation (degrees from horizontal)	Impact Acceleration (*g*)	Impact Force (lb)
1	0	19.3	$8.69(10)^5$
	5	5.2	$2.34(10)^5$
	10	4.2	$1.89(10)^5$
	15	3.9	$1.76(10)^5$
	20	3.8	$1.71(10)^5$
	25	3.7	$1.67(10)^5$
	30	3.8	$1.71(10)^5$
	35	4.1	$1.85(10)^5$
	40	4.4	$1.98(10)^5$
	45	4.8	$2.16(10)^5$
	50	5.3	$2.39(10)^5$
	55	5.9	$2.66(10)^5$
	60	6.5	$2.93(10)^5$
	65	8.2	$3.69(10)^5$
	70	9.3	$4.19(10)^5$
	75	10.9	$4.91(10)^5$
	80	13.2	$5.94(10)^5$
	85	17.9	$8.06(10)^5$
	90	42.5	$1.91(10)^6$
30	0	81.2	$3.65(10)^6$
	5	48.1	$2.16(10)^6$
	10	33.1	$1.49(10)^6$
	15	32.3	$1.45(10)^6$
	20	30.5	$1.37(10)^6$
	25	30.3	$1.36(10)^6$
	30	31.1	$1.40(10)^6$
	35	32.9	$1.48(10)^6$
	40	35.5	$1.60(10)^6$
	45	38.6	$1.74(10)^6$
	50	42.4	$1.91(10)^6$
	55	46.3	$2.08(10)^6$
	60	50.7	$2.28(10)^6$
	65	56.2	$2.53(10)^6$
	70	60.1	$2.70(10)^6$
	75	66.7	$3.00(10)^6$
	80	77.5	$3.49(10)^6$
	85	90.7	$4.08(10)^6$
	90	89.7	$4.04(10)^6$

Table 2.10.3-12 – Maximum Package Responses as a Function of Initial Impact Angle (140 ºF Cases)

Drop Height (ft)	Package Orientation (degrees from horizontal)	Impact Acceleration (*g*)	Impact Force (lb)
1	0	12.4	$5.58(10)^5$
	5	4.0	$1.82(10)^5$
	10	3.3	$1.49(10)^5$
	15	3.0	$1.36(10)^5$
	20	2.8	$1.26(10)^5$
	25	2.7	$1.21(10)^5$
	30	2.8	$1.25(10)^5$
	35	3.0	$1.33(10)^5$
	40	3.3	$1.47(10)^5$
	45	3.6	$1.63(10)^5$
	50	3.8	$1.72(10)^5$
	55	4.3	$1.94(10)^5$
	60	5.1	$2.29(10)^5$
	65	6.6	$2.97(10)^5$
	70	7.2	$3.24(10)^5$
	75	8.2	$3.69(10)^5$
	80	10.1	$4.55(10)^5$
	85	14.0	$6.30(10)^5$
	90	28.6	$1.29(10)^6$
30	0	68.9	$3.10(10)^6$
	5	44.3	$1.99(10)^6$
	10	21.8	$9.79(10)^5$
	15	22.5	$1.01(10)^6$
	20	23.6	$1.06(10)^6$
	25	24.9	$1.12(10)^6$
	30	26.1	$1.18(10)^6$
	35	28.2	$1.27(10)^6$
	40	31.3	$1.41(10)^6$
	45	35.2	$1.58(10)^6$
	50	39.6	$1.78(10)^6$
	55	42.4	$1.91(10)^6$
	60	46.1	$2.07(10)^6$
	65	49.9	$2.25(10)^6$
	70	48.9	$2.20(10)^6$
	75	50.1	$2.25(10)^6$
	80	48.5	$2.18(10)^6$
	85	46.9	$2.11(10)^6$
	90	51.1	$2.30(10)^6$

Table 2.10.3-13 – Summary of Impact Limiter Separation Moments

Drop Height (ft)	Impact Limiter Temperature (ºF)	Limiter Separation Moment (in-lb)
1	-20	$2.16(10)^6$
	140	$1.06(10)^6$
30	-20	$2.76(10)^6$
	140	$1.36(10)^6$

Table 2.10.3-14 – Time-History Details from the Maximum Impact Force Condition SLAPDOWN Analyses (NCT, -20 ºF, 1-foot Drop)

θ_o (degrees)	θ (radians)①	$\partial\theta/\partial t$ (rad/sec)②	$\partial^2\theta/\partial t^2$ (rad/sec^2)③	$\partial^2 y/\partial t^2$ (in/sec^2)④	F_{max} (lb)⑤
5	0.0762	-1.10	-68.4	$2.02(10)^3$	$2.34(10)^5$
10	0.159	-1.17	-54.2	$1.62(10)^3$	$1.89(10)^5$
15	0.242	-1.22	-48.2	$1.51(10)^3$	$1.76(10)^5$
20	0.327	-1.26	-43.7	$1.46(10)^3$	$1.71(10)^5$
25	0.411	-1.30	-39.6	$1.43(10)^3$	$1.67(10)^5$
30	0.495	-1.32	-37.0	$1.48(10)^3$	$1.71(10)^5$
35	0.580	-1.33	-34.7	$1.57(10)^3$	$1.85(10)^5$
40	0.667	-1.30	-32.5	$1.70(10)^3$	$1.98(10)^5$
45	0.754	-1.23	-29.8	$1.85(10)^3$	$2.16(10)^5$
50	0.844	-1.11	-26.8	$2.05(10)^3$	$2.39(10)^5$
55	0.937	-0.917	-22.9	$2.28(10)^3$	$2.66(10)^5$
60⑥	1.031	-0.656	-17.9	$2.53(10)^3$	$2.93(10)^5$

Notes:

① Package orientation at moment of maximum force.

② Rotational velocity.

③ Rotational acceleration.

④ Linear acceleration.

⑤ Maximum impact force.

⑥ For orientation angles greater than 60º, the quasi-static program CASKDROP was conservatively used.

Table 2.10.3-15 – Time-History Details from the Maximum Impact Force Condition SLAPDOWN Analyses (HAC, -20 ºF, 30-foot Drop)

θ_o (degrees)	θ (radians)①	$\partial\theta/\partial t$ (rad/sec)②	$\partial^2\theta/\partial t^2$ (rad/sec^2)③	$\partial^2 y/\partial t^2$ (in/sec^2)④	F_{max} (lb)⑤
5	0.0442	-5.16	$-1.74(10)^2$	$1.86(10)^4$	$2.16(10)^6$
10	0.130	-5.34	$-3.66(10)^2$	$1.28(10)^4$	$1.49(10)^6$
15	0.210	-5.48	$-3.44(10)^2$	$1.25(10)^4$	$1.45(10)^6$
20	0.288	-5.62	$-3.01(10)^2$	$1.18(10)^4$	$1.37(10)^6$
25	0.368	-5.74	$-2.94(10)^2$	$1.17(10)^4$	$1.36(10)^6$
30	0.449	-5.87	$-2.85(10)^2$	$1.20(10)^4$	$1.40(10)^6$
35	0.532	-5.99	$-2.83(10)^2$	$1.27(10)^4$	$1.48(10)^6$
40	0.617	-6.07	$-2.85(10)^2$	$1.37(10)^4$	$1.60(10)^6$
45	0.702	-6.16	$-2.88(10)^2$	$1.49(10)^4$	$1.74(10)^6$
50	0.788	-6.26	$-2.88(10)^2$	$1.61(10)^4$	$1.91(10)^6$
55	0.879	-6.14	$-2.94(10)^2$	$1.79(10)^4$	$2.08(10)^6$
60⑥	0.970	-6.05	$-2.96(10)^2$	$1.96(10)^4$	$2.28(10)^6$

Notes:

① Package orientation at moment of maximum force.

② Rotational velocity.

③ Rotational acceleration.

④ Linear acceleration.

⑤ Maximum impact force.

⑥ For orientation angles greater than 60º, the quasi-static program CASKDROP was conservatively used.

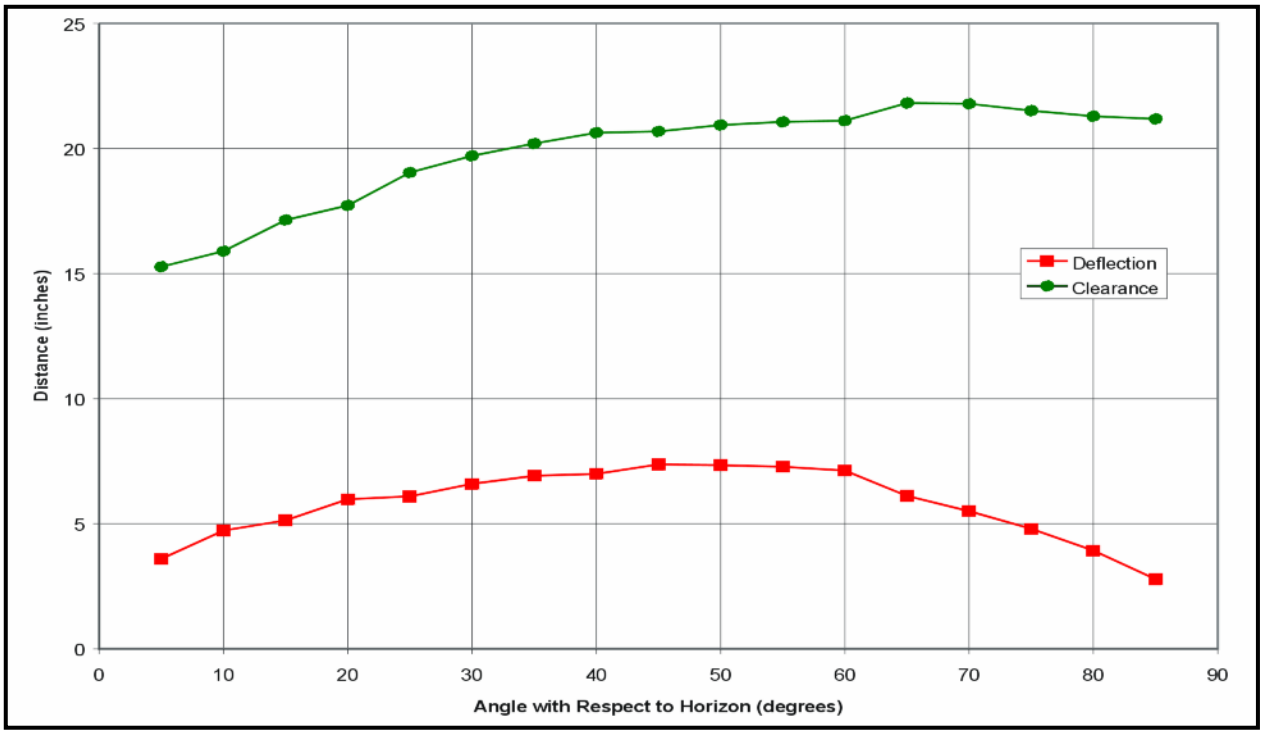

Figure 2.10.3-1 – Impact Limiter Deflection and Residual Clearance for the NCT Oblique Drop, Cold (-20 ºF)

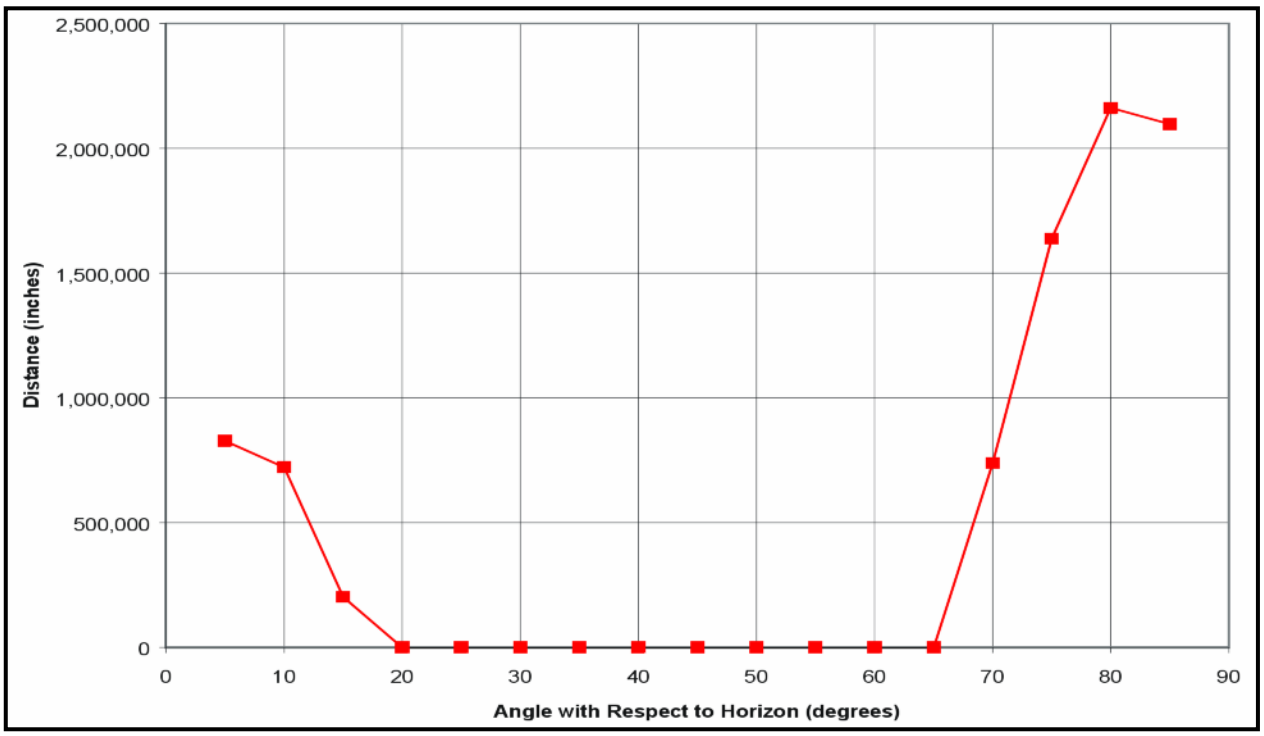

Figure 2.10.3-2 – Impact Limiter Separation Moments for the NCT Oblique Drop, Cold (-20 ºF)

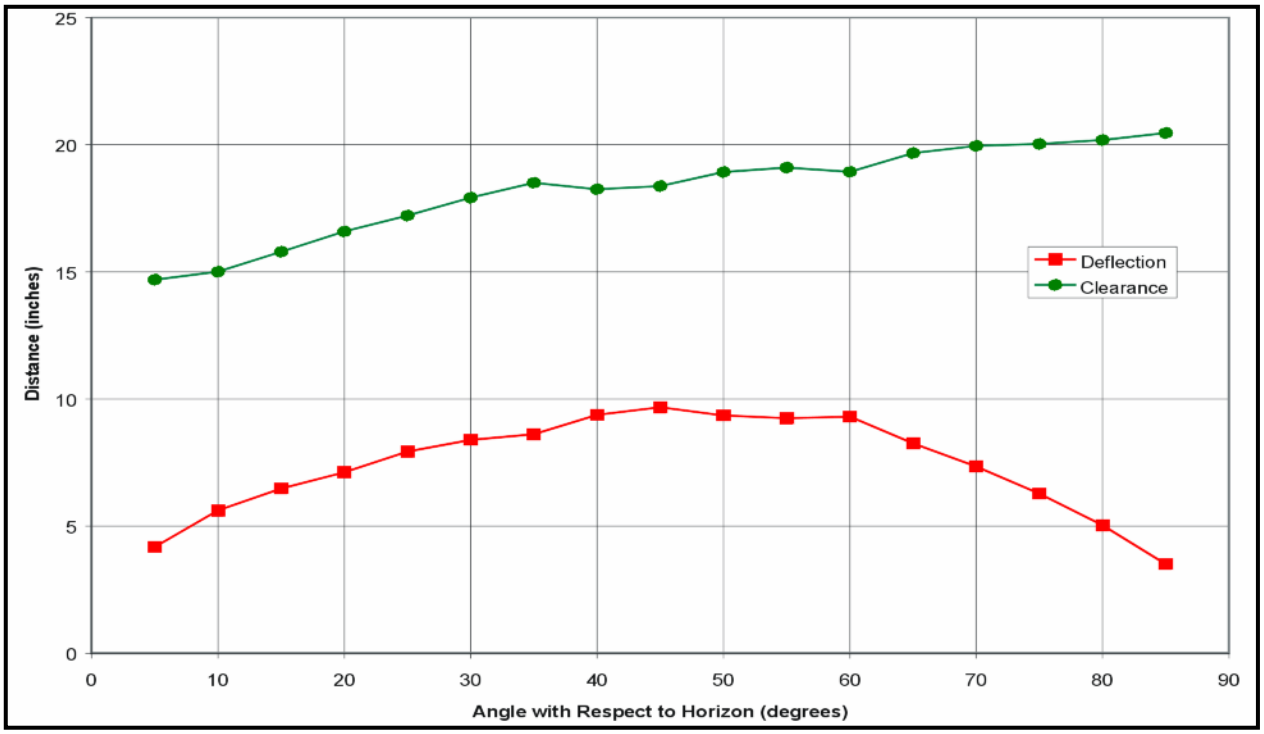

Figure 2.10.3-3 – Impact Limiter Deflection and Residual Clearance for the NCT Oblique Drop, Warm (140 ºF)

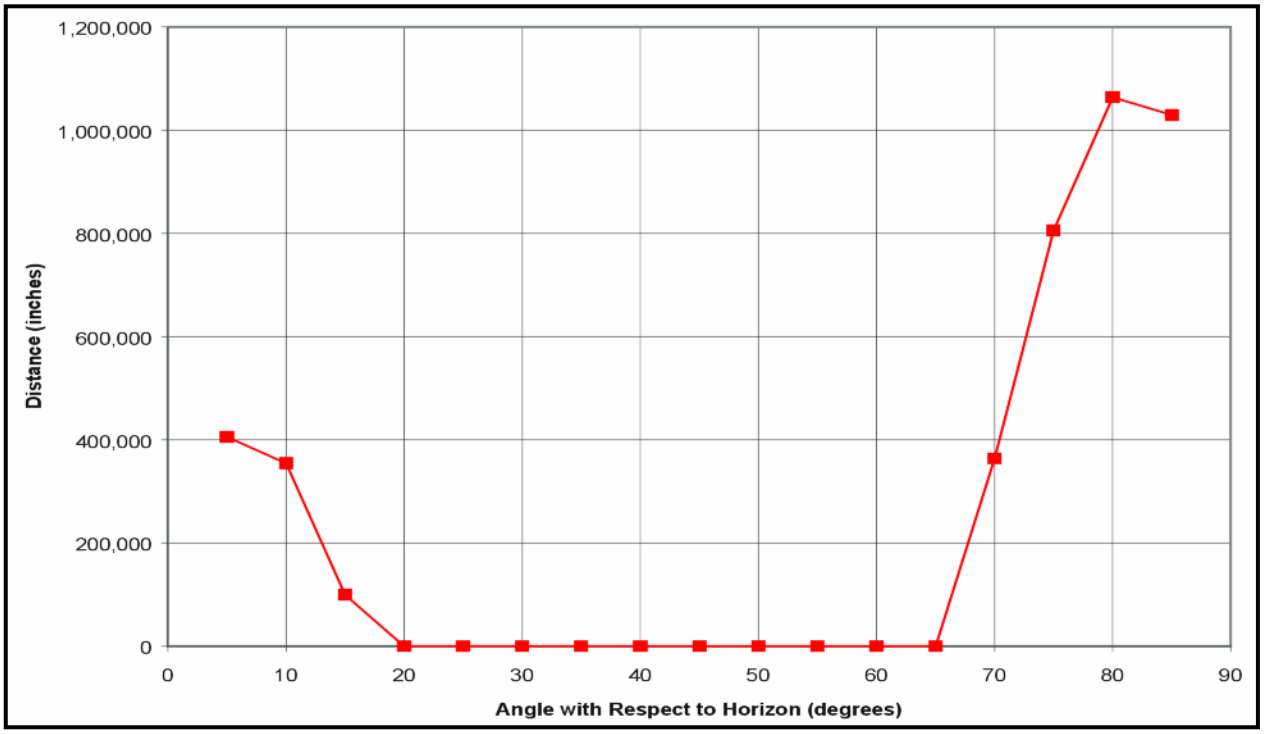

Figure 2.10.3-4 – Impact Limiter Separation Moments for the NCT Oblique Drop, Warm (140 ºF)

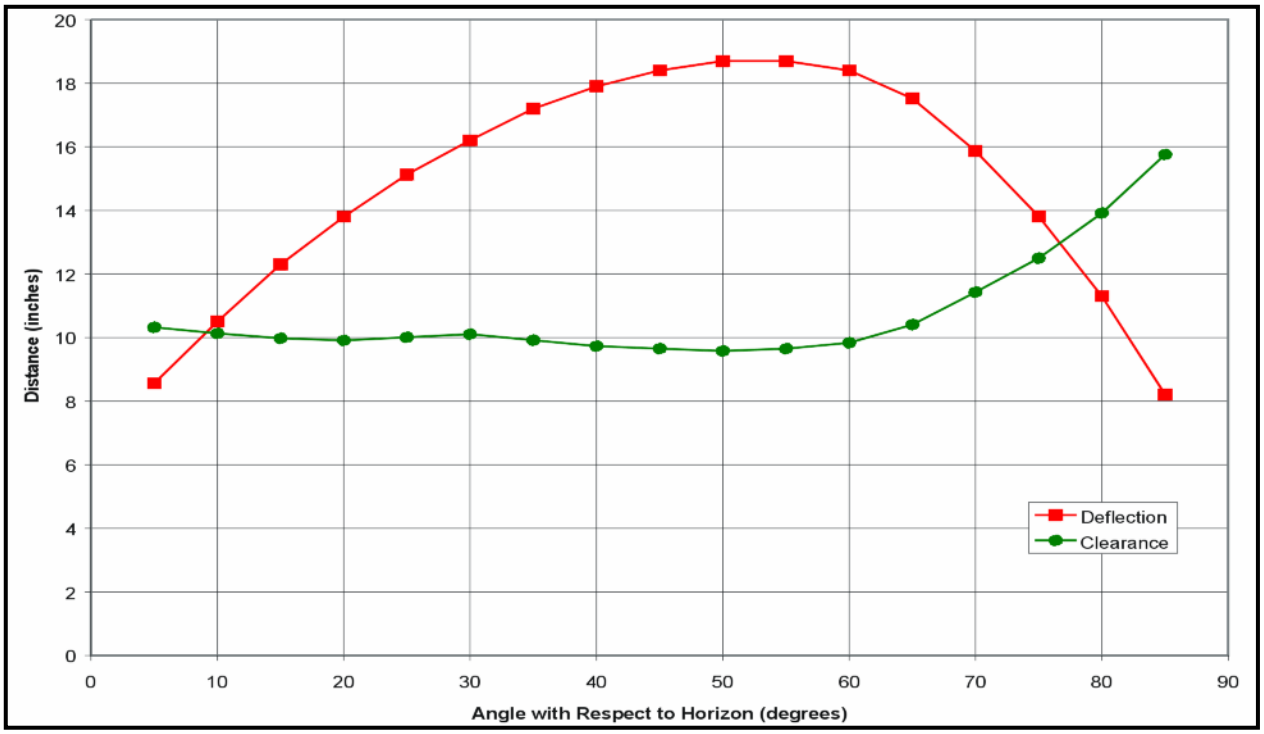

Figure 2.10.3-5 – Impact Limiter Deflection and Residual Clearance for the HAC Oblique Drop, Cold (-20 ºF)

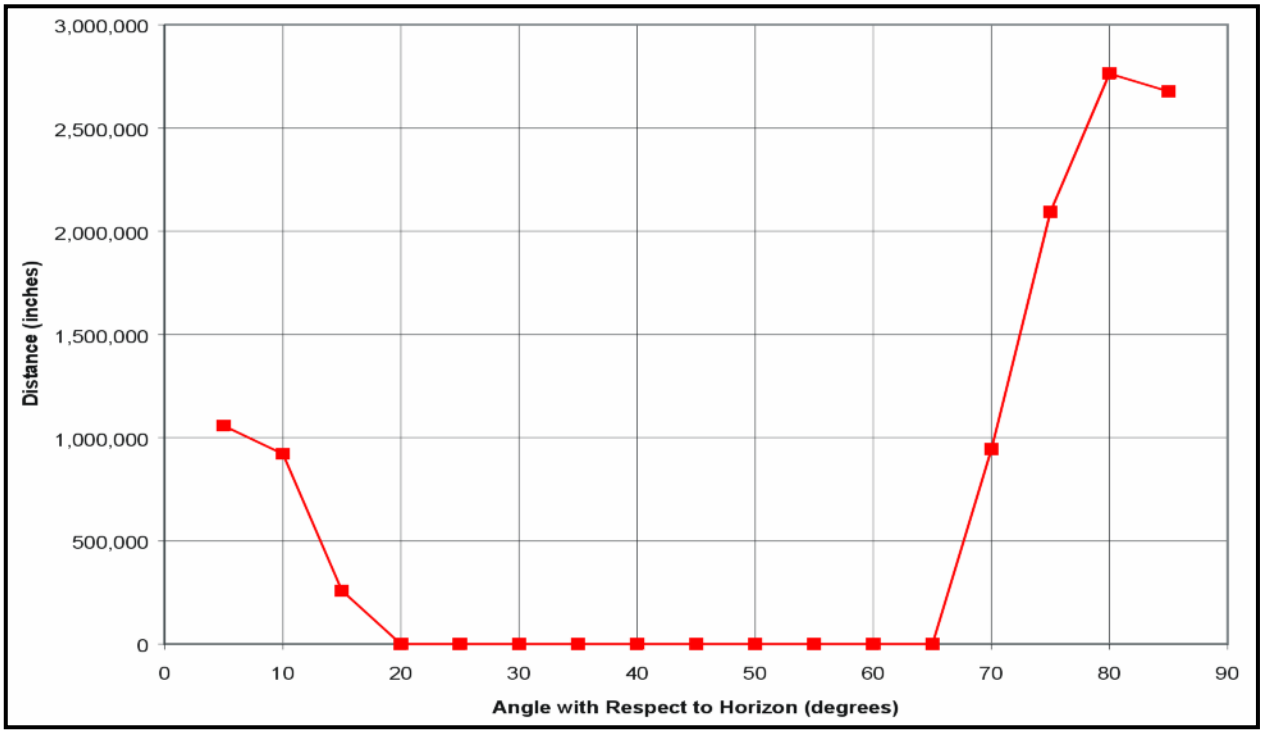

Figure 2.10.3-6 – Impact Limiter Separation Moments for the HAC Oblique Drop, Cold (-20 ºF)

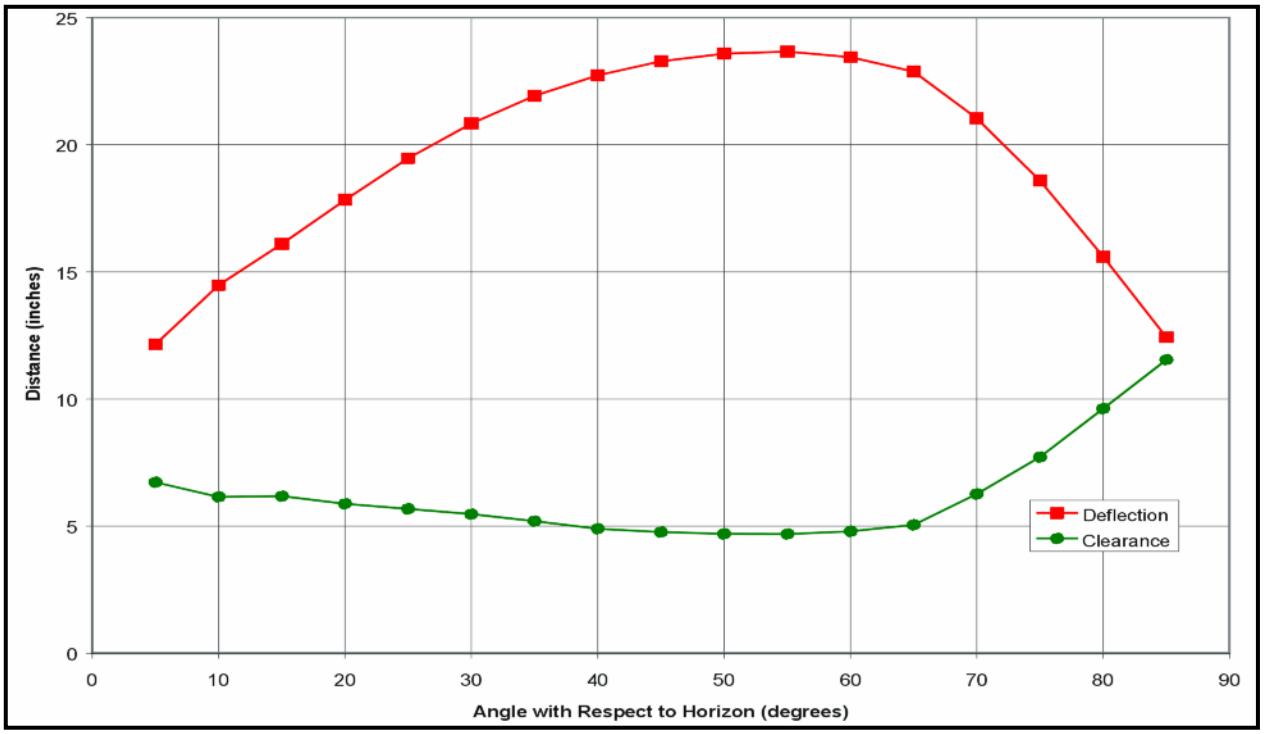

Figure 2.10.3-7 – Impact Limiter Deflection and Residual Clearance for the HAC Oblique Drop, Warm (140 ºF)

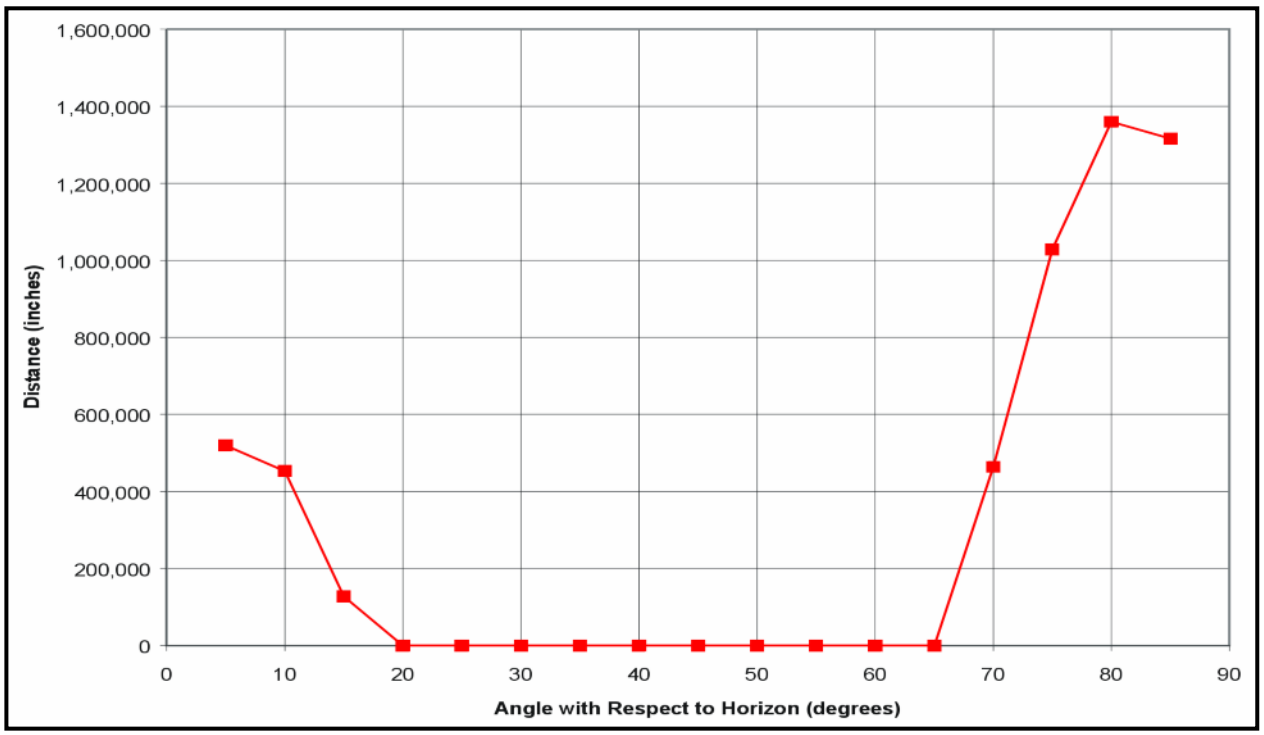

Figure 2.10.3-8 – Impact Limiter Separation Moments for the HAC Oblique Drop, Warm (140 ºF)

2.10.4 Slapdown Assessment

This appendix presents an evaluation of the RH-TRU 72-B package for potential secondary impacts, or slapdowns, following the primary impacts associated with 30-foot corner or oblique drop events. The conclusion reached is that stresses associated with slapdown are within allowable hypothetical accident condition (HAC) stresses. Additionally, impact limiter deformations resulting from slapdown are acceptable as they will not allow "bottoming out" on any package external surface (i.e., trunnions and the package body itself). The basic analytic approach is summarized in Section 2.10.2.2, *Description of the SLAPDOWN Computer Code*.

2.10.4.1 Slapdown Response – Force and Deflection

After an initial impact on the primary limiter, slapdown occurs on the secondary limiter. The secondary impact occurs at an angle very close to horizontal, so the side drop (0º) force deflection curve (calculated by CASKDROP) is used in the analysis. Therefore, the maximum impact force can be obtained by interpolating on the force-deflection curve for the maximum deflection calculated by SLAPDOWN.

Table 2.10.4-1 and Table 2.10.4-2 show secondary impact deformations for 5º, 10º, 15º, and 20º primary impact angles, and corresponding maximum impact forces based on the force-deflection curve for horizontal impact (see Table 2.10.4-3). Calculations are for both cold and warm HAC.

2.10.4.2 Slapdown Response – Maximum Bending Moment

Considering the free-body diagram in Figure 2.10.4-1, the maximum moment occurring in the package as a result of slapdown can be determined.

From force equilibrium:

$$F = m\ddot{y} = \omega_1 L_2$$

or,

$$\omega_1 = \frac{F}{L_2}$$

From moment equilibrium:

$$\frac{FL_2}{2} = 2\left(\frac{\omega_2}{2}\right)\left(\frac{L_2}{2}\right)\left(\frac{2}{3}\right)\left(\frac{L_2}{2}\right) = \frac{\omega_2 L_2^2}{6} = I\ddot{\Theta}$$

or,

$$\omega_2 = \frac{3F}{L_2}$$

Shear and moment as a function of position, x, are given in Table 2.10.4-4. The corresponding shear and moment diagrams are shown in Figure 2.10.4-2 and Figure 2.10.4-3.

The maximum moment is seen to occur at 2/3 the package length, and is equal to $(4/27)FL_2$. The results of this analysis are used in Section 2.10.4.4, *Slapdown Response – Deflections Versus Allowable Stress Limits*, to show that package stresses associated with this maximum bending moment, as well as axial thrust, are within allowable stress limits.

2.10.4.3 Slapdown Response – Thrust Loadings and Package Stresses

As the previous sections considered slapdown orientations slightly off horizontal, a slight amount of axial thrust can develop in the package. This thrust loading, T, is equal to the slapdown force, F, times the sine of the slapdown orientation angle. In addition, the slapdown moment, $(4/27)FL_2$, determined in Section 2.10.4.2, *Slapdown Response – Maximum Bending Moment*, can be multiplied by the cosine of the slapdown orientation angle. Using these formulas and the impact limiter force data from Section 2.10.4.1, *Slapdown Response – Force and Deflection*, the thrusts and moments due to slapdown are calculated and given in Table 2.10.4-5 and Table 2.10.4-6.

For shallow angle cases, calculated time histories show that primary and secondary impacts overlap during the impact event. Thus, the slapdown force is a superposition of the primary and secondary impacts. For remaining angles, only secondary impact forces are used.

By considering the outer cask (OC) geometry, the effect of the thrust loading on the overall response of the package can be seen to be small. For the OC, per Paragraph (3) in Section 2.6.7.2, *Corner and Oblique Drops*, the cross-sectional area, A = 292 in^2, the moment of inertia, I = 51,334 in^4, and c = 20.565 inches.

Per Table 2.1-1 in Section 2.1.2.1.1, *Containment Structures*, the HAC allowable membrane-plus-bending stress, σ_a, is the lesser of $3.6S_m$ (72,000 psi) or S_u (72,600 psi) at 160 ºF. Thus, the allowable stress, σ_a, = 72,000 psi.

Converting the tabulated thrust and moment data to a stress magnitude ($\sigma = T/A + Mc/I$) and computing the margin of safety ($MS = \sigma_a/\sigma - 1$) yields the results given in Table 2.10.4-7 and Table 2.10.4-8.

The lowest margin of safety is +2.60, therefore, the RH-TRU 72-B package is within allowable stress limits for slapdown.

2.10.4.4 Slapdown Response – Deflections Versus Allowable Stress Limits

The impact limiter deflections required to absorb the available slapdown energy were determined in Section 2.10.4.1, *Slapdown Response – Force and Deflection*. A maximum allowable deformation can be established which guarantees that the package body and trunnions are not directly impacted in a slapdown event. This allowable deformation will conservatively equal the distance between the ground and a bottom positioned trunnion during a 0º impact. This allowable can be conservatively applied to all slapdown orientation angles. Based on the package geometry, the maximum allowable deformation will equal 38.000 – 23.695 = 14.305 inches, where 38.000 inches is the impact limiter radius and 23.695 inches is the half-distance across trunnions.

Table 2.10.4-9 compares the allowable deformation with the predicted deformations found in Section 2.10.4.3, *Slapdown Response – Thrust Loadings and Package Stresses*. Only the warm foam case is considered as it results in the maximum impact limiter deformations.

Table 2.10.4-1 – Impact Force and Maximum Deflections for Cold (-20 ºF) HAC Slapdown Cases

Slapdown Orientation (degrees from horizontal)	5º	10º	15º	20º
Force (lb)	$2.13(10)^6$	$2.08(10)^6$	$2.07(10)^6$	$2.06(10)^6$
Deflection (in)	9.23	9.02	9.01	8.95

Table 2.10.4-2 – Impact Force and Maximum Deflections for Warm (140 ºF) HAC Slapdown Cases

Slapdown Orientation (degrees from horizontal)	5º	10º	15º	20º
Force (lb)	$2.30(10)^6$	$2.25(10)^6$	$2.19(10)^6$	$2.20(10)^6$
Deflection (in)	12.93	12.86	12.76	12.77

Table 2.10.4-3 – Force-Deflection Data for Cold (-20 ºF) and Warm (140 ºF) HAC 0º Slapdowns

Deflection (in)	Force at -20 ºF (lb)	Force at 140 ºF (lb)
0.0	0	0
0.5	$1.62(10)^5$	$7.98(10)^4$
1.0	$3.95(10)^5$	$1.94(10)^5$
1.5	$5.72(10)^5$	$2.82(10)^5$
2.0	$6.99(10)^5$	$3.44(10)^5$
2.5	$8.13(10)^5$	$4.00(10)^5$
3.0	$9.28(10)^5$	$4.56(10)^5$
3.5	$1.04(10)^6$	$5.12(10)^5$
4.0	$1.15(10)^6$	$5.66(10)^5$
4.5	$1.25(10)^6$	$6.16(10)^5$
5.0	$1.35(10)^6$	$6.62(10)^5$
5.5	$1.44(10)^6$	$7.07(10)^5$
6.0	$1.53(10)^6$	$7.51(10)^5$
6.5	$1.61(10)^6$	$7.94(10)^5$
7.0	$1.70(10)^6$	$8.35(10)^5$
7.5	$1.77(10)^6$	$8.72(10)^5$
8.0	$1.86(10)^6$	$9.15(10)^5$
8.5	$1.96(10)^6$	$9.64(10)^5$
9.0	$2.07(10)^6$	$1.02(10)^6$
9.5	$2.21(10)^6$	$1.09(10)^6$
10.0	$2.38(10)^6$	$1.17(10)^6$
10.5	$2.58(10)^6$	$1.27(10)^6$
11.0	$2.83(10)^6$	$1.39(10)^6$
11.5	$3.14(10)^6$	$1.54(10)^6$
12.0	$3.55(10)^6$	$1.75(10)^6$
12.5	$4.10(10)^6$	$2.02(10)^6$
13.0	$4.77(10)^6$	$2.34(10)^6$
13.5	$5.53(10)^6$	$2.84(10)^6$
14.0	$6.36(10)^6$	$3.92(10)^6$
14.5	$7.25(10)^6$	$5.80(10)^6$
15.0	$8.19(10)^6$	$8.37(10)^6$
15.5	$9.18(10)^6$	$1.14(10)^7$
16.0	$1.02(10)^7$	$1.49(10)^7$
16.5	$1.13(10)^7$	$1.87(10)^7$

Table 2.10.4-4 – Shear and Moment During Slapdown

Position, x	Shear	Moment
0	0	0
$L_2/6$	(0.2500)F	$(0.02315)FL_2$
$L_2/3$	(0.3333)F	$(0.07407)FL_2$
$L_2/2$	(0.2500)F	$(0.12500)FL_2$
$2L_2/3$	0	$(0.14815)FL_2$
$5L_2/6$	(-0.4166)F	$(0.11574)FL_2$
L_2	(-1.0000)F	0

Table 2.10.4-5 – Thrust and Moment Due to HAC Cold (-20 ºF) Slapdown Cases

θ (degrees from horizontal)	5º	10º	15º	20º
Impact Limiter Force, F, lb	$2.13(10)^6$	$2.08(10)^6$	$2.07(10)^6$	$2.06(10)^6$
Thrust, T = F(sin θ), lb	$1.86(10)^5$	$3.61(10)^5$	$5.36(10)^5$	$7.05(10)^5$
Moment, M = $(0.14815)FL_2(\cos\theta)$, in-lb①	$4.46(10)^7$	$4.30(10)^7$	$4.20(10)^7$	$4.07(10)^7$

Notes:

① L_2 = 141.75 inches.

Table 2.10.4-6 – Thrust and Moment Due to HAC Warm (140 ºF) Slapdown Cases

θ (degrees from horizontal)	5º	10º	15º	20º
Impact Limiter Force, F, lb	$2.30(10)^6$	$2.25(10)^6$	$2.19(10)^6$	$2.20(10)^6$
Thrust, T = F(sin θ), lb	$2.00(10)^5$	$3.91(10)^5$	$5.67(10)^5$	$7.52(10)^5$
Moment, M = $(0.14815)FL_2(\cos\theta)$, in-lb①	$4.81(10)^7$	$4.65(10)^7$	$4.44(10)^7$	$4.34(10)^7$

Notes:

① L_2 = 141.75 inches.

Table 2.10.4-7 – Stresses and Margins of Safety Due to HAC Cold (-20 ºF) Slapdown

θ (degrees from horizontal)	5º	10º	15º	20º
T/A, psi	636	$1.24(10)^3$	$1.83(10)^3$	$2.41(10)^3$
Mc/I, psi	$1.79(10)^4$	$1.72(10)^4$	$1.68(10)^4$	$1.63(10)^4$
σ = T/A + Mc/I, psi	$1.85(10)^4$	$1.85(10)^4$	$1.87(10)^4$	$1.87(10)^4$
MS = $\sigma_a/\sigma - 1$	+2.89	+2.90	+2.86	+2.85

Table 2.10.4-8 – Stresses and Margins of Safety Due to HAC Warm (140 ºF) Slapdown

θ (degrees from horizontal)	5º	10º	15º	20º
T/A, psi	687	$1.34(10)^3$	$1.94(10)^3$	$2.58(10)^3$
Mc/I, psi	$1.93(10)^4$	$1.86(10)^4$	$1.78(10)^4$	$1.74(10)^4$
σ = T/A + Mc/I, psi	$2.00(10)^4$	$2.00(10)^4$	$1.97(10)^4$	$2.00(10)^4$
MS = $\sigma_a/\sigma - 1$	+2.61	+2.60	+2.65	+2.61

Table 2.10.4-9 – Comparison of Allowable and Predicted Deformations for Warm (140 ºF) Slapdown

θ (degrees from horizontal)	5º	10º	15º	20º
Allowable Deformation, inches	14.305	14.305	14.305	14.305
Deformation, inches	12.93	12.86	12.760	12.77
Clearance, inches	1.375	1.445	1.545	1.535

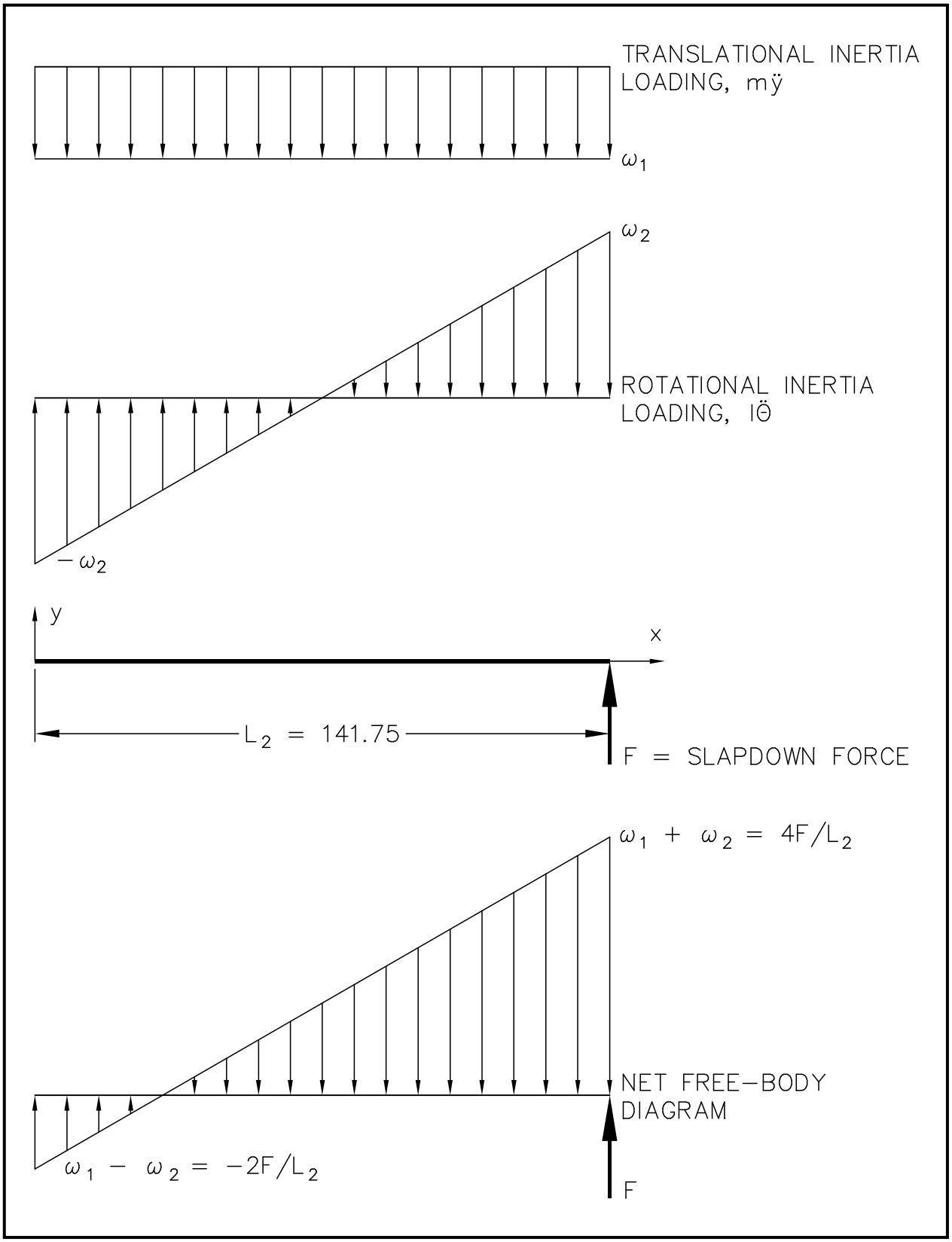

Figure 2.10.4-1 – Free-Body Diagram for Slapdown Loads

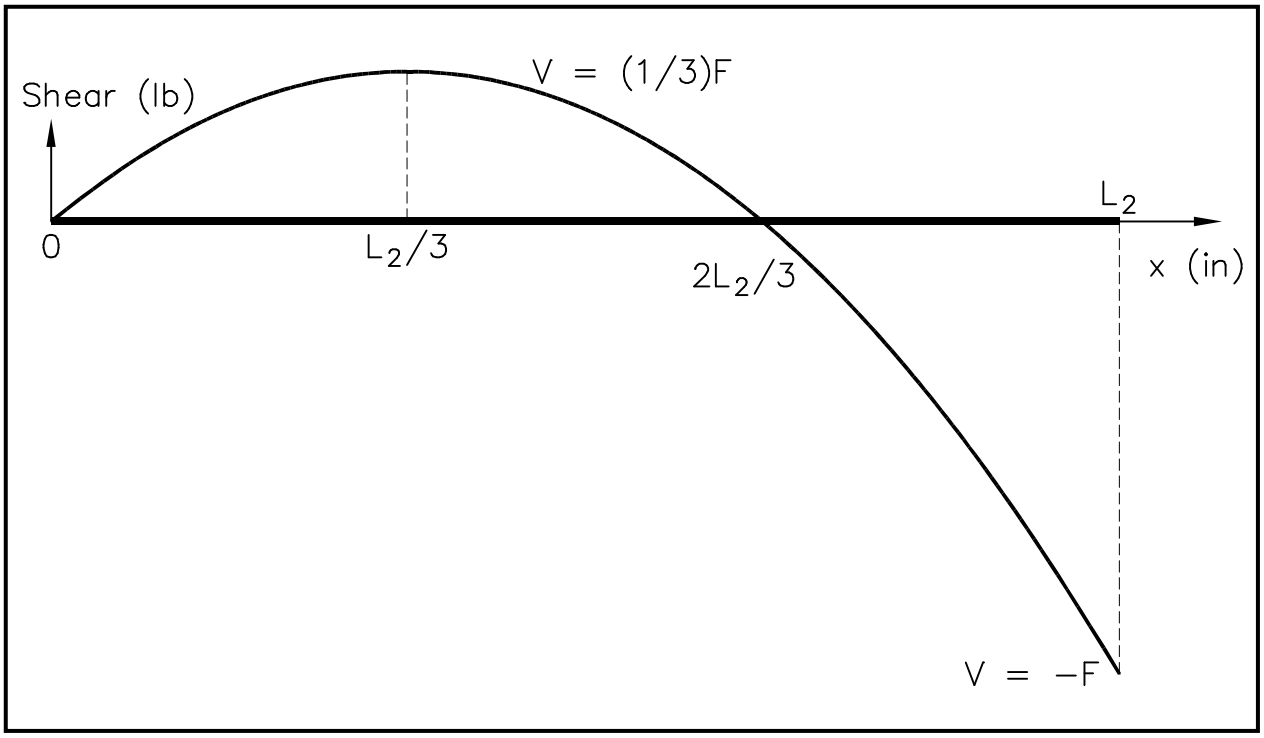

Figure 2.10.4-2 – Shear Diagram for Package During Slapdown

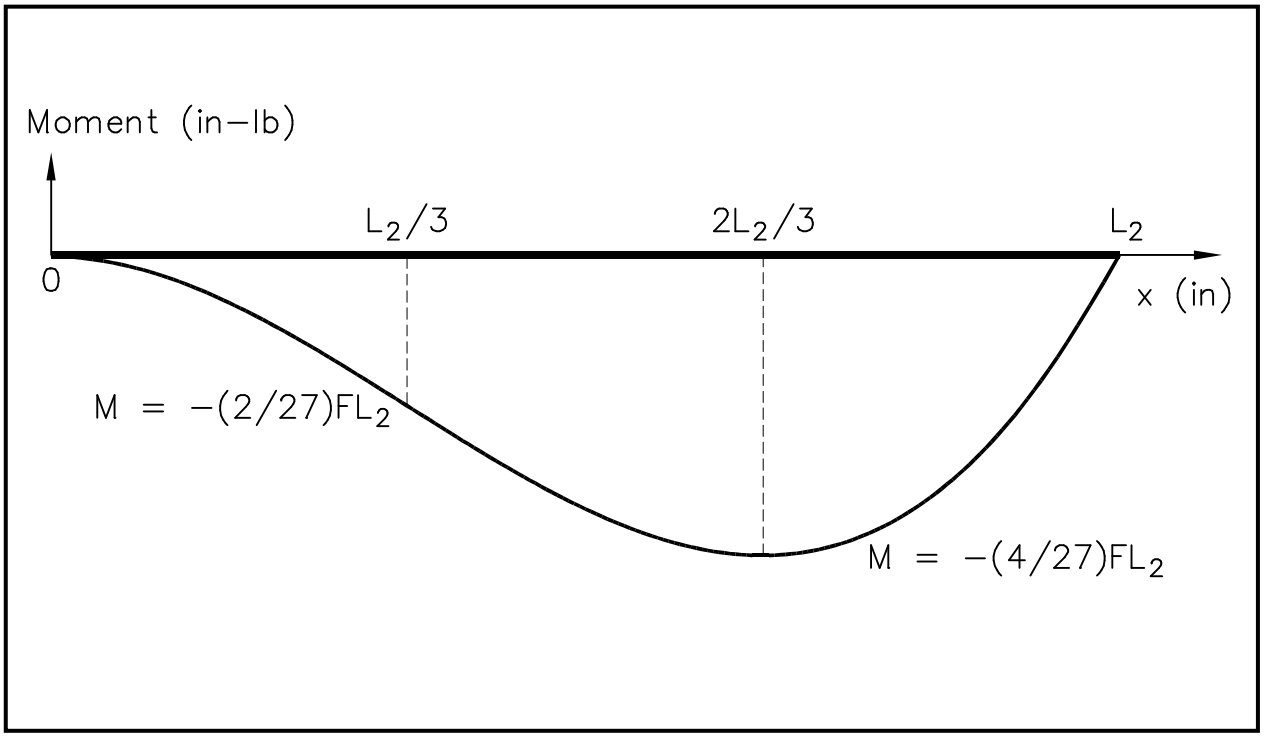

Figure 2.10.4-3 – Moment Diagram for Package During Slapdown

2.10.5 Buckling Design Criteria and Detailed Evaluation

The buckling criteria selected for use in analyzing the RH-TRU 72-B package is that presented in Code Case N-284[1] of the ASME Boiler and Pressure Vessel Code. By demonstrating that the requirements specified in ASME Code Case N-284[1] are met, the buckling requirement of Paragraph C.5 of Regulatory Guide 7.6[2] (i.e., buckling should not occur as the result of any normal or accident condition loading) is considered to have been satisfied. Consistent with Regulatory Guide 7.6 philosophy, ASME Code Level A service condition allowables are used for Regulatory Guide 7.6 defined normal conditions of transport (NCT), and ASME Level D service condition allowables are used for hypothetical accident conditions (HAC) in performing the buckling assessment. It is also noted that Paragraph F-1331.5(c) in Appendix F of the ASME Code[3] (for Level D Service Loadings) specifically identifies use of "a Code Case for metal containment shell buckling" as an acceptable means of addressing buckling issues.

ASME Code Case N-284 addresses both elastic and inelastic buckling and employs a factor of safety of 2.0 for Level A (NCT) conditions and a factor of safety of 1.34 for Level D (HAC) conditions. Interaction equations are employed which account for the effect of combined hoop compressive, axial compressive, and in plane shear loadings. The basic analytic approach is summarized as follows.

1. Theoretical elastic buckling stresses are determined using classical theory.
2. Capacity reduction factors are applied which account for the difference between classical theory and predicted instability stresses for fabricated shells.
3. Plasticity reduction factors are applied for those cases where elastically determined buckling stresses are above the proportional limit.
4. Elastic and inelastic buckling checks which employ appropriate factors of safety and appropriate interaction equations are made using worst case applied compressive and in-plane shear stresses.

All terminology used herein is consistent with that in ASME Code Case N-284[1].

2.10.5.1 Theoretical Elastic Buckling Stresses

The geometry and geometric parameters and the material property data required to carry out the buckling evaluation are presented in Table 2.10.5-1 and Table 2.10.5-2. Using this data, Table 2.10.5-3 and Table 2.10.5-4 are developed to give stress values as a function of the modulus of elasticity, E, as a temperature-dependent property, and Table 2.10.5-4 gives the stresses at the temperatures of interest. The basic equations used in the development of these two tables are

[1] American Society of Mechanical Engineers (ASME) Boiler and Pressure Vessel Code, Section III, *Rules for Construction of Nuclear Power Plant Components*, Division 1, Class MC, Code Case N-284, *Metal Containment Shell Buckling Design Methods*, August 25, 1980.

[2] U. S. Nuclear Regulatory Commission, Regulatory Guide 7.6, *Design Criteria for the Structural Analysis of Shipping Package Containment Vessels*, Revision 1, March 1978.

[3] American Society of Mechanical Engineers (ASME) Boiler and Pressure Vessel Code, Section III, *Rules for Construction of Nuclear Power Plant Components*, Division 1, Subsection NB and Appendices, 1986 Edition.

directly available from Paragraph –1712 of ASME Code Case N-284[1], and are summarized below (note the capacity reduction factors, C_i, are geometric dependent parameters).

a) For axial compression, the theoretical axial buckling stress, $\sigma_{\phi eL}$, is:

$$\sigma_{\phi eL} = C_\phi \frac{Et}{R}$$

where:

$$C_\phi = \frac{0.904}{M_\phi^2} + (0.1013)M_\phi^2 \qquad \text{if } 1.5 \le M_\phi < 1.73$$

$$C_\phi = 0.605 \qquad \text{if } M_\phi \ge 1.73$$

Note: The theoretical elastic buckling stress for axial compression of cylinders is also directly applicable for the case of bending of cylinders per ASME Code Case N-284[1].

b) For External Pressure:

i) No End Pressure ($\sigma_\phi = 0$), the theoretical hoop buckling stress for case of no end pressure, $\sigma_{\theta eL}$, is:

$$\sigma_{\theta eL} = \sigma_{reL} = C_{\theta r} \frac{Et}{R}$$

where:

$$C_{\theta r} = \frac{2.41}{M_\phi^{1.49} - 0.338} \qquad \text{if } 1.5 \le M_\phi < 3.0$$

$$C_{\theta r} = \frac{0.92}{M_\phi - 1.17} \qquad \text{if } 3.0 \le M_\phi < (1.65)(R/t)$$

$$C_{\theta r} = (0.275)\left(\frac{t}{R}\right) + \left(\frac{2.1}{M_\phi^4}\right)\left(\frac{R}{t}\right)^3 \qquad \text{if } M_\phi \ge (1.65)(R/t)$$

ii) ii. End Pressure Included ($\sigma_\phi = ½\sigma_\theta$), the theoretical hoop buckling stress for case of end pressure included, $\sigma_{\theta eL}$, is:

$$\sigma_{\theta eL} = \sigma_{heL} = C_{\theta h} \frac{Et}{R}$$

where:

$$C_{\theta h} = \frac{1.08}{M_\phi^{1.07} - 0.45} \qquad \text{if } 1.5 \le M_\phi < 3.0$$

$$C_{\theta h} = \frac{0.92}{M_\phi - 0.636} \qquad \text{if } 3.0 \le M_\phi < (1.65)(R/t)$$

$$C_{\theta h} = (0.275)\left(\frac{t}{R}\right) + \left(\frac{2.1}{M_\phi^4}\right)\left(\frac{R}{t}\right)^3 \quad \text{if } M_\phi \geq (1.65)(R/t)$$

c) <u>For Shear</u>, the theoretical in-plane shear buckling stress, $\sigma_{\phi\theta eL}$, is:

$$\sigma_{\phi\theta eL} = C_{\phi\theta}\frac{Et}{R}$$

where:

$$C_{\phi\theta} = \left(\frac{4.82}{M_\phi^2}\right)\sqrt{1 + (0.0239)M_\phi^3} \quad \text{if } 1.5 \leq M_\phi < 26$$

$$C_{\phi\theta} = \frac{0.746}{\sqrt{M_\phi}} \quad \text{if } 26 \leq M_\phi < (8.69)(R/t)$$

$$C_{\phi\theta} = 0.253\sqrt{\frac{t}{R}} \quad \text{if } M_\phi \geq (8.69)(R/t)$$

2.10.5.2 Capacity Reduction Factors

Capacity reduction factors which account for the difference between classical theory and predicted instability stresses for fabricated shells are directly determined using Paragraph –1500 of ASME Code Case N-284[1]. For the RH-TRU 72-B package shell geometries, the basic governing equations are as follows.

a) <u>For Axial Compression</u>, the larger of (i) or (ii) is used:

i) <u>Effect of R/t</u>:

$$\alpha_{\phi L} = 0.207 \quad \text{if } R/t \geq 600$$

$$\alpha_{\phi L} = 1.52 - (0.473)\log_{10}(R/t)$$
$$\alpha_{\phi L} = (10^{-5})\sigma_y - 0.033$$
if R/t < 600 (use smaller value)

ii) <u>Effect of Length</u>:

$$\alpha_{\phi L} = 0.837 - (0.14)M \quad \text{if } 1.5 \leq M < 1.73$$

$$\alpha_{\phi L} = \frac{0.837}{M^{0.6}} \quad \text{if } 1.73 \leq M < 10$$

$$\alpha_{\phi L} = 0.207 \quad \text{if } M \geq 10$$

<u>Note</u>: The capacity reduction factor for cylinders under axial compression is also employed for the case of bending of cylinders. This is slightly conservative based on an inspection of Figure 10-9 and Figure 10-13 of ASME Code Case N-284[1]. In other words, advantage is not taken of the fact that the critical buckling stress for cylinders under axial compression is slightly less than the critical buckling stress for cylinders in bending.

b) For Hoop Compression:

$$\alpha_{\theta L} = 0.8$$

c) For Shear:

$$\alpha_{\phi\theta L} = 0.8 \qquad \text{if } R/t \le 250$$

$$\alpha_{\phi\theta L} = 1.323 - (0.218)\log_{10}(R/t) \qquad \text{if } 250 < R/t < 1000$$

Direct application of these equations results in the capacity reduction factors presented in Table 2.10.5-5 as a function of temperature.

In order to directly use the above defined capacity reduction factors, the tolerance requirements of Paragraph NE-4220 of the ASME Code[4] must be met. Per Paragraph NE-4221.1 and Paragraph NE-4221.2, limits on "maximum difference in cross-sectional diameters" and "maximum deviation from true theoretical form for external pressure" must be met. Per the general arrangement drawing in Appendix 1.3.1, *Packaging General Arrangement Drawings*, these requirements are met for the outer cask (OC) outer and inner shells, and inner vessel (IV) shell.

2.10.5.3 Plasticity Reduction Factors

Plasticity reduction factors for cases where the elastically determined buckling stresses are above the proportional limit are directly determined using Paragraph –1600 of ASME Code Case N-284[1]. The magnitude of the reduction factor is directly related to the magnitude of the applied compressive or in-plane shear stress, σ_i, as indicated by the applicable equations below.

a) For Axial Compression:

$$\eta_\phi = 1.0 \qquad \text{if } \sigma_\phi(FS)/\sigma_y \le 0.55$$

$$\eta_\phi = \frac{0.18}{1 - \dfrac{(0.45)\sigma_y}{(FS)\sigma_\phi}} \qquad \text{if } 0.55 < \sigma_\phi(FS)/\sigma_y \le 0.738$$

$$\eta_\phi = 1.31 - \frac{(1.15)\sigma_\phi(FS)}{\sigma_y} \qquad \text{if } 0.738 < \sigma_\phi(FS)/\sigma_y \le 1.0$$

b) For Hoop Compression:

$$\eta_\theta = 1.0 \qquad \text{if } \sigma_\theta(FS)/\sigma_y \le 0.67$$

$$\eta_\theta = 2.53 - \frac{(2.29)\sigma_\theta(FS)}{\sigma_y} \qquad \text{if } 0.67 < \sigma_\theta(FS)/\sigma_y \le 1.0$$

c) For Shear:

$$\eta_{\phi\theta} = 1.0 \qquad \text{if } \sigma_{\phi\theta}(FS)/\sigma_y \le 0.48$$

[4] American Society of Mechanical Engineers (ASME) Boiler and Pressure Vessel Code, Section III, *Rules for Construction of Nuclear Power Plant Components*, Division 1, Subsection NE, 1986 Edition.

$$\eta_{\phi\theta} = \frac{0.1}{1 - \frac{(0.43)\sigma_y}{(FS)\sigma_{\phi\theta}}} \qquad \text{if } 0.48 < \sigma_{\phi\theta}(FS)/\sigma_y \leq 0.6$$

As plasticity reduction factors depend directly on applied compressive or in-plane shear stress magnitudes, numerical values for reduction factors cannot be presented at this point in the evaluation.

2.10.5.4 Development of Upper-Bound Magnitudes for Compressive Stresses and In-Plane Shear Stresses

Per Paragraph –1600 of ASME Code Case N-284[1], as an upper limit, σ_ϕ and σ_θ must be less than σ_y divided by the applicable Factor of Safety (FS). Similarly, for shear, $\sigma_{\phi\theta}$ must be less than or equal to $(0.6)\sigma_y$ divided by the applicable Factor of Safety (FS). With a Factor of Safety of 2.0 for NCT, and 1.34 for HAC, the maximum (upper-bound) permitted values for elastically determined axial, σ_ϕ, or hoop, σ_θ, compressive stresses, and for shear, $\sigma_{\phi\theta}$, are presented in Table 2.10.5-6. Under no circumstances can these upper-bound limits be exceeded. However, satisfying these limits alone is not sufficient to demonstrate that buckling will not occur. As discussed in Section 2.10.5.5, *Interaction Equations*, interaction equations must also be satisfied.

2.10.5.5 Interaction Equations

Elastic and inelastic interaction equations must be satisfied for all states of compressive and in-plane shear stress. The interaction equations for cylindrical shells are directly available from Paragraphs –1713.1.1 and –1713.2.1 of ASME Code Case N-284[1]. Once a stress state is established for a specific shell, plasticity reduction factors can be determined and all appropriate interaction equations checked.

Elastic interaction equations must be satisfied, and if any of the uniaxial critical stress values exceed the proportional limit of the fabricated material, the inelastic interaction equations must also be satisfied.

2.10.5.6 Stress Summary

Applied compressive membrane and in-plane shear stresses for each load condition and for each shell of the RH-TRU 72-B package are summarized in Table 2.10.5-7, Table 2.10.5-8, and Table 2.10.5-9. Appropriate worst-case combinations of these stresses are provided in Table 2.10.5-10, Table 2.10.3-11, and Table 2.10.5-12, thus allowing plasticity reduction factors to be explicitly determined and interaction equations to be checked.

In general, stresses provided in the tables correspond to cold condition (-20 ºF) impact loadings, whereas buckling checks are conservatively performed at upper bound shell temperatures of 160 ºF. The only exceptions to this are for the cases of HAC oblique and side drops, where for the OC outer shell and IV shell, advantage is taken of the lower impact loadings associated with hot conditions. For these two cases, both hot and cold conditions are specifically checked for potential buckling. In addition, with one exception (see below), all buckling checks of the OC shells ignore lead shrinkage induced stresses. This is done recognizing the displacement limited nature of these stresses (i.e., if buckling modes were to initiate, lead-induced stresses would be

relieved). More significantly, if lead is in direct contact with a shell, the shell buckling modes are significantly altered and the presence of the surrounding lead is actually of much more benefit to increasing the buckling resistance of the shell than are the detrimental effects of any imposed displacement limited stresses. This is especially true for the RH-TRU 72-B OC, given the relatively low magnitude of lead shrinkage-induced stresses reported in Appendix 2.10.8, *Fabrication Stresses Due to Lead Pour* (as summarized in Appendix 2.10.8.8, *Summary*). Further, due to creep effects, the actual initial stress state for the OC shells associated with differential expansion of the lead and shells is dependent on the specific thermal cycle history of a package. As such, any beneficial lead shrinkage-induced shell support may have fully crept away prior to a hypothesized drop event. Given the above, lead shrinkage-induced stresses are generally ignored herein, and no benefit is taken for the presence of lead improving buckling resistance. The only exception is for the case of end drop, where the stress analyses from Section 2.6.7, *Free Drop*, and Section 2.7.1, *Free Drop*, do not readily allow removal of lead-induced axial stresses. Thus, for end drop, lead-induced axial compressive stresses are conservatively included, without taking any advantage of their beneficial effect on increased buckling resistance.

2.10.5.7 Detailed Buckling Evaluations, Plasticity Reduction Factor Determinations, and Interaction Equation Checks

By using the worst-case load combinations available in Table 2.10.5-10, Table 2.10.3-11, and Table 2.10.5-12, and the various data available in previous sections, the methods outlined in ASME Code Case N-284[1] can be directly applied to the RH-TRU 72-B package shells. By way of example, Load Combination 6 for the OC inner shell (Table 2.10.5-10) is considered as follows. The step-by-step procedure is that specified in Paragraph –1800 of ASME Code Case N-284[1].

Step 1: Stresses for each specified loading are per Table 2.10.5-7 herein. The specified loadings for Load Combination 6 are NCT differential expansion and HAC oblique drop at 160 ºF.

Step 2: Combined stresses are per Table 2.10.5-10 herein. For Load Combination 6, the combined stresses are:

$$\sigma_\phi = 17{,}049 \text{ psi}$$

$$\sigma_\theta = 724 \text{ psi}$$

$$\sigma_{\phi\theta} = 4{,}796 \text{ psi}$$

Step 3: For HAC, the Factor of Safety (FS) is 1.34. Multiplying the stress components by this Factor of Safety yields:

$$(FS)\sigma_\phi = 22{,}846 \text{ psi}$$

$$(FS)\sigma_\theta = 970 \text{ psi}$$

$$(FS)\sigma_{\phi\theta} = 6{,}427 \text{ psi}$$

Step 4: Capacity reduction factors are available from Section 2.10.5.2, *Capacity Reduction Factors*, and are as follows for Load Combination 6 at a temperature of 160 ºF.

$$\alpha_{\phi L} = 0.237$$

$$\alpha_{\theta L} = 0.8$$

$$\alpha_{\phi\theta L} = 0.8$$

Step 5: Plasticity reduction factors are determined using the equations presented in Section 2.10.5.3, *Plasticity Reduction Factors*, as follows, (the yield strength, σ_y, at 160 ºF is available from Table 2.10.5-2).

a) For axial compression:

$$\frac{(FS)\sigma_\phi}{\sigma_y} = \frac{22{,}846}{27{,}000} = 0.846 \Rightarrow \eta_\phi = 1.31 - \frac{(1.15)(FS)\sigma_\phi}{\sigma_y} = 1.31 - \frac{(1.15)(22{,}846)}{27{,}000} = 0.337$$

b) For hoop compression:

$$\frac{(FS)\sigma_\theta}{\sigma_y} = \frac{970}{27{,}000} = 0.036 \quad \Rightarrow \quad \eta_\theta = 1.0$$

c) For shear:

$$\frac{(FS)\sigma_{\phi\theta}}{\sigma_y} = \frac{6{,}427}{27{,}000} = 0.238 \quad \Rightarrow \quad \eta_\theta = 1.0$$

Step 6: Compute the elastic stress components:

$$\sigma_{\phi s} = \frac{(FS)\sigma_\phi}{\alpha_{\phi L}} = \frac{22{,}846}{0.237} = 96{,}397 \text{ psi}$$

$$\sigma_{\theta s} = \frac{(FS)\sigma_\theta}{\alpha_{\theta L}} = \frac{970}{0.8} = 1{,}213 \text{ psi}$$

$$\sigma_{\phi\theta s} = \frac{(FS)\sigma_{\phi\theta}}{\alpha_{\phi\theta L}} = \frac{6{,}427}{0.8} = 8{,}034 \text{ psi}$$

Step 7: Compute the inelastic stress components:

$$\sigma_{\phi p} = \frac{\sigma_{\phi s}}{\eta_\phi} = \frac{96{,}397}{0.337} = 286{,}045 \text{ psi}$$

$$\sigma_{\theta p} = \frac{\sigma_{\theta s}}{\eta_\theta} = \frac{1{,}213}{1.0} = 1{,}213 \text{ psi}$$

$$\sigma_{\phi\theta p} = \frac{\sigma_{\phi\theta s}}{\eta_{\phi\theta}} = \frac{8{,}034}{1.0} = 8{,}034 \text{ psi}$$

Step 8: For the RH-TRU 72-B package, the buckling evaluation approach consistent with the vessel design and method of analysis is that of Paragraph –1710 of ASME Code Case N-284[1].

Step 9: The following assumptions apply to the buckling analyses:

a) Discontinuity stresses from NCT differential expansion are included and conservatively used without any modification.

b) No corrections are made for discontinuity stresses.

c) Classical uniaxial buckling values are available from Section 2.10.5.1, *Theoretical Elastic Buckling Stresses*. For the OC inner shell at 160 ºF, these classical values are as follows:

$$\sigma_{\phi eL} = 1{,}007{,}722 \text{ psi}$$

$$\sigma_{\theta eL} = \sigma_{reL} = 48{,}400 \text{ psi}$$

$$\sigma_{\theta eL} = \sigma_{heL} = 48{,}400 \text{ psi}$$

$$\sigma_{\phi\theta eL} = 228{,}071 \text{ psi}$$

d) Applicable elastic and inelastic interaction equations in Paragraph –1713.1.1 and Paragraph –1713.2.1 of ASME Code Case N-284[1] are checked as follows:

i) Elastic buckling per Paragraph –1713.1.1 of ASME Code Case N-284[1]:

(a) Axial compression-plus-hoop compression ($\sigma_{\phi s} < \frac{1}{2}\sigma_{\theta s}$):

Not Applicable (n/a)

(b) Axial compression-plus-hoop compression ($\sigma_{\phi s} \geq \frac{1}{2}\sigma_{\theta s}$):

$$\frac{\sigma_{\phi s} - \frac{1}{2}\sigma_{heL}}{\sigma_{\phi eL} - \frac{1}{2}\sigma_{heL}} + \left(\frac{\sigma_{\theta s}}{\sigma_{heL}}\right)^2 \leq 1.0$$

$$\frac{96{,}397 - \frac{1}{2}(48{,}400)}{1{,}007{,}722 - \frac{1}{2}(48{,}400)} + \left(\frac{1{,}213}{48{,}400}\right)^2 = 0.074 \leq 1.0$$

(c) Axial compression-plus-shear:

$$\frac{\sigma_{\phi s}}{\sigma_{\phi eL}} + \left(\frac{\sigma_{\phi\theta s}}{\sigma_{\phi\theta eL}}\right)^2 \leq 1.0$$

$$\frac{96{,}397}{1{,}007{,}722} + \left(\frac{8{,}034}{228{,}071}\right)^2 = 0.097 \leq 1.0$$

(d) Hoop compression-plus-shear:

$$\frac{\sigma_{\theta s}}{\sigma_{reL}} + \left(\frac{\sigma_{\phi\theta s}}{\sigma_{\phi\theta eL}}\right)^2 \leq 1.0$$

$$\frac{1{,}213}{48{,}400} + \left(\frac{8{,}034}{228{,}071}\right)^2 = 0.026 \le 1.0$$

(e) Axial compression-plus-hoop compression-plus-shear:

$$K = 1 - \left(\frac{\sigma_{\varphi\theta s}}{\sigma_{\varphi\theta eL}}\right)^2 = 1 - \left(\frac{8{,}034}{228{,}071}\right)^2 \approx 1.00$$

and equations **(a)** and **(b)** above remain unchanged.

ii) Inelastic buckling per Paragraph –1713.2.1 of ASME Code Case N-284[1]:

(a) Axial compression:

$$\frac{\sigma_{\phi p}}{\sigma_{\phi eL}} \le 1.0 \quad \Rightarrow \quad \frac{286{,}045}{1{,}007{,}722} = 0.284 \le 1.0$$

(b) Hoop compression:

$$\frac{\sigma_{\theta p}}{\sigma_{\theta eL}} \le 1.0 \quad \Rightarrow \quad \frac{1{,}213}{48{,}400} = 0.025 \le 1.0$$

(c) Axial compression-plus-shear:

$$\left(\frac{\sigma_{\phi p}}{\sigma_{\phi eL}}\right)^2 + \left(\frac{\sigma_{\phi\theta p}}{\sigma_{\phi\theta eL}}\right)^2 \le 1.0$$

$$\left(\frac{286{,}045}{1{,}007{,}722}\right)^2 + \left(\frac{8{,}034}{228{,}071}\right)^2 = 0.082 \le 1.0$$

(d) Hoop compression-plus-shear:

$$\left(\frac{\sigma_{\theta p}}{\sigma_{reL}}\right)^2 + \left(\frac{\sigma_{\phi\theta p}}{\sigma_{\phi\theta eL}}\right)^2 \le 1.0$$

$$\left(\frac{1{,}213}{48{,}400}\right)^2 + \left(\frac{8{,}034}{228{,}071}\right)^2 = 0.002 \le 1.0$$

(e) Stiffeners not needed:

As all interaction equations are satisfied and there are no concentrated loads on the shell that cause localized buckling, buckling of the OC inner shell will not occur.

Table 2.10.5-13 summarizes results from the interaction equations for all shells under the worst-case load combinations. As shown, all interaction equations yield values less than 1.0; thus, it is concluded that buckling will not occur for any RH-TRU 72-B package shell component.

Table 2.10.5-1 – Geometry, Geometric Parameters, and Material Data Used in Buckling Evaluations

Parameter	Outer Cask		Inner Vessel
	Outer Shell	Inner Shell	
R (radius, inches)	19.815	16.69	15.8125
t (thickness, inches)	1.5	1.0	0.375
$(Rt)^{0.5}$	5.45	4.085	2.435
L_ϕ (length, inches)	121.62	121.25	111.75
$L_\theta = 2\pi R$ (circumference, inches)	124.5	104.87	99.35
$M_\phi = L_\phi/(Rt)^{0.5}$	22.31	29.68	45.89
$M_\theta = L_\theta/(Rt)^{0.5}$	22.84	25.67	40.80
M (lesser of M_ϕ or M_θ)	22.31	25.67	40.80
μ (Poisson's ratio)	0.3	0.3	0.3
E (Young's modulus, psi)	Temperature Dependent①		
σ_y (yield strength, psi)	Temperature Dependent①		

Notes:

① Potential temperatures of interest are -20 ºF, 70 ºF, and 160 ºF (see Table 2.10.5-2).

Table 2.10.5-2 – Temperature Dependent Material Properties for Type 304 Stainless Steel

Parameter	Temperature		
	-20 ºF	70 ºF	160 ºF
E (Young's modulus, psi)	$28.8(10)^6$	$28.3(10)^6$	$27.8(10)^6$
σ_y (yield strength, psi)	36,000①	31,500①	27,000

Notes:

① The yield strength, σ_y, at -20 ºF and 70 ºF is linearly extrapolated from Table 2.3-1 in Section 2.3, *Mechanical Properties of Materials*

Table 2.10.5-3 – Theoretical Elastic Buckling Stress Values (General Temperature Independent Form)

Elastic Buckling Stress①	Outer Cask		Inner Vessel
	Outer Shell	Inner Shell	
$\sigma_{\phi eL} = C_{\phi}Et/R$ (axial)	(0.045799)E	(0.036249)E	(0.014348)E
$\sigma_{\theta eL} = \sigma_{reL} = C_{\theta r}Et/R$ (hoop, without end pressure)	(0.003052)E	(0.001741)E	(0.000488)E
$\sigma_{\theta eL} = \sigma_{heL} = C_{\theta h}Et/R$ (hoop, with end pressure)	(0.003052)E	(0.001741)E	(0.000482)E
$\sigma_{\phi\theta eL} = C_{\phi\theta}Et/R$ (shear)	(0.011962)E	(0.008204)E	(0.002612)E

Notes:

① Elastic buckling stress formulas are given in Appendix 2.10.5.1, *Theoretical Elastic Buckling Stresses*. The tabulated values are the resultant numerical values with the modulus of elasticity, E, retained as a temperature dependent parameter, and C_i, t, and R are geometric parameters.

Table 2.10.5-4 – Temperature Dependent Theoretical Elastic Buckling Stresses for Each RH-TRU 72-B Package Shell

Shell	Temperature		
	-20 ºF	70 ºF	160 ºF
$\sigma_{\phi eL}$ = theoretical axial buckling stress (psi)			
Outer Cask Outer Shell	1,319,011	1,296,112	1,273,212
Outer Cask Inner Shell	1,043,971	1,025,847	1,007,722
Inner Vessel	413,222	406,048	398,874
$\sigma_{\theta eL} = \sigma_{reL}$ = theoretical hoop buckling stress with no end pressure (psi)			
Outer Cask Outer Shell	87,898	86,372	84,846
Outer Cask Inner Shell	50,141	49,270	48,400
Inner Vessel	14,054	13,810	13,566
$\sigma_{\theta eL} = \sigma_{heL}$ = theoretical hoop buckling stress with end pressure (psi)			
Outer Cask Outer Shell	87,898	86,372	84,846
Outer Cask Inner Shell	50,141	49,270	48,400
Inner Vessel	13,882	13,641	13,400
$\sigma_{\phi\theta eL}$ = theoretical in-plane shear buckling stress (psi)			
Outer Cask Outer Shell	344,506	338,525	332,544
Outer Cask Inner Shell	236,275	232,173	228,071
Inner Vessel	75,226	73,920	72,614

Table 2.10.5-5 – Temperature Dependent Capacity Reduction Factors

Capacity Reduction Factor	Temperature		
	-20 ºF	70 ºF	160 ºF
$\alpha_{\phi L}$ (axial)	0.327	0.282	0.237
$\alpha_{\theta L}$ (hoop)	0.8	0.8	0.8
$\alpha_{\phi\theta L}$(shear)	0.8	0.8	0.8

Table 2.10.5-6 – Upper Bounds for Compressive Stresses and In-Plane Shear Stresses

Stress Condition	Load Condition	Temperature		
		-20 ºF	70 ºF	160 ºF
Upper-bound permitted compressive stress σ_ϕ or σ_θ (psi)	NCT	18,000	15,750	13,500
	HAC	26,866	23,507	20,149
Upper-bound permitted in-plane shear stress $\sigma_{\phi\theta}$ (psi)	NCT	10,800	9,450	8,100
	HAC	16,120	14,104	12,089

Table 2.10.5-7 – Compressive Membrane and In-Plane Shear Stress Summary for the Outer Cask Inner Shell

Load Condition	σ_{axial}	σ_{hoop}	τ	Reference
(a) NCT Differential Thermal Expansion	0	724	0	§2.6.1.2
(b) NCT End Drop at 160 ºF①	6,067	0	0	§2.6.7.1, ¶(6)
(c) NCT Oblique Drop (85º from horizontal) at 160 ºF	6,463	0	608	§2.6.7.2, ¶(4)
(d) NCT Side Drop Maximum Moment Location at 160 ºF	3,881	0	0	§2.6.7.3, ¶(4)
(e) NCT Side Drop Maximum Shear Location at 160 ºF	0	0	1,255	§2.6.7.3, ¶(4)
(f) HAC End Drop at 160 ºF①	12,801	0	0	§2.7.1.1, ¶(6)
(g) HAC Oblique Drop (5º from horizontal) at 160 ºF	17,049	0	4,796	§2.7.1.2, ¶(4)
(h) HAC Side Drop Maximum Moment Location at 160 ºF	16,331	0	0	§2.7.1.3, ¶(4)
(i) HAC Side Drop Maximum Shear Location at 160 ºF	0	0	5,554	§2.7.1.3, ¶(4)
(j) Side Pin Punch Maximum Moment Location at 160 ºF	8,526	0	0	§2.7.3.2
(k) Side Pin Punch Maximum Shear Location at 160 ºF	0	0	4,546	§2.7.3.2

Notes:

① The lead is assumed to be initially shrunk onto the OC inner shell which, for the OC inner shell, is worse than assuming the lead is initially stress-free.

Table 2.10.5-8 – Compressive Membrane and In-Plane Shear Stress Summary for the Outer Cask Outer Shell

Load Condition	σ_{axial}	σ_{hoop}	τ	Reference
(a) NCT Differential Thermal Expansion	0	724	0	§2.6.1.2
(b) NCT End Drop at 160 ºF①	3,550	0	0	§2.6.7.1, ¶(7)
(c) NCT Oblique Drop (85º from horizontal) at 160 ºF	7,348	0	608	§2.6.7.2, ¶(4)
(d) NCT Side Drop Maximum Moment Location at 160 ºF	4,607	0	0	§2.6.7.3, ¶(4)
(e) NCT Side Drop Maximum Shear Location at 160 ºF	0	0	1,255	§2.6.7.3, ¶(4)
(f) HAC End Drop at 160 ºF①	7,493	0	0	§2.7.1.1, ¶(7)
(g1) HAC Oblique Drop (5º from horizontal) at -20 ºF	20,212	0	4,796	§2.7.1.2, ¶(4)
(g2) HAC Oblique Drop (5º from horizontal) at 160 ºF	18,615②	0	4,796	§2.7.1.2, ¶(4)
(h1) HAC Side Drop Maximum Moment Location at -20 ºF	19,388	0	0	§2.7.1.3, ¶(4)
(h2) HAC Side Drop Maximum Moment Location at 160 ºF	16,460③	0	0	§2.7.1.3, ¶(4)
(i) HAC Side Drop Maximum Shear Location at 160 ºF	0	0	5,554	§2.7.1.3, ¶(4)
(j) Side Pin Punch Maximum Moment Location at 160 ºF	10,119	0	0	§2.7.3.2
(k) Side Pin Punch Maximum Shear Location at 160 ºF	0	0	4,546	§2.7.3.2

Notes:

① The lead is assumed to be initially stress-free which, for the OC outer shell, is worse than assuming the lead is initially shrunk onto the OC inner shell.

② For the 160 ºF oblique drop case, the axial stress component from the -20 ºF case is multiplied by the ratio of impact accelerations at temperature; from Table 2.10.3-11 and Table 2.10.3-12 in Appendix 2.10.3, *Drop Impact Evaluation Results*, the appropriate ratio for a 5º oblique drop is 44.3/48.1 = 0.921. Although shear stress could have been similarly reduced, it is conservatively left at the higher magnitude associated with the -20 ºF conditions.

③ For the 160 ºF side drop case, the axial stress component from the -20 ºF case is multiplied by the ratio of impact accelerations at temperature; from Table 2.10.3-11 and Table 2.10.3-12 in Appendix 2.10.3, *Drop Impact Evaluation Results*, the appropriate ratio for a 0º side drop is 68.9/81.2 = 0.849.

Table 2.10.5-9 – Compressive Membrane and In-Plane Shear Stress Summary for the Inner Vessel

Load Condition	σ_{axial}	σ_{hoop}	τ	Reference
(a) NCT Differential Thermal Expansion	0	1,208	0	§2.6.1.2
(b) NCT End Drop at 160 ºF①	4,185	0	0	§2.6.7.1, ¶(5)
(c) NCT Oblique Drop (85º from horizontal) at 160 ºF	5,247	0	2,099	§2.6.7.2, ¶(5)
(d) NCT Side Drop Maximum Moment Location at 160 ºF	4,661	0	0	§2.6.7.3, ¶(5)
(e) NCT Side Drop Maximum Shear Location at 160 ºF	0	0	2,214	§2.6.7.3, ¶(5)
(f) HAC End Drop at 160 ºF①	11,995	0	0	§2.7.1.1, ¶(5)
(g1) HAC Oblique Drop (5º from horizontal) at -20 ºF	21,372	0	7,503	§2.7.1.2, ¶(5)
(g2) HAC Oblique Drop (5º from horizontal) at 160 ºF	18,194②	0	7,503	§2.7.1.2, ¶(5)
(h1) HAC Side Drop Maximum Moment Location at -20 ºF	19,611	0	0	§2.7.1.3, ¶(5)
(h2) HAC Side Drop Maximum Moment Location at 160 ºF	16,650③	0	0	§2.7.1.3, ¶(5)
(i) HAC Side Drop Maximum Shear Location at 160 ºF	0	0	9,317	§2.7.1.3, ¶(5)

Notes:

① The bottom end drop is the worst case for the IV.

② Axial stress for this 160 ºF case is reduced from the value of 21,372 psi presented in Paragraph (5) of Section 2.7.1.2, *Corner and Oblique Drops*, which corresponds to -20 ºF conditions. The reduction recognizes the lower impact acceleration of 44.3*g* at 160 ºF compared to 48.1*g* at -20 ºF (see Note 2 of Table 2.10.5-8). More significantly, from an inspection of Figure 2.10.1-9 in Appendix 2.10.1.4, *Containment Assembly Analysis for Oblique Drops*, and Figure 2.7-11, Figure 2.7-12, and Figure 2.7-13 in Paragraph (3) of Section 2.7.1.2, *Corner and Oblique Drops*, it is clear that the maximum moment of 44.3/48.1 × 4,260,000 = 3,923,451 in-lb (where 4,260,000 in-lb is from the last paragraph of Paragraph (3) of Section 2.7.1.2, *Corner and Oblique Drops*) occurs at IV node 211, which corresponds to the centerline of the 10-inch wide payload canister support ring. However, the nearest location where buckling of the IV shell can actually occur is 5 inches away (i.e., at the outer edge of the payload canister support ring); that location is addressed as follows. From Figure 2.7-12, the shear force at the point of maximum moment is approximately -60,000 pounds. As such, at a point 5 inches away, the bending moment becomes 3,923,451 – 5(60,000) = 3,623,451 in-lb. Finally, as was done in Paragraph (3) of Section 2.7.1.2, *Corner and Oblique Drops*, the 3,623,451 in-lb moment must be increased by a factor of 1.49 to 5,398,942 in-lb. Repeating the IV membrane stress calculation in Paragraph (5) of Section 2.7.1.2, *Corner and Oblique Drops*, using a bending moment of 5,398,942 in-lb instead of 6,347,400 in-lb, results in an axial stress of 18,194 psi. Although stresses due to shear and thrust loads could have been similarly reduced, they are conservatively left at the higher magnitudes associated with the -20 ºF conditions.

③ For the 160 ºF side drop case, the axial stress component from the -20 ºF case is multiplied by the ratio of impact accelerations at temperature; from Table 2.10.3-11 and Table 2.10.3-12 in Appendix 2.10.3, *Drop Impact Evaluation Results*, the appropriate ratio for a 0º side drop is 68.9/81.2 = 0.849.

Table 2.10.5-10 – Worst-Case Load Combinations for the Outer Cask Inner Shell

Combination① (Table 2.10.5-7)	Regulatory Condition	Shell Temperature (ºF)	σ_ϕ (psi)	σ_θ (psi)	$\sigma_{\theta\phi}$ (psi)
(1) (a) + (b)	NCT	160	6,067	724	0
(2) (a) + (c)	NCT	160	6,463	724	608
(3) (a) + (d)	NCT	160	3,881	724	0
(4) (a) + (e)	NCT	160	0	724	1,255
(5) (a) + (f)	HAC	160	12,801	724	0
(6) (a) + (g)	HAC	160	17,049	724	4,796
(7) (a) + (h)	HAC	160	16,331	724	0
(8) (a) + (i)	HAC	160	0	724	5,554

Notes:

① Combining load condition (a) with load conditions (j) or (k) would not result in a governing worst-case.

Table 2.10.5-11 – Worst-Case Load Combinations for the Outer Cask Outer Shell

Combination① (Table 2.10.5-8)	Regulatory Condition	Shell Temperature (ºF)	σ_ϕ (psi)	σ_θ (psi)	$\sigma_{\theta\phi}$ (psi)
(1) (a) + (b)	NCT	160	3,550	724	0
(2) (a) + (c)	NCT	160	7,348	724	608
(3) (a) + (e)	NCT	160	0	724	1,255
(4) (a) + (f)	HAC	160	7,493	724	0
(5a) (a) + (g_1)	HAC	-20	20,212	724	4,796
(5b) (a) + (g_2)	HAC	160	18,615	724	4,796
(6) (a) + (i)	HAC	160	0	724	5,554

Notes:

① Combining load condition (a) with load conditions (d), (h_1), (h_2), (j), or (k) would not result in a governing worst-case.

Table 2.10.5-12 – Worst-Case Load Combinations for the Inner Vessel

Combination① (Table 2.10.5-9)	Regulatory Condition	Shell Temperature (ºF)	σ_ϕ (psi)	σ_θ (psi)	$\sigma_{\theta\phi}$ (psi)
(1) (a) + (c)	NCT	160	5,247	1,208	2,099
(2) (a) + (e)	NCT	160	0	1,208	2,214
(3a) (a) + (g_1)	HAC	-20	21,372	1,208	7,503
(3b) (a) + (g_2)	HAC	160	18,194	1,208	7,503
(4) (a) + (i)	HAC	160	0	1,208	9,317

Notes:

① Combining load condition (a) with load conditions (b), (d), (f), (h_1), or (h_2) would not result in a governing worst-case.

This page intentionally left blank.

Table 2.10.5-13 – Interaction Equation Checks

Combination	Elastic Interaction per –1713.1.1						Inelastic Interaction per –1713.1.2			
	(a)①	(b)②	(c)③	(d)④	(e)(1)⑤	(e)(2)⑥	(a)⑦	(b)⑧	(c)③	(d)④
Outer Cask Inner Shell per Table 2.10.5-10										
(1) (a) + (b)	n/a	0.029	0.051	0.037	n/a	0.029	⑩	⑩	⑨	⑨
(2) (a) + (c)	n/a	0.032	0.054	0.037	n/a	0.032	⑩	⑩	⑩	⑩
(3) (a) + (d)	n/a	0.010	0.032	0.037	n/a	0.010	⑩	⑩	⑨	⑨
(4) (a) + (e)	n/a	n/a	0.000	0.038	n/a	n/a	⑩	⑩	⑩	⑩
(5) (a) + (f)	n/a	0.050	0.072	0.025	n/a	0.050	0.116	0.025	0.014	0.001
(6) (a) + (g)	n/a	0.074	0.097	0.026	n/a	0.074	0.284	0.025	0.082	0.002
(7) (a) + (h)	n/a	0.070	0.092	0.025	n/a	0.070	0.242	0.025	0.059	0.001
(8) (a) + (i)	n/a	n/a	0.002	0.027	n/a	n/a	⑩	⑩	⑩	⑩
Outer Cask Outer Shell per Table 2.10.3-11										
(1) (a) + (b)	n/a	n/a	0.024	0.021	n/a	n/a	⑩	⑩	⑨	⑨
(2) (a) + (c)	n/a	0.016	0.049	0.021	n/a	0.016	⑩	⑩	⑩	⑩
(3) (a) + (e)	n/a	n/a	0.000	0.021	n/a	n/a	⑩	⑩	⑩	⑩
(4) (a) + (f)	n/a	n/a	0.033	0.013	n/a	n/a	⑩	⑩	⑨	⑨
(5a) (a) + (g_1)	n/a	0.031	0.063	0.014	n/a	0.031	0.141	0.014	0.020	0.001
(5b) (a) + (g_2)	n/a	0.051	0.083	0.015	n/a	0.051	0.334	0.014	0.112	0.001
(6) (a) + (i)	n/a	n/a	0.001	0.015	n/a	n/a	⑩	⑩	⑩	⑩
Inner Vessel per Table 2.10.5-12										
(1) (a) + (c)	n/a	0.147	0.116	0.228	n/a	0.148	⑩	⑩	⑩	⑩
(2) (a) + (e)	n/a	n/a	0.006	0.228	n/a	n/a	⑩	⑩	⑩	⑩
(3a) (a) + (g_1)	n/a	0.220	0.240	0.172	n/a	0.227	0.536	0.144	0.316	0.049
(3b) (a) + (g_2)	n/a	0.268	0.288	0.179	n/a	0.278	0.950	0.149	0.932	0.052
(4) (a) + (i)	n/a	n/a	0.046	0.195	n/a	n/a	⑩	⑩	⑩	⑩

Notes for Table 2.10.5-13:

① Axial Compression + Hoop Compression ($\sigma_{\phi s} < (0.5)\sigma_{\theta s}$)

② Axial Compression + Hoop Compression ($\sigma_{\phi s} \geq (0.5)\sigma_{\theta s}$)

③ Axial Compression + Shear

④ Hoop Compression + Shear

⑤ Axial Compression + Hoop Compression + Shear ($\sigma_{\phi s} < (0.5)\sigma_{\theta s}$)

⑥ Axial Compression + Hoop Compression + Shear ($\sigma_{\phi s} \geq (0.5)\sigma_{\theta s}$)

⑦ Axial Compression

⑧ Hoop Compression

⑨ No Shear

⑩ Elastic Stresses Only

2.10.6 Closure Bolt Stress Evaluations

2.10.6.1 Analysis Results

The closure bolt stress analyses consider impact loads, pressure loads and bolt preloads. Bolt stress analysis results are summarized in the following eight tables:

- Table 2.10.6-1 – Outer Cask NCT Bolt Stresses, Torque Coefficient = 0.13
- Table 2.10.6-2 – Outer Cask NCT Bolt Stresses, Torque Coefficient = 0.20
- Table 2.10.6-3 – Inner Vessel NCT Bolt Stresses, Torque Coefficient = 0.13
- Table 2.10.6-4 – Inner Vessel NCT Bolt Stresses, Torque Coefficient = 0.20
- Table 2.10.6-5 – Outer Cask HAC Bolt Stresses, Torque Coefficient = 0.13
- Table 2.10.6-6 – Outer Cask HAC Bolt Stresses, Torque Coefficient = 0.20
- Table 2.10.6-7 – Inner Vessel HAC Bolt Stresses, Torque Coefficient = 0.13
- Table 2.10.6-8 – Inner Vessel HAC Bolt Stresses, Torque Coefficient = 0.20

Each table is preceded by an explicit listing of relevant geometry, taken directly from Appendix 1.3.1, *Packaging General Arrangement Drawings*, and loading data (torque, pressure).

Impact loads are expressed in acceleration *g*-loads, as given within Appendix 2.10.3, *Drop Impact Evaluation Results*. For conservatism, these loads are based upon the -20 ºF "cold" foam stress-strain relations, and bolt allowable stresses are taken at the "hot" temperature of 160 ºF.

Consistent with the ASME Code[1], the normal conditions of transport (NCT) allowable stress, $S_a = 2.0S_m$, and the hypothetical accident conditions (HAC) allowable stress, $S_a = 3.0S_m$ per Paragraph NB-3232 of the ASME Code[1]. For conservatism, external energy absorber reaction forces, which resist separation of the outer cask lid and body, are completely neglected in all calculations.

Analysis methodology, allowable stresses, and basic assumptions used are consistent with conventional design/analysis codes, such as AISC[2] and Section III of the ASME Code[1], specifically Appendix F (Paragraph F-1335). However, the analysis presented herein is more conservative, including stresses associated with preloads. Conventional design/analysis codes consider only externally applied loads and ignore preloads.

Like the ASME Code methodology given in Paragraph F-1335, this analysis uses nominal tensile and shear stresses based upon the tabulated "stress area" of the bolts. It should be noted that the elliptic interaction equations of Paragraph F-1335 and the approach used here give nearly identical results when adjustments in loadings are made to account for the differing treatment of preload tension (ASME ignores preload effects, while this method includes them).

The structural adequacy of the internally threaded base material, when Type 304 stainless steel (S_y = 30,000 psi) or the optional plated carbon steel threaded inserts (Sy = 140,000 psi), to resist the shear loads due to the worst-case bolt tensile loads is easily demonstrated. Of the two, the

[1] American Society of Mechanical Engineers (ASME) Boiler and Pressure Vessel Code, Section III, *Rules for Construction of Nuclear Power Plant Components*, Division 1, Subsection NB and Appendices, 1986 Edition.

[2] American Institute of Steel Construction, *Manual of Steel Construction*, Eighth Edition, American Institute of Steel Construction, Chicago, IL, 1980.

weakest configuration is threading directly into the Type 304 stainless steel base material. Since the optional threaded inserts have a larger outer diameter and a finer thread pitch, the insert/base material interface will be stronger than threading directly into the base metal.

From Table 2.10.6-1 through Table 2.10.6-8, the maximum NCT tensile bolt loads for the outer cask (OC) and inner vessel (IV) for all load combinations and torque coefficients are 54,945 pounds and 21,871 pounds, respectively, and the maximum HAC tensile bolt loads for the OC and IV are 75,794 pounds and 21,871 pounds, respectively.

Per Table 2.1-1 in Section 2.1.2.1.1, *Containment Structures*, the allowable shear stress for NCT is $0.6S_m = (0.6)(20{,}000) = 12{,}000$ psi at 160 ºF, and the allowable shear stress for HAC is $0.42S_u = (0.42)(67{,}700) = 28{,}430$ psi, where material properties for Type F304 stainless steel is taken from Table 2.3-1 in Section 2.3, *Mechanical Properties of Materials*. Each closure bolt hole is analyzed separately.

OC Closure Bolt Hole (1¼-7UNC-2B): From Table 2.10.6-1, the maximum NCT tensile bolt load is 54,945 pounds. For a 1¼-7 UNC-2B thread, the minimum shear area for an internal thread is 2.9441 in^2/in of engagement[3]. The OC closure bolts have a minimum engagement length of 1.75 inches. Therefore, the maximum shear stress, τ, and resulting margin of safety, MS, is:

$$\tau = \frac{54{,}945}{(2.9441)(1.75)} = 10{,}664 \text{ psi}$$

$$\text{MS} = \frac{12{,}000}{10{,}664} - 1.0 = +0.13$$

From Table 2.10.6-5, the maximum HAC tensile bolt load is 75,794 pounds. For a 1¼-7 UNC-2B thread, the minimum shear area for an internal thread is 2.9441 in^2/in of engagement. The OC closure bolts have a minimum engagement length of 1.75 inches. Therefore, the maximum shear stress, τ, and resulting margin of safety, MS, is:

$$\tau = \frac{75{,}794}{(2.9441)(1.75)} = 14{,}711 \text{ psi}$$

$$\text{MS} = \frac{28{,}430}{14{,}711} - 1.0 = +0.93$$

IV Closure Bolt Hole (7/8-9UNC-2B): From Table 2.10.6-3, the maximum NCT tensile bolt load is 21,871 pounds. For a 7/8-9UNC-2B thread, the minimum shear area for an internal thread is 2.0252 in^2/in of engagement[3]. The IV closure bolts have an engagement length of 1.06 inches. Therefore, the maximum shear stress, τ, and resultant minimum margin of safety, MS, is:

$$\tau = \frac{21{,}871}{(2.0252)(1.06)} = 10{,}188 \text{ psi}$$

[3] Raymond C. Boucher, *Table Speeds Calculation of Strength of Threads*, Product Engineering, November 27, 1961, Pages 41-49.

$$MS = \frac{12{,}000}{10{,}188} - 1.0 = +0.18$$

From Table 2.10.6-7, the maximum HAC tensile bolt load is 21,871 pounds. For a 7/8-9UNC-2B thread, the minimum shear area for an internal thread is 2.0252 in^2/in of engagement[3]. The IV closure bolts have an engagement length of 1.06 inches. Therefore, the maximum shear stress, τ, and resultant minimum margin of safety, MS, is:

$$\tau = \frac{21{,}871}{(2.0252)(1.06)} = 10{,}188 \text{ psi}$$

$$MS = \frac{28{,}430}{10{,}188} - 1.0 = +1.79$$

As demonstrated by these results, the internal threads for the RH-TRU 72-B package closure bolts have sufficient strength for all NCT and HAC.

2.10.6.2 Analysis Methodology

A description of terms and the methodology used in Table 2.10.6-1 through Table 2.10.6-8 is described in detail below. The data from Table 2.10.6-1 for the OC with a torque coefficient of 0.13 is used for the following descriptions:

a) Longitudinal Weight, W_A: the weight acting in the longitudinal (axial) direction, and reacted by the lid bolts.

i) OC: W_A includes the OC lid (1,667 pounds), IV (4,023 pounds), and a fully-loaded canister (8,000 pounds):

$$W_A = 1{,}667 + 4{,}023 + 8{,}000 = 13{,}690 \text{ lb}$$

ii) IV: Longitudinal loads are transferred directly to OC lid. Both are flat and parallel, and the OC lid is thicker and stiffer; thus, $W_A = 0$.

b) Lateral Weight, W_L: the weight acting in the lateral (transverse) direction, and amounts to the lid weight only (1,667 pounds for OC, and 1,382 pounds for IV). The IV bolt analysis conservatively ignores lateral support of the IV lid by the OC inner shell.

c) Bolt Preload, F_i: the bolt preload calculated from the torque relation for cadmium plated bolts (i.e., torque coefficient = 0.13[4]). Each bolt analysis is also calculated for non-cadmium plated bolts in successive tables (i.e., torque coefficient = 0.20).

$$F_i = \frac{12T}{(0.13)d} = 51{,}692 \text{ lb}$$

[4] Unbrako Manufacturer's Catalog, *Unbrako Socket Screws*, SPS Technologies, Jenkintown, PA, 1980, pp. 8–9, when ratioing the recommended torques for non-plated and cadmium plated bolts results in a torque coefficient of 0.15; Fastenal's *Technical Reference Guide*, S7028, Rev. 4, Fastenal Company, Winona, MN, reports torque coefficients for cadmium plated bolts of 0.11 – 0.15, and torque coefficients for lubricated bolts of 0.15; thus, a value of 0.13 is reasonable (see http://www.fastenal.com/content/documents/FastenalTechnicalReferenceGuide.pdf).

where the preload torque, T = 700 lb-ft, and the nominal bolt diameter, d = 1.25 inches.

d) Bolt Pressure Load, F_P:

$$F_P = \frac{P_P A_P}{N} = 7{,}083 \text{ pounds for 18 bolts}$$

where the internal pressure, P_P = 150 psig, the pressure area, A_P = 850 in^2 (based on a seal diameter of 32.896 inches), and the number of bolts, N = 18.

e) Bolt Stiffness, K_b:

$$K_b = \frac{A_b E}{L} = 1.44(10)^7 \text{ lb/in}$$

where the bolt cross-sectional area, A_b = 1.23 in^2, the elastic modulus, E = 27.3(10)^6 psi at 160 ºF (see Table 2.3-1 in Section 2.3, *Mechanical Properties of Materials*, for ASTM A320, Grade L43, fasteners), and the effective bolt length, L = (grip length, L_g) + ½(nominal bolt diameter, D) = 1.70 + ½(1.25) = 2.33 inches.

f) Lid Stiffness, K_m:

$$K_m = \frac{A_L E}{L_g} = 1.61(10)^8 \text{ lb/in}$$

where the assumed cross-sectional area is equal to a cylinder with an inside diameter equal to the nominal bolt diameter, D, and an outside diameter equal to three times the nominal bolt diameter, $A_L = (\pi/4)[(3D)^2 - D^2] = 2\pi D^2 = 2\pi(1.25)^2 = 9.8175$ in^2, the elastic modulus, E = 27.8(10)^6 psi at 160 ºF (see Table 2.3-1 in Section 2.3, *Mechanical Properties of Materials*, for Type 304 stainless steel, and the bolt grip length, L_g = 1.70 inches.

g) Impact Acceleration, n_g: based on impact force predictions with a total package weight of 45,000 pounds per Appendix 2.10.3, *Drop Impact Evaluation Results*.

h) Tensile Impact Loads – Uniform Bolt Force Distribution, F_A: only applicable to the 90º end impact case for the OC for NCT.

$$F_A = \frac{P_A}{N} = \frac{n_g W_A (\sin\theta)}{N} = 32{,}324 \text{ lb}$$

where the impact acceleration, $n_g = 42.5g$, the longitudinal weight, W_A = 13,690 pounds, the impact angle, θ = 90º, and the number of bolts, N = 18.

i) Tensile Impact Load – Triangular Bolt Force Distribution, F_A:

$$F_A = P_A\left(\frac{R_L(R_L + R_B)}{I_o}\right)A_B = n_g W_A(\sin\theta)\left(\frac{R_L(R_L + R_B)}{I_o}\right)A_B = 18{,}258 \text{ lb}$$

where the impact acceleration, $n_g = 17.9g$, the longitudinal weight, W_A = 13,690 pounds, the impact angle, θ = 85º, the lid radius, R_L = ½(37.60) = 18.80 inches, the bolt circle radius, R_B = ½(35.20) = 17.60 inches, the bolt shank area, A_B = 0.969 in^2, and the bolt circle moment of inertia, I_o, is:

$$I_o = \pi R_B^3 t + A_b N R_L^2 = \pi(17.60)^3(0.158) + (0.969)(18)(18.80)^2 = 8{,}866\,\text{in}^4$$

where the number of bolts, N = 18, and the equivalent ring thickness, t, is:

$$t = \frac{A_b N}{2\pi R_B} = \frac{(0.969)(18)}{2\pi(17.60)} = 0.158\,\text{inches}$$

The derivation of the triangular force distribution relationship is as follows.

Tensile bolt stresses are calculated by assuming the lid pivots about the outer edge of the lid, point "o", and assuming the bolts are approximated as a thin, circular ring with the thickness equivalent to the total bolt area (ring area).

The equivalent ring thickness, t, is derived from:

$$A = A_b N = 2\pi R_B t \quad \Rightarrow \quad t = \frac{A_b N}{2\pi R_B} = \frac{(0.969)(18)}{2\pi(17.60)} = 0.158\,\text{inches}$$

The moment of inertia of the bolt ring about point "o" is:

$$I_o = I_{cg} + Ad^2 = \pi R_B^3 t + A_b N R_L^2 = \pi(17.60)^3(0.158) + (0.969)(18)(18.80)^2 = 8{,}866\,\text{in}^4$$

The applied bending moment about point "o" due to the impact force, P_A, is $M_o = P_A R_L$. Thus, the maximum tensile stress in the bolt, f_a, is found as:

$$f_A = \frac{Mc}{I} = P_A\left(\frac{R_L(R_L + R_B)}{I_o}\right)$$

and,

$$F_A = P_A\left(\frac{R_L(R_L + R_B)}{I_o}\right)A_B = 18{,}258\,\text{lb}$$

<u>Note</u>: In this analysis, which sweeps from vertical, or end impacts through side impacts, there is a transition from one bolt tension relation to the other at some orientation angle. Both conservatively neglect restoring reaction forces from external energy absorbers. This neglect is extraordinarily conservative for near vertical impacts, but becomes more realistic as the package approaches side impact orientations. Specifically, the center of pressure of the external energy absorber reaction force upon the lid moves from the center of the lid towards the impacting corner of the package as the impact orientation moves from near-vertical to near-horizontal.

j) <u>Lateral (Shear) Bolt Load</u>, F_L:

$$F_L = \frac{P_L}{N} = \frac{n_g W_L(\cos\theta)}{N} = 144\,\text{lb}$$

where the impact acceleration, $n_g = 17.9g$, the lateral weight, W_L = 1,667 pounds, the impact angle, $\theta = 85°$, and the number of bolts, N = 18.

k) Total External Bolt Load, P:

$$P = F_P + F_A = 25{,}341\,\text{lb}$$

where the pressure load, F_P = 7,083 pounds, and the impact load, F_A = 18,258 pounds at an impact angle of 85º.

l) Net Bolt Tension, F_b: the net bolt tension, considering applied external loads and pretension loads.

$$F_b = P\left(\frac{K_b}{K_b + K_m}\right) + F_i \qquad F_m < 0$$

$$F_b = P \qquad F_m \geq 0$$

where the total external bolt load, P = 25,341 pounds at an impact angle of 85º, the bolt stiffness, $K_b = 1.44(10)^7$ lb/in, the lid stiffness, $K_m = 1.61(10)^8$ lb/in, the preload, F_i = 51,692 pounds, and the clamping force, F_m, is:

$$F_m = P\left(\frac{K_m}{K_b + K_m}\right) - F_i = -28{,}431\,\text{lb}$$

Since $F_m < 0$, the net bolt tension, F_b, is:

$$F_b = P\left(\frac{K_b}{K_b + K_m}\right) + F_i = 53{,}784\,\text{lb}$$

m) Bolt Tensile Stress, f_b:

$$f_b = \frac{F_b}{A_b} = 55{,}504\,\text{psi}$$

where the net bolt tension, F_b = 53,784 pounds, and the bolt area, $A_b = 0.969\ \text{in}^2$, is the lesser of the shank area ($1.23\ \text{in}^2$) and the tensile stress area ($0.969\ \text{in}^2$).

n) Nominal Bolt Shear Stress, f_v:

$$f_v = \frac{F_L}{A_b} = 149\,\text{psi}$$

where the lateral bolt load, F_L = 144 pounds, and the bolt area, $A_b = 0.969\ \text{in}^2$, is the lesser of the shank area ($1.23\ \text{in}^2$) and the tensile stress area ($0.969\ \text{in}^2$).

o) Principal Stresses, σ_1 and σ_2:

$$\sigma_{1,2} = \frac{f_b}{2} \pm \sqrt{\left(\frac{f_b}{2}\right)^2 + f_v^2} = 0,\ 55{,}505\,\text{psi (at } \theta = 85°)$$

where the bolt tensile stress, f_b = 55,504 psi, and the nominal bolt shear stress, f_v = 149 psi.

p) Stress Intensity, SI:

$$SI = |\sigma_1 - \sigma_2| = 55{,}505 \text{ psi (at } \theta = 85°)$$

where the principal stresses, σ_1 = 0 psi, and σ_2 = 55,5045 psi.

q) Margin of Safety, MS:

$$MS = \frac{S_a}{SI} - 1 = \frac{2.0S_m}{SI} - 1 = \frac{67{,}600}{55{,}505} - 1 = +0.22$$

This page intentionally left blank.

Table 2.10.6-1 – Outer Cask NCT Bolt Stresses, Torque Coefficient = 0.13

Parameter	Value	Parameter	Value	Parameter	Value
Nominal Thread Diameter (in)	1.25	Preload Torque (lb-ft)	700	Package Weight (lb)	45,000
Number of Bolts	18	Bolt Circle Diameter (in)	35.2	Longitudinal Weight (lb)	13,690
Allowable Stress, $2S_m$ (psi)	67,600	Lid Diameter (in)	37.6	Lateral Weight (lb)	1,667
Shank Area (in^2)	1.23	Impact Limiter Radius (in)	38.0	Torque Coefficient, K	0.13
Stress Area (in^2)	0.969	Package Radius (in)	20.8	Bolt Preload (lb)	51,692
Grip Length (in)	1.7	Bolt Circle Moment of Inertia (in^4)	8,866	Bolt Pressure Load (lb)	7,083
Maximum Pressure (psi)	150	Bolt Elastic Modulus (psi)	$2.73(10)^7$	Bolt Stiffness (lb/in)	14,442,581
Seal Diameter (in)	32.896	Lid Elastic Modulus (psi)	$2.78(10)^7$	Lid Stiffness (lb/in)	$1.61(10)^8$

Angle from Horizontal (degrees)	Impact Acceleration (*g*)	Bolt Force Distribution	Impact Forces		Bolt Tensions		Direct Stresses		Principal Stresses		Stress Intensity	MS
			Tension	Shear	Applied	Net	Tension	Shear	σ_1	σ_2		
90	42.5	Uniform	32,324	0	39,406	54,945	56,702	0	56,702	0	56,702	+0.19
85	17.9	Triangular	18,258	144	25,341	53,784	55,504	149	55,505	0	55,505	+0.22
80	13.2	Triangular	13,310	212	20,393	53,375	55,083	219	55,084	-1	55,085	+0.23
75	10.9	Triangular	10,780	261	17,863	53,167	54,868	270	54,869	-1	54,870	+0.23
70	9.3	Triangular	8,948	295	16,031	53,015	54,711	304	54,713	-2	54,715	+0.24
65	8.2	Triangular	7,609	321	14,692	52,905	54,597	331	54,599	-2	54,601	+0.24
60	6.5	Triangular	5,764	301	12,846	52,753	54,440	311	54,442	-2	54,444	+0.24
55	5.9	Triangular	4,948	313	12,031	52,685	54,371	323	54,373	-2	54,375	+0.24
50	5.3	Triangular	4,157	316	11,240	52,620	54,303	326	54,305	-2	54,307	+0.24
45	4.8	Triangular	3,475	314	10,558	52,564	54,245	324	54,247	-2	54,249	+0.25
40	4.4	Triangular	2,896	312	9,978	52,516	54,196	322	54,198	-2	54,200	+0.25
35	4.1	Triangular	2,408	311	9,490	52,476	54,154	321	54,156	-2	54,158	+0.25
30	3.8	Triangular	1,945	305	9,028	52,437	54,115	315	54,117	-2	54,119	+0.25
25	3.7	Triangular	1,601	311	8,684	52,409	54,086	320	54,088	-2	54,089	+0.25
20	3.8	Triangular	1,331	331	8,413	52,387	54,063	341	54,065	-2	54,067	+0.25
15	3.9	Triangular	1,034	349	8,116	52,362	54,037	360	54,040	-2	54,042	+0.25
10	4.2	Triangular	747	383	7,829	52,339	54,013	395	54,016	-3	54,019	+0.25
5	5.2	Triangular	464	480	7,547	52,315	53,989	495	53,993	-5	53,998	+0.25
0	19.3	Triangular	0	1,787	7,083	52,277	53,949	1,845	54,012	-63	54,075	+0.25

Table 2.10.6-2 – Outer Cask NCT Bolt Stresses, Torque Coefficient = 0.20

Parameter	Value	Parameter	Value	Parameter	Value
Nominal Thread Diameter (in)	1.25	Preload Torque (lb-ft)	700	Package Weight (lb)	45,000
Number of Bolts	18	Bolt Circle Diameter (in)	35.2	Longitudinal Weight (lb)	13,690
Allowable Stress, $2S_m$ (psi)	67,600	Lid Diameter (in)	37.6	Lateral Weight (lb)	1,667
Shank Area (in^2)	1.23	Impact Limiter Radius (in)	38.0	Torque Coefficient, K	0.20
Stress Area (in^2)	0.969	Package Radius (in)	20.8	Bolt Preload (lb)	33,600
Grip Length (in)	1.7	Bolt Circle Moment of Inertia (in^4)	8,866	Bolt Pressure Load (lb)	7,083
Maximum Pressure (psi)	150	Bolt Elastic Modulus (psi)	$2.73(10)^7$	Bolt Stiffness (lb/in)	14,442,581
Seal Diameter (in)	32.896	Lid Elastic Modulus (psi)	$2.78(10)^7$	Lid Stiffness (lb/in)	$1.61(10)^8$

Angle from Horizontal (degrees)	Impact Acceleration (*g*)	Bolt Force Distribution	Impact Forces		Bolt Tensions		Direct Stresses		Principal Stresses		Stress Intensity	MS
			Tension	Shear	Applied	Net	Tension	Shear	σ_1	σ_2		
90	42.5	Uniform	32,324	0	39,406	39,406	40,667	0	40,667	0	40,667	+0.66
85	17.9	Triangular	18,258	144	25,341	35,691	36,833	149	36,834	0	36,835	+0.84
80	13.2	Triangular	13,310	212	20,393	35,283	36,412	219	36,413	-1	36,415	+0.86
75	10.9	Triangular	10,780	261	17,863	35,074	36,196	270	36,198	-2	36,200	+0.87
70	9.3	Triangular	8,948	295	16,031	34,923	36,040	304	36,043	-3	36,045	+0.88
65	8.2	Triangular	7,609	321	14,692	34,813	35,926	331	35,929	-3	35,932	+0.88
60	6.5	Triangular	5,764	301	12,846	34,660	35,769	311	35,772	-3	35,775	+0.89
55	5.9	Triangular	4,948	313	12,031	34,593	35,700	323	35,703	-3	35,706	+0.89
50	5.3	Triangular	4,157	316	11,240	34,528	35,632	326	35,635	-3	35,638	+0.90
45	4.8	Triangular	3,475	314	10,558	34,471	35,574	324	35,577	-3	35,580	+0.90
40	4.4	Triangular	2,896	312	9,978	34,424	35,525	322	35,528	-3	35,531	+0.90
35	4.1	Triangular	2,408	311	9,490	34,383	35,483	321	35,486	-3	35,489	+0.90
30	3.8	Triangular	1,945	305	9,028	34,345	35,444	315	35,447	-3	35,449	+0.91
25	3.7	Triangular	1,601	311	8,684	34,317	35,415	320	35,417	-3	35,420	+0.91
20	3.8	Triangular	1,331	331	8,413	34,294	35,392	341	35,395	-3	35,398	+0.91
15	3.9	Triangular	1,034	349	8,116	34,270	35,366	360	35,370	-4	35,374	+0.91
10	4.2	Triangular	747	383	7,829	34,246	35,342	395	35,346	-4	35,351	+0.91
5	5.2	Triangular	464	480	7,547	34,223	35,318	495	35,325	-7	35,332	+0.91
0	19.3	Triangular	0	1,787	7,083	34,185	35,278	1,845	35,374	-96	35,471	+0.91

Table 2.10.6-3 – Inner Vessel NCT Bolt Stresses, Torque Coefficient = 0.13

Parameter	Value	Parameter	Value	Parameter	Value
Nominal Thread Diameter (in)	0.875	Preload Torque (lb-ft)	200	Package Weight (lb)	45,000
Number of Bolts	8	Bolt Circle Diameter (in)	30.0	Longitudinal Weight (lb)	0
Allowable Stress, $2S_m$ (psi)	67,600	Lid Diameter (in)	32.0	Lateral Weight (lb)	1,382
Shank Area (in^2)	0.407	Impact Limiter Radius (in)	38.0	Torque Coefficient, K	0.13
Stress Area (in^2)	0.407	Package Radius (in)	20.8	Bolt Preload (lb)	21,099
Grip Length (in)	2.75	Bolt Circle Moment of Inertia (in^4)	1,200	Bolt Pressure Load (lb)	11,545
Maximum Pressure (psi)	150	Bolt Elastic Modulus (psi)	$2.73(10)^7$	Bolt Stiffness (lb/in)	3,485,835
Seal Diameter (in)	28.0	Lid Elastic Modulus (psi)	$2.78(10)^7$	Lid Stiffness (lb/in)	$4.86(10)^7$

Angle from Horizontal (degrees)	Impact Acceleration (*g*)	Bolt Force Distribution	Impact Forces		Bolt Tensions		Direct Stresses		Principal Stresses		Stress Intensity	MS
			Tension	Shear	Applied	Net	Tension	Shear	σ_1	σ_2		
90	42.5	Uniform	0	0	11,545	21,871	53,737	0	53,737	0	53,737	+0.26
85	17.9	Uniform	0	270	11,545	21,871	53,737	662	53,746	-8	53,754	+0.26
80	13.2	Uniform	0	396	11,545	21,871	53,737	973	53,755	-18	53,773	+0.26
75	10.9	Uniform	0	487	11,545	21,871	53,737	1,197	53,764	-27	53,791	+0.26
70	9.3	Uniform	0	549	11,545	21,871	53,737	1,350	53,771	-34	53,805	+0.26
65	8.2	Uniform	0	599	11,545	21,871	53,737	1,471	53,778	-40	53,818	+0.26
60	6.5	Uniform	0	561	11,545	21,871	53,737	1,379	53,773	-35	53,808	+0.26
55	5.9	Uniform	0	585	11,545	21,871	53,737	1,436	53,776	-38	53,814	+0.26
50	5.3	Uniform	0	589	11,545	21,871	53,737	1,446	53,776	-39	53,815	+0.26
45	4.8	Uniform	0	586	11,545	21,871	53,737	1,441	53,776	-39	53,815	+0.26
40	4.4	Uniform	0	582	11,545	21,871	53,737	1,431	53,775	-38	53,814	+0.26
35	4.1	Uniform	0	580	11,545	21,871	53,737	1,426	53,775	-38	53,813	+0.26
30	3.8	Uniform	0	569	11,545	21,871	53,737	1,397	53,774	-36	53,810	+0.26
25	3.7	Uniform	0	579	11,545	21,871	53,737	1,423	53,775	-38	53,813	+0.26
20	3.8	Uniform	0	617	11,545	21,871	53,737	1,516	53,780	-43	53,823	+0.26
15	3.9	Uniform	0	651	11,545	21,871	53,737	1,599	53,785	-48	53,832	+0.26
10	4.2	Uniform	0	715	11,545	21,871	53,737	1,756	53,795	-57	53,852	+0.26
5	5.2	Uniform	0	895	11,545	21,871	53,737	2,199	53,827	-90	53,917	+0.25
0	19.3	Uniform	0	3,334	11,545	21,871	53,737	8,192	54,958	-1,221	56,179	+0.20

Table 2.10.6-4 – Inner Vessel NCT Bolt Stresses, Torque Coefficient = 0.20

Parameter	Value	Parameter	Value	Parameter	Value
Nominal Thread Diameter (in)	0.875	Preload Torque (lb-ft)	200	Package Weight (lb)	45,000
Number of Bolts	8	Bolt Circle Diameter (in)	30.0	Longitudinal Weight (lb)	0
Allowable Stress, $2S_m$ (psi)	67,600	Lid Diameter (in)	32.0	Lateral Weight (lb)	1,382
Shank Area (in^2)	0.407	Impact Limiter Radius (in)	38.0	Torque Coefficient, K	0.20
Stress Area (in^2)	0.407	Package Radius (in)	20.8	Bolt Preload (lb)	13,714
Grip Length (in)	2.75	Bolt Circle Moment of Inertia (in^4)	1,200	Bolt Pressure Load (lb)	11,545
Maximum Pressure (psi)	150	Bolt Elastic Modulus (psi)	$2.73(10)^7$	Bolt Stiffness (lb/in)	3,485,835
Seal Diameter (in)	28.0	Lid Elastic Modulus (psi)	$2.78(10)^7$	Lid Stiffness (lb/in)	$4.86(10)^7$

Angle from Horizontal (degrees)	Impact Acceleration (*g*)	Bolt Force Distribution	Impact Forces		Bolt Tensions		Direct Stresses		Principal Stresses		Stress Intensity	MS
			Tension	Shear	Applied	Net	Tension	Shear	σ_1	σ_2		
90	42.5	Uniform	0	0	11,545	14,487	35,593	0	35,593	0.00	35,593	+0.90
85	17.9	Uniform	0	270	11,545	14,487	35,593	662	35,606	-12	35,618	+0.90
80	13.2	Uniform	0	396	11,545	14,487	35,593	973	35,620	-27	35,647	+0.90
75	10.9	Uniform	0	487	11,545	14,487	35,593	1,197	35,634	-40	35,674	+0.89
70	9.3	Uniform	0	549	11,545	14,487	35,593	1,350	35,645	-51	35,696	+0.89
65	8.2	Uniform	0	599	11,545	14,487	35,593	1,471	35,654	-61	35,715	+0.89
60	6.5	Uniform	0	561	11,545	14,487	35,593	1,379	35,647	-53	35,700	+0.89
55	5.9	Uniform	0	585	11,545	14,487	35,593	1,436	35,651	-58	35,709	+0.89
50	5.3	Uniform	0	589	11,545	14,487	35,593	1,446	35,652	-59	35,711	+0.89
45	4.8	Uniform	0	586	11,545	14,487	35,593	1,441	35,652	-58	35,710	+0.89
40	4.4	Uniform	0	582	11,545	14,487	35,593	1,431	35,651	-57	35,708	+0.89
35	4.1	Uniform	0	580	11,545	14,487	35,593	1,426	35,650	-57	35,707	+0.89
30	3.8	Uniform	0	569	11,545	14,487	35,593	1,397	35,648	-55	35,703	+0.89
25	3.7	Uniform	0	579	11,545	14,487	35,593	1,423	35,650	-57	35,707	+0.89
20	3.8	Uniform	0	617	11,545	14,487	35,593	1,516	35,658	-64	35,722	+0.89
15	3.9	Uniform	0	651	11,545	14,487	35,593	1,599	35,665	-72	35,737	+0.89
10	4.2	Uniform	0	715	11,545	14,487	35,593	1,756	35,680	-86	35,766	+0.89
5	5.2	Uniform	0	895	11,545	14,487	35,593	2,199	35,729	-135	35,864	+0.88
0	19.3	Uniform	0	3,334	11,545	14,487	35,593	8,192	37,388	-1,795	39,183	+0.73

Table 2.10.6-5 – Outer Cask HAC Bolt Stresses, Torque Coefficient = 0.13

Parameter	Value	Parameter	Value	Parameter	Value
Nominal Thread Diameter (in)	1.25	Preload Torque (lb-ft)	700	Package Weight (lb)	45,000
Number of Bolts	18	Bolt Circle Diameter (in)	35.2	Longitudinal Weight (lb)	13,690
Allowable Stress, $3S_m$ (psi)	101,400	Lid Diameter (in)	37.6	Lateral Weight (lb)	1,667
Shank Area (in^2)	1.23	Impact Limiter Radius (in)	38.0	Torque Coefficient, K	0.13
Stress Area (in^2)	0.969	Package Radius (in)	20.8	Bolt Preload (lb)	51,692
Grip Length (in)	1.7	Bolt Circle Moment of Inertia (in^4)	8,866	Bolt Pressure Load (lb)	7,074
Maximum Pressure (psi)	150	Bolt Elastic Modulus (psi)	$2.73(10)^7$	Bolt Stiffness (lb/in)	14,442,581
Seal Diameter (in)	32.876	Lid Elastic Modulus (psi)	$2.78(10)^7$	Lid Stiffness (lb/in)	$1.61(10)^8$

Angle from Horizontal (degrees)	Impact Acceleration (*g*)	Bolt Force Distribution	Impact Forces		Bolt Tensions		Direct Stresses		Principal Stresses		Stress Intensity	MS
			Tension	Shear	Applied	Net	Tension	Shear	σ_1	σ_2		
90	89.7	Uniform	68,222	0	75,296	75,296	77,705	0	77,705	0	77,705	+0.30
85	90.7	Uniform	68,720	732	75,794	75,794	78,219	756	78,226	-7	78,233	+0.30
80	77.5	Uniform	58,048	1,246	65,122	65,122	67,205	1,286	67,230	-25	67,254	+0.51
75	66.7	Triangular	65,966	1,599	73,040	73,040	75,377	1,650	75,413	-36	75,449	+0.34
70	60.1	Triangular	57,825	1,904	64,899	64,899	66,975	1,965	67,033	-58	67,090	+0.51
65	56.2	Triangular	52,151	2,200	59,225	59,225	61,120	2,270	61,204	-84	61,288	+0.65
60	50.7	Triangular	44,956	2,348	52,030	55,987	57,778	2,423	57,879	-101	57,981	+0.75
55	46.3	Triangular	38,833	2,459	45,907	55,481	57,256	2,538	57,368	-112	57,481	+0.76
50	42.4	Triangular	33,256	2,524	40,330	55,021	56,781	2,605	56,900	-119	57,020	+0.78
45	38.6	Triangular	27,946	2,528	35,020	54,583	56,329	2,609	56,449	-121	56,570	+0.79
40	35.5	Triangular	23,364	2,519	30,438	54,205	55,939	2,599	56,059	-121	56,180	+0.80
35	32.9	Triangular	19,321	2,496	26,395	53,871	55,594	2,576	55,713	-119	55,832	+0.82
30	31.1	Triangular	15,921	2,494	22,996	53,590	55,305	2,574	55,424	-120	55,544	+0.83
25	30.3	Triangular	13,111	2,543	20,185	53,358	55,065	2,625	55,190	-125	55,315	+0.83
20	30.5	Triangular	10,681	2,654	17,755	53,158	54,858	2,739	54,995	-136	55,131	+0.84
15	32.3	Triangular	8,560	2,889	15,634	52,983	4,678	2,982	54,840	-162	55,002	+0.84
10	33.1	Triangular	5,885	3,019	12,959	52,762	54,450	3,115	54,628	-178	54,805	+0.85
5	48.1	Triangular	4,292	4,438	11,366	52,630	54,314	4,580	54,698	-383	55,081	+0.84
0	81.2	Triangular	0	7,520	7,074	52,276	53,949	7,761	55,043	-1,094	56,137	+0.81

Table 2.10.6-6 – Outer Cask HAC Bolt Stresses, Torque Coefficient = 0.20

Parameter	Value	Parameter	Value	Parameter	Value
Nominal Thread Diameter (in)	1.25	Preload Torque (lb-ft)	700	Package Weight (lb)	45,000
Number of Bolts	18	Bolt Circle Diameter (in)	35.2	Longitudinal Weight (lb)	13,690
Allowable Stress, $3S_m$ (psi)	101,400	Lid Diameter (in)	37.6	Lateral Weight (lb)	1,667
Shank Area (in^2)	1.23	Impact Limiter Radius (in)	38.0	Torque Coefficient, K	0.20
Stress Area (in^2)	0.969	Package Radius (in)	20.8	Bolt Preload (lb)	33,600
Grip Length (in)	1.7	Bolt Circle Moment of Inertia (in^4)	8,866	Bolt Pressure Load (lb)	7,074
Maximum Pressure (psi)	150	Bolt Elastic Modulus (psi)	$2.73(10)^7$	Bolt Stiffness (lb/in)	14,442,581
Seal Diameter (in)	32.876	Lid Elastic Modulus (psi)	$2.78(10)^7$	Lid Stiffness (lb/in)	$1.61(10)^8$

Angle from Horizontal (degrees)	Impact Acceleration (*g*)	Bolt Force Distribution	Impact Forces		Bolt Tensions		Direct Stresses		Principal Stresses		Stress Intensity	MS
			Tension	Shear	Applied	Net	Tension	Shear	σ_1	σ_2		
90	89.7	Uniform	68,222	0	75,296	75,296	77,705	0	77,705	0	77,705	+0.30
85	90.7	Uniform	68,720	732	75,794	75,794	78,219	756	78,226	-7	78,233	+0.30
80	77.5	Uniform	58,048	1,246	65,122	65,122	67,205	1,286	67,230	-25	67,254	+0.51
75	66.7	Triangular	65,966	1,599	73,040	73,040	75,377	1,650	75,413	-36.10	75,449	+0.34
70	60.1	Triangular	57,825	1,904	64,899	64,899	66,975	1,965	67,033	-58	67,090	+0.51
65	56.2	Triangular	52,151	2,200	59,225	59,225	61,120	2,270	61,204	-84	61,288	+0.65
60	50.7	Triangular	44,956	2,348	52,030	52,030	53,695	2,423	53,804	-109	53,913	+0.88
55	46.3	Triangular	38,833	2,459	45,907	45,907	47,375	2,538	47,511	-136	47,647	+1.13
50	42.4	Triangular	33,256	2,524	40,330	40,330	41,620	2,605	41,783	-162	41,945	+1.42
45	38.6	Triangular	27,946	2,528	35,020	36,490	37,658	2,609	37,838	-180	38,017	+1.67
40	35.5	Triangular	23,364	2,519	30,438	36,112	37,268	2,599	37,448	-180	37,628	+1.69
35	32.9	Triangular	19,321	2,496	26,395	35,779	36,923	2,576	37,102	-179	37,281	+1.72
30	31.1	Triangular	15,921	2,494	22,996	35,498	36,634	2,574	36,814	-180	36,994	+1.74
25	30.3	Triangular	13,111	2,543	20,185	35,266	36,394	2,625	36,583	-188	36,771	+1.76
20	30.5	Triangular	10,681	2,654	17,755	35,065	36,187	2,739	36,393	-206	36,600	+1.77
15	32.3	Triangular	8,560	2,889	15,634	34,890	36,007	2,982	36,252	-245	36,497	+1.78
10	33.1	Triangular	5,885	3,019	12,959	34,670	35,779	3,115	36,048	-269	36,317	+1.79
5	48.1	Triangular	4,292	4,438	11,366	34,538	35,643	4,580	36,222	-579	36,801	+1.76
0	81.2	Triangular	0	7,520	7,074	34,184	35,277	7,761	36,909	-1,632	38,541	+1.63

Table 2.10.6-7 – Inner Vessel HAC Bolt Stresses, Torque Coefficient = 0.13

Parameter	Value	Parameter	Value	Parameter	Value
Nominal Thread Diameter (in)	0.875	Preload Torque (lb-ft)	200	Package Weight (lb)	45,000
Number of Bolts	8	Bolt Circle Diameter (in)	30.0	Longitudinal Weight (lb)	0
Allowable Stress, $3S_m$ (psi)	101,400	Lid Diameter (in)	32.0	Lateral Weight (lb)	1,382
Shank Area (in^2)	0.407	Impact Limiter Radius (in)	38.0	Torque Coefficient, K	0.13
Stress Area (in^2)	0.407	Package Radius (in)	20.8	Bolt Preload (lb)	21,099
Grip Length (in)	2.75	Bolt Circle Moment of Inertia (in^4)	1,200	Bolt Pressure Load (lb)	11,545
Maximum Pressure (psi)	150	Bolt Elastic Modulus (psi)	$2.73(10)^7$	Bolt Stiffness (lb/in)	3,485,835
Seal Diameter (in)	28.0	Lid Elastic Modulus (psi)	$2.78(10)^7$	Lid Stiffness (lb/in)	$4.86(10)^7$

Angle from Horizontal (degrees)	Impact Acceleration (*g*)	Bolt Force Distribution	Impact Forces		Bolt Tensions		Direct Stresses		Principal Stresses		Stress Intensity	MS
			Tension	Shear	Applied	Net	Tension	Shear	σ_1	σ_2		
90	89.7	Uniform	0	0	11,545	21,871	53,737	0	53,737	0	53,737	+0.89
85	90.7	Uniform	0	1,366	11,545	21,871	53,737	3,355	53,946	-209	54,155	+0.87
80	77.5	Uniform	0	2,325	11,545	21,871	53,737	5,712	54,338	-600	54,938	+0.85
75	66.7	Triangular	0	2,982	11,545	21,871	53,737	7,327	54,719	-981	55,700	+0.82
70	60.1	Triangular	0	3,551	11,545	21,871	53,737	8,725	55,118	-1,381	56,499	+0.79
65	56.2	Triangular	0	4,103	11,545	21,871	53,737	10,081	55,566	-1,829	57,395	+0.77
60	50.7	Triangular	0	4,379	11,545	21,871	53,737	10,760	55,812	-2,074	57,886	+0.75
55	46.3	Triangular	0	4,588	11,545	21,871	53,737	11,272	56,006	-2,269	58,275	+0.74
50	42.4	Triangular	0	4,708	11,545	21,871	53,737	11,568	56,122	-2,384	58,506	+0.73
45	38.6	Triangular	0	4,715	11,545	21,871	53,737	11,585	56,129	-2,391	58,520	+0.73
40	35.5	Triangular	0	4,698	11,545	21,871	53,737	11,543	56,112	-2,374	58,486	+0.73
35	32.9	Triangular	0	4,656	11,545	21,871	53,737	11,439	56,071	-2,334	58,405	+0.74
30	31.1	Triangular	0	4,653	11,545	21,871	53,737	11,432	56,068	-2,331	58,399	+0.74
25	30.3	Triangular	0	4,744	11,545	21,871	53,737	11,656	56,157	-2,419	58,576	+0.73
20	30.5	Triangular	0	4,951	11,545	21,871	53,737	12,165	56,363	-2,626	58,989	+0.72
15	32.3	Triangular	0	5,390	11,545	21,871	53,737	13,242	56,824	-3,086	59,910	+0.69
10	33.1	Triangular	0	5,631	11,545	21,871	53,737	13,836	57,090	-3,353	60,444	+0.68
5	48.1	Triangular	0	8,278	11,545	21,871	53,737	20,338	60,567	-6,830	67,396	+0.50
0	81.2	Triangular	0	14,027	11,545	21,871	53,737	34,465	70,570	-16,832	87,402	+0.16

Table 2.10.6-8 – Inner Vessel HAC Bolt Stresses, Torque Coefficient = 0.20

Parameter	Value	Parameter	Value	Parameter	Value
Nominal Thread Diameter (in)	0.875	Preload Torque (lb-ft)	200	Package Weight (lb)	45,000
Number of Bolts	8	Bolt Circle Diameter (in)	30.0	Longitudinal Weight (lb)	0
Allowable Stress, $3S_m$ (psi)	101,400	Lid Diameter (in)	32.0	Lateral Weight (lb)	1,382
Shank Area (in^2)	0.407	Impact Limiter Radius (in)	38.0	Torque Coefficient, K	0.20
Stress Area (in^2)	0.407	Package Radius (in)	20.8	Bolt Preload (lb)	13,714
Grip Length (in)	2.75	Bolt Circle Moment of Inertia (in^4)	1,200	Bolt Pressure Load (lb)	11,545
Maximum Pressure (psi)	150	Bolt Elastic Modulus (psi)	$2.73(10)^7$	Bolt Stiffness (lb/in)	3,485,835
Seal Diameter (in)	28.0	Lid Elastic Modulus (psi)	$2.78(10)^7$	Lid Stiffness (lb/in)	$4.86(10)^7$

Angle from Horizontal (degrees)	Impact Acceleration (*g*)	Bolt Force Distribution	Impact Forces		Bolt Tensions		Direct Stresses		Principal Stresses		Stress Intensity	MS
			Tension	Shear	Applied	Net	Tension	Shear	σ_1	σ_2		
90	89.7	Uniform	0	0	11,545	14,487	35,593	0	35,593	0	35,593	+1.85
85	90.7	Uniform	0	1,366	11,545	14,487	35,593	3,355	35,907	-314	36,220	+1.80
80	77.5	Uniform	0	2,325	11,545	14,487	35,593	5,712	36,488	-894	37,382	+1.71
75	66.7	Triangular	0	2,982	11,545	14,487	35,593	7,327	37,043	-1,449	38,492	+1.63
70	60.1	Triangular	0	3,551	11,545	14,487	35,593	8,725	37,617	-2,024	39,640	+1.56
65	56.2	Triangular	0	4,103	11,545	14,487	35,593	10,081	38,250	-2,657	40,907	+1.48
60	50.7	Triangular	0	4,379	11,545	14,487	35,593	10,760	38,593	-3,000	41,593	+1.44
55	46.3	Triangular	0	4,588	11,545	14,487	35,593	11,272	38,863	-3,269	42,132	+1.41
50	42.4	Triangular	0	4,708	11,545	14,487	35,593	11,568	39,023	-3,429	42,452	+1.39
45	38.6	Triangular	0	4,715	11,545	14,487	35,593	11,585	39,032	-3,439	42,470	+1.39
40	35.5	Triangular	0	4,698	11,545	14,487	35,593	11,543	39,009	-3,415	42,424	+1.39
35	32.9	Triangular	0	4,656	11,545	14,487	35,593	11,439	38,953	-3,359	42,312	+1.40
30	31.1	Triangular	0	4,653	11,545	14,487	35,593	11,432	38,949	-3,355	42,304	+1.40
25	30.3	Triangular	0	4,744	11,545	14,487	35,593	11,656	39,071	-3,477	42,548	+1.38
20	30.5	Triangular	0	4,951	11,545	14,487	35,593	12,165	39,354	-3,760	43,114	+1.35
15	32.3	Triangular	0	5,390	11,545	14,487	35,593	13,242	39,980	-4,386	44,366	+1.29
10	33.1	Triangular	0	5,631	11,545	14,487	35,593	13,836	40,339	-4,746	45,084	+1.25
5	48.1	Triangular	0	8,278	11,545	14,487	35,593	20,338	44,822	-9,229	54,051	+0.88
0	81.2	Triangular	0	14,027	11,545	14,487	35,593	34,465	56,585	-20,992	77,577	+0.31

2.10.7 Static and Dynamic Testing

This section describes the testing performed on the RH-TRU 72-B impact limiters. Testing was performed to verify that the impact analyses documented in Appendix 2.10.3, *Drop Impact Evaluation Results*, properly predict the performance of the impact limiters during normal conditions of transport (NCT) and hypothetical accident conditions (HAC). The test program included both static and dynamic tests on half-scale, prototypic test specimens. Static testing is documented in Appendix 2.10.7.1, *Static Test Program*, and dynamic testing in Appendix 2.10.7.2, *Dynamic Test Program*.

2.10.7.1 Static Test Program

Static testing was performed by crushing half-scale impact limiter test articles at a fixed orientation in a laboratory test machine. Two prototypic test articles were tested in a total of three crush orientations. Test results were in the form of static force-deflection curves for crush at the tested orientation.

The purpose of static testing was to confirm that the analytical tools used to calculate impact limiter performance possess adequate accuracy. To the degree that test results and analysis predictions differed, a correction factor was formed, which was used to adjust analytical results. The correction factor formed on the basis of static testing was combined with a similar factor formed on the basis of dynamic testing, as discussed in Appendix 2.10.7.2, *Dynamic Test Program*. Impact magnitudes are calculated in Appendix 2.10.3, *Drop Impact Evaluation Results*.

An additional purpose of testing was to confirm the acceptable behavior of the impact limiters, including the ability to adequately predict such behavior, at relatively high foam strains, i.e., between 80% – 90%. Testing was performed at the University of Washington Structures Research Laboratory in Seattle, Washington, on January 6th, 1999.

2.10.7.1.1 Test Article Configuration

The test was conducted using half-scale, prototypic test articles, including attachment bolts. Therefore, all test article dimensions were half of those given in Appendix 1.3.1, *Packaging General Arrangement Drawings*. Drawings of the test articles are provided in Appendix 2.10.7.4, *Drawings*. Only two differences existed between the test articles and the full-scale prototypic impact limiters:

1. The bolt access hole debris ring was not used in testing. This component is an annular disk made of 11-gage sheet metal, held to the limiter using quarter-turn screws, and that is used to cover the impact limiter attachment bolt holes. The omission of this component had no effect on the crush strength of the impact limiters.
2. The polyurethane foam used in the test articles was nominally 12.5 lb/ft^3 density, whereas the density of the foam used in the full-scale production limiters is 11.5 lb/ft^3. This small difference came about as a consequence of the test program. As described in this appendix, the impact limiters exhibited a greater strength than expected, necessitating a small reduction in the full-scale production foam nominal density to 11.5 lb/ft^3. The test program was not repeated with the lighter foam since the difference in foam strength is modest. Furthermore,

it is of secondary importance, since the results of testing are not utilized directly, but rather as an adjustment factor that can be applied to foam strengths which are not necessarily identical to the one actually tested[1].

The test articles were designated No. 1 and No. 2.

2.10.7.1.2 Test Facilities

Testing was performed using a Baldwin test machine capable of 2.4 million pounds of crush force, and was calibrated for the purposes of this test to a load of 1.2 million pounds. The test fixture, with the test article mounted in the desired orientation, was placed within the test machine. The test fixture rested on the lower platen of the machine at floor level, and the upper platen was used to load the test article. The actual configuration of test article, test fixture, and test machine platens depended on the test orientation, and is discussed in further detail below. The test machine operated at a crush deflection rate of approximately one inch per minute.

The test articles were mounted to a massive steel test fixture which was capable of reconfiguration into each of the required orientations. The fixture was designed to have negligible deflection under test loads. The mandrel of the fixture (the component of the fixture which simulated the package and which interfaced with the test article) had a diameter of 20.8 inches, which was half of the full-scale package diameter of 41⅝ inches. This difference is negligible and had no effect on testing. The mandrel was fully engaged with the test articles, and provided for prototypic attachment of the test articles.

The crush deflection was measured using linear variable-differential transformer (LVDT) measuring devices. The instantaneous deflection values from the LVDTs, along with force values from the test machine, were sampled by a PC-based data acquisition system and recorded as force-deflection pairs.

2.10.7.1.3 Technical Basis for Tests

The orientations chosen for static testing were taken from the overall governing analysis cases. As shown in Table 2.10.3-11 in Appendix 2.10.3, *Drop Impact Evaluation Results*, the governing orientations for maximum impact are the end (85º to 90º from horizontal) and side (0º from horizontal). As shown in

Figure 2.10.3-7 (oblique impact deflection) in Appendix 2.10.3, *Drop Impact Evaluation Results*, and Table 2.10.3-12 (hot side drop results) in Appendix 2.10.3, *Drop Impact Evaluation Results*, the governing cases for maximum deflection are the 55º from the horizontal orientation and the side orientation[2]. Combining all of these orientations, static tests of end, side, and 55º from the horizontal were performed. Due to the interest in maximum deflection cases, each test was carried out to the maximum practicable deflection. To prevent excessive accumulation of damage on a single test article, two test articles were used. Test article No. 1 was tested in the end orientation and test article No. 2 was tested in the side and oblique (55º) orientations. In the

[1] Note that nominal density is utilized as a convenient means of designating a particular foam's general strength level; however, actual foam behavior is ultimately determined only by its individual stress-strain characteristics.

[2] Maximum impacts assume upper-bound foam properties and maximum deflections assume lower-bound foam properties.

latter case, the damage was separated by 180º of azimuth. The tests and orientations are summarized in Table 2.10.7-1.

2.10.7.1.4 Test Description and Results

Details pertaining to each test orientation and test results are discussed below. After testing was completed, the test data was plotted against the corresponding analysis-generated prediction. It was found that, for all three tests, an increase factor on foam crush stress of 1.19 was needed to bring the test results and predictions into good agreement. The "static factor" of 1.19 was applied universally as a multiplying factor to all polyurethane foam crush stress values, and the same factor was found to apply to each of the three tests. As discussed below, the application of the static factor led to extremely good agreement between test results and test predictions. Due to the good agreement and universal applicability of the static factor, it is used consistently in all of the impact analyses performed in Appendix 2.10.3, *Drop Impact Evaluation Results*[3].

Analytical predictions were prepared using the computer program CASKDROP, documented in Appendix 2.10.2.1.1, *Using CASKDROP to Determine Impact Limiter Deformation Behavior*. The basic polyurethane foam stress-strain data was taken from the foam pour records of the test articles. For the end orientation, the prediction was prepared using the parallel-to-rise[4] data from test article No. 1, pour 1, since only pour 1 foam was crushed in the test. For the side orientation, the perpendicular-to-rise data for pour 2 in test article No. 2 was used. Use of data from a single pour was sufficient since the stress-strain difference between the pours was negligible. For the oblique orientation, a combination of parallel-to-rise and perpendicular-to-rise data for pour 2 was used. The data was combined using interpolation, as described in Appendix 2.10.2.1.1, *Using CASKDROP to Determine Impact Limiter Deformation Behavior*. This stress-strain data, taken from test article acceptance test records, is given in Table 2.10.7-2. The stress-strain properties used in the analytical predictions (as adjusted for temperature) are shown in Table 2.10.7-3, Table 2.10.7-4, and Table 2.10.7-5.

The ambient temperature and the temperature of the foam within the test articles during all of the testing was approximately 65 ºF to 70 ºF.

2.10.7.1.4.1 End Orientation

Figure 2.10.7-1 shows the configuration of the end orientation static test. As shown, the only part of the test fixture needed for the test was the mandrel portion; the main framework of the fixture was not used. The mandrel was placed, axis vertical, in the test machine, and test article No. 1 was placed on top of it, with the flat, outer end of the article facing upward toward the upper platen. To avoid contact between the deformed impact limiter and the flange of the mandrel, solid steel spacers (equaling a thickness of three inches) were placed on top of the mandrel before installing the test article as shown. Furthermore, since in the end orientation there is no loading applied to the attachment bolts (since the load is applied parallel to the mandrel axis), the test article was not bolted to the mandrel. Non-prototypic bolts were used to

[3] Note that a "dynamic factor" is also used, based on the results of dynamic testing. The total combined static and dynamic factor, used to increase the foam crush stress for all orientations, is 1.52. Details of the dynamic test results, and a further discussion of these correction factors, are given in Section 2.10.7.3, *Correction Factors*.

[4] Rise direction is defined to be the vertical direction during foam pour, i.e., the axial direction for all test articles.

attach the test article only to the steel spacer plates. These differences in attachment had no effect on the test. The mounted test article was placed in the approximate center of the test machine. A steel plate of 3/8-inch thickness was used to cover the upper platen. The LVDT measured the change in distance between the upper and lower platens of the test machine.

The post-test configuration of the test article is shown in a side view in Figure 2.10.7-2. As shown, the deformation exhibited by the impact limiter was completely of an inside-out nature. That is, the mandrel pushed into the impact limiter from the inside, rather than the flat bottom of the limiter crushing down from the outside. This mode of deformation means that the inner shell of the limiter moved axially relative to the outer shell, drawing the end annular shell down into the impact limiter opening as shown in Figure 2.10.7-3. As the end annular shell was drawn into the opening, it developed the radial wrinkles shown in the figure. Eventually, at a crush deflection of approximately 5.9 inches (52.4% foam crush), the seam between the end annular shell and the inner cylindrical shell of the test article separated adjacent to the weld, extending over an arc of approximately 200º around the circumference of the seam as shown in Figure 2.10.7-3. The crush test was continued to a total of 7.25 inches (65% foam strain), but due to a higher than expected crush strength, the force measuring equipment saturated at a crush of approximately 6.6 inches (59% foam strain). Note that the maximum predicted foam strain in the end drop for lower bound foam properties is 38.5%, which is less than the point at which the seam separated (see Table 2.10.3-7 in Appendix 2.10.3, *Drop Impact Evaluation Results*). The vertical height of the test article and fixture before testing was 35.5 inches, and after load removal after the test was 29 inches, for a difference of 6.5 inches.

As shown by Figure 2.10.7-2, the end annular shell of the test article came in contact with the ribs of the mandrel flange. However, as seen in Figure 2.10.7-3, the impression of the ribs is slight (less than 1/4-inch), demonstrating that this occurred late in the test, in fact, after the force measuring instrumentation had saturated. Therefore, the interference with the ribs had no effect on the data collected.

One feature of an inside-out crush deformation is that the foam undergoes two kinds of deformation: 1) ordinary compressive crush within the diameter of the inner shell of the limiter, and 2) shear cutting around the circumference of the inner shell. Only the former type of deformation is accounted for directly in the analysis software used. To account for the shear force developed, an equivalent increase in the diameter of the inner shell is assumed. Therefore, for purposes of analysis, the inner shell is assumed to have a diameter essentially equal to the outer diameter of the impact limiter, or for the case of the half-scale test article, a diameter of 37.9 inches (the outer diameter of the limiter is 38 inches). This assumption is designated the "end fully effective" case, and accounts for all of the energy absorption actually occurring in the impact limiter. When combined with the 19% increase in foam strength (the static factor of 1.19), the analysis prediction is in good agreement with test results, as shown in Figure 2.10.7-4. The CASKDROP end crush prediction results are given in Table 2.10.7-3.

2.10.7.1.4.2 Side Orientation

Figure 2.10.7-5 shows the configuration of the side orientation static test. Test article No. 2 was placed, axis horizontal, on the mandrel and attached with six, prototypic attachment bolts tightened to the appropriate half-scale torque value of 80±5 lb-ft. As shown, an upper platen load fixture was used due to the design of the test fixture. The upper platen load fixture was

rigid and completely covered the crush plane of the test article. The LVDT measured the change in distance between the upper platen and the top of the main test fixture.

The post-test configuration is shown in an end view in Figure 2.10.7-6. In this case, the deformation was largely of the outside-in variety. Some shearing of the foam did occur, but not as much as in the end orientation. In this case, the end thickness of the limiter (the portion which extends beyond, and is unsupported by, the mandrel) did not crush as much as did the annular portion (surrounding the mandrel). Instead, this portion underwent both partial crush and partial shear, with the shear plane being the plane of the bottom of the inner shell. Other than the expected deformations, there was no damage to the shells or welds, except that the welds which connected the bottom shell to the two bolt access tubes nearest the crush zone separated. The amount of exposed foam was negligible. The crush was carried out for a total crush distance of approximately 7.1 inches (84% foam strain). Upon unloading, the force-deflection curve did not reach zero force until the displacement had returned to approximately 6 inches.

As in the case of the end orientation, the crush force prediction must account for both the crush and the shearing action of the foam. For the side orientation, a fictitious increase in the inner shell is again considered, but in this case the length, rather than the diameter, is increased. The end distance of the half-scale test article, i.e., the thickness of foam beyond the end of the inner shell, is 11.25 inches. For the purposes of analysis, however, the inner shell is assumed to lengthen through half of this distance, so that the end distance is 11.25/2 = 5.625 inches. This assumption is designated the "side fully effective" case, and analytically accounts for all of the energy absorption actually occurring in the impact limiter. When combined with the 19% increase in foam strength (the static factor of 1.19), the analysis prediction is in good agreement with test results, as shown in Figure 2.10.7-7. The CASKDROP side crush prediction results are given in Table 2.10.7-4.

Examination of Figure 2.10.7-7 shows that above a crush of approximately 6 inches in the half-scale (70% foam strain), the analysis force-deflection curve diverges significantly from the test data curve. This difference is conservative, however, since it leads to an overprediction of crush force (i.e., impact) levels while at the same time conservatively overpredicting deflection. This is possible since the analytical prediction curve represents a lower rate of energy absorption than the test data curve. In fact, the energy beneath the curves becomes equivalent only at the end of the test, at a crush of 7 inches (82% foam strain). At that point, the test data curve represents $2.29(10)^6$ in-lb of energy, and the analytical prediction curve $2.24(10)^6$ in-lb. At any lesser crush, the analysis (since it underestimates absorbed energy) will overpredict deflection. Whether the crush force is overpredicted depends on the deflection distance. Below the curve crossover point at 5.5 inches (65% foam strain), the greater predicted deflection will lead to crush force levels approximately on par with the test data. Above the crossover point, the crush force levels will be conservatively overpredicted.

2.10.7.1.4.3 Oblique Orientation

Figure 2.10.7-8 shows the configuration of the oblique orientation static test. The same test article used in the side orientation, No. 2, was used for this test also. Since several of the attachment bolthole access tubes were deformed in the side orientation crush, making access to the attachment bolts impossible, the bolts were left undisturbed and the limiter was re-oriented by rotating the mandrel on the fixture through 180º. In this way, the crush began on the outer corner of the test article farthest away from the side orientation test damage. With a

reconfiguration of the main test fixture, the axis of the test article was oriented at an angle of 55º from the plane of the upper platen[5]. For this test, the upper platen load fixture was removed and the 3/8 inch thick plate reinstalled. Since the total deflection in this test exceeded the stroke of a single LVDT, two were arranged in parallel, with an adequate offset. The second LVDT was set to begin readings before the first one reached the end of its stroke. In this way, the entire range of test travel was accommodated. The LVDTs measured the change in distance between the upper platen and the top of the main test fixture.

The post-test configuration is shown in Figure 2.10.7-9 and Figure 2.10.7-10. (Figure 2.10.7-9 shows the relative juxtaposition of the side and oblique crush damage zones.) In this orientation, essentially all the crush was of the outside-in variety. As seen in the post-test figures, the crush damage caused the welds between the bottom shell and the bolt access tubes to separate, but exposure of foam was negligible. The crush was continued for a total distance of 13.8 inches (97% foam strain). Upon unloading, the force-deflection curve did not reach zero force until the displacement had returned to approximately 12 inches.

Unlike the other two orientations, no alteration to the inner shell dimensions is necessary for the oblique case. Using the 19% increase in foam strength (static factor of 1.19), the analysis prediction is in good agreement with test results, as shown in Figure 2.10.7-11. The CASKDROP oblique crush prediction results are given in Table 2.10.7-5.

2.10.7.1.4.4 Summary

The RH-TRU 72-B package impact limiters were statically crush tested in half-scale, and force-deflection curves were developed. Two test articles were tested in end, side, and 55º from horizontal oblique orientations to deflections that were larger than the maximum deflections predicted for the worst case HAC drop events. Analytical tools were used to predict the test results, and with the utilization of a correction factor of 1.19 on the basic input foam crush stress levels, the agreement between test and predictions is good.

2.10.7.2 Dynamic Test Program

Dynamic testing was performed by dropping half-scale impact limiter test articles from a height of 30 feet onto a flat, horizontal, essentially unyielding surface, in accordance with 10 CFR 71.73(c)(1)[6]. Two test articles were used together with a test package, and were dropped in a total of three orientations, which corresponded to the orientations used in static testing. The test package possessed prototypic weight and impact limiter attachment features. Test results took the form of measured impact deformations. The purpose of dynamic testing was to confirm that the analytical tools used to calculate impact limiter performance possess adequate accuracy. To the degree that test results and analysis predictions differed, a correction factor was formed, which was used to adjust analytical results. The correction factor formed on the basis of dynamic testing was inclusive of the factor formed on the basis of static testing as discussed in

[5] The test fixture and inner shell were oriented at 55º from horizontal; due to prior damage in the side test, the outer shell was oriented at approximately 60º from horizontal.

[6] Title 10, Code of Federal Regulations, Part 71 (10 CFR 71), *Packaging and Transportation of Radioactive Material*, Final Rule, 01-26-04.

Section 2.10.7.1, *Static Test Program*. Impact magnitudes are calculated in Appendix 2.10.3, *Drop Impact Evaluation Results*.

An additional purpose of testing was to confirm the dynamic integrity of the impact limiter in an impact event, and to demonstrate that impact limiter attachments are adequate to prevent loss of a limiter due to impact. Testing was performed in Richland, Washington, on January 18 and February 4, 1999.

2.10.7.2.1 Test Article Configuration

A description of the test articles is given in Section 2.10.7.1.1, *Test Article Configuration*. Dynamic testing was performed using test articles designated No. 3 and No. 4. These articles had the same construction and polyurethane foam specification as did the test articles used in static testing (No. 1 and No. 2). The bolt access hole debris ring was not used in dynamic testing. This omission had no effect on test results. Drawings of the test articles are provided in Appendix 2.10.7.4, *Drawings*.

2.10.7.2.2 Test Facilities

Free drop testing was performed using the drop pad located in the 300 Area of the Department of Energy Hanford Site in Richland, Washington. The pad is made of highly reinforced concrete and covered with an 8½-inch thick steel plate. The pad weighs an estimated 110 tons, which is more than 38 times the weight of the test package, and easily qualifies as an essentially unyielding surface.

The free drop height was 30 feet, +3/-0 inches, measured from the point of the impact limiter nearest the ground. The orientation of the test package for all drops was verified using an inclinometer. When necessary due to wind conditions, guy ropes were used to control the position of the package prior to release to ensure that the package struck within the boundaries of the pad's steel top plate. However, inclination to the horizontal was not affected by wind. The drop from the specified height was completely free.

The test package was made from a thick walled, mild steel pipe with thick end plates, as shown on the drawings included in Appendix 2.10.7.4, *Drawings*. To attain the necessary weight, solid steel bars were securely welded to the inside of the pipe. One additional bar was located in the center of the pipe, and securely welded to one end plate. The space between the steel bars was packed with sand. The test package was 20.8 inches in diameter, which was half of the full-scale package diameter of 41⅝ inches. This difference is negligible and had no effect on testing. The length of the package was 70.9 inches. The impact limiter test articles were attached to the package using prototypic attachment bolts tightened to 80±5 lb-ft. If impact distortion did not render the bolt heads inaccessible, this torque was restored between separate drop tests. For the end drop, only a lower impact limiter test article was needed, and therefore a test plate, which simulated the weight of an impact limiter, was attached to the upper end of the test package in place of an impact limiter. The total weight of the test package in the end drop case was 5,736 pounds. In the side and oblique drop cases, both impact limiter test articles were in place, and the weight of the test package in these drop cases was 5,781 pounds. These weights are within 3% of the half-scale maximum package weight of 45,000 × 1/8 = 5,625 pounds, where 45,000 pounds is the full-scale weight from Section 2.2, *Weights and Centers of Gravity*, and the 1/8 factor is the scale factor on weight, equal to $(1/2)^3$.

A complete record of all drop test activities was made using still and conventional speed video photography.

2.10.7.2.3 Technical Basis for Tests

The orientations chosen for dynamic testing were based on the orientations used in static testing. As discussed in Section 2.10.7.1.3, *Technical Basis for Tests*, these orientations are chosen based on the overall governing analysis cases. The dynamic tests further confirm the adequacy of the analytical methods to properly predict maximum impacts and deformations presented in Appendix 2.10.3, *Drop Impact Evaluation Results*. Another reason for including the end drop among the free drops performed is because the end drop orientation represents the largest[7] impact level, and thus caused the greatest amount of damage to the impact limiter. To prevent excessive accumulation of damage on a single test article, two test articles were used. Test article No. 3 was tested in the end drop and test article No. 4 was tested in the side and oblique (55º) drops. (Test article No. 3 was also present as a prop for the side and oblique drops). As for the static testing, the side and the oblique impact damage zones were separated by 180º of azimuth. The tests and orientations are summarized in Table 2.10.7-6.

2.10.7.2.4 Test Description and Results

Details pertaining to each test orientation and test results are discussed below. Aside from ordinary physical examination, noting types and degree of impact damage, the principal form of free drop test result was the measurement of impact deflection. Due to the presence of significant elastic recovery of the polyurethane foam, crush gages were used in the end and side drop cases to accurately record the maximum crush deflection of the test articles, as described in more detail below. (Measurement of the oblique impact deflection was made using physical measurements of the test article). The measured maximum deflection was used to formulate a correction factor for use with the analytical prediction method ("dynamic factor"). Discussion of the dynamic factor, and its relationship to the static factor, is given in Appendix 2.10.7.3, *Correction Factors*.

Analytical predictions of maximum deflection were prepared using the code CASKDROP, documented in Appendix 2.10.2.1.1, *Using CASKDROP to Determine Impact Limiter Deformation Behavior*. The basic polyurethane foam stress-strain data was taken from the foam pour records of the test articles. For the end drop, the prediction was prepared using the parallel-to-rise data from test article No. 3, pour 1, since only pour 1 foam was crushed in the test. For the side drop, the perpendicular-to-rise data in test article No. 4 for pour 3 was used. (Use of data from a single pour was sufficient since the stress-strain difference between the pours was negligible). For the oblique orientation, a combination of parallel-to-rise and perpendicular-to-rise data for pour 3 was used. The data was combined using interpolation, as described in Appendix 2.10.2.1.1, *Using CASKDROP to Determine Impact Limiter Deformation Behavior*. The stress-strain data, taken from test article acceptance test records, is given in Table 2.10.7-7.

Prior to each test, the temperature of the foam in the test article was measured using short holes drilled into the foam beneath each of the three plastic pipe plug ports. In preparing the test

[7] The 85º oblique drop has a very slightly higher impact than the end drop: 90.7*g* vs 89.7*g* (see Table 2.10.3-11 in Appendix 2.10.3, *Drop Impact Evaluation Results*).

predictions, the properties of the foam were adjusted for temperature using factors developed using the General Plastics foam property database. Since the pour's stress-strain data was taken at room temperature (approximately 73 ºF), the adjustment factor was equal to the ratio of the strength at test temperature to the strength at 73 ºF.

The database foam chosen to create this ratio had a strength level essentially the same as the test article foam.

2.10.7.2.4.1 End Free Drop

Figure 2.10.7-12 shows the configuration of the end drop. Test article No. 3 was attached to the bottom of the test package using 6 prototypic bolts, tightened as discussed in Appendix 2.10.7.2.2, *Test Facilities*. The test plate, simulating the weight of a half-scale impact limiter, was attached to the top of the test package. The axis of the test package was at an angle of 90º from horizontal. To ensure that a record of maximum deflection would be made, independent of elastic recovery, measurement of the bolt access tubes was made both prior to and after the test. The tubes are located on the bottom of the inner shell and are positioned parallel to the package axis (the direction of crush). During impact, the tubes deform by crippling, with essentially no change in their overall position. To ensure that the elastic recovery of the foam did not re-lengthen the deformed tubes, the weld connecting the tube to the bottom shell of test article No. 3 was severed on three of the six tubes. In this way, a tensile load could not be applied to the deformed tube after the maximum deflection had occurred. Therefore, the maximum deflection of the impact limiter was the difference between the length of the deformed and undeformed tubes. The average temperature of the foam in the test article was 42 ºF.

Figure 2.10.7-13 shows the post-test configuration of the end drop test. As in the static end orientation case, the deformation is completely inside-out. That is, the test package pushed into the impact limiter from the inside, rather than the flat bottom of the limiter crushing in from the outside. In fact, the deformation pattern and nature was identical to the static end test, but with a lesser magnitude. There was no failure of the shell anywhere on the test article.

The average length of the three tubes before testing (measured from the flat end of the limiter to the attachment bolt head) was 8.57 inches. After testing, the average length was 6.05 inches, for a difference equal to the maximum deflection of 8.57 – 6.05 = 2.52 inches. To obtain this same deflection value using the CASKDROP code using test article foam data adjusted for a temperature of 42 ºF required that an increase factor of 1.52 be applied to the input foam stress-strain data. Further discussion of this factor is given in Appendix 2.10.7.3, *Correction Factors*. The CASKDROP end drop prediction results are given in Table 2.10.7-8.

Immediately after impact, the elastic recovery in the foam caused the ends of the three gage tubes to recede below the bottom surface of the impact limiter. The difference in length between the top of the three gage tubes and the bottom of the limiter was an average of 1.4 inches. The amount of elastic recovery, or "springback", was therefore 1.4/2.52 × 100 = 56%.

2.10.7.2.4.2 Side Free Drop

Figure 2.10.7-14 shows the configuration of the side drop. Test article No. 3 was attached to the bottom of the package as in the end drop. Since the bolt tubes were crippled, retightening of the attachment bolts was not possible. Test article No. 4 was attached to the top end of the package

using 6 prototypic bolts and tightened, as discussed in Appendix 2.10.7.2.2, *Test Facilities*. The axis of the package was horizontal. The damage to test article No. 3 from the end drop was modest, and did not significantly affect the impact behavior of the new test article, No. 4. To ensure that a record of maximum deflection would be made, independent of elastic recovery, two independent crush gages were secured to the lower side of the test package, as shown in Figure 2.10.7-15[8]. The gages consisted of square tubes, approximately 3.5 inches on a side, made from 1/16 inch thick soft aluminum sheet. The axis of the tubes was parallel to the direction of deflection of the impact limiters during impact. During impact, the gages crippled and retained the maximum deflection of the limiters. The force required to deform the gages was negligible. The average temperature of the foam in the test article was 45 ºF.

Figure 2.10.7-16 shows the post-test configuration of the side drop test. In this case, the nature of the deflection is essentially all outside-in. As for the end drop, the deformation of the test article was similar to that from the corresponding static test, but of a lesser magnitude. The only (minimal) exposure of foam was from the separation of the weld between the two bolt access tubes nearest the ground and the bottom sheet of the limiter.

Figure 2.10.7-16 also shows the post-test configuration of the test article No. 4 crush gage. The gages had an undeformed length of 7.0 inches. There was also a clearance between the end of the gage and the ground of 1.5 inches. After the test, the test article No. 4 gage had a length of 4.94 inches. Thus, the maximum deflection of test article No. 4 in the side drop was 7.0 –4.94 + 1.5 = 3.56 inches. (In the side drop, test article No. 3 was considered only as a backup, due to the prior damage it received in the end drop. Therefore, since good data was collected from test article No. 4, no further consideration of test article No. 3 was needed.) CASKDROP predicted, using test article foam data corrected for temperature and using the dynamic factor of 1.52 as a multiplying factor on foam strength, a deflection of 4.04 inches, which is in reasonable agreement with the test results. The CASKDROP side drop prediction results are given in Table 2.10.7-9.

However, note is taken of the fact that, as seen in Figure 2.10.7-7 in Appendix 2.10.7.1.4.2, *Side Orientation*, the static test force-deflection curve in the region below 4 – 5 inches of deflection lies somewhat above the CASKDROP predicted curve. Therefore, the actual test force-deflection curve could be expected to absorb the drop test energy with slightly less deflection than the predicted curve. In fact, when the actual static test force-deflection curve is used to form the dynamic prediction, the deflection result is identical with the test data. How this was done is now briefly described.

First, the static test force-deflection curve was adjusted for temperature, which was done the same way as for foam strength as described above. Next, the curve was adjusted for the dynamic effect. In the end drop, an overall factor (including both static and dynamic effects) was found to be 1.52. The dynamic share of this factor is 1.52/1.19 = 1.277, where 1.19 is the static factor found in Appendix 2.10.7.1.4, *Test Description and Results*. The static force-deflection curve is then increased by the "temperature factor" × "dynamic factor".

The resulting curve is integrated to give the total absorbed energy of crush. When the absorbed energy equals the kinetic energy of the test package, the solution is reached. (This is the same quasi-static approach utilized in the CASKDROP code). The total kinetic energy of the test

[8] For clarity in the photograph, the test package has been rolled so that the axis of the gages is horizontal. During the drop, the axis of the gages is vertical.

package is W × (360 + δ), where W is the weight of the test package, 360 is the drop height in inches, and δ is the crush deflection of the impact limiters. The solution for δ is 3.56 inches, identical with the test data, and an impact of 155.9*g*. Although less accurate, the CASKDROP prediction is still conservative for both deflection and impact, since it predicts 4.04 inches and 156.4*g*.

Measurements of the post-test flat on test article No. 4 were also made to compare with the crush gage. Using the package body as a reference, the apparent deflection in the side drop was 1.87 inches. The elastic recovery, or "springback", was therefore (3.56 – 1.87)/3.56 × 100 = 47%.

2.10.7.2.4.3 Oblique Free Drop

Figure 2.10.7-17 shows the configuration of the oblique drop. Test articles No. 3 and No. 4 were attached to the test package as in the side drop. Since five of the attachment bolts of test article No. 4 were still accessible, they were retightened to specification. The amount of retightening needed was modest. The primary impact occurred on test article No. 4, at the corner of the limiter which was 180º opposite the side drop damage. A slapdown occurred on test article No. 3. The axis of the test package was actually 53º from horizontal. The average temperature of the foam in the test article was again 45 ºF.

Figure 2.10.7-18 and Figure 2.10.7-19 show the post-test configuration of the oblique drop test. In this case, no separate crush gages were used, since the nature of the oblique impact damage made determination of the maximum deflection somewhat more straightforward. In the oblique case, there is a reduction in surface area over the impact plane, and this accounts for the strongly wrinkled state of the impact surface. In addition, the same reduction in surface area causes local scrubbing of the steel drop pad, transferring a heavy coat of rust to the test article, and making the actual extent of the maximum impact surface quite distinct. Figure 2.10.7-20 shows how the maximum deflection was calculated using the edges of contact. The maximum deflection, measured along the direction of crush, was 7.3 inches. The corresponding prediction was prepared using both CASKDROP and SLAPDOWN, the latter code (see Appendix 2.10.2.2, *Description of the SLAPDOWN Computer Code*) being necessary since the impact is unstable with some of the drop energy going into package rotation. As in the previous two cases, the basic test article foam data was corrected for temperature and increased by the dynamic factor of 1.52 as a multiplying factor on foam strength. The force-deflection curve produced by CASKDROP was fed into SLAPDOWN, which performed a dynamic analysis. The resulting maximum predicted deflection of the primary impact limiter (test article No. 4), was 8.76 inches, which is in reasonable agreement with the test results, and again represents a conservative overprediction of deflection. The CASKDROP and SLAPDOWN oblique drop prediction results are given in Table 2.10.7-10 and Table 2.10.7-11, respectively.

After the oblique drop test, of the four remaining accessible bolts, only one had less than full torque.

2.10.7.2.5 Summary

The RH-TRU 72-B impact limiters were tested in half-scale, 30-foot free drop tests. Two test articles were tested in end, side, and 55º from horizontal oblique orientations. Based on a correction factor developed on the basis of the end drop test, the predictions of the side and oblique drops were in good to excellent agreement with the test results, as summarized in Table 2.10.7-12.

A further result of testing was to demonstrate the structural integrity of both limiter shells and attachments, in a range of impact orientations.

2.10.7.3 Correction Factors

As discussed in Appendix 2.10.7.1.4, *Test Description and Results*, a factor was developed which was used to bring the static test results and test predictions into good agreement. The fact that the same factor (1.19) could be applied to all cases gives confidence that the basic prediction technique is acceptable. However, as described in Appendix 2.10.7.2.4, *Test Description and Results*, further adjustments to the results due to dynamic effects are also necessary. The adjustment factor in that case was found to be 1.52. This was developed on the basis of the end drop test, but when applied to the side and oblique drop cases, good agreement to test results was again obtained. Similar to the static factor, the universal applicability of the dynamic factor gives confidence that the analysis predictions are correct.

These correction factors are used in the impact predictions in Appendix 2.10.3, *Drop Impact Evaluation Results*, in the following way. For HAC drops from 30 feet, the overall factor of 1.52 is used, consistent with the test results discussed in this section. (The static factor of 1.19 is contained within the overall factor, and therefore does not need to be separately applied). For NCT free drops from 1 foot, only the static factor of 1.19 is applied. This is because the strain rate (and therefore, any dynamic effect) in the 1-foot drop is negligible compared to the 30-foot drop. The development of the foam strength used in the impact predictions, including the application of the correction factors, is discussed in Appendix 2.10.3, *Drop Impact Evaluation Results*.

2.10.7.4 Drawings

The following drawings are included in this section:

- 9715-015, *RH-72B Dummy Package*, Sheet 1 (Figure 2.10.7-21)
- 9715-015, *RH-72B Dummy Package*, Sheet 2 (Figure 2.10.7-22)
- 9715-010, *Impact Limiter Test Article RH-72B*, Sheet 1 (Figure 2.10.7-23)
- 9715-010, *Impact Limiter Test Article RH-72B*, Sheet 2 (Figure 2.10.7-24)
- 9715-010, *Impact Limiter Test Article RH-72B*, Sheet 3 (Figure 2.10.7-25)
- 9715-010, *Impact Limiter Test Article RH-72B*, Sheet 4 (Figure 2.10.7-26)

Table 2.10.7-1 – Static Crush Test Summary

Test No.	Unit No.	Orientation from Horizontal	Azimuth Orientation	Purpose of Test
1	1	End (90º)	—	Maximum Impact Case
2	2	Side (0º)	0º	High Impact Case (Cold), High Deflections (Warm)
3	2	Oblique (55º)	180º	Maximum Deflection Case (Warm)

Table 2.10.7-2 – Static Test Article Stress-Strain Properties

Strain, %	Crush Stress at 73ºF (psi)		
	No. 1, Pour 1 Parallel-to-Rise	No. 2, Pour 2 Parallel-to-Rise	No. 2, Pour 2 Perpendicular-to-Rise
5	488	420	363
10	516	423	390
20	510	438	415
30	544	479	458
40	630	549	534
50	822	683	674
60	1,187	972	972
65	1,533	1,278	1,292
70	2,078	1,762	1,864
75	—	2,625	2,750
80	—	4,509	4,849
87	—	14,731	16,403

Table 2.10.7-3 – End Crush CASKDROP Output

End Drop
02-02-1999, 14:00:20

*** PACKAGING TECHNOLOGY ***

CASKDROP, v2.31
Nov 13, 1997

72-B End Crush Test Prediction (Half Scale), fully effective			
Impact Limiter Weight (each) -	313 lbs	Cask and Payload Weight -	5,000 lbs
Impact Limiter Outside Diameter -	38.0000 in	Cask Outside Diameter -	37.9000 in
Impact Limiter Overall Length -	23.0000 in	Cask Overall Length -	70.9000 in
Impact Limiter Conical Diameter -	0.0000 in	Dynamic Unloading Modulus -	1.000E+07 lbs/in
Impact Limiter Conical Length -	0.0000 in	Rad Mass Moment of Inertia -	9,468 lb-in-s²
Impact Limiter End Thickness -	11.2500 in	Frictional Coefficient -	0.0000
Impact Limiter Hole Diameter -	0.0000 in	Drop Height -	30.0000 ft
Impact Limiter Hole Length -	0.0000 in	Drop Angle from Horizontal -	90.0000°
Unbacked Area Threshhold Strain -	0.0000 in/in	Crush Analysis Theory -	Global
Unbacked Area Crush Stress -	0 psi	Number of Integration Incs -	50

VARIABLE CRUSH STRESS	
ε (in/in)	σ (psi)
0.000	0.0
0.050	580.0
0.060	610.0
0.100	614.0
0.120	612.6
0.150	610.5
0.200	607.0
0.300	647.0
0.400	750.0
0.500	979.0
0.600	1,412.0
0.650	1,824.0
0.700	2,473.0

DEFL (in)	MAX ε (%)	AREA (in²)	VOLUME (in³)	XBAR (in)	IMPACT FORCE (lbs)	ACCEL (g's)	I/L MOMENT (in-lbs)	STRAIN ENERGY (in-lbs)	KINETIC ENERGY (in-lbs)	SE/KE RATIO
0.500	4.44	1,134	567	0.00	618,243	109.9	0	30,912	2,027,813	0.02
0.600	5.33	1,134	680	0.00	669,350	119.0	0	95,292	2,028,375	0.05
0.700	6.22	1,134	794	0.00	692,297	123.1	0	163,374	2,028,938	0.08
0.800	7.11	1,134	907	0.00	701,658	124.7	0	233,072	2,029,500	0.11
0.900	8.00	1,134	1,021	0.00	702,463	124.9	0	303,278	2,030,063	0.15
1.000	8.89	1,134	1,134	0.00	698,515	124.2	0	373,327	2,030,625	0.18
1.500	13.33	1,134	1,701	0.00	690,652	122.8	0	719,470	2,033,438	0.35
2.000	17.78	1,134	2,268	0.00	685,219	121.8	0	1,063,448	2,036,250	0.52
2.500	22.22	1,134	2,835	0.00	688,517	122.4	0	1,406,225	2,039,063	0.69
3.000	26.67	1,134	3,402	0.00	707,622	125.8	0	1,754,699	2,041,875	0.86
3.500	31.11	1,134	3,969	0.00	738,526	131.3	0	2,115,848	2,044,688	1.03
4.000	35.56	1,134	4,536	0.00	781,508	138.9	0	2,495,203	2,047,500	1.22
4.500	40.00	1,134	5,104	0.00	846,115	150.4	0	2,901,032	2,050,313	1.41
5.000	44.44	1,134	5,671	0.00	941,113	167.3	0	3,346,559	2,053,125	1.63
5.500	48.89	1,134	6,238	0.00	1,067,868	189.8	0	3,847,543	2,055,938	1.87
6.000	53.33	1,134	6,805	0.00	1,228,583	218.4	0	4,420,013	2,058,750	2.15
6.500	57.78	1,134	7,372	0.00	1,448,800	257.6	0	5,086,229	2,061,563	2.47
7.000	62.22	1,134	7,939	0.00	1,768,481	314.4	0	5,885,487	2,064,375	2.85
7.500	66.67	1,134	8,506	0.00	2,279,317	405.2	0	6,887,367	2,067,188	3.33
8.000	71.11	1,134	9,073	0.00	2,966,120	527.3	0	8,196,035	2,070,000	3.96
8.500	75.56	1,134	9,640	0.00	3,670,901	652.6	0	9,855,290	2,072,813	4.75
9.000	80.00	1,134	10,207	0.00	4,375,682	777.9	0	11,866,936	2,075,625	5.72
9.500	84.44	1,134	10,774	0.00	5,080,464	903.2	0	14,230,973	2,078,438	6.85
10.000	88.89	1,134	11,341	0.00	5,785,245	1,028.5	0	16,947,400	2,081,250	8.14
10.500	93.33	1,134	11,908	0.00	6,490,026	1,153.8	0	20,016,218	2,084,063	9.60
11.000	97.78	1,134	12,475	0.00	7,194,808	1,279.1	0	23,437,426	2,086,875	11.23

Note: For the purpose of this analysis, only the indicated columns are relevant.

Table 2.10.7-4 – Side Crush CASKDROP Output

Side Drop
02-24-1999, 13:54:29

*** PACKAGING TECHNOLOGY ***

CASKDROP, v2.31
Nov 13, 1997

72-B Side Crush Prediction (Half Scale), fully effective			
Impact Limiter Weight (each) -	313 lbs	Cask and Payload Weight -	5,000 lbs
Impact Limiter Outside Diameter -	38.0000 in	Cask Outside Diameter -	21.0000 in
Impact Limiter Overall Length -	23.0000 in	Cask Overall Length -	70.9000 in
Impact Limiter Conical Diameter -	0.0000 in	Dynamic Unloading Modulus -	1.000E+07 lbs/in
Impact Limiter Conical Length -	0.0000 in	Rad Mass Moment of Inertia -	7,526 lb-in-s²
Impact Limiter End Thickness -	5.6250 in	Frictional Coefficient -	0.0000
Impact Limiter Hole Diameter -	0.0000 in	Drop Height -	30.0000 ft
Impact Limiter Hole Length -	0.0000 in	Drop Angle from Horizontal -	0.0000°
Unbacked Area Threshhold Strain -	0.1000 in/in	Crush Analysis Theory -	Global
Unbacked Area Crush Stress -	464 psi	Number of Integration Incs -	50

VARIABLE CRUSH STRESS	
ε (in/in)	σ (psi)
0.000	0.0
0.050	431.0
0.100	464.0
0.200	494.0
0.300	545.0
0.400	635.0
0.500	802.0
0.600	1,157.0
0.650	1,537.0
0.700	2,218.0
0.750	3,273.0
0.800	5,770.0
0.870	19,520.0

DEFL (in)	MAX ε (%)	AREA (in²)	VOLUME (in³)	XBAR (in)	IMPACT FORCE (lbs)	ACCEL (g's)	I/L MOMENT (in-lbs)	STRAIN ENERGY (in-lbs)	KINETIC ENERGY (in-lbs)	SE/KE RATIO
0.500	5.88	398	133	0.00	112,001	19.9	0	28,000	2,027,813	0.01
1.000	11.76	560	375	0.00	198,795	35.3	0	105,699	2,030,625	0.05
1.500	17.65	681	686	0.00	265,260	47.2	0	221,713	2,033,438	0.11
2.000	23.53	781	1,052	0.00	331,071	58.9	0	370,796	2,036,250	0.18
2.500	29.41	867	1,465	0.00	390,680	69.5	0	551,233	2,039,063	0.27
3.000	35.29	943	1,917	0.00	446,952	79.5	0	760,641	2,041,875	0.37
3.500	41.17	1,011	2,406	0.00	502,477	89.3	0	997,999	2,044,688	0.49
4.000	47.05	1,073	2,927	0.00	558,063	99.2	0	1,263,134	2,047,500	0.62
4.500	52.93	1,130	3,478	0.00	629,479	111.9	0	1,560,019	2,050,313	0.76
5.000	58.82	1,182	4,056	0.00	727,804	129.4	0	1,899,340	2,053,125	0.93
5.205	61.23	1,202	4,301	0.00	781,000	138.8	0	2,054,280	2,054,280	1.00
5.500	64.70	1,230	4,659	0.00	876,240	155.8	0	2,300,351	2,055,938	1.12
6.000	70.58	1,275	5,286	0.00	1,121,838	199.4	0	2,799,870	2,058,750	1.36
6.500	76.46	1,316	5,934	0.00	1,524,711	271.1	0	3,461,508	2,061,563	1.68
7.000	82.34	1,355	6,602	0.00	2,568,055	456.5	0	4,484,699	2,064,375	2.17
7.500	88.22	1,391	7,289	0.00	5,588,834	993.6	0	6,523,921	2,067,188	3.16
8.000	94.10	1,425	7,993	0.00	10,065,785	1,789.5	0	10,437,576	2,070,000	5.04
8.500	99.99	1,457	8,714	0.00	15,477,921	2,751.6	0	16,823,502	2,072,813	8.12

Note: The column labeled "Impact Force" represents the sum of two identical forces on each impact limiter. For the purpose of this analysis, only the indicated columns are relevant.

Table 2.10.7-5 – Oblique Crush CASKDROP Output

Corner Drop
02-05-1999, 17:00:46

*** PACKAGING TECHNOLOGY ***

CASKDROP, v2.31
Nov 13, 1997

72-B 55 Deg Crush Prediction (Half Scale), fully effective			
Impact Limiter Weight (each) -	313 lbs	Cask and Payload Weight -	5,000 lbs
Impact Limiter Outside Diameter -	38.0000 in	Cask Outside Diameter -	21.0000 in
Impact Limiter Overall Length -	23.0000 in	Cask Overall Length -	70.9000 in
Impact Limiter Conical Diameter -	0.0000 in	Dynamic Unloading Modulus -	1.000E+07 lbs/in
Impact Limiter Conical Length -	0.0000 in	Rad Mass Moment of Inertia -	8,136 lb-in-s²
Impact Limiter End Thickness -	11.2500 in	Frictional Coefficient -	0.0000
Impact Limiter Hole Diameter -	0.0000 in	Drop Height -	30.0000 ft
Impact Limiter Hole Length -	0.0000 in	Drop Angle from Horizontal -	55.0000°
Unbacked Area Threshhold Strain -	0.1000 in/in	Crush Analysis Theory -	Global
Unbacked Area Crush Stress -	489 psi	Number of Integration Incs -	50
		Maximum Non-Convergence -	0.0000%

VARIABLE CRUSH STRESS	
ε (in/in)	σ (psi)
0.000	0.0
0.050	474.0
0.100	489.0
0.200	512.0
0.300	561.0
0.400	647.0
0.500	809.0
0.600	1,157.0
0.650	1,526.0
0.700	2,134.0
0.750	3,170.0
0.800	5,489.0
0.870	18,116.0

DEFL (in)	MAX ε (%)	AREA (in²)	VOLUME (in³)	XBAR (in)	IMPACT FORCE (lbs)	ACCEL (g's)	I/L MOMENT (in-lbs)	STRAIN ENERGY (in-lbs)	KINETIC ENERGY (in-lbs)	SE/KE RATIO
0.500	69.32	8	2	-11.64	6,847	1.2	0	1,712	2,027,813	0.00
1.000	69.25	23	9	-12.05	19,199	3.4	0	8,223	2,030,625	0.00
1.500	69.17	42	25	-12.45	34,960	6.2	0	21,763	2,033,438	0.01
2.000	69.09	64	51	-12.86	53,340	9.5	0	43,838	2,036,250	0.02
2.500	69.01	88	89	-13.26	73,842	13.1	0	75,634	2,039,063	0.04
3.000	68.97	115	140	-13.66	96,056	17.1	0	118,108	2,041,875	0.06
3.500	68.95	144	204	-14.05	119,686	21.3	0	172,044	2,044,688	0.08
4.000	68.95	174	284	-14.43	144,505	25.7	0	238,092	2,047,500	0.12
4.500	68.95	206	379	-14.81	170,324	30.3	0	316,799	2,050,313	0.15
5.000	68.96	240	490	-15.18	196,936	35.0	0	408,614	2,053,125	0.20
5.500	68.96	274	619	-15.55	224,255	39.9	0	513,911	2,055,938	0.25
6.000	68.96	310	765	-15.90	252,107	44.8	0	633,002	2,058,750	0.31
6.500	68.95	347	929	-16.25	280,412	49.9	0	766,131	2,061,563	0.37
7.000	68.93	384	1,112	-16.60	309,061	54.9	0	913,499	2,064,375	0.44
7.500	68.90	422	1,313	-16.93	337,933	60.1	0	1,075,248	2,067,188	0.52
8.000	68.86	461	1,534	-17.25	366,846	65.2	0	1,251,443	2,070,000	0.60
8.500	68.81	500	1,774	-17.57	395,795	70.4	0	1,442,103	2,072,813	0.70
9.000	68.74	540	2,034	-17.87	424,614	75.5	0	1,647,206	2,075,625	0.79
9.500	68.67	580	2,314	-18.16	453,147	80.6	0	1,866,646	2,078,438	0.90
10.000	69.84	620	2,614	-18.34	485,247	86.3	0	2,101,245	2,081,250	1.01
10.500	73.59	660	2,934	-18.22	533,409	94.8	0	2,355,909	2,084,063	1.13
11.000	77.36	701	3,274	-18.09	589,096	104.7	0	2,636,535	2,086,875	1.26
11.500	81.11	741	3,635	-17.80	664,802	118.2	0	2,950,010	2,089,688	1.41
12.000	84.64	781	4,015	-17.32	782,469	139.1	0	3,311,827	2,092,500	1.58
12.500	88.17	822	4,416	-16.59	978,863	174.0	0	3,752,160	2,095,313	1.79
13.000	91.69	861	4,837	-15.86	1,282,291	228.0	0	4,317,449	2,098,125	2.06
13.500	95.22	901	5,277	-15.26	1,713,019	304.5	0	5,066,277	2,100,938	2.41
14.000	98.75	940	5,737	-14.85	2,279,355	405.2	0	6,064,370	2,103,750	2.88

Note: For the purpose of this analysis, only the indicated columns are relevant.

Table 2.10.7-6 – Dynamic Drop Test Summary

Test No.	Unit No.	Orientation from Horizontal	Azimuth Orientation	Purpose of Test
1	3	End (90º)	—	Maximum Impact Case, Structural Integrity Case
2	4	Side (0º)	0º	High Impact Case (Cold), High Deflections (Warm)
3	4	Oblique (55º)	180º	Maximum Deflection Case (Warm)

Table 2.10.7-7 – Dynamic Test Article Stress-Strain Properties

Strain, %	Crush Stress at 73ºF (psi)		
	No. 3, Pour 1 Parallel-to-Rise	No. 4, Pour 3 Parallel-to-Rise	No. 4, Pour 3 Perpendicular-to-Rise
5	438	459	384
10	458	457	426
20	473	467	446
30	513	505	483
40	585	565	548
50	734	703	685
60	1,055	994	994
65	1,341	1,265	1,305
70	1,850	1,709	1,788
75	2,689	2,475	2,578

Table 2.10.7-8 – End Drop CASKDROP Output

End Drop *** PACKAGING TECHNOLOGY *** CASKDROP, v2.31
02-02-1999, 09:38:21 Nov 13, 1997

72-B End Drop Analysis (Half Scale @ 42 Deg F, incl. nec. factors)			
Impact Limiter Weight (each) -	0 lbs	Cask and Payload Weight -	5,736 lbs
Impact Limiter Outside Diameter -	38.0000 in	Cask Outside Diameter -	37.9000 in
Impact Limiter Overall Length -	23.0000 in	Cask Overall Length -	70.9000 in
Impact Limiter Conical Diameter -	0.0000 in	Dynamic Unloading Modulus -	1.000E+07 lbs/in
Impact Limiter Conical Length -	0.0000 in	Rad Mass Moment of Inertia -	7,552 lb-in-s²
Impact Limiter End Thickness -	11.2500 in	Frictional Coefficient -	0.0000
Impact Limiter Hole Diameter -	0.0000 in	Drop Height -	30.0000 ft
Impact Limiter Hole Length -	0.0000 in	Drop Angle from Horizontal -	90.0000°
Unbacked Area Threshhold Strain -	0.1000 in/in	Crush Analysis Theory -	Global
Unbacked Area Crush Stress -	813 psi	Number of Integration Incs -	50

VARIABLE CRUSH STRESS	
ε (in/in)	σ (psi)
0.000	0.0
0.050	778.0
0.100	813.0
0.200	838.0
0.300	907.0
0.400	1,030.0

DEFL (in)	MAX ε (%)	AREA (in²)	VOLUME (in³)	XBAR (in)	IMPACT FORCE (lbs)	ACCEL (g's)	I/L MOMENT (in-lbs)	STRAIN ENERGY (in-lbs)	KINETIC ENERGY (in-lbs)	SE/KE RATIO
0.500	4.44	1,134	567	0.00	823,303	143.5	0	205,826	2,067,900	0.10
1.000	8.89	1,134	1,134	0.00	948,200	165.3	0	648,702	2,070,768	0.31
1.500	13.33	1,134	1,701	0.00	888,817	154.9	0	1,107,956	2,073,636	0.53
2.000	17.78	1,134	2,268	0.00	923,511	161.0	0	1,561,038	2,076,504	0.75
2.500	22.22	1,134	2,835	0.00	971,329	169.3	0	2,034,748	2,079,373	0.98
2.546	22.63	1,134	2,888	0.00	974,589	169.9	0	2,079,637	2,079,637	1.00
3.000	26.67	1,134	3,402	0.00	1,002,104	174.7	0	2,528,106	2,082,241	1.21
3.500	31.11	1,134	3,969	0.00	1,039,374	181.2	0	3,038,476	2,085,109	1.46
4.000	35.56	1,134	4,536	0.00	1,097,285	191.3	0	3,572,641	2,087,977	1.71
4.500	40.00	1,134	5,104	0.00	1,166,845	203.4	0	4,138,673	2,090,845	1.98
5.000	44.44	1,134	5,671	0.00	1,238,346	215.9	0	4,739,971	2,093,713	2.26
5.500	48.89	1,134	6,238	0.00	1,309,846	228.3	0	5,377,019	2,096,581	2.56
6.000	53.33	1,134	6,805	0.00	1,381,347	240.8	0	6,049,817	2,099,449	2.88
6.500	57.78	1,134	7,372	0.00	1,452,848	253.3	0	6,758,366	2,102,317	3.21
7.000	62.22	1,134	7,939	0.00	1,524,349	265.7	0	7,502,665	2,105,185	3.56
7.500	66.67	1,134	8,506	0.00	1,595,850	278.2	0	8,282,715	2,108,054	3.93
8.000	71.11	1,134	9,073	0.00	1,667,351	290.7	0	9,098,515	2,110,922	4.31
8.500	75.56	1,134	9,640	0.00	1,738,851	303.1	0	9,950,065	2,113,790	4.71
9.000	80.00	1,134	10,207	0.00	1,810,352	315.6	0	10,837,366	2,116,658	5.12
9.500	84.44	1,134	10,774	0.00	1,881,853	328.1	0	11,760,418	2,119,526	5.55
10.000	88.89	1,134	11,341	0.00	1,953,354	340.5	0	12,719,219	2,122,394	5.99
10.500	93.33	1,134	11,908	0.00	2,024,855	353.0	0	13,713,771	2,125,262	6.45
11.000	97.78	1,134	12,475	0.00	2,096,355	365.5	0	14,744,074	2,128,130	6.93

Table 2.10.7-9 – Side Drop CASKDROP Output

Side Drop *** PACKAGING TECHNOLOGY *** CASKDROP, v2.31
02-05-1999, 09:45:29 Nov 13, 1997

72-B Side Drop Analysis (Half Scale @ 45 Deg F, incl. harder foam)			
Impact Limiter Weight (each) -	0 lbs	Cask and Payload Weight -	5,736 lbs
Impact Limiter Outside Diameter -	38.0000 in	Cask Outside Diameter -	21.0500 in
Impact Limiter Overall Length -	23.0000 in	Cask Overall Length -	70.9000 in
Impact Limiter Conical Diameter -	0.0000 in	Dynamic Unloading Modulus -	1.000E+07 lbs/in
Impact Limiter Conical Length -	0.0000 in	Rad Mass Moment of Inertia -	6,630 lb-in-s²
Impact Limiter End Thickness -	5.6250 in	Frictional Coefficient -	0.0000
Impact Limiter Hole Diameter -	0.0000 in	Drop Height -	30.0000 ft
Impact Limiter Hole Length -	0.0000 in	Drop Angle from Horizontal -	0.0000°
Unbacked Area Threshhold Strain -	0.1000 in/in	Crush Analysis Theory -	Global
Unbacked Area Crush Stress -	776 psi	Number of Integration Incs -	50

VARIABLE CRUSH STRESS	
ε (in/in)	σ (psi)
0.000	0.0
0.050	699.0
0.100	776.0
0.200	808.0
0.300	870.0
0.400	979.0
0.500	1,221.0
0.600	1,762.0
0.650	2,311.0
0.700	3,154.0
0.750	4,559.0

DEFL (in)	MAX ε (%)	AREA (in²)	VOLUME (in³)	XBAR (in)	IMPACT FORCE (lbs)	ACCEL (g's)	I/L MOMENT (in-lbs)	STRAIN ENERGY (in-lbs)	KINETIC ENERGY (in-lbs)	SE/KE RATIO
0.500	5.90	398	133	0.00	181,706	31.7	0	45,426	2,067,900	0.02
1.000	11.80	560	375	0.00	328,211	57.2	0	172,906	2,070,768	0.08
1.500	17.70	681	686	0.00	437,973	76.4	0	364,452	2,073,636	0.18
2.000	23.60	781	1,052	0.00	542,231	94.5	0	609,503	2,076,504	0.29
2.500	29.50	867	1,465	0.00	636,048	110.9	0	904,073	2,079,373	0.43
3.000	35.39	943	1,917	0.00	722,512	126.0	0	1,243,713	2,082,241	0.60
3.500	41.29	1,011	2,406	0.00	805,517	140.4	0	1,625,720	2,085,109	0.78
4.000	47.19	1,073	2,927	0.00	887,891	154.8	0	2,049,072	2,087,977	0.98
4.044	47.71	1,078	2,975	0.00	897,107	156.4	0	2,088,228	2,088,228	1.00
4.500	53.09	1,130	3,478	0.00	995,265	173.5	0	2,519,861	2,090,845	1.21
5.000	58.99	1,182	4,056	0.00	1,145,686	199.7	0	3,055,099	2,093,713	1.46
5.500	64.89	1,230	4,659	0.00	1,373,480	239.4	0	3,684,890	2,096,581	1.76
6.000	70.79	1,275	5,286	0.00	1,716,836	299.3	0	4,457,469	2,099,449	2.12
6.500	76.69	1,316	5,934	0.00	2,270,132	395.8	0	5,454,211	2,102,317	2.59
7.000	82.58	1,355	6,602	0.00	2,982,596	520.0	0	6,767,394	2,105,185	3.21
7.500	88.48	1,391	7,289	0.00	3,799,797	662.4	0	8,462,992	2,108,054	4.01
8.000	94.38	1,425	7,993	0.00	4,697,081	818.8	0	10,587,212	2,110,922	5.02

Table 2.10.7-10 – Oblique Drop CASKDROP Output

Corner Drop
02-09-1999, 09:22:12

*** PACKAGING TECHNOLOGY ***

CASKDROP, v2.31
Nov 13, 1997

72-B Oblique Analysis (Half Scale @ 50 Deg F, incl. harder foam)			
Impact Limiter Weight (each) -	313 lbs	Cask and Payload Weight -	5,736 lbs
Impact Limiter Outside Diameter -	38.0000 in	Cask Outside Diameter -	20.8000 in
Impact Limiter Overall Length -	23.0000 in	Cask Overall Length -	70.9000 in
Impact Limiter Conical Diameter -	0.0000 in	Dynamic Unloading Modulus -	1.000E+07 lbs/in
Impact Limiter Conical Length -	0.0000 in	Rad Mass Moment of Inertia -	6,621 lb-in-s²
Impact Limiter End Thickness -	11.2500 in	Frictional Coefficient -	0.0000
Impact Limiter Hole Diameter -	0.0000 in	Drop Height -	30.0000 ft
Impact Limiter Hole Length -	0.0000 in	Drop Angle from Horizontal -	55.0000°
Unbacked Area Threshhold Strain -	0.1000 in/in	Crush Analysis Theory -	Global
Unbacked Area Crush Stress -	784 psi	Number of Integration Incs -	50

VARIABLE CRUSH STRESS	
ε (in/in)	σ (psi)
0.000	0.0
0.050	762.0
0.100	784.0
0.200	811.0
0.300	877.0
0.400	986.0
0.500	1,224.0
0.600	1,755.0
0.650	2,266.0
0.700	3,067.0
0.750	4,527.0

DEFL (in)	MAX ε (%)	AREA (in²)	VOLUME (in³)	XBAR (in)	IMPACT FORCE (lbs)	ACCEL (g's)	I/L MOMENT (in-lbs)	STRAIN ENERGY (in-lbs)	KINETIC ENERGY (in-lbs)	SE/KE RATIO
0.500	3.33	8	2	-11.43	2,016	0.4	0	504	2,067,900	0.00
1.000	6.66	23	9	-11.66	10,144	1.8	0	3,544	2,070,768	0.00
1.500	9.99	42	25	-11.92	22,992	4.0	0	11,828	2,073,636	0.01
2.000	13.33	64	51	-12.20	38,254	6.7	0	27,140	2,076,504	0.01
2.500	16.66	88	89	-12.47	55,384	9.7	0	50,549	2,079,373	0.02
3.000	20.00	115	140	-12.73	74,452	13.0	0	83,008	2,082,241	0.04
3.500	23.33	144	204	-12.99	95,586	16.7	0	125,518	2,085,109	0.06
4.000	26.67	174	284	-13.25	118,742	20.7	0	179,100	2,087,977	0.09
4.500	30.01	206	379	-13.50	143,787	25.1	0	244,732	2,090,845	0.12
5.000	33.37	240	490	-13.76	170,586	29.7	0	323,325	2,093,713	0.15
5.500	36.96	274	619	-14.01	199,086	34.7	0	415,743	2,096,581	0.20
6.000	40.59	310	765	-14.25	229,343	40.0	0	522,850	2,099,449	0.25
6.500	44.26	347	929	-14.48	261,478	45.6	0	645,556	2,102,317	0.31
7.000	47.85	384	1,112	-14.71	295,700	51.5	0	784,850	2,105,185	0.37
7.500	51.27	422	1,313	-14.93	332,210	57.9	0	941,827	2,108,054	0.45
8.000	54.69	461	1,534	-15.13	371,510	64.8	0	1,117,757	2,110,922	0.53
8.500	58.11	500	1,774	-15.32	414,175	72.2	0	1,314,179	2,113,790	0.62
9.000	61.66	540	2,034	-15.49	461,292	80.4	0	1,533,045	2,116,658	0.72
9.500	65.31	580	2,314	-15.64	514,169	89.6	0	1,776,911	2,119,526	0.84
10.000	68.98	620	2,614	-15.75	574,167	100.1	0	2,048,995	2,122,394	0.97
10.127	69.92	630	2,693	-15.78	591,060	103.0	0	2,123,124	2,123,124	1.00
10.500	72.67	660	2,934	-15.83	644,808	112.4	0	2,353,739	2,125,262	1.11
11.000	76.39	701	3,274	-15.85	730,237	127.3	0	2,697,500	2,128,130	1.27
11.500	80.14	741	3,635	-15.84	833,472	145.3	0	3,088,427	2,130,998	1.45
12.000	83.91	781	4,015	-15.81	956,356	166.7	0	3,535,884	2,133,866	1.66
12.500	87.71	822	4,416	-15.76	1,100,030	191.8	0	4,049,981	2,136,735	1.90
13.000	91.53	861	4,837	-15.71	1,265,463	220.6	0	4,641,354	2,139,603	2.17
13.500	95.22	901	5,277	-15.69	1,455,425	253.7	0	5,321,576	2,142,471	2.48
14.000	98.75	940	5,737	-15.68	1,670,416	291.2	0	6,103,036	2,145,339	2.84

Note: Only the force-deflection relationship from this output is relevant to the oblique test; the dynamic result is given in Table 2.10.7-11.

Table 2.10.7-11 – Oblique Drop SLAPDOWN Output

```
PROGRAM SLAPDOWN  VERSION 2.1
 TITLE: 72-B 55 DEG OBLIQUE DROP TEST PREDICTION

 02/18/1999     10:59:08

 ****** NOSE PROPERTIES ******

 LENGTH FROM NOSE TO CG (Z1)            3.545E+01
 RADIUS OF PACKAGE AT NOSE (R1)            1.040E+01
 SQUARE END
 COEFFICIENT OF FRICTION AT NOSE (CF1)  0.000E+00

        NOSE SPRING DEFINITION

        DISPLACEMENT     FORCE
          0.000E+00    0.000E+00
          5.000E-01    2.016E+03
          1.000E+00    1.014E+04
          1.500E+00    2.299E+04
          2.000E+00    3.825E+04
          2.500E+00    5.538E+04
          3.000E+00    7.445E+04
          3.500E+00    9.559E+04
          4.000E+00    1.187E+05
          4.500E+00    1.438E+05
          5.000E+00    1.706E+05
          5.500E+00    1.991E+05
          6.000E+00    2.293E+05
          6.500E+00    2.615E+05
          7.000E+00    2.957E+05
          7.500E+00    3.322E+05
          8.000E+00    3.715E+05
          8.500E+00    4.142E+05
          9.000E+00    4.613E+05
          9.500E+00    5.142E+05
          1.000E+01    5.742E+05
          1.050E+01    6.448E+05
          1.100E+01    7.302E+05
          1.150E+01    8.335E+05
          1.200E+01    9.564E+05
          1.250E+01    1.100E+06
          1.300E+01    1.265E+06
          1.350E+01    1.455E+06
          1.400E+01    1.670E+06

 UNLOADING MODULUS FOR NOSE SPRING      1.000E+07


 ****** TAIL PROPERTIES ******

 LENGTH FROM TAIL TO CG (Z2)            3.545E+01
 RADIUS OF PACKAGE AT TAIL (R2)            1.040E+01
 COEFFICIENT OF FRICTION AT TAIL (CF2)  0.000E+00
 ROUND END

        TAIL SPRING DEFINITION

        DISPLACEMENT     FORCE
          0.000E+00    0.000E+00
          5.000E-01    9.135E+04
          1.000E+00    1.616E+05
          1.500E+00    2.143E+05
          2.000E+00    2.658E+05
          2.500E+00    3.122E+05
          3.000E+00    3.551E+05
          3.500E+00    3.960E+05
          4.000E+00    4.358E+05
          4.500E+00    4.896E+05
          5.000E+00    5.673E+05
          5.500E+00    6.816E+05
          6.000E+00    8.506E+05
          6.500E+00    1.129E+06
          7.000E+00    1.491E+06
          7.500E+00    1.908E+06
          8.000E+00    2.366E+06

 UNLOADING MODULUS FOR TAIL SPRING      1.000E+07
```

```
****** MASS, MOMENT OF INERTIA, AND INITIAL CONDITION DATA ******

 MASS OF BODY                            1.484E+01
 MOMENT OF INERTIA                       8.706E+03
 RADIUS OF GYRATION                      2.422E+01
 INITIAL VERTICAL VELOCITY (pos. up)    -5.275E+02
 GRAVITATIONAL ACCELERATION (pos. up)   -3.860E+02
 INITIAL ANGLE (positive CCW)             5.500E+01

 TIME STEP SCALE FACTOR                  1.000E-02
 FRICTION SCALE FACTOR                   0.000E+00
 WRITE PLOT DATA EVERY STEP


 72-B 55 DEG OBLIQUE DROP TEST PREDICTION

 ****** SEQUENCE OF EVENTS ******

 ** NOSE HIT     AT TIME  0.000E+00, VELOCITY = -5.275E+02, RATIO =  1.00
 ** NOSE REBOUND AT TIME  2.312E-02, VELOCITY =  1.050E+02, RATIO =  -.20
 ** NOSE UNLOAD  AT TIME  2.449E-02, VELOCITY =  1.636E+02, RATIO =  -.31
 ** TAIL HIT     AT TIME  8.990E-02, VELOCITY = -6.965E+02, RATIO =  1.32
 ** TAIL REBOUND AT TIME  1.001E-01, VELOCITY =  2.625E-01, RATIO =   .00
 ** TAIL UNLOAD  AT TIME  1.012E-01, VELOCITY =  6.767E+01, RATIO =  -.13


 ****** RESULTS ******

 Event over at time    1.012E-01, Time step size  1.177E-05
 Time step multiplier  1.000E-02, 8601 Plot times written to database


           DISPLACEMENT     VELOCITY     ACCELERATION

   NOSE      8.756E+00      3.152E+02      6.270E+04 (MAX)
                           -5.278E+02     -3.477E+04 (MIN)

   TAIL      4.331E+00      6.767E+01      9.753E+04 (MAX)
                           -6.967E+02     -5.843E+03 (MIN)

     CG                    4.987E+01      3.138E+04 (MAX)
                           -5.279E+02     -3.860E+02 (MIN)

 ANGULAR                   5.094E-01      1.893E+03 (MAX)
                           -1.425E+01     -1.270E+03 (MIN)

 MAXIMUM ENERGIES:  1.423E+06 (NOSE),  1.157E+06 (TAIL)
 TAIL IMPACT ANGLE =       -4.363187 DEG.
```

Table 2.10.7-12 – Free Drop Test Result Summary

Drop Test Case	Test Result Deflection (inches)	Analytical Prediction (inches)	Comment
End Drop (90º)	2.52	2.52	Basis of Dynamic Correction Factor
Side Drop (0º)	3.56	4.04	Using Analytical Tools
—	—	3.56	Using Static Force-deflection Curve
Oblique Drop (55º)	7.30	8.76	Using Analytical Tools

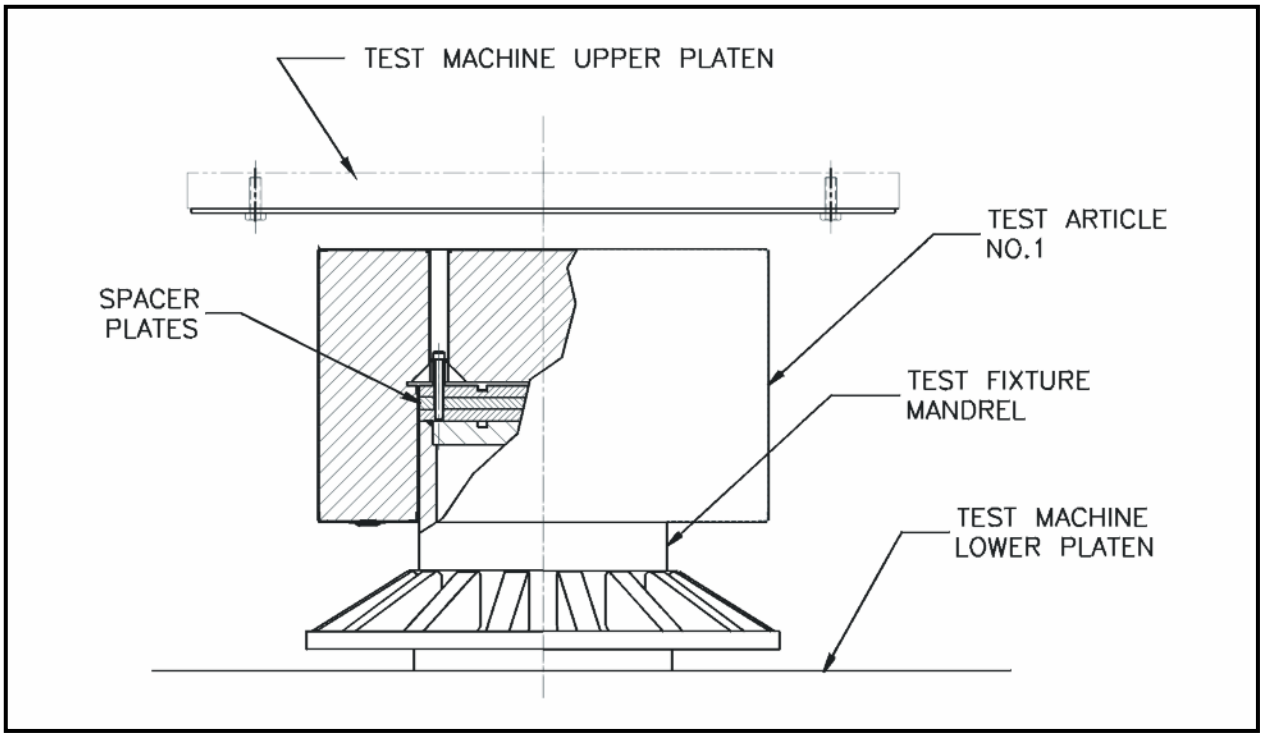

Figure 2.10.7-1 – End Orientation Test

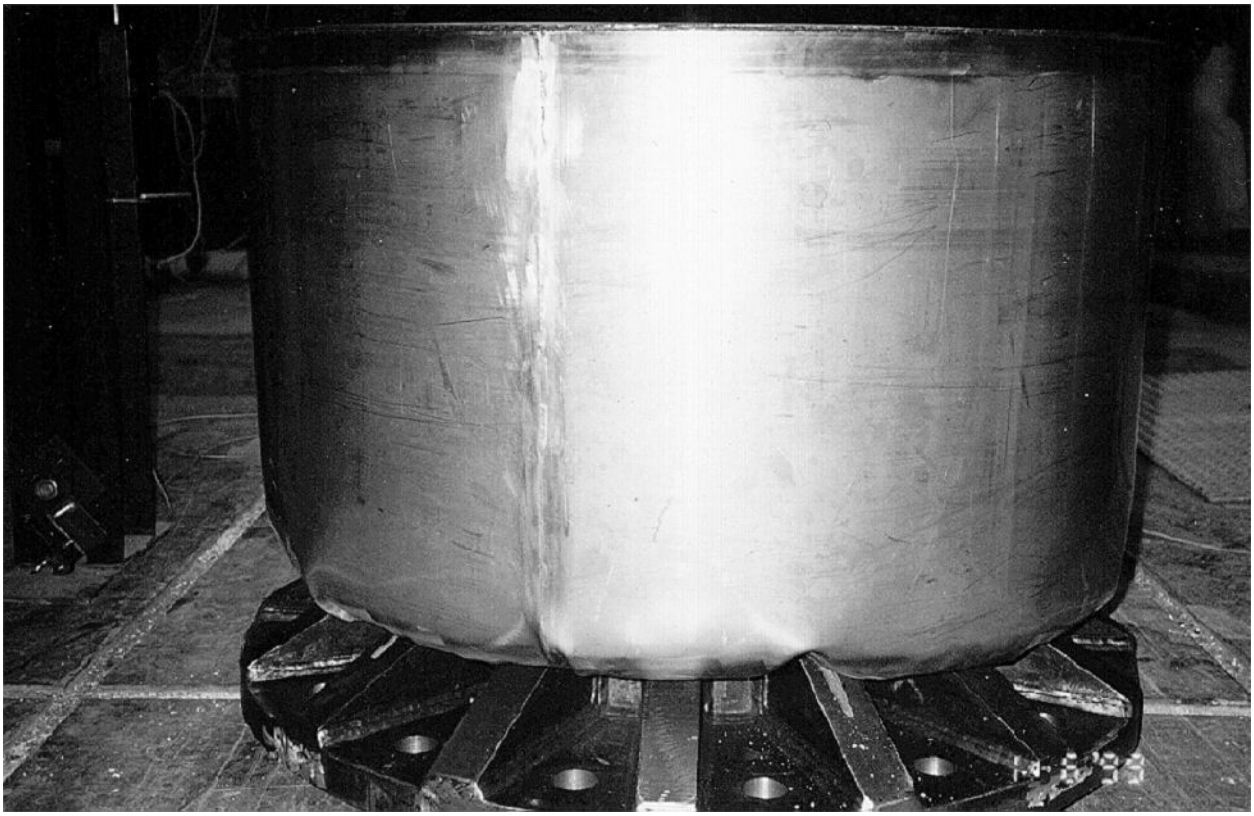

Figure 2.10.7-2 – End Orientation, Post-Test Configuration

Figure 2.10.7-3 – End Orientation, View of Open End

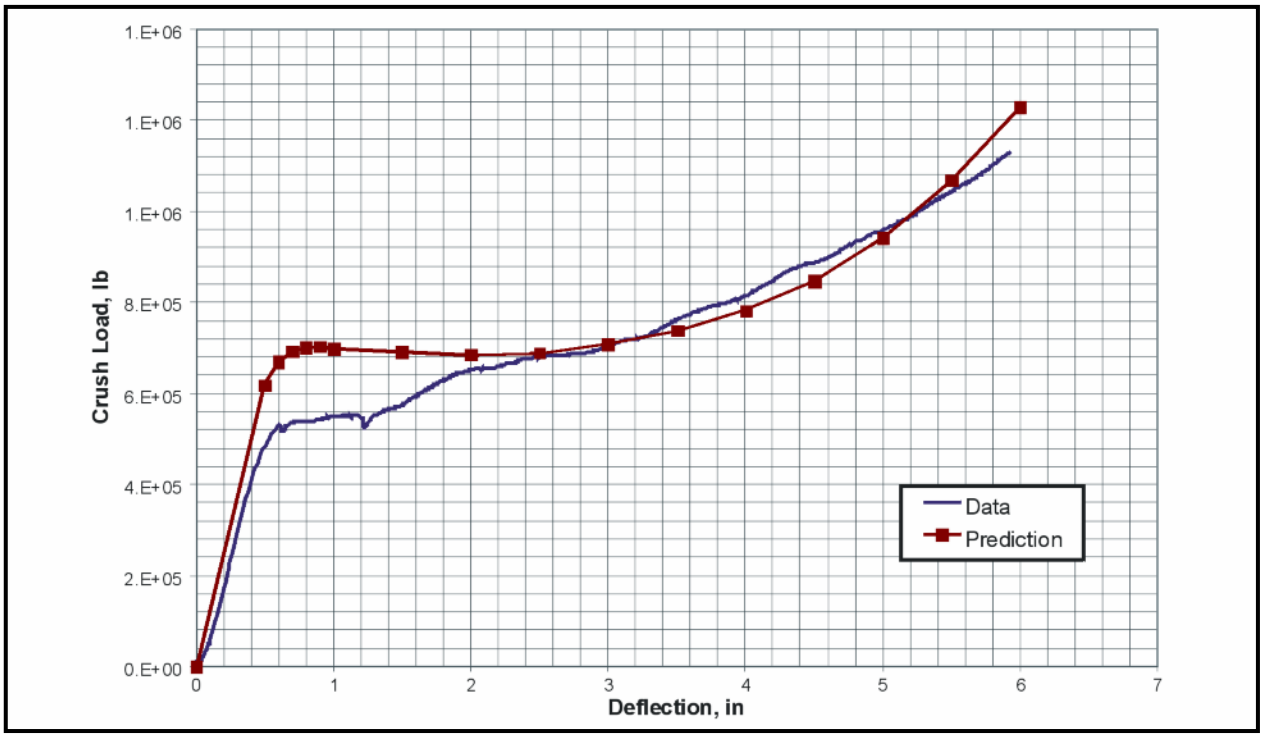

Figure 2.10.7-4 – End Crush Data Versus Prediction

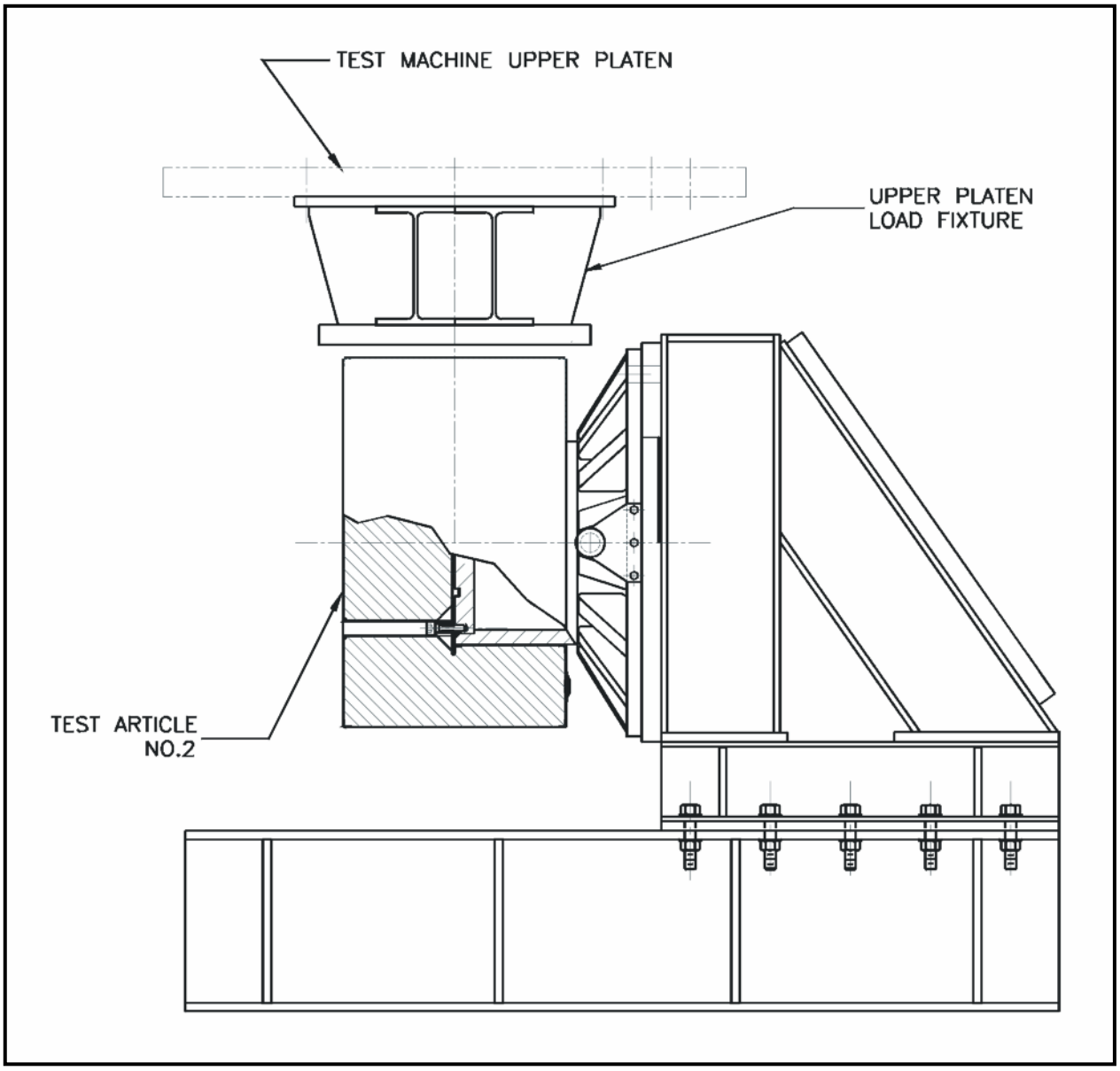

Figure 2.10.7-5 – Side Orientation Test

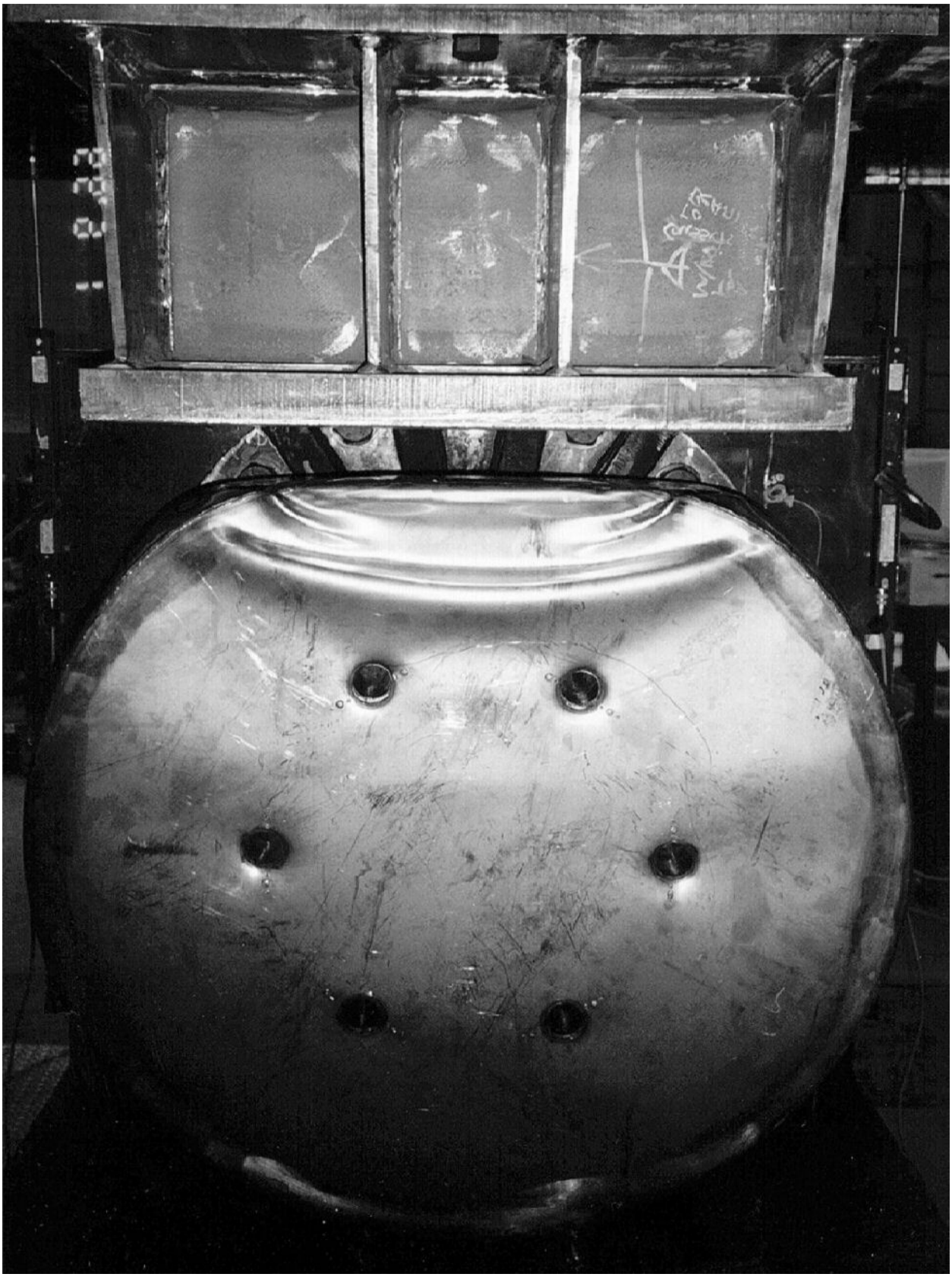

Figure 2.10.7-6 – Side Orientation, Post-Test Configuration

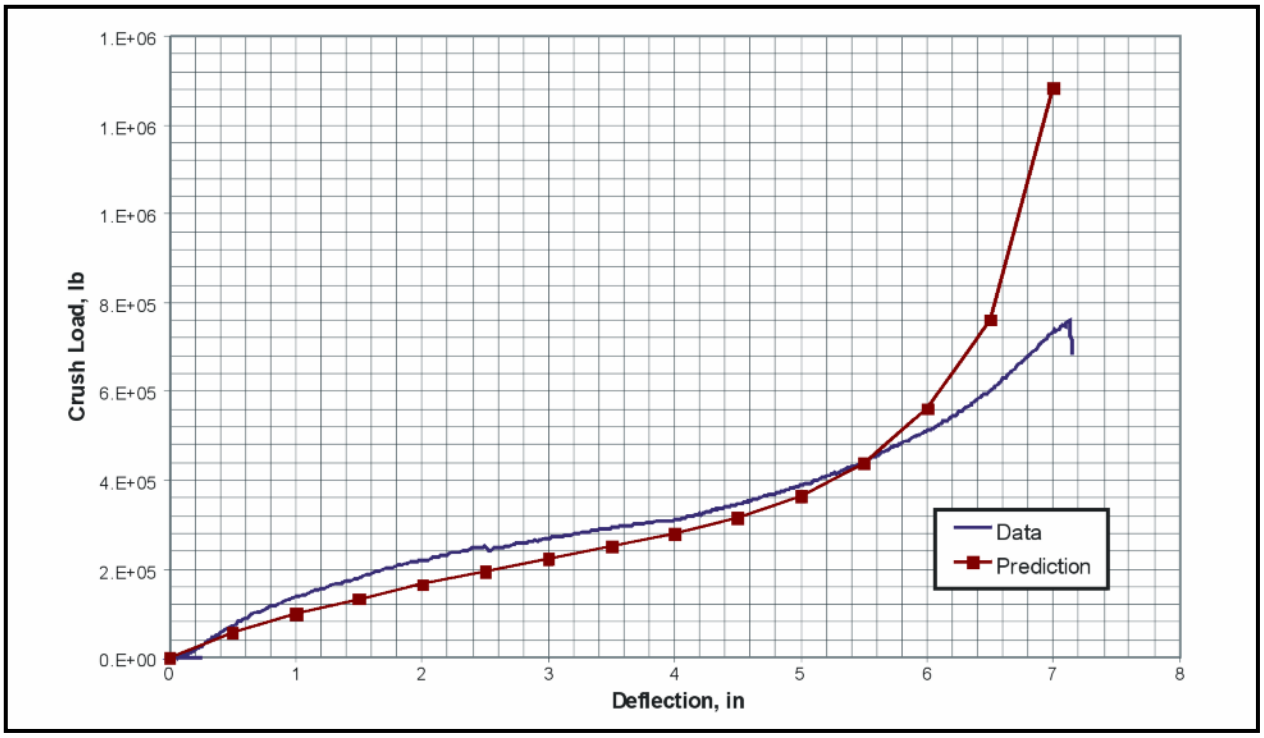

Figure 2.10.7-7 – Side Crush Data Versus Prediction

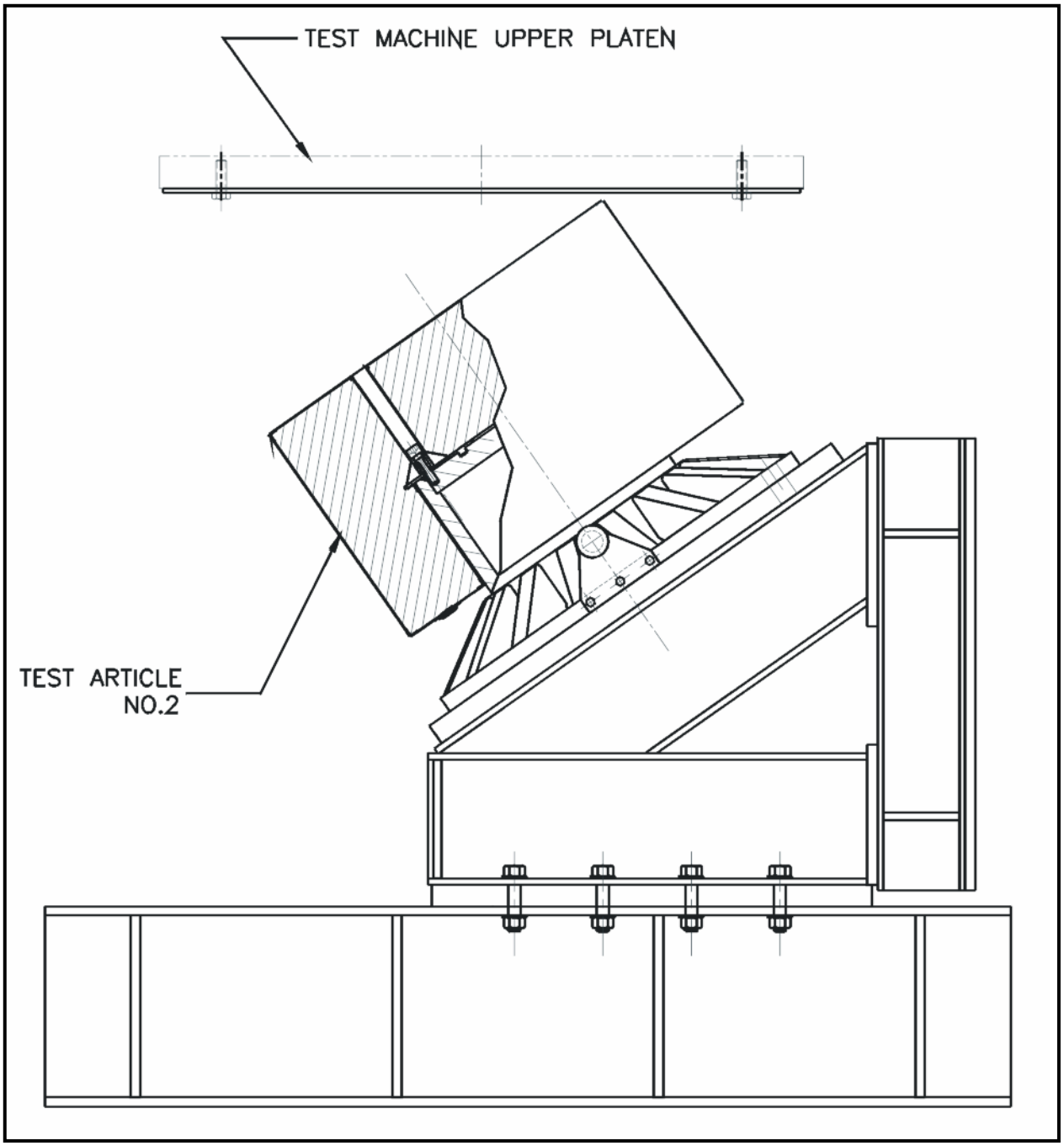

Figure 2.10.7-8 – Oblique Orientation Test

Figure 2.10.7-9 – Oblique Orientation, Post-Test Configuration

Figure 2.10.7-10 – Oblique Orientation, Post-Test Side View

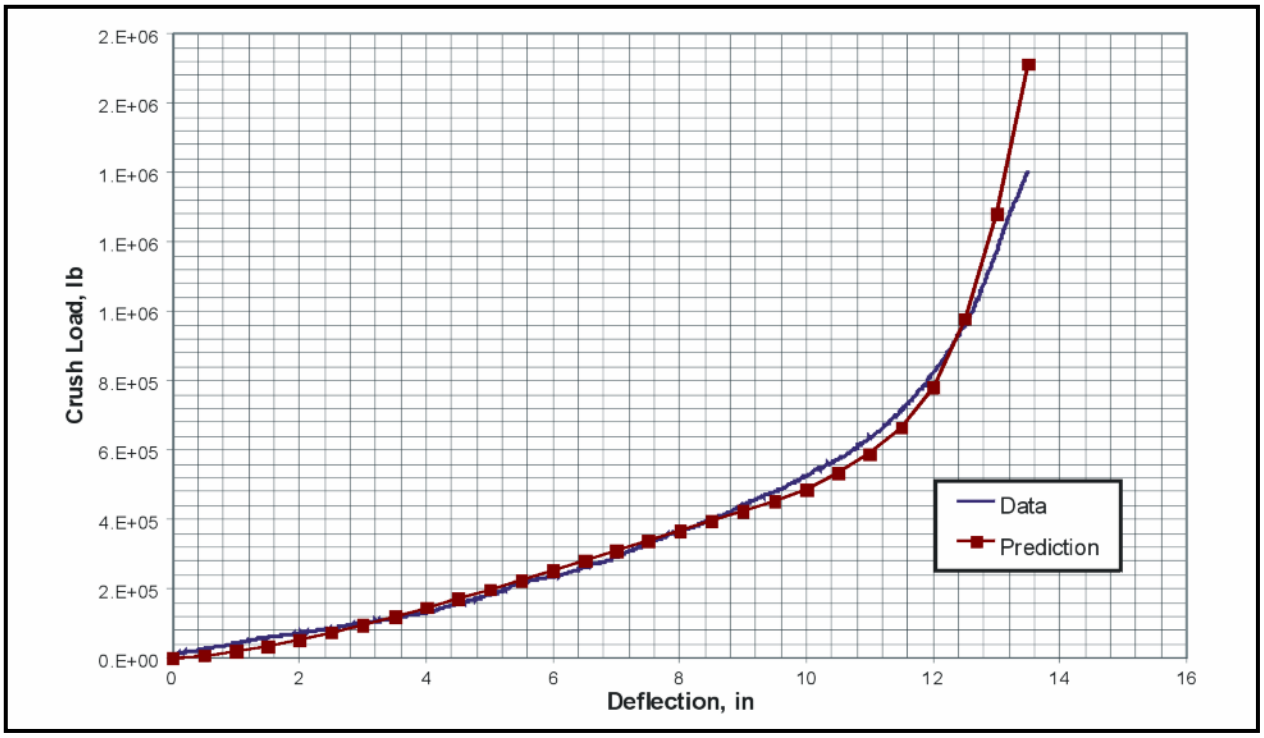

Figure 2.10.7-11 – Oblique Crush Data Versus Prediction

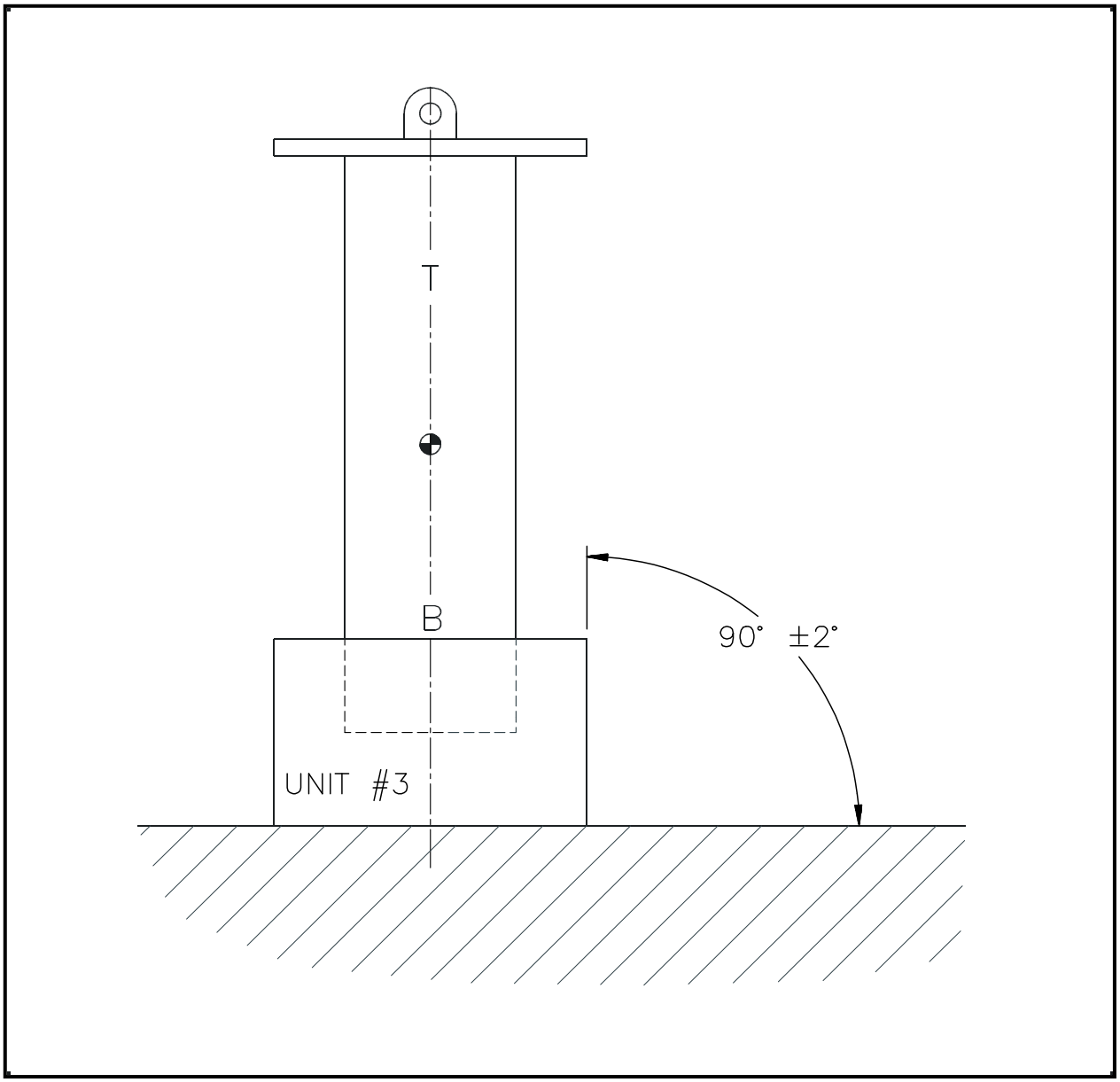

Figure 2.10.7-12 – End Drop Configuration

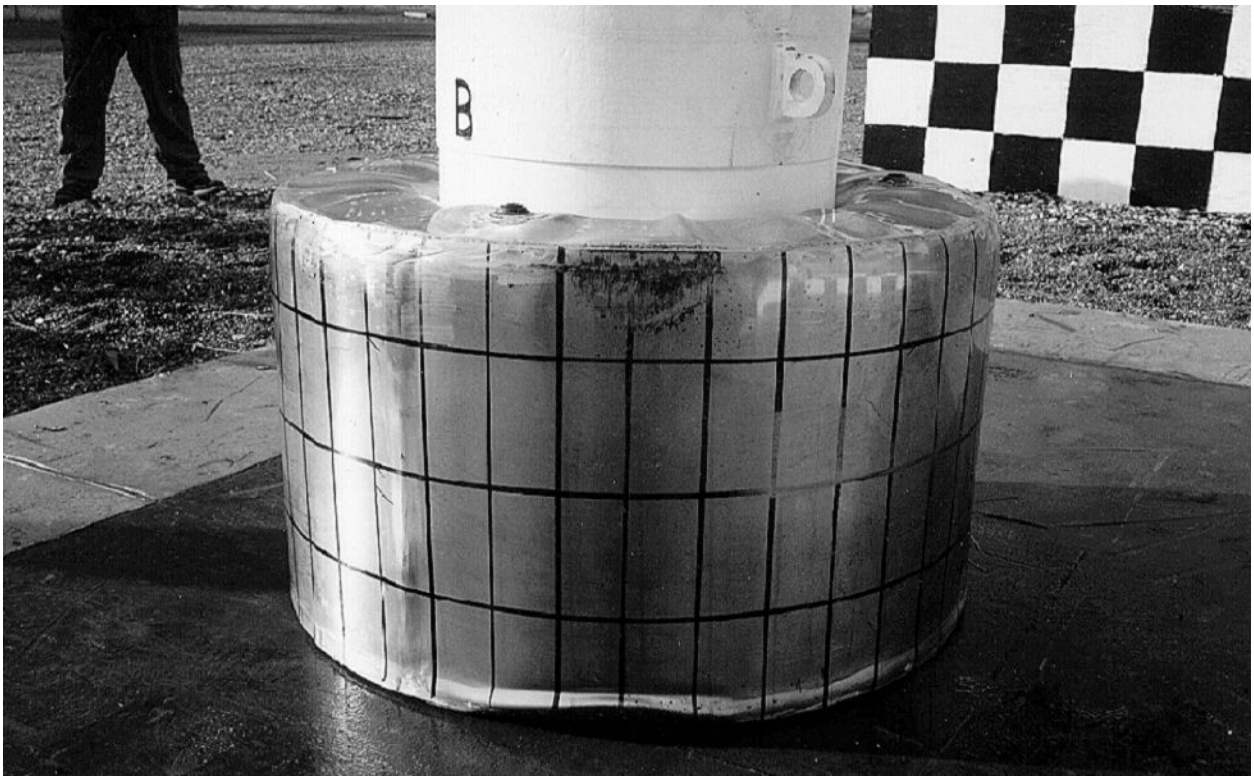

Figure 2.10.7-13 – End Drop, Post-Test Configuration

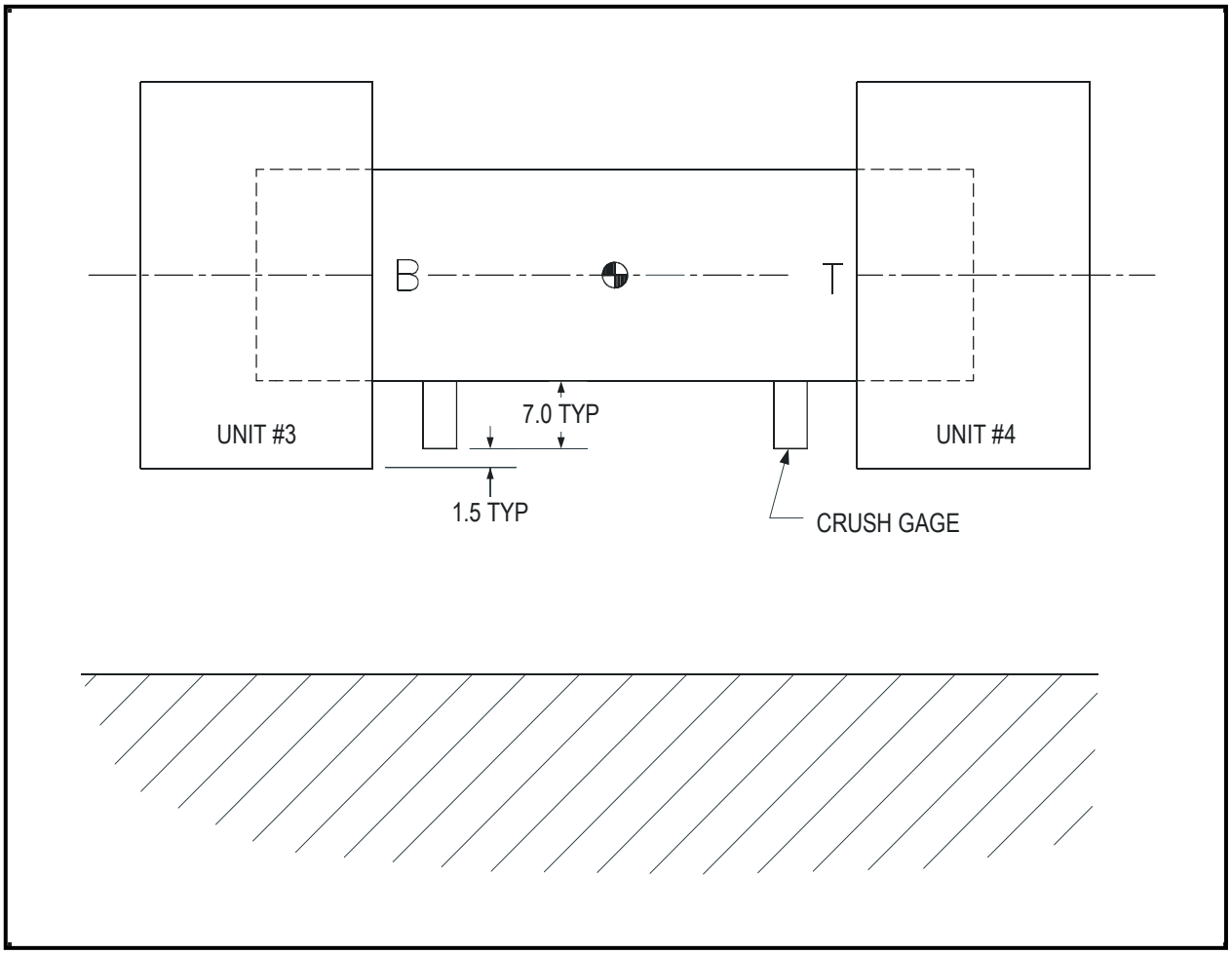

Figure 2.10.7-14 – Side Drop Configuration

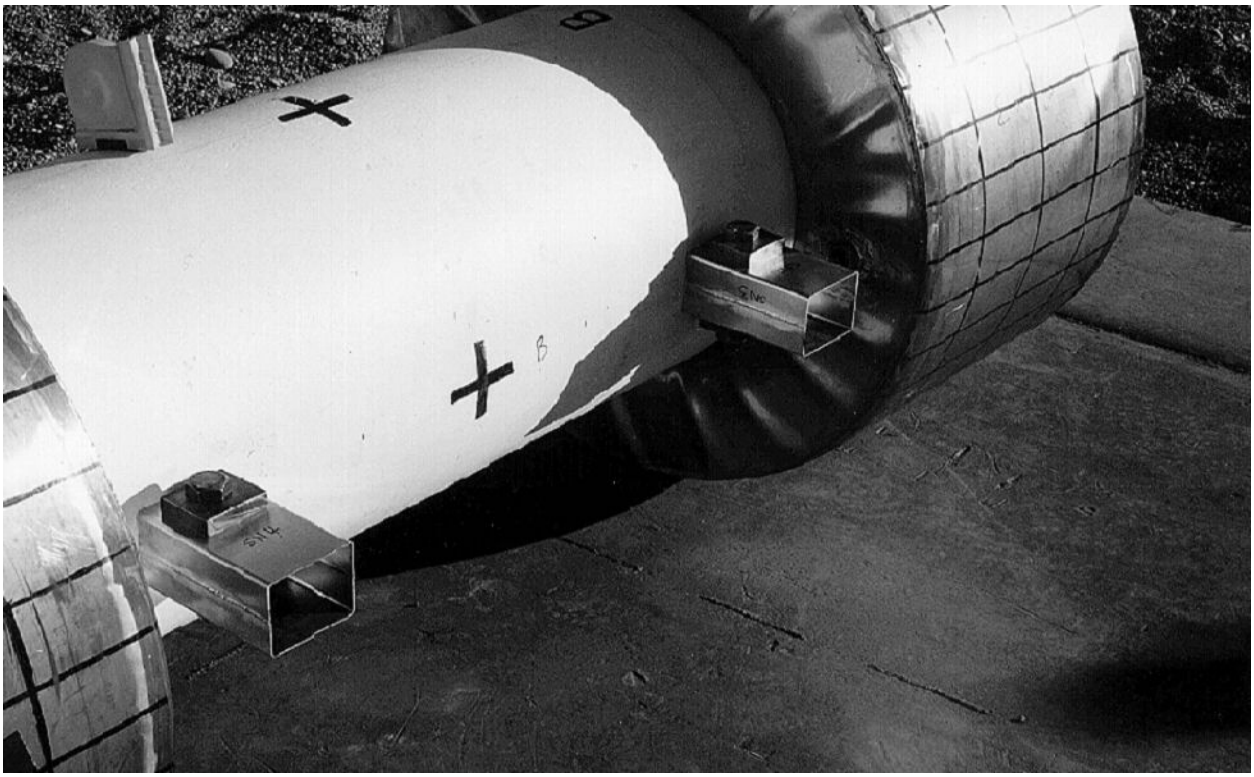

Figure 2.10.7-15 – Side Drop, Crush Gage Detail (Before Test)

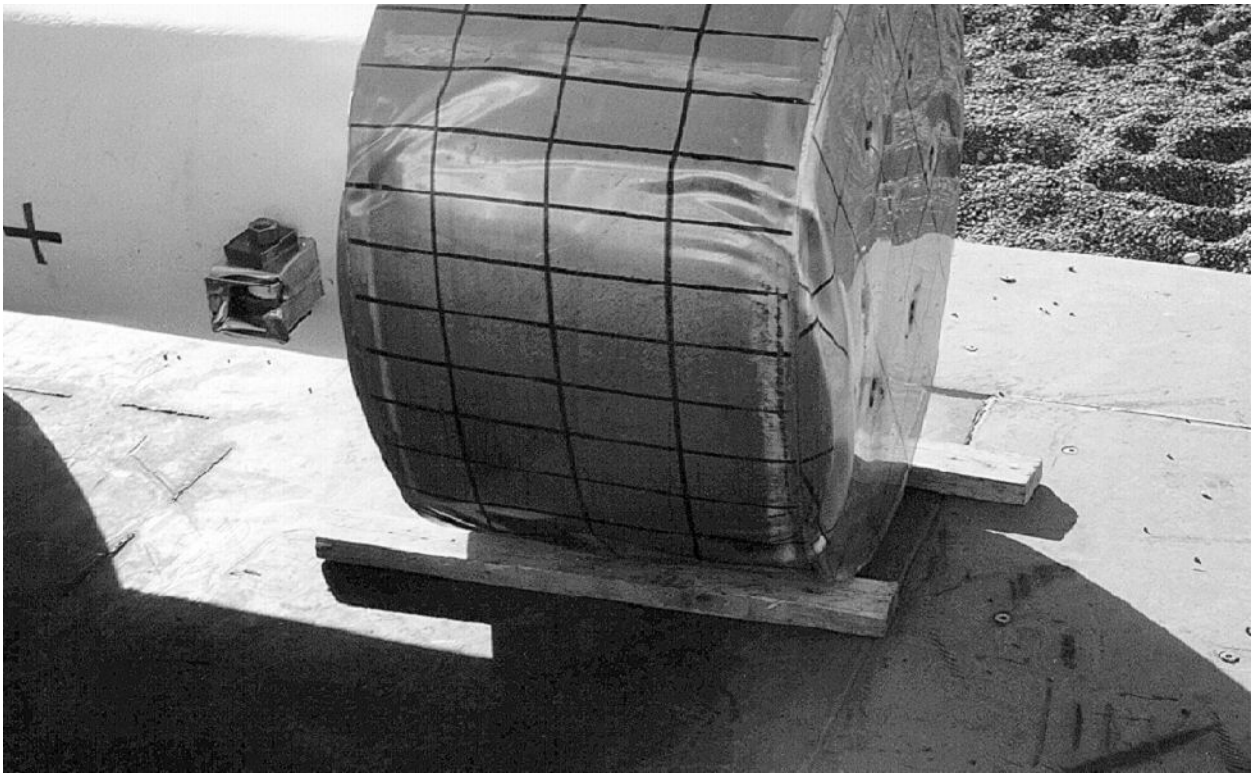

Figure 2.10.7-16 – Side Drop, Post-Test Configuration

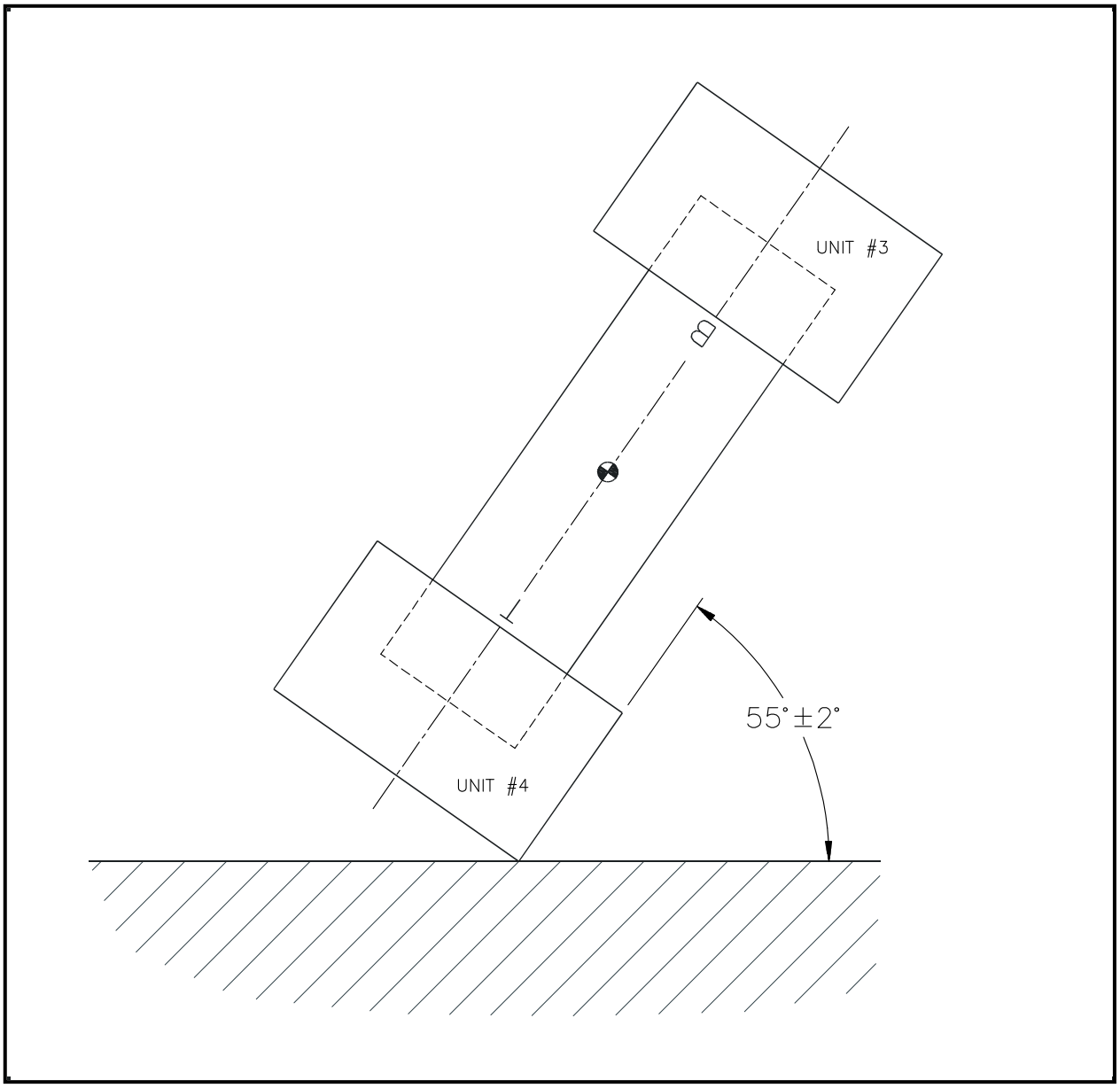

Figure 2.10.7-17 – Oblique Drop Configuration

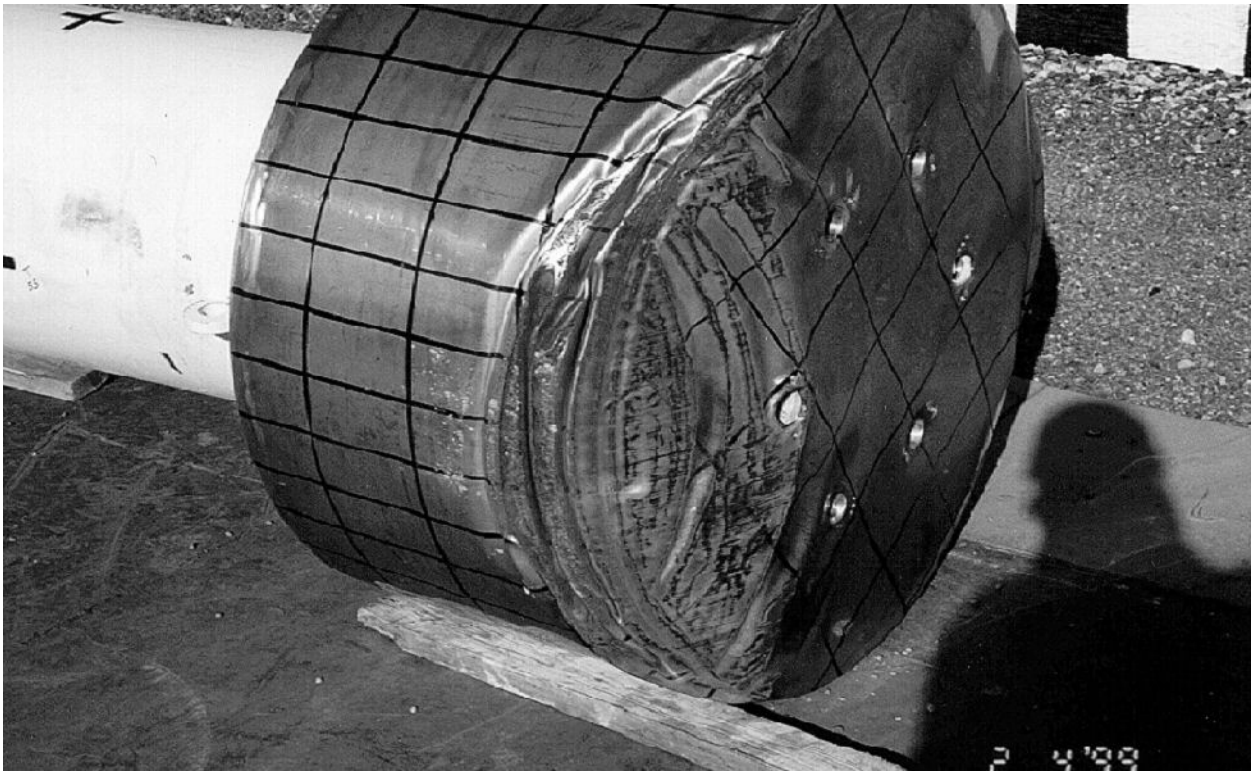

Figure 2.10.7-18 – Oblique Drop, Post-Test Configuration

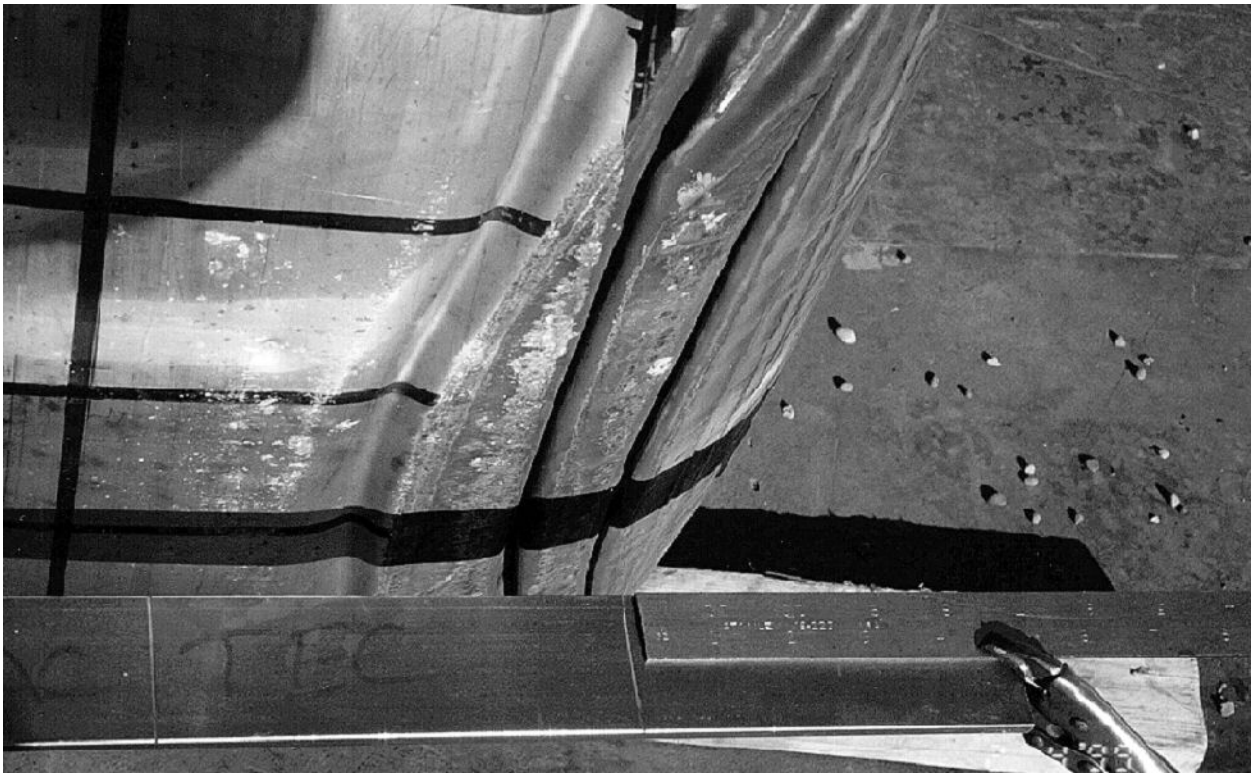

Figure 2.10.7-19 – Oblique Drop, Post-Test Configuration (Detail)

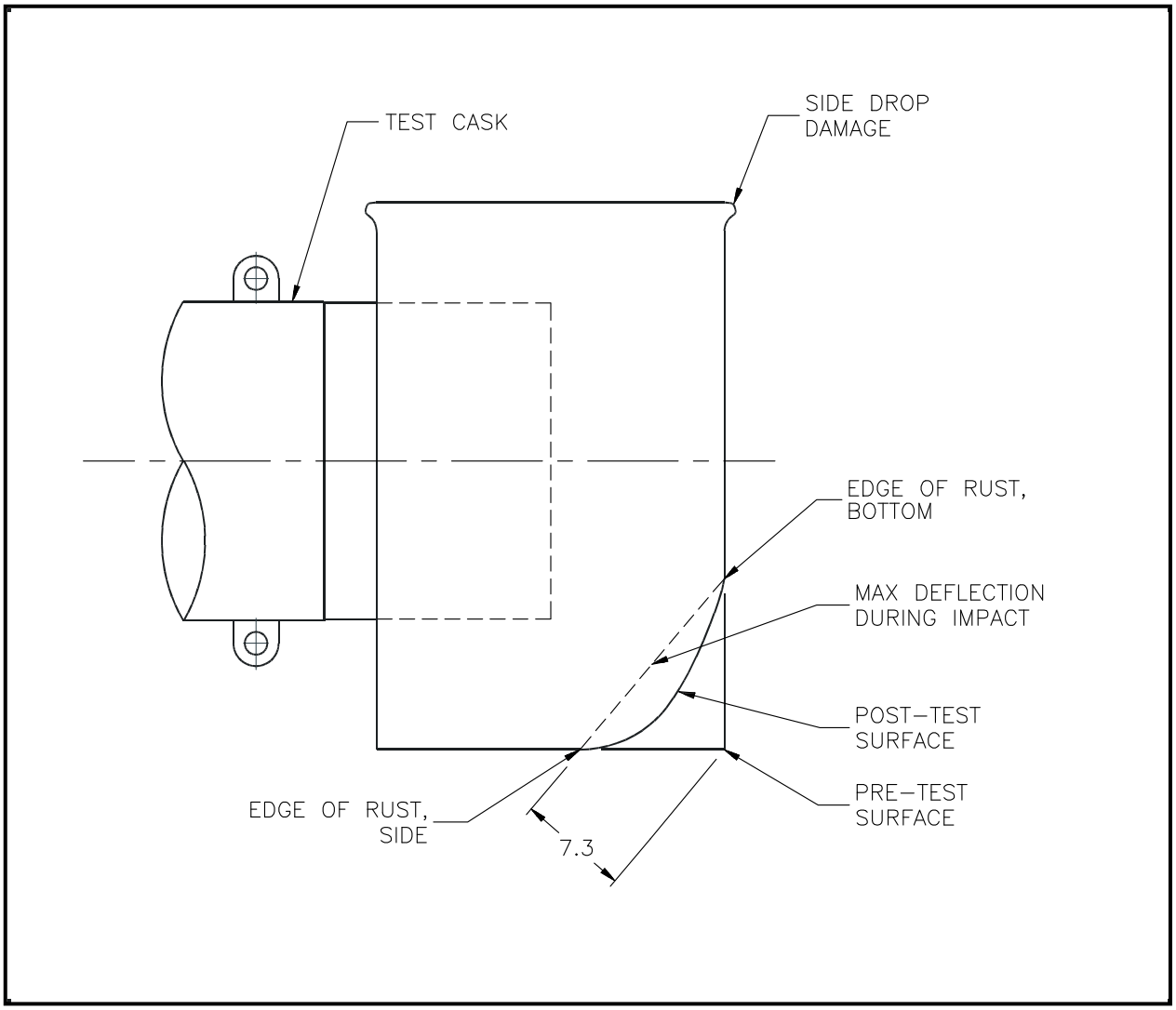

Figure 2.10.7-20 – Oblique Free Drop, Measurement of Deflection

This page intentionally left blank.

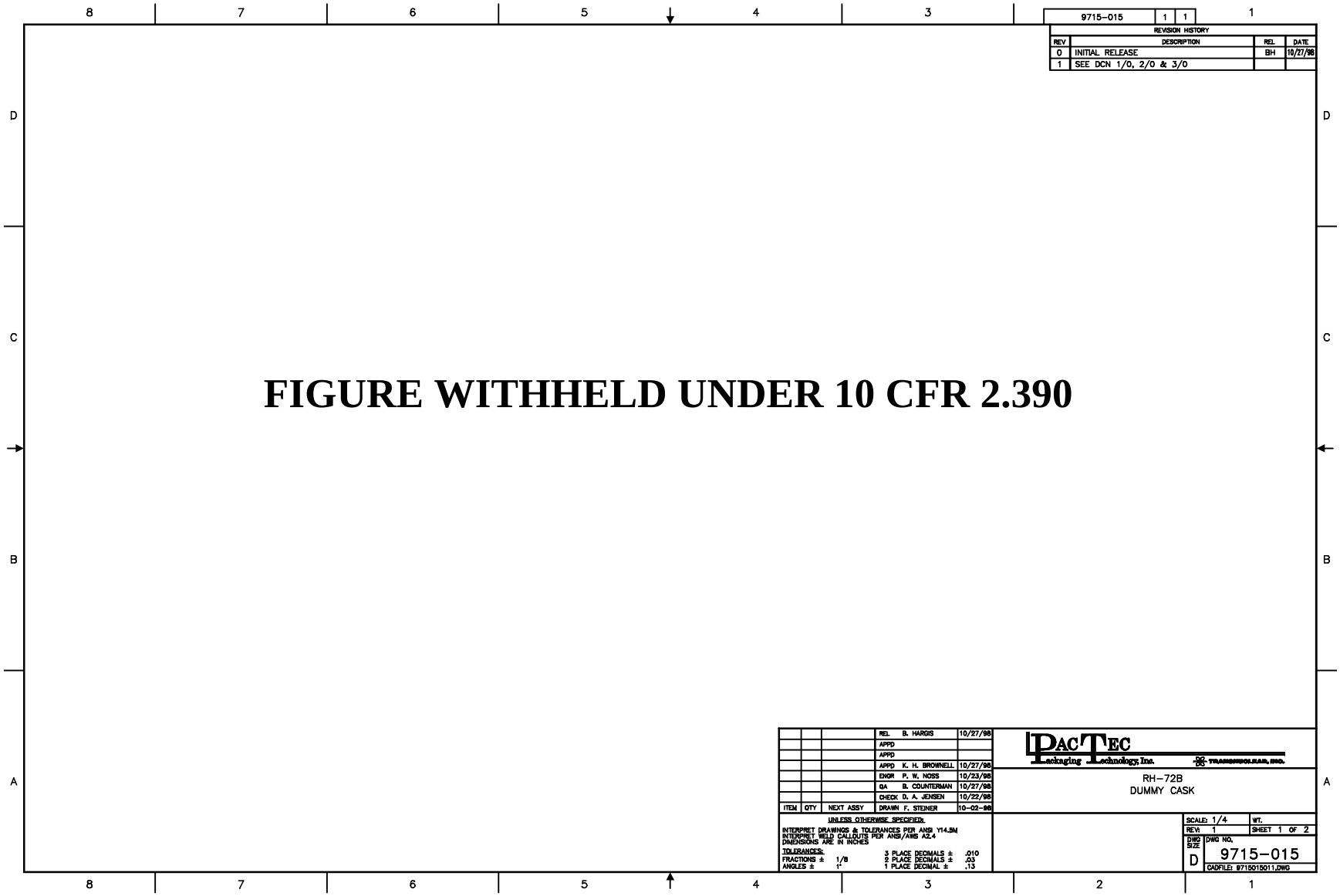

Figure 2.10.7-21 – Drawing 9715-015, *RH-72B Dummy Package*, Sheet 1

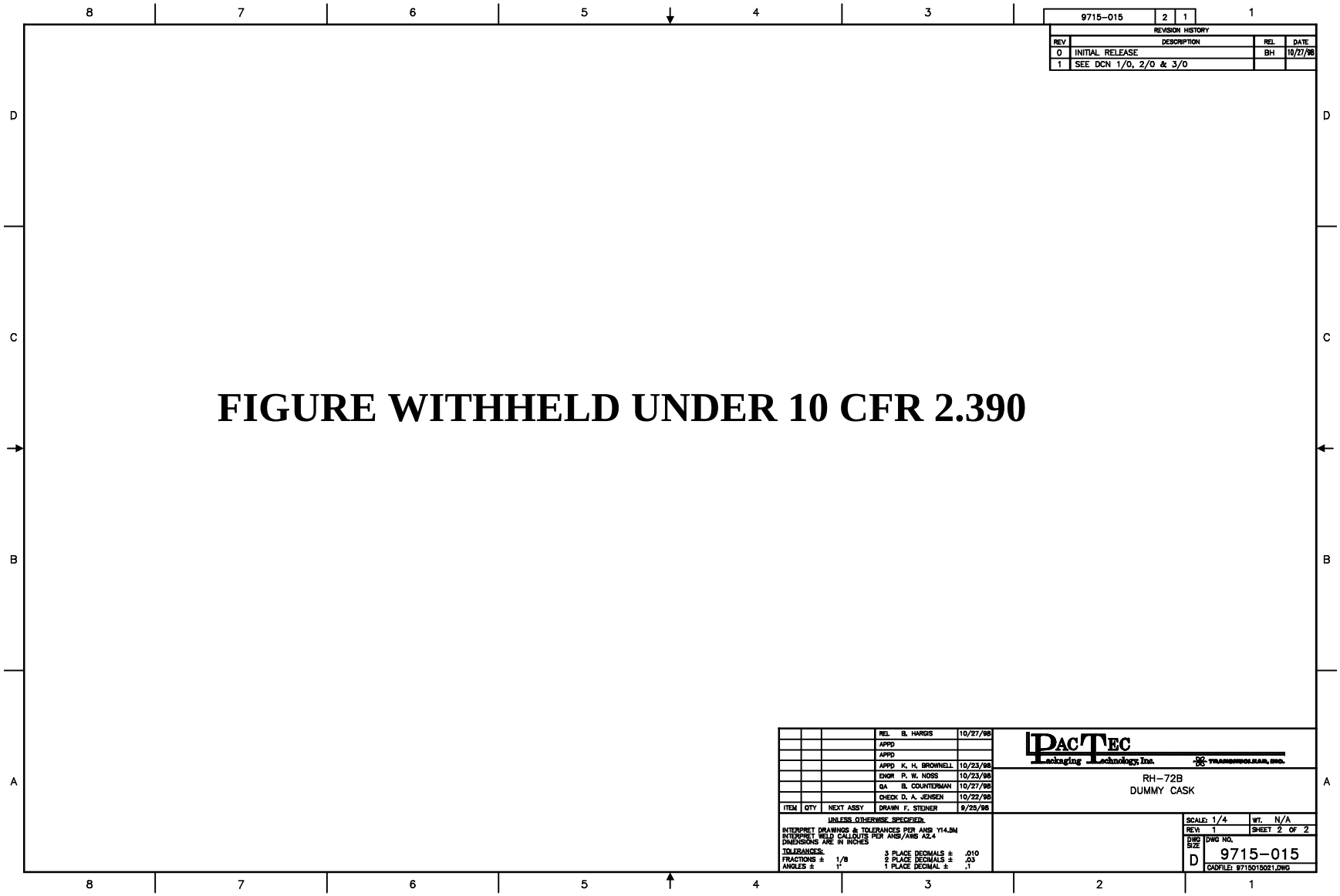

Figure 2.10.7-22 – Drawing 9715-015, *RH-72B Dummy Package*, Sheet 2

9715-010 | 1 | 1

REVISION HISTORY

REV	DESCRIPTION	REL	DATE
0	INITIAL RELEASE	BH	10/15/98
1	SEE DCN 1/0 THRU 7/0		

NOTES, UNLESS OTHERWISE SPECIFIED:

1. FABRICATE IN ACCORDANCE WITH PACTEC SPECIFICATION GF-001. SEE ALSO GENERAL NOTE 14.
2. MATERIALS LISTED IN THE MATERIAL COLUMN ARE FOR REFERENCE ONLY. MANUFACTURER SHALL CONFIRM ACTUAL REQUIREMENTS PRIOR TO FABRICATION.
3. ALL WELDING PROCEDURES AND PERSONNEL SHALL BE QUALIFIED IN ACCORDANCE WITH AWS D1.3 OR ASME CODE, SECTION IX AS APPLICABLE. WELD PROCEDURES AND WELDER QUALIFICATIONS SHALL BE AVAILABLE FOR AUDIT OR REVIEW.
4. WELDS SHALL BE LIQUID PENETRANT INSPECTED ON FINAL PASS IN ACCORDANCE WITH ASME CODE, SECTION III, DIVISION 1, SUBSECTION NB, ARTICLE NB-5000 AND SECTION V, ARTICLE 6.

5> INSTALL ASSEMBLY OF PARTS 5, 22 & 23 AND WELD TO PART 4 AFTER FOAMING.

6> HOLD FOR INTERIOR INSPECTION PRIOR TO MAKING FINAL ASSEMBLY WELD. SEE ALSO FLAG NOTES 8 & 11.

1 7> INSTALL FOAM PER PACTEC SPECIFICATION FP-020.

8. APPLY JOHNSON PASTE WAX TO ALL INTERIOR CAVITY SURFACES PRIOR TO FINAL CLOSURE WELDS.

9> VERIFY AND MATCH WITH OUTSIDE DIAMETER OF ITEM 1.

10> VERIFY AND MATCH WITH INSIDE DIAMETER OF ITEM 2.

11> PRIOR TO FINAL ASSEMBLY, COVER ALL 1/4 TURN FASTENER RECEPTACLES WITH LOW CHLORIDE DUCT TAPE, SEALING ALL AROUND.

12> CLEAN UP O.D. OF ITEM 18 TO ASSURE SMOOTH FIT OF ITEM 15 PRIOR TO WELDING.

13> ITEMS 7 & 8 SHALL BE CADIMIUM PLATED PER QQ-P-416c TYPE 1.

14. THIS WELDMENT IS A 1/2 SIZE TEST ARTICLE. THEREFORE WELD TOLERANCES NOTED IN GF-001, SEC 4.5 SHALL BE 1/2 THE TOLERANCE LISTED.

1 15> OPTION: ITEM 14 MAY BE TUBE MATERIAL, ASTM-A511, TYPE MT 304.

A3	A2	A1	ITEM	PART NO.	DESCRIPTION	
		24	28	97519A003	RIVET, DOME HEAD, ø3/32	MCMASTER-CARR
		12	27	R35	STUD RECEPTICLE	DZUS
		12	26	SR35-SS	STUD RETAINER SNAP RING	DZUS
		12	25	A35T12	1/4-TURN FASTENER	DZUS
		A/R	24		POLYURETHANE FOAM	GENERAL PLASTICS, FR3700 SERIES, 12.5 PCF
		3	23		WELDING SPUD, 3/4 NPT	LADISH 300 SERIES SST
		3	22		PIPE PLUG, 3/4 NPT, HEX SOCKET	PLASTIC
			21			
	1		20		PLATE, 3/8" THK X 11.0 O.D. X 9.5 I.D.	ASTM-A240, TYPE 304
	6		19		PLATE, 1/4" THK X 1.5 X 7.8	ASTM-A240, TYPE 304
	6		18		TUBE, ø1.5 O.D. X .25 WALL X 1.8	ASTM-A511, TYPE MT 304
	12		17		PLATE, 1/4" THK X 1.5 X 1.5	ASTM-A240, TYPE 304
	1		16		PLATE, 1/4" THK X ø23.0	ASTM-A240, TYPE 304
1			15		TUBE, ø1-5/8 O.D. X .06 WALL X 9.7	ASTM-A249 OR A269, TYPE 304
1			14		PLATE, 1/4" THK X ø2.0 O.D. X ø1.5 I.D.	ASTM-A240, TYPE 304
	1	1	13		ANGLE, FORMED, 16 GA (.06) SEE DETAIL	ASTM-A240, TYPE 304
		2	12		ANGLE, FORMED, 16 GA (.06) SEE DETAIL	ASTM-A240, TYPE 304
			11			
			10			
		6	8		SOC HD, 1" BLANK X 3.5 LG	ASTM-A320 L43
		6	7		SOC HD, 1" BLANK X 5.0 LG	ASTM-A320 L43
		1	6		SHEET, 16 GA (.06) X ø19.7	ASTM-A240, TYPE 304
		3	5		SHEET, 16 GA (.06) X ø3.1	ASTM-A240, TYPE 304
		1	4		SHEET, 16 GA (.06) X ø37.7 O.D.	ASTM-A240, TYPE 304
		1	3		SHEET, 16 GA (.06) X ø37.7 O.D.	ASTM-A240, TYPE 304
		1	2		SHEET, 16 GA (.06) X 22.63 X 119	ASTM-A240, TYPE 304
		1	1		SHEET, 13 GA (.09) X 11.5 X 66.5	ASTM-A240, TYPE 304
X		6	A3		BOLT ACCESS TUBE WELDMENT	
	X	1	A2		MOUNTING PLATE WELDMENT	
		X	A1		IMPACT LIMITER ASSEMBLY	

ASSEMBLY & QUANTITY — LIST OF MATERIAL

REL	B. HARGIS	10/15/98
APPD		
APPD		
APPD	K. H. BROWNELL	10/15/98
ENGR	R. A. JOHNSON	10/15/98
QA	B. COUNTERMAN	10/15/98
CHECK	F. STEINER	10/15/98
DRAWN	T. WAAGAN	9/14/98

ITEM | QTY | NEXT ASSY

UNLESS OTHERWISE SPECIFIED:
INTERPRET DRAWINGS & TOLERANCES PER ANSI Y14.5M
INTERPRET WELD CALLOUTS PER ANSI/AWS A2.4
DIMENSIONS ARE IN INCHES
TOLERANCES:
FRACTIONS ± N/A
ANGLES ± N/A
3 PLACE DECIMALS ± N/A
2 PLACE DECIMALS ± N/A
1 PLACE DECIMAL ± N/A

PACTEC Packaging Technology, Inc. — TRANSNUCLEAR, INC.

IMPACT LIMITER
TEST ARTICLE
RH-72 B

SCALE: NONE | WT. N/A
REV: 1 | SHEET 1 OF 4
DWG SIZE D | DWG NO. 9715-010
CADFILE: 971501011.DWG

Figure 2.10.7-23 – Drawing 9715-010, *Impact Limiter Test Article RH-72B*, Sheet 1

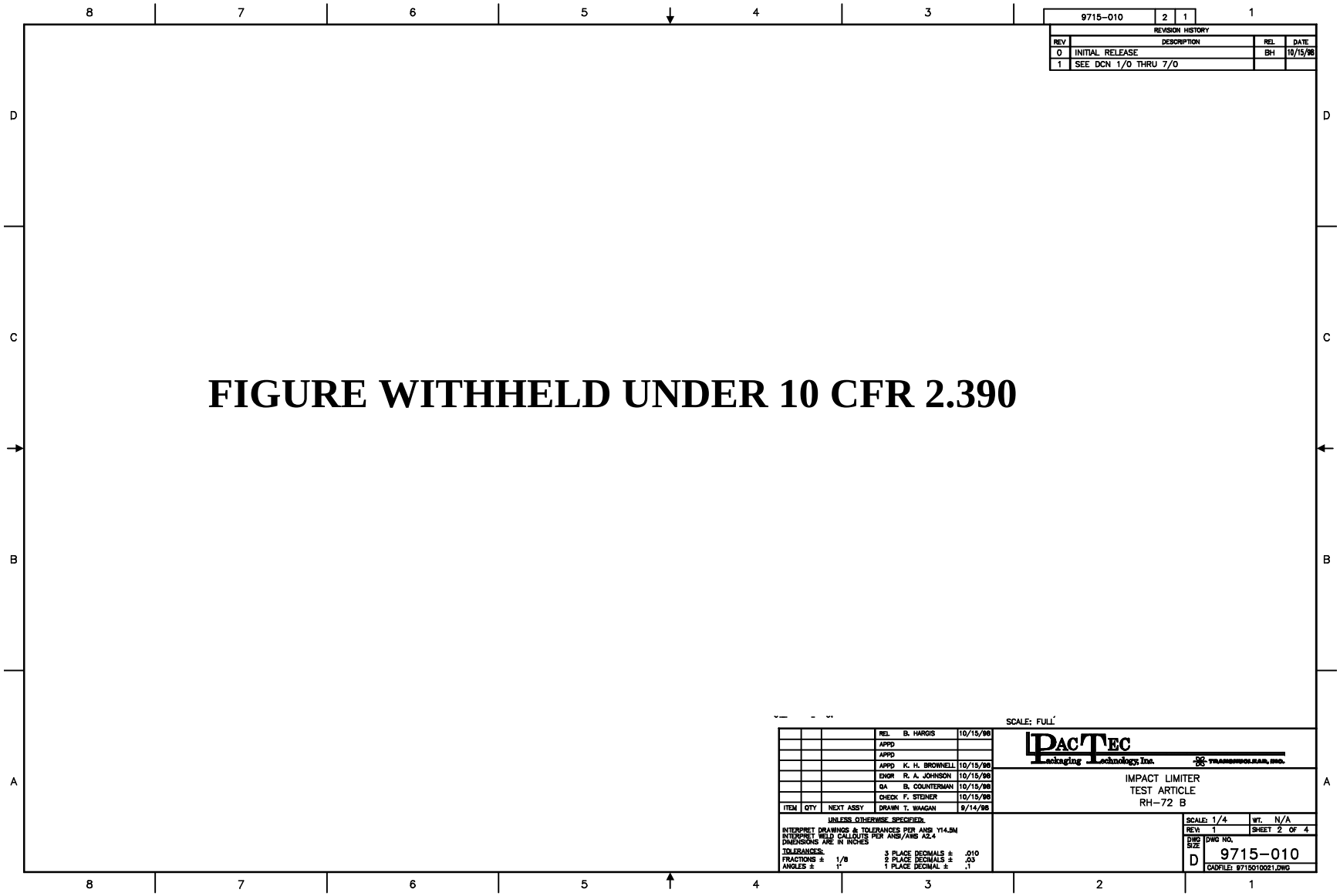

Figure 2.10.7-24 – Drawing 9715-010, *Impact Limiter Test Article RH-72B*, Sheet 2

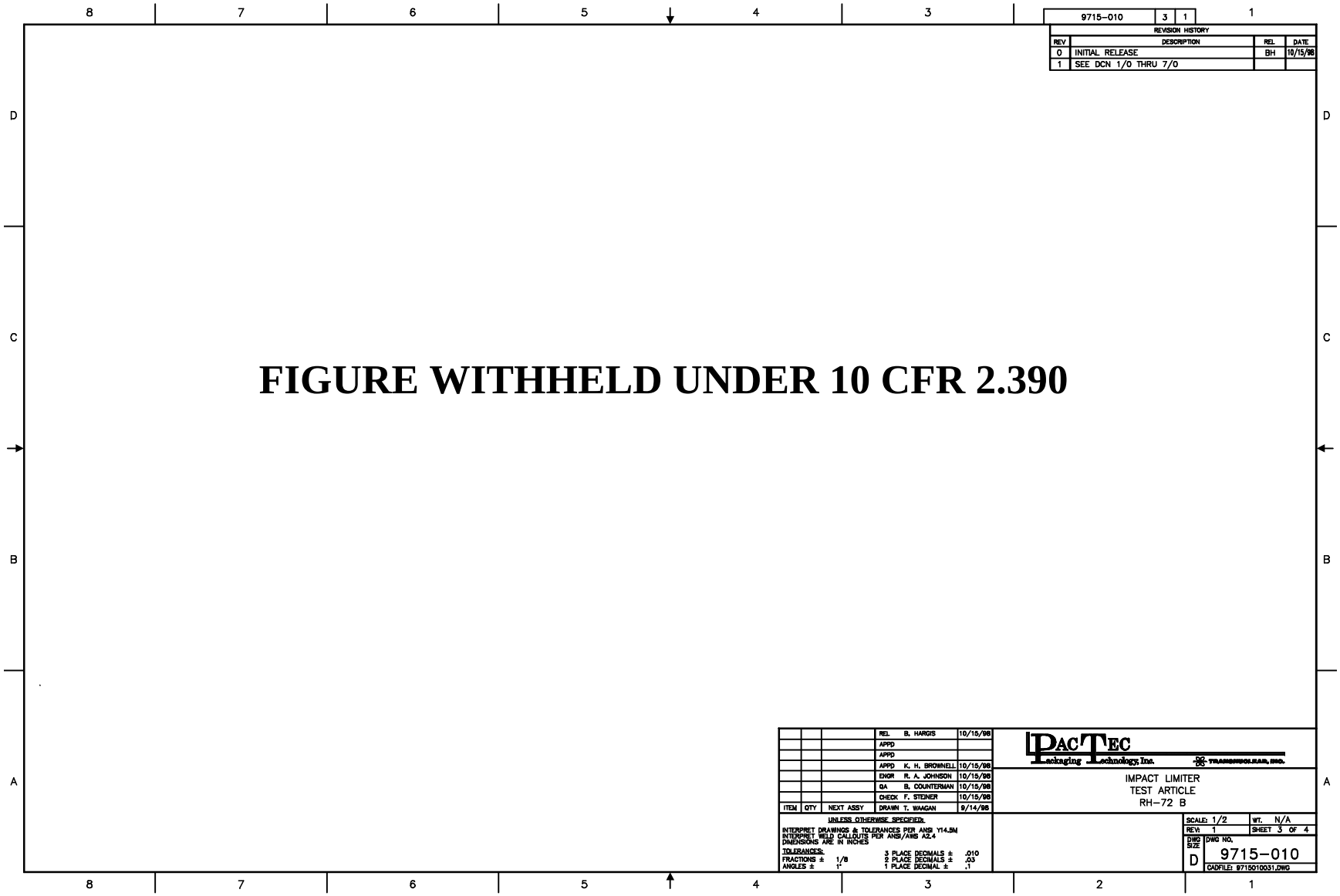

Figure 2.10.7-25 – Drawing 9715-010, *Impact Limiter Test Article RH-72B*, Sheet 3

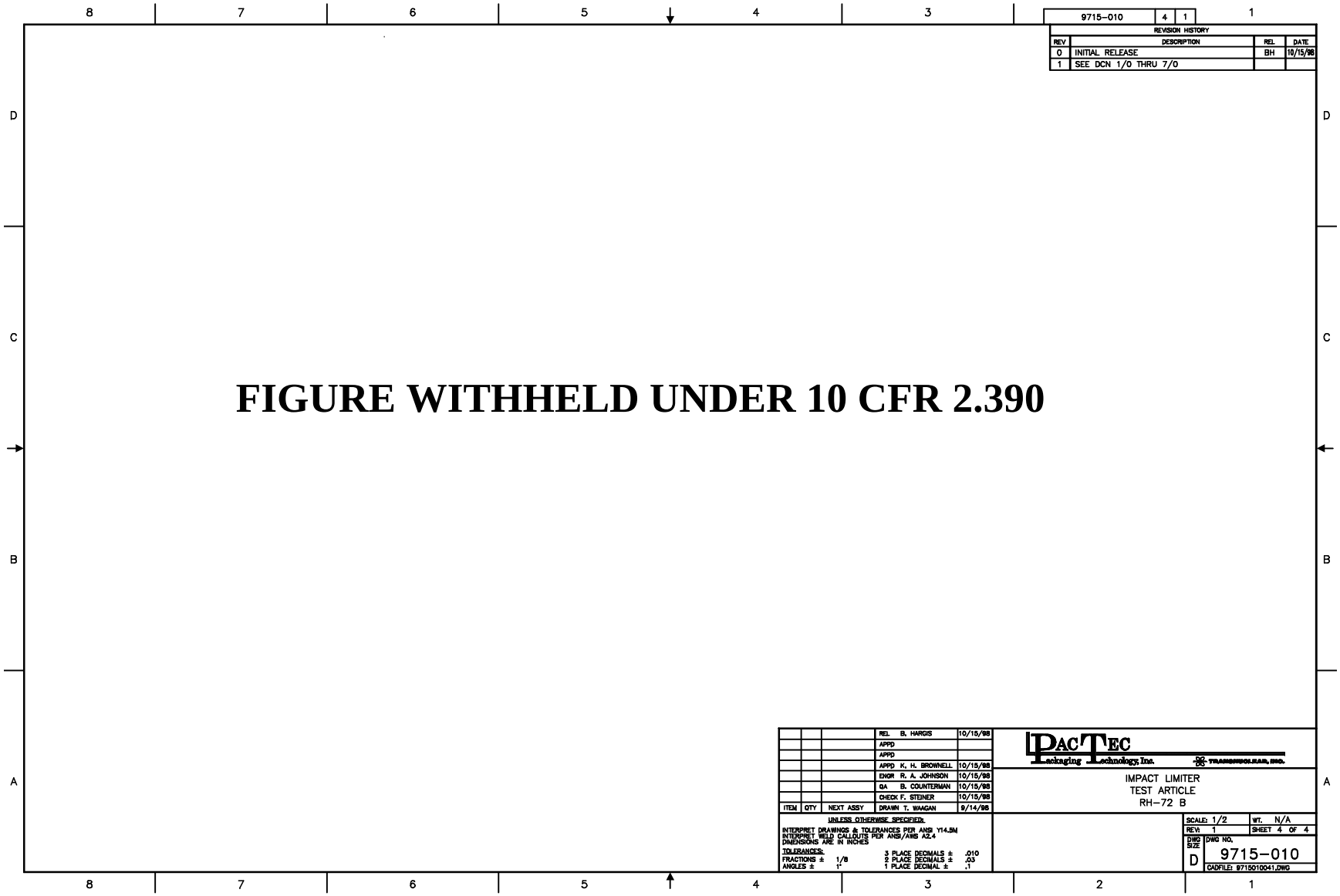

Figure 2.10.7-26 – Drawing 9715-010, *Impact Limiter Test Article RH-72B*, Sheet 4

2.10.8 Fabrication Stresses Due to Lead Pour

To determine fabrication stresses due to lead pour, assume a uniform steel and lead temperature of 620 ºF. The static head (pressure) due to a column of lead, p, is simply:

$$p = \gamma h = 54.1\,\text{psi}$$

where the specific weight of liquid lead, $\gamma = 0.386$ lb/in^3, and the height of the lead column, assuming an additional 11.0 inches for the overflow standpipe, h = 129.25 + 11.0 = 140.25 inches.

The physical properties of ASTM A240, Type 304, stainless steel used for the outer cask (OC) inner and outer shells are extracted from Table 2.3-1 in Section 2.3, *Mechanical Properties of Materials*, and are given in Table 2.10.8-1. The physical properties of lead (copperized) are extracted from Table 2.3-2 in Section 2.3, *Mechanical Properties of Materials*, and are given in Table 2.10.8-2. In the tables, E is Young's (elasticity) modulus, α is the coefficient of thermal expansion (mean from 70 ºF), and μ is Poisson's ratio.

At 70 ºF, the steel shell geometry is presented in Table 2.10.8-3.

2.10.8.1 Hoop Stress Evaluation after Heatup from 70 ºF to 620 ºF

At 620 ºF, without lead, the shells grow in radius and thickness in the following manner:

$$R' = R(1 + \alpha\Delta T)$$

$$t' = t(1 + \alpha\Delta T)$$

where the mean radius is R, the thickness is t, the coefficient of thermal expansion for stainless steel, $\alpha = 9.56(10)^{-6}$ in/in/ºF at 620 ºF, and the change in temperature, $\Delta T = 620 - 70 = 550$ ºF. Then, for each shell, given the dimensions in Table 2.10.8-3, the resulting dimensions are:

$$R'_i = (16.69)\left[1 + 9.56(10)^{-6}(550)\right] = 16.778\,\text{in}$$

$$t'_i = (1.00)\left[1 + 9.56(10)^{-6}(550)\right] = 1.005\,\text{in}$$

$$R'_o = (19.813)\left[1 + 9.56(10)^{-6}(550)\right] = 19.917\,\text{in}$$

$$t'_o = (1.50)\left[1 + 9.56(10)^{-6}(550)\right] = 1.508\,\text{in}$$

When filled with lead, the inner and outer OC shells are subjected to the 54.1 psi pressure head. This pressure head decreases the radius of the inner shell and increases the radius of the outer shell. Utilizing Table 29, Case 1b, of Roark[1], the change in radius of each shell, ΔR, is:

[1] R. J. Roark, W. C. Young, *Formulas for Stress and Strain*, 5th Edition, McGraw-Hill, Inc., New York, NY, 1975.

$$\Delta R'_i = \frac{q(R'_i)^2}{Et'_i} = \frac{(-54.1)(16.778)^2}{[25.2(10)^6](1.005)} = -0.000601\,\text{in}$$

$$\Delta R'_o = \frac{q(R'_o)^2}{Et'_o} = \frac{(54.1)(19.917)^2}{[25.2(10)^6](1.508)} = 0.000565\,\text{in}$$

In summary, as given in Table 2.10.8-4, the initial condition of the steel shells just before lead solidification at 620 ºF is:

$$R = R' + \Delta R' \pm \frac{t'}{2}$$

Lead experiences a decrease in volume of approximently 3.85% upon solidification. The lead pour fabrication process in Appendix 8.3.1, *Lead Installation Procedure*, carefully controls the solidification process such that lead solidification progresses upward from the bottom of the column. As the lead solidifies, it shrinks and liquid lead from above fills in between the solidifying lead and the OC inner and outer shells, thus maintaining a 54.1 psi pressure on the shells.

Eventually, the full annular region between the stainless steel shells is filled with lead, subjected to a pressure loading, as illustrated in Figure 2.10.8-1. (Note: the 54.1 psi pressure actually only exists at the base of the lead column, and linearly decreases to 6.2 psi at the top of the column; use of a uniform 54.1 psi pressure is, therefore, conservative.)

Under this loading, the outer radius of the inner shell, R_{iL} = 17.280 inches, and the inner radius of the outer shell, R_{oL} = 19.164 inches. The geometry of the unloaded lead shell is determined as follows:

$$R_{oL} = a + \Delta a \quad \Rightarrow \quad \Delta a = R_{oL} - a$$

$$R_{iL} = b + \Delta b \quad \Rightarrow \quad \Delta b = R_{iL} - b$$

$$t = L + \Delta L \quad \Rightarrow \quad \Delta L = t - L$$

where a, b, and L, are determined by superimposing Cases 1b and 1d from Table 32 of Roark[1]:

$$\Delta a = \frac{qab^2(2-\mu)}{E(a^2-b^2)} - \frac{qa[a^2(1-2\mu)+b^2(1+\mu)]}{E(a^2-b^2)} = R_{oL} - a$$

$$\Delta b = \frac{qb[a^2(1+\mu)+b^2(1-2\mu)]}{E(a^2-b^2)} - \frac{qa^2b(2-\mu)}{E(a^2-b^2)} = R_{iL} - b$$

$$\Delta L = \frac{qLb^2(1-2\mu)}{E(a^2-b^2)} - \frac{qLa^2(1-2\mu)}{E(a^2-b^2)} = t - L$$

Solving simultaneously,

$$a = 19.164076\,\text{in} \quad \Rightarrow \quad \Delta a = -7.6(10)^{-5}\,\text{in}$$

$$b = 17.280069\,\text{in} \quad \Rightarrow \quad \Delta b = -6.9(10)^{-5}\ \text{in}$$

$$L = 1.0000040\,\text{in} \quad \Rightarrow \quad \Delta L = -4.0(10)^{-6}\ \text{in}$$

where, at 620 ºF, the pressure, q = 54.1 psi, the elastic modulus of lead, $E = 1.36(10)^6$ psi, Poisson's ratio, $\mu = 0.45$, $R_{oL} = 19.164$ inches, $R_{iL} = 17.280$ inches, and t = 1.0 inch. These displacements are negligible, and are therefore subsequently ignored.

At this point, the hoop stress in the OC inner stainless steel shell, σ_i, is:

$$\sigma_i = \frac{pR_i}{t_i} = \frac{p\left(\frac{R_{iL} + R_{iS}}{2}\right)}{R_{iL} - R_{iS}} = -903\,\text{psi}$$

where the pressure, p = 54.1 psi, the inner shell outer radius, $R_{iL} = 17.280$ inches, and the inner shell inner radius, $R_{iS} = 16.275$ inches.

The hoop stress in the OC outer stainless steel shell, σ_o, is:

$$\sigma_o = \frac{pR_o}{t_o} = \frac{p\left(\frac{R_{oS} + R_{oL}}{2}\right)}{R_{oS} - R_{oL}} = 715\,\text{psi}$$

where the pressure, p = 54.1 psi, the outer shell outer radius, $R_{oS} = 20.672$ inches, and the outer shell inner radius, $R_{oL} = 19.164$ inches.

2.10.8.2 Hoop Stress Evaluation after Cooldown from 620 ºF to 70 ºF

In cooling from lead solidification at 620 ºF to a nominal ambient temperature of 70 ºF, the lead shell, with its greater coefficient of thermal expansion/contraction, tends to shrink onto the inner stainless steel shell. If the lead is allowed to cool freely and there is no interference, the cooling lead shell would assume the following geometry:

$$R'_L = R_L(1 + \alpha\Delta T) = 18.018\,\text{in}$$

$$t'_L = t_L(1 + \alpha\Delta T) = 1.863\,\text{in}$$

and,

$$R'_{oL} = R'_L + \frac{t'_L}{2} = 18.950\,\text{in}$$

$$R'_{iL} = R'_L - \frac{t'_L}{2} = 17.087\,\text{in}$$

where the coefficient of thermal expansion for lead, $\alpha = 20.39(10)^{-6}$ in/in/ºF at 620 ºF (a conservative value), the change in temperature, $\Delta T = 70 - 620 = -550$ ºF, the lead mean radius, $R_L = ½(R_{oL} + R_{iL}) = 18.222$ inches, and the lead thickness, $t_L = R_{oL} - R_{iL} = 1.884$ inches.

Stress-free dimensions for the OC inner shell have been previously determined and are repeated once again for convenience in Table 2.10.8-5.

The interference between the lead and stainless steel inner shell, δ, is thus the difference between the unstressed lead inner radius and the unstressed inner shell outer radius at 70 ºF:

$$\delta = 17.190 - 17.087 = 0.103 \text{ in}$$

Using a press (interference) fit equation, Equation 7.33 of Juvinall[2], the interference pressure, p, at a temperature of 70 ºF is:

$$\delta = \frac{b_L p}{E_L}\left(\frac{c^2 + b_L^2}{c^2 - b_L^2} + \mu_L\right) + \frac{b_S p}{E_S}\left(\frac{b_S^2 + a^2}{b_S^2 - a^2} - \mu_S\right)$$

Rearranging terms,

$$p = \frac{\delta}{\frac{b_L}{E_L}\left(\frac{c^2 + b_L^2}{c^2 - b_L^2} + \mu_L\right) + \frac{b_S}{E_S}\left(\frac{b_S^2 + a^2}{b_S^2 - a^2} - \mu_S\right)} = 1{,}225 \text{ psi}$$

where, from Table 2.10.8-5, the inner stainless steel shell inner radius, a = 16.190 inches, the inner stainless steel shell outer radius, b_S = 17.190 inches, the lead shell inner radius, b_L = 17.087 inches, the lead shell outer radius, c = 18.950 inches, the stainless steel elastic modulus and Poisson's ratio, $E_S = 28.3(10)^6$ psi and $\mu_S = 0.3$, respectively (from Table 2.10.8-1) at 70 ºF, the lead elastic modulus and Poisson's ratio, $E_L = 2.34(10)^6$ psi and $\mu_L = 0.45$, respectively (from Table 2.10.8-2) at 70 ºF, and the interface deflection, $\delta = b_S - b_L = 0.103$ inches.

An interface pressure of 1,225 psi corresponds to a lead shell hoop stress, σ_L, of:

$$\sigma_L = p\left(\frac{c^2 + b_L^2}{c^2 - b_L^2}\right) = 11{,}881 \text{ psi}$$

Because of lead's low yield strength, this stress level cannot be sustained.

To fully accommodate the 0.103-inch radial interference, the lead would be required to see a strain of 0.103/17.087 = 0.00603 in/in, or 0.603%. Extrapolating from Figure 2.3-5 in Section 2.3, *Mechanical Properties of Materials*, a hoop stress of approximately 820 psi would exist in the lead for this strain. With this hoop stress, the effective interface pressure, p, would then be:

$$p = \frac{\sigma_L}{\left(\frac{c^2 + b_L^2}{c^2 - b_L^2}\right)} = 84.6 \text{ psi}$$

[2] Robert C. Juvinall, *Engineering Considerations of Stress, Strain, and Strength*, McGraw-Hill Book Company, New York, NY, 1967.

Note that the deflection, δ, for the inner stainless steel shell with a pressure of -84.6 psi is:

$$\delta = \frac{b_S p}{E_S}\left(\frac{b_S^2 + a^2}{b_S^2 - a^2} - \mu_S\right) = -0.00084\,\text{in}$$

which can be conservatively neglected for the inner stainless steel shell hoop stress calculations.

For a pressure of -84.6 psi at 70 ºF, the hoop stress in the inner stainless steel shell, σ_S, is:

$$\sigma_S = p\left(\frac{b_S^2 + a^2}{b_S^2 - a^2}\right) = -1{,}413\,\text{psi}$$

From Figure 2.3-8 in Section 2.3, *Mechanical Properties of Materials*, it is concluded that in 2-to-3 weeks, at 70 ºF, the lead hoop stress, σ_L, would creep to a value of approximately 300 psi (holding an essentially constant 0.603% strain in the lead). The corresponding interface pressure, p, and inner stainless steel shell hoop stress, σ_S, would be:

$$p = \frac{\sigma_L}{\left(\frac{c^2 + b_L^2}{c^2 - b_L^2}\right)} = 31.0\,\text{psi}$$

$$\sigma_S = -p\left(\frac{b_S^2 + a^2}{b_S^2 - a^2}\right) = -518\,\text{psi}$$

To determine the stress-free temperature, T_o, unloading with heat-up would be elastic and, thus, using the previous interference fit equation:

$$\delta = \frac{b_L p}{E_L}\left(\frac{c^2 + b_L^2}{c^2 - b_L^2} + \mu_L\right) + \frac{b_S p}{E_S}\left(\frac{b_S^2 + a^2}{b_S^2 - a^2} - \mu_S\right) = R(\alpha_L - \alpha_S)(T_o - 70)$$

Rewriting the equation in terms of the stress-free temperature, T_o, gives:

$$T_o = \frac{\frac{b_L p}{E_L}\left(\frac{c^2 + b_L^2}{c^2 - b_L^2} + \mu_L\right) + \frac{b_S p}{E_S}\left(\frac{b_S^2 + a^2}{b_S^2 - a^2} - \mu_S\right)}{R(\alpha_L - \alpha_S)} + 70 = 89.9\,°\text{F}$$

where, as before, from Table 2.10.8-5, the inner stainless steel shell inner radius, a = 16.190 inches, the inner stainless steel shell outer radius, b_S = 17.190 inches, the lead shell inner radius, b_L = 17.087 inches, the lead shell outer radius, c = 18.950 inches, the stainless steel elastic modulus, Poisson's ratio, and coefficient of thermal expansion, $E_S = 28.3(10)^6$ psi, $\mu_S = 0.3$, and $\alpha_S = 8.46(10)^{-6}$ in/in/ºF, respectively (from Table 2.10.8-1) at 70 ºF, the lead elastic modulus, Poisson's ratio, and coefficient of thermal expansion, $E_L = 2.34(10)^6$ psi, $\mu_L = 0.45$, and $\alpha_L = 16.07(10)^{-6}$ in/in/ºF, respectively (from Table 2.10.8-2) at 70 ºF, the inner steel/lead interface radius, R = b_s = 17.190 inches, and the interface pressure, p = 31.0 psi.

2.10.8.3 Hoop Stress Evaluation after Cooldown from 90 ºF to -20 ºF

Next, consider cooling to -20 ºF (ΔT = 110 ºF) for determining the worst-case hoop stress on the inner stainless steel shell during all regulatory drop events. The stainless steel and lead shell initial conditions are determined based on the previously defined dimensions of a, b_S, b_L, and c at 70 ºF as follows:

$$a = (16.190)(1 + \alpha_S \Delta T) = 16.175 \text{ in}$$

$$b_S = (17.190)(1 + \alpha_S \Delta T) = 17.174 \text{ in}$$

$$b_L = (17.087)(1 + \alpha_L \Delta T) = 17.058 \text{ in}$$

$$c = (18.950)(1 + \alpha_L \Delta T) = 18.917 \text{ in}$$

$$\delta = b_S - b_L = 0.116 \text{ in}$$

where the thermal expansion coefficient for stainless steel, $\alpha_S = 8.21(10)^{-6}$ in/in/ºF (extrapolated from Table 2.10.8-1) at -20 ºF, and the thermal expansion coefficient for lead, $\alpha_L = 15.7(10)^{-6}$ in/in/ºF (extrapolated from Table 2.10.8-2) at -20 ºF.

To fully accommodate the 0.116-inch radial interference, the lead would be required to see a strain of 0.116/17.058 = 0.00680 in/in, or 0.680%. Extrapolating from Figure 2.3-5 in Section 2.3, *Mechanical Properties of Materials*, a hoop stress, σ_L, of approximately 1,060 psi would exist in the lead for this strain. With this hoop stress, the effective interface pressure, p, would then be:

$$p = \frac{\sigma_L}{\left(\frac{c^2 + b_L^2}{c^2 - b_L^2}\right)} = 109 \text{ psi}$$

For a pressure of -109 psi at -20 ºF, and conservatively neglecting the beneficial effects of lead creep, the hoop stress in the inner stainless steel shell, σ_S, is:

$$\sigma_S = -p\left(\frac{b_S^2 + a^2}{b_S^2 - a^2}\right) = -1{,}821 \text{ psi}$$

2.10.8.4 Hoop Stress Evaluation after Cooldown from 90 ºF to -40 ºF

Finally, consider cooling to -40 ºF (ΔT = 130 ºF) for determining the worst-case hoop stress on the inner stainless steel shell. The stainless steel and lead shell initial conditions are determined based on the previously defined dimensions of a, b_S, b_L, and c at 70 ºF as follows:

$$a = (16.190)(1 + \alpha_S \Delta T) = 16.173 \text{ in}$$

$$b_S = (17.190)(1 + \alpha_S \Delta T) = 17.172 \text{ in}$$

$$b_L = (17.087)(1+\alpha_L \Delta T) = 17.052 \text{ in}$$

$$c = (18.950)(1+\alpha_L \Delta T) = 18.912 \text{ in}$$

$$\delta = b_S - b_L = 0.120 \text{ in}$$

where the thermal expansion coefficient for stainless steel, $\alpha_S = 8.15(10)^{-6}$ in/in/ºF (extrapolated from Table 2.10.8-1) at -40 ºF, and the thermal expansion coefficient for lead, $\alpha_L = 15.6(10)^{-6}$ in/in/ºF (extrapolated from Table 2.10.8-2) at -40 ºF.

To fully accommodate the 0.120-inch radial interference, the lead would be required to see a strain of 0.120/17.052 = 0.00704 in/in, or 0.704%. Extrapolating from Figure 2.3-5 in Section 2.3, *Mechanical Properties of Materials*, a hoop stress, σ_L, of approximately 1,070 psi would exist in the lead for this strain. With this hoop stress, the effective interface pressure, p, would then be:

$$p = \frac{\sigma_L}{\left(\frac{c^2 + b_L^2}{c^2 - b_L^2}\right)} = 110 \text{ psi}$$

For a pressure of -110 psi at -40 ºF, and conservatively neglecting the beneficial effects of lead creep, the hoop stress in the inner stainless steel shell, σ_S, is:

$$\sigma_S = p\left(\frac{b_S^2 + a^2}{b_S^2 - a^2}\right) = -1{,}837 \text{ psi}$$

2.10.8.5 Axial Stress Evaluation after Cooldown from 620 ºF to -20 ºF

The preceeding calculations deal only with the determination of hoop stresses. Axial stresses will also develop in the inner stainless steel shell and lead shell due to axial shrinkage of the lead. In cooling from 620 ºF to 90 ºF (stress-free condition of the lead), then from 90 ºF to -20 ºF, the axial strain in the lead, ε, assuming bonding of the lead to the inner stainless steel shell, would be:

$$\varepsilon = \left[(\alpha_L - \alpha_S)\Delta T\right]_{620} + \left[(\alpha_L - \alpha_S)\Delta T\right]_{-20} = 0.00656 \text{ in/in} = 0.656\% \text{ strain (tensile)}$$

where, for cooldown from 620 ºF to 90 ºF, the lead and stainless steel coefficients of thermal expansion, $\alpha_S = 9.56(10)^{-6}$ in/in/ºF (from Table 2.10.8-1) and $\alpha_L = 20.39(10)^{-6}$ in/in/ºF (from Table 2.10.8-2), respectively, and ΔT = 620 – 90 = 530 ºF, and for cooldown from 90 ºF to -20 ºF, the lead and stainless steel coefficients of thermal expansion, $\alpha_S = 8.21(10)^{-6}$ in/in/ºF (extrapolated from Table 2.10.8-1) and $\alpha_L = 15.7(10)^{-6}$ in/in/ºF (extrapolated from Table 2.10.8-2), respectively, and ΔT = 90 – (-20) = 110 ºF.

Extrapolating from Figure 2.3-5 in Section 2.3, *Mechanical Properties of Materials*, an axial stress, σ_L, of approximately 1,040 psi would exist in the lead for this strain. The effective axial force in the lead shell, P_a, would then be:

$$P_a = \sigma_L A_L = 205{,}532 \text{ lb}$$

where the cross-sectional area of the lead shell, $A_L = \pi(c^2 - b_S^2) = 197.627$ in^2, the outer lead shell radius, c = 18.917 inches, and the inner stainless steel shell outer radius, $b_S = 17.174$ inches, respectively (from Appendix 2.10.8.3, *Hoop Stress Evaluation after Cooldown from 90 ºF to -20 ºF*).

From equilibrium, this same force could develop in the inner stainless steel shell. Thus, at a temperature of -20 ºF, the compressive axial stress in the inner steel shell would be:

$$\sigma_a = \frac{P_a}{A_S} = -1{,}963 \text{ psi}$$

where the axial force, P_a = -205,532 lb, and the cross-sectional area of the inner stainless steel shell, $A_S = \pi(b_S^2 - a^2) = 104.664$ in^2, and the inner and outer lead shell radii, $b_S = 17.174$ inches and a = 16.175 inches, respectively (from Appendix 2.10.8.3, *Hoop Stress Evaluation after Cooldown from 90 ºF to -20 ºF*.

This stress value is a conservative estimate in that it assumes the OC inner shell is incompressible under axial load and that no load would develop in the outer shell (i.e., any compressibility of the inner shell would reduce the lead strain and resultant axial forces and stresses).

2.10.8.6 Axial Stress Evaluation after Cooldown from 620 ºF to -40 ºF

In cooling from 620 ºF to 90 ºF (stress-free condition of the lead), then from 90 ºF to -40 ºF, the axial strain in the lead, ε, assuming bonding of the lead to the inner stainless steel shell, would be:

$$\varepsilon = \left[(\alpha_L - \alpha_S)\Delta T\right]_{620} + \left[(\alpha_L - \alpha_S)\Delta T\right]_{-40} = 0.00671 \text{ in/in} = 0.671\% \text{ strain (tensile)}$$

where, for cooldown from 620 ºF to 90 ºF, the lead and stainless steel coefficients of thermal expansion, $\alpha_S = 9.56(10)^{-6}$ in/in/ºF (from Table 2.10.8-1) and $\alpha_L = 20.39(10)^{-6}$ in/in/ºF (from Table 2.10.8-2), respectively, and ΔT = 620 – 90 = 530 ºF, and for cooldown from 90 ºF to -40 ºF, the lead and stainless steel coefficients of thermal expansion, $\alpha_S = 8.15(10)^{-6}$ in/in/ºF (extrapolated from Table 2.10.8-1) and $\alpha_L = 15.6(10)^{-6}$ in/in/ºF (extrapolated from Table 2.10.8-2), respectively, and ΔT = 90 – (-40) = 130 ºF.

Extrapolating from Figure 2.3-5 in Section 2.3, *Mechanical Properties of Materials*, an axial stress, σ_L, of approximately 1,050 psi would exist in the lead for this strain. The effective axial force in the lead shell, P_a, would then be:

$$P_a = \sigma_L A_L = 207{,}111 \text{ lb}$$

where the cross-sectional area of the lead shell, $A_L = \pi(c^2 - b_S^2) = 197.248$ in^2, the outer lead shell radius, c = 18.912 inches, and the inner stainless steel shell outer radius, $b_S = 17.172$ inches, respectively (from Appendix 2.10.8.4, *Hoop Stress Evaluation after Cooldown from 90 ºF to -40 ºF*).

From equilibrium, this same force could develop in the inner stainless steel shell. Thus, at a temperature of -40 ºF, the compressive axial stress in the inner steel shell would be:

$$\sigma_a = \frac{P_a}{A_S} = -1{,}979 \text{ psi}$$

where the axial force, P_a = -207,111 lb, and the cross-sectional area of the inner stainless steel shell, $A_S = \pi(b_S^2 - a^2) = 104.652$ in^2, and the inner and outer lead shell radii, b_S = 17.172 inches and a = 16.173 inches, respectively (from Appendix 2.10.8.4, *Hoop Stress Evaluation after Cooldown from 90 ºF to -40 ºF*.

Again, this calculation conservatively assumes that the OC inner shell is incompressible under an axial load and that no load develops in the outer shell.

2.10.8.7 Transient Effects

The preceding calculations in this appendix are based on the assumption that the OC inner and outer shells and the lead between them are always at the same temperature during cooldown. Although this ideal condition could never be fully achieved in practice, the procedures used for lead pour (see Appendix 8.3.1, *Lead Installation Procedure*) are set up to minimize the temperature differences that could occur. To control the cooldown process, thermocouples are used to monitor temperatures of the OC inner and outer shells. Thermocouples on the outer shell are located directly opposite those on the inner shell, and the maximum acceptable temperature difference indicated by any opposing pair of thermocouples is limited to 300 ºF. Temperature differences are not expected to ever be this great in practice, but even if they were, the following calculations indicate that they would be acceptable. An additional control is placed on the thermocouple readings so that no single thermocouple reading may change by more than 100 ºF in any 30-minute period. Recognizing the good conductivity exhibited by stainless steel and lead, this control essentially eliminates the consequences of transient effects.

Temperature differences between the inner and outer shells are of little consequence since the axial tie between the shells is made after lead cooldown, when a uniform temperature exists throughout the OC. By welding the outer shell to the base after the cooldown process, temperature differences between the two shells will not cause axial stresses to develop in the shells during cooldown. It can be shown that if the weld were made prior to lead pour, a condition where the inner shell is 300 ºF hotter than the outer shell will result in elastically calculated axial stresses that would be unacceptable, thus establishing the need for final welding after cooldown.

The remaining issue to be addressed is that of temperature differences between the inner shell and the lead. The 300 ºF maximum difference in temperature between the inner and outer shells could conservatively be used as the maximum temperature difference between the inner shell and the lead. Furthermore, if the inner shell is cooler than the lead, the previous calculations will remain conservative. Specifically, with lower temperatures for the inner shell than for the lead, the interference and associated contact pressure between the shell and lead would be reduced, thus reducing the stresses within the inner shell.

When a uniform temperature is finally achieved throughout the OC, the lead would have “caught up” with the inner shell and the previous calculations would be directly applicable.

The remaining case of the inner shell being 300 ºF hotter than the lead is addressed as follows, but considering the lead as being at 70 ºF and the inner shell as being at 370 ºF. The analytical method is identical to the methodology previously used in this appendix.

Per Table 2.10.8-5, the lead inner radius at 70 ºF, assuming no interference with the inner shell, is b_L = 17.087 inches. The outer radius of the inner shell at 370 ºF, b_S, and the inner radius of the inner shell at 370 ºF, a, assuming no interference with the lead, are:

$$b_S = (17.190)(1 + \alpha_S \Delta T) = 17.237 \text{ in}$$

$$a = (16.190)(1 + \alpha_S \Delta T) = 16.234 \text{ in}$$

where the thermal expansion coefficient for stainless steel, $\alpha_S = 9.133(10)^{-6}$ in/in/ºF (interpolated from Table 2.10.8-1) at 370 ºF, and ΔT = 300 ºF.

The resulting interference, δ, is:

$$\delta = b_S - b_L = 0.150 \text{ in}$$

and the maximum strain in the lead, ε, therefore becomes:

$$\varepsilon = \frac{\delta}{b_L} = 0.00878 \text{ in/in} = 0.878\% \text{ strain (tensile)}$$

Extrapolating from Figure 2.3-5 in Section 2.3, *Mechanical Properties of Materials*, a hoop stress, σ, of approximately 900 psi would exist in the lead for this strain. The effective interface pressure, p, would then be:

$$p = \frac{\sigma}{\left(\frac{c^2 + b_L^2}{c^2 - b_L^2}\right)} = 92.8 \text{ psi}$$

where, from Table 2.10.8-5, the outer and inner lead shell radii, c = 18.950 inches and b_L = 17.087 inches, respectively.

For a pressure of 92.8 psi at 370 ºF, and conservatively neglecting the beneficial effects of lead creep, the hoop stress in the inner stainless steel shell, σ_S, is:

$$\sigma_S = -p\left(\frac{b_S^2 + a^2}{b_S^2 - a^2}\right) = -1{,}551 \text{ psi}$$

where, from above, the outer and inner radii of the inner stainless steel shell, b_S = 17.237 inches and a = 16.234 inches, respectively.

The -1,551 psi hoop stress compares with the previously determined hoop stress in the inner shell of -1,413 psi, and only would exist during the fabrication cooldown process (i.e., when the shell is 300 ºF hotter than the lead). When the inner shell continues to cool, this hoop stress would reduce, and it is concluded that the -1,551 psi hoops stress case is independent and would not combine with other loads such as those resulting from hypothesized drop events.

Regarding axial stresses, with the lead at 70 ºF and the inner shell at 370 ºF, and interpolating data from Table 2.10.8-1 and Table 2.10.8-2, the axial strain in the lead, ε_a, assuming bonding, would be:

$$\varepsilon_a = [\alpha_L - \alpha_S)\Delta T]_{620} + [\alpha_S \Delta T]_{370} = 0.00870 \text{ in/in} = 0.870\% \text{ strain (tensile)}$$

where, for cooldown from 620 ºF to 70 ºF, the lead and stainless steel coefficients of thermal expansion, $\alpha_S = 9.56(10)^{-6}$ in/in/ºF (from Table 2.10.8-1) and $\alpha_L = 20.39(10)^{-6}$ in/in/ºF (from Table 2.10.8-2), respectively, and $\Delta T = 620 - 70 = 550$ ºF, and for heatup from 70 ºF to 370 ºF, the stainless steel coefficient of thermal expansion, $\alpha_S = 9.133(10)^{-6}$ in/in/ºF (interpolated from Table 2.10.8-1), and $\Delta T = 370 - 70 = 300$ ºF.

Extrapolating from Figure 2.3-5 in Section 2.3, *Mechanical Properties of Materials*, an axial stress, σ_L, of approximately 900 psi would exist in the lead for this strain.

The corresponding axial stressing the inner shell, σ_a = -1,662 psi. Continued cooling of the inner stell to 70 ºF would reduce this axial compressive stress. Further cooling of the lead and inner shell to -20 ºF or -40 ºF would result in axial stresses no worse than previously determined for these temperatures.

2.10.8.8 Summary

The preceding calculations indicate that stress levels resulting from lead pour and subsequent cooldown would be relatively small. In particular, with compressive stress magnitudes in the neighborhood of 1,500 psi to 2,000 psi, as calculated herein, it is concluded that buckling of the OC inner shell should not occur due to the lead pour procedure (i.e., critical buckling stresses, as determined in Appendix 2.10.5, *Buckling Design Criteria and Detailed Evaluation*, for the OC inner shell, are well above the predicted stress levels).

Table 2.10.8-1 – Mechanical Properties of Stainless Steel (Type 304)

Temperature (ºF)	E (10^6 psi)	α (10^{-6} in/in/ºF)	μ
70	28.3	8.46	0.3
100	28.2	8.55	0.3
200	27.6	8.79	0.3
300	27.0	9.00	0.3
400	26.5	9.19	0.3
500	25.8	9.37	0.3
600	25.3	9.53	0.3
620	25.2	9.56	0.3

Table 2.10.8-2 – Mechanical Properties of Lead (Copperized)

Temperature (ºF)	E (10^6 psi)	α (10^{-6} in/in/ºF)	μ
70	2.34	16.07	0.45
100	2.30	16.21	0.45
200	2.16	16.70	0.45
300	2.00	17.34	0.45
400	1.82	18.17	0.45
500	1.61	19.13	0.45
600	1.40	20.18	0.45
620	1.36	20.39	0.45

Table 2.10.8-3 – Steel Shell Geometry at 70 ºF

Geometry (at 70 ºF)	Inner Shell (in)	Outer Shell (in)
Inside Diameter, D_i	32.38	38.13
Outside Diameter, D_o	34.38	41.13
Shell Thickness, t	1.00	1.50

Table 2.10.8-4 – Initial Shell Conditions Before Lead Solidification

Shell	Inner Radius (in)	Outer Radius (in)
Inner	16.275	17.280
Outer	19.164	20.672

Table 2.10.8-5 – Stress-Free OC Inner Shell Dimensions

Item	Radius (in)		
	620 ºF	70 ºF	ΔR
Stainless Steel Inner Shell Inner Radius	16.275	16.190	0.085
Stainless Steel Inner Shell Outer Radius	17.280	17.190	0.090
Lead Inner Radius	17.280	17.087	0.193
Lead Outer Radius	19.164	18.950	0.214

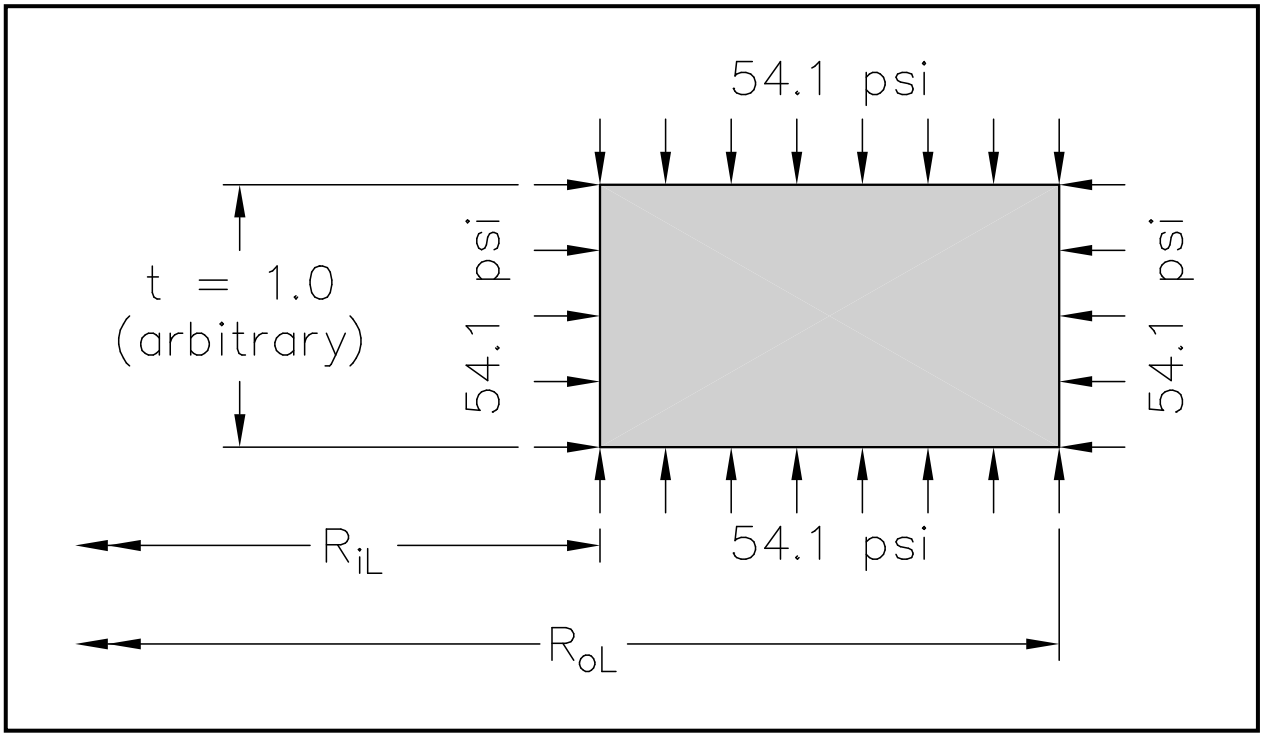

Figure 2.10.8-1 – Free-Body Diagram of Molten Lead in the Lead Column

This page intentionally left blank.

3.0 THERMAL EVALUATION

This section identifies and describes the principal thermal engineering design aspects of the RH-TRU 72-B package important to compliance with the thermal performance requirements of 10 CFR 71[1]. For a more detailed discussion of the package and its key features, see Chapter 1.0, *General Information*.

3.1 Discussion

The RH-TRU 72-B package is designed with a totally passive thermal system. The principal physical characteristics of this system consist of one external thermal fire shield surrounding the outer cask (OC) exterior wall. The fire shield consists of a 10-gauge stainless steel sheet (0.135-inch thick) offset from the OC body by a 12-gauge stainless steel wire wrap (0.105-inch diameter) on a 3-inch pitch. The cylindrical OC consists of a 1.50 inch thick, 41⅛-inch outside diameter stainless steel outer shell, a 1⅞-inch thick lead shield, and a 1-inch thick, 32⅜-inch inside diameter stainless steel inner shell. The OC bottom end plate is 5-inch thick stainless steel, while the OC lid is 6-inch thick stainless steel.

The 32-inch outside diameter inner vessel (IV) is constructed of 3/8-inch thick stainless steel, with a 1½-inch thick stainless steel bottom end plate and a 6½-inch thick stainless steel lid.

Hypothetical accident condition (HAC) impact protection is provided by polyurethane foam impact limiters covering each end of the OC. The polyurethane impact limiters also provide thermal protection during the HAC fire event.

Thermal analyses are performed using the SINDA '85/FLUINT heat transfer code[2]. This is a finite difference, lumped parameter code capable of analyzing steady state and transient thermal conditions. Three principal heat transfer analyses were run as follows:

(1) Steady state analysis at an ambient temperature of 100 ºF, with insolation, for normal conditions of transport (NCT).

(2) Steady state analysis at an ambient temperature of 100 ºF, without insolation, as initial conditions for the HAC fire event.

(3) Transient analysis with damaged impact limiters during the HAC fire event.

HAC boundary conditions initiate at steady state conditions without insolation and consist of exposure to a 1,475 ºF radiation and convection source with an average emissivity coefficient of at least 0.9 and an average flame temperature of at least 1,475 ºF for thirty minutes. This sequence is followed by exposure to 100 ºF ambient air with maximum insolation for a time sufficient to maximize temperatures throughout the package.

The OC outer surface and impact limiters may be optionally painted. The analyses herein use unpainted surface (i.e., bare stainless steel) thermal properties. Since painted surfaces have

[1] Title 10, Code of Federal Regulations, Part 71 (10 CFR 71), *Packaging and Transportation of Radioactive Material*, Final Rule, 01-26-04.

[2] SINDA '85/FLUINT, *Systems Improved Numerical Differencing Analyzer and Fluid Integrator*, Version 2.1, NASA/Martin Marietta Corporation, 1988.

higher emissivities that allow for better decay heat rejection than unpainted surfaces, the use of unpainted surface thermal properties is conservative.

Each analysis assumes bounding payload decay heat loads of 50 and 300 watts, with the 50-watt payload consisting mainly of paper products and the 300-watt payload consisting mainly of metallic items. Further details of the payload heat transfer model are provided in Section 3.4, *Thermal Evaluation for Normal Conditions of Transport*.

Table 3.1-1 and Table 3.1-2 present the maximum temperatures determined by these analyses for the major components of the RH-TRU 72-B package. Details of the analyses are presented in Section 3.4, *Thermal Evaluation for Normal Conditions of Transport*, and Section 3.5, *Hypothetical Accident Thermal Evaluation*. The maximum pressure during NCT is 150.0 psig, from Section 3.4.4.3, *Maximum Pressure for Normal Conditions of Transport*, which is equal to the design pressure of 150 psig. The maximum pressure during HAC is 178.8 psig, from Section 3.5.4, *Maximum Internal Pressure*, which is below the analysis pressure of 300 psig. The thermal criteria for the packaging materials are described in Section 3.3, *Technical Specifications of Components*.

Table 3.1-1 – Maximum NCT Temperatures for RH-TRU 72-B Package

Location	With Insolation (ºF)		Without Insolation (ºF)		Allowable Limits (ºF)
	50 W	300 W	50 W	300 W	
Waste Centerline	217	181	196	164	①
Payload Canister Shell	132	167	110	149	N/A
IV Shell	127	150	105	130	N/A
OC Inner Shell	126	143	104	123	N/A
OC Lead Shield	126	143	104	123	620
OC Outer Shell	126	143	104	123	N/A
OC Thermal Shield	125	142	103	122	N/A
OC Upper Ring Forging	126	137	104	116	N/A
IV O-Ring Seal	126	140	104	120	-40 to 400
OC O-Ring Seal	126	137	104	117	-40 to 400
IV Lid	127	141	105	121	N/A
OC Lid	126	137	104	117	N/A
Impact Limiter Foam	132	143	104	121	300
Impact Limiter Shell	133	142	104	122	N/A

Notes:

① The temperature limit for the waste material is discussed in Appendix 4.6 of the *RH-TRU Payload Appendices*[3].

[3] U.S. Department of Energy (DOE), *RH-TRU Payload Appendices*, U.S. Department of Energy, Carlsbad Field Office, Carlsbad, New Mexico.

Table 3.1-2 – Maximum HAC Temperatures for RH-TRU 72-B Package

Location	Payload (ºF)		Allowable Limits (ºF)
	50 W	300 W	
Waste Centerline	219	196	①
Payload Canister Shell	263	247	N/A
IV Shell	327	343	N/A
OC Inner Shell	488	497	N/A
OC Lead Shield	544	554	620
OC Outer Shell	601	611	N/A
OC Thermal Shield	1,232	1,231	N/A
OC Upper Ring Forging	154	166	N/A
IV O-Ring Seal	150	159	-40 to 400
OC O-Ring Seal	149	158	-40 to 400
IV Lid	148	157	N/A
OC Lid	150	159	N/A
Impact Limiter Foam	420	421	300②
Impact Limiter Shell	1,424	1,425	N/A
Center-Pivot Trunnion	961	967	N/A
Lift Trunnion	998	1,001	N/A

Notes:

① The temperature limit for the waste material is discussed in Appendix 4.6 of the *RH-TRU Payload Appendices*[3].

② In the analysis, foam at temperatures greater than 400 ºF is assumed to be charred, but charring only affects the top foam layer. The remaining foam still protects the payload during the fire transient.

3.2 Summary of Thermal Properties of Materials

The RH-TRU 72-B package is fabricated primarily of Type 304 stainless steel, lead, and polyurethane foam. The void spaces within the package are assumed to be filled with air at one atmosphere. Air also fills the gap between the outer cask (OC) outer shell and the thermal shield. The various waste containers to be transported will be constructed of carbon or stainless steel, while the waste itself is allowed to vary from primarily paper-based waste (with a total maximum allowable decay heat of 50 watts) to a mostly metallic waste (with a total maximum allowable decay heat of 300 watts). A more detailed description of the waste is contained in the *Remote-Handled Transuranic Waste Authorized Methods for Payload Control* (RH-TRAMPAC)[1].

Table 3.2-1 lists the thermal properties used in the model and the sources from which they were obtained. Note that the polyurethane foam density is approximately 10% above 11.5 pcf. This higher density will have a negligible effect under hypothetical accident condition (HAC), and no effect during normal conditions of transport (NCT). Table 3.2-2 lists the conductivity of air as a function of temperature as utilized in the thermal analyses.

The conductivity of the metallic waste is calculated in the following manner (see Appendix 3.6.1, *Thermal Model Details*, for details). A weighted conductivity of the metallic waste is calculated assuming the metal is encased in a cementitious material. The relative amount of these materials is determined by adjusting the portions to achieve a maximum allowable payload weight with three completely filled 55-gallon drums. The heat generation is assumed to be evenly distributed throughout the drums.

An important parameter in radiative heat transfer is the selection of an emissivity (ε) value for each radiating surface. Table 3.2-3 lists the emissivity values and the surface absorptivities (α) used in this analysis, along with the sources.

For thermal modeling purposes, a payload canister wall emissivity of 0.8, corresponding to carbon steel, is used. As shown below, an emissivity of 0.5 (corresponding to stainless steel) would only modestly increase the payload canister wall temperature (on the order of 6 ºF). Since a conservative value of 200 ºF is used for structural evaluations of the payload canister shell (see Chapter 2.0, *Structural Evaluation*), any payload canister emissivity in the 0.5 to 0.8 range is acceptable.

The inner vessel (IV) wall temperature is essentially independent of the payload canister temperature (i.e., IV wall temperature is primarily a function of internal heat load, external solar load, and total thermal resistance between the inner surface of the IV shell and outer surface of the OC thermal shield). Given this, and recognizing that heat transfer between the payload canister and the IV shell will be primarily via radiation, due to the relatively large radial gap between the payload canister and IV shell, the impact of a change in payload canister emissivity from 0.8 to 0.5 is readily established from first principles. From the analysis specifically performed herein for a carbon steel canister, the maximum IV shell temperature is 150 ºF and the corresponding maximum payload canister shell temperature is 167 ºF. The following calculation

[1] U.S. Department of Energy (DOE), *Remote-Handled Transuranic Waste Authorized Methods for Payload Control* (RH-TRAMPAC), U.S. Department of Energy, Carlsbad Field Office, Carlsbad, New Mexico.

establishes the change in payload canister shell temperature due to a change in its emissivity from 0.8 to 0.5.

$$\varepsilon_{e\,csc}\left(T_{cs}^4 - T_{IV}^4\right) = \varepsilon_{essc}\left(T_{ss}^4 - T_{IV}^4\right)$$

where the carbon steel payload canister emissivity, $\varepsilon_{cs} = 0.8$, the stainless steel payload canister and stainless steel IV emissivity, $\varepsilon_{ss} = 0.5$, the temperature of the carbon steel payload canister shell, $T_{cs} = 167$ ºF = 627 ºR, the temperature of the IV shell, $T_{IV} = 150$ ºF = 610 ºR, and the effective emissivity of the carbon steel payload canister, ε_{ecs}, is:

$$\varepsilon_{ecs} = \frac{1}{\frac{1}{\varepsilon_{IV}} + \frac{1}{\varepsilon_{cs}} - 1} = 0.44$$

and, the effective emissivity of the stainless steel payload canister, ε_{ess}, is:

$$\varepsilon_{ess} = \frac{1}{\frac{1}{\varepsilon_{IV}} + \frac{1}{\varepsilon_{ss}} - 1} = 0.33$$

Solving yields a stainless steel payload canister temperature, $T_{ss} = 632.4$ ºR = 172.4 ºF.

Due to the relative thinness of the payload canister shell (1/4-inch thick), and the modest axial and through-wall temperature gradients for the shell, the difference in conductivity for carbon steel versus stainless steel payload canister construction will have a negligible effect on payload canister and packaging temperatures.

Optionally painting the OC and impact limiter outer surfaces significantly increases the emissivity; therefore, use of the lower value of emissivity of $\varepsilon = 0.3$ is conservative[2].

During the HAC transient analyses, all exposed surfaces are assigned emissivities of 0.8 as per 10 CFR §71.73(c)(4)[3]. Therefore, the thermal shield, trunnion, and impact limiter shell emissivities are set at 0.8 in the transient analyses instead of the 0.3 normally used for stainless steel.

[2] Rohsenow, W. M. and J. P. Hartnett, *Handbook of Heat Transfer*, McGraw-Hill, New York, 1973, Section 15, Table 5. This provides an effective emissivity for painted surfaces from 0.81 for oil based paint on polished iron to 0.95 for enamel based paints. Per Table 3.2-3, the package surface emissivity used in this analysis is 0.5.

[3] Title 10, Code of Federal Regulations, Part 71 (10 CFR 71), *Packaging and Transportation of Radioactive Material*, Final Rule, 01-26-04.

Table 3.2-1 – Thermal Properties of Materials

Material	Conductivity (Btu/hr-ft-ºF)	Density (lb/ft^3)	Specific Heat (Btu/lb-ºF)	Reference
Stainless Steel, Type 304	10.0 @ 212 ºF	488	0.11	①
Carbon Steel, A516, Grade 55	25.0 @ 212 ºF	487	0.113	②
Lead	19.3 @ 212 ºF	710	0.031	②
Polyurethane Foam	0.0188 @ 212 ºF	11.5	0.300	③
Payload (paper)	0.02	100	0.55	④
Payload (metallic)	9.47	272.0	0.168	④
Air	Table 3.2-2	0.071	0.240	⑤⑥

Notes:

① General Electric, *Heat Transfer and Fluid Flow Data Books*, Genium Publishing Corporation, Schenectady, NY.

② Rohsenow and Hartnett, *Handbook of Heat Transfer*, McGraw-Hill, New York, NY, 1973, Chapter 2, Table 28.

③ General Plastics, *Last-a-Foam FR-3700® for Crash and Fire Protection of Nuclear Material Shipping Containers*, General Plastics Manufacturing Company, 4910 Burlington Way, Tacoma, Washington, February 1990.

④ The thermal material properties for paper and metallic waste are discussed in Appendix 3.6.1, *Thermal Model Details*.

⑤ Frank Kreith, Principles of Heat Transfer, 3rd Edition, McGraw-Hill, New York, NY, 1973, Table A-3.

⑥ Rohsenow and Hartnett, *Handbook of Heat Transfer*, McGraw-Hill, New York, NY, 1973, Chapter 2, Tables 35 and 39, et al.

Table 3.2-2 – Conductivity of Air

Temperature (ºF)	Air Conductivity (Btu/hr-ft-ºF)
32	0.0140
100	0.0154
300	0.0193
500	0.0231
1,000	0.0319
1,500	0.0400

Table 3.2-3 – Radiation Properties of Materials

Component	Material	ε	α	Reference
Payload Canister Shell	Carbon Steel	0.8	—	①
	Stainless Steel	0.5	—	②③
IV	Stainless Steel	0.5	—	②③
OC Inner Surface	Stainless Steel	0.5	—	②③
OC Outer Surface	Stainless Steel	0.5	—	②③
Trunnions	Stainless Steel	0.3	0.52	②③
Thermal Shield	Stainless Steel	0.3	0.52	②③
Impact Limiter Shell	Stainless Steel	0.3	0.52	②③

Notes:

① General Electric, *Heat Transfer and Fluid Flow Data Books*, et. al., the emissivity for painted surfaces ranges from 0.53 to 0.98, depending on pigment color and surface temperature.

② J. P. Holman, *Heat Transfer*, McGraw-Hill, New York, NY, 1963, Table A-10 gives values of 0.54 to 0.63.

③ Frank Kreith, *Radiation Heat Transfer*, International Textbook Company, 1962, Table 2[5] gives values of 0.43 to 0.78.

3.3 Technical Specifications of Components

The materials used in the RH-TRU 72-B package that are considered to be temperature sensitive are the butyl used for the O-ring seals and the polyurethane foam used in the impact limiters.

O-ring seals should be replaced annually or when required due to seal damage or failure to pass a leak test. The specification for the O-ring seal material used in the RH-TRU 72-B package (Rainier Rubber compound RR0405-70[1], or equivalent) is ASTM D2000 M4AA710 A13 B13 F17 F48 Z Trace Element (see Appendix 3.6.4, *Designating an Alternative Seal Material*, for more information). The butyl O-ring seals have an allowable temperature range of -40 ºF to 400 ºF[2]. The results summarized in Table 3.1-1 and Table 3.1-2 show the O-ring seal temperatures are within these limits.

The minimum operational temperature of polyurethane foam is -20 ºF, since this is the lowest initial temperature at which the packaging must perform. The allowable temperature range for the polyurethane foam during impact loadings is -20 ºF to 300 ºF[3]. In addition, temperature excursions to -40 ºF for the foam will not permanently degrade its properties. Foam performance under hypothetical accident condition (HAC) transient conditions is discussed in Section 3.5, *Hypothetical Accident Thermal Evaluation*. Foam strength sensitivity to temperature is addressed in Chapter 2.0, *Structural Evaluation*.

Other package materials are stainless steel and lead. The melting points for these materials are 2,600 ºF and 620 ºF, respectively. The carbon steel, which may be used in the waste containers and the payload canister, has a melting temperature of approximately 2,750 ºF.

[1] Rainier Rubber Company, Seattle, WA.

[2] U.S. Department of Energy (DOE), *Safety Analysis Report for the TRUPACT-II Shipping Package*, USNRC Certificate of Compliance 71-9218, U.S. Department of Energy, Carlsbad Field Office, Carlsbad, New Mexico.

[3] General Plastics, *Last-a-Foam FR 3700® for Crash and Fire Protection of Nuclear Material Shipping Containers*, General Plastics Manufacturing Company, 4910 Burlington Way, Tacoma, Washington, February 1990.

This page intentionally left blank.

3.4 Thermal Evaluation for Normal Conditions of Transport

This section presents the thermal analyses of the RH-TRU 72-B package for normal conditions of transport (NCT). The thermal conditions considered are those specified in 10 CFR §71.71. Per 10 CFR §71.71(c)(1)[1], a 100 ºF ambient temperature with insolation values per Table 3.4-1 are used for heat input to the exterior package surfaces.

3.4.1.1 Analytical Model

The thermal model chosen represents a two-dimensional, axisymmetric model of the RH-TRU 72-B package. The distribution of the waste within the waste containers is assumed to be uniform. The relatively low expected total decay heat loads of 50 watts and 300 watts means that changes in this assumption will not have a significant effect on the resultant temperature distributions.

The location and number of nodes are chosen to achieve an accurate determination of the temperature distribution in the major packaging components. For a more detailed description of the lumped parameter model, see Appendix 3.6.1, *Thermal Model Details*. The model utilizes the thermal properties presented in Section 3.2, *Summary of Thermal Properties of Materials*. For simplicity's sake, fixed values of thermal conductivity are used for the metals and insolation since changes with temperature are relatively small over the temperature range of interest. In contrast, the thermal conductivity of air is computed as a function of temperature since its conductivity variation is relatively significant.

Heat transfer across all other voids is calculated using a combination of conductive and radiative heat transfer. The heat transfer analyses assumes that the payload canister, inner vessel (IV), outer cask (OC), etc., are concentric cylinders which means that the air gaps surrounding these components are uniform and essentially no direct contact occurs between adjacent components.

Free convection of heat from the exterior surfaces is computed as a function of temperature and orientation of the surface using standard equations of free convection for cylinders and vertical surfaces (see Appendix 3.6.1, *Thermal Model Details*, for details).

Two packaging features that required special consideration in the finite difference model are the O-ring seals (IV and OC) and the center-pivot and lift/tie-down trunnions. Node locations are chosen to provide accurate modeling of the O-ring sealing areas (for additional details, see Appendix 3.6.1, *Thermal Model Details*).

Two payload models are used, one consisting of a paper-based waste with a decay heat of 50 watts, and the other consisting of metallic-based waste with a decay heat of 300 watts. The paper waste payload is modeled with a conductivity approaching that of air. The metallic waste is modeled with a conductivity calculated as discussed in Section 3.2, *Summary of Thermal Properties of Materials*, taking into account the assumed conductivity of the metal and the surrounding material. The two payload models represent the bounding conditions for all payloads, because the established payload parameter limits do not approach the conditions represented by the models.

[1] Title 10, Code of Federal Regulations, Part 71 (10 CFR 71), *Packaging and Transportation of Radioactive Material*, Final Rule, 01-26-04.

RH-TRU 72-B package payloads are restricted by the amount of gas generation that may occur during the course of an assumed worst-case (longest duration) shipment. For organic materials, hydrogen generation is the primary concern. For these payloads, very little heat generation can be tolerated.

For inorganic materials, little gas generation is expected, and higher decay heat values (and correspondingly higher payload temperatures) are acceptable. As detailed in the *Remote-Handled Transuranic Waste Authorized Methods for Payload Control* (RH-TRAMPAC)[2], the decay heat of these hotter payloads is controlled by calculations utilizing payload isotopic inventory information.

The two heat generation limits evaluated therefore perform the dual function of ensuring that neither temperature nor pressure limits of the RH-TRU 72-B package are exceeded.

3.4.1.2 Test Model

This section is not applicable as no thermal testing for NCT is performed for the RH-TRU 72-B package.

3.4.2 Maximum Temperatures

The maximum temperatures noted for normal conditions of transportation (i.e., 100 ºF ambient temperature, with insolation per Table 3.4-1, and 50 and 300 watt decay heat loads) are presented in Table 3.4-2 for the major components of the package.

The thermal shield and impact limiter shell represent the only accessible surfaces of the RH-TRU 72-B package during transportation. As shown in Table 3.4-2, the maximum temperatures for these components for any payload remain at or below the regulatory maximum temperature of 122 ºF for a non-exclusive use shipment per 10 CFR §71.43(g).

3.4.3 Minimum Temperatures

The minimum temperature distribution for the RH-TRU 72-B package will occur with no decay heat load and an ambient air temperature of -40 ºF (per 10 CFR §71.71(c)(2)[1]). Since the steady state analysis of these conditions represents a trivial case, no computerized thermal calculations are performed. Instead, it was assumed that all packaging components would reach the -40 ºF temperature under steady state conditions. For a package with the thermal capacitances of the RH-TRU 72-B package, prolonged exposure to low temperature environments is required to significantly depress package temperatures. As a potential initial condition for all NCT or HAC events, a -20 ºF minimum uniform temperature must be considered in performing the tests of 10 CFR §71.71(b) and §71.73(b).

3.4.4 Maximum Internal Pressure

Evaluation of the maximum internal pressure for the RH-TRU 72-B package considers the factors which affect pressure to demonstrate that pressure increases are below the allowable

[2] U.S. Department of Energy (DOE), *Remote-Handled Transuranic Waste Authorized Methods for Payload Control* (RH -TRAMPAC), U.S. Department of Energy, Carlsbad Field Office, Carlsbad, New Mexico.

pressure for the package. Included in the evaluation is a demonstration that accumulation of potentially flammable gases is precluded. Structural loads do not affect the maximum pressure capability of the packaging for NCT.

3.4.4.1 Design Pressure and Maximum Normal Operating Pressure

The RH-TRU 72-B package has a design pressure of 150 psig. Assuming an external pressure of 14.7 psia, the maximum normal operating pressure (MNOP) is 164.7 psia for the IV at the maximum normal operating temperature. Chapter 2.0, *Structural Evaluation*, discusses the ability of the package to withstand MNOP for both NCT and HAC.

3.4.4.2 Factors Affecting Pressure

The gauge pressure within the sealed IV of the RH-TRU 72-B package may potentially be changed (increased of decreased) due to one or more of the following factors that can affect pressure:

- Radiolytic gas generation (or consumption),
- Temperature-related pressure change,
- Barometric pressure change,
- Chemical reactions,
- Biological gas generation, and/or
- Thermal decomposition.

Each of these factors is discussed in the following sections. Depending on the payload, the relative contribution from each factor may vary from negligible to a significant fraction of the total pressure change. Section 3.4.4.3, *Maximum Pressure for Normal Conditions of Transport*, evaluates the worst-case combination of conditions for pressure increases within a payload.

3.4.4.2.1 Radiolytic Gas Generation

Radiolytic gas generation (radiolysis of the payload materials by the radioactive contaminants) is a potentially significant factor affecting pressure for some payloads. Radiolytic gases are generated when materials absorb radiation energy and produce gas molecules. Oxygen in the initial atmosphere within an RH-TRU package IV may also be consumed in some radiolytic processes. Gases are generated from radiolysis due to alpha, beta, gamma, or neutron interactions with matter. The radiation breaks chemical bonds in the target (potentially gas producing material) and causes chemical reactions to occur in the payload materials and in the atmosphere of the payload cavity. This may result in the net generation or consumption of gases. During transport, radiolysis of waste materials in the RH-TRU 72-B package payloads could result in either the net increase or decrease of pressure within the IV.

The gas generation rate, n_g (moles/sec), is determined from the following equation (see Appendix 2.1 of the *RH-TRU Payload Appendices*[3]):

[3] U.S. Department of Energy (DOE), *RH-TRU Payload Appendices*, U.S. Department of Energy, Carlsbad Field Office, Carlsbad, New Mexico.

$$n_g = W \times F \times G \times C \quad (1)$$

where W is the total decay heat (watts), F is the fraction of total ionizing radiation that is absorbed by target material (potential gas producing material), G is the number of gas molecules generated per unit (100 ev) ionizing radiation absorbed by target material, and C is the conversion factor based on units of measurement.

The gas generation rate depends on the G-value of the material (molecules of gas produced per 100 ev of energy absorbed), the fraction, F, of the emitted energy which is absorbed by the target material, and the emitted energy available from the form of alpha, beta, gamma or neutron radiation. The G-value may be positive (in the case of hydrogen, carbon dioxide, etc.) or negative (often in the case of oxygen). The variable, F, depends on the type of radiation emitted, the spatial distribution of the radioactive contaminants, and the target materials inside the payload container.

In experiments designed to measure the G-values of a material, care is taken to obtain intimate contact between the radionuclides and the target material. The F-factor then approaches 1.0 (100% of the emitted energy is absorbed). In RH-TRU wastes, the F-factor is unlikely to be equal to 1.0 due to the presence of non-target materials and the distribution of source and target materials. Since special care is needed to achieve an F-factor of 1.0 in laboratory conditions, the F-factor in actual waste materials will usually be much less than 1.0; hence, the energy absorbed by the target materials will be only a fraction of the energy emitted.

For payloads in the RH-TRU 72-B package, the analysis of potential gas production in the payload materials is based on an effective G-value (or the product of F and G). When several different waste materials may be present and the distribution of TRU radionuclides is not well known, all of the energy is assumed to be absorbed by the material having the highest G-value. By using this approach, if actual values for gas generation are measured from a specific payload container, results would be bounded by the analytic prediction. A detailed discussion of how effective G-values are assigned to content codes is provided in Appendix 2.2 of the *RH-TRU Payload Appendices*[3]. The effective G-value for each content code is used to determine the allowable gas generation rate to restrict the hydrogen concentration within the innermost confinement volume of the waste to a value less than 5 molar percent and to calculate the decay heat limit for each content code.

The discussion of effective G-value in Appendix 2.2 of the *RH-TRU Payload Appendices*[3] considers both the G-value for materials and the process for selecting an appropriate F-factor for a content code. The F-factor used in calculations varies depending on the waste materials and the configuration of confinement layers.

Appendix 2.2 of the *RH-TRU Payload Appendices*[3] also discusses the reduction in the rate of hydrogen gas generation (G-value) over time based on the total dose of alpha and beta radiation received by the target matrix in the vicinity of the TRU radionuclides. Over time and with constant exposure to radiation, hydrogen is removed from the hydrogenous waste or packaging material (the matrix), thus decreasing the number of hydrogen bonds available for further radiolytic breakdown (the matrix is depleted). As the amount of available hydrogen is reduced over time, the effective G-value decreases with increasing dose to a value that is defined as the "dose-dependent G-value". Because of the characteristics of alpha, beta, and gamma radiation,

only the matrix depletion effects of alpha and beta radiation are considered. No credit is taken for the matrix depletion effects of gamma radiation.

3.4.4.2.2 Temperature Related Pressure Change

Temperature affects package pressure changes in two ways. The first is the thermal expansion of the gases (air, and radiolytic gases) within the IV cavity, caused by an increase in temperature. This increase is calculated utilizing the ideal gas law equation: PV = nRT. The temperature, T, of the IV internal gas (essentially air) is calculated by considering an area average surface temperature of IV and payload canister walls. This value varies depending on decay heat wattage assumed in the thermal analysis for the payload. For NCT and 50 watts (indicative of paper wastes), Table 3.1-1 shows maximum IV and payload canister wall temperatures of 127 ºF and 132 ºF, respectively. Thus, the internal package gas temperature would be 130 ºF; similarly, at 300 watts (indicative of metallic wastes), the gas temperature would be 158 ºF. For HAC, and similar calculations, Table 3.5-1 in Section 3.5.3, *Package Temperatures*, shows that the calculated internal gas temperatures would be 295 ºF for 50 watts and 295 ºF for 300 watts (averaging the canister and IV shell temperatures).

Table 3.4-3 and Table 3.4-4 give significant NCT package temperatures versus decay heat values at decay heat values less than those of Table 3.1-1. These data are also plotted in Figure 3.4-1 and Figure 3.4-2. Similar data for HAC are not necessary as explained in Section 3.5.4, *Maximum Internal Pressure*.

The second pressure increase related to temperature is the partial pressure of moisture and potentially volatile chemicals within the RH-TRU 72-B IV cavity. The assumption for both payloads is that sufficient water exists to maintain a saturated atmosphere. The partial pressure exerted by water vapor is combined with other pressure contributions using Dalton's Law. The water vapor pressure is obtained from the steam tables, based on the coolest wall temperature within the IV, which is the temperature at which the moisture condenses. The partial pressure contribution from potentially volatile chemicals in the waste is assumed to be insignificant. Appendix 4.4 of the *RH-TRU Payload Appendices*[3] evaluates the contribution to the overall pressure in the IV by the vapor pressure that might be exerted by potentially flammable VOCs. (Appendix 4.3 of the *RH-TRU Payload Appendices* evaluates the compatibility of VOCs with the butyl-rubber O-ring seals of the RH-TRU 72-B package).

3.4.4.2.3 Barometric Pressure Change

The design of the RH-TRU 72-B package meets the regulatory requirement for an external pressure of 3.5 psia per 10 CFR §71.71(c)(3)[1]. This external pressure is well below the maximum barometric pressure decrease expected during transport due to elevation and weather changes. The expected maximum barometric pressure decrease would only result in an external pressure of approximately 8 psia.

The conservative approach of using the regulatory requirement of 3.5 psia reduces the safe pressure increase limit by 11.2 psi for a maximum allowable internal pressure of 150 psig. Thus, barometric pressure changes are accounted for by reducing the maximum allowable internal pressure to 150 – 11.2 = 138.8 psig, or adding 11.2 psia to the cumulative pressure increases from other sources.

3.4.4.2.4 Chemical Reactions

Potential pressure increases from gas-producing or exothermic chemical reactions in the payload materials are considered. The chemical compatibility evaluation performed in Appendix 4.1 of the *RH-TRU Payload Appendices*[3] determines the potential for chemical reactions. The chemical list for each content code in the *RH-TRUCON*[4] is restricted to preclude the occurrence of chemical reactions that produce excessive gas or heat.

These chemical lists are evaluated for potential incompatibilities in accordance with the U.S. Environmental Protection Agency (EPA) method that looks at gas production and exothermic reactions[5]. This method is discussed in Appendix 4.1 of the *RH-TRU Payload Appendices*. Use of the EPA method ensures that incompatible chemicals do not contribute to increased pressures in the RH-TRU 72-B package IV.

3.4.4.2.5 Biological Gas Generation

Several different types of microorganisms have the potential to cause gas production from biological decomposition of materials in the payload. These include aerobic, anaerobic, facultative anaerobes, and obligate anaerobes. Each of these microorganisms requires a specific environment to multiply and produce gas.

Cellulosic materials within the payload materials can serve as substrate for microorganisms. However, additional conditions are required for gas generation than just the presence of cellulosic materials. The environment within the payload is hostile and incompatible for these microorganisms due to insufficient nutrients (associated with suitable substrate [nitrogen and phosphorus]), segregation of waste types, a high pH (in some waste types), excess oxygen (for some microorganisms), and/or insufficient water content. These factors will greatly reduce the potential for biological gas generation during the 60-day shipping period. Aerobic bacteria, which are the most likely microorganism to be present, will deplete oxygen and produce CO_2, causing no net increase in pressure. The limited potential for biological gas generation in the RH-TRU 72-B package payload is discussed in Appendix 4.5 of the *RH-TRU Payload Appendices*[3].

3.4.4.2.6 Thermal Decomposition

When heated above a threshold temperature, some materials become chemically unstable, decompose, and produce gases. Usually these temperatures are close to the combustion temperature or phase-change temperature of the material.

As demonstrated in the thermal evaluation (Section 3.4.2, *Maximum Temperatures*), the temperatures of the payloads within the RH-TRU 72-B package are relatively low. In most cases, the temperatures are well below the high end of the usage range for the material. When exposed to the increased temperatures for NCT and HAC, thermal decomposition will not occur.

---

[4] U.S. Department of Energy (DOE), *Remote-Handled Transuranic Content Codes* (RH-TRUCON), DOE/WIPP 90-045, U.S. Department of Energy, Carlsbad Field Office, Carlsbad, New Mexico.

[5] H. K. Hatayama, J. J. Chen, E. R. de Vera, R. D. Stephens, D. L. Storm, *A Method for Determining the Compatibility of Hazardous Wastes*, EPA 600/2 80 076, U.S. Environmental Protection Agency, Cincinnati, Ohio, 1980.

Thermal decomposition as a factor affecting pressure is discussed in detail in Appendix 4.6 of the *RH-TRU Payload Appendices*[3].

3.4.4.3 Maximum Pressure for Normal Conditions of Transport

The maximum pressure within the RH-TRU 72-B package IV under NCT is calculated below for two hypothetical example content codes that provide bounding values for the pressure calculations. One bounding hypothetical example content code is a payload consisting of inorganic waste (identified as "NewMet"), and the second bounding hypothetical example content code is a payload consisting of organic waste (identified as "NewPaper").

As discussed in Section 3.4.4.2, *Factors Affecting Pressure*, the major factors affecting the IV internal pressure are radiolytic gas generation, thermal expansion of gases, and the vapor pressure of water within the IV cavity. Barometric changes that affect external pressure, and hence the gauge pressure of the IV, are bound by the regulatory condition of 3.5 psia external pressure. Thus, upon loading at standard conditions of 14.7 psia, the internal pressure rise allowed is the package design pressure difference, 150 psig minus (14.7 – 3.5) or 138.8 psig; or barometric pressure contributes an administrative 11.2 psia before the other physical factors mentioned above are added. Subsequently, it will become obvious that barometric pressure effects are negligible based upon the low increases in pressure found due to the other factors. IV internal pressure does not increase significantly due to chemical reactions, biological gas generation, or thermal decomposition (see Appendix 4.1, 4.5, and 4.6 of the *RH-TRU Payload Appendices*[3]).

Calculation of maximum pressure in the IV considers immediate release of gases from the innermost confinement containers to the IV. The canister and IV void volumes are assumed to be filled with air at 70 ºF and 14.7 psia when the IV is sealed for transport. It is conservatively assumed that the canister and IV void volumes (190.5 + 493 = 683.5 liters) are the only volumes available in calculating pressures under NCT (no credit is taken for available void volume within any confinement layers). Sufficient water is assumed to be present for saturated water vapor at any temperature. The pressure increase due to water vapor is obtained from the tabulated thermodynamic properties of saturated water and steam.

The maximum pressure in the IV is calculated for the maximum shipping period of 60 days. The use of a 60-day shipping period in the calculation of MNOP is consistent with 10 CFR §71.41(c)[1]. As specified in 10 CFR §71.41(c), this section shows that the "…controls proposed to be exercised by the shipper are demonstrated to be adequate to provide equivalent safety of the shipment." The use of this shipping period is consistent with the analysis presented in Appendix 2.3 of the *RH-TRU Payload Appendices*[3], which shows that the maximum normal shipping period will be less than 60 days by a large margin of safety. As described in Appendix 2.3 of the *RH-TRU Payload Appendices*, routine monitoring of shipments includes the use of the TRANSCOM system at the Waste Isolation Pilot Plant, which provides continuous tracking of shipments from the shipping site to its destination.

The maximum IV pressures for bounding cases for organic and inorganic materials at the end of a 60-day shipping period, are provided in Table 3.4-5. The calculated pressure increases for the bounding cases are at or below the limit for the RH-TRU 72-B package. For the bounding organic materials example (NewPaper) with a decay heat of 23.5 watts, the pressure increase at the end of 60 days is 138.8 psig, equal to the design limit. Therefore, the maximum decay heat

limit for the bounding organic waste payload is 23.5 watts in order to comply with the design pressure limit at the end of the 60-day shipping period. Hydrogen gas generation limits are expected to be controlling for organic payloads with decay heat limits well below this upper bound. Also, as shown in Appendix 2.5 of the *RH-TRU Payload Appendices*[3], for decay heat values greater than 23.5 watts, compliance with the applicable hydrogen gas generation limit ensures compliance with the pressure limit.

For the bounding inorganic materials example (NewMet) with a decay heat of 300 watts, the pressure increase at the end of 60 days is 7.28 psig, well below the maximum allowable pressure increase of 138.8 psig. For this example, the decay heat is the limiting parameter, and the pressure increase is not a controlling factor.

The method used to calculate the maximum IV pressure is provided below. The number of g-moles per second of total gas generated by radiolysis is calculated from the following equation:

$$n_g = G_{eff(T)} \times W \times C \qquad (2)$$

where n_g is the rate of radiolytic gas generation (g-moles/sec), $G_{eff(T)}$ is the temperature-corrected effective G-value (the total number of molecules of gas generated per 100 eV of energy emitted (molecules/100 eV) at the temperature of the target material), W is the total decay heat (watts), and C is the conversion constant for the units used = $1.04(10)^{-5}$ (g-moles)(eV)/(molecule)(watt-sec).

The effective G-values are discussed in Appendix 2.2 of the *RH-TRU Payload Appendices*[3]. A value of F = 1.0, from equation (1), will be utilized for conservatism. The methodology for determing the decay heat limit for each content code is discussed and provided in the RH-TRAMPAC[2].

As discussed in Appendix 2.2 of the *RH-TRU Payload Appendices*[3], the effective G-values provided at room temperature (T_{RT}) are a function of temperature based on the activation energy (E_a) for the material. They are increased, as a result of increased payload average contents temperature, using the corresponding activation energy values obtained from Appendix 2.2 of the *RH-TRU Payload Appendices*. The total increase in pressure for a 60-day shipping period for the bounding payloads is summarized below:

<u>Bounding Content Code NewPaper</u>: From Table 3.4-5, the effective G-value at room temperature is 8.4 molecules/100 eV, and the activation energy is 2.1 kcal/g mole. The average content temperature is 149.2 ºF per Table 3.4-5. The temperature-corrected effective G-value, $G_{eff(T)}$, is calculated using the following equation:

$$G_{eff(T)} = G_{eff(RT)} e^{\left\{\left(\frac{E_a}{R}\right)\left[\frac{T-T_{RT}}{(T)(T_{RT})}\right]\right\}} \qquad (3)$$

where $G_{eff(RT)}$ is the effective G-value at room temperature (molecules/100 eV; the number of molecules of gas generated per 100 eV of energy for target material at room temperature), E_a is the activation energy for the target material (kcal/g-mole), the ideal gas constant, R = $1.99(10)^{-3}$ kcal/g-mole-K, T is the temperature of the target material, average contents temperature (ºC), and room temperature, T_{RT} = room temperature = 21.1 ºC.

Thus, the temperature-corrected effective G-value from Equation (3) is:

$$G_{eff(T)} = \left(8.4\frac{\text{molecules}}{100\text{ eV}}\right)e^{\left\{\left(\frac{2.1\frac{\text{kcal}}{\text{g-mole}}}{1.99(10)^{-3}\frac{\text{kcal}}{\text{g-mole-K}}}\right)\left[\frac{338.3\text{ K}-294.1\text{ K}}{(338.3\text{ K})(294.1\text{ K})}\right]\right\}} = 13.40\frac{\text{molecules}}{100\text{ eV}}$$

Using this temperature-corrected effective G-value, the radiolytic gas generation rate from Equation (2) and Table 3.4-5 is:

$$n_g = \left(13.40\frac{\text{molecules}}{100\text{ eV}}\right)\times(23.5\text{ watts})\times\left(1.04(10)^{-5}\frac{\text{g-mole-eV}}{\text{molecule-watt-sec}}\right) = 3.27(10)^{-5}\frac{\text{g}-\text{moles}}{\text{sec}}$$

The total liters of radiolytic gases generated at STP at the end of 60 days would be:

$$V_R = \left(3.27(10)^{-5}\frac{\text{g}-\text{moles}}{\text{sec}}\right)\times(60\text{ days})\times\left(86{,}400\frac{\text{sec}}{\text{day}}\right)\times\left(22.4\frac{\text{liters}}{\text{g-mole}}\right) = 3{,}796.9\text{ liters at STP}$$

The generated volume of radiolytic gases is heated to the average IV gas temperature of 126.1 ºF per Table 3.4-5. The corresponding volume occupied is:

$$V_{rg} = (3{,}796.9\text{ liters at STP})\times\left(\frac{126.1\,^\circ\text{F}+460\,^\circ\text{R}}{32\,^\circ\text{F}+460\,^\circ\text{R}}\right) = 4{,}523.1\text{ liters at }126.1\,^\circ\text{F}$$

This gas contributes a pressure of:

$$P_{rg} = \frac{4{,}523.1\text{ liters}}{493\text{ liters total void volume}} = 9.2\text{ atm (135.24 psia) at }126.1\,^\circ\text{F}$$

The initial pressure of gas present in the IV at 70 ºF is 14.7 psia. This gas is also heated to 126.1 ºF for bounding content code NewPaper. The increased pressure associated with this increase in temperature is:

$$P_{hu} = (14.7\text{ psia})\times\left(\frac{126.1\,^\circ\text{F}+460\,^\circ\text{R}}{70\,^\circ\text{F}+460\,^\circ\text{R}}\right) = 16.26\text{ psia}$$

The water vapor pressure is based on the temperature of the coolant or condensing surface of the IV, 125.3 ºF per Table 3.4-5. The water vapor pressure, P_{wv}, from the steam tables is 1.95 psia.

Thus, the maximum IV pressure at the end of 60 days for bounding content code NewPaper is:

$$P_{max} = P_{rg} + P_{hu} + P_{wv} - P_{atm} = 135.27 + 16.26 + 1.95 - 14.7 = 138.8\text{ psig}$$

<u>Bounding Content Code NewMet</u>: From Table 3.4-5, the effective G-value at room temperature is 0.012 molecules/100 eV, and the activation energy is 0.0 kcal/g mole. The average content temperature is 178.1 ºF per Table 3.4-5. The temperature-corrected effective G-value from Equation (3) is:

$$G_{eff(T)} = \left(0.012\frac{\text{molecules}}{100\text{ eV}}\right)e^{\left\{\left(\frac{0.0\frac{\text{kcal}}{\text{g-mole}}}{1.99(10)^{-3}\frac{\text{kcal}}{\text{g-mole-K}}}\right)\left[\frac{354.3\text{ K}-294.1\text{ K}}{(354.3\text{ K})(294.1\text{ K})}\right]\right\}} = 0.012\frac{\text{molecules}}{100\text{ eV}}$$

Using this temperature-corrected effective G-value, the radiolytic gas generation rate from Equation (2) and Table 3.4-5 is:

$$n_g = \left(0.012\frac{\text{molecules}}{100\text{ eV}}\right)\times(300\text{ watts})\times\left(1.04(10)^{-5}\frac{\text{g-mole-eV}}{\text{molecule-watt-sec}}\right) = 3.74(10)^{-7}\frac{\text{g-moles}}{\text{sec}}$$

The total liters of radiolytic gases generated at STP at the end of 60 days would be:

$$V_R = \left(3.74(10)^{-7}\frac{\text{g-moles}}{\text{sec}}\right)\times(60\text{ days})\times\left(86{,}400\frac{\text{sec}}{\text{day}}\right)\times\left(22.4\frac{\text{liters}}{\text{g-mole}}\right) = 43.5\text{ liters at STP}$$

The generated volume of radiolytic gases is heated to the average IV gas temperature of 154.9 ºF per Table 3.4-5. The corresponding volume occupied is:

$$V_{rg} = (43.5\text{ liters at STP})\times\left(\frac{154.9\,^\circ\text{F}+460\,^\circ\text{R}}{32\,^\circ\text{F}+460\,^\circ\text{R}}\right) = 54.3\text{ liters at }154.9\,^\circ\text{F}$$

This gas contributes a pressure of:

$$P_{rg} = \frac{54.3\text{ liters}}{493\text{ liters total void volume}} = 0.110\text{ atm (1.62 psia) at }154.9\,^\circ\text{F}$$

The initial pressure of gas present in the IV at 70 ºF is 14.7 psia. This gas is also heated to 154.9 ºF for bounding content code NewMet. The increased pressure associated with this increase in temperature is:

$$P_{hu} = (14.7\text{ psia})\times\left(\frac{154.9\,^\circ\text{F}+460\,^\circ\text{R}}{70\,^\circ\text{F}+460\,^\circ\text{R}}\right) = 17.05\text{ psia}$$

The water vapor pressure is based on the temperature of the coolant or condensing surface of the IV, 145.4 ºF per Table 3.4-5. The water vapor pressure, P_{wv}, from the steam tables is 3.31 psia.

Thus, the maximum IV pressure at the end of 60 days for bounding content code NewMet is:

$$P_{max} = P_{rg} + P_{hu} + P_{wv} - P_{atm} = 1.62 + 17.05 + 3.31 - 14.7 = 7.28\text{ psig}$$

The theorectical bounding decay heat loads for organic waste and inorganic waste are 23.5 watts and 300 watts, respectively. For organic waste, the 23.5 watts corresponds to the maximum allowable pressure increase of 138.8 psig. For inorganic waste, the 300 watts yields a pressure increase of 7.28 psig, well below the design limit. As described in Section 5.4 of the RH-TRAMPAC[2], beyond this theorectical analysis compliance with the flammable gas generation rate limits will ensure compliance with the total gas generation rate limits for all cases.

3.4.5 Maximum Thermal Stresses

Maximum NCT thermal stresses are determined using the temperature results from Section 3.4.2, *Maximum Temperatures*, and Section 3.4.3, *Minimum Temperatures*. NCT thermal stresses are discussed in Section 2.6.1, *Heat*, and Section 2.6.2, *Cold*. As input to Chapter 2.0, *Structural Evaluation*, the minimum temperature is taken as -40 ºF (-20 ºF when combined with any other load cases), and the maximum temperature is taken as 160 ºF for any RH-TRU 72-B packaging component.

3.4.6 Evaluation of Package Performance for Normal Conditions of Transport

The component temperatures associated with the more extreme NCT thermal conditions presented in Section 3.4.2, *Maximum Temperatures*, and Section 3.4.3, *Minimum Temperatures*, are all within the allowable limits for the respective materials per Section 3.3, *Technical Specifications of Components*.

Table 3.4-1 – Insolation Values

Form and Location of Surface	Total Insolation for a 12-Hour Period	
	(gcal/cm^2)	(Btu/in^2)
Flat surfaces transported horizontally:		
• Base	None	None
• Other surfaces	800	20.49
Flat surfaces not transported horizontally	200	5.12
Curved surfaces	400	10.24

Table 3.4-2 – Maximum NCT Temperatures (ºF) for RH-TRU 72-B Package

Location	With Insolation (ºF)		Without Insolation (ºF)	
	50 W	300 W	50 W	300 W
Waste Centerline	217	181	196	164
Payload Canister Shell	132	167	110	149
IV Shell	127	150	105	130
OC Inner Shell	126	143	104	123
OC Lead Shield	126	143	104	123
OC Outer Shell	126	143	104	123
OC Thermal Shield	125	142	103	122
OC Upper Ring Forging	126	137	104	116
IV O-Ring Seal	126	140	104	120
OC O-Ring Seal	126	137	104	117
IV Lid	127	141	105	121
OC Lid	126	137	104	117
Impact Limiter Foam	132	143	104	121
Impact Limiter Shell	133	142	104	122

Table 3.4-3 – Paper Waste NCT Package Temperature Variations with Decay Heat

Wattage (watts)	Average Payload Temperature (ºF)	Average Canister Wall Temperature (ºF)	Average IV Wall Temperature (ºF)	Average IV Air Temperature (ºF)
0	123.51	123.51	123.50	123.50
10	134.44	125.00	124.25	124.63
20	145.32	126.40	124.99	125.70
30	156.14	127.82	125.72	126.77
40	166.92	129.25	126.46	127.86
50	177.66	130.65	127.19	128.92

Table 3.4-4 – Metallic Waste NCT Package Temperature Variations with Decay Heat

Wattage (watts)	Average Payload Temperature (ºF)	Average Canister Wall Temperature (ºF)	Average IV Wall Temperature (ºF)	Average IV Air Temperature (ºF)
0	123.77	123.73	123.68	123.70
50	133.40	130.77	127.22	128.99
100	142.99	137.87	130.92	134.40
150	152.25	144.81	134.60	139.71
200	161.11	151.50	138.19	144.85
250	169.75	158.10	141.81	149.96
300	178.07	164.50	145.36	154.93

Table 3.4-5 – RH-TRU 72-B Pressure Increase Contributions

Parameter	Bounding Content Code	
	NewMet	NewPaper
Pressure Increase at 60 Days (limit = 138.8), psig	7.28	138.8
Water Vapor Added, psia	3.31	1.95
IV Wall Temperature, ºF (T_{IV})	145.4	125.3
Initial Gas Pressure Increase, psia	17.05	16.26
Radiolytic Gas Pressure Added at 60 Days, psia	1.62	135.27
IV Average Gas (Air) Temperature, ºF (T_{air})	154.9	126.1
Radiolytic Gas Generation Over 60 Days, liters @ STP	43.5	3,808.5
Radiolytic Gas Generation Over 60 Days, liters @ T_{air}	54.3	4,536.7
Radiolytic Gas Generation Over 60 Days, g-moles/sec	$3.74(10)^{-7}$	$3.28(10)^{-5}$
Temperature-Corrected Effective G, molecules/100 eV	0.012	13.40
Activation Energy, kcal/g-mole	0	2.1
Effective G for Total Gas, molecules/100 eV	0.012	8.4
Average Payload Contents Temperature, ºF (T_c)	178.1	149.2
Total Decay Heat per Payload Canister, watts	300	23.5
Decay Heat per Payload Container, watts	300	23.5

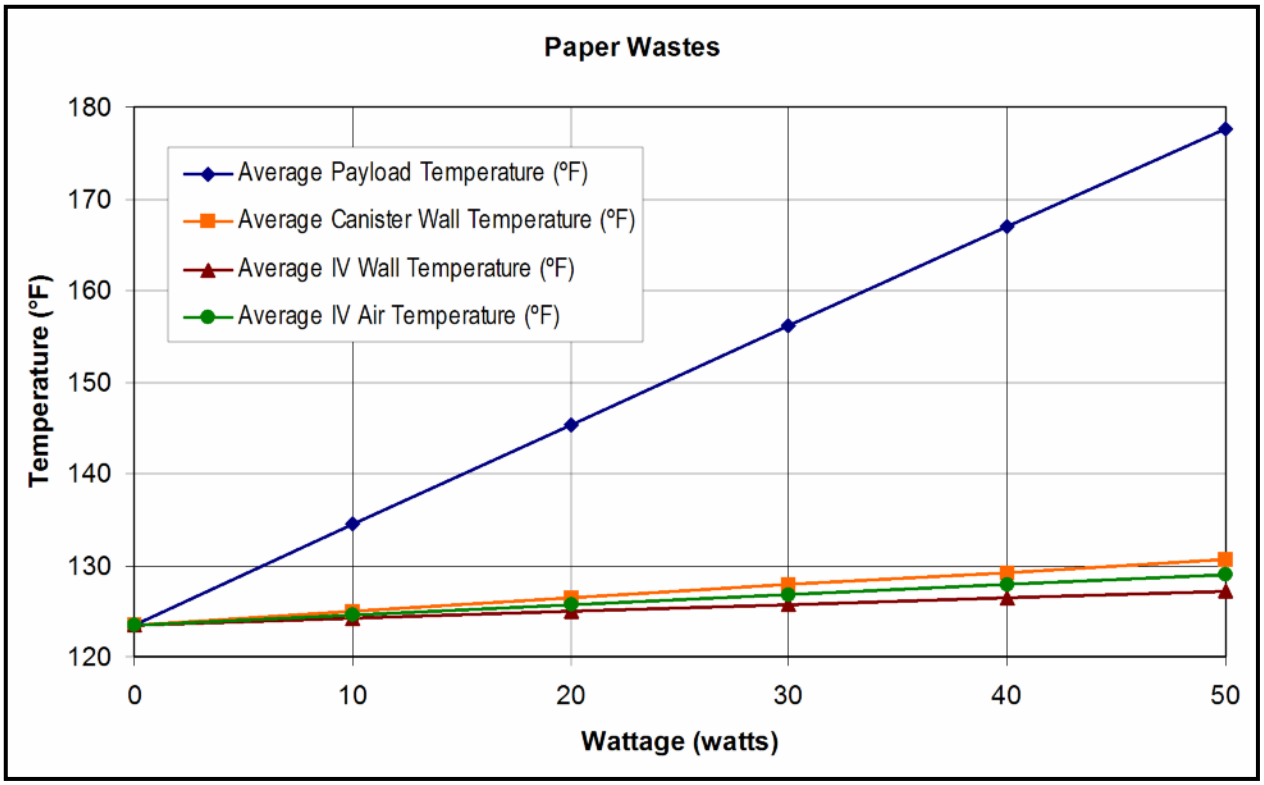

Figure 3.4-1 – Paper Waste NCT Package Temperature Versus Decay Heat

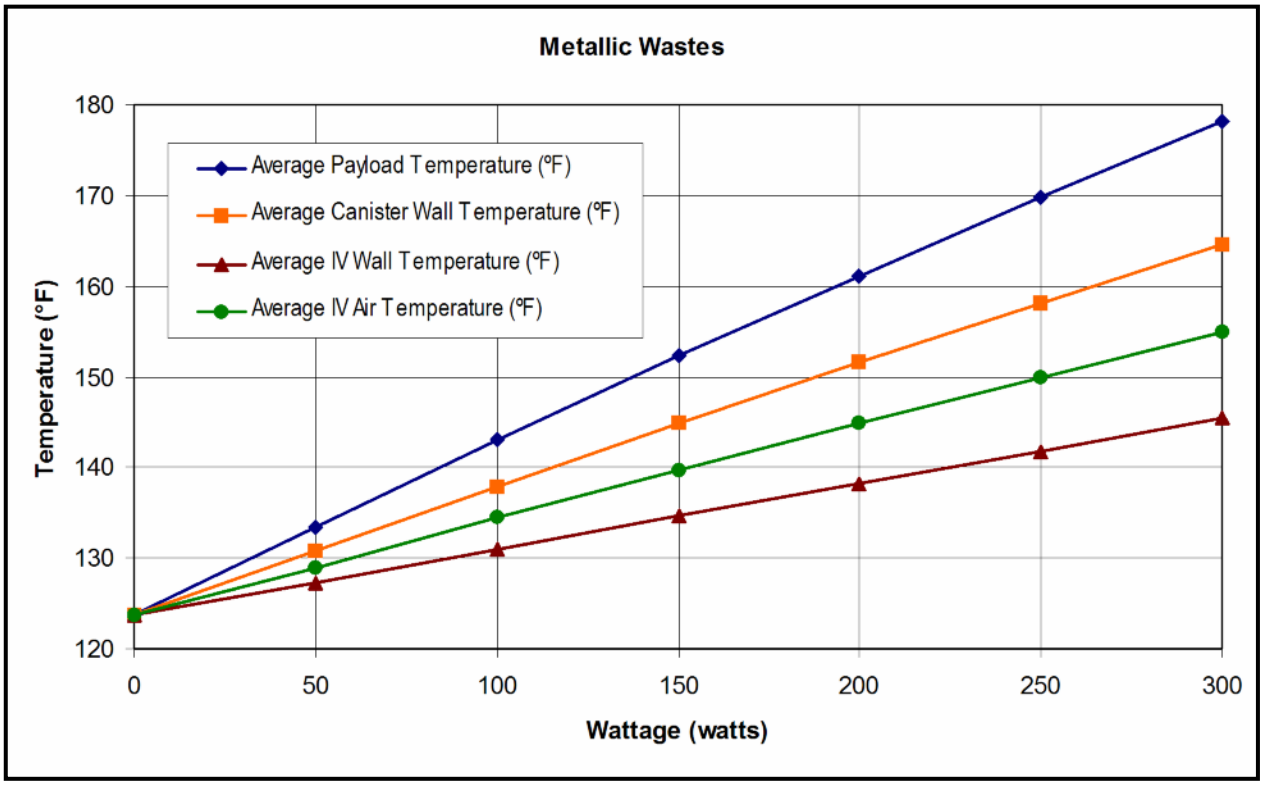

Figure 3.4-2 – Metallic Waste NCT Package Temperature Versus Decay Heat

3.5 Hypothetical Accident Thermal Evaluation

This section presents the thermal analyses of the RH-TRU 72-B package for the hypothetical accident condition (HAC) specified in 10 CFR §71.73(c)(4)[1]. The initial temperature distribution in the package prior to the HAC fire is taken as that corresponding to a 100 ºF steady state condition, without insolation, in accordance with 10 CFR §71.73(b). To determine the effects of the HAC fire event, the package is analytically exposed to a 1,475 ºF radiation and convection source for 30 minutes. The thermal boundary is then returned to the 100 ºF ambient air condition with maximum insolation. The transient analysis is continued for time sufficient to determine maximum values for all temperatures within the package. A time limit of 40 hours was used in these analyses, since this period permitted all packaging components to reach their maximum temperatures.

3.5.1 Thermal Model

3.5.1.1 Analytical Model

The analytical model used to evaluate the HAC fire event is nearly identical to that described in Section 3.4.1.1, *Analytical Model*. In the HAC model, greater detail is modeled into the package, with emphasis on the outer cask (OC) and inner vessel (IV) lid region, and lid-end impact limiter. This was done to allow modeling of the HAC drop-imposed damage to the impact limiter, and to better define temperatures near the damaged areas.

3.5.1.2 Test Model

HAC thermal testing was not performed for the RH-TRU 72-B package. However, thermal tests to evaluate the polyurethane foam used in the impact limiters were performed as part of the NuPac 125-B cask certification[2]. Results of these tests are documented in Appendix 3.6.3, *Polyurethane Foam Performance Tests*. These tests, covering a range of boundary condition assumptions, demonstrate three major findings:

(1) Foam char under direct flame impingement on exposed foam, amounts to approximately 4 inches, completely consistent with thermal modeling assumptions. Importantly, these tests were conducted with a flame temperature of approximately 1,800 ºF, significantly higher than the regulatory requirement of 1475 ºF.

(2) Following termination of the impinging flame, the combustion process is self-extinguishing, regardless of thermal boundary conditions in the tests.

(3) Minor tears or ruptures of the energy absorbing impact limiter shells (up to approximately 3/4-inch) are of no thermal consequence because the intumescent character of the foam char tends to seal and heal the opening in the impact limiter shell by the extrusion of char “plug”.

---

[1] Title 10, Code of Federal Regulations, Part 71 (10 CFR 71), *Packaging and Transportation of Radioactive Material*, Final Rule, 01-26-04.

[2] Nuclear Packaging, Inc., *Safety Analysis Report for the NuPac 125-B Fuel Shipping Package*, USNRC Certificate of Compliance 71-9200, U.S. Department of Energy, Washington, D.C.

3.5.2 Package Conditions and Environment

Two damage conditions are considered for the HAC thermal evaluation. The first damage condition is imposed by the 30-foot side drop. This HAC drop crushes both impact limiters inward 13.0 inches on the side where the impact occurs (see Table 2.10.3-10 in Appendix 2.10.3, *Drop Impact Evaluation Results*). Thus, the effective polyurethane foam thickness in the area of the impact damage is reduced from 16.8 inches to a minimum of 3.8 inches at the centerline of the impact zone. The density and conductivity of the polyurethane foam in the model are changed to reflect those of the crushed foam. The closed-cell polyurethane foam used in the impact limiters retains its compressive strength and charring characteristics over time. Foam samples aged for twenty years have been tested and the compressive strength, elastic modulus, and charring ability compare favorably with nominal design values[3]. Due to the relatively small thickness of polyurethane foam after being crushed, the foam in the impact zone is assumed to be completely charred during the HAC transient fire event. For modeling purposes, the polyurethane foam characteristics are changed to simulate the damage experienced. The foam conductivity in the damaged area is increased to account for the increased density and shortened conduction path to the OC surface. Charred foam is not explicitly modeled in non-crushed areas since its conductivity does not change appreciably, and since the underlying foam is of sufficient thickness to prevent any heat from the fire event from reaching the OC surface through the impact limiter.

The second damage condition results from a 40-inch drop onto a 6-inch diameter puncture bar. Damage for this case is assumed to consist of a 6-inch diameter hole in the impact limiter side, extending down to the inner impact limiter shell near the upper end of the package, thus allowing maximum heat transmission from the fire event to the lid seal area region. The entry hole of the puncture bar through the impact limiter is assumed to be in the side drop damaged region of the impact limiter and to be conical in shape, thus allowing full exposure of the inner limiter shell to the fire environment. This maximizes heat input into the package seals. Appendix 3.6.1.6, *Damaged Impact Limiter*, provides a detailed description of the package damage and how it was modeled.

Damage from these two HAC scenarios is included in a single model. One accident analysis for each payload is run using the damaged package model.

If the optional paint is present on the OC and impact limiter exterior surfaces, the HAC fire test would be conservative because of the relatively high emissivity of paint ($\varepsilon > 0.90$) compared to that of bare stainless steel ($\varepsilon = 0.5$). The higher emissivity results in higher heat flow into the package during the HAC fire test, but the net affect is negligible since the paint burns away very shortly after the start of the fire.

Other damage assumptions could be made, but those assumed herein conservatively cover the concerns for the RH-TRU 72-B package. End and oblique drop cases do far less damage to the impact limiter than what is assumed for the side drop analysis case.

[3] General Plastics, *Last-a-Foam FR 3700® for Crash and Fire Protection of Nuclear Material Shipping Containers*, General Plastics Manufacturing Company, 4910 Burlington Way, Tacoma, Washington, February 1990.

3.5.3 Package Temperatures

The maximum temperatures noted for the HAC fire event described above are presented in Table 3.5-1 for the major components of the package. The transient temperature distributions are given in Figure 3.5-1 through Figure 3.5-10.

3.5.4 Maximum Internal Pressure

3.5.4.1 Temperature Control

The maximum HAC fire event pressure increase from NCT is primarily due to increased temperature and water vapor. Radiolytic gas generation effects are negligible because the period of the HAC fire event is relatively short. All other factors, as mentioned in Section 3.4.4, *Maximum Internal Pressure*, are negligible. Furthermore, the internal pressure rises and falls during the HAC fire event along with, and driven by, local IV and payload canister surface temperature transients. Thus, peak internal pressure occurs with peak surrounding temperatures during the HAC fire transient. Structural loads do not affect the maximum pressure capability of the RH-TRU 72-B packaging for HAC.

Table 3.5-1 lists peak payload canister and IV shell temperatures of 263 ºF and 327 ºF for paper wastes (50 watts maximum expected decay heat), and 247 ºF and 343 ºF for metallic wastes (300 watts maximum expected decay heat). Calculation of water vapor pressure employs the steam tables and IV temperatures. Calculation of increased internal air temperature employs Charles' Law with an average surface temperature essentially equal to the average of the peak payload canister and IV shell temperatures. The worst-case for either type of wastes results in an IV shell temperature of 263 ºF, and an average air temperature of (263 + 327)/2 = 295 ºF.

The initial pressure of gas present in the IV at 70 ºF is 14.7 psia. This gas is heated to 295 ºF. Thus, the increased pressure associated with this increase in temperature is:

$$P_{hu} = (14.7\ \text{psia}) \times \left(\frac{295\,^{\circ}\text{F} + 460\,^{\circ}\text{R}}{70\,^{\circ}\text{F} + 460\,^{\circ}\text{R}} \right) = 20.9\ \text{psia}$$

The water vapor pressure is based on the temperature of the coolant or condensing surface of the IV, 263 ºF. Thus, the water vapor pressure, P_{wv}, from the steam tables is 37.3 psia.

The calculated radiolytic gas pressure, P_{rg} = 135.27 psia, for bounding content code NewPaper is taken from Section 3.4.4.3, *Maximum Pressure for Normal Conditions of Transport*. Thus, the maximum IV pressure at the end of 60 days for bounding content code NewPaper is:

$$P_{max} = P_{rg} + P_{hu} + P_{wv} - P_{atm} = 135.27 + 20.9. + 37.3 - 14.7 = 178.8\ \text{psig}$$

The above is the worst-case possible transient pressure rise for the 60-day shipping period, and is still appreciably below the HAC analysis pressure of 300 psig used in Section 2.7.4, *Thermal*. Thus, the maximum HAC pressure does not affect the performance of the RH-TRU 72-B package.

3.5.4.2 Flammable Gas Control

Radiolytic gas generation effects are negligible because the period of the accident event is relatively short. All other factors as mentioned in Section 3.4.4, *Maximum Internal Pressure*, are negligible. Thus, flammable gas generation during the HAC fire event is no more severe than for NCT. It is assumed that RH-TRU waste materials breach the layers of confinement and also the payload containers under hypothetical accident conditions.

From a hydrogen concentration viewpoint, the worst case is when the layers of internal confinement and the payload containers are intact under normal conditions of transport. In this case, the maximum number of barriers to the release of gases generated within the innermost layer will be present, and flammable gas concentrations will increase from the outside of the payload container to the innermost layer of confinement. During accident conditions, if breaching the payload containers and layers of confinement would occur, the result would be a decrease in the number of barriers to release of generated gases. This would result in more mixing of the gases between layers of confinement and reduced concentrations in each. Hence, the controls placed on the payload to ensure flammability limits are met for normal conditions, also ensure compliance for accident conditions.

3.5.5 Maximum Thermal Stresses

Thermal stresses associated with the HAC fire event can be classified as secondary, displacement limited stresses. The significance of the thermal stresses is discussed in Section 2.7.4, *Thermal*.

3.5.6 Evaluation of Package Performance for the Hypothetical Accident Thermal Conditions

None of the temperatures noted from the HAC fire transient analyses exceed the temperature limitations of the respective materials, as defined in Section 3.3, *Technical Specifications of Components*. The highest lead temperature noted is 66 ºF below the melting point of lead, while the highest O-ring seal temperature noted is 91 ºF below the recommended upper operating limit for the butyl O ring seals of 250 ºF. As expected, the highest OC outer shell and lead temperatures are noted at nodes 551 and 546 due to the presence of the heat paths provided by the center-pivot trunnions.

The package O-ring seals see minimal temperature rise during the HAC fire transient due to a combination of the thermal protection provided by the impact limiter, the physical distance of the O-ring seals from the high temperature regions near the trunnions, and the relatively large mass (i.e., high heat capacity) of the package.

Figure 3.5-1 and Figure 3.5-6 show the behavior of the IV and OC O-ring seals after the HAC fire event. During the HAC fire transient analysis with a paper payload, the IV and OC O-ring seals experience a rise in temperature of only 44 ºF each. For the HAC fire scenario with a metallic payload, the IV and OC O-ring seals experience a 39 ºF and 41 ºF rise in temperature, respectively.

The two different types of payload material analyzed behave differently during the transient analysis. For the paper payload cases, the inner three annular node sets did not peak in temperature after 40 hours, while the outer two annular node sets did peak. To give some

indication of the peak payload temperature, a numerical average of 5 payload nodes at a single cross-section is calculated. As seen in Figure 3.5-2, this numerical average indicates that the payload temperature as a whole is decreasing after approximately 20 hours. Therefore, the maximum payload temperature can be taken as 263 ºF, as shown for node 37, reoccurring at about 5 hours. Note that the temperature of node 37 (263 ºF) is much higher than any of the other payload nodes since node 37 is in contact with the highly conductive carbon steel payload canister (node 515), whose temperature it closely tracks. Unlike the paper payload, the metallic payload nodes all peak in temperature within approximately 15 hours, and then began cooling. The maximum temperature of the metallic payload is reported as 196 ºF after the HAC fire event.

Other RH-TRU 72-B package component temperature histories are shown in Figure 3.5-3, Figure 3.5-4, Figure 3.5-5, Figure 3.5-6, and Figure 3.5-7 for the package with paper payload, and Figure 3.5-8, Figure 3.5-9, and Figure 3.5-10 for the package with metallic payload. The package component temperature histories shown in these figures include the center-pivot trunnion, thermal shield, OC outer shell, lead shield, OC inner shell, IV, and payload canister.

Table 3.5-1 – Maximum HAC Temperatures for RH-TRU 72-B Package

Location	50 W	300 W
Waste Centerline	219	196
Payload Canister Shell	263	247
IV Shell	327	343
OC Inner Shell	488	497
OC Lead Shield	544	554
OC Outer Shell	601	611
OC Thermal Shield	1,232	1,231
OC Upper Ring Forging	154	166
IV O-Ring Seal	150	159
OC O-Ring Seal	149	158
IV Lid	148	157
OC Lid	150	159
Impact Limiter Foam	420	421
Impact Limiter Shell	1,424	1,425

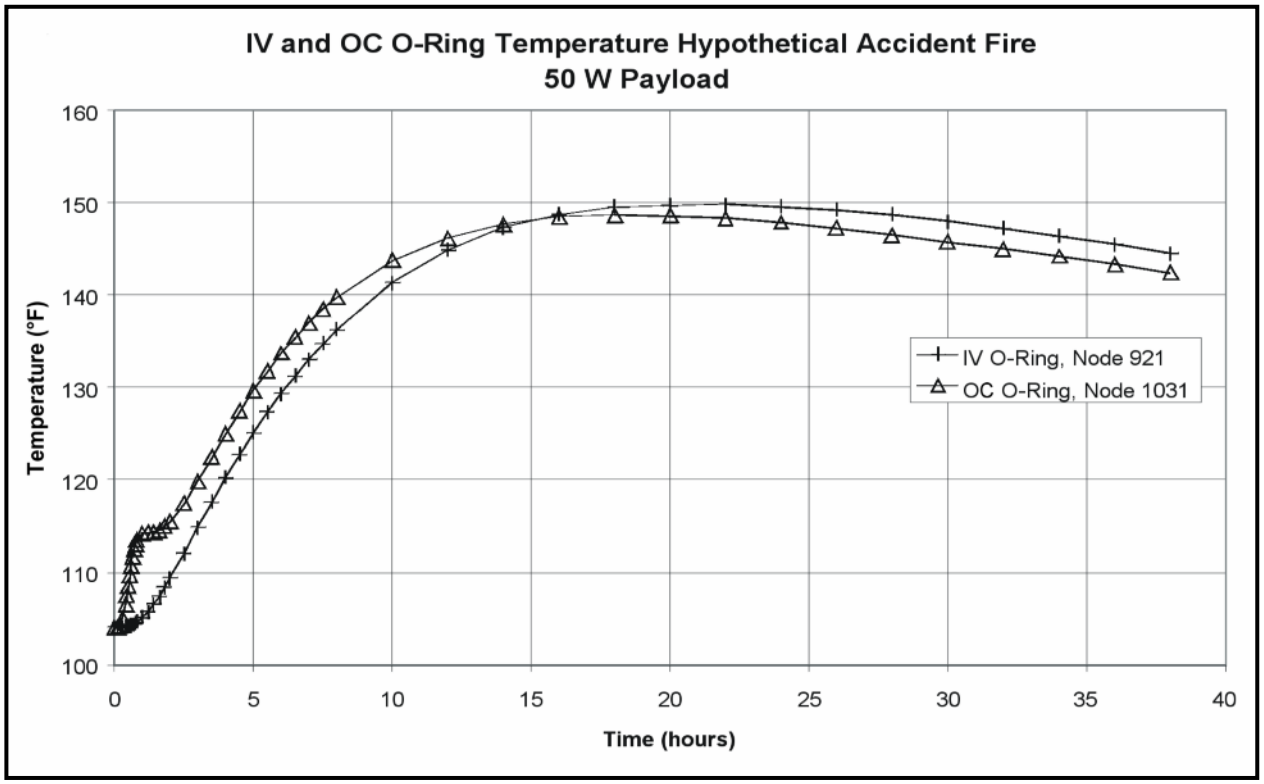

Figure 3.5-1 – IV and OC O-ring Seal Temperatures – 50W Payload

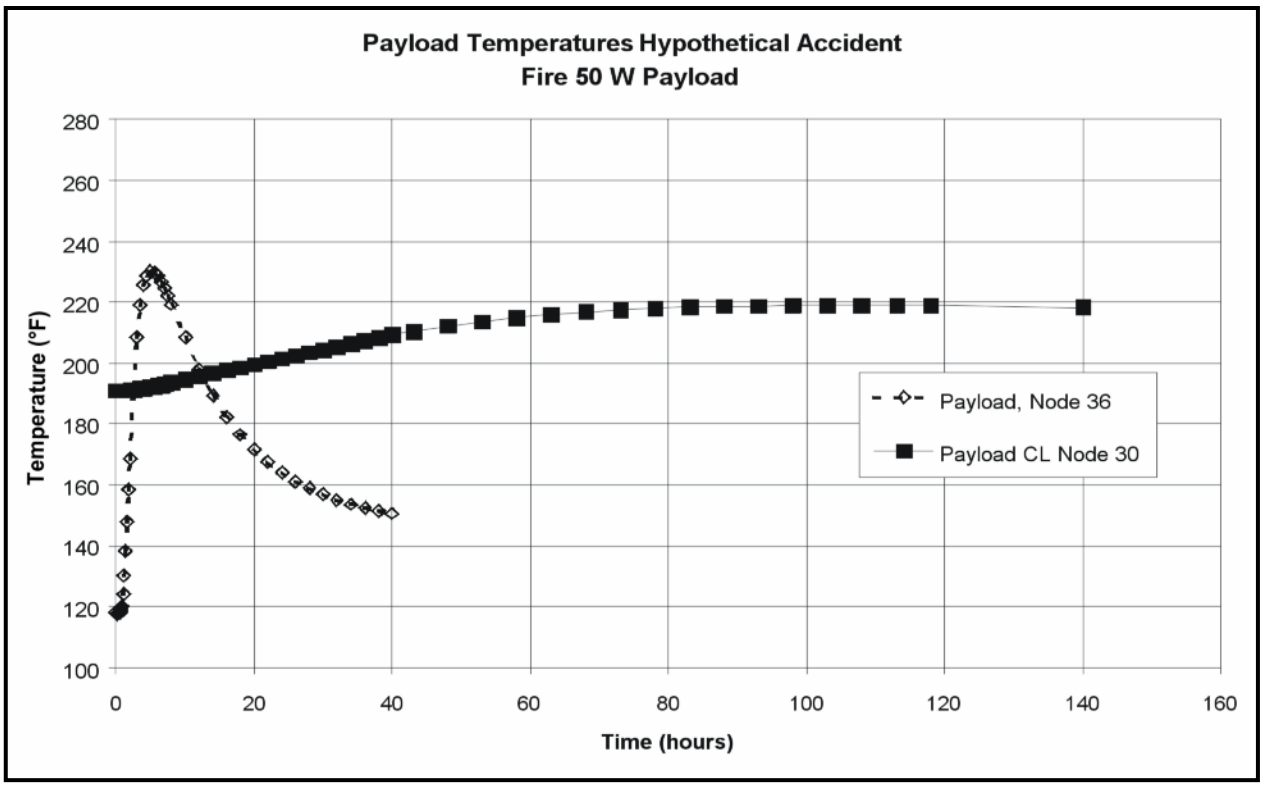

Figure 3.5-2 – Payload Temperatures – 50W Payload

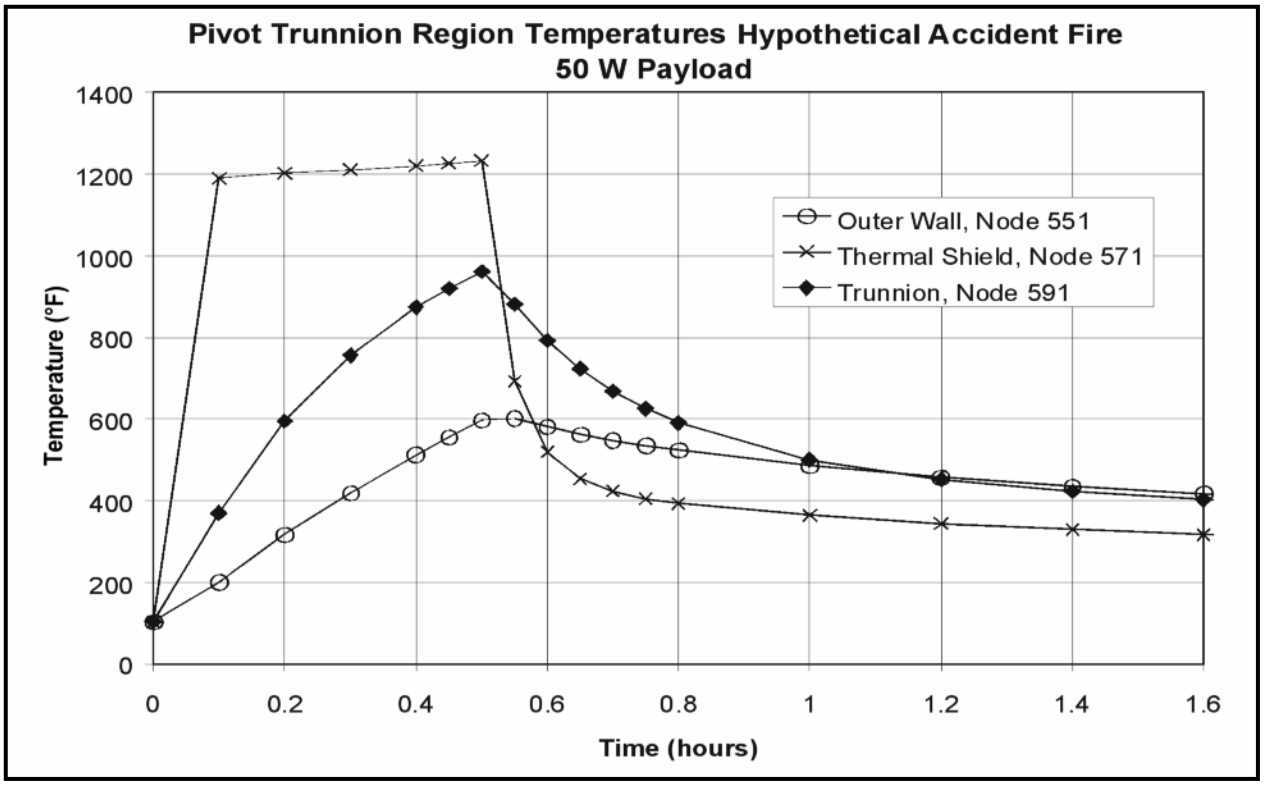

Figure 3.5-3 – Center-Pivot Trunnion Region Temperatures – 50W Payload

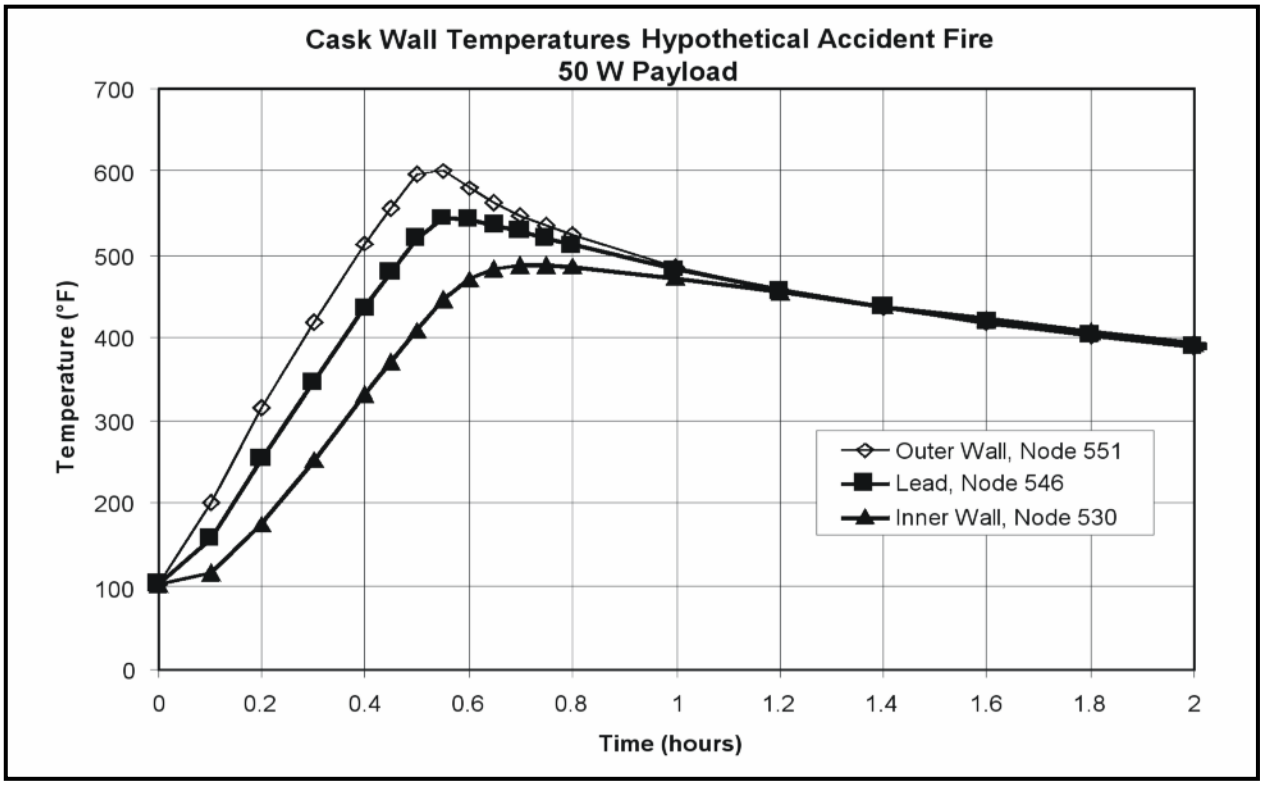

Figure 3.5-4 – OC Wall Temperatures – 50W Payload

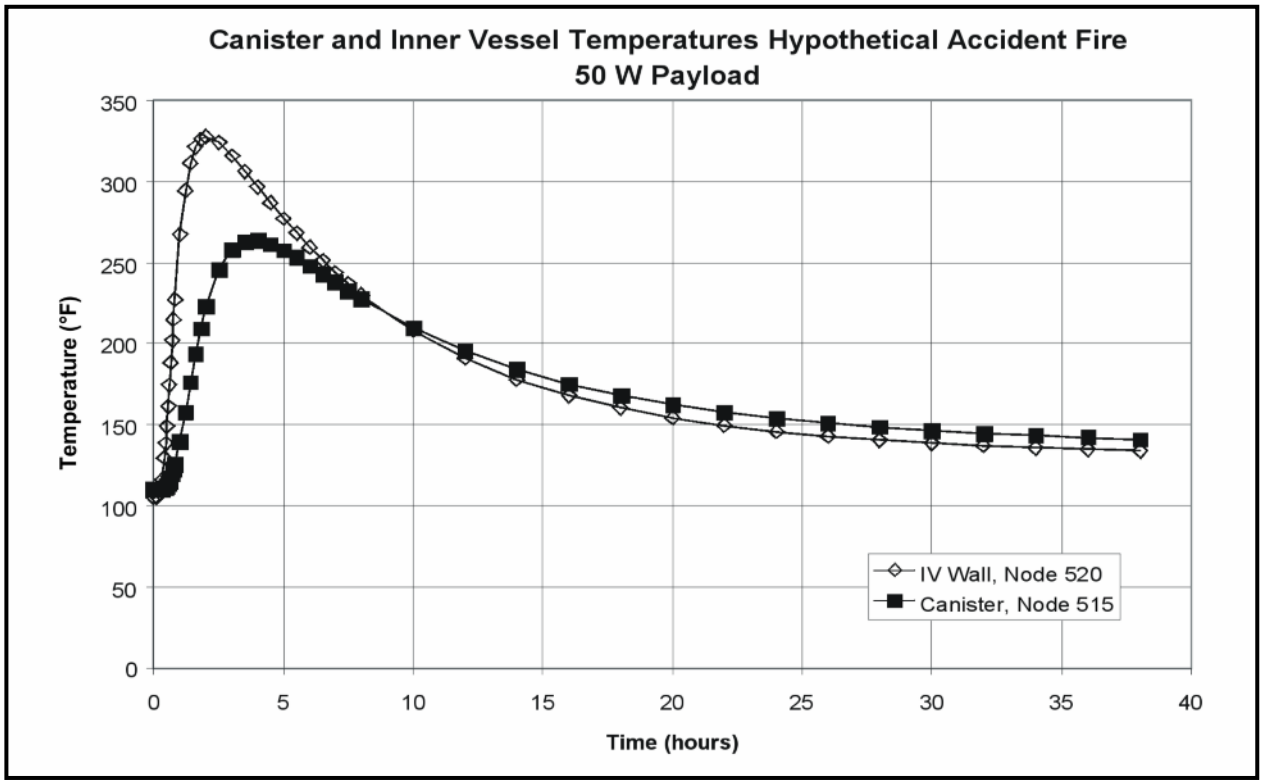

Figure 3.5-5 – Payload Temperatures – 50W Payload

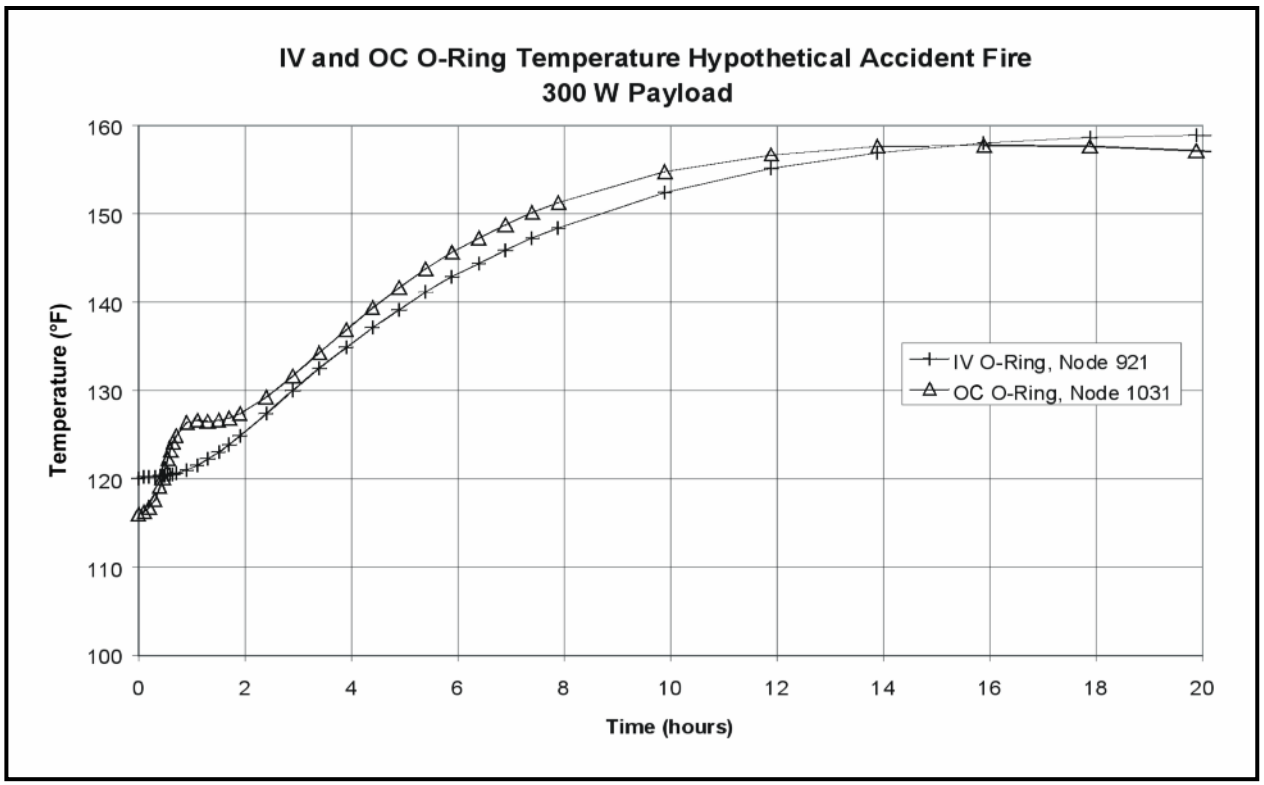

Figure 3.5-6 – IV and OC O-ring Seal Temperatures – 300W Payload

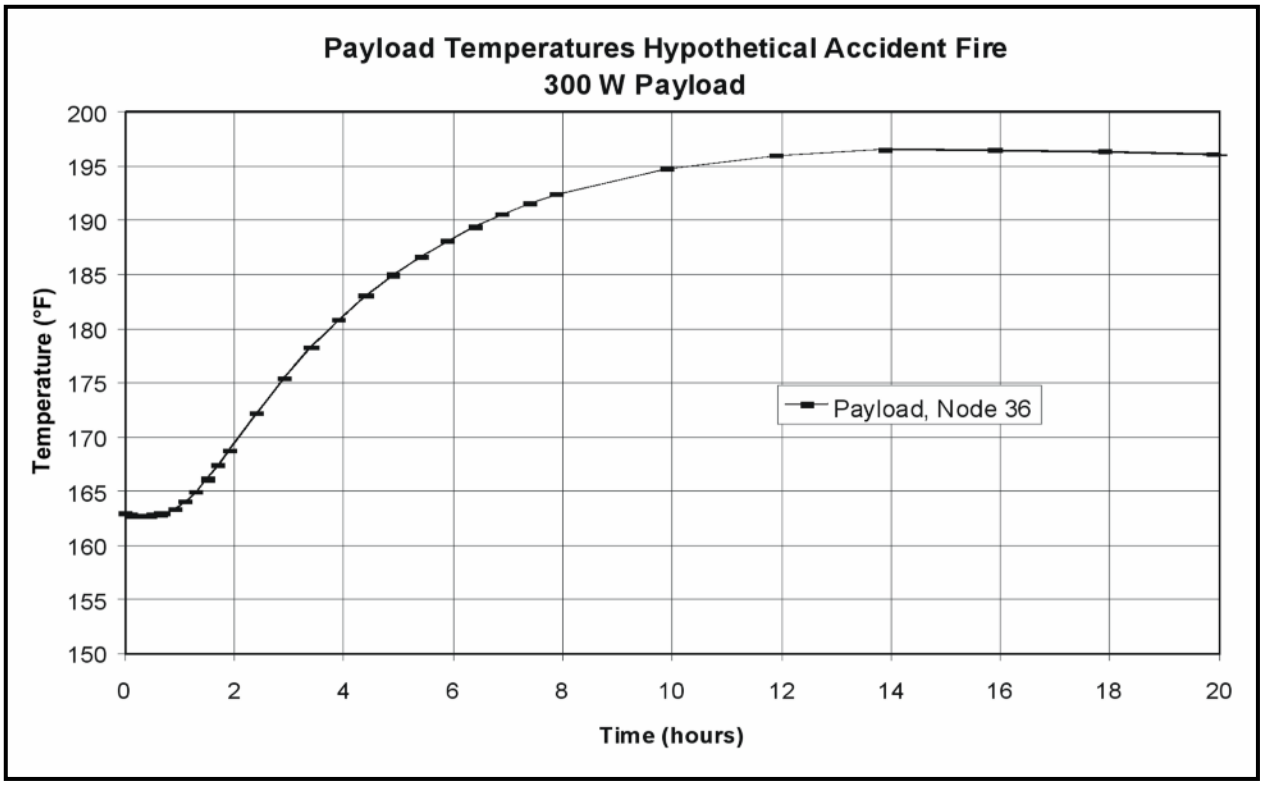

Figure 3.5-7 – Payload Temperatures – 300W Payload

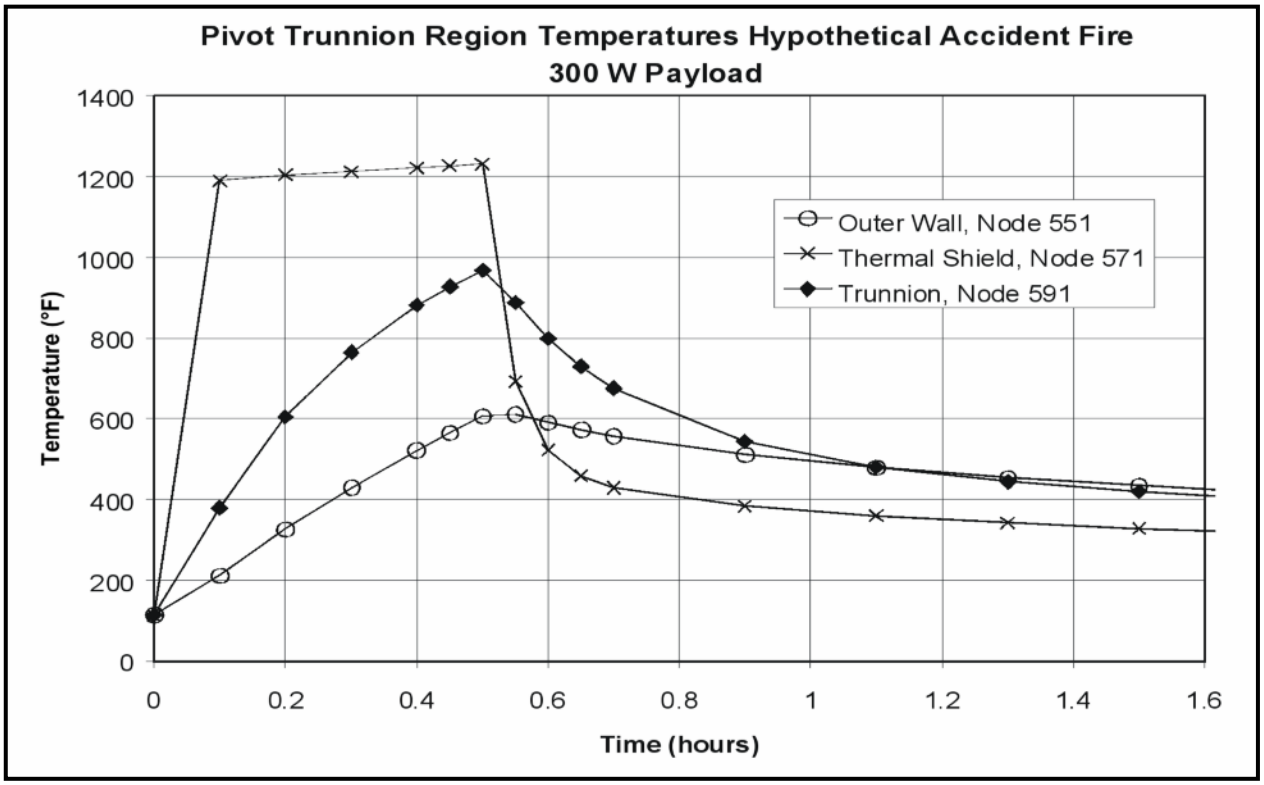

Figure 3.5-8 – Center-Pivot Trunnion Region Temperatures – 300W Payload

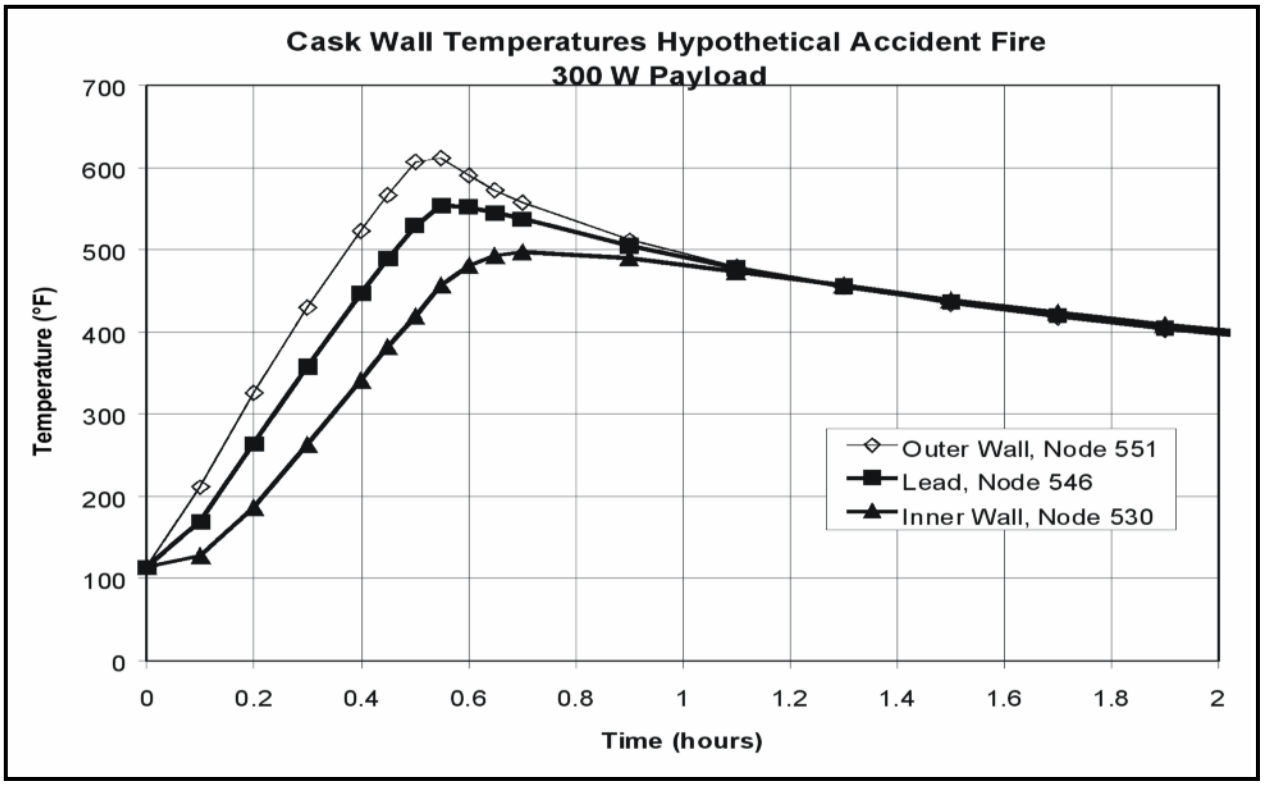

Figure 3.5-9 – OC Wall Temperatures – 300W Payload

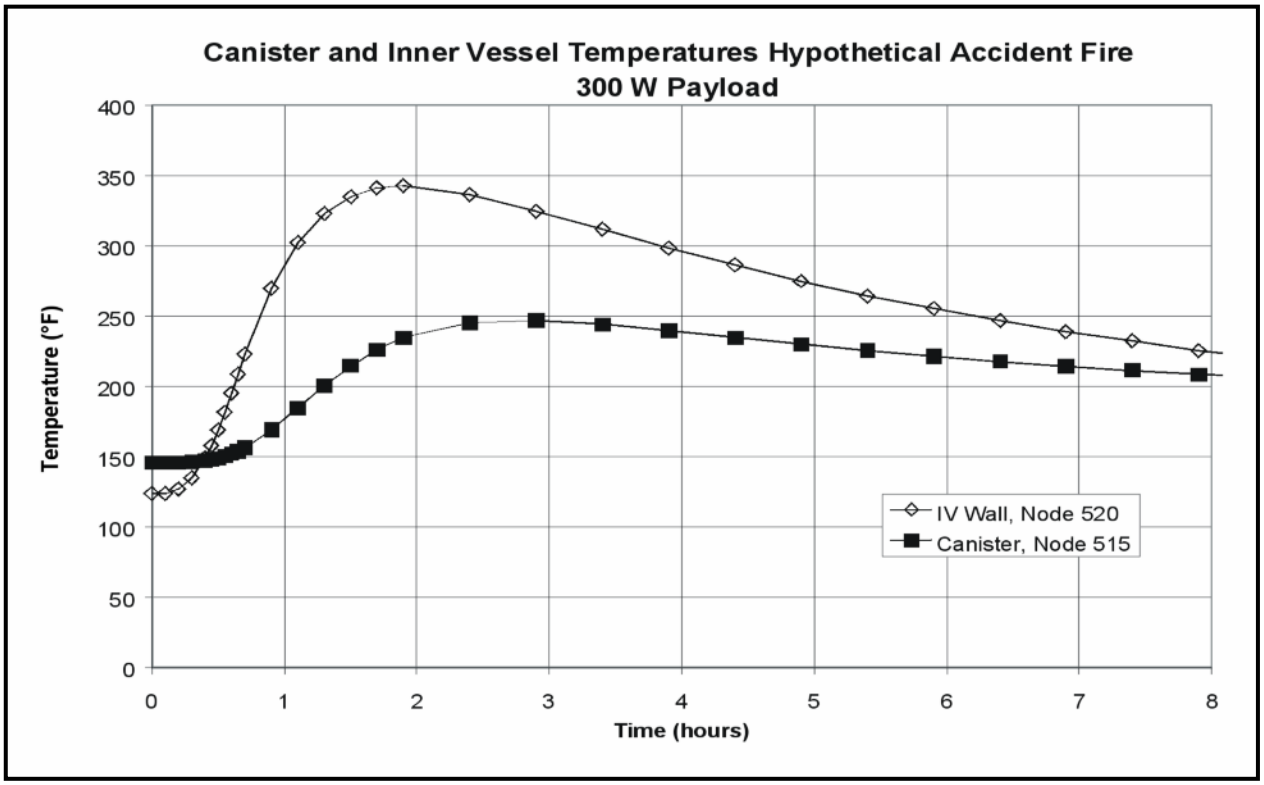

Figure 3.5-10 – Payload Temperatures – 300W Payload

3.6 Appendices

3.6.1 *Thermal Model Details*

3.6.2 *Finite Difference Thermal Analysis and Results*

3.6.3 *Polyurethane Foam Performance Tests*

3.6.4 *Designating an Alternative Seal Material*

This page intentionally left blank.

3.6.1 Thermal Model Details

The development of the thermal model used to analyze the RH-TRU 72B package is described herein. All thermal analyses use the SINDA '85/FLUINT finite difference code[1].

3.6.1.1 Basis of Analysis

(1) Analysis to follow the requirements of 10 CFR 71[2].

(2) SINDA '85/FLUINT is used for the evaluation; see Figure 3.6.1-1 through Figure 3.6.1-7 for nodal maps of the model.

(3) All internal voids are assumed to be filled with air at one (1) atmosphere.

(4) Paper based payload with 50 watts of decay heat.

(5) Metallic based payload with 300 watts of decay heat.

(6) Solar heat loads (insolation) are taken from 10 CFR §71.71(c)(1); see Table 3.4-1 in Section 3.4, *Thermal Evaluation for Normal Conditions of Transport*.

(7) Solar heat input is based on the full surface area of the package, applying solar absorbtivity, $\alpha = 0.3$.

(8) Thermal properties of materials used in the analyses are presented in Table 3.6.1-1 and Table 3.6.1-2. The thermal conductivity of air is approximated by linear interpolation between values given in Table 3.6.1-2.

3.6.1.2 External Heat Transfer

Solar loads for the thermal model are listed in Table 3.6.1-3. Solar loads are calculated using a full package area and are multiplied by an absorbtivity of 0.3 for normal conditions of transport (NCT) and an absorptivity of 0.8 for hypothetical accident conditions (HAC) post-fire. The insolation applied to the package surfaces is calculated by assuming the 10 CFR §71.71(c)(1)[2] values discussed in Paragrah (6) of Section 3.6.1.1, *Basis of Analysis*, are applied for 24 hours. Per 10 CFR §71.73(c)(4), no insolation is applied during the HAC fire event, but is applied for the post-fire transient.

3.6.1.2.1 External Convection

External free convection is included in the model for NCT and for HAC pre- and post-fire conditions. These convection coefficients are calculated internally by computing a local Nusselt number based on local air temperature (average of the local external surface temperature and ambient temperature) and surface area. The Nusselt number is calculated as a function of the Grashof and Prandtl numbers.

---

[1] SINDA '85/FLUINT, *Systems Improved Numerical Differencing Analyzer and Fluid Integrator*, Version 2.1, NASA/Martin Marietta Corporation, 1988.

[2] Title 10, Code of Federal Regulations, Part 71 (10 CFR 71), *Packaging and Transportation of Radioactive Material*, Final Rule, 01-26-04.

3.6.1.2.1.1 Forced Convection During the HAC Hydrocarbon-Fueled Fire

During a worst-case HAC hydrocarbon-fueled fire, the heated gases surrounding the package achieve significant velocities, sufficient to induce forced convection on the surface of the package. Measurements taken during actual hydrocarbon-fueled fire tests predicted average induced gas velocities of between 6 and 9 m/s (19.7 – 29.5 ft/s)[3]. It should be noted that although peak velocities as high as 15 m/s (49.2 ft/s) were measured at 6.1 meters (20 feet) from the fire surface, peak velocities 2.2 meters from the fire surface (7.2 feet), a location more commensurate with the hottest portion of the fire, were under 10 m/s (32.8 ft/s)[4].

Assuming a gas velocity of 9 m/s (29.5 ft/s) and a horizontally oriented package with an outer diameter of 3.47 feet, per *Elements of Heat Transfer*[5], the convection coefficient can be expressed as:

$$h = Nu\frac{k}{L} = \text{Btu/hr - ft}^2\text{ - °F}$$

where k is the conductivity of the gas at the film temperature (Btu/hr-ft-ºF), and L is the effective length of the vertical surface or cylinder diameter (feet). For a horizontal cylinder being subjected to turbulent flow, the Nusselt number can be expressed as:

$$Nu = 0.3 + \frac{0.62\,Re^{1/2}\,Pr^{1/3}}{\left[1+(0.4/Pr)^{2/3}\right]^{1/4}}\left[1+\left(\frac{Re}{282{,}000}\right)^{1/2}\right]$$

Reynold's number, Re, is:

$$Re = \frac{u_\infty D}{\nu}$$

where u_∞ is average air velocity, D is package diameter, ν is dynamic viscosity.

Initial calculations determine that the surface of the package exceeds 1,200 ºF in under 10 minutes; therefore, a film temperature of 1,350 ºF is assumed for determining air material properties. Specifically, Pr = 0.702, k = 0.039 Btu/hr ft-ºF, and ν = 0.00129 ft^2/sec. The resulting Reynold's number is 78,400, the Nusselt number is 207.1, and the heat transfer coefficient is 2.33 Btu/hr-ft^2-ºF. Conservatively, a coefficient of 2.5 Btu/hr-ft^2-ºF is applied to the entire exposed surface of the package for the duration of the half-hour fire simulation.

3.6.1.2.1.2 External Radiation

External radiation from packaging and impact limiter surfaces is calculated using the following equation:

$$Q = \sigma\varepsilon A\left(T^4 - T_\infty^4\right)$$

---

[3] J. J. Gregory, R. Mata, and N. R. Keltner, *Thermal Measurements in a Series of Large Pool Fires*, SAND85-0196, TTC-0659, UC-71, Sandia National Laboratories, Albuquerque, NM, August 1987.

[4] M. E. Schneider, L. A. Kent, *Measurement of Gas Velocities and Temperatures in a Large Open Pool Fire*, Heat and Mass Transfer in Fire, HTD Vol. 73.

[5] Y. Bayazitoglu, M. Ozisik, *Elements of Heat Transfer*, McGraw-Hill Publishing, New York, 1988, pp. 211-212.

Necessary input data are the emissivity and surface area associated with each node's surface. The values for emissivity and area are provided in Table 3.6.1-4.

3.6.1.3 Conductivity Calculations for Conduction and Radiation Elements

3.6.1.3.1 Radial Conduction

Calculations for radial modes of conduction are performed using the following expression:

$$Q = K(\Delta T) = \frac{2\pi K_{mat} L}{\ln\left(r_o / r_i\right)}(\Delta T)$$

where Q is the rate of heat transfer, K is the conductivity, ΔT is the temperature difference, K_{mat} is the material's thermal conductivity, L is the length, r_o is the outer radius, and r_i is the inner radius.

3.6.1.3.2 Axial Conduction

Axial modes of conduction are calculated using the following expression:

$$Q = K(\Delta T) = \frac{K_{mat} A}{L}(\Delta T)$$

where Q is the rate of heat transfer, K is the conductivity, ΔT is the temperature difference, K_{mat} is the material's thermal conductivity, A is the cross-sectional area, and L is the length.

3.6.1.3.3 Radiative Heat Transfer

Radiation between components of the package and payload is calculated using the following expression:

$$Q = \frac{\sigma A_1\left(T_1^4 - T_2^4\right)}{\left(\frac{1}{\varepsilon_1} - 1\right) + \frac{1}{\Im_{1\to 2}} + \left(\frac{A_1}{A_2}\right)\left(\frac{1}{\varepsilon_2} - 1\right)}$$

where σ is the Stefan-Boltzman constant, ε is the emissivity, A is the surface area, ℑ is the view factor, and T is the temperature.

3.6.1.4 Center-Pivot Trunnions

The center-pivot trunnions are modeled on both sides of the package. This was done by breaking the center section of the axisymmetric model into four 90º segments. Two opposing segments are used as locations of the trunnions. Approximately 50% of the segment area is covered by the trunnion baseplate. The remaining area is modeled as being covered by the thermal shield. The trunnion baseplate is connected to the outer cask (OC) outer shell, and is assumed to have full contact with the outer shell. The trunnion is modeled as a cylinder attached to the baseplate. Both baseplate and trunnion are attached to the external convection and radiation nodes in order to accurately model the local heat transfer processes.

3.6.1.5 Lift/Tie-Down Trunnions

The lift/tie-down trunnions are modeled as single nodes at each end of the package. The capacitance and surface area of the trunnions and baseplates are combined and used for the single node. This provides for proper heat transfer to and from the environment, but spreads the heat transfer into the package equally around the OC surface. Thus, actual temperatures immediately under the trunnions are higher than predicted. However, this is considered acceptable since the more accurate modeling of the much larger center-pivot trunnion is considered to provide worst-case wall temperatures.

3.6.1.6 Damaged Impact Limiter

The damaged impact limiter is modeled by changing portions of the model to provide three-dimensional modeling of the damaged area of the impact limiter. The axisymmetric elements representing the package's lid region and attached impact limiter are divided into radial layers and then into five 72º segments. One of the segments is additionally subdivided into three 24º segments. The properties of the original nodes are adjusted accordingly, and additional conductors are added to connect the additional nodes. The smaller segments are properly modified to reflect the crushed portion due to the HAC side drop, and a roughly conical opening is formed by changing the properties of several nodes and associated conductors to simulate the HAC puncture bar damage. To simulate puncture damage, node 2481 on the inner impact limiter skin is assumed to be exposed by the HAC puncture event and is directly connected to external radiation and convection nodes. In this way, the heat input due from the HAC fire event is maximized for the region nearest the packaging's lid and O-ring seals.

3.6.1.7 Payload Model

3.6.1.7.1 Paper Payload

The paper payload is assumed to consist of organic material such as paper or paper-like products. The total decay heat output for this payload is specified to be 50 watts. The waste containers are assumed to be completely filled and therefore the heat is transferred to the waste container walls via conduction only. The conductivity of the waste is 0.02 Btu/hr-ft-ºF. Two waste containers are contained in each of three 17H, 30-gallon drums. Heat is transferred to the payload canister walls via conduction across the air gaps and radiation between container surfaces.

3.6.1.7.2 Metallic Payload

The metallic payload is specified to have 300 watts output from irradiated metallic waste of various forms. It is normally loaded into 55-gallon drums and covered with a cement-like material to fix the metal pieces in place. This configuration is modeled by assuming the drums are filled with a mixture of cement and steel that was ratioed to allow the maximum allowed weight of the payload to be reached. Three drums with this load, each producing 100 watts, are placed into the payload canister. Heat is assumed to be produced uniformly throughout the 55-gallon drums. Thermal capacitance and conductivity are calculated to reflect the metal/cement mixture.

Table 3.6.1-1 – Thermal Properties of Materials

Material	Conductivity (Btu/hr-ft-ºF)	Density (lb/ft^3)	Specific Heat (Btu/lb-ºF)	Reference
Stainless Steel, Type 304	10.0 @ 212 ºF	488	0.11	①
Carbon Steel, A516, Grade 55	25.0 @ 212 ºF	487	0.113	②
Lead	19.3 @ 212 ºF	710	0.031	②
Polyurethane Foam	0.0188 @ 212 ºF	11.5	0.300	③
Payload (paper)	0.02	100	0.55	④
Payload (metallic)	9.47	272.0	0.168	④
Air	Table 3.6.1-2	0.071	0.240	⑤⑥

Notes:

① General Electric, *Heat Transfer and Fluid Flow Data Books*, Genium Publishing Corporation, Schenectady, NY.

② Rohsenow and Hartnett, *Handbook of Heat Transfer*, McGraw-Hill, New York, NY, 1973, Chapter 2, Table 28.

③ General Plastics, *Last-a-Foam FR 3700® for Crash and Fire Protection of Nuclear Material Shipping Containers*, General Plastics Manufacturing Company, 4910 Burlington Way, Tacoma, Washington, February 1990.

④ The thermal material properties for paper and metallic waste are discussed in Appendix 3.6.1.7, *Payload Model*.

⑤ Frank Kreith, Principles of Heat Transfer, 3rd Edition, McGraw-Hill, New York, NY, 1973, Table A-3.

⑥ Rohsenow and Hartnett, *Handbook of Heat Transfer*, McGraw-Hill, New York, NY, 1973, Chapter 2, Tables 35 and 39, et al.

Table 3.6.1-2 – Conductivity of Air

Temperature (ºF)	Air Conductivity (Btu/hr-ft-ºF)	Specific Heat (Btu/lb-ºF)	Absolute Viscosity (lb/ft-hr)
32	0.0140	0.2402	0.04194
100	0.0154	0.2402	0.04626
300	0.0193	0.2432	0.05796
500	0.0231	0.2472	0.06804
1,000	0.0319	0.2622	0.08892
1,500	0.0400	0.2762	0.10800

Table 3.6.1-3 – Solar Loads (Insolation) for the Thermal Model

Node	Surface Type	Surface Area (ft^2)	Solar Load (Btu/hr)
370	curved	16.22	634.73
470	curved	18.15	710.19
570	curved	4.54	177.55
571	curved	4.54	177.55
572	curved	4.54	177.55
573	curved	4.54	177.55
670	curved	18.15	710.19
770	curved	16.22	634.73
2,000	curved	76.27	2,984.17
3,000	curved	76.27	2,984.17
2,010	flat	31.50	1,934.93
3,010	flat	31.50	1,934.93
2,100	flat	21.84	1,341.18
3,100	flat	21.84	1,341.18
380	curved	1.08	39.13
581	flat	2.72	166.76
583	flat	2.72	166.76
591	flat	1.55	48.20
593	flat	1.71	48.20
780	curved	2.16	39.123

Table 3.6.1-4 – External Radiation Input for the Thermal Model

Node	Emissivity	Surface Area (ft^2)
370	0.3	16.22
470	0.3	18.15
570	0.3	4.54
571	0.3	4.54
572	0.3	4.54
573	0.3	4.54
670	0.3	18.15
770	0.3	16.22
2,000	0.3	76.27
3,000	0.3	76.27
2,010	0.3	31.50
3,010	0.3	31.50
2,100	0.3	21.84
3,100	0.3	21.84
380	0.3	1.08
581	0.3	2.72
583	0.3	2.72
591	0.3	1.55
593	0.3	1.71
780	0.3	2.16

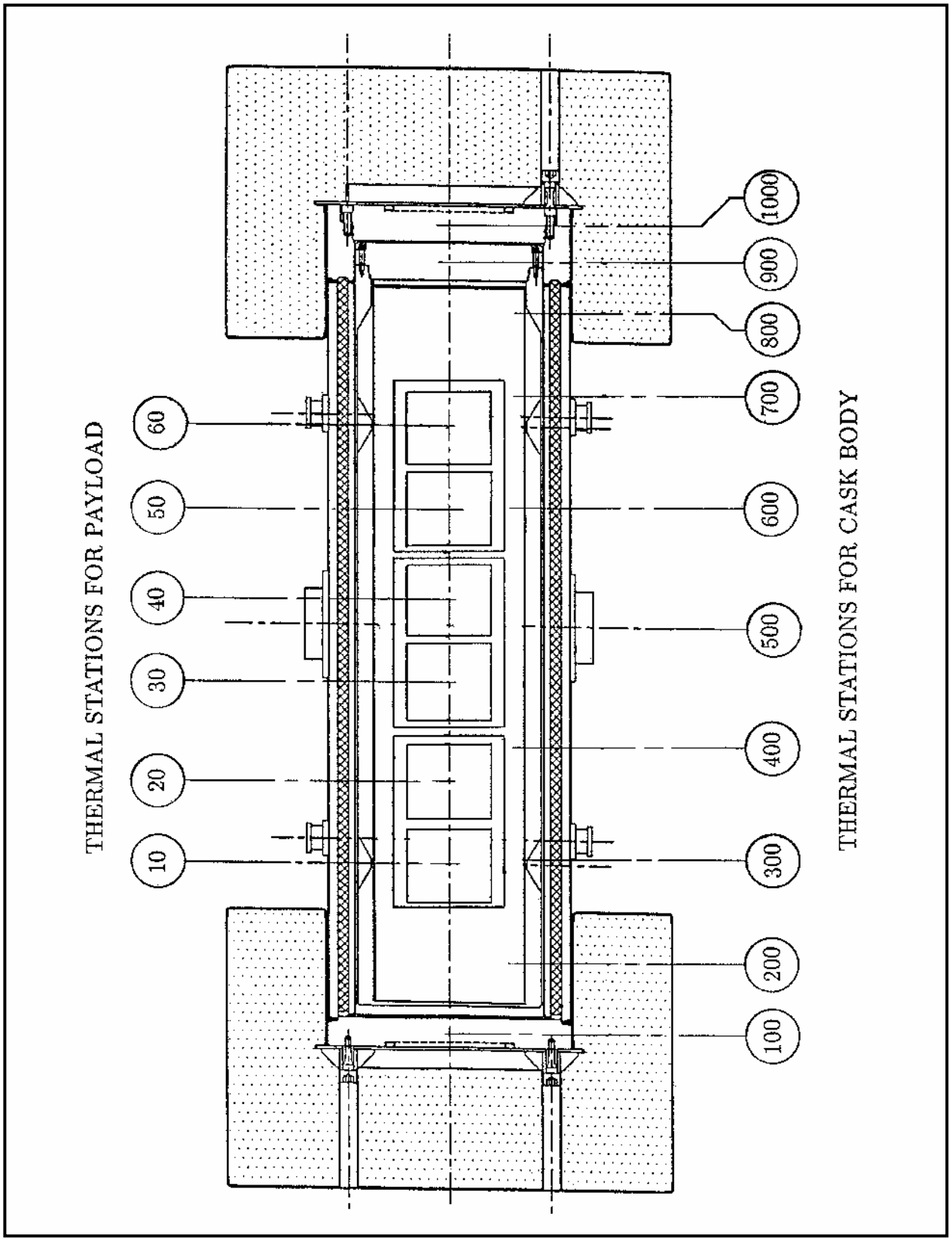

Figure 3.6.1-1 – Thermal Model Stations for RH-TRU 72-B Package Model

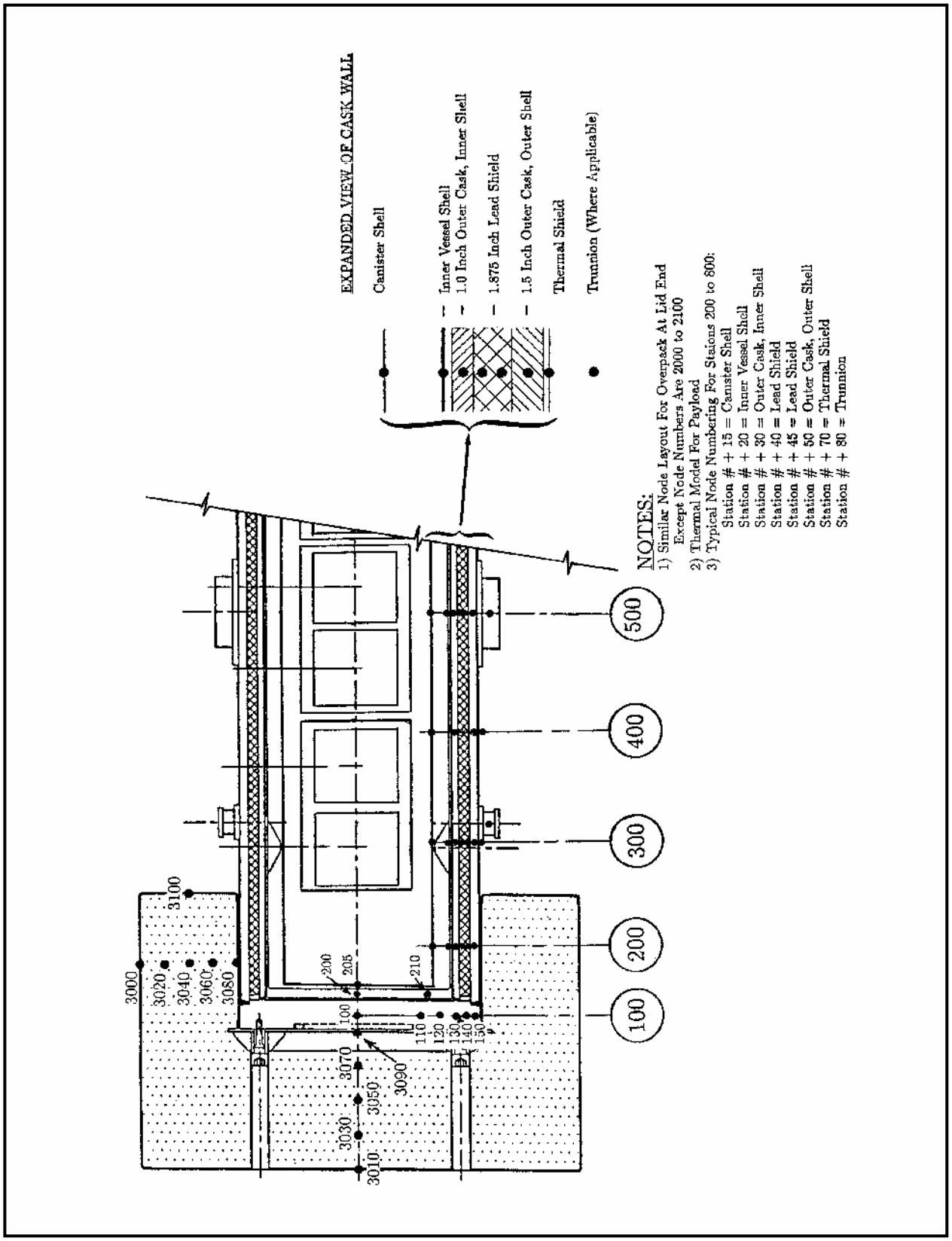

Figure 3.6.1-2 – Node Layout for the Impact Limiters and Packaging Body

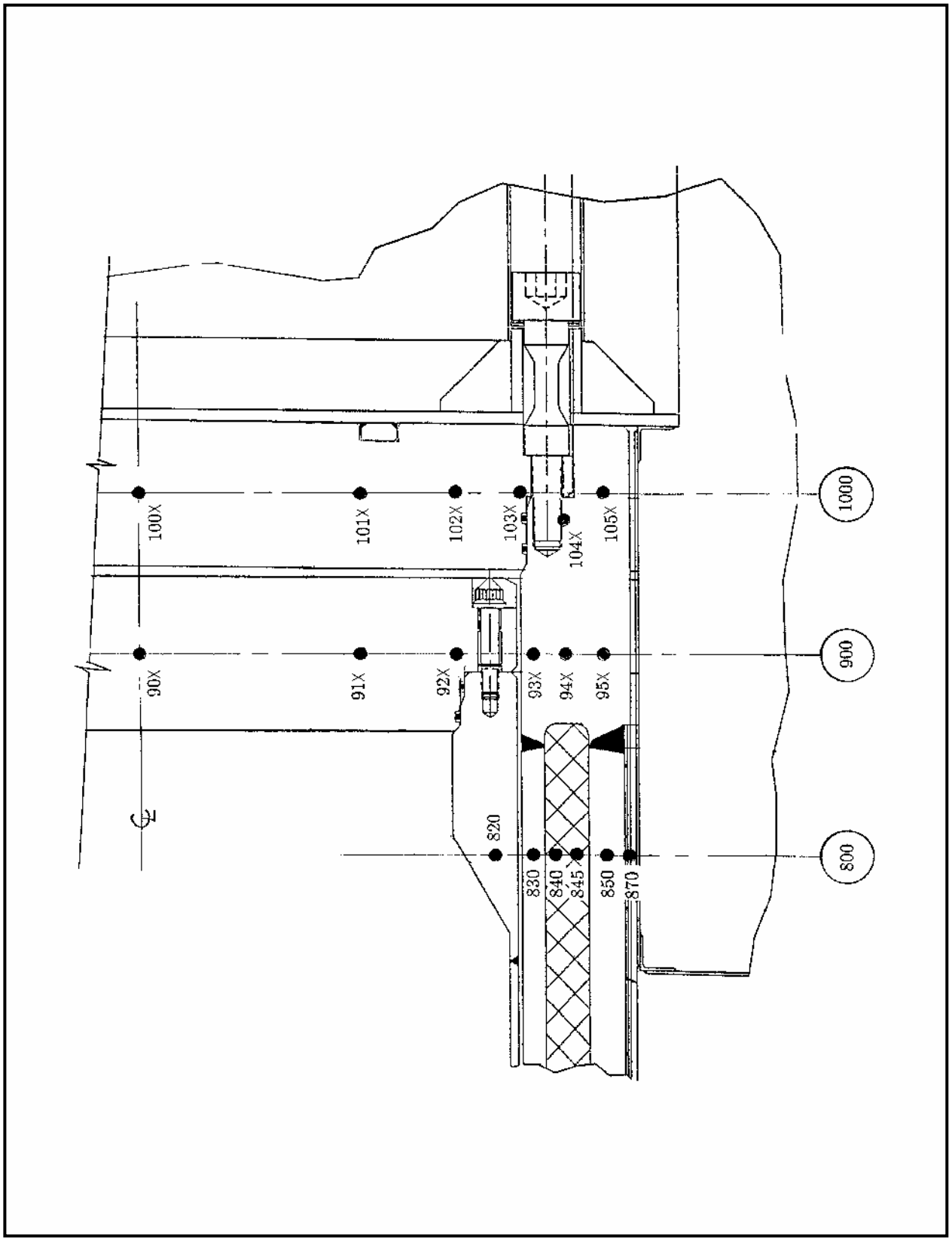

Figure 3.6.1-3 – Thermal Model Node Layout at the Package Lid-End

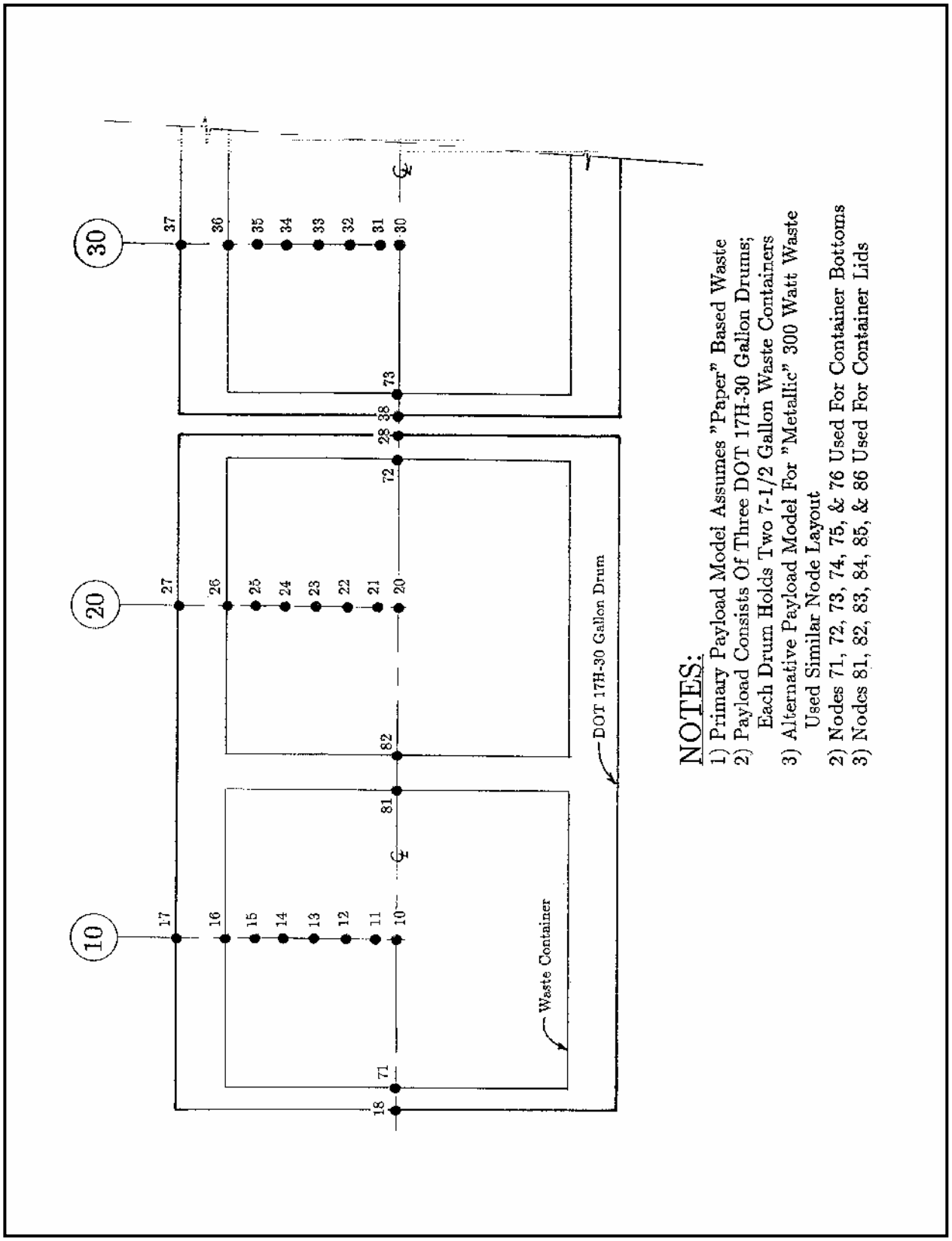

Figure 3.6.1-4 – Payload Node Layout (Non-Metallic Shown)

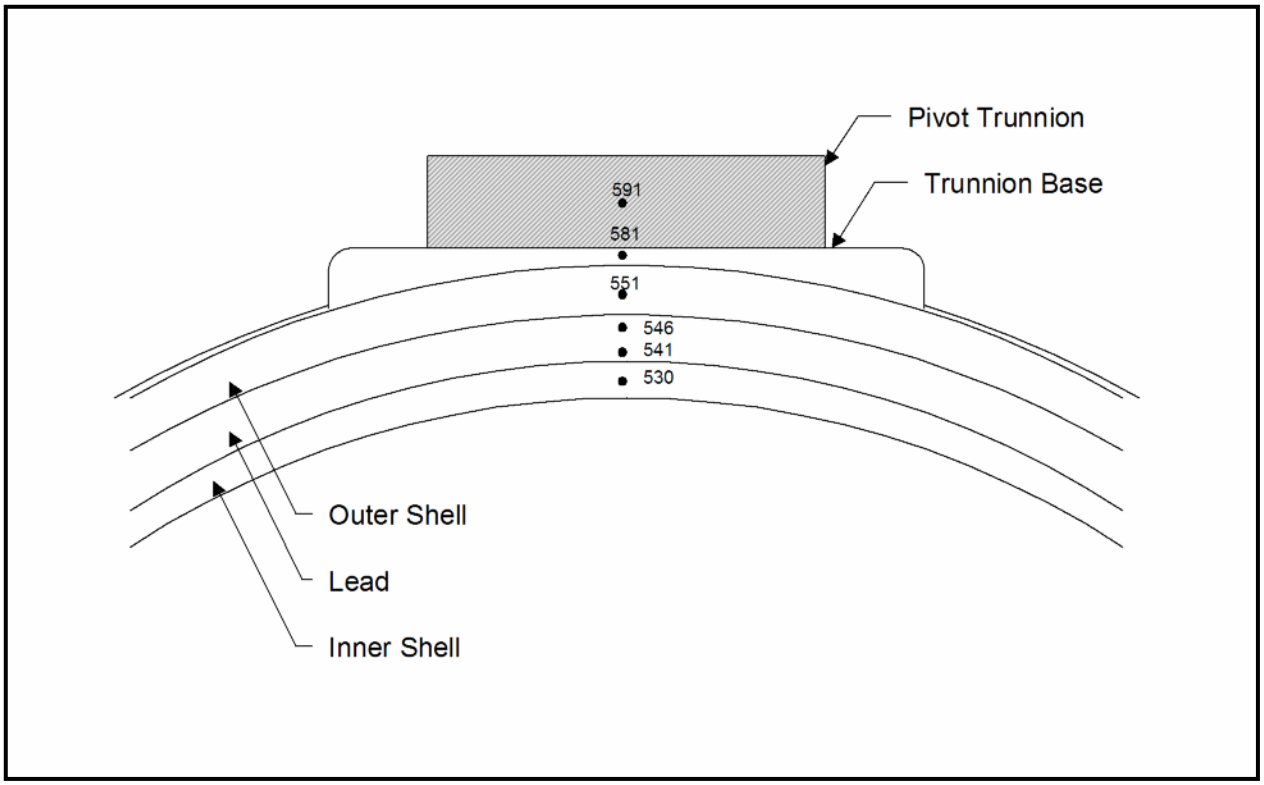

Figure 3.6.1-5 – Center-Pivot Trunnion Node Layout

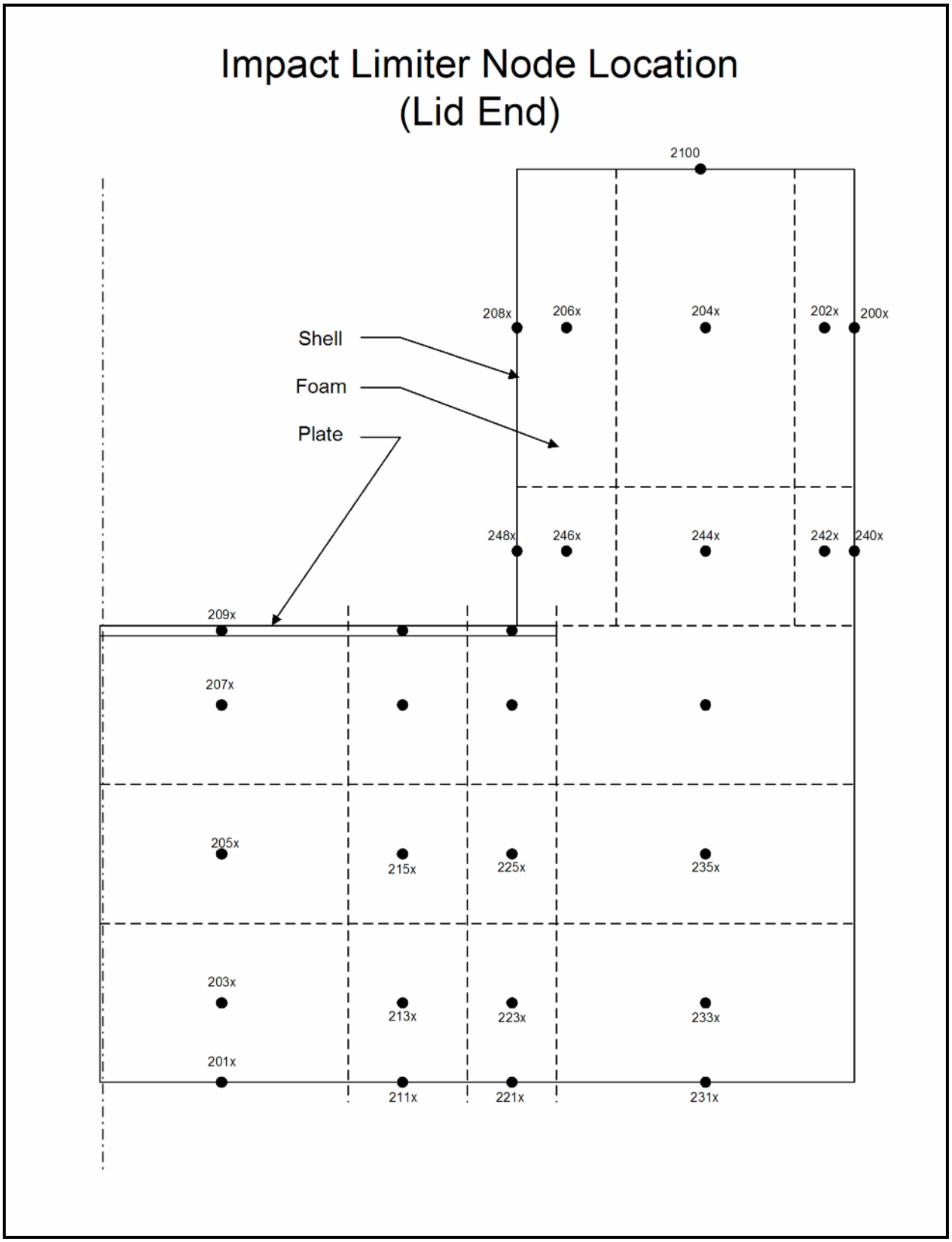

Figure 3.6.1-6 – Lid-End Impact Limiter Node Layout

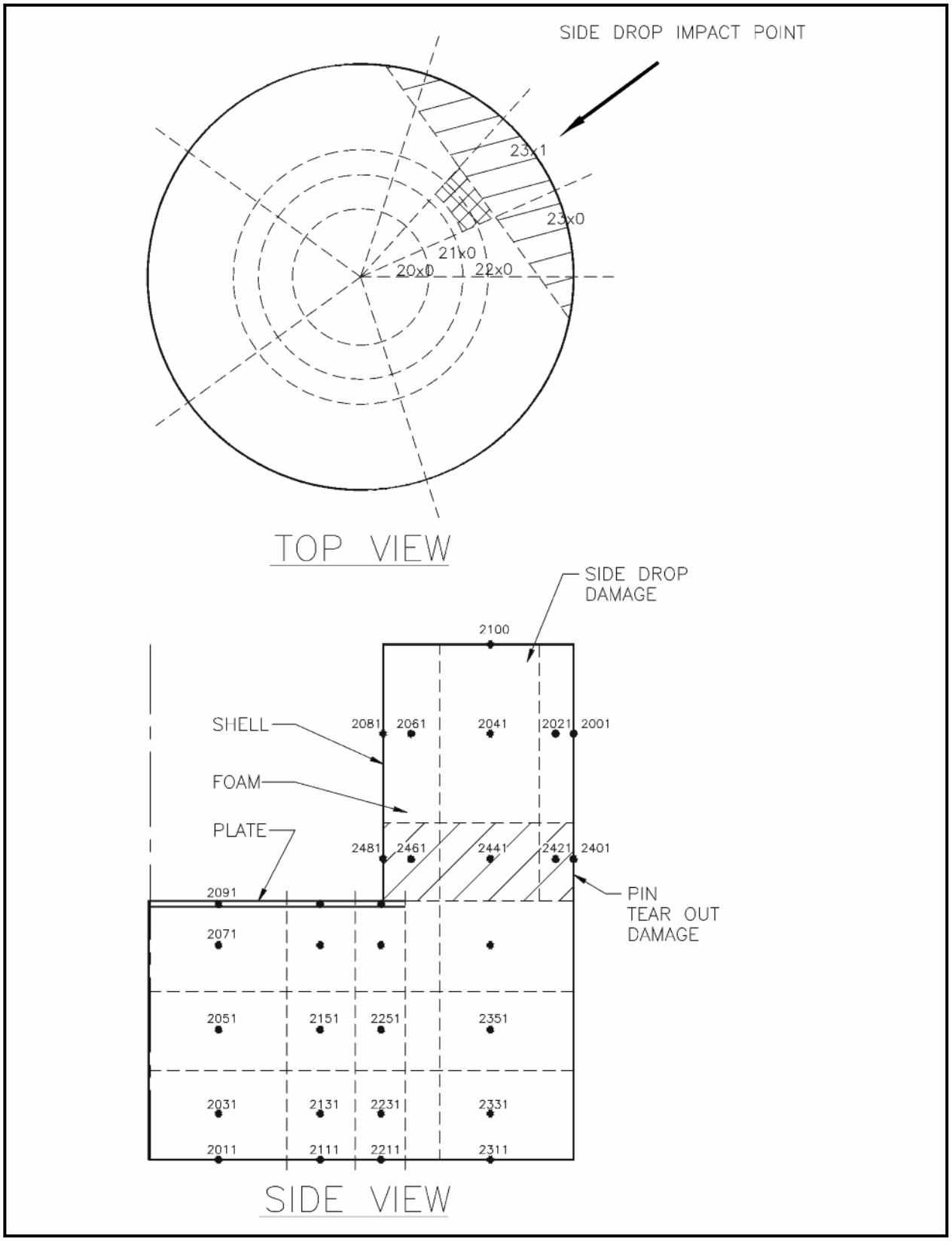

Figure 3.6.1-7 – Side Drop and Puncture Bar Damage Node Layout

3.6.2 Finite Difference Thermal Analysis and Results

Input and output files for the normal conditions of transport (NCT) and hypothetical accident condition (HAC) steady-state SINDA '85/FLUINT[1] runs are included herein. In addition, the input files for the HAC transient analyses are included.

The following input files are included here, with corresponding output files contained within *Data Package for the RH-TRU 72-B Waste Shipping Package*[2].

Normal Conditions of Transport:

3.6.2.1 *50-Watt Steady-State Input File (With and Without Insolation)*

3.6.2.2 *300-Watt Steady-State Input File (With and Without Insolation)*

Hypothetical Accident Conditions:

3.6.2.3 *50-Watt Transient Conditions Input File (Damaged Package Model)*

3.6.2.4 *300-Watt Transient Conditions Input File (Damaged Package Model)*

3.6.2.1 50-Watt Steady-State Input File (With and Without Insolation)

```
HEADER OPTIONS DATA
TITLE 72B FUEL CASK, BASELINE W/ 50W W SOLAR, Trunnion
      MODEL= 72BCASK
      OUTPUT = SST50W.sol
      PPOUT = ALL1
C*********************************************************************
HEADER NODE DATA, CASK
C*********************************************************************
C  *************************
C  PAYLOAD MODEL
C  *************************
       GEN  10,  6,  10,  230.,   0.21013 * 100.0 * 0.25
       GEN  11,  6,  10,  210.,   0.21013 * 100.0 * 0.25
       GEN  12,  6,  10,  180.,   0.21013 * 100.0 * 0.25
       GEN  13,  6,  10,  170.,   0.21013 * 100.0 * 0.25
       GEN  14,  6,  10,  140.,   0.21013 * 100.0 * 0.25
       GEN  15,  6,  10,  125.,   0.21013 * 100.0 * 0.25
       GEN  16,  6,  10,  120.,   6.660 * 0.113
       GEN  17,  6,  10,  117.,   10.976* 0.113
       GEN  18,  6,  10,  120.,   3.5958* 0.113
       GEN  71,  6,   1,  120.,   1.9260* 0.113
       GEN  81,  6,   1,  120.,   1.9260* 0.113
C  *************************
C  OVERPACK   IMPACT LIMITER MODEL
C  *************************
      GEN  2000,  2,  1000,  125.,  371.614* 0.11
      GEN  2020,  2,  1000,  125.,  109.155* 0.30
      GEN  2040,  2,  1000,  127.,  286.960* 0.30
      GEN  2060,  2,  1000,  131.,  117.600* 0.30
      GEN  2080,  2,  1000,  133.,  161.362* 0.11
      GEN  2100,  2,  1000,  133.,  106.561* 0.11
      GEN  2010,  2,  1000,  135.,  153.736* 0.11
      GEN  2030,  2,  1000,  134.,   80.176* 0.30
      GEN  2050,  2,  1000,  133.,   70.154* 0.30
      GEN  2070,  2,  1000,  132.,   75.165* 0.30
      GEN  2090,  2,  1000,  130.,  231.616* 0.11
C  *************************
C  CASK BODY NODES
```

[1] SINDA '85/FLUINT, *Systems Improved Numerical Differencing Analyzer and Fluid Integrator*, Version 2.1, NASA/Martin Marietta Corporation, 1988.

[2] U.S. Department of Energy, *Data Package for the RH-TRU 72-B Waste Shipping Package*, Current Revision, U.S. Department of Energy, Carlsbad Field Office, Carlsbad, New Mexico.

```
C  *************************
C      OUTER CASK BASE PLATE
     100,   131.,   400.353* 0.11
     110,   130.,   292.780* 0.11
     120,   130.,   469.627* 0.11
     130,   130.,   148.075* 0.11
     140,   130.,   301.554* 0.11
     150,   130.,   306.823* 0.11
C      CANISTER
     205,   175.,   100.253* 0.11
     212,   175.,   339.938* 0.031
     215,   175.,   99.224* 0.11
     315,   175.,   101.882* 0.11
     415,   175.,   113.994* 0.11
     515,   175.,   113.994* 0.11
     615,   175.,   113.994* 0.11
     715,   175.,   101.882* 0.11
     805,   175.,   189.583* 0.11
     812,   175.,   570.760* 0.031
     815,   175.,    71.709* 0.11
C      INNER VESSEL
     200,   130.,   120.106* 0.11         $ BASE PLATE
     210,   130.,   240.800* 0.11         $ BASE PLATE
     220,   130.,   185.446* 0.11         $ INNER VESSEL SHELL
     320,   130.,   188.076* 0.11         $ INNER VESSEL SHELL
     420,   130.,   210.435* 0.11         $ INNER VESSEL SHELL
     520,   130.,   210.435* 0.11         $ INNER VESSEL SHELL
     620,   130.,   210.435* 0.11         $ INNER VESSEL SHELL
     720,   130.,   188.076* 0.11         $ INNER VESSEL SHELL
     820,   130.,   608.129* 0.11         $ INNER VESSEL SHELL
C      OUTER CASK, INNER VESSEL
     230,   128.,   533.071* 0.11
     330,   128.,   529.369* 0.11
     430,   128.,   592.300* 0.11
     530,   128.,   592.300* 0.11
     630,   128.,   592.300* 0.11
     730,   128.,   529.369* 0.11
     830,   128.,   299.852* 0.11
C      LEAD SHIELD
     240,   123.,   767.199* 0.031
     340,   118.,   761.870* 0.031
     440,   116.,   852.443* 0.031
C     540,   114.,   852.443* 0.031
     GEN  540,  4,  1,  114.,  0.25*852.443*0.031
     640,   114.,   852.443* 0.031
     740,   114.,   761.870* 0.031
     840,   116.,   431.550* 0.031
     245,   123.,   812.252* 0.031
     345,   118.,   806.610* 0.031
     445,   116.,   902.503* 0.031
C     545,   114.,   902.503* 0.031
     GEN  545,  4,  1,  114.,  0.25*902.503*0.031
     645,   114.,   902.503* 0.031
     745,   114.,   806.610* 0.031
     845,   116.,   456.890* 0.031
C      OUTER CASK, OUTER SHELL
     250,   123.,   949.323* 0.11
     350,   118.,   942.730* 0.11
     450,   116.,  1054.803* 0.11
C     550,   114.,  1054.803* 0.11
     GEN  550,  4,  1,  114.,  0.25*1054.803*0.11
     650,   114.,  1054.803* 0.11

     750,   114.,   942.730* 0.11
     850,   116.,   533.994* 0.11
C      THERMAL SHIELD
     270,   122.,    90.933* 0.11
     370,   115.,    89.726* 0.11
     470,   113.,   100.393* 0.11
C     570,   111.,   100.393* 0.11
     GEN  570,  2,  2,  111.,  0.25*100.393*0.11
     GEN  571,  2,  2,  111.,  0.125*100.393*0.11
     670,   111.,   100.393* 0.11
     770,   112.,    89.726* 0.11
     870,   116.,    50.824* 0.11
C      TRUNNIONS
    380,    117.,   2.*16.857* 0.11    $ 2 LIFTING TRUNNIONS
    581,    112.,   98.53 * 0.11   $  TRANSPORT TRUNNION
    583,    112.,   98.53 * 0.11
    591,    112.,   92.62 * 0.11
    593,    112.,   92.62 * 0.11
```

```
    780,    114.,   4.*16.857* 0.11    $ 4 LIFTING TRUNNIONS
C      INNER VESSEL LID
     900,   130.,   520.459* 0.11
     910,   130.,   380.613* 0.11
     920,   130.,   442.163* 0.11
     930,   130.,   192.498* 0.11
     940,   130.,   392.020* 0.11
     950,   130.,   398.869* 0.11
C      OUTER CASK LID
    1000,   130.,   480.424* 0.11
    1010,   130.,   351.335* 0.11
    1020,   130.,   488.741* 0.11
    1030,   130.,   309.372* 0.11
    1040,   130.,   216.013* 0.11
    1050,   130.,   511.242* 0.11
C  *************************
C  EXTERNAL BOUNDARY NODES
C  *************************
       99,  100.,    1.
       98,  100.,    1.
C*********************************************************************
HEADER CONDUCTOR DATA, CASK
C*********************************************************************
C  *************************
C  PAYLOAD  CONDUCTORS
C  *************************
C  *************************
C  PAYLOAD  TO CASK CONDUCTORS
C  *************************
C       RADIAL CONDUCTANCE
     1011,   10,11, 20,21, 30,31, 40,41, 50,51, 60,61,  7.566* 0.02
     1112,   11,12, 21,22, 31,32, 41,42, 51,52, 61,62, 26.355* 0.02
     1213,   12,13, 22,23, 32,33, 42,43, 52,53, 62,63, 36.473* 0.02

     1314,   13,14, 23,24, 33,34, 43,44, 53,54, 63,64, 53.657* 0.02
     1415,   14,15, 24,25, 34,35, 44,45, 54,55, 64,65, 63.720* 0.02
     1516,   15,16, 25,26, 35,36, 45,46, 55,56, 65,66, 149.30* 0.02
C       AXIAL CONDUCTANCE
     1071,   10,71, 20,72, 30,73, 40,74, 50,75, 60,76,  .7445* 0.02
     1171,   11,71, 21,72, 31,73, 41,74, 51,75, 61,76,  .7445* 0.02
     1271,   12,71, 22,72, 32,73, 42,74, 52,75, 62,76,  .7445* 0.02
     1371,   13,71, 23,72, 33,73, 43,74, 53,75, 63,76,  .7445* 0.02
     1471,   14,71, 24,72, 34,73, 44,74, 54,75, 64,76,  .7445* 0.02
     7115,   15,71, 25,72, 35,73, 45,74, 55,75, 65,76,  .7445* 0.02
     1081,   10,81, 20,82, 30,83, 40,84, 50,85, 60,86,  .7445* 0.02
     1181,   11,81, 21,82, 31,83, 41,84, 51,85, 61,86,  .7445* 0.02
     1281,   12,81, 22,82, 32,83, 42,84, 52,85, 62,86,  .7445* 0.02
     1381,   13,81, 23,82, 33,83, 43,84, 53,85, 63,86,  .7445* 0.02
     1481,   14,81, 24,82, 34,83, 44,84, 54,85, 64,86,  .7445* 0.02
     8115,   15,81, 25,82, 35,83, 45,84, 55,85, 65,86,  .7445* 0.02
C       PAYLOAD TO 30 GALLON DRUMS
     1617,   16,17, 26,27, 36,37, 46,47, 56,57, 66,67, 26.366* 0.0154
     1716,   16,17, 26,27, 36,37, 46,47, 56,57, 66,67, 3.7474*1.7141E 9
     7118,   71,18, 72,28, 73,38, 74,48, 75,58, 76,68, 56.958* 0.0154
     1871,   71,18, 72,28, 73,38, 74,48, 75,58, 76,68, .84718*1.7141E 9
     8182,   81,82, 83,84, 85,86,  56.958* 0.0154
     8281,   81,82, 83,84, 85,86,  .79110*1.7141E 9
     7116,   71,16, 72,26, 73,36, 74,46, 75,56, 76,66,  0.0139* 25.0
     8116,   81,16, 82,26, 83,36, 84,46, 85,56, 86,66,  0.0139* 25.0
     1727,   17,27, 37,47, 57,67,  0.01492* 25.0
     2838,   28,38, 48,58,  94.510* 0.0154
     3828,   28,38, 48,58,  1.3130*1.7141E 9
C  *************************
C  PAYLOAD  TO CASK CONDUCTORS
C  *************************
     18205,  18,212,  68,812,    0.56920*1.7141E 9
     18215,  18,215,  65,815,    1.10020*1.7141E 9
     17215,  17,215,  57,515,  67,615,    0.51980*1.7141E 9
     17315,  17,315,  57,615,  67,715,    3.81130*1.7141E 9
     17415,  17,415,  57,715,  67,815,    0.41869*1.7141E 9
     27315,  27,315,            1.18131*1.7141E 9
     27415,  27,415,            3.50350*1.7141E 9
     27515,  27,515,            0.21220*1.7141E 9
     37315,  37,315,            0.15968*1.7141E 9
     37415,  37,415,            2.40563*1.7141E 9
     37515,  37,515,            2.52010*1.7141E 9
     47415,  47,415,            0.21220*1.7141E 9
     47515,  47,515,            3.35322*1.7141E 9
     47315,  47,315,            1.38911*1.7141E 9
C  *************************
C      CASK BODY RADIAL CONDUCTORS
```

```
C  *************************
     100110,  100,110,    2.753* 10.0
     110120,  110,120,    9.860* 10.0
     120130,  120,130,    17.291* 10.0
     130140,  130,140,    31.676* 10.0
     140150,  140,150,    29.422* 10.0
C      STATION 200
     200210,  200,210,    0.808* 10.0
     210220,  210,220,    0.313* 10.0
     220230,  220,230,    798.369* 0.0154
     230220,  220,230,    2.2176* 1.7141E 9
     230240,  230,240,    1276.159
     240245,  240,245,    182.284* 19.3
     245250,  245,250,    1829.40
     250270,  250,270,    1923.72* 0.0154
     270250,  250,270,    5.4015*1.7141E 9
     251270,  250,270,    2.2700* 10.0         $ WIRE WRAP
C      STATION 300
     320330,  320,330,  720,730,    792.820* 0.0154
     330320,  320,330,  720,730,    2.2173* 1.7141E 9
     330340,  330,340,  730,740,    1267.297
     340345,  340,345,  740,745,    181.018* 19.3
     345350,  345,350,  745,750,    1816.673
     350370,  350,370,  750,770,    1910.36* 0.0154
     370350,  350,370,  750,770,    5.3640*1.7141E 9
     351370,  350,370,  750,770,    2.2500* 10.0         $ WIRE WRAP
C      STATIONS 400,500, & 600
     420430,  420,430, 520,530, 620,630,     887.080* 0.0154
     430420,  420,430, 520,530, 620,630,     2.4976* 1.7141E 9
     430440,  430,440, 630,640,     1417.937
     530540,  530,540, 530,541, 530,542, 530,543,  0.25*1417.937
     440445,  440,445, 640,645,     202.540* 19.3
     540545,  540,545, 541,546, 542,547, 543,548, 0.25*202.540* 19.3
     445450,  445,450, 645,650,     2037.906
     545550,  545,550, 546,551, 547,552, 548,553, 0.25*2037.906
     450470,  450,470, 650,670,     2137.47*0.0154
     550570,  550,570, 552,572, 0.25*2137.47*0.0154
     553570,  551,571, 553,573, 0.125*2137.47*0.0154
     470450,  450,470, 650,670,     6.0017*1.7141E 9
     570550,  550,570, 552,572,  0.25*6.0017*1.7141E 9
     571550,  551,571, 553,573,  0.125*6.0017*1.7141E 9
     451470,  450,470, 650,670,     2.5200* 10.0  $ WIRE WRAP
     551570,  551,571, 553,573,  0.125*2.520*10.0  $wire wrap
     552570,  550,570, 552,572,  0.25*2.520*10.0  $wire wrap
C
C      STATION 800
     820830,  820,830,     449.080* 0.0154
     830820,  820,830,     1.2560* 1.7141E 9
     830840,  830,840,     717.8158
     840845,  840,845,     102.530* 19.3
     845850,  845,850,     1029.0523
     850870,  850,870,     1082.09* 0.0154
     870850,  850,870,     2.9001*1.7141E 9
     851870,  850,870,     1.2800*10.0         $ WIRE WRAP

C      STATION 900
     900910,  900,910,     4.0530* 10.0
     910920,  910,920,     13.855* 10.0
     820930,  820,930,     110.885*0.0154
     930820,  820,930,     0.3101* 1.7141E 9
     920930,  920,930,     177.415*0.0154
     930920,  920,930,     0.4962* 1.7141E 9
     930940,  930,940,     41.179* 10.0
     940950,  940,950,     38.248* 10.0
C      STATION 1000
     10001010, 1000,1010,  3.7410* 10.0
     10101020, 1010,1020,  12.563* 10.0
     10201030, 1020,1030,  13.442* 10.0
     10301040, 1030,1040,  0.6140* 10.0
     10401030, 1030,1040,  1.5000* 40.0
     10501030, 1030,1050,  0.4280* 1.7141E 9
     10301050, 1030,1050,  581.98* 0.0154
     10401050, 1040,1050,  15.816* 10.0
C      CANISTER TO INNER VESSEL
     215220,  215,220,     44.482* 0.0154
     220215,  215,220,     2.6223* 1.7141E 9
     215320,  215,320,  215,210,     0.7137* 1.7141E 9
     315320,  315,320, 715,720     50.887* 0.0154
     320315,  315,320, 715,720    2.999* 1.7141E 9
     315420,  315,420,  315,220,     0.7137* 1.7141E 9
     415420,  415,420,  515,520,  615,620,    56.937* 0.0154
```

```
     420415,  415,420,  515,520,  615,620,    3.3565* 1.7141E 9
     415520,  415,520,  415,320,  515,620,  515,420,  0.7986* 1.7141E 9
     615520,  615,520,  615,720,                      0.7986* 1.7141E 9
     815820,  815,820,     27.401* 0.0154
     820815,  815,820,     1.6992* 1.7141E 9
     815720,  815,720,  815,920,     0.4895* 1.7141E 9
     200205,  200,205,  805,900,   88.488* 0.0154
     805900,  805,900,     1.0660* 1.7141E 9
     205200,  205,200,     1.4417* 1.7141E 9
C
C      TRUNNION TO OUTER SHELL
C
     380350,   380,350,    1.9053* 10.0
     581551,   581,551,    38.32* 10.0
     583553,   583,553,    38.32* 10.0
     591581,   581,591,  583,593,  5.244 * 10.0
     780750,   780,750,    3.8106* 10.0
C  *************************
C      CASK BODY AXIAL CONDUCTORS
C  *************************
     100200,  100,200,     63.006* 0.0154
     200100,  100,200,     0.3470* 1.7141E 9
     110210,  110,210,     46.077* 0.0154
     210110,  110,210,     0.2540* 1.7141E 9
     120210,  120,210,     69.638* 0.0154

     210120,  120,210,     0.3840* 1.7141E 9
     130230,  130,230,     0.7600* 10.0
     140240,  140,240,  140,245,   0.774* 19.3
     150250,  150,250,     1.3533* 10.0
C      INNER VESSEL
     220320,  220,320,     0.1731* 10.0
     320420,  320,420,  620,720,   0.1640* 10.0
     420520,  420,520,  520,620,   0.1550* 10.0
     720820,  720,820,     0.2220* 10.0
     820920,  820,920,     0.0740* 10.0
     920820,  820,920,     1.2000* 40.0
C      OUTER CASK, INNER SHELL
     230330,  230,330,     0.4870* 10.0
     330430,  330,430,  630,730,   0.4610* 10.0
     430530,  430,530,  530,630,   0.4370* 10.0
     730830,  730,830,     0.6240* 10.0
     830930,  830,930,     1.0510* 10.0
C
C      LEAD
C
     240340,  240,340,     0.4820* 19.3
     340440,  340,440,  640,740,   0.4560* 19.3
C     440540,  440,540,  540,640,   0.4320* 19.3
     440540,  440,540, 440,541, 440,542, 440,543, 0.25*0.4320* 19.3
     640540,  640,540, 640,541, 640,542, 640,543, 0.25*0.4320* 19.3
     740840,  740,840,     0.6170* 19.3
     840940,  840,940,     14.80762
C
C      LEAD
C
     245345,  245,345,     0.5100* 19.3
     345445,  345,445,  645,745,   0.4830* 19.3
C     445545,  445,545,  545,645,   0.4580* 19.3
     445545,  445,545, 445,546, 445,547, 445,548,  0.25*0.4580* 19.3
     645545,  645,545, 645,546, 645,547, 645,548,  0.25*0.4580* 19.3
     745845,  745,845,     0.6540* 19.3
     845940,  845,940,     15.67441
C
C      OUTER CASK, OUTER SHELL
C
     250350,  250,350,     0.8680* 10.0
     350450,  350,450,  650,750,   0.8220* 10.0
C     450550,  450,550,  550,650,   0.7780* 10.0
     450550,  450,550, 450,551, 450,552, 450,553, 0.25* 0.7780* 10.0
     650550,  650,550, 650,551, 650,552, 650,553, 0.25* 0.7780* 10.0
     581450,  581,450, 583,450, 581,650, 583,650, 0.025* 0.7780* 10.0
     750850,  750,850,     1.1120* 10.0
     850950,  850,950,     1.8720* 10.0
C

C      THERMAL SHIELD
C
     270370,  270,370,     0.0811* 10.0
     370470,  370,470,  670,770,   0.0768* 10.0
     470570,  470,570, 470,572, 570,670, 572,670,  0.25 * 0.0727* 10.0
```

```
     471570,  470,571, 470,573, 571,670, 573,670,  0.125 * 0.0727* 10.0
     580470,  470,581, 470,583, 670,581, 670,583, 0.125 * 0.0727* 10.0
     770870,  770,870,     0.1039* 10.0
C      CASK LID
     9001000, 900,1000,    63.006* 0.0154
     1000900, 900,1000,    0.3470* 1.7141E 9
     9101010, 910,1010,    46.077* 0.0154
     1010910, 910,1010,    0.2540* 1.7141E 9
     9201020, 920,1020,    69.639* 0.0154
     1020920, 920,1020,    0.3840* 1.7141E 9
     9301040, 930,1040,    1.8400* 10.0
     9401040, 940,1040,    2.5770* 10.0
     9501050, 950,1050,    3.3790* 10.0
C
C      CANISTER
C
     215315,  215,315,     0.1010* 25.0
     315415,  315,415,  615,715,    0.0890* 25.0
     415515,  415,515,  515,615,    0.0843* 25.0
     715815,  715,815,     0.1226* 25.0
     205212,  205,212,    403.0
     805812,  805,812,    231.3
     205215,   205,215,   0.179*25.0
     805815,   805,815,   0.364*25.0
     212215,   212,215,   0.590*19.3
     812815,   812,815,   0.987*19.3
C  *************************
C      OVERPACK CONDUCTORS
C  *************************
     20002020,  2000,2020,  3000,3020, 299.022* 0.019
     20202040,  2020,2040,  3020,3040, 67.0590* 0.019
     20402060,  2040,2060,  3040,3060, 46.1890* 0.019
     20602080,  2060,2080,  3060,3080, 107.068* 0.019
     20102030,  2010,2030,  3010,3030, 28.8630* 0.019
     20302050,  2030,2050,  3030,3050, 15.3940* 0.019
     20502070,  2050,2070,  3050,3070, 15.3940* 0.019
     20702090,  2070,2090,  3070,3090, 28.8630* 0.019
     20002010,  2000,2010,  3000,3010, 0.05399* 10.0
     20002100,  2000,2100,  3000,3100, 0.08162* 10.0
     21002080,  2100,2080,  3100,3080, 0.07954* 10.0
     20902080,  2090,2080,  3090,3080, 0.05658* 10.0
C      OVERPACK TO CASK CONDUCTORS
     20801050,  2080,1050,    279.382* 0.0154
     10502080,  2080,1050,    1.94398*1.7141E 9
     2080950,   2080,950,     284.860* 0.0154
     9502080,   2080,950,     1.98210*1.7141E 9
     2080850,   2080,850,     443.724* 0.0154
     8502080,   2080,850,     3.08750*1.7141E 9
     3080150,   3080,150,     219.123* 0.0154
     1503080,   3080,150,     1.52469*1.7141E 9
     3080250,   3080,250,     788.843* 0.0154
     2503080,   3080,250,     5.48889*1.7141E 9
     20901000,  2090,1000,  3090,200,  236.2740* 0.0154
     10002090,  2090,1000,  3090,200,  0.65630*1.7141E 9
     20901010,  2090,1010,  3090,110,  172.7880* 0.0154
     10102090,  2090,1010,  3090,110,  0.4800* 1.7141E 9
     20901020,  2090,1020,  3090,120,  240.3650* 0.0154
     10202090,  2090,1020,  3090,120,  0.6677* 1.7141E 9
     20901030,  2090,1030,  3090,140,  246.5820* 0.0154
     10302090,  2090,1030,  3090,140,  .68495* 1.7141E 9
     20901050,  2090,1050,  3090,150,  211.1920* 0.0154
     10502090,  2090,1050,  3090,150,  .58664* 1.7141E 9
C
C     CIRCUMFRENTIAL CASK WALL CONDUCTORS
      540541,  540,541, 541,542, 542,543, 543,540,  0.056 * 19.3
      545546,  545,546, 546,547, 547,548, 548,545,  0.053 * 19.3
      550551,  550,551, 551,552, 552,553, 553,550,  0.080 * 10.0
      570571,  570,571, 571,572, 572,573, 573,570,  0.007 * 10.0
      581571,  581,571, 583,573,  0.0140 * 10.0
C
C     EXTERNAL RADIATION HEAT TRANSFER
      7098,   370,98,   770,98,   .3*16.223*1.7141E 9  $ THERMAL SHIELD
      9870, 470,98, 670,98, .3*18.151*1.7141E 9 $ THERMAL SHIELD
      98570,  570,98, 572,98, 0.25*.3*18.151*1.7141E 9 $ THERMAL SHIELD
      98571,  571,98, 573,98, 0.125*.3*18.151*1.7141E 9 $ THERMAL SHIELD
      200098, 2000,98,  3000,98,  .3*76.271*1.7141E 9  $ OVERPACK SHELL
      201098, 2010,98,  3010,98,  .3*31.503*1.7141E 9  $ OVERPACK SHELL
      210098, 2100,98,  3100,98,  .3*21.836*1.7141E 9  $ OVERPACK SHELL
      38098,  380,98,             .3*1.0800*1.7141E 9  $ LIFT TRUNNION
      58098,  581,98, 583,98,      .3*2.715*1.7141E 9  $ CENTER TRUNNION
      59098,  591,98, 593,98,      .3*1.545*1.7141E 9  $ CENTER TRUNNION
```

```
      78098,  780,98,             .3*2.1600*1.7141E 9  $ LIFT TRUNNION
C
C     EXTERNAL CONVECTION HEAT TRANSFER
C           ACTUAL RATE DETERMINED BY INTERNAL ROUTINE
      7099,   370,99,   770,99,   1.0                  $ THERMAL SHIELD
      9970, 470,99, 670,99, 1.0                $ THERMAL SHIELD
      9972, 570,99, 572,99, 1.0
      9971, 571,99, 573,99, 1.0
      200099, 2000,99,  3000,99,  1.0                  $ OVERPACK SHELL
      201099, 2010,99,  3010,99,  1.0                  $ OVERPACK SHELL
      210099, 2100,99,  3100,99,  1.0                  $ OVERPACK SHELL
      38099,  380,99,             1.0                  $ LIFT TRUNNION
      58099,  581,99, 583,99,     1.0                  $ CENTER TRUNNION
      59099,  591,99, 593,99,     1.0                  $ CENTER TRUNNION
      78099,  780,99,             1.0                  $ LIFT TRUNNION
C*********************************************************************
HEADER CONTROL DATA, GLOBAL
C*********************************************************************
      ABSZRO  =  459.67
      SIGMA   =    1.0
      EXTLIM  =    1.0
      ITHOLD  =    1
      ITERXT  =    3
      DRLXCA  =     .0001
      ARLXCA  =     .0001
      ATMPCA  =   10.
      DTMPCA  =    2.
      EBALSA  =     .05
      EBALNA  =     .05
      NLOOPS  = 14000
      ITEROT  = 14001
      NLOOPT  =   80
      OUTPUT  =    0.05
      DTIMEI  =    0.00025
      DTIMEH  =    0.00025
C*********************************************************************
C*********************************************************************
HEADER USER DATA, GLOBAL
C*********************************************************************
      GCONST = 32.2
C*********************************************************************
HEADER USER DATA, CASK
C*********************************************************************
      10 = 32.2     $ GC
C*********************************************************************
HEADER ARRAY DATA, CASK
C*********************************************************************
      1 = 32.,.00958,  212.,.0123,  392.,.0147,  572.,.0169  $arg cond
      2 = 32.,.014,  100.,.0154,  300.,.0193,  500.,.0231    $air cond
      3 = 32.,0.2402, 100.,0.2402, 300.,0.2432, 500.,0.2472  $air cp
      4 = 32.,0.04194, 100.,0.04626, 300.,0.05796, 500.,0.06804 $air mu
C*********************************************************************
HEADER OUTPUT CALLS, CASK
C*********************************************************************
      CALL SORTPR('CASK',0)
C      CALL GPRINT('CASK')
C*********************************************************************
HEADER OPERATION DATA
C*********************************************************************
BUILD 72BCASK, CASK
      CALL STDSTL
C     TIMEND =  10.0
C     TSTEPO = .1
C     TSTEPI = .01666666666666
C     ITEROT = 0
C     FWDBCK
C*********************************************************************
HEADER VARIABLES 1, CASK
C*********************************************************************
C DECAY HEAT PRODUCTION   50 WATTS MAX.
      Q10=  50. *3.413/36.
      Q11=  50. *3.413/36.
      Q12=  50. *3.413/36.
      Q13=  50. *3.413/36.
      Q14=  50. *3.413/36.
      Q15=  50. *3.413/36.
      Q20=  50. *3.413/36.
      Q21=  50. *3.413/36.
      Q22=  50. *3.413/36.
      Q23=  50. *3.413/36.
      Q24=  50. *3.413/36.
```

```
      Q25=  50. *3.413/36.
      Q30=  50. *3.413/36.
      Q31=  50. *3.413/36.
      Q32=  50. *3.413/36.
      Q33=  50. *3.413/36.
      Q34=  50. *3.413/36.
      Q35=  50. *3.413/36.
      Q40=  50. *3.413/36.
      Q41=  50. *3.413/36.
      Q42=  50. *3.413/36.
      Q43=  50. *3.413/36.
      Q44=  50. *3.413/36.
      Q45=  50. *3.413/36.
      Q50=  50. *3.413/36.
      Q51=  50. *3.413/36.
      Q52=  50. *3.413/36.
      Q53=  50. *3.413/36.
      Q54=  50. *3.413/36.
      Q55=  50. *3.413/36.
      Q60=  50. *3.413/36.
      Q61=  50. *3.413/36.
      Q62=  50. *3.413/36.
      Q63=  50. *3.413/36.
      Q64=  50. *3.413/36.
      Q65=  50. *3.413/36.
C  EXTERNAL SOLAR HEATING
      Q370 = 0.52*634.73                      $ BASED ON PROJECTED AREA
      Q470 = 0.52*710.193                     $ BASED ON PROJECTED AREA
      Q570 = 0.25*0.52*710.193                 $ BASED ON PROJECTED AREA
      Q571 = 0.125*0.52*710.193
      Q572 = 0.25*0.52*710.193
      Q573 = 0.125*0.52*710.193
      Q670 = 0.52*710.193                     $ BASED ON PROJECTED AREA
      Q770 = 0.52*634.73                      $ BASED ON PROJECTED AREA
      Q2000= 0.52*2984.17                     $ BASED ON PROJECTED AREA
      Q3000= 0.52*2984.17                     $ BASED ON PROJECTED AREA
      Q2010= 0.52*1934.93                     $ BASED ON PROJECTED AREA
      Q3010= 0.52*1934.93                     $ BASED ON PROJECTED AREA
      Q2100= 0.52*1341.18                     $ BASED ON PROJECTED AREA
      Q3100= 0.52*1341.18                     $ BASED ON PROJECTED AREA
      Q380 = 0.52*1.0800*39.126
      Q581 = 0.52*166.76
      Q583 = 0.52*166.76
      Q591 = 0.52*48.20
      Q593 = 0.52*48.20
      Q780 = 0.52*2.1600*39.126
C  EXTERNAL BOUNDARY TEMPERATURES
      T99 = 100.
      T98 = 100.
C     DISABLE WIRE WRAP CONDUCTANCE FOR NORMAL CONDITIONS
C      G251270 = 1.0E 12
C      G351370 = 1.0E 12
C      G451470 = 1.0E 12
C      G851870 = 1.0E 12
C      IF(TIMEN .LT. .01 .OR. TIMEN .GT. .51) GO TO 50
C      T99 = 1475.
C      T98 = 1424.7
C      G7098  = .8*16.223*1.7141E 9
C      G9870  = .8*18.151*1.7141E 9
C      G98570  = 0.25*.8*18.151*1.7141E 9 $ THERMAL SHIELD
C      G98571  = 0.125*.8*18.151*1.7141E 9 $ THERMAL SHIELD
C      G200098 =.8*76.271*1.7141E 9
C      G201098 =.8*31.503*1.7141E 9
C      G210098 =.8*21.836*1.7141E 9
C      G38098  =.8*1.0800*1.7141E 9
C      G58098  = .8*2.715*1.7141E 9  $ CENTER TRUNNION
C      G59098  = .8*1.545*1.7141E 9  $ CENTER TRUNNION
C      G78098  = .8*2.1600*1.7141E 9
C     ENABLE WIRE WRAP CONDUCTANCE FOR ACCIDENT CONDITIONS
C      G251270 = 2.2700* 10.0
C      G351370 = 2.2500* 10.0
C      G451470 = 2.5200* 10.0
C      G851870 =  1.2800*10.0
C  50  CONTINUE
C
C  CALCULATE VARIABLE CONVECTIVE HEAT TRANSFER RATE
      CALL FRCVV(G7099,T370,T99,16.223,3.4667,XK10,0.,
     *      A3,A2,A4,0.,14.7,53.35)
      CALL FRCVV(G9970,T570,T99,18.151,3.4667,XK10,0.,
     *      A3,A2,A4,0.,14.7,53.35)
      CALL FRCVV(G9972,T570,T99,4.5378,3.46670,XK10,0.0,
```

```
     *      A3,A2,A4,0.0,14.70,53.350)
      CALL FRCVV(G9971,T571,T99,2.2689,3.46670,XK10,0.0,
     *      A3,A2,A4,0.0,14.70,53.350)
      CALL FRCVV(G200099,T2000,T99,76.271,6.3333,XK10,0.,
     *      A3,A2,A4,0.,14.7,53.35)
      CALL FRCVV(G201099,T2010,T99,31.503,6.3333,XK10,0.,
     *      A3,A2,A4,0.,14.7,53.35)
      CALL FRCVV(G210099,T2100,T99,21.836,6.3333,XK10,0.,
     *      A3,A2,A4,0.,14.7,53.35)
      CALL FRCVV(G38099, T380, T99,1.0800,6.3333,XK10,0.,
     *      A3,A2,A4,0.,14.7,53.35)
      CALL FRCVV(G58099, T581, T99,2.715,6.33330,XK10,0.0,
     *      A3,A2,A4,0.0,14.70,53.350)
      CALL FRCVV(G59099, T591, T99,1.545,6.33330,XK10,0.0,
     *      A3,A2,A4,0.0,14.70,53.350)
      CALL FRCVV(G78099, T780, T99,2.1600,6.3333,XK10,0.,
     *      A3,A2,A4,0.,14.7,53.35)
C
C  *************************
C  CALCULATE VARIABLE CONDUCTOR VALUES
C  *************************
      CALL D1D1WM(T46, A2, 26.3660,G1617)
      CALL D1D1WM(T74, A2, 56.9580,G7118)
      CALL D1D1WM(T84, A2, 56.9580,G8182)
      CALL D1D1WM(T38, A2, 94.5100,G2838)
      CALL D1D1WM(T220, A2, 798.3690,G220230)
      CALL D1D1WM(T250, A2, 1923.720,G250270)
      CALL D1D1WM(T320, A2, 792.8200,G320330)
      CALL D1D1WM(T350, A2, 1910.360,G350370)
      CALL D1D1WM(T520, A2, 887.0800,G420430)
      CALL D1D1WM(T450, A2, 2137.470,G450470)
      CALL D1D1WM(T550, A2, 534.3675,G550570)
      CALL D1D1WM(T553, A2, 267.1838,G553570)
      CALL D1D1WM(T820, A2, 449.080,G820830)
      CALL D1D1WM(T850, A2, 1082.09,G850870)
      CALL D1D1WM(T820, A2, 110.885,G820930)
      CALL D1D1WM(T920, A2, 177.415,G920930)
      CALL D1D1WM(T1040, A2, 581.980,G10401050)
      CALL D1D1WM(T215,  A2, 44.4820,G215220)
      CALL D1D1WM(T315,  A2, 50.8870,G315320)
      CALL D1D1WM(T515,  A2, 56.9370,G415420)
      CALL D1D1WM(T815,  A2, 27.4010,G815820)
      CALL D1D1WM(T205,  A2, 88.4880,G200205)
      CALL D1D1WM(T200, A2, 63.0060,G100200)
      CALL D1D1WM(T210, A2, 46.0770,G110210)
      CALL D1D1WM(T210, A2, 69.6380,G120210)
      CALL D1D1WM(T900, A2, 63.0060,G9001000)
      CALL D1D1WM(T910, A2,  46.077,G9101010)
      CALL D1D1WM(T920, A2,  69.639,G9201020)
      CALL D1D1WM(T2080, A2, 279.382,G20801050)
      CALL D1D1WM(T2080, A2, 284.860,G2080950)
      CALL D1D1WM(T2080, A2, 443.724,G2080850)
      CALL D1D1WM(T3080, A2, 219.123,G3080150)
      CALL D1D1WM(T3080, A2, 788.843,G3080250)
      CALL D1D1WM(T2090, A2, 47.2550,G20901000)
      CALL D1D1WM(T2090, A2, 34.5575,G20901010)

      CALL D1D1WM(T2090, A2, 48.0729,G20901020)
      CALL D1D1WM(T2090, A2, 49.3165,G20901030)
      CALL D1D1WM(T2090, A2, 42.2383,G20901050)
C  RESET OUTPUT INTERVAL
C      TSTEPO = .1
C    IF(TIMEN .GT. 0.5000001) TSTEPO = .050
C      IF(TIMEN .GT. 0.8000001) TSTEPO = .100
C      IF(TIMEN .GT. 1.5000001) TSTEPO = .125
C      IF(TIMEN .GT. 3.0000001) TSTEPO = .250
C      IF(TIMEN .GT. 5.0000001) TSTEPO = .500
C*********************************************************************
END OF DATA
```

3.6.2.2 300-Watt Steady-State Input File (With and Without Insolation)

```
HEADER OPTIONS DATA
TITLE 72 B FUEL CASK, DAMAGED 300W
      MODEL= 72B CASK
      OUTPUT = TRN300W.out
      PPOUT = ALL1
      USER1 = STORE72B.DAT
C*********************************************************************
HEADER NODE DATA, CASK
```

```
C*********************************************************************
C  *************************
C  PAYLOAD MODEL
C  *************************
      GEN  10,  3,  20,  165.,   1.093 * 272.0 * 0.168
      GEN  11,  3,  20,  164.,   1.093 * 272.0 * 0.168
      GEN  12,  3,  20,  164.,   1.093 * 272.0 * 0.168
      GEN  13,  3,  20,  164.,   1.093 * 272.0 * 0.168
      GEN  14,  3,  20,  164.,   1.093 * 272.0 * 0.168
      GEN  15,  3,  20,  164.,   1.093 * 272.0 * 0.168
      GEN  16,  3,  20,  164.,   1.093 * 272.0 * 0.168
      GEN  17,  3,  20,  164.,   33.221 * 0.113
      GEN  18,  3,  20,  163.,    6.015 * 0.113
      GEN  28,  3,  20,  164.,    7.525 * 0.113
C  *************************
C  OVERPACK   IMPACT LIMITER MODEL
C  *************************
      GEN  2000,  2,  1000,  100.,  371.614* 0.11
      GEN  2020,  2,  1000,  101.,  109.155* 0.30
      GEN  2040,  2,  1000,  106.,  286.960* 0.30
      GEN  2060,  2,  1000,  112.,  117.600* 0.30
      GEN  2080,  2,  1000,  115.,  161.382* 0.11
      GEN  2100,  2,  1000,  101.,  106.561* 0.11
C     GEN  2010,  2,  1000,  100.,  153.736* 0.11
      GEN  2010,  3,  1,  100.,  1.1090 * 0.11
      GEN  2013,  4,  1,  100.,  3.3271 * 0.11
      GEN  2110,  3,  1,  100.,  1.3202* 0.11
      GEN  2113,  4,  1,  100.,  3.9605* 0.11
      GEN  2210,  3,  1,  100.,  1.3255* 0.11
      GEN  2213,  4,  1,  100.,  3.9765* 0.11
      GEN  2310,  3,  1,  100.,  6.4944* 0.11
      GEN  2313,  4,  1,  100., 19.4834* 0.11
C     GEN  2030,  2,  1000,  100.,   80.176* 0.30
      GEN  2030,  3,  1,  100.,  1.89380* 0.30
      GEN  2033,  4,  1,  100.,  5.68141* 0.30
      GEN  2130,  3,  1,  100.,  2.25438* 0.30
      GEN  2133,  4,  1,  100.,  6.76314* 0.30
      GEN  2230,  3,  1,  100.,  2.26347* 0.30
      GEN  2233,  4,  1,  100.,  6.79041* 0.30
      GEN  2330,  3,  1,  100.,  11.0911* 0.30
      GEN  2333,  4,  1,  100.,  33.2733* 0.30
C     GEN  2050,  2,  1000,  108.,   70.154* 0.30
      GEN  2050,  3,  1,  108.,  0.875 * 1.89380* 0.30
      GEN  2053,  4,  1,  108.,  0.875 * 5.68141* 0.30
      GEN  2150,  3,  1,  108.,  0.875 * 2.25438* 0.30
      GEN  2153,  4,  1,  108.,  0.875 * 6.76314* 0.30
      GEN  2250,  3,  1,  108.,  0.875 * 2.26347* 0.30
      GEN  2253,  4,  1,  108.,  0.875 * 6.79041* 0.30
      GEN  2350,  3,  1,  108.,  0.875 * 11.0911* 0.30
      GEN  2353,  4,  1,  108.,  0.875 * 33.2733* 0.30
C     GEN  2070,  2,  1000,  113.,   75.165* 0.30
      GEN  2070,  3,  1,  113.,  1.7754* 0.30
      GEN  2073,  4,  1,  113.,  5.3263* 0.30
      GEN  2170,  3,  1,  113.,  2.1135* 0.30
      GEN  2173,  4,  1,  113.,  6.3404* 0.30
      GEN  2270,  3,  1,  113.,  2.1220* 0.30
      GEN  2273,  4,  1,  113.,  6.3660* 0.30
      GEN  2370,  3,  1,  113., 10.3979* 0.30
      GEN  2373,  4,  1,  126., 31.1937* 0.30
C     GEN  2090,  2,  1000,  116.,  231.616* 0.11
      GEN  2090,  3,  1,  116.,  5.4449* 0.11
      GEN  2093,  4,  1,  116.,  16.3347* 0.11
      GEN  2190,  3,  1,  116.,  6.4816* 0.11
      GEN  2193,  4,  1,  116.,  19.4448* 0.11
      GEN  2290,  3,  1,  116.,  0.54* 6.5078* 0.11
      GEN  2293,  4,  1,  116.,  0.54*19.5232* 0.11
C
C  REAR OVERPACK   IMPACT LIMITER MODEL
C
      3010,  100.,  153.736* 0.11
      3030,  104.,   80.176* 0.30
      3050,  113.,   70.154* 0.30
      3070,  121.,   75.165* 0.30
      3090,  125.,  231.616* 0.11
C  *************************
C  CASK BODY NODES
C  *************************
C      OUTER CASK BASE PLATE
     100,   124.,   400.353* 0.11
     110,   124.,   292.780* 0.11
     120,   124.,   469.627* 0.11
```

```
     130,   123.,   148.075* 0.11
     140,   123.,   301.554* 0.11
     150,   123.,   306.823* 0.11
C      CANISTER
     205,   149.,   100.253* 0.11
     212,   149.,   339.938* 0.031
     215,   150.,   99.224* 0.11
     315,   150.,   101.882* 0.11
     415,   147.,   113.994* 0.11
     515,   146.,   113.994* 0.11
     615,   144.,   113.994* 0.11
     715,   145.,   101.882* 0.11
     805,   133.,   189.583* 0.11
     812,   133.,   570.760* 0.031
     815,   133.,    71.709* 0.11
C      INNER VESSEL
     200,   134.,   120.106* 0.11         $ BASE PLATE
     210,   132.,   240.800* 0.11         $ BASE PLATE
     220,   130.,   185.446* 0.11         $ INNER VESSEL SHELL
     320,   128.,   188.076* 0.11         $ INNER VESSEL SHELL
     420,   126.,   210.435* 0.11         $ INNER VESSEL SHELL
     520,   124.,   210.435* 0.11         $ INNER VESSEL SHELL
     620,   123.,   210.435* 0.11         $ INNER VESSEL SHELL
     720,   123.,   188.076* 0.11         $ INNER VESSEL SHELL
     820,   120.,   608.129* 0.11         $ INNER VESSEL SHELL
C      OUTER CASK, INNER SHELL
     230,   123.,   533.071* 0.11
     330,   119.,   529.370* 0.11
     430,   116.,   592.300* 0.11
     530,   114.,   592.300* 0.11
     630,   114.,   592.300* 0.11
     730,   114.,   529.370* 0.11
     830,   116.,   299.850* 0.11
C      LEAD SHIELD
     240,   123.,   767.199* 0.031
     340,   118.,   761.870* 0.031
     440,   116.,   852.443* 0.031
     540,   114.,   852.443* 0.031
     640,   114.,   852.443* 0.031
     740,   114.,   761.870* 0.031
     840,   116.,   431.550* 0.031
     245,   123.,   812.252* 0.031
     345,   118.,   806.610* 0.031
     445,   116.,   902.503* 0.031
     545,   114.,   902.503* 0.031
     645,   114.,   902.503* 0.031
     745,   114.,   806.610* 0.031
     845,   116.,   456.890* 0.031
C      OUTER CASK, OUTER SHELL
     250,   123.,   949.323* 0.11
     350,   118.,   942.730* 0.11
     450,   116.,  1054.803* 0.11
     550,   114.,  1054.803* 0.11
     650,   114.,  1054.803* 0.11
     750,   114.,   942.730* 0.11
     850,   116.,   533.990* 0.11
C      THERMAL SHIELD
     270,   122.,    90.933* 0.11
     370,   115.,    89.726* 0.11
     470,   113.,   99.719* 0.11
     570,   111.,   99.719* 0.11
     670,   111.,   99.719* 0.11
     770,   112.,    89.726* 0.11
     870,   116.,    50.824* 0.11
C      TRUNNIONS
    380,    117.,   2.*16.857* 0.11    $ 2 LIFTING TRUNNIONS
    580,    112.,   2.*193.706* 0.11   $ 2 TRANSPORT TRUNNIONS
    780,    114.,   4.*16.857* 0.11    $ 4 LIFTING TRUNNIONS
C      INNER VESSEL LID
C    900,   121.,   520.459* 0.11
      GEN  900, 3,  1,   121.,   0.066667 * 520.459* 0.11
      GEN  903, 4,  1,   121.,   0.200000 * 520.459* 0.11
C    910,   121.,   380.613* 0.11
      GEN  910, 3,  1,   121.,   0.066667 * 380.613* 0.11
      GEN  913, 4,  1,   121.,   0.200000 * 380.613* 0.11
C    920,   120.,   442.163* 0.11
      GEN  920, 3,  1,   120.,   0.066667 * 442.163* 0.11
      GEN  923, 4,  1,   120.,   0.200000 * 442.163* 0.11
C    930,   116.,   192.498* 0.11
      GEN  930, 3,  1,   116.,   0.066667 * 192.498* 0.11
      GEN  933, 4,  1,   116.,   0.200000 * 192.498* 0.11
```

```
C    940,   116.,   392.020* 0.11
      GEN  940, 3,  1,   116.,   0.066667 * 392.020* 0.11
      GEN  943, 4,  1,   116.,   0.200000 * 392.020* 0.11
C    950,   116.,   398.869* 0.11
      GEN  950, 3,  1,   116.,   0.066667 * 398.869* 0.11
      GEN  953, 4,  1,   116.,   0.200000 * 398.869* 0.11
C      OUTER CASK LID
C   1000,   117.,   480.424* 0.11
      GEN 1000, 3,  1,   117.,   0.066667 * 480.424* 0.11
      GEN 1003, 4,  1,   117.,   0.200000 * 480.424* 0.11
C   1010,   117.,   351.335* 0.11
      GEN 1010, 3,  1,   117.,   0.066667 * 351.335* 0.11
      GEN 1013, 4,  1,   117.,   0.200000 * 351.335* 0.11
C   1020,   117.,   488.741* 0.11
      GEN 1020, 3,  1,   117.,   0.066667 * 488.741* 0.11
      GEN 1023, 4,  1,   117.,   0.200000 * 488.741* 0.11
C   1030,   116.,   309.372* 0.11
      GEN 1030, 3,  1,   116.,   0.066667 * 309.372* 0.11
      GEN 1033, 4,  1,   116.,   0.200000 * 309.372* 0.11
C   1040,   116.,   216.013* 0.11
      GEN 1040, 3,  1,   116.,   0.066667 * 216.013* 0.11
      GEN 1043, 4,  1,   116.,   0.200000 * 216.013* 0.11
C   1050,   116.,   511.242* 0.11
      GEN 1050, 3,  1,   116.,   0.066667 * 511.242* 0.11
      GEN 1053, 4,  1,   116.,   0.200000 * 511.242* 0.11
C  *************************
C  EXTERNAL BOUNDARY NODES
C  *************************
       99,  100.,    1.
       98,  100.,    1.
C*********************************************************************
HEADER CONDUCTOR DATA, CASK
C*********************************************************************
C  *************************
C  PAYLOAD  CONDUCTORS
C  *************************
C       RADIAL CONDUCTANCE   PAYLOAD TO 55 GAL DRUM
     1011,   10,11, 30,31, 50,51, 31.697*9.47
     1112,   11,12, 31,32, 51,52, 68.183*9.47
     1213,   12,13, 32,33, 52,53, 103.465*9.47
     1314,   13,14, 33,34, 53,54, 138.564*9.47
     1415,   14,15, 34,35, 54,55, 173.512*9.47
     1516,   15,16, 35,36, 55,56, 208.594*9.47
     1617,   16,17, 36,37, 56,57, 468.945*9.47
     1718,   17,18, 17,28, 0.016*10.0
     3738,   37,38, 37,48, 0.016*10.0
     5758,   57,58, 57,68, 0.016*10.0
C       AXIAL CONDUCTANCE   PAYLOAD TO 55 GAL DRUMS
     1018,   10,18, 11,18, 12,18, 13,18, 14,18, 15,18, 16,18,  0.285*9.47
     1028,   10,28, 11,28, 12,28, 13,28, 14,28, 15,28, 16,28,  0.285*9.47
     3038,   30,38, 31,38, 32,38, 33,38, 34,38, 35,38, 36,38,  0.285*9.47
     3048,   30,48, 31,48, 32,48, 33,48, 34,48, 35,48, 36,48,  0.285*9.47
     5058,   50,58, 51,58, 52,58, 53,58, 54,58, 55,58, 56,58,  0.285*9.47
     5068,   50,68, 51,68, 52,68, 53,68, 54,68, 55,68, 56,68,  0.285*9.47
C       55 GALLON DRUMS TO CANISTER
     18212,   18,212, 68,812,  28.978*0.0154
     21218,   18,212, 68,812,  0.8085*1.7141E 9
     17315,   17,315, 17,215, 37,415, 37,515, 57,615, 57,715,  84.575*0.0154
     31517,   17,315, 17,215, 37,415, 37,515, 57,615, 57,715,  6.3314*1.7141E 9
     2838,   28,38, 48,58,  18.014* 0.0154
     3828,   28,38, 48,58,  2.060*1.7141E 9
C  *************************
C      CASK BODY RADIAL CONDUCTORS
C  *************************
     100110,  100,110,    2.753* 10.0
     110120,  110,120,    9.860* 10.0
     120130,  120,130,    17.291* 10.0
     130140,  130,140,    31.676* 10.0
     140150,  140,150,    29.422* 10.0
C      STATION 200
     200210,  200,210,    0.808* 10.0
     210220,  210,220,    0.313* 10.0
     220230,  220,230,    798.369* 0.0154
     230220,  220,230,    2.2176* 1.7141E 9
     230240,  230,240,    1276.159
     240245,  240,245,    182.284* 19.3
     245250,  245,250,    1829.40
     250270,  250,270,    1923.72* 0.0154
     270250,  250,270,    5.384*1.7141E 9
     251270,  250,270,    2.2700* 10.0         $ WIRE WRAP
C      STATION 300
```

```
     320330,  320,330,  720,730,    792.820* 0.0154
     330320,  320,330,  720,730,    2.2022* 1.7141E 9
     330340,  330,340,  730,740,    1267.297
     340345,  340,345,  740,745,    181.018* 19.3
     345350,  345,350,  745,750,    1816.673
     350370,  350,370,  750,770,    1910.36* 0.0154
     370350,  350,370,  750,770,    5.347*1.7141E 9
     351370,  350,370,  750,770,    2.2500* 10.0         $ WIRE WRAP
C      STATIONS 400,500, & 600
     420430,  420,430, 520,530, 620,630,     887.080* 0.0154
     430420,  420,430, 520,530, 620,630,     2.4640* 1.7141E 9
     430440,  430,440, 530,540, 630,640,     1417.937
     440445,  440,445, 540,545, 640,645,     202.540* 19.3
     445450,  445,450, 545,550, 645,650,     2037.906
     450470,  450,470, 550,570, 650,670,     2137.47* 0.0154
     470450,  450,470, 550,570, 650,670,     5.982*1.7141E 9
     451470,  450,470, 550,570, 650,670,     2.5200* 10.0  $WIRE WRAP
C      STATION 800
     820830,  820,830,     449.080* 0.0154
     830820,  820,830,     1.2474* 1.7141E 9
     830840,  830,840,     717.8158
     840845,  840,845,     102.530* 19.3
     845850,  845,850,     1029.0523
     850870,  850,870,     1082.09* 0.0154
     870850,  850,870,     3.029*1.7141E 9
     851870,  850,870,     1.280* 10.0         $ WIRE WRAP
C      STATION 900
C    820930,  820,930,     110.885*0.0154
   820930,  820,930,  820,931, 820,932,           .0666667*110.885*.0154
   820933,  820,933,  820,934, 820,935, 820,936,  .200000*110.885*.0154
C    930820,  820,930,     0.3080* 1.7141E 9
   930820,  820,930,  820,931, 820,932,           .0205333*1.7141E 9
   933820,  820,933,  820,934, 820,935, 820,936,  .0616000*1.7141E 9
C    900910,  900,910,     4.0530* 10.0
   900910,  900,910,  901,911, 902,912,            .0666667*4.0530* 10.0
   903913,  903,913,  904,914, 905,915, 906,916,   .2000000*4.0530* 10.0
C    910920,  910,920,     13.855* 10.0
   910920,  910,920,  911,921, 912,922,            .0666667*13.855* 10.0
   913923,  913,923,  914,924, 915,925, 916,926,   .2000000*13.855* 10.0
C    920930,  920,930,    177.415* 0.0154
   920930,  920,930,  921,931, 922,932,           .0666667*177.415*.0154
   923933,  923,933,  924,934, 925,935, 926,936,  .2000000*177.415*.0154
C    930920,  920,930,     0.4930* 1.7141E 9
  930920,  920,930,  921,931, 922,932,          .0666667*.4930*1.7141E 9
  933923,  923,933,  924,934, 925,935, 926,936, .2000000*.4930*1.7141E 9
C    930940,  930,940,     41.179* 10.0
   930940,  930,940,  931,941, 932,942,            .0666667*41.179*10.0
   933943,  933,943,  934,944, 935,945, 936,946,   .2000000*41.179*10.0
C    940950,  940,950,     38.248* 10.0
   940950,  940,950,  941,951, 942,952,            .0666667*38.248*10.0
   943953,  943,953,  944,954, 945,955, 946,956,   .2000000*38.248*10.0
C      STATION 900 TO 900
   900901,  900,901,  901,902,                     1.715278* 10.0
   902903,  902,903,  906,900,                     0.857639* 10.0
   903904,  903,904,  904,905,  905,906,           0.571759* 10.0
   910911,  910,911,  911,912,                     0.353261* 10.0
   912913,  912,913,  916,910,                     0.176630* 10.0
   913914,  913,914,  914,915,  915,916,           0.117754* 10.0
   920921,  920,921,  921,922,                     0.317560* 10.0
   922923,  922,923,  926,920,                     0.158780* 10.0
   923924,  923,924,  924,925,  925,926,           0.105853* 10.0
   930931,  930,931,  931,932,                     0.077381* 10.0
   932933,  932,933,  936,930,                     0.038690* 10.0
   933934,  933,934,  934,935,  935,936,           0.025794* 10.0
   940941,  940,941,  941,942,                     0.133635* 10.0
   942943,  942,943,  946,940,                     0.066820* 10.0
   943944,  943,944,  944,945,  945,946,           0.044545* 10.0
   950951,  950,951,  951,952,                     0.097892* 10.0
   952953,  952,953,  956,950,                     0.048946* 10.0
   953954,  953,954,  954,955,  955,956,           0.032631* 10.0
C      STATION 1000
C    10001010, 1000,1010,  3.7410* 10.0
  10001010, 1000,1010, 1001,1011, 1002,1012,       .0666667*3.7410*10.0
  10031013, 1003,1013, 1004,1014, 1005,1015, 1006,1016,  .20*3.7410*10.0
C    10101020, 1010,1020,  12.563* 10.0
  10101020, 1010,1020, 1011,1021, 1012,1022,       .0666667*12.563*10.0
  10131023, 1013,1023, 1014,1024, 1015,1025, 1016,1026,  .2*12.563*10.0
C    10201030, 1020,1030,  13.442* 10.0
  10201030, 1020,1030, 1021,1031, 1022,1032,       .0666667*13.442*10.0
  10231033, 1023,1033, 1024,1034, 1025,1035, 1026,1036,  .2*13.442*10.0
C    10301040, 1030,1040,  0.6140* 10.0
```

```
  10301040, 1030,1040, 1031,1041, 1032,1042,       .0666667*0.6140*10.0
  10331043, 1033,1043, 1034,1044, 1035,1045, 1036,1046,  .2*0.6140*10.0
C    10401030, 1030,1040,  1.5000* 40.
  10401030, 1040,1030, 1041,1031, 1042,1032,       .0666667*1.50*40.
  10431033, 1043,1033, 1044,1034, 1045,1035, 1046,1036,  .2*1.50*40.
C    10501030, 1030,1050,  0.4270* 1.7141E 9
  10501030, 1030,1050, 1031,1051, 1032,1052, .0666667*0.427*1.7141E 9
  10531033, 1033,1053, 1034,1054, 1035,1055, 1036,1056, .2*0.427*1.7141E 9
C    10301050, 1030,1050,  581.98* 0.0154
  10301050, 1030,1050, 1031,1051, 1032,1052,       .0666667*581.98*.0154
  10331053, 1033,1053, 1034,1054, 1035,1055, 1036,1056,  .2*581.98*.0154
C    10401050, 1040,1050,  15.816* 10.0
  10401050, 1040,1050, 1041,1051, 1042,1052,       .0666667*15.816* 10.0
  10431053, 1043,1053, 1044,1054, 1045,1055, 1046,1056,  .2*15.816* 10.0
C      STATION 1000 TO 1000
   10001001,  1000,1001,  1001,1002,                    1.583333* 10.0
   10021003,  1002,1003,  1006,1000,                    0.791667* 10.0
   10031004,  1003,1004,  1004,1005,  1005,1006,        0.527777* 10.0
   10101011,  1010,1011,  1011,1012,                    0.326087* 10.0
   10121013,  1012,1013,  1016,1010,                    0.163044* 10.0
   10131014,  1013,1014,  1014,1015,  1015,1016,        0.108696* 10.0
   10201021,  1020,1021,  1021,1022,                    0.275424* 10.0
   10221023,  1022,1023,  1026,1020,                    0.137712* 10.0
   10231024,  1023,1024,  1024,1025,  1025,1026,        0.091808* 10.0
   10301031,  1030,1031,  1031,1032,                    0.190972* 10.0
   10321033,  1032,1033,  1036,1030,                    0.095486* 10.0
   10331034,  1033,1034,  1034,1035,  1035,1036,        0.063657* 10.0
   10401041,  1040,1041,  1041,1042,                    0.141438* 10.0
   10421043,  1042,1043,  1046,1040,                    0.070719* 10.0
   10431044,  1043,1044,  1044,1045,  1045,1046,        0.047146* 10.0
   10501051,  1050,1051,  1051,1052,                    0.125915* 10.0
   10521053,  1052,1053,  1056,1050,                    0.062957* 10.0
   10531054,  1053,1054,  1054,1055,  1055,1056,        0.041972* 10.0
C
C      CANISTER TO INNER VESSEL
C
     215220,  215,220,     44.482* 0.0154
     220215,  215,220,     2.6440* 1.7141E 9
     215320,  215,320,  215,210,     0.5460* 1.7141E 9
     315320,  315,320,  715,720    50.887* 0.0154
     320315,  315,320,  715,720     3.0247* 1.7141E 9
     315420,  315,420,  315,220,  715,620,  715,820,     0.6154* 1.7141E 9
     415420,  415,420,  515,520,  615,620,    56.937* 0.0154
     420415,  415,420,  515,520,  615,620,    3.3840* 1.7141E 9
     415520,  415,520,  415,320,  515,620,  515,420,  0.6885* 1.7141E 9
     615520,  615,520,  615,720,                      0.6885* 1.7141E 9
     815820,  815,820,     27.401* 0.0154
     820815,  815,820,     1.6287* 1.7141E 9
C    815720,  815,720,  815,920,     0.3313* 1.7141E 9
     815720,  815,720,              0.3313* 1.7141E 9
     815920,  815,920, 815,921, 815,922,   0.066667* 0.3313* 1.7141E 9
     815923,  815,923, 815,924, 815,925, 815,926,  0.2*0.3313* 1.7141E 9
C    200205,  200,205,  805,900,   88.488* 0.0154
     200205,  200,205,            88.488* 0.0154
     805900,  805,900,  805,901, 805,902,     0.066667*  88.488* 0.0154
     805903,  805,903,  805,904, 805,905, 805,906,   0.2*88.488* 0.0154
C    805900,  805,900,  205,200,   1.0289* 1.7141E 9
     205200,  200,205,            1.0289* 1.7141E 9
     900805,  805,900,  805,901, 805,902,     0.066667*1.0289* 1.7141E 9
     903805,  805,903,  805,904, 805,905, 805,906,  0.2*1.0289*1.7141E 9
C
C      TRUNNION TO OUTER SHELL
C
     380350,   380,350,    1.9053* 10.0
     580550,   580,550,    2.5000* 10.0
     780750,   780,750,    3.8106* 10.0
C  *************************
C      CASK BODY AXIAL CONDUCTORS
C  *************************
     100200,  100,200,     63.006* 0.0154
     200100,  100,200,     0.3470* 1.7141E 9
     110210,  110,210,     46.077* 0.0154
     210110,  110,210,     0.2540* 1.7141E 9
     120210,  120,210,     69.638* 0.0154
     210120,  120,210,     0.3840* 1.7141E 9
     130230,  130,230,     0.7600* 10.0
     140240,  140,240,  140,245,   0.774* 19.3
     150250,  150,250,     1.3533* 10.0
C
C      INNER VESSEL
C
```

```
     220320,  220,320,     0.1731* 10.0
     320420,  320,420,  620,720,   0.1640* 10.0
     420520,  420,520,  520,620,   0.1550* 10.0
     720820,  720,820,     0.2220* 10.0
C    820920,  820,920,     0.0740* 10.0
     820920,  820,920, 820,921, 820,922, 0.066667*0.0740* 10.0
     820923,  820,923, 820,924, 820,925, 820,926, 0.20*0.0740* 10.0
C    920820,  820,920,     1.2000* 40.
     920820,  820,920, 820,921, 820,922, 0.066667*1.200* 40.
     923820,  820,923, 820,924, 820,925, 820,926, 0.20*1.200* 40.
C
C      OUTER CASK, INNER SHELL
C
     230330,  230,330,     0.4870* 10.0
     330430,  330,430,  630,730,   0.4610* 10.0
     430530,  430,530,  530,630,   0.4370* 10.0
     730830,  730,830,     0.6240* 10.0
C    830930,  830,930,     1.0510* 10.0
     830930,  830,930, 830,931, 830,932, 0.066667*1.051* 10.
     830933,  830,933, 830,934, 830,935, 830,936, 0.20*1.051* 10.
C
C      LEAD
C
     240340,  240,340,     0.4820* 19.3
     340440,  340,440,  640,740,   0.4560* 19.3
     440540,  440,540,  540,640,   0.4320* 19.3
     740840,  740,840,     0.6170* 19.3
C    840940,  840,940,     14.80762
     840940,  840,940, 840,941, 840,942, 0.066667*14.80762
     840943,  840,943, 840,944, 840,945, 840,946, 0.20*14.80762
C
C      LEAD
C
     245345,  245,345,     0.5100* 19.3
     345445,  345,445,  645,745,   0.4830* 19.3
     445545,  445,545,  545,645,   0.4580* 19.3
     745845,  745,845,     0.6540* 19.3
C    845940,  845,940,     15.67441
     845940,  845,940, 845,941, 845,942, 0.066667*15.67441
     845943,  845,943, 845,944, 845,945, 845,946, 0.20*15.67441
C
C      OUTER CASK, OUTER SHELL
C
     250350,  250,350,     0.8680* 10.0
     350450,  350,450,  650,750,   0.8220* 10.0
     450550,  450,550,  550,650,   0.7780* 10.0
     750850,  750,850,     1.1120* 10.0
C    850950,  850,950,     1.8720* 10.0
     850950,  850,950, 850,951, 850,952, 0.066667*1.8720* 10.0
     850953,  850,953, 850,954, 850,955, 850,956, 0.20*1.8720* 10.0
C
C      THERMAL SHIELD
C
     270370,  270,370,     0.0811* 10.0
     370470,  370,470,  670,770,   0.0768* 10.0
     470570,  470,570,  570,670,   0.0727* 10.0
     770870,  770,870,     0.1039* 10.0
C
C      CASK LID
C
C    9001000, 900,1000,    63.006* 0.0154
     9001000, 900,1000, 901,1001, 902,1002,   .0666667*63.006* 0.0154
     9031003, 903,1003, 904,1004, 905,1005, 906,1006, .2*63.006* 0.0154
C    1000900, 900,1000,    0.3470* 1.7141E 9
     1000900, 900,1000, 901,1001, 902,1002,   .0666667*.3470*1.7141E 9
     1003903, 903,1003, 904,1004, 905,1005, 906,1006, .2*.3470*1.7141E 9
C    9101010, 910,1010,    46.077* 0.0154
     9101010, 910,1010, 911,1011, 912,1012,   .0666667*46.077* 0.0154
     9131013, 913,1013, 914,1014, 915,1015, 916,1016, .2*46.077* 0.0154
C    1010910, 910,1010,    0.2540* 1.7141E 9
     1010910, 910,1010, 911,1011, 912,1012,   .0666667*.2540*1.7141E 9
     1013913, 913,1013, 914,1014, 915,1015, 916,1016, .2*.2540*1.7141E 9
C    9201020, 920,1020,    69.639* 0.0154
     9201020, 920,1020, 921,1021, 922,1022,   .0666667*69.639* 0.0154
     9231023, 923,1023, 924,1024, 925,1025, 926,1026,  .2*69.639* 0.0154
C    1020920, 920,1020,    0.3840* 1.7141E 9
     1020920, 920,1020, 921,1021, 922,1022,   .0666667*.3840*1.7141E 9
     1023923, 923,1023, 924,1024, 925,1025, 926,1026, .2*.3840*1.7141E 9
C    9301040, 930,1040,    1.8400* 10.0
     9301040, 930,1040, 931,1041, 932,1042,   .0666667*1.840 * 10.0
     9331043, 933,1043, 934,1044, 935,1045, 936,1046,   .20*1.840*10.0
```

```
C    9401040, 940,1040,    2.5770* 10.0
     9401040, 940,1040, 941,1041, 942,1042,   .0666667*2.5770* 10.0
     9431043, 943,1043, 944,1044, 945,1045, 946,1046,   .2*2.5770* 10.0
C    9501050, 950,1050,    3.3790* 10.0
     9501050, 950,1050, 951,1051, 952,1052,   .0666667*3.3790* 10.0
     9531053, 953,1053, 954,1054, 955,1055, 956,1056,   .20*3.3790* 10.0
C
C      CANISTER
C
     215315,  215,315,     0.1010* 25.0
     315415,  315,415,  615,715,    0.0890* 25.0
     415515,  415,515,  515,615,    0.0843* 25.0
     715815,  715,815,     0.1226* 25.0
     205212,  205,212,    403.0
     805812,  805,812,    231.3
     205215,   205,215,   0.179*25.0
     805815,   805,815,   0.364*25.0
     212215,   212,215,   0.590*19.3
     812815,   812,815,   0.987*19.3
C  *************************
C      OVERPACK CONDUCTORS
C  *************************
     20002020,  2000,2020,  3000,3020, 299.022* 0.019
     20202040,  2020,2040,  3020,3040, 67.0590* 0.019
     20402060,  2040,2060,  3040,3060, 46.1890* 0.019
     20602080,  2060,2080,  3060,3080, 107.068* 0.019
C    20002010,  2000,2010,  3000,3010, 0.05399* 10.0
     20002310,  2000,2310,  2000,2311, 2000,2312, 0.066667*0.05399* 10.0
     20002313,  2000,2313,  2000,2314, 2000,2315, 2000,2016, 0.20*0.05399* 10.0
     30003010,              3000,3010, 0.05399* 10.0
     20002100,  2000,2100,  3000,3100, 0.08162* 10.0
     21002080,  2100,2080,  3100,3080, 0.07954* 10.0
C    20902080,  2090,2080,  3090,3080, 0.05658* 10.0
     20802290,  2080,2290,  2080,2291, 2080,2292, 0.066667*0.05658* 10.0
     20802293,  2080,2293,  2080,2294, 2080,2295, 2080,2296,  0.200*0.05658* 10.0
     30803090,              3090,3080, 0.05658* 10.0
C    20102030,  2010,2030,  3010,3030, 28.8630* 0.019
C    20302050,  2030,2050,  3030,3050, 15.3940* 0.019
C    20502070,  2050,2070,  3050,3070, 15.3940* 0.019
C    20702090,  2070,2090,  3070,3090, 28.8630* 0.019
C
C  STATION 2010 TO 2030
     20102030,  2010,2030,  2011,2031, 2012,2032,   0.681777*0.019
     20132033,  2013,2033,  2014,2034, 2015,2035, 2016,2036, 2.045331*0.019
     21102130,  2110,2130,  2111,2131, 2112,2132,   0.811578*0.019
     21132133,  2113,2133,  2114,2134, 2115,2135, 2116,2136, 2.434734*0.019
     22102230,  2210,2230,  2211,2231, 2212,2232,   0.814851*0.019
     22132233,  2213,2233,  2214,2234, 2215,2235, 2216,2236, 2.444553*0.019
     23102330,  2310,2330,  2311,2331, 2312,2332,   3.992441*0.019
     23132333,  2313,2333,  2314,2334, 2315,2335, 2316,2336, 11.977323*0.019
C
C  STATION 2030 TO 2050 & 2050 TO 2070
     20302050,  2030,2050,  2031,2051, 2032,2052
                2050,2070,  2051,2071, 2052,2072,   0.363614*0.019
     20332053,  2033,2053,  2034,2054, 2035,2055, 2036,2056
          2053,2073,  2054,2074, 2055,2075, 2056,2076,  1.090842*0.019

     21302150,  2130,2150,  2131,2151, 2132,2152
                2150,2170,  2151,2171, 2152,2172,   0.432842*0.019
     21332153,  2133,2153,  2134,2154, 2135,2155, 2136,2156
            2153,2173,  2154,2174, 2155,2175, 2156,2176,  1.298526*0.019
     22302250,  2230,2250,  2231,2251, 2232,2252
                2250,2270,  2251,2271, 2252,2272,   0.434587*0.019
     22332253,  2233,2253,  2234,2254, 2235,2255, 2236,2256
            2253,2273,  2254,2274, 2255,2275, 2256,2276,  1.303761*0.019
     23302350,  2330,2350,  2331,2351, 2332,2352
                2350,2370,  2351,2371, 2352,2372,   2.129302*0.019
     23332353,  2333,2353,  2334,2354, 2335,2355, 2336,2356
            2353,2373,  2354,2374, 2355,2375, 2356,2376,  6.387906*0.019
C
C  STATION 2070 TO 2090
     20702090,  2070,2090,  2071,2091, 2072,2092,   0.681777*0.019
     20732093,  2073,2093,  2074,2094, 2075,2095, 2076,2096, 2.045331*0.019
     21702190,  2170,2190,  2171,2191, 2172,2192,   0.811578*0.019
     21732193,  2173,2193,  2174,2194, 2175,2195, 2176,2196, 2.434734*0.019
     22702290,  2270,2290,             2272,2292,   0.814851*0.019
     22712291,              2271,2291,              0.814851*0.019
     22732293,  2273,2293,  2274,2294, 2275,2295, 2276,2296, 2.444553*0.019
C    23702390,  2370,2390,  2371,2391, 2372,2392,   3.992441*0.019
C    23732393,  2373,2393,  2374,2394, 2375,2395, 2376,2396, 11.977323*0.019
C
```

```
C
C  REAR OVERPACK   IMPACT LIMITER
     30103030,  3010,3030, 28.8630* 0.019
     30303050,  3030,3050, 15.3940* 0.019
     30503070,  3050,3070, 15.3940* 0.019
     30703090,  3070,3090, 28.8630* 0.019
C
C      OVERPACK TO CASK CONDUCTORS
C    20801050,  2080,1050,    279.382* 0.0154
C    10502080,  2080,1050,    1.92859*1.7141E 9
     20801050,  2080,1050, 2080,1051, 2080,1052, 0.0666667*279.382* 0.0154
     20801053,  2080,1053, 2080,1054, 2080,1055, 2080,1056, 0.20*279.382* 0.0154
C    10502080,  2080,1050,    1.92859*1.7141E 9
     10502080,  2080,1050, 2080,1051, 2080,1052, 0.0666667*1.92859*1.7141E 9
     10532080,  2080,1053, 2080,1054, 2080,1055, 2080,1056, 0.20*1.92859*1.7141E 9
C    2080950,   2080,950,     284.860* 0.0154
     2080950,  2080,950, 2080,951, 2080,952,  0.0666667*284.860*0.0154
     2080953,  2080,953, 2080,954, 2080,955, 2080,956, 0.20*284.860*0.0154
C    9502080,   2080,950,     1.96641*1.7141E 9
     9502080,  2080,950, 2080,951, 2080,952, 0.0666667*1.96641*1.7141E 9
     9532080,  2080,953, 2080,954, 2080,955, 2080,956, 0.20*1.96641*1.7141E 9
     2080850,   2080,850,     443.724* 0.0154
     8502080,   2080,850,     3.06310*1.7141E 9
     3080150,   3080,150,     219.123* 0.0154
     1503080,   3080,150,     1.51262*1.7141E 9
     3080250,   3080,250,     788.843* 0.0154
     2503080,   3080,250,     5.44543*1.7141E 9
C    20901000,  2090,1000,  3090,200,  47.2550* 0.0154
C    10002090,  2090,1000,  3090,200,  0.65630*1.7141E 9
     20901000,  2090,1000,  2091,1001, 2092,1002,  3.15033* 0.0154
C    10002090,  2090,1000,  2091,1001, 2092,1002,  0.04375*1.7141E 9
C     10002090,  2090,1000,  2091,1001, 2092,1002,  100.
     20931003,  2093,1003,  2094,1004, 2095,1005, 2096,1006,  9.45100* 0.0154
C    10032093,  2093,1003,  2094,1004, 2095,1005, 2096,1006, 0.13126*1.7141E 9
     10032093,  2093,1003,  2094,1004, 2095,1005, 2096,1006, 100.
C  NEXT LINE WAS CHANGED FROM 200 TO 100
     3090100,               3090,100,  47.2550* 0.0154
     1003090,               3090,100,  0.65630*1.7141E 9
C    20901010,  2090,1010,  3090,110,  34.5575* 0.0154
C    10102090,  2090,1010,  3090,110,  0.4800* 1.7141E 9
     20901010,  2090,1010,  2091,1011, 2092,1012,  2.30383* 0.0154
C    10102090,  2090,1010,  2091,1011, 2092,1012,  0.0320* 1.7141E 9
C     10102090,  2090,1010,  2091,1011, 2092,1012,  100.
     20931013,  2093,1013,  2094,1014, 2095,1015, 2096,1016, 6.91150* 0.0154
C    10132093,  2093,1013,  2094,1014, 2095,1015, 2096,1016, 0.0960* 1.7141E 9
C
     10132093,  2093,1013,  2094,1014, 2095,1015, 2096,1016, 100.
     3090110,               3090,110,  34.5575* 0.0154
     1103090,               3090,110,  0.4800* 1.7141E 9
C    20901020,  2090,1020,  3090,120,  48.0729* 0.0154
C    10202090,  2090,1020,  3090,120,  0.6677* 1.7141E 9
     21901020,  2190,1020,  2191,1021, 2192,1022,  3.20486* 0.0154
C    10202190,  2190,1020,  2191,1021, 2192,1022,  0.04451*1.7141E 9
C     10202190,  2190,1020,  2191,1021, 2192,1022,  100.
     21931023,  2193,1023,  2194,1024, 2195,1025, 2196,1026, 9.61458* 0.0154
C    10232193,  2193,1023,  2194,1024, 2195,1025, 2196,1026, 0.13354*1.7141E 9
C
     10232193,  2193,1023,  2194,1024, 2195,1025, 2196,1026, 100.
     3090120,               3090,120,  48.0729* 0.0154
     1203090,               3090,120,  0.6677* 1.7141E 9
C    20901030,  2090,1030,  3090,140,  49.3165* 0.0154
C    10302090,  2090,1030,  3090,140,  .68495* 1.7141E 9
     21901030,  2190,1030,  2191,1031, 2192,1032,  3.28777* 0.0154
C    10302190,  2190,1030,  2191,1031, 2192,1032,  .04566* 1.7141E 9
C     10302190,  2190,1030,  2191,1031, 2192,1032,  100.
     21931033,  2193,1033,  2194,1034, 2195,1035, 2196,1036, 9.86333* 0.0154
C    10332193,  2193,1033,  2194,1034, 2195,1035, 2196,1036, 0.13699*1.7141E 9
C
     10332193,  2193,1033,  2194,1034, 2195,1035, 2196,1036, 100.
     3090140,               3090,140,  49.3165* 0.0154
     1403090,               3090,140,  .68495* 1.7141E 9
C    20901050,  2090,1050,  3090,150,  42.2383* 0.0154
C    10502090,  2090,1050,  3090,150,  .58664* 1.7141E 9
     22901050,  2290,1050,  2291,1051, 2292,1052,  2.815887*0.0154
C    10502290,  2290,1050,  2291,1051, 2292,1052,  .039109*1.7141E 9
C     10502290,  2290,1050,  2291,1051, 2292,1052,  100.
     22931053,  2293,1053,  2294,1054, 2295,1055, 2296,1056, 8.44766* 0.0154

C    10532293,  2293,1053,  2294,1054, 2295,1055, 2296,1056,  0.11732*1.7141E 9
C
     10532293,  2293,1053,  2294,1054, 2295,1055, 2296,1056,100.
```

```
     3090150,              3090,150,  42.2383* 0.0154
     1503090,              3090,150,  .58664* 1.7141E 9
C
C     EXTERNAL RADIATION HEAT TRANSFER
      7098,   370,98,   770,98,   .3*16.223*1.7141E 9  $ THERMAL SHIELD
      9870, 470,98, 570,98, 670,98, .3*18.151*1.7141E 9 $ THERMAL SHIELD
      200098, 2000,98,  3000,98,  .3*76.271*1.7141E 9  $ OVERPACK SHELL
C     201098, 2010,98,  3010,98,  .3*31.503*1.7141E 9  $ OVERPACK SHELL
      301098,           3010,98,  .3*31.503*1.7141E 9  $ OVERPACK SHELL
      201098, 2010,98,  2011,98, 2012,98,  .3*.227256* 1.7141E 9
      201398, 2013,98,  2014,98, 2015,98, 2016,98, .3*.681768* 1.7141E 9
      211098, 2110,98,  2111,98, 2112,98,  .3*.270526* 1.7141E 9
      211398, 2113,98,  2114,98, 2115,98, 2116,98, .3*.811578* 1.7141E 9
      221098, 2210,98,  2211,98, 2212,98,  .3*.271617* 1.7141E 9
      221398, 2213,98,  2214,98, 2215,98, 2216,98, .3*.814851* 1.7141E 9
      231098, 2310,98,  2311,98, 2312,98,  .3*1.33081* 1.7141E 9
      231398, 2313,98,  2314,98, 2315,98, 2316,98, .3*3.99243* 1.7141E 9
      210098, 2100,98,  3100,98,  .3*21.836*1.7141E 9  $ OVERPACK SHELL
      38098,  380,98,             .3*1.0800*1.7141E 9  $ LIFT TRUNNION
      58098,  580,98,             .3*7.2320*1.7141E 9  $ CENTER TRUNNION
      78098,  780,98,             .3*2.1600*1.7141E 9  $ LIFT TRUNNION
C
C    DAMAGE RADIATION CONDUCTORS
       105198,  1051,98,           0.01*.8*1.7141E 9
       227198,  2271,98,           0.01*.8*1.7141E 9
       225098,  2250,98,           0.01*.8*1.7141E 9
       225298,  2252,98,           0.01*.8*1.7141E 9
C
C     EXTERNAL CONVECTION HEAT TRANSFER
C           ACTUAL RATE DETERMINED BY INTERNAL ROUTINE
      7099,   370,99,   770,99,   1.0                  $ THERMAL SHIELD
      9970, 470,99, 570,99, 670,99, 1.0                $ THERMAL SHIELD
      200099, 2000,99,  3000,99,  1.0                  $ OVERPACK SHELL
C     201099, 2010,99,  3010,99,  1.0                  $ OVERPACK SHELL
      301099,           3010,99,  1.0                  $ OVERPACK SHELL
      201099, 2010,99,  2011,99, 2012,99,  1.0
      201399, 2013,99,  2014,99, 2015,99, 2016,99,   1.0
      211099, 2110,99,  2111,99, 2112,99,  1.0
      211399, 2113,99,  2114,99, 2115,99, 2116,99,   1.0
      221099, 2210,99,  2211,99, 2212,99,  1.0
      221399, 2213,99,  2214,99, 2215,99, 2216,99,   1.0
      231099, 2310,99,  2311,99, 2312,99,  1.0
      231399, 2313,99,  2314,99, 2315,99, 2316,99,   1.0
      210099, 2100,99,  3100,99,  1.0                  $ OVERPACK SHELL
      38099,  380,99,             1.0                  $ LIFT TRUNNION
      58099,  580,99,             1.0                  $ CENTER TRUNNION
      78099,  780,99,             1.0                  $ LIFT TRUNNION
C*********************************************************************
HEADER CONTROL DATA, GLOBAL
C*********************************************************************
      ABSZRO  =  459.67
      SIGMA   =    1.0
      EXTLIM  =    1.0
      ITHOLD  =    1
      ITERXT  =    3
      DRLXCA  =     .001
      ARLXCA  =     .001
      ATMPCA  =   10.
      DTMPCA  =   20.
      EBALSA  =     .05
      EBALNA  =     .05
      NLOOPS  = 14000
      ITEROT  = 14001
      NLOOPT  =   80
      OUTPUT  =    0.1
      DTIMEI  =    0.00025
      TIMEO = 0.0
      TIMEND =  10.0
      DTIMEH  =    0.00025
C*********************************************************************
HEADER USER DATA, GLOBAL
C*********************************************************************
      GCONST = 32.2
C*********************************************************************
HEADER USER DATA, CASK
C*********************************************************************
      10 = 32.2     $ GC
C*********************************************************************
HEADER ARRAY DATA, CASK
C*********************************************************************
      1 =   $ARGON CONDUCTIVITY   BTU/HR FT F
```

```
      32.,.00958,  212.,.0123,  392.,.0147,  572.,.0169
      932.,.0208
      2 =   $AIR CONDUCTIVITY   BTU/HR FT F
      32.,.014,  100.,.0154,  300.,.0193,  500.,.0231
      1000.,.0319,  1500.,.040
      3 =   $AIR SPECIFIC HEAT   BTU/LB F
      32.,0.2402,  100.,0.2402,  300.,0.2432,  500.,0.2472
      1000.,0.2622,  1500.,0.2762
      4 =  $AIR ABSOLUTE VISCOSITY   LB/FT HR
      32.,0.04194,  100.,0.04626,  300.,0.05796
      500.,0.06804,  1000.,0.08892,  1500.,0.1080
C***********************************************************************
HEADER OUTPUT CALLS, CASK
C***********************************************************************
      CALL SORTPR('CASK',0)
C***********************************************************************
HEADER OPERATION DATA
C***********************************************************************
BUILD 72BCASK, CASK
C      CALL STDSTL
      CALL FWDBCK
C***********************************************************************
HEADER VARIABLES 1, CASK
C***********************************************************************
C DECAY HEAT PRODUCTION   300 WATTS MAX.
      Q10=  300.* 3.413 /3/7
      Q11=  300. * 3.413/3/7
      Q12=  300. * 3.413/3/7
      Q13=  300. * 3.413/3/7
      Q14=  300. * 3.413/3/7
      Q15=  300. * 3.413/3/7
      Q16=  300. * 3.413/3/7
      Q30=  300. * 3.413/3/7
      Q31=  300. * 3.413/3/7
      Q32=  300. * 3.413/3/7
      Q33=  300. * 3.413/3/7
      Q34=  300. * 3.413/3/7
      Q35=  300. * 3.413/3/7
      Q36=  300. * 3.413/3/7
      Q50=  300. * 3.413/3/7
      Q51=  300. * 3.413/3/7
      Q52=  300. * 3.413/3/7
      Q53=  300. * 3.413/3/7
      Q54=  300. * 3.413/3/7
      Q55=  300. * 3.413/3/7
      Q56=  300. * 3.413/3/7
      IF(TIMEN .LT. 1.51) GO TO 40
C  EXTERNAL SOLAR HEATING
      Q370 = 0.52*634.73                  $ BASED ON PROJECTED AREA
      Q470 = 0.52*710.193                 $ BASED ON PROJECTED AREA
      Q570 = 0.52*710.193                 $ BASED ON PROJECTED AREA
      Q670 = 0.52*710.193                 $ BASED ON PROJECTED AREA
      Q770 = 0.52*634.73                  $ BASED ON PROJECTED AREA
      Q2000= 0.52*2984.17                 $ BASED ON PROJECTED AREA
      Q3000= 0.52*2984.17                 $ BASED ON PROJECTED AREA
C      Q2010= 0.52*1934.93                 $ BASED ON PROJECTED AREA
      Q2010= 0.52*13.95809                $ BASED ON PROJECTED AREA
      Q2011= 0.52*13.95809                $ BASED ON PROJECTED AREA
      Q2012= 0.52*13.95809                $ BASED ON PROJECTED AREA
      Q2013= 0.52*41.87427                $ BASED ON PROJECTED AREA
      Q2014= 0.52*41.87427                $ BASED ON PROJECTED AREA
      Q2015= 0.52*41.87427                $ BASED ON PROJECTED AREA
      Q2016= 0.52*41.87427                $ BASED ON PROJECTED AREA
      Q2110= 0.52*16.61571                $ BASED ON PROJECTED AREA
      Q2111= 0.52*16.61571                $ BASED ON PROJECTED AREA
      Q2112= 0.52*16.61571                $ BASED ON PROJECTED AREA
      Q2113= 0.52*49.84713                $ BASED ON PROJECTED AREA
      Q2114= 0.52*49.84713                $ BASED ON PROJECTED AREA
      Q2115= 0.52*49.84713                $ BASED ON PROJECTED AREA
      Q2116= 0.52*49.84713                $ BASED ON PROJECTED AREA
      Q2210= 0.52*16.682708               $ BASED ON PROJECTED AREA
      Q2211= 0.52*16.682708               $ BASED ON PROJECTED AREA
      Q2212= 0.52*16.682708               $ BASED ON PROJECTED AREA
      Q2213= 0.52*50.048124               $ BASED ON PROJECTED AREA
      Q2214= 0.52*50.048124               $ BASED ON PROJECTED AREA
      Q2215= 0.52*50.048124               $ BASED ON PROJECTED AREA
      Q2216= 0.52*50.048124               $ BASED ON PROJECTED AREA
      Q2310= 0.52*81.738569               $ BASED ON PROJECTED AREA
      Q2311= 0.52*81.738569               $ BASED ON PROJECTED AREA
      Q2312= 0.52*81.738569               $ BASED ON PROJECTED AREA
      Q2313= 0.52*245.21571               $ BASED ON PROJECTED AREA
```

```
      Q2314= 0.52*245.21571              $ BASED ON PROJECTED AREA
      Q2315= 0.52*245.21571              $ BASED ON PROJECTED AREA
      Q2316= 0.52*245.21571              $ BASED ON PROJECTED AREA
      Q3010= 0.52*1934.93                $ BASED ON PROJECTED AREA
      Q2100= 0.52*1341.18                $ BASED ON PROJECTED AREA
      Q3100= 0.52*1341.18                $ BASED ON PROJECTED AREA
      Q380 = 0.52*1.0800*39.126
      Q580 = 0.52*6.1760*39.126
      Q780 = 0.52*2.1600*39.126
 40   CONTINUE
C  EXTERNAL BOUNDARY TEMPERATURES
      T99 = 100.
      T98 = 100.
C  DISABLE WIRE WRAP CONDUCTANCE FOR NORMAL CONDITIONS
C      G251270 = 1.0E 12
C      G351370 = 1.0E 12
C      G451470 = 1.0E 12
C      G851870 = 1.0E 12
      IF(TIMEN .LT. 1.01 .OR. TIMEN .GT. 1.51) GO TO 50
      T99 = 1475.
      T98 = 1424.7
C  ACTIVATE DAMAGE CONDITION CONDUCTORS
      G22712291=1.2* .814851*0.019
      G105198 = .8*  .0872664*1.7141E 9
      G227198 = .8*  .14366*1.7141E 9
      G225098 = .8*  .50000*1.7141E 9
      G225298 = .8*  .50000*1.7141E 9
      G7098   = .8*16.223*1.7141E 9
      G9870   = .8*18.151*1.7141E 9
      G200098 = .8*76.271*1.7141E 9
      G301098 = .8*31.503*1.7141E 9
      G201098 = .8*  .227256* 1.7141E 9
      G201398 = .8*  .681768* 1.7141E 9
      G211098 = .8*  .270526* 1.7141E 9
      G211398 = .8*  .811578* 1.7141E 9
      G221098 = .8*  .271617* 1.7141E 9
      G221398 = .8*  .814851* 1.7141E 9
      G231098 = .8* 1.33081* 1.7141E 9
      G231398 = .8* 3.99243* 1.7141E 9
      G210098 = .8*21.836*1.7141E 9
      G38098  = .8* 1.0800*1.7141E 9
      G58098  = .8* 7.2320*1.7141E 9
      G78098  = .8* 2.1600*1.7141E 9
C     ENABLE WIRE WRAP CONDUCTANCE FOR ACCIDENT CONDITIONS
      G251270 = 2.2700* 10.0
      G351370 = 2.2500* 10.0
      G451470 = 2.5200* 10.0
      G851870 =  1.280* 10.0
  50  CONTINUE
C
C  CALCULATE VARIABLE CONVECTIVE HEAT TRANSFER RATE
      CALL FRCVV(G7099,T370,T99,16.2230,3.46670,XK10,0.0,
     *      A3,A2,A4,0.0,14.70,53.350)
      CALL FRCVV(G9970,T570,T99,18.1510,3.46670,XK10,0.0,
     *      A3,A2,A4,0.0,14.70,53.350)
      CALL FRCVV(G200099,T2000,T99,76.2710,6.33330,XK10,0.0,
     *      A3,A2,A4,0.0,14.70,53.350)
C     CALL FRCVV(G201099,T2010,T99,31.5030,6.33330,XK10,0.0,
C    *      A3,A2,A4,0.0,14.70,53.350)
      CALL FRCVV(G301099,T3010,T99,31.5030,6.33330,XK10,0.0,
     *      A3,A2,A4,0.0,14.70,53.350)
      CALL FRCVV(G201099,T2010,T99,.227260,6.33330,XK10,0.0,
     *      A3,A2,A4,0.0,14.70,53.350)
      CALL FRCVV(G201399,T2014,T99,.681780,6.33330,XK10,0.0,
     *      A3,A2,A4,0.0,14.70,53.350)
      CALL FRCVV(G211099,T2110,T99,.270530,6.33330,XK10,0.0,
     *      A3,A2,A4,0.0,14.70,53.350)
      CALL FRCVV(G211399,T2114,T99,.811590,6.33330,XK10,0.0,
     *      A3,A2,A4,0.0,14.70,53.350)
      CALL FRCVV(G221099,T2210,T99,.271620,6.33330,XK10,0.0,
     *      A3,A2,A4,0.0,14.70,53.350)
      CALL FRCVV(G221399,T2214,T99,.814860,6.33330,XK10,0.0,
     *      A3,A2,A4,0.0,14.70,53.350)
      CALL FRCVV(G231099,T2310,T99,1.33080,6.33330,XK10,0.0,
     *      A3,A2,A4,0.0,14.70,53.350)
      CALL FRCVV(G231399,T2314,T99,3.99240,6.33330,XK10,0.0,
     *      A3,A2,A4,0.0,14.70,53.350)
      CALL FRCVV(G210099,T2100,T99,21.8360,6.33330,XK10,0.0,
     *      A3,A2,A4,0.0,14.70,53.350)
      CALL FRCVV(G38099, T380, T99,1.08000,6.33330,XK10,0.0,
     *      A3,A2,A4,0.0,14.70,53.350)
```

```
      CALL FRCVV(G58099, T580, T99,7.23200,6.33330,XK10,0.0,
     *      A3,A2,A4,0.0,14.70,53.350)

      CALL FRCVV(G78099, T780, T99,2.16000,6.33330,XK10,0.0,
     *      A3,A2,A4,0.0,14.70,53.350)
C
C  *************************
C  CALCULATE VARIABLE CONDUCTOR VALUES
C  *************************
      CALL D1D1WM(T38, A2, 94.5100,G2838)
      CALL D1D1WM(T220, A2, 798.3690,G220230)
      CALL D1D1WM(T250, A2, 1923.720,G250270)
      CALL D1D1WM(T320, A2, 792.8200,G320330)
      CALL D1D1WM(T350, A2, 1919.360,G350370)
      CALL D1D1WM(T520, A2, 887.0800,G420430)
      CALL D1D1WM(T550, A2, 2137.470,G450470)
      CALL D1D1WM(T820, A2, 449.0800,G820830)
      CALL D1D1WM(T820, A2, 7.392330,G820930)
      CALL D1D1WM(T820, A2,22.176990,G820933)
      CALL D1D1WM(T850, A2, 1082.090,G850870)
C     CALL D1D1WM(T920, A2, 177.4150,G920930)
      CALL D1D1WM(T921, A2, 11.82770,G920930)
      CALL D1D1WM(T924, A2, 35.48310,G923933)
C     CALL D1D1WM(T1030, A2, 581.9800,G10301050)
      CALL D1D1WM(T1031, A2, 38.79870,G10301050)
      CALL D1D1WM(T1034, A2,116.39610,G10331053)
      CALL D1D1WM(T215,  A2, 44.48200,G215220)
      CALL D1D1WM(T315,  A2, 50.88700,G315320)
      CALL D1D1WM(T515,  A2, 56.93700,G415420)
      CALL D1D1WM(T815,  A2, 27.40100,G815820)
C     CALL D1D1WM(T205,  A2, 88.48800,G200205)
      CALL D1D1WM(T205,  A2, 88.48800,G200205)
      CALL D1D1WM(T901,  A2, 5.899200,G805900)
      CALL D1D1WM(T904,  A2, 17.69760,G805903)
      CALL D1D1WM(T200, A2, 63.00600,G100200)
      CALL D1D1WM(T210, A2, 46.07700,G110210)
      CALL D1D1WM(T210, A2, 69.63800,G120210)
C     CALL D1D1WM(T900, A2, 63.00600,G9001000)
      CALL D1D1WM(T901, A2, 4.200400,G9001000)
      CALL D1D1WM(T904, A2,12.601200,G9031003)
C     CALL D1D1WM(T910, A2,  46.0770,G9101010)
      CALL D1D1WM(T911, A2,  3.07180,G9101010)
      CALL D1D1WM(T914, A2, 9.215400,G9131013)
C     CALL D1D1WM(T920, A2,  69.6390,G9201020)
      CALL D1D1WM(T921, A2,  4.64260,G9201020)
      CALL D1D1WM(T924, A2, 13.92780,G9231023)
C     CALL D1D1WM(T2080, A2, 279.3820,G20801050)
      CALL D1D1WM(T2080, A2, 18.62550,G20801050)
      CALL D1D1WM(T2080, A2, 55.87640,G20801053)
C     CALL D1D1WM(T2080, A2, 284.8600,G2080950)
      CALL D1D1WM(T2080, A2, 18.99070,G2080950)
      CALL D1D1WM(T2080, A2, 56.97200,G2080953)
      CALL D1D1WM(T2080, A2, 443.7240,G2080850)
      CALL D1D1WM(T3080, A2, 219.1230,G3080150)
      CALL D1D1WM(T3080, A2, 788.8430,G3080250)
C     CALL D1D1WM(T2090, A2, 47.25500,G20901000)
      CALL D1D1WM(T2091, A2, 3.150330,G20901000)
      CALL D1D1WM(T2094, A2, 9.450990,G20931003)
      CALL D1D1WM(T3090, A2, 47.25500,G3090100)
C     CALL D1D1WM(T2090, A2, 34.55750,G20901010)
      CALL D1D1WM(T3090, A2, 34.55750,G3090110)
      CALL D1D1WM(T2091, A2, 2.303830,G20901010)
      CALL D1D1WM(T2094, A2, 6.911490,G20931013)
C     CALL D1D1WM(T2090, A2, 48.07290,G20901020)
      CALL D1D1WM(T2191, A2, 3.204860,G21901020)
      CALL D1D1WM(T2194, A2, 9.614580,G21931023)
      CALL D1D1WM(T3090, A2, 48.07290,G3090120)
C     CALL D1D1WM(T2090, A2, 49.31650,G20901030)
      CALL D1D1WM(T2191, A2, 3.287770,G21901030)
      CALL D1D1WM(T2194, A2, 9.863310,G21931033)
      CALL D1D1WM(T3090, A2, 49.31650,G3090140)
C     CALL D1D1WM(T2090, A2, 42.23830,G20901050)
      CALL D1D1WM(T2291, A2, 2.815890,G22901050)
      CALL D1D1WM(T2294, A2, 8.447670,G22931053)
      CALL D1D1WM(T3090, A2, 42.23830,G3090150)
C  RESET OUTPUT INTERVAL
      OUTPUT = .1
      IF(TIMEN .GT. 1.40000001) OUTPUT = .050
      IF(TIMEN .GT. 1.80000001) OUTPUT = .200
      IF(TIMEN .GT. 3.00000001) OUTPUT = .5
C      IF(TIMEN .GT. 3.00000001) OUTPUT = .250
```

```
C      IF(TIMEN .GT. 5.00000001) OUTPUT = .500
END OF DATA
```

3.6.2.3 50-Watt Transient Conditions Input File (Damaged Package Model)

```
HEADER OPTIONS DATA
TITLE 72 B FUEL CASK,HAC FIRE, 50W DAMAGED 14.5 inch IL crush 2/99
      MODEL= 72B CASK
      OUTPUT = 72b5014c.sot
      PPOUT = ALL1
C*********************************************************************
HEADER NODE DATA, CASK
C*********************************************************************
C  *************************
C  PAYLOAD MODEL
C  *************************
      GEN  10,  6,  10,  191.,   0.21013 * 100.0 * 0.25
      GEN  11,  6,  10,  174.,   0.21013 * 100.0 * 0.25
      GEN  12,  6,  10,  163.,   0.21013 * 100.0 * 0.25
      GEN  13,  6,  10,  151.,   0.21013 * 100.0 * 0.25
      GEN  14,  6,  10,  138.,   0.21013 * 100.0 * 0.25
      GEN  15,  6,  10,  125.,   0.21013 * 100.0 * 0.25
      GEN  16,  6,  10,  118.,   6.660 * 0.113
      GEN  17,  6,  10,  113.,   10.976* 0.113
      GEN  18,  6,  10,  110.,   3.5958* 0.113
      GEN  71,  6,   1,  113.,   1.9260* 0.113
      GEN  81,  6,   1,  127.,   1.9260* 0.113
C  *************************
C  OVERPACK   IMPACT LIMITER MODEL
C  *************************
C      GEN  2000,  2,  1000,  100.,  371.614* 0.11
      3000,    100.,  371.614* 0.11
      GEN  2000,  3,     1,  100.,  .06667*.6667*371.614*0.11
      GEN  2003,  4,     1,  100.,  .2*.6667*371.614*0.11
      GEN  2400,  3,     1,  100.,  .06667*.3333*371.614*0.11
      GEN  2403,  4,     1,  100.,  .2*.3333*371.614*0.11
C      GEN  2020,  2,  1000,  100.,  109.155* 0.30
      3020,    100.,  109.155* 0.30
      GEN  2020,  3,     1,  100.,  .06667*.6667*109.155* 0.30
      GEN  2023,  4,     1,  100.,  .2*.6667*109.155* 0.30
      GEN  2420,  3,     1,  100.,  .06667*.3333*109.155* 0.30
      GEN  2423,  4,     1,  100.,  .2*.3333*109.155* 0.30
C      GEN  2040,  2,  1000,  101.,  286.960* 0.30
      3040,  101.,  286.960* 0.30
      GEN  2040,  3,     1,  100.,  .06667*.6667*286.960* 0.30
      GEN  2043,  4,     1,  100.,  .2*.6667*286.960* 0.30
      GEN  2440,  3,     1,  100.,  .06667*.3333*286.960* 0.30
      GEN  2443,  4,     1,  100.,  .2*.3333*286.960* 0.30
C      GEN  2060,  2,  1000,  103.,  117.600* 0.30
      3060, 103.,  117.600* 0.30
      GEN  2060,  3,     1,  100.,  .06667*.6667*117.600* 0.30
      GEN  2063,  4,     1,  100.,  .2*.6667*117.600* 0.30
      GEN  2460,  3,     1,  100.,  .06667*.3333*117.600* 0.30
      GEN  2463,  4,     1,  100.,  .2*.3333*117.600* 0.30
C      GEN  2080,  2,  1000,  103.,  161.382* 0.11
      3080, 103.,  161.382* 0.11
      GEN  2080,  3,     1,  100.,  .06667*.6667*161.382* 0.11
      GEN  2083,  4,     1,  100.,  .2*.6667*161.382* 0.11
      GEN  2480,  3,     1,  100.,  .06667*.3333*161.382* 0.11
      GEN  2483,  4,     1,  100.,  .2*.3333*161.382* 0.11
C
      GEN  2100,  2,  1000,  100.,  106.561* 0.11
C     GEN  2010,  2,  1000,  100.,  153.736* 0.11
      GEN  2010,  3,  1,  100.,  1.1090 * 0.11
      GEN  2013,  4,  1,  100.,  3.3271 * 0.11
      GEN  2110,  3,  1,  100.,  1.3202* 0.11
      GEN  2113,  4,  1,  100.,  3.9605* 0.11
      GEN  2210,  3,  1,  100.,  1.3255* 0.11
      GEN  2213,  4,  1,  100.,  3.9765* 0.11
      GEN  2310,  3,  1,  100.,  6.4944* 0.11
      GEN  2313,  4,  1,  100., 19.4834* 0.11
C     GEN  2030,  2,  1000,  101.,   80.176* 0.30
      GEN  2030,  3,  1,  101.,  1.89380* 0.30
      GEN  2033,  4,  1,  101.,  5.68141* 0.30
      GEN  2130,  3,  1,  101.,  2.25438* 0.30
      GEN  2133,  4,  1,  101.,  6.76314* 0.30
      GEN  2230,  3,  1,  101.,  2.26347* 0.30
      GEN  2233,  4,  1,  101.,  6.79041* 0.30
      GEN  2330,  3,  1,  101.,  11.0911* 0.30
      GEN  2333,  4,  1,  101.,  33.2733* 0.30
```

```
C     GEN  2050,  2,  1000,  102.,   70.154* 0.30
      GEN  2050,  3,  1,  102.,  0.875 * 1.89380* 0.30
      GEN  2053,  4,  1,  102.,  0.875 * 5.68141* 0.30
      GEN  2150,  3,  1,  102.,  0.875 * 2.25438* 0.30
      GEN  2153,  4,  1,  102.,  0.875 * 6.76314* 0.30
      GEN  2250,  3,  1,  102.,  0.875 * 2.26347* 0.30
      GEN  2253,  4,  1,  102.,  0.875 * 6.79041* 0.30
      GEN  2350,  3,  1,  102.,  0.875 * 11.0911* 0.30
      GEN  2353,  4,  1,  102.,  0.875 * 33.2733* 0.30
C     GEN  2070,  2,  1000,  103.,   75.165* 0.30
      GEN  2070,  3,  1,  103.,  1.7754* 0.30
      GEN  2073,  4,  1,  103.,  5.3263* 0.30
      GEN  2170,  3,  1,  103.,  2.1135* 0.30
      GEN  2173,  4,  1,  103.,  6.3404* 0.30
      GEN  2270,  3,  1,  103.,  2.1220* 0.30
      GEN  2273,  4,  1,  103.,  6.3660* 0.30
      GEN  2370,  3,  1,  103., 10.3979* 0.30
      GEN  2373,  4,  1,  103., 31.1937* 0.30
C     GEN  2090,  2,  1000,  103.,  231.616* 0.11
      GEN  2090,  3,  1,  103.,  5.4449* 0.11
      GEN  2093,  4,  1,  103.,  16.3347* 0.11
      GEN  2190,  3,  1,  103.,  6.4816* 0.11
      GEN  2193,  4,  1,  103.,  19.4448* 0.11
      GEN  2290,  3,  1,  103.,  0.54* 6.5078* 0.11
      GEN  2293,  4,  1,  103.,  0.54*19.5232* 0.11
C
C  REAR OVERPACK   IMPACT LIMITER MODEL
C
      3010,  100.,  153.736* 0.11
      3030,  101.,   80.176* 0.30
      3050,  102.,   70.154* 0.30
      3070,  104.,   75.165* 0.30
      3090,  104.,  231.616* 0.11
C  *************************
C  CASK BODY NODES
C  *************************
C      OUTER CASK BASE PLATE
     100,   104.,   400.353* 0.11
     110,   104.,   292.780* 0.11
     120,   104.,   469.627* 0.11
     130,   104.,   148.075* 0.11
     140,   104.,   301.554* 0.11
     150,   104.,   306.823* 0.11
C      CANISTER
     205,   107.,   100.253* 0.11
     212,   107.,   339.938* 0.031
     215,   107.,   99.224* 0.11
     315,   110.,   101.882* 0.11
     415,   110.,   113.994* 0.11
     515,   110.,   113.994* 0.11
     615,   108.,   113.994* 0.11
     715,   108.,   101.882* 0.11
     805,   107.,   189.583* 0.11
     812,   107.,   570.760* 0.031
     815,   107.,    71.709* 0.11
C      INNER VESSEL
     200,   105.,   120.106* 0.11         $ BASE PLATE
     210,   105.,   240.800* 0.11         $ BASE PLATE
     220,   105.,   185.446* 0.11         $ INNER VESSEL SHELL
     320,   105.,   188.076* 0.11         $ INNER VESSEL SHELL
     420,   105.,   210.435* 0.11         $ INNER VESSEL SHELL
     520,   105.,   210.435* 0.11         $ INNER VESSEL SHELL
     620,   104.,   210.435* 0.11         $ INNER VESSEL SHELL
     720,   104.,   188.076* 0.11         $ INNER VESSEL SHELL
     820,   104.,   608.129* 0.11         $ INNER VESSEL SHELL
C      OUTER CASK, INNER SHELL
     230,   104.,   533.071* 0.11
     330,   104.,   529.370* 0.11
     430,   103.,   592.300* 0.11
     530,   103.,   592.300* 0.11
     630,   103.,   592.300* 0.11
     730,   103.,   529.370* 0.11
     830,   103.,   299.850* 0.11
C      LEAD SHIELD
     240,   104.,   767.199* 0.031
     340,   104.,   761.870* 0.031
     440,   103.,   852.443* 0.031
C     540,   103.,   852.443* 0.031
     GEN  540,  4,  1,  103.,  0.25*852.443*0.031
     640,   103.,   852.443* 0.031
     740,   103.,   761.870* 0.031
```

```
     840,   103.,   431.550* 0.031
     245,   103.,   812.252* 0.031
     345,   103.,   806.610* 0.031
     445,   103.,   902.503* 0.031
C     545,   103.,   902.503* 0.031
     GEN  545,  4,  1,  103.,  0.25*902.503*0.031
     645,   103.,   902.503* 0.031
     745,   103.,   806.610* 0.031
     845,   103.,   456.890* 0.031
C      OUTER CASK, OUTER SHELL
     250,   104.,   949.323* 0.11
     350,   104.,   942.730* 0.11
     450,   103.,  1054.803* 0.11
C     550,   103.,  1054.803* 0.11
     GEN  550,  4,  1,  103.,  0.25*1054.803*0.11
     650,   103.,  1054.803* 0.11
     750,   103.,   942.730* 0.11
     850,   103.,   533.994* 0.11
C      THERMAL SHIELD
     270,   104.,    90.933* 0.11
     370,   103.,    89.726* 0.11
     470,   103.,   99.719* 0.11
C     570,   103.,   100.393* 0.11
     GEN  570,  2,  2,  103.,  0.25*100.393*0.11
     GEN  571,  2,  2,  103.,  0.125*100.393*0.11
     670,   103.,   99.719* 0.11
     770,   103.,    89.726* 0.11
     870,   103.,    50.824* 0.11
C      TRUNNIONS
    380,    103.,   2.*16.857* 0.11    $ 2 LIFTING TRUNNIONS
    581,    103.,   98.53 * 0.11   $  TRANSPORT TRUNNION
    583,    103.,   98.53 * 0.11
    591,    103.,   92.62 * 0.11
    593,    103.,   92.62 * 0.11
    780,    103.,   4.*16.857* 0.11    $ 4 LIFTING TRUNNIONS
C      INNER VESSEL LID
C    900,   105.,   520.459* 0.11
      GEN  900, 3,  1,   105.,   0.066667 * 520.459* 0.11
      GEN  903, 4,  1,   105.,   0.200000 * 520.459* 0.11
C    910,   104.,   380.613* 0.11
      GEN  910, 3,  1,   104.,   0.066667 * 380.613* 0.11
      GEN  913, 4,  1,   104.,   0.200000 * 380.613* 0.11
C    920,   104.,   442.163* 0.11
      GEN  920, 3,  1,   104.,   0.066667 * 442.163* 0.11
      GEN  923, 4,  1,   104.,   0.200000 * 442.163* 0.11
C    930,   103.,   192.498* 0.11
      GEN  930, 3,  1,   103.,   0.066667 * 192.498* 0.11
      GEN  933, 4,  1,   103.,   0.200000 * 192.498* 0.11
C    940,   103.,   392.020* 0.11
      GEN  940, 3,  1,   103.,   0.066667 * 392.020* 0.11
      GEN  943, 4,  1,   103.,   0.200000 * 392.020* 0.11
C    950,   103.,   398.869* 0.11
      GEN  950, 3,  1,   103.,   0.066667 * 398.869* 0.11
      GEN  953, 4,  1,   103.,   0.200000 * 398.869* 0.11
C      OUTER CASK LID
C   1000,   104.,   480.424* 0.11
      GEN 1000, 3,  1,   104.,   0.066667 * 480.424* 0.11
      GEN 1003, 4,  1,   104.,   0.200000 * 480.424* 0.11
C   1010,   104.,   351.335* 0.11
      GEN 1010, 3,  1,   104.,   0.066667 * 351.335* 0.11
      GEN 1013, 4,  1,   104.,   0.200000 * 351.335* 0.11
C   1020,   104.,   488.741* 0.11
      GEN 1020, 3,  1,   104.,   0.066667 * 488.741* 0.11
      GEN 1023, 4,  1,   104.,   0.200000 * 488.741* 0.11
C   1030,   104.,   309.372* 0.11
      GEN 1030, 3,  1,   104.,   0.066667 * 309.372* 0.11
      GEN 1033, 4,  1,   104.,   0.200000 * 309.372* 0.11
C   1040,   104.,   216.013* 0.11
      GEN 1040, 3,  1,   104.,   0.066667 * 216.013* 0.11
      GEN 1043, 4,  1,   104.,   0.200000 * 216.013* 0.11
C   1050,   103.,   511.242* 0.11
      GEN 1050, 3,  1,   103.,   0.066667 * 511.242* 0.11
      GEN 1053, 4,  1,   103.,   0.200000 * 511.242* 0.11
C  *************************
C  EXTERNAL BOUNDARY NODES
C  *************************
       99,  100.,    1.
       98,  100.,    1.
C*********************************************************************
HEADER CONDUCTOR DATA, CASK
C*********************************************************************
```

```
C  *************************
C  PAYLOAD  CONDUCTORS
C  *************************
C       RADIAL CONDUCTANCE
     1011,   10,11, 20,21, 30,31, 40,41, 50,51, 60,61,  7.566* 0.02
     1112,   11,12, 21,22, 31,32, 41,42, 51,52, 61,62, 26.355* 0.02
     1213,   12,13, 22,23, 32,33, 42,43, 52,53, 62,63, 36.473* 0.02
     1314,   13,14, 23,24, 33,34, 43,44, 53,54, 63,64, 53.657* 0.02
     1415,   14,15, 24,25, 34,35, 44,45, 54,55, 64,65, 63.720* 0.02
     1516,   15,16, 25,26, 35,36, 45,46, 55,56, 65,66, 149.30* 0.02
C       AXIAL CONDUCTANCE
     1071,   10,71, 20,72, 30,73, 40,74, 50,75, 60,76,  .7445* 0.02
     1171,   11,71, 21,72, 31,73, 41,74, 51,75, 61,76,  .7445* 0.02
     1271,   12,71, 22,72, 32,73, 42,74, 52,75, 62,76,  .7445* 0.02
     1371,   13,71, 23,72, 33,73, 43,74, 53,75, 63,76,  .7445* 0.02
     1471,   14,71, 24,72, 34,73, 44,74, 54,75, 64,76,  .7445* 0.02
     7115,   15,71, 25,72, 35,73, 45,74, 55,75, 65,76,  .7445* 0.02
     1081,   10,81, 20,82, 30,83, 40,84, 50,85, 60,86,  .7445* 0.02
     1181,   11,81, 21,82, 31,83, 41,84, 51,85, 61,86,  .7445* 0.02
     1281,   12,81, 22,82, 32,83, 42,84, 52,85, 62,86,  .7445* 0.02
     1381,   13,81, 23,82, 33,83, 43,84, 53,85, 63,86,  .7445* 0.02
     1481,   14,81, 24,82, 34,83, 44,84, 54,85, 64,86,  .7445* 0.02
     8115,   15,81, 25,82, 35,83, 45,84, 55,85, 65,86,  .7445* 0.02
C       PAYLOAD TO 30 GALLON DRUMS
     1617,   16,17, 26,27, 36,37, 46,47, 56,57, 66,67, 26.366* 0.0154
     1716,   16,17, 26,27, 36,37, 46,47, 56,57, 66,67, 3.7474*1.7141E 9
     7118,   71,18, 72,28, 73,38, 74,48, 75,58, 76,68, 56.958* 0.0154
     1871,   71,18, 72,28, 73,38, 74,48, 75,58, 76,68, .84718*1.7141E 9
     8182,   81,82, 83,84, 85,86,  56.958* 0.0154
     8281,   81,82, 83,84, 85,86,  .79110*1.7141E 9
     7116,   71,16, 72,26, 73,36, 74,46, 75,56, 76,66,  0.0139* 25.0
     8116,   81,16, 82,26, 83,36, 84,46, 85,56, 86,66,  0.0139* 25.0
     1727,   17,27, 37,47, 57,67,  0.01492* 25.0
     2838,   28,38, 48,58,  94.510* 0.0154
     3828,   28,38, 48,58,  1.3130*1.7141E 9
C  *************************
C  PAYLOAD  TO CASK CONDUCTORS
C  *************************
     18205,  18,212,  68,812,    0.56920*1.7141E 9
     18215,  18,215,  65,815,    1.10020*1.7141E 9
     17215,  17,215,  57,515,  67,615,    0.51980*1.7141E 9
     17315,  17,315,  57,615,  67,715,    3.81130*1.7141E 9
     17415,  17,415,  57,715,  67,815,    0.41869*1.7141E 9
     27315,  27,315,            1.18131*1.7141E 9
     27415,  27,415,            3.50350*1.7141E 9
     27515,  27,515,            0.21220*1.7141E 9
     37315,  37,315,            0.15968*1.7141E 9
     37415,  37,415,            2.40563*1.7141E 9
     37515,  37,515,            2.52010*1.7141E 9
     47415,  47,415,            0.21220*1.7141E 9
     47515,  47,515,            3.35322*1.7141E 9
     47315,  47,315,            1.38911*1.7141E 9
C  *************************
C      CASK BODY RADIAL CONDUCTORS
C  *************************
     100110,  100,110,    2.753* 10.0
     110120,  110,120,    9.860* 10.0
     120130,  120,130,    17.291* 10.0
     130140,  130,140,    31.676* 10.0
     140150,  140,150,    29.422* 10.0
C      STATION 200
     200210,  200,210,    0.808* 10.0
     210220,  210,220,    0.313* 10.0
     220230,  220,230,    798.369* 0.0154
     230220,  220,230,    1.9227* 1.7141E 9
     230240,  230,240,    1276.159
     240245,  240,245,    182.284* 19.3
     245250,  245,250,    1829.40
     250270,  250,270,    1923.72* 0.0154
     270250,  250,270,    5.4015*1.7141E 9
     251270,  250,270,    2.2700* 10.0         $ WIRE WRAP
C      STATION 300
     320330,  320,330,  720,730,    792.820* 0.0154
     330320,  320,330,  720,730,    2.2173* 1.7141E 9
     330340,  330,340,  730,740,    1267.297
     340345,  340,345,  740,745,    181.018* 19.3
     345350,  345,350,  745,750,    1816.673
     350370,  350,370,  750,770,    1910.36* 0.0154
     370350,  350,370,  750,770,    5.364*1.7141E 9
     351370,  350,370,  750,770,    2.2500* 10.0         $ WIRE WRAP
C      STATIONS 400,500, & 600
```

```
     420430,  420,430, 520,530, 620,630,     887.080* 0.0154
     430420,  420,430, 520,530, 620,630,     2.4976* 1.7141E 9
     430440,  430,440, 630,640,     1417.937
     530540,  530,540, 530,541, 530,542, 530,543,  0.25*1417.937
     440445,  440,445, 640,645,     202.540* 19.3
     540545,  540,545, 541,546, 542,547, 543,548, 0.25*202.540* 19.3
     445450,  445,450, 645,650,     2037.906
     545550,  545,550, 546,551, 547,552, 548,553, 0.25*2037.906
     450470,  450,470, 650,670,     2137.47*0.0154
     550570,  550,570, 552,572, 0.25*2137.47*0.0154
     553570,  551,571, 553,573, 0.125*2137.47*0.0154
     470450,  450,470, 650,670,     6.0017*1.7141E 9
     570550,  550,570, 552,572,  0.25*6.0017*1.7141E 9
     571550,  551,571, 553,573,  0.125*6.0017*1.7141E 9
     451470,  450,470, 650,670,     2.5200* 10.0  $ WIRE WRAP
     551570,  551,571, 553,573,  0.125*2.520*10.0  $wire wrap
     552570,  550,570, 552,572,  0.25*2.520*10.0  $wire wrap
C      STATION 800
     820830,  820,830,     449.080* 0.0154
     830820,  820,830,     1.2560* 1.7141E 9
     830840,  830,840,     717.8158
     840845,  840,845,     102.530* 19.3
     845850,  845,850,     1029.0523
     850870,  850,870,     1082.09* 0.0154
     870850,  850,870,     2.9001*1.7141E 9
     851870,  850,870,     1.280* 10.0         $ WIRE WRAP
C      STATION 900
C    820930,  820,930,     110.885*0.0154
   820930,  820,930,  820,931, 820,932,           .0666667*110.885*.0154
   820933,  820,933,  820,934, 820,935, 820,936,  .200000*110.885*.0154
C    930820,  820,930,     0.3101* 1.7141E 9
   930820,  820,930,  820,931, 820,932,           .0205333*1.7141E 9
   933820,  820,933,  820,934, 820,935, 820,936,  .0616000*1.7141E 9
C    900910,  900,910,     4.0530* 10.0
   900910,  900,910,  901,911, 902,912,            .0666667*4.0530* 10.0
   903913,  903,913,  904,914, 905,915, 906,916,   .2000000*4.0530* 10.0
C    910920,  910,920,     13.855* 10.0
   910920,  910,920,  911,921, 912,922,            .0666667*13.855* 10.0
   913923,  913,923,  914,924, 915,925, 916,926,   .2000000*13.855* 10.0
C    920930,  920,930,    177.415* 0.0154
   920930,  920,930,  921,931, 922,932,           .0666667*177.415*.0154
   923933,  923,933,  924,934, 925,935, 926,936,  .2000000*177.415*.0154
C    930920,  920,930,     0.4962* 1.7141E 9
  930920,  920,930,  921,931, 922,932,          .0666667*0.4962*1.7141E 9
  933923,  923,933,  924,934, 925,935, 926,936, .2000000*0.4962*1.7141E 9
C    930940,  930,940,     41.179* 10.0
   930940,  930,940,  931,941, 932,942,            .0666667*41.179*10.0
   933943,  933,943,  934,944, 935,945, 936,946,   .2000000*41.179*10.0
C    940950,  940,950,     38.248* 10.0
   940950,  940,950,  941,951, 942,952,            .0666667*38.248*10.0
   943953,  943,953,  944,954, 945,955, 946,956,   .2000000*38.248*10.0
C      STATION 900 TO 900
   900901,  900,901,  901,902,                     1.715278* 10.0
   902903,  902,903,  906,900,                     0.857639* 10.0
   903904,  903,904,  904,905,  905,906,           0.571759* 10.0
   910911,  910,911,  911,912,                     0.353261* 10.0
   912913,  912,913,  916,910,                     0.176630* 10.0
   913914,  913,914,  914,915,  915,916,           0.117754* 10.0
   920921,  920,921,  921,922,                     0.317560* 10.0
   922923,  922,923,  926,920,                     0.158780* 10.0
   923924,  923,924,  924,925,  925,926,           0.105853* 10.0
   930931,  930,931,  931,932,                     0.077381* 10.0
   932933,  932,933,  936,930,                     0.038690* 10.0
   933934,  933,934,  934,935,  935,936,           0.025794* 10.0
   940941,  940,941,  941,942,                     0.133635* 10.0
   942943,  942,943,  946,940,                     0.066820* 10.0
   943944,  943,944,  944,945,  945,946,           0.044545* 10.0
   950951,  950,951,  951,952,                     0.097892* 10.0
   952953,  952,953,  956,950,                     0.048946* 10.0
   953954,  953,954,  954,955,  955,956,           0.032631* 10.0
C      STATION 1000
C    10001010, 1000,1010,  3.7410* 10.0
  10001010, 1000,1010, 1001,1011, 1002,1012,       .0666667*3.7410*10.0
  10031013, 1003,1013, 1004,1014, 1005,1015, 1006,1016,  .20*3.7410*10.0
C    10101020, 1010,1020,  12.563* 10.0
  10101020, 1010,1020, 1011,1021, 1012,1022,       .0666667*12.563*10.0
  10131023, 1013,1023, 1014,1024, 1015,1025, 1016,1026,  .2*12.563*10.0
C    10201030, 1020,1030,  13.442* 10.0
  10201030, 1020,1030, 1021,1031, 1022,1032,       .0666667*13.442*10.0
  10231033, 1023,1033, 1024,1034, 1025,1035, 1026,1036,  .2*13.442*10.0
C    10301040, 1030,1040,  0.6140* 10.0
```

```
  10301040, 1030,1040, 1031,1041, 1032,1042,       .0666667*0.6140*10.0
  10331043, 1033,1043, 1034,1044, 1035,1045, 1036,1046,  .2*0.6140*10.0
C    10401030, 1030,1040,  1.5000* 40.
  10401030, 1040,1030, 1041,1031, 1042,1032,       .0666667*1.50*40.
  10431033, 1043,1033, 1044,1034, 1045,1035, 1046,1036,  .2*1.50*40.
C    10501030, 1030,1050,  0.4280* 1.7141E 9
  10501030, 1030,1050, 1031,1051, 1032,1052, .0666667*0.428*1.7141E 9
  10531033, 1033,1053, 1034,1054, 1035,1055, 1036,1056, .2*0.428*1.7141E 9
C    10301050, 1030,1050,  581.98* 0.0154
  10301050, 1030,1050, 1031,1051, 1032,1052,       .0666667*581.98*.0154
  10331053, 1033,1053, 1034,1054, 1035,1055, 1036,1056,  .2*581.98*.0154
C    10401050, 1040,1050,  15.816* 10.0
  10401050, 1040,1050, 1041,1051, 1042,1052,       .0666667*15.816* 10.0
  10431053, 1043,1053, 1044,1054, 1045,1055, 1046,1056,  .2*15.816* 10.0
C      STATION 1000 TO 1000
   10001001,  1000,1001,  1001,1002,                    1.583333* 10.0
   10021003,  1002,1003,  1006,1000,                    0.791667* 10.0
   10031004,  1003,1004,  1004,1005,  1005,1006,        0.527777* 10.0
   10101011,  1010,1011,  1011,1012,                    0.326087* 10.0
   10121013,  1012,1013,  1016,1010,                    0.163044* 10.0
   10131014,  1013,1014,  1014,1015,  1015,1016,        0.108696* 10.0
   10201021,  1020,1021,  1021,1022,                    0.275424* 10.0
   10221023,  1022,1023,  1026,1020,                    0.137712* 10.0
   10231024,  1023,1024,  1024,1025,  1025,1026,        0.091808* 10.0
   10301031,  1030,1031,  1031,1032,                    0.190972* 10.0
   10321033,  1032,1033,  1036,1030,                    0.095486* 10.0
   10331034,  1033,1034,  1034,1035,  1035,1036,        0.063657* 10.0
   10401041,  1040,1041,  1041,1042,                    0.141438* 10.0
   10421043,  1042,1043,  1046,1040,                    0.070719* 10.0
   10431044,  1043,1044,  1044,1045,  1045,1046,        0.047146* 10.0
   10501051,  1050,1051,  1051,1052,                    0.125915* 10.0
   10521053,  1052,1053,  1056,1050,                    0.062957* 10.0
   10531054,  1053,1054,  1054,1055,  1055,1056,        0.041972* 10.0
C
C      CANISTER TO INNER VESSEL
C
     215220,  215,220,     44.482* 0.0154
     220215,  215,220,     2.6223* 1.7141E 9
     215320,  215,320,  215,210,     0.7137* 1.7141E 9
     315320,  315,320,  715,720,    50.887* 0.0154
     320315,  315,320,  715,720,     2.9999* 1.7141E 9
     315420,  315,420,  315,220,  715,620,  715,820,  0.7137* 1.7141E 9
     415420,  415,420,  515,520,  615,620,    56.937* 0.0154
     420415,  415,420,  515,520,  615,620,    3.3565* 1.7141E 9
     415520,  415,520,  415,320,  515,620,  515,420,  0.7986* 1.7141E 9
     615520,  615,520,  615,720,                      0.7986* 1.7141E 9
     815820,  815,820,     27.401* 0.0154
     820815,  815,820,     1.6992* 1.7141E 9
C    815720,  815,720,  815,920,     0.4895* 1.7141E 9
     815720,  815,720,              0.4895* 1.7141E 9
     815920,  815,920, 815,921, 815,922,   0.066667* 0.4895* 1.7141E 9
     815923,  815,923, 815,924, 815,925, 815,926,  0.2*0.4895* 1.7141E 9
C    200205,  200,205,  805,900,   88.488* 0.0154
     200205,  200,205,            88.488* 0.0154
     805900,  805,900,  805,901, 805,902,     0.066667*  88.488* 0.0154
     805903,  805,903,  805,904, 805,905, 805,906,   0.2*88.488* 0.0154
C    805900,  805,900,  205,200,   1.0660* 1.7141E 9
     205200,  200,205,            1.4417* 1.7141E 9
     900805,  805,900,  805,901, 805,902,     0.066667*1.0660* 1.7141E 9
     903805,  805,903,  805,904, 805,905, 805,906,  0.2*1.0660*1.7141E 9
C
C      TRUNNION TO OUTER SHELL
C
     380350,   380,350,    1.9053* 10.0
     581551,   581,551,    38.32* 10.0
     583553,   583,553,    38.32* 10.0
     591581,   581,591,  583,593,  5.244 * 10.0
     780750,   780,750,    3.8106* 10.0
C  *************************
C      CASK BODY AXIAL CONDUCTORS
C  *************************
     100200,  100,200,     63.006* 0.0154
     200100,  100,200,     0.3470* 1.7141E 9
     110210,  110,210,     46.077* 0.0154
     210110,  110,210,     0.2540* 1.7141E 9
     120210,  120,210,     69.638* 0.0154
     210120,  120,210,     0.3840* 1.7141E 9
     130230,  130,230,     0.7600* 10.0
     140240,  140,240,  140,245,   0.774* 19.3
     150250,  150,250,     1.3533* 10.0
C
```

```
C      INNER VESSEL
C
     220320,  220,320,     0.1731* 10.0
     320420,  320,420,  620,720,   0.1640* 10.0
     420520,  420,520,  520,620,   0.1550* 10.0
     720820,  720,820,     0.2220* 10.0
C    820920,  820,920,     0.0740* 10.0
     820920,  820,920, 820,921, 820,922, 0.066667*0.0740* 10.0
     820923,  820,923, 820,924, 820,925, 820,926, 0.20*0.0740* 10.0
C    920820,  820,920,     1.2000* 40.
     920820,  820,920, 820,921, 820,922, 0.066667*1.200* 40.
     923820,  820,923, 820,924, 820,925, 820,926, 0.20*1.200* 40.
C
C      OUTER CASK, INNER SHELL
C
     230330,  230,330,     0.4870* 10.0
     330430,  330,430,  630,730,   0.4610* 10.0
     430530,  430,530,  530,630,   0.4370* 10.0
     730830,  730,830,     0.6240* 10.0
C    830930,  830,930,     1.0510* 10.0
     830930,  830,930, 830,931, 830,932, 0.066667*1.051* 10.
     830933,  830,933, 830,934, 830,935, 830,936, 0.20*1.051* 10.
C
C      LEAD
C
     240340,  240,340,     0.4820* 19.3
     340440,  340,440,  640,740,   0.4560* 19.3
C     440540,  440,540,  540,640,   0.4320* 19.3
     440540,  440,540, 440,541, 440,542, 440,543, 0.25*0.4320* 19.3
     640540,  640,540, 640,541, 640,542, 640,543, 0.25*0.4320* 19.3
     740840,  740,840,     0.6170* 19.3
C    840940,  840,940,     14.80762
     840940,  840,940, 840,941, 840,942, 0.066667*14.80762
     840943,  840,943, 840,944, 840,945, 840,946, 0.20*14.80762
C
C      LEAD
C
     245345,  245,345,     0.5100* 19.3
     345445,  345,445,  645,745,   0.4830* 19.3
C     445545,  445,545,  545,645,   0.4580* 19.3
     445545,  445,545, 445,546, 445,547, 445,548,  0.25*0.4580* 19.3
     645545,  645,545, 645,546, 645,547, 645,548,  0.25*0.4580* 19.3
     745845,  745,845,     0.6540* 19.3
C    845940,  845,940,     15.67441
     845940,  845,940, 845,941, 845,942, 0.066667*15.67441
     845943,  845,943, 845,944, 845,945, 845,946, 0.20*15.67441
C
C      OUTER CASK, OUTER SHELL
C
     250350,  250,350,     0.8680* 10.0
     350450,  350,450,  650,750,   0.8220* 10.0
C     450550,  450,550,  550,650,   0.7780* 10.0
     450550,  450,550, 450,551, 450,552, 450,553, 0.25* 0.7780* 10.0
     650550,  650,550, 650,551, 650,552, 650,553, 0.25* 0.7780* 10.0
     581450,  581,450, 583,450, 581,650, 583,650, 0.025* 0.7780* 10.0
     750850,  750,850,     1.1120* 10.0
C    850950,  850,950,     1.8720* 10.0
     850950,  850,950, 850,951, 850,952, 0.066667*1.8720* 10.0
     850953,  850,953, 850,954, 850,955, 850,956, 0.20*1.8720* 10.0
C
C      THERMAL SHIELD
C
     270370,  270,370,     0.0811* 10.0
     370470,  370,470,  670,770,   0.0768* 10.0
     470570,  470,570, 470,572, 570,670, 572,670,  0.25 * 0.0727* 10.0
     471570,  470,571, 470,573, 571,670, 573,670,  0.125 * 0.0727* 10.0
     580470,  470,581, 470,583, 670,581, 670,583, 0.125 * 0.0727* 10.0
     770870,  770,870,     0.1039* 10.0
C
C      CASK LID
C
C    9001000, 900,1000,    63.006* 0.0154
     9001000, 900,1000, 901,1001, 902,1002,   .0666667*63.006* 0.0154
     9031003, 903,1003, 904,1004, 905,1005, 906,1006, .2*63.006* 0.0154
C    1000900, 900,1000,    0.3470* 1.7141E 9
     1000900, 900,1000, 901,1001, 902,1002,   .0666667*.3470*1.7141E 9
     1003903, 903,1003, 904,1004, 905,1005, 906,1006, .2*.3470*1.7141E 9
C    9101010, 910,1010,    46.077* 0.0154
     9101010, 910,1010, 911,1011, 912,1012,   .0666667*46.077* 0.0154
     9131013, 913,1013, 914,1014, 915,1015, 916,1016, .2*46.077* 0.0154
C    1010910, 910,1010,    0.2540* 1.7141E 9
```

```
     1010910, 910,1010, 911,1011, 912,1012,   .0666667*.2540*1.7141E 9
     1013913, 913,1013, 914,1014, 915,1015, 916,1016, .2*.2540*1.7141E 9
C    9201020, 920,1020,    69.639* 0.0154
     9201020, 920,1020, 921,1021, 922,1022,   .0666667*69.639* 0.0154
     9231023, 923,1023, 924,1024, 925,1025, 926,1026,  .2*69.639* 0.0154
C    1020920, 920,1020,    0.3840* 1.7141E 9
     1020920, 920,1020, 921,1021, 922,1022,   .0666667*.3840*1.7141E 9
     1023923, 923,1023, 924,1024, 925,1025, 926,1026, .2*.3840*1.7141E 9
C    9301040, 930,1040,    1.8400* 10.0
     9301040, 930,1040, 931,1041, 932,1042,   .0666667*1.840 * 10.0
     9331043, 933,1043, 934,1044, 935,1045, 936,1046,   .20*1.840*10.0
C    9401040, 940,1040,    2.5770* 10.0
     9401040, 940,1040, 941,1041, 942,1042,   .0666667*2.5770* 10.0
     9431043, 943,1043, 944,1044, 945,1045, 946,1046,   .2*2.5770* 10.0
C    9501050, 950,1050,    3.3790* 10.0
     9501050, 950,1050, 951,1051, 952,1052,   .0666667*3.3790* 10.0
     9531053, 953,1053, 954,1054, 955,1055, 956,1056,   .20*3.3790* 10.0
C
C      CANISTER
C
     215315,  215,315,     0.1010* 25.0
     315415,  315,415,  615,715,    0.0890* 25.0
     415515,  415,515,  515,615,    0.0843* 25.0
     715815,  715,815,     0.1226* 25.0
     205212,  205,212,    403.0
     805812,  805,812,    231.3
     205215,   205,215,   0.179*25.0
     805815,   805,815,   0.364*25.0
     212215,   212,215,   0.590*19.3
     812815,   812,815,   0.987*19.3
C  *************************
C      OVERPACK CONDUCTORS
C  *************************
C     20002020,  2000,2020,  3000,3020, 299.022* 0.019
     30003020,  3000,3020, 299.022* 0.019
     20002020,  2000,2020,  2001,2021, 2002,2022, .06667*.6667*299.022* 0.019*1000. $Damage
     24002420,  2400,2420,  2401,2421, 2402,2422, .06667*.3333*299.022* 0.019*1000. $Damage
     20032023,  2003,2023,  2004,2024, 2005,2025, 2006,2026, .20*.6667*299.022* 0.019
     24032423,  2403,2423,  2404,2424, 2405,2425, 2406,2426, .20*.3333*299.022* 0.019
C
C     20202040,  2020,2040,  3020,3040, 67.0590* 0.019
     30203040,  3020,3040, 67.0590* 0.019
     20202040,  2020,2040,  2022,2042, .06667*.6667*67.0590* 0.019*1000. $Damage
     24202440,  2420,2440,  2422,2442, .06667*.3333*67.0590* 0.019*1000. $Damage
     20212041,  2021,2041, .06667*.6667*67.0590* 0.019*1000. $Damage
     24212441,  2421,2441, .06667*.3333*67.0590* 0.019*1000. $Damage
     20232043,  2023,2043,  2024,2044, 2025,2045, 2026,2046, .20*.6667*67.0590* 0.019
     24232443,  2423,2443,  2424,2444, 2425,2445, 2426,2446, .20*.3333*67.0590* 0.019
C
C     20402060,  2040,2060,  3040,3060, 46.1890* 0.019
     30403060,  3040,3060, 46.1890* 0.019
     20402060,  2040,2060,  2041,2061, 2042,2062, .06667*.6667*46.1890*1000.*0.019$Damage
     24402460,  2440,2460,  2441,2461, 2442,2462, .06667*.3333*46.1890*1000.*0.019$Damage
     20432063,  2043,2063,  2044,2064, 2045,2065, 2046,2066, .20*.6667*46.1890* 0.019
     24432463,  2443,2463,  2444,2464, 2445,2465, 2446,2466, .20*.3333*46.1890* 0.019
C
C     20602080,  2060,2080,  3060,3080, 107.068* 0.019
     30603080,  3060,3080, 107.068* 0.019
     20602080,  2060,2080,  2061,2081, 2062,2082, .06667*.6667*46.1890* 0.019
     24602480,  2460,2480,  2461,2481, 2462,2482, .06667*.3333*46.1890* 0.019
     20632083,  2063,2083,  2064,2084, 2065,2085, 2066,2086, .20*.6667*46.1890* 0.019
     24632483,  2463,2483,  2464,2484, 2465,2485, 2466,2486, .20*.3333*46.1890* 0.019
C
C    20002010,  2000,2010,  3000,3010, 0.05399* 10.0
     24002310,  2400,2310,  2401,2311, 2402,2312, 0.066667*0.05399* 10.0
     24032313,  2403,2313,  2404,2314, 2405,2315, 2406,2016, 0.20*0.05399* 10.0
     30003010,  3000,3010, 0.05399* 10.0
     30003100,  3000,3100, 0.08162* 10.0
     20002100,  2000,2100, 2001,2100, 2002,2100, .06667* 0.08162* 10.0
     20032100,  2003,2100, 2004,2100, 2005,2100, 2006,2100, .20* 0.08162* 10.0
C
C    21002080,  2100,2080,  3100,3080, 0.07954* 10.0
     21002080,  2100,2080, 2100,2081, 2100,2082, .06667*0.07954* 10.0
     21002083,  2100,2083, 2100,2084, 2100,2085, 2100,2086, .20* 0.07954* 10.0
     31003080,  3100,3080, 0.07954* 10.0
C
C    20902080,  2090,2080,  3090,3080, 0.05658* 10.0
     24802290,  2480,2290,  2481,2291, 2482,2292, 0.066667*0.05658* 10.0
     24832293,  2483,2293,  2484,2294, 2485,2295, 2486,2296,  0.200*0.05658* 10.0
     30803090,              3090,3080, 0.05658* 10.0
C
```

```
     20002400,  2000,2400,  2001,2401,  2002,2402, .06667*0.463*10.0
     20032403,  2003,2403,  2004,2404,  2005,2405, 2006,2406, .2*0.463*10.0
C
     20202420,  2020,2420,  2021,2421,  2022,2422, .06667*9.512*0.019
     20232423,  2023,2423,  2024,2424,  2025,2425,  2026,2426, .2*9.512*0.019
C
     20402440,  2040,2440,  2041,2441,  2042,2442, .06667*25.005*0.019
     20432443,  2043,2443,  2044,2444,  2045,2445,  2046,2446,  .2*25.005*0.019
C
     20602460,  2060,2460,  2061,2461,  2062,2462, .06667*10.350*0.019
     20632463,  2063,2463,  2064,2464,  2065,2465,  2066,2466, .2*10.350*0.019
C
     20802480,  2080,2480,  2081,2481,  2082,2482, .06667*0.258*10.0
     20832483,  2083,2483,  2084,2484,  2085,2485,  2086,2486, .2*0.258*10.0
C
     20002001,  2000,2001,  2001,2002,  0.011*10.0
     20032004,  2003,2004,  2004,2005,  2005,2006,  0.004*10.0
     20022003,  2002,2003,  2006,2000,  0.005*10.0
C
     20202021,  2020,2021,  2021,2022,  0.240*0.019
     20232024,  2023,2024,  2024,2025,  2025,2026,  0.080*0.019
     20222023,  2022,2023,  2026,2020,  0.120*0.019
C
     20402041,  2040,2041,  2041,2042,  0.900*0.019
     20432044,  2043,2044,  2044,2045,  2045,2046,  0.300*0.019
     20422043,  2042,2043,  2046,2040,  0.450*0.019
C
     20602061,  2060,2061,  2061,2062,  0.696*0.019
     20632064,  2063,2064,  2064,2065,  2065,2066,  0.232*0.019
     20622063,  2062,2063,  2066,2060,  0.348*0.019
C
     20802081,  2080,2081,  2081,2082,  0.019*10.0
     20832084,  2083,2084,  2084,2085,  2085,2086,  0.006*10.0
     20822083,  2082,2083,  2086,2080,  0.010*10.0
C
     24002401,  2400,2401,  2401,2402,  0.005*10.0
     24032404,  2403,2404,  2404,2405,  2405,2406,  0.002*10.0
     24022403,  2402,2403,  2406,2400,  0.003*10.0
C
     24202421,  2420,2421,  2421,2422,  0.120*0.019
     24232424,  2423,2424,  2424,2425,  2425,2426,  0.040*0.019
     24222423,  2422,2423,  2426,2420,  0.060*0.019
C
     24402441,  2440,2441,  2441,2442,  0.450*0.019
     24432444,  2443,2444,  2444,2445,  2445,2446,  0.150*0.019
     24422443,  2442,2443,  2446,2440,  0.225*0.019
C
     24602461,  2460,2461,  2461,2462,  0.348*0.019
     24632464,  2463,2464,  2464,2465,  2465,2466,  0.116*0.019
     24622463,  2462,2463,  2466,2460,  0.174*0.019
C
     24802481,  2480,2481,  2481,2482,  0.010*10.0
     24832484,  2483,2484,  2484,2485,  2485,2486,  0.003*10.0
     24822483,  2482,2483,  2486,2480,  0.005*10.0
C
C    20102030,  2010,2030,  3010,3030, 28.8630* 0.019
C    20302050,  2030,2050,  3030,3050, 15.3940* 0.019
C    20502070,  2050,2070,  3050,3070, 15.3940* 0.019
C    20702090,  2070,2090,  3070,3090, 28.8630* 0.019
C
C  STATION 2010 TO 2030
     20102030,  2010,2030,  2011,2031, 2012,2032,   0.681777*0.019
     20132033,  2013,2033,  2014,2034, 2015,2035, 2016,2036, 2.045331*0.019
     21102130,  2110,2130,  2111,2131, 2112,2132,   0.811578*0.019
     21132133,  2113,2133,  2114,2134, 2115,2135, 2116,2136, 2.434734*0.019
     22102230,  2210,2230,  2211,2231, 2212,2232,   0.814851*0.019
     22132233,  2213,2233,  2214,2234, 2215,2235, 2216,2236, 2.444553*0.019
     23102330,  2310,2330,  2311,2331, 2312,2332,   3.992441*0.019*1000. $Damage
     23132333,  2313,2333,  2314,2334, 2315,2335, 2316,2336, 11.977323*0.019
C
C  STATION 2030 TO 2050 & 2050 TO 2070
     20302050,  2030,2050,  2031,2051, 2032,2052
                2050,2070,  2051,2071, 2052,2072,   0.363614*0.019
     20332053,  2033,2053,  2034,2054, 2035,2055, 2036,2056
          2053,2073,  2054,2074, 2055,2075, 2056,2076,  1.090842*0.019
     21302150,  2130,2150,  2131,2151, 2132,2152
                2150,2170,  2151,2171, 2152,2172,   0.432842*0.019
     21332153,  2133,2153,  2134,2154, 2135,2155, 2136,2156
            2153,2173,  2154,2174, 2155,2175, 2156,2176,  1.298526*0.019
     22302250,  2230,2250,  2231,2251, 2232,2252
                2250,2270,  2251,2271, 2252,2272,   0.434587*0.019
```

```
     22332253,  2233,2253,  2234,2254, 2235,2255, 2236,2256
            2253,2273,  2254,2274, 2255,2275, 2256,2276,  1.303761*0.019
     23302350,  2330,2350,  2331,2351, 2332,2352
                2350,2370,  2351,2371, 2352,2372,   2.129302*0.019*1000. $Damage
     23332353,  2333,2353,  2334,2354, 2335,2355, 2336,2356
            2353,2373,  2354,2374, 2355,2375, 2356,2376,  6.387906*0.019
C
C  STATION 2070 TO 2090
     20702090,  2070,2090,  2071,2091, 2072,2092,   0.681777*0.019
     20732093,  2073,2093,  2074,2094, 2075,2095, 2076,2096, 2.045331*0.019
     21702190,  2170,2190,  2171,2191, 2172,2192,   0.811578*0.019
     21732193,  2173,2193,  2174,2194, 2175,2195, 2176,2196, 2.434734*0.019
     22702290,  2270,2290,             2272,2292,   0.814851*0.019
     22712291,             2271,2291,              0.814851*0.019
     22732293,  2273,2293,  2274,2294, 2275,2295, 2276,2296, 2.444553*0.019
C    23702390,  2370,2390,  2371,2391, 2372,2392,   3.992441*0.019
C    23732393,  2373,2393,  2374,2394, 2375,2395, 2376,2396, 11.977323*0.019
C
C
C  REAR OVERPACK   IMPACT LIMITER
     30103030,  3010,3030, 28.8630* 0.019
     30303050,  3030,3050, 15.3940* 0.019
     30503070,  3050,3070, 15.3940* 0.019
     30703090,  3070,3090, 28.8630* 0.019
C
C      OVERPACK TO CASK CONDUCTORS
C    20801050,  2080,1050,    279.382* 0.0154
     24801050,  2480,1050, 2481,1051, 2482,1052, 0.0666667*279.382* 0.0154*1000.  $Damage
     24831053,  2483,1053, 2484,1054, 2485,1055, 2486,1056, 0.20*279.382* 0.0154
C    10502080,  2080,1050,    1.94398*1.7141E 9
     10502080,  2480,1050, 2481,1051, 2482,1052, 0.0666667*1.94398*1.7141E 9
     10532080,  2483,1053, 2484,1054, 2485,1055, 2486,1056, 0.20*1.94398*1.7141E 9
C    2080950,   2080,950,     284.860* 0.0154
     2080950,  2080,950, 2081,951, 2082,952,  0.0666667*284.860*0.0154*1000.  $Damage
     2083953,  2083,953, 2084,954, 2085,955, 2086,956, 0.20*284.860*0.0154
C    9502080,   2080,950,      1.98210*1.7141E 9
     9502080,  2080,950, 2081,951, 2082,952, 0.0666667* 1.98210*1.7141E 9
     9532080,  2083,953, 2084,954, 2085,955, 2086,956, 0.20* 1.98210*1.7141E 9
C     2080850,   2080,850,     443.724* 0.0154
     2080850,  2080,850,  2081,850, 2082,850, 0.0667*443.724* 0.0154
     2083850,  2083,850,  2084,850,  2085,850, 2086,850, 0.2*443.724* 0.0154*1000.  $Damage
C     8502080,   2080,850,     3.08750*1.7141E 9
     8502080,  2080,850,  2081,850,  2082,850, 0.0667*3.08750*1.7141E 9
     8502083,  2083,850,  2084,850,  2085,850, 2086,850, 0.2*3.08750*1.7141E 9
     3080150,   3080,150,     219.123* 0.0154
     1503080,   3080,150,     1.52469*1.7141E 9
     3080250,   3080,250,     788.843* 0.0154
     2503080,   3080,250,     5.48889*1.7141E 9
C    20901000,  2090,1000,  3090,100,  236.2740* 0.0154
C    10002090,  2090,1000,  3090,100,  0.65630*1.7141E 9
     20901000,  2090,1000,  2091,1001, 2092,1002,  15.7517* 0.0154*1000.  $Damage
C    10002090,  2090,1000,  2091,1001, 2092,1002,  0.04375*1.7141E 9
     20931003,  2093,1003,  2094,1004, 2095,1005, 2096,1006,  47.2550* 0.0154
C    10032093,  2093,1003,  2094,1004, 2095,1005, 2096,1006, 0.13126*1.7141E 9
C
     3090100,               3090,100,  236.2740* 0.0154
     1003090,               3090,100,  0.65630*1.7141E 9
C    20901010,  2090,1010,  3090,110,  172.7880* 0.0154
C    10102090,  2090,1010,  3090,110,  0.4800* 1.7141E 9
     20901010,  2090,1010,  2091,1011, 2092,1012,  11.5192* 0.0154*1000.  $Damage
C    10102090,  2090,1010,  2091,1011, 2092,1012,  0.0320* 1.7141E 9
     20931013,  2093,1013,  2094,1014, 2095,1015, 2096,1016, 34.5575* 0.0154
C    10132093,  2093,1013,  2094,1014, 2095,1015, 2096,1016, 0.0960* 1.7141E 9
C
     3090110,               3090,110,  172.7880* 0.0154
     1103090,               3090,110,  0.4800* 1.7141E 9
C    20901020,  2090,1020,  3090,120,  240.3650* 0.0154
C    10202090,  2090,1020,  3090,120,  0.6677* 1.7141E 9
     21901020,  2190,1020,  2191,1021, 2192,1022,  16.0243* 0.0154*1000.  $Damage
C    10202190,  2190,1020,  2191,1021, 2192,1022,  0.04451*1.7141E 9
     21931023,  2193,1023,  2194,1024, 2195,1025, 2196,1026, 48.0729* 0.0154
C    10232193,  2193,1023,  2194,1024, 2195,1025, 2196,1026, 0.13354*1.7141E 9
C
     3090120,               3090,120,  240.3650* 0.0154
     1203090,               3090,120,  0.6677* 1.7141E 9
C    20901030,  2090,1030,  3090,140,  246.5820* 0.0154
C    10302090,  2090,1030,  3090,140,  .68495* 1.7141E 9
     21901030,  2190,1030,  2191,1031, 2192,1032,  16.4839* 0.0154*1000.  $Damage
C    10302190,  2190,1030,  2191,1031, 2192,1032,  .04566* 1.7141E 9
     21931033,  2193,1033,  2194,1034, 2195,1035, 2196,1036, 49.3167* 0.0154
C    10332193,  2193,1033,  2194,1034, 2195,1035, 2196,1036, 0.13699*1.7141E 9
```

```
C
     3090140,              3090,140,  246.5820* 0.0154
     1403090,              3090,140,  .68495* 1.7141E 9
C    20901050,  2090,1050,  3090,150,  211.1920* 0.0154
C    10502090,  2090,1050,  3090,150,  .58664* 1.7141E 9
     22901050,  2290,1050,  2291,1051, 2292,1052,  14.0794*0.0154*1000.  $Damage
C    10502290,  2290,1050,  2291,1051, 2292,1052,  .039109*1.7141E 9
     22931053,  2293,1053,  2294,1054, 2295,1055, 2296,1056, 42.2383* 0.0154
C    10532293,  2293,1053,  2294,1054, 2295,1055, 2296,1056,  0.11732*1.7141E 9
C
     3090150,              3090,150,  211.1920* 0.0154
     1503090,              3090,150,  .58664* 1.7141E 9
C
C     CIRCUMFERENTIAL CASK WALL CONDUCTORS
      540541,  540,541, 541,542, 542,543, 543,540,  0.056 * 19.3
      545546,  545,546, 546,547, 547,548, 548,545,  0.053 * 19.3
      550551,  550,551, 551,552, 552,553, 553,550,  0.080 * 10.0
      570571,  570,571, 571,572, 572,573, 573,570,  0.007 * 10.0
      581571,  581,571, 583,573,  0.0140 * 10.0
C
C     EXTERNAL RADIATION HEAT TRANSFER
      7098,   370,98,   770,98,   .8*16.223*1.7141E 9  $ THERMAL SHIELD
      9870, 470,98, 670,98, .8*18.151*1.7141E 9 $ THERMAL SHIELD
      98570,  570,98, 572,98, 0.25*.8*18.151*1.7141E 9 $ THERMAL SHIELD
      98571,  571,98, 573,98, 0.125*.8*18.151*1.7141E 9 $ THERMAL SHIELD
C      200098, 2000,98,  3000,98,  .8*76.271*1.7141E 9  $ OVERPACK SHELL
      200098, 2000,98, 2001,98, 2002,98, 0.0667*.6667*.8*76.271*1.7141E 9
      200398, 2003,98, 2004,98, 2005,98, 2006,98, 0.2*.6667*.8*76.271*1.7141E 9
      240098, 2400,98, 2401,98, 2402,98, 0.0667*.333*.8*76.271*1.7141E 9
      240398, 2403,98, 2404,98, 2405,98, 2406,98, 0.2*.333*.8*76.271*1.7141E 9
      300098, 3000,98,  .8*76.271*1.7141E 9
C     201098, 2010,98,  3010,98,  .8*31.503*1.7141E 9  $ OVERPACK SHELL
      301098,           3010,98,  .8*31.503*1.7141E 9  $ OVERPACK SHELL
      201098, 2010,98,  2011,98, 2012,98,  .8*.227256* 1.7141E 9
      201398, 2013,98,  2014,98, 2015,98, 2016,98, .8*.681768* 1.7141E 9
      211098, 2110,98,  2111,98, 2112,98,  .8*.270526* 1.7141E 9
      211398, 2113,98,  2114,98, 2115,98, 2116,98, .8*.811578* 1.7141E 9
      221098, 2210,98,  2211,98, 2212,98,  .8*.271617* 1.7141E 9
      221398, 2213,98,  2214,98, 2215,98, 2216,98, .8*.814851* 1.7141E 9
      231098, 2310,98,  2311,98, 2312,98,  .8*1.33081* 1.7141E 9
      231398, 2313,98,  2314,98, 2315,98, 2316,98, .8*3.99243* 1.7141E 9
      210098, 2100,98,  3100,98,  .8*21.836*1.7141E 9  $ OVERPACK SHELL
      38098,  380,98,             .8*1.0800*1.7141E 9  $ LIFT TRUNNION
      58098,  581,98, 583,98,      .8*2.715*1.7141E 9  $ CENTER TRUNNION
      59098,  591,98, 593,98,      .8*1.545*1.7141E 9  $ CENTER TRUNNION
      78098,  780,98,             .8*2.1600*1.7141E 9  $ LIFT TRUNNION
C
C    DAMAGE RADIATION CONDUCTORS
       248198,  2481,98,           0.0872664*.8*1.7141E 9
C       227198,  2271,98,           0.01*.8*1.7141E 9
C       225098,  2250,98,           0.01*.8*1.7141E 9
C       225298,  2252,98,           0.01*.8*1.7141E 9
C
C     EXTERNAL CONVECTION HEAT TRANSFER
C           ACTUAL RATE DETERMINED BY INTERNAL ROUTINE
      7099,   370,99,   770,99,   1.0                  $ THERMAL SHIELD
      9970, 470,99, 670,99, 1.0                $ THERMAL SHIELD
      9972, 570,99, 572,99, 1.0
      9971, 571,99, 573,99, 1.0
C      200099, 2000,99,  3000,99,  1.0                  $ OVERPACK SHELL
      300099, 3000,99,  1.0                         $ OVERPACK SHELL
      200099, 2000,99, 2001,99, 2002,99,  1.0
      200399, 2003,99, 2004,99, 2005,99, 2006,99, 1.0
      240099, 2400,99, 2401,99, 2402,99,  1.0
      240399, 2403,99, 2404,99, 2405,99, 2406,99, 1.0
C     201099, 2010,99,  3010,99,  1.0                  $ OVERPACK SHELL
      301099,           3010,99,  1.0                  $ OVERPACK SHELL
      201099, 2010,99,  2011,99, 2012,99,  1.0
      201399, 2013,99,  2014,99, 2015,99, 2016,99,   1.0
      211099, 2110,99,  2111,99, 2112,99,  1.0
      211399, 2113,99,  2114,99, 2115,99, 2116,99,   1.0
      221099, 2210,99,  2211,99, 2212,99,  1.0
      221399, 2213,99,  2214,99, 2215,99, 2216,99,   1.0
      231099, 2310,99,  2311,99, 2312,99,  1.0
      231399, 2313,99,  2314,99, 2315,99, 2316,99,   1.0
      210099, 2100,99,  3100,99,  1.0                  $ OVERPACK SHELL
      38099,  380,99,             1.0                  $ LIFT TRUNNION
      58099,  581,99, 583,99,     1.0                  $ CENTER TRUNNION
      59099,  591,99, 593,99,     1.0                  $ CENTER TRUNNION
      78099,  780,99,             1.0                  $ LIFT TRUNNION
      248199, 2481,99,           0.0872664             $PIN PUNCTURE AREA
```

```
C*********************************************************************
HEADER CONTROL DATA, GLOBAL
C*********************************************************************
      ABSZRO  =  459.67
      SIGMA   =    1.0
      EXTLIM  =    1.0
      ITHOLD  =    1
      ITERXT  =    3
      DRLXCA  =     .001
      ARLXCA  =     .001
      ATMPCA  =   10.
      DTMPCA  =   20.
      EBALSA  =     .05
      EBALNA  =     .05
      NLOOPS  = 14000
      ITEROT  = 14001
      NLOOPT  =   80
      OUTPUT  =    0.2
      DTIMEI  =    0.00025
      TIMEO = 0.0
      TIMEND =  40.
      DTIMEH  =    0.00025
C*********************************************************************
HEADER USER DATA, GLOBAL
C*********************************************************************
      GCONST = 32.2
C*********************************************************************
HEADER USER DATA, CASK
C*********************************************************************
      10 = 32.2     $ GC
      11 = 0.0
      12 = 0.0
      13 = 0.0
C*********************************************************************
HEADER ARRAY DATA, CASK
C*********************************************************************
      1 = 32.,.00958,  212.,.0123,  392.,.0147,  572.,.0169  $arg cond
      2 = 32.,.014,  100.,.0154,  300.,.0193,  500.,.0231    $air cond
      3 = 32.,0.2402, 100.,0.2402, 300.,0.2432, 500.,0.2472  $air cp
      4 = 32.,0.04194, 100.,0.04626, 300.,0.05796, 500.,0.06804 $air mu
C*********************************************************************
HEADER OUTPUT CALLS, CASK
C*********************************************************************
      CALL SORTPR('CASK',0)
      WRITE(6,*)'TIME (HRS) ',TIMEM
      WRITE(6,*)'O RINGS (921, 1031) ',T921,T1031
      WRITE(6,*)'CASK UPPER FORGING (1051) ',T1051
      WRITE(6,*)'CASK/IV LID CENTER (900, 1000) ',T900,T1000
      WRITE(6,*)'CASK BASE (100) ',T100
      WRITE(6,*)'IV/CENTER BASE (205, 200) ',T205, T200
      WRITE(6,*)'WALL TEMPS (551, 520, 515) ',T551, T520, T515
      WRITE(6,*)'PIVOT TRUNNION AREA (571, 591, 546) ', T571, T591, T546
      WRITE(6,*)'CANISTER (805, 515) ', T805, T515
      WRITE(6,*)'CASK INNER WALL/OUTER WALL (530, 551) ',T530, T551
      WRITE(6,*)'LEAD SHIELD (541, 546) ', T541, T546
      WRITE(6,*)'PAYLOAD (10) ',T10
C*********************************************************************
HEADER OPERATION DATA
C*********************************************************************
BUILD 72BCASK, CASK
C      CALL STDSTL
      CALL FWDBCK
C*********************************************************************
HEADER VARIABLES 1, CASK
C*********************************************************************
C DECAY HEAT PRODUCTION   50 WATTS MAX.
      Q10=  50. *3.413/36.
      Q11=  50. *3.413/36.
      Q12=  50. *3.413/36.
      Q13=  50. *3.413/36.
      Q14=  50. *3.413/36.
      Q15=  50. *3.413/36.
      Q20=  50. *3.413/36.
      Q21=  50. *3.413/36.
      Q22=  50. *3.413/36.
      Q23=  50. *3.413/36.
      Q24=  50. *3.413/36.
      Q25=  50. *3.413/36.
      Q30=  50. *3.413/36.
      Q31=  50. *3.413/36.
      Q32=  50. *3.413/36.
```

```
      Q33=  50. *3.413/36.
      Q34=  50. *3.413/36.
      Q35=  50. *3.413/36.
      Q40=  50. *3.413/36.
      Q41=  50. *3.413/36.
      Q42=  50. *3.413/36.
      Q43=  50. *3.413/36.
      Q44=  50. *3.413/36.
      Q45=  50. *3.413/36.
      Q50=  50. *3.413/36.
      Q51=  50. *3.413/36.
      Q52=  50. *3.413/36.
      Q53=  50. *3.413/36.
      Q54=  50. *3.413/36.
      Q55=  50. *3.413/36.
      Q60=  50. *3.413/36.
      Q61=  50. *3.413/36.
      Q62=  50. *3.413/36.
      Q63=  50. *3.413/36.
      Q64=  50. *3.413/36.
      Q65=  50. *3.413/36.
      IF(TIMEN .LT. 0.51) GO TO 40
C  EXTERNAL SOLAR HEATING
      Q370 = 0.80*634.73                  $ BASED ON PROJECTED AREA
      Q470 = 0.80*710.193                 $ BASED ON PROJECTED AREA
      Q570 = 0.25*0.80*710.193                 $ BASED ON PROJECTED AREA
      Q571 = 0.125*0.80*710.193
      Q572 = 0.25*0.80*710.193
      Q573 = 0.125*0.80*710.193
      Q670 = 0.80*710.193                 $ BASED ON PROJECTED AREA
      Q770 = 0.80*634.73                  $ BASED ON PROJECTED AREA
C       Q2000= 0.80*2984.17                 $ BASED ON PROJECTED AREA
      Q2000= 0.80*.6667*0.0667*2984.17
      Q2001= 0.80*.6667*0.0667*2984.17
      Q2002= 0.80*.6667*0.0667*2984.17
      Q2003= 0.80*.6667*0.2*2984.17
      Q2004= 0.80*.6667*0.2*2984.17
      Q2005= 0.80*.6667*0.2*2984.17
      Q2006= 0.80*.6667*0.2*2984.17
      Q2400= 0.80*.333*0.0667*2984.17
      Q2401= 0.80*.333*0.0667*2984.17
      Q2402= 0.80*.333*0.0667*2984.17
      Q2403= 0.80*.333*0.2*2984.17
      Q2404= 0.80*.333*0.2*2984.17
      Q2405= 0.80*.333*0.2*2984.17
      Q2406= 0.80*.333*0.2*2984.17
      Q3000= 0.80*2984.17                 $ BASED ON PROJECTED AREA
C       Q2010= 0.80*1934.93                 $ BASED ON PROJECTED AREA
      Q2010= 0.80*13.95809                $ BASED ON PROJECTED AREA
      Q2011= 0.80*13.95809                $ BASED ON PROJECTED AREA
      Q2012= 0.80*13.95809                $ BASED ON PROJECTED AREA
      Q2013= 0.80*41.87427                $ BASED ON PROJECTED AREA
      Q2014= 0.80*41.87427                $ BASED ON PROJECTED AREA
      Q2015= 0.80*41.87427                $ BASED ON PROJECTED AREA
      Q2016= 0.80*41.87427                $ BASED ON PROJECTED AREA
      Q2110= 0.80*16.61571                $ BASED ON PROJECTED AREA
      Q2111= 0.80*16.61571                $ BASED ON PROJECTED AREA
      Q2112= 0.80*16.61571                $ BASED ON PROJECTED AREA
      Q2113= 0.80*49.84713                $ BASED ON PROJECTED AREA
      Q2114= 0.80*49.84713                $ BASED ON PROJECTED AREA
      Q2115= 0.80*49.84713                $ BASED ON PROJECTED AREA
      Q2116= 0.80*49.84713                $ BASED ON PROJECTED AREA
      Q2210= 0.80*16.682708               $ BASED ON PROJECTED AREA
      Q2211= 0.80*16.682708               $ BASED ON PROJECTED AREA
      Q2212= 0.80*16.682708               $ BASED ON PROJECTED AREA
      Q2213= 0.80*50.048124               $ BASED ON PROJECTED AREA
      Q2214= 0.80*50.048124               $ BASED ON PROJECTED AREA
      Q2215= 0.80*50.048124               $ BASED ON PROJECTED AREA
      Q2216= 0.80*50.048124               $ BASED ON PROJECTED AREA
      Q2310= 0.80*81.738569               $ BASED ON PROJECTED AREA
      Q2311= 0.80*81.738569               $ BASED ON PROJECTED AREA
      Q2312= 0.80*81.738569               $ BASED ON PROJECTED AREA
      Q2313= 0.80*245.21571               $ BASED ON PROJECTED AREA
      Q2314= 0.80*245.21571               $ BASED ON PROJECTED AREA
      Q2315= 0.80*245.21571               $ BASED ON PROJECTED AREA
      Q2316= 0.80*245.21571               $ BASED ON PROJECTED AREA
      Q3010= 0.80*1934.93                 $ BASED ON PROJECTED AREA
      Q2100= 0.80*1341.18                 $ BASED ON PROJECTED AREA
      Q3100= 0.80*1341.18                 $ BASED ON PROJECTED AREA
      Q380 = 0.80*1.0800*39.126
      Q581 = 0.80*166.76
```

```
      Q583 = 0.80*166.76
      Q591 = 0.80*48.20
      Q593 = 0.80*48.20
      Q780 = 0.80*2.1600*39.126
      Q2481 = 0.8*5.363                  $ Radiation to Pin Puncture Area
 40   CONTINUE
C  EXTERNAL BOUNDARY TEMPERATURES
      T99 = 100.
      T98 = 100.
      IF(TIMEN .LT. 0.01 .OR. TIMEN .GT. 0.51) GO TO 50
      T99 = 1475.
      T98 = 1424.7
 50  CONTINUE
C
C  CALCULATE VARIABLE CONVECTIVE HEAT TRANSFER RATE
M      CALL D1DEG1((T370+T99)/2,A4,XK10)
M      CALL D1DEG1((T370+T99)/2,A3,XK11)
M      CALL D1DEG1((T370+T99)/2,A2,XK12)
      CALL AIRVCV3(T370,T99,16.223,3.4667,4.173E8,XK10,XK11,XK12,0.0810,G7099)
      IF(TIMEN .LT. 0.51000000) G7099 = 16.223*2.5
C      CALL FRCVV(G7099,T370,T99,16.2230,3.46670,XK10,0.0,
C     *      A3,A2,A4,0.0,14.70,53.350)
M      CALL D1DEG1((T470+T99)/2,A4,XK10)
M      CALL D1DEG1((T470+T99)/2,A3,XK11)
M      CALL D1DEG1((T470+T99)/2,A2,XK12)
      CALL AIRVCV3(T470,T99,18.1510,3.46670,4.173E8,XK10,XK11,XK12,0.0810,G9970)
      IF(TIMEN .LT. 0.51000000) G9970 = 18.1510*2.5
C      CALL FRCVV(G9970,T570,T99,18.1510,3.46670,XK10,0.0,
C     *      A3,A2,A4,0.0,14.70,53.350)
M      CALL D1DEG1((T570+T99)/2,A4,XK10)
M      CALL D1DEG1((T570+T99)/2,A3,XK11)
M      CALL D1DEG1((T570+T99)/2,A2,XK12)
      CALL AIRVCV3(T570,T99,4.5378,3.46670,4.173E8,XK10,XK11,XK12,0.0810,G9972)
      IF(TIMEN .LT. 0.51000000) G9972 = 4.5378*2.5
C      CALL FRCVV(G9972,T570,T99,4.5378,3.46670,XK10,0.0,
C     *      A3,A2,A4,0.0,14.70,53.350)
M      CALL D1DEG1((T571+T99)/2,A4,XK10)
M      CALL D1DEG1((T571+T99)/2,A3,XK11)
M      CALL D1DEG1((T571+T99)/2,A2,XK12)
      CALL AIRVCV3(T571,T99,2.2689,3.46670,4.173E8,XK10,XK11,XK12,0.0810,G9971)
      IF(TIMEN .LT. 0.51000000) G9971 = 2.2689*2.5
C      CALL FRCVV(G9971,T571,T99,2.2689,3.46670,XK10,0.0,
C     *      A3,A2,A4,0.0,14.70,53.350)
CC      CALL FRCVV(G200099,T2000,T99,76.2710,6.33330,XK10,0.0,
CC     *      A3,A2,A4,0.0,14.70,53.350)
M      CALL D1DEG1((T3000+T99)/2,A4,XK10)
M      CALL D1DEG1((T3000+T99)/2,A3,XK11)
M      CALL D1DEG1((T3000+T99)/2,A2,XK12)
      CALL AIRVCV3(T3000,T99,76.271,6.3333,4.173E8,XK10,XK11,XK12,0.0810,G300099)
      IF(TIMEN .LT. 0.51000000) G9970 = 76.271*2.5
C      CALL FRCVV(G300099,T2000,T99,76.2710,6.33330,XK10,0.0,
C     *      A3,A2,A4,0.0,14.70,53.350)
M      CALL D1DEG1((T2000+T99)/2,A4,XK10)
M      CALL D1DEG1((T2000+T99)/2,A3,XK11)
M      CALL D1DEG1((T2000+T99)/2,A2,XK12)
      CALL AIRVCV3(T2000,T99,3.3917,6.3333,4.173E8,XK10,XK11,XK12,0.0810,G200099)
      IF(TIMEN .LT. 0.51000000) G9970 = 3.3917*2.5
C      CALL FRCVV(G200099,T2000,T99,3.3917,6.33330,XK10,0.0,
C     *      A3,A2,A4,0.0,14.70,53.350)
M      CALL D1DEG1((T2003+T99)/2,A4,XK10)
M      CALL D1DEG1((T2003+T99)/2,A3,XK11)
M      CALL D1DEG1((T2003+T99)/2,A2,XK12)
      CALL AIRVCV3(T2003,T99,10.1751,6.3333,4.173E8,XK10,XK11,XK12,0.0810,G200399)
      IF(TIMEN .LT. 0.51000000) G200399 = 10.1751*2.5
C      CALL FRCVV(G200399,T2000,T99,10.1751,6.33330,XK10,0.0,
C     *      A3,A2,A4,0.0,14.70,53.350)
M      CALL D1DEG1((T2400+T99)/2,A4,XK10)
M      CALL D1DEG1((T2400+T99)/2,A3,XK11)
M      CALL D1DEG1((T2400+T99)/2,A2,XK12)
      CALL AIRVCV3(T2400,T99,1.6958,6.3333,4.173E8,XK10,XK11,XK12,0.0810,G240099)
      IF(TIMEN .LT. 0.51000000) G240099 = 1.6958*2.5
C      CALL FRCVV(G240099,T2000,T99,1.6958,6.33330,XK10,0.0,
C     *      A3,A2,A4,0.0,14.70,53.350)
M      CALL D1DEG1((T2403+T99)/2,A4,XK10)
M      CALL D1DEG1((T2403+T99)/2,A3,XK11)
M      CALL D1DEG1((T2403+T99)/2,A2,XK12)
      CALL AIRVCV3(T2403,T99,5.0876,6.3333,4.173E8,XK10,XK11,XK12,0.0810,G240399)
      IF(TIMEN .LT. 0.51000000) G240399 = 5.0876*2.5
C      CALL FRCVV(G240399,T2000,T99,5.0876,6.33330,XK10,0.0,
C     *      A3,A2,A4,0.0,14.70,53.350)
CC      CALL FRCVV(G201099,T2010,T99,31.5030,6.33330,XK10,0.0,
```

```
CC    *      A3,A2,A4,0.0,14.70,53.350)
M      CALL D1DEG1((T3010+T99)/2,A4,XK10)
M      CALL D1DEG1((T3010+T99)/2,A3,XK11)
M      CALL D1DEG1((T3010+T99)/2,A2,XK12)
      CALL AIRVCV3(T3010,T99,31.5030,6.3333,4.173E8,XK10,XK11,XK12,0.0810,G301099)
      IF(TIMEN .LT. 0.51000000) G301099 = 31.5030*2.5
C      CALL FRCVV(G301099,T3010,T99,31.5030,6.33330,XK10,0.0,
C    *      A3,A2,A4,0.0,14.70,53.350)
M      CALL D1DEG1((T2010+T99)/2,A4,XK10)
M      CALL D1DEG1((T2010+T99)/2,A3,XK11)
M      CALL D1DEG1((T2010+T99)/2,A2,XK12)
      CALL AIRVCV3(T2010,T99,.22726,6.3333,4.173E8,XK10,XK11,XK12,0.0810,G201099)
      IF(TIMEN .LT. 0.51000000) G201099 = .22726*2.5
C      CALL FRCVV(G201099,T2010,T99,.227260,6.33330,XK10,0.0,
C     *      A3,A2,A4,0.0,14.70,53.350)
M      CALL D1DEG1((T2014+T99)/2,A4,XK10)
M      CALL D1DEG1((T2014+T99)/2,A3,XK11)
M      CALL D1DEG1((T2014+T99)/2,A2,XK12)
      CALL AIRVCV3(T2014,T99,.68178,6.3333,4.173E8,XK10,XK11,XK12,0.0810,G201399)
      IF(TIMEN .LT. 0.51000000) G201399 = .681780*2.5
C      CALL FRCVV(G201399,T2014,T99,.681780,6.33330,XK10,0.0,
C     *      A3,A2,A4,0.0,14.70,53.350)
M      CALL D1DEG1((T2110+T99)/2,A4,XK10)
M      CALL D1DEG1((T2110+T99)/2,A3,XK11)
M      CALL D1DEG1((T2110+T99)/2,A2,XK12)
      CALL AIRVCV3(T2110,T99,.27053,6.3333,4.173E8,XK10,XK11,XK12,0.0810,G211099)
      IF(TIMEN .LT. 0.51000000) G211099 = .27053*2.5
C      CALL FRCVV(G211099,T2110,T99,.270530,6.33330,XK10,0.0,
C     *      A3,A2,A4,0.0,14.70,53.350)
M      CALL D1DEG1((T2114+T99)/2,A4,XK10)
M      CALL D1DEG1((T2114+T99)/2,A3,XK11)
M      CALL D1DEG1((T2114+T99)/2,A2,XK12)
      CALL AIRVCV3(T2114,T99,0.81159,6.3333,4.173E8,XK10,XK11,XK12,0.0810,G211399)
      IF(TIMEN .LT. 0.51000000) G211399 = .81159*2.5
C      CALL FRCVV(G211399,T2114,T99,.811590,6.33330,XK10,0.0,
C     *      A3,A2,A4,0.0,14.70,53.350)
M      CALL D1DEG1((T2210+T99)/2,A4,XK10)
M      CALL D1DEG1((T2210+T99)/2,A3,XK11)
M      CALL D1DEG1((T2210+T99)/2,A2,XK12)
      CALL AIRVCV3(T2210,T99,0.27162,6.3333,4.173E8,XK10,XK11,XK12,0.0810,G221099)
      IF(TIMEN .LT. 0.51000000) G221099 = 0.27162*2.5
C      CALL FRCVV(G221099,T2210,T99,.271620,6.33330,XK10,0.0,
C     *      A3,A2,A4,0.0,14.70,53.350)
M      CALL D1DEG1((T2213+T99)/2,A4,XK10)
M      CALL D1DEG1((T2213+T99)/2,A3,XK11)
M      CALL D1DEG1((T2213+T99)/2,A2,XK12)
      CALL AIRVCV3(T2213,T99,.81486,6.3333,4.173E8,XK10,XK11,XK12,0.0810,G221399)
      IF(TIMEN .LT. 0.51000000) G221399 = .81486*2.5
C      CALL FRCVV(G221399,T2214,T99,.814860,6.33330,XK10,0.0,
C     *      A3,A2,A4,0.0,14.70,53.350)
M      CALL D1DEG1((T2310+T99)/2,A4,XK10)
M      CALL D1DEG1((T2310+T99)/2,A3,XK11)
M      CALL D1DEG1((T2310+T99)/2,A2,XK12)
      CALL AIRVCV3(T2310,T99,1.3308,6.3333,4.173E8,XK10,XK11,XK12,0.0810,G231099)
      IF(TIMEN .LT. 0.51000000) G231099 = 1.3308*2.5
C      CALL FRCVV(G231099,T2310,T99,1.33080,6.33330,XK10,0.0,
C     *      A3,A2,A4,0.0,14.70,53.350)
M      CALL D1DEG1((T2314+T99)/2,A4,XK10)
M      CALL D1DEG1((T2314+T99)/2,A3,XK11)
M      CALL D1DEG1((T2314+T99)/2,A2,XK12)
      CALL AIRVCV3(T2314,T99,3.9924,6.3333,4.173E8,XK10,XK11,XK12,0.0810,G231399)
      IF(TIMEN .LT. 0.51000000) G231399 = 3.9924*2.5
C      CALL FRCVV(G231399,T2314,T99,3.99240,6.33330,XK10,0.0,
C     *      A3,A2,A4,0.0,14.70,53.350)
M      CALL D1DEG1((T2100+T99)/2,A4,XK10)
M      CALL D1DEG1((T2100+T99)/2,A3,XK11)
M      CALL D1DEG1((T2100+T99)/2,A2,XK12)
      CALL AIRVCV3(T2100,T99,21.836,6.3333,4.173E8,XK10,XK11,XK12,0.0810,G210099)
      IF(TIMEN .LT. 0.51000000) G210099 = 21.836*2.5
C      CALL FRCVV(G210099,T2100,T99,21.8360,6.33330,XK10,0.0,
C     *      A3,A2,A4,0.0,14.70,53.350)
M      CALL D1DEG1((T380+T99)/2,A4,XK10)
M      CALL D1DEG1((T380+T99)/2,A3,XK11)
M      CALL D1DEG1((T380+T99)/2,A2,XK12)
      CALL AIRVCV3(T380,T99,1.08000,6.3333,4.173E8,XK10,XK11,XK12,0.0810,G38099)
      IF(TIMEN .LT. 0.51000000) G38099 = 1.08000*2.5
C      CALL FRCVV(G38099, T380, T99,1.08000,6.33330,XK10,0.0,
C     *      A3,A2,A4,0.0,14.70,53.350)
M      CALL D1DEG1((T581+T99)/2,A4,XK10)
M      CALL D1DEG1((T581+T99)/2,A3,XK11)
M      CALL D1DEG1((T581+T99)/2,A2,XK12)
```

```
      CALL AIRVCV3(T581,T99,2.715,6.3333,4.173E8,XK10,XK11,XK12,0.0810,G58099)
      IF(TIMEN .LT. 0.51000000) G58099 = 2.715*2.5
C      CALL FRCVV(G58099, T581, T99,2.715,6.33330,XK10,0.0,
C     *      A3,A2,A4,0.0,14.70,53.350)
M      CALL D1DEG1((T591+T99)/2,A4,XK10)
M      CALL D1DEG1((T591+T99)/2,A3,XK11)
M      CALL D1DEG1((T591+T99)/2,A2,XK12)
      CALL AIRVCV3(T591,T99,1.545,6.3333,4.173E8,XK10,XK11,XK12,0.0810,G59099)
      IF(TIMEN .LT. 0.51000000) G59099 = 1.545*2.5
C      CALL FRCVV(G59099, T591, T99,1.545,6.33330,XK10,0.0,
C     *      A3,A2,A4,0.0,14.70,53.350)
M      CALL D1DEG1((T780+T99)/2,A4,XK10)
M      CALL D1DEG1((T780+T99)/2,A3,XK11)
M      CALL D1DEG1((T780+T99)/2,A2,XK12)
      CALL AIRVCV3(T780,T99,2.16,6.3333,4.173E8,XK10,XK11,XK12,0.0810,G78099)
      IF(TIMEN .LT. 0.51000000) G78099 = 2.16*2.5
C      CALL FRCVV(G78099, T780, T99,2.16000,6.33330,XK10,0.0,
C     *      A3,A2,A4,0.0,14.70,53.350)
M      CALL D1DEG1((T2481+T99)/2,A4,XK10)
M      CALL D1DEG1((T2481+T99)/2,A3,XK11)
M      CALL D1DEG1((T2481+T99)/2,A2,XK12)
      CALL AIRVCV3(T2481,T99,0.0873,0.33330,4.173E8,XK10,XK11,XK12,0.0810,G248199)
      IF(TIMEN .LT. 0.51000000) G248199 = 0.0873*2.5
C
C  *************************
C  CALCULATE VARIABLE CONDUCTOR VALUES
C  *************************
      CALL D1D1WM(T46, A2, 26.3660,G1617)
      CALL D1D1WM(T74, A2, 56.9580,G7118)
      CALL D1D1WM(T84, A2, 56.9580,G8182)
      CALL D1D1WM(T38, A2, 94.5100,G2838)
      CALL D1D1WM(T220, A2, 798.3690,G220230)
      CALL D1D1WM(T250, A2, 1923.720,G250270)
      CALL D1D1WM(T320, A2, 792.8200,G320330)
      CALL D1D1WM(T350, A2, 1919.360,G350370)
      CALL D1D1WM(T520, A2, 887.0800,G420430)
      CALL D1D1WM(T450, A2, 2137.470,G450470)
      CALL D1D1WM(T550, A2, 534.3675,G550570)
      CALL D1D1WM(T553, A2, 267.1838,G553570)
      CALL D1D1WM(T820, A2, 449.0800,G820830)
      CALL D1D1WM(T820, A2, 7.392330,G820930)
      CALL D1D1WM(T820, A2,22.176990,G820933)
      CALL D1D1WM(T850, A2, 1082.090,G850870)
C     CALL D1D1WM(T920, A2, 177.4150,G920930)
      CALL D1D1WM(T921, A2, 11.82770,G920930)
      CALL D1D1WM(T924, A2, 35.48310,G923933)
C     CALL D1D1WM(T1030, A2, 581.9800,G10301050)
      CALL D1D1WM(T1031, A2, 38.79870,G10301050)
      CALL D1D1WM(T1034, A2,116.39610,G10331053)
      CALL D1D1WM(T215,  A2, 44.48200,G215220)
      CALL D1D1WM(T315,  A2, 50.88700,G315320)
      CALL D1D1WM(T515,  A2, 56.93700,G415420)
      CALL D1D1WM(T815,  A2, 27.40100,G815820)
      CALL D1D1WM(T205,  A2, 88.48800,G200205)
      CALL D1D1WM(T205,  A2, 88.48800,G200205)
      CALL D1D1WM(T901,  A2, 5.899200,G805900)
      CALL D1D1WM(T904,  A2, 17.69760,G805903)
      CALL D1D1WM(T200, A2, 63.00600,G100200)
      CALL D1D1WM(T210, A2, 46.07700,G110210)
      CALL D1D1WM(T210, A2, 69.63800,G120210)
C     CALL D1D1WM(T900, A2, 63.00600,G9001000)
      CALL D1D1WM(T901, A2, 4.200400,G9001000)
      CALL D1D1WM(T904, A2,12.601200,G9031003)
C     CALL D1D1WM(T910, A2,  46.0770,G9101010)
      CALL D1D1WM(T911, A2,  3.07180,G9101010)
      CALL D1D1WM(T914, A2, 9.215400,G9131013)
C     CALL D1D1WM(T920, A2,  69.6390,G9201020)
      CALL D1D1WM(T921, A2,  4.64260,G9201020)
      CALL D1D1WM(T924, A2, 13.92780,G9231023)
C     CALL D1D1WM(T2080, A2, 279.3820,G20801050)
      CALL D1D1WM(T2480, A2, 18.62550,G24801050)
      CALL D1D1WM(T2480, A2, 55.87640,G24831053)
C     CALL D1D1WM(T2080, A2, 284.8600,G2080950)
      CALL D1D1WM(T2080, A2, 18.99070,G2080950)
      CALL D1D1WM(T2080, A2, 56.97200,G2083953)
C      CALL D1D1WM(T2080, A2, 443.7240,G2080850)
      CALL D1D1WM(T2080, A2, 29.5813,G2083850)
      CALL D1D1WM(T2080, A2, 88.7440,G2083850)
      CALL D1D1WM(T3080, A2, 219.1230,G3080150)
      CALL D1D1WM(T3080, A2, 788.8430,G3080250)
C     CALL D1D1WM(T2090, A2, 236.27400,G20901000)
```

```
      CALL D1D1WM(T2091, A2, 3.150330,G20901000)
      CALL D1D1WM(T2094, A2, 9.450990,G20931003)
      CALL D1D1WM(T3090, A2, 236.27400,G3090100)
C     CALL D1D1WM(T2090, A2, 172.78800,G20901010)
      CALL D1D1WM(T3090, A2, 172.78800,G3090110)
      CALL D1D1WM(T2091, A2, 2.303830,G20901010)
      CALL D1D1WM(T2094, A2, 6.911490,G20931013)
C     CALL D1D1WM(T2090, A2, 240.36500,G20901020)
      CALL D1D1WM(T2191, A2, 3.204860,G21901020)
      CALL D1D1WM(T2194, A2, 9.614580,G21931023)
      CALL D1D1WM(T3090, A2, 240.36500,G3090120)
C     CALL D1D1WM(T2090, A2, 246.58200,G20901030)
      CALL D1D1WM(T2191, A2, 3.287770,G21901030)
      CALL D1D1WM(T2194, A2, 9.863310,G21931033)
      CALL D1D1WM(T3090, A2, 246.58200,G3090140)
C     CALL D1D1WM(T2090, A2, 211.19200,G20901050)
      CALL D1D1WM(T2291, A2, 2.815890,G22901050)
      CALL D1D1WM(T2294, A2, 8.447670,G22931053)
      CALL D1D1WM(T3090, A2, 211.19200,G3090150)
C  RESET OUTPUT INTERVAL
      OUTPUT = .1
      IF(TIMEN .GT. 0.40000001) OUTPUT = .050
      IF(TIMEN .GT. 0.80000001) OUTPUT = .200
      IF(TIMEN .GT. 2.00000001) OUTPUT = .5
      IF(TIMEN .GT. 8.00000001) OUTPUT = 2.0
C*************************************************************
HEADER SUBROUTINE DATA
C*********************************************************
include AIRVCV3.F
END OF DATASupport has ended
Support has ended
Support has ended
Support has ended
Support has ended
```

3.6.2.4 300-Watt Transient Conditions Input File (Damaged Package Model)

```
HEADER OPTIONS DATA
TITLE 72 B FUEL CASK, TRAN DAMAGED 300W w/14.5 Inch impact limiter crush
      MODEL= 72B CASK
      OUTPUT = 72b14crs.sot
      PPOUT = ALL1
C*********************************************************************
HEADER NODE DATA, CASK
C*********************************************************************
C  *************************
C  PAYLOAD MODEL
C  *************************
      GEN  10,  3,  20,  164.,   1.093 * 272.0 * 0.168
      GEN  11,  3,  20,  164.,   1.093 * 272.0 * 0.168
      GEN  12,  3,  20,  163.,   1.093 * 272.0 * 0.168
      GEN  13,  3,  20,  163.,   1.093 * 272.0 * 0.168
      GEN  14,  3,  20,  163.,   1.093 * 272.0 * 0.168
      GEN  15,  3,  20,  163.,   1.093 * 272.0 * 0.168
      GEN  16,  3,  20,  163.,   1.093 * 272.0 * 0.168
      GEN  17,  3,  20,  163.,   33.221 * 0.113
      GEN  18,  3,  20,  162.,    6.015 * 0.113
      GEN  28,  3,  20,  163.,    7.525 * 0.113
C  *************************
C  OVERPACK   IMPACT LIMITER MODEL
C  *************************
C      GEN  2000,  2,  1000,  100.,  371.614* 0.11
      3000,    100.,  371.614* 0.11
      GEN  2000,  3,     1,  100.,  .06667*.6667*371.614*0.11
      GEN  2003,  4,     1,  100.,  .2*.6667*371.614*0.11
      GEN  2400,  3,     1,  100.,  .06667*.3333*371.614*0.11
      GEN  2403,  4,     1,  100.,  .2*.3333*371.614*0.11
C      GEN  2020,  2,  1000,  100.,  109.155* 0.30
      3020,    100.,  109.155* 0.30
      GEN  2020,  3,     1,  100.,  .06667*.6667*109.155* 0.30
      GEN  2023,  4,     1,  100.,  .2*.6667*109.155* 0.30
      GEN  2420,  3,     1,  100.,  .06667*.3333*109.155* 0.30
      GEN  2423,  4,     1,  100.,  .2*.3333*109.155* 0.30
C      GEN  2040,  2,  1000,  101.,  286.960* 0.30
      3040,  101.,  286.960* 0.30
      GEN  2040,  3,     1,  100.,  .06667*.6667*286.960* 0.30
      GEN  2043,  4,     1,  100.,  .2*.6667*286.960* 0.30
      GEN  2440,  3,     1,  100.,  .06667*.3333*286.960* 0.30
      GEN  2443,  4,     1,  100.,  .2*.3333*286.960* 0.30
C      GEN  2060,  2,  1000,  103.,  117.600* 0.30
```

```
      3060, 103.,  117.600* 0.30
      GEN  2060,  3,     1,  100.,  .06667*.6667*117.600* 0.30
      GEN  2063,  4,     1,  100.,  .2*.6667*117.600* 0.30
      GEN  2460,  3,     1,  100.,  .06667*.3333*117.600* 0.30
      GEN  2463,  4,     1,  100.,  .2*.3333*117.600* 0.30
C      GEN  2080,  2,  1000,  103.,  161.382* 0.11
      3080, 103.,  161.382* 0.11
      GEN  2080,  3,     1,  100.,  .06667*.6667*161.382* 0.11
      GEN  2083,  4,     1,  100.,  .2*.6667*161.382* 0.11
      GEN  2480,  3,     1,  100.,  .06667*.3333*161.382* 0.11
      GEN  2483,  4,     1,  100.,  .2*.3333*161.382* 0.11
C
      GEN  2100,  2,  1000,  100.,  106.561* 0.11
C     GEN  2010,  2,  1000,  100.,  153.736* 0.11
      GEN  2010,  3,  1,  100.,  1.1090 * 0.11
      GEN  2013,  4,  1,  100.,  3.3271 * 0.11
      GEN  2110,  3,  1,  100.,  1.3202* 0.11
      GEN  2113,  4,  1,  100.,  3.9605* 0.11
      GEN  2210,  3,  1,  100.,  1.3255* 0.11
      GEN  2213,  4,  1,  100.,  3.9765* 0.11
      GEN  2310,  3,  1,  100.,  6.4944* 0.11
      GEN  2313,  4,  1,  100., 19.4834* 0.11
C     GEN  2030,  2,  1000,  101.,   80.176* 0.30
      GEN  2030,  3,  1,  101.,  1.89380* 0.30
      GEN  2033,  4,  1,  101.,  5.68141* 0.30
      GEN  2130,  3,  1,  101.,  2.25438* 0.30
      GEN  2133,  4,  1,  101.,  6.76314* 0.30
      GEN  2230,  3,  1,  101.,  2.26347* 0.30
      GEN  2233,  4,  1,  101.,  6.79041* 0.30
      GEN  2330,  3,  1,  101.,  11.0911* 0.30
      GEN  2333,  4,  1,  101.,  33.2733* 0.30
C     GEN  2050,  2,  1000,  102.,   70.154* 0.30
      GEN  2050,  3,  1,  102.,  0.875 * 1.89380* 0.30
      GEN  2053,  4,  1,  102.,  0.875 * 5.68141* 0.30
      GEN  2150,  3,  1,  102.,  0.875 * 2.25438* 0.30
      GEN  2153,  4,  1,  102.,  0.875 * 6.76314* 0.30
      GEN  2250,  3,  1,  102.,  0.875 * 2.26347* 0.30
      GEN  2253,  4,  1,  102.,  0.875 * 6.79041* 0.30
      GEN  2350,  3,  1,  102.,  0.875 * 11.0911* 0.30
      GEN  2353,  4,  1,  102.,  0.875 * 33.2733* 0.30
C     GEN  2070,  2,  1000,  103.,   75.165* 0.30
      GEN  2070,  3,  1,  103.,  1.7754* 0.30
      GEN  2073,  4,  1,  103.,  5.3263* 0.30
      GEN  2170,  3,  1,  103.,  2.1135* 0.30
      GEN  2173,  4,  1,  103.,  6.3404* 0.30
      GEN  2270,  3,  1,  103.,  2.1220* 0.30
      GEN  2273,  4,  1,  103.,  6.3660* 0.30
      GEN  2370,  3,  1,  103., 10.3979* 0.30
      GEN  2373,  4,  1,  103., 31.1937* 0.30
C     GEN  2090,  2,  1000,  103.,  231.616* 0.11
      GEN  2090,  3,  1,  103.,  5.4449* 0.11
      GEN  2093,  4,  1,  103.,  16.3347* 0.11
      GEN  2190,  3,  1,  103.,  6.4816* 0.11
      GEN  2193,  4,  1,  103.,  19.4448* 0.11
      GEN  2290,  3,  1,  103.,  0.54* 6.5078* 0.11
      GEN  2293,  4,  1,  103.,  0.54*19.5232* 0.11
C
C  REAR OVERPACK   IMPACT LIMITER MODEL
C
      3010,  100.,  153.736* 0.11
      3030,  104.,   80.176* 0.30
      3050,  113.,   70.154* 0.30
      3070,  121.,   75.165* 0.30
      3090,  125.,  231.616* 0.11
C  *************************
C  CASK BODY NODES
C  *************************
C      OUTER CASK BASE PLATE
     100,   124.,   400.353* 0.11
     110,   124.,   292.780* 0.11
     120,   124.,   469.627* 0.11
     130,   124.,   148.075* 0.11
     140,   123.,   301.554* 0.11
     150,   123.,   306.823* 0.11
C      CANISTER
     205,   148.,   100.253* 0.11
     212,   148.,   339.938* 0.031
     215,   149.,   99.224* 0.11
     315,   149.,   101.882* 0.11
     415,   146.,   113.994* 0.11
     515,   146.,   113.994* 0.11
```

```
     615,   144.,   113.994* 0.11
     715,   145.,   101.882* 0.11
     805,   132.,   189.583* 0.11
     812,   132.,   570.760* 0.031
     815,   132.,    71.709* 0.11
C      INNER VESSEL
     200,   135.,   120.106* 0.11         $ BASE PLATE
     210,   133.,   240.800* 0.11         $ BASE PLATE
     220,   130.,   185.446* 0.11         $ INNER VESSEL SHELL
     320,   128.,   188.076* 0.11         $ INNER VESSEL SHELL
     420,   126.,   210.435* 0.11         $ INNER VESSEL SHELL
     520,   124.,   210.435* 0.11         $ INNER VESSEL SHELL
     620,   123.,   210.435* 0.11         $ INNER VESSEL SHELL
     720,   123.,   188.076* 0.11         $ INNER VESSEL SHELL
     820,   120.,   608.129* 0.11         $ INNER VESSEL SHELL
C      OUTER CASK, INNER SHELL
     230,   123.,   533.071* 0.11
     330,   119.,   529.369* 0.11
     430,   116.,   592.300* 0.11
     530,   114.,   592.300* 0.11
     630,   114.,   592.300* 0.11
     730,   114.,   529.369* 0.11
     830,   116.,   299.852* 0.11
C      LEAD SHIELD
     240,   123.,   767.199* 0.031
     340,   118.,   761.870* 0.031
     440,   116.,   852.443* 0.031
C     540,   114.,   852.443* 0.031
     GEN  540,  4,  1,  114.,  0.25*852.443*0.031
     640,   114.,   852.443* 0.031
     740,   114.,   761.870* 0.031
     840,   116.,   431.550* 0.031
     245,   123.,   812.252* 0.031
     345,   118.,   806.610* 0.031
     445,   116.,   902.503* 0.031
C     545,   114.,   902.503* 0.031
     GEN  545,  4,  1,  114.,  0.25*902.503*0.031
     645,   114.,   902.503* 0.031
     745,   114.,   806.610* 0.031
     845,   116.,   456.890* 0.031
C      OUTER CASK, OUTER SHELL
     250,   123.,   949.323* 0.11
     350,   118.,   942.730* 0.11
     450,   116.,  1054.803* 0.11
C     550,   114.,  1054.803* 0.11
     GEN  550,  4,  1,  114.,  0.25*1054.803*0.11
     650,   114.,  1054.803* 0.11
     750,   114.,   942.730* 0.11
     850,   116.,   533.994* 0.11
C      THERMAL SHIELD
     270,   122.,    90.933* 0.11
     370,   115.,    89.726* 0.11
     470,   113.,   100.393* 0.11
C     570,   111.,   100.393* 0.11
     GEN  570,  2,  2,  111.,  0.25*100.393*0.11
     GEN  571,  2,  2,  111.,  0.125*100.393*0.11
     670,   111.,   100.393* 0.11
     770,   112.,    89.726* 0.11
     870,   116.,    50.824* 0.11
C      TRUNNIONS
    380,    117.,   2.*16.857* 0.11    $ 2 LIFTING TRUNNIONS
    581,    114.,   98.53 * 0.11   $  TRANSPORT TRUNNION
    583,    114.,   98.53 * 0.11
    591,    114.,   92.62 * 0.11
    593,    114.,   92.62 * 0.11
    780,    114.,   4.*16.857* 0.11    $ 4 LIFTING TRUNNIONS
C      INNER VESSEL LID
C    900,   121.,   520.459* 0.11
      GEN  900, 3,  1,   121.,   0.066667 * 520.459* 0.11
      GEN  903, 4,  1,   121.,   0.200000 * 520.459* 0.11
C    910,   121.,   380.613* 0.11
      GEN  910, 3,  1,   121.,   0.066667 * 380.613* 0.11
      GEN  913, 4,  1,   121.,   0.200000 * 380.613* 0.11
C    920,   120.,   442.163* 0.11
      GEN  920, 3,  1,   120.,   0.066667 * 442.163* 0.11
      GEN  923, 4,  1,   120.,   0.200000 * 442.163* 0.11
C    930,   116.,   192.498* 0.11
      GEN  930, 3,  1,   116.,   0.066667 * 192.498* 0.11
      GEN  933, 4,  1,   116.,   0.200000 * 192.498* 0.11
C    940,   116.,   392.020* 0.11
      GEN  940, 3,  1,   116.,   0.066667 * 392.020* 0.11
```

```
      GEN  943, 4,  1,   116.,   0.200000 * 392.020* 0.11
C    950,   116.,   398.869* 0.11
      GEN  950, 3,  1,   116.,   0.066667 * 398.869* 0.11
      GEN  953, 4,  1,   116.,   0.200000 * 398.869* 0.11
C      OUTER CASK LID
C   1000,   117.,   480.424* 0.11
      GEN 1000, 3,  1,   117.,   0.066667 * 480.424* 0.11
      GEN 1003, 4,  1,   117.,   0.200000 * 480.424* 0.11
C   1010,   117.,   351.335* 0.11
      GEN 1010, 3,  1,   117.,   0.066667 * 351.335* 0.11
      GEN 1013, 4,  1,   117.,   0.200000 * 351.335* 0.11
C   1020,   117.,   488.741* 0.11
      GEN 1020, 3,  1,   117.,   0.066667 * 488.741* 0.11
      GEN 1023, 4,  1,   117.,   0.200000 * 488.741* 0.11
C   1030,   116.,   309.372* 0.11
      GEN 1030, 3,  1,   116.,   0.066667 * 309.372* 0.11
      GEN 1033, 4,  1,   116.,   0.200000 * 309.372* 0.11
C   1040,   116.,   216.013* 0.11
      GEN 1040, 3,  1,   116.,   0.066667 * 216.013* 0.11
      GEN 1043, 4,  1,   116.,   0.200000 * 216.013* 0.11
C   1050,   116.,   511.242* 0.11
      GEN 1050, 3,  1,   116.,   0.066667 * 511.242* 0.11
      GEN 1053, 4,  1,   116.,   0.200000 * 511.242* 0.11
C  *************************
C  EXTERNAL BOUNDARY NODES
C  *************************
       99,  100.,    1.
       98,  100.,    1.
C*********************************************************************
HEADER CONDUCTOR DATA, CASK
C*********************************************************************
C  *************************
C  PAYLOAD  CONDUCTORS
C  *************************
C       RADIAL CONDUCTANCE   PAYLOAD TO 55 GAL DRUM
     1011,   10,11, 30,31, 50,51, 31.697*9.47
     1112,   11,12, 31,32, 51,52, 68.183*9.47
     1213,   12,13, 32,33, 52,53, 103.465*9.47
     1314,   13,14, 33,34, 53,54, 138.564*9.47
     1415,   14,15, 34,35, 54,55, 173.512*9.47
     1516,   15,16, 35,36, 55,56, 208.594*9.47
     1617,   16,17, 36,37, 56,57, 468.945*9.47
     1718,   17,18, 17,28, 0.016*10.0
     3738,   37,38, 37,48, 0.016*10.0
     5758,   57,58, 57,68, 0.016*10.0
C       AXIAL CONDUCTANCE   PAYLOAD TO 55 GAL DRUMS
     1018,   10,18, 11,18, 12,18, 13,18, 14,18, 15,18, 16,18,  0.285*9.47
     1028,   10,28, 11,28, 12,28, 13,28, 14,28, 15,28, 16,28,  0.285*9.47
     3038,   30,38, 31,38, 32,38, 33,38, 34,38, 35,38, 36,38,  0.285*9.47
     3048,   30,48, 31,48, 32,48, 33,48, 34,48, 35,48, 36,48,  0.285*9.47
     5058,   50,58, 51,58, 52,58, 53,58, 54,58, 55,58, 56,58,  0.285*9.47
     5068,   50,68, 51,68, 52,68, 53,68, 54,68, 55,68, 56,68,  0.285*9.47
C       55 GALLON DRUMS TO CANISTER
     18212,   18,212, 68,812,  28.978*0.0154
     21218,   18,212, 68,812,  0.8085*1.7141E 9
     17315,   17,315, 17,215, 37,415, 37,515, 57,615, 57,715,  84.575*0.0154
     31517,   17,315, 17,215, 37,415, 37,515, 57,615, 57,715,  6.3314*1.7141E 9
     2838,   28,38, 48,58,  18.014* 0.0154
     3828,   28,38, 48,58,  2.060*1.7141E 9
C  *************************
C      CASK BODY RADIAL CONDUCTORS
C  *************************
     100110,  100,110,    2.753* 10.0
     110120,  110,120,    9.860* 10.0
     120130,  120,130,    17.291* 10.0
     130140,  130,140,    31.676* 10.0
     140150,  140,150,    29.422* 10.0
C      STATION 200
     200210,  200,210,    0.808* 10.0
     210220,  210,220,    0.313* 10.0
     220230,  220,230,    798.369* 0.0154
     230220,  220,230,    1.9227* 1.7141E 9
     230240,  230,240,    1276.159
     240245,  240,245,    182.284*19.3
     245250,  245,250,    1829.40
     250270,  250,270,    1923.72* 0.0154
     270250,  250,270,    5.4015*1.7141E 9
     251270,  250,270,    2.2700* 10.0         $ WIRE WRAP
C      STATION 300
     320330,  320,330,  720,730,    792.820* 0.0154
     330320,  320,330,  720,730,    2.2173* 1.7141E 9
```

```
     330340,  330,340,  730,740,    1267.297
     340345,  340,345,  740,745,    181.018*19.3
     345350,  345,350,  745,750,    1816.673
     350370,  350,370,  750,770,    1910.36*0.0154
     370350,  350,370,  750,770,    5.3640*1.7141E 9
     351370,  350,370,  750,770,    2.2500* 10.0         $ WIRE WRAP
C      STATIONS 400,500, & 600
     420430,  420,430, 520,530, 620,630,     887.080* 0.0154
     430420,  420,430, 520,530, 620,630,     2.4976* 1.7141E 9
     430440,  430,440, 630,640,     1417.937
     530540,  530,540, 530,541, 530,542, 530,543,  0.25*1417.937
     440445,  440,445, 640,645,     202.540* 19.3
     540545,  540,545, 541,546, 542,547, 543,548, 0.25*202.540* 19.3
     445450,  445,450, 645,650,     2037.906
     545550,  545,550, 546,551, 547,552, 548,553, 0.25*2037.906
     450470,  450,470, 650,670,     2137.47*0.0154
     550570,  550,570, 552,572, 0.25*2137.47*0.0154
     553570,  551,571, 553,573, 0.125*2137.47*0.0154
     470450,  450,470, 650,670,     6.0017*1.7141E 9
     570550,  550,570, 552,572,  0.25*6.0017*1.7141E 9
     571550,  551,571, 553,573,  0.125*6.0017*1.7141E 9
     451470,  450,470, 650,670,     2.5200* 10.0  $ WIRE WRAP
     551570,  551,571, 553,573,  0.125*2.520*10.0  $wire wrap
     552570,  550,570, 552,572,  0.25*2.520*10.0  $wire wrap
C      STATION 800
     820830,  820,830,     449.080* 0.0154
     830820,  820,830,     1.2560* 1.7141E 9
     830840,  830,840,     717.8158
     840845,  840,845,     102.530* 19.3
     845850,  845,850,     1029.0523
     850870,  850,870,     1082.09* 0.0154
     870850,  850,870,     2.9001*1.7141E 9
     851870,  850,870,     1.2800*10.0         $ WIRE WRAP
C      STATION 900
C    820930,  820,930,     110.885*0.0154
   820930,  820,930,  820,931, 820,932,           .0666667*110.885*.0154
   820933,  820,933,  820,934, 820,935, 820,936,  .200000*110.885*.0154
C    930820,  820,930,    0.3101* 1.7141E 9
   930820,  820,930,  820,931, 820,932,           .0666667* 0.3101*1.7141E 9
   933820,  820,933,  820,934, 820,935, 820,936,  .200000*0.3101*1.7141E 9
C    900910,  900,910,     4.0530* 10.0
   900910,  900,910,  901,911, 902,912,            .0666667*4.0530* 10.0
   903913,  903,913,  904,914, 905,915, 906,916,   .2000000*4.0530* 10.0
C    910920,  910,920,     13.855* 10.0
   910920,  910,920,  911,921, 912,922,            .0666667*13.855* 10.0
   913923,  913,923,  914,924, 915,925, 916,926,   .2000000*13.855* 10.0
C    920930,  920,930,    177.415* 0.0154
   920930,  920,930,  921,931, 922,932,           .0666667*177.415*.0154
   923933,  923,933,  924,934, 925,935, 926,936,  .2000000*177.415*.0154
C    930920,  920,930,     0.4962* 1.7141E 9
  930920,  920,930,  921,931, 922,932,          .0666667*0.4962*1.7141E 9
  933923,  923,933,  924,934, 925,935, 926,936, .2000000*0.4962*1.7141E 9
C    930940,  930,940,     41.179* 10.0
   930940,  930,940,  931,941, 932,942,            .0666667*41.179*10.0
   933943,  933,943,  934,944, 935,945, 936,946,   .2000000*41.179*10.0
C    940950,  940,950,     38.248* 10.0
   940950,  940,950,  941,951, 942,952,            .0666667*38.248*10.0
   943953,  943,953,  944,954, 945,955, 946,956,   .2000000*38.248*10.0
C      STATION 900 TO 900
   900901,  900,901,  901,902,                     1.715278* 10.0
   902903,  902,903,  906,900,                     0.857639* 10.0
   903904,  903,904,  904,905,  905,906,           0.571759* 10.0
   910911,  910,911,  911,912,                     0.353261* 10.0
   912913,  912,913,  916,910,                     0.176630* 10.0
   913914,  913,914,  914,915,  915,916,           0.117754* 10.0
   920921,  920,921,  921,922,                     0.317560* 10.0
   922923,  922,923,  926,920,                     0.158780* 10.0
   923924,  923,924,  924,925,  925,926,           0.105853* 10.0
   930931,  930,931,  931,932,                     0.077381* 10.0
   932933,  932,933,  936,930,                     0.038690* 10.0
   933934,  933,934,  934,935,  935,936,           0.025794* 10.0
   940941,  940,941,  941,942,                     0.133635* 10.0
   942943,  942,943,  946,940,                     0.066820* 10.0
   943944,  943,944,  944,945,  945,946,           0.044545* 10.0
   950951,  950,951,  951,952,                     0.097892* 10.0
   952953,  952,953,  956,950,                     0.048946* 10.0
   953954,  953,954,  954,955,  955,956,           0.032631* 10.0
C      STATION 1000
C    10001010, 1000,1010,  3.7410* 10.0
  10001010, 1000,1010, 1001,1011, 1002,1012,       .0666667*3.7410*10.0
  10031013, 1003,1013, 1004,1014, 1005,1015, 1006,1016,  .20*3.7410*10.0
```

```
C    10101020, 1010,1020,  12.563* 10.0
  10101020, 1010,1020, 1011,1021, 1012,1022,       .0666667*12.563*10.0
  10131023, 1013,1023, 1014,1024, 1015,1025, 1016,1026,  .2*12.563*10.0
C    10201030, 1020,1030,  13.442* 10.0
  10201030, 1020,1030, 1021,1031, 1022,1032,       .0666667*13.442*10.0
  10231033, 1023,1033, 1024,1034, 1025,1035, 1026,1036,  .2*13.442*10.0
C    10301040, 1030,1040,  0.6140* 10.0
  10301040, 1030,1040, 1031,1041, 1032,1042,       .0666667*0.6140*10.0
  10331043, 1033,1043, 1034,1044, 1035,1045, 1036,1046,  .2*0.6140*10.0
C    10401030, 1030,1040,  1.5000* 40.
  10401030, 1040,1030, 1041,1031, 1042,1032,       .0666667*1.50*40.
  10431033, 1043,1033, 1044,1034, 1045,1035, 1046,1036,  .2*1.50*40.
C    10501030, 1030,1050,  0.4280* 1.7141E 9
  10501030, 1030,1050, 1031,1051, 1032,1052, .0666667*0.428*1.7141E 9
  10531033, 1033,1053, 1034,1054, 1035,1055, 1036,1056, .2*0.428*1.7141E 9
C    10301050, 1030,1050,  581.98* 0.0154
  10301050, 1030,1050, 1031,1051, 1032,1052,       .0666667*581.98*.0154
  10331053, 1033,1053, 1034,1054, 1035,1055, 1036,1056,  .2*581.98*.0154
C    10401050, 1040,1050,  15.816* 10.0
  10401050, 1040,1050, 1041,1051, 1042,1052,       .0666667*15.816* 10.0
  10431053, 1043,1053, 1044,1054, 1045,1055, 1046,1056,  .2*15.816* 10.0
C      STATION 1000 TO 1000
   10001001,  1000,1001,  1001,1002,                    1.583333* 10.0
   10021003,  1002,1003,  1006,1000,                    0.791667* 10.0
   10031004,  1003,1004,  1004,1005,  1005,1006,        0.527777* 10.0
   10101011,  1010,1011,  1011,1012,                    0.326087* 10.0
   10121013,  1012,1013,  1016,1010,                    0.163044* 10.0
   10131014,  1013,1014,  1014,1015,  1015,1016,        0.108696* 10.0
   10201021,  1020,1021,  1021,1022,                    0.275424* 10.0
   10221023,  1022,1023,  1026,1020,                    0.137712* 10.0
   10231024,  1023,1024,  1024,1025,  1025,1026,        0.091808* 10.0
   10301031,  1030,1031,  1031,1032,                    0.190972* 10.0
   10321033,  1032,1033,  1036,1030,                    0.095486* 10.0
   10331034,  1033,1034,  1034,1035,  1035,1036,        0.063657* 10.0
   10401041,  1040,1041,  1041,1042,                    0.141438* 10.0
   10421043,  1042,1043,  1046,1040,                    0.070719* 10.0
   10431044,  1043,1044,  1044,1045,  1045,1046,        0.047146* 10.0
   10501051,  1050,1051,  1051,1052,                    0.125915* 10.0
   10521053,  1052,1053,  1056,1050,                    0.062957* 10.0
   10531054,  1053,1054,  1054,1055,  1055,1056,        0.041972* 10.0
C
C      CANISTER TO INNER VESSEL
C
     215220,  215,220,     44.482* 0.0154
     220215,  215,220,     2.6223* 1.7141E 9
     215320,  215,320,  215,210,     0.7137* 1.7141E 9
     315320,  315,320, 715,720,     50.887* 0.0154
     320315,  315,320, 715,720,    2.999* 1.7141E 9
     315420,  315,420,  315,220,     0.7137* 1.7141E 9
     415420,  415,420,  515,520,  615,620,    56.937* 0.0154
     420415,  415,420,  515,520,  615,620,    3.3565* 1.7141E 9
     415520,  415,520,  415,320,  515,620,  515,420,  0.7986* 1.7141E 9
     615520,  615,520,  615,720,                      0.7986* 1.7141E 9
     815820,  815,820,     27.401* 0.0154
     820815,  815,820,     1.6992* 1.7141E 9
C    815720,  815,720,  815,920,     0.4895* 1.7141E 9
     815720,  815,720,              0.4895* 1.7141E 9
     815920,  815,920, 815,921, 815,922,   0.066667* 0.4895* 1.7141E 9
     815923,  815,923, 815,924, 815,925, 815,926,  0.2*0.4895* 1.7141E 9
C    200205,  200,205,  805,900,   88.488* 0.0154
     200205,  200,205,             88.488* 0.0154
     805900,  805,900,  805,901, 805,902,     0.066667*  88.488* 0.0154
     805903,  805,903,  805,904, 805,905, 805,906,   0.2*88.488* 0.0154
C    805900,  805,900,  205,200,   1.0660* 1.7141E 9
     205200,  200,205,             1.4417* 1.7141E 9
     900805,  805,900,  805,901, 805,902,     0.066667*1.0660* 1.7141E 9
     903805,  805,903,  805,904, 805,905, 805,906,  0.2*1.0660*1.7141E 9
C
C      TRUNNION TO OUTER SHELL
C
     380350,   380,350,    1.9053* 10.0
     581551,   581,551,    38.32* 10.0
     583553,   583,553,    38.32* 10.0
     591581,   581,591,  583,593,  5.244 * 10.0
     780750,   780,750,    3.8106* 10.0
C  *************************
C      CASK BODY AXIAL CONDUCTORS
C  *************************
     100200,  100,200,     63.006* 0.0154
     200100,  100,200,     0.3470* 1.7141E 9
     110210,  110,210,     46.077* 0.0154
```

```
     210110,  110,210,     0.2540* 1.7141E 9
     120210,  120,210,     69.638* 0.0154
     210120,  120,210,     0.3840* 1.7141E 9
     130230,  130,230,     0.7600* 10.0
     140240,  140,240,  140,245,   0.774* 19.3
     150250,  150,250,     1.3533* 10.0
C
C      INNER VESSEL
C
     220320,  220,320,     0.1731* 10.0
     320420,  320,420,  620,720,   0.1640* 10.0
     420520,  420,520,  520,620,   0.1550* 10.0
     720820,  720,820,     0.2220* 10.0
C    820920,  820,920,     0.0740* 10.0
     820920,  820,920, 820,921, 820,922, 0.066667*0.0740* 10.0
     820923,  820,923, 820,924, 820,925, 820,926, 0.20*0.0740* 10.0
C    920820,  820,920,     1.2000* 40.
     920820,  820,920, 820,921, 820,922, 0.066667*1.200* 40.
     923820,  820,923, 820,924, 820,925, 820,926, 0.20*1.200* 40.
C
C      OUTER CASK, INNER SHELL
C
     230330,  230,330,     0.4870* 10.0
     330430,  330,430,  630,730,   0.4610* 10.0
     430530,  430,530,  530,630,   0.4370* 10.0
     730830,  730,830,     0.6240* 10.0
C    830930,  830,930,     1.0510* 10.0
     830930,  830,930, 830,931, 830,932, 0.066667*1.051* 10.
     830933,  830,933, 830,934, 830,935, 830,936, 0.20*1.051* 10.
C
C      LEAD
C
     240340,  240,340,     0.4820* 19.3
     340440,  340,440,  640,740,   0.4560* 19.3
C     440540,  440,540,  540,640,   0.4320* 19.3
     440540,  440,540, 440,541, 440,542, 440,543, 0.25*0.4320* 19.3
     640540,  640,540, 640,541, 640,542, 640,543, 0.25*0.4320* 19.3
     740840,  740,840,     0.6170* 19.3
C    840940,  840,940,     14.80762
     840940,  840,940, 840,941, 840,942, 0.066667*14.80762
     840943,  840,943, 840,944, 840,945, 840,946, 0.20*14.80762
C
C      LEAD
C
     245345,  245,345,     0.5100* 19.3
     345445,  345,445,  645,745,   0.4830* 19.3
C     445545,  445,545,  545,645,   0.4580* 19.3
     445545,  445,545, 445,546, 445,547, 445,548,  0.25*0.4580* 19.3
     645545,  645,545, 645,546, 645,547, 645,548,  0.25*0.4580* 19.3
     745845,  745,845,     0.6540* 19.3
C    845940,  845,940,     15.67441
     845940,  845,940, 845,941, 845,942, 0.066667*15.67441
     845943,  845,943, 845,944, 845,945, 845,946, 0.20*15.67441
C
C      OUTER CASK, OUTER SHELL
C
     250350,  250,350,     0.8680* 10.0
     350450,  350,450,  650,750,   0.8220* 10.0
C     450550,  450,550,  550,650,   0.7780* 10.0
     450550,  450,550, 450,551, 450,552, 450,553, 0.25* 0.7780* 10.0
     650550,  650,550, 650,551, 650,552, 650,553, 0.25* 0.7780* 10.0
     581450,  581,450, 583,450, 581,650, 583,650, 0.025* 0.7780* 10.0
     750850,  750,850,     1.1120* 10.0
C    850950,  850,950,     1.8720* 10.0
     850950,  850,950, 850,951, 850,952, 0.066667*1.8720* 10.0
     850953,  850,953, 850,954, 850,955, 850,956, 0.20*1.8720* 10.0
C
C      THERMAL SHIELD
C
     270370,  270,370,     0.0811* 10.0
     370470,  370,470,  670,770,   0.0768* 10.0
     470570,  470,570, 470,572, 570,670, 572,670,  0.25 * 0.0727* 10.0
     471570,  470,571, 470,573, 571,670, 573,670,  0.125 * 0.0727* 10.0
     580470,  470,581, 470,583, 670,581, 670,583, 0.125 * 0.0727* 10.0
     770870,  770,870,     0.1039* 10.0
C
C      CASK LID
C
C    9001000, 900,1000,    63.006* 0.0154
     9001000, 900,1000, 901,1001, 902,1002,   .0666667*63.006* 0.0154
     9031003, 903,1003, 904,1004, 905,1005, 906,1006, .2*63.006* 0.0154
```

```
C    1000900, 900,1000,    0.3470* 1.7141E 9
     1000900, 900,1000, 901,1001, 902,1002,   .0666667*.3470*1.7141E 9
     1003903, 903,1003, 904,1004, 905,1005, 906,1006, .2*.3470*1.7141E 9
C    9101010, 910,1010,    46.077* 0.0154
     9101010, 910,1010, 911,1011, 912,1012,   .0666667*46.077* 0.0154
     9131013, 913,1013, 914,1014, 915,1015, 916,1016, .2*46.077* 0.0154
C    1010910, 910,1010,    0.2540* 1.7141E 9
     1010910, 910,1010, 911,1011, 912,1012,   .0666667*.2540*1.7141E 9
     1013913, 913,1013, 914,1014, 915,1015, 916,1016, .2*.2540*1.7141E 9
C    9201020, 920,1020,    69.639* 0.0154
     9201020, 920,1020, 921,1021, 922,1022,   .0666667*69.639* 0.0154
     9231023, 923,1023, 924,1024, 925,1025, 926,1026,  .2*69.639* 0.0154
C    1020920, 920,1020,    0.3840* 1.7141E 9
     1020920, 920,1020, 921,1021, 922,1022,   .0666667*.3840*1.7141E 9
     1023923, 923,1023, 924,1024, 925,1025, 926,1026, .2*.3840*1.7141E 9
C    9301040, 930,1040,    1.8400* 10.0
     9301040, 930,1040, 931,1041, 932,1042,   .0666667*1.840 * 10.0
     9331043, 933,1043, 934,1044, 935,1045, 936,1046,   .20*1.840*10.0
C    9401040, 940,1040,    2.5770* 10.0
     9401040, 940,1040, 941,1041, 942,1042,   .0666667*2.5770* 10.0
     9431043, 943,1043, 944,1044, 945,1045, 946,1046,   .2*2.5770* 10.0
C    9501050, 950,1050,    3.3790* 10.0
     9501050, 950,1050, 951,1051, 952,1052,   .0666667*3.3790* 10.0
     9531053, 953,1053, 954,1054, 955,1055, 956,1056,   .20*3.3790* 10.0
C
C      CANISTER
C
     215315,  215,315,     0.1010* 25.0
     315415,  315,415,  615,715,    0.0890* 25.0
     415515,  415,515,  515,615,    0.0843* 25.0
     715815,  715,815,     0.1226* 25.0
     205212,  205,212,    403.0
     805812,  805,812,    231.3
     205215,   205,215,   0.179*25.0
     805815,   805,815,   0.364*25.0
     212215,   212,215,   0.590*19.3
     812815,   812,815,   0.987*19.3
C  *************************
C      OVERPACK CONDUCTORS
C  *************************
C     20002020,  2000,2020,  3000,3020, 299.022* 0.019
     30003020,  3000,3020, 299.022* 0.019
     20002020,  2000,2020,  2001,2021, 2002,2022, .06667*.6667*299.022* 0.019*1000. $Damage
     24002420,  2400,2420,  2401,2421, 2402,2422, .06667*.3333*299.022* 0.019*1000. $Damage
     20032023,  2003,2023,  2004,2024, 2005,2025, 2006,2026, .20*.6667*299.022* 0.019
     24032423,  2403,2423,  2404,2424, 2405,2425, 2406,2426, .20*.3333*299.022* 0.019
C
C     20202040,  2020,2040,  3020,3040, 67.0590* 0.019
     30203040,  3020,3040, 67.0590* 0.019
     20202040,  2020,2040,  2022,2042, .06667*.6667*67.0590* 0.019*1000. $Damage
     24202440,  2420,2440,  2422,2442, .06667*.3333*67.0590* 0.019*1000. $Damage
     20212041,  2021,2041, .06667*.6667*67.0590* 0.019*1000. $Damage
     24212441,  2421,2441, .06667*.3333*67.0590* 0.019*1000. $Damage
     20232043,  2023,2043,  2024,2044, 2025,2045, 2026,2046, .20*.6667*67.0590* 0.019
     24232443,  2423,2443,  2424,2444, 2425,2445, 2426,2446, .20*.3333*67.0590* 0.019
C
C     20402060,  2040,2060,  3040,3060, 46.1890* 0.019
     30403060,  3040,3060, 46.1890* 0.019
     20402060,  2040,2060,  2041,2061, 2042,2062, .06667*.6667*46.1890*1000.*0.019  $ Damage
     24402460,  2440,2460,  2441,2461, 2442,2462, .06667*.3333*46.1890*1000.*0.019  $ Damage
     20432063,  2043,2063,  2044,2064, 2045,2065, 2046,2066, .20*.6667*46.1890* 0.019
     24432463,  2443,2463,  2444,2464, 2445,2465, 2446,2466, .20*.3333*46.1890* 0.019
C
C     20602080,  2060,2080,  3060,3080, 107.068* 0.019
     30603080,  3060,3080, 107.068* 0.019
     20602080,  2060,2080,  2061,2081, 2062,2082, .06667*.6667*46.1890* 0.019
     24602480,  2460,2480, 2461,2481,  2462,2482, .06667*.3333*46.1890* 0.019
     20632083,  2063,2083,  2064,2084, 2065,2085, 2066,2086, .20*.6667*46.1890* 0.019
     24632483,  2463,2483,  2464,2484, 2465,2485, 2466,2486, .20*.3333*46.1890* 0.019
C
C    20002010,  2000,2010,  3000,3010, 0.05399* 10.0
     24002310,  2400,2310,  2401,2311, 2402,2312, 0.066667*0.05399* 10.0
     24032313,  2403,2313,  2404,2314, 2405,2315, 2406,2016, 0.20*0.05399* 10.0
     30003010,  3000,3010, 0.05399* 10.0
     30003100,  3000,3100, 0.08162* 10.0
     20002100,  2000,2100, 2001,2100, 2002,2100, .06667* 0.08162* 10.0
     20032100,  2003,2100, 2004,2100, 2005,2100, 2006,2100, .20* 0.08162* 10.0
C
C    21002080,  2100,2080,  3100,3080, 0.07954* 10.0
     21002080,  2100,2080, 2100,2081, 2100,2082, .06667*0.07954* 10.0
     21002083,  2100,2083, 2100,2084, 2100,2085, 2100,2086, .20* 0.07954* 10.0
```

```
     31003080,  3100,3080, 0.07954* 10.0
C
C    20902080,  2090,2080,  3090,3080, 0.05658* 10.0
     24802290,  2480,2290,  2481,2291, 2482,2292, 0.066667*0.05658* 10.0
     24832293,  2483,2293,  2484,2294, 2485,2295, 2486,2296,  0.200*0.05658* 10.0
     30803090,              3090,3080, 0.05658* 10.0
C
     20002400,  2000,2400,  2001,2401,  2002,2402, .06667*0.463*10.0
     20032403,  2003,2403,  2004,2404,  2005,2405, 2006,2406, .2*0.463*10.0
C
     20202420,  2020,2420,  2021,2421,  2022,2422, .06667*9.512*0.019
     20232423,  2023,2423,  2024,2424,  2025,2425,  2026,2426, .2*9.512*0.019
C
     20402440,  2040,2440,  2041,2441,  2042,2442, .06667*25.005*0.019
     20432443,  2043,2443,  2044,2444,  2045,2445,  2046,2446,  .2*25.005*0.019
C
     20602460,  2060,2460,  2061,2461,  2062,2462, .06667*10.350*0.019
     20632463,  2063,2463,  2064,2464,  2065,2465,  2066,2466, .2*10.350*0.019
C
     20802480,  2080,2480,  2081,2481,  2082,2482, .06667*0.258*10.0
     20832483,  2083,2483,  2084,2484,  2085,2485,  2086,2486, .2*0.258*10.0
C
     20002001,  2000,2001,  2001,2002,  0.011*10.0
     20032004,  2003,2004,  2004,2005,  2005,2006,  0.004*10.0
     20022003,  2002,2003,  2006,2000,  0.005*10.0
C
     20202021,  2020,2021,  2021,2022,  0.240*0.019
     20232024,  2023,2024,  2024,2025,  2025,2026,  0.080*0.019
     20222023,  2022,2023,  2026,2020,  0.120*0.019
C
     20402041,  2040,2041,  2041,2042,  0.900*0.019
     20432044,  2043,2044,  2044,2045,  2045,2046,  0.300*0.019
     20422043,  2042,2043,  2046,2040,  0.450*0.019
C
     20602061,  2060,2061,  2061,2062,  0.696*0.019
     20632064,  2063,2064,  2064,2065,  2065,2066,  0.232*0.019
     20622063,  2062,2063,  2066,2060,  0.348*0.019
C
     20802081,  2080,2081,  2081,2082,  0.019*10.0
     20832084,  2083,2084,  2084,2085,  2085,2086,  0.006*10.0
     20822083,  2082,2083,  2086,2080,  0.010*10.0
C
     24002401,  2400,2401,  2401,2402,  0.005*10.0
     24032404,  2403,2404,  2404,2405,  2405,2406,  0.002*10.0
     24022403,  2402,2403,  2406,2400,  0.003*10.0
C
     24202421,  2420,2421,  2421,2422,  0.120*0.019
     24232424,  2423,2424,  2424,2425,  2425,2426,  0.040*0.019
     24222423,  2422,2423,  2426,2420,  0.060*0.019
C
     24402441,  2440,2441,  2441,2442,  0.450*0.019
     24432444,  2443,2444,  2444,2445,  2445,2446,  0.150*0.019
     24422443,  2442,2443,  2446,2440,  0.225*0.019
C
     24602461,  2460,2461,  2461,2462,  0.348*0.019
     24632464,  2463,2464,  2464,2465,  2465,2466,  0.116*0.019
     24622463,  2462,2463,  2466,2460,  0.174*0.019
C
     24802481,  2480,2481,  2481,2482,  0.010*10.0
     24832484,  2483,2484,  2484,2485,  2485,2486,  0.003*10.0
     24822483,  2482,2483,  2486,2480,  0.005*10.0
C
C    20102030,  2010,2030,  3010,3030, 28.8630* 0.019
C    20302050,  2030,2050,  3030,3050, 15.3940* 0.019
C    20502070,  2050,2070,  3050,3070, 15.3940* 0.019
C    20702090,  2070,2090,  3070,3090, 28.8630* 0.019
C
C  STATION 2010 TO 2030
     20102030,  2010,2030,  2011,2031, 2012,2032,   0.681777*0.019
     20132033,  2013,2033,  2014,2034, 2015,2035, 2016,2036, 2.045331*0.019
     21102130,  2110,2130,  2111,2131, 2112,2132,   0.811578*0.019
     21132133,  2113,2133,  2114,2134, 2115,2135, 2116,2136, 2.434734*0.019
     22102230,  2210,2230,  2211,2231, 2212,2232,   0.814851*0.019
     22132233,  2213,2233,  2214,2234, 2215,2235, 2216,2236, 2.444553*0.019
     23102330,  2310,2330,  2311,2331, 2312,2332,   3.992441*0.019*1000. $Damage
     23132333,  2313,2333,  2314,2334, 2315,2335, 2316,2336, 11.977323*0.019
C
C  STATION 2030 TO 2050 & 2050 TO 2070
     20302050,  2030,2050,  2031,2051, 2032,2052
                2050,2070,  2051,2071, 2052,2072,   0.363614*0.019
     20332053,  2033,2053,  2034,2054, 2035,2055, 2036,2056
```

```
          2053,2073,  2054,2074, 2055,2075, 2056,2076,  1.090842*0.019
     21302150,  2130,2150,  2131,2151, 2132,2152
                2150,2170,  2151,2171, 2152,2172,   0.432842*0.019
     21332153,  2133,2153,  2134,2154, 2135,2155, 2136,2156
            2153,2173,  2154,2174, 2155,2175, 2156,2176,  1.298526*0.019
     22302250,  2230,2250,  2231,2251, 2232,2252
                2250,2270,  2251,2271, 2252,2272,   0.434587*0.019
     22332253,  2233,2253,  2234,2254, 2235,2255, 2236,2256
            2253,2273,  2254,2274, 2255,2275, 2256,2276,  1.303761*0.019
     23302350,  2330,2350,  2331,2351, 2332,2352
                2350,2370,  2351,2371, 2352,2372,   2.129302*0.019*1000. $Damage
     23332353,  2333,2353,  2334,2354, 2335,2355, 2336,2356
            2353,2373,  2354,2374, 2355,2375, 2356,2376,  6.387906*0.019
C
C  STATION 2070 TO 2090
     20702090,  2070,2090,  2071,2091, 2072,2092,   0.681777*0.019
     20732093,  2073,2093,  2074,2094, 2075,2095, 2076,2096, 2.045331*0.019
     21702190,  2170,2190,  2171,2191, 2172,2192,   0.811578*0.019
     21732193,  2173,2193,  2174,2194, 2175,2195, 2176,2196, 2.434734*0.019
     22702290,  2270,2290,             2272,2292,   0.814851*0.019
     22712291,              2271,2291,              0.814851*0.019
     22732293,  2273,2293,  2274,2294, 2275,2295, 2276,2296, 2.444553*0.019
C    23702390,  2370,2390,  2371,2391, 2372,2392,   3.992441*0.019
C    23732393,  2373,2393,  2374,2394, 2375,2395, 2376,2396, 11.977323*0.019
C
C
C  REAR OVERPACK   IMPACT LIMITER
C
     30103030,  3010,3030, 28.8630* 0.019
     30303050,  3030,3050, 15.3940* 0.019
     30503070,  3050,3070, 15.3940* 0.019
     30703090,  3070,3090, 28.8630* 0.019
C
C      OVERPACK TO CASK CONDUCTORS
C
C    20801050,  2080,1050,    279.382* 0.0154
     24801050,  2480,1050, 2481,1051, 2482,1052, 0.0666667*279.382* 0.0154*1000.  $Damage
     24831053,  2483,1053, 2484,1054, 2485,1055, 2486,1056, 0.20*279.382* 0.0154
C    10502080,  2080,1050,    1.94398*1.7141E 9
     10502480,  2480,1050, 2481,1051, 2482,1052, 0.0666667*1.94398*1.7141E 9
     10532480,  2483,1053, 2484,1054, 2485,1055, 2486,1056, 0.20*1.94398*1.7141E 9
C    2080950,   2080,950,     284.860* 0.0154
     2080950,  2080,950, 2081,951, 2082,952,  0.0666667*284.860*0.0154*1000.  $Damage
     2083953,  2083,953, 2084,954, 2085,955, 2086,956, 0.20*284.860*0.0154
C    9502080,   2080,950,      1.98210*1.7141E 9
     9502080,  2080,950, 2081,951, 2082,952, 0.0666667* 1.98210*1.7141E 9
     9532080,  2083,953, 2084,954, 2085,955, 2086,956, 0.20* 1.98210*1.7141E 9
C     2080850,   2080,850,     443.724* 0.0154
     2080850,  2080,850,  2081,850, 2082,850, 0.0667*443.724* 0.0154*1000.  $Damage
     2083850,  2083,850,  2084,850,  2085,850, 2086,850, 0.2*443.724* 0.0154
C     8502080,   2080,850,     3.08750*1.7141E 9
     8502080,  2080,850,  2081,850,  2082,850, 0.0667*3.08750*1.7141E 9
     8502083,  2083,850,  2084,850,  2085,850, 2086,850, 0.2*3.08750*1.7141E 9
     3080150,   3080,150,     219.123* 0.0154
     1503080,   3080,150,     1.52469*1.7141E 9
     3080250,   3080,250,     788.843* 0.0154
     2503080,   3080,250,     5.48889*1.7141E 9
C    20901000,  2090,1000,  3090,100,  236.2740* 0.0154
C    10002090,  2090,1000,  3090,100,  0.65630*1.7141E 9
     20901000,  2090,1000,  2091,1001, 2092,1002,  15.7517* 0.0154*1000. $Damage
C    10002090,  2090,1000,  2091,1001, 2092,1002,  0.04375*1.7141E 9
     20931003,  2093,1003,  2094,1004, 2095,1005, 2096,1006,  47.2550* 0.0154
C    10032093,  2093,1003,  2094,1004, 2095,1005, 2096,1006, 0.13126*1.7141E 9
C
     3090100,               3090,100,  236.2740* 0.0154
     1003090,               3090,100,  0.65630*1.7141E 9
C    20901010,  2090,1010,  3090,110,  172.7880* 0.0154
C    10102090,  2090,1010,  3090,110,  0.4800* 1.7141E 9
     20901010,  2090,1010,  2091,1011, 2092,1012,  11.5192* 0.0154*1000. $Damage
C    10102090,  2090,1010,  2091,1011, 2092,1012,  0.0320* 1.7141E 9
     20931013,  2093,1013,  2094,1014, 2095,1015, 2096,1016, 34.5575* 0.0154
C    10132093,  2093,1013,  2094,1014, 2095,1015, 2096,1016, 0.0960* 1.7141E 9
C
     3090110,               3090,110,  172.7880* 0.0154
     1103090,               3090,110,  0.4800* 1.7141E 9
C    20901020,  2090,1020,  3090,120,  240.3650* 0.0154
C    10202090,  2090,1020,  3090,120,  0.6677* 1.7141E 9
     21901020,  2190,1020,  2191,1021, 2192,1022,  16.0243* 0.0154*1000.  $Damage
C    10202190,  2190,1020,  2191,1021, 2192,1022,  0.04451*1.7141E 9
     21931023,  2193,1023,  2194,1024, 2195,1025, 2196,1026, 48.0729* 0.0154
C    10232193,  2193,1023,  2194,1024, 2195,1025, 2196,1026, 0.13354*1.7141E 9
```

```
C
     3090120,               3090,120,  240.3650* 0.0154
     1203090,               3090,120,  0.6677* 1.7141E 9
C    20901030,  2090,1030,  3090,140,  246.5820* 0.0154
C    10302090,  2090,1030,  3090,140,  .68495* 1.7141E 9
     21901030,  2190,1030,  2191,1031, 2192,1032,  16.4839* 0.0154*1000. $Damage
C    10302190,  2190,1030,  2191,1031, 2192,1032,  .04566* 1.7141E 9
     21931033,  2193,1033,  2194,1034, 2195,1035, 2196,1036, 49.3167* 0.0154
C    10332193,  2193,1033,  2194,1034, 2195,1035, 2196,1036, 0.13699*1.7141E 9
C
     3090140,               3090,140,  246.5820* 0.0154
     1403090,               3090,140,  .68495* 1.7141E 9
C    20901050,  2090,1050,  3090,150,  211.1920* 0.0154
C    10502090,  2090,1050,  3090,150,  .58664* 1.7141E 9
     22901050,  2290,1050,  2291,1051, 2292,1052,  14.0794*0.0154*1000.  $Damage
C    10502290,  2290,1050,  2291,1051, 2292,1052,  .039109*1.7141E 9
     22931053,  2293,1053,  2294,1054, 2295,1055, 2296,1056, 42.2383* 0.0154
C    10532293,  2293,1053,  2294,1054, 2295,1055, 2296,1056,  0.11732*1.7141E 9
C
     3090150,               3090,150,  211.1920* 0.0154
     1503090,               3090,150,  .58664* 1.7141E 9
C
C     CIRCUMFRENTIAL CASK WALL CONDUCTORS
      540541,  540,541, 541,542, 542,543, 543,540,  0.056 * 19.3
      545546,  545,546, 546,547, 547,548, 548,545,  0.053 * 19.3
      550551,  550,551, 551,552, 552,553, 553,550,  0.080 * 10.0
      570571,  570,571, 571,572, 572,573, 573,570,  0.007 * 10.0
      581571,  581,571, 583,573,  0.0140 * 10.0
C
C     EXTERNAL RADIATION HEAT TRANSFER
      7098,   370,98,   770,98,   .8*16.223*1.7141E 9  $ THERMAL SHIELD
      9870, 470,98, 670,98, .8*18.151*1.7141E 9 $ THERMAL SHIELD
      98570,  570,98, 572,98, 0.25*.8*18.151*1.7141E 9 $ THERMAL SHIELD
      98571,  571,98, 573,98, 0.125*.8*18.151*1.7141E 9 $ THERMAL SHIELD
C      200098, 2000,98,  3000,98,  .8*76.271*1.7141E 9  $ OVERPACK SHELL
      200098, 2000,98, 2001,98, 2002,98, 0.0667*.6667*.8*76.271*1.7141E 9
      200398, 2003,98, 2004,98, 2005,98, 2006,98, 0.2*.6667*.8*76.271*1.7141E 9
      240098, 2400,98, 2401,98, 2402,98, 0.0667*.333*.8*76.271*1.7141E 9
      240398, 2403,98, 2404,98, 2405,98, 2406,98, 0.2*.333*.8*76.271*1.7141E 9
      300098, 3000,98,  .8*76.271*1.7141E 9
C     201098, 2010,98,  3010,98,  .8*31.503*1.7141E 9  $ OVERPACK SHELL
      301098,           3010,98,  .8*31.503*1.7141E 9  $ OVERPACK SHELL
      201098, 2010,98,  2011,98, 2012,98,  .8*.227256* 1.7141E 9
      201398, 2013,98,  2014,98, 2015,98, 2016,98, .8*.681768* 1.7141E 9
      211098, 2110,98,  2111,98, 2112,98,  .8*.270526* 1.7141E 9
      211398, 2113,98,  2114,98, 2115,98, 2116,98, .8*.811578* 1.7141E 9
      221098, 2210,98,  2211,98, 2212,98,  .8*.271617* 1.7141E 9
      221398, 2213,98,  2214,98, 2215,98, 2216,98, .8*.814851* 1.7141E 9
      231098, 2310,98,  2311,98, 2312,98,  .8*1.33081* 1.7141E 9
      231398, 2313,98,  2314,98, 2315,98, 2316,98, .8*3.99243* 1.7141E 9
      210098, 2100,98,  3100,98,  .8*21.836*1.7141E 9  $ OVERPACK SHELL
      38098,  380,98,             .8*1.0800*1.7141E 9  $ LIFT TRUNNION
      58098,  581,98, 583,98,      .8*2.715*1.7141E 9  $ CENTER TRUNNION
      59098,  591,98, 593,98,      .8*1.545*1.7141E 9  $ CENTER TRUNNION
      78098,  780,98,             .8*2.1600*1.7141E 9  $ LIFT TRUNNION
C
C    DAMAGE RADIATION CONDUCTORS
       248198,  2481,98,           0.0872664*.8*1.7141E 9
C       227198,  2271,98,           0.01*.8*1.7141E 9
C       225098,  2250,98,           0.01*.8*1.7141E 9
C       225298,  2252,98,           0.01*.8*1.7141E 9
C
C     EXTERNAL CONVECTION HEAT TRANSFER
C           ACTUAL RATE DETERMINED BY INTERNAL ROUTINE
      7099,   370,99,   770,99,   1.0                  $ THERMAL SHIELD
      9970, 470,99, 670,99, 1.0                $ THERMAL SHIELD
      9972, 570,99, 572,99, 1.0
      9971, 571,99, 573,99, 1.0
C      200099, 2000,99,  3000,99,  1.0                  $ OVERPACK SHELL
      300099, 3000,99,  1.0                          $ OVERPACK SHELL
      200099, 2000,99, 2001,99, 2002,99,  1.0
      200399, 2003,99, 2004,99, 2005,99, 2006,99, 1.0
      240099, 2400,99, 2401,99, 2402,99,  1.0
      240399, 2403,99, 2404,99, 2405,99, 2406,99, 1.0
C     201099, 2010,99,  3010,99,  1.0                  $ OVERPACK SHELL
      301099,           3010,99,  1.0                  $ OVERPACK SHELL
      201099, 2010,99,  2011,99, 2012,99,  1.0
      201399, 2013,99,  2014,99, 2015,99, 2016,99,   1.0
      211099, 2110,99,  2111,99, 2112,99,  1.0
      211399, 2113,99,  2114,99, 2115,99, 2116,99,   1.0
      221099, 2210,99,  2211,99, 2212,99,  1.0
```

```
      221399, 2213,99,  2214,99, 2215,99, 2216,99,   1.0
      231099, 2310,99,  2311,99, 2312,99,  1.0
      231399, 2313,99,  2314,99, 2315,99, 2316,99,   1.0
      210099, 2100,99,  3100,99,  1.0                  $ OVERPACK SHELL
      38099,  380,99,             1.0                  $ LIFT TRUNNION
      58099,  581,99, 583,99,     1.0                  $ CENTER TRUNNION
      59099,  591,99, 593,99,     1.0                  $ CENTER TRUNNION
      78099,  780,99,             1.0                  $ LIFT TRUNNION
      248199, 2481,98,           0.0872664             $PIN PUNCTURE AREA
C*********************************************************************
HEADER CONTROL DATA, GLOBAL
C*********************************************************************
      ABSZRO  =  459.67
      SIGMA   =    1.0
      EXTLIM  =    1.0
      ITHOLD  =    1
      ITERXT  =    3
      DRLXCA  =     .001
      ARLXCA  =     .001
      ATMPCA  =   10.
      DTMPCA  =   20.
      EBALSA  =     .05
      EBALNA  =     .05
      NLOOPS  = 14000
      ITEROT  = 14001
      NLOOPT  =   80
      OUTPUT  =    0.1
      DTIMEI  =    0.00025
      TIMEO   =    0.0
      TIMEND  =   40.0
      DTIMEH  =    0.00025
C*********************************************************************
HEADER USER DATA, GLOBAL
C*********************************************************************
      GCONST = 32.2
C*********************************************************************
HEADER USER DATA, CASK
C*********************************************************************
      10 = 32.2     $ GC
      11 = 0.0
      12 = 0.0
      13 = 0.0
      14 = 0.0
      15 = 0.0
C*********************************************************************
HEADER ARRAY DATA, CASK
C*********************************************************************
      1 =   $ARGON CONDUCTIVITY   BTU/HR FT F
      32.,.00958,  212.,.0123,  392.,.0147,  572.,.0169
      932.,.0208
      2 =   $AIR CONDUCTIVITY   BTU/HR FT F
      32.,.014,  100.,.0154,  300.,.0193,  500.,.0231
      1000.,.0319,  1500.,.040
      3 =   $AIR SPECIFIC HEAT   BTU/LB F
      32.,0.2402,  100.,0.2402,  300.,0.2432,  500.,0.2472
      1000.,0.2622,  1500.,0.2762
      4 =  $AIR ABSOLUTE VISCOSITY   LB/FT HR
      32.,0.04194,  100.,0.04626,  300.,0.05796
      500.,0.06804,  1000.,0.08892,  1500.,0.1080
C*********************************************************************
HEADER OUTPUT CALLS, CASK
C*********************************************************************
      CALL SORTPR('CASK',0)
      WRITE(6,*)'TIME (HRS) ',TIMEM
      WRITE(6,*)'O RINGS (921, 1031) ',T921,T1031
      WRITE(6,*)'CASK UPPER FORGING (1051) ',T1051
      WRITE(6,*)'CASK/IV LID CENTER (900, 1000) ',T900,T1000
      WRITE(6,*)'CASK BASE (100) ',T100
      WRITE(6,*)'IV/CENTER BASE (205, 200) ',T205, T200
      WRITE(6,*)'WALL TEMPS (551, 520, 515) ',T551, T520, T515
      WRITE(6,*)'PIVOT TRUNNION AREA (571, 591, 546) ', T571, T591, T546
      WRITE(6,*)'CANISTER (805, 515) ', T805, T515
      WRITE(6,*)'CASK INNER WALL/OUTER WALL (530, 551) ',T530, T551
      WRITE(6,*)'LEAD SHIELD (541, 546) ', T541, T546
      WRITE(6,*)'PAYLOAD (36) ',T36
C*********************************************************************
HEADER OPERATION DATA
C*********************************************************************
BUILD 72BCASK, CASK
C      CALL STDSTL
      CALL FWDBCK
```

```
C*********************************************************************
HEADER VARIABLES 1, CASK
C*********************************************************************
C DECAY HEAT PRODUCTION   300 WATTS MAX.
      Q10=  300.* 3.413 /3/7
      Q11=  300. * 3.413/3/7
      Q12=  300. * 3.413/3/7
      Q13=  300. * 3.413/3/7
      Q14=  300. * 3.413/3/7
      Q15=  300. * 3.413/3/7
      Q16=  300. * 3.413/3/7
      Q30=  300. * 3.413/3/7
      Q31=  300. * 3.413/3/7
      Q32=  300. * 3.413/3/7
      Q33=  300. * 3.413/3/7
      Q34=  300. * 3.413/3/7
      Q35=  300. * 3.413/3/7
      Q36=  300. * 3.413/3/7
      Q50=  300. * 3.413/3/7
      Q51=  300. * 3.413/3/7
      Q52=  300. * 3.413/3/7
      Q53=  300. * 3.413/3/7
      Q54=  300. * 3.413/3/7
      Q55=  300. * 3.413/3/7
      Q56=  300. * 3.413/3/7
       IF(TIMEN .LT. 0.51) GO TO 40
C  EXTERNAL SOLAR HEATING
       Q370 = 0.8*634.73                  $ BASED ON PROJECTED AREA
       Q470 = 0.8*710.193                 $ BASED ON PROJECTED AREA
       Q570 = 0.25*0.8*710.193                 $ BASED ON PROJECTED AREA
       Q571 = 0.125*0.8*710.193
       Q572 = 0.25*0.8*710.193
       Q573 = 0.125*0.8*710.193
       Q670 = 0.8*710.193                 $ BASED ON PROJECTED AREA
       Q770 = 0.8*634.73                  $ BASED ON PROJECTED AREA
C        Q2000= 0.52*2984.17                 $ BASED ON PROJECTED AREA
       Q2000= 0.8*.6667*0.0667*2984.17
       Q2001= 0.8*.6667*0.0667*2984.17
       Q2002= 0.8*.6667*0.0667*2984.17
       Q2003= 0.8*.6667*0.2*2984.17
       Q2004= 0.8*.6667*0.2*2984.17
       Q2005= 0.8*.6667*0.2*2984.17
       Q2006= 0.8*.6667*0.2*2984.17
       Q2400= 0.8*.333*0.0667*2984.17
       Q2401= 0.8*.333*0.0667*2984.17
       Q2402= 0.8*.333*0.0667*2984.17
       Q2403= 0.8*.333*0.2*2984.17
       Q2404= 0.8*.333*0.2*2984.17
       Q2405= 0.8*.333*0.2*2984.17
       Q2406= 0.8*.333*0.2*2984.17
       Q3000= 0.8*2984.17                 $ BASED ON PROJECTED AREA
C        Q2010= 0.52*1934.93                 $ BASED ON PROJECTED AREA
       Q2010= 0.8*13.95809                $ BASED ON PROJECTED AREA
       Q2011= 0.8*13.95809                $ BASED ON PROJECTED AREA
       Q2012= 0.8*13.95809                $ BASED ON PROJECTED AREA
       Q2013= 0.8*41.87427                $ BASED ON PROJECTED AREA
       Q2014= 0.8*41.87427                $ BASED ON PROJECTED AREA
       Q2015= 0.8*41.87427                $ BASED ON PROJECTED AREA
       Q2016= 0.8*41.87427                $ BASED ON PROJECTED AREA
       Q2110= 0.8*16.61571                $ BASED ON PROJECTED AREA
       Q2111= 0.8*16.61571                $ BASED ON PROJECTED AREA
       Q2112= 0.8*16.61571                $ BASED ON PROJECTED AREA
       Q2113= 0.8*49.84713                $ BASED ON PROJECTED AREA
       Q2114= 0.8*49.84713                $ BASED ON PROJECTED AREA
       Q2115= 0.8*49.84713                $ BASED ON PROJECTED AREA
       Q2116= 0.8*49.84713                $ BASED ON PROJECTED AREA
       Q2210= 0.8*16.682708               $ BASED ON PROJECTED AREA
       Q2211= 0.8*16.682708               $ BASED ON PROJECTED AREA
       Q2212= 0.8*16.682708               $ BASED ON PROJECTED AREA
       Q2213= 0.8*50.048124               $ BASED ON PROJECTED AREA
       Q2214= 0.8*50.048124               $ BASED ON PROJECTED AREA
       Q2215= 0.8*50.048124               $ BASED ON PROJECTED AREA
       Q2216= 0.8*50.048124               $ BASED ON PROJECTED AREA
       Q2310= 0.8*81.738569               $ BASED ON PROJECTED AREA
       Q2311= 0.8*81.738569               $ BASED ON PROJECTED AREA
       Q2312= 0.8*81.738569               $ BASED ON PROJECTED AREA
       Q2313= 0.8*245.21571               $ BASED ON PROJECTED AREA
       Q2314= 0.8*245.21571               $ BASED ON PROJECTED AREA
       Q2315= 0.8*245.21571               $ BASED ON PROJECTED AREA
       Q2316= 0.8*245.21571               $ BASED ON PROJECTED AREA
       Q3010= 0.8*1934.93                 $ BASED ON PROJECTED AREA
```

```
      Q2100= 0.8*1341.18                $ BASED ON PROJECTED AREA
      Q3100= 0.8*1341.18                $ BASED ON PROJECTED AREA
      Q380 = 0.8*1.0800*39.126
      Q581 = 0.8*166.76
      Q583 = 0.8*166.76
      Q591 = 0.8*48.20
      Q593 = 0.8*48.20
      Q780 = 0.8*2.1600*39.126
C Pin Puncture Area
      Q2481 = 0.8*5.363
  40  CONTINUE
C  EXTERNAL BOUNDARY TEMPERATURES
      T99 = 100.
      T98 = 100.
      IF(TIMEN .LT. 0.01 .OR. TIMEN .GT. 0.51) GO TO 50
      T99 = 1475.
      T98 = 1424.7
 50   CONTINUE
C
C  CALCULATE VARIABLE CONVECTIVE HEAT TRANSFER RATE
M      CALL D1DEG1((T370+T99)/2,A4,XK10)
M      CALL D1DEG1((T370+T99)/2,A3,XK11)
M      CALL D1DEG1((T370+T99)/2,A2,XK12)
      CALL AIRVCV3(T370,T99,16.2230,3.46670,4.173E8,XK10,XK11,XK12,0.081,G7099)
      IF(TIMEN .LT. 0.51000000) G7099 = 16.2230*2.5
M      CALL D1DEG1((T470+T99)/2,A4,XK10)
M      CALL D1DEG1((T470+T99)/2,A3,XK11)
M      CALL D1DEG1((T470+T99)/2,A2,XK12)
      CALL AIRVCV3(T470,T99,18.1510,3.46670,4.173E8,XK10,XK11,XK12,0.081,G9970)
      IF(TIMEN .LT. 0.51000000) G9970 = 18.150*2.5
M      CALL D1DEG1((T570+T99)/2,A4,XK10)
M      CALL D1DEG1((T570+T99)/2,A3,XK11)
M      CALL D1DEG1((T570+T99)/2,A2,XK12)
      CALL AIRVCV3(T570,T99,4.5378,3.46670,4.173E8,XK10,XK11,XK12,0.081,G9972)
      IF(TIMEN .LT. 0.51000000) G9972 = 4.5378*2.5
M      CALL D1DEG1((T571+T99)/2,A4,XK10)
M      CALL D1DEG1((T571+T99)/2,A3,XK11)
M      CALL D1DEG1((T571+T99)/2,A2,XK12)
      CALL AIRVCV3(T571,T99,2.2689,3.46670,4.173E8,XK10,XK11,XK12,0.081,G9971)
      IF(TIMEN .LT. 0.51000000) G9971 = 2.2689*2.5
M      CALL D1DEG1((T3000+T99)/2,A4,XK10)
M      CALL D1DEG1((T3000+T99)/2,A3,XK11)
M      CALL D1DEG1((T3000+T99)/2,A2,XK12)
      CALL AIRVCV3(T3000,T99,76.2710,6.33330,4.173E8,XK10,XK11,XK12,0.081,G300099)
      IF(TIMEN .LT. 0.51000000) G300099 = 76.2710*2.5
M      CALL D1DEG1((T2000+T99)/2,A4,XK10)
M      CALL D1DEG1((T2000+T99)/2,A3,XK11)
M      CALL D1DEG1((T2000+T99)/2,A2,XK12)
      CALL AIRVCV3(T2000,T99,3.3917,6.33330,4.173E8,XK10,XK11,XK12,0.081,G200099)
      IF(TIMEN .LT. 0.51000000) G200099 = 3.3917*2.5
M      CALL D1DEG1((T2400+T99)/2,A4,XK10)
M      CALL D1DEG1((T2400+T99)/2,A3,XK11)
M      CALL D1DEG1((T2400+T99)/2,A2,XK12)
      CALL AIRVCV3(T2400,T99,1.6958,6.33330,4.173E8,XK10,XK11,XK12,0.081,G240099)
      IF(TIMEN .LT. 0.51000000) G240099 = 1.6958*2.5
M      CALL D1DEG1((T2003+T99)/2,A4,XK10)
M      CALL D1DEG1((T2003+T99)/2,A3,XK11)
M      CALL D1DEG1((T2003+T99)/2,A2,XK12)
      CALL AIRVCV3(T2003,T99,10.751,6.33330,4.173E8,XK10,XK11,XK12,0.081,G200399)
      IF(TIMEN .LT. 0.51000000) G200399 = 10.751*2.5
M      CALL D1DEG1((T2403+T99)/2,A4,XK10)
M      CALL D1DEG1((T2403+T99)/2,A3,XK11)
M      CALL D1DEG1((T2403+T99)/2,A2,XK12)
      CALL AIRVCV3(T2403,T99,5.0876,6.33330,4.173E8,XK10,XK11,XK12,0.081,G240399)
      IF(TIMEN .LT. 0.51000000) G240399 = 5.0876*2.5
M      CALL D1DEG1((T3010+T99)/2,A4,XK10)
M      CALL D1DEG1((T3010+T99)/2,A3,XK11)
M      CALL D1DEG1((T3010+T99)/2,A2,XK12)
      CALL AIRVCV3(T3010,T99,31.5030,6.33330,4.173E8,XK10,XK11,XK12,0.081,G301099)
      IF(TIMEN .LT. 0.51000000) G201099 = 31.503*2.5
M      CALL D1DEG1((T2010+T99)/2,A4,XK10)
M      CALL D1DEG1((T2010+T99)/2,A3,XK11)
M      CALL D1DEG1((T2010+T99)/2,A2,XK12)
      CALL AIRVCV3(T2010,T99,0.22726,6.33330,4.173E8,XK10,XK11,XK12,0.081,G201099)
      IF(TIMEN .LT. 0.51000000) G201099 = 0.22726*2.5
M      CALL D1DEG1((T2013+T99)/2,A4,XK10)
M      CALL D1DEG1((T2013+T99)/2,A3,XK11)
M      CALL D1DEG1((T2013+T99)/2,A2,XK12)
      CALL AIRVCV3(T2013,T99,0.681780,6.33330,4.173E8,XK10,XK11,XK12,0.081,G201399)
      IF(TIMEN .LT. 0.51000000) G201399 = 0.68178*2.5
M      CALL D1DEG1((T2110+T99)/2,A4,XK10)
```

```
M      CALL D1DEG1((T2110+T99)/2,A3,XK11)
M      CALL D1DEG1((T2110+T99)/2,A2,XK12)
      CALL AIRVCV3(T2110,T99,0.270530,6.33330,4.173E8,XK10,XK11,XK12,0.081,G211099)
      IF(TIMEN .LT. 0.51000000) G211099 = 0.270530*2.5
M      CALL D1DEG1((T2113+T99)/2,A4,XK10)
M      CALL D1DEG1((T2113+T99)/2,A3,XK11)
M      CALL D1DEG1((T2113+T99)/2,A2,XK12)
      CALL AIRVCV3(T2113,T99,0.811590,6.33330,4.173E8,XK10,XK11,XK12,0.081,G211399)
      IF(TIMEN .LT. 0.51000000) G211399 = .811590*2.5
M      CALL D1DEG1((T2210+T99)/2,A4,XK10)
M      CALL D1DEG1((T2210+T99)/2,A3,XK11)
M      CALL D1DEG1((T2210+T99)/2,A2,XK12)
      CALL AIRVCV3(T2210,T99,0.271620,6.33330,4.173E8,XK10,XK11,XK12,0.081,G221099)
      IF(TIMEN .LT. 0.51000000) G221099 = 0.271620*2.5
M      CALL D1DEG1((T2213+T99)/2,A4,XK10)
M      CALL D1DEG1((T2213+T99)/2,A3,XK11)
M      CALL D1DEG1((T2213+T99)/2,A2,XK12)
      CALL AIRVCV3(T2213,T99,0.818460,6.33330,4.173E8,XK10,XK11,XK12,0.081,G221399)
      IF(TIMEN .LT. 0.51000000) G221399 = 0.818460*2.5
M      CALL D1DEG1((T2310+T99)/2,A4,XK10)
M      CALL D1DEG1((T2310+T99)/2,A3,XK11)
M      CALL D1DEG1((T2310+T99)/2,A2,XK12)
      CALL AIRVCV3(T2310,T99,1.33080,6.33330,4.173E8,XK10,XK11,XK12,0.081,G231099)
      IF(TIMEN .LT. 0.51000000) G231099 = 1.33080*2.5
M      CALL D1DEG1((T2313+T99)/2,A4,XK10)
M      CALL D1DEG1((T2313+T99)/2,A3,XK11)
M      CALL D1DEG1((T2313+T99)/2,A2,XK12)
      CALL AIRVCV3(T2313,T99,3.99240,6.33330,4.173E8,XK10,XK11,XK12,0.081,G231399)
      IF(TIMEN .LT. 0.51000000) G231399 = 3.99240*2.5
M      CALL D1DEG1((T2100+T99)/2,A4,XK10)
M      CALL D1DEG1((T2100+T99)/2,A3,XK11)
M      CALL D1DEG1((T2100+T99)/2,A2,XK12)
      CALL AIRVCV3(T2100,T99,21.8360,6.33330,4.173E8,XK10,XK11,XK12,0.081,G210099)
      IF(TIMEN .LT. 0.51000000) G210099 = 21.8360*2.5
M      CALL D1DEG1((T380+T99)/2,A4,XK10)
M      CALL D1DEG1((T380+T99)/2,A3,XK11)
M      CALL D1DEG1((T380+T99)/2,A2,XK12)
      CALL AIRVCV3(T380,T99,1.08000,6.33330,4.173E8,XK10,XK11,XK12,0.081,G38099)
      IF(TIMEN .LT. 0.51000000) G38099 = 1.08000*2.5
M      CALL D1DEG1((T581+T99)/2,A4,XK10)
M      CALL D1DEG1((T581+T99)/2,A3,XK11)
M      CALL D1DEG1((T581+T99)/2,A2,XK12)
      CALL AIRVCV3(T581,T99,2.715,6.33330,4.173E8,XK10,XK11,XK12,0.081,G58099)
      IF(TIMEN .LT. 0.51000000) G58099 = 2.715*2.5
M      CALL D1DEG1((T591+T99)/2,A4,XK10)
M      CALL D1DEG1((T591+T99)/2,A3,XK11)
M      CALL D1DEG1((T591+T99)/2,A2,XK12)
      CALL AIRVCV3(T591,T99,1.545,6.33330,4.173E8,XK10,XK11,XK12,0.081,G59099)
      IF(TIMEN .LT. 0.51000000) G59099 = 1.545*2.5
M      CALL D1DEG1((T780+T99)/2,A4,XK10)
M      CALL D1DEG1((T780+T99)/2,A3,XK11)
M      CALL D1DEG1((T780+T99)/2,A2,XK12)
      CALL AIRVCV3(T780,T99,2.160,6.33330,4.173E8,XK10,XK11,XK12,0.081,G78099)
      IF(TIMEN .LT. 0.51000000) G78099 = 2.160*2.5
C Pin Puncture Area
M      CALL D1DEG1((T2481+T99)/2,A4,XK10)
M      CALL D1DEG1((T2481+T99)/2,A3,XK11)
M      CALL D1DEG1((T2481+T99)/2,A2,XK12)
      CALL AIRVCV3(T2481,T99,0.0873,0.33330,4.173E8,XK10,XK11,XK12,0.081,G248199)
      IF(TIMEN .LT. 0.51000000) G248199 = 0.0873*2.5
CC    CALL FRCVV(G7099,T370,T99,16.2230,3.46670,XK10,0.0,
CC   *      A3,A2,A4,0.0,14.70,53.350)
CC    CALL FRCVV(G9970,T470,T99,18.1510,3.46670,XK10,0.0,
CC   *      A3,A2,A4,0.0,14.70,53.350)
CC    CALL FRCVV(G9972,T570,T99,4.5378,3.46670,XK10,0.0,
CC   *      A3,A2,A4,0.0,14.70,53.350)
CC    CALL FRCVV(G9971,T571,T99,2.2689,3.46670,XK10,0.0,
CC   *      A3,A2,A4,0.0,14.70,53.350)
C      CALL FRCVV(G200099,T2000,T99,76.2710,6.33330,XK10,0.0,
C     *      A3,A2,A4,0.0,14.70,53.350)
CC     CALL FRCVV(G300099,T2000,T99,76.2710,6.33330,XK10,0.0,
CC     *      A3,A2,A4,0.0,14.70,53.350)
CC      CALL FRCVV(G200099,T2000,T99,3.3917,6.33330,XK10,0.0,
CC     *      A3,A2,A4,0.0,14.70,53.350)
CC     CALL FRCVV(G200399,T2000,T99,10.1751,6.33330,XK10,0.0,
CC     *      A3,A2,A4,0.0,14.70,53.350)
CC      CALL FRCVV(G240099,T2000,T99,1.6958,6.33330,XK10,0.0,
CC     *      A3,A2,A4,0.0,14.70,53.350)
CC      CALL FRCVV(G240399,T2000,T99,5.0876,6.33330,XK10,0.0,
CC     *      A3,A2,A4,0.0,14.70,53.350)
C      CALL FRCVV(G201099,T2010,T99,31.5030,6.33330,XK10,0.0,
```

```
C     *      A3,A2,A4,0.0,14.70,53.350)
CC      CALL FRCVV(G301099,T3010,T99,31.5030,6.33330,XK10,0.0,
CC     *      A3,A2,A4,0.0,14.70,53.350)
CC      CALL FRCVV(G201099,T2010,T99,.227260,6.33330,XK10,0.0,
CC     *      A3,A2,A4,0.0,14.70,53.350)
CC      CALL FRCVV(G201399,T2014,T99,.681780,6.33330,XK10,0.0,
CC     *      A3,A2,A4,0.0,14.70,53.350)
CC      CALL FRCVV(G211099,T2110,T99,.270530,6.33330,XK10,0.0,
CC     *      A3,A2,A4,0.0,14.70,53.350)
CC      CALL FRCVV(G211399,T2114,T99,.811590,6.33330,XK10,0.0,
CC     *      A3,A2,A4,0.0,14.70,53.350)
CC      CALL FRCVV(G221099,T2210,T99,.271620,6.33330,XK10,0.0,
CC     *      A3,A2,A4,0.0,14.70,53.350)
CC      CALL FRCVV(G221399,T2214,T99,.814860,6.33330,XK10,0.0,
CC     *      A3,A2,A4,0.0,14.70,53.350)
CC      CALL FRCVV(G231099,T2310,T99,1.33080,6.33330,XK10,0.0,
CC     *      A3,A2,A4,0.0,14.70,53.350)
CC      CALL FRCVV(G231399,T2314,T99,3.99240,6.33330,XK10,0.0,
CC     *      A3,A2,A4,0.0,14.70,53.350)
CC      CALL FRCVV(G210099,T2100,T99,21.8360,6.33330,XK10,0.0,
CC     *      A3,A2,A4,0.0,14.70,53.350)
CC      CALL FRCVV(G38099, T380, T99,1.08000,6.33330,XK10,0.0,
CC     *      A3,A2,A4,0.0,14.70,53.350)
CC      CALL FRCVV(G58099, T581, T99,2.715,6.33330,XK10,0.0,
CC     *      A3,A2,A4,0.0,14.70,53.350)
CC      CALL FRCVV(G59099, T591, T99,1.545,6.33330,XK10,0.0,
CC     *      A3,A2,A4,0.0,14.70,53.350)
CC      CALL FRCVV(G78099, T780, T99,2.16000,6.33330,XK10,0.0,
CC     *      A3,A2,A4,0.0,14.70,53.350)
C
C  *************************
C  CALCULATE VARIABLE CONDUCTOR VALUES
C  *************************
      CALL D1D1WM(T38, A2, 94.5100,G2838)
      CALL D1D1WM(T220, A2, 798.3690,G220230)
      CALL D1D1WM(T250, A2, 1923.720,G250270)
      CALL D1D1WM(T320, A2, 792.8200,G320330)
      CALL D1D1WM(T350, A2, 1919.360,G350370)
      CALL D1D1WM(T520, A2, 887.0800,G420430)
      CALL D1D1WM(T450, A2, 2137.470,G450470)
      CALL D1D1WM(T550, A2, 534.3675,G550570)
      CALL D1D1WM(T553, A2, 267.1838,G553570)
      CALL D1D1WM(T820, A2, 449.0800,G820830)
      CALL D1D1WM(T820, A2, 7.392330,G820930)
      CALL D1D1WM(T820, A2,22.176990,G820933)
      CALL D1D1WM(T850, A2, 1082.090,G850870)
C     CALL D1D1WM(T920, A2, 177.4150,G920930)
      CALL D1D1WM(T921, A2, 11.82770,G920930)
      CALL D1D1WM(T924, A2, 35.48310,G923933)
C     CALL D1D1WM(T1030, A2, 581.9800,G10301050)
      CALL D1D1WM(T1031, A2, 38.79870,G10301050)
      CALL D1D1WM(T1034, A2,116.39610,G10331053)
      CALL D1D1WM(T215,  A2, 44.48200,G215220)
      CALL D1D1WM(T315,  A2, 50.88700,G315320)
      CALL D1D1WM(T515,  A2, 56.93700,G415420)
      CALL D1D1WM(T815,  A2, 27.40100,G815820)
      CALL D1D1WM(T205,  A2, 88.48800,G200205)
      CALL D1D1WM(T205,  A2, 88.48800,G200205)
      CALL D1D1WM(T901,  A2, 5.899200,G805900)
      CALL D1D1WM(T904,  A2, 17.69760,G805903)
      CALL D1D1WM(T200, A2, 63.00600,G100200)
      CALL D1D1WM(T210, A2, 46.07700,G110210)
      CALL D1D1WM(T210, A2, 69.63800,G120210)
C     CALL D1D1WM(T900, A2, 63.00600,G9001000)
      CALL D1D1WM(T901, A2, 4.200400,G9001000)
      CALL D1D1WM(T904, A2,12.601200,G9031003)
C     CALL D1D1WM(T910, A2,  46.0770,G9101010)
      CALL D1D1WM(T911, A2,  3.07180,G9101010)
      CALL D1D1WM(T914, A2, 9.215400,G9131013)
C     CALL D1D1WM(T920, A2,  69.6390,G9201020)
      CALL D1D1WM(T921, A2,  4.64260,G9201020)
      CALL D1D1WM(T924, A2, 13.92780,G9231023)
C     CALL D1D1WM(T2080, A2, 279.3820,G20801050)
      CALL D1D1WM(T2480, A2, 18.62550,G24801050)
      CALL D1D1WM(T2480, A2, 55.87640,G24831053)
C     CALL D1D1WM(T2080, A2, 284.8600,G2080950)
      CALL D1D1WM(T2080, A2, 18.99070,G2080950)
      CALL D1D1WM(T2080, A2, 56.97200,G2083953)
C      CALL D1D1WM(T2080, A2, 443.7240,G2080850)
      CALL D1D1WM(T2080, A2, 29.5813,G2083850)
      CALL D1D1WM(T2080, A2, 88.7440,G2083850)
```

```
      CALL D1D1WM(T3080, A2, 219.1230,G3080150)
      CALL D1D1WM(T3080, A2, 788.8430,G3080250)
C     CALL D1D1WM(T2090, A2, 236.27400,G20901000)
      CALL D1D1WM(T2091, A2, 3.150330,G20901000)
      CALL D1D1WM(T2094, A2, 9.450990,G20931003)
      CALL D1D1WM(T3090, A2, 236.27400,G3090100)
C     CALL D1D1WM(T2090, A2, 172.78800,G20901010)
      CALL D1D1WM(T3090, A2, 172.78800,G3090110)
      CALL D1D1WM(T2091, A2, 2.303830,G20901010)
      CALL D1D1WM(T2094, A2, 6.911490,G20931013)
C     CALL D1D1WM(T2090, A2, 240.36500,G20901020)
      CALL D1D1WM(T2191, A2, 3.204860,G21901020)
      CALL D1D1WM(T2194, A2, 9.614580,G21931023)
      CALL D1D1WM(T3090, A2, 240.36500,G3090120)
C     CALL D1D1WM(T2090, A2, 246.58200,G20901030)
      CALL D1D1WM(T2191, A2, 3.287770,G21901030)
      CALL D1D1WM(T2194, A2, 9.863310,G21931033)
      CALL D1D1WM(T3090, A2, 246.58200,G3090140)
C     CALL D1D1WM(T2090, A2, 211.19200,G20901050)
      CALL D1D1WM(T2291, A2, 2.815890,G22901050)
      CALL D1D1WM(T2294, A2, 8.447670,G22931053)
      CALL D1D1WM(T3090, A2, 211.19200,G3090150)
C  RESET OUTPUT INTERVAL
      OUTPUT = .1
      IF(TIMEN .GT. 0.40000001) OUTPUT = .050
      IF(TIMEN .GT. 0.70000001) OUTPUT = .200
      IF(TIMEN .GT. 2.00000001) OUTPUT = .5
      IF(TIMEN .GT. 8.00000001) OUTPUT = 2.0
C*************************************************************
HEADER SUBROUTINE DATA
C*********************************************************
include AIRVCV3.F
END OF DATA
Support has ended
Support has ended
Support has ended
Support has ended
Support has ended
Support has ended
Support has ended
The environment variable SINDA_LOC could not be found
Check your .login, .cshrc, .profile or whatever is appropriate
SINDA/FLUINT is not licensed for this machine.
Demo limit of 50 nodes or 10 lumps exceeded.
The environment variable SINDA_LOC could not be found
Check your .login, .cshrc, .profile or whatever is appropriate
SINDA/FLUINT is not licensed for this machine.
Demo limit of 50 nodes or 10 lumps exceeded.
The environment variable SINDA_LOC could not be found
Check your .login, .cshrc, .profile or whatever is appropriate
SINDA/FLUINT is not licensed for this machine.
Demo limit of 50 nodes or 10 lumps exceeded.
The environment variable SINDA_LOC could not be found
Check your .login, .cshrc, .profile or whatever is appropriate
SINDA/FLUINT is not licensed for this machine.
Demo limit of 50 nodes or 10 lumps exceeded.
```

3.6.3 Polyurethane Foam Performance Tests

3.6.3.1 Introduction

(1) During the design phase of the NuPac 125-B cask[1], a rigid unicellular polyurethane foam was selected for the impact absorption medium in the overpacks. The specific product, *LAST-A-FOAM* FR-3700, with a nominal density of 12 lb/ft^3 . The foam, when at a 12 lb/ft^3 density, was designated as "FR-3712".

(2) The NuPac 125-B quarter-scale impact limiters were filled with this product and performed well during the engineering development drop test series. Therefore, the foam in the stated density was selected as the primary impact limiting medium for the full-scale impact limiters.

(3) A series of thermal evaluation tests were conducted on May 2, 1985, to evaluate the foam's performance when subjected to high-temperature thermal input and flame impingement[2]. This was done to assure that the foam would allow the impact limiter to survive the fire test and protect the containment seals from degradation as required by 10 CFR 71[3].

(4) The tests were conducted in accordance with the referenced NuPac test procedure.

3.6.3.2 Test Discussion

(1) A total of three (3) new 5-gallon steel cans were filled with the FR-3712 foam under the same process controls utilized in production. The steel cans were selected to simulate a general impact limiter configuration (the foam encased in a steel shell).

(2) The three (3) foamed cans were then configured for the test series as follows:

(a) One can was left in the as-foamed configuration with the end uncovered. This configuration was selected to simulate a basically undamaged impact limiter with a single opening to expose the foam to flame impingement.

(b) One can was crushed to elongate it approximately 20% at the can diameter. The can was then punctured approximately halfway down one side to a depth of 2 – 3 inches into the foam with a hole approximately 1¼ inches in diameter. The opposite side was cut and the steel shell torn away to expose the foam over a 3/4-inch wide by 3-inch long by 1/4-inch deep area. The can opening was left uncovered. The foam was cracked longitudinally from one end to the other due to crushing. The crack opening was from 1/8-inch to 1/2-inch in width.

This configuration was selected to simulate a severely damaged impact limiter.

---

[1] Nuclear Packaging, Inc., *Safety Analysis Report for the NuPac 125-B Fuel Shipping Package*, USNRC Certificate of Compliance 71-9200, U.S. Department of Energy, Washington, D.C.

[2] General Plastics, *Last-a-Foam FR-3700® for Crash and Fire Protection of Nuclear Material Shipping Containers*, General Plastics Manufacturing Company, 4910 Burlington Way, Tacoma, Washington, February 1990.

[3] Title 10, Code of Federal Regulations, Part 71 (10 CFR 71), *Packaging and Transportation of Radioactive Material*, Final Rule, 01-26-04.

(c) One can was left undamaged and wrapped with two (2) layers of thick fiberglass mat. The can was then closed off with a steel lid. The lid was punctured to exposed the foam to the atmosphere over an area approximately 3 square inches. The puncture extended approximately 2 inches deep into the foam.

This configuration was selected to subject the foam to a high level of heat retention and gas production within the foamed impact limiter. This was done to simulate a relatively undamaged, but highly heated impact limiter.

(3) The foam height was 13¼ inches to 13½ inches in each can.

(4) Each can was instrumented with a thermocouple at the end farthest from the flame.

(5) Each can was then subjected to a 1,800 to 1,850 ºF flame for thirty (30) minutes.

(6) All tests were fully documented with video equipment.

3.6.3.3 Test Results

(1) The undamaged can described in Paragraph (2)(a) of Appendix 3.6.3.2, *Test Discussion*, performed well during the flame test. The test can was sectioned after the flame test. Inspection of the sectioned specimen indicated that the foam exposed to the flame developed a char layer approximately 6 inches high. However, the undamaged foam height only decreased from 13½ inches to 10½ inches. The foam below the char line exhibited no damage, discoloration, or other degradation.

The temperature at the back of the foam opposite the flame increased to 134 ºF during the test. This indicated very good thermal insulation properties for the foam. When the flame was removed, the foam self-extinguished very quickly.

A summary of the test results follows:

- Final Temperature in the Foam at the End Opposite the Flame: 134 ºF
- Remaining Foam Height: 10½ inches
- Char Height: 6 inches
- Duration of Foam Burn after Flame Removal: 1 minute, 26 seconds

(2) The damaged can as described in Paragraph (2)(b) of Appendix 3.6.3.2, *Test Discussion*, also performed well during the flame test. Due to the crushing of the can, the foam was highly cracked. This provided a number of routes for flame progression into the foam. Inspection of the sectioned can showed that the flame had progressed all the way to the bottom of the can. However, observation during the test indicated that about 10 minutes into the 30-minute test many of the flame routes had been closed down by the self-healing properties of the developing char layer.

In particular, the foam char pushing out of the penetrations on the sides of the can completely closed off the flow of flame to the inside of the can at those locations after 10 minutes of the test. This resulted in self-healing of the foam and no further foam damage below the char line in those areas.

The basic foam height remaining after the flame test was 9½ inches of the original 13½ inches. Foam under the char at the various crack lines exhibited no damage or discoloration.

The foam self-extinguished just as quickly after flame removal as the undamaged can discussed in Paragraph (1).

Thermal insulation performance was excellent. Even though the 1,850 ºF flame traveled down the crack network and charred the foam until a distance approximately 3/4 inches from the thermocouple, the temperature at the back of the foam did not exceed 482 ºF.

A summary of the test results follows:

- Final Temperature in the Foam at the End Opposite the Flame: 482 ºF
- Remaining Foam Height: 9½ inches
- Char Height: 6 inches
- Duration of Foam Burn after Flame Removal: 1 minute, 31 seconds

(3) The undamaged and fiberglass-wrapped can described in Paragraph (2)(c) of Appendix 3.6.3.2, *Test Discussion*, performed better than predicted during the flame test. This configuration performed very well in the area of thermal insulation. The maximum temperature noted at the back of the foam was 89 ºF.

The foam continued to burn very slowly through the one hole in the can cover for approximately 5 minutes after the flame was removed. This was due to the gases generated by the retained heat within the foam inside the can. However, the amount of gas, the intensity of the burn and its duration were all lower than expected and therefore, very satisfactory.

Inspection of the sectioned can showed that the char was only 3 inches high due to the restraint provided by the can cover. The remaining foam height was 10¼ inches from a pretest height of 13¼ inches. The foam below the char line was totally undamaged and intact, and appeared as new.

A summary of the test results follows:

- Final Temperature in the Foam at the End Opposite the Flame: 89 ºF
- Remaining Foam Height: 10¼ inches
- Char Height: 2⅜ inches
- Duration of Foam Burn after Flame Removal: 4 minute, 58 seconds

3.6.3.4 Summary

(1) The foam performed very well in the thermal performance evaluation series. The highly damaged sample sustained greater damage due to the cracking and resulting additional flame impingement and convection routes they presented. However, the damaged sample still demonstrated good temperature attenuation and quick self-extinguishing after the flame removal.

The final can, with the fiberglass wrap, was configured to present the worst-case for flame self-extinguishing. It did take the longest to self-extinguish, but still performed far better than expected in the areas of thermal insulation, self-extinguishing, and foam condition after test.

(2) Foam char performance was very good in all cases, with less than 30% of the foam turning to char in the worst case.

(3) Therefore, it is recommended that the FR-3700 series of rigid polyurethane foam be approved for use as the impact absorbing medium in impact limiters subjected to the fire test requirements of 10 CFR 71[3] for Type B containers.

Details of this test program have been incorporated into General Plastics', *Last-a-Foam FR-3700® for Crash and Fire Protection of Nuclear Material Shipping Containers*[2].

3.6.4 Designating an Alternative Seal Material

Rainier Rubber RR0405-70 butyl rubber compound is utilized based on extensive TRUPACT-II qualification testing that closely simulated the required performance characterized by package performance testing[1]. The actual ability of the O-ring seals to meet these requirements is based on the seal material's basic characteristics.

TRUPACT-II qualification testing identified certain key parameters that are important to seal performance. Of these, two important parameters for this application are resistance to helium permeation and acceptable resiliency at cold temperatures. Butyl rubber performs very well resisting helium permeation, and the TR-10 test in ASTM D1329[2] provides an acceptable method for determining cold temperature material resiliency, with the properties of the RR0405-70 acting as a baseline for the required resiliency.

The ability of the compound to withstand elevated temperatures while not having significant reduction in material properties is also required to maintain seal integrity after the hypothetical accident condition thermal event. Material properties in elastomers are reduced through the process of de-polymerization, an aging phenomenon. Elastomer aging can be accelerated by the application of energy (heat). The effect of aging can be quantified by measuring the reduction of physical properties after maintaining the seal material at an elevated temperature for a specific length of time. For the same amount of reduction in properties, a shorter time can be used at a higher temperature, or a longer time can be used at a lower temperature. ASTM D573[3] provides an acceptable method for determining the effects of temperature aging on elastomeric compounds.

ASTM D395[4] provides an acceptable method for determining the effects of compression set. RR0405-70 butyl rubber compound uses an acceptance criterion of less than 25% compression set for 22 hours at an elevated temperature of 70 ºC.

ASTM D2137[5] provides an acceptable method for determining an elastomeric material's ability to withstand cold temperatures and remain pliable. Although the TR-10 test in ASTM D1329 demonstrates the seal material's resiliency at a much lower temperature, this test verifies the seal material's lack of brittleness at the minimum regulatory temperature of -40 ºC.

Hardness or durometer along with tensile strength and elongation are defined and checked to ensure durability of the seal material during operation. ASTM D2240[6] provides an acceptable

---

[1] U.S. Department of Energy (DOE), *Safety Analysis Report for the TRUPACT-II Shipping Package*, USNRC Certificate of Compliance 71-9218, U.S. Department of Energy, Carlsbad Field Office, Carlsbad, New Mexico.

[2] ASTM D1329-88 (re-approved 1998), *Standard Test Method for Evaluating Rubber Property – Retraction at Lower Temperatures (TR Test),* American Society for Testing and Materials, Philadelphia, PA, Volume 09.01, 2001.

[3] ASTM D573-99, *Standard Test Method for Rubber – Deterioration in an Air Oven,* American Society for Testing and Materials, Philadelphia, PA, Volume 09.01, 2001.

[4] ASTM D395-01, *Standard Test Methods for Rubber Property – Compression Set,* American Society for Testing and Materials, Philadelphia, PA, Volume 09.01, 2001.

[5] ASTM D2137-94 (re-approved 2000), *Standard Test Methods for Rubber Property – Brittleness Point of Flexible Polymers and Coated Fabrics,* American Society for Testing and Materials, Philadelphia, PA, Volume 09.02, 2001.

[6] ASTM D2240-00, *Standard Test Method for Rubber Property – Durometer Hardness,* American Society for Testing and Materials, Philadelphia, PA, Volume 09.01, 2002.

method for determining the required 70 ±5 durometer, and ASTM D412[7] provides an acceptable method for determining the required minimum 10 MPa (1,450 psi) tensile strength and minimum 250% elongation, with the properties of the RR0405-70 acting as a baseline for the required hardness, tensile strength, and elongation.

For proprietary seal materials that have fairly demanding requirements such as the RR0405-70 butyl rubber compound, the compound is commonly specified by a company designator and subsequently checked against exacting performance standards. Specifying an elastomeric compound by its chemistry alone is difficult considering the shear number of parameters that affect seal performance. However, by applying the above nationally recognized standards to a material batch, the important parameters are defined for verifying the performance of the seal material.

ASTM D1414[8] is the standard method for testing O-ring seals, and covers most, but not all, of the required testing delineated above. However, due to the overall size of the O-ring seals and the additional testing specified, ASTM D2000[9] provides a better standard classification system.

Each batch of compounded material requires testing, where a "batch" represents the chemical compounding of the material before vulcanizing and a "lot" refers to the quantity of finished product made at any one time.

Using the ASTM D2000 designator, O-ring seals with properties equivalent to RR0405-70 butyl rubber material are classified as follows; this designator callout is currently being specified for the RR0405-70 butyl rubber material, as discussed above, and summarized in the table below:

M4AA710 A13 B13 F17 F48 Z Trace Element

Designator	Condition
M	Metric units designator (default condition)
4	Grade 4 acceptance criteria for the tests specified
AA	Butyl rubber compound
7	70 Shore A durometer hardness per ASTM D2240
10	Tensile strength and elongation per ASTM D 412; acceptance criteria are a minimum 10 MPa (1,450 psi) tensile strength and a minimum 250% elongation
A13	Heat resistance test per ASTM D573; the acceptance criteria are a maximum 10 Shore A durometer hardness increase, a maximum reduction in tensile strength of 25%, and a maximum reduction in ultimate elongation of 25% at 70 ºC

[7] ASTM D412-98a, *Standard Test Methods for Vulcanized Rubber and Thermoplastic Rubbers and Thermoplastic Elastomers – Tension,* American Society for Testing and Materials, Philadelphia, PA, Volume 09.01, 2001.

[8] ASTM D1414-94 (re-approved 1999), *Standard Test Methods for Rubber O-Rings,* American Society for Testing and Materials, Philadelphia, PA, Volume 09.02, 2001.

[9] ASTM D2000-01, *Standard Classification System for Rubber Products in Automotive Applications,* American Society for Testing and Materials, Philadelphia, PA, Volume 09.02, 2001.

Designator	Condition
B13	Compression set per Method B of ASTM D395; acceptance criterion is a maximum 25% compression set after 22 hours at 70 ºC
F17	Cold temperature resistance specifying low temperature brittleness per Method A, 9.3.2, of ASTM D2137; non-brittle after 3 minutes at -40 ºC
F48	Cold temperature resiliency, where F is for cold temperature resistance, and 4 specifies testing to the TR-10 test of ASTM D1329; 8 indicates a TR-10 temperature of -50 ºC (-58 ºF), or less
Z Trace Element	Z designator allows specific notes to be added; "Z Trace Element" allows trace elements to be added to the elastomeric compound to meet the seal material requirements

Using the above seal material designator, the acceptable seal material for the RH-TRU 72-B package are O-ring seals meeting the SAR drawing requirements and specified as:

> "Butyl rubber material per Rainier Rubber RR0405-70, or equivalent, meeting the requirements of ASTM D2000 M4AA710 A13 B13 F17 F48 Z Trace Element"

This page intentionally left blank.

4.0 CONTAINMENT

4.1 Containment Boundary

This section identifies the containment boundary considered for the RH-TRU 72-B package.

4.1.1 Containment Vessel

Two independent levels of containment are established within the RH-TRU 72-B package. In general, each containment vessel is constructed primarily of ASTM A240, Type 304, austenitic stainless steel for the shells, and ASTM A240, Type 304, or ASTM A182, Type F304, austenitic stainless steel for the lids and end closures. The exceptions are so noted in the following detailed descriptions.

4.1.1.1 Inner Vessel

The inner vessel (IV) containment boundary is identified as the 32-inch outside diameter by 3/8-inch thick shell, the 1½-inch thick bottom closure, the lid-end forging, and the 6½-inch thick IV lid, complete with the lid's middle O-ring seal, the gas sampling port closure bolt with the closure bolt outer O-ring seal, and the backfill port closure bolt with the closure bolt O-ring seal. The sealing surfaces are machined to a maximum of 125 RMS micro-finish for sealing reliability.

With reference to Appendix 1.3.1, *Packaging General Arrangement Drawings*, the IV containment boundary consists of the following components:

1. A 1½-inch thick, Type 304 or Type F304 stainless steel bottom closure,

2. A 3/8-inch thick, 32-inch outside diameter, Type 304 stainless steel shell, with a full length, full penetration seam weld,

3. A full-penetration girth weld joining the shell to the bottom forging,

4. An upper end (lid-end), Type F304 stainless steel ring forging,

5. A full-penetration girth weld joining the upper end ring forging to the shell,

6. A 6½-inch thick, Type 304 or Type F304 stainless steel lid,

7. A butyl containment O-ring seal that forms the seal between the upper end forging and the lid (the containment O-ring seal is the middle of the three IV closure seals),

8. A Type 304 or Type 316 stainless steel gas sampling port insert, containing a Nitronic 60 closure bolt with butyl O-ring seal (the upper O-ring seal is the containment seal),

9. A 1/4-inch bevel weld which seals the gas sampling port insert to the lid,

10. A Type 304 or Type 316 stainless steel backfill port insert, containing a Nitronic 60 closure bolt with butyl O-ring seal,

11. A 1/4-inch bevel weld which seals the backfill port insert to the lid,

12. A Type 304 or Type 316 stainless steel test port insert, and

13. A 1/4-inch bevel weld which seals the test port insert to the lid.

The inside diameter of the IV is 31¼ inches. Two (2) intermediate support rings and a pair of optional guide rails are located inside the IV for payload canister support. Including the support rings, guide rails, and upper forging, a 26½-inch diameter by 121½-inch long cavity is provided within the IV for the packaging payload.

The specific IV containment components are illustrated in Figure 4.1-1.

The weight of the IV is approximately 4,023 pounds (1,825 kg), the overall length is 130 inches, and the outside diameter is 32 inches.

The non-Type 304 stainless steel components utilized in the IV containment boundary are the butyl O-ring seals (containment seals for the gas sampling port closure bolt, backfill port closure bolt, and the lid), and the Nitronic 60 gas sampling port and backfill port closure bolts.

4.1.1.2 Outer Cask

The outer cask (OC) containment boundary is identified as the 32 3/8-inch inside diameter by 1-inch thick inner shell, the 5-inch thick OC bottom end plate, the closure end forging, and the 6-inch thick OC lid, complete with the lid inner O-ring seal and the gas sampling port closure bolt with closure bolt O-ring seal. The sealing surfaces are machined to a maximum of 125 RMS micro-finish for sealing reliability.

With reference to Appendix 1.3.1, *Packaging General Arrangement Drawings*, the OC containment boundary consists of the following components:

1. A 5-inch thick, Type 304 or Type F304 stainless steel bottom closure,

2. A 1-inch thick, 34⅜-inch outside diameter, Type 304 stainless steel inner shell, with a full length, full penetration seam weld,

3. A full-penetration girth weld joining the inner shell to the bottom forging,

4. An upper end (lid-end), Type F304 stainless steel ring forging,

5. A full-penetration girth weld joining the upper end ring forging to the inner shell,

6. A 6-inch thick, Type 304 or Type F304 stainless steel lid,

7. A butyl containment O-ring seal that forms the seal between the upper end forging and the lid (the containment O-ring seal is the innermost of the two OC closure seals),

8. A Type 304 or Type 316 stainless steel gas sampling port insert, containing a Nitronic 60 closure bolt with butyl O-ring seal,

9. A 1/4-inch bevel weld which seals the gas sampling port insert to the lid,

10. A Type 304 or Type 316 stainless steel test port insert, and

11. A 1/4-inch bevel weld which seals the test port insert to the lid,

12. A 32⅜-inch diameter by 130¾-inch long cavity is provided within the OC for the IV.

The specific OC containment components are illustrated in Figure 4.1-2.

The non-Type 304 stainless steel components utilized in the OC containment boundary are the butyl O-ring seals (containment seals for the gas sampling port closure bolt and the lid), and the Nitronic 60 gas sampling port closure bolt.

Inadvertent opening of the package closures cannot occur for the RH-TRU 72-B package. Following installation of the packaging payload, the IV lid is secured via eight (8), 7/8-9UNC bolts. The OC closure lid is then secured via eighteen (18), 1¼-7UNC bolts, thus eliminating access to the IV closure. The closure-end impact limiter is attached using six (6), 1¼-7UNC bolts. When installed, the impact limiter eliminates access to the OC closure. With this double closure design coupled with the presence of the impact limiter, inadvertent opening of the package cannot occur.

4.1.2 Containment Penetrations

The only containment penetrations into each of the two containment vessels, the IV and OC, are the test and gas sampling ports, and the lids themselves. In addition, the IV has a backfill port. The detail of each penetration is shown in Appendix 1.3.1, *Packaging General Arrangement Drawings*. Each penetration is designed to maintain a leakage rate not to exceed 1×10^{-7} standard cubic centimeters per second (scc/sec), air, so defined as "leaktight" per ANSI N14.5[1], for all normal conditions of transport (NCT) and hypothetical accident conditions (HAC). All IV penetrations are covered by the OC lid, and all OC penetrations are covered by the impact limiters. These coverings, along with tamper-indicating lock wires, ensure that unauthorized operation is precluded.

4.1.3 Seals and Welds

4.1.3.1 Seals

Seals affecting containment are described above. A summary of seal testing prior to first use, during routine maintenance, and upon assembly for transportation is as follows.

4.1.3.1.1 Fabrication Leakage Rate Test

During fabrication, following the pressure testing per Section 8.1.2.2, *Inner Vessel and Outer Cask Pressure Testing*, both the OC and IV shall be individually tested per the *Fabrication Leakage Rate Test*, delineated in Section 8.1.3, *Fabrication Leakage Rate Tests*. This test verifies the containment integrity of the RH-TRU 72-B package to a leakage rate not to exceed 1×10^{-7} scc/sec, air.

4.1.3.1.2 Maintenance Leakage Rate Tests

The *Maintenance Leakage Rate Test* delineated in Section 8.2.2, *Maintenance/Periodic Leakage Rate Tests*, shall be performed on the package annually. Additionally, upon repair of an O-ring sealing surface, and/or replacement of a containment O-ring seal, a gas sampling port closure bolt, or a backfill port closure bolt (IV only), the appropriate section of the *Maintenance Leakage*

[1] ANSI N14.5-1997, *American National Standard for Radioactive Materials – Leakage Tests on Packages for Shipment,* American National Standards Institute, Inc. (ANSI).

Rate Test delineated in Section 8.2.2, *Maintenance/Periodic Leakage Rate Tests*, shall be performed to verify that the repaired or replaced component is maintained to be "leaktight" per ANSI N14.5[1]. This test verifies the sealing integrity of the RH-TRU 72-B package to a leakage rate not to exceed 1×10^{-7} scc/sec, air.

4.1.3.1.3 Preshipment Leakage Rate Test

Prior to shipment of the loaded RH-TRU 72-B package, the OC shall be leakage rate tested per the *Preshipment Leakage Rate Test* delineated in Appendix 7.4.1, *Preshipment Leakage Rate Test*. As an option, the IV may also be leakage rate tested per the *Preshipment Leakage Rate Test* delineated in Appendix 7.4.1, *Preshipment Leakage Rate Test*.

As an option, the *Maintenance Leakage Rate Test* delineated in Section 8.2.2, *Maintenance/Periodic Leakage Rate Tests*, may be performed in lieu of the *Preshipment Leakage Rate Test*.

4.1.3.2 Welds

All containment vessel welds are full penetration welds that have been radiographic or ultrasonic test inspected to ensure structural integrity. All containment boundary welds are confirmed to be leaktight per the *Fabrication Leakage Rate Test*, delineated in Section 8.1.3, *Fabrication Leakage Rate Tests*.

4.1.4 Closure

4.1.4.1 Outer Cask Closure

Closure of the OC is effected by eighteen (18), ASTM A320, Grade L43, alloy steel, 1¼-7UNC cap screws tightened to 600 – 700 lb-ft torque.

4.1.4.2 Inner Vessel Closure

Closure of the IV is effected by the eight (8), ASTM A320, Grade L43, alloy steel, 7/8-9UNC cap screws tightened to 100 – 200 lb-ft torque.

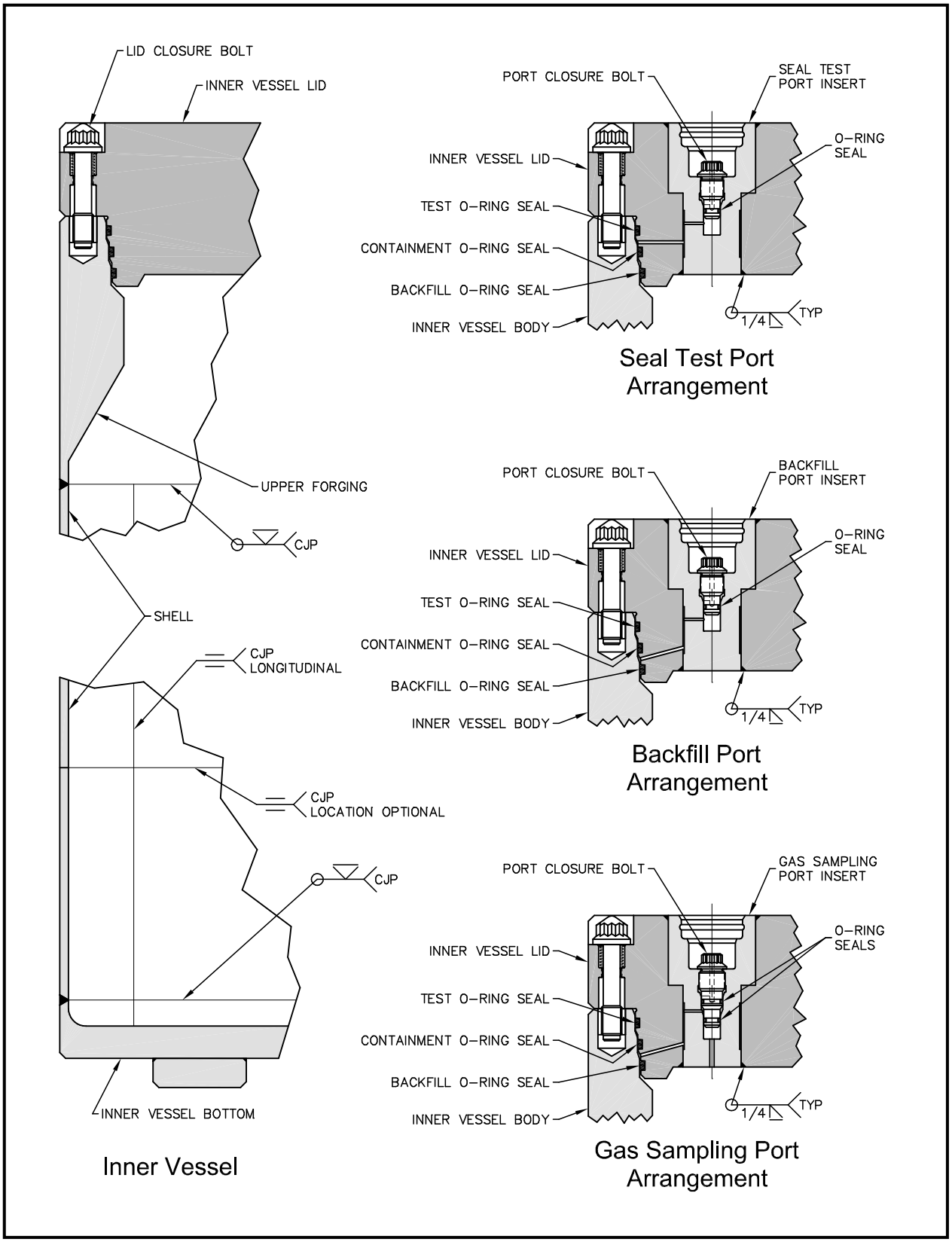

Figure 4.1-1 – Inner Vessel Containment Components

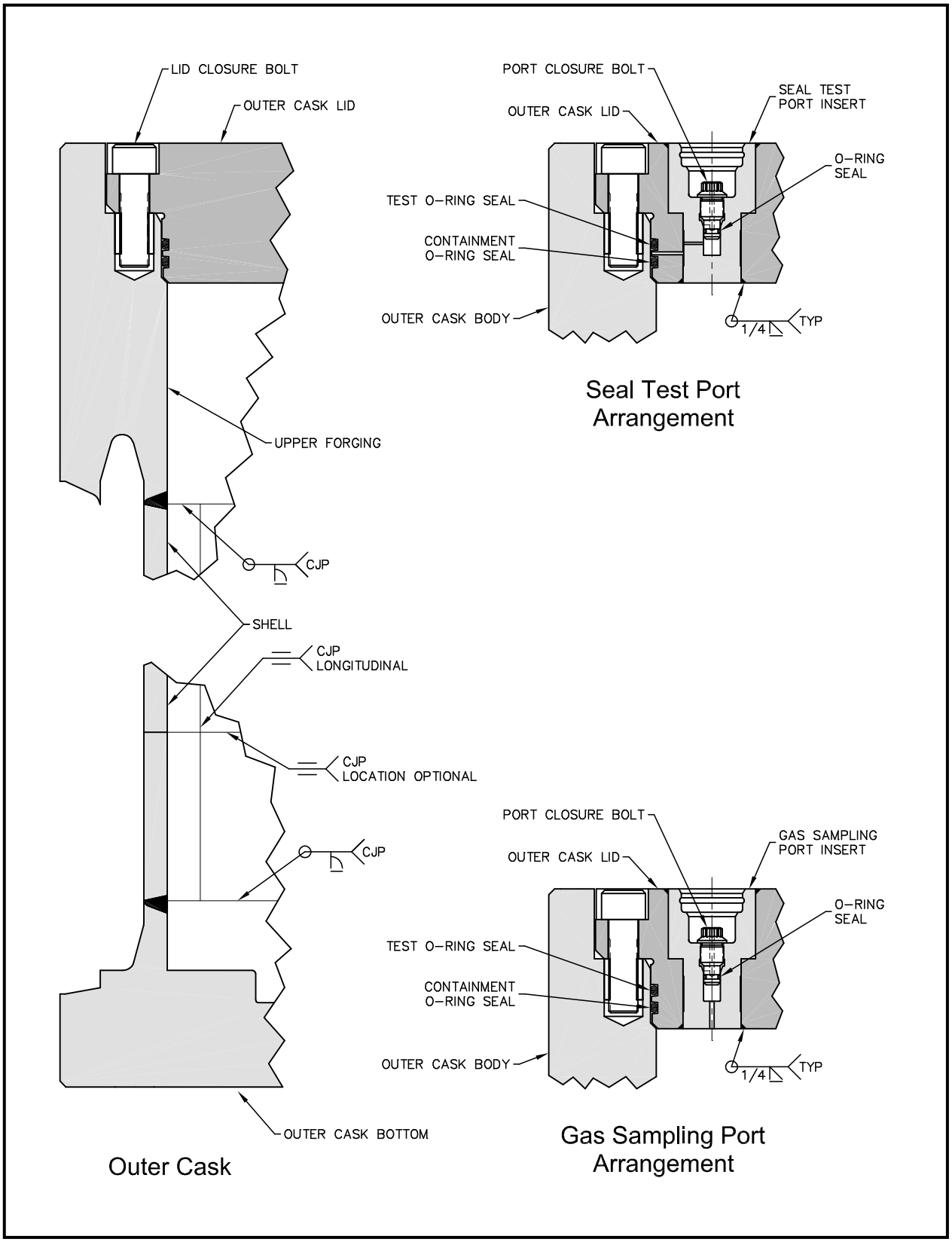

Figure 4.1-2 – Outer Cask Containment Components

4.2 Requirements for Normal Conditions of Transport

The results of the structural analyses performed in Chapter 2.0, *Structural Evaluation*, and the thermal analyses performed in Chapter 3.0, *Thermal Evaluation*, verify that there will be no release of radioactive materials per the "leaktight" criterion of ANSI N14.5[1] under any of the normal conditions of transport (NCT).

4.2.1 Containment of Radioactive Material

The "leaktight" containment criterion of ANSI N14.5[1] specified for the structure and seals of the RH-TRU 72-B package ensures that the requirements of 10 CFR §71.51[2] are satisfied under NCT.

4.2.2 Pressurization of Containment Vessel

The design pressure of both the RH-TRU 72-B package's inner vessel (IV) and outer cask (OC) is 150 psig. Results from the analyses presented in Section 3.4.4, *Maximum Internal Pressure*, verify that any increase in pressure, due to an increase in temperature of the initial package gas atmosphere or due to the water vapor pressure from the water assumed present in the vessel cavity, will be equal to or less than 150 psig within both the IV and OC. A pressure increase to 150 psig in either containment vessel will not reduce the effectiveness of the RH-TRU 72-B package to maintain containment integrity per Section 4.2.1, *Containment of Radioactive Material*.

4.2.3 Containment Criterion

The IV and OC shall be leakage rate tested as described in Section 4.1.3.1.1, *Fabrication Leakage Rate Test*, Section 4.1.3.1.2, *Maintenance Leakage Rate Tests*, and Section 4.1.3.1.3, *Preshipment Leakage Rate Test*, to demonstrate the containment criterion of Section 4.2.1, *Containment of Radioactive Material*, at the completion of fabrication, for maintenance, or for assembly verification prior to transport, respectively.

[1] ANSI N14.5-1997, *American National Standard for Radioactive Materials – Leakage Tests on Packages for Shipment,* American National Standards Institute, Inc. (ANSI).

[2] Title 10, Code of Federal Regulations, Part 71 (10 CFR 71), *Packaging and Transportation of Radioactive Material*, Final Rule, 01-26-04.

This page intentionally left blank.

4.3 Containment Requirements for the Hypothetical Accident Conditions

The results of the structural analyses performed in Chapter 2.0, *Structural Evaluation*, and the thermal analyses performed in Chapter 3.0, *Thermal Evaluation*, verify that there will be no release of radioactive materials per the "leaktight" criterion of ANSI N14.5[1] under any of the hypothetical accident conditions (HAC).

The RH-TRU 72-B package containment O-ring seals are fabricated from Rainier Rubber butyl compound RR0405-70, or equivalent, per ASTM D2000 M4AA710 A13 B13 F17 F48 Z Trace Element. This compound was extensively tested under a wide range of compression and temperature conditions during the development program for the TRUPACT-II package (NRC Certificate of Compliance No. 71-9218) [2]. The worst service condition for the O-ring seals was found to be at the minimum temperature of -20 ºF. At this low temperature, the loss of seal material resiliency is greatest. Consequently, sudden offset of the lid could result in loss of leaktight sealing capability. The TRUPACT-II package test conditions included imposing nominal seal compression (centered lid condition) at the minimum service temperature, followed immediately by minimum compression (simulating full lid offset). Under these test conditions, it was determined that a minimum residual compression of approximately 15% was required to maintain consistent "leaktight" sealing capability for the butyl seal material. Additional testing of Rainier Rubber Butyl Compound RR0405-70 was performed during development of the RTG Package (DOE Certificate of Compliance No. 71-9904)[3]. That testing demonstrated that compressions as low as 10% will still result in a "leaktight" seal at both hot (at and above 350 ºF) and cold (-40 ºF) conditions.

The inner vessel (IV) closure seal configuration consists of three O-ring bore seals, each located on a different diameter of the IV lid (see Appendix 1.3.1, *Packaging General Arrangement Drawings*, for details). The middle O-ring seal is defined as the containment boundary (the inner O-ring seal retains the test gas for helium leakchecking, while the outer O-ring seal provides an annulus in which to establish a vacuum for leakchecking). In order to determine the minimum compression that may occur on the IV containment O-ring seal, the largest tolerance stackup on the lid, flange, and O-ring seal groove dimensions are utilized. The smallest radial gap occurs at the location of

---

[1] ANSI N14.5-1997, *American National Standard for Radioactive Materials – Leakage Tests on Packages for Shipment,* American National Standards Institute, Inc. (ANSI).

[2] U.S. Department of Energy (DOE), *Safety Analysis Report for the TRUPACT-II Shipping Package*, USNRC Certificate of Compliance 71-9218, U.S. Department of Energy, Carlsbad Field Office, Carlsbad, New Mexico.

[3] DOE Docket No. 94-6-9904, *Radioisotope Thermoelectric Generator Transportation System Safety Analysis Report for Packaging*, WHC-SD-RTG-SARP-001, prepared for the U.S. Department of Energy Office of Nuclear Energy under Contract No. DE-AC06-87RL10930 by Westinghouse Hanford Company, Richland, WA. Per Appendix 2.10.6 of the TRUPACT-II SAR, elevated temperature tests were performed on Rainier Rubber Company butyl rubber compound No. RR0405-70 O-ring seals with seal compressions as low as 10%. The specific time-temperature test parameters evaluated were 380 ºF for 24 hours followed by 350 ºF for 144 hours, for a total of 168 hours (1 week). At these temperatures, all elastomeric compounds are susceptible to relatively high helium permeability; thus, helium leak testing was not performed. Instead, a hard vacuum of less than 0.0029 psia (20 Pa) was maintained on the test O-ring seals with no measurable pressure loss that would indicate leakage. At the end of the entire test sequence, the test O-ring seals were stabilized at -20 ºF and shown, via helium leak testing, to be leaktight (i.e., a leakage rate less than 1×10^{-7} standard cubic centimeters per second (scc/s), air leakage).

the upper O-ring seal. The maximum upper flange inside diameter at this location is 28.006 inches. The minimum IV lid diameter at the same location is 27.990 – 0.005 = 27.985 inches. Therefore, the maximum possible radial clearance for a centered lid is ½(28.006 – 27.985) = 0.0105 inches (round to 0.011 inches).

The minimum containment O-ring seal groove diameter is 27.368 inches. The maximum upper flange diameter at this point is 27.806 inches, for a maximum radial space for the containment O-ring seal with a centered lid of of ½(27.806 – 27.368) = 0.219 inches. The maximum possible clearance between the bottom of the O-ring seal groove and the adjacent sealing surface on the upper flange for a shifted lid is thus 0.011 + 0.219 = 0.230 inches. The minimum IV O-ring seal cross-sectional diameter is 0.275 – 0.003 = 0.272 inches. The minimum possible residual O-ring seal compression is thus (0.272 – 0.230)/0.272 × 100% = 15%. Given the O-ring seal test results, the current IV containment seal design is adequate to ensure that a minimum residual O-ring seal compression will be maintained under worst-case tolerance stackup and lid offset conditions.

The outer cask (OC) closure seal configuration consists of two O-ring bore seals, both at the same diameter on the OC lid (see Appendix 1.3.1, *Packaging General Arrangement Drawings*, for details). The inner O-ring seal is defined as the containment seal (the outer O-ring seal provides a vacuum annulus for helium leakchecking, where the test gas is contained in the void space between the IV and OC). The OC upper flange diameter at the containment O-ring seal location is 32.893 ± 0.003 inches.

The maximum possible OC lid offset condition will occur when the lid outside diameter is at its minimum value (32.861 inches), and the flange inside diameter is maximum (32.896 inches). In this case, the maximum possible radial clearance for a centered lid is ½(32.896 – 32.861) = 0.0175 inches. The maximum containment O-ring seal diameter is 32.265 inches. The maximum radial space for the containment O-ring seal with a centered lid is therefore ½(32.896 – 32.265) = 0.3155 inches. The maximum possible clearance between the bottom of the O-ring seal groove and the adjacent flange sealing surface for a shifted lid is thus 0.0175 + 0.3155 = 0.333 inches. Minimum O-ring seal compression will therefore be (0.387 – 0.333)/0.387 × 100% = 14% residual O-ring seal squeeze, which is above the required minimum value of 10%, as determined by seal test results.

4.3.1 Fission Gas Products

There are no fission gas products in the RH-TRU 72-B package.

4.3.2 Containment of Radioactive Material

The "leaktight" containment criterion of ANSI N14.5[1] specified for the structure and seals of the RH-TRU 72-B package ensures that the requirements of 10 CFR §71.51[4] are satisfied under HAC. The "leaktight" containment design will be verified by the fabrication leak checks of the initial production packaging (refer to Section 8.1.3, *Fabrication Leakage Rate Tests*, for details).

[4] Title 10, Code of Federal Regulations, Part 71 (10 CFR 71), *Packaging and Transportation of Radioactive Material*, Final Rule, 01-26-04.

4.3.3 Containment Criterion

The RH-TRU 72-B package has been designed, constructed, and verified by leakage rate testing to meet the "leaktight" criterion established in ANSI N14.5[1].

The results of the structural analyses performed in Chapter 2.0, *Structural Evaluation*, and the thermal analyses performed in Chapter 3.0, *Thermal Evaluation*, verify that the RH-TRU 72-B package will meet the "leaktight" criterion of ANSI N14.5[1] under HAC (refer specifically to Section 2.7.8, *Summary of Damage*). These results verify, structurally, there is no compromise of the containment boundary for HAC. These results verify, thermally, that seal surface temperatures remain low enough to prevent deformation of the sealing materials such that the "leaktight" criterion is maintained.

The only damage arising from normal conditions of transport (NCT) involves minor deformations to the impact limiter(s) that have no effect on packaging containment ability. The analyses presented in Section 2.7.1, *Free Drop*, through Section 2.7.7, *Deep Water Immersion Test*, show that the HAC test sequence will not result in any significant structural damage to the RH-TRU 72 B packaging. Nearly all permanent damage occurs in the external impact limiters, as desired. Minor amounts of damage can occur to packaging components as follows:

In the HAC 30-foot free drop event, a conservatively maximum bounding lead slump of 0.513 inches is estimated, as delineated in Paragraph (9) of Section 2.7.1.1, *Flat End Drop*. However, as demonstrated in testing of the NuPac 125-B cask[5], no measurable lead slump would actually be expected to occur in the RH-TRU 72-B package as a result of flat end drop. For the 40-inch drop on a 6-inch diameter puncture bar, occurring on the side of the package at midlength, localized OC damage can occur at the impact point. However, overall bending response of the package remains elastic. Additionally, the OC outer shell will not be perforated, and no melting of the lead shielding would occur in the ensuing HAC fire event.

Localized puncture damage would occur in the form of a reduction in lead thickness adjacent to the point of impact of the puncture bar. Pin punch results from the NuPac 125-B quarter-scale drop tests[5] were analyzed to provide a conservative estimate of similar damage that could be expected for the RH-TRU 72-B package. It was determined that a 40-inch side drop on the puncture bar causes, at most, a 35% localized reduction in the thickness of the lead shielding on the NuPac 125-B cask. This estimate is conservative for the RH-TRU 72-B package because it is significantly lighter in weight than the NuPac 125-B cask, and therefore puncture-induced deformations would be expected to be less.

As documented in Section 2.7.3, *Puncture*, puncture on the lid-end of the package can result in a slight, permanent inward deformation of the OC lid. However, stress levels remain modest, and the inward deformation is very small and has been shown to increase containment O-ring seal compression. As such, the lid-end puncture event does not adversely affect containment integrity.

These permanent deformations are of little consequence for the RH-TRU 72-B package as they represent only minor changes in packaging geometry. In particular, damage is not sufficient to compromise "leaktightness" of the IV or OC containment boundaries. Lead deformation is only

[5] Nuclear Packaging, Inc., *Safety Analysis Report for the NuPac 125-B Fuel Shipping Package*, USNRC Certificate of Compliance 71-9200, U.S. Department of Energy, Washington, D.C.

of concern relative to shielding. The worst-case puncture damage is therefore addressed in the shielding evaluation in Chapter 5.0, *Shielding Evaluation*. For these reasons, the integrity of the package is not considered to be compromised by the HAC test sequence set forth in 10 CFR 71[4].

Finally, as detailed in Section 4.3, *Containment Requirements for the Hypothetical Accident Conditions*, full lateral offset of the IV and OC lids that might result from side drop or side puncture will not compromise the containment seals leaktight capability. This is because, as demonstrated in the referenced section, O-ring seal compression remains above the minimum 10% required value under worst-case tolerance stackup and lid offset.

5.0 SHIELDING EVALUATION

The RH-TRU 72-B packaging provides sufficient shielding to ensure that for the authorized contents, the package will comply with the radiation dose rate limits given in 10 CFR §71.47(b)[1] for normal conditions of transport (NCT) and §71.51(a)(2) for hypothetical accident conditions (HAC). Compliance with the NCT radiation dose rate limits is demonstrated by pre-shipment radiological surveys of the package after loading. For the *General Payload Case*, compliance with the HAC dose rate limit is achieved by imposing activity limits for individual radionuclides and using the method of summing partial fractions for multiple radionuclide payloads. For the *Controlled Self-Shielding Payload Case*, the HAC dose rate limit is met by compliance with the NCT dose rate limits in addition to being supplemented by imposing activity limits for individual radionuclides and using the method of summing partial fractions for multiple radionuclide payloads.

5.1 Discussion and Results

The RH-TRU 72-B package transports payload canisters that contain gamma and neutron sources. The gamma sources are primarily fission products or bi-product material mixed in various waste forms that are of sufficient strength to require shielding. The neutron source material is of lower source strength, and specific neutron shielding is not required.

The steel canister, steel inner vessel (IV), and the steel and lead outer cask (OC) provide the required gamma shielding in the radial direction for the authorized contents. The impact limiters provide modest neutron shielding and spacing that reduces the magnitude of the surface dose rate near the ends of the package. Thick steel end plates and lids, along with the impact limiters, provide shielding and spacing to reduce the dose rates to acceptable levels out the ends of the package. The shielding evaluation is based on the radial direction because it represents the worst case: the relative spacing between the source and the detector location is least, and the effective shielding, including puncture damage, is lowest. The effects of the impact limiters are conservatively ignored.

There are two categories of authorized contents:

- *General Payload Case*
- *Controlled Self-Shielding Payload Case*

The *General Payload Case* bounds any authorized contents, regardless of form or configuration. The NCT dose rate limits are met by measurement, but because the payload form and configuration are not controlled, the HAC dose rate limits are met by restricting the allowable activity of the contents. The HAC model is described in Section 5.3, *Model Specification*. The HAC activity limits are given in Table 5.1-1 for all radionuclides known in the RH inventory as given in Table 5.1-2. Additionally, radionuclides may be assigned HAC activity limits through the methodologies defined in Appendix 5.5.3, *Screening Methodology for Neutron Emitting Isotopes*, and Appendix 5.5.4, *Screening Methodology for Gamma Emitting Isotopes*.

[1] Title 10, Code of Federal Regulations, Part 71 (10 CFR 71), *Packaging and Transportation of Radioactive Material*, Final Rule, 01-26-04.

For waste that is constrained in terms of payload form and configuration, as certified by the processes defined in *Remote-Handled Transuranic Waste Authorized Methods for Payload Control* (RH-TRAMPAC)[2], the *Controlled Self-Shielding Payload Case* applies. Evaluations in Appendix 5.5.5, *Evaluation of the Effect of NCT to HAC Changes on Neutron Dose Rates*, and Appendix 5.5.6, *Evaluation of the Effect of NCT-to-HAC Changes on Gamma Dose Rates*, demonstrate that the HAC limits are satisfied by meeting the NCT dose rate limits at the time of shipment. Additionally, HAC dose rate compliance through NCT surveys is supplemented by limiting the activity of radionuclides in the *Controlled Self-Shielding Payload Case* to 15 times the values calculated for the *General Payload Case*.

NCT and HAC shielding requirements are established by the following criteria:

Normal Conditions of Transport:

The RH-TRU 72-B package is transported by exclusive use shipment. The NCT radiation dose rate limits given in 10 CFR §71.47(b)[1] are conservatively adapted for the shielding evaluation as follows:

- A maximum of 200 mrem/hr at the external surface of the package, as presented for transport,
- A maximum of 10 mrem/hr at any point 2 meters from the external surface of the package, as presented for transport, and
- A maximum of 2 mrem/hr in any normally occupied space.

Compliance with these limits is verified at time of shipment by preshipment radiological survey of the loaded package and transporter, using a calibrated radiation detector under the control of the quality assurance program.

Hypothetical Accident Conditions:

The maximum dose rate under HAC given in 10 CFR §71.51(a)(2)[1] is 1,000 mrem/hr at any point one meter from the package. The RH-TRU 72-B package undergoes damage as a result of the HAC events. The shielding evaluations leading to the Table 5.1-1 HAC activity limits and the Appendix 5.5.3, *Screening Methodology for Neutron Emitting Isotopes*, and Appendix 5.5.4, *Screening Methodology for Gamma Emitting Isotopes*, screening methods represent a conservative model of the effects of the damage (see Figure 5.1-1):

- The impact limiters are assumed to be absent. Although they sustain crush damage during the HAC events, they are shown in Chapter 2.0, *Structural Evaluation*, to remain in place. Since the presence of the impact limiters in the radial direction offers little shielding or spacing in the HAC shielding calculation, neglecting the impact limiters is a minor, but conservative effect.
- Puncture damage is conservatively modeled to provide maximum damage in the location that causes the greatest effect. The distance from the package to the detector location is measured from the puncture damage.

[2] U.S. Department of Energy (DOE), *Remote-Handled Transuranic Waste Authorized Methods for Payload Control* (RH-TRAMPAC), U.S. Department of Energy, Carlsbad Field Office, Carlsbad, New Mexico.

- The radiological source is assumed to reconfigure to a point source oriented at the location, just inside the payload canister, closest to the puncture damage location.
- The payload canister is assumed to be pressed to the inside of the IV wall.

Each inventory radionuclide is evaluated to determine its gamma and/or neutron source spectrum. The maximum activity of each isotope is then found by calculating the activity that leads to the dose rate limit for the HAC model. The gamma evaluation given in Section 5.4.1, *Gamma Shielding Evaluation*, involves discrete point source calculations, in one dimension, and ignores any self-shielding. The neutron evaluation given in Section 5.4.2, *Neutron Shielding Evaluation*, includes a three-dimensional Monte Carlo N-Particle Transport Code (MCNP[3]) dose rate calculation for each isotope, adjusted with a derived conservative subcritical multiplication factor (Appendix 5.5.2, *Derivation of MCNP Neutron Subcritical Multiplication Factor*). The neutron source strength is based on a uranium oxide matrix to account for alpha-n production, but conservatively neglects self-shielding effects. Mixtures of isotopes are limited by the sum of the fractions method given in Section 5.4.3, *Total Radiation Source*.

[3] J. F. Breismeister, Editor, *MCNP – A General Monte Carlo Code N-Particle Transport Code, Version 4B*, LA-12625-M, Los Alamos National Laboratory, Los Alamos, New Mexico, 1997.

Table 5.1-1 – Summary of HAC Activity Limits

Radionuclide Name	Gamma Emitter	Neutron Emitter	HAC @ 1-m Maximum Allowable Activity (Ci), A_{GN}	Radionuclide Name	Gamma Emitter	Neutron Emitter	HAC @ 1-m Maximum Allowable Activity (Ci), A_{GN}
^{3}H			unlimited	^{93m}Nb	×		unlimited
^{10}Be			unlimited	^{94}Nb	×		1.887E+02
^{14}C			unlimited	^{95}Nb	×		4.578E+02
^{22}Na	×		7.040E+01	^{95m}Nb	×		1.520E+06
^{32}P			unlimited	^{99}Tc	×		unlimited
^{33}P			unlimited	^{99m}Tc	×		unlimited
^{35}S			unlimited	^{103}Ru	×		7.161E+03
^{45}Ca	×		unlimited	^{106}Ru			unlimited
^{46}Sc	×		7.058E+01	^{103m}Rh	×		unlimited
^{49}V			unlimited	^{106}Rh	×		2.180E+03
^{51}Cr	×		unlimited	^{107}Pd			unlimited
^{54}Mn	×		2.938E+02	^{108}Ag	×		5.931E+04
^{55}Fe			unlimited	^{108m}Ag	×		5.064E+02
^{59}Fe	×		8.578E+01	^{109m}Ag	×		unlimited
^{57}Co	×		5.245E+05	^{110}Ag	×		1.971E+04
^{58}Co	×		3.122E+02	^{110m}Ag	×		6.301E+01
^{60}Co	×		3.643E+01	^{109}Cd	×		unlimited
^{59}Ni			unlimited	^{113m}Cd	×		unlimited
^{63}Ni			unlimited	^{115m}Cd	×		3.938E+03
^{64}Cu	×		1.255E+04	^{114}In	×		4.741E+04
^{65}Zn	×		2.044E+02	^{114m}In	×		1.674E+04
^{73}As	×		unlimited	^{115m}In	×		9.296E+06
^{79}Se			unlimited	^{119m}Sn	×		unlimited
^{85}Kr	×		1.534E+06	^{121m}Sn	×		unlimited
^{86}Rb	×		1.316E+03	^{123}Sn	×		1.752E+04
^{87}Rb			unlimited	^{126}Sn	×		unlimited
^{89}Sr	×		2.180E+06	^{124}Sb	×		5.003E+01
^{90}Sr			unlimited	^{125}Sb	×		4.166E+03
^{88}Y	×		2.485E+01	^{126}Sb	×		1.907E+02
^{90}Y	×		unlimited	^{126m}Sb	×		4.589E+02
^{90m}Y	×		1.495E+04	^{123}Te			unlimited
^{91}Y	×		3.201E+04	^{123m}Te	×		unlimited
^{88}Zr	×		2.204E+05	^{125m}Te	×		unlimited
^{90}Zr			unlimited	^{127}Te	×		8.177E+06
^{90m}Zr			unlimited	^{127m}Te	×		7.946E+06

Radionuclide Name	Gamma Emitter	Neutron Emitter	HAC @ 1-m Maximum Allowable Activity (Ci), A_{GN}	Radionuclide Name	Gamma Emitter	Neutron Emitter	HAC @ 1-m Maximum Allowable Activity (Ci), A_{GN}
^{93}Zr	×		unlimited	^{129}Te	×		1.231E+04
^{95}Zr	×		5.574E+02	^{129m}Te	×		1.695E+04
^{125}I	×		unlimited	^{210}Pb	×		unlimited
^{129}I	×		unlimited	^{211}Pb	×		6.387E+03
^{131}I	×		1.189E+04	^{212}Pb	×		6.065E+07
^{134}Cs	×		2.444E+02	^{214}Pb	×		1.967E+04
^{135}Cs			unlimited	^{207}Bi	×		1.112E+02
^{137}Cs	×		1.268E+03	^{210}Bi			unlimited
^{133}Ba	×		1.967E+06	^{211}Bi	×		2.446E+07
^{137}Ba			unlimited	^{212}Bi	×		1.342E+03
^{137m}Ba	×		1.198E+03	^{213}Bi	×		1.887E+04
^{141}Ce	×		unlimited	^{214}Bi	×		5.576E+01
^{142}Ce			unlimited	^{209}Po	×		4.694E+04
^{144}Ce	×		unlimited	^{210}Po	×		2.819E+07
^{143}Pr	×		unlimited	^{211}Po	×		3.639E+04
^{144}Pr	×		2.393E+03	^{212}Po			unlimited
^{144m}Pr	×		7.371E+04	^{213}Po	×		8.565E+06
^{146}Pm	×		9.394E+02	^{214}Po			unlimited
^{147}Pm	×		unlimited	^{215}Po	×		unlimited
^{148}Pm	×		1.760E+02	^{216}Po	×		1.780E+07
^{148m}Pm	×		2.576E+02	^{218}Po			unlimited
^{146}Sm			unlimited	^{211}At	×		3.290E+05
^{147}Sm			unlimited	^{217}At	×		1.673E+07
^{151}Sm	×		unlimited	^{219}Rn	×		1.019E+06
^{150}Eu	×		2.750E+02	^{220}Rn	×		3.373E+06
^{152}Eu	×		1.149E+02	^{222}Rn	×		9.315E+06
^{154}Eu	×		1.108E+02	^{221}Fr	×		6.687E+07
^{155}Eu	×		unlimited	^{223}Fr	×		4.101E+04
^{152}Gd			unlimited	^{223}Ra	×		7.495E+05
^{153}Gd	×		unlimited	^{224}Ra	×		2.257E+07
^{160}Tb	×		1.379E+02	^{225}Ra	×		unlimited
^{166m}Ho	×		2.564E+02	^{226}Ra	×		unlimited
^{168}Tm	×		3.067E+02	^{228}Ra	×		unlimited
^{182}Ta	×		8.964E+01	^{225}Ac	×		2.925E+06
^{198}Au	×		3.074E+04	^{227}Ac	×		unlimited
^{207}Tl	×		8.436E+04	^{228}Ac	×		1.730E+02

Radionuclide Name	Gamma Emitter	Neutron Emitter	HAC @ 1-m Maximum Allowable Activity (Ci), A_{GN}	Radionuclide Name	Gamma Emitter	Neutron Emitter	HAC @ 1-m Maximum Allowable Activity (Ci), A_{GN}
^{208}Tl	×		1.617E+01	^{227}Th	×		1.610E+06
^{209}Tl	×		3.819E+01	^{228}Th	×		unlimited
^{209}Pb			unlimited	^{229}Th	×		unlimited
^{230}Th	×	×	1.000E+06	^{243}Pu	×		6.373E+07
^{231}Th	×		unlimited	^{244}Pu		×	4.500E+00
^{232}Th	×	×	2.090E+06	^{241}Am	×	×	5.455E+05
^{234}Th	×		unlimited	^{242}Am	×		unlimited
^{231}Pa	×	×	7.288E+05	^{242m}Am	×	×	2.780E+07
^{233}Pa	×		3.117E+06	^{243}Am	×	×	6.199E+05
^{234}Pa	×		1.370E+02	^{245}Am	×		unlimited
^{234m}Pa	×		8.465E+03	^{240}Cm		×	9.500E+04
^{232}U	×	×	6.389E+05	^{242}Cm	×	×	6.109E+04
^{233}U	×	×	8.720E+05	^{243}Cm	×	×	5.830E+04
^{234}U	×	×	8.909E+05	^{244}Cm	×	×	3.410E+03
^{235}U	×	×	9.472E+05	^{245}Cm	×	×	2.140E+04
^{236}U	×	×	9.680E+05	^{246}Cm		×	1.480E+01
^{237}U	×		unlimited	^{247}Cm	×		1.774E+05
^{238}U	×	×	1.180E+04	^{248}Cm		×	4.870E-02
^{239}U	×		3.108E+04	^{250}Cm		×	5.710E-03
^{240}U	×		unlimited	^{247}Bk	×		unlimited
^{237}Np	×	×	9.030E+05	^{249}Bk	×	×	4.590E+06
^{238}Np	×		2.211E+02	^{250}Bk	×		1.547E+02
^{239}Np	×		4.986E+07	^{249}Cf	×	×	1.685E+05
^{240}Np	×		2.510E+02	^{250}Cf	×	×	4.580E+00
^{240m}Np	×		8.149E+02	^{251}Cf	×	×	4.580E+05
^{236}Pu	×	×	4.325E+05	^{252}Cf	×	×	1.190E-01
^{238}Pu	×	×	4.638E+05	^{254}Cf		×	3.640E-03
^{239}Pu	×	×	7.014E+05	^{252}Es	×		1.657E+03
^{240}Pu	×	×	9.140E+04	^{253}Es	×	×	3.569E+04
^{241}Pu	×	×	unlimited	^{254}Es	×	×	8.959E+04
^{242}Pu	×	×	1.060E+03	^{254m}Es	×	×	7.165E+00

Notes:

① Ci = curie(s).

② HAC = hypothetical accident conditions.

③ m = meter(s).

Table 5.1-2 – RH-TRU Radionuclide Inventory

^{3}H	^{90m}Zr	^{123m}Te	^{160}Tb	^{223}Fr	^{236}Pu
^{10}Be	^{93}Zr	^{125m}Te	^{166m}Ho	^{223}Ra	^{238}Pu
^{14}C	^{95}Zr	^{127}Te	^{168}Tm	^{224}Ra	^{239}Pu
^{22}Na	^{93m}Nb	^{127m}Te	^{182}Ta	^{225}Ra	^{240}Pu
^{32}P	^{94}Nb	^{129}Te	^{198}Au	^{226}Ra	^{241}Pu
^{33}P	^{95}Nb	^{129m}Te	^{207}Tl	^{228}Ra	^{242}Pu
^{35}S	^{95m}Nb	^{125}I	^{208}Tl	^{225}Ac	^{243}Pu
^{45}Ca	^{99}Tc	^{129}I	^{209}Tl	^{227}Ac	^{244}Pu
^{46}Sc	^{99m}Tc	^{131}I	^{209}Pb	^{228}Ac	^{241}Am
^{49}V	^{103}Ru	^{134}Cs	^{210}Pb	^{227}Th	^{242}Am
^{51}Cr	^{106}Ru	^{135}Cs	^{211}Pb	^{228}Th	^{242m}Am
^{54}Mn	^{103m}Rh	^{137}Cs	^{212}Pb	^{229}Th	^{243}Am
^{55}Fe	^{106}Rh	^{133}Ba	^{214}Pb	^{230}Th	^{245}Am
^{59}Fe	^{107}Pd	^{137}Ba	^{207}Bi	^{231}Th	^{240}Cm
^{57}Co	^{108}Ag	^{137m}Ba	^{210}Bi	^{232}Th	^{242}Cm
^{58}Co	^{108m}Ag	^{141}Ce	^{211}Bi	^{234}Th	^{243}Cm
^{60}Co	^{109m}Ag	^{142}Ce	^{212}Bi	^{231}Pa	^{244}Cm
^{59}Ni	^{110}Ag	^{144}Ce	^{213}Bi	^{233}Pa	^{245}Cm
^{63}Ni	^{110m}Ag	^{143}Pr	^{214}Bi	^{234}Pa	^{246}Cm
^{64}Cu	^{109}Cd	^{144}Pr	^{209}Po	^{234m}Pa	^{247}Cm
^{65}Zn	^{113m}Cd	^{144m}Pr	^{210}Po	^{232}U	^{248}Cm
^{73}As	^{115m}Cd	^{146}Pm	^{211}Po	^{233}U	^{250}Cm
^{79}Se	^{114}In	^{147}Pm	^{212}Po	^{234}U	^{247}Bk
^{85}Kr	^{114m}In	^{148}Pm	^{213}Po	^{235}U	^{249}Bk
^{86}Rb	^{115m}In	^{148m}Pm	^{214}Po	^{236}U	^{250}Bk
^{87}Rb	^{119m}Sn	^{146}Sm	^{215}Po	^{237}U	^{249}Cf
^{89}Sr	^{121m}Sn	^{147}Sm	^{216}Po	^{238}U	^{250}Cf
^{90}Sr	^{123}Sn	^{151}Sm	^{218}Po	^{239}U	^{251}Cf
^{88}Y	^{126}Sn	^{150}Eu	^{211}At	^{240}U	^{252}Cf
^{90}Y	^{124}Sb	^{152}Eu	^{217}At	^{237}Np	^{254}Cf
^{90m}Y	^{125}Sb	^{154}Eu	^{219}Rn	^{238}Np	^{252}Es
^{91}Y	^{126}Sb	^{155}Eu	^{220}Rn	^{239}Np	^{253}Es
^{88}Zr	^{126m}Sb	^{152}Gd	^{222}Rn	^{240}Np	^{254}Es
^{90}Zr	^{123}Te	^{153}Gd	^{221}Fr	^{240m}Np	^{254m}Es

FIGURE WITHHELD UNDER 10 CFR 2.390

Figure 5.1-1 – HAC Radial Shielding Configuration

5.2 Source Specification

Radiation sources in the contents include fission, activation and actinide products. The RH-TRU inventory of expected isotopes is given in Table 5.1-2. Generally, each content code is expected to have only a few radionuclides in any significant amounts, with trace amounts of other radionuclides. There are two types of sources: *General Payload* or *Controlled Self-Shielding Payload*.

General Payload Case:

The isotopic *General Payload* source activity limits, controlled by the HAC dose rate limit, are given in Table 5.1-1. The source activity limits for gamma and neutron isotopes not listed in Table 5.1-1 or neutron sources not bounded by the assumed UO_2 source matrix may be determined by following the procedures given in Appendix 5.5.3, *Screening Methodology for Neutron Emitting Isotopes*, and Appendix 5.5.4, *Screening Methodology for Gamma Emitting Isotopes*. The *General Payload* source is characterized by the following:

- There are no restrictions on payload form, location, distribution, self-shielding properties, or physical response to HAC.
- NCT dose rate requirements are met by performing preshipment radiological surveys.
- HAC dose rate requirements are met by imposing activity limits (and the sum of fractions for multiple-radionuclide payloads) that are derived based on an assumed point source located against the payload canister wall just inside the puncture location (see Figure 5.1-1).

Table 5.1-1 presents the limiting quantities (i.e., activities in Curies) that equal, but do not exceed, the HAC allowable dose rate for each nuclide provided in Table 5.1-2. The maximum allowable activities listed in Table 5.1-1 account for pure gamma (A_G), pure neutron (A_N), or combined gamma/neutron (A_{GN}) emission where $A_{GN} = 1/[(1/A_G)+(1/A_N)]$. All radionuclides that do not have gamma energies and do not undergo spontaneous fission or whose maximum allowable activity is calculated to be greater than 1×10^8 curies are classified as "unlimited."

Controlled Self-Shielding Payload Case:

The *Controlled Self-Shielding Payload* shielding source is constrained by the measured NCT dose rates and supplemented by source activity limits by isotope which are 15 times those applied to the *General Payload Case*. Evaluations are performed in Appendix 5.5.5, *Evaluation of the Effect of NCT to HAC Changes on Neutron Dose Rates*, and Appendix 5.5.6, *Evaluation of the Effect of NCT-to-HAC Changes on Gamma Dose Rates*, that demonstrate the measured NCT dose rates ensure compliance with both NCT and HAC dose rate limits. The *Controlled Self-Shielding Payload* shielding source is characterized by the following:

- There are no restrictions on payload location or distribution, but the form of the waste is such that self-shielding properties and the physical response to HAC are constrained through the following payload requirements:

- The payload is a homogeneous solid/sludge, as certified by the processes defined in *Remote-Handled Transuranic Waste Authorized Methods for Payload Control* (RH-TRAMPAC)[1] that naturally precludes the loss of greater than 8 inches of water/polyethylene or 1 inch of steel equivalent self-shielding material in response to HAC, or
- The payload is compacted and fills greater than 90% of the payload canister internal volume, as certified by the processes defined in RH-TRAMPAC[1], such that it precludes the loss of greater than 8 inches of water/polyethylene or 1 inch of steel equivalent self-shielding material in response to HAC.

- NCT dose rate requirements are met by performing preshipment radiological surveys.
- HAC dose rate requirements are met by performing preshipment NCT radiological surveys that are shown to be limiting per the analyses provided in Appendix 5.5.5, *Evaluation of the Effect of NCT to HAC Changes on Neutron Dose Rates*, and Appendix 5.5.6, *Evaluation of the Effect of NCT-to-HAC Changes on Gamma Dose Rates*. Additionally, HAC dose rate compliance is supplemented by imposing activity limits (and the sum of fractions for multiple-radionuclide payloads) that are 15 times the limits derived for the *General Payload Case*.

5.2.1 Gamma Source

General Payload Case:

The allowable gamma source strength for the payload canister is derived from Table 5.1-2 based on a conservative evaluation of the maximum activity within the HAC limit. Table 5.1-1 lists these isotopes and their allowable HAC quantities (activities) calculated based on a point source in air, adjacent to the interior surface of the payload canister, at the puncture damage location. For gamma emitting isotopes not listed in Table 5.1-1, HAC activity limits may be determined by following the procedures given in Appendix 5.5.4, *Screening Methodology for Gamma Emitting Isotopes*.

Controlled Self-Shielding Payload Case:

As shown in Appendix 5.5.6, *Evaluation of the Effect of NCT-to-HAC Changes on Gamma Dose Rates*, compliance with the NCT measurements at the time of shipment ensure that the NCT and HAC dose rate limits will not be exceeded. Additionally, HAC dose rate compliance is supplemented by imposing activity limits that are 15 times the limits derived for the *General Payload Case*.

5.2.2 Neutron Source

General Payload Case:

The allowable neutron source strength for the payload canister is derived from Table 5.1-2 based on a conservative evaluation of the maximum activity at the HAC limit. Table 5.1-1 lists the

[1] U.S. Department of Energy (DOE), *Remote-Handled Transuranic Waste Authorized Methods for Payload Control* (RH-TRAMPAC), U.S. Department of Energy, Carlsbad Field Office, Carlsbad, New Mexico.

resulting maximum allowable activity for each neutron-generating isotope. For neutron-generating isotopes not identified in Table 5.1-1 or in a source matrix not bounded by the UO_2 assumption, HAC activity limits may be determined by following the procedures given in Appendix 5.5.3, *Screening Methodology for Neutron Emitting Isotopes*.

The derivation of the neutron source strength is complex. Although the assumption of the HAC point source is geometrically conservative, it does not include subcritical multiplication or production of neutrons by alpha-n reactions. In order to develop a reasonably correct, but bounding, neutron source, the point source assumption is maintained for the source geometry. However, alpha-n production is assumed to occur as though there is a homogeneous media of the source isotope and UO_2, and a subcritical multiplication factor is developed and applied to the source. In this manner, the activity limits bound the authorized payloads.

The neutron source for each isotope is developed using the computer code SOURCES-4A[2]. The code generates neutron production rates for spontaneous fission and alpha-n reactions (based on the assumed source matrix, UO_2). In addition, the code outputs the average neutron energy and spectra, by isotope. The neutron source strength by isotope, and the corresponding neutron spectra by energy group, is developed in the PacTec Report, *Neutron Source Rates for TRU Waste*[3].

The shielding subcritical multiplication factor is derived in Appendix 5.5.2, *Derivation of MCNP Neutron Subcritical Multiplication Factor*. The factor, 2.7, is applied in the neutron dose rate calculations in Table 5.4-5 in Section 5.4, *Shielding Evaluation*.

Controlled Self-Shielding Payload Case:

As shown in Appendix 5.5.5, *Evaluation of the Effect of NCT to HAC Changes on Neutron Dose Rates*, compliance with NCT measurements at the time of shipment ensure that the NCT and HAC dose rate limits are not exceeded. Additionally, HAC dose rate compliance is supplemented by imposing activity limits that are 15 times the limits derived for the *General Payload Case*.

[2] Los Alamos National Laboratory, *SOURCES 4A: A Code for Calculating (α,n), Spontaneous Fission, and Delayed Neutron Sources and Spectra*, LA-13639-MS, Los Alamos, New Mexico, September 1999.

[3] Packaging Technology, Inc., *Neutron Source Rates for TRU Waste*, ED-042, Tacoma, WA, November 2000.

This page intentionally left blank.

5.3 Model Specification

This section describes the models for the RH-TRU 72-B package shielding evaluations.

5.3.1 Description of Radial and Axial Shielding Configuration

The HAC radial shielding model is illustrated in Figure 5.1-1. The radial shielding model assumes an isotropic point-source geometry directly adjacent to the payload canister shell. The payload canister shell, in-turn, is assumed adjacent to the inner vessel (IV) shell (i.e., ignoring the radial spacers), and the IV shell is assumed adjacent to the OC inner shell. This configuration minimizes the distance between the point source and the receptor at a distance of one (1) meter from the outside surface of the thermal shield. Only the attenuating effects of the carbon or stainless steel payload canister, stainless steel inner IV, and OC inner shell, lead, outer shell, and thermal shield shell are included in the dose rate calculations.

In addition, the model includes the reduction of lead shielding thickness of 35% (i.e., locally reduced from 1.875 inches thick to 1.219 inches thick) due to localized puncture bar damage. The OC outer shell and thermal shield are assumed to translate radially inward corresponding to the amount of radial lead deformation.

5.3.2 Shield Regional Densities

The shielding models are comprised of plain carbon steel (payload canister shell), Type 304 stainless steel (IV and OC shells), and lead; with material densities of 490 lb/ft^3 (7.8526 g/cc), 500 lb/ft^3 (8.0128 g/cc), and 708 lb/ft^3 (11.3500 g/cc), respectively. The use of carbon steel versus slightly higher density stainless steel for the canister shell is the worst case for shielding evaluations. Table 5.3-1 summarizes the shield regional densities for each of these gamma-attenuating materials.

Table 5.3-1 – Summary of Shield Regional Densities

Element	Carbon Steel		Type 304 Stainless Steel		Lead	
	Percent	Partial Density (g/cc)	Percent	Partial Density (g/cc)	Percent	Partial Density (g/cc)
Silicon	—	—	1%	0.0801	—	—
Chromium	—	—	19%	1.5224	—	—
Manganese	—	—	2%	0.1603	—	—
Iron	100%	7.8526	68%	5.4487	—	—
Nickel	—	—	10%	0.8013	—	—
Lead	—	—	—	—	100%	11.3500
Total	*100%*	*7.8526*	*100%*	*8.0128*	*100%*	*11.3500*

5.4 Shielding Evaluation

5.4.1 Gamma Shielding Evaluation

General Payload Case:

The gamma shielding evaluation to determine the HAC activity limits delineated in Table 5.1-1 conservatively utilizes an isotropic point-source geometry, as described in Section 5.3.1, *Description of Radial and Axial Shielding Configuration*. This point source geometry allows the use of hand calculations that produce results that are conservative in comparison to those obtained from a full Monte Carlo analysis. The dose rate from an isotropic point-source, as a function of gamma energy, is simply[1]:

$$D(E) = \frac{S(E)B(E,x)K(E)}{4\pi R^2} e^{-x}$$

where D(E) is the dose rate as a function of gamma energy, E (mrem/hr), S(E) is the source strength as a function of gamma energy, E (γ/s; 1 curie = $3.7(10)^{10}$ γ/s), B(E,x) is the buildup factor as a function of gamma energy, E, and mean free paths, x(E), K(E) is the gamma flux-to-dose rate conversion factor (γ/cm²-s to mrem/hr), and R is the radial distance from the source to the receptor (cm; see Figure 5.1-1).

Gamma energy and intensity data is provided in Kinsey, et al.[2] All gamma energies less than 0.100 MeV are conservatively rounded to 0.100 MeV for the purpose of linear interpolation in Table 5.4-1, Table 5.4-2, and Table 5.4-3.

The number of mean free paths, x(E), is:

$$x(E) = \sum_{i=1}^{n} \mu_i(E) t_i$$

where $\mu_i(E)$ is the attenuation coefficient (as a function of gamma energy) of shield "i", and t_i is the thickness of shield "i" in centimeters. The number of mean free paths is a non-dimensional number.

The attenuation coefficient for shield "i" is:

$$\mu_i(E) = \left[\frac{\mu_1(E)}{\rho}\right]\rho_1 + \left[\frac{\mu_2(E)}{\rho}\right]\rho_2 + \left[\frac{\mu_3(E)}{\rho}\right]\rho_3 + \cdots + \left[\frac{\mu_n(E)}{\rho}\right]\rho_n$$

[1] T. Rockwell III, et al, *Reactor Shielding Design Manual*, TID-7004, First Edition, U.S. Atomic Energy Commission, Oak Ridge, Tennessee, March 1956, Chapter 1, Section 3.2, Equation 1.

[2] R.R. Kinsey, et al., *The NUDAT/PCNUDAT Program for Nuclear Data*, paper submitted to the 9th International Symposium of Capture Gamma-Ray Spectroscopy and Related Topics, Budapest, Hungary, October 1996; data extracted from the NUDAT database, version September 7, 2000, CD-ROM.

where, for a material containing "n" different elements, $\mu_x(E)$ and ρ_x are the mass attenuation coefficient (as a function of gamma energy) and partial density for element "x." The units for the attenuation coefficient are cm^{-1}. The units for mass attenuation coefficient are cm^2/g. Table 5.3-1 presents a summary of the partial density for each major element of the three gamma attenuation materials (i.e., carbon steel, Type 304 stainless steel, and lead). Table 5.4-1 summarizes the mass attenuation coefficients for each element as a function of gamma energy, as taken from ANSI/ANS 6.4.3-1991[3]. Mass attenuation coefficients used in the subsequent shielding calculations are linearly interpolated from the data in Table 5.4-1.

Gamma-ray isotropic point-source buildup factors are determined by conservatively assuming iron as the dominant shielding material. Although the actual buildup factors will lie somewhere between iron (atomic number, Z = 26) and lead (Z = 82), use of iron as the buildup factor will conservatively bound the maximum isotopic quantity (curies) allowed for transport because the buildup factor increases as the atomic number decreases.

Buildup factors are determined using the geometric progression (G-P) function as presented in ANSI/ANS 6.4.3-1991[3]. The G-P function accurately reproduces buildup factor data for deep penetrations in shields (i.e., >20 mean free paths thick). The buildup factor, as a function of gamma energy, E, and mean free paths, x, using the G-P function is:

$$B(E,x) = 1 + (b-1)\frac{(K^x - 1)}{(K-1)} \quad \text{for } K \neq 1$$

$$B(E,x) = 1 + (b-1)x \quad \text{for } K = 1$$

$$K(x) = cx^a + d\left[\frac{\tanh\left(\frac{x}{X_k} - 2\right) - \tanh(-2)}{1 - \tanh(-2)}\right]$$

The coefficients a, b, c, d, and X_K, as a function of gamma energy, are provided in Table 5.4-2. The subsequent shielding analyses calculate the buildup factors over the range of gamma energies for a given number of mean free paths. The resulting buildup factors are then linearly interpolated for the gamma energy associated with the number of mean free paths to arrive at the actual buildup factor used in the dose rate calculation.

Gamma flux-to-dose rate conversion factors are determined using the values delineated in ANSI/ANS 6.1.1-1977[4], and presented in Table 5.4-3. The data in Table 5.4-3 are linearly interpolated to determine the conversion factor for a given gamma energy.

Table 5.1-1 presents the limiting quantities (i.e., activities in curies) that equal, but do not exceed, the HAC allowable dose rate for each gamma emitting nuclide provided in Table 5.1-2. Again, the maximum allowable activities listed in Table 5.1-1 account for pure gamma (A_G),

[3] ANSI/ANS 6.4.3-1991, *Gamma-Ray Attenuation Coefficients & Buildup Factors for Engineering Materials*, American Nuclear Society (ANS), La Grange Park, Illinois.

[4] ANSI/ANS 6.1.1-1977, *Neutron and Gamma-Ray Flux-To-Dose-Rate Factors*, American Nuclear Society (ANS), La Grange Park, Illinois.

pure neutron (A_N), or combined gamma/neutron (A_{GN}) emission where $A_{GN} = 1/[(1/A_G)+(1/A_N)]$. Examples of the gamma dose rate calculations are presented in Appendix 5.5.1, *HAC at 1m Co-60 Point Source Gamma Shielding Analysis*.

Controlled Self-Shielding Payload Case:

Calculations given in Appendix 5.5.5, *Evaluation of the Effect of NCT to HAC Changes on Neutron Dose Rates*, verify that compliance with the NCT measurements at time of shipment ensure that the NCT and HAC dose rate limits will not be exceeded. Additionally, HAC dose rate compliance is supplemented by imposing activity limits that are 15 times the limits derived for the *General Payload Case*.

5.4.2 Neutron Shielding Evaluation

General Payload Case:

Activity limits are developed for each of the neutron generating isotopes identified in Table 5.1-2 using the same basic geometrical arrangement that is used to develop the gamma activity limits, as shown in Figure 5.1-1.

The actual neutron source spectra for each isotope is input into the computer code MCNP[5] normalized as a unit source strength. The resulting dose rate is then multiplied by the respective source strength for each isotope[6] and the subcritical neutron multiplication factor developed in Appendix 5.5.2, *Derivation of MCNP Neutron Subcritical Multiplication Factor*. This product is then divided into 1,000 to establish the HAC allowable activity for each isotope (see Table 5.4-5).

The MCNP computer code, developed at the Los Alamos National Laboratory (LANL), is now used extensively both in the United States and throughout the world. The MCNP code is a general-purpose neutron and photon transport code with a very powerful geometry package.

An MCNP representation of the KENO package model developed and described in Chapter 6.0, *Criticality Evaluation*, is used for these calculations. The unit sources are modeled as point sources near the package wall, with puncture damage added into the model, as shown in Figure 5.4-1. Flux-to-dose rate conversion factors are given in Table 5.4-4. Table 5.4-5 presents the limiting quantities (i.e., activities in Curies) that equal, but do not exceed, the HAC allowable dose rate for each neutron emitting nuclide provided in Table 5.1-2. The activity limits listed in Table 5.4-5 account for pure neutron (A_N) emission only. Sample input files are provided in Appendix 5.5.7, *MCNP Input Files for the Shielding Analyses*.

Controlled Self-Shielding Payload Case:

Calculations given in Appendix 5.5.5, *Evaluation of the Effect of NCT to HAC Changes on Neutron Dose Rates*, verify that compliance with the NCT measurements at time of shipment ensure that the NCT and HAC dose rate limits will not be exceeded. Additionally, HAC dose rate compliance is supplemented by imposing activity limits that are 15 times the limits derived for the *General Payload Case*.

---

[5] J. F. Breismeister, Editor, *MCNP – A General Monte Carlo Code N-Particle Transport Code, Version 4B*, LA-12625-M, Los Alamos National Laboratory, Los Alamos, New Mexico, 1997.

[6] Packaging Technology, Inc., *Neutron Source Rates for TRU Waste*, ED-042, Tacoma, WA, November 2000.

5.4.3 Total Radiation Source

The dose rate is linearly proportional to the source magnitude for an isotropic point source geometry (i.e., doubling the curie content will double the resulting dose rate). Therefore, the method of summing "partial fractions" is appropriately utilized to determine pre-shipment acceptability for any combination radionuclides present in the waste. The method of summing partial fractions is similarly used in Appendix A.IV of 10 CFR 71[7] for determination of the maximum quantity of mixed isotopes that may be shipped in a Type A package.

General Payload Case:

For the *General Payload Case*, the sum of dose rate partial fractions for any combination of the radionuclides must be less than or equal to unity, or:

$$\sum_{i=1}^{n} \frac{a_i}{A_{GN_i}} \leq 1$$

where, for a particular payload mix, a_i is the actual curie content of radionuclide "i" and A_{GNi} is the limiting curie content of radionuclide "i" given in Table 5.1-1 or calculated from the methodologies outlined in Appendix 5.5.3, *Screening Methodology for Neutron Emitting Isotopes*, or Appendix 5.5.4, *Screening Methodology for Gamma Emitting Isotopes*.

For example, 36.43 curies of ^{60}Co, 557.4 curies of ^{95}Zr, and 1,060 curies of ^{242}Pu each result in a limiting HAC dose rate of one (1) rem per hour at a distance of one (1) meter from the package surface. The sum of the partial fractions for a payload containing 20.0 curies of ^{60}Co, 38.0 curies of ^{95}Zr, and 155 curies of ^{242}Pu is:

$$\frac{a_{60_{Co}}}{A_{GN_{60_{Co}}}} + \frac{a_{95_{Zr}}}{A_{GN_{95_{Zr}}}} + \frac{a_{242_{Pu}}}{A_{GN_{242_{Pu}}}} = \frac{20}{36.43} + \frac{38}{557.4} + \frac{155}{1{,}060} = 0.55 + 0.07 + 0.15 = 0.77 \leq 1.00$$

Thus, the combination of isotopes for the above example will not exceed the HAC limiting dose rate of one (1) rem per hour at a distance of one (1) meter from the package surface.

Additionally, the sum of dose rate partial fractions must be less than 0.1 to limit the dose contribution from radionuclides whose activity limits are calculated by the procedures outlined in Appendix 5.5.3, *Screening Methodology for Neutron Emitting Isotopes*, and/or Appendix 5.5.4, *Screening Methodology for Gamma Emitting Isotopes*, to 10% of the total, or:

$$\sum_{i=1}^{n} \frac{a_i}{A_{GN_i}} \leq 0.1$$

where, for a particular payload mix, a_i is the actual curie content of radionuclide "i" and A_{GNi} is the limiting curie content of radionuclide "i" calculated from the methodologies outlined in Appendix 5.5.3, *Screening Methodology for Neutron Emitting Isotopes*, or Appendix 5.5.4, *Screening Methodology for Gamma Emitting Isotopes*.

[7] Title 10, Code of Federal Regulations, Part 71 (10 CFR 71), *Packaging and Transportation of Radioactive Material*, Final Rule, 01-26-04.

Controlled Self-Shielding Payload Case:

For the *Controlled Self-Shielding Payload Case*, the sum of dose rate partial fractions for any combination of the radionuclides must be less than or equal to unity, or:

$$\sum_{i=1}^{n} \frac{a_i}{15 \times A_{GN_i}} \leq 1$$

where, for a particular payload mix, a_i is the actual curie content of radionuclide "i" and A_{GNi} is the limiting curie content of radionuclide "i" given in Table 5.1-1 or calculated from the methodologies outlined in Appendix 5.5.3, *Screening Methodology for Neutron Emitting Isotopes*, or Appendix 5.5.4, *Screening Methodology for Gamma Emitting Isotopes*.

Additionally, the sum of dose rate partial fractions must be less than 0.1 to limit the dose contribution from isotopes whose activity limits are calculated by the procedures outlined in Appendix 5.5.3, *Screening Methodology for Neutron Emitting Isotopes*, and/or Appendix 5.5.4, *Screening Methodology for Gamma Emitting Isotopes*, to 10% of the total, or:

$$\sum_{i=1}^{n} \frac{a_i}{15 \times A_{GN_i}} \leq 0.1$$

where, for a particular payload mix, a_i is the actual curie content of radionuclide "i" and A_{GNi} is the limiting curie content of radionuclide "i" calculated from the methodologies outlined in Appendix 5.5.3, *Screening Methodology for Neutron Emitting Isotopes*, or Appendix 5.5.4, *Screening Methodology for Gamma Emitting Isotopes*.

The justification for the 15× factor used in the *Controlled Self-Shielding Payload Case* total radiation source equations is given in Appendix 5.5.5, *Evaluation of the Effect of NCT to HAC Changes on Neutron Dose Rates*, and Appendix 5.5.6, *Evaluation of the Effect of NCT-to-HAC Changes on Gamma Dose Rates*.

As described in *Remote-Handled Transuranic Waste Authorized Methods for Payload Control* (RH-TRAMPAC)[8], all other payload limits (decay heat, FGE, etc.) will also have to be met for all shipments in the RH-TRU 72-B package.

[8] U.S. Department of Energy (DOE), *Remote-Handled Transuranic Waste Authorized Methods for Payload Control* (RH-TRAMPAC), U.S. Department of Energy, Carlsbad Field Office, Carlsbad, New Mexico.

Table 5.4-1 – Mass Attenuation Coefficients from ANSI/ANS 6.4.3-1991

γ-Energy (MeV)	Silicon	Chromium	Manganese	Iron	Nickel	Lead
0.100	1.73E-01	2.92E-01	3.10E-01	3.43E-01	4.10E-01	5.36E+00
0.150	1.40E-01	1.67E-01	1.72E-01	1.83E-01	2.05E-01	1.92E+00
0.200	1.25E-01	1.31E-01	1.32E-01	1.38E-01	1.49E-01	9.43E-01
0.300	1.07E-01	1.04E-01	1.03E-01	1.06E-01	1.11E-01	3.77E-01
0.400	9.54E-02	9.04E-02	8.95E-02	9.20E-02	9.53E-02	2.17E-01
0.500	8.70E-02	8.17E-02	8.07E-02	8.28E-02	8.55E-02	1.51E-01
0.600	8.04E-02	7.52E-02	7.42E-02	7.61E-02	7.84E-02	1.18E-01
0.800	7.06E-02	6.57E-02	6.49E-02	6.64E-02	6.83E-02	8.47E-02
1.000	6.34E-02	5.90E-02	5.82E-02	5.96E-02	6.12E-02	6.84E-02
1.500	5.17E-02	4.81E-02	4.75E-02	4.86E-02	4.99E-02	5.10E-02
2.000	4.47E-02	4.20E-02	4.15E-02	4.25E-02	4.37E-02	4.54E-02
3.000	3.67E-02	3.55E-02	3.51E-02	3.61E-02	3.73E-02	4.20E-02
4.000	3.23E-02	3.23E-02	3.20E-02	3.30E-02	3.44E-02	4.18E-02
5.000	2.96E-02	3.05E-02	3.04E-02	3.14E-02	3.28E-02	4.26E-02

Table 5.4-2 – Iron Exposure Buildup Factor Coefficients from ANSI/ANS 6.4.3-1991

γ-Energy (MeV)	b	c	a	X_K	d
0.100	1.389	0.557	0.144	14.11	-0.0791
0.150	1.660	0.743	0.079	14.12	-0.0476
0.200	1.839	0.911	0.034	13.23	-0.0334
0.300	1.973	1.095	-0.009	11.86	-0.0183
0.400	1.992	1.187	-0.027	10.72	-0.0140
0.500	1.967	1.240	-0.039	8.34	-0.0074
0.600	1.947	1.247	-0.040	8.20	-0.0096
0.800	1.906	1.233	-0.038	7.93	-0.0110
1.000	1.841	1.250	-0.048	19.49	0.0140
1.500	1.750	1.197	-0.040	15.90	0.0110
2.000	1.712	1.123	-0.021	7.97	-0.0057
3.000	1.627	1.059	-0.005	11.99	-0.0132
4.000	1.553	1.026	0.005	12.93	-0.0191
5.000	1.483	1.009	0.012	13.12	-0.0258

Table 5.4-3 – Gamma Flux-to-Dose Rate Conversion Factors from ANSI/ANS 6.1.1-1977

γ-Energy (MeV)	$DF_g(E)$ (γ/cm²-s to mrem/hr)	γ-Energy (MeV)	$DF_g(E)$ (γ/cm²-s to mrem/hr)
0.100	2.83E-04	0.800	1.68E-03
0.150	3.79E-04	1.000	1.98E-03
0.200	5.01E-04	1.400	2.51E-03
0.250	6.31E-04	1.800	2.99E-03
0.300	7.59E-04	2.200	3.42E-03
0.350	8.78E-04	2.600	3.82E-03
0.400	9.85E-04	2.800	4.01E-03
0.450	1.08E-03	3.250	4.41E-03
0.500	1.17E-03	3.750	4.83E-03
0.550	1.27E-03	4.250	5.23E-03
0.600	1.36E-03	4.750	5.60E-03
0.650	1.44E-03	5.000	5.80E-03
0.700	1.52E-03		

Table 5.4-4 – Neutron Flux-to-Dose Rate Conversion Factors from ANSI/ANS 6.1.1-1977

η-Energy (MeV)	$DF_g(E)$ (η/cm²-s to rem/hr)	Quality Factor	η-Energy (MeV)	$DF_g(E)$ (η/cm²-s to rem/hr)	Quality Factor
2.50E-08	3.67E-06	2.0	5.00E-01	9.26E-05	11.0
1.00E-07	3.67E-06	2.0	1.0	1.32E-04	11.0
1.00E-06	4.46E-06	2.0	2.5	1.25E-04	9.0
1.00E-05	4.54E-06	2.0	5.0	1.56E-04	8.0
1.00E-04	4.18E-06	2.0	7.0	1.47E-04	7.0
1.00E-03	3.76E-06	2.0	10.0	1.47E-04	6.5
1.00E-02	3.56E-06	2.5	14.0	2.08E-04	7.5
1.00E-01	2.17E-05	7.5	20.0	2.27E-04	8.0

Table 5.4-5 – Neutron Dose Rate Calculations

Radionuclide	Source Strength (η/s/g)	Dose Rate from 1 η/s Point Source (mrem/h)	Neutron Multiplication Factor	Mass for 1000 mrem/h at 1 Meter (g)	Specific Activity (Ci/g)	Activity for 1000 mrem/h at 1 Meter (Ci), A_N
^{230}Th	9.13E+00	8.52E-07	2.70	4.76E+07	2.10E-02	1.00E+06
^{232}Th	2.28E-05	8.58E-07	2.70	1.90E+13	1.10E-07	2.09E+06
^{231}Pa	2.64E+01	8.49E-07	2.70	1.65E+07	4.70E-02	7.77E+05
^{232}U	1.50E+04	8.50E-07	2.70	2.90E+04	2.20E+01	6.39E+05
^{233}U	4.83E+00	8.53E-07	2.70	8.99E+07	9.70E-03	8.72E+05
^{234}U	3.03E+00	8.50E-07	2.70	1.44E+08	6.20E-03	8.91E+05
^{235}U	1.02E-03	8.43E-07	2.70	4.31E+11	2.20E-06	9.49E+05
^{236}U	2.94E-02	8.47E-07	2.70	1.49E+10	6.50E-05	9.68E+05
^{238}U	1.37E-02	7.81E-07	2.70	3.46E+10	3.40E-07	1.18E+04
^{237}Np	3.43E-01	8.49E-07	2.70	1.27E+09	7.10E-04	9.03E+05
^{236}Pu	5.33E+05	8.50E-07	2.70	8.17E+02	5.30E+02	4.33E+05
^{238}Pu	1.62E+04	8.40E-07	2.70	2.73E+04	1.70E+01	4.64E+05
^{239}Pu	3.86E+01	8.47E-07	2.70	1.13E+07	6.20E-02	7.02E+05
^{240}Pu	1.17E+03	7.98E-07	2.70	3.97E+05	2.30E-01	9.14E+04
^{241}Pu	1.35E+00	8.44E-07	2.70	3.24E+08	1.00E+02	3.24E+10
^{242}Pu	1.72E+03	7.94E-07	2.70	2.71E+05	3.90E-03	1.06E+03
^{244}Pu	1.90E+03	7.80E-07	2.70	2.50E+05	1.80E-05	4.50E+00
^{241}Am	2.71E+03	8.48E-07	2.70	1.61E+05	3.40E+00	5.48E+05
^{242m}Am①	7.39E+16	8.00E-07	2.70	6.26E-09	3.30E+12	2.07E+04
^{242m}Am②	1.65E+02	8.10E-07	2.70	2.78E+06	1.00E+01	2.78E+07
^{243}Am	1.40E+02	8.48E-07	2.70	3.12E+06	2.00E-01	6.25E+05
^{240}Cm	9.48E+07	8.23E-07	2.70	4.75E+00	2.00E+04	9.50E+04
^{242}Cm	2.48E+07	8.07E-07	2.70	1.85E+01	3.30E+03	6.11E+04
^{243}Cm	4.10E+05	8.07E-07	2.70	1.12E+03	5.20E+01	5.83E+04
^{244}Cm	1.09E+07	8.05E-07	2.70	4.21E+01	8.10E+01	3.41E+03
^{245}Cm	3.82E+03	8.04E-07	2.70	1.24E+05	1.72E-01	2.14E+04
^{246}Cm	9.68E+06	8.02E-07	2.70	4.77E+01	3.10E-01	1.48E+01
^{248}Cm	4.03E+07	7.93E-07	2.70	1.16E+01	4.20E-03	4.87E-02
^{250}Cm③	1.25E+10	7.76E-07	2.70	3.81E-02	1.50E-01	5.71E-03
^{249}Bk③	1.65E+05	7.82E-07	2.70	2.87E+03	1.60E+03	4.59E+06
^{249}Cf③	6.26E+03	8.37E-07	2.70	7.07E+04	4.10E+00	2.90E+05
^{250}Cf③	1.08E+10	8.23E-07	2.70	4.17E-02	1.10E+02	4.58E+00
^{251}Cf	1.52E+03	8.50E-07	2.70	2.86E+05	1.60E+00	4.58E+05
^{252}Cf③	2.05E+12	8.19E-07	2.70	2.20E-04	5.40E+02	1.19E-01
^{254}Cf③	1.05E+15	8.26E-07	2.70	4.28E-07	8.50E+03	3.64E-03
^{253}Es③	3.13E+08	8.29E-07	2.70	1.43E+00	2.50E+04	3.57E+04
^{254}Es③	9.43E+06	8.33E-07	2.70	4.72E+01	1.90E+03	8.96E+04
^{254m}Es③	1.94E+13	8.23E-07	2.70	2.32E-05	3.10E+05	7.20E+00

Notes:

① 2.2 MeV; used modified Sources 4A data file.

② 0.048 MeV; used modified Sources 4A data file.

③ Used modified Sources 4A data file.

FIGURE WITHHELD UNDER 10 CFR 2.390

Figure 5.4-1 – Axial View for MCNP Neutron Point Source Calculations

This page intentionally left blank.

5.5 Appendices

5.5.1 *HAC at 1m Co-60 Point Source Gamma Shielding Analysis*

5.5.2 *Derivation of MCNP Neutron Subcritical Multiplication Factor*

5.5.3 *Screening Methodology for Neutron Emitting Isotopes*

5.5.4 *Screening Methodology for Gamma Emitting Isotopes*

5.5.5 *Evaluation of the Effect of NCT to HAC Changes on Neutron Dose Rates*

5.5.6 *Evaluation of the Effect of NCT-to-HAC Changes on Gamma Dose Rates*

5.5.7 *MCNP Input Files for the Shielding Analyses*

This page intentionally left blank.

5.5.1 HAC at 1m Co-60 Point Source Gamma Shielding Analysis

Unit Definition: Units not standard to MathCAD and additional constants are defined as follows:

$\gamma := Bq \cdot s$ $\quad \nu := \gamma$ $\quad Ci := 3.7 \cdot 10^{10} \cdot Bq$ $\quad eV := 1.60 \cdot 10^{-19} \cdot J$

$KeV := 1 \cdot 10^{3} \cdot eV$ $\quad MeV := 1 \cdot 10^{6} \cdot eV$ $\quad mrem := \frac{hr \cdot \gamma}{cm^2 \cdot s}$

Mass Attentuation Coefficients from ANSI/ANS 6.4.3-1991: Tabular mass attenuation coefficients as a function of gamma energy for 1) silicon, 2) chromium, 3) manganese, 4) iron, 5) nickel, and 6) lead are imported and assigned to the following variables:

$Ti :=$ D:\..\mass_attenuation_coefficients.xls $\quad i := 0 .. rows(Ti) - 2$

$Ei_i := Ti_{i,0} \cdot MeV$ $\quad \mu 1_{\rho_i} := Ti_{i,1} \cdot \frac{cm^2}{g}$ $\quad \mu 2_{\rho_i} := Ti_{i,2} \cdot \frac{cm^2}{g}$ $\quad \mu 3_{\rho_i} := Ti_{i,3} \cdot \frac{cm^2}{g}$

$\mu 4_{\rho_i} := Ti_{i,4} \cdot \frac{cm^2}{g}$ $\quad \mu 5_{\rho_i} := Ti_{i,5} \cdot \frac{cm^2}{g}$ $\quad \mu 6_{\rho_i} := Ti_{i,6} \cdot \frac{cm^2}{g}$

Iron Exposure Build Up Factor Coefficients from ANSI/ANS 6.4.3-1991: Tabular iron exposure build up factor coefficients as function of gamma energy are imported and assigned to the following variables:

$Tj :=$ D:\..\iron_buildup_coefficients.xls $\quad j := 0 .. rows(Tj) - 2$

$Ej_j := Tj_{j,0} \cdot MeV$ $\quad a_j := Tj_{j,1}$ $\quad b_j := Tj_{j,2}$

$c_j := Tj_{j,3}$ $\quad d_j := Tj_{j,4}$ $\quad x_{k_j} := Tj_{j,5}$

Flux to Dose Rate Conversion Factors from ANSI/ANS 6.1.1-1977: Tabular flux to dose rate conversion factors as a function of gamma energy are imported and assigned to the following variables:

$Tk :=$ D:\..\flux_doserate_factors.xls $\quad k := 0 .. rows(Tk) - 2$

$Ek_k := Tk_{k,0} \cdot MeV$ $\quad Kk_k := Tk_{k,1}$

Shield Composition Definition: The following table defines the thickness, density, and percent composition of the shielding materials. The percent composition is defined by 1) silicon, 2) chromium, 3) manganese, 4) iron, 5) nickel, and 6) lead.

$m := 0 .. 5$

Tm :=

	Thickness	Density	%Silicon	%Chrom	%Mang	%Iron	%Nickel	%Lead
	0	1	2	3	4	5	6	7
0	0.2500	7.8526	0.0000	0.0000	0.0000	100.0000	0.0000	0.0000
1	0.3750	8.0128	1.0000	19.0000	2.0000	68.0000	10.0000	0.0000
2	1.0000	8.0128	1.0000	19.0000	2.0000	68.0000	10.0000	0.0000
3	1.2190	11.3500	0.0000	0.0000	0.0000	0.0000	0.0000	100.0000
4	1.5000	8.0128	1.0000	19.0000	2.0000	68.0000	10.0000	0.0000
5	0.1350	8.0128	1.0000	19.0000	2.0000	68.0000	10.0000	0.0000
6								
7								

$t_m := Tm_{m,0} \cdot in$ $\quad p1_m := Tm_{m,2} \cdot \%$ $\quad p3_m := Tm_{m,4} \cdot \%$ $\quad p5_m := Tm_{m,6} \cdot \%$

$\rho_m := Tm_{m,1} \cdot \frac{g}{cm^3}$ $\quad p2_m := Tm_{m,3} \cdot \%$ $\quad p4_m := Tm_{m,5} \cdot \%$ $\quad p6_m := Tm_{m,7} \cdot \%$

<u>Detector Distance and Dose Limit Definition</u>: The dose limit is defined as $D := 1000 \cdot mrem \cdot hr^{-1}$ when measured at a distance of 1 meter from the surface of the package. The following table defines the horizontal and vertical distance from each point source to the detector and calculates the resulting radial distance.

$nn := 0 \quad n := 0..nn$

Tn :=

	Horizontal	Vertical
	0	1
0	43.8490	0.0000
1	0.0000	0.0000
2	0.0000	0.0000
3	0.0000	0.0000
4	0.0000	0.0000
5	0.0000	0.0000
6	0.0000	0.0000
7	0.0000	0.0000
8	0.0000	0.0000
9	0.0000	0.0000
10	0.0000	0.0000
11	0.0000	0.0000
12	0.0000	0.0000
13	0.0000	0.0000

$$R_n := \sqrt{\left(Tn_{n,0}\right)^2 + \left(Tn_{n,1}\right)^2} \cdot in$$

Radionuclide Gamma Energy and Intensity: For the specified radionuclide, the gamma energies and gamma intensities are imported and assigned to the following variables:

$Tl :=$ D:\..\radionuclide_data.xls $\qquad$ $index := 6$

$$ll := \left| \begin{array}{l} i \leftarrow 0 \\ \text{while } Tl_{i,0} \neq index \\ \quad i \leftarrow i + 1 \\ ll \leftarrow Tl_{i,1} - 1 \end{array} \right. \qquad l := 0..ll$$

$$E := \left| \begin{array}{l} i \leftarrow 0 \\ \text{while } Tl_{i,0} \neq index \\ \quad i \leftarrow i + 1 \\ ll \leftarrow Tl_{i,1} - 1 \\ \text{for } j \in 0..ll \\ \quad E_j \leftarrow \left| \begin{array}{ll} 100 & \text{if } Tl_{i+j,2} < 100 \\ Tl_{i+j,2} & \text{otherwise} \end{array} \right. \\ E \cdot KeV \end{array} \right. \qquad I := \left| \begin{array}{l} i \leftarrow 0 \\ \text{while } Tl_{i,0} \neq index \\ \quad i \leftarrow i + 1 \\ ll \leftarrow Tl_{i,1} - 1 \\ \text{for } j \in 0..ll \\ \quad I_j \leftarrow Tl_{i+j,3} \\ I \cdot \% \end{array} \right.$$

Free Mean Path Calculations: The following equations utilize mass attenuation coefficients as a function of gamma energy and the shield composition definition to calculate the number of mean free paths for each of the gamma energies and shield materials:

$$\mu_{m,l} := \left(linterp\left(Ei, \mu 1_{\rho}, E_l\right) \cdot \rho_m \cdot p1_m\right) + \left(linterp\left(Ei, \mu 2_{\rho}, E_l\right) \cdot \rho_m \cdot p2_m\right) + \left(linterp\left(Ei, \mu 3_{\rho}, E_l\right) \cdot \rho_m \cdot p3_m\right) \ldots$$
$$+ \left(linterp\left(Ei, \mu 4_{\rho}, E_l\right) \cdot \rho_m \cdot p4_m\right) + \left(linterp\left(Ei, \mu 5_{\rho}, E_l\right) \cdot \rho_m \cdot p5_m\right) + \left(linterp\left(Ei, \mu 6_{\rho}, E_l\right) \cdot \rho_m \cdot p6_m\right)$$

$$x_{m,l} := \mu_{m,l} \cdot t_m$$

$$x_{total_l} := \sum x^{\langle l \rangle}$$

Build Up Factor Calculations: The following G-P geometric progression equations (ANSI/ANS 6.4.3-1991) is utilized along with iron buildup factor coefficients and the number of mean free paths to calculate a buildup factor for each of the gamma energies:

$$Kx_l := linterp\left(Ej, c, E_l\right) \cdot \left(x_{total_l}\right)^{linterp\left(Ej, a, E_l\right)} + linterp\left(Ej, d, E_l\right) \cdot \frac{\left[\tanh\left[\left(\frac{x_{total_l}}{linterp\left(Ej, x_k, E_l\right)}\right) - 2\right] - \tanh(-2)\right]}{1 - \tanh(-2)}$$

$$B_l := \left| \begin{array}{ll} 1 + \left(linterp\left(Ej, b, E_l\right) - 1\right) \cdot \left[\frac{\left[\left(Kx_l\right)^{x_{total_l}} - 1\right]}{\left(Kx_l - 1\right)}\right] & \text{if } Kx_l \neq 1 \\ 1 + \left(linterp\left(Ej, b, E_l\right) - 1\right) \cdot x_{total_l} & \text{if } Kx_l = 1 \end{array} \right.$$

Maximum Activity Calculations: The following equations calculate the total gamma dose resulting from 1 Ci of the specified radionuclide, then ratio the total dose to calculate the activity required to meet the limiting dose rate. The limiting activity is then utilized to calculate the individual gamma dose contributions from each point source. The gamma dose calculations utilize Rockwell's methodology.

$$K_l := \mathrm{linterp}(Ek, Kk, E_l)$$

$$D_{ratiocomp_{l,n}} := \left[\frac{Ci \cdot I_l \cdot B_l \cdot K_l}{4 \cdot \pi \cdot (R_n)^2}\right] \cdot e^{-x_{total_l}}$$

$$D_{ratiototal_n} := \sum D_{ratiocomp}^{\langle n \rangle}$$

$$D_{ratiolimit} := \sum D_{ratiototal}$$

$$A_{limit} := Ci \cdot \frac{D}{(D_{ratiolimit})}$$

$$D_{limitcomp_{l,n}} := \left[\frac{A_{limit} \cdot I_l \cdot B_l \cdot K_l}{4 \cdot \pi \cdot (R_n)^2}\right] \cdot e^{-x_{total_l}}$$

$$D_{limittotal_n} := \sum D_{limitcomp}^{\langle n \rangle}$$

$$D_{limit} := \sum D_{limittotal}$$

Summary of Results: The gamma energies and intensities for radionuclide $index = 6$ are as follows:

$$E^T = \left[346.9300 \;\; 826.2800 \;\; 1.1732 \cdot 10^3 \;\; 1.3325 \cdot 10^3 \;\; 2.1588 \cdot 10^3 \;\; 2.5050 \cdot 10^3\right] \cdot KeV$$

$$I^T = \left[7.6000 \cdot 10^{-3} \;\; 7.6000 \cdot 10^{-3} \;\; 99.9736 \;\; 99.9856 \;\; 1.1100 \cdot 10^{-3} \;\; 2.0000 \cdot 10^{-6}\right] \cdot \%$$

The mass attenuation coefficients and the number of mean free paths for each of the gamma energies and shield materials are

$$\mu^T = \begin{bmatrix} 0.7808 & 0.7970 & 0.7970 & 3.4267 & 0.7970 & 0.7970 \\ 0.5144 & 0.5254 & 0.5254 & 0.9370 & 0.5254 & 0.5254 \\ 0.4381 & 0.4474 & 0.4474 & 0.7079 & 0.4474 & 0.4474 \\ 0.4106 & 0.4193 & 0.4193 & 0.6450 & 0.4193 & 0.4193 \\ 0.3258 & 0.3326 & 0.3326 & 0.5092 & 0.3326 & 0.3326 \\ 0.3084 & 0.3147 & 0.3147 & 0.4958 & 0.3147 & 0.3147 \end{bmatrix} \cdot \frac{1}{cm} \text{ and}$$

$$x^T = \begin{bmatrix} 0.4958 & 0.7592 & 2.0245 & 10.6100 & 3.0367 & 0.2733 \\ 0.3266 & 0.5005 & 1.3346 & 2.9013 & 2.0019 & 0.1802 \\ 0.2782 & 0.4262 & 1.1365 & 2.1919 & 1.7047 & 0.1534 \\ 0.2607 & 0.3994 & 1.0651 & 1.9971 & 1.5977 & 0.1438 \\ 0.2069 & 0.3168 & 0.8447 & 1.5765 & 1.2671 & 0.1140 \\ 0.1958 & 0.2998 & 0.7994 & 1.5351 & 1.1991 & 0.1079 \end{bmatrix},$$

such that the total mean free path for each gamma energy is

$$x_{total}^T = (17.1995 \;\; 7.2451 \;\; 5.8909 \;\; 5.4638 \;\; 4.3260 \;\; 4.1371).$$

The buildup factors and flux-to-dose rate conversion factors for each of the gamma energies are

$B^T = (34.4640 \;\; 11.2272 \;\; 7.6782 \;\; 6.7031 \;\; 4.4661 \;\; 4.0905)$ and

$K^T = \left[8.7069 \cdot 10^{-4} \;\; 1.7194 \cdot 10^{-3} \;\; 2.2095 \cdot 10^{-3} \;\; 2.4206 \cdot 10^{-3} \;\; 3.3757 \cdot 10^{-3} \;\; 3.7250 \cdot 10^{-3}\right]$.

The distances from each of the point-sources to the detector location are

$R^T = (43.85) \cdot in,$

such that the individual gamma dose contributions from each gamma energy and point sources are

$$D_{limitcomp}^T = \left[6.6883 \cdot 10^{-7} \;\; 9.0551 \cdot 10^{-3} \;\; 405.4765 \;\; 594.4953 \;\; 0.0191 \;\; 4.2085 \cdot 10^{-5}\right] \cdot \frac{mrem}{hr}.$$

Therefore, the total limiting dose of $D_{limit} = 1000 \cdot \frac{mrem}{hr}$ is obtained with a total limiting point source activity of $A_{limit}(nn+1) = 36.4345 \cdot Ci$.

This page intentionally left blank.

5.5.2 Derivation of MCNP Neutron Subcritical Multiplication Factor

The actual distribution of isotopes in the package is not specifically defined for the *General Payload Case*. In order to ensure the hypothetical accident condition (HAC) dose rate limit is met, a point source geometry is used to calculate the maximum allowable activity. Subcritical multiplication will increase the effective neutron source dependent on the source distribution and payload matrix. In order to account for subcritical neutron multiplication, a neutron multiplication factor is derived.

The factor is developed by assuming a point neutron source imbedded in a theoretical sphere of homogenized ^{239}Pu and a 30% polyethylene and 70% water mixture. It is assumed that 325 grams of ^{239}Pu are in the "target" matrix. The 30% polyethylene and 70% water mixture is assumed to be a representative matrix in the package for multiplication. Calculations are done for varying source spheres using MCNP with the effect of subcritical multiplication enabled. These calculations are then compared to the equivalent point source calculation to determine the effective increase, or multiplication, in dose rate. The calculation results are presented in Table 5.5.2-1. A sample MCNP[1] input file is included at the end of this appendix.

The neutron multiplication dose rate calculations are made by making minor modifications to the point source geometry described in Section 5.4*, Shielding Evaluation*. The modifications include:

1. Moving the point source radially inward far enough to accommodate a sphere centered about the point source, where the far radial extent of the sphere just touches the inside of the package radial shield.
2. The material within the sphere is a mix of 30% polyethylene and 70% water mixture (density = 0.976 g/cm^3) and ^{239}Pu (density (theoretical) = 19.84 g/cm^3). The total allowed maximum mass of ^{239}Pu is 325 grams, which corresponds to a full density volume of 16.3811 cm^3. For a sphere of radius, r, and corresponding volume, V, the volume fraction of ^{239}Pu is 16.3811/V, and the volume fraction of the polyethylene is 1 – (16.3811/V). The total density of the mix and the composition of the mix is then determined from these volume fractions of the full density of material.
3. The calculations are made for various sphere radii and the increase in the dose rate from neutron multiplication is just the ratio of the dose rate with the sphere in place (point source in center of the sphere) to the dose rate with the point source without the sphere. The MCNP[1] geometry with a sphere is shown in Figure 5.5.2-1, Figure 5.5.2-2, and Figure 5.5.2-3, and a typical MCNP input file is listed in Table 5.5.5-2.
4. Calculations are made with a 30% polyethylene and 70% water mixture reflector. The reflector geometry shown in Figure 5.5.2-1, Figure 5.5.2-2, and Figure 5.5.2-3 utilizes the (30% polyethylene and 70% water mixture ^{239}Pu) sphere, and includes a 30.48 cm thick 30% polyethylene and 70% water mixture reflector, as shown in Figure 5.5.2-1. This reflector is replaced with a void inside a cylinder (with the same radius as the sphere next to the shield) for most of the calculations to eliminate that attenuation to the detector.

[1] J. F. Breismeister, Editor, *MCNP – A General Monte Carlo Code N-Particle Transport Code, Version 4B*, LA-12625-M, Los Alamos National Laboratory, Los Alamos, New Mexico, 1997.

The first series of calculations summarized in Table 5.5.2-1 are for the ^{252}Cf source, which has nearly the highest average neutron energy (2.53 MeV) of the authorized isotopes. The base case is the point source (no sphere) right inside the shield. The optimum sphere radius corresponds to H/Pu atom ratios between 700 and 900, and gives a dose rate factor of about 2.2 from the neutron multiplication. The next two calculations in the table are for a higher energy 5 MeV neutron source. This shows the dose factor from neutron multiplication decreases with increasing neutron energy because there is less neutron attenuation at higher energies so the source neutron escapes the sphere more easily.

The last eight cases in Table 5.5.2-1 are for the ^{238}U source, which has the lowest average neutron energy (1.69 MeV) of the authorized isotopes. The dose factor from neutron multiplication is larger for this lower source energy with a maximum of 2.60. A factor of 2.70 is applied to the point source calculations to conservatively include neutron multiplication.

The third from the last case of Table 5.5.2-1, case *sm090un*, replaces the void cylindrical region between the sphere and the inner shield with the (30%polyethylene, 70% water) reflector. This additional reflector increases the multiplication factor, but it also provides more attenuation for neutrons to reach the detector. Since the ratio for this case is a little less than that for case *sm090u*, the attenuation is more important. Cases *sm090n4* and *sm090n8* at the bottom of Table 5.5.2-1 are like case *sm090un*, except the sphere is moved inward four inches and eight inches respectively. Again the attenuation is more important than any change in the multiplication from the reflector modification.

Table 5.5.2-1 – Dose Rate Increase from Neutron Multiplication

Case①	Sphere Radius (cm)	H/Pu Atom Ratio	Neutron Dose Rate at 1 Meter (mrem/hr)			
			This Case	σ (%)	No Multiplier	Ratio
^{252}Cf point unit neutron source surrounded by a sphere of 325 grams ^{239}Pu mixed with (30% polyethylene,70% water) and reflected with 1-foot (30.48 cm) of (30% polyethylene,70% water).						
smbase	0.0	none	8.19E-07	0.4	8.19E-07	1.00
sm000	1.5755	0	1.03E-06	0.9	8.19E-07	1.25
sm0001	1.8836	1	8.38E-07	0.9	8.19E-07	1.02
sm001	3.1627	10	6.60E-07	1.0	8.19E-07	0.81
sm010	6.5512	100	7.19E-07	1.2	8.19E-07	0.88
sm050	11.1608	500	1.55E-06	1.6	8.19E-07	1.89
sm070	12.4821	700	1.82E-06	1.7	8.19E-07	2.22
sm080	13.0491	800	1.81E-06	1.8	8.19E-07	2.21
*sm090*②	13.5707	900	1.78E-06	1.8	8.19E-07	2.17
sm100	14.0551	1,000	1.74E-06	1.8	8.19E-07	2.13
sm110	14.5082	1,100	1.60E-06	1.8	8.19E-07	1.95
sm150	16.0865	1,500	1.12E-06	1.7	8.19E-07	1.37
*sm090n*③	13.5707	900	1.76E-06	2.1	8.19E-07	2.15
5 MeV point unit neutron source surrounded by a sphere of 325 grams ^{239}Pu mixed with (30% polyethylene,70% water) and reflected with 1-foot (30.48 cm) of (30% polyethylene,70% water).						
s5mbase	0.0	none	9.21E-07	0.4	9.21E-07	1.00
s5m090	13.5707	900	1.23E-06	2.2	9.21E-07	1.33
^{238}U point unit neutron source surrounded by a sphere of 325 grams ^{239}Pu mixed with (30% polyethylene,70% water) and reflected with 1-foot (30.48 cm) of (30% polyethylene,70% water).						
Smbaseu	0.0	none	7.81E-07	0.4	7.81E-07	1.00
sm070u	12.4821	700	1.98E-06	1.7	7.81E-07	2.53
sm080u	13.0491	800	2.00E-06	1.8	7.81E-07	2.56
sm090u	13.5707	900	2.03E-06	1.8	7.81E-07	2.60
sm100u	14.0551	1,000	1.87E-06	1.8	7.81E-07	2.39
*sm090un*④	13.5707	900	1.98E-06	2.0	7.81E-07	2.54
*sm090n4*⑤	13.5707	900	2.95E-07	2.4	7.81E-07	0.38
*sm090n8*⑥	13.5707	900	6.95E-08	3.6	7.81E-07	0.09

Notes for Table 5.5.2-1:

① The MCNP input file name is this case name preceded by an "i" and the MCNP output file is this case name preceded by an "o".

② The k_{eff} value for case *sm090* is 0.9144.

③ This is like case *sm090*, except there is no void cylindrical region between the sphere and the inner shield.

④ This is like case *sm090u*, except there is no void cylindrical region between the sphere and the inner shield.

⑤ This is like case *sm090un*, except the sphere is moved inward 4 inches.

⑥ This is like case *sm090un*, except the sphere is moved inward 8 inches.

Table 5.5.2-2 – Typical MCNP Input File for the Neutron Multiplication Calculations

```
 72-b Cask, single with h/pu=900 [30% poly, 70% water], shield mult ,ism090u
c    u-238 spectrum
c    dimensions for cask taken from figure 6.3-1 of original chapter 6
c    *****interior of cask
    1 41  -1.00552  -1                      $ mix in sphere
    2 42  -0.976    -2  1 -11 (-7:(7 6))    $ 12" reflector
    3  0            -6  1 -11  7            $ front void
    4  0           -11  2 -24 23 (-7:(7 6)) $ remaining void of interior
c    *****radial of cask, except along 6" puncture bar for lead and outer
   11  3  -8.020   -12 11 -24 23            $ inner radial steel
   12 51 -11.340   -13 12 -24 23 (22:-21)   $ lead
   13  3  -8.020   -14 13 -24 23 (22:-21)   $ ss outer cask, outer shell
c    *****radial of cask for 6" puncture bar for lead and outer
   17 51 -11.340   -13 12 -22 21 -15        $ lead
   18  3  -8.020   -14    -22 21 -16 (15:13) $ ss outer cask, outer shell
c    *****bottom of cask
   21  3  -8.020   -14    -23 25            $ next to inside
   22  3  -8.020   -14    -25 27            $ intermediate
   23  3  -8.020   -14    -27 29            $ outer
c    *****top of cask
   24  3  -8.020   -14    -26 24            $ next to inside
   25  3  -8.020   -14    -28 26            $ intermediate
   26  3  -8.020   -14    -30 28            $ outer
c    *****beyond cask
   31 77  -0.00123  -8    -42 41            $ air to beyond detector
         ((14:-29:30):(16 -22 21))
   32 77  -0.00123  -9    -44 43 (8:-41:42) $ air on beyond
   33  0            (9:-43:44)              $ outside world
c          inside cask
    1  sx   26.1158  13.5707 $ sphere for mix
    2  sx   26.1158  44.0507 $ reflector
    6  cx   13.5707          $ forward cylinder for reflector
    7  px   26.1158          $ plane for reflector
c          radial cask
   11  cz   39.6875          $ inner radial of cask
   12  cz   43.1800          $ inner steel
   13  cz   47.9425          $ lead
   14  cz   52.0700          $ outer steel
   15  px   46.27626         $ lead at puncture bar
   16  px   50.40376         $ outer steel at puncture bar
c          axial cask
   21  pz   -7.620           $ bottom of puncture bar
   22  pz    7.620           $ top of puncture bar
   23  pz -154.305           $ bottom inside of cask
   24  pz  154.305           $ top inside of cask
   25  pz -159.808           $ bottom first intermediate
   26  pz  165.317           $ top first intermediate
   27  pz -165.312           $ bottom second intermediate
   28  pz  176.318           $ top second intermediate
   29  pz -170.815           $ bottom outside of cask
   30  pz  187.325           $ top outside of cask
c          air beyond cask
   41  pz -320.815           $ 150 cm below
   42  pz  337.325           $ 150 cm above
   43  pz -670.815           $ 500 cm below
   44  pz  687.325           $ 500 cm above
    8  cz  202.070           $ 150 cm beyond
```

```
    9  cz  552.070          $ 500 cm beyond

mode   n
imp:n    1 15r 0.25 0
print
cut:n    j j 0 0
nps    50000
ctme   300.
c     point unit source from u-238
sdef x=26.1158 y=0. z=0. erg=d7 wgt=1.0
sc7   u-238
si7   0.1 0.5     1.0     2.0     3.0     4.0     6.0     8.0
          10.0  12.0
sp7   0.00E+00  1.99E-03  2.76E-03  4.52E-03  2.53E-03
      1.15E-03  6.57E-04  9.05E-05  1.07E-05  1.25E-06
c    SS-304L from Nuclear Systems Materials Handbook Rev. 36
m3     6000.60c -0.0003  25055.50c -0.02    15031.50c -0.01
      28000.50c -0.0925  24000.50c -0.19    26000.55c -0.6872
c     mix for 30% poly and 70% water with pu-239
m41    1001.60c -.117160  6000.60c -.234670  94239.60c -.030874
       8016.60c -.617295
mt41   poly.01t
m42    1001.60c -.120893  6000.60c -.242146   8016.60c -.636961 $ poly,w
mt42   poly.01t
m51   82000.50c -1.00                            $ lead
m77    8016.60c  0.220    7014.60c  0.780        $ air
c      ansi/ans-6.1.1-1977 fluence-to-dose,neutrons(mrem/hr/(n/cm**2/s)
de0    log   2.5e-08 1.0e-07 1.0e-06 1.0e-05 1.0e-04
             .001     .01     .1      .5      1.0
              2.5     5.0     7.0     10.0    14.0  20.0
df0    log   3.67e-3 3.67e-3 4.46e-3 4.54e-3  4.18e-3
             3.76e-3 3.56e-3 2.17e-2 9.26e-2  .132
              .125    .156    .147    .147    .208  .227
fc5    dose rate in mrem/hr at 1 meter from outer surface
f5:n    150.40376  0. 0. 20.
```

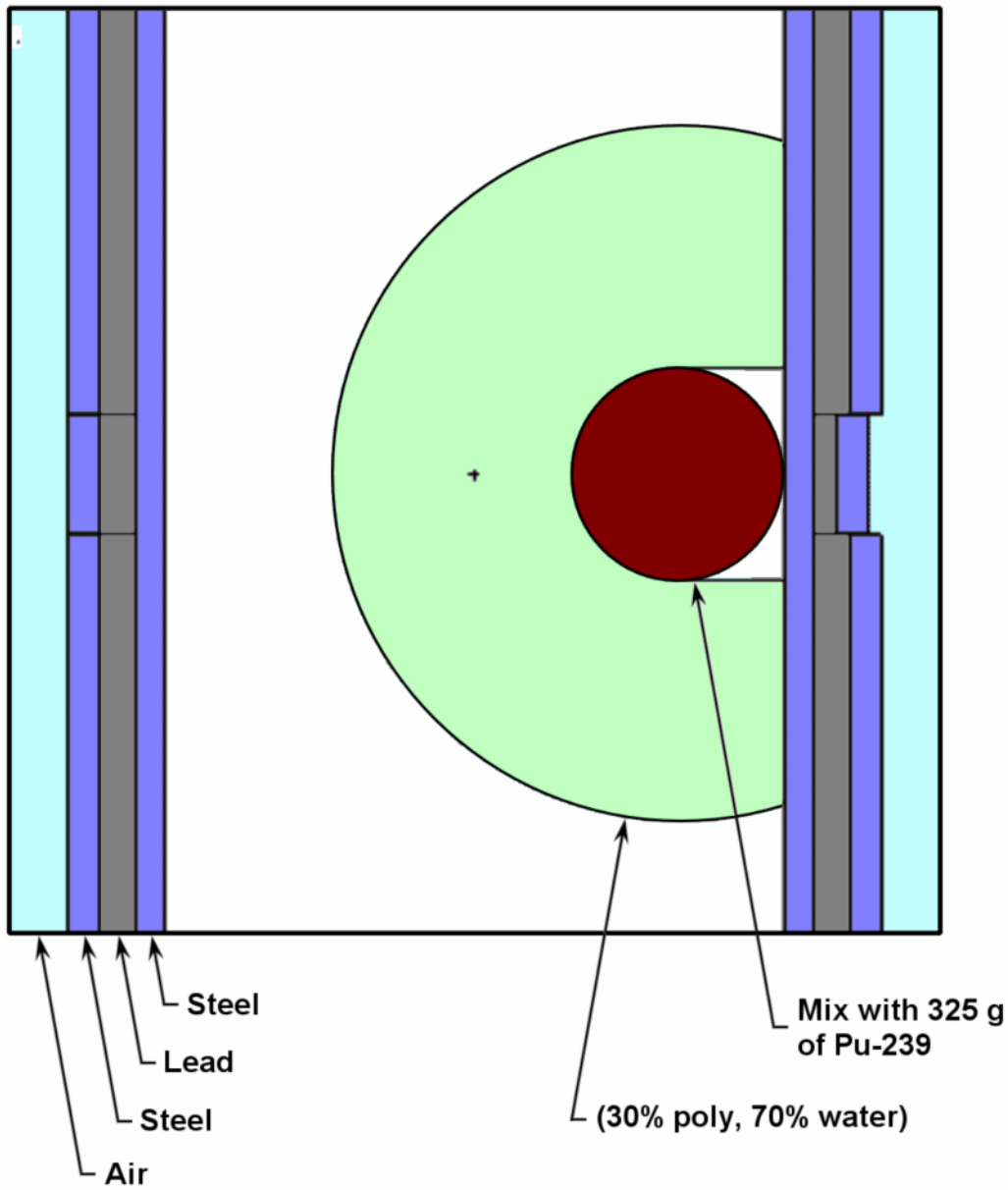

Note: The packaging geometry is consistent with the criticality model, except for the puncture bar (Δr for lead decreases from 1.875 inches to 1.219 inches). The point source is in the center of the sphere; sphere and reflector are (30% poly/70% water).

Figure 5.5.2-1 – Axial View of Geometry Model for Neutron Multiplication Showing Sphere, Reflector, and Puncture Bar Vicinity

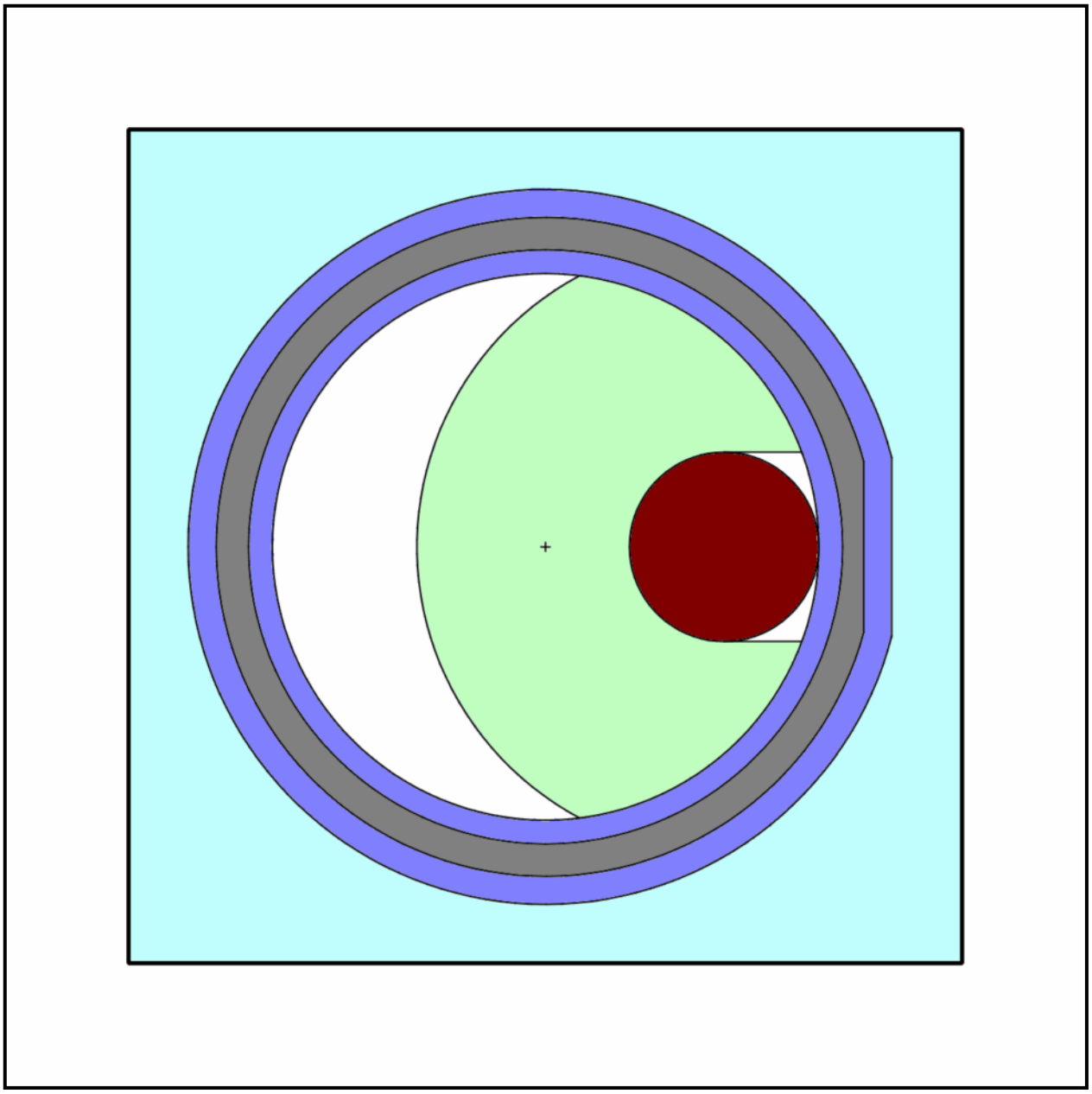

Figure 5.5.2-2 – Plan View of Geometry Model for Neutron Multiplication Showing Sphere, Reflector, and Puncture Bar Vicinity

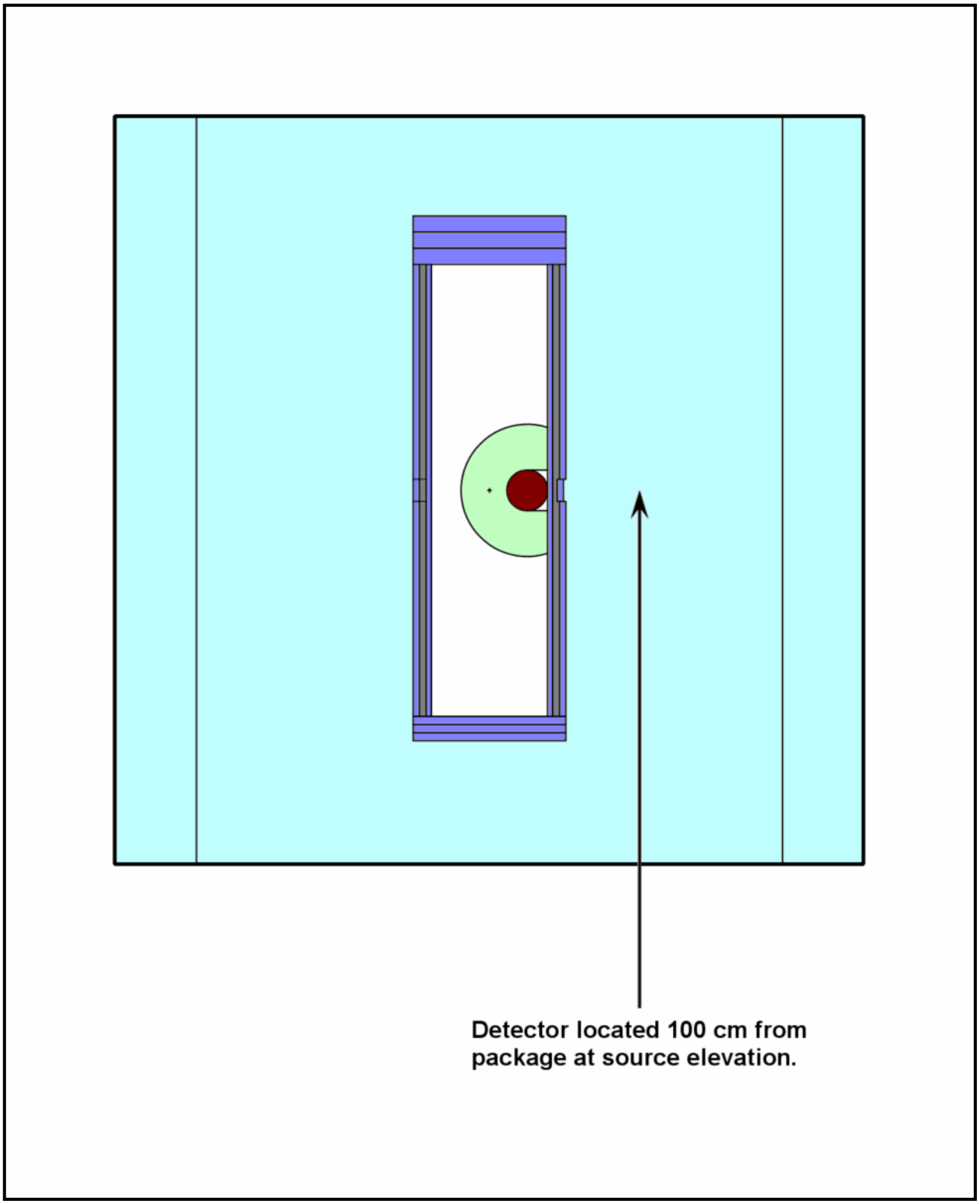

Figure 5.5.2-3 – Expanded Axial View for Neutron Multiplication Showing Detector

5.5.3 Screening Methodology for Neutron Emitting Isotopes

The maximum allowable activity for each of the neutron source isotopes, based on the hypothetical accident conditions limit, are presented in Table 5.1-1 in Section 5.1, *Discussion and Results*. A methodology is developed herein for screening or calculating the maximum allowable activity of neutron source isotopes that are either newly identified by the shipper or require additional consideration due to a waste form matrix that produces more neutrons than the uranium oxide assumed in the development of the alpha-n component of the total neutron source strengths.

Evaluation of the Sources 4A[1] output and the MCNP[2] dose rate calculations discussed in Section 5.2.2, *Neutron Source,* and Section 5.4.2, *Neutron Shielding Evaluation,* reveals the following:

- The total source strength for each isotope is the sum of the alpha-n and spontaneous fission contributions. This source strength is a characteristic of the specific isotope and the assumed target matrix (in this case uranium oxide).
- The neutron source strength for each isotope has a unique neutron energy spectrum, and a corresponding average energy.
- The average energies for the evaluated isotopes all fall between 1.5 and 2.6 MeV.
- The dose rate calculations for the evaluated isotopes show no functional relationship between average energy and dose rate. In fact, the calculated dose rates for unit neutron sources generated with the unique neutron energy spectra, are all within about 5% of the mean.
- Figure 5.5.3-1 shows that the neutron source strength required to reach the dose rate limit is not directly related to the average neutron energy. This is probably the case, in part, because the spectra are different.
- The characteristic source strength per curie for the isotopes (including the subcritical multiplication factor) is inversely proportional to the activity required to reach the limit (see Figure 5.5.3-2).

Figure 5.5.3-2 shows the total neutrons per second per curie (for each radionuclide) is a function of the maximum allowable activity as predicted by MCNP[2]. Plotted on a log-log scale, the data falls on a nearly straight line. In order to fit the data to a curve, the log of the total neutrons per second per curie data is compared with the log of the maximum allowable activity.

A linear curve fit of the log-log data results in the following functional relationship:

$$\log \eta = -1.0025 \log A_N + 8.663$$

where η is the total number of total neutrons per second per curie, and A_N is the maximum allowable activity in curies. Solving for η, the equation may be rewritten as:

---

[1] Los Alamos National Laboratory, *SOURCES 4A: A Code for Calculating (α,n), Spontaneous Fission, and Delayed Neutron Sources and Spectra*, LA-13639-MS, Los Alamos, New Mexico, September 1999.

[2] J. F. Breismeister, Editor, *MCNP – A General Monte Carlo Code N-Particle Transport Code, Version 4B*, LA-12625-M, Los Alamos National Laboratory, Los Alamos, New Mexico, 1997.

$$\eta = \frac{10^{8.663}}{A_N^{1.0025}} = \frac{4.60 \times 10^8}{A_N^{1.0025}}$$

This relationship may be used for screening additional radionuclides based on their characteristic total "neutrons per second per curie." Setting A_N equal to 10^8 Ci and solving for η in the above equation yields a screening value for total neutrons per second per curie of 4.40 η/s-Ci. Thus, a radionuclide having a neutron source strength per curie of less than 4.40 η/s-Ci and an average neutron source energy between 1.5 and 2.6 MeV may be shipped without restriction.

Alternately, the formula may be used to calculate the maximum allowable activity based on the neutron source strength per curie. Rearranging the equation to solve for A_N gives the following:

$$A_N = \frac{4.37 \times 10^8}{\eta^{0.998}}$$

This equation should only be used for source spectra that have an average neutron source energy between 1.5 and 2.6 MeV. The code Sources 4A[1] can be used to develop the source strength per curie based on the isotopic characteristics and the target matrix assumption, as described in Section 5.2.2, *Neutron Source*.

In summary, the screening method can be applied to neutron isotopes that have an average neutron source energy between 1.5 and 2.6 MeV. If the actual waste matrix is bounded by the uranium oxide matrix assumption for alpha-n production, then the isotope can be shipped without restriction if its neutron source strength is less than or equal to 4.40 η/s-Ci. Otherwise, the maximum allowable activity can be calculated directly by using the above equation and a known neutron source strength.

The maximum allowable activity for isotopes with gamma and neutron emissions (A_{GN}) is calculated by using this Appendix for the neutron activity limit (A_N), Appendix 5.5.4, *Screening Methodology for Gamma Emitting Isotopes*, for the gamma activity limit (A_G), and the following equation:

$$A_{GN} = \frac{1}{\left[\left(\frac{1}{A_G}\right) + \left(\frac{1}{A_N}\right)\right]}$$

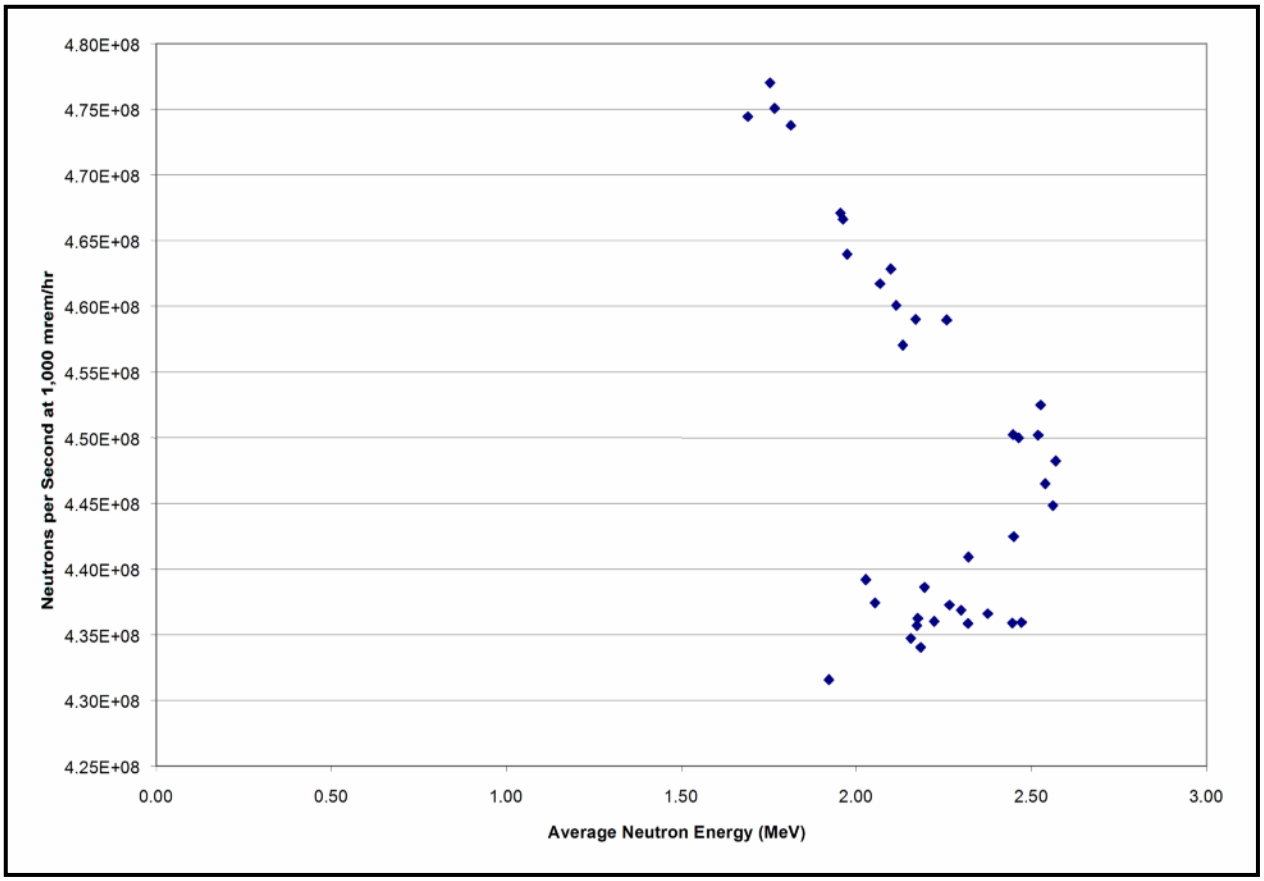

Figure 5.5.3-1 – Neutron Source Strength at 1,000 mrem/hr vs. Average Neutron Energy

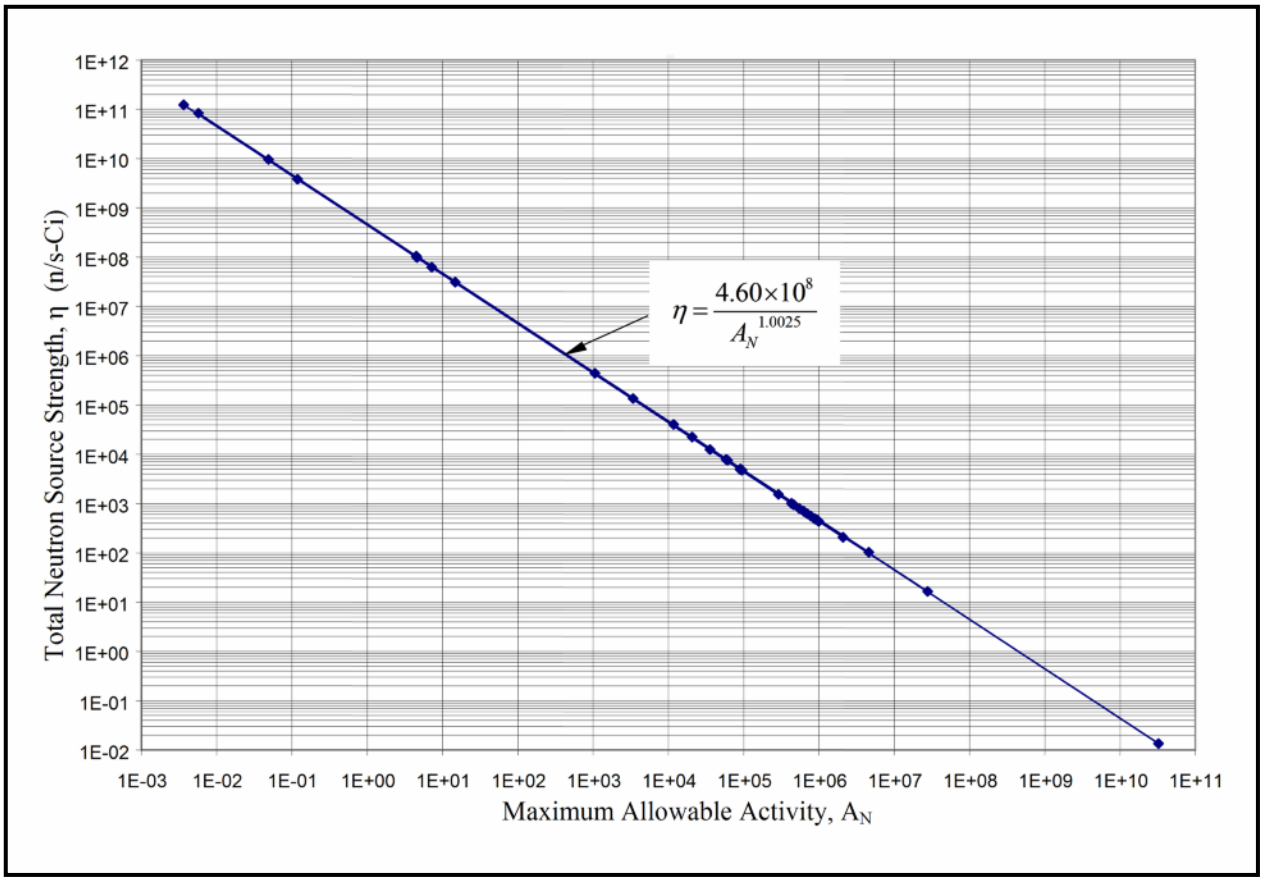

Figure 5.5.3-2 – Total Neutron Source Strength per Curie as a Function of Maximum Allowable Activity (Curies)

5.5.4 Screening Methodology for Gamma Emitting Isotopes

The maximum allowable activity for each of the gamma source isotopes, based on the hypothetical accident conditions (HAC) limit, are presented in Table 5.1-1 in Section 5.1, *Discussion and Results*. A methodology is developed herein for screening or calculating the maximum allowable activity of gamma source isotopes that are newly identified by the shipper.

Calculations were performed using the same technique given in Section 5.4.1, *Gamma Shielding Evaluation,* to evaluate the relationship of gamma energy vs. gamma intensity to reach the 1000 mrem/h dose rate limit for a given activity of 1×10^8 curies. Evaluation of the results reveals the following:

- The maximum allowable gamma source effective activity is related to the gamma energy (see Figure 5.5.4-2).
- Gamma energies less than 0.3 MeV are acceptable, and require no additional screening or evaluation.

Figure 5.5.4-1 shows that the percent intensity to reach the dose rate limit is a function of the gamma energy. Plotted on a semi-log scale, the data falls on a nearly smooth curve. Curve fitting the data yields the equation:

$$\log[\log(I) + 7.1] = (-1.6281)\log(\gamma) + 0.989$$

where I is the intensity factor (as a fraction where 1.00 = 100%), and γ is the gamma energy (MeV). This equation may be re-arranged in order to solve for I as follows:

$$\mathrm{I} = 10^{\left(1.256\gamma^{-1.6281} - 7.1\right)}$$

This functional relationship is shown in Figure 5.5.4-1 as the "fit curve." Because this curve fit overpredicts allowable gamma intensity at lower energies, its use would not be conservative. Consequently, to ensure conservative results for gamma energies below ~1.0 MeV, and the entire energy range, a curve that just falls below data points was derived. This curve slightly underpredicts allowable gamma intensity, as shown in Figure 5.5.4-1, "bounding curve." Thus, the following bounding equation was derived:

$$\mathrm{I}_{\mathrm{critical}} = 10^{\left(0.952\gamma^{-1.6281} - 7.1\right)}$$

This relationship may be used for screening additional radionuclides based on their characteristic gamma energy intensities. For an isotope with a single gamma energy, setting γ equal to the gamma energy in MeV and solving for $\mathrm{I}_{\mathrm{critical}}$ in the above equation, yields the maximum allowable intensity (as a fraction). Thus, a radionuclide having a single gamma energy and an associated gamma intensity less than $\mathrm{I}_{\mathrm{critical}}$ may be shipped without restriction.

For radionuclides that have multiple gamma energies the method described above is followed for each gamma energy to show that the radionuclide may be shipped without restriction.

In addition to screening radionuclides that may be shipped without restriction, the relationship derived in Figure 5.5.4-1 can be extended to calculate the maximum allowable activity for individual gamma energies. Figure 5.5.4-2 is the same as Figure 5.5.4-1, except the intensity

scale has been changed to effective activity. Figure 5.5.4-2 shows the effective activity for a given gamma energy to reach the 1000 mrem/h dose rate limit. Given a single gamma energy in MeV, its maximum allowable activity may be determined by using the following equation, or Figure 5.5.4-2 adjusted by the respective I_γ:

$$A_\gamma = A_{critical}\left(\frac{I_{critical}}{I_\gamma}\right) = 10^8\left(\frac{10^{\left(0.952\gamma^{-1.6281}-7.1\right)}}{I_\gamma}\right) = \frac{10^{\left(0.952\gamma^{-1.6281}+0.9\right)}}{I_\gamma}$$

Note that I_γ represents the gamma intensity for the specific gamma energy, and is represented as a fraction (e.g., 0.5 is 50%) and $A_{critical}$ is the maximum allowable activity limit of 1×10^8 curies.

For radionuclides that have multiple gamma energies, the above process is followed to calculate the maximum allowable activity for each gamma energy. The maximum allowable activity for all gamma emissions from a particular radionuclide is calculated as follows:

$$A_G = \frac{1}{\sum_{i=1}^{n}\frac{1}{A_{\gamma_i}}}$$

In summary, the screening method can be applied to gamma isotopes that have gamma energies ranging between 0 and 5 MeV. A gamma isotope can be shipped without restriction if all of its gamma energies are less than or equal to 0.3 MeV or if all of its gamma energies have an associated gamma intensity that is less than the critical gamma intensity. Otherwise, the maximum allowable activity can be calculated directly by using the above equations for A_γ and A_G.

The maximum allowable activity for isotopes with gamma and neutron emissions (A_{GN}) is calculated by using this Appendix for the gamma activity limit (A_G), Appendix 5.5.3, *Screening Methodology for Neutron Emitting Isotopes*, for the neutron activity limit (A_N), and the following equation:

$$A_{GN} = \frac{1}{\left[\left(\frac{1}{A_G}\right)+\left(\frac{1}{A_N}\right)\right]}$$

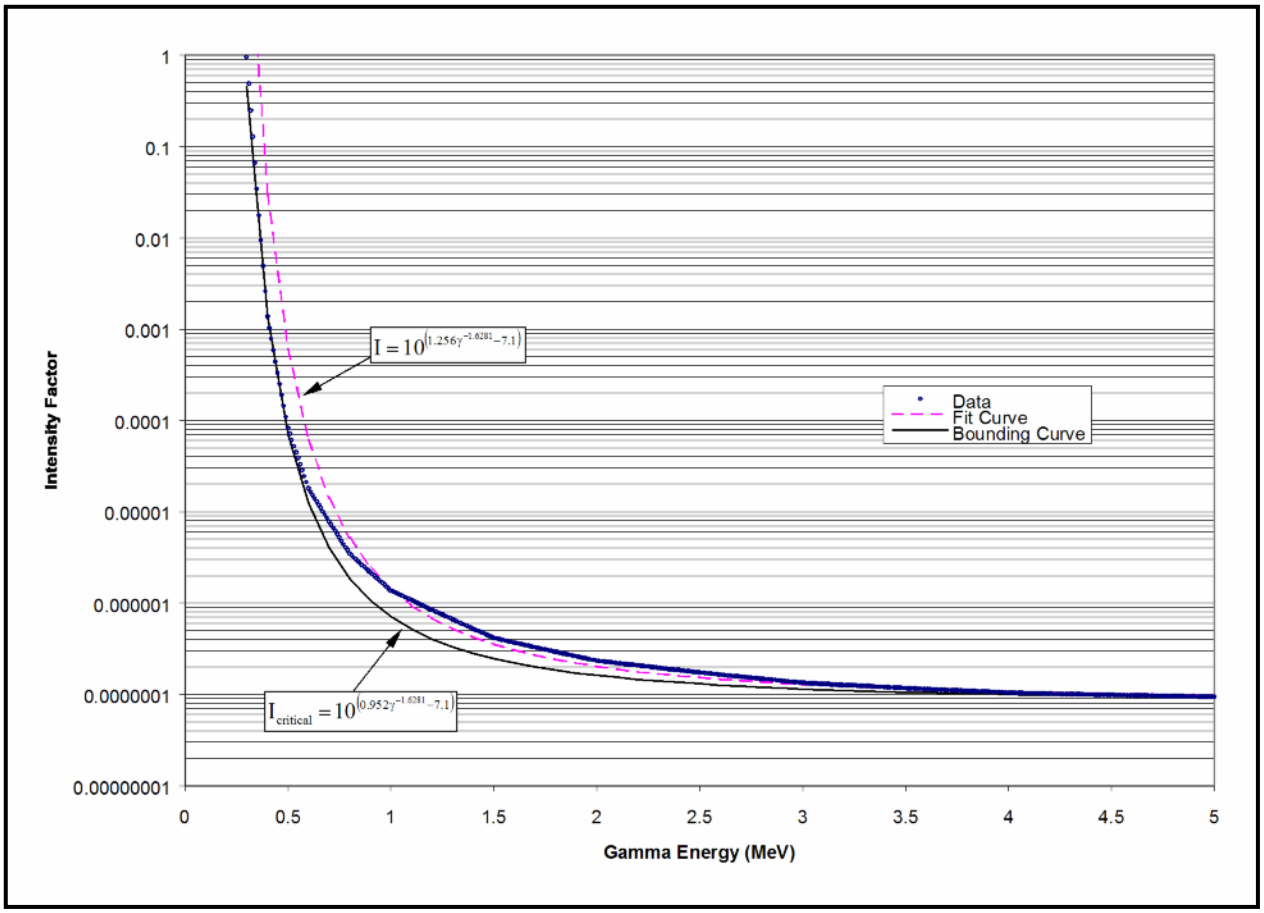

Figure 5.5.4-1 – Intensity Factor vs. Gamma Energy for a Dose Rate of 1,000 mrem/hr at 1 Meter with a 1×10^8 Curie Source Activity

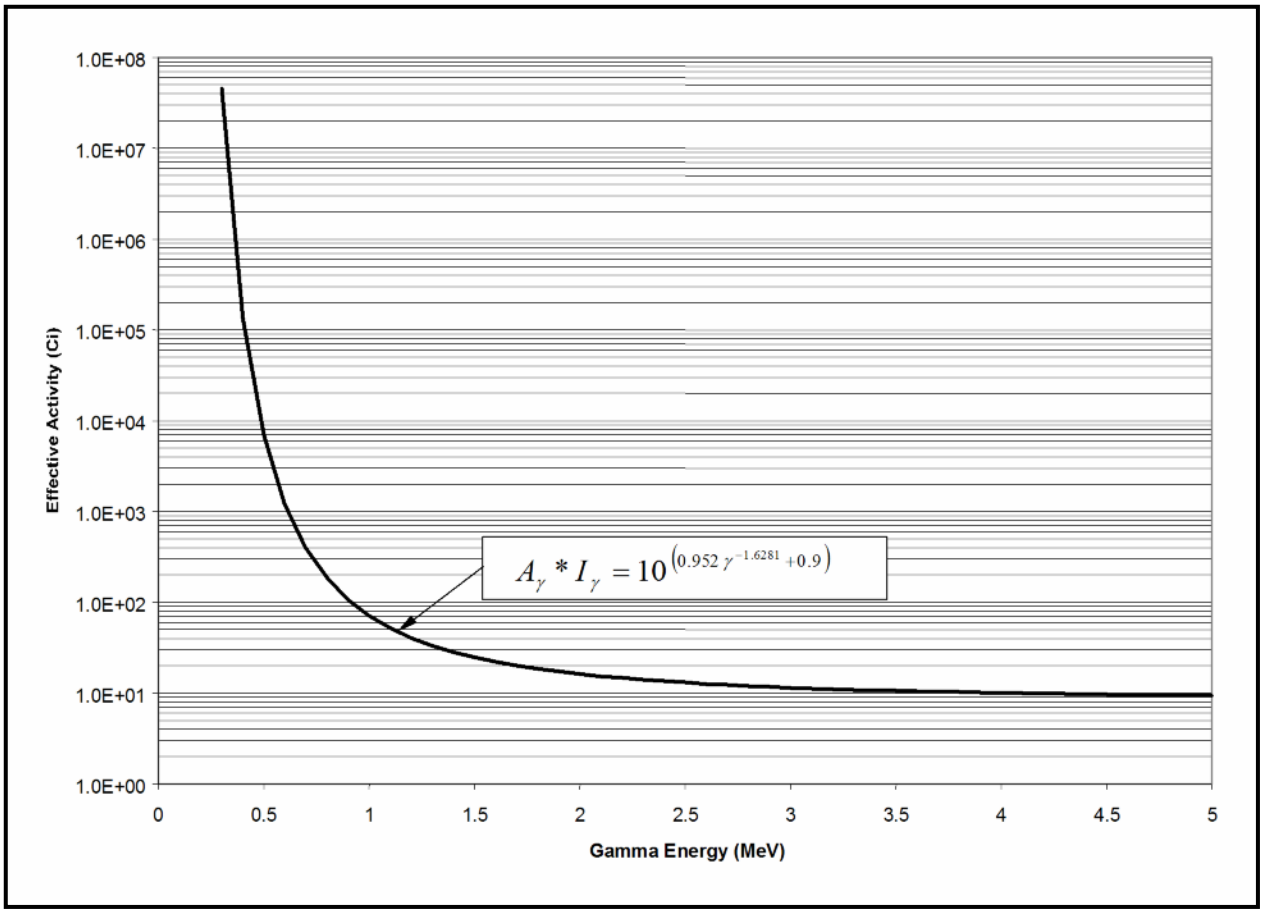

Figure 5.5.4-2 – Effective Activity vs. Gamma Energy for a Dose Rate of 1,000 mrem/hr at 1 Meter

5.5.5 Evaluation of the Effect of NCT to HAC Changes on Neutron Dose Rates

This appendix evaluates the conditions that are required for the normal conditions of transport (NCT) measured dose rates to be more restrictive than the hypothetical accident conditions (HAC) dose rate acceptance criteria. The evaluation considers relocation of the neutron source and self-shielding displacement in the RH-TRU 72-B package. The NCT dose rates are measured at the time of shipment and provide a direct confirmation of the package activity loading. When the NCT dose rates are limiting, the HAC dose rates can also be verified. Movement of the source isotopes or displacement of internal self shielding under HAC may cause the external dose rates to increase. The purpose of this appendix is to evaluate whether the HAC dose rate acceptance criteria could be exceeded due to source or self-shielding displacement in the RH-TRU 72-B package, if the NCT measured dose rates (at time of shipment) meet the acceptance criteria.

The results indicate that the NCT dose rate criteria is sufficient to ensure meeting the HAC dose rate requirements for any source relocation combined with an effective loss of up to 8 inches of 30% polyethylene and 70% water mixture.

5.5.5.1 Source Displacement Effects

Two source distributions are selected to represent the NCT conditions that maximizes allowable source activity: a point source at the package center, and a uniformly distributed source. One source distribution is selected to represent the HAC condition that minimizes allowable source activity, i.e., a point source just inside the puncture location. The ratio of the 1-meter dose rates under the NCT and HAC distributions represents a reasonable approximation of the maximum increase in HAC dose rate due to source displacement.

Calculations are performed using MCNP[1] to assess the effect of source displacement. A point neutron source of unit strength (using the Pu^{239} spectrum) is placed at the center of the package, and calculations are performed for the radial surface, 1-meter and 2-meter dose rates (see Figure 5.5.5-1). The source strength is then scaled to normalize to the applicable NCT acceptance criteria limit. In this case, the surface limit of 200 mrem/hr is limiting (case *nopun*). A separate case is then run with puncture damage (case *pun*), with the source still at the center of the package (see Figure 5.1-1 in Section 5.1, *Discussion and Results*). The calculated dose rate at 1 meter from the damaged surface is found to be 23.4 mrem/hr (see Table 5.5.5-1). This is approximately 43× below the HAC limit.

Cases are also run with the same source uniformly distributed inside the package. The results are given in Table 5.5.5-1 (cases *pun5* and *nopun4*), and the 1-meter dose rate is found to be 15.9 mrem/hr. However, for the uniform distribution case, the 2-meter dose rate is limiting. Consequently, the relevant 1-meter dose rate with the distributed source is (10/6.99) × 15.9 = 22.7 mrem/hr. This is approximately 44× below the HAC limit.

[1] J. F. Breismeister, Editor, *MCNP – A General Monte Carlo Code N-Particle Transport Code, Version 4B*, LA-12625-M, Los Alamos National Laboratory, Los Alamos, New Mexico, 1997.

Calculations are then performed for the case where the point source is moved to the radial side of the package (case *pun3*), just inside the puncture damage. The calculated 1-meter dose rate is found to be 45.2 mrem/hr. Consequently, the maximum HAC dose rate increase due to point source displacement is 45.2/23.4 = 2×.

5.5.5.2 Self-Shielding Reduction Effects

Calculations are performed with the unit source in the center of the package and two self-shielding cases, using 30% polyethylene and 70% water mixture spheres, with the results given in Table 5.5.5-1. For a sphere of 4 inches, the calculated 1-meter dose rate is 7.32 mrem/hr (case *pun6*). Removal of self-shielding leads to an increase in HAC dose rate of 23.4/7.32 = 3.2×. Removal of 8 inches of self-shielding leads to an increase in the HAC dose rate of 23.4/1.27 = 18.4× (case *pun7*).

5.5.5.3 Combined Effects

Based on the Table 5.5.5-1 results, maximum neutron point source displacement under HAC increases the 1-meter dose rate by no more than 2×. The 1-meter dose rate could increase by a greater factor if a uniform source is able to reconfigure into a point source at the puncture bar location. However, if the package experiences a side drop, the contents would tend to displace horizontally, and the axial orientation of the source would not change. Consequently, the point source displacement case would bound. If the package experiences an end drop, the contents would tend to displace axially. The radial puncture location could correspond to a location that would effectively see an increase in source strength. This is like a case where the distributed source is compressed into a disk. However, because the authorized contents are constrained, the compression would be much less than 50%, and the corresponding increase in HAC dose rate would be no more than a factor of two.

Events that would cause the effective displacement of 4 inches of self-shielding (30% polyethylene, 70% water) would increase the HAC dose rate by a maximum of 3.2×, and the effective loss of 8 inches of self-shielding would increase the HAC dose rate by a maximum of 18.4×. Conservatively, the total displacement of the neutron source combined with the effective loss of 8 inches of self-shielding would increase the HAC dose rate by no more than 2.0 × 18.4 = 37×. This is below the 43× needed to reach the limit. Therefore, for contents that meet the criteria given in Section 5.2, *Source Specification,* as a *Controlled Self-Shielding Payload* in the RH-TRU 72-B package, neutron source movements and self-shielding displacements are not sufficient to cause the HAC limit to be exceeded, if the NCT measured dose rates meet the acceptance criteria.

5.5.5.4 Maximum HAC Activity Limits for the Controlled Self-Shielding Payload Case

When the internal shielding, self-shielding, and source location can be assumed to remain intact following the HAC, the NCT dose rate limit will continue to have more restrictive activity limits than the HAC dose rate criteria. Thus, the maximum *Controlled Self-Shielding Payload* will be based on the most limiting payload activity for the measured NCT dose rate, thermal heat load, gas generation, and the payload mass. The maximum HAC *Controlled Self-Shielding Activity Limits* are set at 15× the *General Payload* as given in Section 5.2, *Source Specification,* and

Remote-Handled Transuranic Waste Authorized Methods for Payload Control (RH-TRAMPAC)[2]. This provides maximum limits for the radionuclide activities and limits the amount of credit that can be taken for internal self-shielding. For comparison, the reduction in the 1-meter dose rate provided by 8 inches of polyethylene/water shield around a ^{239}Pu source, as used above, is 18×. The maximum HAC activity limit of 15 times the *General Payload* limits is applied to both gamma and neutron emitting isotopes.

5.5.5.5 MCNP Input Files

The case *nopun4* is the same as the listing for case *nopun*, except the neutron source is distributed uniformly throughout the interior instead of at the center of the package.

The case *pun* is the same as the neutron input file for the point isotopic source case "pu239", except the point source is at the center, a surface tally is included for the contact dose rate, and a point detector tally of the 2-meter dose rate is included.

The cases *pun3* and *pun5* are the same as the listing of case *pun*, except for the appropriate change in the source location or distribution. The cases *pun6* and *pun7* are also the same as the listing of case *pun*, except there is a sphere of (30% polyethylene, 70% water) surrounding the point source of radius 4 inches and 8 inches, respectively.

[2] U.S. Department of Energy (DOE), *Remote-Handled Transuranic Waste Authorized Methods for Payload Control* (RH-TRAMPAC), U.S. Department of Energy, Carlsbad Field Office, Carlsbad, New Mexico.

Table 5.5.5-1 – Dose Rates as a Function of Neutron Source (Pu-239) Location and Self-Shielding

Case①	Puncture Damage	Source Location	Source (η/s)	Dose Rate (mrem/hr)		
				Surface②	1 Meter③	2 Meter④
nopun	no	Center	5.32E+07	2.00E+02	2.23E+01	8.33E+00
pun	yes	Center	5.32E+07	2.35E+02	2.34E+01	8.63E+00
nopun4	no	Uniform	5.32E+07	7.54E+01	1.56E+01	6.99E+00
pun5	yes	Uniform	5.32E+07	9.26E+01	1.59E+01	7.08E+00
pun3	yes	+x	5.32E+07	3.82E+03	4.52E+01	1.36E+01
pun6	yes	Center, 4-inch⑤	5.32E+07	7.59E+01	7.32E+00	2.71E+00
pun7	yes	Center, 8-inch⑥	5.32E+07	—	1.27E+00	4.67E-01

Notes:

① The MCNP input file name is this case name preceded by an "i" and the MCNP output file is this case name preceded by an "o".

② This surface dose rate is at +x (next to the puncture damage when it exists). The one standard deviation statistical uncertainties are about 5% except for case *opun3*, which is 0.7%, and *opun7*, which has a large statistical uncertainty and so is not given.

③ This dose rate is at 1 meter from the outside surface (outside surface of puncture damage when there is puncture damage) in the +x direction, where the puncture damage is at +x. The one standard deviation statistical uncertainties are about 0.2% except for case *opun6*, which is 0.42%, and *opun7*, which is 2.1%.

④ This dose rate is at 2 meters from the outside surface (outside surface of puncture damage when there is puncture damage) in the +x direction, where the puncture damage is at +x. The one standard deviation statistical uncertainties are about 0.3% except for case *opun6*, which is 0.37%, and *opun7*, which is 1.8%.

⑤ The source is a point at the center of the package and in the center of a 4-inch radius sphere of (30% polyethylene, 70% water).

⑥ The source is a point at the center of the package and in the center of a 8-inch radius sphere of (30% polyethylene, 70% water).

General Notes:

① The "+x" source location means the source is just inside the shield by the puncture bar damage.

② The "uniform" source location means that the source is distributed uniformly throughout the inside of the package.

③ The source strength is normalized to give the 200 mrem/hr surface limit without puncture bar damage when the source is a point in the center of the package.

Table 5.5.5-2 – Listing of MCNP File for Neutron Case “nopun”; No Puncture Bar Damage

```
72-b Cask, dose rates without puncture, pu239 point source, center, inopun
c    dimensions for cask taken from figure 6.3-1 of original chapter 6
c    *****interior of cask
    1  0           -11    -24 23            $ interior
c    *****radial of cask, no puncture bar
   11  3  -8.020   -12 11 -24 23            $ inner radial steel
   12 51 -11.340   -13 12 -24 23            $ lead
   13  3  -8.020   -14 13 -24 23            $ ss outer cask, outer shell
c    *****radial of cask for 6" puncture bar for lead and outer
c     17 51 -11.340   -13 12 -22 21 -15        $ lead
c     18  3  -8.020   -14    -22 21 -16 (15:13) $ ss outer cask, outer shell
c    *****bottom of cask
   21  3  -8.020   -14    -23 25            $ next to inside
   22  3  -8.020   -14    -25 27            $ intermediate
   23  3  -8.020   -14    -27 29            $ outer
c    *****top of cask
   24  3  -8.020   -14    -26 24            $ next to inside
   25  3  -8.020   -14    -28 26            $ intermediate
   26  3  -8.020   -14    -30 28            $ outer
c    *****beyond cask
   31 77  -0.00123  -8    -42 41            $ air to beyond detector
         (14:-29:30)
   32 77  -0.00123  -9    -44 43 (8:-41:42) $ air on beyond
   33  0            (9:-43:44)              $ outside world

c          radial cask
   11  cz   39.6875          $ inner radial of cask
   12  cz   43.1800          $ inner steel
   13  cz   47.9425          $ lead
   14  cz   52.0700          $ outer steel
   15  px   46.27626         $ lead at puncture bar
   16  px   50.40376         $ outer steel at puncture bar
c          axial cask
   21  pz   -7.620           $ bottom of puncture bar
   22  pz    7.620           $ top of puncture bar
   23  pz -154.305           $ bottom inside of cask
   24  pz  154.305           $ top inside of cask
   25  pz -159.808           $ bottom first intermediate
   26  pz  165.317           $ top first intermediate
   27  pz -165.312           $ bottom second intermediate
   28  pz  176.318           $ top second intermediate
   29  pz -170.815           $ bottom outside of cask
   30  pz  187.325           $ top outside of cask
c          air beyond cask
   41  pz -320.815           $ 150 cm below
   42  pz  337.325           $ 150 cm above
   43  pz -670.815           $ 500 cm below
   44  pz  687.325           $ 500 cm above
    8  cz  202.070           $ 150 cm beyond
    9  cz  552.070           $ 500 cm beyond
   51  cx    5.08            $ cyl for tally of surface dose
   52  px    0.0

mode   n
imp:n    1 10r 0.25 0
print
cut:n    j j 0 0
nps   1000000
ctme    120.
c     point unit source just inside shield, midway puncture bar
sdef  x=0.0  y=0. z=0. erg=d7 wgt=1.0
sc7   PU239
si7   0.1 0.5     1.0     2.0     3.0     4.0     6.0     8.0
          10.0  12.0
sp7    0.00E+00  1.73E+00  1.71E+00  9.29E+00  1.88E+01
       6.84E+00  2.85E-01  4.58E-04  9.66E-05  2.28E-05
c    SS-304L from Nuclear Systems Materials Handbook Rev. 36
m3     6000.60c -0.0003  25055.50c -0.02    15031.50c -0.01
      28000.50c -0.0925  24000.50c -0.19    26000.55c -0.6872
m51   82000.50c -1.00                              $ lead
m77    8016.60c  0.220    7014.60c  0.780         $ air
c      ansi/ans-6.1.1-1977 fluence-to-dose,neutrons(mrem/hr/(n/cm**2/s)
de0    log   2.5e-08 1.0e-07 1.0e-06 1.0e-05 1.0e-04
             .001     .01     .1      .5      1.0
              2.5     5.0     7.0     10.0    14.0  20.0
df0    log   3.67e-3 3.67e-3 4.46e-3 4.54e-3  4.18e-3
             3.76e-3 3.56e-3 2.17e-2 9.26e-2  .132
              .125    .156    .147    .147    .208  .227
fc2    dose rate on puncture surface (2" radius), second tally
f2:n    14
fs2    -52 -51 t
sd2    1.0  81.156   1.0 1.0
fc5    dose rate in mrem/hr at 1 meter from outer surface
f5:n    152.07     0. 0. 20.
fc15   dose rate in mrem/hr at 2 meter from outer surface
f15:n   252.07     0. 0. 20.
```

Table 5.5.5-3 – Listing of MCNP File for Neutron Case "pun"; Includes Puncture Bar Damage

```
72-b Cask, dose rates with puncture, pu239 point source,center  ipun
c    dimensions for cask taken from figure 6.3-1 of original chapter 6
c    *****interior of cask
    1  0            -11    -24 23            $ interior
c    *****radial of cask, except along 6" puncture bar for lead and outer
   11  3  -8.020   -12 11 -24 23            $ inner radial steel
   12 51 -11.340   -13 12 -24 23 (22:-21)   $ lead
   13  3  -8.020   -14 13 -24 23 (22:-21)   $ ss outer cask, outer shell
c    *****radial of cask for 6" puncture bar for lead and outer
   17 51 -11.340   -13 12 -22 21 -15        $ lead
   18  3  -8.020   -14    -22 21 -16 (15:13) $ ss outer cask, outer shell
c    *****bottom of cask
   21  3  -8.020   -14    -23 25            $ next to inside
   22  3  -8.020   -14    -25 27            $ intermediate
   23  3  -8.020   -14    -27 29            $ outer
c    *****top of cask
   24  3  -8.020   -14    -26 24            $ next to inside
   25  3  -8.020   -14    -28 26            $ intermediate
   26  3  -8.020   -14    -30 28            $ outer
c    *****beyond cask
   31 77  -0.00123  -8    -42 41            $ air to beyond detector
         ((14:-29:30):(16 -22 21))
   32 77  -0.00123  -9    -44 43 (8:-41:42) $ air on beyond
   33  0            (9:-43:44)              $ outside world

c          radial cask
   11  cz   39.6875          $ inner radial of cask
   12  cz   43.1800          $ inner steel
   13  cz   47.9425          $ lead
   14  cz   52.0700          $ outer steel
   15  px   46.27626         $ lead at puncture bar
   16  px   50.40376         $ outer steel at puncture bar
c          axial cask
   21  pz   -7.620           $ bottom of puncture bar
   22  pz    7.620           $ top of puncture bar
   23  pz -154.305           $ bottom inside of cask
   24  pz  154.305           $ top inside of cask
   25  pz -159.808           $ bottom first intermediate
   26  pz  165.317           $ top first intermediate
   27  pz -165.312           $ bottom second intermediate
   28  pz  176.318           $ top second intermediate
   29  pz -170.815           $ bottom outside of cask
   30  pz  187.325           $ top outside of cask
c          air beyond cask
   41  pz -320.815           $ 150 cm below
   42  pz  337.325           $ 150 cm above
   43  pz -670.815           $ 500 cm below
   44  pz  687.325           $ 500 cm above
    8  cz  202.070           $ 150 cm beyond
    9  cz  552.070           $ 500 cm beyond
   51  cx    5.08            $ cyl for tally of surface dose

mode   n
imp:n    1 12r 0.25 0
print
cut:n    j j 0 0
nps   1000000
ctme    120.
c     point unit source just inside shield, midway puncture bar
sdef  x=0.0  y=0. z=0. erg=d7 wgt=1.0
sc7   PU239
si7   0.1 0.5     1.0     2.0     3.0     4.0     6.0     8.0
          10.0  12.0
sp7    0.00E+00  1.73E+00  1.71E+00  9.29E+00  1.88E+01
       6.84E+00  2.85E-01  4.58E-04  9.66E-05  2.28E-05
c    SS-304L from Nuclear Systems Materials Handbook Rev. 36
m3     6000.60c -0.0003  25055.50c -0.02    15031.50c -0.01
      28000.50c -0.0925  24000.50c -0.19    26000.55c -0.6872
m51   82000.50c -1.00                              $ lead
m77    8016.60c  0.220    7014.60c  0.780         $ air
c      ansi/ans-6.1.1-1977 fluence-to-dose,neutrons(mrem/hr/(n/cm**2/s)
de0    log   2.5e-08 1.0e-07 1.0e-06 1.0e-05 1.0e-04
             .001     .01     .1      .5      1.0
              2.5     5.0     7.0     10.0    14.0  20.0
df0    log   3.67e-3 3.67e-3 4.46e-3 4.54e-3  4.18e-3
             3.76e-3 3.56e-3 2.17e-2 9.26e-2  .132
              .125    .156    .147    .147    .208  .227
fc2    dose rate on puncture surface (2" radius), first tally
f2:n    16
fs2    -51
sd2    81.0732 1.0
fc5    dose rate in mrem/hr at 1 meter from outer surface
f5:n    150.40376  0. 0. 20.
fc15   dose rate in mrem/hr at 2 meter from outer surface
f15:n   250.40376  0. 0. 20.
```

FIGURE WITHHELD UNDER 10 CFR 2.390

The point source "center" is at the midpoint axially of the puncture bar and in the radial center of the package. The "+x" source is at the same elevation, but next to the inner shield (in +x). The "uniform" source is distributed uniformly throughout the interior of the package. All the sources have a unit total source strength. The "6" and "7" cases have small spheres of material around the point source.

Figure 5.5.5-1 – Axial View for Source and Attenutation Variations (NCT to HAC) Showing Detectors

This page intentionally left blank.

5.5.6 Evaluation of the Effect of NCT-to-HAC Changes on Gamma Dose Rates

This appendix evaluates the conditions that are required for the Normal Conditions of Transport (NCT) measured dose rates to be more restrictive than the Hypothetical Accident Conditions (HAC) dose rate acceptance criteria. The evaluation considers relocation of the gamma source and self-shielding displacement in the RH-TRU 72-B package. The NCT dose rates are measured at the time of shipment and provide a direct confirmation of the package activity loading. When the NCT dose rates are limiting, the HAC dose rates can also be verified. Movement of the source isotopes or displacement of internal self-shielding under HAC may cause the external dose rates to increase. The purpose of this appendix is to evaluate whether the HAC dose rate acceptance criteria could be exceeded due to gamma source or self-shielding displacement in the RH-TRU 72-B package, if the NCT measured dose rates (at time of shipment) meet the acceptance criteria.

Since the shielding effects of the package are a function of gamma energy, two representative gamma source cases are selected: ^{137}Cs and ^{60}Co. Figure 5.5.5-1 in Appendix 5.5.5, *Evaluation of the Effect of NCT to HAC Changes on Neutron Dose Rates*, applies to the subsequent cases.

The results show that the ^{137}Cs case is limiting. Since the absorption coefficient is less for the ^{60}Co gamma energy, the relative effect of the package shielding and subsequent puncture damage is less than for the ^{137}Cs case.

The results indicate that the NCT dose rate criteria is sufficient to ensure meeting the HAC dose rate requirements for any source relocation combined with an effective loss of up to either 8 inches of 30% polyethylene and 70% water mixture or 1 inch of steel.

5.5.6.1 Cs-137 (0.6617 MeV)

5.5.6.1.1 Source Displacement Effects

Two source distributions are selected to represent the NCT conditions that maximize allowable source activity: a point source at the package center, and a uniformly distributed source. One source distribution is selected to represent the HAC condition that minimizes allowable source activity, i.e., a point source just inside the puncture location. The ratio of the 1-meter dose rates under the NCT and HAC distributions represents a reasonable approximation of the maximum increase in HAC dose rate due to source displacement.

Calculations are performed using MCNP[1] to assess the effect of source displacement. A point source of unit strength is placed at the center of the package, and calculations are performed for the radial surface, 1-meter, and 2-meter dose rates. The source strength is then scaled to normalize to the applicable NCT acceptance criteria limit. In this case, the surface limit of 200 mrem/hr is limiting (case *mnopun*). A separate case is then run with puncture bar damage (case *mpun*) with the source still at the center of the package (see Figure 5.1-1 in Section 5.1, *Discussion and Results*). The calculated dose rate at 1 meter from the damaged surface is found to be 58.3 mrem/hr (see Table 5.5.6-1). This is approximately 17× below the HAC limit.

[1] J. F. Breismeister, Editor, *MCNP – A General Monte Carlo Code N-Particle Transport Code, Version 4B*, LA-12625-M, Los Alamos National Laboratory, Los Alamos, New Mexico, 1997.

Cases are then run with the same source uniformly distributed inside the package. The results are given in Table 5.5.6-1 (cases *mpun5* and *mnopun4*). The 1-meter dose rate is found to be 6.61 mrem/hr. For the uniform distribution case, the 2-meter dose rate is limiting. Consequently, the relevant 1-meter dose rate with the distributed source is (10/2.3) × 6.61 = 28.8 mrem/hr. This is approximately 35× below the HAC limit.

Calculations are then performed for the case where the point source is moved to the radial side of the package (case *mpun3*), just inside the puncture bar damage. The calculated 1-meter dose rate is found to be 187 mrem/hr. Consequently, the maximum HAC dose rate increase due to point source displacement is 187/58.3 = 3.2×.

5.5.6.1.2 Self-Shielding Reduction Effects

Calculations are performed with the point source at the center of the package and five self-shielding cases, two using 30% polyethylene and 70% water mixture spheres, and three using steel spheres, with the results given in Table 5.5.6-1. For a 30% polyethylene and 70% water mixture sphere of 4 inches, the calculated 1-meter dose rate is 28.3 mrem/hr (case *mpun6*). Removal of this self-shielding leads to an increase in HAC dose rate of 58.3/28.3 = 2.1×. Removal of 8 inches of 30% polyethylene and 70% water mixture self shielding leads to an increase in the HAC dose rate of 58.3/12.4 = 4.7× (case *mpun7*). Removal of 0.5 inches (case *mpun8*), 1 inch (case *mpun9*), and 2 inches (case *mpun0*) of steel shielding leads to HAC dose rate increases of 1.9×, 3.7×, and 12.6×, respectively.

5.5.6.1.3 Combined Effects

Puncture bar damage measurably increases the HAC dose rate, even without other effects. Based on the point source case, the HAC dose rate increase due to the puncture bar is a maximum of 58.3/18.0 = 3.2×.

Based on the Table 5.5.6-1 results, maximum gamma source displacement under HAC, for the point source case, increases the HAC dose rate by no more than 3.2×. The HAC dose rate could increase by a greater factor if a uniform source is able to reconfigure into a point source at the puncture bar location. However, if the package experiences a side drop, the contents would tend to displace horizontally, and the axial orientation of the source would not change. Consequently, the point source displacement case bounds. If the package experiences an end drop, the contents would tend to displace axially. The radial puncture location could correspond to a location that would effectively see an increase in source strength. This is like a case where the distributed source is compressed into a disk. However, because the authorized contents are constrained, the compression would be much less than 50%, and the corresponding increase in HAC dose rate would be no more than a factor of two.

HAC damage, displacement of the gamma source, and the effective loss of 8 inches of 30% polyethylene and 70% water mixture self-shielding or 1 inch of steel increases the HAC dose rate by no more than 3.2 × 3.2 × 4.7 = 48×. Since the maximum NCT conditions dose rate at 1 meter is 18 mrem/hr, the maximum HAC dose rate is 48 × 18 = 864 mrem/hr. This is below the HAC limit of 1,000 mrem/hr. Therefore, for contents that meet the criteria given in Section 5.2, *Source Specification,* for a *Controlled Self-Shielding Payload*, gamma source movements and self-shielding displacements are not sufficient to cause the HAC limit to be exceeded, if the NCT measured dose rates meet the acceptance criteria.

5.5.6.2 Co-60 (1.21 MeV)

5.5.6.2.1 Source Displacement Effects

The same calculational method used in the Section 5.5.6.1, *Cs-137 (0.6617 MeV)*, evaluation is used in this case.

Calculations are performed using MCNP[1] to assess the effect of source displacement. A point source of unit strength is placed in the center of the package, and calculations are performed for the radial surface, 1-meter, and 2-meter dose rates. The source strength is then scaled to normalize to the applicable NCT acceptance criteria limit. In this case, the surface limit of 200 mrem/hr is limiting (case *hnopun*). A separate case is then run with puncture bar damage (case *hpun*), with the source still at the center of the package (see Figure 5.1-1 in Section 5.1, *Discussion and Results*). The calculated dose rate at 1 meter from the damaged surface is found to be 32.2 mrem/hr (see Table 5.5.6-2). This is approximately 31× below the HAC limit.

Cases are then run with the same source uniformly distributed inside the package. The results are given in Table 5.5.6-2 (cases *hpun5* and *hnopun4*). The 1-meter dose rate is found to be 6.59 mrem/hr. For the uniform distribution case, the 2-meter dose rate is limiting. Consequently, the relevant 1-meter dose rate with the distributed source is (10/2.9) × 6.59 = 22.7 mrem/hr. This is approximately 44× below the HAC limit.

Calculations are then performed for the case where the point source is moved to the radial side of the package, just inside the puncture bar damage. The calculated 1-meter dose rate is found to be 84.2 mrem/hr. Consequently, the maximum HAC dose rate increase due to point source displacement is 84.2/32.2 = 2.6×.

5.5.6.2.2 Self-Shielding Reduction Effect

Calculations are performed with the point source in the center of the package and four self-shielding cases, one using a 30% polyethylene and 70% water mixture sphere, and three using steel spheres, with the results given in Table 5.5.6-2. For a 30% polyethylene and 70% water mixture sphere of 8 inches, the calculated 1-meter dose rate is 11.7 mrem/hr (case *hpun7*). Removal of this shielding leads to an increase in HAC dose rate of 32.2/11.7 = 2.7×. Removal of 0.5 inches (case *hpun8*), 1 inch (case *hpun9*), and 2 inches (case *hpun0*) of steel shielding leads to HAC dose rate increases of 1.5×, 2.3×, and 6.0×, respectively.

5.5.6.2.3 Combined Effects

Puncture damage increases the 1-meter dose rate, even without other effects. However, the effect of the puncture damage is less for this gamma energy than is found for the Cs^{137} evaluation. Based on the uniform source case, the HAC dose rate increase due to the puncture is a maximum of 1.1×, and 1.8× for the point source located in the center of the package.

Based on the Table 5.5.6-2 results, maximum gamma point source displacement under HAC increases the 1-meter dose rate by no more than 2.6×. The HAC dose rate could increase by a greater factor if a uniform source is able to reconfigure into a point source at the puncture bar location. However, if the package experiences a side drop, the contents would tend to displace horizontally, and the axial orientation of the source would not change. Consequently, the point source displacement case bounds. If the package experienced an end drop, the contents would

tend to displace axially. The radial puncture location could correspond to a location that would effectively see an increase in source strength. This is like a case where the distributed source is compressed into a disk. However, because the authorized contents are constrained, the compression would be much less than 50%, and the corresponding increase in HAC dose rate would be no more than a factor of two.

HAC damage, displacement of the gamma source, and the effective loss of 8 inches of 30% polyethylene and 70% water mixture self-shielding or 2 inches of steel increases the HAC dose rate by no more than 1.8 × 2.6 × 6 = 28×. Since the maximum NCT conditions dose rate at 1 meter is 18.4 mrem/hr, the maximum HAC dose rate would be 28 × 18.4 = 515 mrem/hr. This is below the HAC limit of 1,000 mrem/hr. Therefore, for contents that meet the criteria given in Section 5.2, *Source Specification*, for a *Controlled Self-Shielding Payload*, gamma source movements and self-shielding displacements are not sufficient to cause the HAC limit to be exceeded, if the NCT measured dose rates meet the acceptance criteria.

5.5.6.3 Maximum HAC Activity Limits for the Controlled Self-Shielding Payload Case

When the internal shielding, self-shielding, and source location can be assumed to remain intact following the HAC, the NCT dose rate limit will continue to have more restrictive activity limits than the HAC dose rate criteria. Thus, the maximum *Controlled Self-Shielding Payload* will be based on the most limiting payload activity for the measured NCT dose rate, thermal heat load, gas generation, and the payload mass. The maximum HAC *Controlled Self-Shielding Activity Limits* are set at 15× the *General Payload*, as given in Section 5.2, *Source Specification*, and *Remote-Handled Transuranic Waste Authorized Methods for Payload Control* (RH-TRAMPAC)[2]. This provides maximum limits for the radionuclide activities and limits the amount of credit that can be taken for internal self-shielding. For comparison, the reduction in the 1-meter dose rate provided by 2 inches of steel around a ^{137}Cs source is 13×. The maximum HAC activity limit of 15 times the *General Payload* limits is applied to both gamma and neutron emitting isotopes.

5.5.6.4 MCNP Input Files

The corresponding cases for the photons are the same as the listings in Appendix 5.5.5, *Evaluation of the Effect of NCT to HAC Changes on Neutron Dose Rates*, except the mode is changed from “n” to “p” with the appropriate card changes to go to a photon calculation, including changing the source and the flux-to-dose conversion factors from neutron to photon. There are three cases where the sphere of material is steel instead of the (poly/water) mix, with three smaller radii. The cases for the ^{137}Cs source have a “m” in front of the corresponding neutron case number, and the cases for a ^{60}Co source have a “h” in front of the corresponding neutron case number. The input files for cases “mpun” and “hpun” are listed in Table 5.5.6-3 and Table 5.5.6-4, respectively.

[2] U.S. Department of Energy (DOE), *Remote-Handled Transuranic Waste Authorized Methods for Payload Control* (RH-TRAMPAC), U.S. Department of Energy, Carlsbad Field Office, Carlsbad, New Mexico.

Table 5.5.6-1 – Dose Rates as a Function of a Representative Photon Cs-137 Source (E = 0.6617 MeV) Location and Self-Shielding

Case①	Puncture Damage	Source Location	Source (γ/s)	Dose Rate (mrem/hr)		
				Surface②	1 Meter③	2 Meter④
mnopun	no	center	1.86E+13	2.00E+02	1.80E+01	6.00E+00
mpun	yes	center	1.86E+13	1.41E+03	5.83E+01	1.89E+01
mpun3	yes	+x	1.86E+13	2.40E+04	1.87E+02	5.07E+01
mpun5	yes	uniform	1.86E+13	1.16E+02	6.61E+00	2.69E+00
nopun4	no	uniform	1.86E+13	—	4.84E+00	2.30E+00
mpun6	yes	center, 4-inch⑤	1.86E+13	6.60E+02	2.83E+01	9.24E+00
mpun7	yes	center, 8-inch⑥	1.86E+13	3.18E+02	1.24E+01	4.16E+00
mpun8	yes	center, ½-inch⑦	1.86E+13	7.14E+02	3.12E+01	1.02E+01
mpun9	yes	center, 1-inch⑧	1.86E+13	3.87E+02	1.58E+01	5.20E+00
mpun0	yes	center, 2-inch⑨	1.86E+13	1.11E+02	4.62E+00	1.40E+00

Notes:

① The MCNP input file name is this case name preceded by an "i" and the MCNP output file is this case name preceded by an "o".

② This surface dose rate is at +x (next to the puncture bar damage, when it exists). The one standard deviation statistical uncertainties are 11.2%, 4.5%, 1.1%, 13.8%, 37%, 5.2%, 7.0%, 5.1%, 6.7%, and 8.8%, respectively; case *mnopun4* is not given since the uncertainty is so large.

③ This dose rate is at 1-meter from the outside surface (outside surface of puncture bar damage, when it exists) in the +x direction, where the puncture bar damage is at +x. The one standard deviation statistical uncertainties are less than 4%, except for case *ompun5*, which is 6.9%, case *mnopun4*, which is 9.4%, and case *mpun9*, which is 5.2% .

④ This dose rate is at 2 meters from the outside surface (outside surface of puncture bar damage when it exists) in the +x direction, where the puncture bar damage is at +x. The one standard deviation statistical uncertainties are less than 4.0% for all cases.

⑤ The source is a point in the center of the package and at the center of a 4-inch radius sphere of (30% polyethylene, 70% water).

⑥ The source is a point in the center of the package and at the center of a 8-inch radius sphere of (30% polyethylene, 70% water).

⑦ The source is a point in the center of the package and at the center of a 0.5-inch radius sphere of steel.

⑧ The source is a point in the center of the package and at the center of a 1-inch radius sphere of steel.

⑨ The source is a point in the center of the package and at the center of a 2-inch radius sphere of steel.

General Notes:

① The "+x" source location means the source is just inside the shield by the puncture bar damage.

② The "uniform" source location means that the source is distributed uniformly throughout the inside of the package.

③ The source strength is normalized to give the 200 mrem/hr surface limit without puncture bar damage when the source is a point in the center of the package. A fairly large statistical uncertainty of 11.2% occurs at this normalization point.

Table 5.5.6-2 – Dose Rates as a Function of a Representative Photon Co-60 Source (E = 1.21 MeV) Location and Self-Shielding

Case①	Puncture Damage	Source Location	Source (γ/s)	Dose Rate (mrem/hr)		
				Surface②	1 Meter③	2 Meter④
hnopun	no	center	3.17E+11	2.00E+02	1.84E+01	6.33E+00
hpun	yes	center	3.17E+11	5.13E+02	3.22E+01	1.09E+01
hpun3	yes	+x	3.17E+11	9.36E+03	8.42E+01	2.26E+01
hpun5	yes	uniform	3.17E+11	6.26E+01	6.59E+00	3.09E+00
hnopun4	no	uniform	3.17E+11	2.34E+01	5.85E+00	2.90E+00
hpun7	yes	center, 8-inch⑤	3.17E+11	1.91E+02	1.17E+01	3.87E+00
hpun8	yes	center, ½-inch⑥	3.17E+11	3.47E+02	2.10E+01	7.16E+00
hpun9	yes	center, 1-inch⑦	3.17E+11	2.20E+02	1.39E+01	4.66E+00
hpun0	yes	center, 2-inch⑧	3.17E+11	9.57E+01	5.33E+00	1.80E+00

Notes:

① The MCNP input file name is this case name preceded by an "i" and the MCNP output file is this case name preceded by an "o".

② This surface dose rate is at +x (next to the puncture bar damage, when it exists). The one standard deviation statistical uncertainties are 2.5%, 1.9%, 0.4%, 4.6%, 8.5%, and 2.3%, respectively.

③ This dose rate is at 1-meter from the outside surface (outside surface of puncture bar damage, when it exists) in the +x direction, where the puncture bar damage is at +x. The one standard deviation statistical uncertainties are less than 2% for all cases.

④ This dose rate is at 2 meters from the outside surface (outside surface of puncture bar damage when it exists) in the +x direction, where the puncture bar damage is at +x. The one standard deviation statistical uncertainties are less than 1.3% for all cases.

⑤ The source is a point in the center of the package and at the center of a 8-inch radius sphere of (30% polyethylene, 70% water).

⑥ The source is a point in the center of the package and at the center of a 0.5-inch radius sphere of steel.

⑦ The source is a point in the center of the package and at the center of a 1-inch radius sphere of steel.

⑧ The source is a point in the center of the package and at the center of a 2-inch radius sphere of steel.

General Notes:

① The "+x" source location means the source is just inside the shield by the puncture bar damage.

② The "uniform" source location means that the source is distributed uniformly throughout the inside of the package.

③ The source strength is normalized to give the 200 mrem/hr surface limit without puncture bar damage when the source is a point in the center of the package.

Table 5.5.6-3 – Listing of MCNP File for Cs-137 Photon Case “mpun”; Includes Puncture Bar Damage

```
 72-b Cask, p dose rates with puncture, cs point source,center  impun
c    dimensions for cask taken from figure 6.3-1 of original chapter 6
c    *****interior of cask
    1  0           -11    -24 23            $ interior
c    *****radial of cask, except along 6" puncture bar for lead and outer
   11  3  -8.020   -12 11 -24 23            $ inner radial steel
   12 51 -11.340   -13 12 -24 23 (22:-21)   $ lead
   13  3  -8.020   -14 13 -24 23 (22:-21)   $ ss outer cask, outer shell
c    *****radial of cask for 6" puncture bar for lead and outer
   17 51 -11.340   -13 12 -22 21 -15        $ lead
   18  3  -8.020   -14    -22 21 -16 (15:13) $ ss outer cask, outer shell
c    *****bottom of cask
   21  3  -8.020   -14    -23 25            $ next to inside
   22  3  -8.020   -14    -25 27            $ intermediate
   23  3  -8.020   -14    -27 29            $ outer
c    *****top of cask
   24  3  -8.020   -14    -26 24            $ next to inside
   25  3  -8.020   -14    -28 26            $ intermediate
   26  3  -8.020   -14    -30 28            $ outer
c    *****beyond cask
   31 77  -0.00123  -8    -42 41            $ air to beyond detector
         ((14:-29:30):(16 -22 21))
   32 77  -0.00123  -9    -44 43 (8:-41:42) $ air on beyond
   33  0            (9:-43:44)              $ outside world

c          radial cask
   11  cz   39.6875          $ inner radial of cask
   12  cz   43.1800          $ inner steel
   13  cz   47.9425          $ lead
   14  cz   52.0700          $ outer steel
   15  px   46.27626         $ lead at puncture bar
   16  px   50.40376         $ outer steel at puncture bar
c          axial cask
   21  pz   -7.620           $ bottom of puncture bar
   22  pz    7.620           $ top of puncture bar
   23  pz -154.305           $ bottom inside of cask
   24  pz  154.305           $ top inside of cask
   25  pz -159.808           $ bottom first intermediate
   26  pz  165.317           $ top first intermediate
   27  pz -165.312           $ bottom second intermediate
   28  pz  176.318           $ top second intermediate
   29  pz -170.815           $ bottom outside of cask
   30  pz  187.325           $ top outside of cask
c          air beyond cask
   41  pz -320.815           $ 150 cm below
   42  pz  337.325           $ 150 cm above
   43  pz -670.815           $ 500 cm below
   44  pz  687.325           $ 500 cm above
    8  cz  202.070           $ 150 cm beyond
    9  cz  552.070           $ 500 cm beyond
   51  cx    5.08            $ cyl for tally of surface dose

mode   p
imp:p    1 1 4 32  4 32   1 5r  32 8 0
pd0     .1 .1 .2 1  .2 1  .1 5r   1 .5 0
print
phys:p   j 1
nps   10000000
ctme     90.
c     point unit source just inside shield, midway puncture bar
sdef  x=0.0  y=0. z=0. erg=.6617 wgt=1.0
c    SS-304L from Nuclear Systems Materials Handbook Rev. 36
m3     6000.60c -0.0003  25055.50c -0.02    15031.50c -0.01
      28000.50c -0.0925  24000.50c -0.19    26000.55c -0.6872
m51   82000.50c -1.00                              $ lead
m77    8016.60c  0.220    7014.60c  0.780         $ air
c      ansi/ans-6.1.1-1977 fluence-to-dose,photons(mrem/hr/(p/cm**2/s)
de0        0.01   0.03   0.05   0.07   0.10   0.15   0.20   0.25   0.30
           0.35   0.40   0.45   0.50   0.55   0.60   0.65   0.70   0.80
           1.00   1.40   1.80   2.20   2.60   2.80   3.25   3.75   4.25
           4.75   5.00   5.25   5.75   6.25   6.75   7.50   9.00   11.0
           13.0   15.0
df0        3.96-3 5.82-4 2.90-4 2.58-4 2.83-4 3.79-4 5.01-4 6.31-4 7.59-4
           8.78-4 9.85-4 1.08-3 1.17-3 1.27-3 1.36-3 1.44-3 1.52-3 1.68-3
           1.98-3 2.51-3 2.99-3 3.42-3 3.82-3 4.01-3 4.41-3 4.83-3 5.23-3
           5.60-3 5.80-3 6.01-3 6.37-3 6.74-3 7.11-3 7.66-3 8.77-3 1.03-2
           1.18-2 1.33-2
fc2    dose rate on puncture surface (2" radius), first tally
f2:p    16
fs2    -51
sd2    81.0732 1.0
fc5    dose rate in mrem/hr at 1 meter from outer surface
f5:p    150.40376  0. 0. 20.
fc15   dose rate in mrem/hr at 2 meter from outer surface
f15:p   250.40376  0. 0. 20.
```

Table 5.5.6-4 – Listing of MCNP File for Co-60 Photon Case “hpun”; Includes Puncture Bar Damage

```
 72-b Cask, p dose rates with puncture, co point source,center  ihpun
c    dimensions for cask taken from figure 6.3-1 of original chapter 6
c    *****interior of cask
    1  0           -11    -24 23            $ interior
c    *****radial of cask, except along 6" puncture bar for lead and outer
   11  3  -8.020   -12 11 -24 23            $ inner radial steel
   12 51 -11.340   -13 12 -24 23 (22:-21)   $ lead
   13  3  -8.020   -14 13 -24 23 (22:-21)   $ ss outer cask, outer shell
c    *****radial of cask for 6" puncture bar for lead and outer
   17 51 -11.340   -13 12 -22 21 -15        $ lead
   18  3  -8.020   -14    -22 21 -16 (15:13) $ ss outer cask, outer shell
c    *****bottom of cask
   21  3  -8.020   -14    -23 25            $ next to inside
   22  3  -8.020   -14    -25 27            $ intermediate
   23  3  -8.020   -14    -27 29            $ outer
c    *****top of cask
   24  3  -8.020   -14    -26 24            $ next to inside
   25  3  -8.020   -14    -28 26            $ intermediate
   26  3  -8.020   -14    -30 28            $ outer
c    *****beyond cask
   31 77  -0.00123  -8    -42 41            $ air to beyond detector
         ((14:-29:30):(16 -22 21))
   32 77  -0.00123  -9    -44 43 (8:-41:42) $ air on beyond
   33  0            (9:-43:44)              $ outside world

c          radial cask
   11  cz   39.6875          $ inner radial of cask
   12  cz   43.1800          $ inner steel
   13  cz   47.9425          $ lead
   14  cz   52.0700          $ outer steel
   15  px   46.27626         $ lead at puncture bar
   16  px   50.40376         $ outer steel at puncture bar
c          axial cask
   21  pz   -7.620           $ bottom of puncture bar
   22  pz    7.620           $ top of puncture bar
   23  pz -154.305           $ bottom inside of cask
   24  pz  154.305           $ top inside of cask
   25  pz -159.808           $ bottom first intermediate
   26  pz  165.317           $ top first intermediate
   27  pz -165.312           $ bottom second intermediate
   28  pz  176.318           $ top second intermediate
   29  pz -170.815           $ bottom outside of cask
   30  pz  187.325           $ top outside of cask
c          air beyond cask
   41  pz -320.815           $ 150 cm below
   42  pz  337.325           $ 150 cm above
   43  pz -670.815           $ 500 cm below
   44  pz  687.325           $ 500 cm above
    8  cz  202.070           $ 150 cm beyond
    9  cz  552.070           $ 500 cm beyond
   51  cx    5.08            $ cyl for tally of surface dose

mode   p
imp:p    1 1 4 16  4 16   1 5r  16 4 0
pd0     .1 .1 .2 1  .2 1  .1 5r   1 .5 0
print
phys:p   j 1
nps   10000000
ctme     90.
c     point unit source just inside shield, midway puncture bar
sdef  x=0.0  y=0. z=0. erg=d7    wgt=1.0
sc7       ORIGEN2 FOR 1 CURIE OF CO-60
c         MEV       phot/s    Mev/s
#         si7         sp7
           l           d
        0.015     1.961E+09 $ 2.942E+07
        0.025     3.388E+08 $ 8.470E+06
        0.0375    1.935E+08 $ 7.256E+06
        0.0575    2.182E+08 $ 1.255E+07
        0.085     8.582E+07 $ 7.295E+06
        0.125     3.296E+07 $ 4.120E+06
        0.225     1.084E+07 $ 2.439E+06
        0.375     3.041E+06 $ 1.140E+06
        0.575     1.746E+05 $ 1.004E+05
        0.85      2.763E+06 $ 2.349E+06
        1.1732    3.700E+10 $ 4.341E+10
        1.3325    3.700E+10 $ 4.930E+10
        2.25      3.921E+05 $ 8.822E+05
        2.75      1.213E+03 $ 3.336E+03
c        Total    7.683E+10 $ 9.279E+10
c    SS-304L from Nuclear Systems Materials Handbook Rev. 36
m3     6000.60c -0.0003  25055.50c -0.02    15031.50c -0.01
      28000.50c -0.0925  24000.50c -0.19    26000.55c -0.6872
m51   82000.50c -1.00                              $ lead
m77    8016.60c  0.220    7014.60c  0.780         $ air
c      ansi/ans-6.1.1-1977 fluence-to-dose,photons(mrem/hr/(p/cm**2/s)
de0        0.01   0.03   0.05   0.07   0.10   0.15   0.20   0.25   0.30
```

```
            0.35   0.40   0.45   0.50   0.55   0.60   0.65   0.70   0.80
            1.00   1.40   1.80   2.20   2.60   2.80   3.25   3.75   4.25
            4.75   5.00   5.25   5.75   6.25   6.75   7.50   9.00   11.0
            13.0   15.0
df0         3.96-3 5.82-4 2.90-4 2.58-4 2.83-4 3.79-4 5.01-4 6.31-4 7.59-4
            8.78-4 9.85-4 1.08-3 1.17-3 1.27-3 1.36-3 1.44-3 1.52-3 1.68-3
            1.98-3 2.51-3 2.99-3 3.42-3 3.82-3 4.01-3 4.41-3 4.83-3 5.23-3
            5.60-3 5.80-3 6.01-3 6.37-3 6.74-3 7.11-3 7.66-3 8.77-3 1.03-2
            1.18-2 1.33-2
fc2     dose rate on puncture surface (2" radius), first tally
f2:p     16
fs2     -51
sd2     81.0732 1.0
fc5     dose rate in mrem/hr at 1 meter from outer surface
f5:p     150.40376  0. 0. 20.
fc15    dose rate in mrem/hr at 2 meter from outer surface
f15:p    250.40376  0. 0. 20.
```

5.5.7 MCNP Input Files for the Shielding Analyses

The following is a listing of case *pu239* for the dose rate from a unit point neutron source just inside package. Each of the input files for the other 37 isotopes is the same as the above listing, except for changes to the spectrum for that isotope on the sp7 card.

```
 72-b Cask, dose rate at 100 cm, point source just inside shield,  iPU239
c    dimensions for cask taken from figure 6.3-1 of original chapter 6
c    *****interior of cask
    1  0          -11    -24 23            $ interior
c    *****radial of cask, except along 6" puncture bar for lead and outer
   11  3  -8.020   -12 11 -24 23           $ inner radial steel
   12 51 -11.340   -13 12 -24 23 (22:-21)   $ lead
   13  3  -8.020   -14 13 -24 23 (22:-21)   $ ss outer cask, outer shell
c    *****radial of cask for 6" puncture bar for lead and outer
   17 51 -11.340   -13 12 -22 21 -15        $ lead
   18  3  -8.020   -14    -22 21 -16 (15:13) $ ss outer cask, outer shell
c    *****bottom of cask
   21  3  -8.020   -14    -23 25            $ next to inside
   22  3  -8.020   -14    -25 27            $ intermediate
   23  3  -8.020   -14    -27 29            $ outer
c    *****top of cask
   24  3  -8.020   -14    -26 24            $ next to inside
   25  3  -8.020   -14    -28 26            $ intermediate
   26  3  -8.020   -14    -30 28            $ outer
c    *****beyond cask
   31 77  -0.00123  -8    -42 41            $ air to beyond detector
         ((14:-29:30):(16 -22 21))
   32 77  -0.00123  -9    -44 43 (8:-41:42) $ air on beyond
   33  0            (9:-43:44)              $ outside world

c          radial cask
   11  cz   39.6875          $ inner radial of cask
   12  cz   43.1800          $ inner steel
   13  cz   47.9425          $ lead
   14  cz   52.0700          $ outer steel
   15  px   46.27626         $ lead at puncture bar
   16  px   50.40376         $ outer steel at puncture bar
c          axial cask
   21  pz   -7.620           $ bottom of puncture bar
   22  pz    7.620           $ top of puncture bar
   23  pz -154.305           $ bottom inside of cask
   24  pz  154.305           $ top inside of cask
   25  pz -159.808           $ bottom first intermediate
   26  pz  165.317           $ top first intermediate
   27  pz -165.312           $ bottom second intermediate
   28  pz  176.318           $ top second intermediate
   29  pz -170.815           $ bottom outside of cask
   30  pz  187.325           $ top outside of cask
c          air beyond cask
   41  pz -320.815           $ 150 cm below
   42  pz  337.325           $ 150 cm above
   43  pz -670.815           $ 500 cm below
   44  pz  687.325           $ 500 cm above
    8  cz  202.070           $ 150 cm beyond
    9  cz  552.070           $ 500 cm beyond

mode   n
imp:n    1 12r 0.25 0
print
cut:n    j j 0 0
nps   200000
ctme    60.
c     point unit source just inside shield, midway puncture bar
sdef  x=39.687  y=0. z=0. erg=d7 wgt=1.0
sc7   PU239
si7   0.1 0.5     1.0     2.0     3.0     4.0     6.0     8.0
          10.0  12.0
sp7    0.00E+00  1.73E+00  1.71E+00  9.29E+00  1.88E+01
       6.84E+00  2.85E-01  4.58E-04  9.66E-05  2.28E-05
c    SS-304L from Nuclear Systems Materials Handbook Rev. 36
m3     6000.60c -0.0003  25055.50c -0.02    15031.50c -0.01
      28000.50c -0.0925  24000.50c -0.19    26000.55c -0.6872
m51   82000.50c -1.00                              $ lead
m77    8016.60c  0.220    7014.60c  0.780         $ air
c      ansi/ans-6.1.1-1977 fluence-to-dose,neutrons(mrem/hr/(n/cm**2/s)
de0    log   2.5e-08 1.0e-07 1.0e-06 1.0e-05 1.0e-04
             .001     .01     .1      .5      1.0
              2.5     5.0     7.0     10.0    14.0  20.0
df0    log   3.67e-3 3.67e-3 4.46e-3 4.54e-3  4.18e-3
             3.76e-3 3.56e-3 2.17e-2 9.26e-2  .132
              .125    .156    .147    .147    .208  .227
fc5    dose rate in mrem/hr at 1 meter from outer surface
f5:n    150.40376  0. 0. 20.
```

This page intentionally left blank.

6.0 CRITICALITY EVALUATION

The following analyses demonstrate that the RH-TRU 72-B package complies with the requirements of 10 CFR §71.55[1]and §71.59. The analyses presented herein show that the criticality requirements are satisfied when limiting the RH-TRU 72-B package as follows for the payloads described in the *Remote-Handling Transuranic Waste Authorization Methods for Payload Control* (RH-TRAMPAC)[2]. These limits are summarized in Table 6.1-1.

- Case A – General Payload: maximum mass limit of 315 fissile gram equivalent (FGE) of ^{239}Pu, of manually compacted waste (i.e., not machine compacted) with less than or equal to 1% of special reflectors by weight. In addition, with 5 grams ^{240}Pu the waste is limited to 325 FGE ^{239}Pu, with 15 grams ^{240}Pu the waste is limited to 350 FGE ^{239}Pu, and with 25 grams ^{240}Pu the waste is limited to 370 FGE ^{239}Pu. These additional limits also require manually compacted waste (i.e., not machine compacted) with less than or equal to 1% of special reflectors by weight.
- Case B – Special Reflector Payload: maximum mass limit of 100 FGE ^{239}Pu, of manually compacted waste (i.e., not machine compacted) with greater than 1% of special reflectors by weight where the fissile material is not chemically or mechanically bound to the special reflector material, and maximum of 305 FGE of ^{239}Pu, where the fissile material is chemically or mechanically bound to the special reflector material.
- Case C – Machine-Compacted Payload: maximum mass limit of 245 FGE ^{239}Pu, of machine-compacted waste with less than or equal to 1% of special reflectors by weight.
- Case D – Low Enriched Uranium (LEU) Payload: maximum enrichment limit of 0.96 wt% ^{235}U fissile equivalent mass (^{235}U FEM), of distributed fissile isotope(s) in the non-fissile ^{238}U, and manually compacted waste (i.e., not machine compacted) with no restriction on special reflector materials.

Based on an unlimited array of undamaged or damaged RH-TRU 72-B packages, the CSI, per 10 CFR §71.59[1], is 0.0.

6.1 Discussion of Results

A comprehensive description of the RH-TRU 72-B packaging is provided in Section 1.2, *Package Description*, and in the packaging drawings in Appendix 1.3.1, *Packaging General Arrangement Drawings*. For the contents of the RH-TRU 72-B package specified in Section 6.2, *Package Contents*, the outer diameter of the package is required to maintain criticality safety for any number of RH-TRU 72-B packages for both normal conditions of transport (NCT) and hypothetical accident conditions (HAC). The stainless steel shells (inner vessel (IV) shell and outer cask (OC) outer shell) and the lead filled cavity between these shells provide better reflection than water such that the package would be further subcritical without it.

[1] Title 10, Code of Federal Regulations, Part 71 (10 CFR 71), *Packaging and Transportation of Radioactive Material*, Final Rule, 01-26-04.

[2] U.S. Department of Energy (DOE), *Remote-Handled Transuranic Waste Authorized Methods for Payload Control* (RH-TRAMPAC), U.S. Department of Energy, Carlsbad Field Office, Carlsbad, New Mexico.

The primary criterion for ensuring that a package (or package array) is safely subcritical is:

$$k_s = k_{eff} + 2\sigma < USL$$

where the quantity k_s is the neutron multiplication factor computed for a given configuration plus twice the uncertainty, σ, in the computed result.

This quantity is computed and reported in order to permit a direct comparison of results against the upper subcritical limit (USL) determined in Section 6.5, *Critical Benchmark Experiments*. The USL is determined on the basis of a benchmark analysis and incorporates the combined effects of code computational bias, the uncertainty in the bias based on both experimental and computational uncertainties, and an administrative margin. Further discussion regarding the USL is provided in Chapter 4, *Determination of Bias and Subcritical Limits*, of NUREG/CR-6361[3].

The fissile mass limits are summarized in Table 6.1-1, and the results of the criticality calculations are summarized in Table 6.1-2. All k_s values are less than the respective USLs of 0.9382 for Pu systems and 0.9257 for the LEU systems. For all cases, the modeled conditions are considered to be extremely conservative and provide an upper limit on k_s. Therefore, the requirements of 10 CFR §71.55 are satisfied when the contents of a single RH-TRU 72-B package is limited in accordance with the limits presented in Table 6.1-1. The application of these limits is described the RH-TRAMPAC[2].

Infinite arrays of both damaged and undamaged RH-TRU 72-B packages, as defined in Section 6.3.4, *Array Models*, are also safely subcritical. The post-accident geometry model for the damaged RH-TRU 72-B package conservatively bounds the damage postulated from HAC analyses documented in Section 2.7, *Hypothetical Accident Conditions*. The model conservatively assumes that the impact limiters are deformed to one-half their initial dimensions.

Calculations performed for Case A of the RH-TRU 72-B package single unit and infinite array of single units of damaged packages indicate that the maximum reactivity of the package arrays are essentially the same as that of the HAC single-unit cases[4] to within the calculated uncertainty of the Monte Carlo analysis (typically about 0.0010). This occurs because:

- The packages are large in comparison with the optimum moderated geometric size of the postulated worst case sphere which results in two effects. First, when full reflection is applied to the optimally moderated spheres, the reflectors tend to isolate the units. Second, since the package is large compared to the spheres, the solid angle to adjacent spheres is small. Both of these effects reduce the interaction between units.
- The package design results in essentially equivalent physical conditions for the NCT and HAC with respect to the IV region. Consequently, the NCT and HAC single-unit models were identical. In the HAC infinite case, the size of the units under HAC is not significantly

[3] J. J. Lichtenwalter, S. M. Bowman, M. D. DeHart, and C. M. Hopper, *Criticality Benchmark Guide for Light-Water Reactor Fuel in Transportation and Storage Packages*, NUREG/CR-6361, ORNL/TM-13211, March 1997.

[4] Note that the NCT and HAC single-unit models were identical since the package contents are optimally located for the NCT model, the damage to the package during the HAC results in no significant structural damage (the impact limiters were conservatively not modeled in the single unit case), and flooding with water is already bounded by the optimum moderator/reflector assumptions of 25% polyethylene/74% water/1% beryllium.

reduced by compression of the impact limiters. Consequently the distance between units remains great enough for unit isolation.

In the Case D, using the postulated representation of the LEU payload, interaction at very low interspersed moderation levels was demonstrated. This is primarily caused by the much larger size of the fissile geometry allowed in the package. This increased size both reduced the solid angle to adjacent spheres (and therefore increased the potential for interaction) and reduced the isolating effects of a reflector. Consequently, the difference between the NCT and HAC single unit and the HAC infinite unit cases differs by 0.5 percent, increasing from 0.9150 to 0.9200 for the poly/water reflected system and 0.9187 to 0.9224 for the special reflector reflected system. However, the low enrichment of the fissile isotope assures a subcritical condition for an infinite system in the absence of significant special reflectors.

For an infinite array of damaged RH-TRU 72-B packages, the maximum calculated k_s values for each case occurred for optimal internal moderation and maximum reflection within the IV and in between the packages. All limits were developed to maintain k_s below the respective USL. The highest k_s from all cases was 0.9370 occurring for Case A in evaluating the 315 FGE unrestricted limit and the 370 FGE limit with 25 g ^{240}Pu present in the waste matrix. These both occurred for infinite arrays of packages at optimal moderation and full reflection. All specific calculations are detailed in Section 6.4.3, *Criticality Results*. These evaluations provide conservative representations of the postulated materials, geometries, and interaction effects from full to decreased volume fractions of interspersed moderation in infinite arrays of units. Therefore, the requirements in 10 CFR §71.59[1] are satisfied for the arrays of RH-TRU 72-B packages under the fissile limitations indicated in Table 6.1-1.

Table 6.1-1 – Fissile Material Limit per RH-TRU 72-B Package

Fissile Content Special Conditions	Fissile Material Limit per RH-TRU 72-B Package①			
	Case A	Case B	Case C	Case D
None②	315 ^{239}Pu FGE	100 ^{239}Pu FGE	245 ^{239}Pu FGE	0.96 wt% ^{235}U FEM
>5 g ^{240}Pu	325 ^{239}Pu FGE	—	—	—
>15 g ^{240}Pu	350 ^{239}Pu FGE	—	—	—
>25 g ^{240}Pu	370 ^{239}Pu FGE	—	—	—
Fissile material bound to special reflector	—	305 ^{239}Pu FGE	—	—

Table 6.1-2 – Summary of Criticality Analysis Results

	Case A	Case B	Case C	Case D
Normal Conditions of Transport (NCT)				
Number of undamaged packages calculated to be subcritical	∞	∞	∞	∞
Single Unit Maximum k_s	Bound by HAC Single Unit k_s	Bound by HAC Infinite Array k_s		Bound by HAC Single Unit k_s
Infinite Array Maximum k_s	Bound by HAC Infinite Array k_s			
Hypothetical Accident Conditions (HAC)				
Number of damaged packages calculated to be subcritical	∞	∞	∞	∞
Single Unit Maximum k_s (0 g ^{240}Pu)	0.9370	Bound by HAC Infinite Array k_s		0.9187
Infinite Array Maximum k_s (0 g ^{240}Pu)	0.9361	0.9086	0.9372	0.9224
Infinite Array Maximum k_s (with ^{240}Pu)	0.9370	—	—	—
Infinite Array Maximum k_s (with fissile material bound to special reflector)	—	0.9340	—	—
Upper Subcritical Limit (USL)	0.9382			0.9257

Notes for Table 6.1-1 and Table 6.1-2:

① Other physical contents limits apply based on each Case A through D. For example, Case A is limited to manually compacted waste (not machine compacted) with up to 1 wt% beryllium. For complete summary of applicability for each case see Section 6.4.3.4, *Applicable Criticality Limits for RH-TRU Waste*.

② These limits apply to the payload regardless of the ^{240}Pu content or the distribution of the ^{239}Pu.

6.2 Package Contents

The payload cavity of an RH-TRU 72-B package can accommodate one payload canister, containing one of four authorized payload types: a General Payload (Case A), a Special Reflected Payload (Case B), a Machine-Compacted Payload (Case C), and a Low Enriched Uranium (LEU) Payload (Case D). The different FGE limits apply depending on the contents of the shipment as discussed in the subsections below.

The quantities of all fissile isotopes other than ^{239}Pu present in the RH-TRU waste matrix may be converted to a FGE using the conversion factors outlined in the *Remote-Handling Transuranic Waste Authorization Methods for Payload Control* (RH-TRAMPAC)[1]. For modeling purposes, the package is assumed to contain ^{239}Pu at the FGE limit. The fissile composition of the RH-TRU waste matrix will typically be as follows:

Nuclide	Weight-Percent
Pu-238	Trace
Pu-239	93.0
Pu-240	5.8
Pu-241	0.4
Pu-242	Trace
Am-241	Trace
All other fissile isotopes	0.7

Additionally, when other fissile isotopes are present in the LEU Payload, the quantities of other contaminating fissile isotopes may be accounted for in the % ^{235}U FEM calculations using the conversion factors also outlined in the RH-TRAMPAC[1].

6.2.1 Applicability of Case A Limits – General Payload

The Case A, General Payload, limits are applicable to canisters of RH-TRU waste material where the ^{239}Pu fissile nuclides (or FGEs of other fissile nuclides), in any form or distribution, with or without ^{240}Pu, are contained in manually compacted (i.e., not machine compacted) wastes and the waste contains less than or equal to 1% of special reflectors by weight. No credit is taken for parasitic neutron absorption of the waste materials and other authorized payload components consisting of the canister, dunnage, and any packing materials, except to the extent that the fissile, moderator, and special reflector elements absorb neutrons. The contents of the RH-TRU 72-B package is conservatively modeled with an optimally moderated sphere of ^{239}Pu and a mixture of 25% polyethylene and 75% water (by volume). The size of the sphere is determined by the specific H/^{239}Pu number density ratio, and this parameter is varied in order to determine the most reactive configuration (i.e., an optimally moderated sphere for a given ^{239}Pu

[1] U.S. Department of Energy (DOE), *Remote-Handled Transuranic Waste Authorized Methods for Payload Control* (RH-TRAMPAC), U.S. Department of Energy, Carlsbad Field Office, Carlsbad, New Mexico.

mass). The RH-TRU waste material and other authorized payload components may contain plastic materials such as anti-contamination clothing, plastic bags, and other plastic refuse that are manually compacted only.

The utilization of polyethylene as the bounding hydrogenous moderating material is justified by the SAIC-1322-001[2] study which concludes that polyethylene is the most reactive moderator that could credibly moderate the transuranic waste in a pure form. A 25% volumetric packing fraction for polyethylene is used as a conservative value which is based on physical testing that bounds the packing fraction of polyethylene in manually compacted TRU waste of 13.36%[3]. Higher packing fractions of up to 100% polyethylene resulting from machine compacted waste are evaluated under the Case C limits presented in Section 6.2.3, *Applicability of Case C Limits – Machine-Compacted Payload*.

This evaluation also addresses the addition of special reflectors in the waste matrix. Materials that can credibly provide better than 25% polyethylene/75% water equivalent reflection are termed "special reflectors" and are not authorized for shipment under the General Payload case in quantities that exceed 1% by weight except in those specific configurations discussed below. Based on the studies of reflector material documented in SAIC-1322-001[2], Be, BeO, C, D_2O, MgO, and depleted uranium (less than 0.72 wt% and greater than or equal to 0.3 wt% ^{235}U) are the only materials considered special reflectors because they provide reflection equivalent to 2 ft thickness of 25% polyethylene and 75% water mixture under the following conditions:

- Less than 5/8-inch thick at 100% of theoretical density[4] in the form of large solids;
- Less than 11/16-inch thick at 70% of theoretical density in the form of tightly-packed particulate solids;
- Less than 20% packing fraction at 24 inches thick in the form of randomly dispersed particulate solids.

The utilization of 1% by volume beryllium in the modeled waste matrix bounds the presence of up to 1 wt% quantities of special reflectors that are randomly dispersed in the payload containers for the purposes of the calculations. This substitution of 1% by volume for 1 wt% is valid based on the large volume of the IV, the maximum allowed payload canister weight allowed in the package, and the low densities of the most reactive payload configurations using the poly/water mixtures. SAIC-1322-001[2] found that beryllium is the bounding special reflector as it provides the best reflection of the system and results in the highest k_s.

Limits for these special reflectors in excess of 1 wt% are addressed in Section 6.2.2, *Applicability of Case B Limits – Special Reflector Payload*.

---

[2] Neeley, G. W., D. L. Newell, S. L. Larson, and R. J. Green, *Reactivity Effects of Moderator and Reflector Materials on a Finite Plutonium System*, SAIC-1322-001, Revision 1, Science Applications International Corporation, Oak Ridge, Tennessee, May 2004.

[3] WP-8-PT.09, *Test Plan to Determine the TRU Waste Polyethylene Packing Fraction*, Washington TRU Solutions, LLC., Revision 0, June 2003.

[4] The theoretical densities used in the study (refer Footnote 2) are 1.85 g/cc for Be, 2.69 g/cc for BeO, 2.1 g/cc for C, 1.1054 g/cc for D_2O, 3.22 g/cc for MgO, and 19.05 g/cc for depleted U.

6.2.2 Applicability of Case B Limits – Special Reflector Payload

The Case B, Special Reflector Payload limit is applicable for contents containing greater than 1% by weight quantities of special reflector materials provided the contents are manually compacted (i.e., not machine compacted). These requirements drive the assumptions regarding the appropriately bounding moderator and reflector materials that are utilized in the analysis to bound the presence of all materials that are authorized for shipment under the Case B FGE limit of 100 g ^{239}Pu. However, if the special reflector materials can be shown to be in thicknesses and/or packing fractions that are less than 25% polyethylene/ 75% water equivalent parameters given in Table 6.2-1, then Case A, General Payload limits can be used. Note that equivalent thicknesses for Be and BeO are not given as, for thin reflectors of these materials, 100% packing fraction does not result in the highest reactivity and the equivalent thickness increases inversely with the packing fraction; thus, only a packing fraction comparison can be used for Be and BeO. The contents model assumptions are provided in Section 6.3.1.2, *Case B, Special Reflector Payload, Contents Model*. A summary discussion of special reflectors is provided in Section 6.4.3.3, *Special Reflectors in RH-TRU Waste*.

The utilization of polyethylene as a bounding hydrogenous moderating material at a 25% packing fraction is consistent with the justification provided in Section 6.2.1, *Applicability of Case A Limits – General Payload*. However, the fissile sphere is moderated with varying volume fractions of beryllium as beryllium was also found in SAIC-1322-001[2] to increase reactivity when significant quantities are included in the moderator. The use of a 100% dense thick Be reflector in the model bounds the presence of other special reflector materials.

To obtain a second less restrictive limit, the fissile isotope is assumed to be chemically or mechanically bound to the special reflector material and the remainder of the waste is assumed to be hydrogenous reflector material consisting of a 25% polyethylene/74% water/1% beryllium mixture. Having the fissile isotope chemically or mechanically bound to the special reflector material allows the higher 305 FGE limit since the material is not available as a reflector (above 1 wt% that represents contamination in the remaining waste matrix) and is not as effective as a moderator. This limit allows for packaging of larger quantities of special reflector material where the fissile isotope is chemically or mechanically bound to the reflector material as a higher concentration contaminant. The use of a variable volume fraction Be moderator in the model bounds the presence of other special reflector materials.

6.2.3 Applicability of Case C Limits – Machine-Compacted Payload

The Case C, Machine-Compacted Payload, limit is applicable provided the contents are machine compacted and contain less than or equal to 1% by weight quantities of special reflector materials. These requirements drive the assumptions regarding the appropriately bounding moderator and reflector materials that are utilized in the analyses to bound the presence of all materials that are authorized for shipment under the Case C 245 FGE limit. The contents model assumptions are provided in Section 6.3.1.3, *Case C, Machine-Compacted Payload, Contents Model*.

The utilization of polyethylene as a bounding hydrogenous moderating material at 100% packing fraction is consistent with the machine compacted polyethylene waste that can be compacted at some facilities under extremely high pressures. Additionally, SAIC-1322-001[2] concluded no material, that could credibly moderate a fissile sphere in a pure form, resulted in a higher

reactivity than the 100% polyethylene moderated system. Thus, compared to Case A, the packing fraction of the moderator is the dominant factor that results in an increase in reactivity and a subsequent lowering of the FGE limit in this Case C. The only inorganic material that increased reactivity when added to the fissile mixture was beryllium, thus up to 1wt% beryllium is modeled in the moderator. The effect of more than 1% by weight quantities of beryllium in the moderator is studied separately under Case B as beryllium is also the leading special reflector. The use of 99% polyethylene and 1% beryllium (by volume) in the reflector region is an appropriately bounding reflector material as it is consistent with the moderator assumption and accounts for the less than or equal to 1% by weight quantities of special reflector materials allowed in the package under the Case C limitations.

6.2.4 Applicability of Case D Limits – LEU Payload

The LEU contents are restricted to material that is primarily uranium (in terms of the heavy metal component) and waste matrix material distributed within a canister in such a manner that the maximum enrichment of the uranium does not exceed 0.96% ^{235}U FEM in any location of the waste material, and there are no variations in the fissile concentration that exceed 0.96% ^{235}U FEM in any location.

Based on subcritical limits published in ANSI/ANS 8.1,[5] the subcritical enrichment limit for uranium oxides mixed homogeneously with water with no limitations on mass or concentration is 0.96 wt% ^{235}U. Uranium nitrates show a higher subcritical limit. The uranium oxide case bounds the low enriched uranium payloads approved in this evaluation. ANSI/ANS 8.12[6] establishes subcritical concentration limits for plutonium-uranium oxide mixtures. A homogenous mixture of plutonium oxide mixed with natural enrichment uranium oxide is assigned a subcritical concentration limit of 0.13 wt% Pu in the mixture of (Pu + U) of unlimited mass. However, these general limits are not equivalent and offer limited application in determining the wt% ^{235}U FEM for any other fissile isotopes that may exist in low concentrations in the waste matrix primarily made or contaminated with ^{238}U. Evaluation of the limit is needed because these standards do not address the higher hydrogen content of the polyethylene/water moderator (the standards are based water reflected aqueous systems only), the special reflector materials allowed in the waste matrix, and the thick steel and lead walls of the package that provide for a higher amount of neutron backscatter. Conversion factors are outlined in the RH-TRAMPAC[1] for calculating the contribution of other fissile isotopes to the % ^{235}U FEM.

A parameter study was performed to determine the maximum k_s under varying 25% polyethylene and 75% water moderator mixtures with the uranium oxide assuming a homogeneous media. Additionally, the presence of special reflector material in the waste matrix was evaluated. The same combinations of special reflector conditions as evaluated in Case B were evaluated for the LEU payload and found to be acceptable with the enrichment limit. The maximum k_s found during these parametric evaluations identified the most reactive waste matrix. The NCT and HAC criticality calculations were then made for the optimum mixtures within the package.

---

[5] ANSI/ANS-8.1 1998, *Nuclear Criticality Safety in Operations with Fissionable Materials Outside Reactors*, American Nuclear Society (ANS), La Grange Park, Illinois.

[6] ANSI/ANS-8.12 1987, *Nuclear Criticality Control and Safety of Plutonium-Uranium Fuel Mixtures Outside Reactors*, American Nuclear Society (ANS), La Grange Park, Illinois.

Table 6.2-1 – Special Reflector Material Parameters that Achieve the Reactivity of a 25%/75% Polyethylene/Water Mixture Reflector

Special Reflector Material	Equivalent Thickness at 100% of Theoretical Density (inches)	Equivalent Thickness at 70% of Theoretical Density (inches)	Equivalent Packing Fraction at 24-inch Thickness (%)
Be	N/A	N/A	7
BeO	N/A	N/A	7
C	0.18	0.25	9
D_2O	0.24	0.27	14
MgO	0.26	0.33	15
U(Natural)	0.08	0.10	1
U(0.6% ^{235}U)	0.14	0.18	1
U(0.5% ^{235}U)	0.18	0.28	2
U(0.4% ^{235}U)	0.33	0.51	3
U(0.3% ^{235}U)	0.56	0.73	5

This page intentionally left blank.

6.3 Model Specifications

6.3.1 Contents Models

Criticality calculations for the RH-TRU 72-B package are performed using the three-dimensional Monte Carlo computer code KENO-V.a[1] by using the CSAS25[2] driver utility module in the SCALE v4.4a software package[3]. Descriptions of the calculational models are given in Section 6.3.1, *Contents Models*, for all cases. A summary of materials and atom densities that are used in the evaluation of the RH-TRU 72-B package is given in Section 6.3.2, *Package Model*.

The limiting mass of fissile material that may be transported in a single RH-TRU 72-B package is shown to provide adequate subcritical margin based on the detailed KENO-V.a analysis. These calculations are performed for an optimally moderated single-unit model and an infinite array model of the RH-TRU 72-B package under both normal conditions of transport (NCT) and hypothetical accident conditions (HAC) for each of the four cases presented.

In all cases, the computational model consists of a contents model and a packaging model. The contents models conservatively represent the package contents, including all authorized payload components and the waste matrix as allowed by each of the cases evaluated. The packaging model represents the remaining structural materials comprising the RH-TRU 72-B packaging. The amount of moderating and reflecting material assumed present in the computational model is varied to maximize reactivity for the single unit and infinite array unit models of the NCT and HAC cases.

6.3.1.1 Case A, General Payload, Contents Model

The Case A, General Payload, contents model is represented as an optimally moderated homogeneous sphere of fissile material with a moderating material consisting of one of the following mixtures: 25% polyethylene and 75% water, or 25% polyethylene, 74% water, and 1% beryllium (each by volume). The remainder of the waste matrix is represented by one or the other of the moderator mixtures only. This representation of the waste matrix conservatively locates the entire fissile isotope mass in one location and provides optimum moderation and reflection using the worst case expected materials allowed in the waste matrix, namely, the hydrogenous polyethylene and water and the trace amounts of special reflector, beryllium. Both mixtures are evaluated to determine which is optimal as a moderated mixture. Based on the expected payload weight, volume of the payload container, the densities of the most reactive systems modeled, and on the density of Be at 1.85 g/cc, modeling the 1% beryllium by volume bounds the limit of 1% by weight.

---

[1] Petrie, L. M., and N. F. Landers, *KENO-V.a: An Improved Monte Carlo Criticality Program with Supergrouping*, ORNL/NUREG/CSD-2/V2/R6, Volume 2, Section F11, March 2000.

[2] Landers, N. F., and L. M. Petrie, *CSAS: Control Module for Enhanced Criticality Safety Analysis Sequences*, NUREG/CR-0200, ORNL/NUREG/CSD-2/V2/R6, Volume 1, Section C4, March 2000.

[3] Oak Ridge National Laboratory (ORNL), *SCALE 4.4a: Modular Code System for Performing Standardized Computer Analyses for Licensing Evaluation for Workstations and Personal Computers*, NUREG/CR-0200, ORNL/NUREG/CSD-2/R6, March 2000.

Since the canister within the package is not credited with containing the waste in any specific configuration, various locations for the Pu sphere are evaluated to determine the effects on package neutron multiplication factor. The sphere is evaluated centered in the container, as shown in Figure 6.3-2, located centered against the thickest end (to evaluate the thick steel reflector conditions at the container top closure) as shown in Figure 6.3-3, and located in the "corner," that is, against the thickest end and displaced radially to the outside of the package, as shown in Figure 6.3-4. Because the payload configuration and IV is unaffected by the HAC conditions, the NCT and HAC contents models are equivalent and the location of the sphere resulting in the maximum neutron multiplication factor is used throughout the remaining evaluations, as applicable.

6.3.1.2 Case B, Special Reflector Payload, Contents Model

The Case B, Special Reflector Payload, contents model also consists of a fissile sphere. The composition of the sphere is modified with the addition of greater amounts of Be and, due to the more efficient Be reflector conditions, the fissile material is reduced to a lower limit of 100 FGE. The first condition assumes that the Pu sphere is optimally moderated with the same mixture as evaluated in Case A, namely, a mixture of 25% polyethylene, 74% water, and 1% beryllium. Since unlimited beryllium is allowed under the limitations of Case B, a beryllium reflector fills the remainder of the IV space. This case evaluates the effect of a pure Be reflector with an optimally moderated Pu sphere. Since the beryllium is a better reflector than steel, the Pu sphere is moved back to the center of the package for this evaluation (scoping calculations showed this to be the most reactive location for the sphere). In order to evaluate voids in the reflector, the volume fraction of beryllium reflector in the IV region is also varied from 100% down to 1%. The second conditions assume that a higher percentage of beryllium is also in the moderator and a solid beryllium reflector exists around the sphere. In order to evaluate this condition, beryllium is added to the sphere and displaces the poly/water mixture raising the volume percent of the beryllium in the moderator from 1% to 80% to evaluate the trend. Between these two evaluations, the waste matrix is evaluated with beryllium at greater than 1% as special reflector of an optimally moderated sphere, with and without significant special reflector in the moderator, thus conservatively evaluating the case where the fissile isotope is not necessarily bound chemically or mechanically to the special reflector material.

A third configuration of the contents is also modeled that assumes that all of the fissile isotope is bound to special reflector material (this also conservatively leaves allowance for 1% by volume special reflector material to be distributed throughout the waste matrix). This contents model evaluates varying volume percents of beryllium displacing the 25% polyethylene/75% water mixture in the moderator with 305 FGE in the sphere. The reflector in the model remains a 25% polyethylene, 74% water, and 1% beryllium (each by volume) mixture that accounts for some special reflector contamination in the remainder of the waste matrix. This contents model is designed to provide a higher fissile loading limit where the waste matrix is known to consist of larger quantities of special reflector materials with higher fissile concentrations chemically or mechanically bound to the special reflector (such as alloys, molds, and crucibles) and where the remainder of the waste matrix is at most contaminated with special reflector (such as, personnel protective equipment, trash, inert packaging material). In this model, the location of the sphere was again found to be most reactive in the "corner" of the IV where neutrons were more effectively backscattered into the hydrogenous reflector region.

6.3.1.3 Case C, Machine-Compacted Payload, Contents Model

The fissile sphere composition in the Case C contents model is moderated with 100% polyethylene and the IV region is filled with a reflector consisting of 99% polyethylene and 1% beryllium (by volume). The 1% beryllium (by volume) accounts for the increased neutron moderation that is caused by less than or equal to 1 wt% special reflector material that is allowed in the Machine-Compacted Payload package. The volume fraction of the 99% polyethylene/1% beryllium reflector in the IV region is varied to assure that voids in the waste matrix are less reactive than the fully compacted conditions.

6.3.1.4 Case D, LEU Payload, Contents Model

Since 0.96 wt% ^{235}U FEM fissile concentrations are so low, the most reactive system from a neutron multiplication factor standpoint grows very large. ANSI/ANS 8.1[4] lists 0.96 wt% ^{235}U as a subcritical enrichment limit for uranium oxides mixed homogenously with water. Consequently, this enrichment should be subcritical for infinite systems.[5] For this waste matrix, uranium oxide at 0.96 wt% ^{235}U is mixed homogenously throughout the IV with varying amounts of 25% polyethylene/ 74% water/ 1% beryllium moderator mixture to represent the worst case waste matrix. The only physical limit placed on the system is that the total mass of the uranium/moderator mixture in the IV does not exceed the contents weight limit of 6,900 pounds. Any voids are filled with the lighter 25% polyethylene/ 74% water/ 1% beryllium reflector mixture used in Case A. The package is filled from the top to the bottom with the U/ 25% polyethylene/ 74% water/ 1% beryllium mixture and followed with the 25% polyethylene/ 74% water/ 1% beryllium reflector mixture to completely fill the container. To evaluate the special reflector materials, the reflector region in the IV was replaced with Be and the percentage of Be in the moderator was increased to evaluate the trend in added special reflector in the moderator. Three different fissile region/reflector region configurations using the Be reflector are evaluated. These are shown in Figure 6.3-6 (these changes in location were evaluated due to results in evaluating Case B). In all cases the additional reflector material is conservatively included in excess of the payload weight limit. A range of H/^{235}U ratios are evaluated to determine the optimum moderated configuration. As before, since the contents model for the NCT and HAC physical conditions are identical, only the HAC conditions are evaluated to represent both.

6.3.2 Package Model

A comprehensive description of the RH-TRU 72-B packaging is provided in Section 1.2, *Package Description*, and in the packaging drawings in Appendix 1.3.1, *Packaging General Arrangement Drawings*. The packaging includes an inner vessel (IV), an outer cask (OC), and impact limiters. The impact limiters cover each end of the OC and are steel shells filled with polyurethane foam. The OC includes a steel shell structure that encloses and supports lead shielding, and surrounds the independent steel IV. The nested IV and OC each provide independent leak-tight containment under NCT.

---

[4] ANSI/ANS 8.1-1998, *Nuclear Criticality Safety in Operations with Fissionable Materials Outside Reactors*, American Nuclear Society (ANS), La Grange Park, Illinois.

[5] Note that the ANSI/ANS 8.1 is applicable to aqueous, water reflected systems. The system modeled in Case D and throughout this evaluation contains some special reflector material and is reflected by significant thicknesses of steel. The presence of both of these materials invalidates the use of the ANSI/ANS 8.1 limits.

The packaging is robust due to the heavy wall design needed to provide gamma shielding. For modeling simplicity, miscellaneous hardware (such as the trunnions) is neglected for both NCT and HAC models. The impact limiters are neglected for all of the single package models of Cases A through D. The impact limiters are assumed to provide one half their respective thicknesses in all directions for infinite array Cases A through D. The modeled impact limiters are assumed to only provide spacing, and are treated in the same manner as the other regions outside of the package. These assumptions conservatively:

- Allow for greater reflection in the single package cases by allowing the water reflector outside the package to be closer fitting;
- Account for array HAC damage to the impact limiters due to crush damage during impact;
- Reduce spacing between packages in infinite array calculations to conservatively increase interaction between packages; and
- Allow greater external interspersed moderation in the infinite array cases by filling the region normally occupied by the impact limiter with interspersed moderator (low density water).

Since the IV and OC sustain little damage during HAC (except for localized puncture damage of the OC) and minor variations in the package dimensions have little effect on the neutron multiplication calculations (due to the large size of the packages), nominal packaging dimensions are used for both NCT and HAC models. The waste canister within the package is not explicitly modeled and no credit is taken for materials or shape of this container. A generalized sphere of the optimally moderated fissile isotope, with an optimized reflector filling the remainder of the package IV void is used to represent the containerized waste matrix. The sphere is evaluated in various locations in the IV to determine the most reactive conditions under NCT and HAC.

The package model represents the IV and OC structural materials as follows. The model consists of nested, right circular cylindrical shells of Type 304 stainless steel (SS304) and lead shielding (Pb). The inner diameter of the IV cavity is modeled with an inner diameter of 31.25 inches (79.375 cm), and an inside length of 121.5 inches (308.61 cm). The IV wall and the inner shell of the OC are represented as a single region of SS304 with a thickness of 1.626 inches (3.493 cm). The lead shield inside the OC inner and outer walls is modeled as 1.875 inches (4.763 cm) thick. Outside of the lead shield, the thermal shield and the OC outer shell are represented as a single SS304 region of 1.625 inches (4.127 cm). All gaps between components are neglected. This representation of the package therefore results in a model that has an outer diameter that is slightly less than the actual outer diameter of the vessel. With respect to the length of the vessel, the end caps are modeled as solid SS304 with a thickness of 13 inches (33.02 cm) on the closure end and 6.5 inches (16.51 cm) on the vessel bottom. This results in an overall package length of 141 inches without the impact limiters. The impact limiters, when used in the models as described above, are modeled in dimension only (with interspersed moderator filling the void) and extend the overall diameter of the package by 16 inches (40.64 cm) and the overall length by 23 inches (58.42 cm).

The RH-TRU 72-B package model for the damaged and undamaged unit is depicted in Figure 6.3-1.

6.3.3 Single Package Models

Compliance with the requirements of 10 CFR §71.55[6] is demonstrated by analyzing optimally moderated damaged and undamaged, single-unit RH-TRU 72-B packages.

The NCT and HAC single-unit model consists of the contents models described in Section 6.3.1, *Contents Models*, combined with the packaging model described in Section 6.3.2, *Package Model*, for each of the four cases evaluated. In all cases, the package with its contents is surrounded with a 12 inch (30.5 cm) thick, close-fitting full density water reflector. This representation of the single unit conservatively replaces the impact limiter volume with full density water which tends to be a better reflector than foam when positioned closer to the fissile region. Representations of the KENO-V.a[1] models are shown in Figure 6.3-2 through Figure 6.3-6 with the contents in the various modeled locations. Since the NCT and HAC configurations are not different under these assumptions, both are represented by the same model. Single-unit calculations are performed with the contents sphere in various locations to determine optimum neutron multiplication of the system.

6.3.4 Array Models

Calculations are performed for infinite arrays of damaged and undamaged RH-TRU 72-B packages in a close packed, square-pitch configuration. Triangular-pitched array configurations are not considered because the size of the package is sufficiently large compared to the size of the most reactive contents configuration that the triangular-pitched configuration is not significant as indicated by the square-pitched array analyses showing that the interaction effects are of minor consequence as compared to the single unit fully reflected cases. For Cases A through B the package includes the impact limiters reduced to half-thickness to simulate the damage under HAC conditions. In Case D, the LEU is essentially subcritical under infinite configurations and the packages were conservatively modeled without the addition of the impact limiters. This reduced spacing (either with or without impact limiters) conservatively bounds the NCT configuration and only the HAC configurations are calculated. A specularly reflective boundary condition is applied to all six faces of the unit cell defining the array configuration in order to represent an infinite array of RH-TRU 72-B packages. The contents sphere is modeled in various locations with in the package to achieve maximum interaction between packages. Additionally, interspersed moderation between RH-TRU 72-B packages is evaluated using various volume fractions up to full density water to evaluate the maximum interaction achievable between units. The contents configuration modeled are described in Section 6.3.1.1, *Case A, General Payload, Contents Model*.

6.3.5 Package Regional Densities

A summary of all material densities and compositions used in the KENO-V.a[1] models for the RH-TRU 72-B package is given in the following tables as indicated by the case study. Specifically, Case A, General Payload, regional densities are recorded in Table 6.3-1 and Table 6.3-2; Case B, Special Reflector Payload, in Table 6.3-3; Case C, Machine-Compacted Payload, in Table 6.3-4; and Case D, LEU Payload, in Table 6.3-5 and Table 6.3-6. The parameters are

[6] Title 10, Code of Federal Regulations, Part 71 (10 CFR 71), *Packaging and Transportation of Radioactive Material*, Final Rule, 01-26-04.

computed based on the SCALE Standard Composition Library[7] provided values of density as follows: plutonium density of 19.84 g/cc, beryllium density of 1.850 g/cc, polyethylene density of 0.9230 g/cc, water density of 0.9982 g/cc, SS304 density of 7.94 g/cc, and lead density of 11.344 g/cc. The materials used to represent the RH-TRU package are Type 304 stainless steel (SS304) and lead (Pb). The SCALE Standard Composition Library identifier "BEBOUND", nuclide identifier 4309, was used to model the beryllium reflector. The cross-section of BEBOUND is based on a beryllium metal whereas the cross-section for standard material BE is based on a free gas representation. BEBOUND is also used to model beryllium in the benchmark cases discussed in Section 6.5, *Critical Benchmark Experiments*.

For Cases A through D with data shown in Table 6.3-1 through Table 6.3-6, the fissile material composition is determined by defining the mass of fissile material (in this case the Pu limit for the specific case or the uranium enrichment) and then inputing the desired H/X ratio to be evaluated. Using these two input parameters the material composition for the arbitrary mixture used to represent the moderated fissile region is calculated. To use an arbitrary mixture in SCALE the percentages by weight of each constituent must be specified. In our modeling, the fissile material and the moderator are treated in a volume additive manner. The moderator is a combination of volume percentages of the indicated combinations of water, polyethylene and beryllium. The process is described for the Pu sphere as follows.

Since the system is evaluated for optimum H/Pu ratio, the desired Pu mass and the H/Pu ratio are used to calculate the mass of hydrogen in the sphere as follows:

$$mH = \frac{H/Pu \times mPu \times MwH}{MwPu}$$

where mH is mass of hydrogen, H/Pu is the hydrogen to plutonium ratio desired, mPu is mass of plutonium, MwH is atomic weight of hydrogen, and MwPu is atomic weight of plutonium.

Once the mass of hydrogen is known for the composition the mass of polyethylene can be shown to equal:

$$mCH_2 = \frac{mH}{2MwH \times \left(\frac{Vol\%H_2O}{Vol\%CH_2} \times \frac{\rho H_2O}{\rho CH_2 \times MwH_2O} + \frac{1}{MwCH_2} \right)}$$

where mCH_2 is the mass of polyethylene, $Vol\%H_2O$ and $Vol\%CH_2$ are the volume percentages of water and polyethylene, respectively, ρH_2O and ρCH_2 are the densities of water and polyethylene, respectively, and MwH_2O and $MwCH_2$ are the molecular weights of water and polyethylene, respectively.

Once the mass of polyethylene is known the mass of O, C, and Be can be shown to equal:

$$mO = mCH_2 \times \frac{Vol\%H_2O}{Vol\%CH_2} \times \frac{\rho H_2O}{\rho CH_2} \times \frac{MwO}{MwH_2O}$$

[7] L. M. Petrie, P. B. Fox and K. Lucius, *Standard Composition Library*, ORNL/NUREG/CSD-2/V3/R6, Volume 3, Section M8, March 2000.

$$mC = \frac{mCH_2}{MwCH_2} \times MwO$$

$$mBe = \frac{Vol\%Be}{Vol\%CH_2} \times mCH_2 \times \frac{\rho Be}{\rho CH_2}$$

where mO, mC, and mBe are the masses of oxygen, carbon, and beryllium, respectively, Vol%C and Vol%Be are the volume percentage of carbon and beryllium, respectively, ρBe is the density of beryllium, and MwO is the atomic weight of oxygen.

Using the masses and densities of Pu and CH_2 in a volume additive manner, the volume of the moderated Pu sphere can be shown to equal:

$$V_s = \frac{mPu}{\rho Pu} + \frac{mCH_2}{\rho CH_2} \times \left(1 + \frac{Vol\%H_2O}{Vol\%CH_2} + \frac{Vol\%Be}{Vol\%CH_2}\right)$$

In the cases with the additional ^{240}Pu (Case A, General Payload, evaluations), the volume of the sphere is increased as follows and all other calculations remain the same:

$$V_s = \frac{m^{240}Pu + m^{239}Pu}{\rho Pu} + \frac{mCH_2}{\rho CH_2} \times \left(1 + \frac{Vol\%H_2O}{Vol\%CH_2} + \frac{Vol\%Be}{Vol\%CH_2}\right).$$

In the Case D evaluation, the same approach was used except ^{235}U was substituted for ^{239}Pu, ^{238}U was substituted for ^{240}Pu, and the values of uranium densities and atomic weights were appropriately substituted for those of Pu in the above equations and the ratio of ^{235}U to ^{238}U was related using the 0.96 wt% enrichment value. Although other approaches are equivalent, this method maintained the evaluations of the Pu and U systems consistent by using a volume additive method between the fissile isotope and the moderator constituents.

Once all of the elemental masses and volume of the mixture are known, total mass of the mixture, the weight percentages for each constituent, and the solution densities are calculated in the usual manner. These weight percentages and solution density values are used in the arbitrary material definition of the Pu sphere composition in the KENO-V.a[1] input file. From these values the number densities are calculated in the usual manner to obtain the number densities reported in Table 6.3-1 through Table 6.3-6. These number densities were compared to those calculated by SCALE as a check of the input. Results agree to within 3 significant digits with differences attributed to round off errors in the various calculations.

Table 6.3-1 – Fissile Contents Model Properties for 315 g Pu Spheres (Case A)①

H/Pu Ratio	Pu Concentration (g Pu/L)	Sphere Radius (cm)	Solution Density (g/cc)	Number Densities (atoms/b-cm)				
				^{239}Pu	H	O	C	Be
25% Polyethylene/75% Water Moderator								
700	39.56	12.3872	1.0170	9.9673E-05	6.9772E-02	2.4990E-02	9.8955E-03	N/A
800	34.63	12.9499	1.0123	8.7236E-05	6.9788E-02	2.4996E-02	9.8979E-03	
900	30.79	13.4676	1.0087	7.7561E-05	6.9806E-02	2.5002E-02	9.9003E-03	
1,000	27.71	13.9483	1.0057	6.9810E-05	6.9811E-02	2.5004E-02	9.9011E-03	
1,100	25.20	14.3979	1.0034	6.3478E-05	6.9826E-02	2.5010E-02	9.9033E-03	
25% Polyethylene/74% Water/1% Beryllium Moderator								
700	39.19	12.4268	1.0252	9.8730E-05	6.9110E-02	2.4659E-02	9.8962E-03	1.2338E-03
800	34.30	12.9914	1.0205	8.6405E-05	6.9124E-02	2.4664E-02	9.8982E-03	1.2341E-03
900	30.49	13.5107	1.0169	7.6821E-05	6.9138E-02	2.4669E-02	9.9002E-03	1.2344E-03
1,000	27.45	13.9929	1.0140	6.9148E-05	6.9148E-02	2.4672E-02	9.9017E-03	1.2345E-03
1,100	24.96	14.4440	1.0116	6.2867E-05	6.9155E-02	2.4675E-02	9.9026E-03	1.2346E-03
1,200	22.88	14.8685	1.0097	5.7639E-05	6.9167E-02	2.4679E-02	9.9044E-03	1.2349E-03
1,300	21.12	15.2701	1.0080	5.3210E-05	6.9172E-02	2.4681E-02	9.9050E-03	1.2350E-03

Notes:

① Number densities in this table are calculated from the raw input data as a check to SCALE. SCALE duplicated these densities to the third significant digit. The differences are attributed to round-off errors.

Table 6.3-2 – Fissile Contents Model Properties for Various Pu Spheres with Pu-240 Added as Indicated (Case A)①

H/Pu Ratio	Pu Concentration (g Pu/L)	Sphere Radius (cm)	Solution Density (g/cc)	Number Densities (atoms/b-cm)					
				^{240}Pu	^{239}Pu	H	O	C	Be
5g ^{240}Pu/325 g ^{235}Pu/25% Polyethylene/74% Water/1% Beryllium Moderator									
700	39.77	12.5595	1.0251	1.5122E-06	9.8661E-05	6.9063E-02	2.4642E-02	9.8895E-03	1.2330E-03
800	34.81	13.1297	1.0205	1.3236E-06	8.6361E-05	6.9088E-02	2.4651E-02	9.8931E-03	1.2335E-03
900	30.95	13.6543	1.0169	1.1761E-06	7.6785E-05	6.9106E-02	2.4657E-02	9.8957E-03	1.2338E-03
1,000	27.86	14.1414	1.0140	1.0583E-06	6.9120E-05	6.9120E-02	2.4662E-02	9.8976E-03	1.2340E-03
1,100	25.33	14.5971	1.0116	9.6187E-07	6.2845E-05	6.9128E-02	2.4665E-02	9.8989E-03	1.2342E-03
15g ^{240}Pu/350 g ^{235}Pu/25% Polyethylene/74% Water/1% Beryllium Moderator									
700	40.80	12.8782	1.0251	4.2074E-06	9.8558E-05	6.8990E-02	2.4616E-02	9.8791E-03	1.2317E-03
800	35.71	13.4623	1.0205	3.6816E-06	8.6282E-05	6.9024E-02	2.4628E-02	9.8840E-03	1.2323E-03
900	31.76	13.9997	1.0169	3.2732E-06	7.6721E-05	6.9049E-02	2.4637E-02	9.8875E-03	1.2328E-03
1,000	28.59	14.4988	1.0140	2.9484E-06	6.9068E-05	6.9068E-02	2.4644E-02	9.8902E-03	1.2331E-03
1,100	26.00	14.9656	1.0116	2.6800E-06	6.2801E-05	6.9082E-02	2.4649E-02	9.8922E-03	1.2334E-03
25g ^{240}Pu/370 g ^{235}Pu/25% Polyethylene/74% Water/1% Beryllium Moderator									
700	41.72	13.1232	1.0251	6.6249E-06	9.8465E-05	6.8925E-02	2.4593E-02	9.8698E-03	1.2306E-03
800	36.53	13.7179	1.0205	5.8015E-06	8.6210E-05	6.8967E-02	2.4608E-02	9.8758E-03	1.2313E-03
900	32.49	14.2650	1.0169	5.1585E-06	7.6665E-05	6.8998E-02	2.4619E-02	9.8802E-03	1.2319E-03
1,000	29.25	14.7732	1.0140	4.6452E-06	6.9022E-05	6.9022E-02	2.4627E-02	9.8836E-03	1.2323E-03
1,100	26.60	15.2485	1.0116	4.2231E-06	6.2763E-05	6.9040E-02	2.4634E-02	9.8861E-03	1.2326E-03

Notes:

① Number densities in this table are calculated from the raw input data as a check to SCALE. SCALE duplicated these densities to the third significant digit. The differences are attributed to round-off errors.

Table 6.3-3 – Fissile Contents Model Properties for 100 g Pu Spheres (Case B)

H/Pu Ratio	Pu Concentration (g Pu/L)	Sphere Radius (cm)	Solution Density (g/cc)	Number Densities (atoms/b-cm)				
				^{239}Pu	H	O	C	Be
25% Polyethylene/74% Water/1% Beryllium Moderator								
600	45.70	8.0536	1.0313	1.1514E-04	6.9082E-02	2.4649E-02	9.8921E-03	1.2333E-03
700	39.19	8.4773	1.0252	9.8730E-05	6.9110E-02	2.4659E-02	9.8962E-03	1.2338E-03
800	34.30	8.8624	1.0205	8.6405E-05	6.9124E-02	2.4664E-02	9.8982E-03	1.2341E-03
900	30.49	9.2167	1.0169	7.6821E-05	6.9138E-02	2.4669E-02	9.9002E-03	1.2344E-03
1,000	27.45	9.5456	1.0140	6.9148E-05	6.9148E-02	2.4672E-02	9.9017E-03	1.2345E-03
1,100	24.96	9.8533	1.0116	6.2867E-05	6.9155E-02	2.4675E-02	9.9026E-03	1.2346E-03
24.5% Polyethylene/73.5% Water/2% Beryllium Moderator								
600	45.22	8.0820	1.0398	1.1393E-04	6.8360E-02	2.4485E-02	9.6953E-03	2.4670E-03
700	38.77	8.5072	1.0336	9.7683E-05	6.8377E-02	2.4491E-02	9.6977E-03	2.4676E-03
800	33.94	8.8937	1.0290	8.5492E-05	6.8394E-02	2.4497E-02	9.7001E-03	2.4682E-03
900	30.17	9.2493	1.0255	7.6014E-05	6.8412E-02	2.4503E-02	9.7026E-03	2.4688E-03
1,000	27.16	9.5794	1.0226	6.8420E-05	6.8419E-02	2.4506E-02	9.7037E-03	2.4691E-03
1,100	24.69	9.8882	1.0203	6.2210E-05	6.8431E-02	2.4510E-02	9.7054E-03	2.4695E-03
24% Polyethylene/72% Water/4% Beryllium Moderator								
600	44.30	8.1376	1.0563	1.1161E-04	6.6968E-02	2.3986E-02	9.4979E-03	4.9342E-03
700	37.98	8.5658	1.0503	9.5699E-05	6.6989E-02	2.3994E-02	9.5009E-03	4.9357E-03
800	33.24	8.9550	1.0458	8.3757E-05	6.7005E-02	2.3999E-02	9.5031E-03	4.9369E-03
900	29.56	9.3130	1.0423	7.4465E-05	6.7017E-02	2.4004E-02	9.5049E-03	4.9378E-03
1,000	26.60	9.6454	1.0395	6.7026E-05	6.7027E-02	2.4007E-02	9.5063E-03	4.9386E-03
1,100	24.19	9.9563	1.0372	6.0941E-05	6.7035E-02	2.4010E-02	9.5074E-03	4.9391E-03
23.5% Polyethylene/70.5% Water/6% Beryllium Moderator								
600	43.38	8.1948	1.0728	1.0929E-04	6.5576E-02	2.3487E-02	9.3004E-03	7.4016E-03
700	37.19	8.6260	1.0669	9.3707E-05	6.5594E-02	2.3494E-02	9.3030E-03	7.4036E-03
800	32.55	9.0179	1.0625	8.2011E-05	6.5610E-02	2.3500E-02	9.3052E-03	7.4054E-03
900	28.94	9.3784	1.0591	7.2914E-05	6.5623E-02	2.3504E-02	9.3071E-03	7.4069E-03
1,000	26.05	9.7132	1.0563	6.5629E-05	6.5629E-02	2.3506E-02	9.3080E-03	7.4076E-03
1,100	23.69	10.0263	1.0541	5.9672E-05	6.5639E-02	2.3510E-02	9.3094E-03	7.4087E-03
23% Polyethylene/69% Water/8% Beryllium Moderator								
600	42.46	8.2536	1.0893	1.0697E-04	6.4183E-02	2.2989E-02	9.1030E-03	9.8692E-03
700	36.40	8.6880	1.0835	9.1712E-05	6.4199E-02	2.2994E-02	9.1052E-03	9.8716E-03
800	31.86	9.0827	1.0792	8.0269E-05	6.4214E-02	2.3000E-02	9.1073E-03	9.8739E-03
900	28.33	9.4458	1.0759	7.1366E-05	6.4228E-02	2.3005E-02	9.1093E-03	9.8761E-03
1,000	25.50	9.7830	1.0732	6.4235E-05	6.4236E-02	2.3008E-02	9.1104E-03	9.8773E-03
1,100	23.18	10.0984	1.0710	5.8402E-05	6.4244E-02	2.3010E-02	9.1114E-03	9.8785E-03

H/Pu Ratio	Pu Concentration (g Pu/L)	Sphere Radius (cm)	Solution Density (g/cc)	Number Densities (atoms/b-cm)				
				^{239}Pu	H	O	C	Be
22.5% Polyethylene/67.5% Water/10% Beryllium Moderator								
600	41.54	8.3142	1.1058	1.0465E-04	6.2791E-02	2.2490E-02	8.9055E-03	1.2337E-02
700	35.61	8.7517	1.1002	8.9727E-05	6.2810E-02	2.2497E-02	8.9081E-03	1.2341E-02
800	31.17	9.1494	1.0960	7.8531E-05	6.2825E-02	2.2502E-02	8.9102E-03	1.2344E-02
900	27.71	9.5152	1.0927	6.9815E-05	6.2834E-02	2.2505E-02	8.9115E-03	1.2346E-02
1,000	24.94	9.8548	1.0901	6.2844E-05	6.2844E-02	2.2509E-02	8.9130E-03	1.2347E-02
1,100	22.68	10.1726	1.0879	5.7134E-05	6.2848E-02	2.2510E-02	8.9135E-03	1.2348E-02
20% Polyethylene/60% Water/20% Beryllium Moderator								
600	36.93	8.6465	1.1883	9.3041E-05	5.5825E-02	1.9995E-02	7.9175E-03	2.4679E-02
700	31.66	9.1015	1.1833	7.9769E-05	5.5838E-02	2.0000E-02	7.9194E-03	2.4685E-02
800	27.71	9.5152	1.1796	6.9813E-05	5.5850E-02	2.0004E-02	7.9211E-03	2.4690E-02
900	24.64	9.8957	1.1767	6.2064E-05	5.5859E-02	2.0007E-02	7.9223E-03	2.4694E-02
1,000	22.18	10.2490	1.1744	5.5866E-05	5.5867E-02	2.0010E-02	7.9234E-03	2.4697E-02
1,100	20.16	10.5794	1.1725	5.0792E-05	5.5872E-02	2.0012E-02	7.9242E-03	2.4700E-02
15% Polyethylene/45% Water/40% Beryllium Moderator								
600	27.71	9.5152	1.3535	6.9814E-05	4.1889E-02	1.5003E-02	5.9409E-03	4.9381E-02
700	23.76	10.0162	1.3498	5.9854E-05	4.1896E-02	1.5006E-02	5.9421E-03	4.9391E-02
800	20.79	10.4716	1.3470	5.2379E-05	4.1902E-02	1.5008E-02	5.9428E-03	4.9397E-02
900	18.48	10.8905	1.3449	4.6564E-05	4.1908E-02	1.5010E-02	5.9438E-03	4.9405E-02
1,000	16.64	11.2794	1.3432	4.1914E-05	4.1913E-02	1.5012E-02	5.9444E-03	4.9410E-02
1,100	15.12	11.6432	1.3418	3.8108E-05	4.1917E-02	1.5013E-02	5.9449E-03	4.9414E-02
10% Polyethylene/30% Water/60% Beryllium Moderator								
600	18.48	10.8905	1.5188	4.6563E-05	2.7937E-02	1.0007E-02	3.9624E-03	7.4104E-02
700	15.84	11.4642	1.5164	3.9918E-05	2.7942E-02	1.0008E-02	3.9629E-03	7.4116E-02
800	13.87	11.9856	1.5146	3.4933E-05	2.7945E-02	1.0009E-02	3.9634E-03	7.4125E-02
900	12.33	12.4652	1.5132	3.1054E-05	2.7948E-02	1.0010E-02	3.9638E-03	7.4132E-02
1,000	11.09	12.9105	1.5120	2.7948E-05	2.7949E-02	1.0011E-02	3.9639E-03	7.4133E-02
1,100	10.09	13.3270	1.5111	2.5411E-05	2.7951E-02	1.0011E-02	3.9642E-03	7.4138E-02
5% Polyethylene/15% Water/80% Beryllium Moderator								
600	9.25	13.7190	1.6843	2.3291E-05	1.3976E-02	5.0056E-03	1.9821E-03	9.8852E-02
700	7.93	14.4420	1.6831	1.9967E-05	1.3976E-02	5.0060E-03	1.9823E-03	9.8859E-02
800	6.94	15.0991	1.6822	1.7473E-05	1.3978E-02	5.0063E-03	1.9824E-03	9.8864E-02
900	6.16	15.7035	1.6815	1.5530E-05	1.3978E-02	5.0065E-03	1.9824E-03	9.8868E-02
1,000	5.55	16.2647	1.6810	1.3980E-05	1.3979E-02	5.0068E-03	1.9826E-03	9.8875E-02
1,100	5.04	16.7896	1.6805	1.2710E-05	1.3979E-02	5.0069E-03	1.9826E-03	9.8875E-02

Table 6.3-4 – Fissile Contents Model Properties for 245 g Pu Spheres (Case C)

H/Pu Ratio	Pu Concentration (g Pu/L)	Sphere Radius (cm)	Solution Density (g/cc)	Number Densities (atoms/b-cm)			
				^{239}Pu	H	C	Be
100% Polyethylene Moderator							
700	44.88	10.9231	0.9658	1.1306E-04	7.9145E-02	3.9572E-02	N/A
800	39.28	11.4192	0.9605	9.8963E-05	7.9170E-02	3.9585E-02	
900	34.92	11.8756	0.9563	8.7983E-05	7.9184E-02	3.9592E-02	
1,000	31.44	12.2994	0.9530	7.9199E-05	7.9199E-02	3.9600E-02	
1,100	28.58	12.6958	0.9503	7.2012E-05	7.9213E-02	3.9606E-02	
99% Polyethylene/1% Beryllium Moderator							
700	44.43	10.9597	1.8939	1.1193E-04	7.8353E-02	3.9177E-02	1.2334E-03
800	38.89	11.4575	1.9048	9.7967E-05	7.8374E-02	3.9187E-02	1.2338E-03
900	34.57	11.9154	1.9133	8.7102E-05	7.8392E-02	3.9196E-02	1.2341E-03
1,000	31.12	12.3406	1.9202	7.8405E-05	7.8404E-02	3.9202E-02	1.2343E-03
1,100	28.30	12.7383	1.9259	7.1285E-05	7.8415E-02	3.9207E-02	1.2345E-03

Table 6.3-5 – Fissile Contents Model Properties for 0.96 wt% U-235 FEM (Case D)

H/^{235}U Ratio	^{235}U Concentration (g ^{235}U/L)	Fissile Cylinder Height (cm)	Mixture Density (g/cc)	Number Densities (atoms/b-cm)					
				^{238}U	^{235}U	H	O	C	Be
25% Polyethylene/74% Water/1% Beryllium Moderator (Cases in Table 6.4-10 through Table 6.4-13)									
300	60.35	91.2100	6.9487	1.5752E-02	1.5464E-04	4.6393E-02	1.6553E-02	6.6432E-03	8.2839E-04
400	49.34	108.1520	5.8605	1.2877E-02	1.2641E-04	5.0566E-02	1.8042E-02	7.2407E-03	9.0270E-04
500	41.72	124.0774	5.1083	1.0889E-02	1.0690E-04	5.3448E-02	1.9071E-02	7.6534E-03	9.5410E-04
600	36.14	139.0790	4.5573	9.4327E-03	9.2599E-05	5.5560E-02	1.9824E-02	7.9559E-03	9.9189E-04
700	31.88	153.2384	4.1362	8.3199E-03	8.1680E-05	5.7175E-02	2.0400E-02	8.1871E-03	1.0207E-03
800	28.51	166.6162	3.8041	7.4422E-03	7.3065E-05	5.8450E-02	2.0855E-02	8.3696E-03	1.0435E-03
900	25.79	179.2845	3.5353	6.7319E-03	6.6090E-05	5.9479E-02	2.1222E-02	8.5170E-03	1.0619E-03
1,000	23.55	191.2971	3.3133	6.1453E-03	6.0327E-05	6.0328E-02	2.1525E-02	8.6387E-03	1.0772E-03

Table 6.3-6 – Fissile Contents Model Properties for 0.96 wt% U-235 FEM (Case D with Variable Beryllium Moderator and H/U-235=500)

Vol% Be①	^{235}U Concentration (g ^{235}U/L)	Fissile Cylinder Height (cm)	Mixture Density (g/cc)	Number Densities (atoms/b-cm)					
				^{238}U	^{235}U	H	O	C	Be
Variable Beryllium in Moderator (Cases in Table 6.4-14)									
1	41.72	124.0774	5.1083	1.0889E-02	1.0690E-04	5.3448E-02	1.9071E-02	7.6534E-03	9.5410E-04
2	41.38	124.7318	5.0815	1.0800E-02	1.0602E-04	5.3010E-02	1.8987E-02	7.5184E-03	1.9131E-03
4	40.72	126.0013	5.0303	1.0629E-02	1.0434E-04	5.2172E-02	1.8686E-02	7.3992E-03	3.8438E-03
6	40.06	127.3124	4.9785	1.0456E-02	1.0264E-04	5.1323E-02	1.8382E-02	7.2788E-03	5.7927E-03
8	39.39	128.6614	4.9263	1.0281E-02	1.0093E-04	5.0466E-02	1.8075E-02	7.1573E-03	7.7599E-03
10	38.72	130.0526	4.8736	1.0105E-02	9.9201E-05	4.9600E-02	1.7766E-02	7.0347E-03	9.7455E-03
20	35.24	137.7161	4.6024	9.1986E-03	9.0308E-05	4.5151E-02	1.6172E-02	6.4037E-03	1.9961E-02
40	27.77	157.7149	4.0188	7.2482E-03	7.1154E-05	3.5578E-02	1.2743E-02	5.0459E-03	4.1942E-02
60	19.50	187.9168	3.3729	5.0897E-03	4.9961E-05	2.4982E-02	8.9482E-03	3.5433E-03	6.6265E-02
80	10.30	238.7916	2.6543	2.6881E-03	2.6388E-05	1.3195E-02	4.7260E-03	1.8714E-03	9.3329E-02
85	7.83	257.4534	2.4619	2.0449E-03	2.0072E-05	1.0038E-02	3.5952E-03	1.4236E-03	1.0058E-01

Notes:

① Volume-% beryllium in the moderator.

Table 6.3-7 – Structural Model Properties for the RH-TRU 72-B Package (All Cases)

Nuclide	SCALE Nuclide Identifier	Percentage of Composition	Number Density (atoms/b-cm)
Type 304 Stainless Steel for RH-TRU 72-B Package Walls and End Caps			
C	6012	0.080 wt%	3.1877E-04
Si	14000	1.000 wt%	1.7025E-03
P	15031	0.045 wt%	6.9468E-05
Cr	24304	19.000 wt%	1.7473E-02
Mn	25055	2.000 wt%	1.7407E-03
Fe	26304	68.375 wt%	5.8545E-02
Ni	28304	9.500 wt%	7.7402E-03
Lead for RH- TRU 72-B Package Shielding			
Pb	82000	100 wt%	3.2969E-02

Table 6.3-8 – Reflector Model Properties for the RH-TRU 72-B Package by Case

Nuclide	SCALE Nuclide Identifier	Number Density (atoms/b-cm)
25% Polyethylene/75% Water IV Reflector used in Case A		
H	1001	6.99063E-02
C	6012	9.91472E-03
O	8016	2.50384E-02
25% Polyethylene/74% Water/1% Beryllium IV Reflector used in Case A and D		
H	1001	6.92387E-02
Bebound	4309	1.23621E-03
C	6012	9.91472E-03
O	8016	2.47046E-02
100% Beryllium IV Reflector used in Case B①		
Bebound	4309	1.23621E-01
99% Polyethylene/1% Beryllium IV Reflector used in Case C		
H	1001	7.85246E-02
Bebound	4309	1.23621E-03
C	6012	3.92623E-02

Notes:

① For the variable density reflector cases of Section 6.4.3.2.2, *Case B, Special Reflector Payload, Infinite Array Results*, this quantity is reduced by the indicated volume fraction multiplier, as shown in Table 6.4-6.

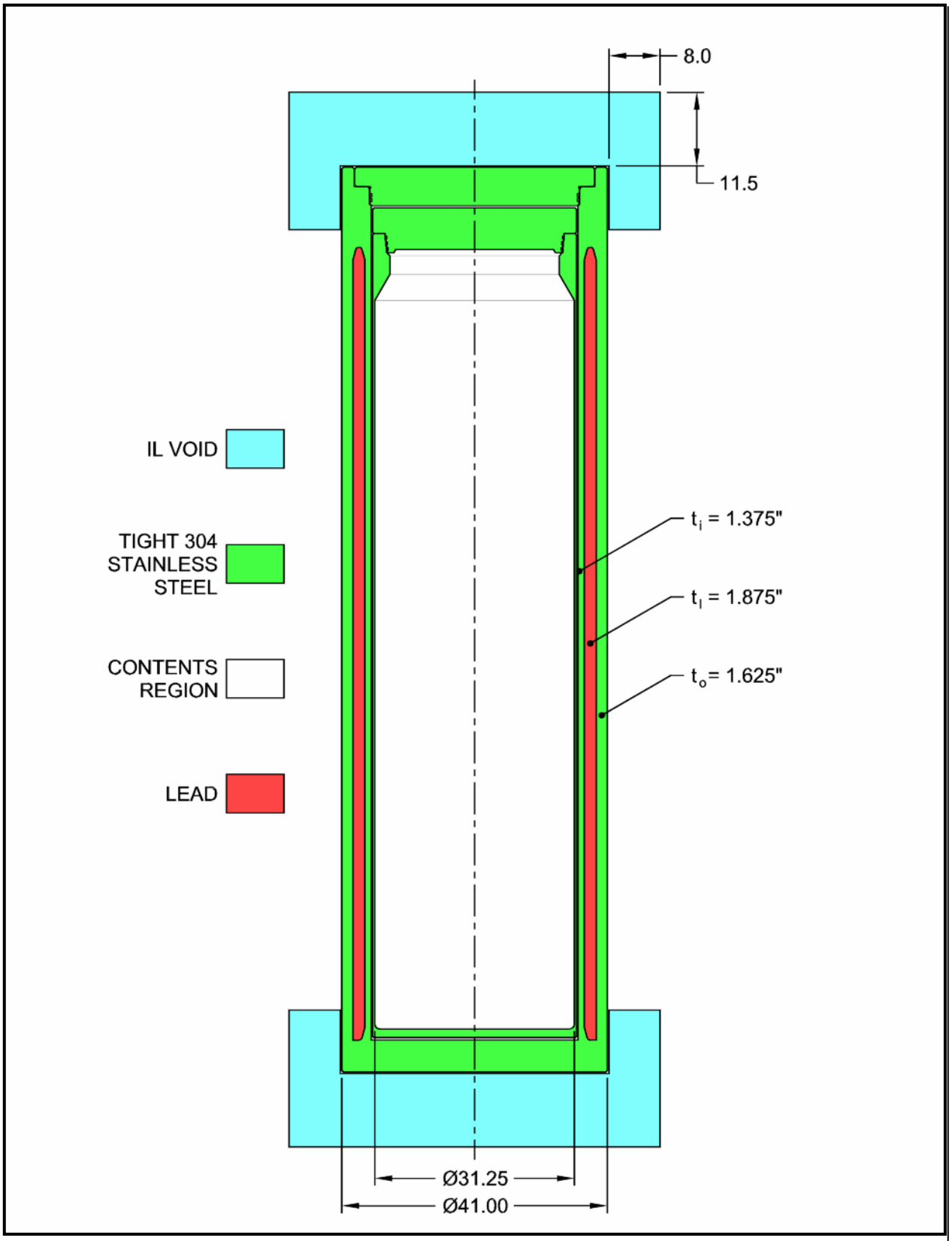

Figure 6.3-1 – Simplified Drawing of RH-TRU 72-B Package

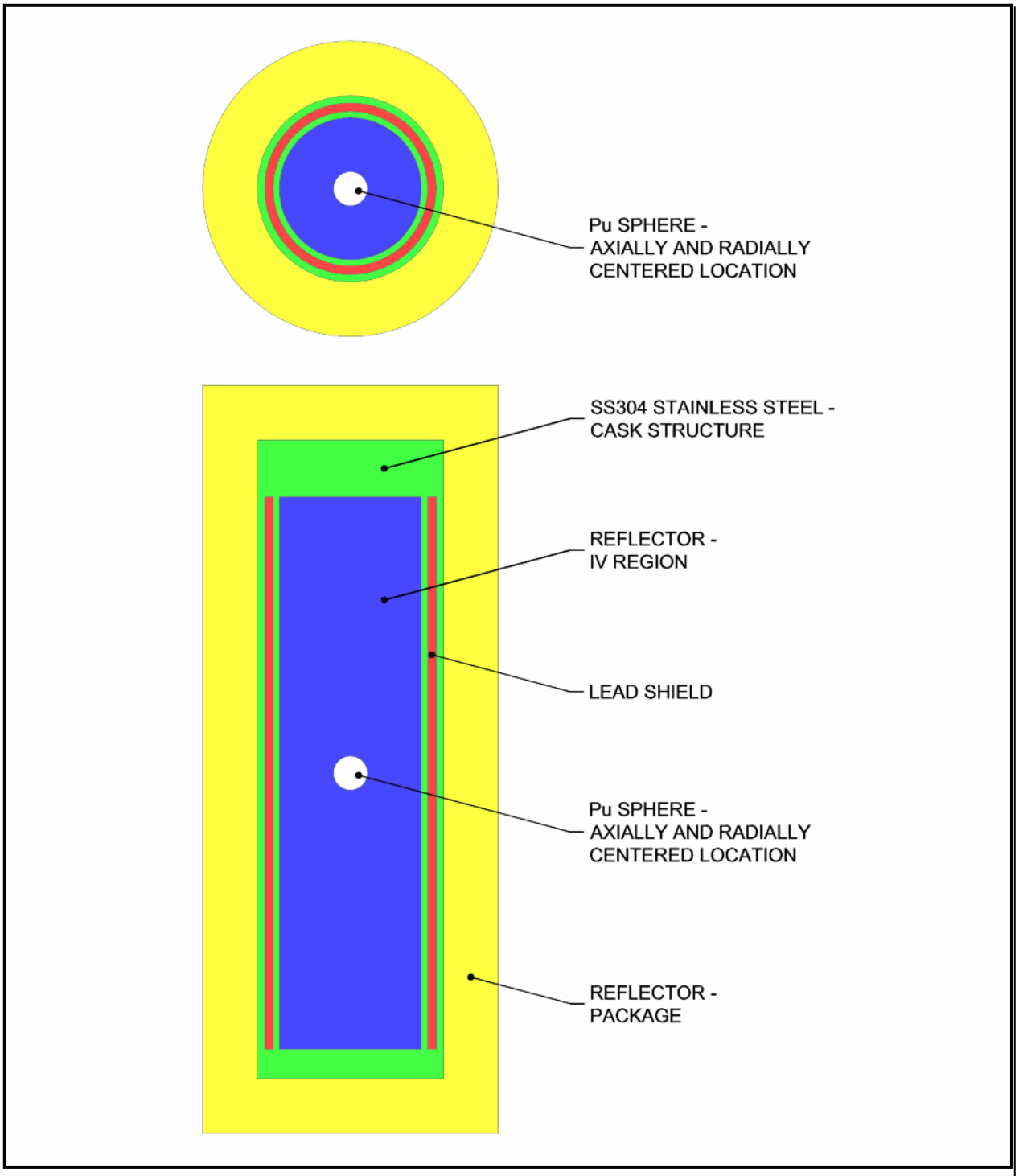

Figure 6.3-2 – KENO-V.a NCT and HAC Single Unit, Case A through C, Sphere Centered Model Representation (Top and Side Views)[8]

[8] Infinite unit depiction is the same with the exception of the outside cylindrical reflector. The infinite unit is modeled with a cuboid shaped outer region that extends a distance of one half the thickness of the impact limiters from all sides of the package and reflected on all sides with a mirror boundary to model an infinite array of packages (see Figure 6.3-5).

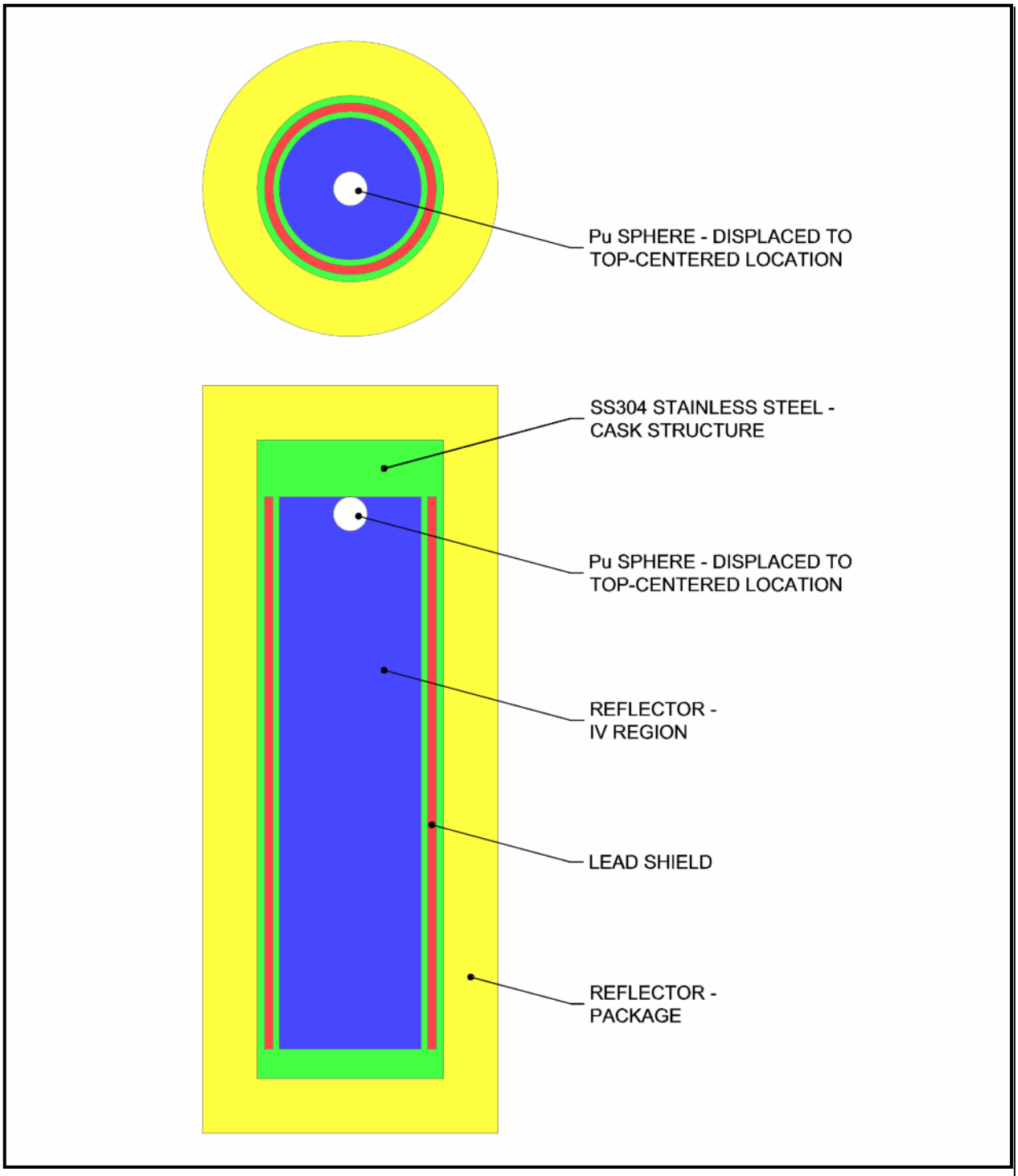

Figure 6.3-3 - KENO-V.a NCT and HAC Single Unit, Case A through C, Sphere Centered Top Model Representation (Top and Side Views)[8]

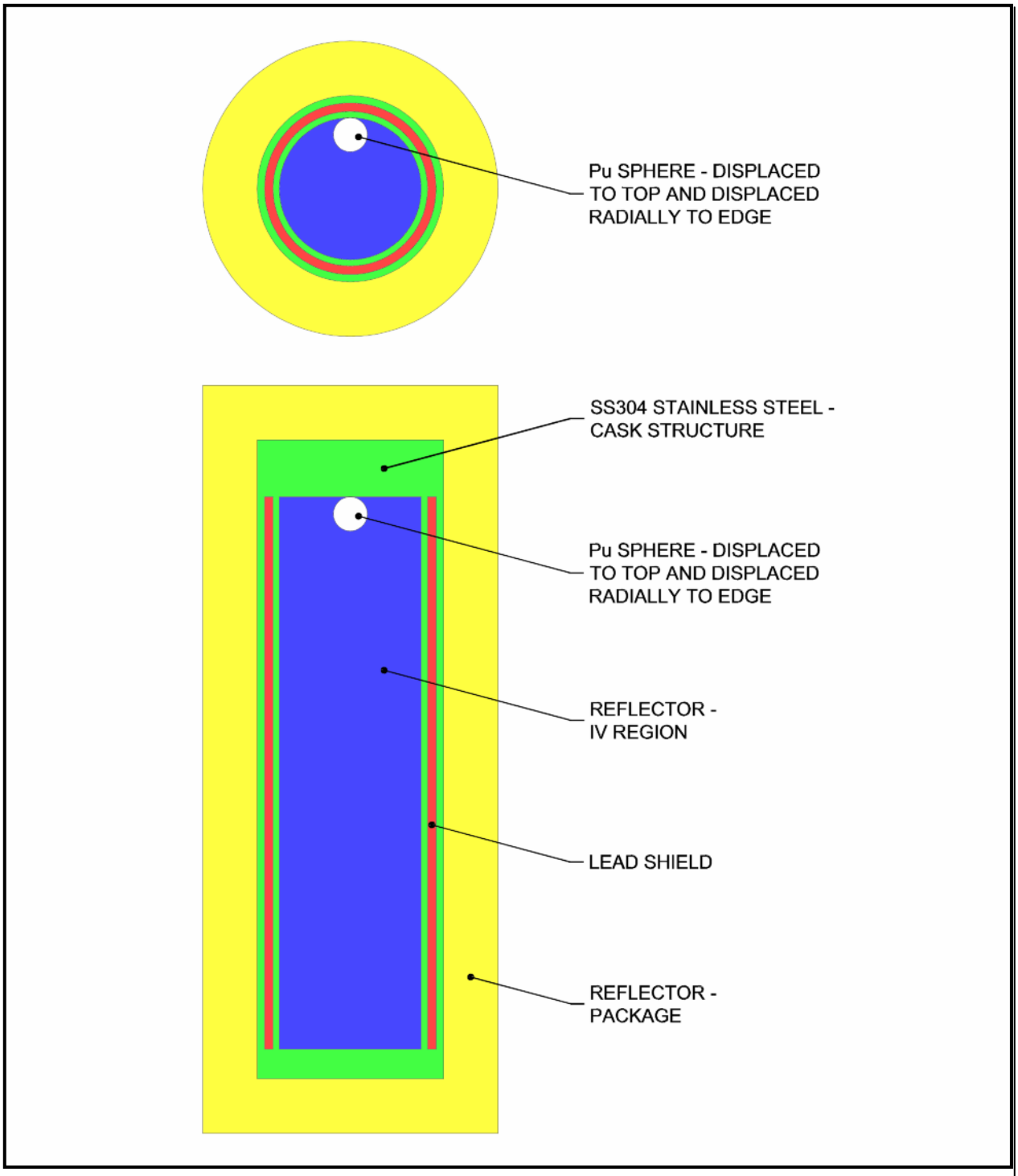

Figure 6.3-4 – KENO-V.a NCT and HAC Single Unit, Case A through C, Sphere Centered Top and Displaced Radially, Model Representation (Top and Side Views)[8]

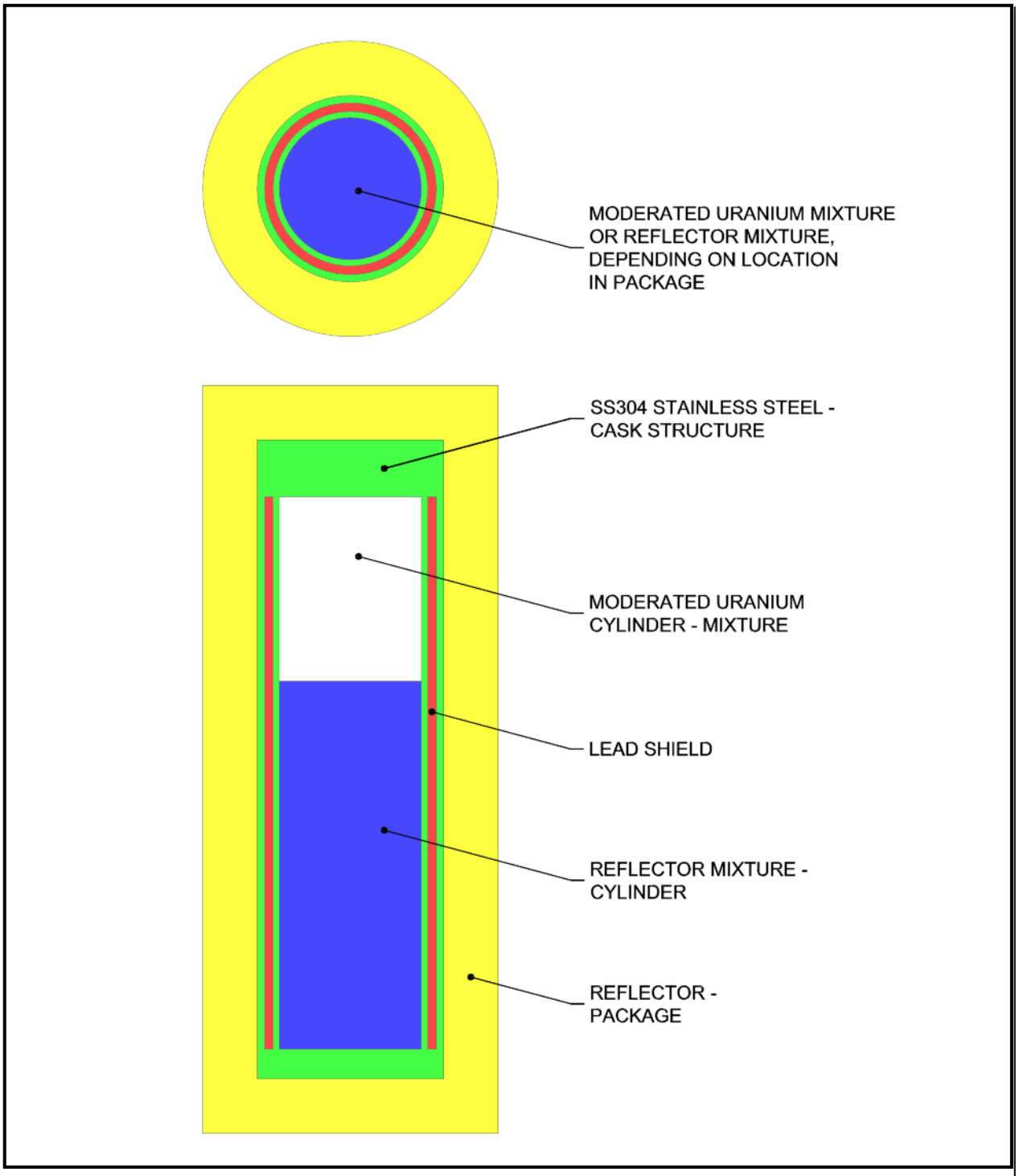

Figure 6.3-5 – KENO-V.a NCT and HAC Infinite Unit, Case D, Cylindrical Fissile Region Model Representation (Top and Side Views)[9]

[9] Both the NCT and HAC models of the single case unit were bounded by this infinite case model based on evaluation of the package during the Case A studies.

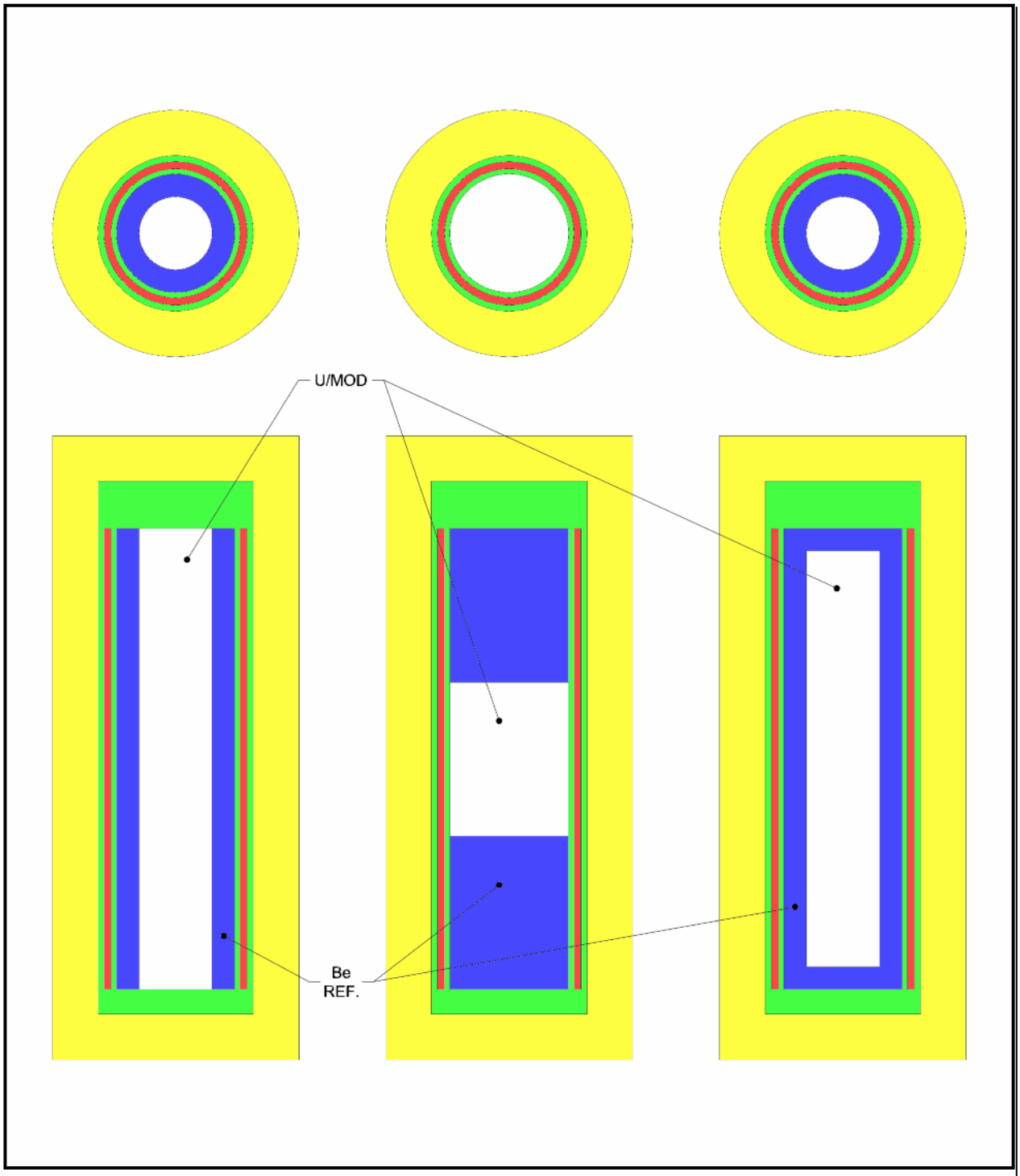

Figure 6.3-6 – KENO-V.a NCT and HAC Single-Unit, Case D, Cylindrical Fissile Region Models with Various Be Reflector Regions (Long, Skinny; Short, Squat; and Encapsulated Location Models both Top and Side Views)

6.4 Criticality Calculations

A description of the criticality calculations performed for the RH-TRU 72-B package is presented in this section. The calculational methodology is discussed in Section 6.4.1, *Calculational or Experimental Method*. The optimization of the payload model is discussed in Section 6.4.2, *Fuel Loading or Other Contents Loading Assumptions*. The results of all calculations are presented in Section 6.4.3, *Criticality Results*.

The intent of the analysis is to demonstrate that the RH-TRU 72-B package is safely subcritical under normal conditions of transport (NCT) and hypothetical accident conditions (HAC) provided the loading limits for each package payload are observed.

6.4.1 Calculational or Experimental Method

Calculations for the RH-TRU 72-B package are performed using the three-dimensional Monte Carlo transport theory code, KENO-V.a[1]. The SCALE-PC v4.4a[2], CSAS25 utility[3] is used as a driver for the KENO code. In this role, CSAS25 determines nuclide number densities, performs resonance processing, and automatically prepares the necessary input for the KENO code based on a simplified input description. The 238 energy-group (238GROUPNDF5), cross-section library based on ENDF/B-V cross-section data[4] is used as the nuclear data library for the KENO-V.a code.

The KENO code has been used extensively in the criticality safety industry for several years. KENO-V.a is an extension of earlier versions of the KENO code and includes many versatile geometry capabilities and screen plots to facilitate geometry verification. The KENO-V.a code and the associated 238GROUPNDF5 cross-section data set are validated for proper operation on the PC platform by performing criticality analyses of a number of relevant benchmark criticality experiments. A description of these benchmark calculations, along with justification for the computed bias in the code and library for the relevant region of applicability, is provided in Section 6.5, *Critical Benchmark Experiments*.

6.4.2 Fuel Loading or Other Contents Loading Assumptions

The allowable fuel loading for a single RH-TRU 72-B package is based on the FGE package fissile loading limit established by this analysis for each of the contents and package Cases A through C and based on the FEM enrichment loading limit established for Case D. The limits for each case are chosen to demonstrate that the RH-TRU 72-B package is safely subcritical under

---

[1] L. M. Petrie and N. F. Landers, *KENO-V.a: An Improved Monte Carlo Criticality Program with Supergrouping*, ORNL/NUREG/CSD-2/V2/R6, Volume 2, Section F11, March 2000.

[2] Oak Ridge National Laboratory (ORNL), *SCALE 4.4a: Modular Code System for Performing Standardized Computer Analyses for Licensing Evaluation for Workstations and Personal Computers*, ORNL/NUREG/CSD-2/R6, March 2000.

[3] N. F. Landers and L. M. Petrie, *CSAS: Control Module for Enhanced Criticality Safety Analysis Sequences*, ORNL/NUREG/CSD-2/V1/R6, Volume 1, Section C4, March 2000.

[4] W. C. Jordan and S. M. Bowman, *Scale Cross-Section Libraries*, ORNL/NUREG/CSD-2/V3/R6, Volume 3, Section M4, March 2000.

NCT and HAC. Calculations are based on the following conservative general assumptions, additional conservative assumptions already addressed in Section 6.3.1, *Contents Models*, and Section 6.3.2, *Package Model*, and upon the specific assumptions discussed during each evaluation in Section 6.4.3.1, *Criticality Results for Single RH-TRU 72-B Package*, and Section 6.4.3.2, *Criticality Results for Infinite Arrays of RH-TRU 72-B Packages*.

(1) ^{239}Pu is present at the FGE limit assigned to the payload type. Special FGE limits with 0 g, 5 g, 15 g, and 25 g ^{240}Pu are calculated for Case A only.

(2) All Pu is assumed to be optimally moderated and reflected with the optimal degree of moderation determined in each case for the applicable moderator (by adjusting the H/Pu ratio and/or by adjusting the Be percentage in the fissile sphere, as applicable). Studies indicate that the presence of voids in the optimal spherical contents model significantly reduces k_{eff} (demonstrated by evaluating a reduced density reflector in the IV region). The presence of less than or equal to 1% by weight beryllium in the moderator was also shown to have a small effect on k_{eff}, and larger quantities are evaluated as a special case (See Case B).

(3) The reflector material is tight fitting around the fissile geometry and assumed to fill the IV at up to 100% of theoretical density of the applicable reflector. In Case B, using a beryllium reflector, results show that the presence of voids in the reflector reduces k_{eff} (again, as demonstrated by evaluating a reduced density reflector in the IV region). Additionally, Case B evaluates special reflector material at greater than 1 wt% that is chemically bound to the fissile material.

(4) The fissile material is represented in a spherical geometry. Calculations performed for other geometries, such as cylinders and cubes, indicate a reduction in k_{eff} for single units for these other geometries and for infinite units with the large spacing provided by the packaging.

(5) All structural materials comprising the authorized payload contents, including the canister, dunnage, and packing material, are conservatively neglected. The waste matrix outside the sphere is represented by a polyethylene/water/beryllium mixture.

The same conservative assumptions that are used to analyze the single-unit RH-TRU 72-B package are used for the infinite array calculations. However, the presence of a variable density interspersed moderator between units in the infinite array cases is evaluated in addition to a full density water interspersed moderator to better evaluate the interaction between units.

6.4.3 Criticality Results

The results of the calculations for the RH-TRU 72-B package criticality evaluation are divided into two sections. Results for the single RH-TRU 72-B package are presented in Section 6.4.3.1, *Criticality Results for Single RH-TRU 72-B Package*, and results for infinite arrays of RH-TRU 72-B packages are presented in Section 6.4.3.2, *Criticality Results for Infinite Arrays of RH-TRU 72-B Packages*. Reported neutron multiplication factors represent the computed k_{eff} values plus twice the standard deviation, σ, for the result calculated, as follows:

$$k_s = k_{eff} + 2\sigma < USL$$

This quantity is then compared with the upper subcritical limit (USL) in order to demonstrate an adequate margin of subcriticality. Generally, the Monte Carlo calculations reported here are performed with sufficient histories to bring the computed relative standard deviation in the result to approximately 0.1% and until other indicators in the output file indicate the source term has converged. Typical KENO parameters required to obtain this level of uncertainty are 1000 generations of 1000 histories per generation, with the information from the initial 50 generations skipped when performing the statistic evaluation of the generations. More generations may have been run when convergence was not indicated using these basic parameters.

6.4.3.1 Criticality Results for Single RH-TRU 72-B Package

With the models described in Section 6.3.3, *Single Package Models*, subcriticality of the RH-TRU 72-B package under both NCT and HAC is demonstrated for each of the cases discussed in Section 6.4.3.1.1, *Case A, General Payload, Single Unit Results*, through Section 6.4.3.1.4, *Case D, LEU Payload, Single Unit Results*, below.

6.4.3.1.1 Case A, General Payload, Single Unit Results

The initial evaluation of the General Payload case was designed to evaluate the optimum combinations of moderator composition, reflector composition, and fissile sphere location for the NCT case. Since this approach optimizes the neutron multiplication factor of the package contents and since the HAC configuration, as modeled, is identical to the NCT configuration, results from this evaluation will be used on subsequent evaluations of single and infinite unit NCT and HAC analyses. Initial scoping calculations showed a limit of 315 FGE was necessary to demonstrate subcriticality with the most reactive configuration in Case A and was used throughout the Case A single unit and infinite array evaluations without ^{240}Pu.

First, the single unit model was evaluated with a sphere located in the center of the RH-TRU 72-B at various H/Pu ratios using a moderator with 25% polyethylene/75% water and a moderator with 25% polyethylene/74% water/1% beryllium by volume. The remainder of the IV was filled with a reflector consisting of 25% polyethylene/75% water or 25% polyethylene/74% water/1% beryllium by volume. Three of the four possible combinations of moderator/reflector conditions were evaluated for comparison with the sphere centered in the package. The results of these three baseline evaluations are shown in Table 6.4-1. This initial evaluation demonstrates that the addition of Be into the moderator (the Pu sphere) and the reflector (the IV region) results in a slightly higher k_s than the system moderated and reflected with the 25% polyethylene/75% water, although all of the results are statistically equivalent. The 25% polyethylene/74% water/1% Be mixture was used in the moderator and reflector as the standard to more accurately reflect the 1% allowable beryllium throughout the waste matrix under the General Payload limits.

To evaluate whether the thick SS304 walls would provide better reflection than the 25% polyethylene/74% water/1% beryllium by volume alone, the sphere was moved to the top center of the container near the 13 inch thick SS304 top closure and into the top, radially displaced corner locations of the cylinder. The results of the evaluation of these two alternate locations are shown in Table 6.4-1 for comparison. The most reactive location is in the top, radially displaced corner. This indicates that the thick steel and lead reflector provided by the top and sides of the vessel is more significant than the poly/water mixture.

To evaluate the effects of a reduced density reflector (for example, to represent voids in the waste matrix), the case with an H/Pu of 900 was evaluated with various volume fractions of the 25% polyethylene/74% water portion of the reflector while leaving the approved 1% beryllium by volume throughout the reflector region (this conservatively captures the presence of the beryllium, up to the allowable limit, for this case while reducing the other postulated reflecting effects of the waste matrix represented by the water/polyethylene mixture). The results of the evaluation are shown in Table 6.4-2. The results indicate that the full density reflector optimizes the single unit neutron multiplication factor. This evaluation demonstrates that any voids reduce the k_s of the package and are allowable.

Based on the above evaluation, the maximum k_s appears under the conditions that result from a Pu sphere optimally moderated with the mixture of 25% polyethylene/74% water /1% beryllium at an H/Pu of 800 – 900. The location of the sphere is at the top of the container near the thick steel closure lids and radially displaced to the outside edge. This combination of steel reflector back scattering neutrons in the direction of the fissile sphere provides a slight increase in k_s over the sphere centered in the package location. This configuration will be used in each of the following evaluations where scoping calculations confirm the maximum reactivity conditions are satisfied.

6.4.3.1.2 Case B, Special Reflector Payload, Single Unit Results

Based on the evaluations of Section 6.4.3.1.1, *Case A, General Payload, Single Unit Results*, and Section 6.4.3.2.1, *Case A, General Payload, Infinite Array Results*, the maximum reactivity of a single unit RH-TRU 72-B package under NCT and HAC conditions is statistically equivalent to that of an infinite array of HAC packages under maximum reflection conditions. Additionally, the due to the large size of the package and the small size of the most reactive fissile sphere, the fully reflected single package and the infinite array of packages with full interspersed moderation are physically identical with the exception of a small amount of water reflection at the contact points. Thus, the analysis given in Section 6.4.3.2.2, *Case B, Special Reflector Payload, Infinite Array Results* is used to evaluate the Case B single-unit analysis.

6.4.3.1.3 Case C, Machine-Compacted Payload, Single Unit Results

Based on the evaluations of Section 6.4.3.1.1, *Case A, General Payload, Single Unit Results*, and Section 6.4.3.2.1, *Case A, General Payload, Infinite Array Results*, the maximum reactivity of a single unit RH-TRU 72-B package under NCT and HAC conditions is statistically equivalent to that of an infinite array of HAC packages under maximum reflection conditions. Additionally, the due to the large size of the package and the small size of the most reactive fissile sphere, the fully reflected single package and the infinite array of packages with full interspersed moderation are physically identical with the exception of a small amount of water reflection at the contact points. Thus the analysis given in Section 6.4.3.2.3, *Case C, Machine-Compacted Payload, Infinite Array Results*, is used to evaluate the Case C single-unit analysis.

6.4.3.1.4 Case D, LEU Payload, Single Unit Results

Due to the change in the form of control from a mass controlled system to an enrichment controlled system and due to the low enrichment level desired for this limiting package, the size of the optimum fissile mass could conceivably fill the RH-TRU 72-B package volume. Unlike

the spherical geometries evaluated in the previous cases, the spheres of optimally moderated LEU would exceed the size of the package and a cylindrical geometry was selected to attain the maximum reactivity of a single unit RH-TRU 72-B package under NCT and HAC conditions. To place a realistic limit on the quantity of fissile material available, the package loading limit of 6,900 pounds was chosen as a bounding amount of waste material to model. 0.96 wt% ^{235}U moderated at optimum H/^{235}U using a 25% polyethylene, 74% water, and 1% beryllium mixture was modeled as filling the container nearest the thick steel reflector at the top and extending through the IV until 6,900 pounds of waste material was placed into the package. The remainder of the void was filled with the same 25% polyethylene, 74% water, and 1% beryllium mixture. The single unit model was then evaluated to identify the optimum H/^{235}U. The results of the evaluation are reported in Table 6.4-10. The optimum H/^{235}U appears near 500 as expected with large, well moderated, uranium systems.

To evaluate the effects of unlimited special reflectors in the container (other than LEU), the single unit case was modified to evaluate three variations of a single unit fissile material region with a Be reflector: a long, skinny cylinder with radially distributed Be; a short, squat cylinder with axially distributed Be (similar to the cases above but moved away from the steel end caps); and a cylinder encapsulated in a Be reflector. In these three single unit cases, the moderated region remained as a 0.96 wt% ^{235}U matrix moderated with a 25% polyethylene, 74% water, and 1% beryllium mixture to various H/^{235}U ratios and the reflector region in the IV was replaced with Be. The outside of the package continued to be modeled with a full density water reflector. Results of these three evaluations as reported in Table 6.4-12. All configurations are subcritical and the most reactive is the short squat cylinder with Be on either side.

Since no new or worse configuration conditions appear under HAC, this single-unit analysis bounds both NCT and HAC and all single case results are less than the USL of 0.9257 for the LEU systems with beryllium.

6.4.3.1.5 Conclusions for Single Unit Calculations

Based on optimum moderation of the fissile contents and maximum reflection conditions modeled by filling the IV with full density materials, as approved for each case, and surrounding the package by an additional 30.5 cm of water, all Case A single unit results are less than the USL. Based on Case A infinite array results, the infinite arrays of units for Case B and C will also bound the results of the single-unit cases. All subsequent cases were evaluated with the infinite array cases bounding the single-unit cases for the Case A, B, and C studies. All infinite arrays cases were found subcritical as discussed and summarized in Section 6.4.3.2, *Criticality Results for Infinite Arrays of RH-TRU 72-B Packages*. The single unit Case D evaluation also found that for a single-unit, optimally moderated low enriched uranium waste stream in the RH-TRU 72-B package remained subcritical under NCT and HAC with no restrictions on special reflectors. Thus, a single RH-TRU 72-B package will remain subcritical under both NCT and HAC conditions and under the prescribed limits for each case A through D above.

6.4.3.2 Criticality Results for Infinite Arrays of RH-TRU 72-B Packages

The infinite array model studies the interaction between the fissile contents in adjacent RH-TRU 72-B packages. The models described in Section 6.3, *Model Specifications*, provide the basis of the KENO-V.a calculations. The only difference in the NCT and HAC models is that the

thickness of the impact limiter changes. OC wall puncturing was ignored as a physical impact to the neutronics model of the package. Since the HAC model provided a closer spacing between units due to the reduced impact limiter dimensions, the HAC model was used to bound the NCT model. The infinite array calculation assumes the presence of interspersed moderation between the packages of the array. This moderation was modeled with various volume fraction of water in the array interstitial space to determine the most reactive conditions.

6.4.3.2.1 Case A, General Payload, Infinite Array Results

As in the single unit analysis for Case A, the contents are assumed to be in an optimal geometry with optimal moderation resulting from the plausible packaging materials including polyethylene wastes and the in leakage of water into the IV. The maximum polyethylene density for the manually compacted waste allowed in the General Payload is assumed to be 25% by volume with 74% water and 1% beryllium filling the remaining void in the IV. The fissile material is assumed to mix homogenously with the same mixture of 25% polyethylene/74% water/1% Be (by volume).

In the infinite-unit Case A evaluation, the RH-TRU 72-B package modeled in an infinite square-pitched array with spacing provided by the half-thickness impact limiters (as described in Section 6.3.2, *Package Model*), is used to represent the HAC infinite-unit configuration which bounds the NCT infinite-unit configuration. The package with its contents is evaluated with full interspersed moderation in the IV region and with full water density interspersed moderation in between units. Additionally, these same regions are modeled with voids. These two evaluations demonstrate the two extreme conditions of interspersed moderation between the spheres contained within the package. For this evaluation, the spheres were located in the most reactive configuration next to the top and radially displaced to the side of the container. This configuration conservatively models the thick steel reflector that does not change during NCT or HAC conditions. Results for these two analyses are shown in Table 6.4-3. These results indicate that the maximum reactivity of the package is achieved under full density reflection conditions. With the IV and exterior regions of the package modeled as a void, the interaction of the packages is presumably maximized, but probably due to the size of the units the infinite array reactivity is less than the fully reflected unit reactivity.

Table 6.4-4 shows the results of evaluating the most reactive moderated fissile spheres from Table 6.4-3 (H/Pu = 900 and 1200 cases) through the range of interspersed moderation in both the IV Region and between the RH-TRU 72-B packages. This range of interspersed moderation between fissile units should reveal significant trends in interaction with increased moderation. The results in Table 6.4-4 demonstrate a smooth rise in k_s as the density of interspersed moderation increases from low to full density values. This result suggests poor coupling between the fissile material in adjacent packagess and indicates that the interaction with adjacent units is minimal.

Based on the results of the evaluation of the unrestricted loading limit of 315 g ^{239}Pu, the alternate limits that include specific measured quantities of ^{240}Pu in addition to the ^{239}Pu are evaluated to demonstrate that the most reactive reflector conditions above (namely, a reflector of 25% polyethylene/74% water/1% Be (by volume) in the IV region and full density water in between packages) is also subcritical for over a range of interstitially moderated fissile spheres with the various combinations of ^{240}Pu and ^{239}Pu. These alternate limits allow more ^{239}Pu

contamination in the waste matrix where the ^{240}Pu is present in known quantities. The k_s for each of these evaluations are shown in Table 6.4-5. Maximum k_s for all three cases stays centered at an H/^{239}Pu of 900, and all are less than the USL of 0.9382.

Note that due to the large size of the package and the small size of the most reactive fissile sphere, each package in the infinite array is essentially a fully reflected single package. Consequently, although the fully reflected infinite array results are slightly lower, the results are statistically equivalent (within one standard deviation) to the fully reflected single-unit results and the infinite arrays can be used to evaluate the single-unit cases in Case B and Case C evaluations. All Case A results are less than the USL of 0.9382.

6.4.3.2.2 Case B, Special Reflector Payload, Infinite Array Results

In the infinite-unit Case B analysis evaluated, the RH-TRU 72-B package modeled in an infinite square-pitched array with spacing provided by the half-thickness impact limiters (as described in Section 6.3.2, *Package Model*) is used to represent the HAC infinite-unit configuration which bounds the NCT infinite unit-configuration just like the Case A study. Two special conditions are evaluated. The first evaluation examines the special reflector material and the Pu in an unbounded state. As such, the special reflector is allowed in unlimited amounts in the waste stream (that is, greater than 1 wt% Be) and with no restriction as to location and proximity to the fissile material. The package was evaluated with the higher percentages of Be in two regions.

First, the Be was added to the reflector region in the IV to determine the effects of high amounts of Be as a reflector around the optimally moderated Pu sphere. This demonstrated the effects of Be as a reflector. Scoping calculations resulted in lowering the mass limit for this Case to 100 FGE to account of the higher reactivity of the system using a special reflector such as Be. The Be reflector was found to be more effective than the steel in the top and sides of the package. Consequently, based on these scoping calculations, the Pu sphere was moved back to the center of the package where the Be reflector could have maximal impact. The package with its contents is evaluated first with variable density Be moderation/reflection in the IV region ranging from 1% to 100% Be (by volume). In all cases, the interspersed moderation outside of the packages was modeled with full density water to obtain optimum reactivity as indicated in evaluation of the Case A results. Results of these calculations are shown in Table 6.4-6. Following this initial evaluation the additional Be was added to the Pu mixture to evaluate the impact of the Be tightly bound to the Pu and having a Be reflector. This model used the full density Be moderator/reflector conditions in the IV and full water density interspersed moderation outside the package. Results of these calculations are also shown in Table 6.4-7. The trends indicate the full density Be in the moderator/reflector region of the IV provide maximum system reactivity and the system is subcritical at this FGE limit for both full density and voided loadings. The evaluation of bound Pu/Be in the Be reflected package indicates that adding Be to the sphere in a manner that displaces the hydrogenous moderator, lowers the system reactivity also resulting in a subcritical package for all concentrations of Be throughout the package as a special reflector.

The results for the second evaluation are shown in Table 6.4-8 using the higher mass content of 305 FGE as obtained during scoping calculations. This evaluation assumes a special condition that the fissile material and the special reflector material are chemically or mechanically bound. The Pu and Be (utilized as the most reactive special reflector) are mixed, also with poly and water in such a manner as to evaluate optimum moderation by varying the weight percent of the

Be in the moderator and leaving the contribution of the poly-to-water at a ratio of about 25% poly to 75% water. Since all of the fissile material is chemically or mechanically bound to the special reflector material in the moderator region and the special reflector material is not as effective as a poly/water moderator, the spheres were evaluated with a higher mass content of 305 FGE and still remained subcritical. The remaining reflection region inside the package was filled with the same 25% by volume with 74% water and 1% beryllium to represent the non-special reflector portion of the waste matrix and still account for some contamination with beryllium in this region. All results from both evaluations are less than the USL of 0.9382.

6.4.3.2.3 Case C, Machine-Compacted Payload, Infinite Array Results

In the infinite-unit Case C analysis evaluated, the RH-TRU 72-B package, modeled in an infinite square-pitched array with spacing provided by the half-thickness impact limiters (as described in Section 6.3.2, *Package Model*), is used to represent the HAC infinite-unit configuration which bounds the NCT infinite unit-configuration just like the Case A study. The spherical contents of 100% polyethylene moderated ^{239}Pu is evaluated with a reflector consisting of 99% polyethylene and 1% beryllium to represent the contents of machine compacted waste. Scoping calculations identified that the full density poly was indeed a better moderator that the poly/water combinations assumed in the Case A studies and that it was necessary to reduce the mass limit for this payload from 315 FGE to 245 FGE to maintain the evaluated cases below the USL. Scoping calculations also confirmed that the maximum reactivity of the package continued to be obtained using the Pu sphere displaced radially at the top of the package as it had shown in the Case A studies. Results for the sphere centered and top centered locations are not reported. Following this evaluation, the moderator was modified to add the 1% beryllium resulting in a 99% polyethylene/1% beryllium (by volume) mixture in both the moderator and reflector region. In all cases, the interspersed moderation outside of the packages was modeled with full density water to obtain optimum reactivity as indicated in evaluation of the Case A results. Results from both of these evaluations using a range of H/Pu values are shown in Table 6.4-9. Optimum conditions are centered on an H/Pu of 900 as in the other poly/water moderated cases and the 1% beryllium in the moderator resulted in a slight increase in reactivity as previously found in the Case A studies. Since the Case A studies identified that the full density reflector was more effective than a reduced density reflector and since the full density polyethylene reflector has similar characteristics, these cases were not reevaluated. Also, since the infinite arrays evaluated in Case A studies were optimum using full density water between packages and the full density polyethylene in the Case C contents model is a more effective reflector, Case C was only evaluated with full density water between packages. All results are less than the USL of 0.9382.

6.4.3.2.4 Case D, LEU Payload, Infinite Array Results

In the infinite-unit Case D analysis evaluated, the RH-TRU 72-B package modeled in an infinite square-pitched array with spacing provided by the half-thickness impact limiters (as described in Section 6.3.2, *Package Model*), is used to represent the HAC infinite-unit configuration which bounds the NCT infinite unit-configuration just like the previous case studies. Using the low enriched uranium limit, the optimally moderated volume is very large with respect to the container. Consequently, the contents are modeled as filling the cylinder at one end as described in Section 6.3.1.4, *Case D, LEU Payload, Contents Model*. The H/^{235}U was varied to identify the optimal moderation of the infinite package. Results for the model using full water density

between units are reported in Table 6.4-11. As with the single unit case evaluated in Section 6.4.3.1.4, *Case D, LEU Payload, Single Unit Results*, the optimum moderation condition occurs at an $H/^{235}U$ of 500. Since physical geometry of this model differs significantly from that evaluated in Section 6.4.3.2.1, *Case A, General Payload, Infinite Array Results*, the model was also evaluated with varying interspersed moderation between packages at the optimum interstitial moderation value of $H/^{235}U = 500$. These results are also reported in Table 6.4-11. Unlike the Pu cases evaluated above, the packages show significantly more interaction at the lower interspersed moderation values with a slight peaking at a volume fraction of 0.1% full density water between packages. As with the previous cases, the results of the evaluation bound both the NCT and HAC.

In evaluating the effects of special reflectors, the most reactive location model (the short, squat cylinder model determined most reactive in the Single Unit evaluations) was used to evaluate the infinite unit Be reflected case (see Figure 6.3-6 center model). The package was initially evaluated using the same fissile material mixture as above at varying $H/^{235}U$ ratios. The results are reported in Table 6.4-13. In this case the addition of Be special reflector material does increase k_s slightly over the poly/water/Be reflected case above. The most reactive case at an $H/^{235}U$ of 400 was run varying the interspersed moderation between units in the infinite array. These results are also reported in Table 6.4-13. As was seen from the poly/water/Be reflected cases above, there is a slight increase in k_s at an interspersed moderation value of 0.1 vol% water. Finally, the uranium moderator region of the infinite model is evaluated for the addition of Be in quantities greater than 1 wt% Be. Table 6.4-14 shows the results of the evaluation over a range of Be volume percent additions to the fissile region. The moderator mixture was maintained such that the water to polyethylene ratio remained at 75% to 25% and the $H/^{235}U$ remained at 500 (near optimum to show the trend). The trend shows that the addition of special reflector material to the moderator causes a smooth reduction in the k_s as moderator concentration increases. This evaluation was conducted in such a manner that the $H/^{235}U$ was maintained constant (without hydrogen moderation the overall k_s is much lower).

All results are less than the USL of 0.9257 and the results are consistent with the ANSI/ANS 8.1[5] standard that states the subcritical limit of 0.96 wt% ^{235}U for aqueous moderated and reflected low enriched uranium systems.

6.4.3.2.5 Conclusions for Infinite Array Calculations

The calculations reported in this section are performed with conservative representations of arrays of undamaged and damaged RH-TRU 72-B packages. The HAC model used bounds the NCT model by using a smaller spacing of one half the impact limiter radius and end thickness. In addition, the results indicated that the reactivity effects of array interaction are less than those of close, full reflection of the package contents. Hence, maximum reactivity results for arrays of RH-TRU 72-B packages under NCT are essentially the same as under HAC at optimum moderation and reflection conditions. Therefore, infinite arrays of RH-TRU 72-B packages are

[5] ANSI/ANS 8.1-1998, *Nuclear Criticality Safety in Operations with Fissionable Materials Outside Reactors*, American Nuclear Society (ANS), La Grange Park, Illinois.

safely subcritical under both NCT and HAC, and the requirements of 10 CFR §71.59[6] are satisfied. Furthermore, a CSI of zero (0.0) is justified.

6.4.3.3 Special Reflectors in RH-TRU Waste

As described previously, the only "special reflectors" credibly applicable to RH-TRU waste criticality analysis are: beryllium (Be), beryllium oxide (BeO), carbon (C), deuterium (D_2O), magnesium oxide (MgO), and depleted uranium (≥0.3 wt% ^{235}U and <0.72 wt% ^{235}U) when present in quantities greater than 1 wt%. Each special reflector with regard to its possible presence in RH-TRU waste is discussed below:

Beryllium and Beryllium Oxide – Be, and/or BeO, may be present in RH-TRU waste in quantities greater than 1 wt% by weight. The limits for payload containers are found in Table 6.1-1 under Case B. As described in Section 6.2.1, *Applicability of Case A Limits – General Payload*, beryllium is the limiting special reflector for RH-TRU waste. Limits for both bound and unbound Be have been evaluated for the Special Reflector Payload in Case B.

Carbon – Carbon is present as a constituent in the RH-TRU waste as discussed below:

(1) Carbon may be present as graphite molds, solids, or crucibles. In these forms the carbon will be chemically and irreversibly bound to the plutonium or other fissile material and cannot separate and may be handled using limits for Special Reflector Payloads with Pu bound to the special reflector;

(2) Carbon may be present in filter media as spent or activated carbon (for example, in activated charcoal filters). The plutonium or other fissile material would then be attached to the carbon media, would not be easily separated, and may be handled using limits for Special Reflector Payloads with Pu bound to the special reflector.

(3) Carbon may also be present in alloys, which are by definition chemically and/or mechanically bound, and may be handled using limits for Special Reflector Payloads with Pu bound to the special reflector.

Deuterium – The presence of liquid waste in the payload containers, except for residual amounts, is prohibited. As specified by the *Remote-Handling Transuranic Waste Authorization Methods for Payload Control* (RH-TRAMPAC)[7], the total volume of residual liquid in a payload container shall be less than 1 percent (volume) of the payload container. This limitation on the authorized contents is such that the D_2O will not be present in greater than 1 wt%, and the waste may be handled using limits for the General Payload with less than or equal to 1 wt% special reflector.

Magnesium Oxide – Magnesium oxide crucibles used in high temperature-controlled applications, such as reduction processes, may be present in solid inorganic waste forms such as glass, metal, and pyrochemical salts. If present, MgO will be bound to the fissile material and would not be easily separated. MgO used for neutralization in solidified material cannot be separated out as it is chemically reacted in the waste generation process. There is no identified mechanism that could cause the magnesium oxide in RH-TRU waste to be reconfigured as a

[6] Title 10, Code of Federal Regulations, Part 71 (10 CFR 71), *Packaging and Transportation of Radioactive Material*, Final Rule, 01-26-04.

[7] U.S. Department of Energy (DOE), *Remote-Handled Transuranic Waste Authorized Methods for Payload Control* (RH-TRAMPAC), U.S. Department of Energy, Carlsbad Field Office, Carlsbad, New Mexico.

reflector. This waste may be handled using limits for Special Reflector Payloads with Pu bound to the special reflector

Depleted Uranium (≥0.3 wt% ^{235}U and < 0.72 wt% ^{235}U) – Depleted uranium may be present in RH-TRU waste, but it will be chemically and/or mechanically bound to the plutonium or physically inseparable because the densities of U and Pu are similar. Separation by mechanical means or by leaching is extremely difficult and is considered highly unlikely in the RH-TRU waste after packaging. Depleted uranium in the RH-TRU waste will, therefore, not be separated from the fissile material and/or reconfigured as a reflector. As such, Case D limits for an LEU Payload should be used.

6.4.3.4 Applicable Criticality Limits for RH-TRU Waste

Case A covers manually compacted (not machine compacted) waste contaminated with up to 1 wt% special reflectors and extends the payload limit from 315 g ^{239}Pu FGE with no ^{240}Pu or unknown ^{240}Pu to 325, 350, and 370 g ^{239}Pu FGE with 5 g ^{240}Pu, 15 g ^{240}Pu, and 25 g ^{240}Pu, respectively. Case B covers manually compacted (not machine compacted) waste containing greater than 1 wt% special reflectors and extends the payload limit from 100 g ^{239}Pu FGE to 305 g ^{239}Pu FGE when the fissile material is known to be chemically or mechanically bound to the special reflector/moderator. Case C covers machine compacted waste contaminated with up to 1 wt% special reflectors and limits the fissile isotope to 245 g ^{239}Pu FGE. Case D covers manually compacted (not machine compacted) waste containing special reflectors and low enriched uranium contaminated with other homogeneously distributed fissile isotopes. The Case D evaluation limits the enrichment of the fissile isotopes to 0.96 wt% ^{235}U FEM, with no restriction on special reflector materials.

In conclusion, the specific payload limits are summarized in Table 6.4-15 for comparison.

Table 6.4-1 – Single-Unit, NCT and HAC, Case A, Sphere Centered, 315 FGE, k_s vs. H/Pu Ratio with Different Moderator/Reflector Combinations[8]

Case	H/Pu	Moderator/Reflector Conditions	k_{eff}	σ	k_s	AEG
Sphere Centered in Package						
NPWPW	700	Moderator and Reflector = 25% Poly/75% Water	0.9166	0.0009	0.9184	216.5
	800		0.9206	0.0009	0.9224	217.1
	900		0.9230	0.0009	**0.9248**	217.5
	1,000		0.9221	0.0009	0.9239	217.8
	1,100		0.9174	0.0009	0.9192	218.1
NPWPWB	700	Moderator = 25% Poly/75% Water, and Reflector = 25% Poly/74% Water/1% Beryllium	0.9173	0.0011	0.9195	216.6
	800		0.9230	0.0009	0.9248	217.1
	900		0.9244	0.0009	**0.9262**	217.5
	1,000		0.9228	0.0010	0.9248	217.8
	1,100		0.9203	0.0010	0.9223	218.1
NPWBPWB	700	Moderator and Reflector = 25% Poly/74% Water/1% Beryllium	0.9187	0.0010	0.9207	216.6
	800		0.9238	0.0010	0.9258	217.1
	900		0.9246	0.0009	**0.9264**	217.5
	1,000		0.9243	0.0009	0.9261	217.8
	1,100		0.9212	0.0010	0.9232	218.1
Sphere Centered at Top of Package						
NPWBPWBTOP	700	Moderator and Reflector = 25% Poly/74% Water/1% Beryllium	0.9246	0.0009	0.9264	216.5
	800		0.9293	0.0009	**0.9311**	217.0
	900		0.9285	0.0009	0.9303	217.4
	1,000		0.9280	0.0009	0.9298	217.8
	1,100		0.9252	0.0009	0.9270	218.1
Sphere at Top and Radially Displaced to Side of Package						
NPWBPWBTOP SIDE	700	Moderator and Reflector = 25% Poly/74% Water/1% Beryllium	0.9298	0.0010	0.9318	216.4
	800		0.9352	0.0009	**0.9370**	217.0
	900		0.9340	0.0009	0.9358	217.4
	1,000		0.9327	0.0009	0.9345	217.7
	1,100		0.9311	0.0010	0.9331	218.0

[8] All of the largest k_ss are highlighted within 1σ of each other.

Table 6.4-2 – Single-Unit, NCT and HAC, Case A, Sphere Top and Radially Displaced, 315 FGE, H/Pu at 900, k_s vs. Variable Interspersed Moderation Volume Fraction in the IV

Case	H/Pu	Moderator/Reflector Conditions	VF	k_{eff}	σ	k_s	AEG
NPWBPWBTOP SIDEIM	900	Moderator (Sphere) = 25% Poly/74% Water/1% Beryllium Reflector (IV Region) = 25% Poly/74% Water at Volume Fraction (VF) Given Maintaining the 1% Beryllium in the Mixture Constant	0.01	0.8256	0.0010	0.8276	216.4
			0.05	0.8351	0.0010	0.8371	216.5
			0.1	0.8481	0.0009	0.8499	216.6
			0.2	0.8673	0.0010	0.8693	216.8
			0.3	0.8855	0.0011	0.8877	217.0
			0.4	0.8975	0.0010	0.8995	217.1
			0.5	0.9058	0.0009	0.9076	217.2
			0.6	0.9154	0.0009	0.9172	217.2
			0.7	0.9204	0.0009	0.9222	217.3
			0.8	0.9242	0.0010	0.9262	217.3
			0.9	0.9307	0.0008	0.9323	217.3
			1	0.9340	0.0009	**0.9358**	217.4

Table 6.4-3 – Infinite-Unit, NCT and HAC, Case A, Sphere Top and Radially Displaced, 315 FGE, k_s vs. H/Pu Ratio with Different Moderator/Interspersed Moderator Combinations

Case	H/Pu	Moderator/Reflector Conditions	k_{eff}	σ	k_s	AEG
IFULL[9]	700	Moderator and Reflector = 25% Poly/74% Water/ 1% Beryllium Interspersed Moderator Between Units = Full Density Water	0.9299	0.0010	0.9319	216.4
	800		0.9333	0.0010	0.9353	217.0
	900		0.9341	0.0010	**0.9361**	217.4
	1,000		0.9330	0.0008	0.9346	217.7
	1,100		0.9282	0.0009	0.9300	218.0
IVOID	700	Moderator (Sphere) = 25% Poly/74% Water/1% Beryllium Reflector (IV Region) and Interspersed Moderator Between Units = Void	0.8150	0.0010	0.8170	215.1
	800		0.8288	0.0010	0.8308	215.8
	900		0.8400	0.0011	0.8422	216.4
	1,000		0.8441	0.0009	0.8459	216.8
	1,100		0.8484	0.0009	0.8502	217.2
	1,200		0.8488	0.0009	**0.8506**	217.5
	1,300		0.8473	0.0009	0.8491	217.8

[9] Set run with random number seed different than the default to correct an unusual trend in this data set (one value significantly higher than expected). The value from this original run (physically the same input file) using the default random number seed is shown in H/Pu=900 entry of Table 6.4-4.

Table 6.4-4 – Infinite-Unit, NCT and HAC, Case A, Sphere Top and Radially Displaced, 315 FGE, k_s vs. Variable Interspersed Moderator at H/Pu Ratios of Interest

Case	H/Pu	Moderator/Reflector Conditions	VF	k_{eff}	σ	k_s	AEG
I900IM[10]	900	Moderator (Sphere) = 25% Poly/ 74% Water/ 1% Beryllium Interspersed Moderator (IV Region) = 25% Poly/ 74% Water/ 1% Beryllium at Given VF Interspersed Moderator (Between Units) = Water at Given VF	0.01	0.8273	0.0009	0.8291	216.4
			0.05	0.8315	0.0010	0.8335	216.5
			0.1	0.8426	0.0010	0.8446	216.6
			0.2	0.8675	0.0009	0.8693	216.8
			0.3	0.8834	0.0010	0.8854	217.0
			0.4	0.8944	0.0010	0.8964	217.1
			0.5	0.9055	0.0010	0.9075	217.2
			0.6	0.9157	0.0009	0.9175	217.2
			0.7	0.9223	0.0009	0.9241	217.3
			0.8	0.9261	0.0009	0.9279	217.3
			0.9	0.9299	0.0009	0.9317	217.3
			1	0.9339	0.0009	**0.9357**	217.4
I1200IM	1,200	Moderator (Sphere) = 25% Poly/ 74% Water/ 1% Beryllium Interspersed Moderator (IV Region) = 25% Poly/ 74% Water/ 1% Beryllium at Given VF Interspersed Moderator (Between Units) = Water at Given VF	0.01	0.8385	0.0009	0.8403	217.5
			0.05	0.8405	0.0009	0.8423	217.6
			0.1	0.8504	0.0009	0.8522	217.7
			0.2	0.8686	0.0010	0.8706	217.9
			0.3	0.8823	0.0009	0.8841	218.0
			0.4	0.8944	0.0009	0.8962	218.0
			0.5	0.9011	0.0009	0.9029	218.1
			0.6	0.9080	0.0009	0.9098	218.1
			0.7	0.9131	0.0009	0.9149	218.2
			0.8	0.9161	0.0009	0.9179	218.2
			0.9	0.9207	0.0009	0.9225	218.2
			1	0.9224	0.0009	**0.9242**	218.2

[10] The case with VF = 1 does not agree with the value in Table 6.4-3. See Footnote 9 explaining the random number seed difference in the runs. This data run is designed to show the k_s trend vs. reduced interspersed moderation values only.

Table 6.4-5 – Infinite-Unit, NCT and HAC, Case A, Sphere Top and Radially Displaced, k_s vs. H/Pu Ratio for Limiting Pu-240/Pu-239 Combinations with Optimum Moderator/Reflector

Case	^{240}Pu (g)	^{239}Pu (g)	H/^{239}Pu	Moderator/Reflector Conditions	k_{eff}	σ	k_s	AEG
I05Pu240	5	325	700	Moderator and Reflector = 25% Poly/ 74% Water/ 1% Beryllium Interspersed Moderator Between Units = Full Density Water	0.9253	0.0009	0.9271	216.4
			800		0.9314	0.0009	0.9332	216.9
			900		0.9327	0.0009	**0.9345**	217.3
			1,000		0.9321	0.0009	0.9339	217.7
			1,100		0.9276	0.0008	0.9292	218.0
I15Pu240	15	350	700		0.9277	0.0011	0.9299	216.3
			800		0.9320	0.0009	0.9338	216.8
			900		0.9345	0.0009	**0.9363**	217.3
			1,000		0.9329	0.0010	0.9349	217.6
			1,100		0.9295	0.0008	0.9311	217.9
I25Pu240	25	370	700		0.9272	0.0010	0.9292	216.2
			800		0.9346	0.0010	0.9366	216.8
			900		0.9352	0.0009	**0.9370**	217.2
			1,000		0.9346	0.0009	0.9364	217.6
			1,100		0.9337	0.0010	0.9357	217.9

Table 6.4-6 – Infinite-Unit, NCT and HAC, Case B, Sphere Centered, 100 FGE, k_s vs. H/Pu Ratio with Different Reflector Conditions

Case	Volume % Beryllium in Reflector	H/Pu	k_{eff}	σ	k_s	AEG
IBEREF100	1	600	0.8975	0.0009	0.8993	215.8
		700	0.9035	0.0009	0.9053	216.5
		800	0.9063	0.0009	**0.9081**	217.0
		900	0.9047	0.0009	0.9065	217.4
		1,000	0.9025	0.0008	0.9041	217.7
		1,100	0.8974	0.0007	0.8988	218.0
IBEREFIM100	0.01	900	0.4468	0.0008	0.4484	215.5
	0.05	900	0.4633	0.0009	0.4651	215.5
	0.1	900	0.4907	0.0008	0.4923	215.6
	0.2	900	0.5491	0.0008	0.5507	215.9
	0.3	900	0.6041	0.0009	0.6059	216.2
	0.4	900	0.6618	0.0008	0.6634	216.5
	0.5	900	0.7115	0.0009	0.7133	216.7
	0.6	900	0.7616	0.0010	0.7636	216.9
	0.7	900	0.8048	0.0008	0.8064	217.0
	0.8	900	0.8408	0.0009	0.8426	217.2
	0.9	900	0.8757	0.0008	0.8773	217.3
	1	900	0.9047	0.0009	**0.9065**	217.4

Table 6.4-7 – Infinite-Unit, NCT and HAC, Case B, Sphere Centered, 100 FGE, k_s vs. H/Pu Ratio with Different Moderator Conditions in 100% Be Reflector

Case	Moderator Mixture	H/Pu	k_{eff}	σ	k_s	AEG
I01TO18BEMOD100	25% Poly/ 74% Water/ 1% Beryllium	600	0.8975	0.0009	0.8993	215.8
		700	0.9035	0.0009	0.9053	216.5
		800	0.9063	0.0009	**0.9081**	217.0
		900	0.9047	0.0009	0.9065	217.4
		1,000	0.9025	0.0008	0.9041	217.7
		1,100	0.8974	0.0007	0.8988	218.0
	24.5% Poly/ 73.5% Water/ 2% Beryllium	600	0.8963	0.0009	0.8981	215.8
		700	0.9026	0.0009	0.9044	216.5
		800	0.9066	0.0009	**0.9084**	217.0
		900	0.9038	0.0009	0.9056	217.4
		1,000	0.9024	0.0009	0.9042	217.7
		1,100	0.8954	0.0009	0.8972	218.0
	24% Poly/ 72% Water/ 4% Beryllium	600	0.8971	0.0010	0.8991	215.8
		700	0.9046	0.0009	0.9064	216.5
		800	0.9058	0.0009	**0.9076**	217.0
		900	0.9044	0.0008	0.9060	217.4
		1,000	0.9007	0.0008	0.9023	217.7
		1,100	0.8981	0.0008	0.8997	218.0
I19TO36BEMOD100	23.5% Poly/ 70.5% Water/ 6% Beryllium	600	0.8977	0.0009	0.8995	215.9
		700	0.9044	0.0008	0.9060	216.5
		800	0.9066	0.0010	**0.9086**	217.0
		900	0.9043	0.0008	0.9059	217.4
		1,000	0.9009	0.0008	0.9025	217.7
		1,100	0.8962	0.0008	0.8978	218.0
	23% Poly/ 69% Water/ 8% Beryllium	600	0.8941	0.0009	0.8959	215.9
		700	0.9046	0.0009	**0.9064**	216.5
		800	0.9043	0.0009	0.9061	217.0
		900	0.9024	0.0009	0.9042	217.4
		1,000	0.9001	0.0009	0.9019	217.8
		1,100	0.8950	0.0008	0.8966	218.0

Case	Moderator Mixture	H/Pu	k_{eff}	σ	k_s	AEG
I19TO36BEMOD100	22.5% Poly/ 67.5% Water/ 10% Beryllium	600	0.8957	0.0009	0.8975	215.9
		700	0.9023	0.0010	0.9043	216.5
		800	0.9060	0.0010	**0.9080**	217.0
		900	0.9025	0.0009	0.9043	217.4
		1,000	0.9002	0.0008	0.9018	217.8
		1,100	0.8955	0.0008	0.8971	218.0
I37TO54BEMOD100	20% Poly/ 60% Water/ 20% Beryllium	600	0.8943	0.0010	0.8963	216.0
		700	0.8997	0.0009	0.9015	216.6
		800	0.9023	0.0010	**0.9043**	217.1
		900	0.9002	0.0009	0.9020	217.5
		1,000	0.8963	0.0008	0.8979	217.8
		1,100	0.8900	0.0008	0.8916	218.1
	15% Poly/ 45% Water/ 40% Beryllium	600	0.8870	0.0009	0.8888	216.3
		700	0.8900	0.0009	0.8918	216.8
		800	0.8915	0.0009	**0.8933**	217.3
		900	0.8899	0.0009	0.8917	217.7
		1,000	0.8860	0.0009	0.8878	218.0
		1,100	0.8793	0.0008	0.8809	218.2
	10% Poly/ 30% Water/ 60% Beryllium	600	0.8706	0.0009	0.8724	216.7
		700	0.8738	0.0009	**0.8756**	217.2
		800	0.8723	0.0008	0.8739	217.6
		900	0.8709	0.0009	0.8727	218.0
		1,000	0.8647	0.0008	0.8663	218.2
		1,100	0.8565	0.0009	0.8583	218.5
I55TO60BEMOD100	5% Poly/ 15% Water/ 80% Beryllium	600	0.8408	0.0010	**0.8428**	217.5
		700	0.8371	0.0009	0.8389	217.9
		800	0.8319	0.0008	0.8335	218.2
		900	0.8227	0.0008	0.8243	218.5
		1,000	0.8152	0.0008	0.8168	218.8
		1,100	0.8043	0.0007	0.8057	218.9

Table 6.4-8 – Infinite-Unit, NCT and HAC, Case B, Sphere Centered, 305 FGE, k_s vs. H/Pu Ratio with the Indicated Moderator Conditions

Case	Moderator Mixture	H/Pu	k_{eff}	σ	k_s	AEG
I01TO12BE	25% Poly/ 74% Water/ 1% Beryllium	600	0.9108	0.0010	0.9128	215.8
		700	0.9229	0.0010	0.9249	216.4
		800	0.9268	0.0009	**0.9286**	216.9
		900	0.9268	0.0009	**0.9286**	217.4
		1,000	0.9266	0.0010	**0.9286**	217.7
		1,100	0.9211	0.0008	0.9227	218.0
	24.5% Poly/ 73.5% Water/ 2% Beryllium	600	0.9137	0.0010	0.9157	215.8
		700	0.9227	0.0011	0.9249	216.4
		800	0.9268	0.0010	**0.9288**	217.0
		900	0.9270	0.0009	**0.9288**	217.4
		1,000	0.9257	0.0010	0.9277	217.7
		1,100	0.9223	0.0010	0.9243	218.0
I13TO24BE	24% Poly/ 72% Water/ 4% Beryllium	600	0.9141	0.0009	0.9159	215.8
		700	0.9221	0.0009	0.9239	216.4
		800	0.9265	0.0009	0.9283	217.0
		900	0.9275	0.0010	**0.9295**	217.4
		1,000	0.9272	0.0009	0.9290	217.7
		1,100	0.9228	0.0009	0.9246	218.0
	23.5% Poly/ 70.5% Water/ 6% Beryllium	600	0.9135	0.0010	0.9155	215.8
		700	0.9227	0.0010	0.9247	216.5
		800	0.9279	0.0010	0.9299	217.0
		900	0.9281	0.0010	**0.9301**	217.4
		1,000	0.9270	0.0010	0.9290	217.7
		1,100	0.9241	0.0009	0.9259	218.0
I25TO36BE	23% Poly/ 69% Water/ 8% Beryllium	600	0.9137	0.0010	0.9157	215.8
		700	0.9233	0.0009	0.9251	216.5
		800	0.9271	0.0009	0.9289	217.0
		900	0.9294	0.0009	**0.9312**	217.4
		1,000	0.9268	0.0009	0.9286	217.7
		1,100	0.9247	0.0008	0.9263	218.0
	22.5% Poly/ 67.5% Water/ 10% Beryllium	600	0.9145	0.0010	0.9165	215.8
		700	0.9241	0.0010	0.9261	216.5
		800	0.9267	0.0010	0.9287	217.0
		900	0.9290	0.0009	0.9308	217.4
		1,000	0.9294	0.0009	**0.9312**	217.8
		1,100	0.9242	0.0009	0.9260	218.0

Case	Moderator Mixture	H/Pu	k_{eff}	σ	k_s	AEG
I37TO48BE	20% Poly/ 60% Water/ 20% Beryllium	600	0.9172	0.0009	0.9190	215.9
		700	0.9272	0.0011	0.9294	216.6
		800	0.9287	0.0010	0.9307	217.1
		900	0.9316	0.0010	**0.9336**	217.5
		1,000	0.9298	0.0010	0.9318	217.8
		1,100	0.9276	0.0010	0.9296	218.1
	15% Poly/ 45% Water/ 40% Beryllium	600	0.9143	0.0009	0.9161	216.2
		700	0.9241	0.0009	0.9259	216.8
		800	0.9289	0.0011	0.9311	217.3
		900	0.9320	0.0010	**0.9340**	217.7
		1,000	0.9291	0.0009	0.9309	218.0
		1,100	0.9256	0.0009	0.9274	218.2
I49TO60BE	10% Poly/ 30% Water/ 60% Beryllium	600	0.9096	0.0010	0.9116	216.6
		700	0.9192	0.0009	0.9210	217.1
		800	0.9239	0.0010	**0.9259**	217.6
		900	0.9234	0.0009	0.9252	217.9
		1,000	0.9193	0.0010	0.9213	218.2
		1,100	0.9170	0.0009	0.9188	218.5
	5% Poly/ 15% Water/ 80% Beryllium	600	0.8954	0.0010	0.8974	217.3
		700	0.9000	0.0010	0.9020	217.8
		800	0.9032	0.0009	**0.9050**	218.2
		900	0.8988	0.0010	0.9008	218.5
		1,000	0.8937	0.0010	0.8957	218.7
		1,100	0.8859	0.0008	0.8875	219.0
I61TO66BE	1.25% Poly/ 3.75% Water/ 95% Beryllium	600	0.8492	0.0009	**0.8510**	219.2
		700	0.8348	0.0008	0.8364	219.5
		800	0.8174	0.0008	0.8190	219.8
		900	0.7990	0.0009	0.8008	219.9
		1,000	0.7786	0.0008	0.7802	220.1
		1,100	0.7597	0.0007	0.7611	220.2

Table 6.4-9 – Infinite Unit, NCT and HAC, Case C, Sphere Top Side, 245 FGE, k_s vs. H/Pu Ratio with Different Moderator/Reflector Combinations

Case	H/Pu	Moderator/Reflector Conditions	k_{eff}	σ	k_s	AEG
ITOPSIDE245	700	Moderator = 100% Poly Reflector = 99% Poly/ 1% Beryllium	0.9307	0.0009	0.9325	216.5
	800		0.9332	0.0010	0.9352	217.0
	900		0.9343	0.0009	**0.9361**	217.4
	1,000		0.9328	0.0009	0.9346	217.7
	1,100		0.9296	0.0009	0.9314	218.0
ITOPSIDEBEMOD245	700	Moderator and Reflector = 99% Poly/ 1% beryllium	0.9287	0.0011	0.9309	216.5
	800		0.9338	0.0010	0.9358	217.0
	900		0.9350	0.0011	**0.9372**	217.4
	1,000		0.9332	0.0009	0.9350	217.7
	1,100		0.9301	0.0009	0.9319	218.0

Table 6.4-10 – Single-Unit, NCT and HAC, Case D, Cylindrical Fissile Region, 0.96 wt% U-235 FEM, k_s vs. H/U-235 Ratio

Case	H/^{235}U	k_{eff}	σ	k_s	AEG
DSIN	300	0.8981	0.0006	0.8993	190.6
	400	0.9111	0.0007	0.9125	197.0
	500	0.9136	0.0007	**0.9150**	201.1
	600	0.9087	0.0006	0.9099	203.9
	700	0.8990	0.0006	0.9002	206.0
	800	0.8852	0.0006	0.8864	207.6
	900	0.8727	0.0006	0.8739	208.8
	1000	0.8580	0.0005	0.8590	209.9

Table 6.4-11 – Infinite-Unit, NCT and HAC, Case D, Cylindrical Fissile Region, 0.96 wt% U-235, k_s vs. H/U-235 Ratio and Variable Density Interspersed Moderation Conditions

Case	Interspersed Moderation Condition	$H/^{235}U$	k_{eff}	σ	k_s	AEG
DINF	1	300	0.8987	0.0007	0.9001	190.6
		400	0.9124	0.0007	0.9138	197.0
		500	0.9144	0.0006	**0.9156**	201.1
		600	0.9070	0.0005	0.9080	203.9
		700	0.8986	0.0006	0.8998	206.0
		800	0.8843	0.0006	0.8855	207.6
		900	0.8721	0.0005	0.8731	208.8
		1000	0.8576	0.0007	0.8590	209.9
DINFIM	0.00001	500	0.9183	0.0007	0.9197	201.2
	0.001	500	0.9188	0.0006	**0.9200**	201.2
	0.01	500	0.9168	0.0005	0.9178	201.1
	0.05	500	0.9156	0.0006	0.9168	201.1
	0.1	500	0.9138	0.0007	0.9152	201.0
	0.2	500	0.9140	0.0006	0.9152	201.0
	0.4	500	0.9132	0.0006	0.9144	201.1
	0.6	500	0.9125	0.0005	0.9135	201.0
	0.8	500	0.9139	0.0006	0.9151	201.0
	1	500	0.9144	0.0006	0.9156	201.1

Table 6.4-12 – Single-Unit, NCT and HAC, Case D, Be Reflected, Cylindrical Fissile Region, 0.96 wt% U-235 FEM, k_s vs. H/U-235 Ratio

Case	IV Region Reflector Condition	$H/^{235}U$	k_{eff}	σ	k_s	AEG
Long Cylinder with Be Reflector Radially Distributed						
LEUBEREFLSIN0	Reflector = 25% poly/ 74% water/ 1% beryllium	300	0.8912	0.0007	0.8926	193.5
		400	0.9033	0.0006	0.9045	198.8
		500	0.9052	0.0005	**0.9062**	202.4
		600	0.8999	0.0006	0.9011	204.9
		700	0.8889	0.0005	0.8899	206.7
		800	0.8770	0.0006	0.8782	208.2
		900	0.8654	0.0005	0.8664	209.4
		1,000	0.8513	0.0006	0.8525	210.3
Short Squat Cylinder with Be Reflector Axially Distributed on Ends						
LEUBEREFLSIN1	Reflector = 25% poly/ 74% water/ 1% beryllium	300	0.9037	0.0006	0.9049	191.1
		400	0.9167	0.0006	0.9179	197.3
		500	0.9168	0.0006	**0.9180**	201.2
		600	0.9088	0.0006	0.9100	204.0
		700	0.9005	0.0006	0.9017	206.1
		800	0.8875	0.0006	0.8887	207.7
		900	0.8740	0.0005	0.8750	208.9
		1,000	0.8590	0.0005	0.8600	210.0
Cylinder with Be Reflector Encapsulating Cylinder						
LEUBEREFLSIN2	Reflector = 25% poly/ 74% water/ 1% beryllium	300	0.8950	0.0006	0.8962	193.2
		400	0.9075	0.0005	0.9085	198.8
		500	0.9080	0.0006	**0.9092**	202.4
		600	0.9020	0.0006	0.9032	204.9
		700	0.8907	0.0007	0.8921	206.7
		800	0.8809	0.0006	0.8821	208.2
		900	0.8678	0.0006	0.8690	209.3
		1,000	0.8527	0.0005	0.8537	210.2

Table 6.4-13 – Infinite-Unit, NCT and HAC, Case D, Be Reflected, Short, Squat, Cylindrical Fissile Region, 0.96 wt% U-235 FEM, k_s vs. H/U-235 Ratio and Variable Interspersed Moderation Between Packages

Case	Interspersed Moderation Condition (vol fraction H_2O)	$H/^{235}U$	k_{eff}	σ	k_s	AEG
Infinite Unit Package Array with Full Density Interspersed Moderation						
LEUBEREFLINF1	1	300	0.9067	0.0007	0.9081	191.1
		400	0.9175	0.0006	**0.9187**	197.3
		500	0.9168	0.0007	0.9182	201.2
		600	0.9111	0.0006	0.9123	204.0
		700	0.8998	0.0006	0.9010	206.1
		800	0.8880	0.0005	0.8890	207.7
		900	0.8733	0.0006	0.8745	208.9
		1,000	0.8585	0.0006	0.8597	210.0
Infinite Unit Package Array at H/X=400 with Variable Density Interspersed Moderation						
LEUBEREFLINF1IM	0.00001	400	0.9228	0.0006	0.9240	197.4
	0.001	400	0.9214	0.0005	**0.9224**	197.4
	0.01	400	0.9206	0.0006	0.9218	197.4
	0.05	400	0.9177	0.0006	0.9189	197.3
	0.1	400	0.9179	0.0007	0.9193	197.3
	0.2	400	0.9165	0.0006	0.9177	197.3
	0.4	400	0.916	0.0006	0.9172	197.3
	0.6	400	0.916	0.0006	0.9172	197.3
	0.8	400	0.9169	0.0006	0.9181	197.3
	1	400	0.9175	0.0006	0.9187	197.3

Table 6.4-14 – Infinite-Unit, NCT and HAC, Case D, Be Reflected, Short, Squat, Cylindrical Fissile Region, 0.96 wt% U-235 FEM, Moderated to H/U-235=500, k_s vs. Be in Moderator

Case	Be in Moderator (Vol% Be)	k_{eff}	σ	k_s	AEG
LEUBEMODREFLINF1	1	0.9168	0.0007	**0.9182**	201.2
	2	0.9166	0.0006	0.9178	201.3
	4	0.916	0.0007	0.9174	201.5
	6	0.9153	0.0007	0.9167	201.7
	8	0.9144	0.0005	0.9154	201.8
	10	0.9151	0.0006	0.9163	202.0
	20	0.9101	0.0007	0.9115	202.9
	40	0.8978	0.0007	0.8992	205.0
	60	0.8705	0.0007	0.8719	207.8
	80	0.8111	0.0006	0.8123	212.0
	85	0.7814	0.0006	0.7826	213.5

Table 6.4-15 – Fissile Payload Limits

Payload Name	Physical Form and Other Contents Restrictions	Fissile Isotope Special Conditions	Fissile Limit per Package (g ^{239}Pu FGE)	Applicable Analysis Case
General Payload	Not Machine Compacted with ≤1% by weight Be	None	315	A
		≥5 g ^{240}Pu	325	A
		≥15 g ^{240}Pu	350	A
		≥25 g ^{240}Pu	370	A
Special Reflector Payload	Not Machine Compacted with >1% by weight Be	Fissile material not bound to Special Reflector	100	B
		Fissile material bound to Special Reflector	305	B
Machine-Compacted Payload	≤1% by weight Be	None	245	C
Payload Name	**Physical Form and Other Contents Restrictions**	**Fissile Isotope Special Conditions**	**Fissile Limit per Package (wt% ^{235}U FEM)**	**Applicable Analysis Case**
Low Enriched Uranium (LEU) Payload	Not Machine Compacted	Primarily uranium (in terms of the heavy metal component) with waste matrix distributed to not exceed enrichment limit	0.96	D

6.5 Critical Benchmark Experiments

The KENO-V.a Monte Carlo criticality code[1] has been used extensively in criticality evaluations. The 238 energy-group, ENDF-B/V cross-section library[2] employed here has been selected based on its relatively fine neutron energy group structure. This section justifies the validity of this computation tool and data library combination for application to the RH-TRU 72-B package criticality analysis.

The ORNL USLSTATS code, described in Appendix C, *User's Manual for USLSTATS V1.0*, of NUREG/CR-6361[3], is used to establish an upper subcriticality limit, USL, for the analysis. Computed neutron multiplication factors, k_{eff}, for the RH-TRU 72-B package are deemed to be adequately subcritical if the computed value of k_{eff} plus two standard deviations is below the USL as follows:

$$k_s = k_{eff} + 2\sigma < USL$$

The USL includes the combined effects of code bias, uncertainty in the benchmark experiments, uncertainty in the computational evaluation of the benchmark experiments, and an administrative margin of subcriticality. The USL is determined using the confidence band with administrative margin technique (USLSTATS Method 1).

The result of the statistical analysis of the Pu fissile isotope benchmark experiments is a USL of 0.9382. Due to the significant positive bias exhibited by the code and library for the benchmark experiments, the USL is constant with respect to the various parameters selected for the benchmark analysis.

The result of the statistical analysis of the LEU benchmark experiments is a USL of 0.9257.

6.5.1 Benchmark Experiments and Applicability

6.5.1.1 PU Benchmarks

A total of 196 benchmark experiments of water-reflected solutions of plutonium nitrate are evaluated using the KENO-V.a[1] Monte Carlo criticality code with the SCALE-PC v4.4a[4] , 238 energy-group, ENDF-B/V cross-section library. The benchmark cases are evaluated with respect to three independent parameters: 1) the H/Pu ratio, 2) the average fission energy group (AEG), and 3) the ratio of ^{240}Pu to total Pu.

---

[1] L. M. Petrie and N. F. Landers, *KENO-V.a: An Improved Monte Carlo Criticality Program with Supergrouping*, ORNL/NUREG/CSD-2/V2/R6, Volume 2, Section F11, March 2000.

[2] W. C. Jordan and S. M. Bowman, *Scale Cross-Section Libraries*, ORNL/NUREG/CSD-2/V3/R6, Volume 3, Section M4, March 2000.

[3] J. J. Lichtenwalter, S. M. Bowman, M. D. DeHart, C. M. Hopper, *Criticality Benchmark Guide for Light-Water-Reactor Fuel in Transportation and Storage Packages*, NUREG/CR-6361, ORNL/TM-13211, March 1997.

[4] Oak Ridge National Laboratory (ORNL), SCALE 4.4a: *Modular Code System for Performing Standardized Computer Analysis for Licensing Evaluation for Workstations and Personal Computers*, ORNL/NUREG/CSD-2/R6, March 2000.

Detailed descriptions of the benchmark experiments are obtained from the OECD Nuclear Energy Agency's *International Handbook of Evaluated Criticality Safety Benchmark Experiments*[5]. The critical experiments selected for this analysis are presented in Table 6.5-1. Experiments with beryllium and Pu as the fissile component are not available. The only experiments with beryllium in the thermal energy range identified from the OECD Handbook contained ^{233}U as the fissile isotope. Thus, 31 benchmarks with ^{233}U and beryllium in the thermal energy range and 15 benchmarks with ^{233}U and no beryllium also in the thermal energy range were evaluated. With respect to validation of polyethylene, CH_2, in the models, some of the ^{233}U benchmarks contained polyethylene and some of the plutonium experiments contained Plexiglas, which also contains carbon. All criticality models of the RH-TRU 72-B package fall within the range of applicability of the benchmark experiments for the H/Pu ratio and AEG trending parameters as follows:

Range of Applicability for Trending Parameters
$45 \leq$ H/Pu Ratio $\leq 2{,}730$
$173 \leq$ AEG ≤ 220
$4.95 \times 10^{-3} \leq {}^{240}Pu/Pu$ Ratio $\leq 2.32 \times 10^{-1}$

The intent of using the $^{240}Pu/Pu$ ratio is to demonstrate the validity of an extension of the range of applicability of this parameter to the RH-TRU 72-B package criticality models. The Case A models include a $^{240}Pu/Pu$ Ratio of up to 6.6×10^{-2}, which is within the range of applicability. Only thermal benchmark experiments are analyzed. Criticality analysis of the RH-TRU 72-B package and package arrays demonstrate that neutron multiplication factors are insignificant when the package contents are unmoderated.

6.5.1.2 0.96 wt% ^{235}U Benchmarks

A total of 82 benchmark experiments of various low enriched uranium experiments ranging from uranium solutions to moderated uranium oxide rod arrays with reflectors ranging from water to polythene (similar in properties to polyethylene with respect to C and H constituents) are evaluated using the KENO-V.a[1] Monte Carlo criticality code with the SCALE-PC v4.4a[4] , 238 energy-group, ENDF-B/V cross-section library[2]. The benchmark case results are evaluated with respect to three parameters: 1) the H/X ratio, 2) the average fission energy group (AEG), and 3) the enrichment of ^{235}U.

Detailed descriptions of the benchmark experiments are obtained from the OECD Nuclear Energy Agency's *International Handbook of Evaluated Criticality Safety Benchmark Experiments*[5]. The critical experiments selected for this analysis are presented in Table 6.5-4. With respect to validation of polyethylene, CH_2, in the models, some of the ^{235}U benchmarks contained polythene (a polymer of the gas ethene -C_2H_4) which also contains carbon and similar C to H ratios as polyethylene. All criticality models of the RH-TRU 72-B package fall within

[5] OECD Nuclear Energy Agency, *International Handbook of Evaluated Criticality Safety Benchmark Experiment*s, NEA/NSC/DOC(95)03, September 2002.

the range of applicability of the benchmark experiments for the H/Pu ratio and AEG trending parameters as follows:

Range of Applicability for Trending Parameters
$300 \leq H/^{235}U \leq 1438$
$168.7 \leq AEG \leq 220$
$2.6 \leq {}^{235}U$ *enrichment* ≤ 10.1

The enrichments at which the package contents are analyzed fall outside of the range of applicability of the benchmark cases. The USL method 1 provides a means of projecting the USL to areas outside the range and this was used to develop a USL for the 0.96 wt% ^{235}U enrichment for comparison only. Since this low enrichment is expected to always be subcritical in aqueous, water-reflected systems according to ANSI/ANS 8.1[6], and since these systems did indeed evaluate to k_s values in the 0.8 to 0.9 region, the calculations are accepted to fall within the range of applicability and the USL, for the purpose of this analysis, is extended to the lower enrichment of 0.96 wt% ^{235}U. The Be analysis described in Section 6.5.1.1, *PU Benchmarks*, also applies here.

6.5.2 Details of Benchmark Calculations

A total of 196 experimental benchmarks with Pu in the thermal energy range were evaluated with the KENO-V.a[1] code with the SCALE-PC v4.4a[4], 238 group, ENDF-B/V cross-section library[2]. Detailed descriptions of these experiments are found in the OECD Handbook. A summary of the experiment titles is provided in Table 6.5-1. The benchmark results were evaluated using the USLSTATS program as discussed in the next section.

A total of 82 experimental benchmarks with LEU in the thermal energy range were evaluated with the KENO-V.a[1] code with the SCALE-PC v4.4a[4], 238 group, ENDF-B/V cross-section library[2]. Detailed descriptions of these experiments are found in the OECD Handbook. A summary of the LEU benchmark experiment titles selected for this study is provided in Table 6.5-4. The benchmark results were evaluated using the USLSTATS program (Version 1.4, April 23, 2003), as discussed in the next section.

6.5.3 Results of Benchmark Calculations

6.5.3.1 PU Benchmarks

Table 6.5-2 summarizes the trending parameter values, computed k_{eff} values, and uncertainties for each case. The uncertainty value, σ_c, assigned to each case is a combination of the benchmark uncertainty for each experiment, σ_{exp}, and the Monte Carlo uncertainty associated with the particular computational evaluation of the case, σ_{comp}, or:

[6] ANSI/ANS 8.1-1998, *Nuclear Criticality Safety in Operations with Fissionable Materials Outside Reactors*, American Nuclear Society (ANS), La Grange Park, Illinois.

$$\sigma_c = \sqrt{\sigma_{exp}^2 + \sigma_{comp}^2}$$

These values were input into the USLSTATS program in addition to the following parameters:

- P, proportion of population falling above lower tolerance level = 0.995
- 1-γ , confidence on fit = 0.95
- α , confidence on proportion P = 0.95
- x_{min}, minimum value of AEG for which USL correlation are computed = N/A, minimum of supplied data used by code
- x_{max}, maximum value of AEG for which USL correlation are computed = N/A, maximum of supplied data used by code
- σ_{eff}, estimate in average standard deviation of all input values of k_{eff} = -1.0, use supplied values
- Δk_m, administrative margin used to ensure subcriticality = 0.05.

This data is followed by triplets of trending parameter value, computed k_{eff}, and uncertainty for each case. The USL Method 1 result was chosen which performs a confidence band analysis on the data for the trending parameter.

Three trending parameters are identified for determination of the bias. First, the AEG is used in order to characterize any code bias with respect to neutron spectral effects. The USL is calculated vs. AEG separately for the Pu experiments, ^{233}U experiments with beryllium and ^{233}U experiments without beryllium in addition to the combined results of the Pu and ^{233}U with beryllium experiments. Because the ^{233}U fissile isotope introduces a component that is not relative to the calculations performed for the RH-TRU 72-B and may have a distinct bias of its own, comparison of the USL for the ^{233}U experiments with beryllium to the USL for those without beryllium allows the effect of the beryllium reflector to be separated from the effect of the ^{233}U isotope. Next, the H/Pu ratio of each experimental case containing Pu is used in order to characterize the material and geometric properties of each sphere. Finally, since all the Pu experiments include ^{240}Pu to some extent and the RH-TRU 72-B models contain varying amount of ^{240}Pu, a trending analysis of the results of the Pu experiments with respect to ^{240}Pu/Pu ratio is performed. The ^{233}U results are not considered in the trending with respect to H/Pu as the optimum H/Pu range will be significantly different for a ^{233}U system vs. a Pu system. For obvious reasons, the ^{233}U results are also not considered in the trending with respect to the ^{240}Pu/Pu ratio.

The USLs calculated using USLSTATS Method 1 for the benchmark combinations discussed above are tabulated in Table 6.5-3. The USL calculated based on the combined results of the ^{233}U with beryllium and Pu experiments of 0.9382 is chosen as the USL for this analysis. This USL value is ~0.001 below that of the Pu experiments alone. The ^{233}U benchmarks without Be result in a lower USL (0.0032) than calculated from the ^{233}U benchmark results without beryllium. This difference is greater than the benchmark uncertainty of each benchmark case (~0.001). Both of the ^{233}U USL values are lower than the Pu experiment USL values indicating that the ^{233}U isotope in the experiments has a more significant effect on the USL than the beryllium. Thus, the USL based on the combined results of the ^{233}U with beryllium and Pu experiments chosen adequately accounts for any bias attributable to beryllium. In addition, the

USLs calculated for the Pu experiments using either H/X or the ^{240}Pu/Pu ratio as the trending parameter do not differ significantly from the Pu USL vs. AEG and are bounded by the chosen USL value of 0.9382. USLSTATS calculated constant USL values with respect to H/Pu and ^{240}Pu/Pu ratio indicating no appreciable trend with respect to these parameters.

6.5.3.2 0.96 wt% ^{235}U Benchmarks

Table 6.5-5 summarizes the computed k_{eff} values, trending parameter values, and uncertainties for each case. The uncertainty value, σ_c, assigned to each case is a combination of the benchmark uncertainty for each experiment, σ_{exp}, and the Monte Carlo uncertainty associated with the particular computational evaluation of the case, σ_{comp}, or:

$$\sigma_c = \sqrt{\sigma_{exp}^2 + \sigma_{comp}^2}$$

These values were input into the USLSTATS program in addition to the following parameters:

- P, proportion of population falling above lower tolerance level = 0.995
- 1-γ , confidence on fit = 0.95
- α , confidence on proportion P = 0.95
- x_{min}, minimum value of AEG for which USL correlation are computed = N/A, minimum of supplied data used by code
- x_{max}, maximum value of AEG for which USL correlation are computed = N/A, maximum of supplied data used by code
- σ_{eff}, estimate in average standard deviation of all input values of k_{eff} = -1.0, use supplied values
- Δk_m, administrative margin used to ensure subcriticality = 0.05.

This data is followed by triplets of trending parameter value, computed k_{eff}, and uncertainty for each case. The USL Method 1 result was chosen which performs a confidence band analysis on the data for the trending parameter.

Three trending parameters are identified for determination of the bias. The data is trended against AEG, H/X, and ^{235}U enrichment to determine bias resulting from all of these parameters. The output values of USLSTATS, USL Method 1 are shown in Table 6.5-6 for comparison. Each value is calculated using the USL Method 1 for the region of interest as indicated by the footnotes. For the region of interest in this evaluation, the enrichment value of 0.96 wt% ^{235}U falls outside of the range of applicability of the benchmark experiments. However, since this value of enrichment is expected to always result in subcritical configurations for the region of interest in this analysis, the USL has been conservatively projected to the 0.96 wt% for comparison with the other USL results. As indicated in Table 6.5-6 the USL based on AEG is the most limiting and the value of 0.9257 will be used in this analysis as the USL for ^{235}U systems.

Table 6.5-1 – ^{239}Pu Benchmark Experiment Description

Series①	Title
PU-SOL-THERM-001	Water-reflected 11.5 inch diameter spheres of plutonium nitrate solutions
PU-SOL-THERM-002	Water-reflected 12 inch diameter spheres of plutonium nitrate solutions
PU-SOL-THERM-003	Water-reflected 13 inch diameter spheres of plutonium nitrate solutions
PU-SOL-THERM-004	Water-reflected 14 inch diameter spheres of plutonium nitrate solutions 0.54% to 3.43% Pu-240
PU-SOL-THERM-005	Water-reflected 14 inch diameter spheres of plutonium nitrate solutions 4.05% and 4.40% Pu-240
PU-SOL-THERM-006	Water-reflected 15 inch diameter spheres of plutonium nitrate solutions
PU-SOL-THERM-007	Water-reflected 11.5 inch diameter spheres partly filled with plutonium nitrate solutions
PU-SOL-THERM-009	Unreflected 48 inch-diameter sphere of plutonium nitrate solution
PU-SOL-THERM-010	Water-reflected 9-, 10-, 11-, and 12 inch-diameter cylinders of plutonium nitrate solutions
PU-SOL-THERM-011	Bare 16- and 18 inch-diameter spheres of plutonium nitrate solutions
PU-SOL-THERM-014	Interacting cylinders of 300-mm diameter with plutonium nitrate solution (115.1gPu/l) in air
PU-SOL-THERM-015	Interacting cylinders of 300-mm diameter with plutonium nitrate solution (152.5gPu/l) in air
PU-SOL-THERM-016	Interacting cylinders of 300-mm and 256-mm diameters with plutonium nitrate solution (152.5 and 115.1gPu/l) and nitric acid (2N) in air
PU-SOL-THERM-017	Interacting cylinders of 256-mm and 300-mm diameters with plutonium nitrate solution (115.1gPu/l) in air
PU-SOL-THERM-020	Water-reflected and water-cadmium reflected 14-inch diameter spheres of plutonium nitrate solutions
PU-SOL-THERM-021	Water-reflected and bare 15.2-inch-diameter spheres of plutonium nitrate solutions
PU-SOL-THERM-024	Slabs of plutonium nitrate solutions reflected by 1-inch-thick Plexiglas
U233-SOL-THERM-001	Unreflected spheres of 233U nitrate solutions
U233-SOL-THERM-003	Paraffin-reflected 5-, 5.4-, 6-, 6.6-, 7.5- 8-, 8.5-, 9- and 12-inch-diameter cylinders of 233U uranyl fluoride solutions
U233-SOL-THERM-015	Uranyl-fluoride (233U) solutions in spherical stainless steel vessels with reflectors of Be, CH2, and Be-CH2 composites

Notes:

① These benchmarks are found under the experimental series noted in the first column in the following reference: OECD Nuclear Energy Agency, *International Handbook of Evaluated Criticality Safety Benchmark Experiment*s, NEA/NSC/DOC(95)03, September 2002.

Table 6.5-2 – ^{239}Pu Benchmark Case Parameters and Computed Results

Case Name①	k_{eff}	σ_{comp}	AEG	H/X②	^{240}Pu/ Pu Ratio	Benchmark Uncertainty σ_{exp}③
PUST001_CASE_1	1.0080	0.0010	212.494	352.9	0.04650	0.0050
PUST001_CASE_2	1.0100	0.0010	209.961	258.1	0.04650	0.0050
PUST001_CASE_3	1.0133	0.0010	207.777	204.1	0.04650	0.0050
PUST001_CASE_4	1.0073	0.0010	206.439	181	0.04650	0.0050
PUST001_CASE_5	1.0111	0.0011	205.757	171.2	0.04650	0.0050
PUST001_CASE_6	1.0089	0.0010	195.766	86.7	0.04650	0.0050
PUST002_CASE_1	1.0074	0.0010	214.693	508	0.03110	0.0047
PUST002_CASE_2	1.0088	0.0011	214.457	489.2	0.03110	0.0047
PUST002_CASE_3	1.0074	0.0010	213.798	437.3	0.03110	0.0047
PUST002_CASE_4	1.0103	0.0010	213.343	407.5	0.03110	0.0047
PUST002_CASE_5	1.0125	0.0011	212.898	380.6	0.03110	0.0047
PUST002_CASE_6	1.0099	0.0010	211.974	333.5	0.03110	0.0047
PUST002_CASE_7	1.0101	0.0010	211.146	299.3	0.03110	0.0047
PUST003_CASE_1	1.0089	0.0010	216.630	774.1	0.01750	0.0047
PUST003_CASE_2	1.0076	0.0011	216.438	742.7	0.01750	0.0047
PUST003_CASE_3	1.0103	0.0010	216.055	677.2	0.03110	0.0047
PUST003_CASE_4	1.0094	0.0010	215.948	660.5	0.03110	0.0047
PUST003_CASE_5	1.0097	0.0010	215.535	607.2	0.03110	0.0047
PUST003_CASE_6	1.0099	0.0011	214.960	545.3	0.03110	0.0047
PUST003_CASE_7	1.0121	0.0009	216.482	714.8	0.03110	0.0047
PUST003_CASE_8	1.0091	0.0011	216.321	692.1	0.03110	0.0047
PUST004_CASE_1	1.0080	0.0010	217.470	981.7	0.00538	0.0047
PUST004_CASE_2	1.0032	0.0009	217.408	898.6	0.04180	0.0047
PUST004_CASE_3	1.0059	0.0008	217.241	864	0.04500	0.0047
PUST004_CASE_4	1.0033	0.0009	217.034	842	0.03260	0.0047
PUST004_CASE_5	1.0043	0.0010	217.257	780.2	0.03630	0.0047
PUST004_CASE_6	1.0074	0.0009	217.195	668	0.00495	0.0047
PUST004_CASE_7	1.0104	0.0010	217.030	573.3	0.00495	0.0047
PUST004_CASE_8	1.0040	0.0009	216.917	865	0.00504	0.0047
PUST004_CASE_9	1.0041	0.0009	216.580	872.2	0.01530	0.0047
PUST004_CASE_10	1.0078	0.0009	215.881	971.6	0.02510	0.0047

Case Name①	k_{eff}	σ_{comp}	AEG	H/X②	^{240}Pu/ Pu Ratio	Benchmark Uncertainty σ_{exp}③
PUST004_CASE_11	1.0041	0.0010	215.106	929.6	0.02330	0.0047
PUST004_CASE_12	1.0094	0.0009	217.031	884.1	0.03160	0.0047
PUST004_CASE_13	1.0042	0.0009	217.074	925.5	0.03350	0.0047
PUST005_CASE_1	1.0072	0.0010	217.069	866.4	0.04030	0.0047
PUST005_CASE_2	1.0084	0.0009	216.909	832.7	0.04030	0.0047
PUST005_CASE_3	1.0092	0.0009	216.749	800.7	0.04030	0.0047
PUST005_CASE_4	1.0091	0.0010	216.360	734.4	0.04030	0.0047
PUST005_CASE_5	1.0102	0.0010	215.906	666.1	0.04030	0.0047
PUST005_CASE_6	1.0112	0.0010	215.451	607.9	0.04030	0.0047
PUST005_CASE_7	1.0099	0.0010	215.004	557.2	0.04030	0.0047
PUST005_CASE_8	1.0024	0.0010	216.903	830.6	0.04030	0.0047
PUST005_CASE_9	1.0078	0.0010	216.687	788.9	0.04030	0.0047
PUST006_CASE_1	1.0059	0.0008	217.615	1028.2	0.03110	0.0035
PUST006_CASE_2	1.0079	0.0009	217.459	986.2	0.03110	0.0035
PUST006_CASE_3	1.0072	0.0010	217.147	910.9	0.03110	0.0035
PUST007_CASE_2	1.0090	0.0011	198.911	102.6	0.04570	0.0047
PUST007_CASE_3	1.0024	0.0010	199.553	110.11	0.04570	0.0047
PUST007_CASE_5	1.0099	0.0010	209.885	253.3	0.04570	0.0047
PUST007_CASE_6	1.0054	0.0011	209.689	247.3	0.04570	0.0047
PUST007_CASE_7	1.0072	0.0010	209.816	250.5	0.04570	0.0047
PUST007_CASE_8	1.0007	0.0012	209.577	246.5	0.04570	0.0047
PUST007_CASE_9	0.9996	0.0011	209.628	246.5	0.04570	0.0047
PUST007_CASE_10	1.0009	0.0011	210.426	275.5	0.04570	0.0047
PUST009_CASE_1	1.0202	0.0007	219.730	2579.3	0.02510	0.0033
PUST009_CASE_2	1.0242	0.0005	219.819	2706.5	0.02510	0.0033
PUST009_CASE_3	1.0232	0.0006	219.830	2729.8	0.02510	0.0033
PUST010_CASE_1.11	1.0158	0.0011	219.830	471.3	0.02840	0.0048
PUST010_CASE_1.12	1.0125	0.0009	214.122	527.7	0.02890	0.0048
PUST010_CASE_1.9	1.0183	0.0012	214.895	259.3	0.02840	0.0048
PUST010_CASE_2.11	1.0124	0.0011	210.075	542.3	0.02840	0.0048
PUST010_CASE_2.12	1.0136	0.0010	214.882	600.5	0.02890	0.0048
PUST010_CASE_2.9	1.0140	0.0011	215.514	346.8	0.02840	0.0048

Case Name①	k_{eff}	σ_{comp}	AEG	H/X②	^{240}Pu/ Pu Ratio	Benchmark Uncertainty σ_{exp}③
PUST010_CASE_3.11	1.0128	0.0011	212.361	542.3	0.02840	0.0048
PUST010_CASE_3.12	1.0208	0.0009	215.036	707	0.02890	0.0048
PUST010_CASE_3.9	1.0120	0.0010	216.250	470.4	0.02840	0.0048
PUST010_CASE_4.11	1.0055	0.0011	214.300	588.7	0.02840	0.0048
PUST010_CASE_4.12	1.0142	0.0009	215.366	825.1	0.02890	0.0048
PUST010_CASE_5.11	1.0068	0.0010	216.852	646.5	0.02840	0.0048
PUST010_CASE_6.11	1.0176	0.0012	215.739	402.3	0.02890	0.0048
PUST010_CASE_7.11	1.0065	0.0010	213.340	519.8	0.02890	0.0048
PUST011_CASE_1.16	1.0135	0.0010	214.790	733	0.04150	0.0052
PUST011_CASE_1.18	1.0001	0.0009	215.818	1157.3	0.04180	0.0052
PUST011_CASE_2.16	1.0196	0.0010	217.686	705.5	0.04150	0.0052
PUST011_CASE_2.18	1.0065	0.0011	215.633	1103.2	0.04180	0.0052
PUST011_CASE_3.16	1.0213	0.0010	217.509	662.8	0.04150	0.0052
PUST011_CASE_3.18	1.0027	0.0010	215.281	1109.8	0.04180	0.0052
PUST011_CASE_4.16	1.0139	0.0011	217.525	653.4	0.04150	0.0052
PUST011_CASE_4.18	0.9991	0.0011	215.196	1053.7	0.04180	0.0052
PUST011_CASE_5.16	1.0113	0.0010	217.313	550.7	0.04150	0.0052
PUST011_CASE_5.18	1.0099	0.0010	214.156	995.4	0.04180	0.0052
PUST011_CASE_6.18	1.0068	0.0010	217.071	870.4	0.04180	0.0052
PUST011_CASE_7.18	1.0050	0.0010	216.471	1056.4	0.04180	0.0052
PUST014_CASE_1	1.0068	0.0012	205.455	210.2	0.04230	0.0032
PUST014_CASE_3	1.0065	0.0010	205.477	210.2	0.04230	0.0032
PUST014_CASE_4	1.0079	0.0011	205.504	210.2	0.04230	0.0032
PUST014_CASE_5	1.0065	0.0011	205.510	210.2	0.04230	0.0032
PUST014_CASE_6	1.0073	0.0013	205.516	210.2	0.04230	0.0032
PUST014_CASE_7	1.0082	0.0012	205.434	210.2	0.04230	0.0043
PUST014_CASE_8	1.0051	0.0012	205.462	210.2	0.04230	0.0032
PUST014_CASE_9	1.0068	0.0012	205.477	210.2	0.04230	0.0032
PUST014_CASE_10	1.0060	0.0011	205.499	210.2	0.04230	0.0032
PUST014_CASE_11	1.0046	0.0010	205.526	210.2	0.04230	0.0032
PUST014_CASE_12	1.0076	0.0010	205.522	210.2	0.04230	0.0032
PUST014_CASE_13	1.0080	0.0011	205.420	210.2	0.04230	0.0043

Case Name①	k_{eff}	σ_{comp}	AEG	H/X②	^{240}Pu/ Pu Ratio	Benchmark Uncertainty σ_{exp}③
PUST014_CASE_14	1.0062	0.0011	205.458	210.2	0.04230	0.0043
PUST014_CASE_15	1.0067	0.0011	205.507	210.2	0.04230	0.0043
PUST014_CASE_16	1.0057	0.0011	205.512	210.2	0.04230	0.0043
PUST014_CASE_17	1.0033	0.0011	205.506	210.2	0.04230	0.0043
PUST014_CASE_18	1.0070	0.0011	205.430	210.2	0.04230	0.0043
PUST014_CASE_19	1.0045	0.0011	205.469	210.2	0.04230	0.0043
PUST014_CASE_20	1.0061	0.0011	205.487	210.2	0.04230	0.0043
PUST014_CASE_21	1.0066	0.0012	205.514	210.2	0.04230	0.0043
PUST014_CASE_22	1.0060	0.0012	205.527	210.2	0.04230	0.0043
PUST014_CASE_23	1.0048	0.0012	205.530	210.2	0.04230	0.0043
PUST014_CASE_24	1.0080	0.0012	205.393	210.2	0.04230	0.0043
PUST014_CASE_25	1.0042	0.0011	205.445	210.2	0.04230	0.0043
PUST014_CASE_26	1.0066	0.0011	205.490	210.2	0.04230	0.0043
PUST014_CASE_27	1.0044	0.0011	205.504	210.2	0.04230	0.0043
PUST014_CASE_28	1.0052	0.0011	205.534	210.2	0.04230	0.0043
PUST014_CASE_29	1.0050	0.0011	205.525	210.2	0.04230	0.0043
PUST014_CASE_30	1.0060	0.0010	205.416	210.2	0.04230	0.0043
PUST014_CASE_31	1.0046	0.0011	205.444	210.2	0.04230	0.0043
PUST014_CASE_33	1.0021	0.0011	205.446	210.2	0.04230	0.0043
PUST014_CASE_34	1.0045	0.0011	205.480	210.2	0.04230	0.0043
PUST015_CASE_1	1.0065	0.0010	201.243	155.3	0.04230	0.0038
PUST015_CASE_2	1.0069	0.0011	201.272	155.3	0.04230	0.0038
PUST015_CASE_3	1.0060	0.0011	201.289	155.3	0.04230	0.0038
PUST015_CASE_4	1.0056	0.0012	201.324	155.3	0.04230	0.0038
PUST015_CASE_5	1.0072	0.0011	201.311	155.3	0.04230	0.0038
PUST015_CASE_6	1.0078	0.0012	201.327	155.3	0.04230	0.0038
PUST015_CASE_7	1.0078	0.0011	201.209	155.3	0.04230	0.0047
PUST015_CASE_8	1.0056	0.0011	201.255	155.3	0.04230	0.0047
PUST015_CASE_9	1.0062	0.0012	201.292	155.3	0.04230	0.0047
PUST015_CASE_10	1.0060	0.0011	201.333	155.3	0.04230	0.0047
PUST015_CASE_11	1.0012	0.0010	201.196	155.3	0.04230	0.0047
PUST015_CASE_12	1.0053	0.0011	201.280	155.3	0.04230	0.0047

Case Name①	k_{eff}	σ_{comp}	AEG	H/X②	^{240}Pu/ Pu Ratio	Benchmark Uncertainty σ_{exp}③
PUST015_CASE_13	1.0084	0.0010	201.307	155.3	0.04230	0.0047
PUST015_CASE_14	1.0065	0.0012	201.335	155.3	0.04230	0.0047
PUST015_CASE_15	1.0082	0.0013	201.196	155.3	0.04230	0.0047
PUST015_CASE_16	1.0064	0.0010	201.222	155.3	0.04230	0.0047
PUST015_CASE_17	1.0067	0.0010	201.299	155.3	0.04230	0.0047
PUST016_CASE_1	1.0077	0.0011	201.225	155.3	0.04230	0.0043
PUST016_CASE_2	1.0048	0.0011	201.265	155.3	0.04230	0.0043
PUST016_CASE_3	1.0072	0.0011	201.295	155.3	0.04230	0.0043
PUST016_CASE_4	1.0075	0.0011	201.318	155.3	0.04230	0.0043
PUST016_CASE_5	1.0054	0.0012	205.463	210.2	0.04230	0.0038
PUST016_CASE_6	1.0047	0.0011	205.476	210.2	0.04230	0.0038
PUST016_CASE_7	1.0093	0.0013	205.511	210.2	0.04230	0.0038
PUST016_CASE_8	1.0072	0.0011	205.508	210.2	0.04230	0.0038
PUST016_CASE_9	1.0070	0.0012	205.607	210.2	0.04230	0.0033
PUST016_CASE_10	1.0065	0.0012	205.556	210.2	0.04230	0.0033
PUST016_CASE_11	1.0063	0.0011	205.516	210.2	0.04230	0.0033
PUST017_CASE_1	1.0076	0.0011	205.535	210.2	0.04230	0.0038
PUST017_CASE_2	1.0050	0.0011	205.488	210.2	0.04230	0.0038
PUST017_CASE_3	1.0041	0.0011	205.492	210.2	0.04230	0.0038
PUST017_CASE_4	1.0054	0.0012	205.482	210.2	0.04230	0.0038
PUST017_CASE_5	1.0066	0.0012	205.488	210.2	0.04230	0.0038
PUST017_CASE_6	1.0056	0.0011	205.479	210.2	0.04230	0.0038
PUST017_CASE_7	1.0069	0.0011	205.485	210.2	0.04230	0.0038
PUST017_CASE_8	1.0051	0.0011	205.497	210.2	0.04230	0.0038
PUST017_CASE_9	1.0071	0.0012	205.525	210.2	0.04230	0.0038
PUST017_CASE_10	1.0060	0.0011	205.500	210.2	0.04230	0.0038
PUST017_CASE_11	1.0050	0.0011	205.531	210.2	0.04230	0.0038
PUST017_CASE_12	1.0057	0.0011	205.509	210.2	0.04230	0.0038
PUST017_CASE_13	1.0047	0.0011	205.490	210.2	0.04230	0.0038
PUST017_CASE_14	1.0049	0.0013	205.487	210.2	0.04230	0.0038
PUST017_CASE_15	1.0072	0.0012	205.533	210.2	0.04230	0.0038
PUST017_CASE_16	1.0075	0.0010	205.522	210.2	0.04230	0.0038

Case Name①	k_{eff}	σ_{comp}	AEG	H/X②	^{240}Pu/ Pu Ratio	Benchmark Uncertainty σ_{exp}③
PUST017_CASE_17	1.0068	0.0012	205.519	210.2	0.04230	0.0038
PUST017_CASE_18	1.0056	0.0010	205.487	210.2	0.04230	0.0038
PUST020_CASE_1	1.0075	0.0010	215.482	596.5	0.04570	0.0059
PUST020_CASE_2	1.0117	0.0010	215.622	615.6	0.04570	0.0059
PUST020_CASE_3	1.0049	0.0009	216.499	743.8	0.04570	0.0059
PUST020_CASE_5	1.0074	0.0010	213.992	462.9	0.04570	0.0059
PUST020_CASE_6	1.0078	0.0009	213.637	450.5	0.04570	0.0059
PUST020_CASE_7	1.0022	0.0009	216.277	722.9	0.04570	0.0059
PUST020_CASE_8	1.0066	0.0011	210.650	341.1	0.04570	0.0059
PUST020_CASE_9	1.0004	0.0010	214.048	543.2	0.04570	0.0059
PUST021_CASE_7	1.0109	0.0011	215.405	662	0.04570	0.0032
PUST021_CASE_8	1.0044	0.0010	197.712	125	0.04570	0.0065
PUST021_CASE_9	1.0117	0.0010	215.136	634	0.04570	0.0032
PUST021_CASE_10	1.0123	0.0008	218.033	1107	0.04570	0.0025
PUST024_CASE_1	1.0018	0.0010	191.676	87.5	0.18400	0.0062
PUST024_CASE_2	0.9999	0.0009	191.828	87.5	0.18400	0.0062
PUST024_CASE_3	1.0002	0.0011	191.933	87.5	0.18400	0.0062
PUST024_CASE_4	1.0020	0.0010	192.026	87.5	0.18400	0.0062
PUST024_CASE_5	0.9986	0.0011	192.017	87.5	0.18400	0.0062
PUST024_CASE_6	0.9988	0.0009	173.477	44.9	0.18400	0.0077
PUST024_CASE_7	1.0072	0.0010	201.097	143.9	0.18400	0.0053
PUST024_CASE_8	1.0073	0.0010	201.200	143.9	0.18400	0.0053
PUST024_CASE_9	1.0068	0.0010	201.253	143.9	0.18400	0.0053
PUST024_CASE_10	1.0090	0.0010	201.353	143.9	0.18400	0.0053
PUST024_CASE_11	1.0065	0.0011	201.418	143.9	0.18400	0.0053
PUST024_CASE_12	1.0069	0.0010	201.452	143.9	0.18400	0.0053
PUST024_CASE_13	1.0066	0.0010	201.493	143.9	0.18400	0.0053
PUST024_CASE_14	1.0019	0.0011	197.708	115.8	0.23200	0.0053
PUST024_CASE_15	1.0033	0.0012	197.781	115.8	0.23200	0.0053
PUST024_CASE_16	1.0017	0.0009	197.845	115.8	0.23200	0.0053
PUST024_CASE_17	1.0026	0.0010	197.990	115.8	0.23200	0.0053
PUST024_CASE_18	1.0085	0.0010	212.039	367.3	0.18400	0.0051

Case Name①	k_{eff}	σ_{comp}	AEG	H/X②	^{240}Pu/ Pu Ratio	Benchmark Uncertainty σ_{exp}③
PUST024_CASE_19	1.0079	0.0009	212.057	367.3	0.18400	0.0051
PUST024_CASE_20	1.0100	0.0010	212.074	367.3	0.18400	0.0051
PUST024_CASE_21	1.0075	0.0010	212.106	367.3	0.18400	0.0051
PUST024_CASE_22	1.0054	0.0010	212.142	367.3	0.18400	0.0051
PUST024_CASE_23	1.0068	0.0011	212.166	367.3	0.18400	0.0051
233ST001CASE_1	0.9975	0.0008	218.415	1531.5	N/A	0.0031
233ST001CASE_2	0.9959	0.0008	218.224	1471.7	N/A	0.0033
233ST001CASE_3	0.9955	0.0007	218.055	1420.1	N/A	0.0033
233ST001CASE_4	0.9970	0.0007	217.875	1369.7	N/A	0.0033
233ST001CASE_5	0.9956	0.0008	217.697	1325.4	N/A	0.0033
233ST003CASE_40	1.0029	0.0011	192.780	74.1	N/A	0.0087
233ST003CASE_41	1.0164	0.0011	191.195	74.1	N/A	0.0151
233ST003CASE_42	1.0002	0.0013	191.824	74.1	N/A	0.0087
233ST003CASE_45	1.0040	0.0013	180.246	45.9	N/A	0.0126
233ST003CASE_55	1.0102	0.0011	176.271	39.4	N/A	0.0122
233ST003CASE_57	1.0196	0.0012	204.026	154	N/A	0.0087
233ST003CASE_58	1.0119	0.0012	209.393	250	N/A	0.0087
233ST003CASE_61	1.0056	0.0011	211.723	329	N/A	0.0087
233ST003CASE_62	1.0079	0.0012	213.031	396	N/A	0.0087
233ST003CASE_65	1.0039	0.0010	216.519	775	N/A	0.0087
233ST015_CASE_1	0.9928	0.0012	175.241	51.58	N/A	0.0075
233ST015_CASE_2	0.9869	0.0013	173.581	51.58	N/A	0.0070
233ST015_CASE_3	0.9863	0.0012	181.133	51.58	N/A	0.0068
233ST015_CASE_4	0.9863	0.0012	181.133	51.58	N/A	0.0041
233ST015_CASE_5	0.9844	0.0012	172.140	51.58	N/A	0.0055
233ST015_CASE_6	0.9750	0.0012	171.626	51.58	N/A	0.0099
233ST015_CASE_7	0.9807	0.0012	179.879	51.58	N/A	0.0070
233ST015_CASE_8	0.9719	0.0012	171.311	51.58	N/A	0.0067
233ST015_CASE_9	0.9664	0.0013	171.019	51.58	N/A	0.0050
233ST015_CASE_10	0.9841	0.0012	174.951	51.58	N/A	0.0051
233ST015_CASE_11	0.9937	0.0012	181.620	64.23	N/A	0.0075
233ST015_CASE_12	0.9942	0.0012	180.243	64.23	N/A	0.0069

Case Name①	k_{eff}	σ_{comp}	AEG	H/X②	^{240}Pu/ Pu Ratio	Benchmark Uncertainty σ_{exp}③
233ST015_CASE_13	0.9924	0.0011	179.562	64.23	N/A	0.0069
233ST015_CASE_14	0.9930	0.0011	187.157	64.23	N/A	0.0036
233ST015_CASE_15	0.9881	0.0012	178.911	64.23	N/A	0.0060
233ST015_CASE_16	0.9877	0.0013	178.599	64.23	N/A	0.0043
233ST015_CASE_17	0.9924	0.0012	186.084	64.23	N/A	0.0029
233ST015_CASE_18	0.9727	0.0014	178.045	64.23	N/A	0.0056
233ST015_CASE_19	0.9728	0.0012	177.964	64.23	N/A	0.0052
233ST015_CASE_20	0.9969	0.0011	193.458	102.54	N/A	0.0079
233ST015_CASE_21	0.9992	0.0012	192.290	102.54	N/A	0.0070
233ST015_CASE_22	0.9966	0.0011	191.669	102.54	N/A	0.0062
233ST015_CASE_23	0.9949	0.0011	191.140	102.54	N/A	0.0055
233ST015_CASE_24	0.9901	0.0013	190.850	102.54	N/A	0.0051
233ST015_CASE_25	0.9917	0.0012	196.919	102.54	N/A	0.0023
233ST015_CASE_26	0.9964	0.0011	204.143	199.4	N/A	0.0066
233ST015_CASE_27	0.9982	0.0011	203.709	199.4	N/A	0.0063
233ST015_CASE_28	0.9948	0.0010	203.459	199.4	N/A	0.0058
233ST015_CASE_29	0.9928	0.0012	203.220	199.4	N/A	0.0051
233ST015_CASE_30	0.9940	0.0011	203.118	199.4	N/A	0.0048
233ST015_CASE_31	0.9946	0.0012	203.041	199.4	N/A	0.0055

Notes:

① All cases were run with 1,000 neutrons per generation for 1,000 generations, with the initial 50 generations skipped.

② X refers to Pu or ^{233}U as applicable for the benchmark cases.

③ The *International Handbook of Evaluated Criticality Safety Benchmark Experiment*s provides a benchmark uncertainty for each case approved for a benchmark. This uncertainty is based on evaluation of the effects of various errors and model simplifications on the calculated k_{eff} of the individual experiment.

Table 6.5-3 – Calculation of Pu-239 USL with Be

Benchmark Set	Number of Cases	USL vs. AEG	USL vs. H/X	USL vs. ^{240}Pu/Pu
^{233}U without Be	15	0.9270	N/A	N/A
^{233}U with Be	31	0.9302 (204.14)①	N/A	N/A
Pu	196	0.9395	0.9393	0.9395
Pu + ^{233}U with Be	227	**0.9382**②	N/A	N/A

Notes:

① This value is calculated at an AEG of 204.14. USL increases with AEG such that this is conservative for the AEG of the calculations (~217).

② Range of applicability is 195.928 < AEG < 219.83.

Table 6.5-4 – Low Enriched U-235 Benchmark Experiment Description

Series①	Title
LEU-SOL-THERM-003	Full and Truncated Bare Spheres of 10% Enriched Uranyl Nitrate Water Solutions
LEU-SOL-THERM-004	STACY: Water-Reflected 10% Enriched Uranyl Nitrate Solution in a 60-cm Diameter Cylindrical Tank
LEU-COMP-THERM-006	Critical Arrays of Low Enriched UO_2 Fuel Rods with Water-to-Fuel Volume Ratios Ranging from 1.5 to 3.0
LEU-COMP-THERM-010	Critical Arrays of Water-Moderated $U(4.31)O_2$ Fuel Rods Reflected by Two Lead, Uranium, or Steel Walls
LEU-COMP-THERM-049	Maracas Program: Polythene Reflected Critical Configurations with Low Enriched and Low Moderated Uranium Dioxide Powder $U(5)O_2$

Notes:

① These benchmarks are found under the experimental series noted in the first column in the following reference: OECD Nuclear Energy Agency, *International Handbook of Evaluated Criticality Safety Benchmark Experiment*s, NEA/NSC/DOC(95)03, September 2002.

Table 6.5-5 – Low Enriched U-235 Benchmark Case Parameters, Computed Results and Reported Experimental Benchmark Uncertainty

Case Name	k_{eff}	σ_{comp}	AEG	H/X①	Enrichment (wt% ^{235}U)	Benchmark Uncertainty σ_{exp}②
LST03C1M238.OUT	1.0007	0.0019	218.0	770	10.07	0.0039
LST03C2M238.OUT	1.0000	0.0016	218.5	878	10.07	0.0042
LST03C3M238.OUT	1.0009	0.0018	218.6	897	10.07	0.0042
LST03C4M238.OUT	0.9955	0.0015	218.7	913	10.07	0.0042
LST03C5M238.OUT	0.9971	0.0014	219.5	1173	10.07	0.0048
LST03C6M238.OUT	0.9995	0.0015	219.6	1213	10.07	0.0049
LST03C7M238.OUT	0.9984	0.0013	219.6	1240	10.07	0.0049
LST03C8M238.OUT	1.0018	0.0012	220.0	1412	10.07	0.0052
LST03C9M238.OUT	0.9994	0.0011	220.0	1438	10.07	0.0052
STACYC01M238.OUT	1.0052	0.0020	217.8	719	9.97	0.0008
STACYC29M238.OUT	1.0059	0.0019	218.1	771	9.97	0.0009
STACYC33M238.OUT	0.9993	0.0015	218.4	842	9.97	0.0009
STACYC34M238.OUT	1.0033	0.0018	218.7	896	9.97	0.0010
STACYC46M238.OUT	1.0038	0.0017	218.8	942	9.97	0.0010
STACYC51M238.OUT	1.0007	0.0015	219.0	983	9.97	0.0011
STACYC54M238.OUT	1.0021	0.0013	219.1	1018	9.97	0.0011
LCT006.OUT - case1	0.9920	0.0008	198.0	167	2.596	0.0020
LCT006.OUT – case 2	0.9927	0.0009	197.8	167	2.596	0.0020
LCT006.OUT – case 3	0.9927	0.0009	197.3	167	2.596	0.0020
LCT006.OUT – case 4	0.9933	0.0008	201.2	203	2.596	0.0020
LCT006.OUT – case 5	0.9934	0.0008	200.9	203	2.596	0.0020
LCT006.OUT – case 6	0.9948	0.0010	200.6	203	2.596	0.0020
LCT006.OUT – case 7	0.9939	0.0009	200.2	203	2.596	0.0020
LCT006.OUT – case 8	0.9927	0.0007	199.9	203	2.596	0.0020
LCT006.OUT – case 9	0.9942	0.0009	204.9	276	2.596	0.0020
LCT006.OUT – case 10	0.9956	0.0009	204.5	276	2.596	0.0020
LCT006.OUT – case 11	0.9938	0.0008	204.2	276	2.596	0.0020
LCT006.OUT – case 12	0.9955	0.0010	204.0	276	2.596	0.0020
LCT006.OUT – case 13	0.9954	0.0008	203.6	276	2.596	0.0020

Case Name	k_{eff}	σ_{comp}	AEG	H/X①	Enrichment (wt% ^{235}U)	Benchmark Uncertainty σ_{exp}②
LCT006.OUT – case 14	0.9942	0.0009	206.9	333	2.596	0.0020
LCT006.OUT – case 15	0.9952	0.0009	206.6	333	2.596	0.0020
LCT006.OUT – case 16	0.9957	0.0009	206.4	333	2.596	0.0020
LCT006.OUT – case 17	0.9956	0.0008	206.1	333	2.596	0.0020
LCT006.OUT – case 18	0.9942	0.0008	205.8	333	2.596	0.0020
LEUCT010-01.OUT	1.0068	0.0009	206.8		4.31	0.0021
LEUCT010-02.OUT	1.0056	0.0008	207.2		4.31	0.0021
LEUCT010-03.OUT	1.0054	0.0009	207.4		4.31	0.0021
LEUCT010-04.OUT	0.9931	0.0009	207.7		4.31	0.0021
LEUCT010-05.OUT	0.9948	0.0008	193.5		4.31	0.0021
LEUCT010-06.OUT	0.9956	0.0008	197.3		4.31	0.0021
LEUCT010-07.OUT	0.9976	0.0009	200.1		4.31	0.0021
LEUCT010-08.OUT	0.9915	0.0009	201.5		4.31	0.0021
LEUCT010-09.OUT	0.9999	0.0010	206.5		4.31	0.0021
LEUCT010-10.OUT	1.0006	0.0009	206.9		4.31	0.0021
LEUCT010-11.OUT	0.9995	0.0008	207.2		4.31	0.0021
LEUCT010-12.OUT	0.9977	0.0009	207.5		4.31	0.0021
LEUCT010-13.OUT	0.9903	0.0009	207.7		4.31	0.0021
LEUCT010-14.OUT	0.9963	0.0010	194.9		4.31	0.0028
LEUCT010-15.OUT	0.9948	0.0009	195.4		4.31	0.0028
LEUCT010-16.OUT	0.9960	0.0008	195.8		4.31	0.0028
LEUCT010-17.OUT	0.9965	0.0009	196.1		4.31	0.0028
LEUCT010-18.OUT	0.9948	0.0009	196.3		4.31	0.0028
LEUCT010-19.OUT	0.9955	0.0008	196.7		4.31	0.0028
LEUCT010-20.OUT	0.9987	0.0009	195.4		4.31	0.0028
LEUCT010-21.OUT	0.9977	0.0009	195.8		4.31	0.0028
LEUCT010-22.OUT	0.9964	0.0008	196.4		4.31	0.0028
LEUCT010-23.OUT	0.9956	0.0009	196.7		4.31	0.0028
LEUCT010-24.OUT	0.9898	0.0010	186.6		4.31	0.0028
LEUCT010-25.OUT	0.9930	0.0009	187.7		4.31	0.0028
LEUCT010-26.OUT	0.9942	0.0009	188.6		4.31	0.0028
LEUCT010-27.OUT	0.9943	0.0010	189.5		4.31	0.0028

Case Name	k_{eff}	σ_{comp}	AEG	H/X①	Enrichment (wt% ^{235}U)	Benchmark Uncertainty σ_{exp}②
LEUCT010-28.OUT	0.9956	0.0010	190.4		4.31	0.0028
LEUCT010-29.OUT	0.9942	0.0011	191.1		4.31	0.0028
LEUCT010-30.OUT	0.9920	0.0010	192.8		4.31	0.0028
LEUCT049-01.OUT	0.9907	0.0009	169.7	40	5	0.0034
LEUCT049-02.OUT	0.9923	0.0008	169.7	40	5	0.0034
LEUCT049-03.OUT	0.9899	0.0009	168.9	40	5	0.0034
LEUCT049-04.OUT	0.9940	0.0008	168.7	40	5	0.0034
LEUCT049-05.OUT	0.9904	0.0008	177.2	50	5	0.0042
LEUCT049-06.OUT	0.9904	0.0009	177.1	50	5	0.0042
LEUCT049-07.OUT	0.9899	0.0009	177.6	50	5	0.0042
LEUCT049-08.OUT	0.9909	0.0008	176.6	50	5	0.0042
LEUCT049-09.OUT	0.9895	0.0009	182.8	60	5	0.0037
LEUCT049-10.OUT	0.9920	0.0009	182.7	60	5	0.0037
LEUCT049-11.OUT	0.9904	0.0009	182.8	60	5	0.0037
LEUCT049-12.OUT	0.9911	0.0009	182.0	60	5	0.0037
LEUCT049-13.OUT	0.9910	0.0009	174.5		5	0.0037
LEUCT049-14.OUT	0.9905	0.0011	174.5		5	0.0037
LEUCT049-15.OUT	0.9931	0.0009	174.4		5	0.0037
LEUCT049-16.OUT	0.9909	0.0010	177.6		5	0.0037
LEUCT049-17.OUT	0.9907	0.0008	176.7		5	0.0037
LEUCT049-18.OUT	0.9934	0.0008	178.8		5	0.0030

Notes:

① X refers to ^{235}U for the benchmark cases in this study. Where sufficient data was available, the effective H/^{235}U was calculated for the heterogeneous system of closely spaced uranium oxide rods and water moderator.

② The *International Handbook of Evaluated Criticality Safety Benchmark Experiment*s provides an benchmark uncertainty for each case approved for a benchmark. This uncertainty is based on evaluation of the effects of various errors and model simplifications on the calculated k_{eff} of the individual experiment.

Table 6.5-6 – Calculation of Low Enriched U-235 USL

Benchmark Set	Number of Cases	USL vs. AEG	USL vs. H/X	USL vs. ^{235}U Enrichment
^{235}U	82 (46)①	0.9339②	0.9393③	0.9353④
^{235}U + ^{233}U w/ Be	113	**0.9257**⑤	N/A	N/A

Notes:

① Calculated H/^{235}U values were provided for only 46 of the cases. The remaining cases consisted of heterogeneous solid fuel rod arrays.

② USL increases with AEG. Calculated benchmark AEGs ranged from 168.7 to 220.0. Range of applicability for this USL is 168.7 ≤ AEG ≤ 220 based on the USL at AEG = 168.7.

③ USL increases with H/^{235}U. Benchmark H/^{235}Us ranged from 40 to 1438. Range of applicability for this USL is 300 ≤ H/^{235}U ≤ 1438 based on the USL at H/^{235}U = 300.

④ USL increases with ^{235}U Enrichment. Benchmark enrichments ranged from 2.6 to 10.1 wt% ^{235}U. There are no benchmark experiments that extend enrichment to 0.96 wt% ^{235}U and based on ANSI/ANS, at and below this enrichment any aqueous, water-reflected systems are always subcritical. Consequently, evaluations of systems at 0.96 wt% ^{235}U will technically, by definition, fall outside the range of applicability of the USL. This USL is based on projections of the USL provided by USLSTATS method 1 equation to an enrichment of 0.96 wt% ^{235}U (which is conservatively lower than the value at 2.6 wt% ^{235}U). Range of applicability for this USL is 0.96 ≤ ^{235}U enrichment ≤ 10.1 based on the projected USL at ^{235}U enrichment of 0.96 wt% ^{235}U.

⑤ USL increases with AEG. Calculated benchmark AEGs ranged from 168.7 to 220.0. Range of applicability for this USL is 168.7 ≤ AEG ≤ 220 based on the USL at AEG = 168.7.

This page intentionally left blank.

7.0 OPERATING PROCEDURES

7.1 Procedures for Loading the Package

Loading the RH-TRU 72-B package for transport involves: 1) prior loading and measuring the payload canisters, 2) dry-loading the prepared payload canister into the RH-TRU 72-B package, 3) leakage rate testing the RH-TRU 72-B package outer cask (OC) and, optionally, the inner vessel (IV) seals, and (4) securing the external impact limiters to the RH-TRU 72-B package.

7.1.1 Loading the Payload Canister

The RH-TRU payload canister shall be prepared in accordance with the *Remote-Handled Transuranic Waste Authorized Methods for Payload Control* (RH-TRAMPAC)[1].

7.1.2 Loading the RH-TRU 72-B Package

This section delineates the procedures for loading the payload canister into the RH-TRU 72-B package. The package may be transported on either of two trailers, the Center-Pivot Trailer (CPT) or the Lift-Off Trailer (LOT). Because of differences in tie-down and loading/unloading method, the following procedures note where the differences exist and provide specific directions for each trailer.

The loading operation shall only be performed in a dry (no precipitation) environment. In the event of sudden precipitation during outdoor loading operations, precautions, such as covering the OC and IV cavities, shall be implemented to prevent water from entering the cavities. If precipitation enters the cavities, the free-standing water shall be removed. For the IV cavity, the payload canister shall be removed from the IV, and the IV cavity shall be dried using a vacuum system or absorbent materials attached to the end of a rod to remove the free-standing water. For the OC cavity, the payload canister shall be removed from the IV, the IV shall be removed from the OC, and the OC cavity shall be dried using a vacuum system or absorbent materials attached to the end of a rod to remove the free-standing water.

Only the lid shall be lifted by the pintle socket. If the IV is to be lifted, either empty or loaded, it shall be lifted using eyebolts in the holes on the lid, as indicated on the drawings in Appendix 1.3.1, *Packaging General Arrangement Drawings*. The approximate weight of the loaded IV is 12,023 pounds.

For all venting, loading, and unloading operations, ensure that appropriate controls are in place to control spread of contamination and protect against excessive personnel radiation exposure. The only special tools, other than standard socket sets for bolts and the lifting equipment for the package, are the leakage rate test tool and standard leakage rate test equipment, including the optional rate-of-rise leakage rate test equipment.

[1] U.S. Department of Energy (DOE), *Remote-Handled Transuranic Waste Authorized Methods for Payload Control* (RH-TRAMPAC), U.S. Department of Energy, Carlsbad Field Office, Carlsbad, New Mexico.

While disassembling the packaging in preparation for loading, the shipping facility personnel shall check the condition of the packaging components for acceptability. Damaged or defective components shall be replaced or suitably repaired before loading and reassembling the package for shipment.

Prior to loading, packaging surfaces shall be radiologically surveyed and checked for contamination, and the results of the checks shall be recorded.

If the OC lid has been removed, proceed directly to Paragraph 7.1.2.4. If both the OC and IV lids have been removed, proceed directly to Paragraph 7.1.2.7. Hereafter, reference to each RH-TRU 72-B package component may be found in Appendix 1.3.1, *Packaging General Arrangement Drawings*.

7.1.2.1 If possible, locate the RH-TRU 72-B package under a temporary structure or in a building where it will not be exposed to precipitation and remove the impact limiters.

CPT: Disconnect the fixed tie-down links, rotate the package to a vertical orientation about the package center-pivot trunnions, and secure.

LOT: Disconnect the main tie-down trunnion caps (may additionally include lower trunnion caps) and attach a lift yoke to the upper trunnions. Upend the package, rotating about the lower trunnions. Remove remaining tie-down caps, as necessary. Lift the package off the trailer and place in a vertical holding fixture, supported by the center-pivot trunnions.

7.1.2.2 Unscrew the OC lid gas sampling port closure bolt. As an option, install appropriate fittings into the OC lid gas sampling port to unscrew the gas sampling port closure bolt. The appropriate fittings will include a specially-designed tool that will allow manipulation of the gas sampling port closure bolt in predetermined increments. This tool will be referred to as a "test port tool".

7.1.2.3 Remove the eighteen (18), 1¼-7UNC bolts from the OC lid. Remove the lid and store in a protected area to preclude damage to the lid sealing surface.

7.1.2.4 If an optional OC sealing area protection device is to be used, install over the sealing area on the OC.

7.1.2.5 Unscrew the IV lid gas sampling port closure bolt. As an option, install a test port tool into the IV lid gas sampling port and rotate the knurled handle to unscrew the gas sampling port closure bolt.

7.1.2.6 Remove the eight (8), 7/8-9UNC bolts from the IV lid. Remove the lid and store in a protected area to preclude damage to the lid sealing surface.

7.1.2.7 If an optional IV sealing area/protection device is to be used, install over the sealing area on the IV. If an optional guide funnel or package loading collar is to be used, install over the package.

7.1.2.8 Transfer the payload canister into the IV. (If a horizontal transfer is planned, the package must be moved to the transfer fixture and downended prior to transfer.)

7.1.2.9 If necessary, upend the package prior to installing lids. If utilized in Paragraph 7.1.2.7, remove the optionally installed guide funnel and/or package loading collar, and remove the IV sealing area protection device from the IV.

7.1.2.10 Optionally clean and visually inspect the three O-ring seals on the IV lid in accordance with Section 8.2.3.4.1, *Sealing Area Routine Inspection and Repair*. Clean and visually inspect both O-ring seals on the OC lid, also in accordance with Section 8.2.3.4.1, *Sealing Area Routine Inspection and Repair*. Sparingly apply new vacuum grease to the seals. Replace the O-ring seals if the inspection reveals any condition that may affect the sealing capability of the elastomer seal. This may be done anytime prior to installation as long as the cleanliness is verified just prior to installation. Inspect and clean as necessary the seals on the test and vent/gas sample ports.

7.1.2.11 Optionally clean and visually inspect the sealing area on the IV body in accordance with Section 8.2.3.4.1, *Sealing Area Routine Inspection and Repair*.

7.1.2.12 Install the IV lid, tightening in a star pattern the eight (8), 7/8-9UNC bolts to 100 – 200 lb-ft torque.

7.1.2.13 If utilized in Paragraph 7.1.2.7, remove the guide funnel or package loading collar from the package.

7.1.2.14 Install the gas sampling port closure bolt and tighten to approximately 15 – 20 lb-ft torque.

7.1.2.15 Optionally perform a *Preshipment Leakage Rate* or *Maintenance Leakage Rate Test* per Appendix 7.4.1, *Preshipment Leakage Rate Test*, or Section 8.2.2, *Maintenance/Periodic Leakage Rate Tests*, respectively, on the IV body (using the seal test port, gas sampling port and backfill port seals).

(Maintenance leakage rate testing per Section 8.2.2, *Maintenance/Periodic Leakage Rate Tests*, is required if any containment O-ring seals are replaced.)

7.1.2.16 If utilized in Paragraph 7.1.2.4, remove the OC sealing area protection device from the OC.

7.1.2.17 Clean and visually inspect the sealing area on the OC body in accordance with Section 8.2.3.4.1, *Sealing Area Routine Inspection and Repair*.

7.1.2.18 Install the OC lid, tightening in a star pattern the eighteen (18), 1¼-7UNC bolts to 600 – 700 lb-ft torque.

7.1.2.19 If not previously done so in Paragraph 7.1.2.2, install a test port tool into the OC lid gas sampling port.

7.1.2.20 Utilizing the test port tool, install the gas sampling port closure bolt (tighten to approximately 15 – 20 lb-ft torque).

7.1.2.21 Perform a *Preshipment Leakage Rate* or *Maintenance Leakage Rate Test* per Appendix 7.4.1, *Preshipment Leakage Rate Test*, or Section 8.2.2, *Maintenance/Periodic Leakage Rate Tests*, respectively, on the OC body (using the seal test port and gas sampling port seals).

7.1.2.22 Monitor the radiation level to ensure the package meets the requirements of 10 CFR §71.47[2] and 49 CFR §173.441[3]. Survey the package surface and ensure that non-fixed contamination levels meet the requirements of 49 CFR §173.443.

7.1.2.23 CPT: Return the RH-TRU 72-B package to a horizontal orientation by rotating it about the center-pivot trunnions.

7.1.2.24 LOT: Return the RH-TRU 72-B package to the transport vehicle and downend it to a horizontal orientation by rotating it about its lower tie-down trunnions. (Lower tie-down trunnion caps may be secured prior to downending the package.)

7.1.2.25 Secure the package to the transport vehicle using the fixed tie-down links (CPT) or trunnion caps (LOT).

7.1.2.26 Install the impact limiters and secure each via the six (6), 1¼-7UNC impact limiter attachment bolts. Tighten the bolts to 600 – 700 lb-ft torque.

7.1.2.27 Install a bolt and flat washers into each of the two impact limiter lifting lugs on each impact limiter to preclude their use as a tie-down devices.

7.1.2.28 Install the tamper-indicating device.

7.1.2.29 Complete all necessary shipping papers in accordance with Subpart C of 49 CFR 172[4].

7.1.2.30 Package marking shall be in accordance with Subpart D, labeling shall be in accordance with Subpart E, and placarding shall be in accordance with Subpart F of 49 CFR 172[4].

---

[2] Title 10, Code of Federal Regulations, Part 71 (10 CFR 71), *Packaging and Transportation of Radioactive Material*, Final Rule, 01-26-04.

[3] Title 49, Code of Federal Regulations, Part 173 (49 CFR 173), *Shippers—General Requirements for Shipments and Packagings*, U.S. Department of Transportation, Washington, D.C., Current Version.

[4] Title 49, Code of Federal Regulations, Part 172 (49 CFR 172), *Hazardous Materials Table, Special Provisions, Hazardous Materials Communications, Emergency Response Information, and Training Requirements*, U.S. Department of Transportation, Washington, D.C., Current Version.

7.2 Procedures for Unloading the Package

In general, procedures for unloading the RH-TRU 72-B package are the reverse of Section 7.1.2, *Loading the RH-TRU 72-B Package*.

Upon receipt of the package, the receiving facility personnel shall check and record the condition of the tamper-indicating device. If the device shows damage, but there is no indication that the packaging containment was breached, the incident should be dispositioned under the requirements of 10 CFR 71[1]. If there are indications that packaging containment has been compromised (this would involve removal of the upper impact limiter, at a minimum), the incident should be treated as a substantial hazard to public safety, and dealt with under the requirements of 10 CFR §71.95 and the requirements of DOE Order 232.1[2].

Upon receipt of the package and removal of the impact limiters, rotate the package to a vertical orientation and secure, if the Center-Pivot Trailer (CPT) is used. The package may be unloaded while still on the CPT or, if desired, remove the trunnion restraints and lift the package off the trailer. If the Lift-Off Trailer (LOT) is used, upend the package, rotating about the lower trunnions, and lift the package off the trailer. After removal from either trailer, place the package into a vertical holding fixture, supported by the center-pivot trunnions. Prior to removing either the OC or IV lids, a test port tool shall be installed in the respective gas sampling port and the containment vessel gas shall be vented. After each vessel has been vented, the respective lid may be removed. Store the lids in a manner such that potential damage to the lids is minimized.

After unloading the package, the receiving facility personnel shall check the internal surfaces for contamination and record the findings. The shipping labeling shall be removed.

[1] Title 10, Code of Federal Regulations, Part 71 (10 CFR 71), *Packaging and Transportation of Radioactive Material*, Final Rule, 01-26-04.

[2] DOE Order 232.1, *Occurrence Reporting and Processing of Operations Information*, U.S. Department of Energy, Washington, D.C., Current Version.

This page intentionally left blank.

7.3 Preparation of an Empty Package for Transport

Previously used and empty (without contents but fully assembled) RH-TRU 72-B packages shall be handled per the requirements of 49 CFR §173.428[1]. Among other stipulations, the referenced regulation requires: 1) verification that the radiation on the external surface of the package does not exceed 0.5 millirem per hour, and 2) affixing an "EMPTY" label to the package. Leakage rate testing of the seals is not required for shipping an empty package meeting the requirements of 49 CFR §173.428.

7.3.1 Shipment of the Package as LSA Material

If the contents and the internal contamination of the package meet the definition of *Low Specific Activity* (LSA) material per 49 CFR §173.403[1], the RH-TRU 72-B package shall be handled per the requirements of 49 CFR §173.427 and shipped in accordance with the following.

7.3.1.1 With the package disassembled, verify that the contents, including internal contamination, meet the requirements of 49 CFR 173.403[1].

7.3.1.2 Close the inner vessel (IV) and outer cask (OC) in accordance with Paragraphs 7.1.2.9 through 7.1.2.13, Paragraphs 7.1.2.16 through 7.1.2.18, and Paragraphs 7.1.2.22 through 7.1.2.28 of Section 7.1.2, *Loading the RH-TRU 72-B Package*. Ensure all containment penetrations (i.e., vent ports, test ports, etc.) are properly sealed and covered.

7.3.1.3 If shipped in accordance with Section 7.3.1, *Shipment of the Package as LSA Material*, the package must be labeled as an LSA material shipment.

[1] Title 49, Code of Federal Regulations, Part 173 (49 CFR 173), *Shippers—General Requirements for Shipments and Packagings*, U.S. Department of Transportation, Washington, D.C., Current Version.

This page intentionally left blank.

7.4 Appendices

7.4.1 *Preshipment Leakage Rate Test*

This page intentionally left blank.

7.4.1 Preshipment Leakage Rate Test

After the RH-TRU 72-B package is assembled and prior to shipment, leakage rate testing shall be performed to confirm proper assembly of the package following the guidelines of Section 7.6, *Preshipment Leakage Rate Test*, and Appendix A.5.2, *Gas Pressure Rise*, of ANSI N14.5[1].

7.4.1.1 Gas Pressure Rise Leakage Rate Test Acceptance Criteria

In order to demonstrate containment integrity in preparation for shipment, no leakage shall be detected when tested to a sensitivity of 1×10^{-3} reference cubic centimeters per second (scc/s) air, or less, per Section 7.6, *Preshipment Leakage Rate Test*, of ANSI N14.5.

7.4.1.2 Determining the Test Volume and Test Time

1. Assemble a leakage rate test apparatus that consists of, at a minimum, the components illustrated in Figure 7.4-1, using a calibrated volume with a range of 100 – 500 cubic centimeters, and a calibrated pressure transducer with a minimum sensitivity of 100 millitorr. Connect the test apparatus to the test volume (i.e., the outer cask (OC) or inner vessel (IV) seal test or vent port, as appropriate).
2. Set the indicated sensitivity on the digital readout of the calibrated pressure transducer, ΔP, to, at a minimum, the resolution (i.e., sensitivity) of the calibrated pressure transducer (e.g, ΔP = 1, 10, or 100 millitorr for a pressure transducer with a 1 millitorr sensitivity).
3. Open all valves (i.e., the vent valve, calibration valve, and vacuum pump isolation valve), and record ambient atmospheric pressure, P_{atm}.
4. Isolate the calibrated volume by closing the vent and calibration valves.
5. Evacuate the test volume to a pressure less than the indicated sensitivity on the digital readout of the calibrated pressure transducer or 0.76 torr, whichever is less.
6. Isolate the vacuum pump from the test volume by closing the vacuum pump isolation valve. Allow the test volume pressure to stabilize and record the test volume pressure, P_{test} (e.g., P_{test} < 1 millitorr for an indicated sensitivity of 1 millitorr).
7. Open the calibration valve and, after allowing the system to stabilize, record the total volume pressure, P_{total}.
8. Knowing the calibrated volume, V_c, calculate and record the test volume, V_t, using the following equation:

$$V_t = V_c \left(\frac{P_{atm} - P_{total}}{P_{total} - P_{test}} \right)$$

9. Knowing the indicated sensitivity on the digital readout of the calibrated pressure transducer, ΔP, calculate and record the test time, t, using the following equation:

$$t = \Delta P(1.32)V_t$$

[1] ANSI N14.5-1997, *American National Standard for Radioactive Materials - Leakage Tests on Packages for Shipment,* American National Standards Institute, Inc. (ANSI).

7.4.1.3 Performing the Gas Pressure Rise Leakage Rate Test

1. Isolate the calibrated volume by closing the calibration valve.
2. Open the vacuum pump isolation valve and evacuate the test volume to a pressure less than the test volume pressure, P_{test}, determined in step 6 of Section 7.4.1.2, *Determining the Test Volume and Test Time*.
3. Isolate the vacuum pump from the test volume by closing the vacuum pump isolation valve. Allow the test volume pressure to stabilize and record the beginning test pressure, P_1. After a period of time equal to "t" seconds, determined in step 9 of Section 7.4.1.2, *Determining the Test Volume and Test Time*, record the ending test pressure, P_2. To be acceptable, there shall be no difference between the final and initial pressures such that the requirements of Section 7.4.1.1, *Gas Pressure Rise Leakage Rate Test Acceptance Criteria*, are met.
4. If, after repeated attempts, the O-ring seal fails to pass the leakage rate test, replace the damaged seal and/or repair the damaged sealing surfaces per Section 8.2.3.4.1, *Sealing Area Routine Inspection and Repair*. Perform verification leakage rate test per the applicable procedure delineated in Section 8.2.2, *Maintenance/Periodic Leakage Rate Tests*.

7.4.1.4 Optional Preshipment Leakage Rate Test

As an option to Section 7.4.1.3, *Performing the Gas Pressure Rise Leakage Rate Test*, Section 8.2.2, *Maintenance/Periodic Leakage Rate Tests*, may be performed.

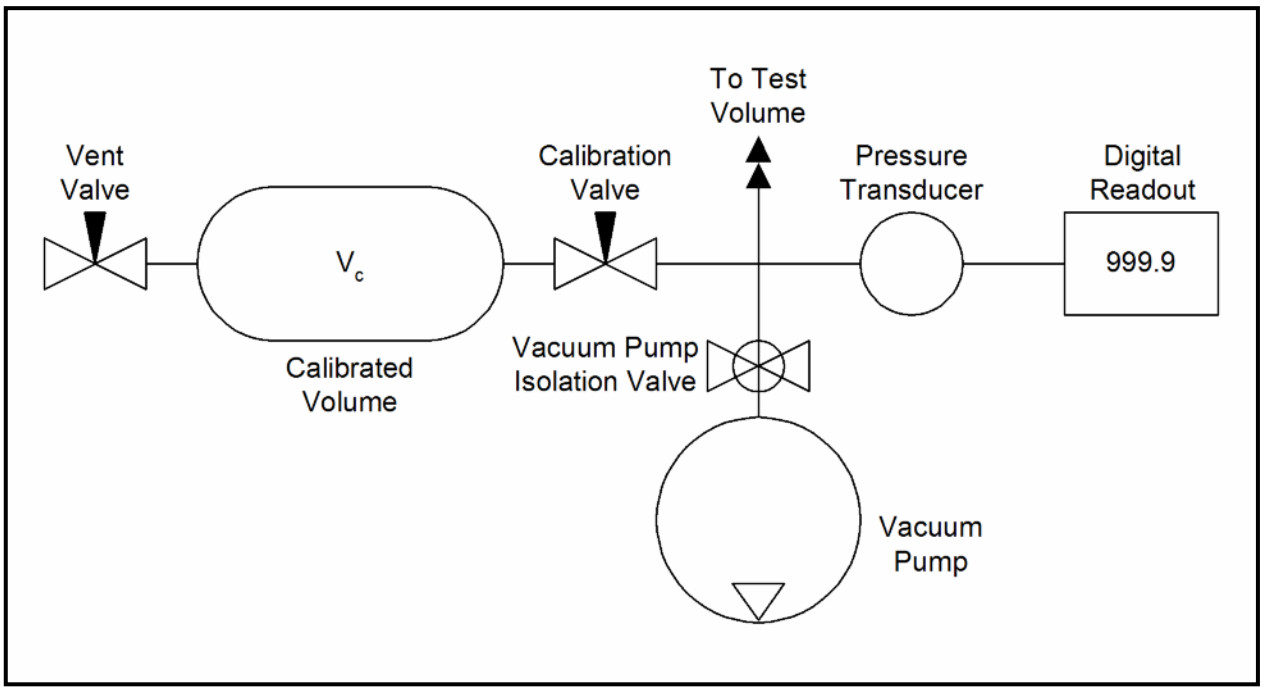

Figure 7.4-1 – Pressure Rise Leakage Rate Test Schematic

8.0 ACCEPTANCE TESTS AND MAINTENANCE PROGRAM

This section describes the acceptance test and the maintenance program that shall be used on the RH-TRU 72-B package in compliance with Subpart G of 10 CFR 71[1].

8.1 Acceptance Tests

This section discusses the tests to be performed prior to first use of the RH-TRU 72-B package.

8.1.1 Visual Inspection

All RH-TRU 72-B packaging materials of construction and welds shall be examined in accordance with requirements delineated on the drawings in Appendix 1.3.1, *Packaging General Arrangement Drawings*, per the requirements of 10 CFR 71.85(a)[1].

Each package shall be visually inspected to ensure that it is conspicuously and durably marked with its model number, serial number, gross weight, and packaging identification number, per the requirements of 10 CFR 71.85(c)[1].

8.1.2 Structural and Pressure Tests

8.1.2.1 Lifting Device Load Testing

The maximum working load for any pair of lifting/tie-down trunnions is 45,000 pounds, or 22,500 pounds per trunnion. Each pair of the lifting/tie-down trunnions shall be load tested to a minimum of 150% of their maximum working load, or 67,500 pounds.

The maximum working load of the two center-pivot trunnions is 45,000 pounds, or 22,500 pounds per trunnion. The pair of center-pivot trunnions shall be load tested to a minimum of 150% of their maximum working load, or 67,500 pounds.

The maximum working load for the inner vessel (IV) lift pintle socket is 4,000 pounds (1,390 pounds for the lid weight, plus 2,610 pounds for residual vacuum and lid separation force due to O-ring seal resistance). The IV lid lift pintle socket shall be load tested to 150% of the maximum working load, or 6,000 pounds.

The maximum working load for the outer cask (OC) lid lift pintle socket is 4,000 pounds (1,670 pounds for the lid weight, plus 2,330 pounds for residual vacuum and lid separation force due to O-ring seal resistance). The OC lid lift pintle socket shall be load tested to 150% of the maximum working load, or 6,000 pounds.

All accessible welds and adjacent base material (minimum 1/2-inch on each side of the weld) directly related to the load testing of the lifting devices shall be visually inspected for plastic deformation or cracking, and liquid penetrant inspected per ASME Boiler and Pressure Vessel

[1] Title 10, Code of Federal Regulations, Part 71 (10 CFR 71), *Packaging and Transportation of Radioactive Material*, Final Rule, 01-26-04.

Code, Section V[2], Article 6, and ASME Boiler and Pressure Vessel Code, Section III[3], Division 1, Subsection NB, Article NB-5000, as delineated on the drawings in Appendix 1.3.1, *Packaging General Arrangement Drawings*. Indications of cracking or distortion shall be recorded on a nonconformance report and dispositioned prior to final acceptance in accordance with the cognizant quality assurance program.

8.1.2.2 Inner Vessel and Outer Cask Pressure Testing

Per the requirements of 10 CFR §71.85(b) [1], the IV and OC shall be pressure tested to 150% of the maximum normal operating pressure (MNOP) to verify structural integrity. The MNOP of the IV and OC is equal to the 150 psig design pressure. Thus, each containment vessel shall be tested to 150 × 1.5 = 225 psig.

Following containment vessel pressure testing, all accessible welds and adjacent base material (minimum 1/2-inch on each side of the weld) directly related to the pressure testing of the containment vessels shall be visually inspected for plastic deformation or cracking, and liquid penetrant inspected per ASME Boiler and Pressure Vessel Code, Section V[2], Article 6, and ASME Boiler and Pressure Vessel Code, Section III[3], Division 1, Subsection NB, Article NB-5000. Indications of cracking or distortion shall be recorded on a nonconformance report and dispositioned prior to final acceptance in accordance with the cognizant quality assurance program.

8.1.3 Fabrication Leakage Rate Tests

Fabrication Leakage Rate Testing shall conform to the requirements of Section 7.3 of ANSI N14.5[4].

The *Fabrication Leakage Rate Test* shall be performed after the structural and/or pressure test(s) delineated in Section 8.1.2, *Structural and Pressure Tests*, above, to verify package configuration and performance to design criteria.

To begin the test, the IV is assumed separate from the OC, and the lids of each are removed. The *Fabrication Leakage Rate Test* is separated into seven (7) tests, four (4) for the IV and three (3) for the OC. The seven (7) separate tests are: 1) IV structure integrity, 2) IV lid seal integrity, 3) IV gas sampling port closure bolt seal integrity, 4) IV backfill port seal integrity, 5) OC structure integrity, 6) OC lid seal integrity, and 7) OC gas sampling port closure bolt seal integrity.

8.1.3.0.1 Obtain a helium mass spectrometer leak detector capable of detecting a leak of 5×10^{-8} standard cubic centimeters per second (scc/s), air, or better (1.3×10^{-7} scc/s, helium).

8.1.3.0.2 Calibrate the leak detector to a minimum sensitivity of 5×10^{-8} scc/s, air (1.3×10^{-7} scc/s, helium).

---

[2] American Society of Mechanical Engineers (ASME) Boiler and Pressure Vessel Code, Section V, *Nondestructive Examination*, 1986 Edition.

[3] American Society of Mechanical Engineers (ASME) Boiler and Pressure Vessel Code, Section III, *Rules for Construction of Nuclear Power Plant Components*, 1986 Edition.

[4] ANSI N14.5-1997, *American National Standard for Radioactive Materials – Leakage Tests on Packages for Shipment,* American National Standards Institute, Inc. (ANSI).

8.1.3.1 Testing the IV Structure Integrity

The *Fabrication Leakage Rate Test* of the IV structure shall be performed per Section A.5.4, *Evacuated Envelope – Gas Detector*, or Section A.5.3, *Gas Filled Envelope – Gas Detector*, of ANSI N14.5[4]. For testing the IV structure integrity using the *Evacuated Envelope Method*, go to Section 8.1.3.1.1, *Testing the IV Structure Integrity – Evacuated Envelope Method*, and for testing the IV structure integrity using the *Gas Filled Envelope Method*, go to Section 8.1.3.1.2, *Testing the IV Structure Integrity – Gas Filled Envelope Method*.

8.1.3.1.1 Testing the IV Structure Integrity – Evacuated Envelope Method

8.1.3.1.1.1 The IV shall be assembled with all three main O-ring seals installed in the IV lid. Assembly is as shown on the drawing in Appendix 1.3.1, *Packaging General Arrangement Drawings*.

8.1.3.1.1.2 Install the assembled IV into a functional OC body.

8.1.3.1.1.3 Install a test port tool into the IV gas sampling port.

8.1.3.1.1.4 Fully retract the IV gas sampling port closure bolt by rotating the cap on the test port tool to the fully open position.

8.1.3.1.1.5 Connect a vacuum pump to the IV gas sampling port.

8.1.3.1.1.6 Evacuate the IV cavity through the gas sampling port to 90% vacuum or better (≤10% ambient atmospheric pressure). Isolate the vacuum pump from the system.

8.1.3.1.1.7 Provide a helium atmosphere in the cavity of the IV by backfilling with helium gas to a pressure slightly greater than atmospheric pressure (+1 psi, -0 psi) and close the valve to isolate the source of helium gas from the system. Correction for tracer gas concentration shall be performed.

8.1.3.1.1.8 Install the IV gas sampling port closure bolt using the test port tool and tighten to 15 – 20 lb-ft torque.

8.1.3.1.1.9 Remove the IV test port tool.

8.1.3.1.1.10 Remove the OC gas sampling port closure bolt and install the OC lid.

8.1.3.1.1.11 Evacuate air from the OC/IV annulus through the OC gas sampling port until the vacuum is sufficient to operate the helium mass spectrometer leak detector.

8.1.3.1.1.12 Perform the leakage rate test to the requirements of Section 8.1.3.8, *Fabrication Leakage Rate Test Acceptance Criteria*. If after repeated attempts, the IV structure fails to pass the leakage rate test, isolate the leak path and, prior to repairing the leak path and repeating the IV structure leakage rate test, record the results of the test and any recommended actions for disposition in accordance with the requirements of the cognizant quality assurance program.

8.1.3.1.2 Testing the IV Structure Integrity – Gas Filled Envelope Method

8.1.3.1.2.1 The IV shall be assembled with all three main O-ring seals installed in the lid. Assembly is as shown on the drawing in Appendix 1.3.1, *Packaging General Arrangement Drawings*.

8.1.3.1.2.2 Remove the IV gas sampling port closure bolt and install the helium mass spectrometer to the IV gas sampling port.

8.1.3.1.2.3 Surround the assembled IV with an envelope.

8.1.3.1.2.4 Evacuate the IV cavity through the IV gas sampling port until the vacuum is sufficient to operate the helium mass spectrometer leak detector.

8.1.3.1.2.5 Provide a helium environment at a pressure slightly above one atmosphere around the exterior of the IV, taking care to purge all other gases from any pockets or cavities adjacent to the vessel.

8.1.3.1.2.6 Determine the leakage rate of the system. Per Section A.3.6, *Tracer Gas Partial Pressure*, of ANSI N14.5[4], the measured leakage rate shall conservatively be multiplied by a factor of two to account for the less than 100% concentration of the helium in the envelope surrounding the IV.

8.1.3.1.2.7 Perform the leakage rate test to the requirements of Section 8.1.3.8, *Fabrication Leakage Rate Test Acceptance Criteria*. If after repeated attempts, the IV structure fails to pass the leakage rate test, isolate the leak path and, prior to repairing the leak path and repeating the IV structure leakage rate test, record the results of the test and any recommended actions for disposition in accordance with the requirements of the cognizant quality assurance program.

8.1.3.2 Testing the IV Lid Seal Integrity

8.1.3.2.1 The *Fabrication Leakage Rate Test* of the IV lid middle seal shall be performed per Section A.5.4, *Evacuated Envelope – Gas Detector*, of ANSI N14.5[4].

8.1.3.2.2 The IV shall be assembled with all three main O-ring seals installed in the IV lid. Assembly is as shown on the drawing in Appendix 1.3.1, *Packaging General Arrangement Drawings*.

8.1.3.2.3 Attach a vacuum pump and a source of helium gas, in parallel, to the backfill port. Fittings will include a specially-designed tool that will maintain a leak-tight interface between the backfill port and the helium supply/vacuum pump, while allowing manipulation of the backfill port closure bolt. This tool will be referred to as a "test port tool." Install valves on each of the lines to allow independent isolation of the vacuum pump and the source of helium gas to the backfill port. Close the valve to the source of helium gas, and open the valve to the vacuum pump. Figure 8.1-1 provides a schematic of this configuration.

8.1.3.2.4 Utilizing the test port tool, rotate the backfill port closure bolt fully open.

8.1.3.2.5 Evacuate the system to 90% vacuum or better (≤10% ambient atmospheric pressure). Isolate the vacuum pump from the system.

8.1.3.2.6 Provide a helium atmosphere inside the evacuated cavity by backfilling with helium gas to a pressure slightly greater than atmospheric pressure (+1 psi, -0 psi) and close the valve to isolate the source of helium gas from the system. Correction for tracer gas concentration shall be performed.

8.1.3.2.7 Utilizing the test port tool, rotate the backfill port closure bolt closed and tighten to 15 – 20 lb-ft torque.

8.1.3.2.8 Remove the helium-contaminated test port tool from the backfill port.

8.1.3.2.9 Install a clean (helium-free) test port tool into the seal test port.

8.1.3.2.10 Attach a leak detector to the test port tool.

8.1.3.2.11 Utilizing the test port tool, rotate the seal test port closure bolt fully open.

8.1.3.2.12 Evacuate the cavity above the lid containment seal until the vacuum is sufficient to operate the leak detector.

8.1.3.2.13 Determine the leakage rate of the system using the leak detector.

8.1.3.2.14 Perform the leakage rate test to the requirements of Section 8.1.3.8, *Fabrication Leakage Rate Test Acceptance Criteria*. If after repeated attempts, the IV lid containment seal fails to pass the leakage rate test, isolate the leak path and, prior to repairing the leak path and repeating the IV lid containment seal leakage rate test, record the results of the test and any recommended actions for disposition in accordance with the requirements of the cognizant quality assurance program.

8.1.3.3 Testing the IV Gas Sampling Port Closure Bolt Seal Integrity

8.1.3.3.1 The *Fabrication Leakage Rate Test* of the IV gas sampling port closure bolt containment seal shall be performed per Section A.5.4, *Evacuated Envelope – Gas Detector*, of ANSI N14.5[4].

8.1.3.3.2 The IV shall be assembled with all three main O-ring seals installed in the IV lid. Assembly is as shown on the drawing in Appendix 1.3.1, *Packaging General Arrangement Drawings*.

8.1.3.3.3 Verify the presence of a helium atmosphere below the gas sampling port closure bolt containment seal, as provided for in Paragraphs 8.1.3.2.3 through 8.1.3.2.8.

8.1.3.3.4 Tighten the IV gas sampling port closure bolt to 15 – 20 lb-ft torque.

8.1.3.3.5 Install a test port tool into the gas sampling port.

8.1.3.3.6 Attach a leak detector to the test port tool.

8.1.3.3.7 Evacuate the cavity above the gas sampling port closure bolt containment seal until the vacuum is sufficient to operate the leak detector.

8.1.3.3.8 Determine the leakage rate of the system using the leak detector.

8.1.3.3.9 Perform the leakage rate test to the requirements of Section 8.1.3.8, *Fabrication Leakage Rate Test Acceptance Criteria*. If after repeated attempts, the IV gas sampling port closure bolt containment seal fails to pass the leakage rate test, isolate the leak path and, prior to repairing the leak path and repeating the IV gas sampling port closure bolt containment seal leakage rate test, record the results of the test and any recommended actions for disposition in accordance with the requirements of the cognizant quality assurance program.

8.1.3.4 Testing the IV Backfill Port Closure Bolt Seal Integrity

8.1.3.4.1 The *Fabrication Leakage Rate Test* of the IV backfill port closure bolt containment seal shall be performed per Section A.5.4, *Evacuated Envelope – Gas Detector*, of ANSI N14.5[4].

8.1.3.4.2 The IV shall be assembled with all three main O-ring seals installed in the IV lid. Assembly is as shown on the drawing in Appendix 1.3.1, *Packaging General Arrangement Drawings*.

8.1.3.4.3 Verify the presence of a helium atmosphere below the backfill port closure bolt containment seal, as provided for in Paragraphs 8.1.3.2.3 through 8.1.3.2.8.

8.1.3.4.4 Install a clean (helium-free) test port tool into the backfill port. Attach a leak detector to the test port tool.

8.1.3.4.5 Evacuate the cavity above the backfill port closure bolt until the vacuum is sufficient to operate the leak detector.

8.1.3.4.6 Determine the leakage rate of the system using the leak detector.

8.1.3.4.7 Perform the leakage rate test to the requirements of Section 8.1.3.8, *Fabrication Leakage Rate Test Acceptance Criteria*. If after repeated attempts, the IV backfill port closure bolt containment seal fails to pass the leakage rate test, isolate the leak path and, prior to repairing the leak path and repeating the IV backfill port closure bolt containment seal leakage rate test, record the results of the test and any recommended actions for disposition in accordance with the requirements of the cognizant quality assurance program.

8.1.3.5 Testing the OC Structure Integrity

8.1.3.5.1 The *Fabrication Leakage Rate Test* of the OC structure shall be performed per Section A.5.3, *Gas Filled Envelope – Gas Detector*, of ANSI N14.5[4]. During fabrication, the OC containment shell shall be leakage rate tested prior to lead installation. Special lids and IV mock ups may be used for this component test. To test the OC structure in its entirety, the following steps shall be used.

8.1.3.5.2 As an option, remove the OC lid and install a functional or mock-up IV within the OC cavity for volume reduction.

8.1.3.5.3 Assemble the OC with both main O-ring seals installed in the OC lid. Assembly is as shown on the drawing in Appendix 1.3.1, *Packaging General Arrangement Drawings*.

8.1.3.5.4 Remove the OC gas sampling port closure bolt and install the helium mass spectrometer leak detector to the OC gas sampling port.

8.1.3.5.5 Surround the assembled OC with an envelope.

8.1.3.5.6 Evacuate the OC internal cavity annulus through the OC gas sampling port until the vacuum is sufficient to operate the helium mass spectrometer leak detector.

8.1.3.5.7 Provide helium at a pressure slightly above one atmosphere about the exterior of the OC, taking care to purge all other gases from any pockets or cavities adjacent to the vessel.

8.1.3.5.8 Determine the leakage rate of the system using the leak detector. Per Section A.3.6, *Tracer Gas Partial Pressure*, of ANSI N14.5[4], the measured leakage rate shall conservatively be multiplied by a factor of two to account for the less than 100% concentration of the helium in the envelope surrounding the OC.

8.1.3.5.9 Perform the leakage rate test to the requirements of Section 8.1.3.8, *Fabrication Leakage Rate Test Acceptance Criteria*. If after repeated attempts, the OC structure fails to pass the leakage rate test, isolate the leak path and, prior to repairing the leak path and repeating the OC structure leakage rate test, record the results for disposition in accordance with the requirements of the cognizant quality assurance program.

8.1.3.6 Testing the OC Lid Seal Integrity

8.1.3.6.1 The Fabrication Leakage Rate Test of the OC lid seal shall be performed per Section A.5.4, *Evacuated Envelope – Gas Detector*, of ANSI N14.5[4].

8.1.3.6.2 The OC shall be assembled with both main O-ring seals installed in the OC lid. Assembly is as shown on the drawing in Appendix 1.3.1, *Packaging General Arrangement Drawings*.

8.1.3.6.3 Install a test port tool into the OC gas sampling port.

8.1.3.6.4 Utilizing the test port tool, rotate the OC gas sampling port closure bolt fully open.

8.1.3.6.5 Attach a vacuum pump and a source of helium gas, in parallel, to the test port tool. Install valves on each of the lines to allow independent isolation of the vacuum pump and the source of helium gas to the test port tool. Close the valve to the source of helium gas, and open the valve to the vacuum pump. Figure 8.1-2 provides a schematic of this configuration.

8.1.3.6.6 Evacuate the system through the gas sampling port to 90% vacuum or better (≤10% ambient atmospheric pressure). Isolate the vacuum pump from the system.

8.1.3.6.7 Backfill with helium gas to a pressure slightly greater than atmospheric pressure (+1 psi, -0 psi) and close the valve to isolate the source of helium gas from the system. Correction for tracer gas concentration shall be performed.

8.1.3.6.8 Utilizing the test port tool, rotate the gas sampling port closure bolt closed, and tighten to 15 – 20 lb-ft torque.

8.1.3.6.9 Remove the helium-contaminated test port tool from the gas sampling port.

8.1.3.6.10 Install a clean (helium-free) test port tool into the seal test port.

8.1.3.6.11 Attach the leak detector to the test port tool.

8.1.3.6.12 Utilizing the test port tool, rotate the seal test port closure bolt fully open.

8.1.3.6.13 Evacuate the system through the test port tool until the vacuum is sufficient to operate the leak detector.

8.1.3.6.14 Determine the leakage rate of the system using the leak detector.

8.1.3.6.15 Perform the leakage rate test to the requirements of Section 8.1.3.8, *Fabrication Leakage Rate Test Acceptance Criteria*. If after repeated attempts, the OC lid containment seal fails to pass the leakage rate test, isolate the leak path and, prior to repairing the leak path and repeating the OC lid containment seal leakage rate test, record the results for disposition in accordance with the requirements of the cognizant quality assurance program.

8.1.3.7 Testing the OC Gas Sampling Port Closure Bolt Seal Integrity

8.1.3.7.1 The *Fabrication Leakage Rate Test* of the OC gas sampling port closure bolt containment seal shall be performed per Section A.5.4, *Evacuated Envelope – Gas Detector*, of ANSI N14.5[4].

8.1.3.7.2 The OC shall be assembled with both main O-ring seals installed in the OC lid. Assembly is as shown on the drawing in Appendix 1.3.1, *Packaging General Arrangement Drawings*.

8.1.3.7.3 Verify the presence of a helium atmosphere below the gas sampling port closure bolt containment seal, as provided for in Paragraphs 8.1.3.6.3 through 8.1.3.6.9.

8.1.3.7.4 Install a clean (helium-free) test port tool into the gas sampling port. Attach a leak detector to the test port tool.

8.1.3.7.5 Evacuate the cavity above the gas sampling port closure bolt until the vacuum is sufficient to operate the leak detector.

8.1.3.7.6 Determine the leakage rate of the system using the leak detector.

8.1.3.7.7 Perform the leakage rate test to the requirements of Section 8.1.3.8, *Fabrication Leakage Rate Test Acceptance Criteria*. If after repeated attempts, the OC gas sampling port closure bolt containment seal fails to pass the leakage rate test, isolate the leak path and, prior to repairing the leak path and repeating the OC gas sampling port closure bolt containment seal leakage rate test, record the results for disposition in accordance with the requirements of the cognizant quality assurance program.

8.1.3.8 Fabrication Leakage Rate Test Acceptance Criteria

8.1.3.8.1 To be acceptable, per Section 6.3.2, *Application of Referenced Air Leakage Rate*, of ANSI N14.5[4], each vessel test and each containment seal test shall demonstrate a leakage rate of 1×10^{-7} scc/s, air, (leaktight) (2.6×10^{-7} helium), or less.

8.1.3.8.2 In order to demonstrate that the package is leaktight, per Section 8.4, *Sensitivity*, of ANSI N14.5[4], the sensitivity of the leakage rate test procedure shall be 5×10^{-8} scc/s, air (1.3×10^{-7} helium), or less.

8.1.3.8.3 Indications of non-conformance with the above stated standards shall be recorded for disposition prior to repair and final acceptance in accordance with the requirements of the cognizant quality assurance program.

8.1.4 Component Tests

8.1.4.1 Polyurethane Foam

This section establishes the requirements and acceptance criteria for installation, inspection, and testing of rigid, closed cell, polyurethane foam utilized within the RH-TRU 72-B packaging.

8.1.4.1.1 Introduction and General Requirements

The polyurethane foam used within the RH-TRU 72-B packaging is comprised of a specific "formulation" of foam constituents that, when properly apportioned, mixed, and reacted, produce a polyurethane foam material with physical characteristics consistent with the requirements given in this section. In practice, the chemical constituents are batched into multiple parts (e.g., parts A and B) for later mixing in accordance with a formulation. Therefore, a foam "batch" is considered to be a specific grouping and apportionment of chemical constituents into separate and controlled vats or bins for each foam formulation part. Portions from each batch part are combined in accordance with the foam formulation requirements to produce the liquid foam material for pouring into a component. Thus, a foam "pour" is defined as apportioning and mixing the batch parts into a desired quantity for subsequent installation (pouring).

The following sections describe the general requirements for chemical composition, constituent storage, foamed component preparation, foam material installation, and foam pour and test data records.

8.1.4.1.1.1 Polyurethane Foam Chemical Composition

The foam supplier shall certify that the chemical composition of the polyurethane foam is as delineated below, with the chemical component weight percents falling within the specified ranges. In addition, the foam supplier shall certify that the finished (cured) polyurethane foam does not contain halogen-type flame retardants or trichloromonofluoromethane (Freon 11).

Carbon	50% – 70%	Phosphorus	0% – 2%
Oxygen	14% – 34%	Silicon	< 1%
Nitrogen	4% – 12%	Chlorine	< 1%
Hydrogen	4% – 10%	Other	< 1%

8.1.4.1.1.2 Polyurethane Foam Constituent Storage

The foam supplier shall certify that the polyurethane foam constituents have been properly stored prior to use, and that the polyurethane foam constituents have been used within their shelf life.

8.1.4.1.1.3 Foamed Component Preparation

Prior to polyurethane foam installation, the foam supplier shall verify that an anti-bond agent, such as Johnson's Wax, has been applied to all of the component shell interior surfaces. In addition, due to the internal pressures generated during the foam pouring/curing process, the foam supplier shall visually verify that adequate bracing/shoring of the component shells is provided to maintain the dimensional configuration throughout the foam pouring/curing process.

8.1.4.1.1.4 Polyurethane Foam Installation

The direction of foam rise shall be vertically aligned with the shell component axis.

The surrounding walls of the component shell where the liquid foam material is to be installed shall be between 55 ºF and 95 ºF prior to foam installation. Measure and record the component shell temperature to an accuracy of ±2 ºF prior to foam installation.

In the case of multiple pours into a single foamed component, the cured level of each pour shall be measured and recorded to an accuracy of ±1 inch.

Measure and record the weight of liquid foam material installed during each pour to an accuracy of ±10 pounds.

All test samples shall be poured into disposable containers at the same time as the actual pour it represents, clearly marking the test sample container with the pour date and a unique pour identification number. All test samples shall be cut from a larger block to obtain freshly cut faces. Prior to physical testing, each test sample shall be cleaned of superfluous foam dust.

8.1.4.1.1.5 Polyurethane Foam Pour and Test Data Records

A production pour and testing record shall be compiled by the foam supplier during the foam pouring operation and subsequent physical testing. Upon completion of production and testing, the foam supplier shall issue certification referencing the production record data and test data pertaining to each foamed component. At a minimum, relevant pour and test data shall include:

- formulation, batch, and pour numbers, with foam material traceability, and pour date,
- foamed component description, part number, and serial number,
- instrumentation description, serial number, and calibration due date,
- pour and test data (e.g., date, temperature, dimensional, and/or weight measurements, thermal conductivity, compressive stress, etc., as applicable), and
- technician and Quality Assurance/Quality Control (QA/QC) sign-off.

8.1.4.1.2 Physical Characteristics

The following subsections define the required physical characteristics of the polyurethane foam material used for the RH-TRU 72-B packaging design.

Testing for the various polyurethane foam physical characteristics is based on a “formulation”, “batch”, or “pour”, as appropriate, as defined in Section 8.1.4.1.1, *Introduction and General Requirements*. The physical characteristics determined for a specific foam formulation are relatively insensitive to small variations in chemical constituents and/or environmental conditions, and therefore include physical testing for thermal conductivity, specific heat, and leachable chlorides. Similarly, the physical characteristics determined for a batch are only slightly sensitive to small changes in formulation and/or environmental conditions during batch mixing, and therefore include physical testing for flame retardancy and intumescence. Finally, the physical characteristics determined for a pour are also only slightly sensitive to small changes in formulation and slightly more sensitive to variations in environmental conditions during pour mixing, and therefore include physical testing for density and compressive stress.

8.1.4.1.2.1 Physical Characteristics Determined for a Foam Formulation

1. Foam material physical characteristics for the following parameters shall be determined once for a particular foam formulation. If multiple components are to be foamed utilizing a specific foam formulation, then additional physical testing, as defined below, need not be performed.

8.1.4.1.2.1.1 Thermal Conductivity

1. The thermal conductivity test shall be performed using a heat flow meter (HFM) apparatus. The HFM establishes steady state unidirectional heat flux through a test specimen between two parallel plates at constant but different temperatures. By measurement of the plate temperatures and plate separation, Fourier's law of heat conduction is used by the HFM to automatically calculate thermal conductivity. Description of a typical HFM is provided in ASTM C518[5]. The HFM shall be calibrated against a traceable reference specimen per the HFM manufacturer's operating instructions.

2. Three (3) test samples shall be taken from the sample pour. Each test sample shall be of sufficient size to enable testing per the HFM manufacturer's operating instructions.

3. Measure and record the necessary test sample parameters as input data to the HFM per the HFM manufacturer's operating instructions.

4. Perform thermal conductivity testing and record the measured thermal conductivity for each test sample following the HFM manufacturer's operating instructions.

5. Determine and record the average thermal conductivity of the three test samples. The numerically averaged thermal conductivity of the three test samples shall be 0.019 Btu/hr-ft-ºF ±20% (i.e., within the range of 0.016 to 0.022 Btu/hr-ft-ºF).

8.1.4.1.2.1.2 Specific Heat

1. The specific heat test shall be performed using a differential scanning calorimeter (DSC) apparatus. The DSC establishes a constant heating rate and measures the differential heat flow into both a test specimen and a reference specimen. Description of a typical DSC is provided in ASTM E1269[6]. The DSC shall be calibrated against a traceable reference specimen per the DSC manufacturer's operating instructions.

2. Three (3) test samples shall be taken from the sample pour. Each test sample shall be of sufficient size to enable testing per the DSC manufacturer's operating instructions.

3. Measure and record the necessary test sample parameters as input data to the DSC per the DSC manufacturer's operating instructions.

4. Perform specific heat testing and record the measured specific heat for each test sample following the DSC manufacturer's operating instructions.

---

[5] ASTM C518-04, *Standard Test Method for Steady-State Heat Flux Measurements and Thermal Transmission Properties by Means of the Heat Flux Meter Apparatus*, American Society for Testing and Materials, Philadelphia, PA, Volume 04.06, 2004.

[6] ASTM E1269-05, *Standard Test Method for Determining Specific Heat Capacity by Differential Scanning Calorimetry*, American Society for Testing and Materials, Philadelphia, PA, Volume 14.02, 2005.

5. Determine and record the average specific heat of the three test specimens. The numerically averaged specific heat at 77 °F of the three test samples shall be 0.30 Btu/lb-ºF ±20% (i.e., within the range of 0.24 to 0.36 Btu/lb-ºF).

8.1.4.1.2.1.3 Leachable Chlorides

1. The leachable chlorides test shall be performed using an ion chromatograph (IC) apparatus. The IC measures inorganic anions of interest (i.e., chlorides) in water. Description of a typical IC is provided in EPA Method 300.0[7]. The IC shall be calibrated against a traceable reference specimen per the IC manufacturer's operating instructions.
2. One (1) test sample shall be taken from the sample pour. The test sample shall be a cube with dimensions of 2.00 ±0.03 inches.
3. Place the test sample in a room (ambient) temperature environment (i.e., 65 ºF to 85 ºF) for sufficient time to thermally stabilize the test sample. Measure and record the room temperature to an accuracy of ±2 ºF.
4. Measure and record the thickness, width, and length of each test sample to an accuracy of ±0.001 inches.
5. Obtain a minimum of 550 ml of distilled or de-ionized water for testing. The test water shall be from a single source to ensure consistent anionic properties for testing control.
6. Obtain a 400 ml, or larger, contaminant free container that is capable of being sealed. Fill the container with 262 ±3 ml of test water. Fully immerse the test sample inside the container for a duration of 72 ±3 hours. If necessary, use an inert standoff to ensure the test sample is completely immersed for the full test duration. Seal the container prior to the 72 hour duration.
7. Obtain a second, identical container to use as a "control". Fill the control container with 262 ±3 ml of the same test water. Seal the control container for a 72 ±3 hour duration.
8. At the end of the test period, measure and record the leachable chlorides in the test water per the IC manufacturer's operating instructions. The leachable chlorides in the test water shall not exceed one part per million (1 ppm).
9. Should leachable chlorides in the test water exceed 1 ppm, measure and record the leachable chlorides in the test water from the "control" container. The difference in leachable chlorides from the test water and "control" water sample shall not exceed 1 ppm.

8.1.4.1.2.2 Physical Characteristics Determined for a Foam Batch

Foam material physical characteristics for the following parameters shall be determined once for a particular foam batch based on the batch definition from Section 8.1.4.1.1, *Introduction and General Requirements*. If a single or multiple components are to be poured utilizing multiple pours from a single foam batch, then additional physical testing, as defined below, need not be performed for each foam pour.

[7] EPA Method 300.0, *Determination of Inorganic Anions in Water by Ion Chromatography*, U.S. Environmental Protection Agency.

8.1.4.1.2.2.1 Flame Retardancy

1. Three (3) test samples shall be taken from a pour from each foam batch. Each test sample shall be a rectangular prism with nominal dimensions of 0.5 inches thick, 3.0 inches wide, and a minimum length of 6.0 inches. In addition, individual sample lengths must not be less than the total burn length observed for the sample when tested.
2. Place the test samples in a room (ambient) temperature environment (i.e., 65ºF to 85ºF) for sufficient time to thermally stabilize the test samples. Measure and record the room temperature to an accuracy of ±2ºF.
3. Measure and record the length of each test sample to an accuracy of ±0.1 inches.
4. Install a Ø3/8 inches (10 mm), or larger, Bunsen or Tirrill burner inside an enclosure of sufficient size to perform flame retardancy testing. Adjust the burner flame height to 1½ ±1/8 inches. Verify that the burner flame temperature is 1,550 ºF, minimum.
5. Support the test sample with the long axis oriented vertically within the enclosure such that the test sample's bottom edge will be 3/4 ±1/16 inches above the top edge of the burner.
6. Move the burner flame under the test sample for an elapsed time of 60 ±2 seconds. As illustrated, align the burner flame with the front edge of the test sample thickness and the center of the test sample width.

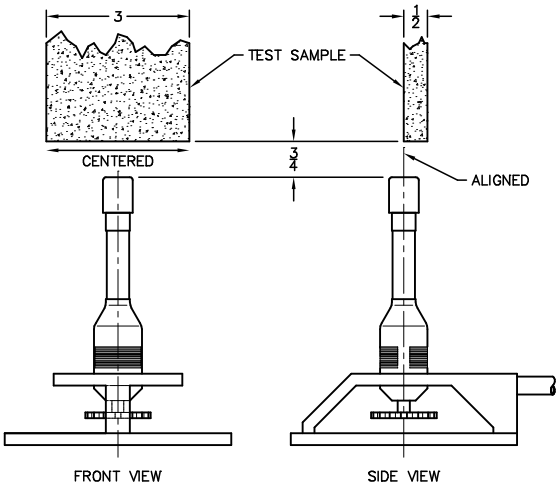

7. Immediately after removal of the test sample from the burner flame, measure and record the following data:
   a. Measure and record, to the nearest second, the elapsed time until flames from the test sample extinguish.
   b. Measure and record, to the nearest second, the elapsed time from the occurrence of drips, if any, until drips from the test sample extinguish.
   c. Measure and record, to the nearest 0.1 inches, the burn length following cessation of all visible burning and smoking.
8. Flame retardancy testing acceptance is based on the following criteria:
   a. The numerically averaged flame extinguishment time of the three test samples shall not exceed fifteen (15) seconds.
   b. The numerically averaged flame extinguishment time of drips from the three test samples shall not exceed three (3) seconds.
   c. The numerically averaged burn length of the three test samples shall not exceed six (6) inches.

8.1.4.1.2.2.2 Intumescence

1. Three (3) test samples shall be taken from a pour from each foam batch. Each test sample shall be a cube with nominal dimensions of 2.0 inches.
2. Place the test samples in a room (ambient) temperature environment (i.e., 65 ºF to 85 ºF) for sufficient time to thermally stabilize the test samples. Measure and record the room temperature to an accuracy of ±2 ºF.
3. Preheat a furnace to 1,475 ºF ±18 ºF.
4. Identify two opposite faces on each test sample as the thickness direction. The thickness dimension shall be in the parallel-to-rise direction. Measure and record the initial thickness (t_i) of each test sample to an accuracy of ±0.01 inches.
5. Mount a test sample onto a fire resistant fiberboard, with one face of the thickness direction contacting to the board. As illustrated above, the test samples may be mounted by installing onto a 12 to 16 gauge wire (Ø0.105 to Ø0.063 inches, respectively) of sufficient length, oriented perpendicular to the fiberboard face. The test samples may be pre-drilled with an undersized hole to allow installation onto the wire.

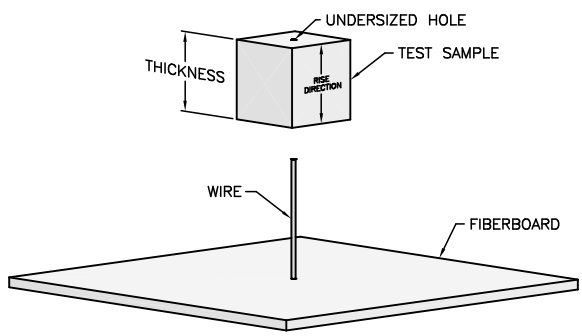

6. Locate the test sample/fiberboard assembly over the opening of the pre-heated furnace for a 90 ±3 second duration. After removal of the test sample/fiberboard assembly from the furnace, gently extinguish any remaining flames and allow the test sample to cool.
7. Measure and record the final thickness (t_f) of the test sample to an accuracy of ±0.1 inches.
8. For each sample tested, determine and record the intumescence, I, as a percentage of the original sample length as follows:

$$I = \frac{t_f - t_i}{t_i} \times 100$$

9. Determine and record the average intumescence of the three test samples. The numerically averaged intumescence of the three test samples shall be a minimum of 50%.

8.1.4.1.2.3 Physical Characteristics Determined for a Foam Pour

Foam material physical characteristics for the following parameters shall be determined for each foam pour based on the pour definition from Section 8.1.4.1.1, *Introduction and General Requirements*

8.1.4.1.2.3.1 Density

1. Three (3) test samples shall be taken from the foam pour. Each test sample shall be a rectangular prism with nominal dimensions of 1.0 inch thick (T) × 2.0 inches wide (W) × 2.0 inches long (L).

2. Place the test samples in a room (ambient) temperature environment (i.e., 65 ºF to 85 ºF) for sufficient time to thermally stabilize the test samples. Measure and record the room temperature to an accuracy of ±2 ºF.
3. Measure and record the weight of each test sample to an accuracy of ±0.01 grams.
4. Measure and record the thickness, width, and length of each test sample to an accuracy of ±0.001 inches.
5. Determine and record the room temperature density of each test sample utilizing the following formula:

$$\rho_{foam}\ (\text{lb/ft}^3) = \frac{\text{Weight (g)}}{453.6\ \text{g/lb}} \times \frac{1{,}728\ \text{in}^3/\text{ft}^3}{\text{T (in)} \times \text{W (in)} \times \text{L (in)}}$$

6. Determine and record the average density of the three test samples. The numerically averaged density of the three test samples shall nominally be 11.5 lb/ft^3 ±15% (i.e., within the range of 9.8 to 13.2 lb/ft^3).

8.1.4.1.2.3.2 Parallel-to-Rise Compressive Stress

1. Three (3) test samples shall be taken from the foam pour. Each test sample shall be a rectangular prism with nominal dimensions of 1.0 inch thick (T) × 2.0 inches wide (W) × 2.0 inches long (L). The thickness dimension shall be the parallel-to-rise direction.
2. Place the test samples in a room (ambient) temperature environment (i.e., 65 ºF to 85 ºF) for sufficient time to thermally stabilize the test samples. Measure and record the room temperature to an accuracy of ±2 ºF.
3. Measure and record the thickness, width, and length of each test sample to an accuracy of ±0.001 inches.

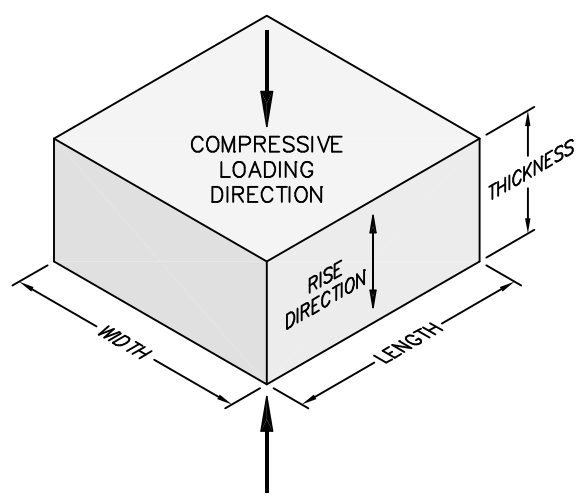

4. Compute and record the surface area of each test sample by multiplying the width by the length (i.e., W × L).
5. Place a test sample in a Universal Testing Machine. Lower the machine's crosshead until it touches the test sample. Set the machine's parameters for the thickness of the test sample.
6. Apply a compressive load to each test sample at a rate of 0.10 ±0.05 inches/minute until a strain of 70%, or greater, is achieved. For each test sample, plot the compressive stress versus strain and record the compressive stress at strains of 10%, 40%, and 70%.
7. Determine and record the average parallel-to-rise compressive stress of the three test samples from each pour. As delineated in Table 8.1-1, the average parallel-to-rise compressive stress for each pour shall be the nominal compressive stress ±15% at strains of 10%, 40%, and 70%.

8. Determine and record the average parallel-to-rise compressive stress of all test samples from each foamed component. As delineated in Table 8.1-1, the average parallel-to-rise compressive stress for a foamed component shall be the nominal compressive stress ±10% at strains of 10%, 40%, and 70%.

8.1.4.1.2.3.3 Perpendicular-to-Rise Compressive Stress

1. Three (3) test samples shall be taken from the foam pour. Each test sample shall be a rectangular prism with nominal dimensions of 1.0 inch thick (T) × 2.0 inches wide (W) × 2.0 inches long (L). The thickness dimension shall be the perpendicular-to-rise direction.

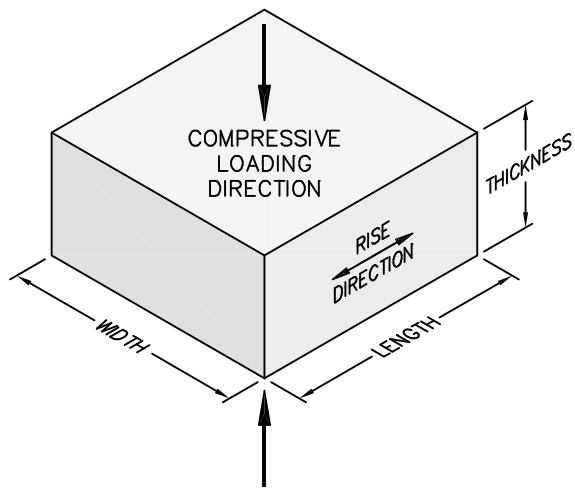

2. Place the test samples in a room (ambient) temperature environment (i.e., 65 ºF to 85 ºF) for sufficient time to thermally stabilize the test samples. Measure and record the room temperature to an accuracy of ±2 ºF.
3. Measure and record the thickness, width, and length of each test sample to an accuracy of ±0.001 inches.
4. Compute and record the surface area of each test sample by multiplying the width by the length (i.e., W × L).
5. Place a test sample in a Universal Testing Machine. Lower the machine's crosshead until it touches the test sample. Set the machine's parameters for the thickness of the test sample.
6. Apply a compressive load to each test sample at a rate of 0.10 ±0.05 inches/minute until a strain of 70%, or greater, is achieved. For each test sample, plot the compressive stress versus strain and record the compressive stress at strains of 10%, 40%, and 70%.
7. Determine and record the average perpendicular-to-rise compressive stress of the three test samples from each pour. As delineated in Table 8.1-1, the average perpendicular-to-rise compressive stress for each pour shall be the nominal compressive stress ±15% at strains of 10%, 40%, and 70%.
8. Determine and record the average perpendicular-to-rise compressive stress of all test samples from each foamed component. As delineated in Table 8.1-1, the average perpendicular-to-rise compressive stress for a foamed component shall be the nominal compressive stress ±10% at strains of 10%, 40%, and 70%.

8.1.5 Tests for Shielding Integrity

Poured lead shielding integrity shall be confirmed via gamma scanning. There are two gamma scan techniques utilized. The main difference is in the method utilized to determine acceptance criteria. Both gamma scan techniques are exactly the same in all other respects and are conducted as follows.

An Eberline E120 probe, or equivalent, is used to scan the OC surface while an iridium-192 or cobalt-60 source of sufficient strength is present at the center of the OC cavity. The source is first placed on the bottom of the package cavity while the outer surface is scanned around its circumference, parallel to the source. The source is then moved up a predetermined distance and the circumference scanned again. This sequence is repeated until the entire package surface is scanned.

The OC outer surface is gridded and a chart is made to reflect the gridded surface. Dose rates are recorded from each grid square by scanning every point in the grid and recording the maximum dose rates in the corresponding grid on the chart. This data then serves as the raw gamma scan results. All dose rates are in milliroentgens per hour (mR/hr).

The dose rates are evaluated by comparing them to predetermined dose rate values for nominal (as designed) lead thickness and nominal less 10% lead thickness. The two different methods utilized to determine acceptance criteria are discussed below.

The first method, the *Laboratory Calibration Method*, utilizes test blocks of the package wall made up of lead and steel sheets. The test blocks simulate nominal, or as designed, and nominal less 10% lead thicknesses. The source is placed behind the nominal test block assembly at a distance equal to the inside radius of the package. The probe is then placed on the outside of the test block assembly and dose readings are recorded. This test sequence is repeated on the nominal less 10% test block assembly. The resultant dose values are then utilized as acceptance criteria for the actual gamma scan. Additionally, the expected dose rate values for nominal and reduced thickness shielding are calculated utilizing attenuation values for steel, lead, and air as correlation verification.

The second method, the *Field Calibration Method*, utilizes a specially fabricated test lid which incorporates a holder for various lead and steel sheet thicknesses. This fixture is installed onto the package to be scanned, with the test lid set up to simulate the nominal lead thickness. The source is placed below the test lid, inside the package, at a distance equal to the inside radius of the package. A dose reading is then recorded. The lead sheet thickness in the test lid holder is then adjusted to establish the nominal less 10% lead thickness configuration. Again, the source is placed below the test lid at a distance equal to the inside radius of the package and a dose reading is recorded. Additional dose readings are taken in 1/8-inch lead thickness increments between and beyond the two base readings until four-to-eight dose readings are obtained. The resultant data is then plotted on a chart for dose values versus lead thickness. The value for nominal less 10% lead thickness is utilized as the maximum acceptable dose value for the inspected package.

Indications of non-conformance with the above stated standards shall be recorded for disposition prior to repair and final acceptance in accordance with the requirements of the cognizant quality assurance program.

8.1.6 Thermal Acceptance Tests

Material properties established in Section 3.2, *Summary of Thermal Properties of Materials*, are consistently conservative for the analyses performed. As such, with the exception of the polyurethane foam (addressed in Section 8.1.4.1, *Polyurethane Foam*), acceptance tests for material thermal properties are not performed.

8.1.7 Lead Installation Tests

Testing during the lead installation process involves pre- and post-pour diameter and straightness measurements of the OC inner shell and close monitoring of the package temperatures during the preheat, lead pour, and cooldown processes. A more detailed description of the lead installation and testing is presented in Appendix 8.3.1, *Lead Installation Procedure*.

Table 8.1-1 – Compressive Stress Ranges at Room Temperature (psi)

	Parallel-to-Rise at Strain, $\varepsilon_{//}$			Perpendicular-to-Rise at Strain, $\varepsilon_{\perp}$		
Sample Range	**ε = 10%**	**ε = 40%**	**ε = 70%**	**ε = 10%**	**ε = 40%**	**ε = 70%**
Nominal –15%	320	382	1,132	296	371	1,185
Nominal –10%	338	404	1,199	313	392	1,255
Nominal	376	449	1,332	348	436	1,394
Nominal +10%	414	494	1,465	383	480	1,533
Nominal +15%	432	516	1,532	400	501	1,603

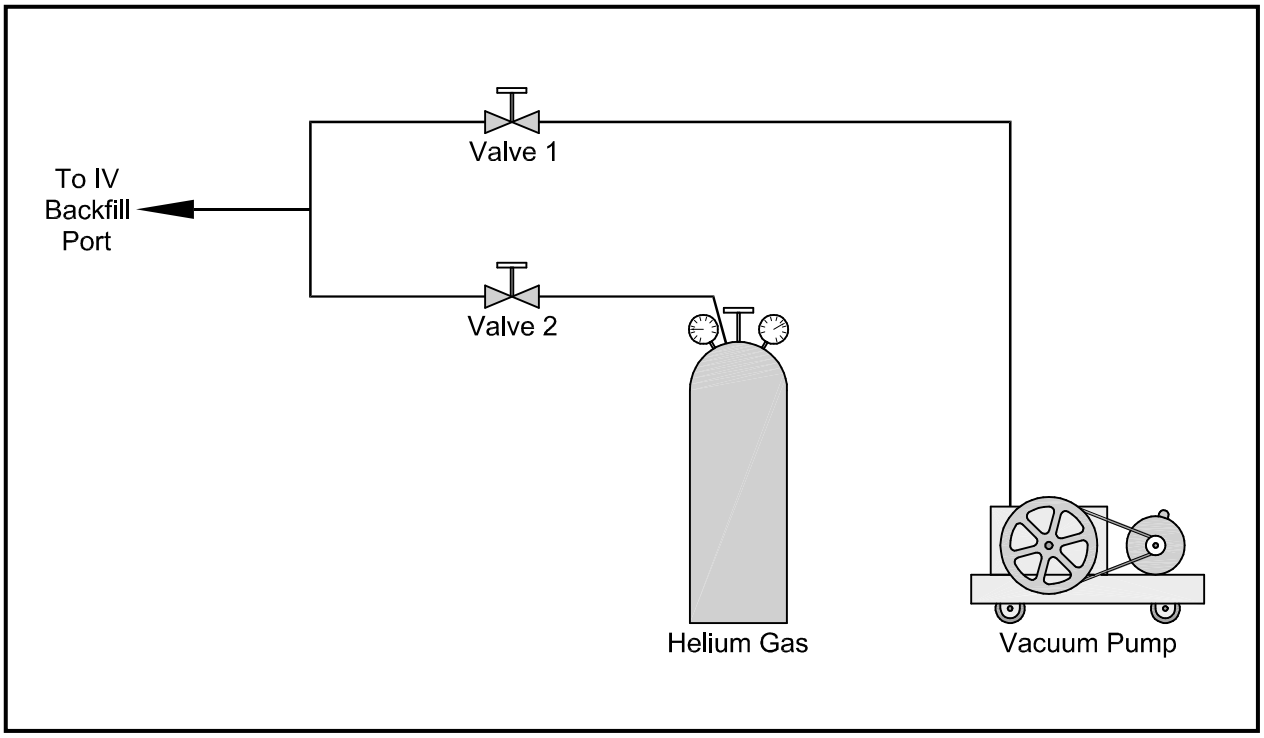

Figure 8.1-1 – Testing the IV Lid Seal Integrity

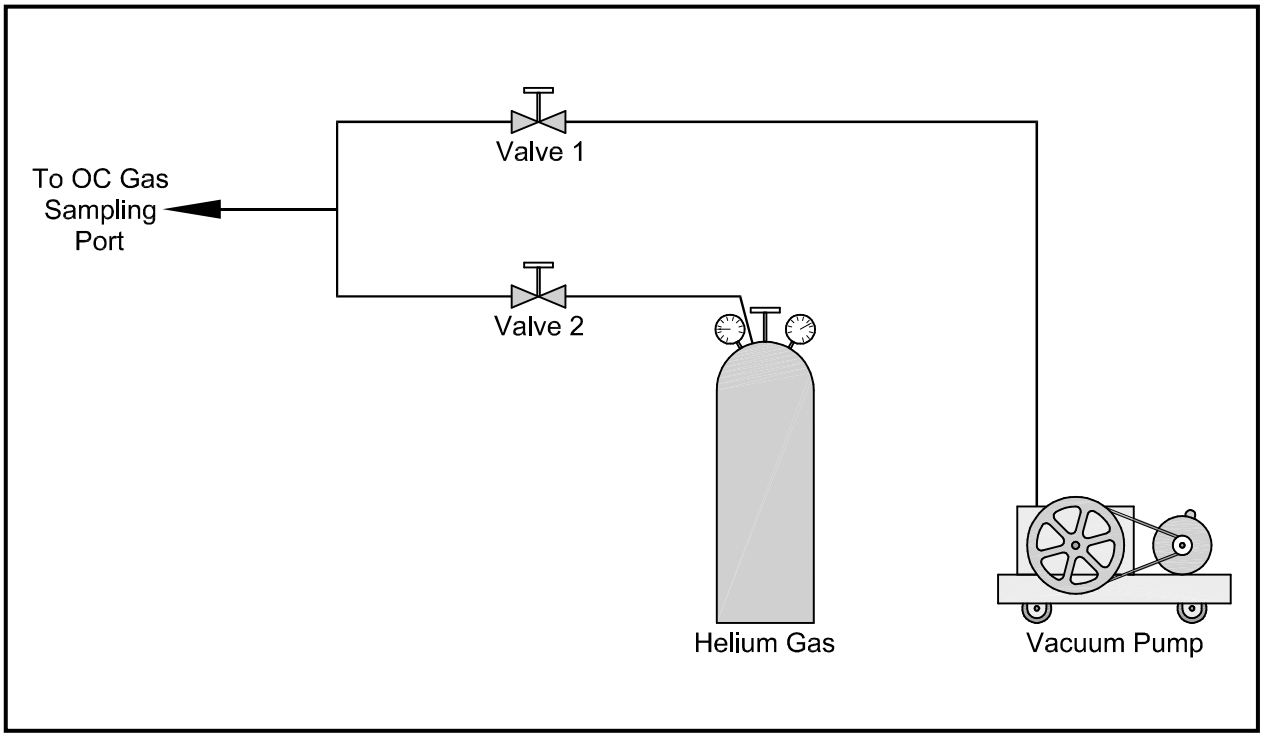

Figure 8.1-2 – Testing the OC Lid Seal Integrity

This page intentionally left blank.

8.2 Maintenance Program

This section describes the maintenance program used to ensure continued performance of the RH-TRU 72-B package.

The criteria for repair of the packaging are dictated by the design, as detailed in the drawings in Appendix 1.3.1, *Packaging General Arrangement Drawings*. When the packaging is not in compliance with the design configuration, it must be removed from service. Repairs will involve returning the packaging to a compliant configuration. Repair verification procedures will be equivalent to fabrication verification procedures.

Packaging repairs fall into two categories, minor and major. Minor repairs are those that can be readily accomplished and require no special tools, supplies, equipment, or highly skilled personnel. Minor repairs would include replacement of damaged consumables, polishing out scratches on the seal surfaces, and so forth. Such repairs can be undertaken by users that have the necessary equipment and qualified personnel.

Major repairs consist of all repairs requiring welding or machining to correct a deficiency that affects the performance integrity of the packaging or its components. Major repairs and major component replacements are the responsibility of the packaging licensee, and will be performed at a facility designated and approved by the licensee.

8.2.1 Structural and Pressure Tests

8.2.1.1 Structural Tests

Other than the stress corrosion tests specified in Section 8.2.1.3, *Inner Vessel Interior Surface Inspection*, and the lifting device load tests required for first use (see Section 8.1.2.1, *Lifting Device Load Testing*), no structural tests are necessary to ensure continuous performance of the package.

8.2.1.2 Containment Vessel Pressure Testing

Other than the acceptance tests required for first use (see Section 8.1.2.2, *Inner Vessel and Outer Cask Pressure Testing*), no pressure tests are necessary to ensure continued performance of the package.

8.2.1.3 Inner Vessel Interior Surface Inspection

Prior to first use and annually thereafter, inspections shall be performed on the accessible interior surfaces of the inner vessel (IV) for evidence of chemically induced stress corrosion. This shall consist of a visual inspection for indication of IV interior surface corrosion. Should evidence of corrosion exist, a liquid penetrant inspection of the IV interior surfaces including accessible shell, head, flange and weld surfaces shall be performed per ASME Boiler and Pressure Vessel Code, Section V[1], Article 6, and ASME Boiler and Pressure Vessel Code, Section III[2], Division

[1] American Society of Mechanical Engineers (ASME) Boiler and Pressure Vessel Code, Section V, *Nondestructive Examination*, 1986 Edition.

[2] American Society of Mechanical Engineers (ASME) Boiler and Pressure Vessel Code, Section III, *Rules for Construction of Nuclear Power Plant Components*, 1986 Edition.

1, Subsection NB, Article NB-5000. Indications of cracking or distortion shall be recorded on a nonconformance report and dispositioned prior to corrective actions.

Once the packaging is put into service, at a maximum interval of five (5) years, inspections shall be performed on the accessible interior surfaces of the IV for evidence of chemically induced stress corrosion. This shall consist of a liquid penetrant inspection of the entire IV interior surfaces, including accessible shell, head, flange and weld surfaces per ASME Boiler and Pressure Vessel Code, Section V[1], Article 6, and ASME Boiler and Pressure Vessel Code, Section III[2], Division 1, Subsection NB, Article NB-5000. Indications of cracking or distortion shall be recorded on a nonconformance report and dispositioned prior to corrective actions in accordance with the cognizant quality assurance program.

8.2.2 Maintenance/Periodic Leakage Rate Tests

Maintenance/Periodic Leakage Rate Testing shall conform to the requirements of Section 7.4, *Maintenance Leakage Rate Test*, of ANSI N14.5[3].

Appropriate sections of the *Maintenance/Periodic Leakage Rate Test* shall be performed during routine maintenance to verify package configuration and performance to design criteria. *Maintenance/Periodic Leakage Rate Tests* of the lid O-ring seals and port closure bolt seals are to be performed upon replacement, but seals need not necessarily be replaced at the same time (i.e., seals are to be replaced annually or when damaged). Sections of the *Maintenance/Periodic Leakage Rate Test* shall be performed upon component failure during the *Preshipment Leakage Rate Test* (see Appendix 7.4.1, *Preshipment Leakage Rate Test*).

To begin the test, it is assumed the IV and OC lids are removed. The *Maintenance Leakage Rate Test* is separated into five (5) tests, three (3) for the IV and two (2) for the outer cask (OC). The five (5) separate tests are: 1) IV lid seal integrity, 2) IV gas sampling port closure bolt seal integrity, 3) IV backfill port closure bolt seal integrity, 4) OC lid seal integrity, and 5) OC gas sampling port closure bolt seal integrity.

8.2.2.0.1 Obtain a helium mass spectrometer leak detector capable of detecting a leak of 5×10^{-8} standard cubic centimeters per second (scc/s), air, or better (1.3×10^{-7} scc/s, helium).

8.2.2.0.2 Calibrate the leak detector to a minimum sensitivity of 5×10^{-8} scc/s, air (1.3×10^{-7} scc/s, helium).

8.2.2.1 Testing the IV Lid Seal Integrity

8.2.2.1.1 Clean and visually inspect the three IV lid O-ring seals. Sparingly apply new vacuum grease to the seals. Install the O-ring seals into the O-ring grooves.

8.2.2.1.2 Clean and visually inspect the sealing area on the IV body. Install the IV lid, tightening the eight (8) 7/8-9UNC bolts to 100 – 200 lb-ft torque.

8.2.2.1.3 Tighten the gas sampling port closure bolt to 15 – 20 lb-ft torque.

[3] ANSI N14.5-1997, *American National Standard for Radioactive Materials – Leakage Tests on Packages for Shipment,* American National Standards Institute, Inc. (ANSI).

8.2.2.1.4 Install a test port tool into the backfill port.

8.2.2.1.5 Attach a vacuum pump and a source of helium gas, in parallel, to the test port tool. Install valves on each of the lines to allow independent isolation of the vacuum pump and the source of helium gas to the test port tool. Close the valve to the source of helium gas, and open the valve to the vacuum pump.

8.2.2.1.6 Utilizing the test port tool, rotate the backfill port closure bolt fully open.

8.2.2.1.7 Evacuate the system through the test port tool to 90% vacuum or better (≤10% ambient atmospheric pressure). Isolate the vacuum pump from the system.

8.2.2.1.8 Backfill the evacuated cavity with helium gas to a pressure slightly greater than atmospheric pressure (+1 psi, -0 psi), and close the valve to isolate the source of helium gas from the system. Correction for tracer gas concentration shall be performed.

8.2.2.1.9 Utilizing the test port tool, rotate the backfill port closure bolt closed and tighten to 15 – 20 lb-ft torque.

8.2.2.1.10 Remove the helium-contaminated test port tool from the backfill port.

8.2.2.1.11 Install a clean (helium-free) test port tool into the seal test port.

8.2.2.1.12 Attach a leak detector to the test port tool.

8.2.2.1.13 Utilizing the test port tool, rotate the seal test port closure bolt fully open.

8.2.2.1.14 Evacuate the cavity above the IV lid containment seal until the vacuum is sufficient to operate the leak detector.

8.2.2.1.15 Determine the leakage rate of the system using the leak detector.

8.2.2.1.16 If the leakage rate of the system exceeds the level indicated in Section 8.2.2.6, *Maintenance/Periodic Leakage Rate Test Acceptance Criteria*, release the vacuum, remove the IV lid and inspect the seals for cuts, tears, or abrasion, and the sealing areas for cleanliness and surface condition. If necessary, replace the defective seal(s) and/or repair the sealing areas. Repeat Paragraphs 8.2.2.1.1 through 8.2.2.1.15. If, after repeated testing, it has been determined that the lid containment seal cannot be made to pass the requirements of Section 8.2.2.6, *Maintenance/Periodic Leakage Rate Test Acceptance Criteria*, utilize appropriate methods to locate/isolate the leak path. Repair the leak path and repeat Paragraphs 8.2.2.1.1 through 8.2.2.1.15 to verify integrity of the IV lid containment seal.

8.2.2.1.17 After successfully completing Paragraphs 8.2.2.1.1 through 8.2.2.1.16, rotate the seal test port closure bolt closed, tighten to 15 – 20 lb-ft torque, and remove the leak detector/test port tool.

8.2.2.2 Testing the IV Gas Sampling Port Closure Bolt Seal Integrity

8.2.2.2.1 Verify the presence of a helium atmosphere below the gas sampling port closure bolt containment seal, as provided for in Paragraphs 8.2.2.1.3 through 8.2.2.1.10.

8.2.2.2.2 Install a test port tool into the gas sampling port.

8.2.2.2.3 Attach a leak detector to the test port tool.

8.2.2.2.4 Evacuate the cavity above the gas sampling port closure bolt containment seal until the vacuum is sufficient to operate the leak detector.

8.2.2.2.5 Determine the leakage rate of the system using the leak detector.

8.2.2.2.6 If the leakage rate of the system exceeds the level indicated in Section 8.2.2.6, *Maintenance/Periodic Leakage Rate Test Acceptance Criteria*, release the vacuum, remove the gas sampling port closure bolt and inspect the seal for cuts, tears, or abrasion, and the sealing areas for cleanliness and surface condition. If necessary, replace the defective components and/or repair the sealing areas. Repeat Paragraphs 8.2.2.2.1 through 8.2.2.2.5. If, after repeated testing, it has been determined that the gas sampling port closure bolt containment seal cannot be made to pass the requirements of Section 8.2.2.6, *Maintenance/Periodic Leakage Rate Test Acceptance Criteria*, utilize appropriate methods to locate/isolate the leak path. Repair the leak path and repeat Paragraphs 8.2.2.2.1 through 8.2.2.2.5 to verify integrity of the gas sampling port closure bolt containment seal.

8.2.2.2.7 After successfully completing Paragraphs 8.2.2.2.1 through 8.2.2.2.6, remove the leak detector/test port tool.

8.2.2.3 Testing the IV Backfill Port Closure Bolt Seal Integrity

8.2.2.3.1 Verify the presence of a helium atmosphere below the backfill port closure bolt containment seal, as provided for in Paragraphs 8.2.2.1.3 through 8.2.2.1.10.

8.2.2.3.2 Install a clean (helium-free) test port tool into the backfill port. Attach a leak detector to the test port tool.

8.2.2.3.3 Evacuate the cavity above the backfill port closure bolt until the vacuum is sufficient to operate the leak detector.

8.2.2.3.4 Determine the leakage rate of the system using the leak detector.

8.2.2.3.5 If the leakage rate of the system exceeds the level indicated in Section 8.2.2.6, *Maintenance/Periodic Leakage Rate Test Acceptance Criteria*, release the vacuum, remove the backfill port closure bolt and inspect the seal for cuts, tears, or abrasion, and the sealing areas for cleanliness and surface condition. If necessary, replace the defective components and/or repair the sealing areas. Repeat Paragraphs 8.2.2.3.1 through 8.2.2.3.4. If, after repeated testing, it has been determined that the backfill port closure bolt containment seal cannot be made to pass the requirements of Section 8.2.2.6, *Maintenance/Periodic Leakage Rate Test Acceptance Criteria*, utilize appropriate methods to locate/isolate the leak path. Repair the leak path and repeat Paragraphs 8.2.2.3.1 through 8.2.2.3.4 to verify integrity of the backfill port closure bolt seal.

8.2.2.3.6 After successfully completing Paragraphs 8.2.2.3.1 through 8.2.2.3.5, remove the leak detector/test port tool.

8.2.2.4 Testing the OC Lid Seal Integrity

8.2.2.4.1 Clean and visually inspect both OC O-ring lid seals. Sparingly apply new vacuum grease to the seals. Install the O-ring seals into the O-ring grooves.

8.2.2.4.2 Clean and visually inspect the sealing area on the OC body. Install the OC lid, tightening the eighteen (18), 1¼-7UNC bolts to 600 – 700 lb-ft torque.

8.2.2.4.3 Install a test port tool into the gas sampling port.

8.2.2.4.4 Utilizing the test port tool, rotate the OC gas sampling port closure bolt fully open.

8.2.2.4.5 Attach a vacuum pump and a source of helium gas, in parallel, to the test port tool. Install valves on each of the lines to allow independent isolation of the vacuum pump and the source of helium gas to the test port tool. Close the valve to the source of helium gas, and open the valve to the vacuum pump.

8.2.2.4.6 Evacuate the system through the test port tool to 90% vacuum or better (≤10% ambient atmospheric pressure). Isolate the vacuum pump from the system.

8.2.2.4.7 Backfill with helium gas to a pressure slightly greater than atmospheric pressure (+1 psi, -0 psi) and close the valve to isolate the source of helium gas from the system. Correction for tracer gas concentration shall be performed.

8.2.2.4.8 Utilizing the test port tool, rotate the OC gas sampling closure bolt closed and tighten to 15 – 20 lb-ft torque.

8.2.2.4.9 Remove the helium-contaminated test port tool from the gas sampling port.

8.2.2.4.10 Install a clean (helium-free) test port tool into the seal test port.

8.2.2.4.11 Attach the leak detector to the test port tool.

8.2.2.4.12 Utilizing the test port tool, rotate the seal test port closure bolt fully open.

8.2.2.4.13 Evacuate the system through the test port tool until the vacuum is sufficient to operate the leak detector.

8.2.2.4.14 Determine the leakage rate of the system using the leak detector.

8.2.2.4.15 If the leakage rate of the system exceeds the level indicated in Section 8.2.2.6, *Maintenance/Periodic Leakage Rate Test Acceptance Criteria*, release the vacuum, remove the OC lid and inspect the closure seals for cuts, tears, or abrasion, and the sealing areas for cleanliness and surface condition. If necessary, replace the defective seal(s) and/or repair the sealing areas. Repeat Paragraphs 8.2.2.4.1 through 8.2.2.4.14. If, after repeated testing, it has been determined that the lid containment seal cannot be made to pass the requirements of Section 8.2.2.6, *Maintenance/Periodic Leakage Rate Test Acceptance Criteria*, utilize appropriate methods to locate/isolate the leak path. Repair the leak path and repeat Paragraphs 8.2.2.4.1 through 8.2.2.4.14 to verify integrity of the OC lid containment seal.

8.2.2.4.16 After successfully completing Paragraphs 8.2.2.4.1 through 8.2.2.4.15, rotate the seal test port closure bolt closed, tighten to 15 – 20 lb-ft torque, and remove the leak detector/test port tool.

8.2.2.5 Testing the OC Gas Sampling Port Closure Bolt Seal Integrity

8.2.2.5.1 Verify the presence of a helium atmosphere below the gas sampling port closure bolt containment seal, as provided for in Paragraphs 8.2.2.4.4 through 8.2.2.4.9.

8.2.2.5.2 Install a clean (helium-free) test port tool into the gas sampling port. Attach a leak detector to the test port tool.

8.2.2.5.3 Evacuate the cavity above the gas sampling port closure bolt until the vacuum is sufficient to operate the leak detector.

8.2.2.5.4 Determine the leakage rate of the system using the leak detector.

8.2.2.5.5 If the leakage rate of the system exceeds the level indicated in Section 8.2.2.6, *Maintenance/Periodic Leakage Rate Test Acceptance Criteria*, release the vacuum, remove the gas sampling port closure bolt and inspect the seal for cuts, tears, or abrasion, and the sealing areas for cleanliness and surface condition. If necessary, replace the defective components and/or repair the sealing areas. Repeat Paragraphs 8.2.2.5.1 through 8.2.2.5.4. If, after repeated testing, it has been determined that the gas sampling port closure bolt containment seal cannot be made to pass the requirements of Section 8.2.2.6, *Maintenance/Periodic Leakage Rate Test Acceptance Criteria*, utilize appropriate methods to locate/isolate the leak path. Repair the leak path and repeat Paragraphs 8.2.2.5.1 through 8.2.2.5.4 to verify integrity of the gas sampling port closure bolt seal.

8.2.2.5.6 After successfully completing Paragraphs 8.2.2.5.1 through 8.2.2.5.5, remove the leak detector/test port tool.

8.2.2.6 Maintenance/Periodic Leakage Rate Test Acceptance Criteria

8.2.2.6.1 To be acceptable, per Section 6.3.2, *Application of Referenced Air Leakage Rate*, of ANSI N14.5[3], each vessel test and each containment seal test shall demonstrate a leakage rate of 1×10^{-7} scc/s, air, (leaktight) (2.6×10^{-7} helium), or less.

8.2.2.6.2 In order to demonstrate that the package is leaktight, per Section 8.4, *Sensitivity*, of ANSI N14.5[3], the sensitivity of the leakage rate test procedure shall be 5×10^{-8} scc/s, air (1.3×10^{-7} helium), or less.

8.2.2.6.3 Indications of non-conformance with the above stated standards shall be recorded for disposition prior to repair and final acceptance in accordance with the requirements of the cognizant quality assurance program.

8.2.3 Subsystems Maintenance

8.2.3.1 Fasteners

All threaded components shall be inspected annually and prior to each use for deformed or stripped threads. Any damaged components shall be replaced prior to further use. At a minimum, OC and IV closure bolts, and impact limiter attachment bolts shall be replaced prior to the completion of 460 service cycles for the OC closure bolts and impact limiter attachment bolts, and 550 service cycles for the IV closure bolts.

8.2.3.2 Impact Limiters

A sound industrial maintenance program should be followed to assure the integrity of the impact limiters. Such a program should include procedures for periodic inspection, cleaning, replacement of damaged consumables (attachment bolts, pipe plugs, lifting lug hinges), and the associated record-keeping and quality assurance controls. Inspections should include surveys of the impact limiter exterior for dents, cuts and/or punctures, indications of loss of weld integrity, and general cleanliness of the outer shell. If any damage is detected which might prevent the impact limiter from performing its design functions, the impact limiter must be removed from service until a detailed evaluation is made and remediation approach can be determined. Remediation of such damage must be carried out in a manner which will return the impact limiter to its original design condition.

Specifically, the impact limiter attachment bolts shall be inspected annually and after each use for damaged or stripped threads. The plastic pipe plugs at the ends of the impact limiters shall be inspected for damage after each use and replaced prior to further use if damage is present. The pipe plugs shall be removed on an annual basis and the foam shall be visually inspected. Inspections of the foam will be for determination of deviations from the design requirements of the foam which might prevent the impact limiter from performing its design functions. Such discrepancies would include discontinuities in the foam, such as cracks or voids, or indications of egress of moisture. If any such discrepancies are detected, and the potential exists that they are widespread (i.e., are not limited to the visible portion of the foam), the impact limiter must be removed from service until a detailed evaluation is made and a remediation approach can be determined. Remediation of such damage must be carried out in a manner which will return the impact limiter to its original design condition. Minor problems, such as ingress of moisture, should be corrected as appropriate, either by the user or the packaging licensee. Loss of integrity of the polyurethane foam (unless it can be conclusively demonstrated to be highly localized) is not considered a repairable condition.

8.2.3.3 Trunnions

The trunnions shall be inspected annually and before each use for excessive wear, galling, or distortion. Trunnions exhibiting such damage shall be corrected prior to further use.

8.2.3.4 Sealing Areas and Grooves

8.2.3.4.1 Sealing Area Routine Inspection and Repair

Before each use, OC and IV sealing surfaces and the visible portion of the O-ring seals and grooves shall be visually inspected for damage that could impair the sealing capabilities of the RH-TRU 72-B packaging. Furthermore, at the time of O-ring seal replacement, visually inspect the O-ring seal grooves for damage that could impair the sealing capabilities of the RH-TRU 72-B packaging. Damage shall be corrected prior to further use (e.g., using 400 – 600 grit emery cloth to polish the sealing surfaces) to the surface finish specified in Section 8.2.3.4.2, *Annual Sealing Area Inspection*.

Upon completion of sealing area and/or groove repairs, perform a sealing area inspection per Section 8.2.3.4.2, *Annual Sealing Area Inspection*, and leakage rate test per the applicable subsection of the *Maintenance Leakage Rate Test* per Section 8.2.2, *Maintenance/Periodic Leakage Rate Tests*.

8.2.3.4.2 Annual Sealing Area Inspection

In order to maintain an effective seal at the OC and IV lid-to-body joint, an annual inspection of the OC and IV body O-ring sealing area surface finishes shall be performed. The surface finish in the containment sealing areas shall be maintained at a maximum 125 RMS micro-inches finish. The following surfaces shall be measured annually:

(1) Bottom surface of each O-ring seal groove, and

(2) Surface of the OC and IV body containment O-ring sealing areas.

If the surface condition of the above sealing areas is determined to exceed 125 RMS micro-inches, repair the sealing area(s) per the requirements of Section 8.2.3.4.1, *Sealing Area Routine Inspection and Repair*.

8.2.4 Valves, Rupture Discs, and Gaskets

This section describes the inspection and replacement schedule for these components.

8.2.4.1 Valves

No valves are used on the RH-TRU 72-B packaging.

8.2.4.2 Rupture Discs

No rupture discs are used on the RH-TRU 72-B packaging.

8.2.4.3 Gaskets

All O-ring seals and gaskets shall be replaced annually or when damaged, per the size and material specifications delineated on the drawings in Appendix 1.3.1, *Packaging General Arrangement Drawings*. Following seal replacement, the seal(s) shall be leakage rate tested to the requirements of Section 8.2.2, *Maintenance/Periodic Leakage Rate Tests*.

8.2.5 Shielding

Other than the tests required prior to first use, no shielding tests are necessary to ensure continued performance of the RH-TRU 72-B packaging.

8.2.6 Thermal

No thermal inspections or tests are necessary to ensure continued performance of the RH-TRU 72-B packaging.

8.2.7 Criticality Control Materials

No materials designed specifically for criticality control are employed in the RH-TRU 72-B packaging. As such, no tests of criticality control materials are necessary to ensure continued performance.

8.3 Appendices

8.3.1 *Lead Installation Procedure*

This page intentionally left blank.

8.3.1 Lead Installation Procedure

The following delineates the procedure for installation of poured lead into the RH-TRU 72-B packaging outer cask (OC). The procedure presents pre-pour, lead pour, gamma scan inspection of the lead shielding, and post-pour requirements. Note that the OC thermal shield is attached after lead pour and cooldown.

8.3.1.1 Interior cavities and surfaces of the OC shells which are to be in contact with the lead shielding shall be swabbed with solvent, wiped down, sandblasted, or otherwise cleansed of loose mill scale, weld slag, and all carbonaceous materials prior to lead pour.

8.3.1.2 All OC inner and outer surfaces shall be supported or braced, as necessary, to prevent distortion during the lead-pouring and cooldown operations.

8.3.1.3 The lead-pouring operation is performed with the packaging inverted (i.e., the OC base plate is up, lid-end is down).

Fill pipes shall be provided through the OC outer shell, adjacent to the lid-end forging, sized as required to allow for rapid and even lead fill.

Standpipes shall be provided through the OC outer shell, adjacent to the base plate, sized as required to allow for easy access of lead during the cooldown operation.

Vent risers shall be provided through the OC base plate to allow for escape of air and impurities.

8.3.1.4 The OC shall be instrumented with thermocouple wires at eight (8) locations on the inside and outside to monitor temperature differentials between the two shells. A total of sixteen (16) thermocouples shall be required. Internal and/or external bracing may be temporarily removed to facilitate thermocouple installation.

The thermocouples shall be mounted opposite each other on the inside and outside shells to assure proper temperature differential measurements. The thermocouple sets shall be mounted at equal intervals over the full length of the OC. The sets shall also be located around the shell circumference so that all areas of the OC are instrumented.

In addition, a calibrated strip recorder with the thermocouples capable of measuring temperatures to 1,000 ºF and plotting time/temperature data every 60 seconds shall be utilized.

Adequate precautions must be taken to assure that the thermocouples are protected from impact or flame impingement during the preheat, lead pour, and cooldown phases.

8.3.1.5 All OC components (i.e., outer shell, inner shell, lid-end forging, and bottom-end closure) shall be uniformly preheated to a temperature of 600 ºF to 700 ºF over the entire surface prior to lead pouring. Preheating shall be done in a suitable enclosure to assure uniform preheating. During preheat, the maximum temperature change for any thermocouple shall not exceed 100 ºF in any thirty (30) minute period.

8.3.1.6 The temperature of the lead at the time of lead pour shall range from 750 ºF to 850 ºF.

8.3.1.7 The rate of lead flow shall be controlled to fill the OC as rapidly and evenly as possible. The lead shall enter the cavity in such a way as to minimize impingement on the OC shells.

8.3.1.8 Heat sources shall be controlled during the cooldown period so that the OC is cooled to ensure that only one solidifying front exists in the lead.

During cooldown, the maximum temperature change for any thermocouple shall not exceed 100 ºF in any thirty (30) minute period, and the maximum difference in temperatures between any pair of thermocouples mounted directly opposite each other (one on the OD and the corresponding one on the ID) shall not exceed 300 ºF at any instant in time.

8.3.1.9 Molten lead at a minimum temperature of 750 ºF shall be added to the standpipes, as necessary, at a rate consistent with normal shrinkage.

8.3.1.10 After all the thermocouples indicate a temperature less than 100 ºF, the thermocouples and any internal and/or external bracing shall be removed and the OC gamma scanned in accordance with the tests delineated in Section 8.1.5, *Tests for Shielding Integrity*.

8.3.1.11 Upon a successful gamma scan, inspection measurements taken after lead pour must meet the requirements specified on the drawings in Appendix 1.3.1, *Packaging General Arrangement Drawings*. (NOTE: Specifically, the tolerance requirements of ASME Boiler and Pressure Vessel Code, Division 1, Section III[1], Subsection NE, Article NE-4220, as defined in drawing Flag Note 27, shall be met.)

8.3.1.12 Remove all fill pipes, vent pipes, and standpipes, clean the holes thoroughly of all lead, and install plugs of identical material as the base material.

[1] American Society of Mechanical Engineers (ASME) Boiler and Pressure Vessel Code, Section III, *Rules for Construction of Nuclear Power Plant Components*, 1986 Edition.

9.0 QUALITY ASSURANCE

This section describes quality assurance (QA) requirements and methods of compliance applicable to the RH-TRU 72-B package.

9.1 Introduction

The RH-TRU 72-B package is designed and shall be built for the U.S. Department of Energy (DOE) and must be approved by the U.S. Nuclear Regulatory Commission (NRC) for the shipment of radioactive material in accordance with the applicable provisions of the U.S. Department of Transportation, described in Subpart I of 49 CFR Part 173[1]. Procurement, design, fabrication, assembly, testing, maintenance, repair, modification, and use of the RH-TRU 72-B package are all done under QA programs that meet all applicable NRC and DOE QA requirements. QA requirements for payloads to be transported in the RH-TRU 72-B package are discussed in the *Remote-Handled Transuranic Waste Authorized Methods for Payload Control* (RH-TRAMPAC)[2].

[1] Title 49, Code of Federal Regulations, Part 173 (49 CFR 173), *Shippers–General Requirements for Shipments and Packagings*, Current Version.

[2] U.S. Department of Energy (DOE), *Remote-Handled Transuranic Waste Authorized Methods for Payload Control* (RH-TRAMPAC), U.S. Department of Energy, Carlsbad Field Office, Carlsbad, New Mexico.

This page intentionally left blank.

9.2 Quality Assurance Requirements

9.2.1 U.S. Nuclear Regulatory Commission

The QA requirements for packaging established by the NRC are described in Subpart H of 10 CFR 71[1]. Subpart H is an 18 criteria QA program based on ANSI/ASME NQA-1[2]. Guidance for QA programs for packaging is described in the NRC Regulatory Guide 7.10[3].

9.2.2 U.S. Department of Energy

The QA requirements of DOE for the use of NRC certified packaging are described in Chapter 4 of DOE Order 460.1[4]. According to Chapter 4.(4)(b), the DOE and its contractors may use NRC certified Type B packaging only under the conditions specified in the certificate of compliance.

9.2.3 Transportation to/from WIPP

Public Law 102-579, enacted by the 102nd Congress, reads as follows:

SEC. 16. TRANSPORTATION.

(a) SHIPPING CONTAINERS. - No transuranic waste may be transported by or for the Secretary [of Energy] to or from WIPP, except in packages -

(1) the design of which has been certified by the Nuclear Regulatory Commission; and

(2) that have been determined by the Nuclear Regulatory Commission to satisfy its quality assurance requirements.

The determination under paragraph (2) shall not be subject to rulemaking or judicial review.

[1] Title 10, Code of Federal Regulations, Part 71 (10 CFR 71), *Packaging and Transportation of Radioactive Material*, Final Rule, 01-26-04.

[2] ANSI/ASME NQA-1, *Quality Assurance Requirements of Nuclear Power Plants*, American National Standards Institute.

[3] U.S. Nuclear Regulatory Commission, Regulatory Guide 7.10, *Establishing Quality Assurance Programs for Packaging Used in the Transport of Radioactive Material,* Revision 1, June 1986.

[4] U.S. Department of Energy Order 460.1, *Packaging and Transportation Safety,* September 1995.

This page intentionally left blank.

9.3 Quality Assurance Program

9.3.1 NRC Regulatory Guide 7.10

Guidance for QA programs applicable to design, fabrication, assembly, and testing of packaging used in transport of radioactive material is covered in Annex 1 of the NRC's Regulatory Guide 7.10[1]; procurement, use, maintenance and repair are covered in Annex 2.

9.3.2 Design

The RH-TRU 72-B package was designed under a QA program approved by the NRC for packaging design. Requests for modification or changes to the design will be submitted to the NRC for approval prior to modification of the RH-TRU 72-B packaging. Any future design changes will be made under an appropriate NRC approved QA program.

9.3.3 Fabrication, Assembly, and Testing

Fabrication, assembly, and testing of each RH-TRU 72-B packaging are performed under a QA program approved by the NRC for these activities.

9.3.4 Procurement

Procurement of each RH-TRU 72B packaging is performed under a QA program that meets the applicable QA requirements of the NRC.

9.3.5 Use

The RH-TRU 72-B package will be used primarily by the DOE for shipments of authorized contents to the WIPP site. However, it may also be used between DOE sites other than WIPP (inter-site) and for DOE on-site shipments within site boundaries (intra-site). The DOE is registered with the NRC as a user of the RH-TRU 72-B package under the general license provisions of 49 CFR §173.471[5]. The RH-TRU 72-B packaging may also be used for non-DOE shipments as authorized by the NRC.

---

[1] U.S. Nuclear Regulatory Commission, Regulatory Guide 7.10, *Establishing Quality Assurance Programs for Packaging Used in the Transport of Radioactive Material,* Revision 1, June 1986.

[5] Title 49, Code of Federal Regulations, Part 173 (49 CFR 173), *Shippers—General Requirements for Shipments and Packagings*, U.S. Department of Transportation, Washington, D.C., Current Version.

9.3.5.1 DOE Shipments to/from WIPP

Use of RH-TRU 72-B packaging for shipments to/from the WIPP site will be made under a QA program that meets the QA requirements of the NRC. The appropriate DOE Field Office(s) shall inspect and approve the QA programs of the DOE contractors that make shipments to or from WIPP in the RH-TRU 72-B package. DOE or the DOE managing and operating contractor for the WIPP shall perform surveillances of the RH-TRU 72-B package users' QA programs to ensure that the package is used in accordance with the requirements of the certificate of compliance.

9.3.5.2 Other DOE Shipments: Non-WIPP

The appropriate DOE Field Office(s) shall inspect and approve the shipper's and receiver's QA programs for equivalency to the NRC's QA program requirements in Subpart H of 10 CFR 71[4]. For example, a contractor working under an 18 criteria QA program per ANSI/ASME NQA-1[7] could be deemed acceptable if the program is applicable to packaging. DOE or the DOE managing and operating contractor for the WIPP shall perform surveillances of the RH-TRU 72-B package users' QA programs to ensure that the package is used in accordance with the requirements of the certificate of compliance.

9.3.5.3 Non-DOE Users of RH-TRU 72-B package

Non-DOE users of RH-TRU 72-B package shall have QA programs approved by the NRC.

9.3.6 Maintenance and Repair

Minor maintenance, such as changing seals or fasteners, may be performed under the user's QA program. Major maintenance, such as cutting or welding a containment boundary, shall be performed under an appropriate QA program that has been approved by the NRC.

[7] ANSI/ASME NQA-1, *Quality Assurance Requirements of Nuclear Power Plants*, American National Standards Institute.